



**FACULTAD DE INGENIERIA U.N.A.M.
DIVISION DE EDUCACION CONTINUA**

***CURSO INTERNACIONAL DE SISTEMAS ELECTRICOS DE
POTENCIA***

MODULO II

SISTEMAS ELECTRICOS DE POTENCIA II

ESTABILIDAD DE SISTEMAS ELECTRICOS DE POTENCIA

1996



...M.A.M.U. AIRBORNE E...
...AMERICAN...
...ELECTRICAL...

INTERNATIONAL SYSTEMS ELECTRIC
POTENTIAL

SYSTEMS ELECTRIC POTENTIAL

INTERNATIONAL SYSTEMS ELECTRIC POTENTIAL

ESTABILIDAD DE LOS SISTEMAS ELECTRICOS DE POTENCIA

CONTENIDO:

- 1 El problema de la estabilidad (FMC).**
 - 2 Máquina Síncrona (FMC).**
 - 3 Estabilidad transitoria. Máquina-bus infinito (FMC).**
 - 4 Método de las áreas iguales (JLHG).**

 - 5 Métodos de solución numérica (FMC).**
 - 6 Sistemas multimáquina (JLHG).**
 - 7 Estabilidad en estado estable (FMC).**
 - 8 Estabilidad dinámica (JLHG).**
- Conclusiones.**

EXPOSITORES:

FMC - Ing. Felipe Martínez Cruz
Cía. de Luz y Fuerza del Centro, S.A.

JLHG - José Leonel Hernández Grimaldo
Cía. de Luz y Fuerza del Centro, S.A.

The first part of the document discusses the importance of maintaining accurate records. It states that records should be kept for a minimum of seven years. This is necessary to ensure that all transactions are properly documented and can be audited if necessary.

The second part of the document outlines the procedures for handling confidential information. It emphasizes that all confidential data must be stored securely and accessed only by authorized personnel. Any breach of confidentiality must be reported immediately to the appropriate authorities.

The third part of the document describes the process for reviewing and updating policies. It notes that policies should be reviewed annually to ensure they remain relevant and effective. Any changes to policies should be approved by the management team and communicated to all staff members.

The fourth part of the document provides information about the company's commitment to environmental sustainability. It highlights the company's efforts to reduce its carbon footprint and promote responsible resource use. This includes initiatives such as recycling, energy conservation, and using eco-friendly products.

The fifth and final part of the document discusses the company's approach to diversity and inclusion. It states that the company is committed to creating a workplace where all employees are treated fairly and have equal opportunities for growth and development. This involves implementing policies and practices that support diversity and foster an inclusive culture.

For more information, please contact our HR department at [phone number] or visit our website at [website URL].

I EL PROBLEMA DE LA ESTABILIDAD

1.1 ESTADO ESTABLE Y ESTADO DINAMICO.

El análisis de los sistemas de potencia implica el cálculo de algunas variables de la red, como voltajes, corrientes, potencias activa y reactiva, frecuencias, etc., bajo un conjunto de condiciones dadas. La figura 1.1 presenta una organización de los estudios sobre sistemas de potencia. La clase de problemas localizados en la parte izquierda de la figura son llamados de estado estable o régimen permanente (steady state) porque en ellos las magnitudes eléctricas del sistema son prácticamente constantes; en este caso la solución se obtiene mediante ecuaciones algebraicas. Esto no significa que el sistema esté estático o inalterable en el momento para el cual se obtiene la solución.

Por el contrario, el sistema puede sufrir cambios bruscos, por ejemplo, una condición de falla. El punto es que resulta mucho más fácil resolver ecuaciones algebraicas que ecuaciones diferenciales. Se ha aprendido a hacer buen uso de las soluciones en estado estable en la planeación del sistema y al determinar la protección de éste. Esto es semejante a tomar un grupo de fotografías del sistema bajo ciertas condiciones específicas. A partir de estas fotografías se pueden diseñar expansiones del sistema y esquemas de protección, y puede uno aprender bastante acerca de las debilidades y fortalezas del sistema.

En los problemas dinámicos mostrados en la parte derecha de la figura 1.1, se hace necesario resolver un grupo de ecuaciones diferenciales para determinar el comportamiento de voltajes, corrientes y otras variables como una función del tiempo.

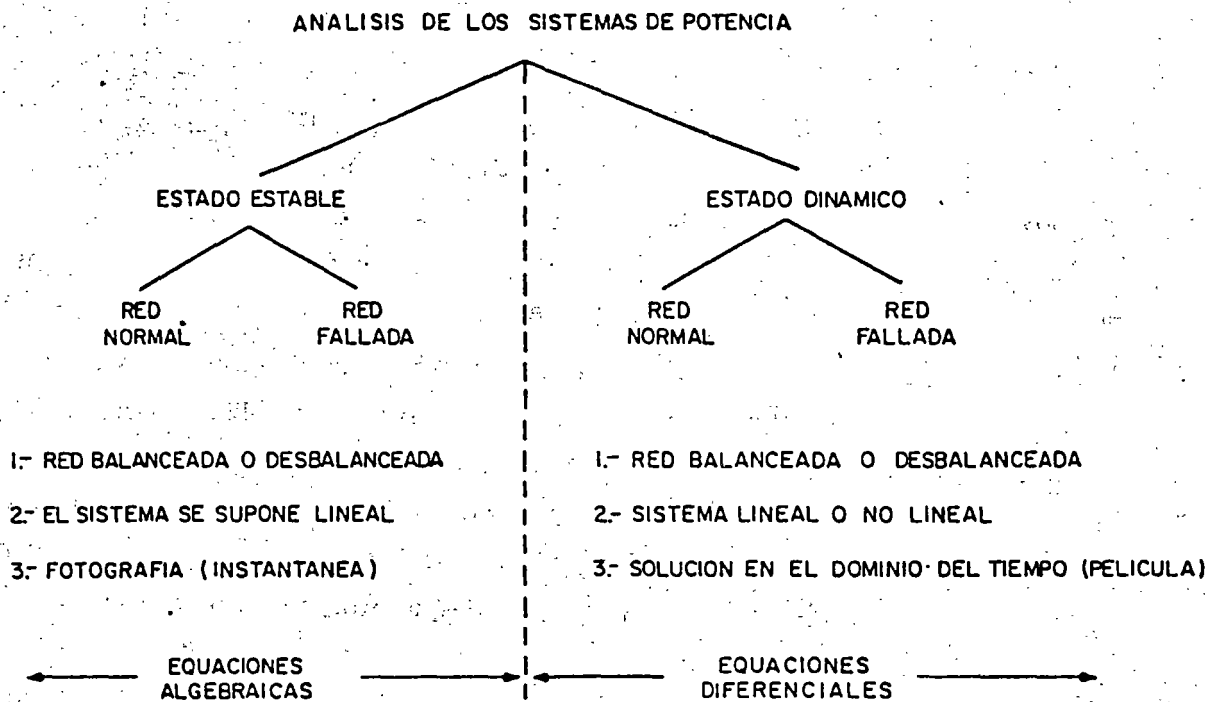


Figura 1.1 Organización de los estudios sobre sistemas de potencia.

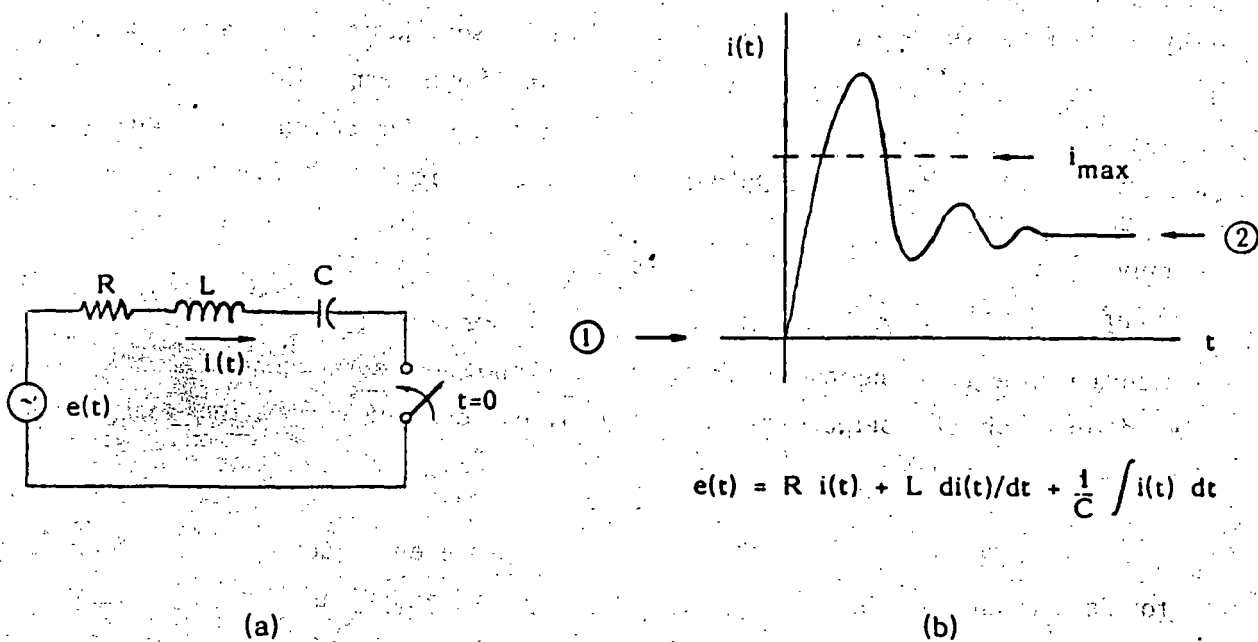


Figura 1.2 Estado transitorio de un circuito eléctrico.

Aunque los estudios en régimen permanente son muy útiles, con ellos no es posible reproducir y detectar condiciones especiales entre dos estados de operación del sistema, las cuales pudieran ser críticas. Esto solo se logra con los estudios dinámicos. A manera de analogía, se presenta el siguiente ejemplo: un circuito serie RLC, como el mostrado en la figura 1.2(a), se energiza en el tiempo $t=0$; después de que el transitorio ocurre, la corriente se estabiliza en un cierto valor. Si lo que uno desea es calcular el valor de estado estable de la corriente, basta con aplicar la ley de Ohm para fasores e impedancias, siendo ésta una ecuación algebraica. Pero si lo que uno desea es conocer el valor instantáneo de la corriente y determinar si rebasó cierto valor crítico $i_{\text{máx}}$, es necesario resolver la ecuación diferencial del circuito. La figura 1.2(b) ilustra de manera objetiva lo explicado.

La figura 1.3 muestra el conjunto de estudios dinámicos que generalmente se realiza para los sistemas de potencia, haciéndose hincapié en la diferencia de tiempos o velocidades de ocurrencia. Dentro de estos fenómenos se incluyen los llamados "problemas o estudios de estabilidad", los cuáles aparecen marcados con un asterisco.

Los estudios de estado estable y los estudios dinámicos son generalmente de una gran dimensión para el caso de los sistemas de potencia. Redes de pocos cientos de nodos y con varias decenas de generadores son muy comunes, ello hace que estos problemas deban orientarse a soluciones computacionales.

1.2 ESTABLECIMIENTO DEL PROBLEMA.

El problema de la estabilidad consiste en estudiar el comportamiento de las máquinas después de que en el sistema ocurre un disturbio. El disturbio puede ser pequeño, como la variación normal de la carga o mayor, como el disparo de un generador, la falla en una línea, etc.

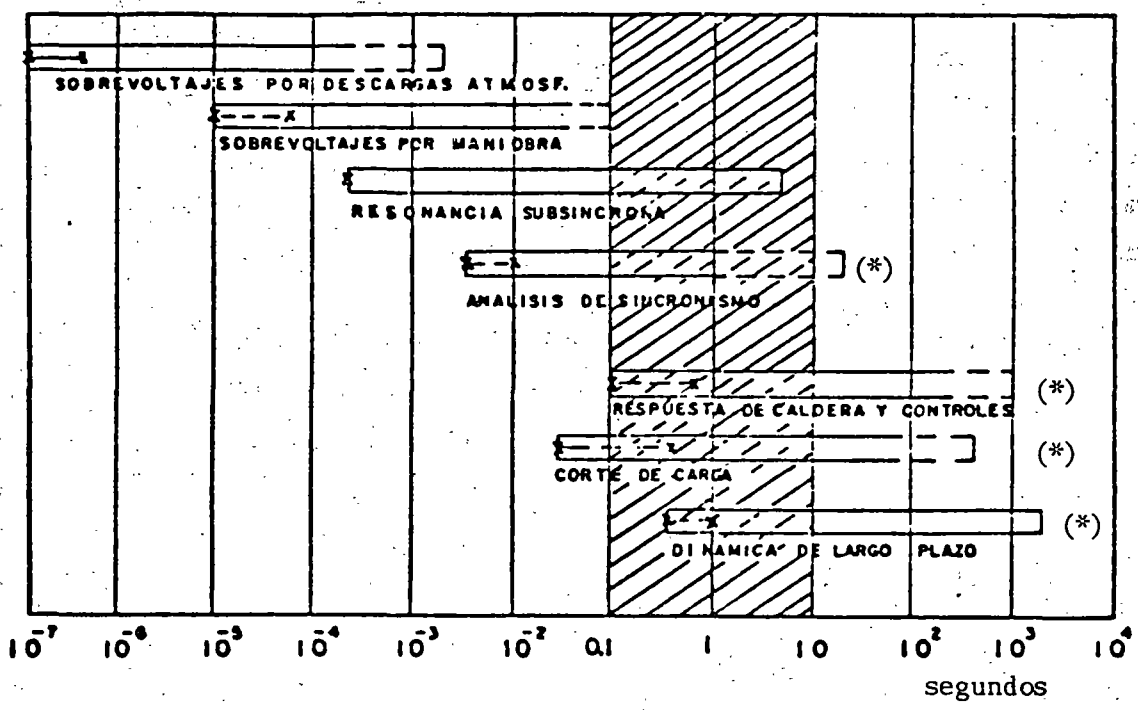


Figura 1.3 Clasificación de los estudios dinámicos.

Si el sistema es estable ante cierto disturbio, todas sus máquinas permanecerán en sincronismo, es decir, seguirán operando en paralelo y a la misma velocidad.

El periodo transitorio o dinámico siguiente al disturbio es oscilatorio por naturaleza, pero si el sistema es estable, estas oscilaciones se amortiguarán hasta dar origen a una nueva condición normal de operación. La figura 1.4 muestra, por ejemplo, la manera en que varía la frecuencia en varios puntos del Sistema Interconectado Mexicano después de cierto disturbio.

Los conceptos anteriores permiten plantear una primera definición de estabilidad de un sistema eléctrico:

"Si la respuesta oscilatoria de un sistema de potencia, durante el periodo transitorio posterior a cierto disturbio es amortiguada y el sistema alcanza en un tiempo finito una nueva condición normal de operación, se dice que el sistema es estable".

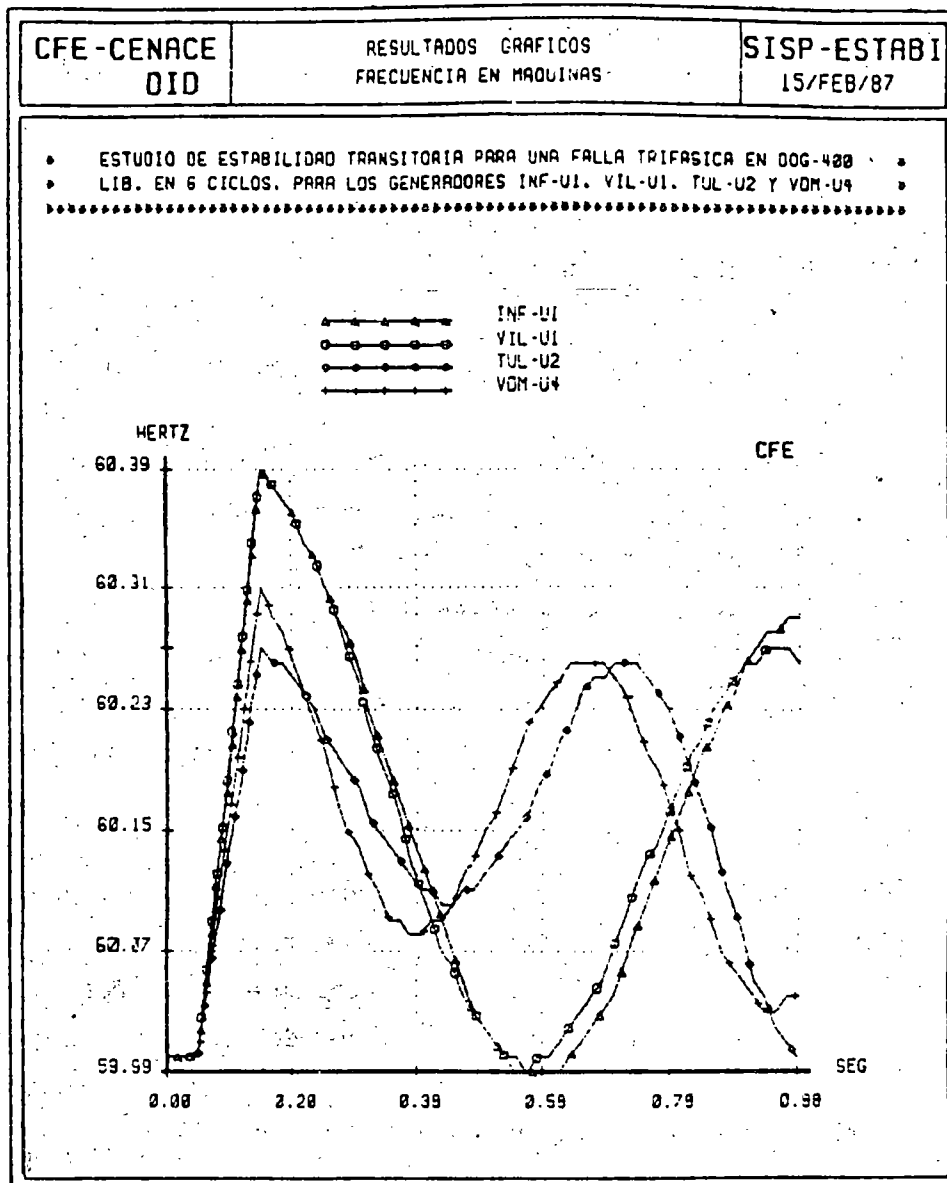


Figura 1.4. Comportamiento de la frecuencia en varios puntos del sistema después de una falla trifásica.

1.3 CLASIFICACION DE LOS ESTUDIOS DE ESTABILIDAD.

Los estudios de estabilidad pueden ser de tres tipos:

- a).- Estabilidad transitoria.
- b).- Estabilidad en régimen permanente o estado estable.
- c).- Estabilidad dinámica.

A continuación se da una breve descripción de cada uno de ellos.

Estabilidad transitoria.- Los estudios de estabilidad transitoria tienen por objeto analizar el sincronismo de las máquinas de un sistema de potencia después de un disturbio mayor. El criterio de estabilidad consiste en verificar si el desplazamiento angular relativo entre los rotors de los generadores no crece indefinidamente. El tiempo de estudio comprende desde el instante del disturbio hasta unos 2 segundos. Dada la rapidez del fenómeno, generalmente se desprecia el efecto de los controles de velocidad y de voltaje de los generadores.

Estabilidad en estado estable.- Estos estudios permiten determinar la máxima transferencia de potencia que puede realizarse entre dos puntos del sistema. Su metodología se basa en considerar pequeños disturbios y determinar su efecto en la operación síncrona del sistema. En este tipo de estudios se supone que la acción de los controles ya tuvo lugar, con el fin de no considerar el estado transitorio o dinámico entre el estado inicial y el estado final.

Estabilidad dinámica.- Los estudios de estabilidad dinámica tienen la finalidad de analizar el comportamiento de las principales variables del sistema después de un disturbio, sobretodo la frecuencia. El resultado del disturbio son oscilaciones con frecuencias típicas de 2 a 4 hertz. En este tipo de estudios es fundamental incluir la respuesta de los controles de velocidad y de voltaje de las máquinas del sistema. Si las oscilaciones producidas por el disturbio se amortiguan por la acción de los controles, se dice que el sistema es dinámicamente estable.

1.4 METODOS DE SOLUCION.

Los estudios de estabilidad se resuelven principalmente mediante las técnicas siguientes:

- a).- Métodos gráficos.
- b).- Simulación digital.
- c).- Simulación analógica.
- d).- Simulación híbrida.

Las técnicas más utilizadas son las dos primeras, por lo que a continuación se explican éstas con mayor detalle.

Métodos gráficos.

En el caso de la estabilidad transitoria se utiliza con cierta frecuencia el método de la áreas iguales, el cual consiste básicamente en investigar si el área de aceleración es igual al área de desaceleración. Para ello se hace uso de las curvas "potencia-ángulo", las que se explicarán en los capítulos siguientes.

Por otro lado, en los estudios de estabilidad en estado estable se utiliza ampliamente el diagrama de Clarke, que permite obtener gráficamente los voltajes internos de las máquinas, valores que son necesarios para determinar el límite de estabilidad.

Simulación digital.

Si se estudia un sistema de potencia con bastantes máquinas, líneas y cargas y se trata de reproducir los efectos de un cierto disturbio, puede pensarse que el problema es de difícil solución. Afortunadamente, las constantes de tiempo de los diferentes componentes del sistema son apreciablemente diferentes, permitiendo que uno se concentre sólo en ciertos elementos clave que afectan el transitorio y el área bajo estudio.

El primer paso consiste en establecer un modelo del sistema para el estado dinámico. Los elementos incluidos en el modelo serán aquellos que afecten la aceleración o desaceleración de los rotores de las máquinas. La complejidad del modelo dependerá del tipo de transitorio y del sistema bajo estudio. Generalmente, los componentes del sistema que afectan los pares eléctricos y mecánicos de las máquinas deben incluirse en el modelo. Estos componentes son:

- 1.- La red (antes, durante y después del disturbio).
- 2.- Las cargas y sus características.
- 3.- Los parámetros de las máquinas síncronas.
- 4.- El sistema de excitación de las máquinas.
- 5.- Las turbinas y su regulador de velocidad.

Así, los ingredientes principales para la solución son: el conocimiento de las condiciones iniciales del sistema antes del disturbio y la descripción matemática de los principales componentes del sistema que afectan el comportamiento dinámico de las máquinas síncronas.

Las ecuaciones diferenciales que resultan del planteamiento matemático se resuelven mediante métodos numéricos, haciendo uso de la computadora digital.

La aparición de la computadora digital en los inicios de los años 50's y su aplicación a los problemas dinámicos de los sistemas de potencia desde el año de 1959, han permitido realizar análisis más completos, más precisos y de mayor magnitud, estimulando el desarrollo de nuevas técnicas de solución y mejorando los conceptos teóricos y filosóficos del comportamiento dinámico de los sistemas eléctricos.

2 MAQUINA SINCRONA

Los generadores síncronos, transformadores y líneas de transmisión constituyen los elementos fundamentales de un sistema eléctrico de potencia. De ellos, la máquina síncrona es el dispositivo más complejo. Esto se debe a que en la máquina se presentan fenómenos eléctricos, magnéticos y mecánicos, todos ellos interrelacionados. Por ejemplo, el campo magnético de la máquina es una variable que depende del tiempo y del espacio debido al movimiento del rotor y a la irregularidad del entrehierro, provocando que las inductancias propias y mutuas de sus devanados no sean constantes como en los transformadores y en las líneas de transmisión.

2.1 CONFIGURACION DE LA MAQUINA.

Una máquina síncrona está formada por dos partes fundamentales: una fija, llamada estator y una móvil, conocida como rotor. En ellas se alojan seis devanados:

- Tres en el estator, uno para cada fase. Estos devanados son idénticos y están simétricamente distribuidos; son de corriente alterna y se conectan al sistema eléctrico.
- Otro en el rotor, llamado "devanado de campo". Este devanado se excita con corriente directa proveniente de una fuente externa y es el que va a inducir las fuerzas electromotrices (fems) en los devanados del estator, al producirse el movimiento del rotor.

Este capítulo es un resumen, con algunas aportaciones personales, obtenido de varias referencias entre las que destaca la siguiente: ELECTRIC ENERGY SYSTEM THEORY de O. L. Elgerd. FMC-880920.

- Dos devanados más en el rotor, uno en cada cabeza polar. Estos, reciben el nombre de "devanados amortiguadores" y están constituidos por barras cortocircuitadas, en las que solo se inducen fems cuando se presenta en la máquina una velocidad diferente a la síncrona.

La figura 2.1 muestra de manera esquemática la disposición física de estos devanados.

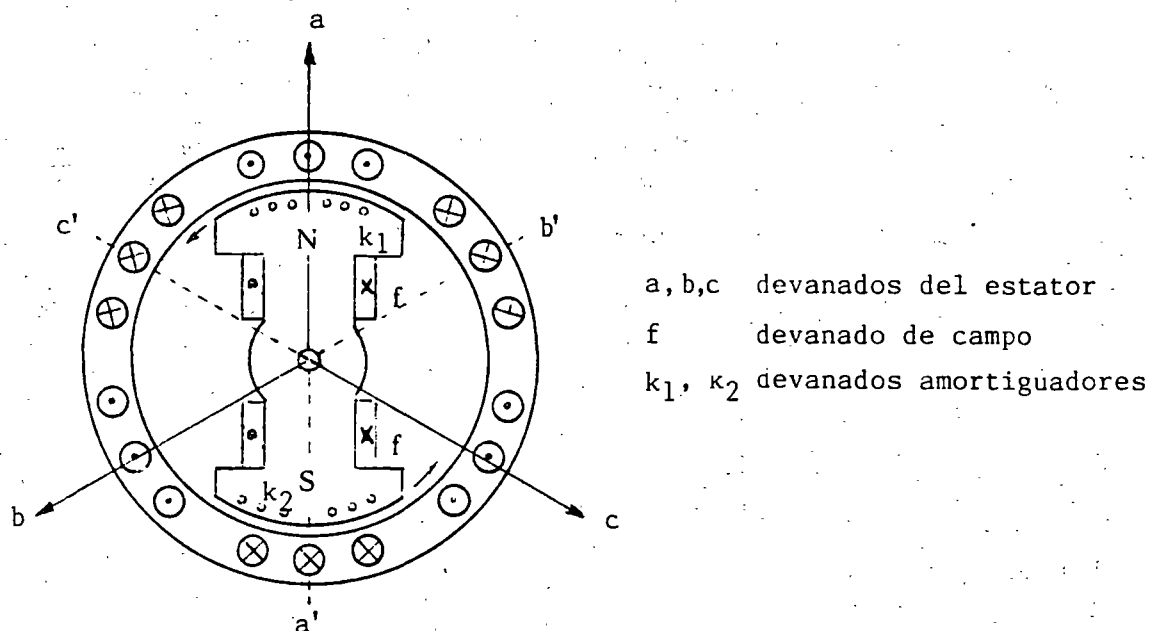


Figura 2.1 Devanados de una máquina síncrona.

2.2 LA MAQUINA SINCRONA Y EL SISTEMA ELECTRICO.

Si la máquina opera como generador, lo cual ocurre generalmente, el rotor es impulsado por un primotor; por ejemplo, una turbina de vapor o una turbina hidráulica.

Un generador síncrono puede operar alimentando una sola carga o en paralelo con otros generadores en una gran red; esto último es también lo más común. En la figura 2.2 se tiene un conjunto de n generadores conectados al sistema. El k -ésimo generador suministra al sistema su potencia

compleja $S_k = P_k + jQ_k$. En las terminales de la máquina se mantiene el voltaje en un valor $|V_k|$ y el sistema en su conjunto funciona en sincronía a la frecuencia f .

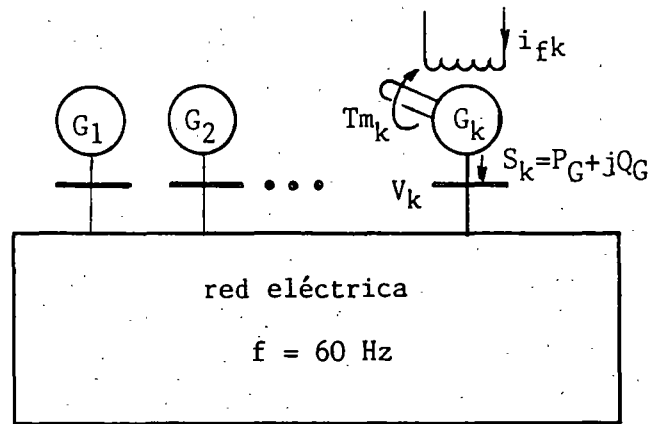
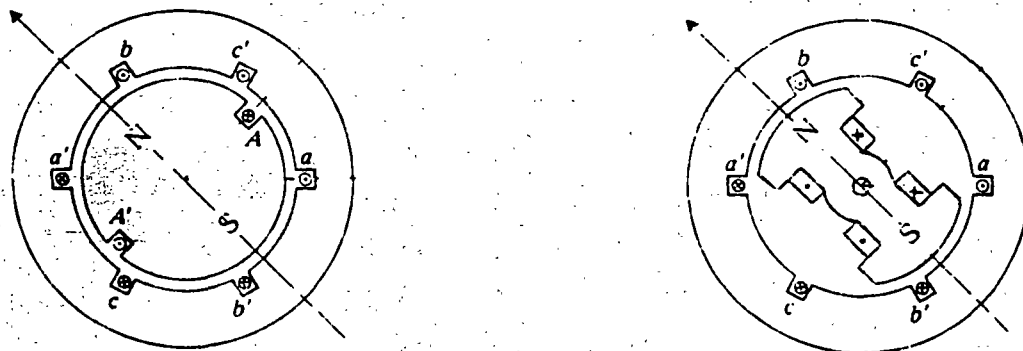


Figura 2.2 Típica operación en paralelo de n generadores.

Existen dos tipos de generadores síncronos, los de polos lisos y aquéllos de polos salientes. Los primeros se usan en velocidades altas, como los turbogeneradores que operan a unas 3600 rpm; los segundos, se utilizan en bajas velocidades, como los hidrogeneradores que operan a unas 400 rpm. La figura 2.3 muestra las diferencias fundamentales de estos dos tipos de máquinas.



(a) Polos lisos

(b) Polos salientes

Figura 2.3 Tipos de máquinas síncronas.

La ecuación que relaciona la velocidad de operación de las máquinas con la frecuencia del sistema es:

$$\omega_m = \frac{120 f}{p} \quad (2.1)$$

Donde:

ω_m = velocidad (mecánica) de rotación, en rpm

f = frecuencia del sistema, en hertz

p = No. de polos de la máquina.

Así, si una máquina de dos polos se conecta a un sistema de 60 hertz, ésta debe girar a 3600 rpm.

Por último, la irregularidad del entrehierro entre el rotor y el estator en las máquinas de polos salientes, recibe el nombre de "saliencia", término que se utilizará más adelante.

2.3 CONTROL DE LAS MAQUINAS SINCRONAS.

Es útil analizar el comportamiento cualitativo de la máquina síncrona antes de intentar abordar sus modelos matemáticos.

Cada máquina del sistema puede controlarse mediante dos variables: la corriente de campo del rotor y el par mecánico del primotor T_m . Cuando una o ambas variables son alteradas, generalmente se producen cambios en las cuatro variables de salida: potencia activa generada P_G , potencia reactiva generada Q_G , voltaje terminal $|V|$ y la frecuencia de operación f . Esta interrelación se muestra en la figura 2.4.

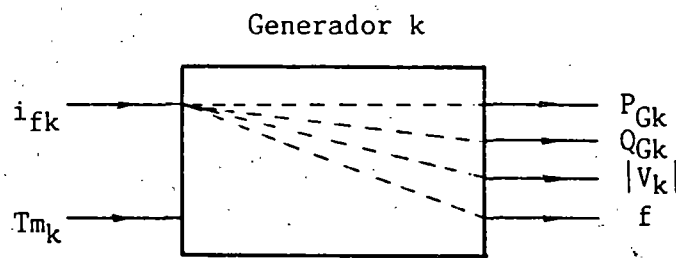


Figura 2.4 Variables de entrada y salida de un generador síncrono.

Desde el punto de vista del sistema, sería deseable tener un comportamiento no interactivo, de tal modo que al manipular una variable de entrada se produjera el cambio en solo una variable de salida. Esto generalmente no es posible. En primer lugar, porque se tienen cuatro variables de salida y solo dos de entrada; además, el comportamiento físico inherente de la máquina es tal que se presenta cierto acoplamiento entre las variables de entrada y las de salida. El grado de acoplamiento dependerá fundamentalmente de la magnitud del sistema. El mejor grado de desacoplamiento se logra cuando el sistema es muy grande, siendo el ideal, el caso denominado "red infinitamente fuerte" o simplemente "bus infinito".

Un bus infinito tiene las siguientes características:

- 1.- Una potencia de cortocircuito disponible infinita.- Lo que equivale a decir que tiene una reactancia de Thevenin igual a cero.
- 2.- Una masa y una inercia, infinitas.
- 3.- Un voltaje y una frecuencia invariables.

En el caso de la conexión de una máquina síncrona a un bus infinito, la frecuencia f del sistema y el voltaje terminal $|V_k|$ son independientes del control de la corriente de campo I_{fk} y el par mecánico de la máquina T_{mk} , y en tal caso las cuatro variables de salida de la figura 2.4 se reducen a dos: la potencia activa P_{Gk} y la potencia reactiva Q_{Gk} . En este caso particular, la condición de desacoplamiento casi está satisfecha. El manejo

de la corriente de campo afectará sólo a la potencia reactiva generada, mientras que un cambio en el par mecánico iniciado por la apertura o cierre de las válvulas de vapor o de agua en el primotor, afectará principalmente a la potencia activa generada. El cambio en el par también afectará, en menor medida a la potencia reactiva; es decir se tiene un pequeño acoplamiento entre T_m y Q_G .

El concepto de bus infinito representa un caso extremo del tamaño del sistema. El otro extremo es representado por un solo generador alimentando una carga única. En este caso, supóngase que se incrementa el par mecánico. Lo que sucede a continuación (si no actúan los controles de velocidad y de voltaje) es que la velocidad del rotor aumentará, y por lo tanto la frecuencia. El aumento de velocidad provocará que las fems inducidas en los devanados del estator se incrementen y entonces el voltaje terminal también se elevará. Finalmente, todos estos cambios producirán alteraciones en las potencias activa y reactiva. En resumen, la alteración en el par mecánico produce cambios en las cuatro variables de salida. Algo similar sucede si la alteración se efectúa en la corriente de campo.

Si en este último caso se considera la respuesta de los controles, la historia es muy diferente. La figura 2.5 servirá de auxiliar para la explicación. El regulador automático de voltaje (RAV) es el encargado de controlar el voltaje terminal del generador síncrono; su funcionamiento de una manera resumida, es el siguiente: cuando el voltaje terminal (medido a través de un transformador de potencial) es diferente a un cierto valor de referencia, se genera una señal que se envía a la fuente de corriente directa para ajustar el valor de la corriente de campo. Si el voltaje era mayor al deseado, el resultado de la acción del regulador automático de voltaje es una disminución de la corriente de campo.

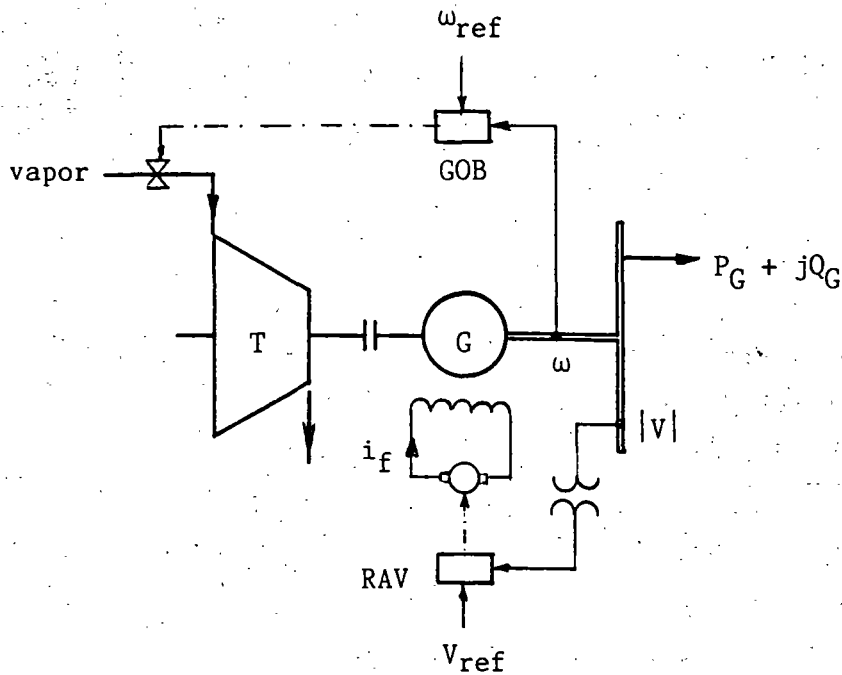


Figura 2.5 Controles de una máquina síncrona.

El gobernador o control de velocidad de una máquina síncrona, es el encargado por un lado, de mantener la velocidad de la máquina en un valor constante, y por el otro, variar la potencia activa de salida P_G . Funciona de manera similar al regulador de voltaje. Si la velocidad de rotación de la máquina es diferente a cierta velocidad de referencia, se generará una señal que abrirá o cerrará las válvulas de vapor o de agua para ajustar el par mecánico. Si la velocidad era menor a la deseada, el gobernador mandará abrir las válvulas para permitir la entrada de más vapor o de más agua.

Para el caso de una máquina conectada a un bus infinito ya se explicó que al cambiar el par mecánico, no se altera la velocidad, pero sí se varía la potencia activa generada. Por lo tanto, para aumentar o disminuir la potencia activa de salida, tendrá que manipularse el gobernador hasta lograr la apertura o cierre de válvulas, respectivamente.

2.4. ECUACIONES FUNDAMENTALES DE LA MAQUINA SINCRONA.

a) Planteamiento.

Existen básicamente dos formas de expresar las ecuaciones de una máquina síncrona: en términos de los enlaces de flujos (ψ) de cada devanado, o en función de los voltajes en los mismos. Aquí se seguirá esta última.

Las ecuaciones que se presentarán parten de las siguientes consideraciones fundamentales:

1.- Se supone que la máquina es magnéticamente lineal; esto significa que se desprecia la saturación del circuito magnético.

2.- Se supone que la máquina se puede representar como un conjunto de circuitos acoplados magnéticamente.

3.- Se desprecia el efecto de los devanados amortiguadores.

4.- Se suponen nulas las resistencias de los devanados.

Después de estos supuestos, la expresión que sirve como punto de partida para el desarrollo de las ecuaciones es:

$$v_{abc} = \frac{d}{dt} [L_{abc}(t)] i_{abc} \quad (2.2)$$

En la ecuación (2.2) la matriz de inductancias $[L_{abc}(t)]$ de 4×4 está formada por las inductancias propias y mutuas de los tres devanados del estator y las del devanado de campo. Todas ellas, a excepción de la inductancia propia del devanado de campo, son dependientes del tiempo, debido al movimiento del rotor y a la saliencia de la máquina.

Para resolver este problema se utiliza una herramienta matemática llamada transformación de Blondel, la cual ha sido aplicada por otros autores como Doherty, Park, etc. Esta transformación transporta el problema del marco de referencia "abc" al marco "dqo"; algo similar a lo que sucede cuando se utilizan las componentes simétricas al resolver circuitos trifásicos desbalanceados.

En el marco dqo existen dos ejes: el "eje directo (d)", que coincide con el eje polar, y el "eje en cuadratura (q)" que se localiza en la línea neutra magnética. Ver figura 2.6.

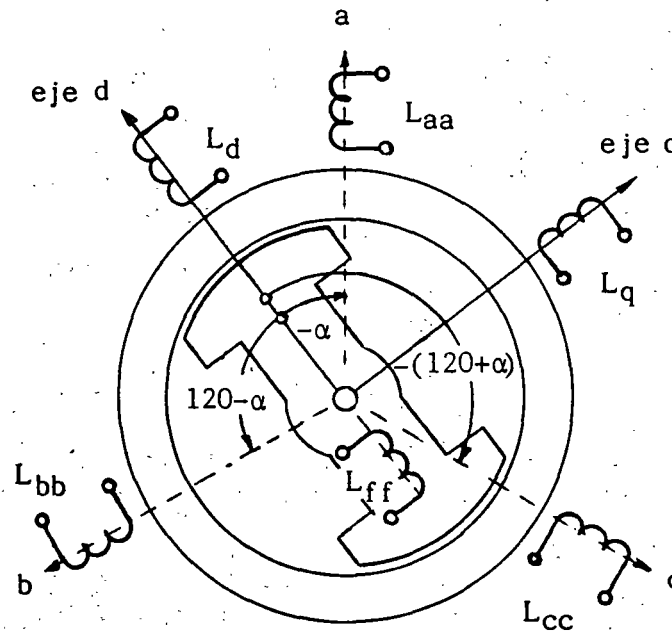


Figura 2.6 Reactancias en los marcos abc y dqo.

La transformación de Blondel simplifica notablemente las ecuaciones, ya que en el marco dqo las inductancias, las corrientes y los voltajes son constantes e independientes de la posición del rotor.

b) El generador con carga balanceada.

Después de establecer la ecuación (2.2) en el marco abc, de aplicar la transformación de Blondel y de expresar en forma fasorial las ecuaciones resultantes para el caso un generador operando con carga trifásica balanceada, se obtienen las siguientes expresiones:

$$V_a = E_a - jX_d I_d - jX_q I_q \quad (2.3)$$

$$I_a = I_d + I_q \quad (2.4)$$

Donde:

$$E_a = \frac{-\omega L_5 i_{f0}}{\sqrt{2}} \quad (2.5)$$

= fem inducida en vacío en la fase a.

$$I_d = j |I| \cos \Psi = \text{corriente de eje directo.} \quad (2.6)$$

$$I_q = - |I| \sin \Psi = \text{corriente de eje en cuadratura.} \quad (2.7)$$

I = Valor máximo de la corriente de cada devanado del estator.

$X_d = \omega L_d$ = reactancia de eje directo.

$X_q = \omega L_q$ = reactancia de eje en cuadratura.

L_5 = Valor máximo de la inductancia mutua entre el devanado de la fase a y el devanado de campo.

i_{f0} = corriente de campo nominal.

Los fasores anteriores se muestran en el diagrama de la figura 2.7. Este diagrama es extremadamente importante, dado que permite obtener de él toda la información esencial relacionada con la operación de una máquina síncrona en condiciones de estado estable equilibrado.

Puesto que existe simetría entre los fasores de cada fase, se ha retirado el subíndice a de los fasores E, V e I. Nótese que el ángulo ϕ es el existente entre el voltaje terminal y la corriente.

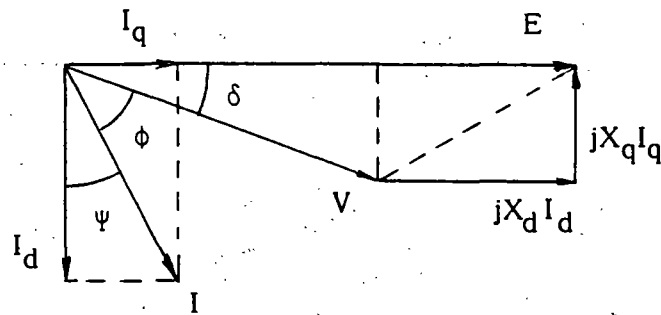


Figura 2.7 Diagrama fasorial de la máquina síncrona en condiciones balanceadas.

c) Potencia activa generada.

Las potencias activa y reactiva entregadas al sistema por un generador síncrono están dadas por:

$$P_G = |V| |I| \cos \phi \quad (2.8)$$

$$Q_G = |V| |I| \sin \phi \quad (2.9)$$

Donde V , I y ϕ están definidos en el diagrama fasorial anterior. P_G y Q_G se consideran positivas si salen del generador hacia el sistema. Del diagrama fasorial:

$$|E| - |I_d| X_d = |V| \cos \delta \quad (2.10.a)$$

$$|I_q| X_q = |V| \sin \delta \quad (2.10.b)$$

$$|I_q| = |I| \sin \psi \quad (2.11.a)$$

$$|I_d| = |I| \cos \psi \quad (2.11.b)$$

$$\phi + \delta + \psi = 90^\circ \quad (2.12)$$

De la ecuación (2.12) se deriva:

$$\cos \phi = \sin \psi \cos \delta + \cos \psi \sin \delta, \text{ por lo tanto:}$$

$$|I| \cos \phi = |I| \sin \psi \cos \delta + |I| \cos \psi \sin \delta \quad (2.13)$$

Haciendo uso de las ecuaciones (2.11), se tiene:

$$|I| \cos \phi = |I_q| \cos \delta + |I_d| \sin \delta \quad (2.14)$$

Sustituyendo (2.14) en (2.8):

$$P_G = |V| |I_q| \cos \delta + |V| |I_d| \sin \delta \quad (2.15)$$

Despejando las corrientes de las ecuaciones (2.10):

$$|I_d| = \frac{|E| - |V| \cos \delta}{X_d} \quad (2.16)$$

$$|I_q| = \frac{|V| \sin \delta}{X_q} \quad (2.17)$$

Sustituyendo (2.16) y (2.17) en (2.15):

$$\begin{aligned} P_G &= |V| \cos \delta \left[\frac{|V| \sin \delta}{X_q} \right] + |V| \sin \delta \left[\frac{|E| - |V| \cos \delta}{X_d} \right] \\ &= \frac{|V|^2 \cos \delta \sin \delta}{X_q} + \frac{|E| |V|}{X_d} \sin \delta - \frac{|V|^2 \cos \delta \sin \delta}{X_d} \end{aligned}$$

$$P_G = \frac{|E| |V|}{X_d} \sin \delta + \frac{|V|^2}{2} \left(\frac{1}{X_q} - \frac{1}{X_d} \right) \sin 2\delta \quad (2.18)$$

ya que $\cos \delta \sin \delta = 1/2 \sin 2\delta$.

Se concluye que para todo propósito práctico, P_G es función únicamente del ángulo de carga δ , existente entre los fasores E y V . Esto se debe a que el voltaje terminal $|V|$ puede suponerse constante si la red es razonablemente grande y $|E|$, la fem inducida, es constante si se mantiene la corriente de campo en un valor fijo.

d) Reactancias típicas.

Si las reactancias de una máquina síncrona se expresan en por unidad de sus valores nominales, se obtienen valores semejantes para cada reactancia, independientemente de la capacidad de la máquina.

La tabla 2.1 muestra los valores de las reactancias principales para los diferentes tipos de máquinas síncronas: las reactancias síncronas de eje directo (X_d) y de eje en cuadratura (X_q); la reactancia transitoria de eje directo (X'_d), la reactancia subtransitoria de eje directo (X''_d), la reactancia de secuencia negativa (X_2) y la reactancia de secuencia cero (X_0).

TABLA 2.1
Reactancias típicas de máquinas síncronas en p.u.

Reactancia	Motores Síncronos	Condensadores Síncronos	Hidro- generadores	Turbo- generadores
X_d	1.00	1.60	1.00	1.15
X_q	0.75	1.00	0.65	1.00
X'_d	0.30	0.40	0.30	0.15
X''_d	0.20	0.25	0.20	0.10
X_2	0.25	0.25	0.20	0.13
X_0	0.06	0.08	0.07	0.04

2.5 MODELO CLASICO DE LA MAQUINA SINCRONA.

Consideración No. 5.- Si se supone que la máquina es de polos lisos, o bien, de polos salientes, pero se ignora el efecto de la saliencia, se tiene que $X_d = X_q$.

En estas condiciones, se obtiene lo que se conoce como el modelo clásico de la máquina síncrona. En este contexto, la ecuación (2.18) se convierte en:

$$P_G = \frac{|E||V|}{X_d} \sin \delta \quad (2.19)$$

Siguiendo un procedimiento similar al usado para deducir la ecuación (2.18), y considerando saliencia despreciable, es posible obtener una expresión para la potencia reactiva Q_G . El resultado es:

$$Q_G = \frac{|E||V|}{X_d} \cos \delta - \frac{|V|^2}{X_d} \quad (2.20)$$

Por otro lado, si $X_d = X_q$, la ecuación (2.3) se transforma en:

$$V = E - j X_d (I_d + I_q) = E - j X_d I \quad (2.21)$$

El diagrama fasorial en estas condiciones se simplifica notablemente, como se observa en la figura 2.8.

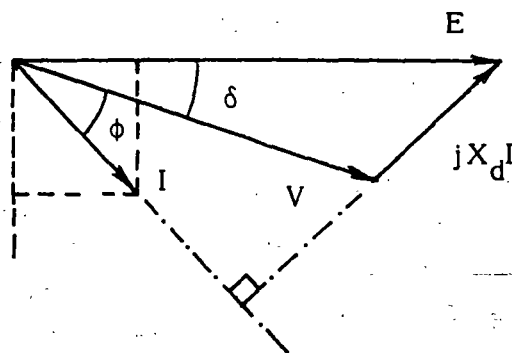


Figura 2.8 Diagrama fasorial para generadores síncronos de polos lisos.

El comportamiento de la máquina descrito por la ecuación (2.21) y el diagrama fasorial de la figura 2.8, es posible reproducirlo mediante un circuito equivalente sumamente simple. Ver figura 2.9.

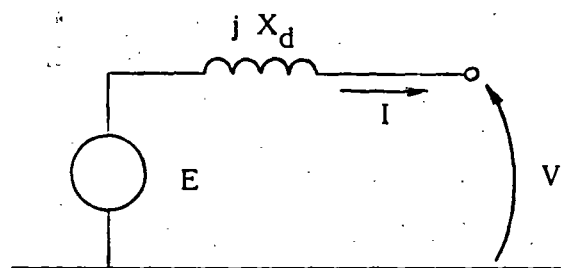


Figura 2.9 Circuito equivalente del generador de polos lisos.

2.6 OPERACION DE LA MAQUINA SINCRONA.

a) Modos de operación.

Las máquinas síncronas tienen tres modos de operación: como generador, cuando la potencia activa va de la máquina al sistema; como condensador síncrono, si la potencia activa es cero, o bien, como motor si la potencia activa va del sistema a la máquina.

Por lo que se refiere a la potencia reactiva, la máquina síncrona tiene dos posibilidades de operación: como capacitor o generador de reactivos, si la máquina entrega potencia reactiva al sistema; o bien, como inductancia o consumidor de reactivos, si absorbe potencia reactiva del sistema.

Es común usar los símbolos (\rightarrow) (\leftrightarrow) para indicar el sentido de la potencia activa y el de la potencia reactiva respectivamente; la figura 2.10 resume los diferentes modos de operación de una máquina síncrona, aclarando que en general los generadores, los condensadores y los motores síncronos, tienen características constructivas diferentes.

	GENERADOR	CONDENSADOR SINCRONO	MOTOR
CAPACITOR (entregando)			
INDUCTANCIA (absorbiendo)			

Figura 2.10 Modos de operación de una máquina síncrona.

b) Límites de operación.

Una "curva de capacidad" o carta de operación de un generador síncrono es una gráfica que contiene una serie de puntos (P,Q), que en conjunto constituyen los límites de funcionamiento de una máquina síncrona. Este documento es un auxiliar de gran utilidad, tanto para el personal de operación de la planta generadora, como para el personal de control y despacho que opera el sistema de potencia.

La figura 2.11 muestra una curva de capacidad típica, en la que pueden observarse los cuatro límites de un generador síncrono:

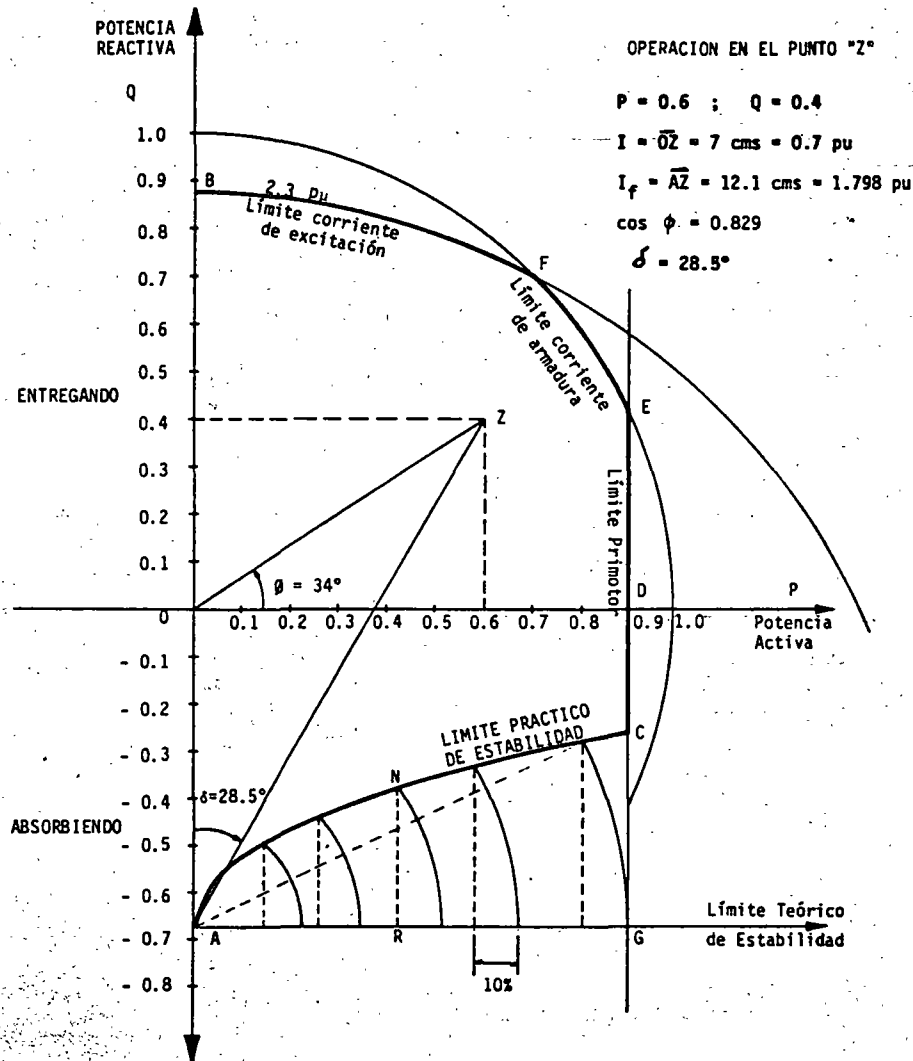


Figura 2.11 Curva de capacidad para un generador de rotor cilíndrico.

- 1) Arco BF - Límite por calentamiento en el rotor provocado por la corriente de campo o corriente de excitación.
- 2) Arco FE - Límite por calentamiento en el estator, provocado por la corriente de armadura.
- 3) Segmento EC - Límite por capacidad mecánica del primotor.
- 4) Arco CA - Límite por estabilidad de la máquina.

El área acotada por estos cuatro límites y el eje de las ordenadas, constituye la región permitida para operar el generador síncrono, dando lugar a una gran cantidad de combinaciones posibles (P,Q).

2.7 EJERCICIOS

Para finalizar el capítulo se presentan dos ejemplos numéricos que ilustran de manera objetiva el comportamiento de un generador síncrono. En ambos, se supone que la máquina es de polos lisos y está conectada a un gran sistema; esto es con el fin de simplificar los análisis y centrar la atención en los aspectos fundamentales.

Ejemplo 1.- Un generador con 400 MVA, 20 kV y 60 Hz nominales opera inicialmente con un ángulo de carga de 30° y una corriente de excitación tal que la fem inducida es de 1.25 pu. Si sus reactancias X_d y X_q son de 1.0 pu, determinar:

- P_G y Q_G para las condiciones iniciales.
- P_G y Q_G si se modifica la corriente de excitación de tal modo que la fem inducida se reduce a 0.7 pu.
- Mostrar el efecto del cambio de excitación mediante curvas "potencia-ángulo" y de diagramas fasoriales.

SOLUCION

$$\begin{aligned} \text{a) } S_r &= 400 \text{ MVA} \\ V_r &= 20 \text{ kv} = 1.0 \text{ pu} \\ \delta &= 30^\circ \\ |E| &= 1.25 \text{ pu} = 1.25 \times 20 = 25 \text{ kV} \end{aligned}$$

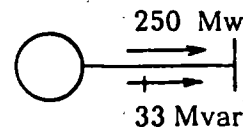
Mediante las ecuaciones (2.19) y (2.20) de este capítulo y trabajando con valores por unidad, se tiene:

$$P_G = \frac{1.25 \times 1.0}{1.0} \sin 30^\circ = 0.625 \text{ pu}$$

$$Q_G = \frac{1.25 \times 1.0}{1.0} \cos 30^\circ - \frac{(1.0)^2}{1.0} = 1.0825 - 1 = 0.0825 \text{ pu}$$

En valores absolutos:

$$\begin{aligned} P_G &= 0.625 \times 400 = 250 \text{ Mw} \\ Q_G &= 0.0825 \times 400 = + 33 \text{ Mvar} \end{aligned}$$

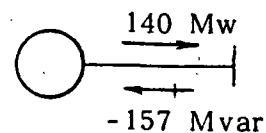


b) CONTROL DE LA EXCITACION

$$|E| = 0.70 \text{ pu}$$

$$P_G = \frac{0.7 \times 1.0}{1.0} \sin 30^\circ = 0.35 \text{ pu} = 140 \text{ Mw}$$

$$Q_G = \frac{0.7 \times 1.0}{1.0} \cos 30^\circ - \frac{(1.0)^2}{1.0} = -0.39 \text{ pu} = -157 \text{ Mvar}$$



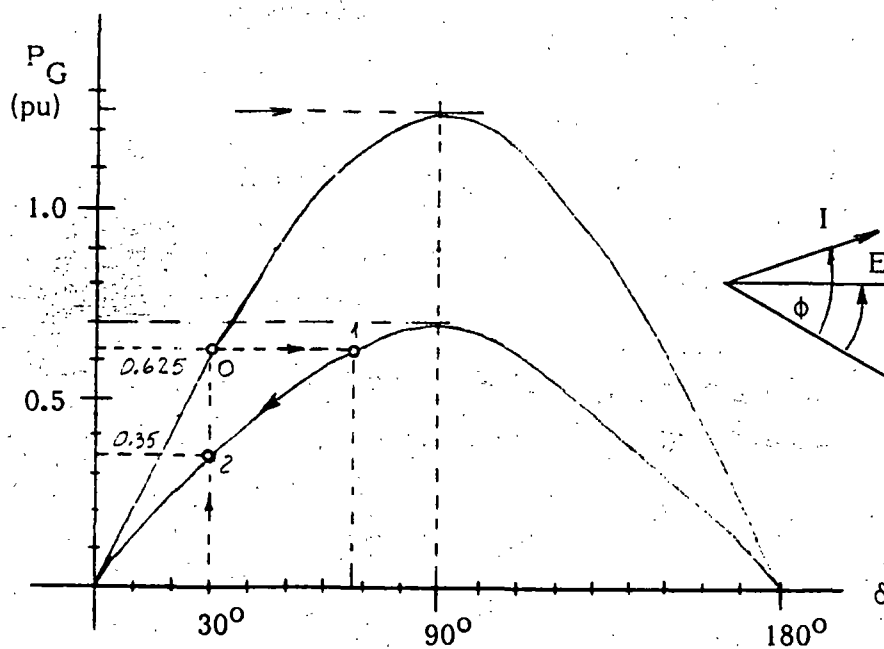
c) Efecto del control de la excitación:

Para el inciso (a):

$$P_{\max} = \frac{|E| |V|}{X_d} \sin 90^\circ = \frac{1.25 \times 1.0}{1.0} = 1.25 \text{ pu}$$

Para el inciso (b):

$$P_{\max} = \frac{0.7 \times 1.0}{1.0} = 0.70 \text{ pu}$$



Ejemplo 2.- El generador del ejemplo 1 está ahora operando con una fem de 1.5 pu y una potencia activa de 0.25 pu. En este caso determinar:

- El ángulo de carga δ y la potencia reactiva Q_G .
- Los mismos valores anteriores, pero después de incrementar el par mecánico al triple.
- Mostrar mediante curvas "potencia-ángulo" y diagramas fasoriales, el resultado del cambio en el par.

SOLUCION

$$|E| = 1.5 \text{ pu}$$

$$P_G = 0.25 \text{ pu} = 100 \text{ Mw}$$

De la ecuación (2.19):

$$\delta = \text{sen}^{-1} \frac{P_G X_d}{|E||V|} = \text{sen}^{-1} \frac{0.25 \times 1.0}{1.5 \times 1.0} = 9.6^\circ$$

$$Q_G = \frac{1.5 \times 1.0}{1.0} \cos 9.6^\circ - \frac{(1.0)^2}{1.0} = 0.48 \text{ pu} = 192 \text{ Mvar}$$

b) CONTROL DEL PAR MECANICO.

Si T_m aumenta al triple, P_G se incrementa en la misma proporción. Por lo tanto:

$$P_G = 3 \times 0.25 = 0.75 \text{ pu} = 300 \text{ Mw}$$

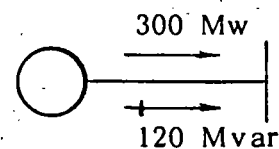
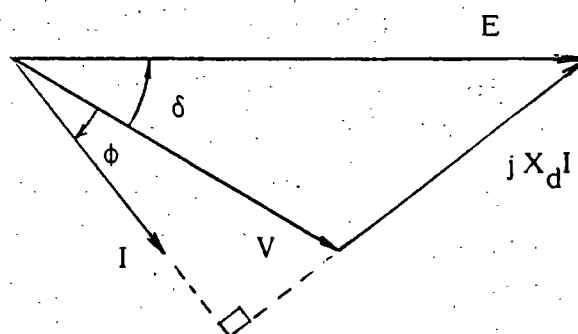
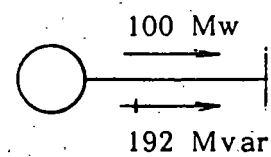
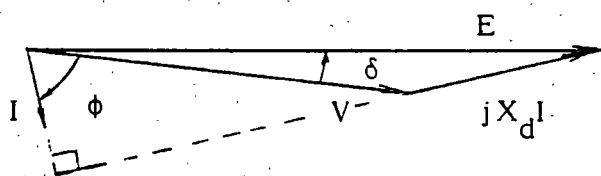
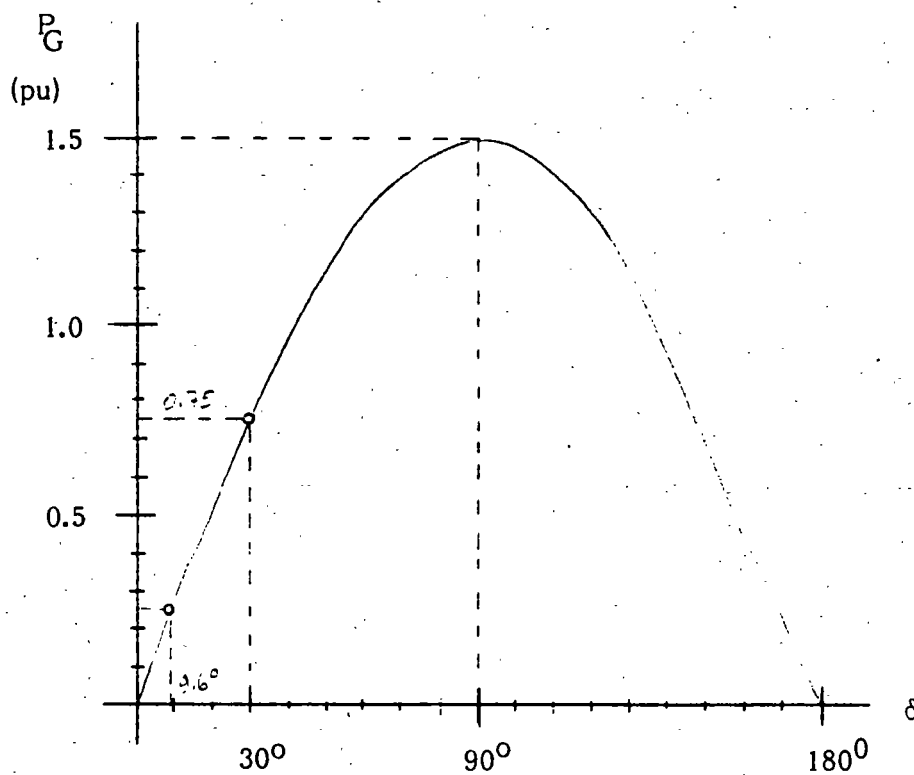
$$\delta = \text{sen}^{-1} \frac{P_G X_d}{|E||V|} = \text{sen}^{-1} \frac{0.75 \times 1.0}{1.5 \times 1.0} = 30^\circ$$

$$Q_G = \frac{1.5 \times 1.0}{1.0} \cos 30^\circ - \frac{(1.0)^2}{1.0} = 0.30 \text{ pu} = 120 \text{ Mvar}$$

Nótese que la potencia reactiva se redujo de 0.48 a 0.30 pu; es decir, solo el 38%, contra el 200% de cambio en la potencia activa.

C) Efecto del control en el par mecánico.

$$P_{\max} = \frac{|E||V|}{X_d} = \frac{1.5 \times 1.0}{1.0} = 1.5 \text{ pu}$$



3 ESTABILIDAD TRANSITORIA. SISTEMA "MAQUINA-BUS INFINITO"

En este capítulo se inicia el análisis de la estabilidad transitoria de un sistema eléctrico de potencia (SEP), llamada también "estabilidad a grandes disturbios" ó "estudios de primera oscilación", que consisten en fenómenos rápidos con duración del orden de 1 segundo. Se introduce también el modelo "máquina-bus infinito", representación simplificada del sistema real, pero que permite obtener conclusiones y resultados con alto grado de aproximación.

3.1 SISTEMA "MAQUINA - BUS INFINITO".

Un SEP está integrado por numerosos generadores síncronos y cargas interconectadas por medio de líneas de transmisión y transformadores. En el comportamiento dinámico del sistema eléctrico interactúan todos los elementos, resultando un problema de gran complejidad por la cantidad de elementos y por el número de ecuaciones necesarias para representarlos.

Sin embargo, es posible simplificar el problema, eliminando el mayor número de componentes y reduciendo al mínimo las ecuaciones representativas de los elementos que permanecen. Con este objetivo en mente, las simplificaciones básicas que dan origen al sistema idealizado llamado "máquina-bus infinito", son:

- 1.- Se eliminan los controles de velocidad y de voltaje de los generadores síncronos, dada la rapidez del fenómeno.
- 2.- Se separa el generador síncrono que se desea estudiar.
- 3.- Se agrupan los generadores restantes y la red eléctrica (líneas, transformadores y cargas), sustituyéndose por un bus infinito (definido en el punto 2.3 de estas notas).

La figura 3.1 muestra gráficamente la simplificación explicada anteriormente. En ella, la barra con pequeñas líneas diagonales representa al bus infinito.

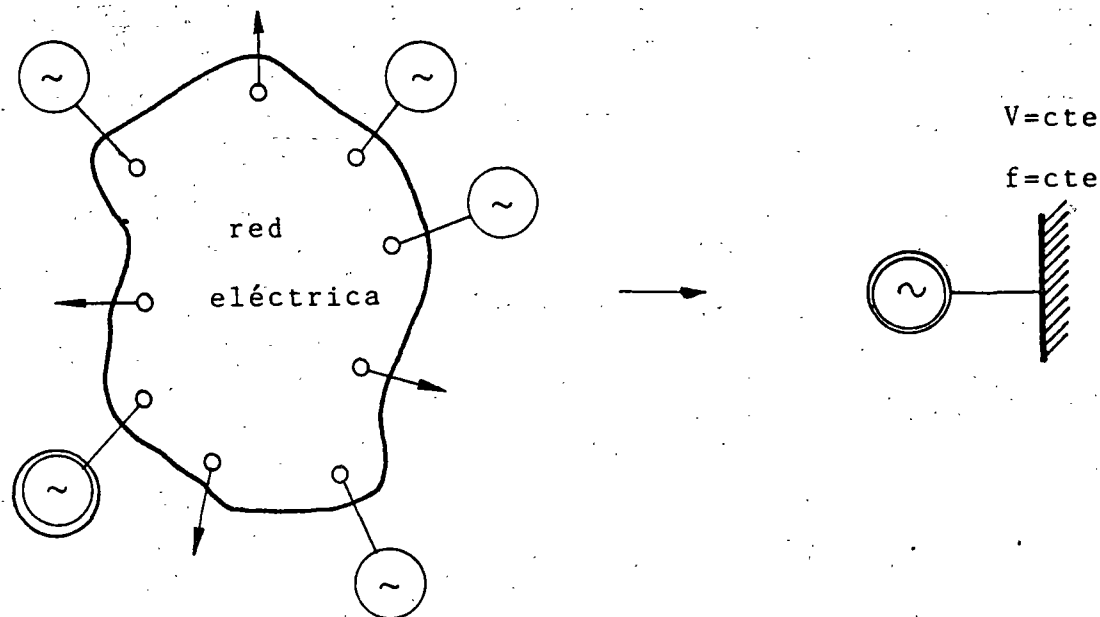


Fig. 3.1 Diagrama esquemático del sistema "máquina - bus infinito"

Este modelo idealizado significa que las unidades generadoras y la red del sistema son de un tamaño bastante mayor que el generador en estudio. Este tamaño relativo evita que eventos que ocurran en la máquina logren afectar el voltaje y la frecuencia del nodo del sistema al cual está conectada.

Es muy amplio el número de problemas que pueden resolverse y la cantidad de conceptos que pueden desarrollarse a partir de este modelo, cuya complejidad está reducida a su mínima expresión.

En el sistema "máquina-bus infinito" pueden también incluirse las líneas y transformadores a través de los cuales se conecta la máquina al sistema, como en el caso mostrado en la figura 3.2.

3.2 DESCRIPCION FISICA DEL FENOMENO DINAMICO.

Antes de incursionar en el análisis cuantitativo del modelo "máquina-bus infinito" se abordará brevemente una descripción del fenómeno dinámico en forma cualitativa.

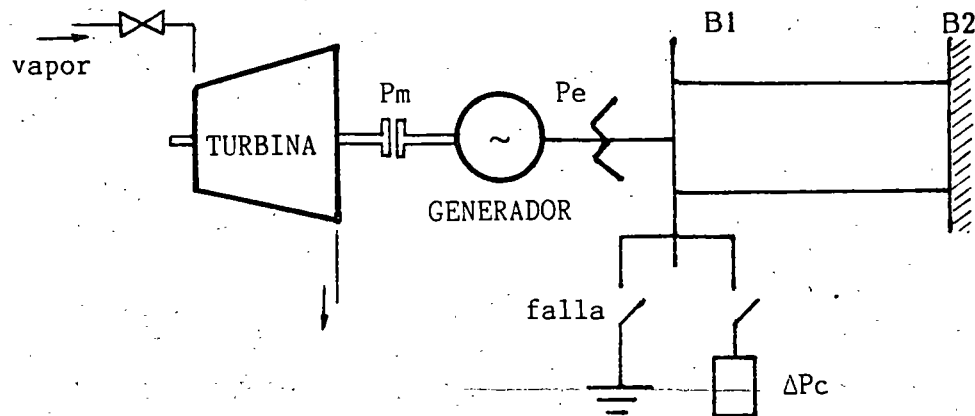


Fig.3.2 Modelo "máquina-bus infinito" incluyendo primotor y elementos de conexión al sistema.

Cuando en la barra B1 ocurre un cortocircuito trifásico se presenta la siguiente secuencia de acontecimientos:

- La potencia eléctrica (P_e) de la máquina se hace CERO inmediatamente, ya que el voltaje en ese punto se abate.
- Debido a la lentitud del control de velocidad, se supone que la potencia mecánica (P_m) permanece constante.
- Las masas rodantes de la MS (rotor, excitatriz, flechas, etc.) absorben la potencia mecánica en forma de energía cinética, aumentando su velocidad.
- El ángulo del rotor de la MS crece, pudiéndose presentar la pérdida de sincronismo, si la falla se prolonga indefinidamente.

El fenómeno opuesto ocurre si en lugar de la falla, se conecta la carga ΔP_c .

En estas circunstancias pueden presentarse tres casos importantes:

- 1.- Si $P_m = P_e$ la MS está en equilibrio y el ángulo de carga se mantiene constante.
- 2.- Si $P_m > P_e$ la MS se acelera y el ángulo de carga crece.
- 3.- Si $P_m < P_e$ la MS se desacelera y el ángulo de carga decrece.

3.3. GENERALIZACION DE LA ECUACION POTENCIA-ANGULO.

La potencia eléctrica de salida de una MS está dada por la ecuación (2.19), la cual por su importancia, aquí se repite:

$$P_e = P_G = \frac{|E| |V|}{X_d} \text{ sen } \delta \quad (2.19)$$

Si la fem E es constante, porque el nivel de la corriente de excitación no se ha alterado, y V también, por estar la máquina conectada a un gran sistema, las únicas variables que resultan son el ángulo de carga (δ) y la potencia eléctrica (P_e). Al graficar estas dos variables, se obtiene la llamada curva "potencia - ángulo" mostrada en la figura 3.3.

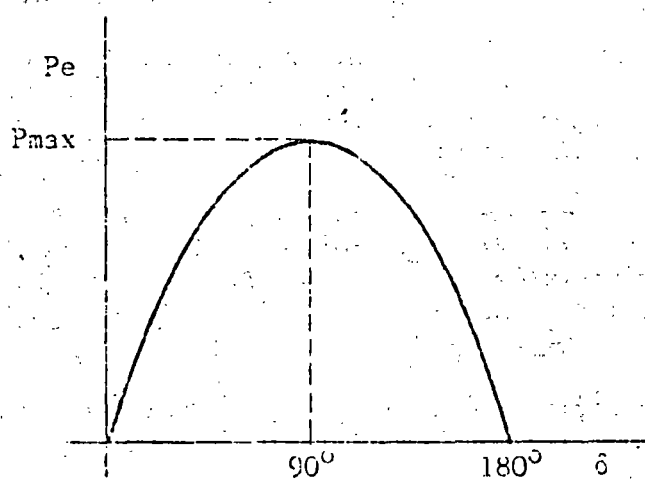


Fig. 3.3 Curva "Potencia-ángulo" para el sistema "máquina-bus infinito"

La potencia máxima de salida (P_{max}) ocurre cuando δ es igual a 90° , por lo tanto:

$$P_{max} = \frac{|E'| |V|}{X_d'} \quad (3.1)$$

Las ecuaciones (2.19) y (3.1) son válidas también para el caso en que la MS se conecte al bus infinito a través de líneas de transmisión y transformadores, siendo necesario sustituir X_d por la reactancia equivalente serie (X) del circuito (ver figura 3.4b). Otra de las adecuaciones requeridas en los estudios de estabilidad transitoria es representar a la MS por su reactancia transitoria de eje directo (X'_d) y el voltaje atrás de ésta (E'). Con ello:

$$P_e = \frac{|E'| |V|}{X} \text{ sen } \delta \quad (3.2)$$

$$P_{max} = \frac{|E'| |V|}{X} \quad (3.3)$$

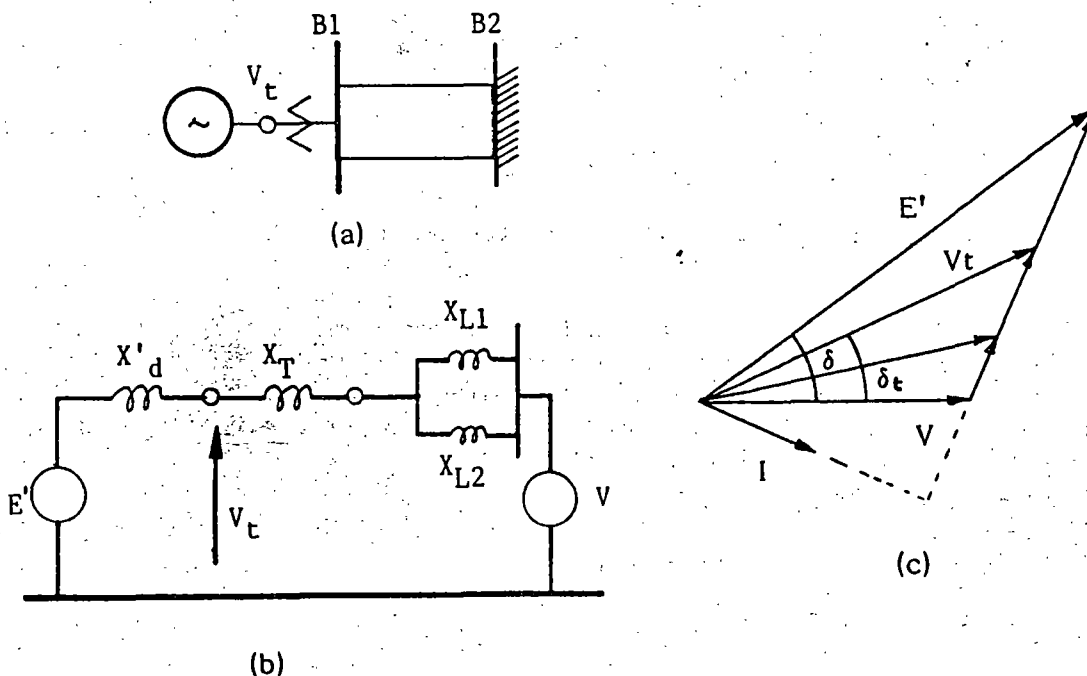


Fig 3.4. Circuito equivalente y diagrama fasorial de un sistema "máquina-bus infinito" que incluye líneas y transformador.

En estas condiciones, δ es el ángulo total existente entre los fasores E' y V (ver figura 3.4c).

La ecuación de la potencia eléctrica (3.2) se puede utilizar también cuando en lugar de conocer E' , se cuenta con el voltaje terminal (V_t) de la MS y el voltaje del bus infinito (V), teniéndose:

$$P_e = \frac{|V_t| |V|}{X_{t00}} \sin \delta_t \quad (3.4)$$

En este caso (δ_t) es el ángulo que existe entre los fasores V_t , V y la reactancia (X_{t00}) es el equivalente serie entre las terminales del generador y el bus infinito.

3.4. BASES PARA EL ESTUDIO CUANTITATIVO DEL MODELO.

El objeto de esta sección es establecer la ecuación que reproduzca el comportamiento del ángulo del rotor de la MS en el tiempo, después de presentarse un desbalance de potencia.

A dicha ecuación se le llama "ecuación de oscilación" y se arribará a ella después de repasar algunos conceptos físicos.

a. - DINAMICA DE TRANSLACION Y DINAMICA DE ROTACION.

Por lo general, existe mucha familiaridad con los fenómenos asociados a movimientos de cuerpos en una sola dirección, pero cuando el movimiento de los cuerpos es giratorio cuesta un poco más de esfuerzo su análisis. Los conceptos y las leyes de la dinámica son aplicables en ambos casos, haciendo las consideraciones convenientes. La tabla 3.1 presenta la comparación de las ecuaciones fundamentales de la dinámica de translación y la de rotación.

TABLA 3.1
COMPARACION DE LAS ECUACIONES PARA EL MOVIMIENTO DE TRANSLACION
CON LAS DEL MOVIMIENTO CIRCULAR

TRANSLACION				ROTACION			
MAGNITUD	SIMBOLO	ECUACION	UNIDAD	MAGNITUD	SIMBOLO	ECUACION	UNIDAD
Longitud	s	-	m	Desplazamiento angular	θ	$\theta = \frac{s}{r}$	rad
Masa	m	-	kg	Momento de inercia	I	$I = \int r^2 dm$	kg m ²
Tiempo	t	-	s	Tiempo	t	-	s
Velocidad	v	$v = ds/dt$	m/s	Velocidad angular	ω	$\omega = d\theta/dt$	rad/s
Aceleración	a	$a = dv/dt$	m/s ²	Aceleración angular	α	$\alpha = d\omega/dt$	rad/s ²
Fuerza	F	$F = ma$	N	Par	T	$T = I\alpha$	N m
Cantidad de movimiento	M'	$M' = mv$	N s	Momento angular cinético	H	$H = I\omega$	s/rad
Trabajo	W	$W = \int F ds$	J	Trabajo	W	$W = \int T d\theta$	J
Potencia	P	$P = dW/dt$ $= Fv$	w	Potencia	P	$P = dH/dt$ $= T\omega$	w
Energía cinética	E_k	$E_k = \frac{1}{2}mv^2$	J	Energía cinética de rotación	E_k	$E_k = \frac{1}{2}I\omega^2$	J

b. - POTENCIA ACELERANTE.

La potencia acelerante (Pa) es la diferencia entre la potencia mecánica aplicada a la MS por su primotor y la potencia eléctrica de salida:

$$P_a = P_m - P_e \quad [MW] \quad (3.5)$$

c. - MOMENTO DE INERCIA.

El momento de inercia es una cantidad física de especial importancia en el estudio de la rotación de cuerpos rígidos, pues mide la capacidad de almacenamiento de energía cuando dichos cuerpos giran alrededor de cierto eje.

El momento de inercia (I) se define como:

$$I = \int r^2 dm = \sum_{i=1}^n m_i r_i^2 \quad [Kg m^2] \quad (3.6)$$

siendo (m) la masa de un elemento pequeño ó diferencial del cuerpo y (r) el radio de giro del elemento.

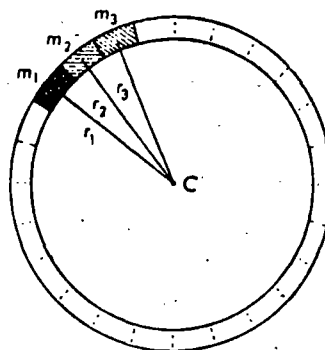


Fig. 3.5 División en masas pequeñas de un anillo girando alrededor del eje C.

Para un anillo como el de la figura 3.5, el momento de inercia resulta:

$$I = (m_1 + m_2 + m_3 \dots + m_n) r^2 = Mr^2$$

siendo M la masa total.

La figura 3.6 proporciona las expresiones para el cálculo del momento de inercia de algunos cuerpos con formas regulares.

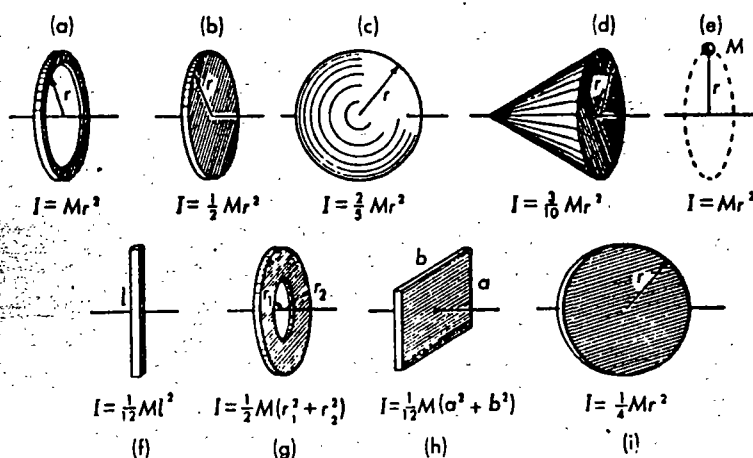


Fig. 3.6 Momento de inercia de algunos cuerpos típicos.

Obsérvese como un cuerpo llega a tener diferentes momentos de inercia, dependiendo del eje de giro seleccionado (ver figuras 3.6b y 3.6i).

d. - CONSTANTE DE INERCIA.

La constante de inercia (H) de una MS se define como:

$$H = \frac{\text{Energía cinética a velocidad síncrona}}{\text{Potencia aparente nominal}}$$

Utilizando las ecuaciones de la tabla 3.1, se obtiene:

$$H = \frac{E_{co}}{S_n} = \frac{1/2 I \omega^2}{S_n} \quad [\text{MJ/MVA ó seg}] \quad (3.7)$$

La constante de inercia es un parámetro de diseño que influye en la estabilidad de manera muy relevante. El valor de H al estar referido a la capacidad nominal propia de cada unidad generadora, cae en un rango estrecho de valores, independientemente del tamaño de la unidad. Desafortunadamente la tendencia en los diseños recientes es hacia una disminución del valor H, de manera que lo que se ha ganado en la mejora de la estabilidad por esquemas de protecciones e interruptores más rápidos, se ha perdido por las constantes de inercia más pequeñas de las nuevas unidades.

El rango de H para unidades generadoras de tipo hidráulico es de 2 a 7 y de tipo térmico de 2 a 5.

e. - SUSTITUCION DEL DESPLAZAMIENTO ANGULAR POR EL ANGULO DE CARGA.

Las ecuaciones que describen la dinámica de rotación de la tabla 3.1 están desarrolladas en base al desplazamiento angular (θ). Este ángulo tiene el inconveniente de que crece permanentemente y esto dificulta el análisis de la posición del rotor. Por tal motivo, se hace uso del ángulo de carga en lugar del desplazamiento angular, bajo las siguientes consideraciones:

El ángulo (θ) mide la posición del rotor con respecto a una referencia fija y (δ) con respecto a una referencia que gira a velocidad síncrona, como se muestra en la figura 3.7. Por lo tanto $\theta = \omega_0 t + \delta$, con lo que:

$$\delta = \theta - \omega_0 t \quad (3.8)$$

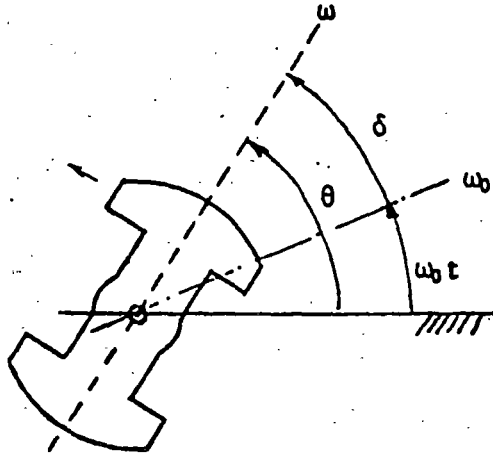


Fig. 3.7 Cambio del ángulo θ por δ .

Si se deriva la ecuación (3.8) con respecto al tiempo, se obtiene:

$$\frac{d\delta}{dt} = \frac{d\theta}{dt} - \omega_0$$

$$\frac{d\delta}{dt} = \omega(t) - \omega_0 \quad (3.9)$$

Esta ecuación es de importancia en los temas subsecuentes y establece que el cambio en ángulo del rotor (δ) depende de la diferencia entre su velocidad real $\omega(t)$ y la velocidad síncrona ω_0 .

Como ω_0 es una constante, al derivar ahora (3.9) se tiene:

$$\frac{d^2\delta}{dt^2} = \frac{d\omega(t)}{dt} \quad (3.10)$$

Sustituyendo P_e en términos de P_{max} :

$$M \frac{d^2 \delta}{dt^2} = P_m - P_{max} \text{ Sen } \delta \quad (3.13)$$

Esta es la llamada ecuación de oscilación, a partir de la cual se obtiene el comportamiento del ángulo δ , después de un desbalance de potencia.

Existen otras versiones de la ecuación de oscilación, las cuales se usan indistintamente y que a continuación se presentan.

Si se introduce la constante de inercia H (ec. 3.7), se obtiene:

$$H = \frac{1/2 I \omega^2}{S_n} = \frac{M \omega}{2 S_n}$$

$$M = \frac{2 S_n H}{\omega} \quad (3.14)$$

Sustituyendo (3.14) en (3.13) y reordenando:

$$\frac{2 S_n H}{\omega} \frac{d^2 \delta}{dt^2} = P_m - P_{max} \text{ sen } \delta$$

$$\frac{d^2 \delta}{dt^2} = \frac{\omega}{2H} (P_m - P_{max} \text{ Sen } \delta) \quad (3.15)$$

donde las potencias se encuentran dadas en por unidad de S_n , al quedar divididas por ella.

Si la velocidad síncrona ω se sustituye por su equivalente $2\pi f_0$, se obtiene una versión más de la ecuación de oscilación:

$$\frac{d^2 \delta}{dt^2} = \frac{\pi f_0}{H} (P_m - P_{max} \text{ sen } \delta) \quad (3.16)$$

La solución de la ecuación de oscilación se efectúa por métodos numéricos mediante la computadora digital ya que no tiene solución analítica.

la derivada de $\omega(t)$ es la aceleración angular y de acuerdo con las ecuaciones de la tabla 3.1, resulta que:

$$\boxed{\frac{d^2\delta}{dt^2} = \frac{d^2\theta}{dt^2}} \quad (3.11)$$

Esta última ecuación nos indica que desde el punto de vista de la aceleración del rotor, es indistinto trabajar con el desplazamiento angular θ , que con el ángulo δ .

f. - ECUACION DE OSCILACION.

La segunda Ley de Newton para el movimiento de translación establece que $F = m (d^2s / dt^2)$. Para el movimiento de rotación:

$$T = I \frac{d^2\delta}{dt^2} \quad (3.12)$$

En esta ecuación, T es el par acelerante. Con esta consideración y haciendo uso de la ec. (3.11) para el cambio en ángulo, se tiene:

$$T_m - T_e = I \frac{d^2\delta}{dt^2}$$

Donde (T_m) es el par mecánico y (T_e) el par eléctrico. Al multiplicar por la velocidad ω :

$$P_m - P_e = I\omega \frac{d^2\delta}{dt^2}$$

Al producto $I\omega$ se le denomina "momento angular cinético" y se designa con la letra M , quedando:

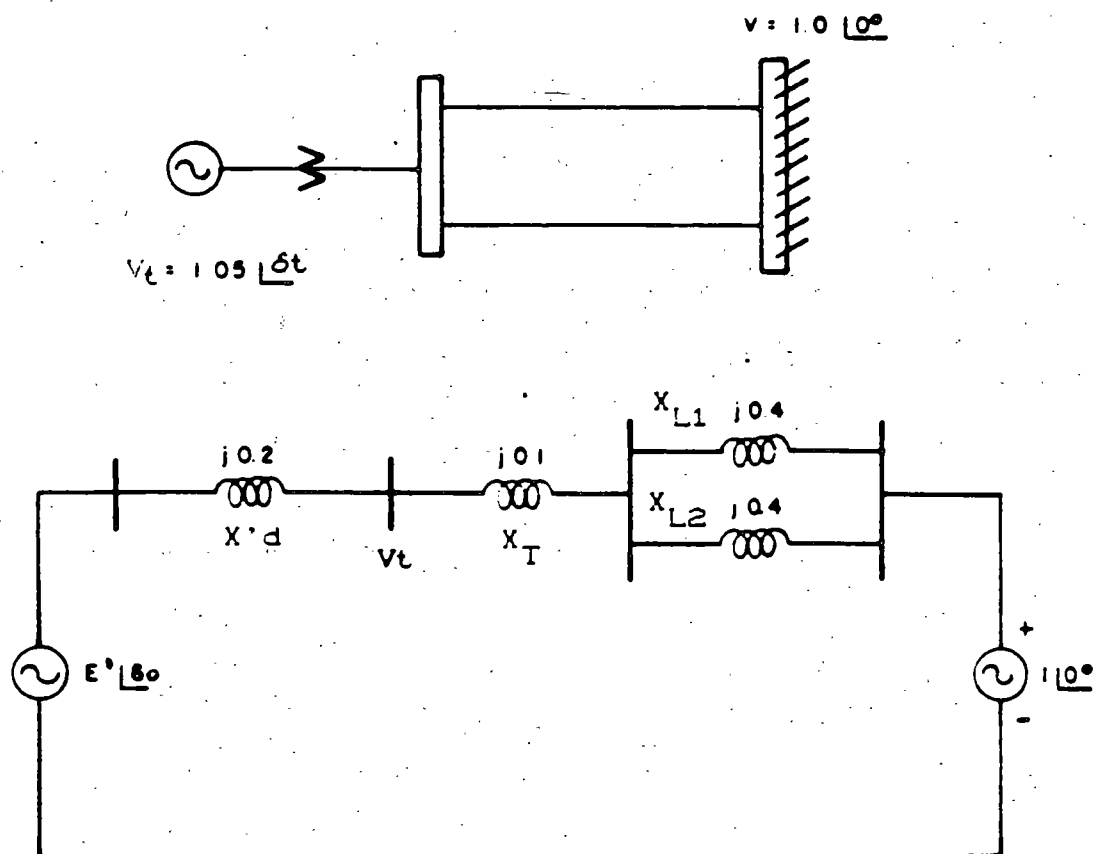
$$P_m - P_e = M \frac{d^2\delta}{dt^2}$$

3.5 EJEMPLO.

Una máquina síncrona está conectada a un bus infinito. Su reactancia transitoria de eje directo ($X'd$) es de 0.2 pu, la reactancia del transformador es 0.1 pu y la de las líneas de 0.4 pu, todas en base a los valores nominales de la máquina.

Inicialmente la máquina está entregando una potencia activa (P) de 0.8 pu con un voltaje terminal (V) de 1.05 pu; la constante de inercia de la máquina (H) es de 5 MJ/Mva y el voltaje en el bus infinito de 1.0 pu.

Determine la ecuación de oscilación para condiciones de prefalla, es decir, para condiciones normales.



SOLUCION

1. Se determina el ángulo del voltaje terminal de la máquina.

$$P_e = \frac{|V_t||V|}{X_{t\infty}} \sin \delta_t \quad (3.4)$$

$$\delta_t = \sin^{-1} \frac{P X_{t\infty}}{|V_t||V|} = \sin^{-1} \frac{0.8 \times 0.3}{1.05 \times 1} = 13.21^\circ$$

2. Se calcula la corriente aportada por el generador.

$$I = \frac{V_t - V}{X_{tcc}} = \frac{1.05 \angle 13.21 - 1.0 \angle 0}{0.3 \angle 90} = 0.803 \angle -5.29$$

3. Se obtiene el voltaje interno de la maquina o fem (E).

$$E' = V_t + jX'd I = 1.05 \angle 13.21 + (0.2 \angle 90) (0.803 \angle -5.29)$$

$$E' = 1.111 \angle 21.09 \text{ pu} \quad \text{Observe que } \delta = 21.09^\circ$$

4. Se determina el valor de la potencia máxima (Pmax).

$$P_{max} = \frac{|E'| |V|}{X} = \frac{1.11 \times 1}{0.5} = 2.222 \text{ pu}$$

5. - Se establece la ecuación de oscilación.

$$\frac{d^2 \delta}{dt^2} = -\frac{\pi f}{H} (P_m - P_{max} \sin \delta)$$

$$\frac{d^2 \delta}{dt^2} = -\frac{60 \pi}{5} (0.8 - 2.222 \sin \delta)$$

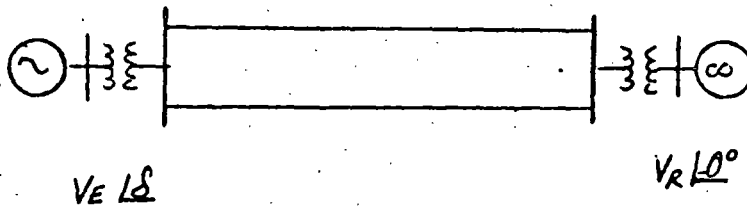
$$\frac{d^2 \delta}{dt^2} = 37.7 (0.8 - 2.222 \sin \delta)$$

4 METODO DE LAS AREAS IGUALES

El método de las áreas iguales es un método directo de solución al problema de la estabilidad transitoria en sistemas eléctricos de potencia, está basado en conceptos de energía y utiliza las gráficas Potencia-Angulo ($P - \delta$) en sus diferentes estados de operación para determinar las condiciones de estabilidad.

METODO DE AREAS IGUALES PARA EL ESTUDIO DE ESTABILIDAD TRANSITORIA

- La ecuación de oscilación (sin considerar amortiguamiento) del generador síncrono de la siguiente fig. es :



$$M \frac{d^2 \delta}{dt^2} = P_{mec} - P_e(t) \quad \dots \dots \dots (1)$$

$$M \frac{d^2 \delta}{dt^2} = P_{mec} - \frac{V_E V_R}{X_{ER}} \text{Sen } \delta_{ER} \quad \dots \dots \dots (2)$$

$$o' \quad M \frac{d\omega}{dt} = P_{mec} - P_{m\acute{a}x} \text{Sen } \delta \quad \dots \dots \dots (3)$$

$$\frac{d\delta}{dt} = \omega - \omega_0 ; \quad \omega_0 = \text{velocidad sincrónica} \quad \dots \dots (4)$$

Dividiendo ec. (3) entre ec. (4) tenemos

$$\frac{M \frac{d\omega}{dt}}{\frac{d\delta}{dt}} = \frac{P_{mec} - P_{m\acute{a}x} \text{Sen } \delta}{\omega - \omega_0}$$

$$M \frac{d\omega}{dt} (\omega - \omega_0) = (P_{mec} - P_{m\acute{a}x} \text{Sen } \delta) \frac{d\delta}{dt}$$

$$M \omega d\omega = (P_{mec} - P_{m\acute{a}x} \text{Sen } \delta) d\delta \quad \dots \dots (5)$$

Integrando la ec. (5) se tiene :

$$M \int_{\omega_0}^{\omega} \omega d\omega = \int_{\delta_0}^{\delta} (P_{mec.} - P_{m\acute{a}x} \text{ Sen } \delta) d\delta$$

$$\frac{1}{2} M \omega^2 - \frac{1}{2} M \omega_0^2 = \int_{\delta_0}^{\delta} (P_{mec.} - P_{m\acute{a}x} \text{ Sen } \delta) d\delta$$

$$\Delta E_c = \int_{\delta_0}^{\delta} P_{ac.} d\delta$$

⑥

ΔE_c = Incremento de energa cinética debido a la velocidad ω .

La ecuación ⑥ indica que la energa acumulada ó disipada en la máquina, provocada por un cambio en la velocidad, puede ser calculada por la integral de la potencia de aceleración. La potencia de aceleración puede ser positiva o negativa.

- o La solución de la ecuación de oscilación (ec. 1), mostrará el comportamiento angular de la máquina (δ) ante alguna contingencia. (Solución analítica).
- o Otra alternativa para observar el comportamiento angular y determinar la estabilidad de la máquina, bajo condiciones transitorias, sin resolver la ec. de oscilación; es el método gráfico llamado "Criterio de Areas Iguales".
- o El método de Areas-Iguales se limita a un generador (s) oscilando contra un bus infinito, ó a 2 grupos de generadores equivalentes que intercambian energa entre sí.

El método de Areas-Iguales está fundamentado en conceptos de energa. De acuerdo a este método, un sistema será estable si ante alguna contingencia la energa acumulada durante la aceleración, es disipada en un período de desaceleración. De lo contrario será inestable.

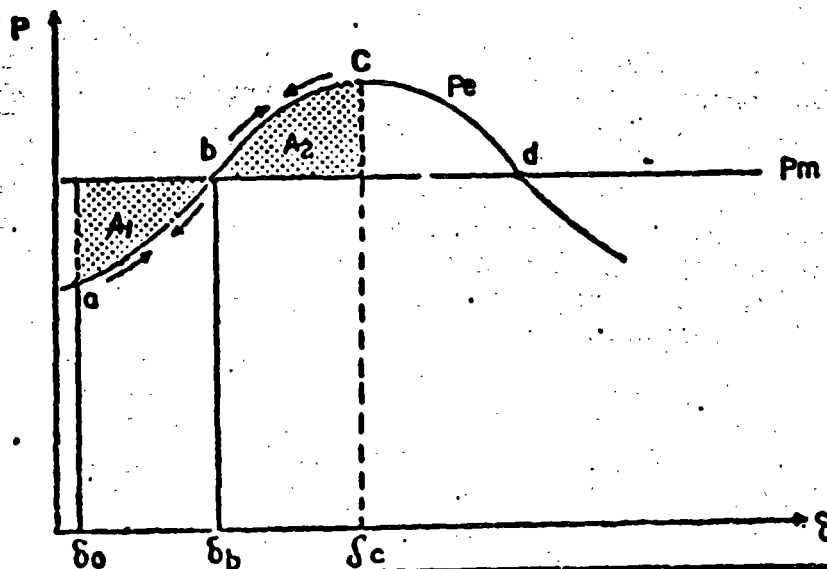
- o Suposiciones del método de Areas-Iguales, en estudios transitorios de 1a. oscilación.
 - La potencia mecánica de la turbina permanece constante.
 - Voltaje constante detrás de la reactancia transitoria.
 - Pares de amortiguamiento despreciados.
 - Efectos resistivos y capacitivos de LT's se desprecian.
 - Por simplicidad se analizan fallas 3Ø ó disparo de -- elementos sin presencia de fallas.

Considerese el caso mostrado en la siguiente fig. donde debido a un disturbio, a partir de δ_0 se tiene una diferencia entre la potencia eléctrica (P_e) y la potencia mecánica (P_m).

En forma analítica, la condición para que sea estable - requiere que $\Delta E_c = 0$, es decir que:

$$\Delta E_c = 0 = \int_{\delta_0}^{\delta_b} (P_m - P_{max} \text{Sen} \delta) d\delta - \int_{\delta_b}^{\delta_c} (P_{max} \text{Sen} \delta - P_m) d\delta$$

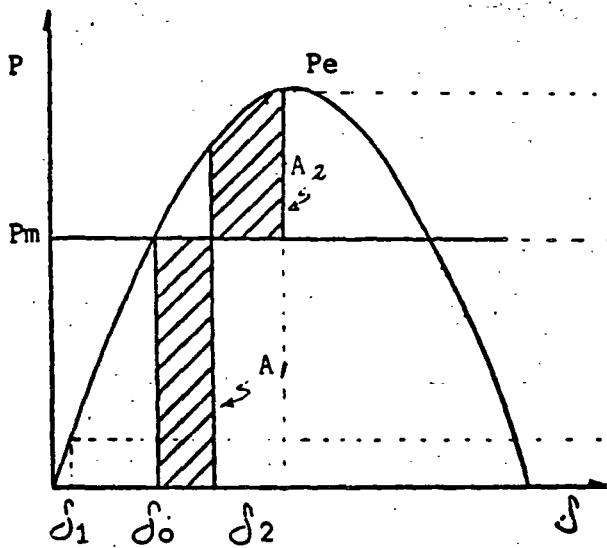
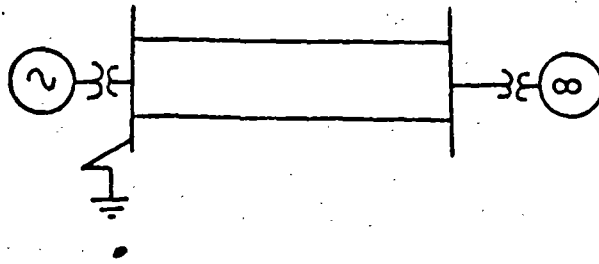
FIG.
CRITERIO AREAS
IGUALES



T A B L A I

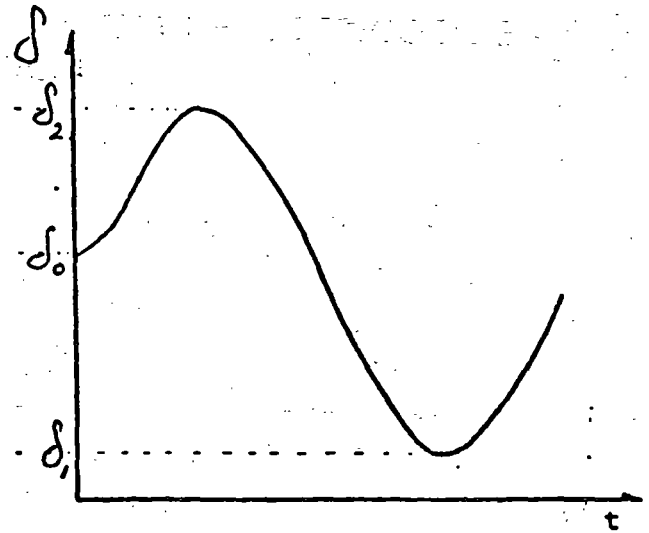
Resumen de variables para el caso analizado en la

Trayectoria	Velocidad Angular	Posición Angular	Aceleración
a - b	$W > W_0$	crece	positiva
b	$W > W_0$ máxima	crece	cero
b - c	$W > W$	crece	negativa
c	$W = W_0$	decrece	negativa (mínima)
c - b	$W < W_0$	decrece	negativa
b	$W < W_0$ mínima	decrece	cero
b - a	$W < W_0$	decrece	positiva
a	$W = W_0$	crece	positiva (máxima)

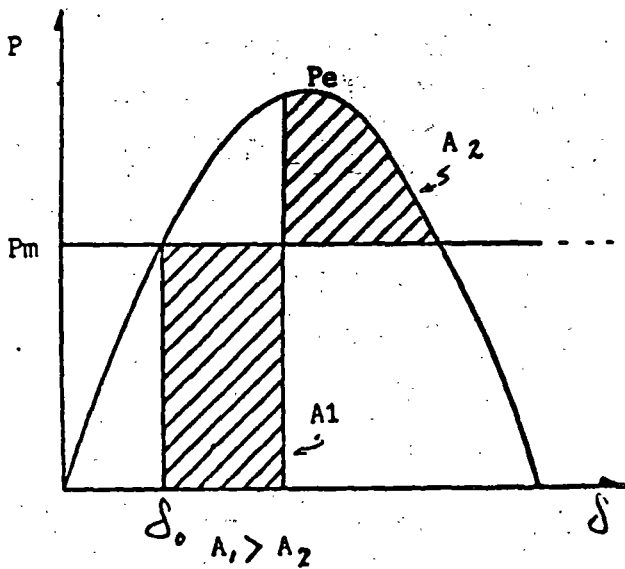


$A_1 = A_2$

(a)



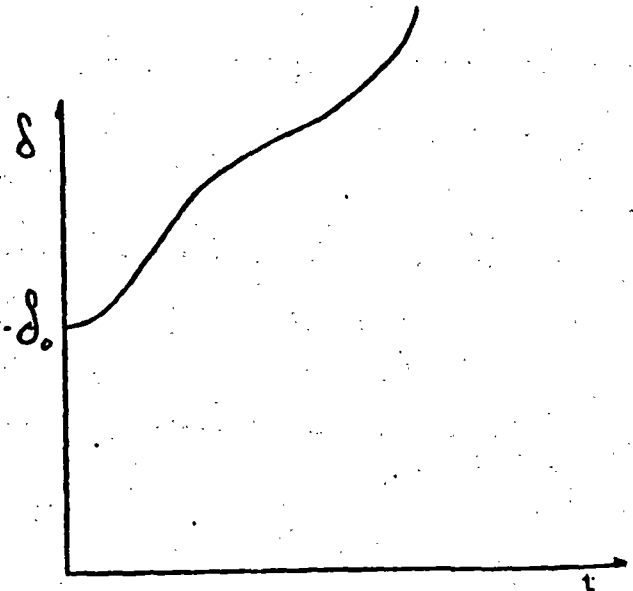
Oscilación de la máquina en una condición estable.

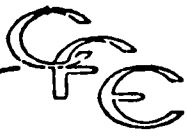


Pérdida de sincronismo de la máquina.

Ejemplo de Máquina-Bus Infinito. Falla 3Ø liberada en 2 tiempos. Caso (a) Estable

(b)

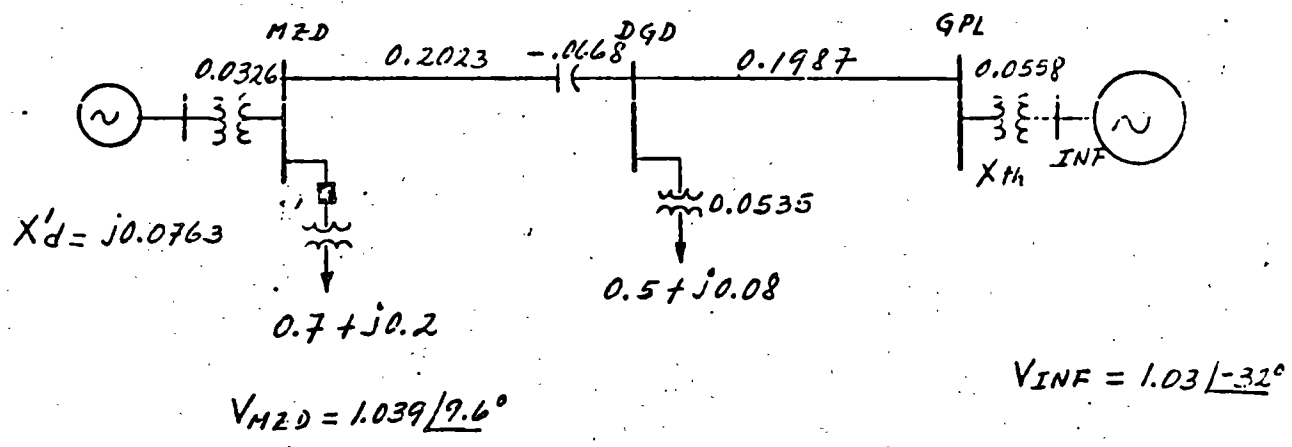




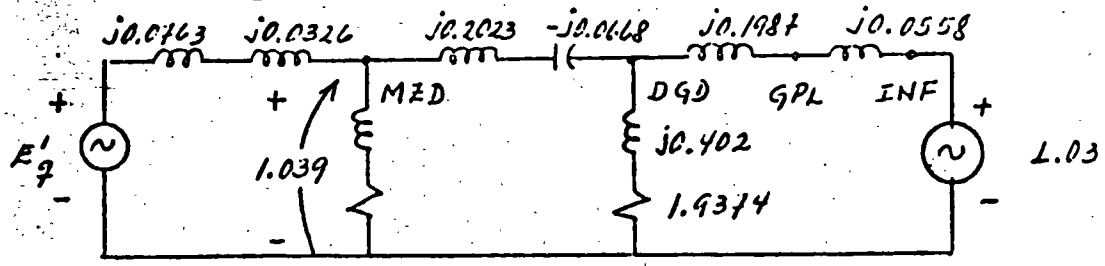
EJEMPLO: ANALISIS DE LA TRANSMISION MZD-GPL POR AREAS IGUALES.

Utilizando el método de Areas iguales (Gráfico), determinar la generación máxima de MZD-U3, para soportar la pérdida -- de la carga de Mazatlán (70 MW) a la hora de demanda máxima sin pérdida de sincronismo de MZD-U3. Representar en GPL - al resto del Sistema Interconectado por un equivalente de Thévenin.

En la siguiente figura se indican los parámetros de los elementos que intervienen en el estudio así como algunos datos obtenidos de una corrida de flujos. Se desprecia el efecto-capacitivo y resistivo de las líneas.



El diagrama de reactancias queda de la siguiente manera:



Para determinar la transferencia de potencia de MZD hacia el bus infinito, se requiere transformar la conexión Y - a una conexión Δ . Nos interesa la impedancia serie entre el nodo MZD y el bus INF.

$$Z_{M2D-INF} = \frac{j0.2625 - 0.05448 - 0.03455 + j0.494 - 0.1025}{1.9374 + j0.402}$$

$$Z_{M2D-INF} = \frac{-0.1915 + j0.7565}{1.9786 \angle 11.7^\circ} = \frac{0.78036 \angle 104.2^\circ}{1.9786 \angle 11.7^\circ}$$

$$Z_{M2D-INF} = 0.394 \angle 92.5^\circ \therefore X_{M2D-INF} \approx j0.394$$

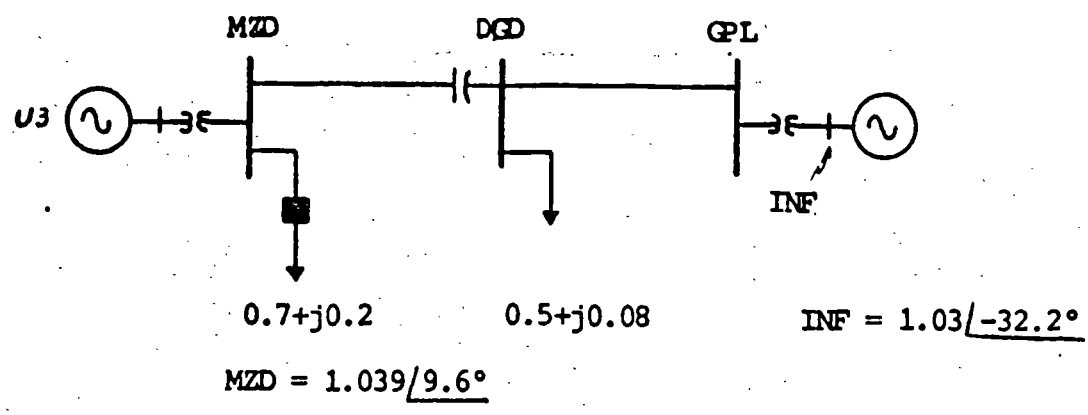
La ecuación de transferencia de potencia de M2D a INF es:

$$P_e = \frac{V_{M2D} V_{INF}}{X_{M2D-INF}} \text{ Sen } \delta = \frac{(1.039)(1.03)}{0.394} \text{ Sen } \delta$$

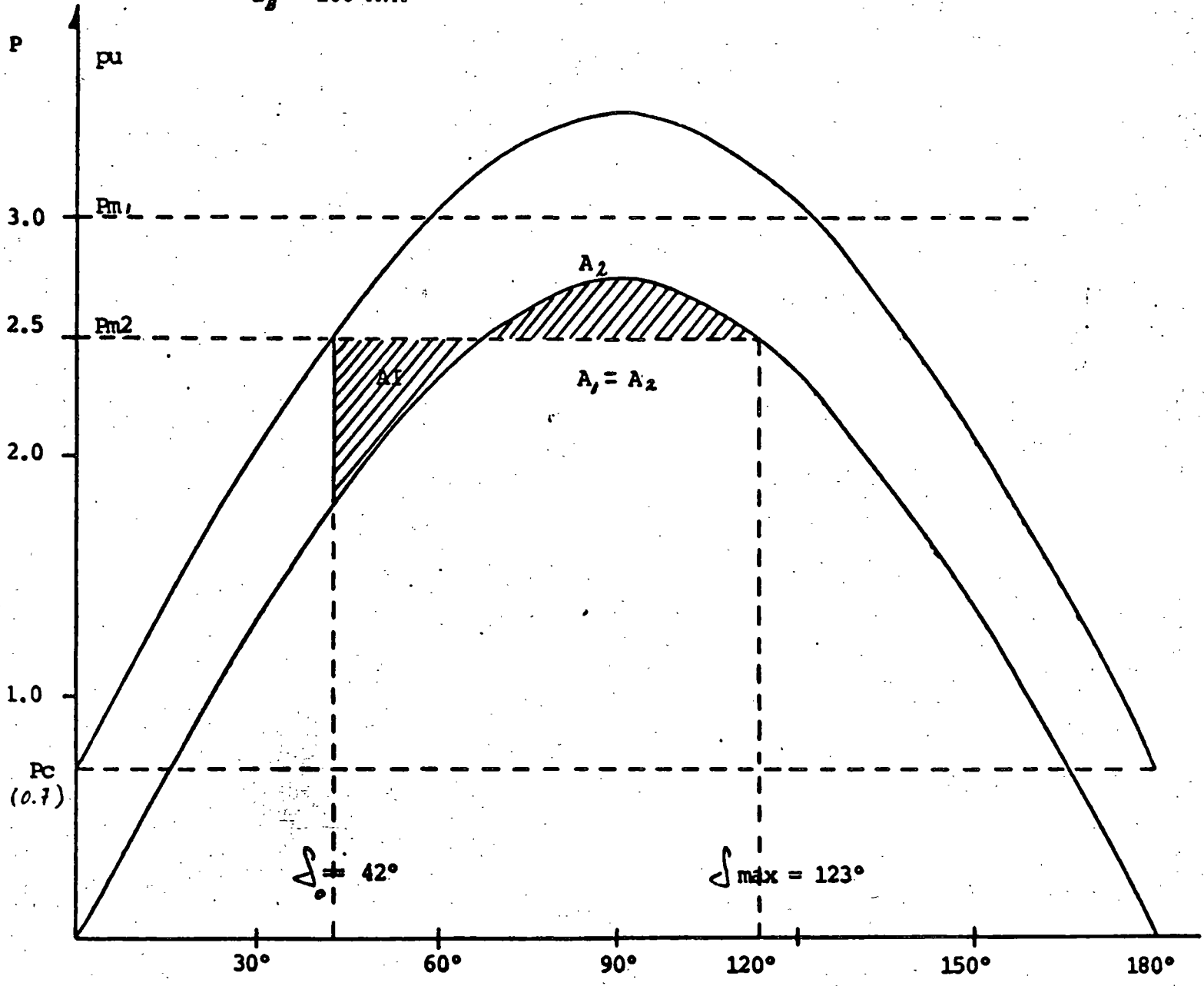
$$P_e = 2.72 \text{ Sen } \delta$$

En la siguiente gráfica P- δ se muestra la característica de transferencia de potencia; la carga de Mazatlán y la potencia mecánica del turbogenerador, para algunos valores de generación.

Efectuando análisis por el método de Arcas Iguales resultó que la generación máxima para M2D-U3 es de aproximadamente 2.5 pu. (250 MW).



$S_B = 100 \text{ MVA}$



Análisis de estabilidad transitoria por el método de Areas Iguales para simular, pérdida de la carga de Mazatlán.

CFE-CENACE
DID

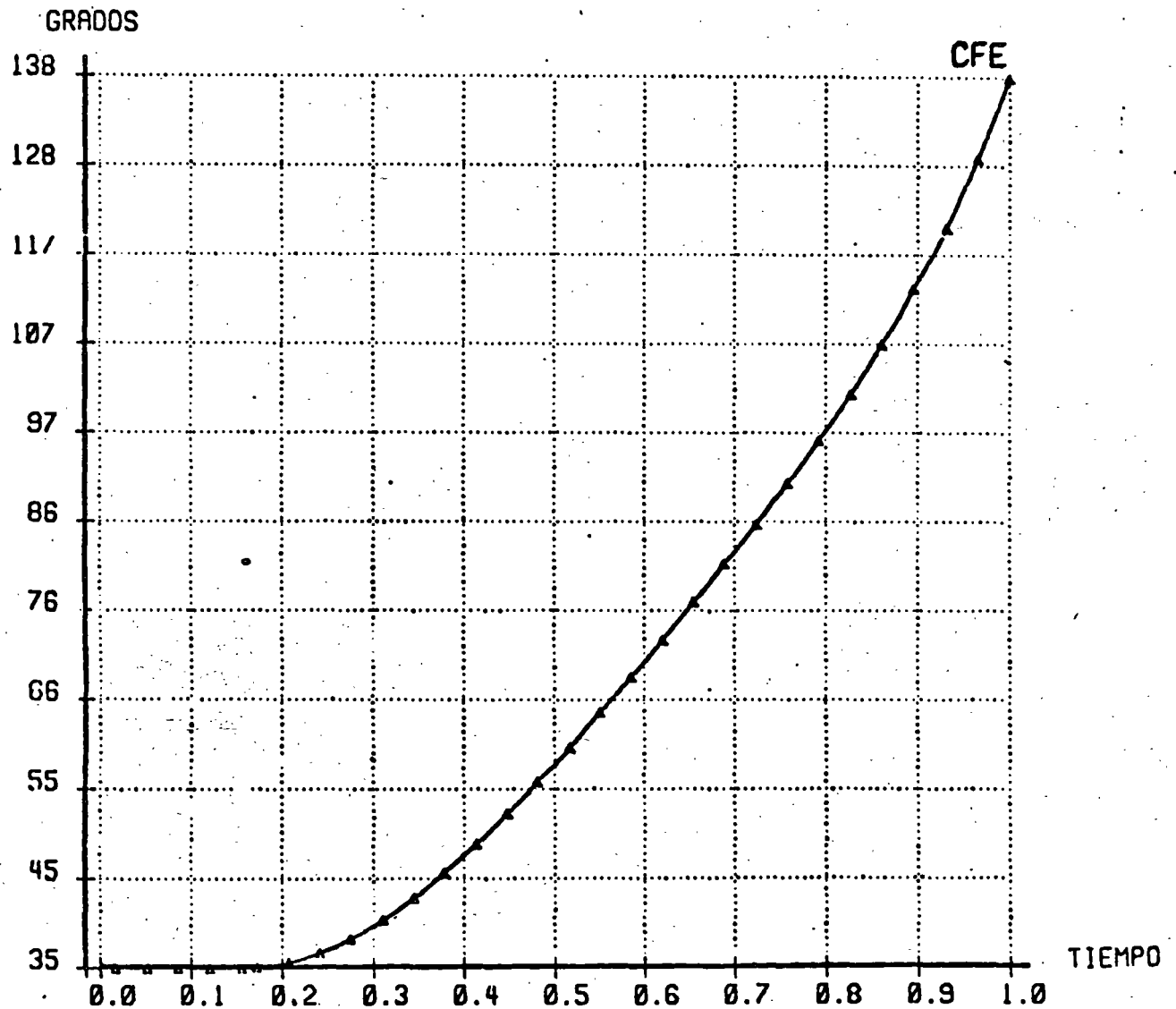
RESULTADOS GRAFICOS
DIFERENCIAS ANGULARES

SISP-ESTABI
27/FEB/86

* PERDIDA DE LA CARGA DE MZD-115 . CONSIDERANDO LA U3 DE MZD Y LA CARGA *
* MZD-115 HACIA EL SIN. *

MADUINA DE REFERENCIA MTY-UI

—————▲————— MZD-U3



CFE-CENACE
DID

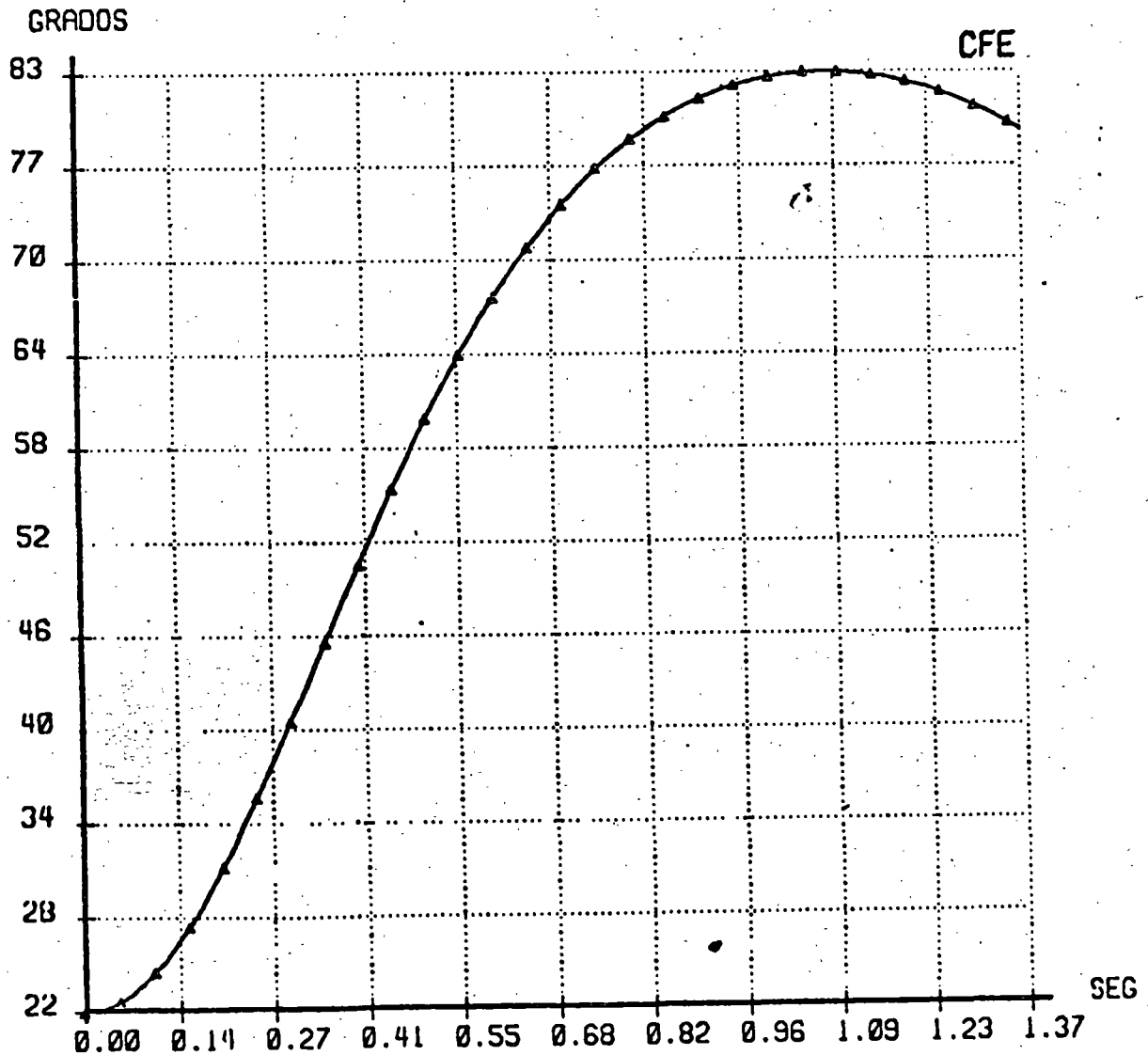
RESULTADOS GRAFICOS
DIFERENCIAS ANGULARES

SISP-ESTABI
28/FEB/86

* PERDIDA DE CARGA EN MZD-115 . U3 DE MZD CON 265 MW *
* * * * *

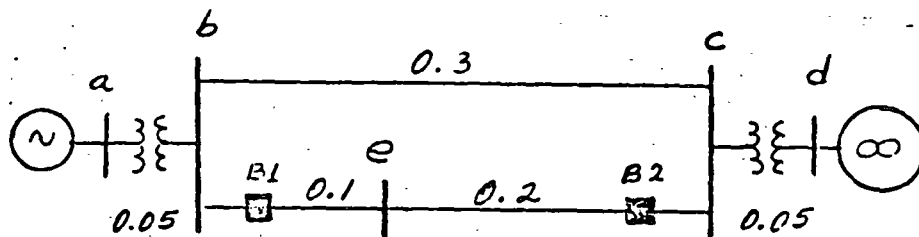
MAQUINA DE REFERENCIA MTY-U1

▲ — ▲ — ▲ — ▲ — ▲ MZD-U3



EJEMPLO No. 1. Considere el sistema de la siguiente figura. Si el bus infinito absorbe $S = 1.0 + j0.2$. Demostrar que los valores correspondientes para E'_g y δ_0 son 1.152 y 20.3° .

Calcular la máxima oscilación del rotor δ_3 , si disparan accidentalmente el I-B1.



$$X'_d = X_g = 0.15$$

$$V_d = 1 \angle 0^\circ$$

$$H = 2.7 \text{ seg.}$$

$$E'_g = V_d + jX'_d I$$

$$I^* = \frac{S}{V_d} = \frac{1.0 + j0.2}{1 \angle 0^\circ} = 1.0 + j0.2$$

$$\therefore I = 1.0 - j0.2$$

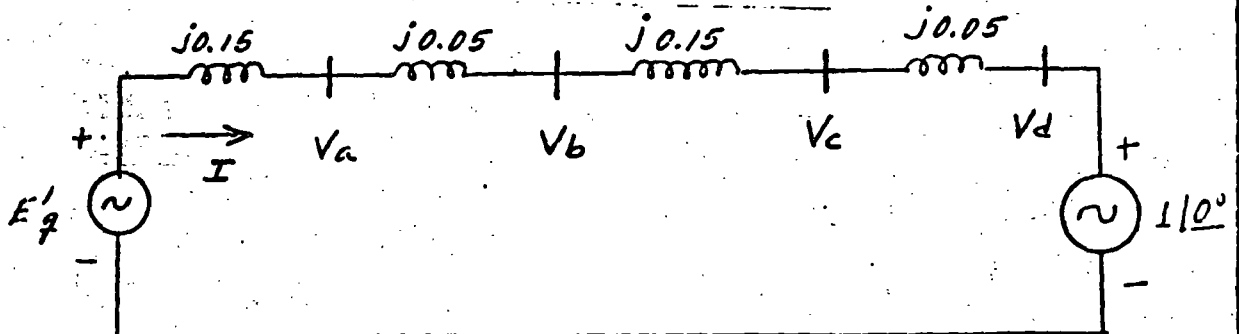


Diagrama de reactancias.

$$E'_g = V_d + jX_T I = 1 \angle 0^\circ + j0.4(1 - j0.2)$$

$$E'_g = 1.152 \angle 20.3^\circ ; \delta_0 = 20.3^\circ$$

$$S = VI^* = (1.152 \angle 20.3^\circ)(1.0198 \angle 11.3^\circ) = 1.1748 \angle 31.6^\circ$$

$$S = P + jQ = 1.0 + j0.616$$

$$\underline{P_e = P_m = 1.0 \text{ pu}}$$

también:

$$P_e = \frac{E'_q V}{X_T} \sin \delta = \frac{(1.152)(1)}{0.4} \sin 20.3^\circ = 1.0 \text{ pu.}$$

$$\underline{P_m = 1.0 \text{ pu.}}$$

$$\Rightarrow \therefore \underline{\text{EN PREFALLA } P_e = 2.88 \sin \delta}$$

$$\frac{d^2 \delta}{dt^2} = \frac{\pi f}{H} (P_m - P_e)$$

$$\boxed{\frac{d^2 \delta}{dt^2} = 69.8 (1 - 2.88 \sin \delta)} \quad \text{Ec. de oscilación.}$$

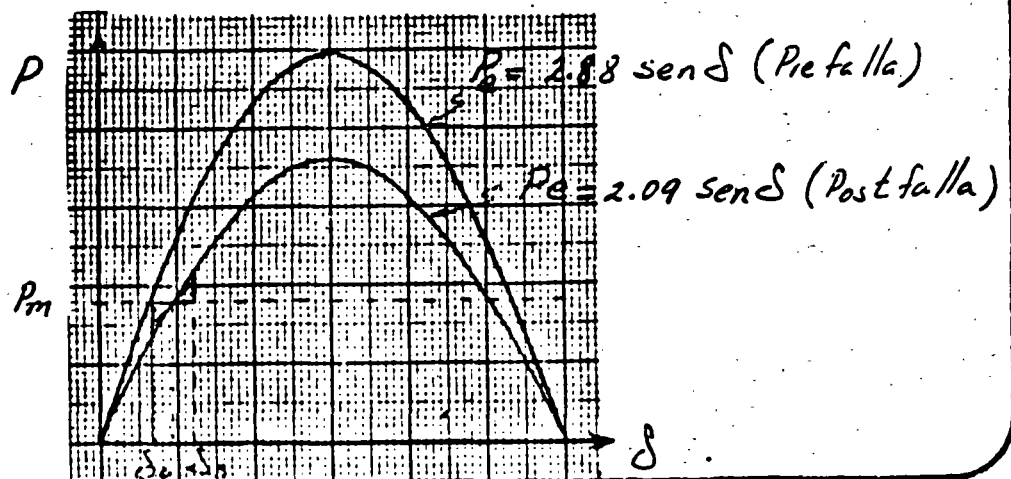
\Rightarrow Al abrirse el I-B1 la X_T es:

$$X_T = 0.15 + 0.05 + 0.03 + 0.05 = 0.55$$

$$P_e = \frac{E'_q V}{X_T} \sin \delta = \frac{(1.152)(1)}{0.55} \sin \delta = 2.09 \sin \delta$$

$$\Rightarrow \therefore \underline{\text{EN POSTFALLA } P_e = 2.09 \sin \delta}$$

$$\boxed{\frac{d^2 \delta}{dt^2} = 69.8 (1 - 2.09 \sin \delta)}$$



Con una linea abierta se tiene que en el cruce de P_m y P_e

$$P_e = P_m = 1.0 \text{ pu.}$$

$$\Rightarrow 1.0 = 2.09 \sin \delta_2$$

$$\delta_2 = \sin^{-1} \frac{1}{2.09} = 28.6^\circ$$

$$\delta_2 = 28.6^\circ \quad \text{ó} \quad \delta_2 = 151.4^\circ$$

$$A_1 = \int_{28.3^\circ}^{28.6^\circ} (1 - 2.09 \sin \delta) d\delta = \delta \Big|_{0.354}^{0.499} + 2.09 \cos \delta \Big|_{0.354}^{0.499}$$

$$A_1 = 0.499 - 0.354 + 1.835 - 1.96 = 0.02$$

$$A_1 = 0.02$$

$$0.02 = \int_{28.6^\circ}^{\delta_3} (2.09 \sin \delta - 1) d\delta$$

$$0.02 = -2.09 \cos \delta \Big|_{0.499}^{\delta_3} - \delta \Big|_{0.499}^{\delta_3}$$

$$0.02 = -2.09 \cos \delta_3 + 1.835 - \delta_3 + 0.499$$

$$\delta_3 + 2.09 \cos \delta_3 = 2.314$$

$$\delta_3 \approx 37^\circ$$

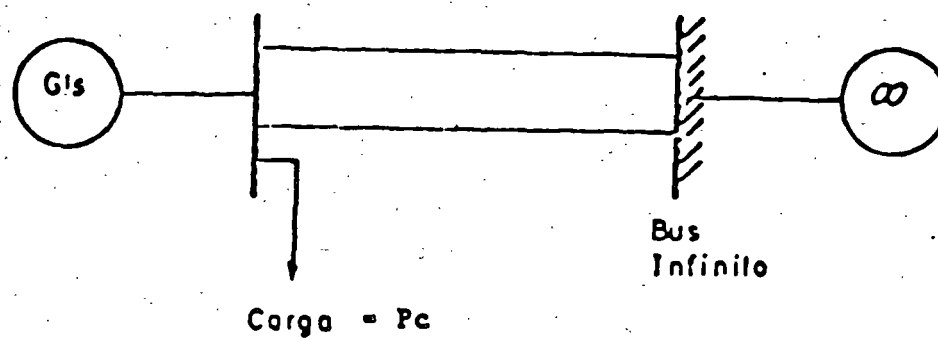
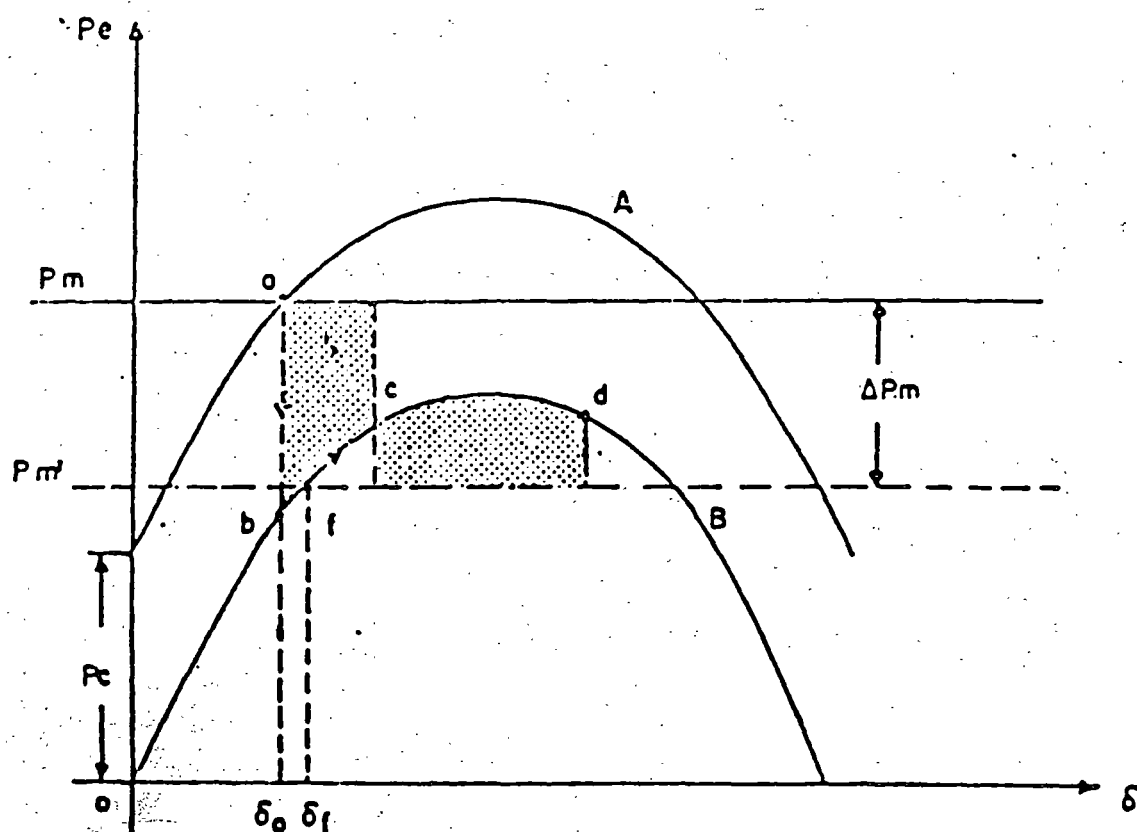


FIG. 9 Sistema de Potencia con Carga en el nodo de Generación.



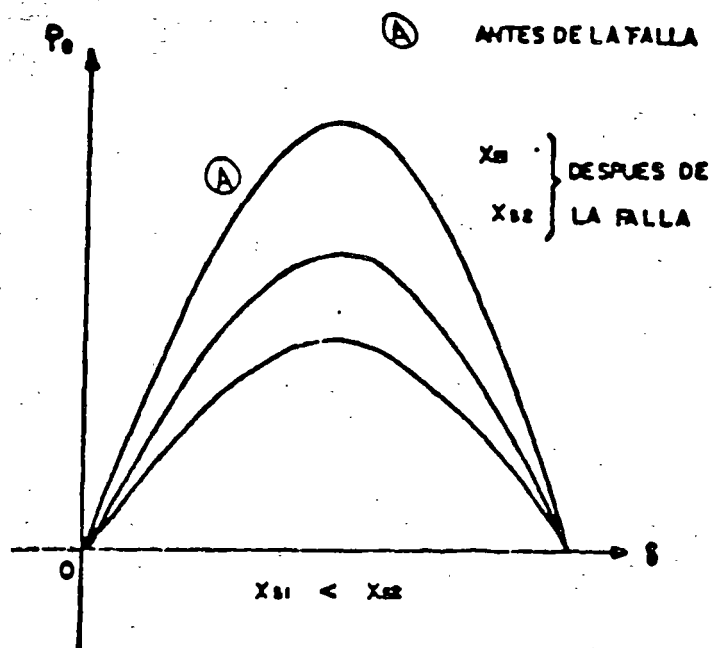
A. Curva Pre-disturbio

B. Curva con pérdida — de carga.

ΔP_m Magnitud del disparo de generación.

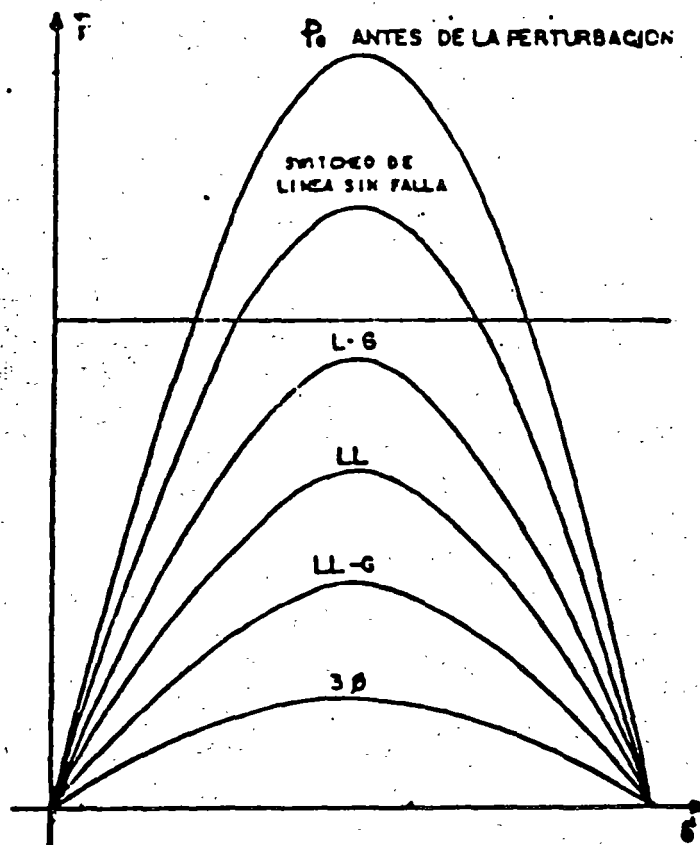
FIG. 10 Método de las Areas Iguales considerando pérdida de Carga y disparo automático de Generación.

FIGURA 20. LA MAGNITUD DE LA REACTANCIA DEL SISTEMA X_B DESPUES DE LA FALLA ES IMPORTANTE.



SE DESEA QUE X_B SEA LO MENOR POSIBLE

FIGURA 21. LA NATURALEZA (TIPO) DE FALLA ES IMPORTANTE.



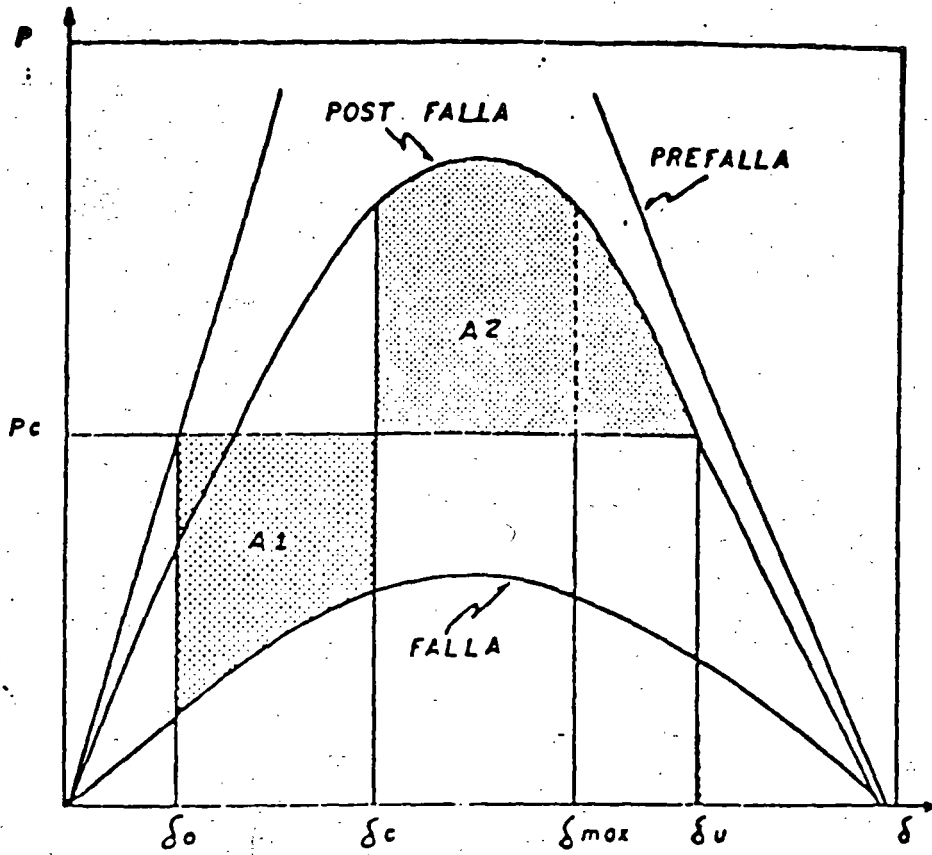


FIGURA 22

MARGEN DE ENERGIA PARA SOPORTAR CONTINGENCIA
EVALUADO CON ESTABILIDAD TRANSITORIA: CASO ELEMENTAL
MAQUINA BUS INFINITO.

MARGEN DE ENERGIA = A₂ - A₁

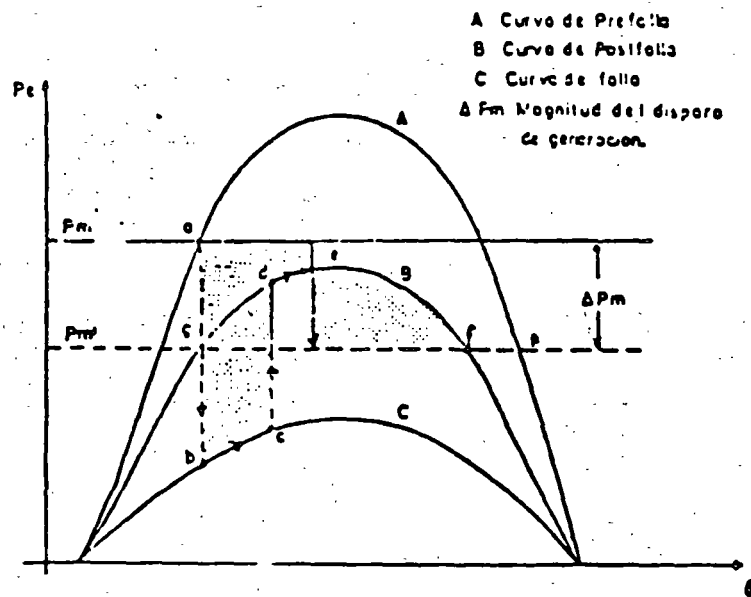


FIG. 8 Método de Areas Iguales considerando disparo Automático de Generación.

4

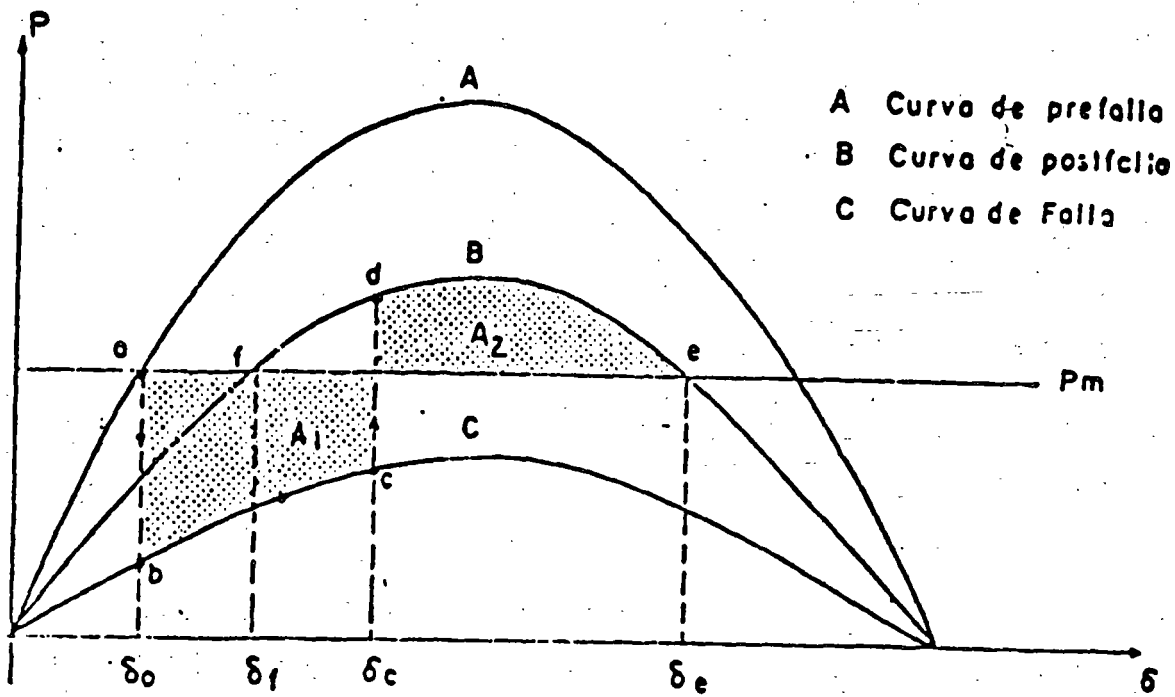
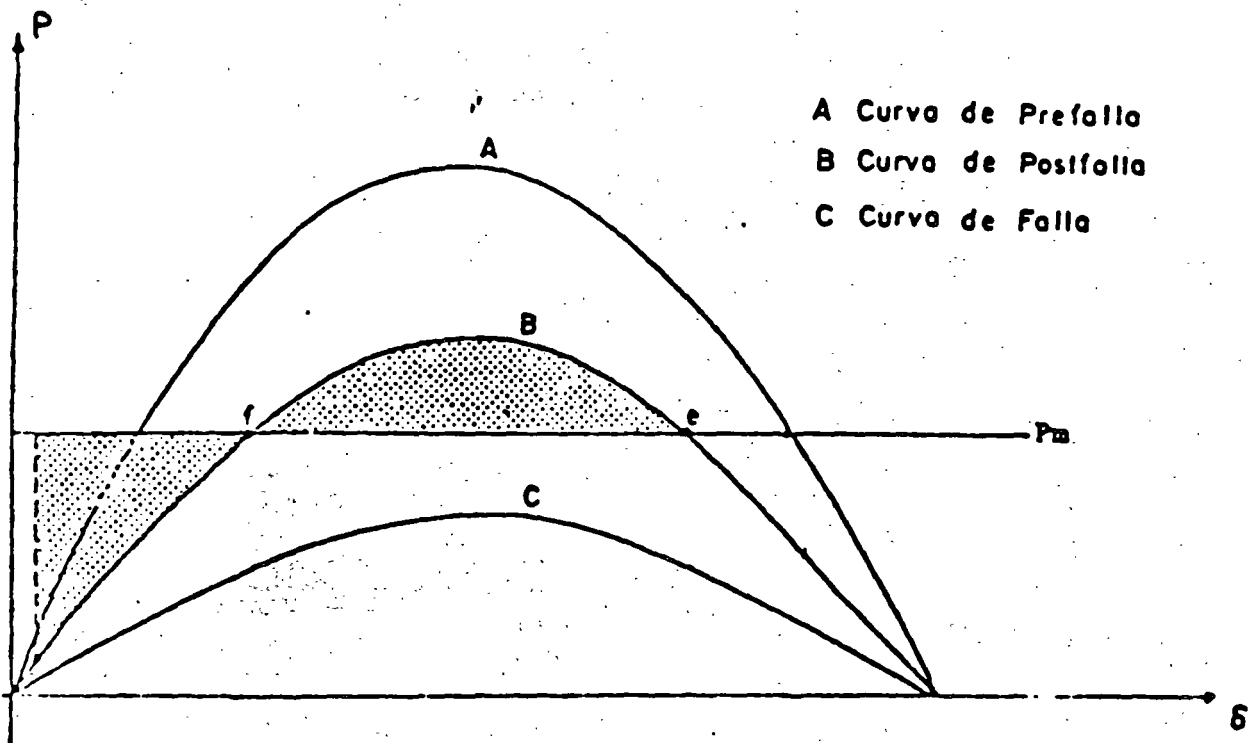


FIG. 6 Curvas de Potencia para las condiciones de Prefallo, falla y Postfallo.



5.1 NECESIDAD DEL USO DE METODOS NUMERICOS.

En el capítulo 3 se expuso que las expresiones matemáticas que describen el comportamiento dinámico de un sistema eléctrico son ecuaciones diferenciales no lineales, las cuales no tienen solución por métodos directos. Es por ello que se hace necesario aplicar métodos numéricos para obtener la solución citada, a través de la computadora digital.

Los métodos más utilizados en este tipo de problemas son:

- Método de Euler.
- Método modificado de Euler.
- Método trapezoidal.
- Método de Runge-Kutta.

Los dos primeros se emplean frecuentemente con fines didácticos, dada su sencillez; aunque desde el punto de vista del tiempo de cómputo no son muy eficientes. Por el contrario, los dos últimos se caracterizan por su alta eficiencia, pero su planteamiento resulta complicado.

En el presente capítulo se describen los dos métodos de Euler y su aplicación a la solución de la ecuación de oscilación que resulta de un sistema "máquina-bus infinito". Al final se dan algunas conclusiones de tipo general en relación con el impacto del tipo, localización y duración de las fallas sobre la estabilidad transitoria de un sistema eléctrico.

5.2 GENERALIDADES DE LOS METODOS.

Regularmente, los métodos numéricos para resolver ecuaciones diferenciales, llamados de integración numérica, utilizan el proceso "paso a paso" para obtener una serie de valores para cada una de las variables dependientes, los cuales corresponden a un conjunto de valores de la variable independiente seleccionados usualmente en intervalos fijos.

La precisión de una solución por integración numérica depende del método escogido y del tamaño del intervalo.

5.3 METODO DE EULER.

El problema de integración numérica consiste en que a partir de una ecuación diferencial de primer orden

$$\frac{dy}{dx} = f(x,y) \quad (5.1)$$

en la que y es la variable dependiente y x la variable independiente, se requiere obtener su solución, la cual es de la forma

$$y = g(x,c) \quad (5.2)$$

En esta expresión, c es una constante obtenida con las condiciones iniciales especificadas. La curva que representa a la ecuación solución (5.2) es como la mostrada en la figura 5.1. Dado que esta curva varía suavemente, es posible aproximarla por medio de segmentos de recta muy cortos. En estas condiciones, en el punto inicial $P_0(x_0, y_0)$ de esta curva se cumple

$$\Delta y \cong \left. \frac{dy}{dx} \right|_0 \Delta x$$

siendo Δy el incremento en la variable dependiente correspondiente al incremento Δx y $dy/dx|_0$ la pendiente de la curva en el punto $P_0(x_0, y_0)$, misma que se obtiene sustituyendo las coordenadas del punto P_0 en la ecuación diferencial (5.1).

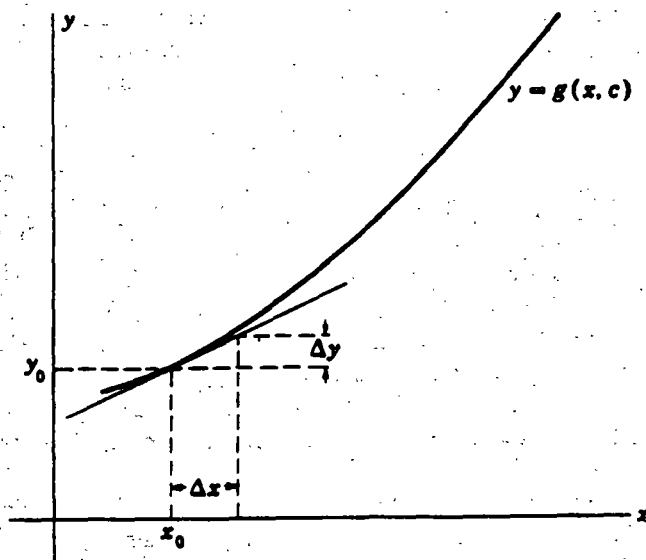


Figura 5.1
Gráfica de la función solución

Por lo tanto, dados los valores iniciales puede obtenerse un nuevo valor de las variables x, y para un incremento Δx especificado. Haciendo $h = \Delta x$, se obtiene

$$x_1 = x_0 + h$$

$$y_1 = y_0 + \Delta y = y_0 + \left. \frac{dy}{dx} \right|_0 h$$

Del mismo modo puede determinarse un segundo valor de las variables:

$$x_2 = x_1 + h$$

$$y_2 = y_1 + \left. \frac{dy}{dx} \right|_1 h = y_1 + f(x_1, y_1) h$$

Este proceso debe repetirse para calcular los valores subsiguientes de x, y

$$x_3 = x_2 + h \quad y_3 = y_2 + \left. \frac{dy}{dx} \right|_2 h$$

$$\dots$$

$$x_n = x_{n-1} + h \quad y_n = y_{n-1} + \left. \frac{dy}{dx} \right|_{n-1} h$$

Una vez realizado el proceso completo, los valores x, y que corresponden a la solución se proporcionan en forma de tabla. La figura 5.2 muestra gráficamente el método descrito.

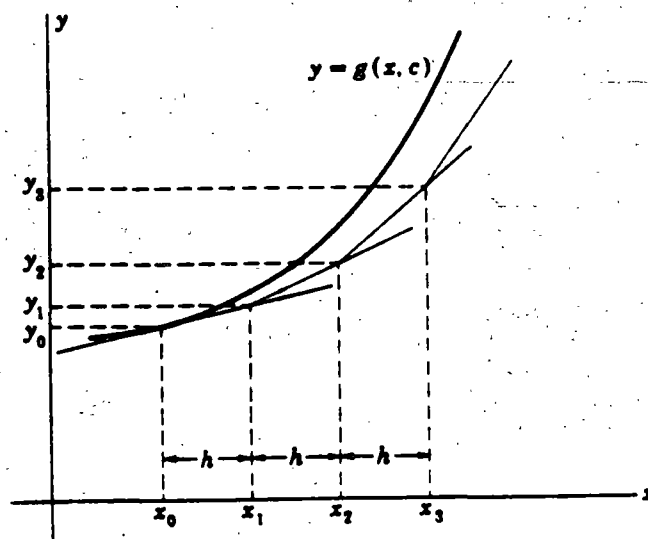


Figura 5.2

Gráfica de la solución estimada por el método de Euler

5.4 METODO MODIFICADO DE EULER.

En el método original de Euler, el valor de la derivada al principio de cada incremento se aplicaba en todo el intervalo. Un perfeccionamiento del método se logra calculando un valor preliminar de y para x_1 como antes

$$x_1 = x_0 + h$$

$$y_1^0 = y_0 + \left. \frac{dy}{dx} \right|_0 h$$

y sustituyendo estos valores en la ecuación (5.1) para calcular el valor de la pendiente al final del intervalo, es decir

$$\left. \frac{dy}{dx} \right|_1 = f(x_1, y_1^0)$$

Entonces, es posible obtener un valor modificado de y más aproximado, usando el promedio de las derivadas o pendientes

$$y_1^1 = y_0 + (1/2) \left[\left. \frac{dy}{dx} \right|_0 + \left. \frac{dy}{dx} \right|_1 \right] h$$

Usando y_1^1 y x_1 se puede calcular una tercera aproximación de y mediante el mismo procedimiento

$$y_1^2 = y_0 + (1/2) \left[\left. \frac{dy}{dx} \right|_0 + \left. \frac{dy}{dx} \right|_1 \right] h$$

El proceso se continúa hasta que en dos estimaciones consecutivas los valores obtenidos de y difieran en un monto menor a una cierta tolerancia preestablecida. Finalmente, las fases del método se repiten en su totalidad para obtener el valor de las variables en los siguientes intervalos. La mayor precisión que se obtiene con el método modificado de Euler se muestra en la figura 5.3.

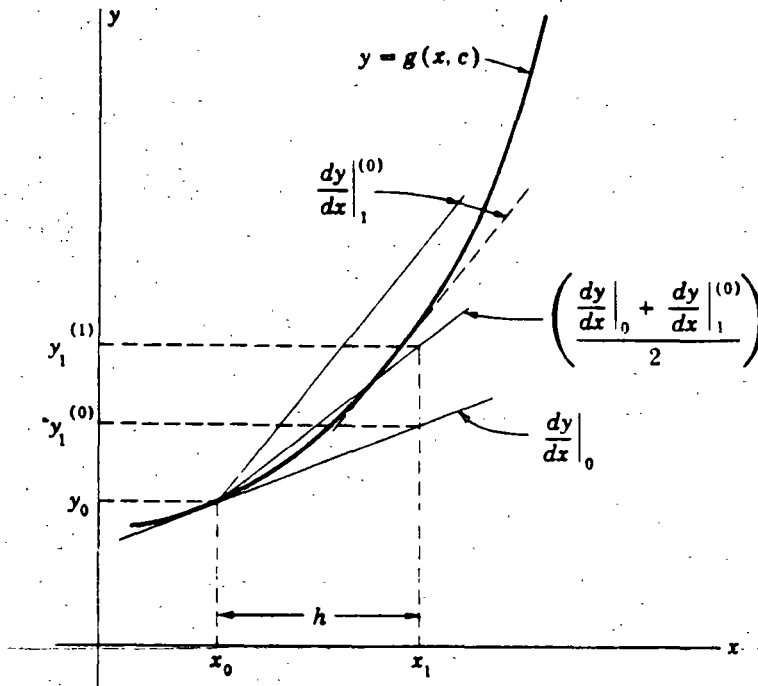


Figura 5.3
Gráfica de la solución por el método modificado de Euler.

5.5 EJEMPLO DE SOLUCION NUMERICA.

Supóngase que se desea resolver la ecuación diferencial

$$\frac{dy}{dx} = 3x^2$$

Es obvio que la solución obtenida por métodos directos es

$$y = x^3$$

pero se aprovechará la sencillez de esta función para mostrar la formulación de los métodos de integración numérica. En la figura 5.4 se muestra el diagrama de flujo correspondiente al algoritmo del método modificado de Euler, en base al cual se elaboró el siguiente programa para computadora en lenguaje basic:

```

10 REM Programa para resolver una ecuación diferencial
15 REM por el método modificado de Euler
20 XF=5 : H=.5 : X0=0 : Y0=0
25 PRINT X0,Y0
30 X1= X0 : Y1=Y0
40 REM Valor preliminar
50 D1=3*X1^2 : X2 = X1+H : Y2P=Y1+D1*H
60 REM Valor corregido
70 D2=3*X2^2 : DPROM=.5*(D1+D2) : Y2C = Y1 + DPROM*H
85 PRINT X2,Y2C
95 IF X2>XF THEN 100 ELSE 97
97 X1=X2 : Y1=Y2C : GOTO 40
100 END

```

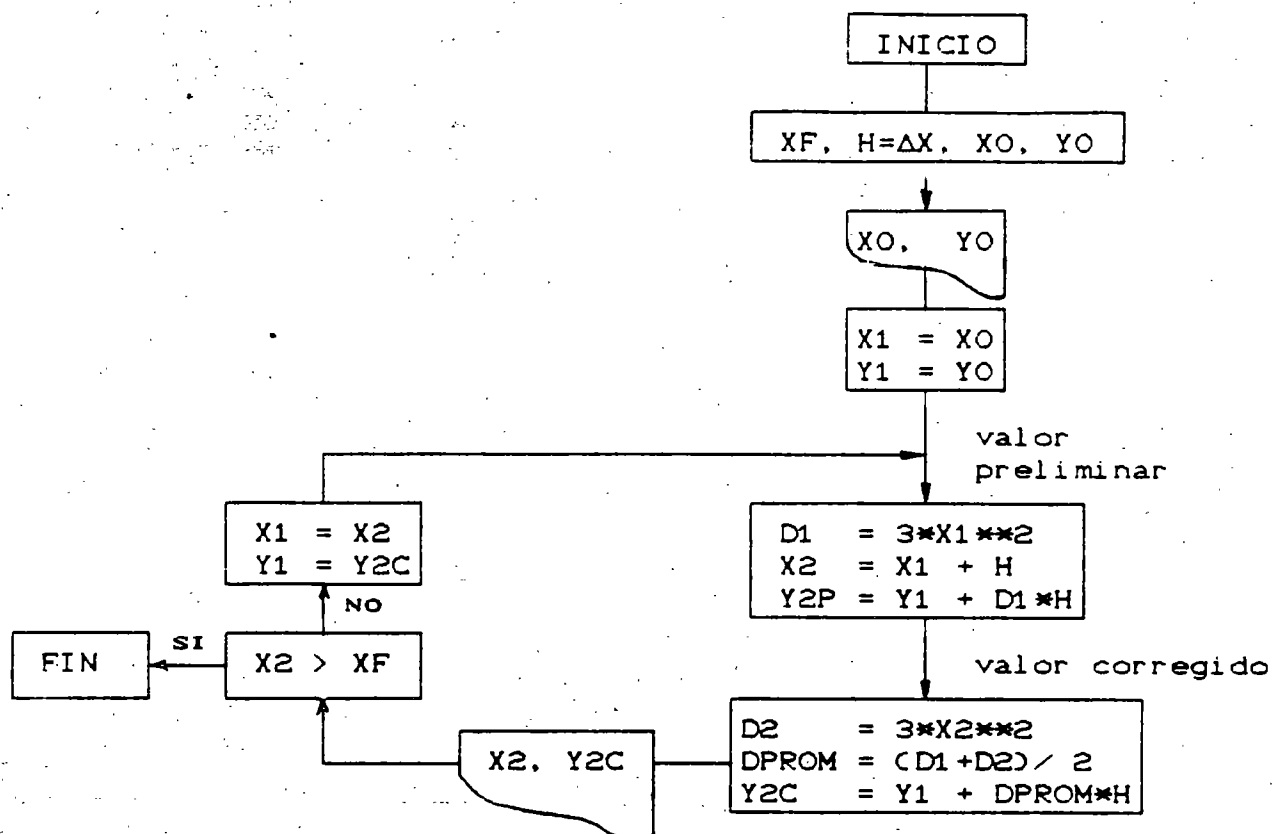


Figura 5.4

Diagrama de flujo para el método modificado de Euler

En el diagrama la variables de entrada son:

XF = Valor final de la variable independiente.
 H = Δx = Tamaño del intervalo de integración.
 (XO, YO) = Condiciones iniciales.

Los resultados son los mostrados en la siguiente tabla:

TABLA DE RESULTADOS DE LA INTEGRACION NUMERICA

X	Y (exacta)	Y (Euler) (h=0.5)	Y (Mod. de Euler) (h=0.5)	Y (Mod. de Euler) (h=0.1)
0	0	0	0	0
1	1	0.4	1.13	1.01
2	8	5.3	8.25	8.01
3	27	20.6	27.38	27.02
4	64	52.5	64.50	64.02
5	125	106.9	125.63	125.02

5.6 ECUACIONES DE OSCILACION PARA LA SOLUCION NUMERICA.

Con el objeto de mostrar el empleo de los métodos de integración numérica en los estudios de estabilidad transitoria, se retoma el ejemplo del sistema presentado en el capítulo 3 y cuya configuración se muestra nuevamente en la figura 5.5. En ella se ha agregado una falla en una de las líneas, representada por la reactancia de valor 0.1 pu. Esta reactancia equivale a una falla trifásica no sólida, o bien, representa a las reactancias de las redes de secuencia negativa y cero en el caso de una falla desbalanceada.

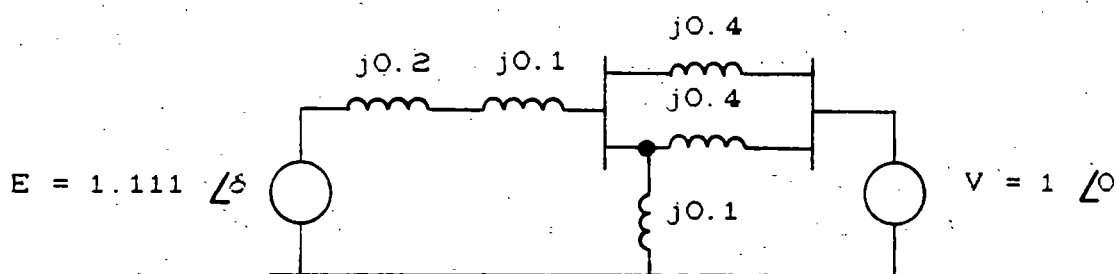


Figura 5.5

Circuito equivalente del sistema "máquina-bus infinito" estudiado en el capítulo 3.

De manera semejante a como ocurrió en el caso del método de las "Áreas Iguales", en la solución de tipo numérico también deben considerarse los tres momentos básicos del sistema:

- Prefalla.
- Falla y
- Postfalla.

a) Condiciones de prefalla.

En el capítulo 3 se determinó que la ecuación de oscilación en condiciones normales o de prefalla para el sistema era:

$$-\frac{d^2\delta}{dt^2} = 37.7 (0.8 - 2.222 \text{ sen } \delta)$$

b) Condiciones de falla.

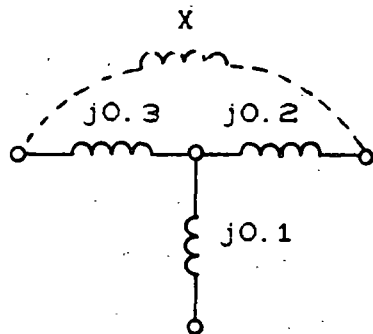
En condiciones de falla las reactancias involucradas quedan conectadas como se muestra en la figura 5.6(a), calculándose la reactancia entre las fuentes de voltaje mediante

reducciones serie-paralelo y conversiones estrella-delta, llegando así a un valor de 1.1 pu. Con ello, la potencia máxima resulta:

$$P_{max} = \frac{|E| |V|}{X} = \frac{(1.111)(1.0)}{1.1} = 1.01$$

y la ecuación de oscilación en condiciones de falla:

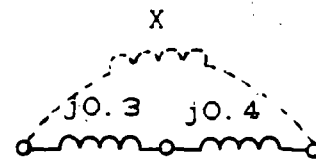
$$\frac{d^2 \delta}{dt^2} = 37.7 (0.8 - 1.01 \text{ sen } \delta)$$



$$X = \frac{0.3 \times 0.2 + 0.2 \times 0.1 + 0.1 \times 0.3}{0.1}$$

$$X = 1.1 \text{ pu}$$

(a)



$$X = 0.3 + 0.4$$

$$X = 0.7 \text{ pu}$$

(b)

Figura 5.6

Reactancia entre las fuentes de voltaje en condiciones de (a) falla y (b) postfalla.

c) Condiciones de postfalla.

Una vez liberada la falla, las reactancias del circuito quedan como se muestra en la figura 5.6(b), con lo que la reactancia equivalente entre las fuentes de voltaje es de 0.7 pu y la potencia máxima igual a

$$P_{\max} = \frac{|E| |V|}{X} = \frac{(1.111)(1.0)}{0.7} = 1.587$$

resultando la ecuación de oscilación para condiciones de postfalla siguiente:

$$-\frac{d^2\delta}{dt^2} = 37.7 (0.8 - 1.587 \text{ sen } \delta)$$

Finalmente, es necesario reemplazar la ecuación de oscilación por dos ecuaciones de primer orden para estar en posibilidades de aplicar los métodos de solución numérica. Para ello se parte del hecho demostrado de que el cambio en el ángulo del rotor δ depende de la diferencia de velocidades angulares:

$$\frac{d\delta(t)}{dt} = \omega(t) - \omega_0 \quad (5.3)$$

Si se deriva la ecuación anterior, se obtiene:

$$\frac{d^2\delta(t)}{dt^2} = \frac{d\omega(t)}{dt}$$

A partir de este resultado, la ecuación de oscilación puede escribirse

$$\frac{d\omega(t)}{dt} = \frac{\omega_0}{2H} (P_m - P_{\max} \text{ sen } \delta) \quad (5.4)$$

Las ecuaciones diferenciales (5.3) y (5.4) serán la base para la solución numérica en los estudios de estabilidad transitoria. La primera, proporciona el cambio en el ángulo y la segunda, el cambio en la velocidad angular.

5.7 APLICACION DE LOS METODOS DE INTEGRACION NUMERICA A LOS ESTUDIOS DE ESTABILIDAD.

En la figura 5.7 se proporciona el diagrama de flujo correspondiente a un programa digital que permite simular un sistema "máquina-bus infinito" sujeto a condiciones de disturbio. El algoritmo utiliza el método modificado de Euler.

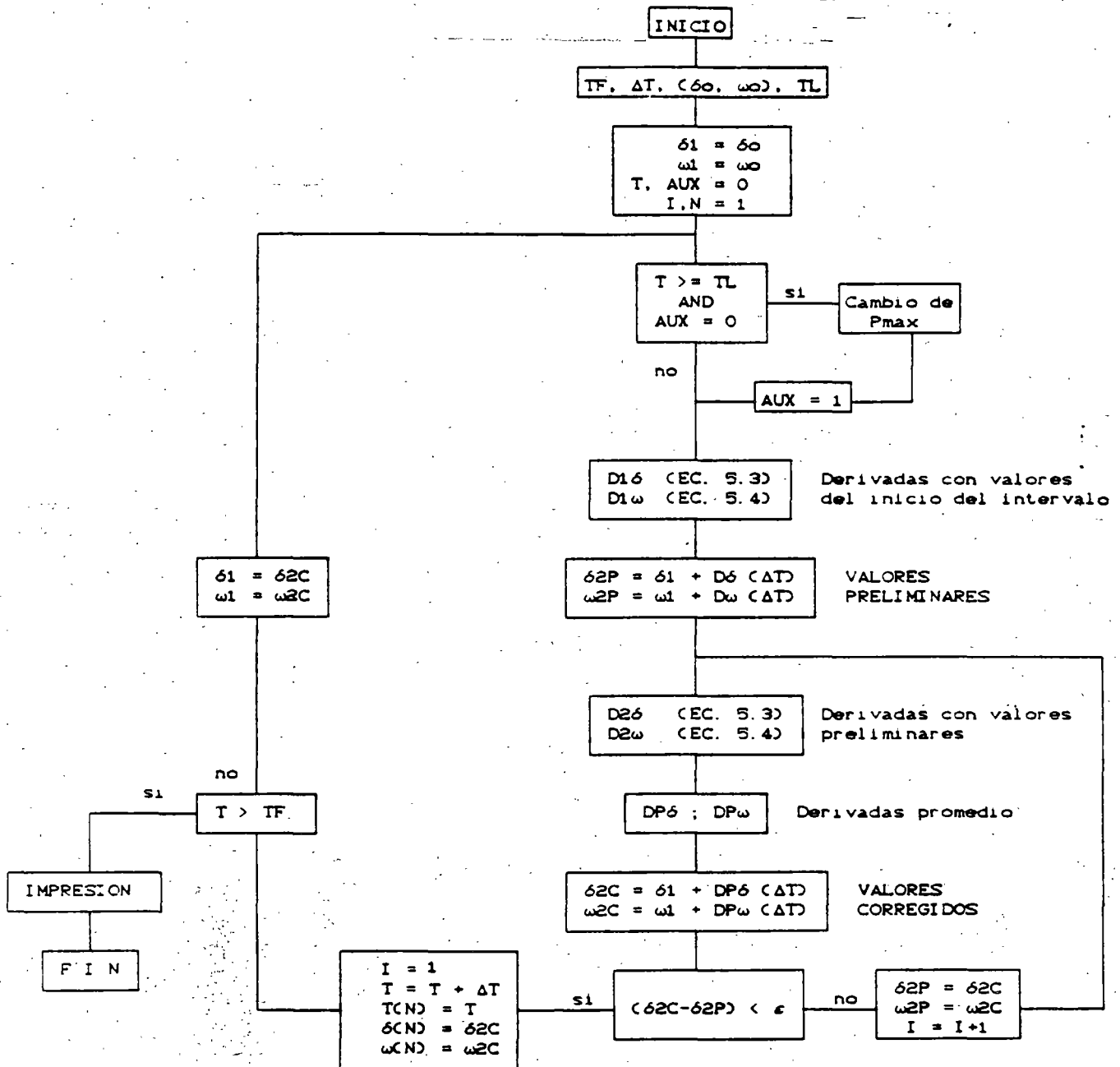


Figura 5.7
 Algoritmo para la simulación de un sistema
 máquina-bus infinito en condiciones de disturbio

Las variables de entrada son:

TF = Tiempo (final) del estudio
 ΔT = Tamaño del intervalo de integración
 (δ_0, ω_0) = Condiciones iniciales
 TL = Tiempo de liberación de la falla

y las de salida:

TCND = Tiempo asociado a cada intervalo
 δ (ND) = Angulo del rotor en cada intervalo
 ω (ND) = Velocidad angular del rotor en cada intervalo

Las etapas del proceso son: una evaluación inicial de las derivadas del ángulo y de la velocidad mediante las ecuaciones (5.3) y (5.4), utilizando los valores correspondientes al principio del intervalo; una estimación preliminar del ángulo y de la velocidad; un cálculo de las derivadas al final del intervalo, empleando los valores preliminares, y un cálculo modificado final aplicando el promedio de las derivadas. La variante en este último diagrama con respecto al de la figura 5.4 consiste en que ahora se incluye un lazo para efectuar las iteraciones que sean necesarias hasta que la diferencia entre el valor preliminar y el corregido esté dentro de la tolerancia deseada (ϵ).

Para realizar una simulación es necesario primeramente, efectuar el estudio del sistema en condiciones de prefalla como se hizo en el capítulo 3, para obtener los valores del ángulo y la velocidad antes del disturbio, es decir, las condiciones iniciales.

Durante el proceso numérico se parte de las condiciones iniciales y se empieza a trabajar con la ecuación de oscilación en condiciones de falla. Cuando el tiempo (T) alcanza o rebasa el tiempo de liberación de la falla (TL), el programa efectúa el cambio de Pmax para que a partir de ese instante se trabaje con la ecuación de oscilación de postfalla.

5.8 OBTENCION DE RESULTADOS Y ALGUNAS CONCLUSIONES GENERALES.

Los valores calculados durante la corrida del programa se imprimen al final de la misma en forma de tabla, usando tres columnas principales: tiempo, ángulo y velocidad angular del rotor. A partir de estos datos es posible obtener gráficas de velocidad contra tiempo o ángulo contra (tiempo como las mostradas al final de este capítulo) con el objeto de concluir si el sistema fué o no estable para el disturbio simulado.

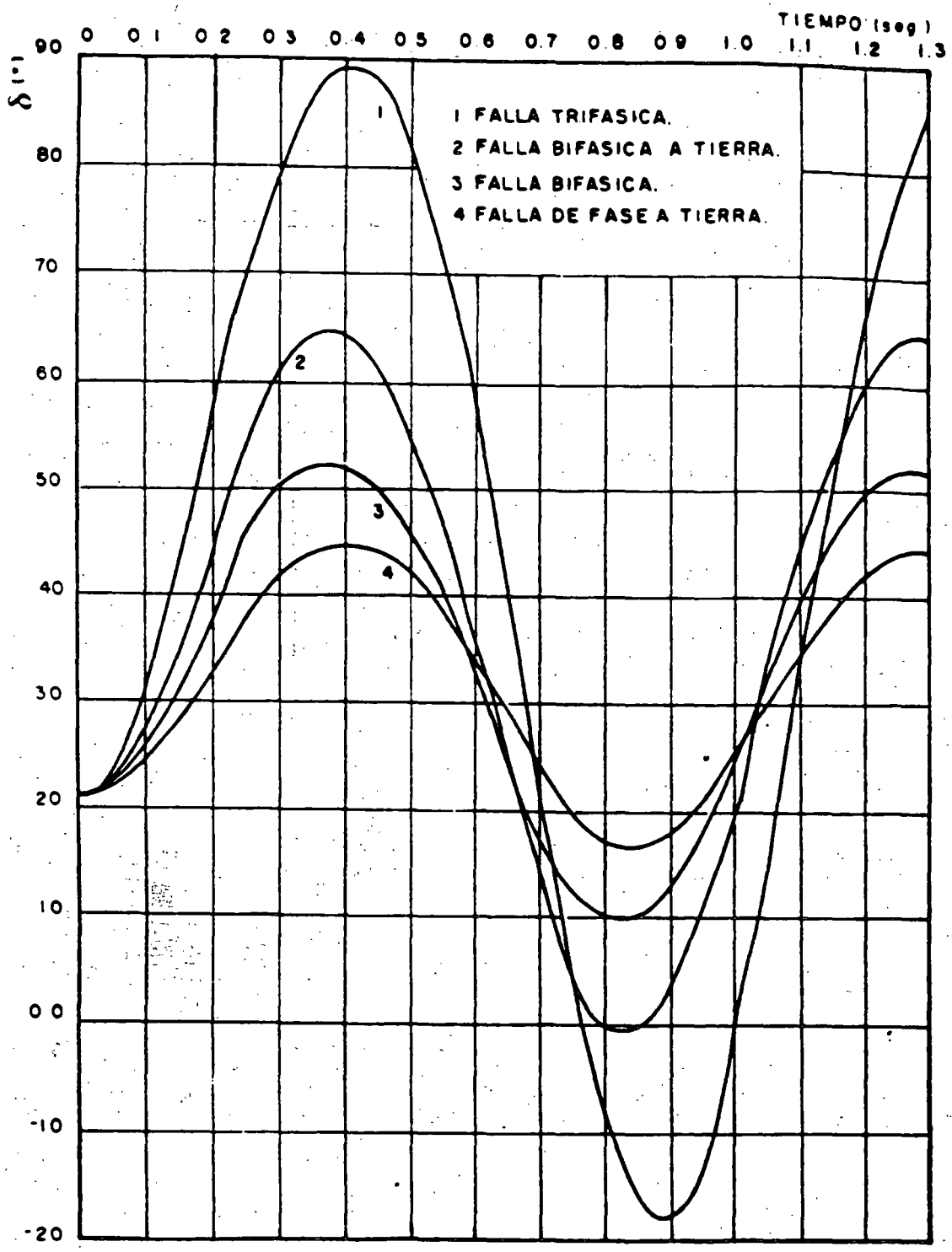
Las curvas ángulo-tiempo de las figuras 5.8 a 5.11 fueron obtenidas a partir de simulaciones mediante un programa digital como el descrito, aplicando diferentes disturbios al sistema "máquina-bus infinito" que se ha venido estudiando. Del comportamiento particular de este sistema es posible obtener algunas conclusiones de carácter general, las cuales son muy importantes:

- 1). La estabilidad de una máquina síncrona depende, entre otras cosas, de la severidad de la falla, siendo la de mayor impacto la falla trifásica y la de menor impacto la de fase a tierra (ver figura 5.8).
- 2). Las fallas tienen un mayor efecto sobre la estabilidad de las máquinas, entre más cercanas a éstas ocurran (figura 5.9).
- 3). La duración de la falla juega un papel de suma importancia en la estabilidad de un sistema (figura 5.10).
- 4). Las máquinas con menor inercia se ven más afectada por las perturbaciones (ver figura 5.11)

EFFECTO DEL TIPO DE FALLA

FRL = 0
TL = 0.19 s

Figura 5.8



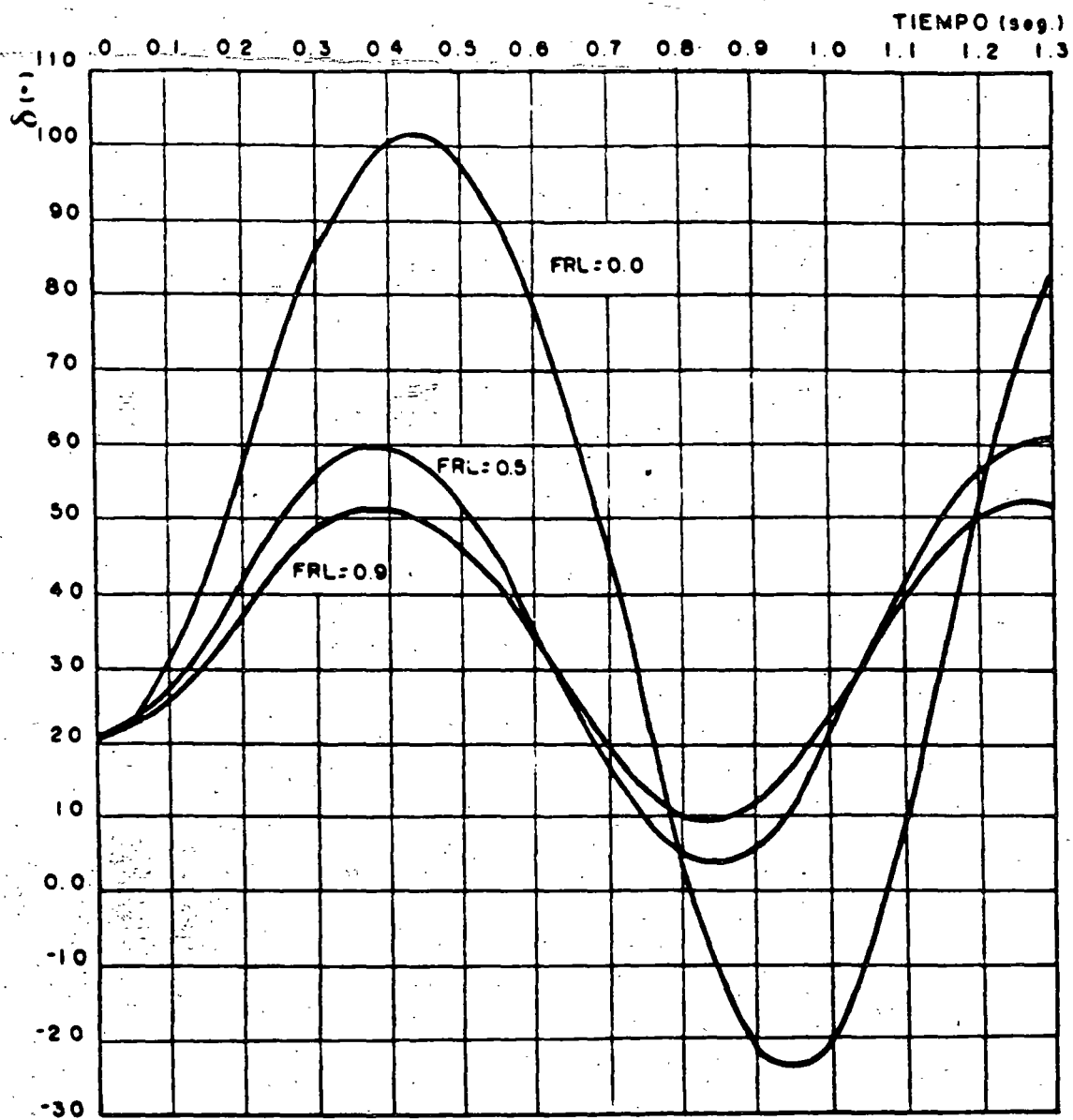
EFECTO DE LA LOCALIZACION DE LA FALLA

TL = 0.21 s

Falla 30

XF = 0

Figura 5.9



EFECTO DE LA DURACION DE LA FALLA

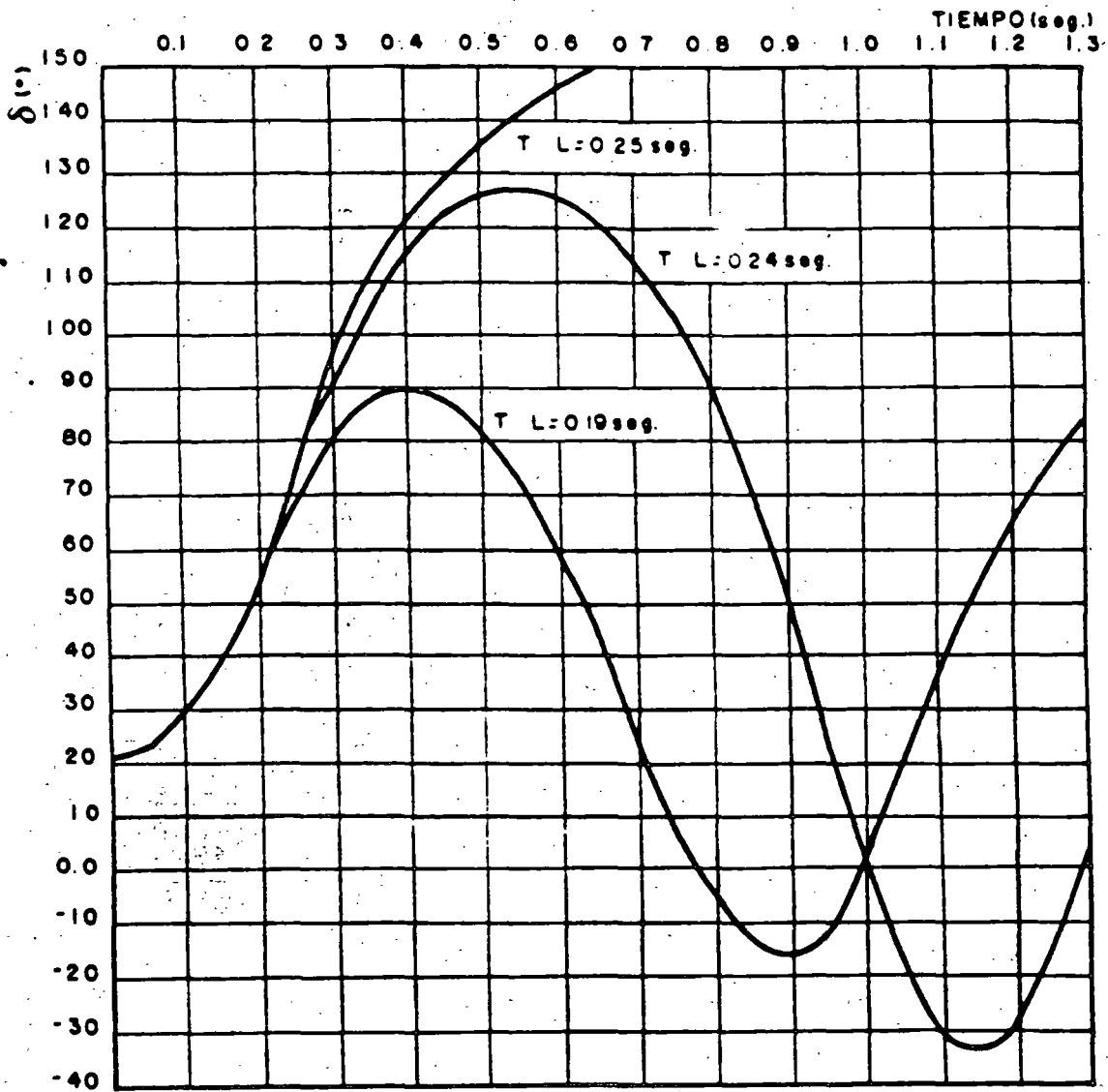
FRL = 0

Falla 3 ϕ

XF = 0

TCL = Tiempo crítico de liberación = 0.24 s

Figura 5.10



EFECTO DE LA INERCIA

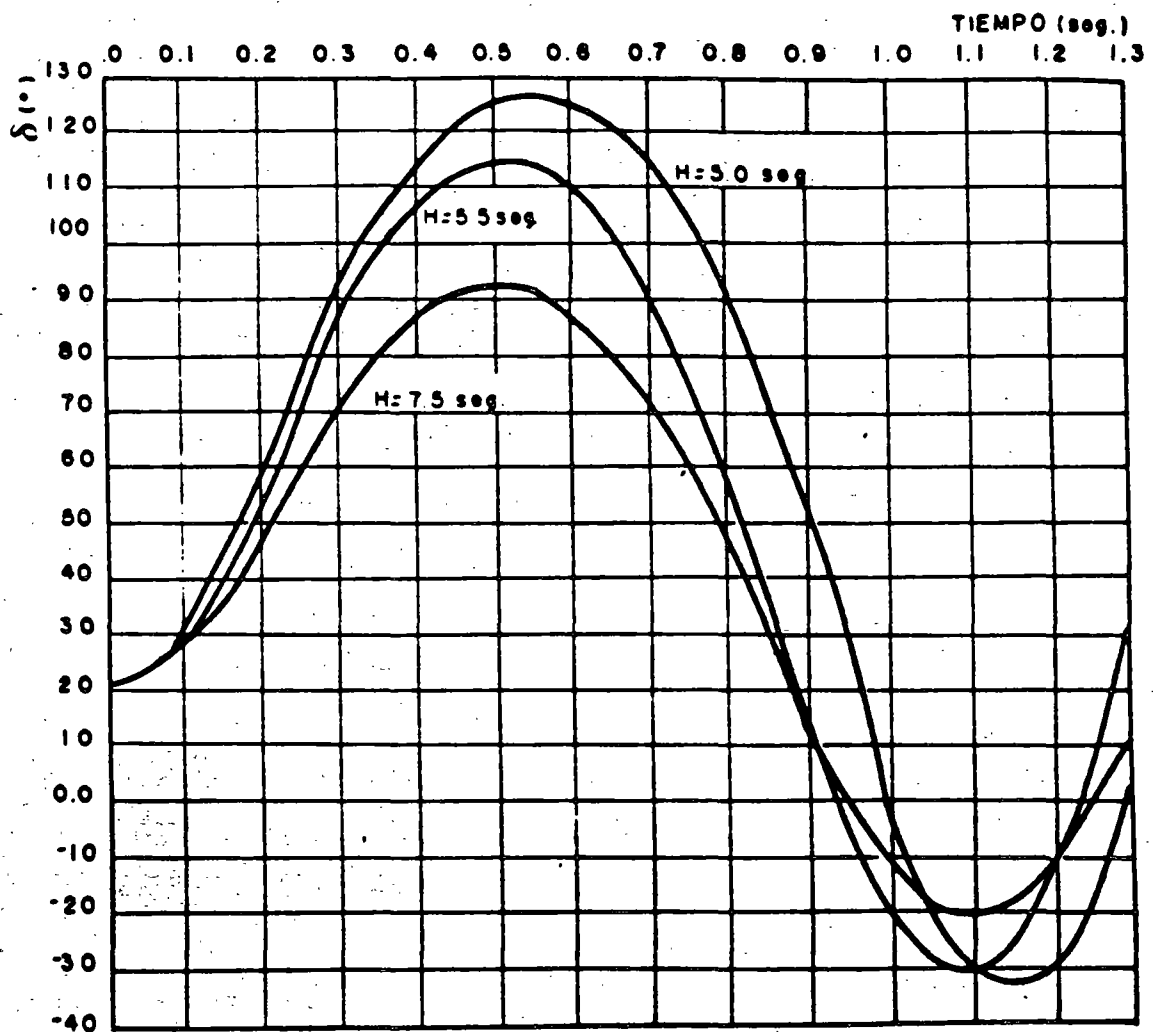
FRL = 0

TL = 0.24 s = TCL

Falla 30

XF = 0

Figura 5.11



6. MODELADO DE SISTEMAS MULTIMAQUINA

Las mismas consideraciones que se hacen para un sistema formado por una máquina y un bus infinito se consideran válidas para un sistema multimáquina.

o La potencia mecánica de entrada se puede considerar constante en el estudio.

o Se desprecia el amortiguamiento y los flujos asíncronos de potencia.

o Se puede usar el modelo más sencillo de la máquina síncrona el cual asume una fuente de voltaje constante atras de la reactancia transitoria.

o El ángulo mecánico del rotor coincide con el ángulo del voltaje atras de la reactancia transitoria.

o Las cargas se modelan por medio de impedancias constantes.

El modelo clásico que se describe es válido para el estudio de estabilidad transitoria conocido como estudio de primera oscilación.

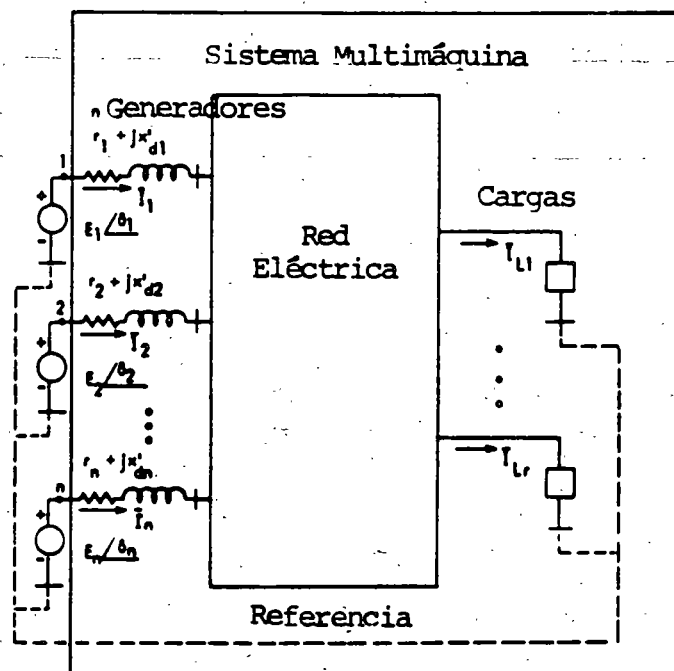
La segunda consideración describe que la característica de amortiguamiento es lineal y un par de amortiguamiento (o potencia D_w frecuentemente se adiciona al par Inercial (o a la potencia) en la ecuación de oscilación. El coeficiente de amortiguamiento D incluye varias componentes del par de amortiguamiento del tipo mecánico y eléctrico. Los valores típicos del par de amortiguamiento es de 1-3 pu. El cual representa el amortiguamiento de la Turbina, el amortiguamiento eléctrico del generador, y el efecto amortiguante de la carga.

La consideración 5 respecto a modelar la carga como una impedancia constante se hace para simplificar la representación del sistema y se usa en los estudios clásicos, pero cabe aclarar que esto no es una restricción.

La carga tiene dinámica propia que generalmente se desconoce su

comportamiento en función del voltaje y la frecuencia, que varía de una representación de Impedancia Constante a una característica de Potencia Constante modificando en forma apreciable la respuesta del sistema y la condición de estabilidad del Sistema.

La red eléctrica asociada a un sistema de n -generadores que se muestra en la figura en la cual se representa un sistema con un nodo de referencia que define el valor de los voltajes internos de las máquinas generadoras referido como el voltaje atras de la reactancia transitoria que se calcula a partir del resultado de un estudio de flujos de carga.



La magnitud del voltaje interno se mantiene en un valor constante en los estudios clásicos de estabilidad. En esta condición el sistema eléctrico se representa por red pasiva entre los n nodos con fuentes activas y la red se puede representar por medio de la matriz de admitancia nodal y se expresa en forma matricial.

$$I = YE$$

Recordando que la matriz de admitancia nodal se forma:

$$Y_{ii} = Y_{ii} \angle \theta_{ii} = G_{ii} + B_{ii}$$

$$Y_{ij} = Y_{ij} \angle \theta_{ij} = \text{Valor negativo de la admitancia de transferencia entre nodos } i \text{ y } j.$$

La inyección de potencia en el nodo i queda:

$$P_i = \operatorname{Re} \{ E_i I_i^* \}$$

Para la potencia eléctrica se tiene:

$$P_{ei} = E_i^2 G_{ii} + \sum E_i E_j Y_{ij} \cos(\theta_{ij} - \delta_i + \delta_j); \quad i = 1, \dots, n$$

La ecuación de oscilación se expresa como:

$$R \frac{2H_i}{\omega} \frac{d\omega_i}{dt} + D_i \omega_i = P_{mi} - [E_i^2 G_{ii} + \sum E_i E_j Y_{ij} \cos(\theta_{ij} - \delta_i + \delta_j)]$$

$$\frac{d\delta_i}{dt} = \omega_i - \omega_R$$

Hay que recordar que para la condición inicial la potencia eléctrica es igual a la potencia mecánica.

Las ecuaciones que describen el comportamiento dinámico es un conjunto de n ecuaciones diferenciales simultáneas de segundo orden que en forma compacta se expresan:

$$\dot{x} = f(x, x_0, t)$$

El vector x tiene una dimensión de $(2n \times 1)$

$$x^t = [\omega_1, \delta_1, \omega_2, \delta_2, \dots, \omega_n, \delta_n]$$

UTILIDAD DE ANALISIS DE ESTABILIDAD

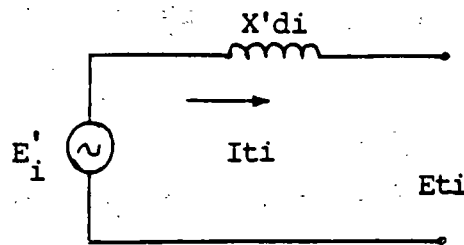
EN

SISTEMAS ELECTRICOS DE POTENCIAETAPA PLANEACION:

- A) DISEÑO DE LA RED.
- B) ESPECIFICACIÓN DE PARÁMETROS DE LOS GENERADORES: $x'd$,
 $x'q$, H , ETC.
- C) TIPOS DE SISTEMAS DE EXCITACIÓN.
- D) EQUIPOS DE CONTROL SUPLEMENTARIOS: VALVULEO RÁPIDO MOMEN
TÁNEO Y SOSTENIDO, INSERCIÓN DE CAPACITORES SERIE, FRENA
DO DINÁMICO, RECIERRE MONOPOLAR, ETC.
- E) COMPENSACIÓN DE POTENCIA REACTIVA: COMPENSADORES ESTÁTI-
COS DE VARS, CAPACITORES SERIE, ETC.

ETAPA OPERACIÓN:

- A) DEFINICIÓN DE LÍMITES DE GENERACIÓN-TRANSMISIÓN.
- B) IMPLANTACIÓN DE ESQUEMAS DE CONTROL SUPLEMENTARIOS (DISP.
AUTOMÁTICOS DE CARGA, GENERACIÓN, LÍNEA, ETC.).
- C) AJUSTES ESQUEMAS DE PROTECCIONES DE DISTANCIA.
- D) SEGREGACIÓN DEL SISTEMA ELÉCTRICO DE POTENCIA ANTE OSCILA
CIONES NO AMORTIGUADAS.
- E) DISEÑO DE ESQUEMAS DE CORTE DE CARGA POR BAJA FRECUENCIA.
- F) ANÁLISIS Y REPRODUCCIÓN DE DISTURBIOS.

EXPRESIONES MATEMÁTICAS DEL GENERADORSUBÍNDICE i = No. DE GENERADOR.

$$I_{ti} = \frac{P_{ti} - jQ_{ti}}{E_{ti}^*} ; E'_i = E_{ti} + jX'd_i I_{ti}$$

$$E'_i = e'_i + jf_i ; \delta_i = \text{tg}^{-1} \frac{f'_i}{e'_i}$$

$$P_{ei} = \text{Re} [I_{ti} E_i'^*] ;$$

$$\frac{d\delta_i}{dt} = W_i(t) - 2\pi f ; \frac{dW_i}{dt} = \frac{\pi f}{H_i} (P_{mi} - P_{ei}(t))$$

EXPRESIONES DEL MÉTODO MODIFICADO DE EULER

$$1. Y_1^o = Y_0 + \left. \frac{dy}{dt} \right|_0 \Delta T$$

$$2. \text{CON } Y_1^o \text{ EVALUAR } \left. \frac{dy}{dt} \right|_1 \text{ EN EL PUNTO FINAL DEL INTERVALO.}$$

$$3. Y_1^i = Y_0 + \left(\frac{\left. \frac{dy}{dt} \right|_0 + \left. \frac{dy}{dt} \right|_1}{2} \right) \Delta T$$

PLANTEAMIENTOS Y CUESTIONAMIENTOS SOBRE ESTUDIOS DE
ESTABILIDAD EN SISTEMAS MULTIMAQUINA

1. SOLUCIÓN AL CONJUNTO DE ECUACIONES ALGEBRAICAS NO LINEALES PARA OBTENER LAS CONDICIONES DE LOS VOLTAJES NODALES EN LAS REDES -- ELÉCTRICAS. "CORRIDAS DE FLUJOS".
2. INFORMACIÓN DE PARÁMETROS DE LOS TURBOGENERADORES Y DE EQUIPO - ASOCIADO; REACTANCIAS TRANSITORIAS, CONSTANTES DE INERCIA, SISTEMAS DE EXCITACIÓN, SISTEMA DE GOBERNACIÓN, PARÁMETROS DE TURBINAS, ETC.
3. SOLUCIÓN AL PROBLEMA DE ESTABILIDAD, RESOLVIENDO LAS ECUACIONES DIFERENCIALES QUE DEFINEN EL COMPORTAMIENTO DINÁMICO DE LOS TURBOGENERADORES Y CONTRALES (SISTEMAS DE EXCITACIÓN, GOBERNADORES, ETC.).
4. INTERPRETACIÓN DE LOS RESULTADOS Y EFECTOS FACTIBLES DE PREDECIR SOBRE LOS SISTEMAS ELÉCTRICOS DE POTENCIA.
 - A) ES ESTABLE UNA Ó UN GRUPO DE UNIDADES.
 - B) ALGUNA PIERDE SINCRONISMO.
 - C) TODAS PIERDEN SINCRONISMO.
 - D) CORTES DE CARGA POR BAJA FRECUENCIA.
 - E) CORTES DE CARGA POR BAJO VOLTAJE.
 - F) OSCILACIONES LENTAS EN EL SISTEMA.
 - G) ETCÉTERA.

SECUENCIA PARA SOLUCION DE LAS ECUACIONES DE OSCILACION
EN UN SISTEMA MULTIMAQUINA

M. EJLER MODIFICADO

1. CONDICIONES INICIALES. CORRIDA DE FLUJOS PARA DETERMINAR: $\delta_i(0)$, $-$
 $W_i(0)$, $E'_i(0)$, $I_{Ti}(0)$, $E_{Ti}(0)$, $P_{Ei}(0)$.

2. DETERMINACION DE $\delta_i^o(\Delta T)$ Y $W_i^o(\Delta T)$.

3. CON $\delta_i^o(\Delta T)$ CALCULAR LAS COMPONENTES DE $E_i^o(\Delta T)$.

4. CORRIDA DE FLUJOS CON $E_i^o(\Delta T)$ PARA DETERMINAR VOLTAJES NODALES EN ΔT .
 $E_{Ti}^o(\Delta T)$.

5. DETERMINAR $I_{Ti}^o(\Delta T)$ Y $P_{Ei}^o(\Delta T)$.

6. CORREGIR PARA DETERMINAR LOS VALORES FINALES (EN ΔT) DE $\delta_i^1(\Delta T)$,
 $W_i^1(\Delta T)$, $E_i^1(\Delta T)$.

7. CORRER FLUJOS CON $E_i^1(\Delta T)$ PARA ENCONTRAR VOLTAJES NODALES $E_{Ti}^1(\Delta T)$.

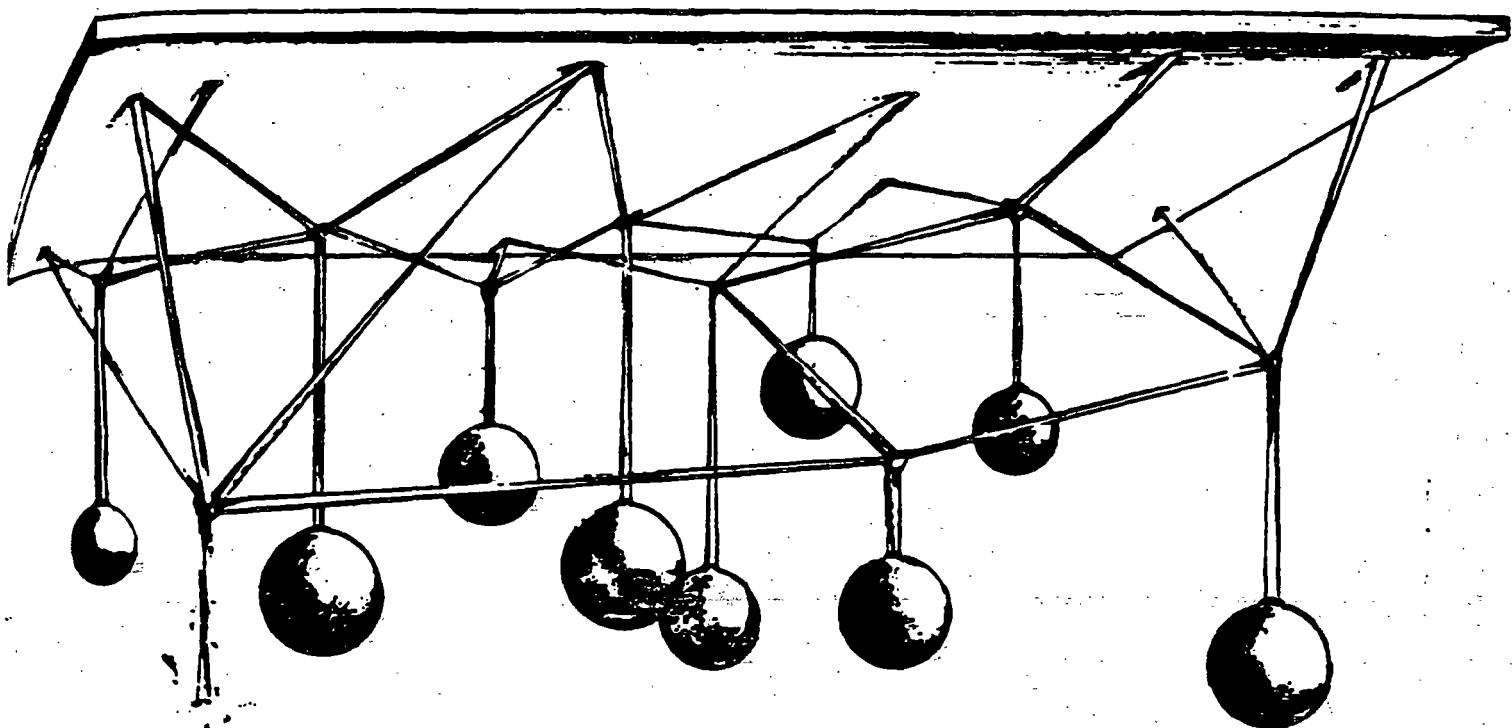
8. DETERMINAR $I_{Ti}^1(\Delta T)$, $P_{Ei}^1(\Delta T)$.

1A. PRIMERA ESTIMACION DE VARIABLES PARA EL PASO DE INTEGRACION AT.

2A. ESTIMACION FINAL DE VARIABLES PARA EL PASO DE INTEGRACION AT.

ANALOGÍA MECÁNICA PARA ILUSTRAR EL PROBLEMA DE ESTABILIDAD TRANSITORIA.

UN NÚMERO DE MASAS DE DIFERENTES PESOS REPRESENTAN A LOS GENERADORES. LAS BANDAS DE HULE (LIGAS) QUE FORMAN LA RED SEMEJAN A LAS LÍNEAS DE TRANSMISIÓN.



EL ANÁLISIS DE ESTABILIDAD TRANSITORIA CONSTARÍA DE LAS SIGUIENTES ETAPAS:

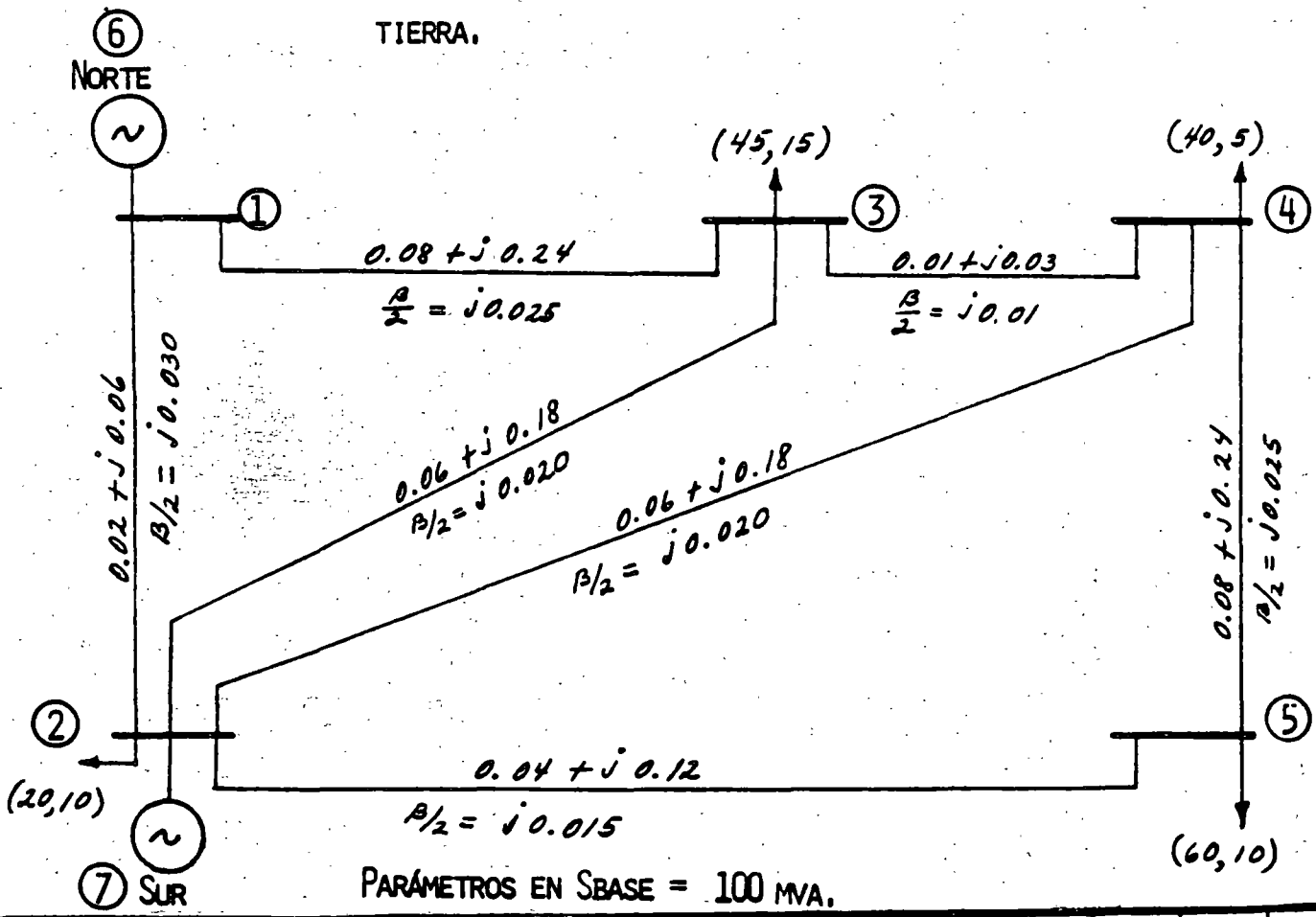
- DETERMINAR EL ESTADO ESTABLE DE PREFALLA.
- INICIAR LA FALLA.
- CALCULAR EL MOVIMIENTO TRANSITORIO DE LAS MASAS Y LAS FUERZAS RESULTANTES EN LAS LIGAS.
- SI LAS FUERZAS NO EXCEDEN LOS PUNTOS DE RUPTURA DE LAS LIGAS - EL SISTEMA SE JUZGARÍA COMO ESTABLE PARA LA FALLA QUE EN PARTICULAR SE LE APLICÓ.

EJEMPLO: ESTABILIDAD MULTIMÁQUINA.

UTILIZANDO EL MÉTODO MODIFICADO DE EULER PARA LA SOLUCIÓN DE LAS ECUACIONES DIFERENCIALES DE OSCILACIÓN, CALCULAR EL COMPORTAMIENTO DE LA VELOCIDAD $W(t)$ Y POSICIÓN ANGULAR $\delta(t)$ EN LAS MÁQUINAS DE LA SIGUIENTE RED, PARA UN TIEMPO $-\ - -$ $\Delta t = 0.02$ SEG.; SI EN $t = 0$ SEG. OCURRE UNA FALLA Φ (TRIFÁSICA) EN LA BARRA 2 DE 0.1 SEG. DE DURACIÓN.

PREMISAS:

- A) VOLTAJE CONSTANTE DETRÁS DE LA REACTANCIA TRANSITORIA.
- B) POTENCIA MECÁNICA CONSTANTE.
- C) LAS CARGAS SON REPRESENTADAS COMO ADMITANCIAS FIJAS A TIERRA.



EN LA TABLA I SE INDICAN LOS DATOS DE LOS GENERADORES EN PU, SOBRE UNA -
SBASE = 100 MVA.

TABLA I

GENERADOR	CONSTANTE DE INERCIA H (SEG.)	REACTANCIA TRANSITORIA EJE DIRECTO X'D
NORTE	50.0	0.25
SUR	1.0	1.50

DESARROLLO

I. A) $T = 0^-$

- CALCULAR CONDICIONES DE PREFALLA.

DE UNA CORRIDA DE FLUJOS ANTES DE LA OCURRENCIA DE LA FALLA SE OB
TUVIERON LOS VOLTAJES NODALES Y GENERACIONES QUE SE MUESTRAN EN -
LA TABLA II.

TABLA II

VOLTAJES NODALES DE PREFALLA

BARRA	VOLTAJE PU.	GENERACIÓN		CARGAS	
		MW	MVAR	MW	MVAR
1	1.060 + j0.0	129.56	-7.48	0.0	0.0
2	1.0462 - j0.05128	40.0	30.0	20.0	10.0
3	1.02032 - j0.0892	0.0	0.0	45.0	15.0
4	1.01917 - j0.09506	0.0	0.0	40.0	5.0
5	1.01209 - j0.10906	0.0	0.0	60.0	10.0

- CALCULAR LOS VOLTAJES ATRÁS DE LAS REACTANCIAS TRANSITORIAS:

PARA EL GENERADOR NORTE SE DESIGNARÁ COMO E'_6

PARA EL GENERADOR SUR SE DESIGNARÁ COMO E'_7

$$E'_i = E_{ti} + j X'_{di} I_{ti} \quad I_{ti} = \frac{P_{ti} - jQ_{ti}}{E'^*_{ti}}$$

GEN. NORTE

$$E'_6 = 1.06 + j0.0 + j0.25 \left(\frac{1.29565 + j0.07480}{1.06 - j0.0} \right)$$

$$E'_6 = 1.04236 + j0.30558 = 1.08623 \quad 16.34^\circ$$

$$\delta_6 = 16.34^\circ \quad \delta = 0.28517 \text{ rad.}$$

$$P_{m6} = 1.29565 \quad pu = P_{e6}$$

GEN. SUR

$$E'_7 = 1.0462 - j0.05128 + j1.5 \left(\frac{0.4 - j0.3}{1.0462 + j0.05128} \right)$$

$$E'_7 = 1.50335 + j0.49981 = 1.58426 \quad 18.39^\circ$$

$$\delta_7 = 18.39^\circ \quad \delta = 0.32097 \text{ rad.}$$

$$P_{m7} = 0.4 \text{ pu.} = P_{e7}$$

B) $T = 0^+$

EN EL INSTANTE DE OCURRIR LA FALLA Y DURANTE LA MISMA, EL VOLTAJE EN LA BARRA 2 ES IGUAL A CERO.

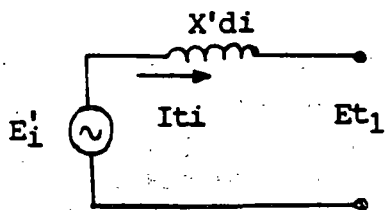
MANTENIENDO LOS VOLTAJES DETRÁS DE LAS REACTANCIAS TRANSITORIAS Y DE LA BARRA 2 FIJOS, SE EFECTÚA UNA CORRIDA DE FLUJOS PARA ENCON-

TRAR LOS VOLTAJES NODALES DE FALLA. EN LA TABLA III SE MUESTRAN LOS VOLTAJES RESULTANTES DE LA CORRIDA DE FLUJOS.

TABLA III
VOLTAJES EN EL INSTANTE DE LA FALLA

BARRA	VOLTAJES NODALES	
1	0.19234	+ j0.00330
2	0.0	+ j0.0
3	0.04707	- j0.00096
4	0.03758	- j0.00118
5	0.01226	- j0.00093
6	1.04236	+ j0.30558
7	1.50335	+ j0.49981

CORRIENTES EN LOS GENERADORES CON LA FALLA



$$I't_i = \frac{E'i - E_{t1}}{x'di}$$

GEN. NORTE $I_6 = \frac{1.04236 + j0.30558 - 0.19234 - j0.0033}{j0.25}$

$$I_6 = 1.20912 - j3.4008 \text{ pu}$$

$$\text{GEN. SUR} \quad I_7 = \frac{1.50335 + j0.49981 - 0.0 - j0.0}{j1.5}$$

$$I_7 = 0.33321 - j1.00223 \text{ pu.}$$

POTENCIA ELÉCTRICA DE LOS GENERADORES EN EL MOMENTO DE LA FALLA.

$$P_{e6} = \text{Re} [I_6 E_6'^*] = \text{Re} [(1.20912 - j3.4008) (1.04236 - j0.30558)]$$

$$P_{e6} = 0.22134 \text{ pu}$$

$$P_{e7} = \text{Re} [I_7 E_7'^*] = \text{Re} [(0.33321 - j1.00223) (1.50335 - j0.49981)]$$

$$P_{e7} = 0.0 \text{ pu}$$

II. A) $T = 0.02 \text{ SEG} = \Delta T$

DETERMINAR $W(T)$ Y $\delta(T)$ PARA LOS GENERADORES.

1RA. ESTIMACIÓN

$$W_i^o(\Delta T) = W_i'(0) + \left. \frac{dW_i}{dt} \right|_{(0)} \Delta T$$

$$\frac{dW_i}{dt} = \frac{\pi f}{H_i} (P_{mi} - P_{ei}(t)) ; \quad \frac{d\delta_i}{dt} = W_i(t) - 2\pi f$$

$$\text{GEN. NORTE} \quad \left. \frac{dW_6}{dt} \right|_{(0)} = \frac{(3.1416)(60)}{50} (1.29565 - 0.22134) = 4.05006$$

$$W_6^o(0.02) = 2(3.1416)(60) + 4.05006(0.02)$$

$$W_6^o(0.02) = 377.073$$

$$\left. \frac{d\delta_6}{dt} \right|_{(0)} = 2\pi f - 2\pi f = 0$$

$$\delta_6(0.02) = 0.28517 + 0 (0.02)$$

$$\delta_6(0.02) = 0.28517 \text{ rad.}$$

$$\text{GEN. SUR} \quad \left. \frac{dw_7}{dt} \right|_{(0)} = \frac{(3.1416) (60)}{1.0} (0.4000 - 0.0) = 75.398$$

$$w_7^{\circ}(0.02) = 2(3.1416) (60) + 75.398 (0.02)$$

$$w_7^{\circ}(0.02) = 378.499$$

$$\left. \frac{d\delta_7}{dt} \right|_{(0)} = 2\pi f - 2\pi f = 0$$

$$\delta_7^{\circ}(0.02) = 0.32097 + 0 (0.02)$$

$$\delta_7^{\circ}(0.02) = 0.32097 \text{ rad.}$$

- B) CON ESTOS ÁNGULOS DE LOS ROTORES DE LOS GENERADORES, QUE SON LOS ÁNGULOS DE FASE DE LOS VOLTAJES DETRÁS DE LAS REACTANCIAS TRANSITORIAS, Y DADO QUE LA MAGNITUD DE ESTOS VOLTAJES ES CONSTANTE, SE CALCULAN LAS COMPONENTES REAL E IMAGINARIA DE LOS VOLTAJES DETRÁS DE LAS REACTANCIAS TRANSITORIAS. EFECTUANDO ASIMISMO, UNA NUEVA CORRIDA DE FLUJOS PARA DETERMINAR LOS VOLTAJES NODALES.

DADO QUE LOS VOLTAJES INTERNOS DE LOS GENERADORES NO HAN SUFRIDO CAMBIO EN SUS ÁNGULOS DE FASE, LA SOLUCION DE LA CORRIDA DE FLUJOS ARROJARÁ -- LOS MISMOS VOLTAJES NODALES, CORRIENTES Y POTENCIAS ELÉCTRICAS EN LAS --

UNIDADES QUE LOS OBTENIDOS EN EL INSTANTE DE LA OCURRENCIA DE LA FALLA
(T_0^+).

LOS VALORES AL FINAL DEL INTERVALO $\Delta T = 0.02$ SEG. DE VELOCIDAD Y APERTU
RA ANGULAR DE LOS ROTORES SERÁN:

$$\text{GEN. NORTE } P_{E6}(T) = P_{E6}^{\circ}(0.02) = 0.22134 \text{ PU.}$$

$$W_6(T) = W_6'(0) = 376.992$$

$$\delta_6(T) = \delta_6'(0) = 0.28517$$

$$\left. \frac{dW_6}{dt} \right|_{(0)} = 4.05006$$

$$\left. \frac{d\delta_6}{dt} \right|_{(0)} = 0$$

$$W_6'(0.02) = W_6'(0) + \left(\frac{\left. \frac{dW_6}{dt} \right|_{(0)} + \left. \frac{dW_6}{dt} \right|_{(0.02)}}{2} \right) 0.02$$

$$\left. \frac{dW_6}{dt} \right|_{(0.02)} = \frac{\pi E}{H_6} (P_{M6} - P_{E6}^{\circ}(0.02))$$

$$\left. \frac{dW_6}{dt} \right|_{(0.02)} = \frac{(3.1416)(60)}{50} (1.29565 - 0.22134)$$

$$\left. \frac{dW_6}{dt} \right|_{(0.02)} = 4.05006$$

$$W_6'(0.02) = 376.992 + \left(\frac{4.05006 + 4.05006}{2} \right) 0.02$$

$$\underline{W_6'(0.02) = 377.073}$$

$$\delta_6'(0.02) = \delta_6'(0) + \left(\frac{\frac{d\delta_6}{dt} \Big|_0 + \frac{d\delta_6}{dt} \Big|(0.02)}{2} \right) 0.02$$

$$\frac{d\delta_6}{dt} \Big|_{(0.02)} = W_6'(0.02) - 2\pi F = 377.073 - 376.992$$

$$\frac{d\delta_6}{dt} \Big|_{(0.02)} = 0.08100$$

$$\delta_6'(0.02) = 0.28517 + \left(\frac{0 + 0.081}{2} \right) 0.02$$

$$\delta_6'(0.02) = 0.28598 \text{ RAD.} = 16.3854^\circ$$

GEN. SUR

$$PE_7(T) = PE_7^0(0.02) = 0.22134$$

$$W_7(T) = W_7'(0) = 376.992$$

$$\delta_7(T) = \delta_7'(0) = 0.32097$$

$$\frac{dW_7}{dt} \Big|_0 = 75.3984$$

$$\frac{d\delta_7}{dt} \Big|_0 = 0.0$$

$$W_7'(0.02) = W_7'(0) + \left(\frac{\frac{dW_7}{dt} \Big|_{(0)} + \frac{dW_7}{dt} \Big|_{(0.02)}}{2} \right) 0.02$$

$$\frac{dW_7}{dt} \Big|_{(0.02)} = \frac{\pi F}{H_7} (P_{M7} - P_{E7}^0(0.02))$$

$$\frac{dW_7}{dt} \Big|_{(0.02)} = \frac{(3.1416)(60)}{1} (0.400 - 0.0) = 75.398$$

$$W_7'(0.02) = 376.992 + \left(\frac{75.398 + 75.398}{2} \right) 0.02 = 378.4997$$

$$\delta_7'(0.02) = \delta_7'(0) + \left(\frac{\frac{d\delta_7}{dt} \Big|_{(0)} + \frac{d\delta_7}{dt} \Big|_{(0.02)}}{2} \right) 0.02$$

$$\frac{d\delta_7}{dt} \Big|_{(0.02)} = W_7'(0.02) - 2\pi F = 378.4997 - 376.992$$

$$\frac{d\delta_7}{dt} \Big|_{(0.02)} = 1.50797$$

$$\delta_7'(0.02) = 0.32097 + \left(\frac{0 + 1.50797}{2} \right) 0.02$$

$$\delta_7'(0.02) = 0.33605 \text{ RAD.} = 19.2592^\circ$$

LOS VOLTAJES INTERNOS DE LOS GENERADORES QUEDAN:

$$E_6' = 1.08523 \quad \underline{16.3854^\circ}$$

$$E_7' = 1.58426 \quad \underline{19.2542^\circ}$$

CON LOS NUEVOS ÁNGULOS DE LOS VOLTAJES E'_6 Y E'_7 Y CON EL VOLTAJE DE LA BARRA 2 IGUAL A CERO SE EFECTÚA UNA CORRIDA DE FLUJOS PARA OBTENER LOS -- NUEVOS VOLTAJES NODALES. EN LA TABLA IV SE INDICAN, ASÍ COMO LOS VOLTAJES INTERNOS DE LOS GENERADORES E'_6 Y E'_7 .

TABLA IV

VOLTAJES EN $AT = 0.02$ SEGUNDOS

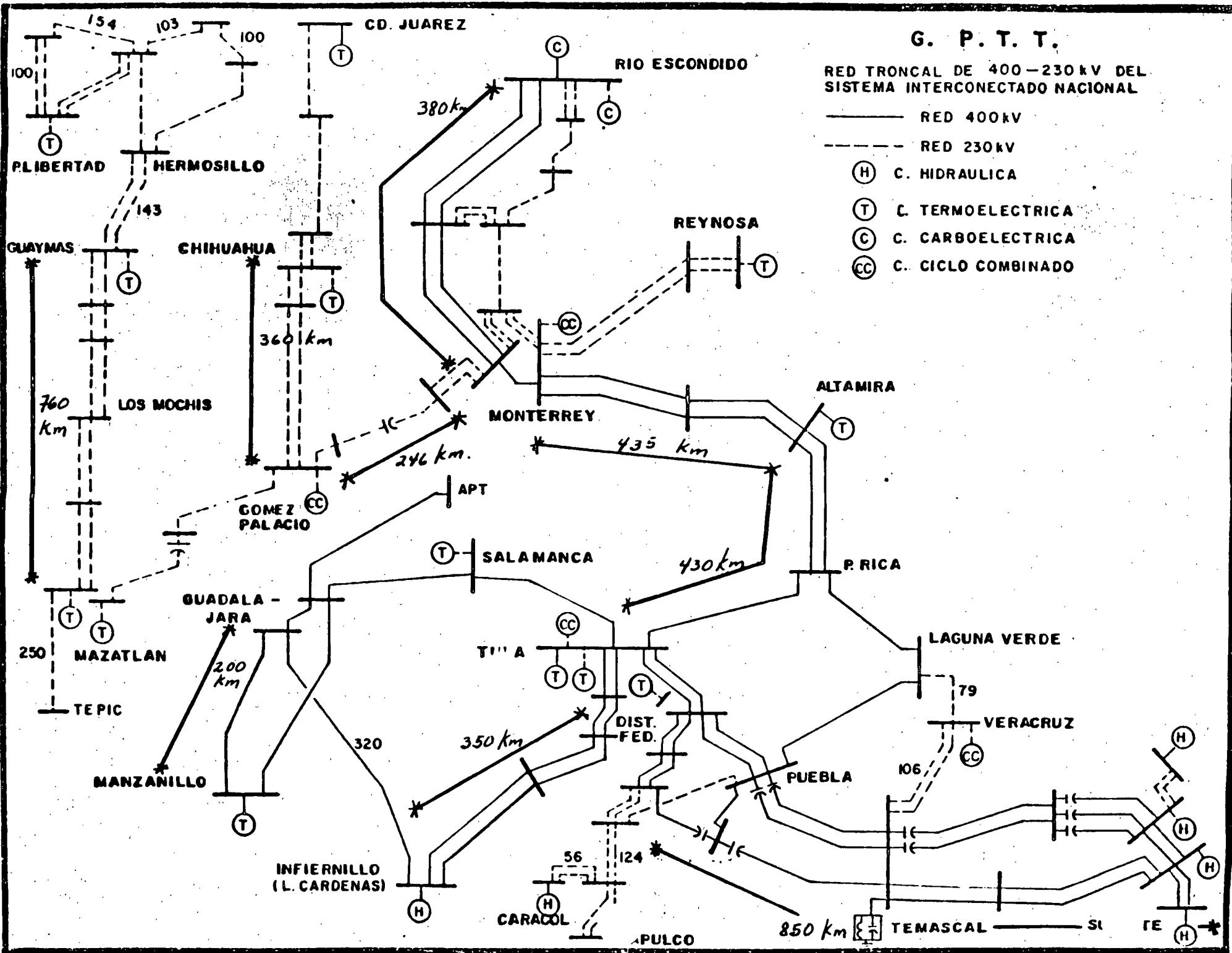
BARRA	VOLTAJES	PU
1	0.19258 +	J0.00353
2	0.0 +	J0.0
3	0.04815 -	J0.00114
4	0.03845 -	J0.00133
5	0.01249 -	J0.00097
6	1.042113 +	J0.30642
7	1.49564 +	J0.52242

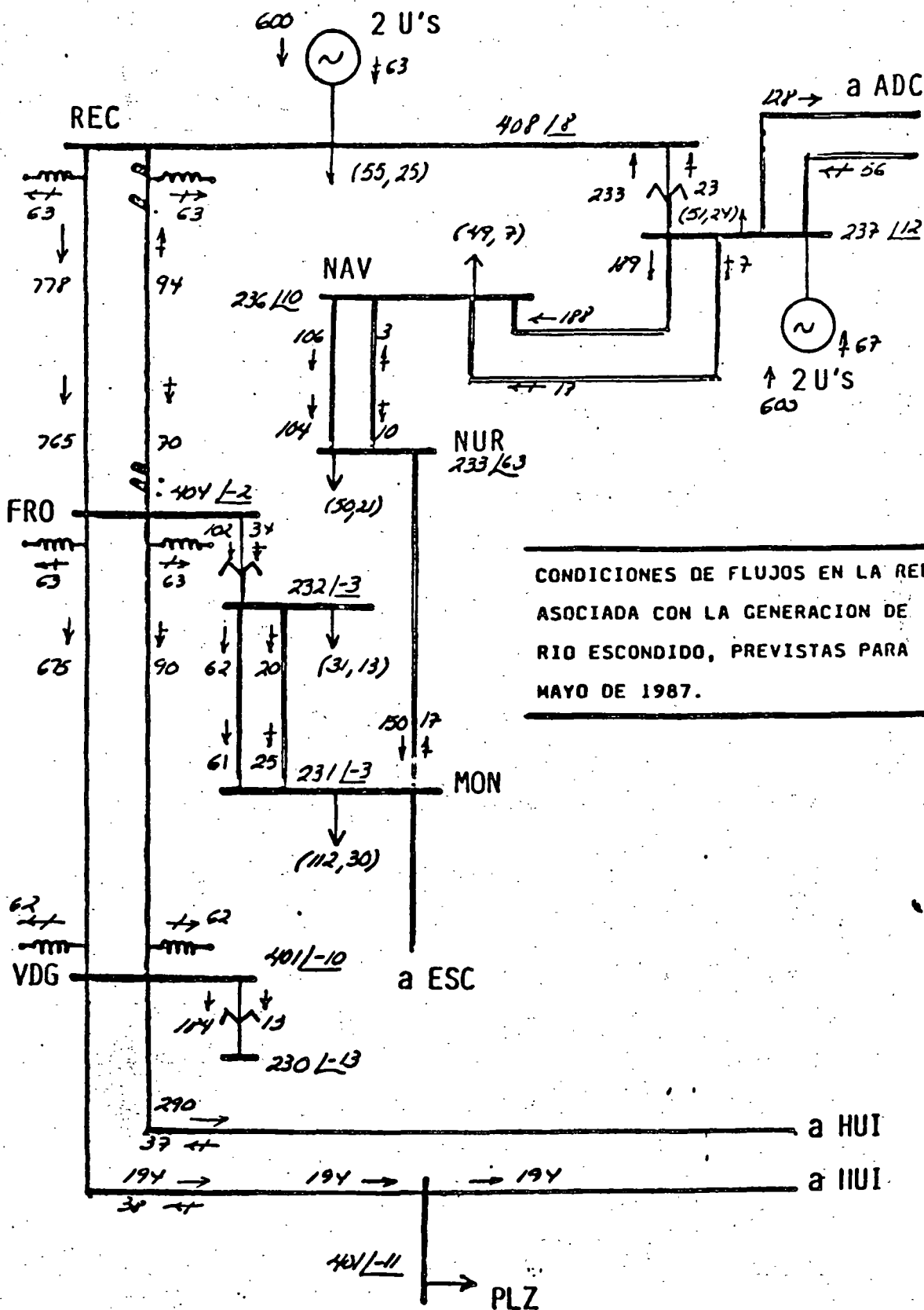
CON LOS VOLTAJES DE TABLA IV SE CALCULAN LAS POTENCIAS ELÉCTRICAS. ÉSTAS SE MUESTRAN EN LA TABLA V.

TABLA V

POTENCIAS ELÉCTRICAS EN $AT = 0.02$ SEGUNDOS

GENERADOR	POTENCIAS ELÉCTRICAS
NORTE (6)	0.22132
SUR (7)	0.0





CONDICIONES DE FLUJOS EN LA RED ASOCIADA CON LA GENERACION DE RIO ESCONDIDO, PREVISTAS PARA MAYO DE 1987.

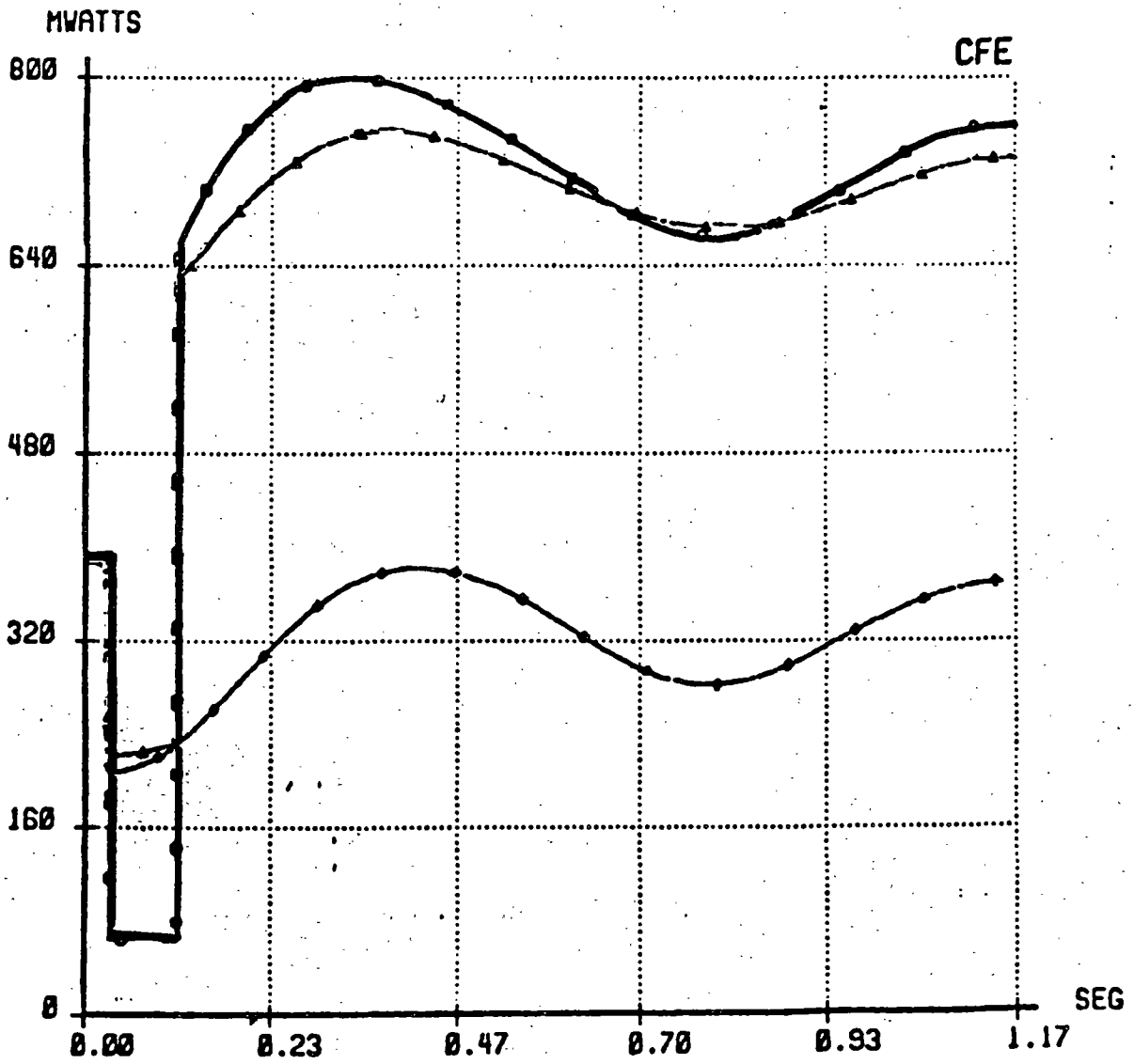
CFE CENACE
DID

RESULTADOS GRAFICOS
FLUJOS DE POTENCIA

SISP-ESTABI
22/OCT/86

* RED DEL SISTEMA INTERCONECTADO PARA 1987 EN DEMANDA MAXIMA. *
 * 1:FALLA 2F, 2:FALLA 3F (EN LT REC-FRO), 3:DISPARO DEL AT DE REC. *

—●— REC-400 -> REC-FRO FALLA 2 0
 —●— REC-C2 -> FRO-C2 FALLA 3 0
 —●— NUR-230 -> MON-230 APERTURA AT de REC



CFE CENACE
DID

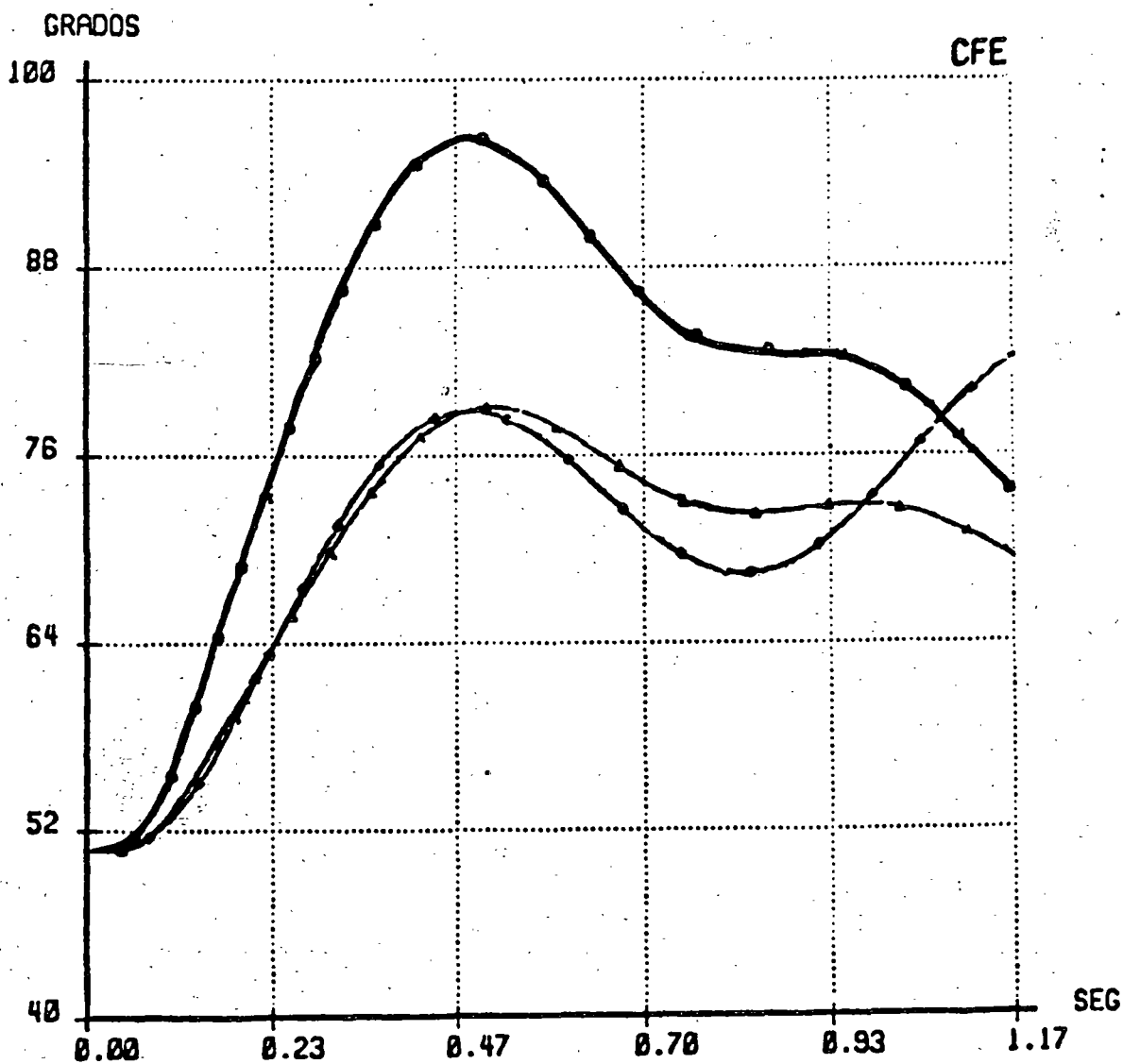
RESULTADOS GRAFICOS
DIFERENCIAS ANGULARES

SISP-ESTABI
22/OCT/86

• RED DEL SISTEMA INTERCONECTADO PARA 1987 EN DEMANDA MAXIMA. •
 • 1:FALLA 2F. 2:FALLA 3F (EN LT REC-FRO). 3:DISPARO DEL AT DE REC. •

MAQUINA DE REFERENCIA TUL-U4

—●—●—●—●—●—	REC-U1	FALLA 2 Ø
—●—●—●—●—●—	CASO2	FALLA 3 Ø
—●—●—●—●—●—	CASO3	APERTURA AT de REC



CFE-CENACE
DID

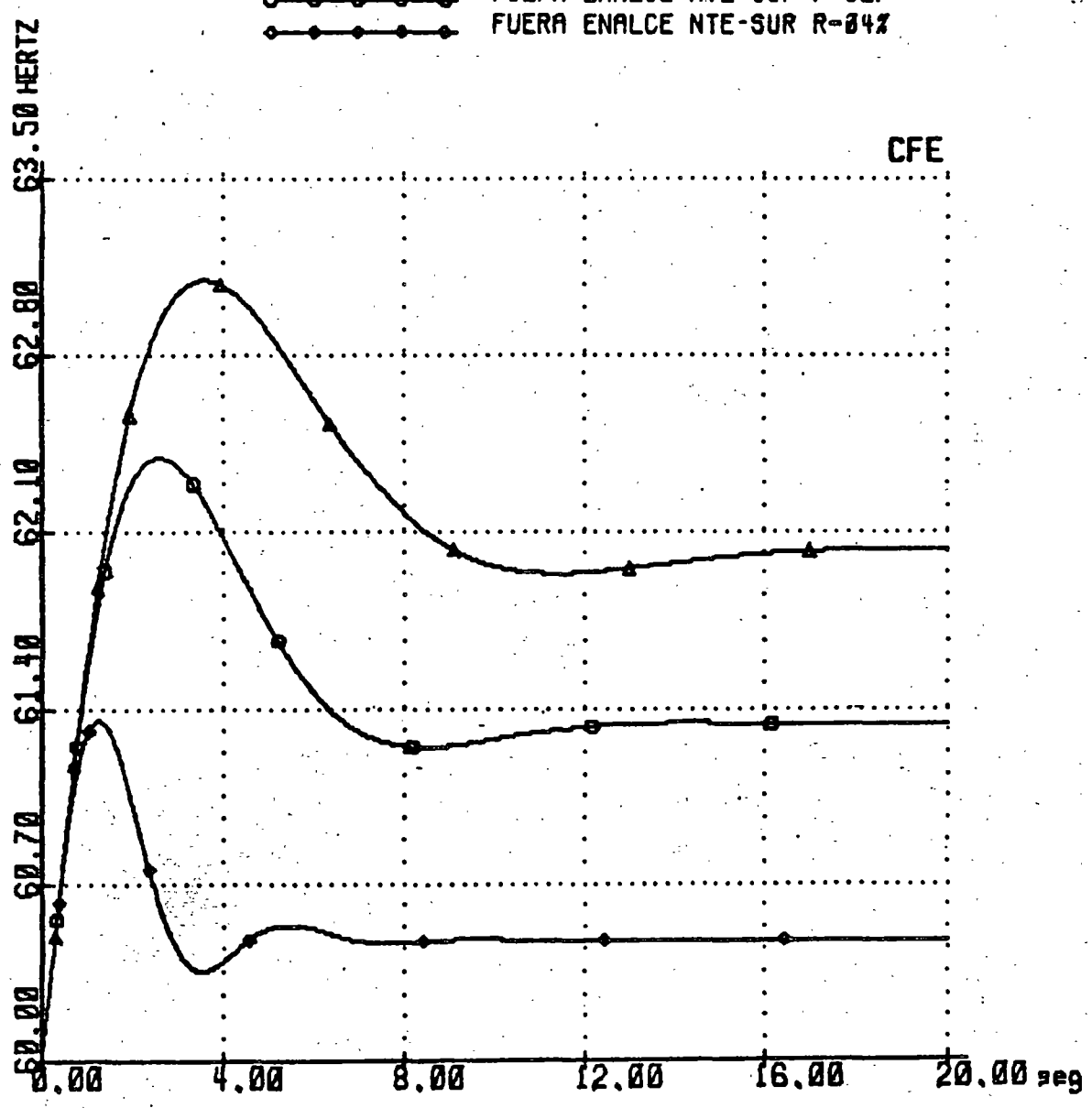
RESULTADOS GRAFICOS

SISP-CARFRE
04/NOV/86

13/15

SIMULACION DE LA SEPARACION DEL NYN Y SIS EL 861020 - 11:47 HRS
EXCEDENTE EN NYN 720 MW; DEFICIT SIS 880 MW.

- ▲-▲-▲-▲-▲ FUERA ENLACE NTE-SUR R=19%
- FUERA ENLACE NTE-SUR R=12%
- FUERA ENLACE NTE-SUR R=04%



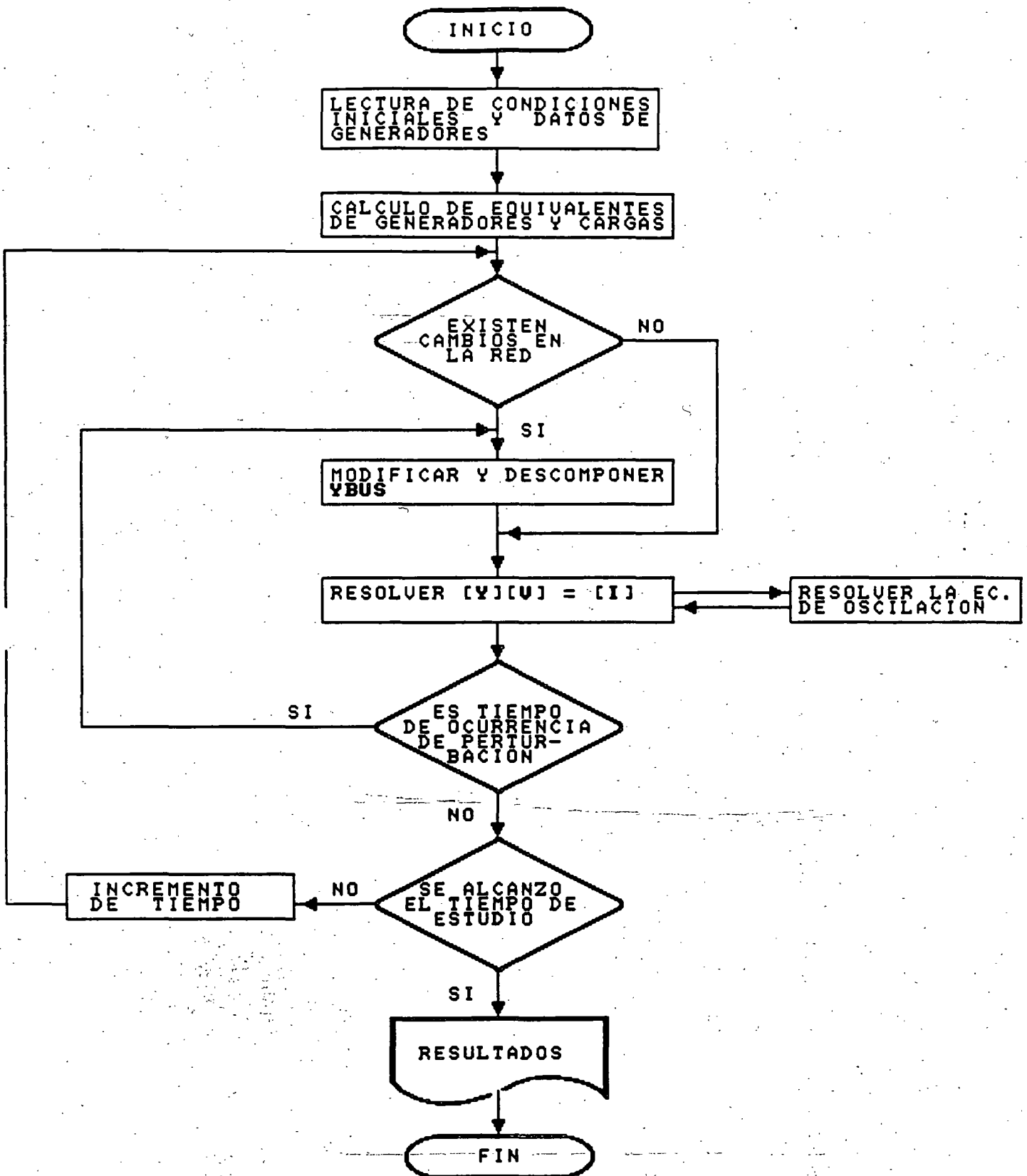


DIAGRAMA DE BLOQUES PARA LA SOLUCION DEL PROBLEMA DE ESTABILIDAD TRANSITORIA EN SISTEMAS MULTIMAQUINAS

ESTABILIDAD TRANSITORIA EN SISTEMAS MULTIMAQUINAS.

DESCRIPCION DEL DIAGRAMA DE BLOQUES.

Lectura de condiciones iniciales y datos de generadores. Del programa de flujos de potencia se extrae la información topológica y nodal necesaria para estudios de estabilidad transitoria. Se graban datos de líneas, Ybus, potencias nodales y de carga así como también voltajes nodales. Como información adicional para los generadores se dan los valores de reactancias, constantes de inercia y los tipos de máquina (polos lisos o polos salientes).

Cálculo de equivalentes de generadores y cargas. De acuerdo al tipo de máquina y al tipo de carga se obtienen sus equivalentes.

Cambios en la red. Cuando existen cambios en la red debidos a una perturbación, es necesario modificar la matriz Ybus, modificar de ser necesario las inyecciones de corriente nodal y resolver para voltajes nodales.

Solución de la ecuación de oscilación. Una vez resuelta para [V] la ecuación $[Y][V]=[I]$ se encuentran δ y ω para ese tiempo utilizando las ecuaciones respectivas de acuerdo al método de solución seleccionado, ajustandose al mismo tiempo el valor de δ con soluciones iterativas de la ecuación $[Y][V]=[I]$.

Simulación de la perturbación. Algunos de los tipos de perturbación que es conveniente tener implementados en los programas de explotación son:

- Fallas paralelo
- Fallas serie
- Salida de línea o transformador
- Salida de generador
- Operación de relevadores
- Recierres

ESTABILIDAD TRANSITORIA EN SISTEMAS MULTIMAQUINAS.

MODIFICACION DE [Y] DE ACUERDO AL TIPO DE FALLA.

a) Falla 3ϕ . Los elementos del renglón k se hacen cero, a excepción de la diagonal principal, el cual toma el valor de $1.0 \angle 0^\circ$ y la inyección de corriente nodal en caso de existir también se hace cero.

b) Falla $\phi - T$. Se modifica únicamente el elemento Y_{kk}

$$Y_{kk_n} = Y_{kk_a} + \frac{1}{Z_{-e_k} + Z_{0e_k}}$$

c) Falla $\phi\phi - T$. En el elemento Y_{kk}

$$Y_{kk_n} = Y_{kk_a} + \frac{\begin{bmatrix} Z_{-e_k} \\ \end{bmatrix} \begin{bmatrix} Z_{0e_k} \\ \end{bmatrix}}{Z_{-e_k} + Z_{0e_k}}$$

d) Falla $\phi - \phi$. En el elemento Y_{kk}

$$Y_{kk_n} = Y_{kk_a} + \frac{1}{Z_{-e_k}}$$

e) ϕ abierta entre los nodos k y l . Se modifica Y_{kk} , Y_{ll} , Y_{kl} y Y_{lk} intercalando en serie la suma del paralelo de las impedancias equivalentes de secuencia positiva y secuencia cero en el nodo donde se simula la apertura.

f) $\phi\phi$ abiertas entre los nodos k y l . Se modifica Y_{kk} , Y_{ll} , Y_{kl} y Y_{lk} . Se conecta en serie en el punto de apertura la suma de las impedancias equivalentes de secuencia positiva y secuencia cero.

ESTABILIDAD TRANSITORIA EN SISTEMAS MULTIMAQUINAS.

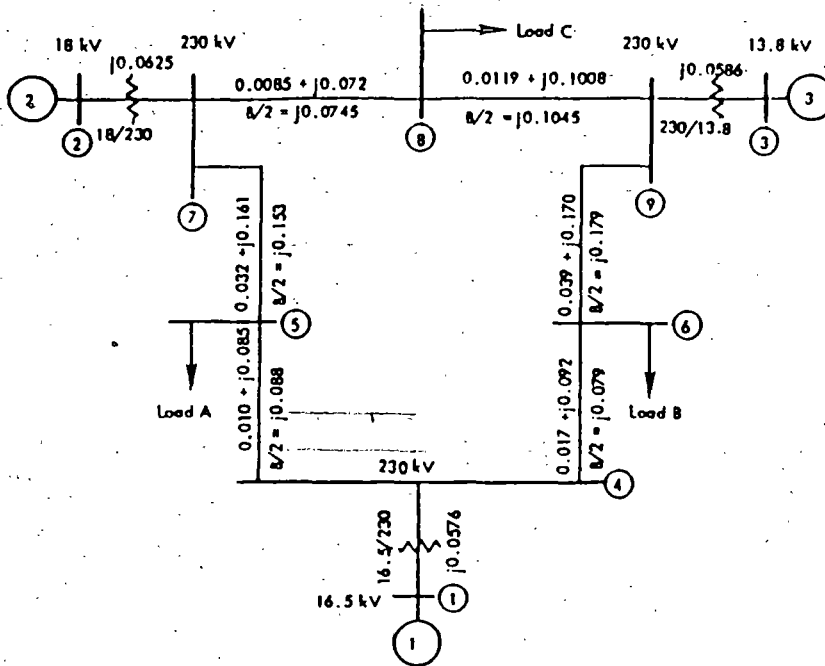
MODIFICACION DE [Y] CON OTRAS PERTURBACIONES.

- g) Salida de línea ó transformador. Es clara la afectación en los elementos mutuos y propios de los nodos en cuestión.
- h) Salida de generador. Se hace cero la inyección de corriente en el nodo correspondiente, y se elimina la admitancia propia de acuerdo al modelo utilizado.
- i) Modificación en la carga. Se modifica el elemento propio de acuerdo al modelo considerado.

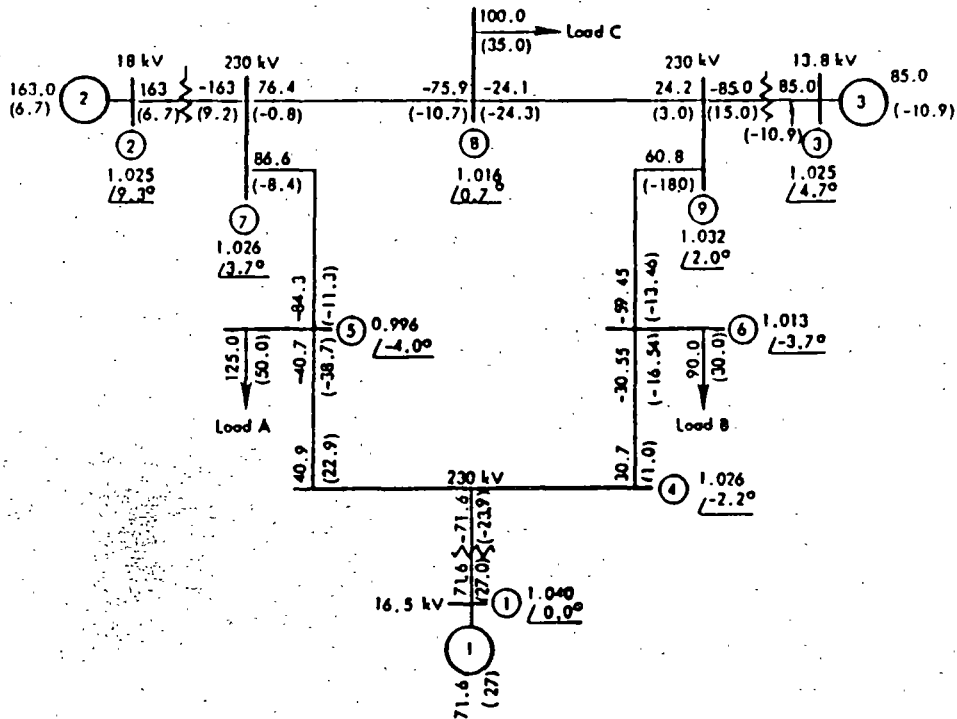
Nota:

- Y_{kk_n} Y_{kk_a} - Admitancias propia en el nodo k , nueva y anterior respectivamente.
- Z_{-e_k} - Impedancia de secuencia negativa equivalente en el nodo k .
- Z_{0e_k} - Impedancia de secuencia cero equivalente en el nodo k .

Chapter 2



Nine-bus system impedance diagram: all impedances are in pu on a 100-MVA base.



Nine-bus system load-flow diagram showing prefault conditions; all flows are in MW and MVAR.

Table 2.1. Generator Data

Generator	1	2	3
Rated MVA	247.5	192.0	128.0
kV	16.5	18.0	13.8
Power factor	1.0	0.85	0.85
Type	hydro	steam	steam
Speed	180 r/min	3600 r/min	3600 r/min
x_d	0.1460	0.8958	1.3125
x_d'	0.0608	0.1198	0.1813
x_q	0.0969	0.8645	1.2578
x_q'	0.0969	0.1969	0.25
x_l (leakage)	0.0336	0.0521	0.0742
r_{do}	8.96	6.00	5.89
r_{po}	0	0.535	0.600
Stored energy at rated speed	2364 MW·s	640 MW·s	301 MW·s

Note: Reactance values are in pu on a 100-MVA base. All time constants are in s. (Several quantities are tabulated that are as yet undefined in this book. These quantities are derived and justified in Chapter 4 but are given here to provide complete data for the sample system.)

***** SISTEMA DE PRUEBA 9 NODOS ANDERSON *****
 ***** JLHG 071091 *****

OMH

FIN

GEN1	00.00	00.00	11	0
2	00.00	00.00	11	0
GEN3	00.00	00.00	11	0
CUATRO	00.00	00.00	11	0
CINCO	125.00	50.00	11	0
SEIS	90.00	30.00	11	0
SIETE	00.00	00.00	11	0
OCHO	100.00	35.00	11	0
NUEVE	00.00	00.00	11	0

FIN

GEN1	CUATRO	300.00	100.00	-100.00	1.04000
GEN2	SIETE	163.00	50.00	-50.00	1.02500
GEN3	NUEVE	85.00	50.00	-50.00	1.02500

FIN

CUATRO	GEN1	0.00000	0.05760	0.00000	1.00000
SIETE	GEN2	0.00000	0.06250	0.00000	1.00000
NUEVE	GEN3	0.00000	0.05860	0.00000	1.00000
CUATRO	CINCO	0.01000	0.08500	0.08800	
CUATRO	SEIS	0.01700	0.09200	0.07900	
CINCO	SIETE	0.03200	0.16100	0.15300	
SEIS	NUEVE	0.03900	0.17000	0.17900	
SIETE	OCHO	0.00850	0.07200	0.07450	
OCHO	NUEVE	0.01190	0.10080	0.10450	

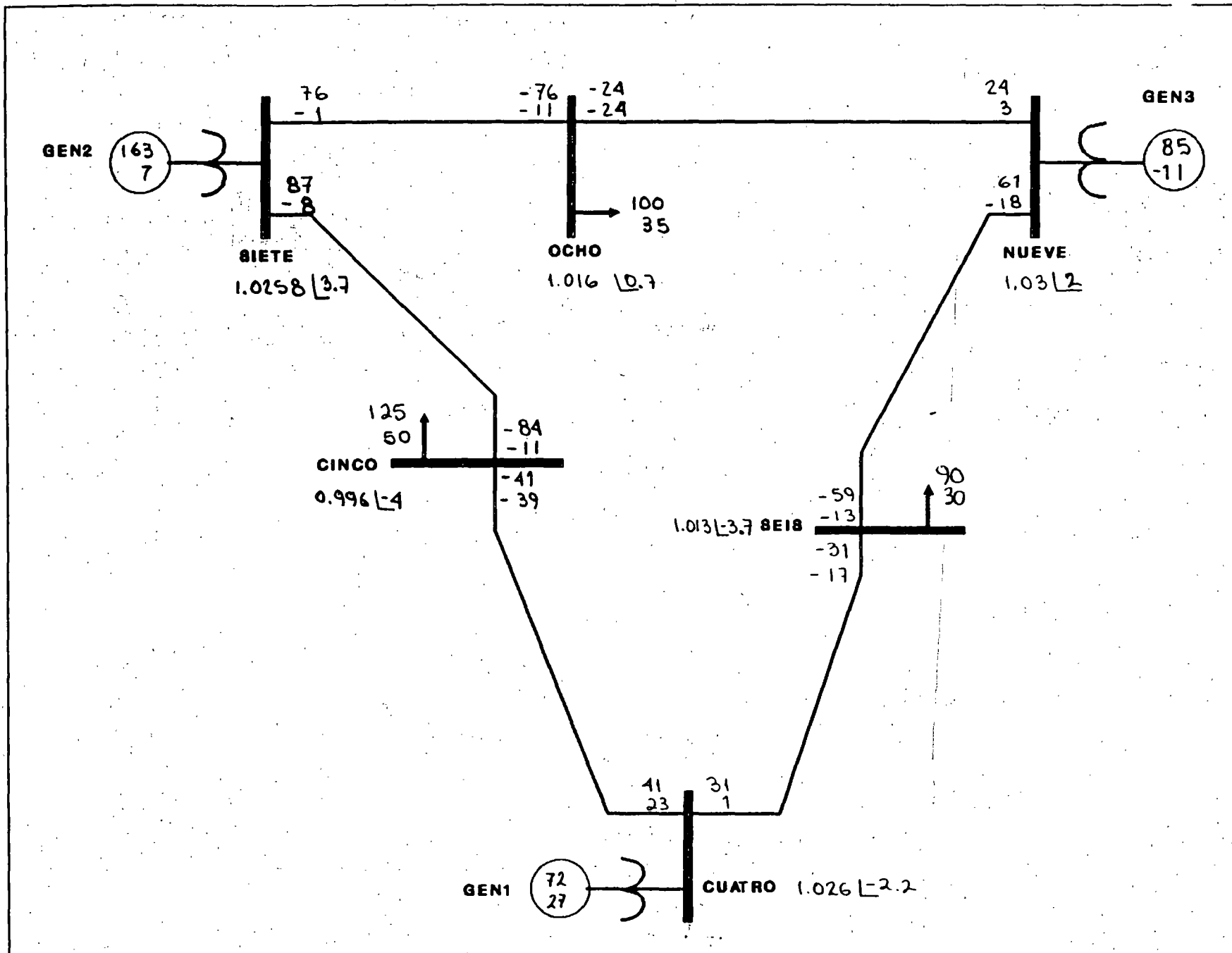
FIN

FIN

OK 20:49:03 0.306 0.115

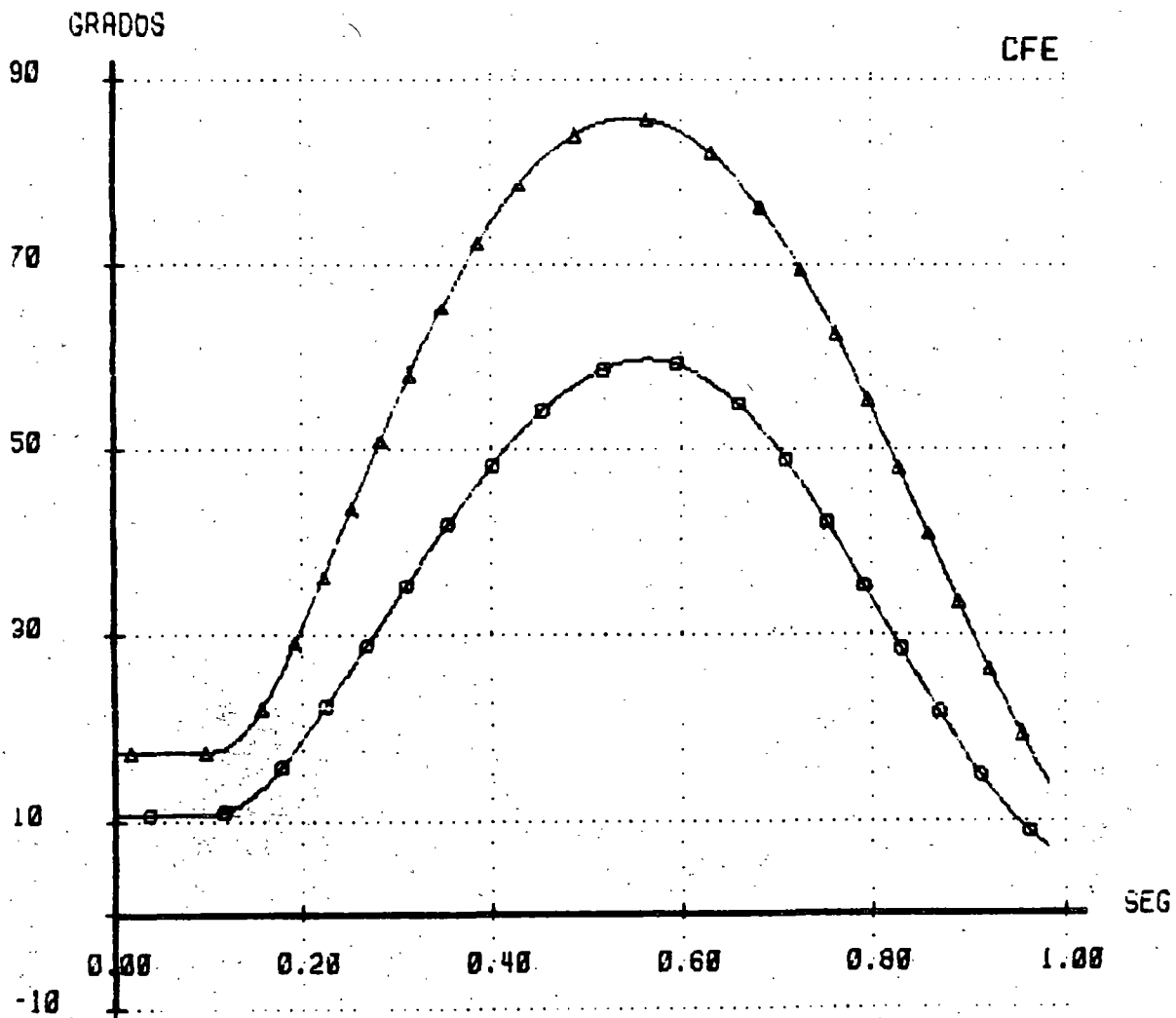
***** SISTEMA DE PRUEBA 9 NODOS ANDERSON *****
 ***** JLHG 071091 *****

DE	1 GEN1	MW	MVAR	MVA	TAP	1.04000	0.00	1
GENERADOR		71.7	27.1R	76.6				
A	4 CUATRO	71.7	27.1	76.6	0.0000	TR		
DE	2 GEN2	MW	MVAR	MVA	TAP	1.02500	9.28	2
GENERADOR		163.0	6.7R	163.1				
A	7 SIETE	163.0	6.7	163.1	0.0000	TR		
DE	3 GEN3	MW	MVAR	MVA	TAP	1.02500	4.66	3
GENERADOR		85.0	-10.8R	85.7				
A	9 NUEVE	85.0	-10.8	85.7	0.0000	TR		
DE	4 CUATRO	MW	MVAR	MVA	TAP	1.02578	-2.22	4
A	1 GEN1	-71.7	-23.9	75.6	1.0000	TR		
A	5 CINCO	40.9	22.9	46.9	0.0000			
A	6 SEIS	30.7	1.0	30.7	0.0000			
DE	5 CINCO	MW	MVAR	MVA	TAP	0.99561	-3.99	5
A	CARGA	125.0	50.0	134.6				
A	4 CUATRO	-40.7	-38.7	56.1	0.0000			
A	7 SIETE	-84.3	-11.3	85.1	0.0000			
DE	6 SEIS	MW	MVAR	MVA	TAP	1.01263	-3.69	6
A	CARGA	90.0	30.0	94.9				
A	4 CUATRO	-30.5	-16.6	34.7	0.0000			
A	9 NUEVE	-59.5	-13.5	61.0	0.0000			
DE	7 SIETE	MW	MVAR	MVA	TAP	1.02576	3.72	7
A	2 GEN2	-163.0	9.2	163.3	1.0000	TR		
A	5 CINCO	86.6	-8.4	87.0	0.0000			
A	8 OCHO	76.4	-0.8	76.4	0.0000			
DE	8 OCHO	MW	MVAR	MVA	TAP	1.01587	0.73	8
A	CARGA	100.0	35.0	105.9				
A	7 SIETE	-75.9	-10.7	76.7	0.0000			
A	9 NUEVE	-24.1	-24.3	34.2	0.0000			
DE	9 NUEVE	MW	MVAR	MVA	TAP	1.03234	1.97	9
A	3 GEN3	-85.0	14.9	86.3	1.0000	TR		
A	6 SEIS	60.8	-18.1	63.4	0.0000			
A	8 OCHO	24.2	3.1	24.4	0.0000			



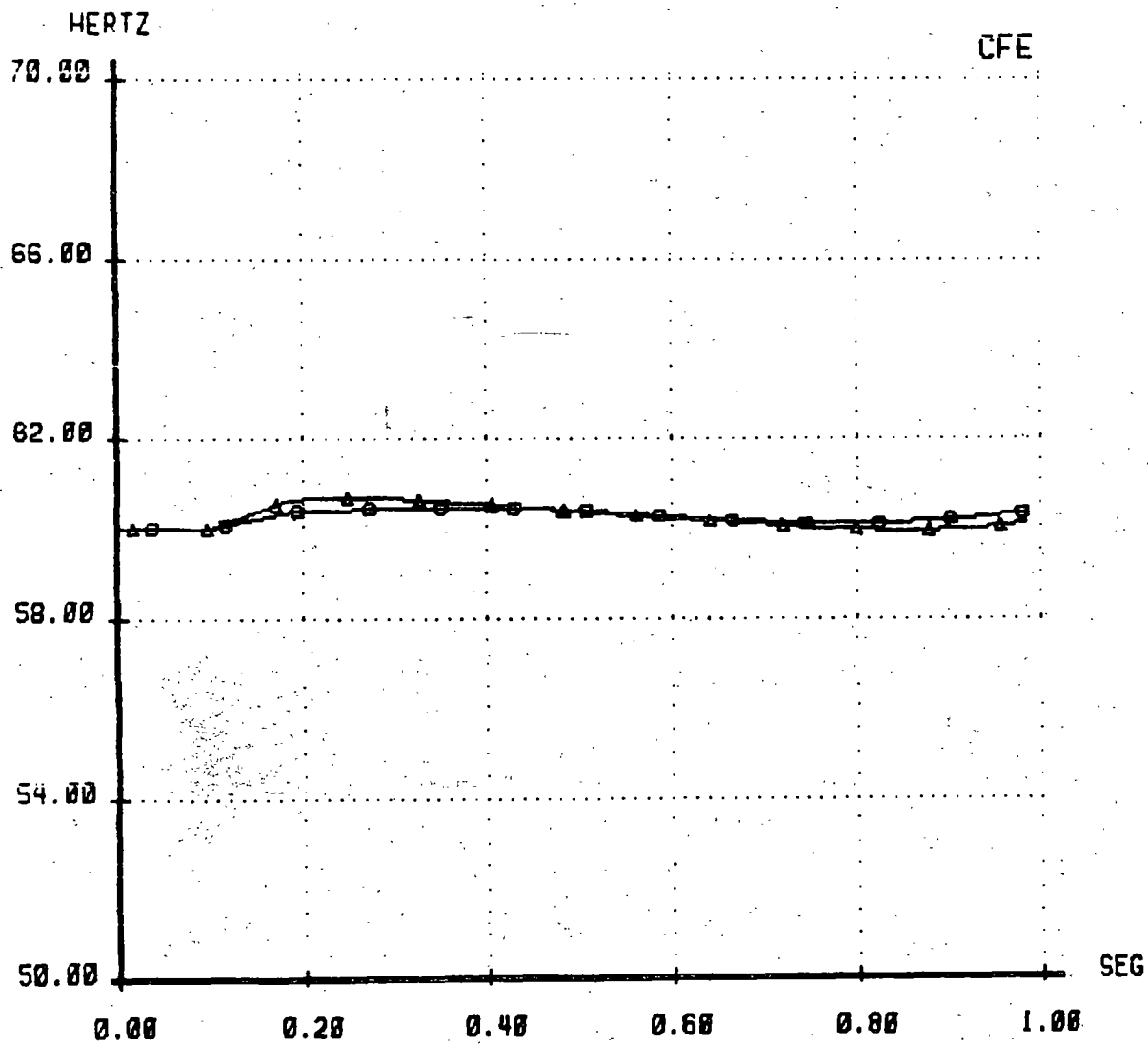
SISTEMA DE PRUEBA DE NUEVE NODOS (ANDERSON). FALLA TRIFASICA EN EL NO
SIETE A LOS 6 CICLOS. SE LIBERA CON LA APERTURA DE CINCO-SIETE EN 11 C
+--- MAQUINA DE REFERENCIA ---+ [GEN1]

---▲--- GEN2
---□--- GEN3

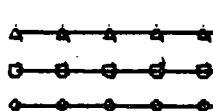


SISTEMA DE PRUEBA DE NUEVE NODOS (ANDERSON). FALLA TRIFASICA EN EL NO
SIETE A LOS 6 CICLOS. SE LIBERA CON LA APERTURA DE CINCO-SIETE EN 11 C

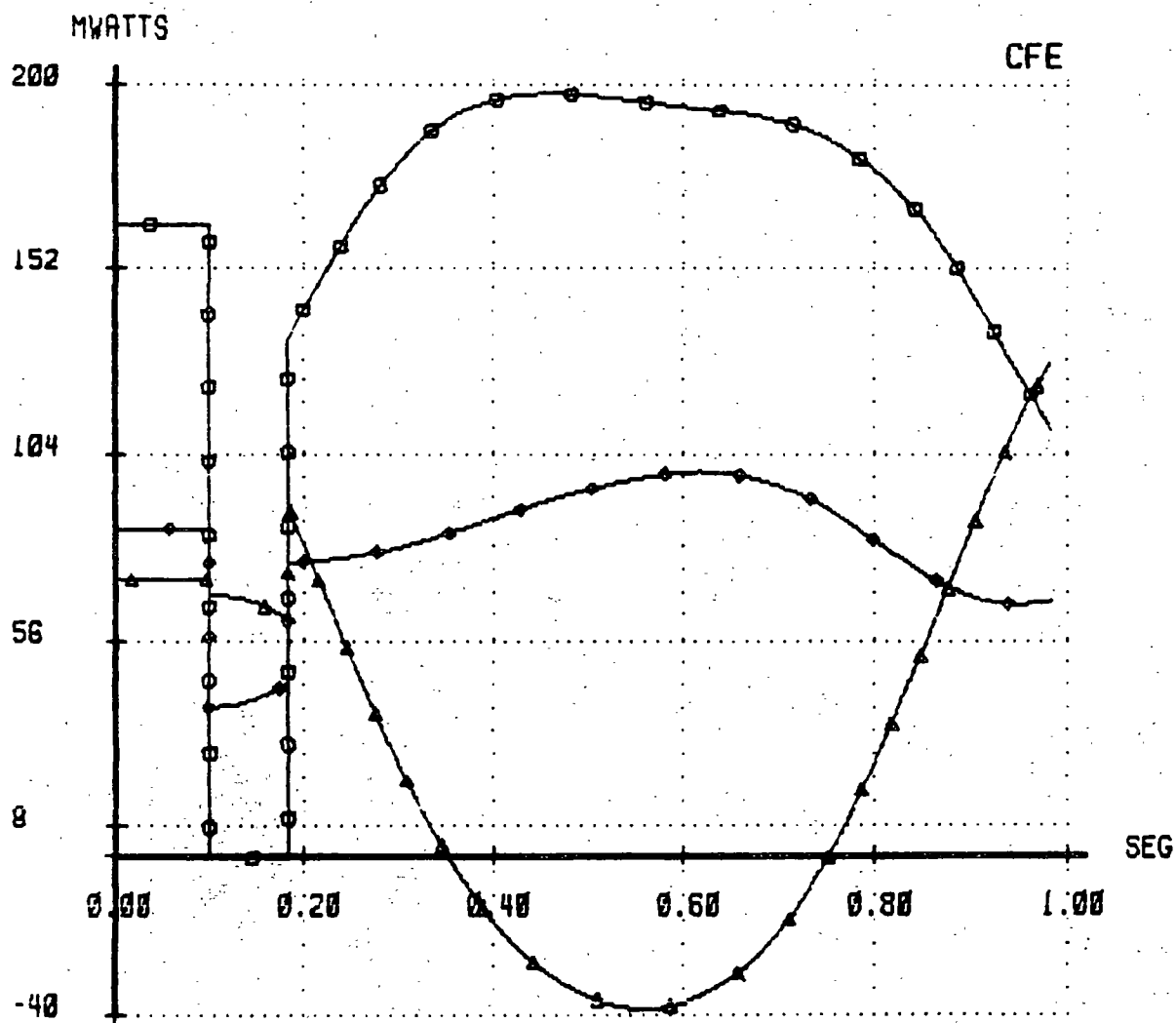
△ △ △ △ △ GEN2
○ ○ ○ ○ ○ GEN3



SISTEMA DE PRUEBA DE NUEVE NODOS (ANDERSON). FALLA TRIFASICA EN EL NO
SIETE A LOS 6 CICLOS. SE LIBERA CON LA APERTURA DE CINCO-SIETE EN 11 C

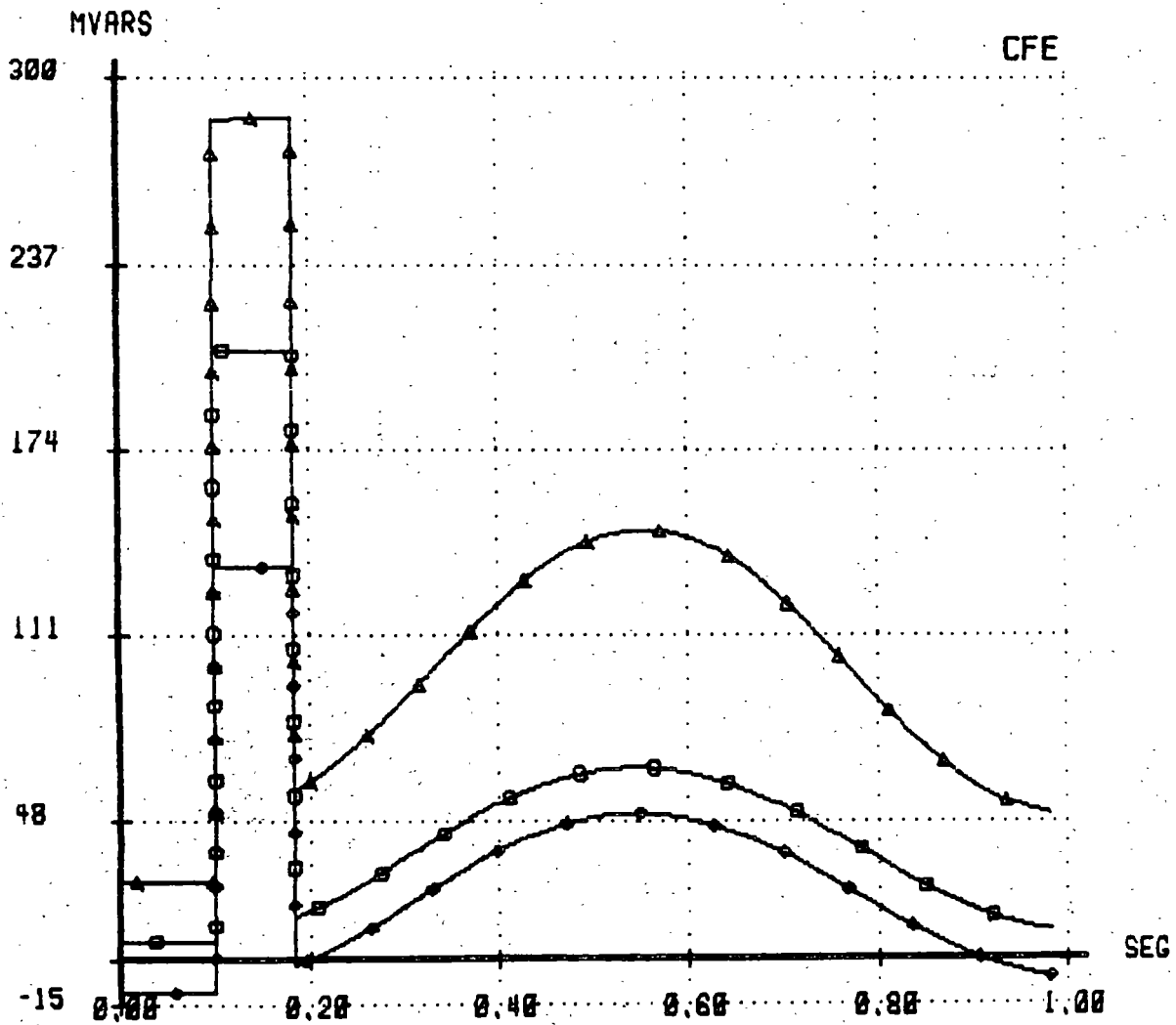


 GEN1
 GEN2
 GEN3



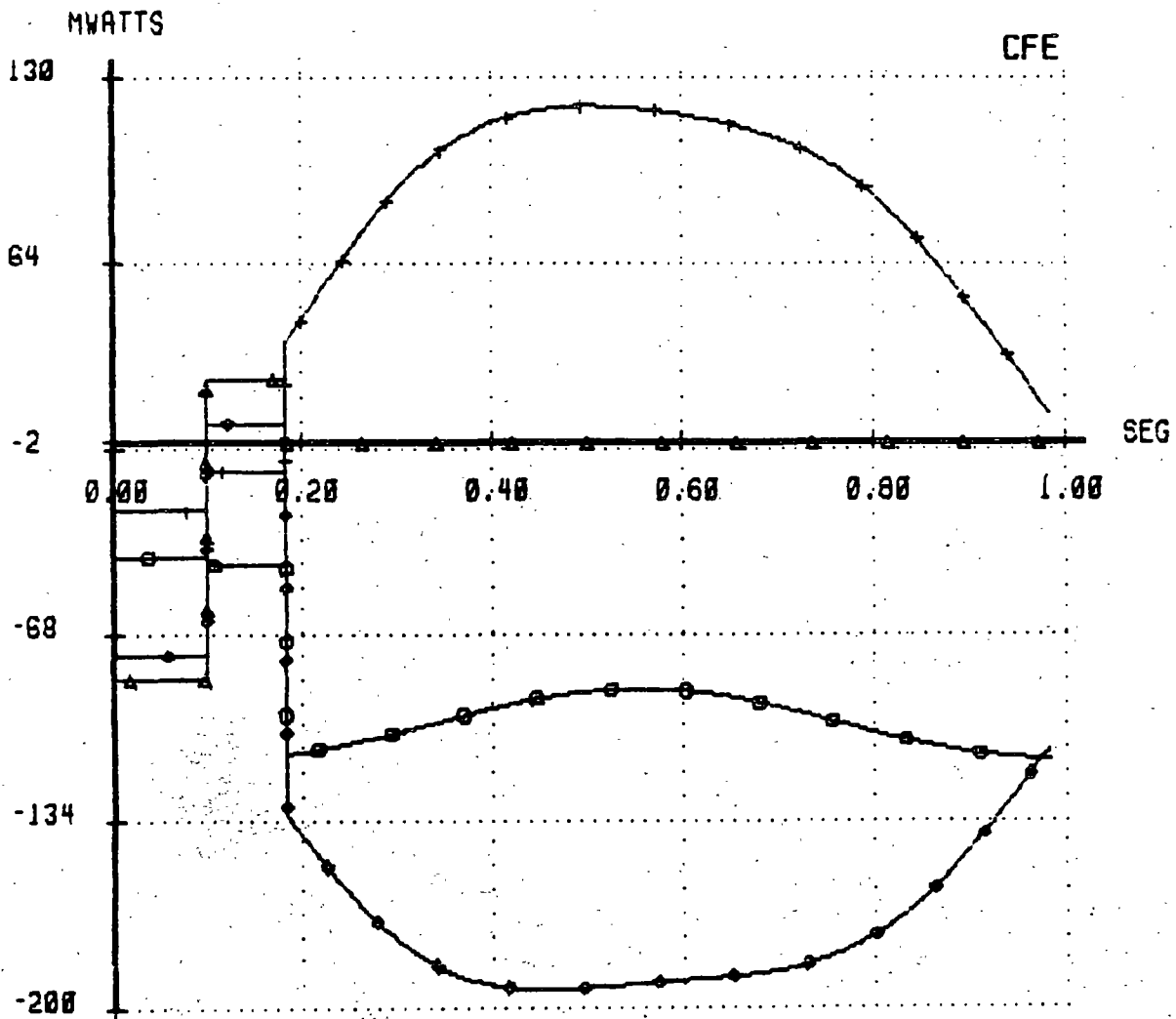
SISTEMA DE PRUEBA DE NUEVE NODOS (ANDERSON). FALLA TRIFASICA EN EL NO
SIETE A LOS 6 CICLOS. SE LIBERA CON LA APERTURA DE CINCO-SIETE EN 11 C

▲ GEN1
□ GEN2
● GEN3



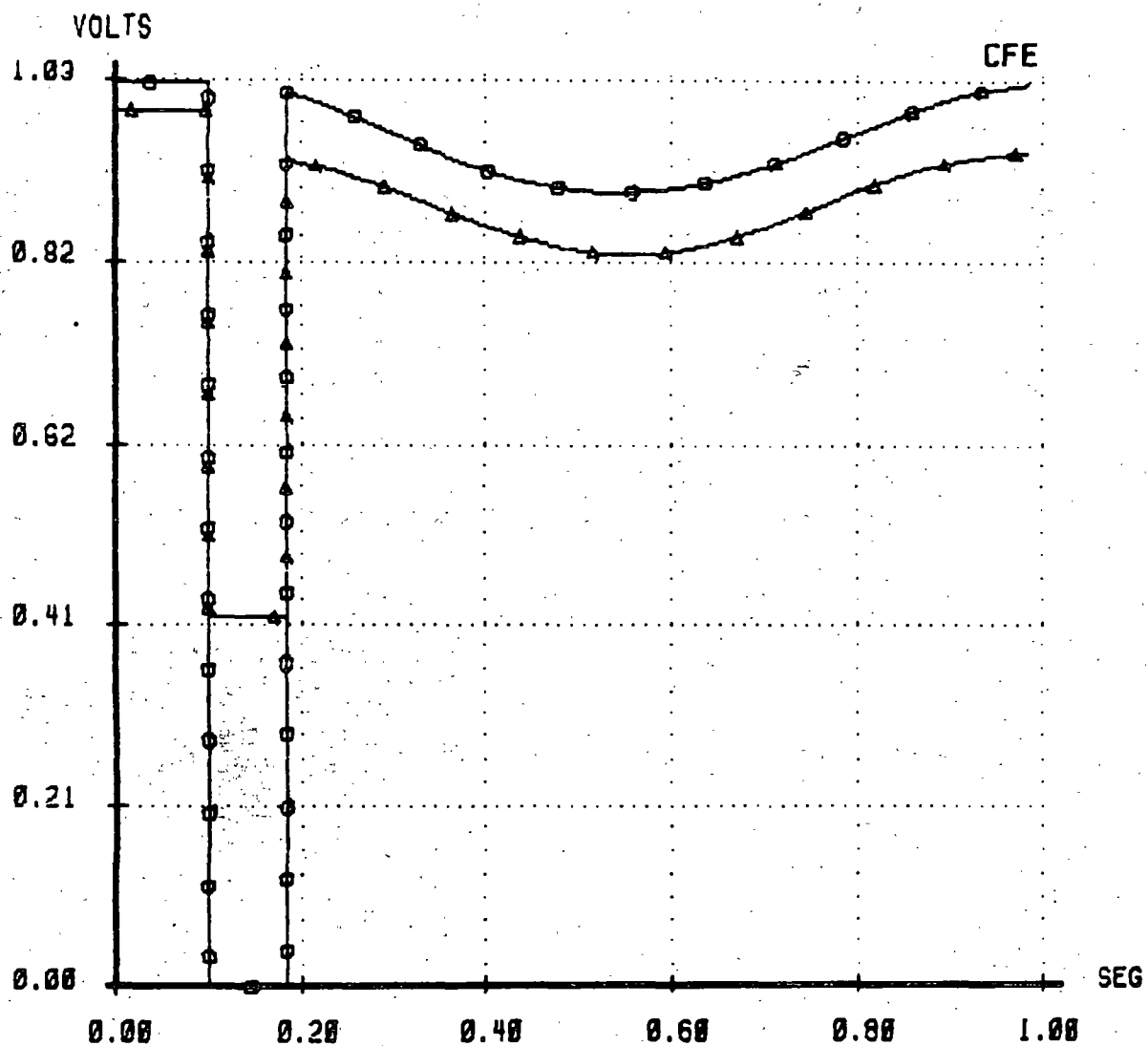
SISTEMA DE PRUEBA DE NUEVE NODOS (ANDERSON). FALLA TRIFASICA EN EL NO SIETE A LOS 6 CICLOS. SE LIBERA CON LA APERTURA DE CINCO-SIETE EN 11 C

—▲—▲—▲—▲—▲—	CINCO	-> SIETE
—○—○—○—○—○—	CINCO	-> CUATRO
—●—●—●—●—●—	OCHO	-> SIETE
—+—+—+—+—+—	OCHO	-> NUEVE



SISTEMA DE PRUEBA DE NUEVE NODOS (ANDERSON). FALLA TRIFASICA EN EL NO
SIETE A LOS 6 CICLOS. SE LIBERA CON LA APERTURA DE CINCO-SIETE EN 11 C

△-△-△-△-△ CINCO
○-○-○-○-○ SIETE



7 ESTABILIDAD EN ESTADO ESTABLE (EEE)

OBJETIVOS:

- Plantear el método de Edith Clarke y algunas técnicas aproximadas para determinar la transferencia de potencia máxima entre dos puntos de un SEP.
- Comentar el caso radial para enfatizar que los métodos anteriores no son aplicables en esta situación.

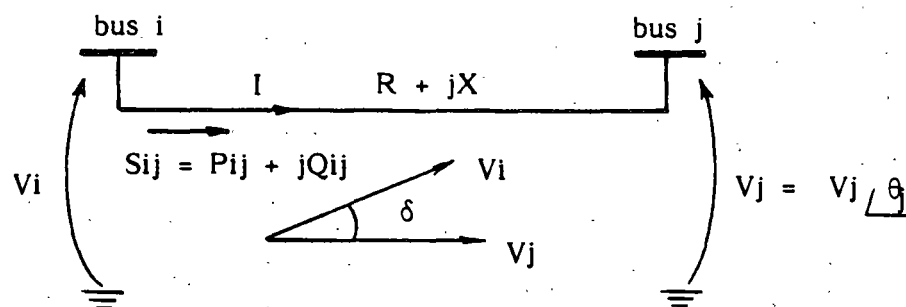
CARACTERISTICAS DE LOS ESTUDIOS DE EEE:

- Métodos sencillos.
- Los límites de EEE son superiores a los encontrados en estabilidad transitoria.
- Se utilizan cuando no se cuenta con recursos de simulación digital:

Límites de EEE + Margen = Límites prácticos

- Punto de atención: sincronismo de las máquinas.

TRANSFERENCIA DE POTENCIA ACTIVA
ENTRE DOS PUNTOS DEL SISTEMA



o Secuencia de solución:

- 1.- $I = (V_i - V_j)/Z$
- 2.- $S_{ij} = P_{ij} + jQ_{ij} = V_i I^*$
- 3.- $\delta = \theta_i - \theta_j$
- 4.- $P_{ij} = \text{Re} (S_{ij})$

o Resultado:

$$P_{ij} = \frac{1}{R^2 + X^2} (R |V_i|^2 - R |V_i| |V_j| \cos \delta + X |V_i| |V_j| \text{sen } \delta)$$

Si se considera $R=0$:

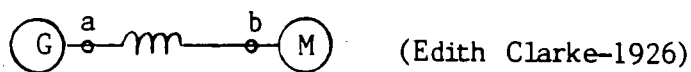
$$P_{ij} = \frac{1}{X^2} (X |V_i| |V_j| \text{sen } \delta)$$

$$P_{ij} = \frac{|V_i| |V_j|}{X} \text{sen } \delta$$

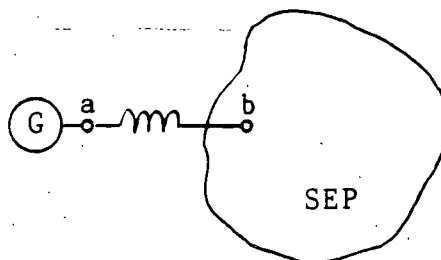
!!!

CASOS DE APLICACION

- Caso 0

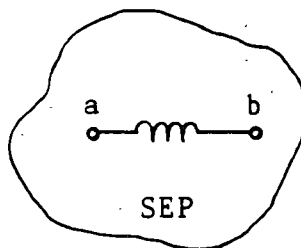


- Caso 1



- Caso 2

SCC
 Tula 13 700 MVA
 Salamanca 5 400
 USA 35 000

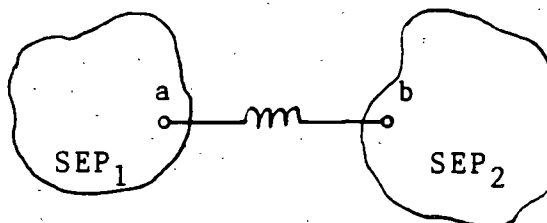


(Dunlop-1979)

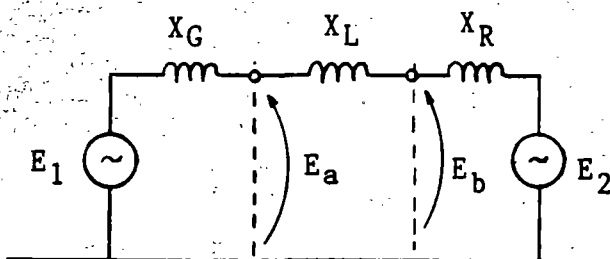
$$X_G = S_B / SCC_a$$

$$X_R = S_B / SCC_b$$

- Caso 3



o Representación General:



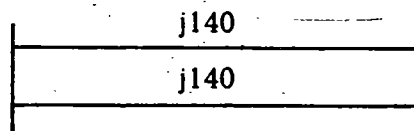
$$LEEE = P_{\max} = \frac{E_1 E_2}{X}$$

$$X = X_G + X_L + X_R$$

ALGUNAS APLICACIONES CUALITATIVAS

$$P_{\max} = \frac{E_1 E_2}{X}$$

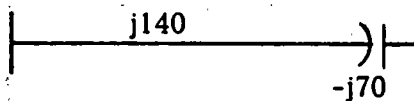
1.- Líneas en paralelo



$$X = \frac{j140}{2} = j70$$

$P_{\max} \uparrow$

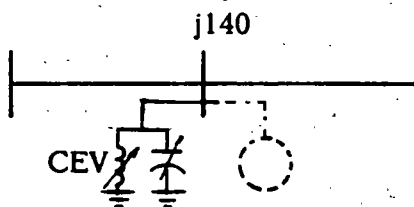
2.- Compensación serie



$$X = j140 - j70 = j70$$

$P_{\max} \uparrow$

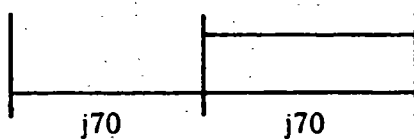
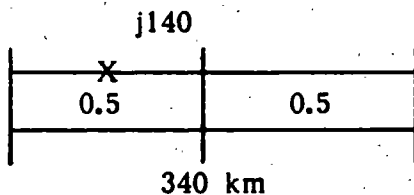
3.- Compensación en paralelo



$$X = \frac{j140}{2} = j70$$

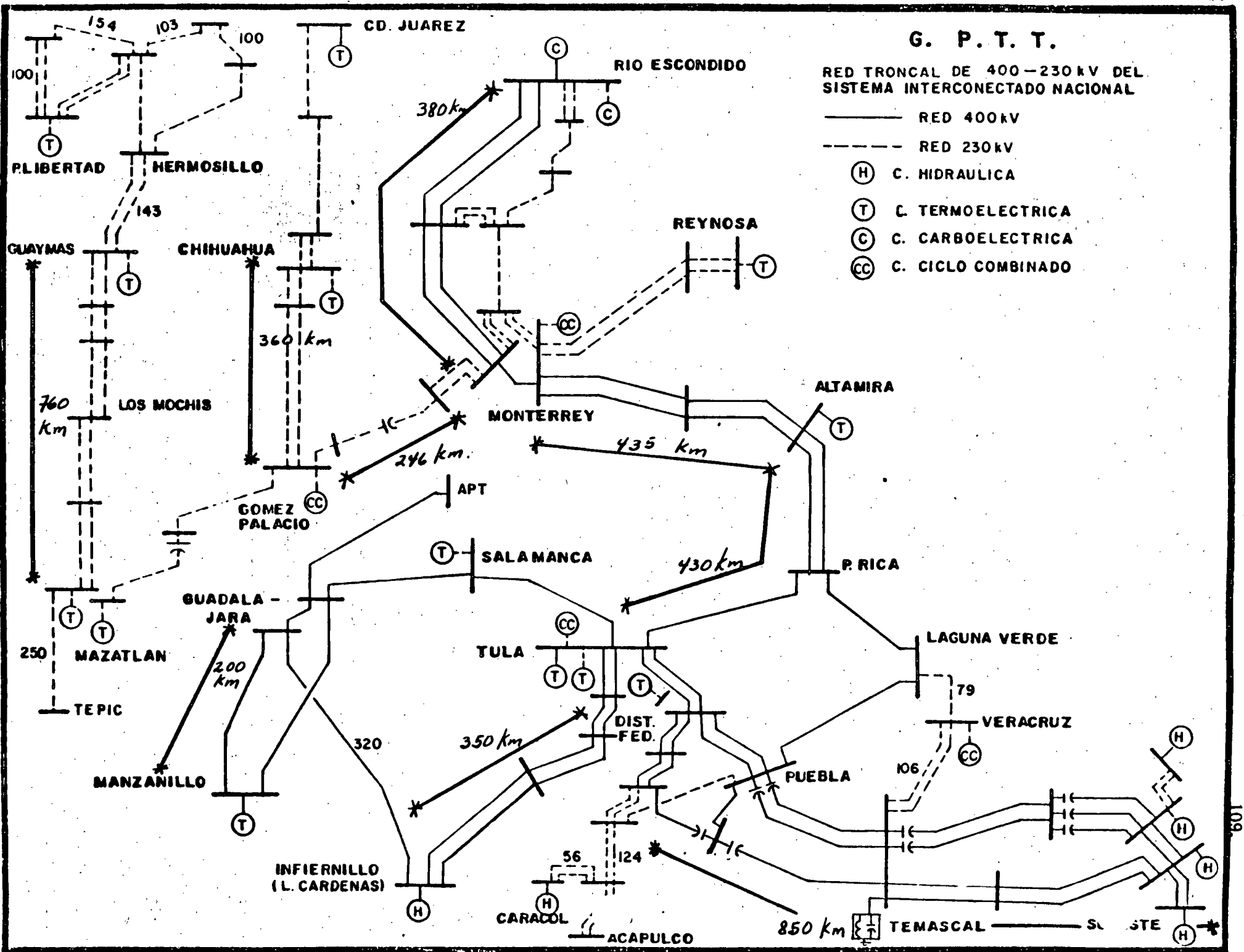
$P_{\max} \uparrow$

4.- Subestación de maniobra.



$$X = j70 + \frac{j70}{2} = j105$$

$P_{\max} \uparrow$



G. P. T. T.

RED TRONCAL DE 400-230 kV DEL SISTEMA INTERCONECTADO NACIONAL

— RED 400 kV

- - - RED 230 kV

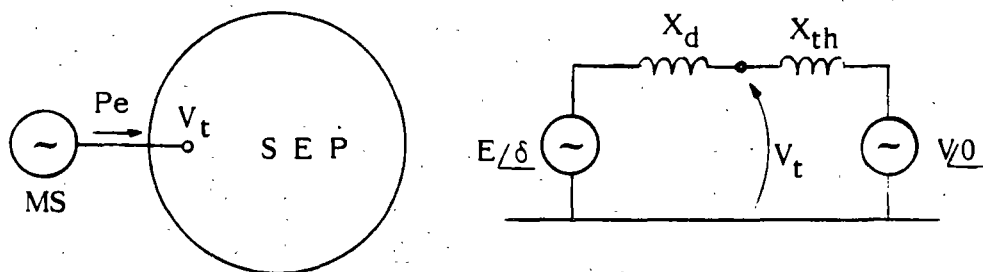
(H) C. HIDRAULICA

(T) C. TERMoeLECTRICA

(C) C. CARBOELECTRICA

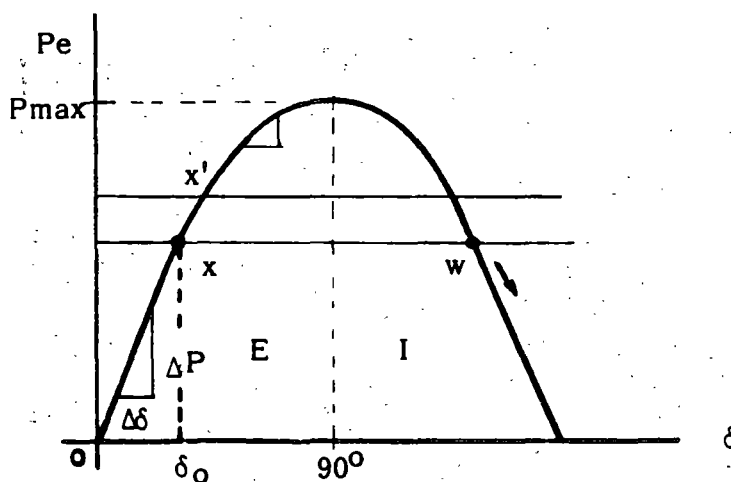
(CC) C. CICLO COMBINADO

MAQUINA - BUS INFINITO



$$P_e = \frac{|E| |V|}{X_d} \sin \delta$$

$$P_{\max} = \frac{|E| |V|}{X_d}$$



El coeficiente de sincronización es una medida de la estabilidad:

$$CS = \frac{\Delta}{d\delta} \frac{dP}{d\delta} \approx \frac{\Delta P}{\Delta \delta}$$

$$\text{en } \delta = 0^\circ : \quad \frac{dP}{d\delta} = \cos(0) = 1$$

$$\text{en } \delta = 90^\circ : \quad \frac{dP}{d\delta} = \cos(90) = 0$$

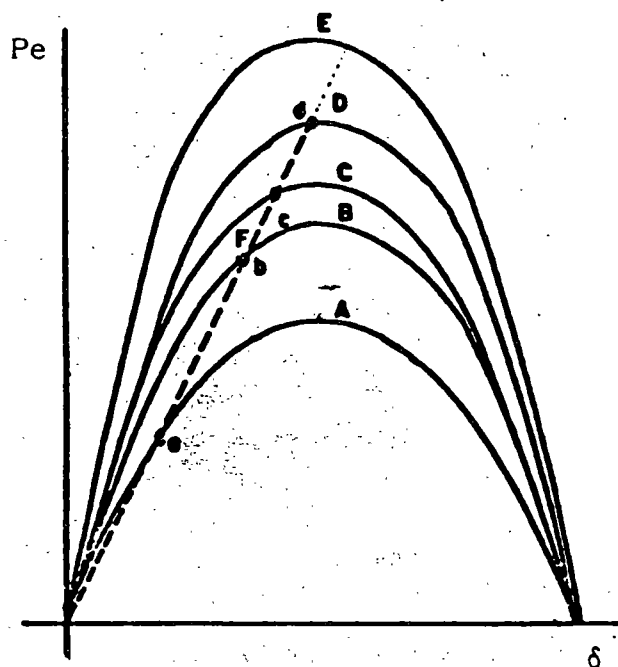
EL CASO GENERAL

o Límite de estabilidad con excitación fija.

$$P_{\max} = LEEE = \frac{E_1 E_2}{X} \sin \delta$$

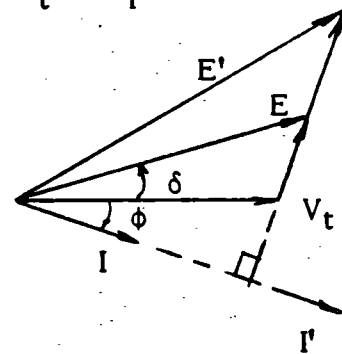
- La transferencia de potencia entre dos puntos del sistema depende de E_1 , E_2 , X y δ
- Se tendrá un límite de transferencia por cada nivel de excitación.
- Idem para cada configuración del sistema.

o Efecto del cambio manual de excitación.



Proceso:

$$\Delta P \rightarrow -\Delta V_t \rightarrow \Delta i_f \rightarrow \Delta E \rightarrow \Delta \delta$$



A-E Curvas con excitación cte.

F Curva con cambio de excitación manual.

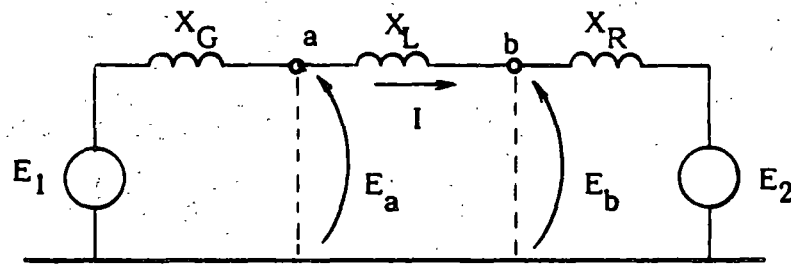
Problema: Se conocen los voltajes externos (E_a, E_b) pero se desconocen los voltajes internos (E_1, E_2) para encontrar P_{\max} .

DIAGRAMA DE (EDITH) CLARKE

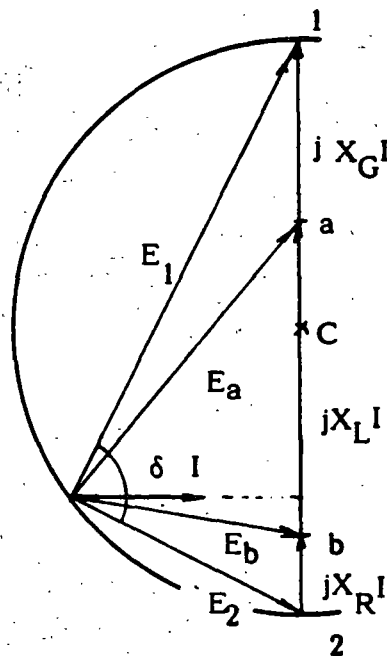
Es un método gráfico directo, para determinar el LEEE en base al diagrama fasorial del circuito.

El límite se obtiene para $\delta = 90^\circ$ y voltajes E_a , E_b especificados.

o Circuito equivalente



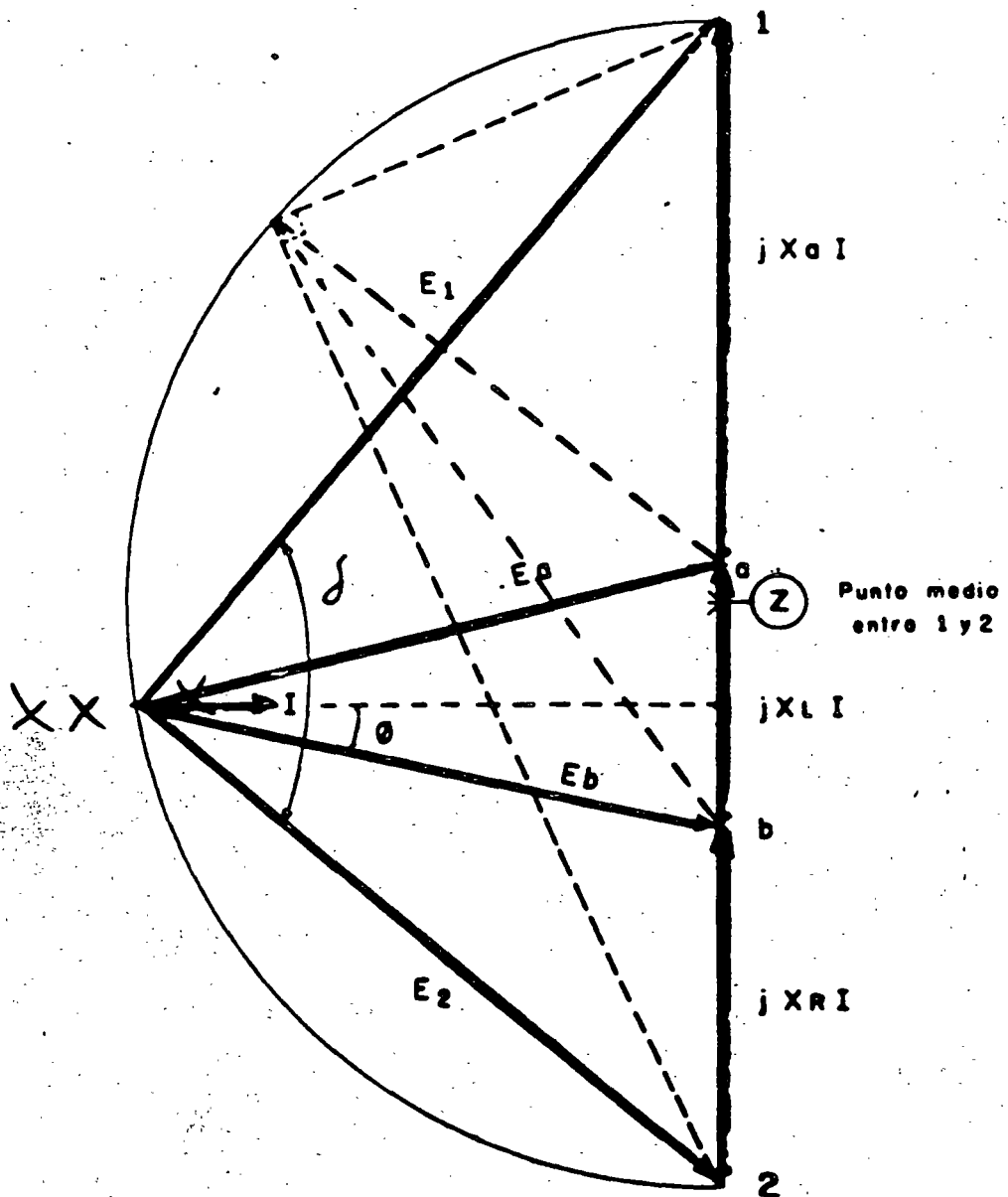
o Diagrama de Clarke



CONSTRUCCION DEL DIAGRAMA:

- 1.- Se trazan (a escala) $X_G I$, $X_L I$, $X_R I$
- 2.- Se dibuja el semicírculo
- 3.- Se obtiene el vértice del diagrama fasorial
- 4.- Se determina la magnitud de I , E_1 , E_2
- 5.- Se obtiene el LEE = P_{max}

$$P_{max} = \frac{E_1 E_2}{X_{12}} = E_b I \cos \phi$$



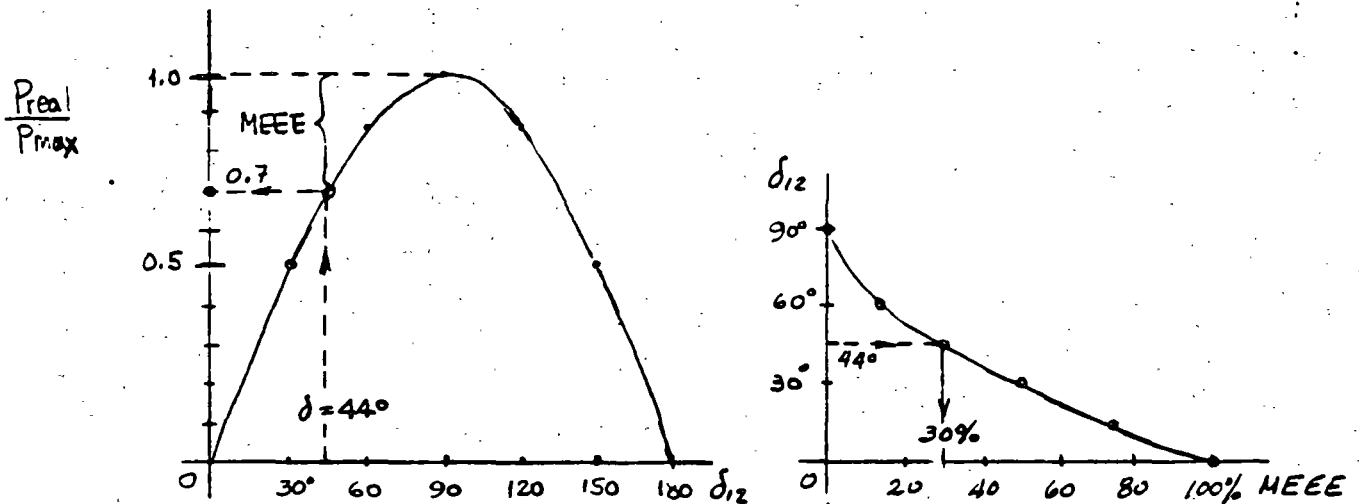
MARGEN DE ESTABILIDAD:

- * $MEEE \triangleq \frac{P_{max} - P_{real}}{P_{max}} \quad (100)$
- * SE SELECCIONA DE TAL MODO QUE EL SISTEMA SOPORTE CUALQUIER DISTURBIO CONCEBIBLE
- * REGLA PRACTICA:

$$MEEE = 30 - 35\%$$

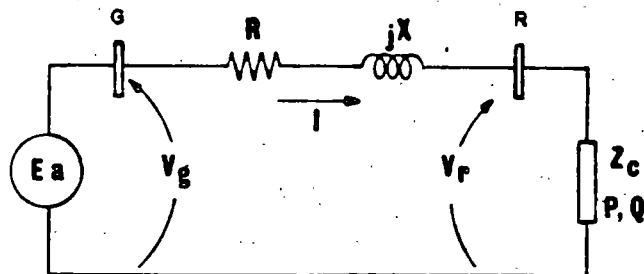
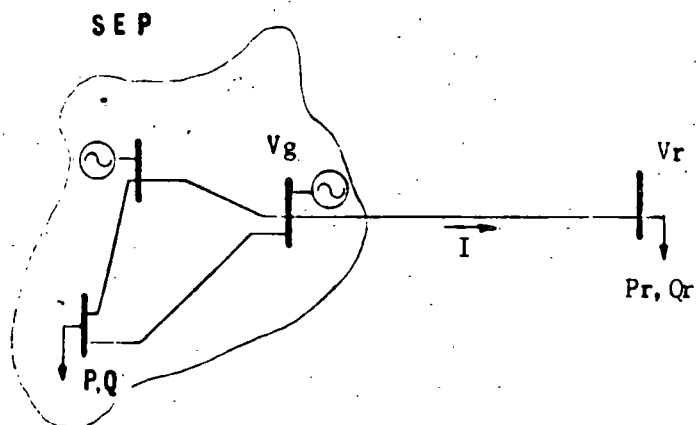
$$\delta_{12} = 44 - 40^\circ$$

$$\delta_{ab} = ?$$

ESTUDIO DE FLUJOS:

- * CONDICIONES DE INESTABILIDAD: PROBLEMAS DE CONVERGENCIA (δ, p anormales)
- * ANGULOS MAYORES A 90° EN EE?
- * NO SE INCLUYE LA REPRESENTACION INTERNA DE MAQUINAS: REGULACION IDEAL
- * LIMITE DE REACTIVOS YA ALCANZADOS

EL CASO RADIAL. Particularidades



Cantidades conocidas: \tilde{V}_g , R , X , P_r , Q_r

Cantidades desconocidas: \tilde{I} , \tilde{V}_r

Método usado anteriormente: Aproximaciones sucesivas

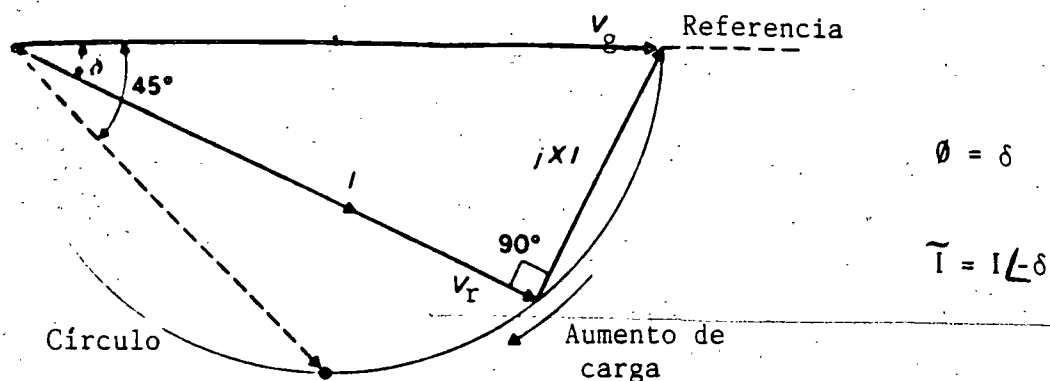
Ecuación básica:

$$\tilde{V}_g = \tilde{V}_r + \tilde{z}\tilde{I} \quad ; \tilde{V}_g \text{ se supone cte.}$$

UN CASO PARTICULAR (Elgerd)

$$R = 0$$

$$Q_r = 0 \quad ; \quad \text{f.p.} = 1$$



En el extremo de envío:

$$S_g = P_g + jQ_g = (V_g \angle 0) (I \angle \delta) = (V_g I \cos \delta) + j(V_g I \sin \delta)$$

$$P_g = V_g I \cos \delta \quad (A)$$

Por inspección:

$$V_r \sin \delta = X I \cos \delta \quad I = \frac{V_r \sin \delta}{X \cos \delta}$$

Sustituyendo la corriente en (A):

$$P_g = \frac{V_g V_r}{X} \sin \delta \quad (B) ?$$

Pero:

$$V_r = V_g \cos \delta \quad (C) !$$

Sustituyendo (C) en (B):

$$P_g = \frac{V_g^2}{2X} \sin 2\delta \quad (D)$$

Finalmente:

$$\boxed{LEEE = P_{max} = \frac{V_g^2}{2X}}$$

Ocurre en : $\delta = 45$ y $V_r = 0.707$ pu

CASO RADIAL. SOLUCION GENERAL

Resultados del artículo "Comportamiento del voltaje en líneas de transmisión radiales "FMC-JLMM":

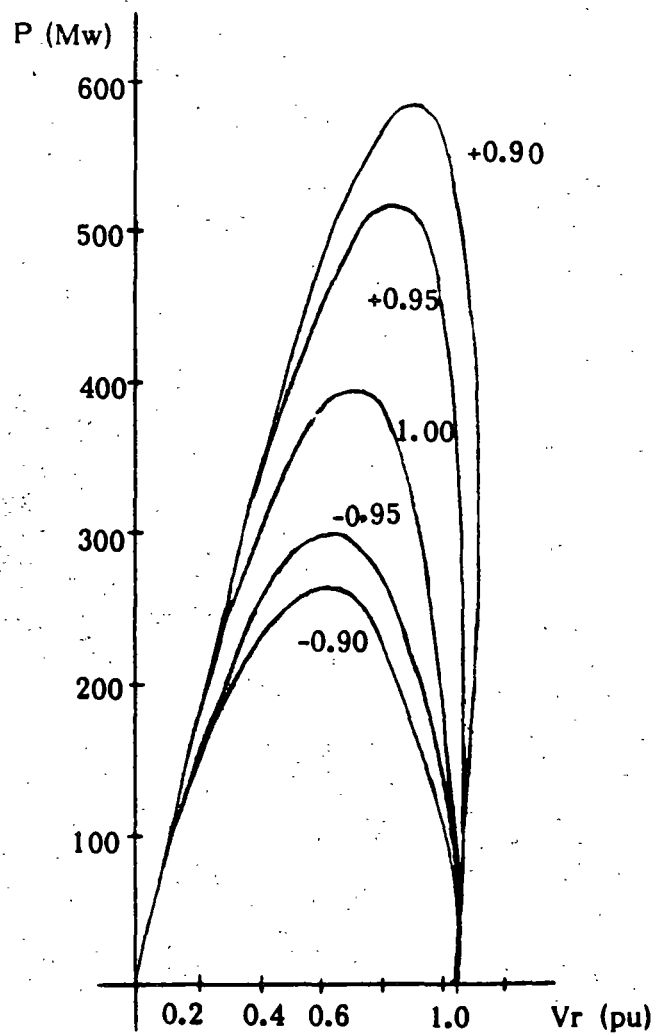
$$V_r = + \sqrt{A \pm \sqrt{D}} \quad (3\emptyset, 1\emptyset, pu)$$

$$A = \frac{V_g^2}{2} - B \cos \alpha \quad ; \quad \alpha = \theta + \phi$$

$$B = \frac{P Z}{\cos \phi}$$

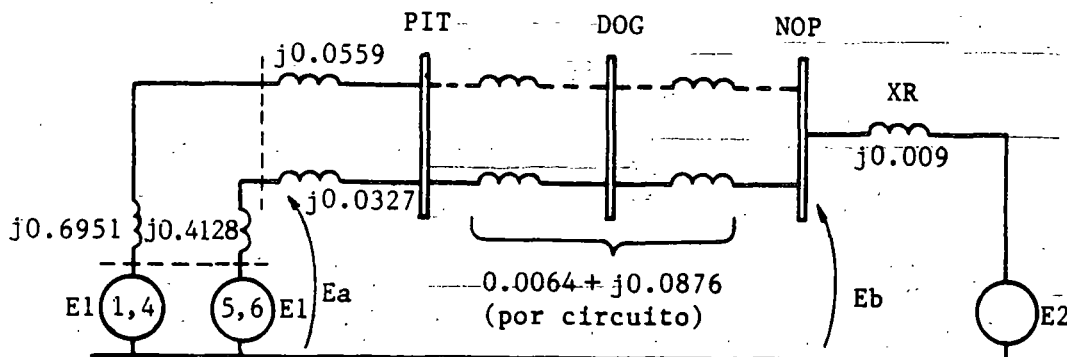
$$D = A^2 - B^2$$

$$LEEE = P_{max} = \frac{V_g^2 \cos \phi}{2 Z (1 + \cos \alpha)}$$



Ejemplo 1.- Determinar el LEEE de una de las líneas de 400 kV pitirera - Nopala.

o Diagrama de reactancias.



$$X_G = 0.0943 \text{ pu}$$

$$S_B = 100 \text{ MVA}$$

$$X_L = 0.0951$$

$$E_a = 410/400 = 1.025 \text{ pu}$$

$$X_R = 0.009$$

$$E_b = 410/400 = 1.025 \text{ pu}$$

o Caídas por reactancias:

$$X_G I = j0.0943 I \quad (94.3 \text{ mm})$$

$$X_L I = j0.0951 I \quad (95.1 \text{ mm})$$

$$X_R I = j0.009 I \quad (9.0 \text{ mm})$$

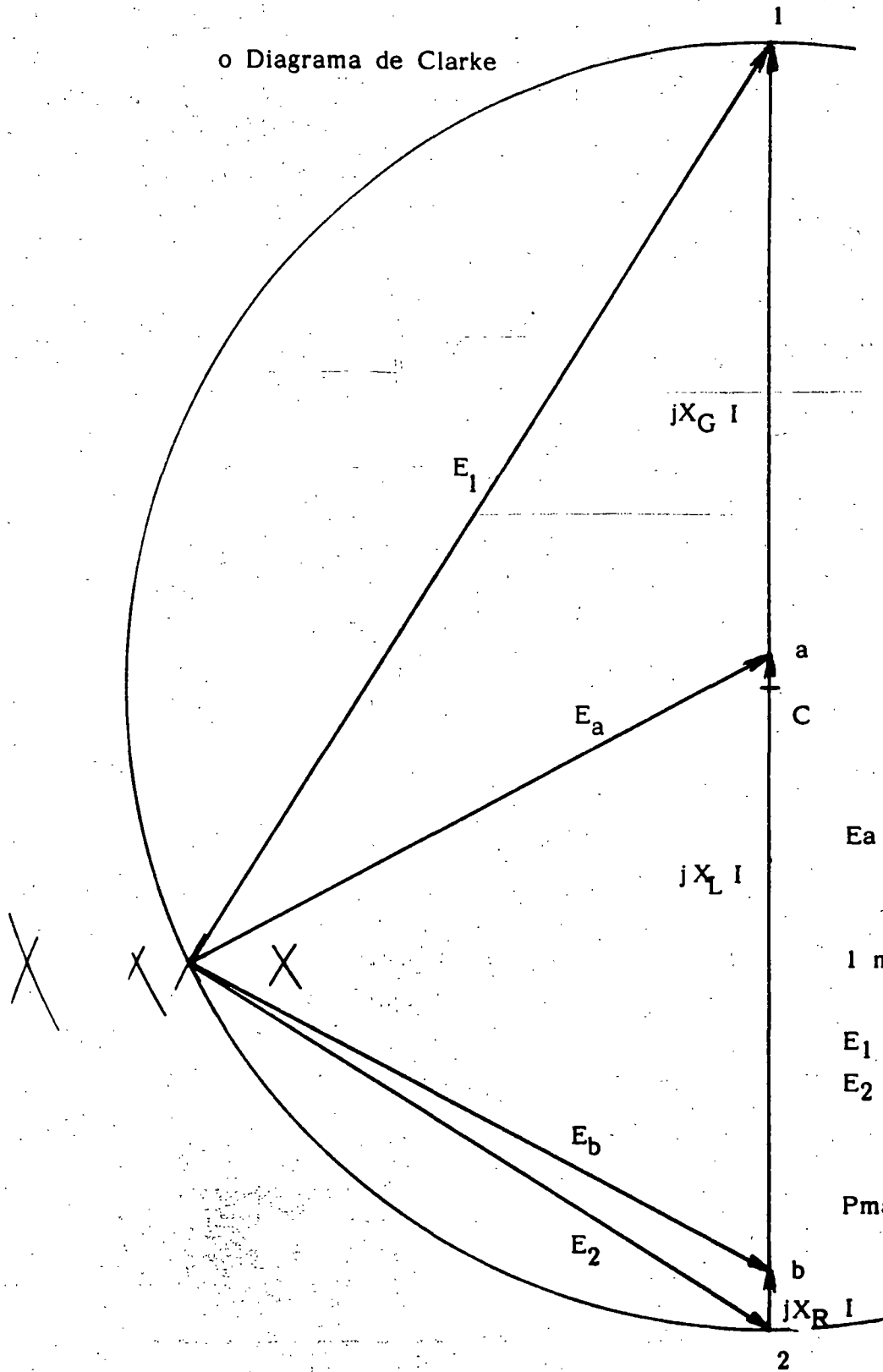
$$X I = 0.1984 I \quad (198.4 \text{ mm})$$

Escala seleccionada: $0.1984 I = 198.4 \text{ mm}$.

o Solución de 3 casos:

Caso	Condiciones	LEEE (Mw/línea)
1	6G's + 1 L	898
2	6G's + 2L's	706
3	2G's + 1 L	570

o Diagrama de Clarke



RESULTADOS:

$$E_a = E_b = 102 \text{ mm} \\ = 1.025 \text{ pu}$$

$$1 \text{ mm} = 0.01005 \text{ pu de } V$$

$$E_1 = 167.5 \text{ mm} = 1.68 \text{ pu}$$

$$E_2 = 105.5 \text{ mm} = 1.06 \text{ pu}$$

$$P_{\max} = \frac{1.68 \times 1.06}{0.1984}$$

$$P_{\max} = 8.98 \text{ pu} \\ = 898 \text{ Mw}$$

TECNICAS APROXIMADAS

- Regla de los 30°

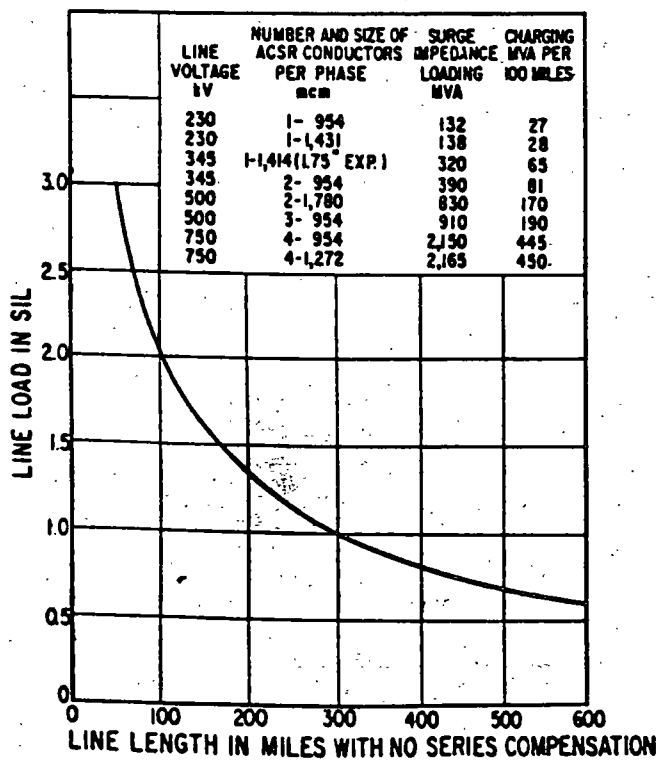
$$LEEE \cong \frac{E_a E_b}{X_{ab}} \text{ sen } 30^\circ$$

EJEMPLO: Determinar el LEEE para una de las líneas de 400 kV entre Infiernillo y Nopala (340 km).

$$X_L = 140.6 \text{ ohms} \quad Z_c = 326 \text{ ohms}$$

$$LEEE = \frac{(410)(410)}{140.6} (0.5) \cong 600 \text{ Mw}$$

- Curva de Clair



SIL = Potencia característica de la línea
(Surge Impedance Loading)

$$Z_c = \sqrt{\frac{L}{C}} = \text{Impedancia característica (surge impedance)}$$

EJEMPLO (Continuación):

$$SIL = \frac{(V_{prom})^2}{Z_c} = \frac{(410)^2}{326} = 515 \text{ Mw}$$

$$l = 340 \text{ km} = 211 \text{ millas}$$

$$LEEE = k SIL \cong (1.26)(515) \cong 650 \text{ Mw}$$

Ejemplo 2.- El Caso Radial.

En el caso 3 del ejemplo 1 se obtuvo un LEEE de 570 Mw. Considerando una línea similar, pero en condiciones radiales, calcular:

- a).- El LEEE con $R = 0$ y $fp = 1$.
 b).- IDEM pero con la ecuación general, considerando el valor de la resistencia y un $fp = 0.9$ inductivo.

SOLUCION

a).-

$$X = X_T + X_L = (j0.0327/2) + j0.0876 = j0.10395$$

$$LEEE = P_{MAX} = \frac{V_G^2}{2X} = \frac{(1.025)^2}{2(0.10395)} = 5.05 \text{ PU}$$

$$LEEE = 505 \text{ MW (CONTRA 570 MW)}$$

b).-

$$Z = 0.0064 + j0.10395 = 0.1041 \angle 86.5^\circ$$

$$\theta = \cos^{-1}(0.9) = 25.8^\circ$$

$$\alpha = \theta + (\theta) = 86.5 + (-25.8^\circ) = 60.7$$

$$LEEE = \frac{V_G^2 \cos \theta}{2Z(1 + \cos \alpha)} = \frac{(1.025)^2 (0.9)}{2(0.1041) (1 + 0.49)}$$

$$LEEE = (505)(0.6) = 305 \text{ MW (CONTRA 570 MW)}$$

8. ESTABILIDAD DINÁMICA

Dentro del análisis del comportamiento dinámico de los sistemas de potencia se ha estudiado la estabilidad transitoria por medio de la cual se puede determinar si un sistema pierde estabilidad en la primera oscilación, sin embargo el problema de estabilidad se puede presentar en oscilaciones posteriores generalmente cuando la perturbación provoca que alguno o algunos de los equipos de control capaces de producir pares de amortiguamiento negativo hagan que el sistema pierda estabilidad. Las consideraciones que se hacen en este estudio son diferentes al de estabilidad transitoria dado que el efecto de los controles es determinate y el tiempo de estudio es mayor. En forma simple se puede decir que la Estabilidad Dinámica estudia el comportamiento del sistema de potencia para periodos de tiempo superiores a la primera oscilación y se deben tomar en cuenta un modelado de cada componente que represente adecuadamente su operación en el periodo de tiempo de interes.

Estudio de Estabilidad Dinámica.

Cuando se analiza la estabilidad dinámica del sistema es conveniente suponer que los disturbios que causan los cambios desaparecen, por ejemplo: El movimiento del sistema es libre, en este caso la estabilidad se asegura si el sistema regresa a su estado inicial.

Si el modelado de SEP se hace por medio de ecuaciones lineales o estas se linealizan, se pueden utilizarlas técnicas del análisis del sistema lineales. El método más común es representar cada componente por su función de transferencia y aplicar las técnicas conocidas en teoría del control clásico como Nyquist, Bode, Root Locus, etc. Actualmente para sistemas multivariables el modelo de variables de estado es el más utilizado y se representa en forma compacta.

$$\dot{x} = Ax + Eu$$

La respuesta libre del sistema se obtiene por el primer método de Lyapunov, el cual consiste en determinar los eigenvalores de la matriz "A". El criterio de estabilidad se establece por la representación de los eigenvalores en el plano asumiendo que el sistema pierde estabilidad cuando cualquier eigenvalor tiene parte real positiva. Si todas las partes reales de los eigenvalores son negativas, se dice que el sistema dinámico es estable o asintóticamente estable.

El método usado para linealizar el sistema de ecuaciones es suponer que la perturbación del sistema es pequeña y ocasiona cambios pequeños en las variables del sistema, tales como $\Delta\delta$, $\Delta\omega$, Δi_d , ΔP , etc.

Las ecuaciones para estas variables se encuentran por medio de la serie de Taylor alrededor del punto X_0 que es la condición de predisturbio y por simplicidad se desprecian los términos de orden mayor a 2 por considerar su efecto poco significativo. Suponiendo que el vector de estado "X" tiene un estado inicial X_0 , al ocurrir un disturbio el vector de estado cambiará ligeramente y queda:

$$X = X_0 + \Delta X$$

El modelo en variables de estado es:

$$\dot{X} = f(X, t)$$

Representando el pequeño cambio se tiene:

$$\dot{X} + \Delta \dot{X} = f(X_0 + \Delta X, t)$$

La expansión en serie de Taylor se expresa:

$$\dot{X}_0 + \Delta \dot{X}_0 = f(X_0, t) + \left. \frac{df}{dx_1} \right|_{X_0} \Delta x_1 + \left. \frac{df}{dx_2} \right|_{X_0} \Delta x_2 + \dots + \left. \frac{df}{dx_n} \right|_{X_0} \Delta x_n$$

Quedando como:

$$\dot{\Delta X} = A_{X_0} \Delta X + B_{X_0} \Delta U$$

La respuesta libre del sistema $\dot{\Delta X} = A \Delta X$ estará dada por los eigenvalores de la matriz A.

$$A = \left[\frac{df}{dX} \right]_{X_0}$$

INTERPRETACION MATEMATICA DE LOS EIGENVALORES Y EIGENVECTORES

Suponiendo que un sistema se expresa por un conjunto de ecuaciones linealmente independientes de la forma:

$$\begin{bmatrix} a_{11} & a_{12} \\ a_{21} & a_{22} \end{bmatrix} \begin{bmatrix} X_1 \\ X_2 \end{bmatrix} = \begin{bmatrix} Y_1 \\ Y_2 \end{bmatrix}$$

En forma compacta:

$$A x = Y$$

El problema es encontrar un vector "X" (llamado Eigenvector, vector propio o columna modal) el cual será transformado por la matriz "A" en un vector "Y" cuyas coordenadas son proporcionales al vector "X" en el espacio vectorial. Esto es, encontrar el vector "X" que satisfaga.

$$Ax = \lambda x$$

λ es llamado eigenvalor, valor característico, número característico, valor propio. Es escalar o complejo que deberá ser calculado.

$$[A - \lambda I] x = 0$$

La matriz resultante de la reducción del parentesis se conoce como matriz característica y representa los coeficientes de un conjunto de ecuaciones lineales simultaneas y homogeneas las cuales tienen una solución que no es trivial.

Los eigenvalores se determinan al obtener las raíces del polinomio resultante del determinante de la matriz característica.

$$\text{Det } [A - \lambda I] = 0$$

La interpretación se puede tomar como que cada punto del espacio n-dimensional se transforma a un nuevo espacio.

INTERPRETACION FISICA DE LOS EIGENVALORES

Para propósitos de estabilidad las interpretaciones son las siguientes:

Un eigenvalor está formado por 2 componentes, una parte real " α " y una parte imaginaria " β ".

La parte real representa la constante de amortiguamiento; y la parte imaginaria es la frecuencia natural del modo oscilación.

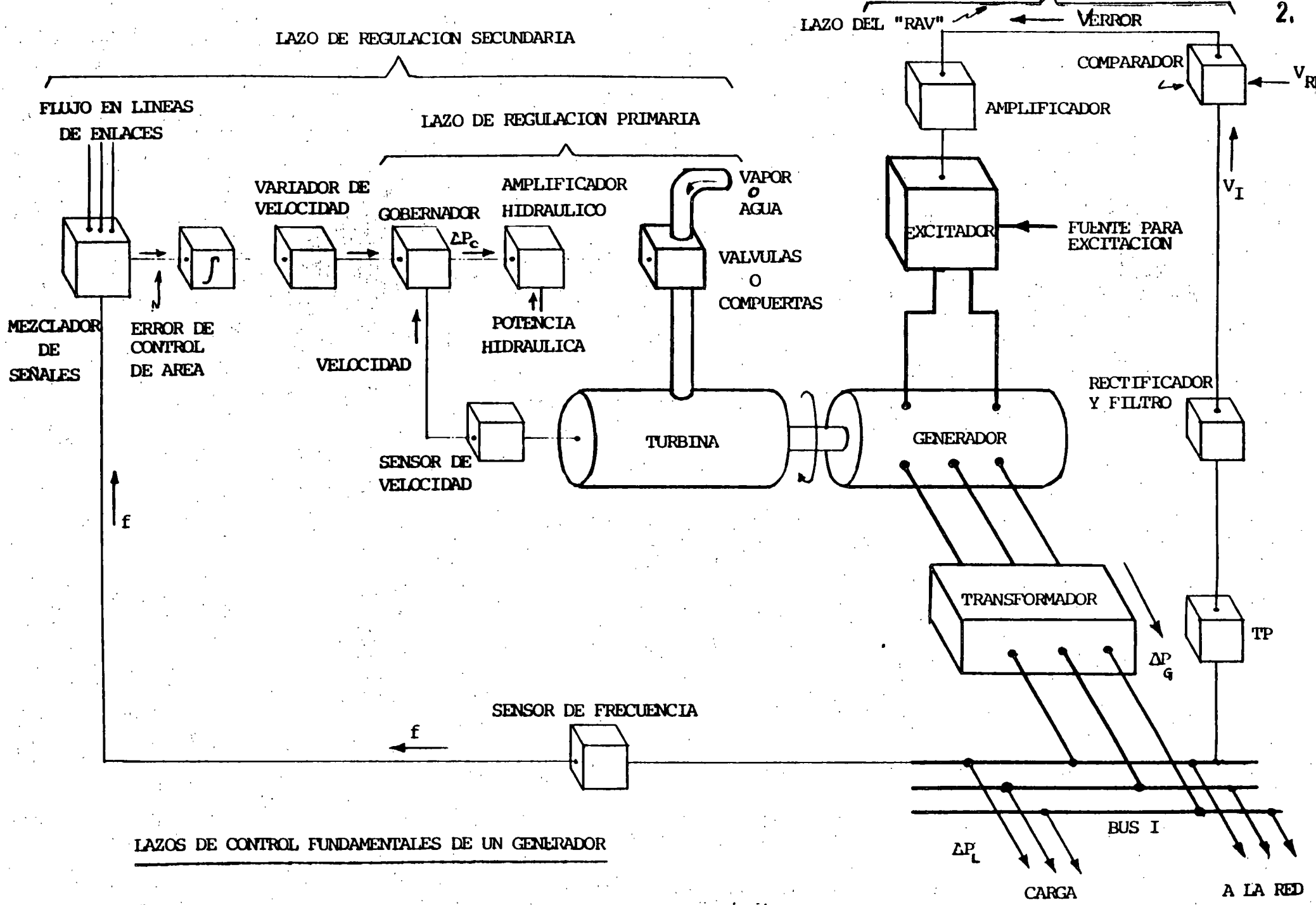
Se pueden analizar algunos puntos significativos en el plano complejo.

Podemos decir que el sistema es estable si los eigenvalores están en el lado izquierdo del plano complejo, e inestable si se encuentra en el lado derecho, en el caso en donde $\alpha=0$ las oscilaciones son constantes y mantenidas.

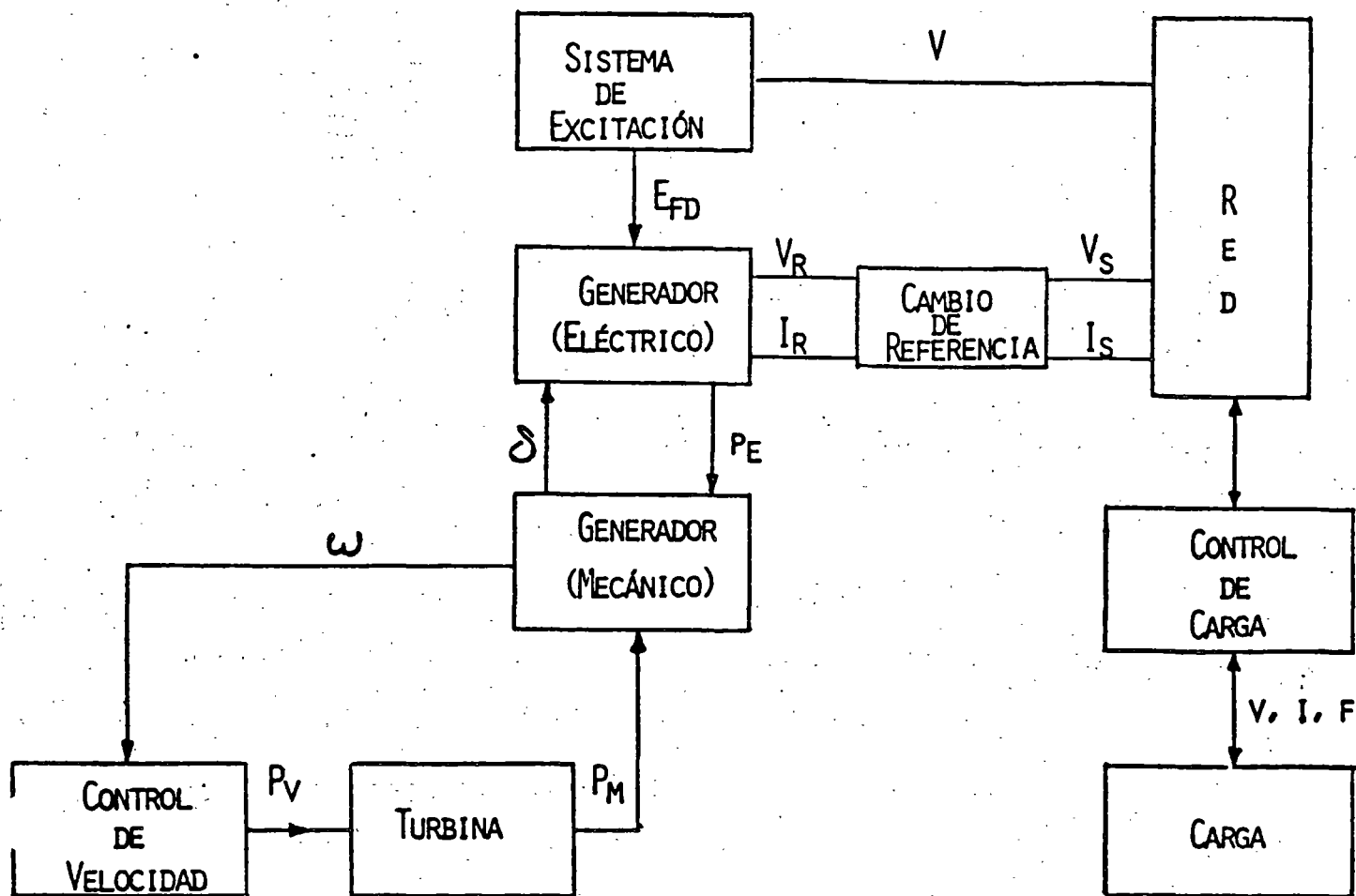
AREA DE INTERÉS

	DINÁMICA DEL GEN. ELECT. (ANÁLISIS DE ESTABILIDAD TRANSITORIA)	REGULACIÓN PRIMARIA Y C A G	DINÁMICA DE LA CALDERA Y CONTROLES
Pocos SEGUNDOS	X		
DE VARIOS SEGUNDOS A POCOS MINU- TOS.		X	
VARIOS MINUTOS			X

CLASIFICACION DE PROBLEMAS DINÁMICOS DE ACUERDO A LA -
DURACIÓN DE LOS EFECTOS PRINCIPALES.



LAZOS DE CONTROL FUNDAMENTALES DE UN GENERADOR

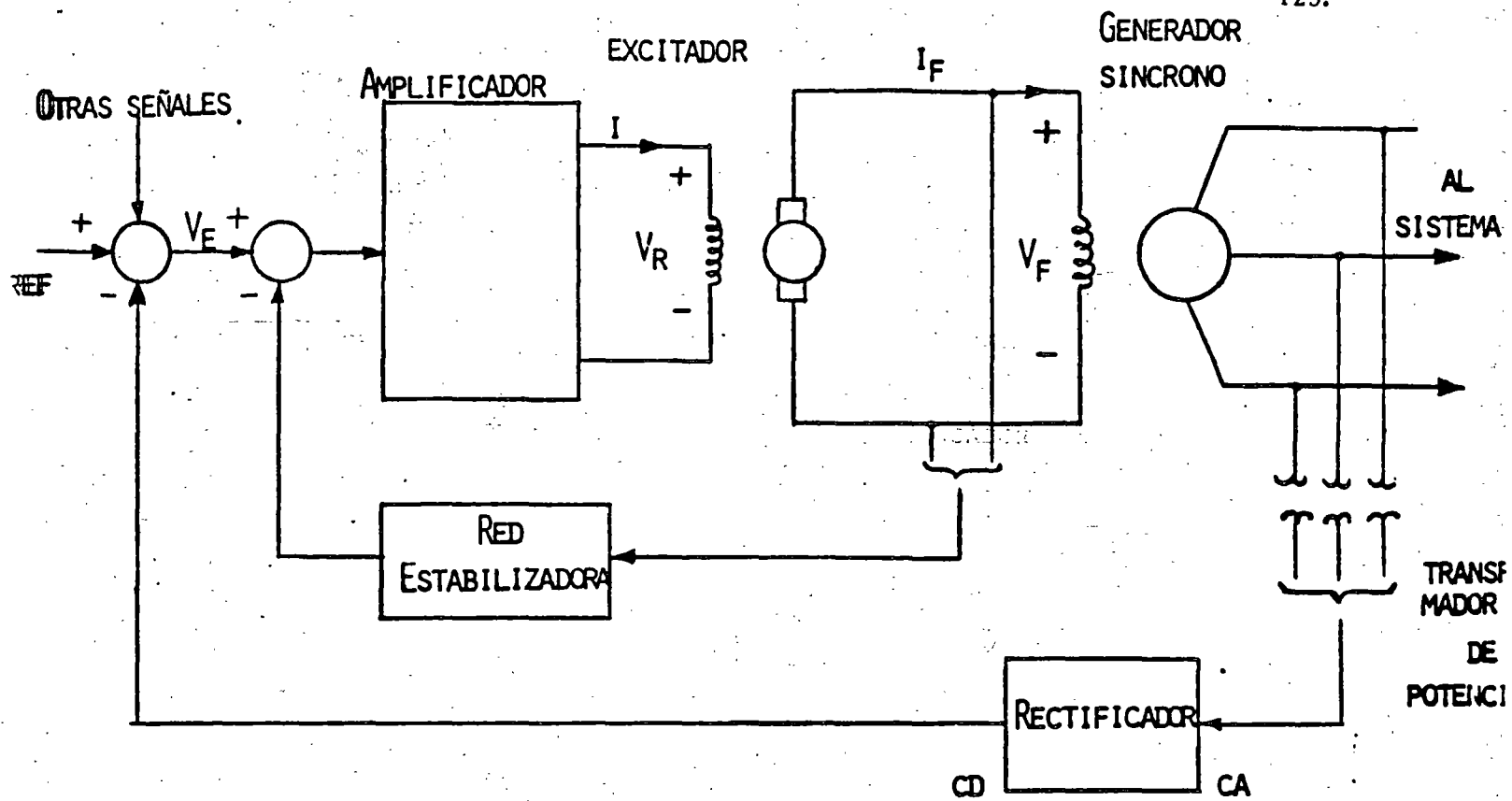


ELEMENTOS QUE INTERVIENEN EN UN ESTUDIO DE ESTABILIDAD DINÁMICA

MODELOS DE COMPONENTES:

LOS SUBSISTEMAS DE MAYOR INFLUENCIA EN EL PROBLEMA DINÁMICO SON:

- CONTROL DE VELOCIDAD.
- CONTROL DE POTENCIA MECÁNICA.
- CARGA;
- RELEVADORES.
- CONTROL DE VOLTAJE.



SISTEMA DE EXCITACION SIMPLIFICADO

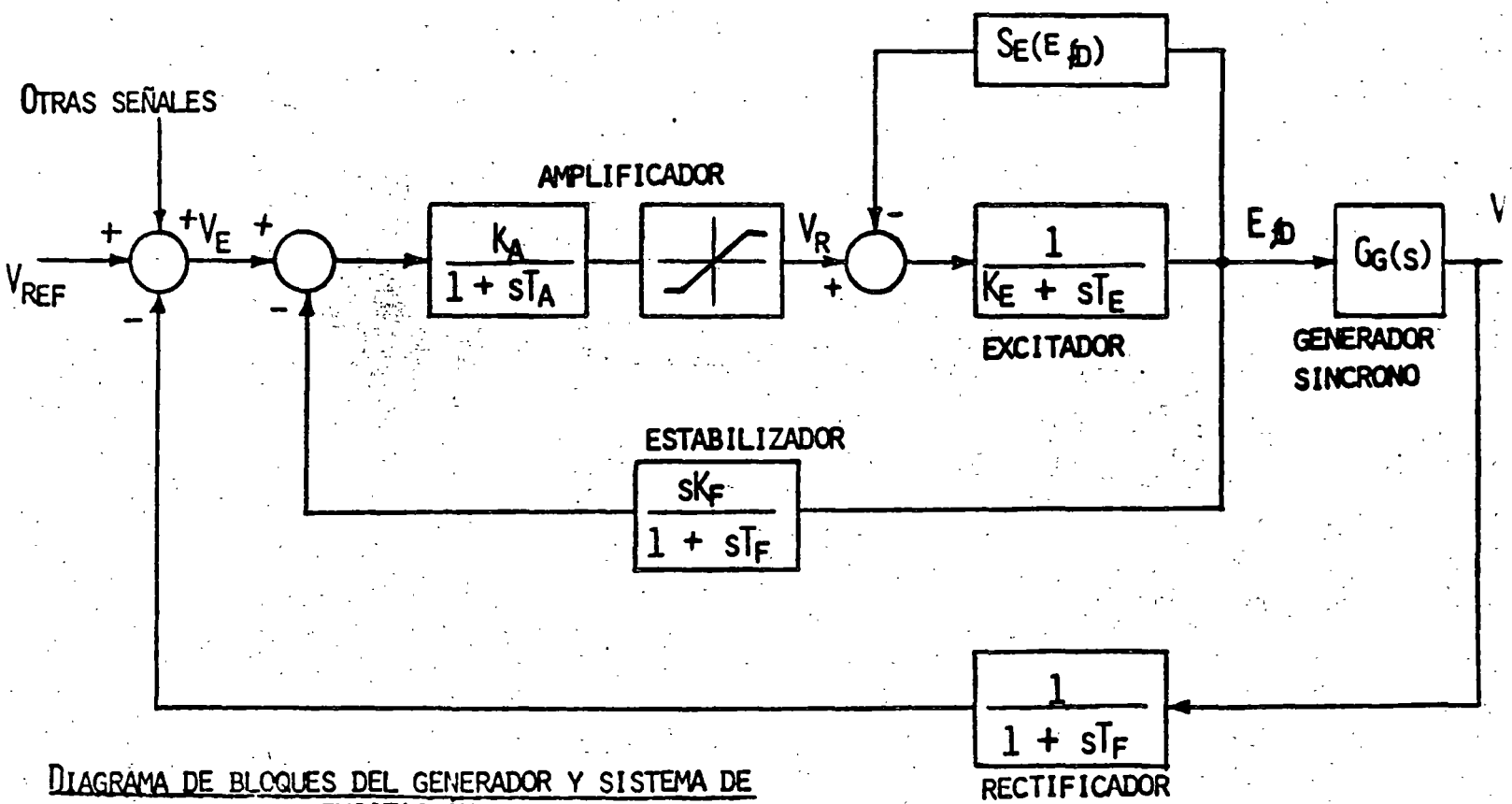
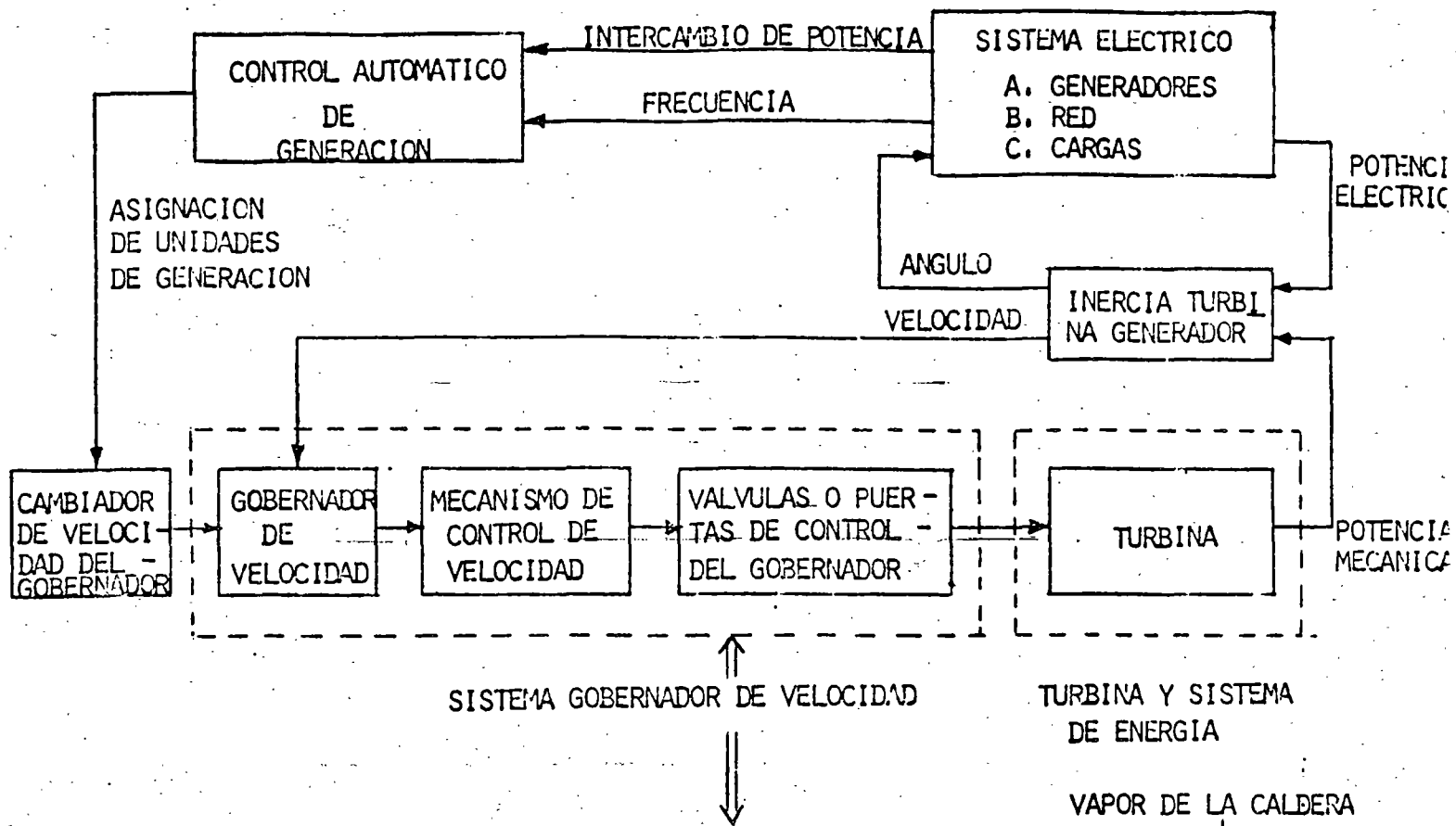


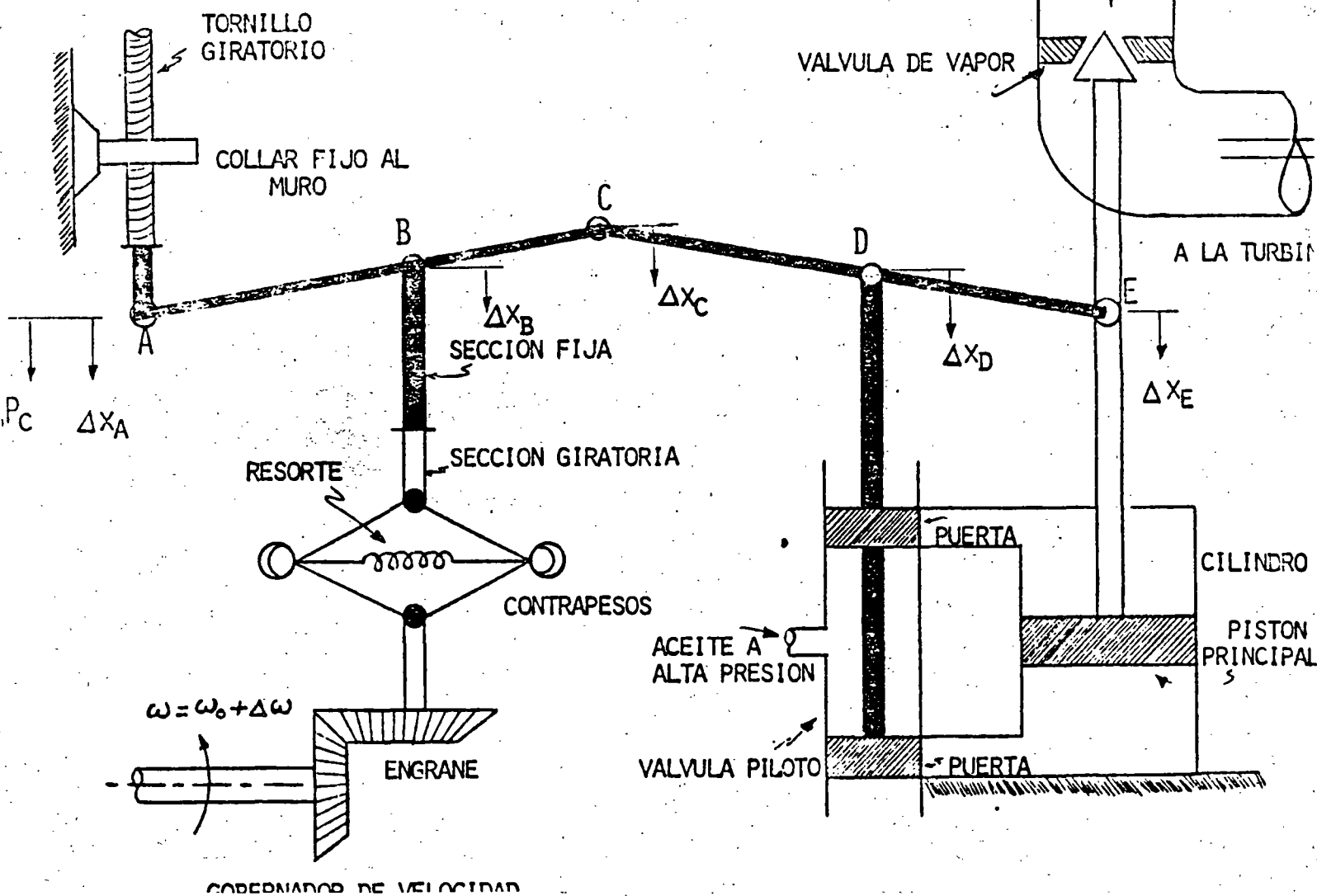
DIAGRAMA DE BLOQUES DEL GENERADOR Y SISTEMA DE EXCITACION

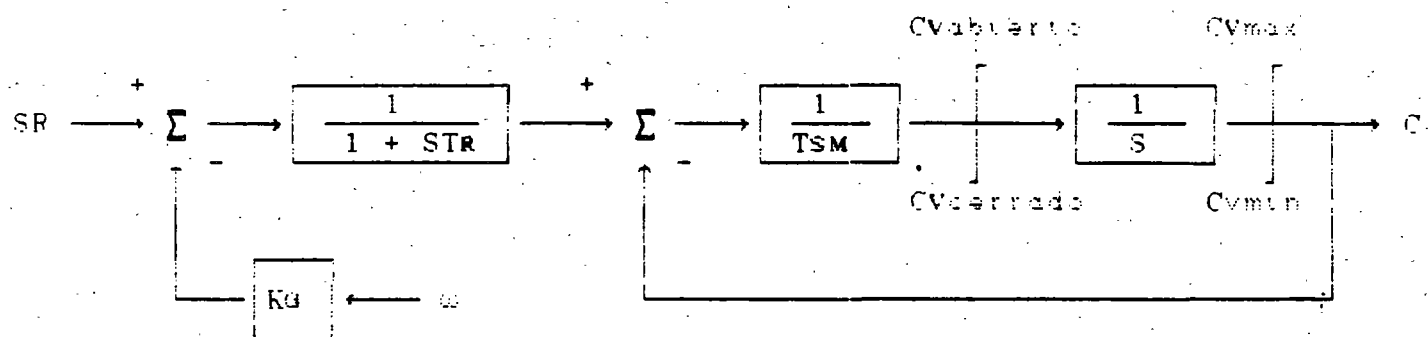


SISTEMA GOBERNADOR DE VELOCIDAD

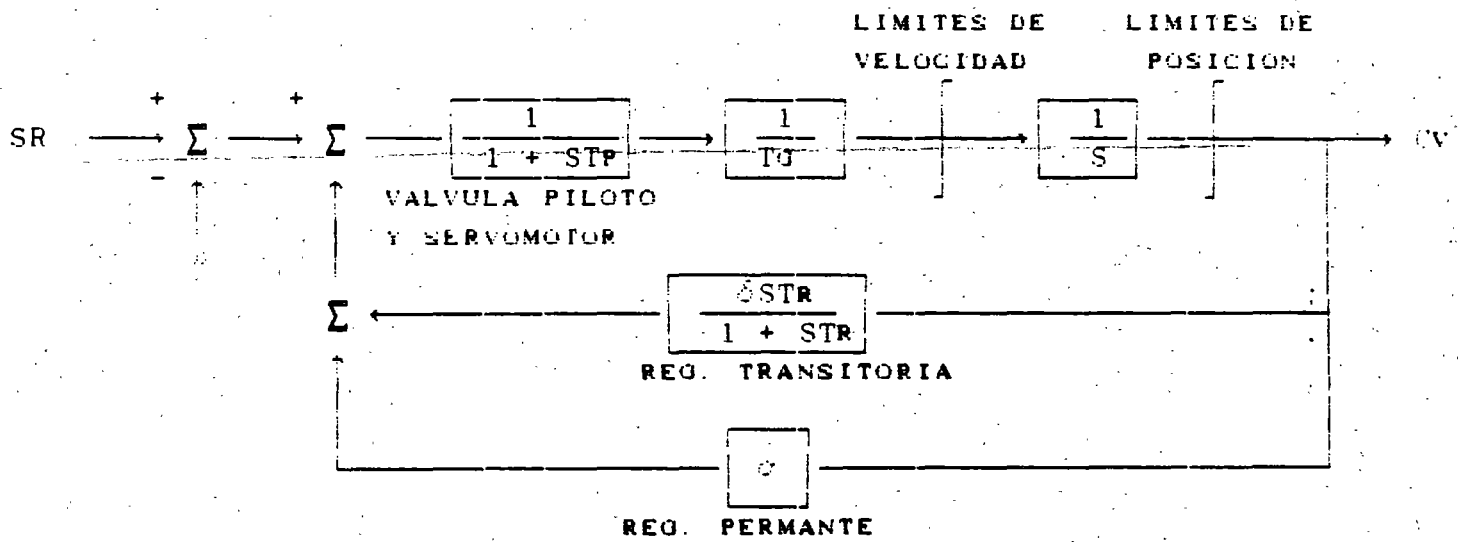
TURBINA Y SISTEMA DE ENERGIA

VAPOR DE LA CALDERA



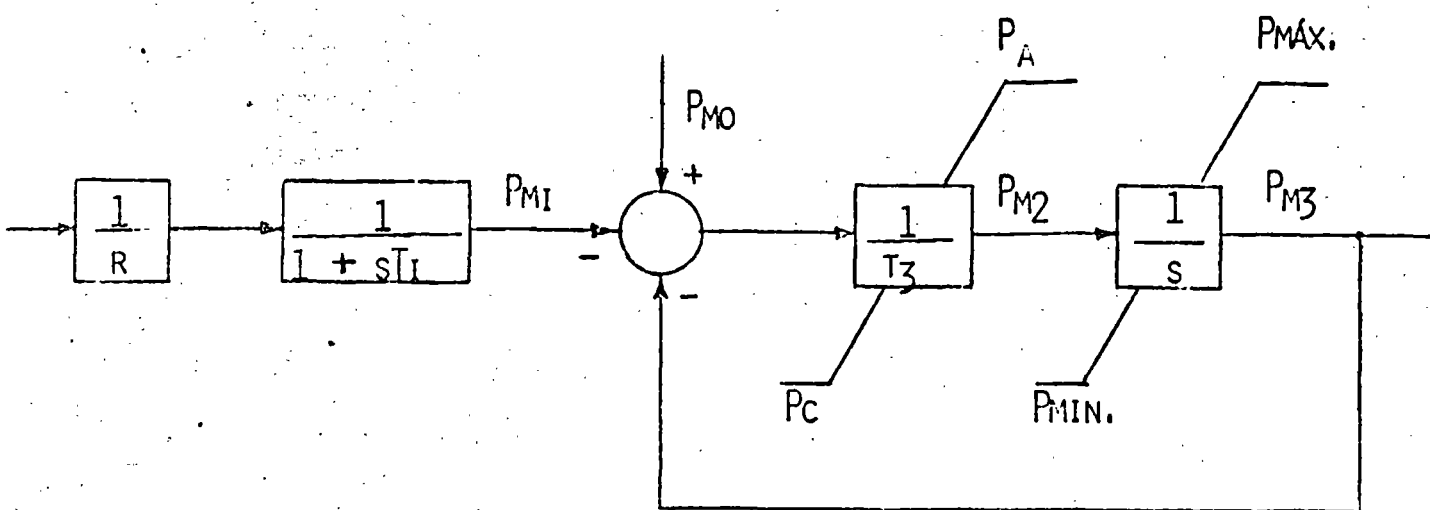


GOBERNADOR MECANICO - HIDRAULICO (TURBO)



GOBERNADOR MECANICO - HIDRAULICO (HIDRO)

DIAGRAMA DE BLOQUES DEL SUBSISTEMA DE CONTROL DE VELOCIDAD DE UNIDADES TÉRMICAS.



R - CARACTERÍSTICAS DE REGULACION EN ESTADO ESTABLE.

T₁ - CONSTANTE DE TIEMPO DEL RELEVADOR DE VELOCIDAD.

T₃ - CONSTANTE DE TIEMPO DEL SERVOMOTOR.

P_A, P_C - VELOCIDAD MÁXIMA PARA LA APERTURA Y CIERRE DE VÁLVULAS.

P_{MÁX.}, P_{MÍN.} - POSICIÓN MÁXIMA Y MÍNIMA DE VÁLVULAS.

P_{M0} - POSICIÓN ACTUAL DE VÁLVULAS.

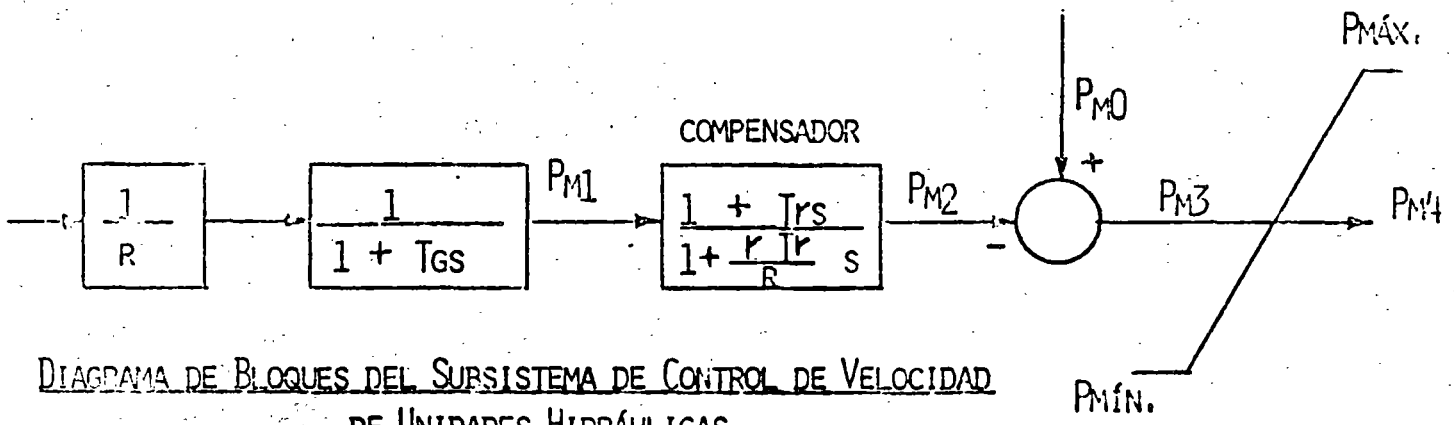


DIAGRAMA DE BLOQUES DEL SUBSISTEMA DE CONTROL DE VELOCIDAD DE UNIDADES HIDRÁULICAS

T_r - CONSTANTE DE TIEMPO DEL DASHPOT.

R - CARACTERÍSTICAS DE REGULACIÓN DE ESTADO ESTABLE.

T_G - TIEMPO PARA PRODUCCIÓN 1.0 P.U. DE APERTURA EN LA VÁLVULA COMO RESPUESTA A UN CAMBIO DE 1.0 P.U. DE VELOCIDAD.

r - CARACTERÍSTICAS DE REGULACIÓN TRANSITORIA.

P_{M0} - POSICIÓN ACTUAL DE VÁLVULA.

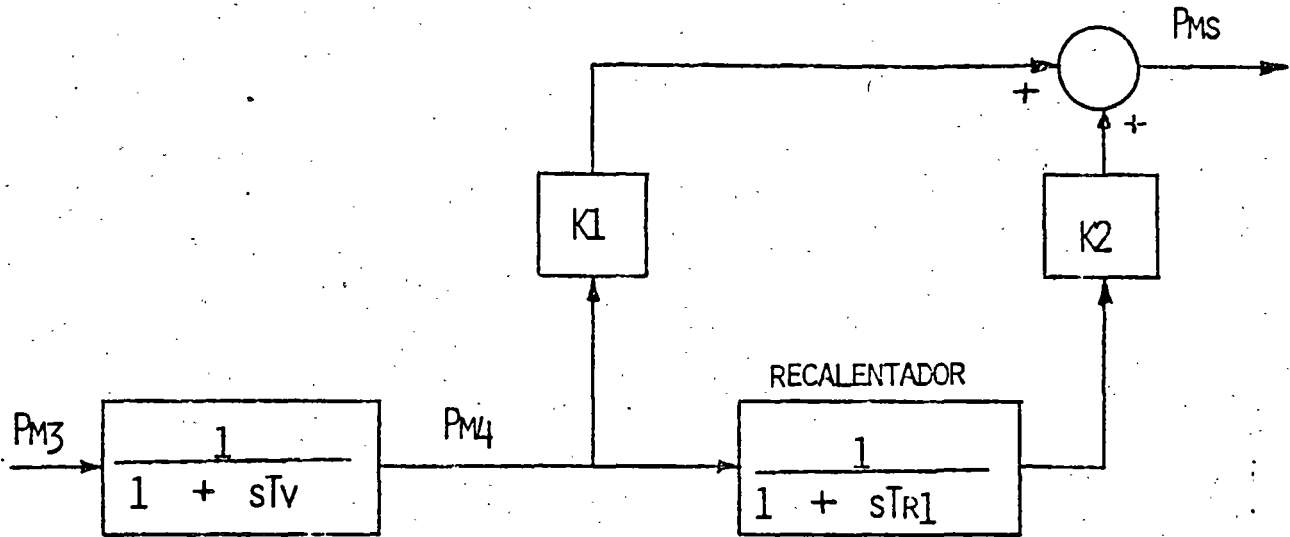
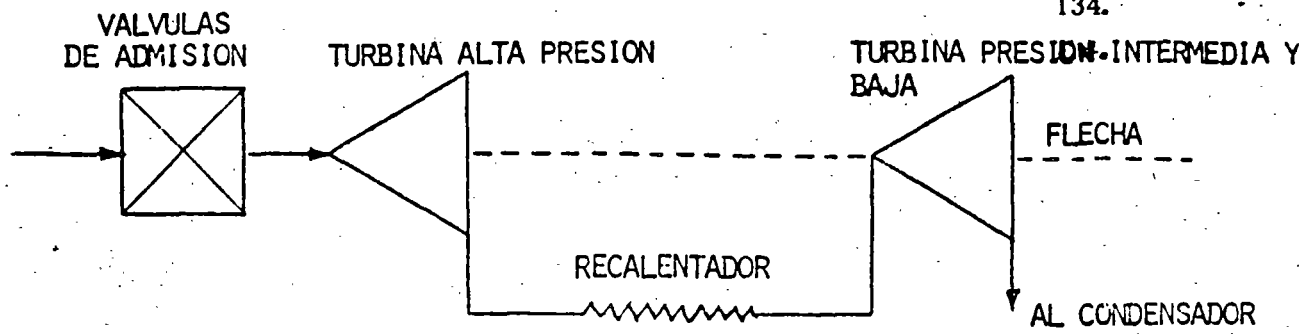


DIAGRAMA DE BLOQUES PARA TURBINAS DE VAPOR

T_V - CONSTANTE DE TIEMPO DEL VOLUMEN DE ENTRADA DE VAPOR.

T_{R1} - CONSTANTE DE TIEMPO DEL RECALENTADOR.

K_1, K_2 - FRACCIONES DE POTENCIA MECÁNICA.

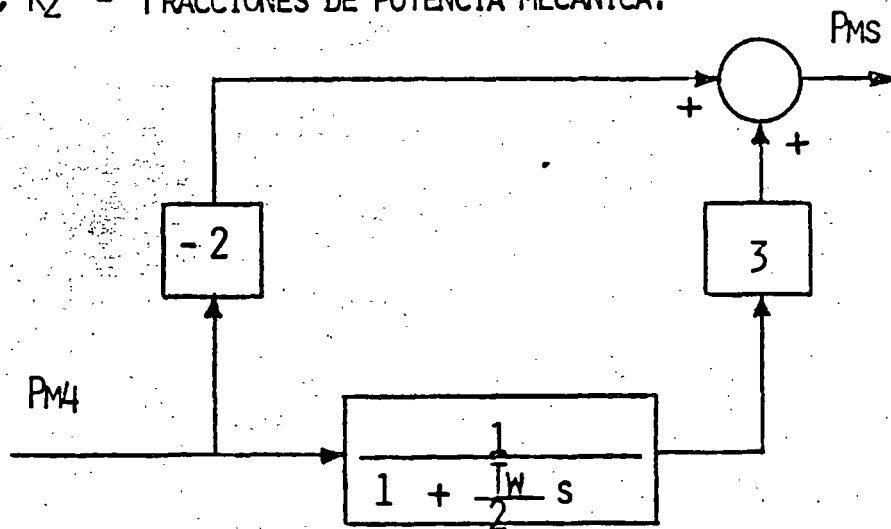


DIAGRAMA DE BLOQUES PARA TURBINAS HIDRÁULICAS

T_W - CONSTANTE DE TIEMPO DE LA INERCIA DEL AGUA.

MODELACIÓN DE LA CARGA

$$P = \left(\frac{F}{F_0} \right)^{f_P} \left(\frac{V}{V_0} \right)^{v_P} P_0$$

$$Q = \left(\frac{F}{F_0} \right)^{f_Q} \left(\frac{V}{V_0} \right)^{v_Q} Q_0$$

(P_0, Q_0) - VALORES BASE DE POTENCIA ACTIVA Y REACTIVA.

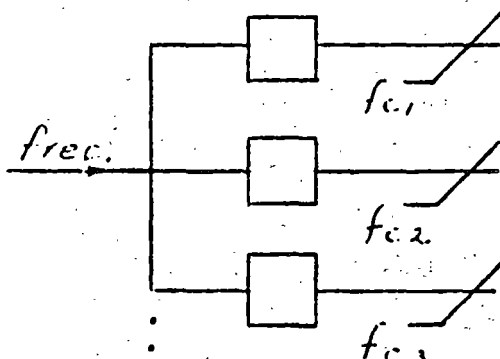
(P, Q) - VALORES DE POTENCIA ACTIVA Y REACTIVA AFECTADOS POR VOLTAJE Y FRECUENCIA.

(V_0, F_0) - VALORES BASE DE VOLTAJE Y FRECUENCIA.

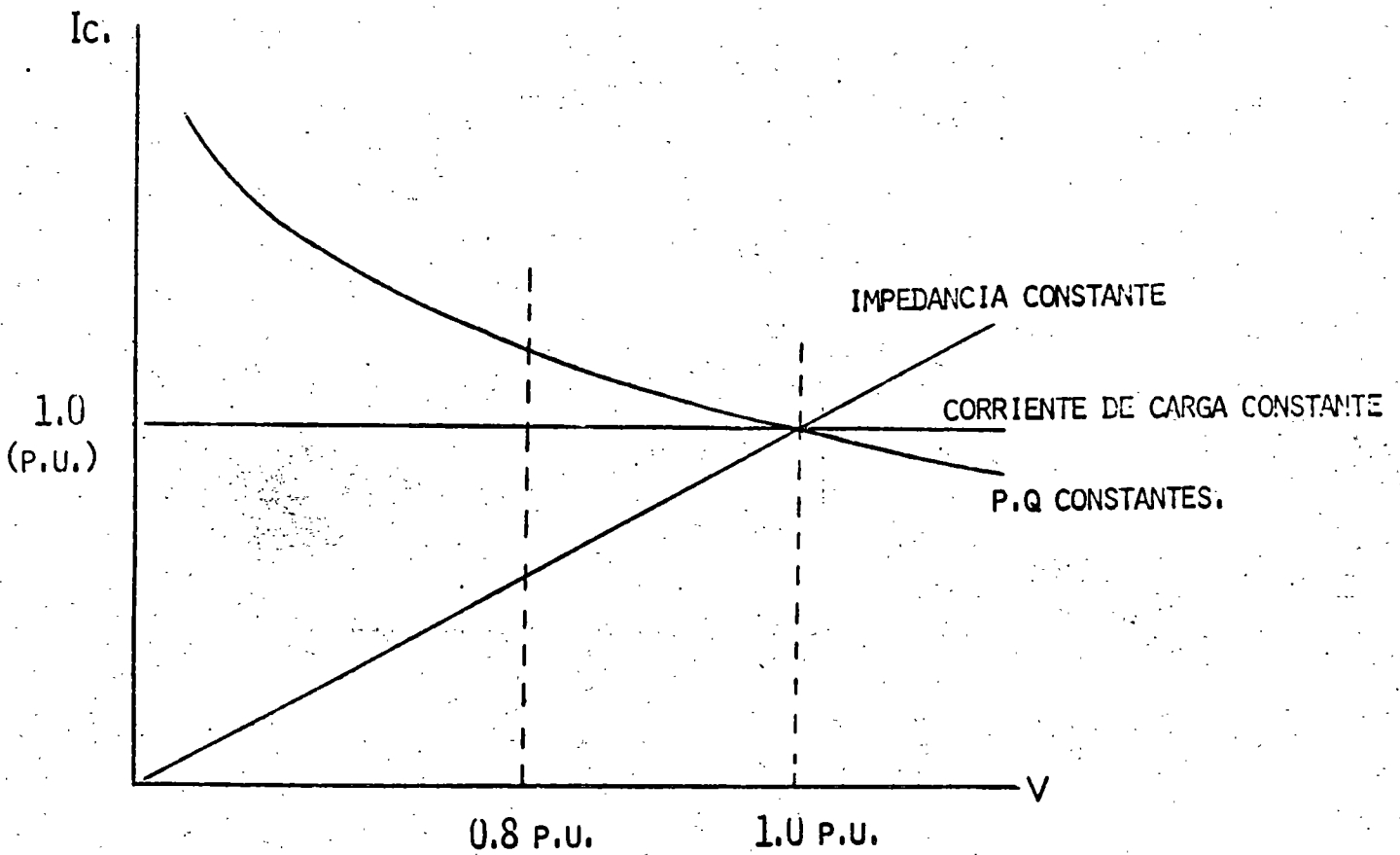
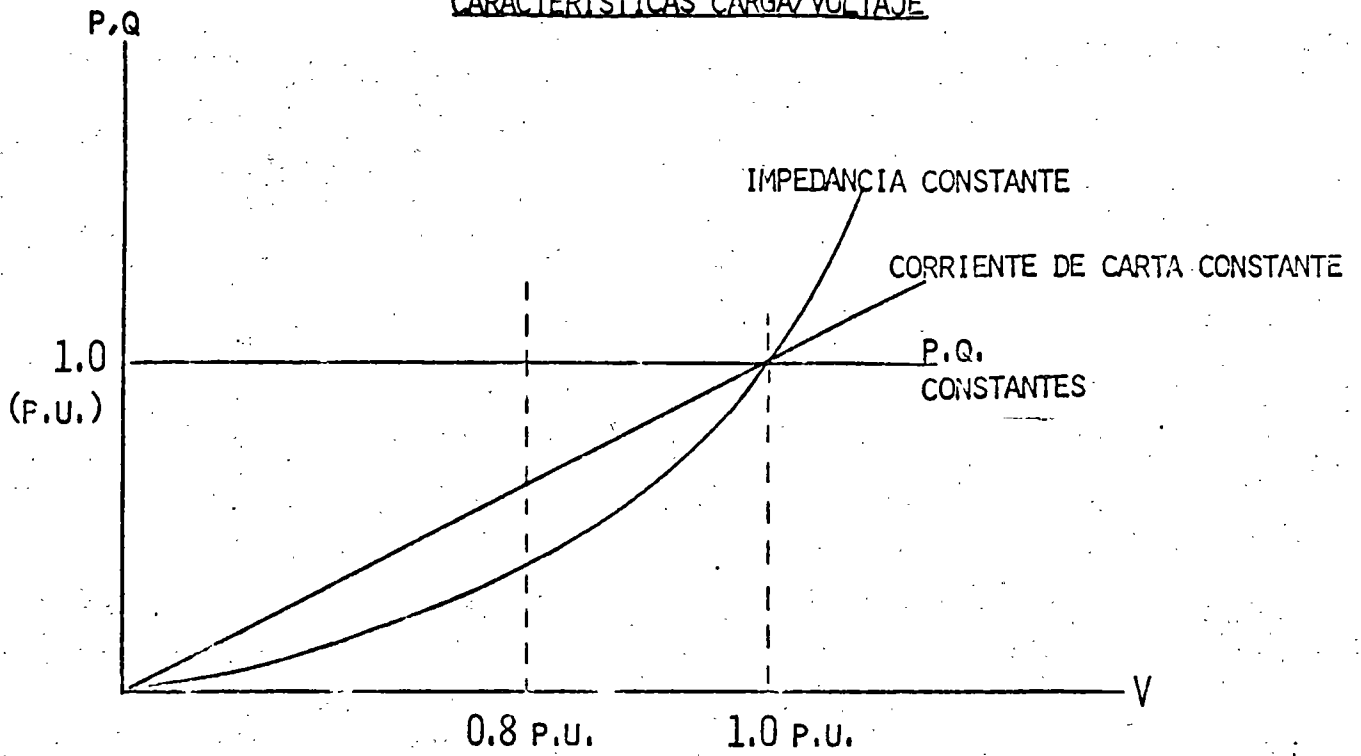
(V, F) - VALORES EN EL TIEMPO DE VOLTAJE Y FRECUENCIA.

TIPOS DE CARGA

f_P	f_Q	v_P	v_Q	C A R G A
0	0	0	0	POTENCIA CONSTANTE
0	0	1	1	CORRIENTE CONSTANTE
0	0	2	2	IMPEDANCIA CONSTANTE
1	1	0	0	DEPENDENCIA LINEAL UNITARIA DE LA FRECUENCIA.

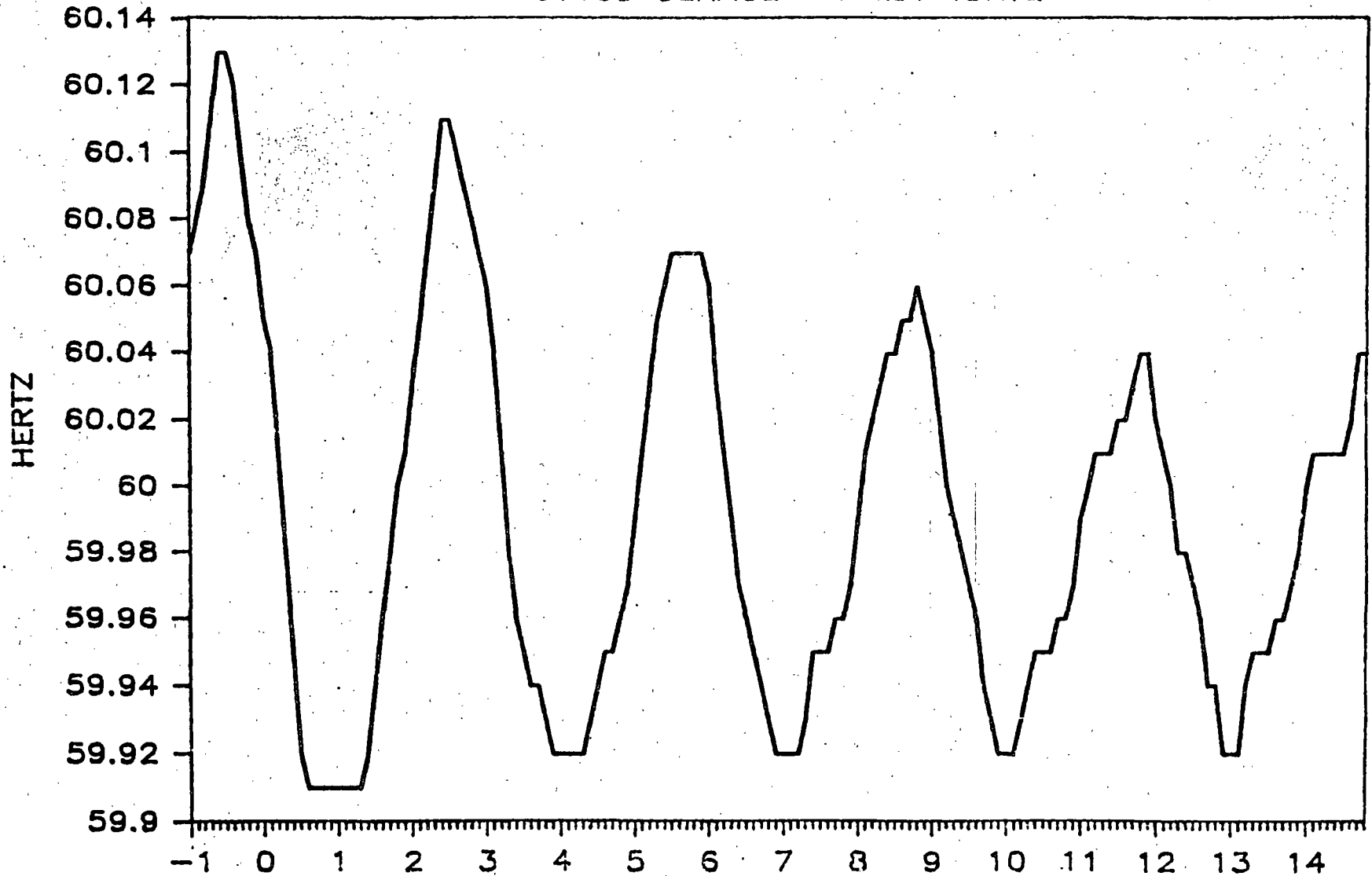
DESCONEXIÓN DE AUTOMÁTICA DE CARGA

$$f_{c1} > f_{c2} > f_{c3}$$

CARACTERÍSTICAS CARGA/VOLTAJECARACTERÍSTICAS CORRIENTE DE CARGA/VOLTAJE

FRECUENCIA GPL-230 POR DISP. PRD - T

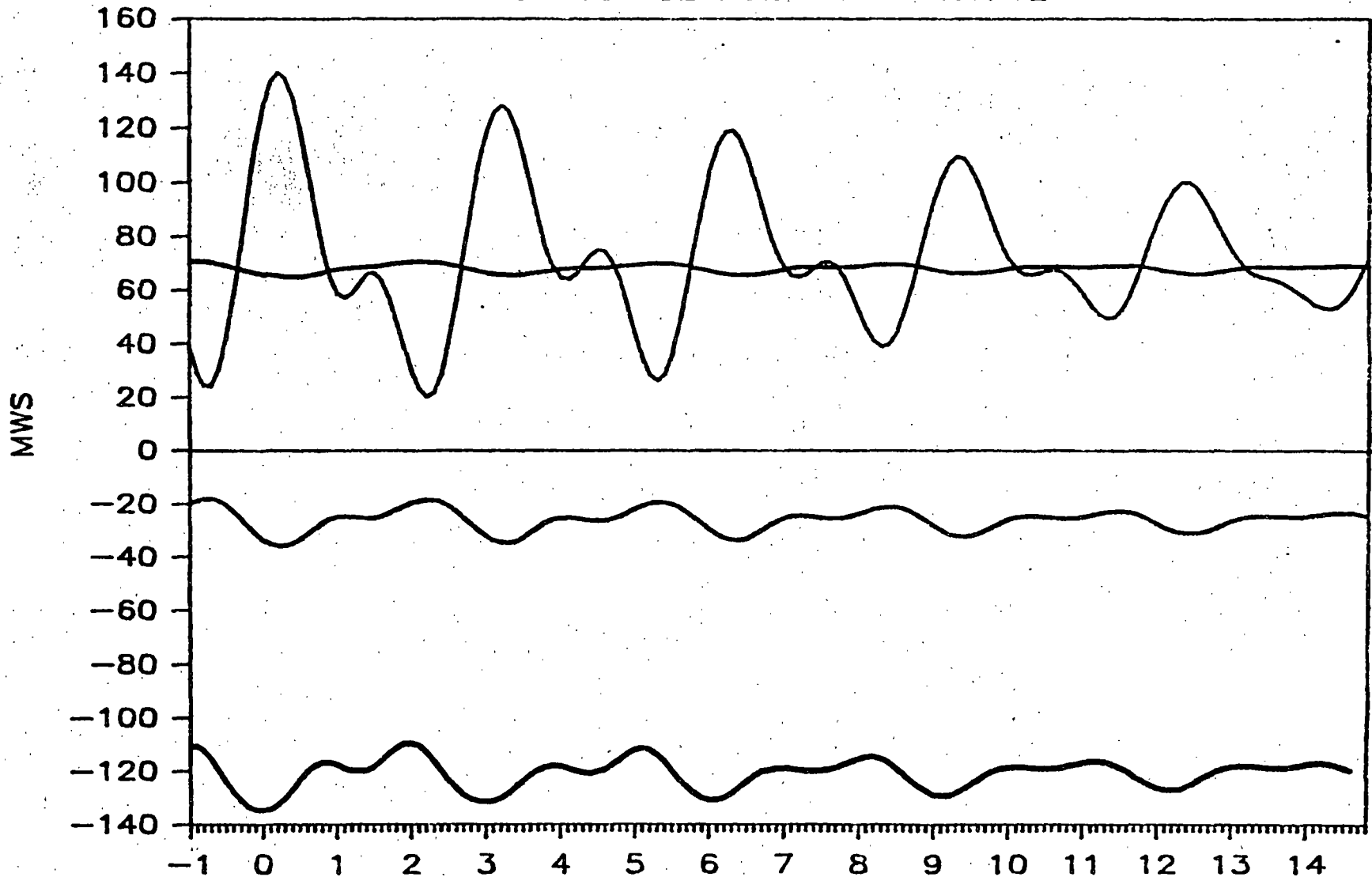
861105 CENACE - AREA NORTE



— SEG.
93020

FLUJOS LINEAS GPL * DISP. PRD-TUL *

861105 CENACE - AREA NORTE



— 93020 — 93030 — 93040 — 92980

SEG.

73050

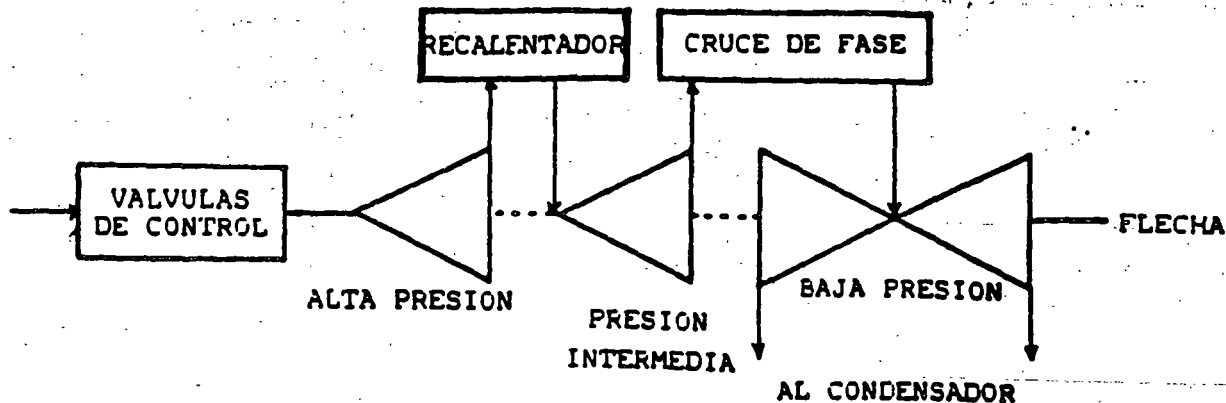


Figura 1. Diagrama esquemático de la turbina térmica con recalentamiento.

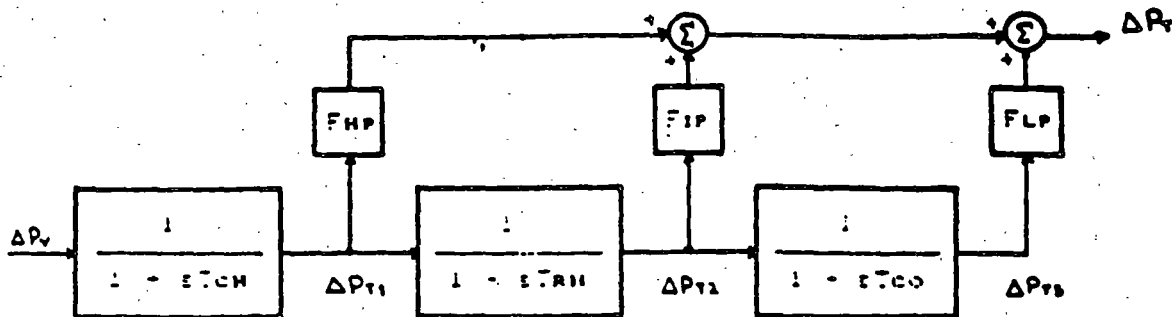


Figura 2. Modelo en bloques de la turbina térmica con recalentamiento.

$$\begin{bmatrix} \Delta F \\ \Delta F_{T3} \\ \Delta F_{T2} \\ \Delta F_{T1} \\ \Delta F_v \end{bmatrix} = \begin{bmatrix} -1 \cdot T_p & F_{LP}/P \cdot T_p & F_{IP}/P \cdot T_p & F_{HP}/P \cdot T_p & 0 \\ 0 & -1 \cdot T_{CO} & 1 \cdot T_{CO} & 0 & 0 \\ 0 & 0 & -1 \cdot T_{RH} & 1 \cdot T_{RH} & 0 \\ 0 & 0 & 0 & -1 \cdot T_{CH} & 1 \cdot T_{CH} \\ -1 \cdot P \cdot T_H & 0 & 0 & 0 & -1 \cdot T_H \end{bmatrix} \begin{bmatrix} \Delta F \\ \Delta F_{T3} \\ \Delta F_{T2} \\ \Delta F_{T1} \\ \Delta F_v \end{bmatrix}$$

$$+ \begin{bmatrix} -1 \cdot P \cdot T_p \\ 0 \\ 0 \\ 0 \\ 0 \end{bmatrix} \Delta P_L + \begin{bmatrix} 0 \\ 0 \\ 0 \\ 0 \\ 1 \cdot T_H \end{bmatrix} \Delta P_{REF}$$

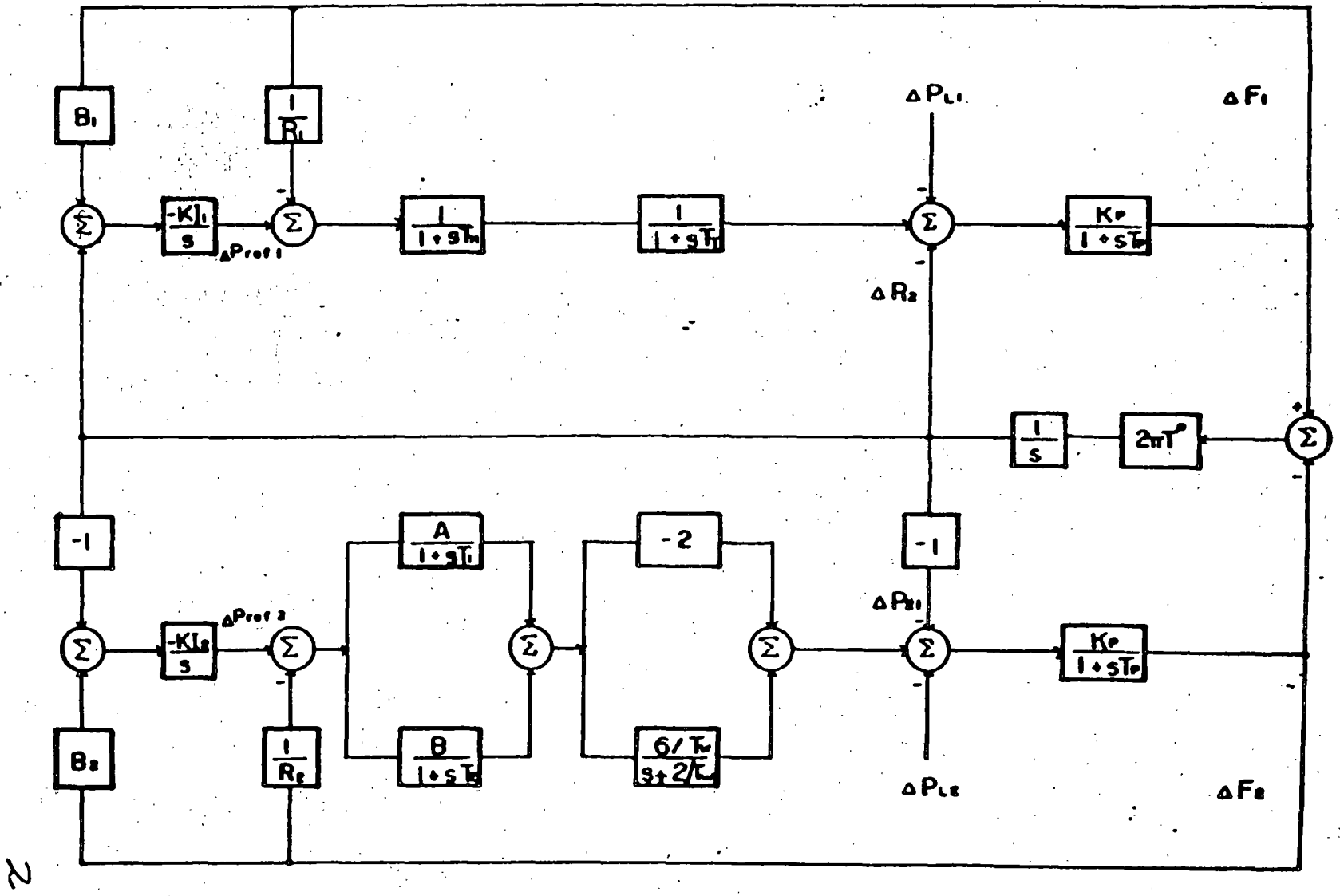


Figura 1 Regulación secundaria para dos áreas con control de interconexiones

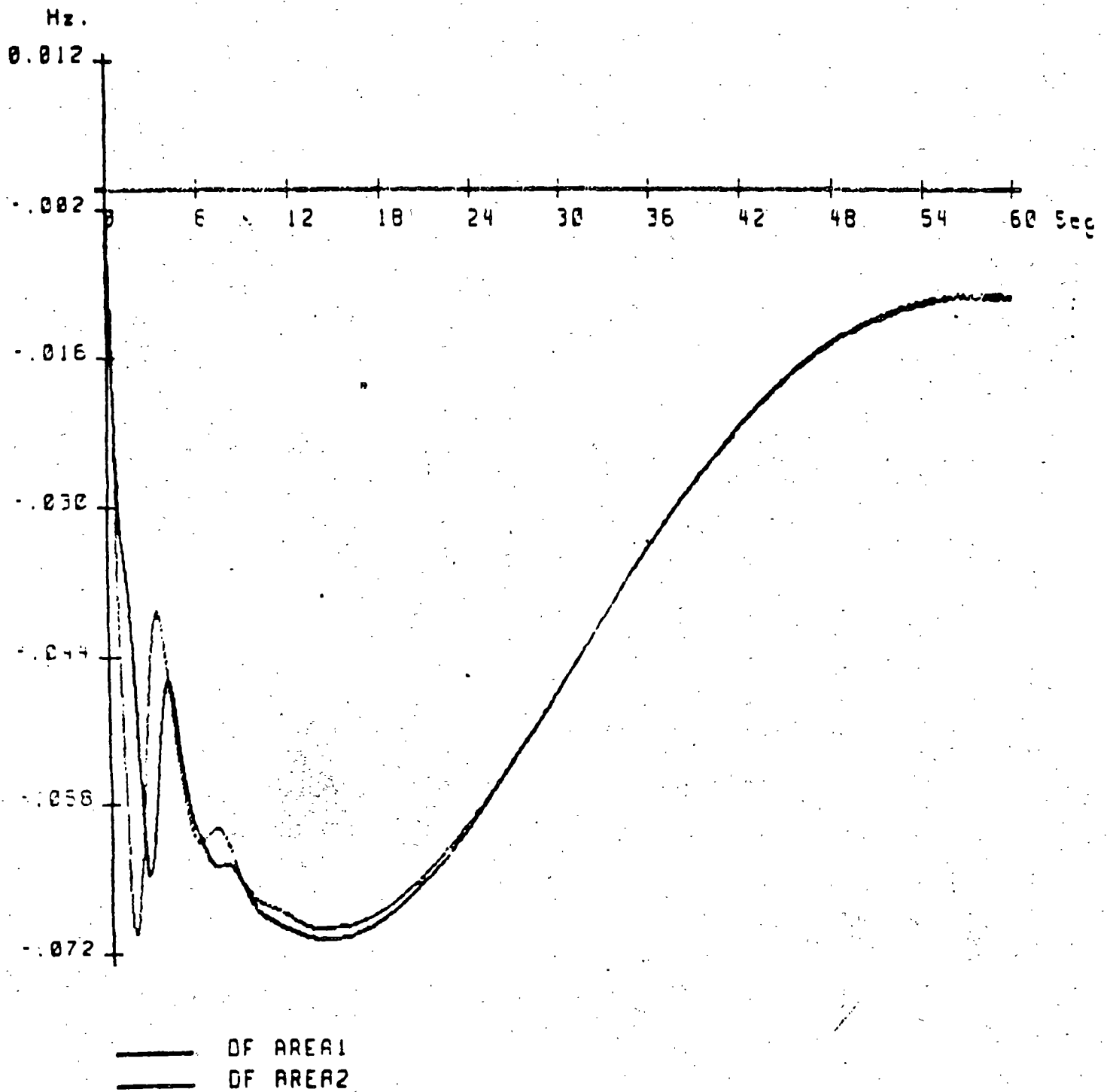
$$A = \begin{bmatrix} \frac{1}{T_P} & 0 & \frac{K_P}{T_P} & 0 & 0 & 0 & 0 & 0 & 0 & 0 & -\frac{K_P}{T_P} \\ 0 & -\frac{1}{T_P} & 0 & \frac{K_P}{T_P} & 0 & -\frac{2K_P}{T_P} & -\frac{2K_P}{T_P} & 0 & 0 & 0 & \frac{K_P}{T_P} \\ 0 & 0 & -\frac{1}{T_T} & 0 & \frac{1}{T_T} & 0 & 0 & 0 & 0 & 0 & 0 \\ 0 & 0 & 0 & -\frac{2}{T_V} & 0 & \frac{6}{T_V} & \frac{6}{T_V} & 0 & 0 & 0 & 0 \\ -\frac{1}{R_1 T_H} & 0 & 0 & 0 & -\frac{1}{T_H} & 0 & 0 & \frac{1}{T_H} & 0 & 0 & 0 \\ 0 & -\frac{A}{R_2 T_1} & 0 & 0 & 0 & -\frac{1}{T_1} & 0 & 0 & \frac{A}{T_1} & 0 & 0 \\ 0 & -\frac{B}{R_2 T_2} & 0 & 0 & 0 & 0 & -\frac{1}{T_2} & 0 & \frac{B}{T_2} & 0 & 0 \\ -K_{I1} B_1 & 0 & 0 & 0 & 0 & 0 & 0 & 0 & 0 & 0 & -K_{I1} \\ 0 & -K_{I2} B_2 & 0 & 0 & 0 & 0 & 0 & 0 & 0 & 0 & K_{I2} \\ 2\pi T^0 & -2\pi T^0 & 0 & 0 & 0 & 0 & 0 & 0 & 0 & 0 & 0 \end{bmatrix}$$

$$X = \begin{bmatrix} \Delta F_1 \\ \Delta F_2 \\ \Delta P_T \\ \Delta P_{T1} \\ \Delta P_V \\ \Delta P_{V1} \\ \Delta P_{V2} \\ \Delta P_{r1} \\ \Delta P_{r2} \\ \Delta P_{i2} \end{bmatrix}$$

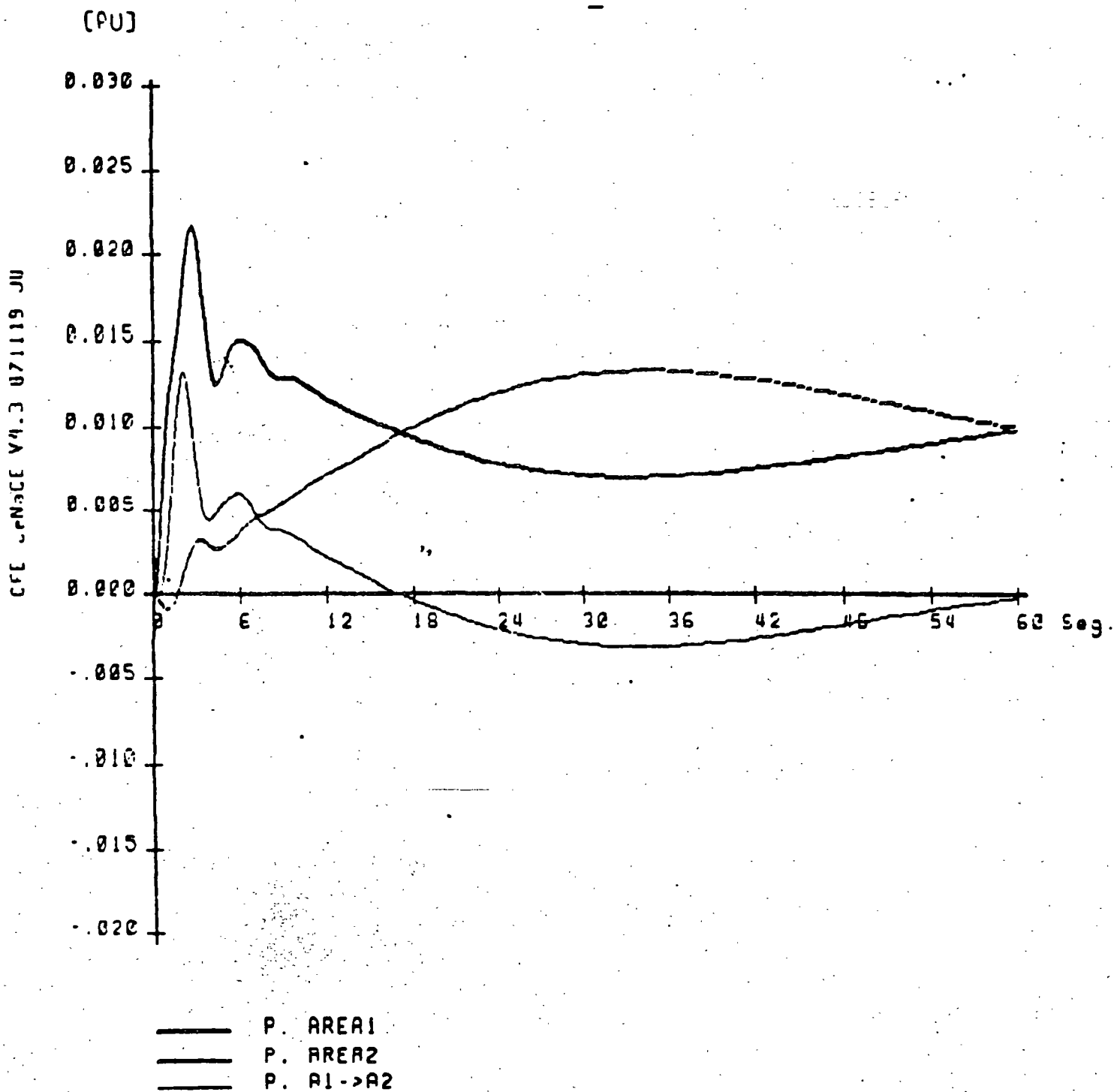
$$BU = \begin{bmatrix} -K_P/T_P \Delta P_{i1} \\ -K_P/T_P \Delta P_{i2} \\ 0 \\ 0 \\ 0 \\ 0 \\ 0 \\ 0 \\ 0 \\ 0 \end{bmatrix}$$

3

GRAFICAS DE VARIACION DE FRECUENCIA (caso 2)



VARIACION DE POTENCIA MECANICA Y DE POTENCIA
DE INTERCONEXION
(caso 2)





**FACULTAD DE INGENIERIA U.N.A.M.
DIVISION DE EDUCACION CONTINUA**

***CURSO INTERNACIONAL DE SISTEMAS ELECTRICOS DE
POTENCIA***

MODULO II

SISTEMAS ELECTRICOS DE POTENCIA II

SOBRETENSIONES Y COORDINACION DE ASILAMENTOS

1996

I. OBJETIVO

El programa de la asignatura de sobretensiones y coordinación de aislamiento debe cumplir con cuatro objetivos primordiales:

1. Ofrecer el conocimiento de las causas y características de los esfuerzos eléctricos o sobretensiones que se presentan en un sistema de potencia, desarrollando en el alumno la capacidad de realizar cálculos analíticos y digitales a partir de modelos del sistema sujeto a estudio. Presentar los medios disponibles para reducir la magnitud de las sobretensiones y proteger los elementos del sistema.

2. Describir el comportamiento de aislamientos gaseosos, líquidos y sólidos bajo diferentes tipos de esfuerzo eléctrico en cuanto a los fenómenos físicos involucrados en la ruptura dieléctrica y la descripción probabilística del aguante. Incluyendo una introducción general a los medios utilizados en laboratorios para reproducir sobretensiones características y los procedimientos de prueba a partir de los cuales se define el aguante de un aislamiento.

3. Combinar los dos elementos anteriores para diseñar el nivel de aislamiento de un sistema de potencia. Llegando a un balance entre el aguante del aislamiento bajo un esfuerzo eléctrico determinado, el costo inherente en la selección del nivel de aislamiento y la fiabilidad de los elementos del sistema.

4. Exponer la importancia económica del tema, lo cual incluye los siguientes aspectos:

* El costo de inversión adicional incurrido por la compañía que ofrece el suministro eléctrico al sobrediseñar el aislamiento de un sistema por falta de conocimiento de la magnitud y probabilidad de ocurrencia de los esfuerzos eléctricos a que está sujeto el mismo.

* La destrucción y deterioro sufridos por los elementos del sistema de potencia debido a los distintos tipos de esfuerzo eléctrico.

* La reducción en la calidad del suministro de energía eléctrica debida a fallas producidas por sobretensiones y el costo de la falla para el usuario de la energía eléctrica.

II. TEMARIO

1. Introducción

- 1.1 Fallas por sobretensiones en la red troncal del sistema interconectado mexicano
- 1.2 Clasificación de sobretensiones
- 1.3 Descripción del aislamiento en base a su aguante a un esfuerzo eléctrico
- 1.4 Nociones de coordinación de aislamiento

2. Ondas viajeras en líneas de transmisión

- 2.1 Modelos de líneas de transmisión
- 2.2 Conductividad finital del terreno
- 2.3 Efecto corona

3. Componentes modales

4. Sobretensiones por descargas atmosféricas

- 4.1 Física y parámetros de una descarga atmosférica
- 4.2 Blindaje de líneas de transmisión
- 4.3 Modelo de una descarga directa a una línea
- 4.4 Flameo inverso
- 4.5 Sobretensiones inducidas por descargas atmosféricas

5. Sobretensiones por maniobra

- 5.1 Cierre y recierre de líneas de transmisión
- 5.2 Maniobras en circuitos inductivos
- 5.3 Interrupción prematura de pequeñas corrientes inductivas
- 5.4 Corte virtual de una corriente inductiva
- 5.5 Reignición del arco en el interruptor
- 5.6 Interrupción de corrientes capacitivas

6. Sobretensiones temporales

6.1 Fallas a tierra

6.2 Cambios repentinos en la carga

6.3 Efecto Ferranti

6.4 Energización de líneas terminadas en transformador

6.5 Ferrðresonancia

7. Transitorios en subestaciones encapsuladas en SF6

8. Medios para reducir esfuerzos eléctricos en sistemas de potencia

8.1 Efecto de los parámetros del sistema en las magnitud y duración de las sobretensiones

8.2 Apartarrayos (historia, descripción, características)

8.3 Selección de apartarrayos

9. Conceptos básicos de ruptura dieléctrica de gases, líquidos y sólidos

10. Probabilidad y estadística aplicada a la coordinación de aislamiento

11. Nivel de aislamiento de un sistema

11.1 Equipos de laboratorio utilizados para reproducir los distintos tipos de sobretensiones

11.2 Definición del aguante de elementos del sistema de potencia en base a pruebas de laboratorio

12. Dimensionamiento de líneas y subestaciones

12.1 Compactación de líneas y subestaciones

13. Estándares nacionales e internacionales de coordinación de aislamiento.

Introduction

Power system networks are subjected to many forms of transient phenomena ranging from the relatively slow electromechanical oscillations associated with synchronous machine instability to the comparatively fast variations in voltage and current brought about by sudden changes in the steady state values of one or other of these quantities. The fast transients contain components with a relatively high frequency, for instance, about 70 kHz in the transient overvoltage produced by the clearance of a 1 km short-line fault.

Sudden changes in voltage and current may be the result of a lightning stroke or some malfunction of the system, or they may be due to the deliberate switching of a part of the system. Lightning is a common cause of faults and subsequent circuit outages, but faults can and do occur for many other reasons. Malfunctioning of the system can occur in numerous ways and has a variety of consequences; e.g. an open circuit of one phase can lead to a rearrangement of circuit inductances and capacitances in such a manner that a resonant circuit is produced and excited with large values of voltage and/or current as a consequence. Other types of malfunctioning may lead to abnormal voltage and current conditions which are sustained rather than transitory in nature. Transient overvoltages are produced by both the opening and closing of a circuit breaker and their calculation and assessment is the particular concern of this monograph.

Because of their importance in the design of switchgear, the transient voltages generated by the opening of a circuit breaker were originally regarded with more interest than those due to circuit breaker closure. These latter do not particularly affect the operation of the circuit breaker and in the past they did not exceed the insulation level of the system which, for the lower operating voltages then in use, was governed entirely by lightning considerations. Over the years, the

voltages at which electrical power is transmitted over long distances have been increasing continually, and many systems are now in operation at 400, 500 and 750 kV and transmission at 1000 kV is under investigation.

Because the magnitudes of lightning surges on transmission lines are not greatly affected by the line design, the lightning performance of the line shows an improvement with increasing operating-voltage level. In contrast, system-generated overvoltages are directly related to the system voltage and their magnitudes increase as the system voltage increases. As a result, at operating voltages of 400 kV and above, system-generated overvoltages play an increasingly large part in determining the insulation level of the system. In this context the overvoltages caused by the energisation of transmission lines are particularly significant since, given the necessary conditions, overvoltage levels of over three times the phase to neutral voltage are possible. Although the system insulation level must be sufficiently high in order not to hazard the reliability of the system, at the same time there are strong economic reasons for keeping it as low as possible. A result of these developments is that a much greater emphasis is being placed on the need for the ability to predict system overvoltages at the planning stage, in order that steps may be taken to reduce their severity and for minimisation of the system insulation level, as far as possible.

For the purpose of calculating switching transients the elements of a power system may be divided into two types: first, those whose parameters are essentially lumped, such as generators, transformers, reactors and capacitors and secondly, overhead lines and underground cables whose parameters are of a distributed nature. When a switching operation takes place these circuit elements are subjected to voltages and currents having a wide frequency range which may extend from 50 Hz to the region of 100 kHz. Over such a range the values of the system parameters and of the earth path are not constant but vary with frequency.

Ideally, the method of calculation used should be capable of representing both lumped and distributed parameters equally well, and of faithfully reproducing the variation of their values with frequency. In addition, it should be able to represent the effect of nonlinearities such as those due to surge diverters, magnetic saturation, corona and the circuit breaker arc. In practice such a method is not easily achieved, and currently use methods represent a compromise in some respect, the particular compromise arrived at being governed by the specific requirements of the user. Difficulties inherent in the calculation of transients are not confined to method alone. The provision of sufficiently

accurate and extensive system data also has its problems, and is of considerable importance, since the accuracy of any calculation cannot be better than the data on which it is based. For the most accurate results, full knowledge of the variation of the circuit elements with frequency is necessary, and this may not always be readily available.

The traditional method of assessing the severity of transient phenomena in power systems has been to use the transient network analyser (TNA) type of analogue computer, which provides facilities for forming a scale model of the system being studied, using lumped values of inductance, capacitance and resistance. Such models have been used by power system engineers for well over thirty years (Peterson, 1939) but by their very nature are liable to a size limitation. Eventually, problems are encountered which are too large to be accommodated without drastic simplification or an expensive extension of the facilities. The TNA can be advantageous in those cases where the exact mechanism of the transient phenomena under investigation is not immediately apparent and where the work is of an exploratory nature. A combination of analogue and digital facilities can be extremely powerful and, to be realistic, the two approaches should be seen as being complementary rather than competitive. Comparisons of the results from the two approaches tend to show a good overall correlation but with differences in the fine detail of the transient waveforms. Sophisticated TNA facilities are in use at the present time (Dickson *et al.*, 1973, Borgonovo *et al.*, 1974) and in some cases are closely linked to digital facilities (Morsztyn *et al.*, 1969, Bowles *et al.*, 1972).

Unfortunately, power supply systems are so complex that a truly analytical solution of any but the simplest problem is virtually impossible. Even a numerical approach was forbidding until the advent of a powerful digital computer which proved not only a necessary tool but also a stimulus to the development of new techniques. It is the purpose of this monograph to describe these developments and their application to practical problems.

The need for these methods as they apply particularly to transmission circuits has been emphasised in recent years. Firstly, by the fact that the use of higher transmission voltages has meant that system insulation level is determined largely by transient switching overvoltages rather than by lightning, and secondly, by the transient phenomena associated with the use of high-voltage underground cable (much of it crossbonded) in order to bring power into the larger centres of population. Since such transients depend to a great extent on the properties of overhead lines and underground cables it is not inappropriate therefore to commence with a consideration of the transmission line equations.

Basic analysis and system parameters

The general transmission-line problem is formulated on the assumption that a network representation is permissible. This is equivalent to postulating plane-wave propagation along the line, although it is known from Maxwell's equations that, in the presence of losses, this is not strictly true. Nevertheless, once the network concept is abandoned the problem has to be dealt with as a field problem, with all its attendant difficulties.

Once formulated in terms of differential equations these are solved for the particular simple cases which have been traditionally considered. However, modern methods of solutions are employed to serve as an introduction to the development of later Chapters.

The remainder of the Chapter is devoted to investigating some of the practical features which are subsequently to be taken into account. In particular, the manner in which the parameters of both lines and cables vary with frequency is discussed and illustrated.

2.1 Equations for multiwire transmission lines

An n -wire line above a conducting earth is generally described in terms of resistances and self-inductances; mutual inductances and capacitances; and capacitance and conductance to the earth. Then with

R_l, M_{ll}, C_{ll}, G_l = resistance, inductance, earth capacitance and conductance respectively, per unit length of the l th wire

M_{lm}, C_{lm} = mutual inductance and capacitance respectively, per unit length between the l th, m th wires

as illustrated in Fig. 2.1, it follows that

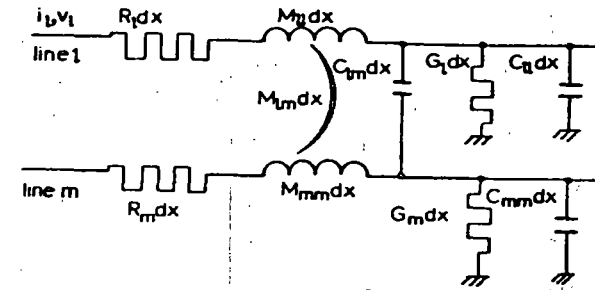


Fig. 2.1 Element of two phases of a multiphase line

$$\frac{\partial v_l}{\partial x} = - \sum_{m=1}^n M_{lm} \frac{\partial i_m}{\partial t} - R_l i_l \quad (2.1)$$

$$\frac{\partial i_l}{\partial x} = - \sum_{m=1}^n C_{lm} \frac{\partial}{\partial t} (v_l - v_m) - C_{ll} \frac{\partial v_l}{\partial t} - G_l v_l \quad (2.2)$$

These equations can be written in the matrix form

$$\frac{\partial v}{\partial x} = -Zi; \quad \frac{\partial i}{\partial x} = -Yv \quad (2.3)$$

where v, i are column matrices of the voltages to earth and currents of the n wires, and Z, Y (the impedance and admittance matrices respectively) are square matrices of order n with the

$$(r, s)\text{th element of } Z = M_{rs} \frac{\partial}{\partial t} + \delta_{rs} R_r \quad (2.4)$$

where $\delta_{rs} = 0$ if $r \neq s, \delta_{rr} = 1$ is the Kronecker delta, and the

$$(r, s)\text{th element of } Y = \begin{cases} -C_{rs} \frac{\partial}{\partial t}, & r \neq s \\ \sum_{q=1}^n C_{rq} \frac{\partial}{\partial t} + G_r, & r = s \end{cases} \quad (2.5)$$

Since Z, Y are each symmetric matrices, eqns. 2.3 can be combined to give

$$\frac{\partial^2 v}{\partial x^2} = Pv; \quad \frac{\partial^2 i}{\partial x^2} = \tilde{P}i \quad (2.6)$$

where $P = ZY$, and it is important to bear in mind that both Z and Y contain the differential operator with respect to time. In general the matrix P is not symmetric.

Whenever it is desired to carry out an integral transform with respect to time, eqns. 2.6 are written

$$\frac{d^2 \bar{v}}{dx^2} = \bar{P} \bar{v}; \quad \frac{d^2 \bar{i}}{dx^2} = \bar{P} \bar{i} \quad (2.7)$$

where $\bar{P} = \bar{Z} \bar{Y}$ and \bar{Z}, \bar{Y} are formed from Z, Y by replacing the time derivative by the transform parameter, provided that the system is quiescent up to time zero.

Although eqns. 2.6 are so readily formulated their solution is far from simple. Indeed, prior to the availability of digital computers, progress was only possible by the introduction of simplifying assumptions and the use of much ingenuity. Since many of the concepts of this early work are developed in later chapters it is instructive to consider briefly some important special cases which include the single-phase and the transposed 3-phase lines.

2.2 Single-phase lines

In a single line with earth return, the expressions in eqn. 2.7 (with the bar referring to the Laplace transform) reduce to

$$\frac{d^2 \bar{v}}{dx^2} = k^2 \bar{v}; \quad \frac{d^2 \bar{i}}{dx^2} = k^2 \bar{i}$$

where, dropping subscripts, $k^2 = (pM + R)(pC + G)$, and it is assumed that the line is charge-free prior to zero time. It is seen in Section 4.1 that the parameter k is related to the propagation constant of the line.

The general solutions are of the form (Lacey, 1941)

$$\bar{v} = A \exp(-kx) + B \exp(kx) \quad (2.8)$$

$$\bar{i} = \frac{1}{z} \{A \exp(-kx) - B \exp(kx)\} \quad (2.9)$$

where

$$z = Z_0 \left(\frac{\alpha + \beta + p}{\alpha - \beta + p} \right)^{1/2}$$

with

$$\alpha = \frac{R}{2M} + \frac{G}{2C}; \quad \beta = \frac{R}{2M} - \frac{G}{2C}; \quad Z_0 = \left(\frac{M}{C} \right)^{1/2}$$

and A, B are determined from the boundary conditions and are generally functions of the transform parameter p . The analysis can be carried further if the line parameters are such that k can be expressed as a linear function of p . This implies that $\beta = 0$ and $k = (p + \alpha)/\nu$, where

$\nu = (MC)^{-1/2}$. Then, on using the Heaviside Shift Theorem, the inverse Laplace transform of eqns. 2.8 and 2.9 assume the form

$$v = \exp(-\alpha t) \{F_1(x - \nu t) + F_2(x + \nu t)\} \quad (2.10)$$

$$i = \exp(-\alpha t) \{F_1(x - \nu t) - F_2(x + \nu t)\} / Z_0 \quad (2.11)$$

where

$$F_1(x - \nu t) \equiv 0 \quad \text{for } x - \nu t < 0$$

$$F_2(x + \nu t) \equiv 0 \quad \text{for } x + \nu t < 0$$

Thus the general solutions are seen to be combinations of a forward and a backward wave each travelling with velocity ν . Since each component of both the current and voltage waves is subject to the same attenuation $\exp(-\alpha t)$ the line is said to be *distortionless*.

In the special case of the *lossless* line $\alpha = R/(2M) = G/(2C) = 0$ so that the waves are propagated without attenuation. This simple treatment forms the basis for two well known graphical approaches; one due to Bewley (1933) and the other due to Schnyder (1929) and Bergeron (1935), which are developed further in Chapter 6.

2.3 3-phase transposed lines

A perfectly transposed line is taken to have the same parameters associated with each phase so that, in terms of the Laplace transform, the (r, s) th element of the \bar{Z}, \bar{Y} matrices can be written respectively as

$$\begin{aligned} pm, r \neq s: & \quad pM + R, r = s \\ \text{and} & \\ -pc, r \neq s; & \quad pC + G, r = s \end{aligned}$$

Then $\bar{P} (= \bar{Z} \bar{Y})$ has the symmetric form

$$\bar{P} = \begin{bmatrix} a & b & b \\ b & a & b \\ b & b & a \end{bmatrix} = \bar{P} \quad (2.12)$$

with

$$a = (pM + R)(pC + G) - 2p^2 mc$$

$$b = -p^2 (Mc + mc - mC) + p(-cR + mG)$$

With this simplification the analysis can be taken further by using the properties of the eigenvalues and eigenvectors of a matrix to convert eqn. 2.7 viz.

$$\frac{d^2 \bar{v}}{dx^2} = \bar{P} \bar{v}$$

into a diagonal form. This involves writing the \bar{v} -matrix in the form

$$\bar{v} = S \bar{v}_m \quad (2.13)$$

where S is a nonsingular matrix of order 3×3 which is independent of x , and \bar{v}_m is a 3×1 column matrix. Then eqn. 2.7 takes the form

$$\frac{d^2 \bar{v}_m}{dx^2} = S^{-1} \bar{P} S \bar{v}_m \quad (2.14)$$

in which S is chosen such that the matrix $(S^{-1} \bar{P} S)$ is diagonal.

To this end it is necessary to find the three scalars λ (the eigenvalues) and column matrices X (the eigenvectors) which satisfy

$$(\bar{P} - \lambda U)X = 0 \quad (2.15)$$

where U is the unit matrix of order 3.

With the \bar{P} of eqn. 2.12 the values of λ are given as the roots of the determinantal equation

$$\begin{vmatrix} a - \lambda & b & b \\ b & a - \lambda & b \\ b & b & a - \lambda \end{vmatrix} = 0$$

i.e. $\lambda = a - b, a - b, a + 2b$.

The corresponding eigenvectors are found by using each of these three eigenvalues in turn in eqn. 2.15. Then with X in the form

$$X = \begin{bmatrix} x_1 \\ x_2 \\ x_3 \end{bmatrix} = (x_1, x_2, x_3)$$

the repeated values of $\lambda = a - b$ yield

$$x_1 + x_2 + x_3 = 0$$

and it is possible to choose two independent solutions to this equation.

Possible choices for X are

$$\{1, (-1 + j\sqrt{3})/2, (-1 - j\sqrt{3})/2\}$$

$$\{1, (-1 - j\sqrt{3})/2, (-1 + j\sqrt{3})/2\}$$

as in the method of symmetrical components. However, this choice introduces complex elements, and it is usual in considering transient phenomena to choose

$$\{1, -\frac{1}{2}, -\frac{1}{2}\} = X_\alpha \text{ say, associated with } \lambda_\alpha = a - b$$

$$\{0, (\sqrt{3})/2, -(\sqrt{3})/2\} = X_\beta \text{ say, associated with } \lambda_\beta = a - b$$

The eigenvector associated with the eigenvalue $\lambda_0 = a + 2b$ can be chosen to be $\{1, 1, 1\} = X_0$, say. If the 3×3 matrix S is constructed from the eigenvectors as

$$S = [X_\alpha, X_\beta, X_0]$$

then it is generally known as the modal transformation matrix. If further D denotes the diagonal matrix of the eigenvalues i.e.

$$D = \begin{bmatrix} \lambda_\alpha & 0 & 0 \\ 0 & \lambda_\beta & 0 \\ 0 & 0 & \lambda_0 \end{bmatrix}$$

it follows that, on using eqn. 2.15

$$\begin{aligned} SD &= [\lambda_\alpha X_\alpha, \lambda_\beta X_\beta, \lambda_0 X_0] \\ &= [\bar{P} X_\alpha, \bar{P} X_\beta, \bar{P} X_0] = \bar{P} S \end{aligned}$$

so that

$$S^{-1} \bar{P} S = D$$

and eqn. 2.14 reduces to

$$\frac{d^2 \bar{v}_m}{dx^2} = D \bar{v}_m$$

or with

$$\bar{v}_m = \{\bar{v}_\alpha, \bar{v}_\beta, \bar{v}_0\}$$

to the three scalar differential equations

$$\frac{d^2 \bar{v}_\alpha}{dx^2} = (a - b) \bar{v}_\alpha; \quad \frac{d^2 \bar{v}_\beta}{dx^2} = (a - b) \bar{v}_\beta; \quad \frac{d^2 \bar{v}_0}{dx^2} = (a + 2b) \bar{v}_0$$

Since \bar{P} is symmetric i.e. $\bar{P} = \bar{P}^T$ it follows from eqn. 2.7 that

$$\frac{d^2 \bar{i}}{dx^2} = \bar{P} \bar{i}$$

so that the same modal transformation matrix S reduces it, with $\bar{i} = S \bar{i}_m$, to

$$\frac{d^2 \bar{i}_m}{dx^2} = D \bar{i}_m$$

which again represents three scalar differential equations in the components $\bar{i}_\alpha, \bar{i}_\beta, \bar{i}_0$ say, of \bar{i}_m .

It is important to note that the modal transformation matrix S is independent of the values of a , b and depends only on their arrangement in the matrix \bar{P} . Both \bar{Z} , \bar{Y} contain only two distinct elements each and their arrangement is precisely that of a , b in \bar{P} , hence it follows that

$$S^{-1}\bar{Z}S = D_1; \quad S^{-1}\bar{Y}S = D_2$$

where D_1 , D_2 are diagonal matrices of the eigenvalues of \bar{Z} , \bar{Y} . Now the Laplace transform of eqn. 2.3 is

$$\frac{d\bar{v}}{dx} = -\bar{Z}\bar{i}; \quad \frac{d\bar{i}}{dx} = -\bar{Y}\bar{v}$$

and on making the substitutions $\bar{v} = S\bar{v}_m$, $\bar{i} = S\bar{i}_m$ these become

$$\frac{d\bar{v}_m}{dx} = -S^{-1}\bar{Z}S\bar{i}_m; \quad \frac{d\bar{i}_m}{dx} = -S^{-1}\bar{Y}S\bar{v}_m$$

which accordingly reduce to

$$\frac{d\bar{v}_m}{dx} = -D_1\bar{i}_m; \quad \frac{d\bar{i}_m}{dx} = -D_2\bar{v}_m$$

Since D_1 , D_2 are diagonal it is apparent that each voltage component v_α , v_β , v_0 is related only to the corresponding current component. Further, for each component the differential equations are of the type discussed in Section 2.2 for the single-phase line.

Since the inverse Laplace transform of eqn. 2.13 gives $v = Sv_m$, $i = Si_m$, the line currents can be written

$$\begin{bmatrix} i_1 \\ i_2 \\ i_3 \end{bmatrix} = \begin{bmatrix} 1 \\ -\frac{1}{2} \\ -\frac{1}{2} \end{bmatrix} i_\alpha + \begin{bmatrix} 0 \\ (\sqrt{3})/2 \\ -(\sqrt{3})/2 \end{bmatrix} i_\beta + \begin{bmatrix} 1 \\ 1 \\ 1 \end{bmatrix} i_0$$

and line voltages are similarly decomposed. The solution can then be regarded as the sum of three modes of propagation, referred to as the α , β , 0 modes. The sum of the phase currents

$$i_1 + i_2 + i_3 = 3i_0$$

is independent of i_α , i_β and the ground current is $3i_0$. Accordingly, the α , β modes of propagation are described as aerial modes, and the 0 mode as the ground mode.

In Section 2.2 it is noted that distortionless propagation is only possible if k is a linear function of the transform parameter. Hence for all three modes to be distortionless it is necessary that both $(a - b)^{1/2}$,

$(a + 2b)^{1/2}$ should be linear functions of p . With the values of a , b given in eqn. 2.12 this necessitates both

$$(M - m)G = (C + c)R$$

and

$$(M + 2m)G = (C - 2c)R$$

For nonzero values of m , M , c , C , both relationships can only be satisfied simultaneously if $R = 0 = G$, i.e. if the line is lossless. In this case it is readily shown that the aerial modes v_α , v_β travel with a velocity $[(M - m)(C + c)]^{-1/2}$ while the ground mode v_0 travels with a velocity $[(M + 2m)(C - 2c)]^{-1/2}$.

The concept of modal propagation is developed further in Chapter 4 where the restrictions imposed here are removed.

2.4 Transmission line parameters

In the analytical work of the previous Sections it has been tacitly assumed that the line parameters are constants, whereas it has long been recognised that the resistive and inductive elements are dependent on frequency, and hence in this sense on waveshape. It is erroneous to describe them as being functions of time. Moreover the capacitances are voltage dependent when corona occurs.

2.4.1 Effect of earth conductivity

In practice some of the salient features of these parameters are influenced by the geological structure and electrical properties of the earth in the neighbourhood of the line. Carson (1926) considered the inductive parameters of a line over a homogeneous conducting earth with unit relative permeability. However, in deriving the earth resistivity from resistance measurements, the value is sometimes found to depend markedly on the electrode separation. For example, in tests on the Ramnäs line, Hylten-Cavallius and Gjerlov (1950) quote 60–800 Ωm , 1000–2000 Ωm for electrode separations of 5 m, 200 m respectively. This variation indicates a stratified earth. Accordingly it is more realistic to consider n sinusoidal line currents of angular frequency ω situated in air above an earth which is supposed to consist of a stratum of uniform thickness, resistivity ρ_2 , relative permeability μ_2 above a semi-infinite stratum with respective properties ρ_3 , μ_3 . Plane-wave propagation is assumed and displacement currents are ignored. Then, if the r th current I_r ($1 \leq r \leq n$) is taken as concentrated at the point (ξ_r, η_r) in the (x, y) -plane, as illustrated in Fig. 2.2, the current density is zero everywhere in the air except at the points (ξ_r, η_r) where it is infinite.

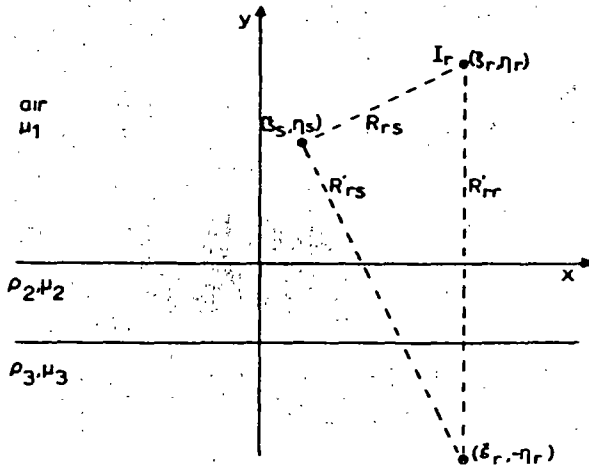


Fig. 2.2 Current-carrying conductor above a stratified earth

The Dirac delta function $\delta(x - a)$ is designed to represent such an idealised situation. It is defined here by

$$\delta(x - a) = \begin{cases} 0 & \text{if } x \neq a \\ \infty & \text{if } x = a \end{cases}$$

in such a way that

$$\int_{-\infty}^{\infty} \delta(x - a) dx = 1$$

implying that if $f(x)$ is continuous at $x = a$ and bounded elsewhere

$$\int_{-\infty}^{\infty} f(x) \delta(x - a) dx = f(a)$$

Hence in the air the current density can be expressed in the form

$$\sum_{r=1}^n k_r \delta(x - \xi_r) \delta(y - \eta_r)$$

On integrating over a small area in the x, y plane including only the r th current it follows immediately from the above definition that $k_r = I_r$. Accordingly Maxwell's equations for the electric field strength can be used to give

$$\frac{\partial^2 E_1}{\partial x^2} + \frac{\partial^2 E_1}{\partial y^2} = m_1^2 \sum_{r=1}^n I_r \delta(x - \xi_r) \delta(y - \eta_r), y \geq 0 \quad (2.16)$$

$$\frac{\partial^2 E_2}{\partial x^2} + \frac{\partial^2 E_2}{\partial y^2} = m_2^2 E_2, 0 \leq y_2 = -y \leq d \text{ (finite stratum)} \quad (2.17)$$

$$\frac{\partial^2 E_3}{\partial x^2} + \frac{\partial^2 E_3}{\partial y^2} = m_3^2 E_3, 0 \leq y_3 = -(y + d) \text{ (infinite stratum)} \quad (2.18)$$

where

$$m_1^2 = j\omega\mu_1\mu_0; \quad m_2^2 = j\omega\mu_2\mu_0/\rho_2; \quad m_3^2 = j\omega\mu_3\mu_0/\rho_3$$

Continuity of the electric field strength, tangential magnetising force, and normal flux density give rise to the following conditions at $y = 0$:

$$E_1 = E_2 = E_0, \text{ say}; \quad \frac{1}{\mu_1} \frac{\partial E_1}{\partial y} = -\frac{1}{\mu_2} \frac{\partial E_2}{\partial y_2}; \quad \frac{\partial E_1}{\partial x} = \frac{\partial E_2}{\partial x}$$

and at $y = -d$

$$E_2 = E_3 = E_d, \text{ say}; \quad \frac{1}{\mu_2} \frac{\partial E_2}{\partial y_2} = \frac{1}{\mu_3} \frac{\partial E_3}{\partial y_3}; \quad \frac{\partial E_2}{\partial x} = \frac{\partial E_3}{\partial x}$$

Taking the infinite complex Fourier transform for x and the infinite or finite sine transforms as appropriate for y , eqns. 2.16, 2.17 and 2.18 become

$$(\lambda^2 + \alpha^2) \bar{E}_1 = -m_1^2 \sum_{r=1}^n I_r \exp(-j\alpha\xi_r) \sin(\lambda\eta_r) + \lambda E_0$$

$$\left\{ \left(\frac{\rho\pi}{d} \right)^2 + \alpha^2 + m_2^2 \right\} \bar{E}_2 = \frac{\rho\pi}{d} \left\{ E_0 - (-1)^p \bar{E}_d \right\}$$

$$\{\lambda^2 + \alpha^2 + m_3^2\} \bar{E}_3 = \lambda \bar{E}_d$$

where

$$\bar{E}_r = \int_{-\infty}^{\infty} \int_0^{\infty} E_r \sin(\lambda y) \exp(-j\alpha x) dx dy, \quad r = 1, 3$$

$$\bar{E}_2 = \int_{-\infty}^{\infty} \int_0^d E_2 \sin(\rho\pi y/d) \exp(-j\alpha x) dx dy$$

and here ρ is a positive integer.

[Readers not familiar with this use of integral transforms are referred to Mullineux *et al* (1970) where the techniques are discussed in relation to this type of problem].

The inverse transform for λ is

$$E_1 = -\frac{2}{\pi} m_1^2 \sum_{r=1}^n I_r \int_0^{\infty} \exp(-j\alpha\xi_r) \frac{\sin(\lambda\eta_r) \sin(\lambda y)}{\lambda^2 + \alpha^2} d\lambda$$

$$+ \frac{2E_0}{\pi} \int_0^{\infty} \frac{\lambda \sin(\lambda y)}{\lambda^2 + \alpha^2} d\lambda$$

$$= -\frac{m_1^2}{2|\alpha|} \sum_{r=1}^n I_r \{ \exp(-|\alpha| |\eta_r - y|) - \exp(-|\alpha| |\eta_r + y|) \} \exp(-j\alpha \xi_r) + \bar{E}_0 \exp(-|\alpha| y) \quad (2.19)$$

on using the calculus of residues to evaluate the integrals. Similarly,

$$\bar{E}_3 = \bar{E}_d \exp(-\gamma_3 \gamma_3), \gamma_3^2 = \alpha^2 + m_3^2 \quad (2.20)$$

The inverse transform with respect to p yields

$$\bar{E}_2 = \frac{2}{d} \sum_{p=1}^{\infty} \left(\frac{p\pi}{d} \right) \frac{\bar{E}_0 - (-1)^p \bar{E}_d}{(p\pi/d)^2 + \gamma_2^2} \sin(p\pi y_2/d), \gamma_2^2 = \alpha^2 + m_2^2$$

This summation can be effected by using the calculus of residues to give

$$\bar{E}_2 = \bar{E}_0 \frac{\sinh\{(d-y_2)\gamma_2\}}{\sinh(d\gamma_2)} + \bar{E}_d \frac{\sinh(y_2\gamma_2)}{\sinh(d\gamma_2)} \quad (2.21)$$

The transformed continuity conditions can now be used to eliminate the unknowns \bar{E}_0, \bar{E}_d from eqns. 2.19, 2.20 and 2.21 giving, after the final inversion,

$$E_1 = -\frac{m_1^2}{4\pi} \sum_{r=1}^n I_r \ln \left\{ \frac{(\eta_r + y)^2 + (x - \xi_r)^2}{(\eta_r - y)^2 + (x - \xi_r)^2} \right\} - \frac{m_1^2}{\pi} \sum_{r=1}^n I_r \int_0^{\infty} \frac{\mu_2 \cos\{\alpha(x - \xi_r)\} \exp\{-\alpha(\eta_r + y)\}}{\mu_2 \alpha + \mu_1 A(\alpha)} d\alpha \quad (2.22)$$

where

$$A(\alpha) = \gamma_2 \frac{\mu_3 \gamma_2 \sinh(d\gamma_2) + \mu_2 \gamma_3 \cosh(d\gamma_2)}{\mu_3 \gamma_2 \cosh(d\gamma_2) + \mu_2 \gamma_3 \sinh(d\gamma_2)} \quad (2.23)$$

Eqn. 2.22 gives the mutual impedance directly per unit length between the r th, s th conductors (since $m_1^2 = j\omega\mu_1\mu_0$) as

$$Z_{rs} = \frac{j\omega\mu_1\mu_0}{2\pi} \ln \frac{R'_{rs}}{R_{rs}} + \frac{j\omega\mu_1\mu_0}{\pi} \int_0^{\infty} \frac{\mu_2 \cos\{\alpha(\xi_s - \xi_r)\} \exp\{-\alpha(\eta_r + \eta_s)\}}{\mu_2 \alpha + \mu_1 A(\alpha)} d\alpha \quad (2.24)$$

where

$$R_{rs}^2 = (\eta_r + \eta_s)^2 + (\xi_s - \xi_r)^2; R'_{rs} = (\eta_r - \eta_s)^2 + (\xi_s - \xi_r)^2$$

Clearly, R_{rs} is the distance between the r th and s th conductors, and R'_{rs} is the distance between the s th conductor and the image point of the r th conductor, with reference to the surface of the earth. The logarithmic term is real and is recognised as the mutual impedance in the classical case of a perfectly conducting earth. In the integral term, $A(\alpha)$

is complex and this leads to a complex mutual impedance which contains a resistive term accounting for losses in the earth. Further, since $A(\alpha)$ is dependent on frequency, the impedances are also frequency dependent.

In practice, the conductors are not filamentary but have a radius R_r , say. The external self impedance of the r th conductor can therefore be estimated from eqn. 2.22 by taking (x, y) to be a point on the surface of the conductor. The negative exponential term in the integral ensures a high rate of convergence and the only contribution to the integral comes from a range of values of α small enough to permit the cosine term being set to unity. Thus the external self-impedance is given by

$$Z_{rr} = \frac{j\omega\mu_1\mu_0}{2\pi} \ln \left(\frac{R'_r}{R_r} \right) + \frac{j\omega\mu_1\mu_0}{\pi} \int_0^{\infty} \frac{\mu_2 \exp(-2\alpha\eta_r)}{\mu_2 \alpha + \mu_1 A(\alpha)} d\alpha \quad (2.25)$$

and is again frequency dependent.

The particular case of a homogeneous earth may be obtained by letting d tend to infinity. Then, from eqn. 2.23, $A(\alpha)$ tends to

$$A(\alpha) = \gamma_2 = \sqrt{(\alpha^2 + m_2^2)}$$

but otherwise eqns. 2.24 and 2.25 remain unchanged. With the relative permeabilities set to unity the expressions derived by Carson (1926) can be obtained by a simple substitution. The integral forms given here, in addition to generalising Carson's equations, are more convenient for computational purposes than his series expressions. In using the integrals of eqns. 2.24 and 2.25 the negative exponential terms ensure rapid convergence. In fact the range of integration can be reduced to as small a range as $0 \leq \alpha \leq 0.2$. A small integration step length is required and 0.001 is suggested. The process outlined can be extended to cover the case of an earth with any number of strata.

Wise (1934) modified Carson's results for a homogeneous earth in an approximate manner to include the effects of displacement currents. Hedman (1965) has shown that the modification has negligible effect at frequencies below 500 kHz. For the stratified earth Wedepohl and Wasley (1966) incorporated similar approximations which modify eqn. 2.23 by replacing γ_2, γ_3 by γ'_2, γ'_3 where, with ϵ as the relative permittivity,

$$\gamma'_2 = \gamma_2 + \omega^2 \mu_0 \epsilon_0 (\mu_1 \epsilon_1 - \mu_2 \epsilon_2)$$

$$\gamma'_3 = \gamma_3 + \omega^2 \mu_0 \epsilon_0 (\mu_1 \epsilon_1 - \mu_3 \epsilon_3)$$

In this approach the effects of displacement currents can become noticeable at frequencies above 60 kHz. However, in practice not only is it rare for the same geological features to extend over the whole

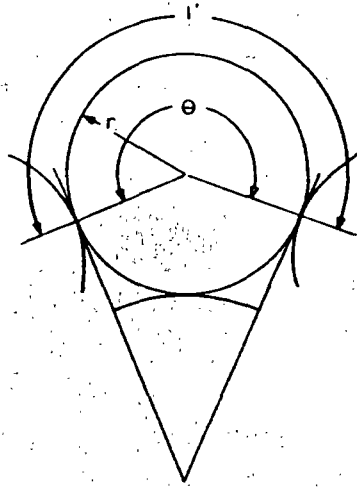


Fig. 2.3 Section of conductor surface

distance of a line, but also precise information on the electrical properties is usually lacking. For these reasons, in the present state of the art, the modifications arising from the effects of displacement currents are generally neglected.

2.4.2 Conductor internal impedance

The internal self impedance of a conductor is small in comparison with the external but may be estimated, for the usual stranded conductor, in the following manner (Galloway *et al.*, 1964).

Part of the cross-section of a stranded conductor is shown in Fig. 2.3. If a sufficiently high frequency is considered, the surface magnetic field intensity H_0 is tangential at all points to the surface of the conductor and proportional to the current density J_0 at the surface. The current density at any depth r normal to the surface of the conductor is

$$J = J_0 \exp(-mr)$$

and

$$H_0 = J_0/m$$

where

$$m = \sqrt{j\omega\mu\mu_0\rho}$$

The total current in the conductor is obtained by integrating a surface element dl , first normal to the surface, and then around the surface. Owing to the largeness of m , the first integration with respect to r may be taken to infinity with small error, and the total current I is consequently

$$I = \int_0^l \int_0^\infty \vec{J}_0 \exp(-mr) dl dr = (1/m) \int_0^l J_0 dl$$

where l is the length of the surface path of the conductor. To calculate the internal impedance, it is necessary to know the total voltage drop, which must be evaluated at the extreme outer radius since the voltage drop in the air path is calculated from this point. At this point, the surface current density is a maximum, and is denoted by J_0 . The voltage drop is $V = \rho \hat{J}_0$. The internal impedance is

$$Z = V/I = m\rho \hat{J}_0 / \int_0^l J_0 dl$$

Since H and J are proportional everywhere this can be expressed in the form

$$Z = m\rho \hat{H}_0 / \int_0^l H_0 dl$$

By symmetry, the field pattern in all outer strands is identical and $l = nr\theta$ where

n = number of outer strands

r = radius of the outer strand

θ = angle subtended by adjacent touching strands at the centre, as shown in Fig. 2.3.

= $(2\pi/n) + \pi$, as is also seen from Fig. 2.3,

and therefore

$$l = r\pi(2 + n).$$

The integral

$$\int_0^l H_0 dl$$

may be obtained by an analogue method using an electrolytic tank for one half of the surface of one strand. Then $\hat{H}_0 l$ is obtained by drawing a straight line as a projection to the initial slope. The factor

$$K = \hat{H}_0 l / \int_0^l H_0 dl$$

has been determined in this way for a number of outer strands commonly used, namely 6, 12, 18 and 24, and it has been found that its value is approximately 2.25.

Thus the formula for the conductor internal impedance is

$$Z_c = \frac{2.25\rho m}{r\pi(2 + n)} \quad (2.26)$$

or

$$R_c = X_c = \frac{2.25\sqrt{(\omega\mu\mu_0\rho)}}{r\pi(2+n)\sqrt{2}}$$

This is most accurate when the depth of penetration is small compared with the radius of one strand. For the conductors in common use the formula should give acceptable accuracy above approximately 2–5 kHz.

2.4.3 Line capacitance

The conductor diameters are small in comparison with their separation so that on the assumption that displacement currents within the earth are negligible, the capacitances are given by the well known expressions [e.g. Bewley (1933)]

$$\left. \begin{aligned} C_{rr} &= 2\pi\epsilon_0/\ln(R'_{rn}/R_{rn}) \\ C_{rr} &= 2\pi\epsilon_0/\ln(R'_{rr}/R_{rr}) \end{aligned} \right\} \quad (2.27)$$

The latter can be suitably increased to account for the insulator capacitance.

Wagner and Lloyd (1955) have measured the charge absorbed when the voltage is such that corona discharges occur on the line. This absorption of charge is equivalent to an increase in capacitance and hence to a reduced speed of travel. Hylten-Cavallius and Gjerlov (1959) have developed the theory for a single conductor above a perfectly conducting earth and discussed the difficulties in applying it in more realistic cases. Their paper contains interesting test results.

Further investigation seems to be necessary before the effect of corona can be taken into account in calculation, particularly on lines in which each phase consists of a bundle of separate conductors in parallel. The general effect is to increase the capacitances and conductance to earth. However, until further quantitative information becomes available, it is customary to treat the capacitance as being independent of voltage and to neglect the earth conductance.

2.4.4 Bundling of sub-conductors

In high voltage systems each phase comprises several subconductors whose centres are spaced at the vertices of a regular polygon which can be circumscribed by a circle of radius a . It is possible to proceed by following mathematically the physical situation, i.e. for a sinusoidal excitation of frequency ω (so that the time derivatives are replaced by $j\omega$) the parameters are calculated for each separate subconductor and the order of the matrix $P(j\omega)$ derived from eqn. 2.6 is reduced by

introducing a common voltage for each subconductor within a given bundle. This method is time consuming and Battisson *et al.* (1969) have shown that the results differ only marginally from those produced using the concept of geometric-mean distance.

In Howes's method (see Dwight, 1954, p. 151) the capacitance between n subconductors of a bundle and a remote p th conductor is calculated on the assumption that each of the n subconductors carries the same charge of $1/n$ coulombs per metre. Then the induced voltage on the p th conductor can be deduced using eqn. 2.27 as

$$\frac{1}{2\pi\epsilon_0} \sum_{i=1}^n \frac{1}{n} \ln \left(\frac{R'_{ip}}{R_{ip}} \right) = \frac{1}{2\pi\epsilon_0} \ln \left\{ \frac{\prod_{i=1}^n (R'_{ip})}{\prod_{i=1}^n (R_{ip})} \right\}^{1/n}$$

so that the capacitance is expressible in terms of the geometric-mean distances

$$\left\{ \prod_{i=1}^n (R'_{ip}) \right\}^{1/n}, \left\{ \prod_{i=1}^n (R_{ip}) \right\}^{1/n}$$

Using Guye's theorem (see Dwight, 1954, p. 104) the term R_{rr} in eqn. 2.28 is replaced by

$$\{na^{n-1}a'\}^{1/n}$$

where

a = radius of circumscribing circle.

a' = radius of subconductor

whilst R'_{rr} is the geometric-mean distance between a bundle and its image with reference to the surface of the earth. Actually the dimensions of power lines are such that the geometric-mean distance between phases is closely approximated to the distance between bundle centres.

If the earth were perfectly conducting so that the integrals in eqns. 2.24 and 2.25 disappear, a similar assumption of equal currents in each subconductor would lead to the use of the same geometric-mean distances in the calculation of the inductive parameters. Battisson *et al.* (1969) have given evidence to indicate that if the integrals are also evaluated using geometric-mean distances, the errors introduced are small.

2.4.5 Earth wires

Multiple earth wires, even when widely separated, can be bundled by the method of the previous Section. After all the bundling is completed the order of the impedance and admittance matrices is one more than the number of phases. If, as is usual, the earth wire is taken to be at zero potential throughout its length, the order of these matrices can be reduced by matrix manipulation to that of the number of phases.

For convenience the steady-state condition is considered and the matrices are partitioned to separate the n phases and the earth wire.

Then, with obvious notation which indicates the order of the matrices, there results

$$\frac{d}{dx} \begin{bmatrix} i_p(n \times 1) \\ i_e(1 \times 1) \end{bmatrix} = - \begin{bmatrix} Y_{pp}(n \times n) & Y_{pe}(n \times 1) \\ Y_{ep}(1 \times n) & Y_{ee}(1 \times 1) \end{bmatrix} \begin{bmatrix} v_p(n \times 1) \\ v_e(1 \times 1) \end{bmatrix}$$

and

$$\frac{d}{dx} \begin{bmatrix} v_p(n \times 1) \\ v_e(1 \times 1) \end{bmatrix} = - \begin{bmatrix} Z_{pp}(n \times n) & Z_{pe}(n \times 1) \\ Z_{ep}(1 \times n) & Z_{ee}(1 \times 1) \end{bmatrix} \begin{bmatrix} i_p(n \times 1) \\ i_e(1 \times 1) \end{bmatrix}$$

With $v_e = 0$ simple manipulation yields

$$\left. \begin{aligned} \frac{d}{dx} i_p &= -Y_{pp} v_p \\ \text{and} \quad \frac{d}{dx} v_p &= -(Z_{pp} - Z_{pe} Z_{ee}^{-1} Z_{ep}) i_p \end{aligned} \right\} \quad (2.28)$$

By convention these new $n \times n$ matrices in eqn. 2.28 are still referred to as the admittance and impedance matrices and denoted by Y, Z ; their order distinguishes them from the original.

2.4.6 Example

To illustrate the dependence of the parameters on frequency the single circuit 400 kV quadruple 0-4 line of Fig. 2.4 is considered. Typical parameters are shown in Fig. 2.5 for both homogeneous and stratified earths. The effect of stratification can be interpreted in terms of the frequency dependent depth of penetration (Poritsky and Jerrard, 1954)

$$\sqrt{2/(\omega\mu\sigma)} \text{ metres}$$

For an earth resistivity of $20 \Omega\text{m}$, the depth of penetration varies from 5.6 km to 5.6 m as ω varies from 1 to 10^6 rad/s. Hence at the lower frequency a top stratum 60 m thick has little effect, but at the higher frequency a top stratum 6 m thick has a pronounced effect on the inductance.

Fig. 2.5 indicates that when a top stratum of low resistivity overlies an earth of high resistivity the inductance approximates that due to a homogeneous earth of high resistivity at low frequencies and of low resistivity at high frequencies. This is in contrast to the resistance which corresponds more closely to that due to a homogeneous earth of high resistivity at all frequencies. The significance of these effects is discussed in Chapter 7.

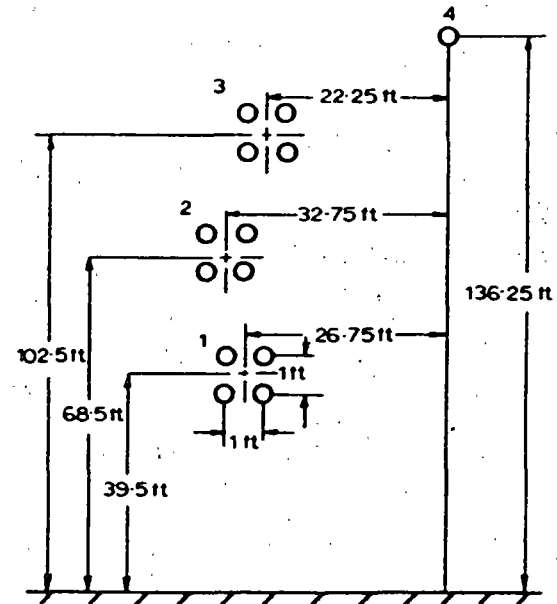


Fig. 2.4 Configuration for a 400 kV line

2.5 Cable parameters

Traditionally, single-core cables have been treated as coaxial transmission lines with the sheath held at zero potential. While this approach has provided sufficiently accurate results for the stress on the main cable insulation, it provides no information about the stress on the insulation between the cable sheath and the surrounding earth. Unlike the effect produced by a breakdown of the main insulation, a puncture of the sheath insulation does not lead to immediate failure of the system. It does however permit the occurrence of corrosion of the sheath and so leads to eventual failure. Accordingly, a single core cable is initially regarded as a 2-conductor device buried in earth of finite conductivity. Then the interaction between the N single-core cables comprising the cable system is considered and the impedance and admittance matrices derived. In contrast to the corresponding matrices for a transmission line these matrices are of order $2N \times 2N$ since the current and voltage in each sheath are included in the calculation.

2.5.1 Single core cable

A sector of the cable is illustrated in Fig. 2.6. Under lossless con

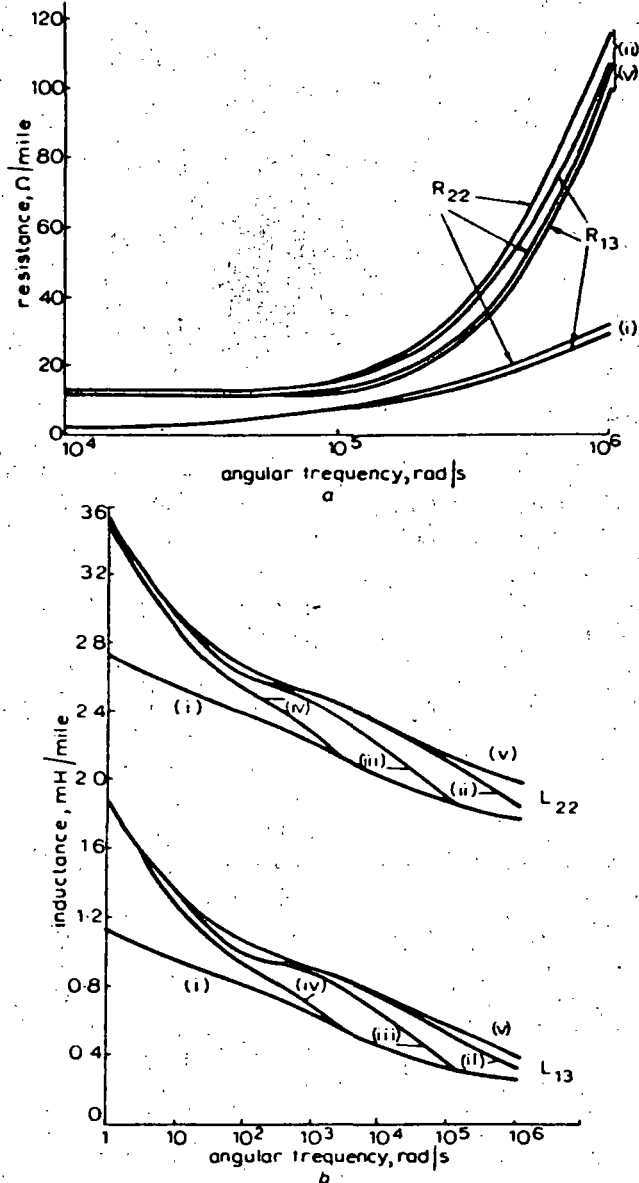


Fig. 2.5 Typical parameters of 400 kV line (earth wire eliminated)
 a Resistance
 b Inductance
 (i) Homogeneous earth, resistivity = 200 Ωm.
 (ii) 0.6 m stratum resistivity = 20 Ωm, above an infinite stratum of resistivity 1000 Ωm
 (iii) 6 m stratum resistivity 1000 Ωm
 (iv) 60 m stratum
 (v) Homogeneous earth, resistivity = 1000 Ωm

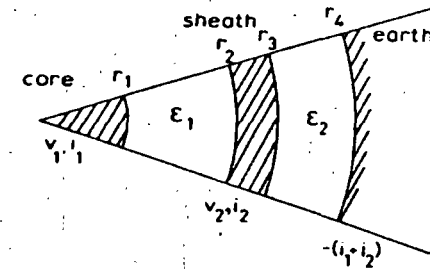


Fig. 2.6 Section of cable

it follows from elementary principles that, ignoring capacitance currents, the inductive elements give

$$v_1 - v_2 = z_2 i_1$$

$$v_2 = z_6 (i_1 + i_2)$$

where

$$z_2 = \frac{j\omega\mu_0}{2} \ln \left(\frac{r_2}{r_1} \right); \quad z_6 = \frac{j\omega\mu_0}{2} \ln \left(\frac{r_4}{r_3} \right) \quad (2.29)$$

and the reason for the choice of subscripts becomes apparent later. The impedance matrix is thus seen to be

$$Z = \begin{bmatrix} z_2 + z_6 & z_6 \\ z_6 & z_6 \end{bmatrix} \quad (2.30)$$

In a similar way consideration of the capacitive elements only gives the admittance matrix as

$$Y = \begin{bmatrix} y_1 & -y_1 \\ -y_1 & y_1 + y_2 \end{bmatrix} \quad (2.31)$$

where

$$y_1 = j\omega 2\pi \epsilon_1 \epsilon_0 / \ln(r_2/r_1)$$

and

$$y_2 = j\omega 2\pi \epsilon_2 \epsilon_0 / \ln(r_4/r_3)$$

When losses are introduced into the system, Wedepohl and Wilcox (1973) point out that, even with a soil of a poor resistivity of 1000 Ωm, the time constant for the diffusion of charge within the soil is about 10⁻⁸s. Hence for practical purposes, when the smallest unit of time is 10⁻⁶s, the admittance matrix given above is unaltered except for the inclusion of the conductances of the main and sheath insulations.

The electromagnetic problem when the core and sheath have finite

conductivity was solved by Shelkunoff (1934) who proved the following two theorems:

Theorem 1: If the return path is wholly external or wholly internal, then the longitudinal electromotive intensity on that surface of a hollow conductor which is nearest to the return path equals the corresponding surface impedance per unit length multiplied by the total current flowing in the conductor; and the intensity on the other surface equals the transfer impedance per unit length multiplied by the total current.

Theorem 2: If the return path is partly external and partly internal, the separate components of the intensity due to the two parts of the total current are calculated by the above theorem and then added to obtain the total intensities.

Accordingly the problem may be solved in terms of seven impedances:

- z_1 the surface impedance of the core
- z_2 the inductive impedance already defined (eqn. 2.29)
- z_3 the impedance of the inner surface of the sheath
- z_4 the transfer impedance between the inner and outer surfaces of the sheath
- z_5 the impedance of the outer surface of the sheath
- z_6 the inductive impedance already defined (eqn. 2.29)
- z_7 the impedance of the earth surface surrounding the cable

Then the above theorems may be used to give

$$v_1 - v_2 = z_1 i_1 + z_2 i_1 + z_3 i_1 - z_4(i_1 + i_2)$$

$$v_2 = -z_4 i_1 + z_5(i_1 + i_2) + z_6(i_1 + i_2) + z_7(i_1 + i_2)$$

from which the impedance matrix follows as

$$Z = \begin{bmatrix} z_1 + z_2 + z_3 + z_5 + z_6 + z_7 - 2z_4 & z_5 + z_6 + z_7 - z_4 \\ z_5 + z_6 + z_7 - z_4 & z_5 + z_6 + z_7 \end{bmatrix} \quad (2.32)$$

Expressions for the constituent impedances z_1, z_3, z_4, z_5 were derived by Shelkunoff (1934) and for z_7 by Pollaczek (1931). Their analytic results, together with approximations which are more convenient for computation, are given in Table 2.1 where it will be noted that these impedances are expressed in terms of a parameter m . Since m is defined by

$$m^2 = j\omega\mu\mu_0/\rho$$

Table 2.1

Impedance	Analytical form, Ω/m	Approximate form, Ω/m	Comments
z_1	$\{\rho m I_0(mr_1)\} / \{2nr_1 I_1(mr_1)\}$	$\{\rho m \coth(0.777mr_1)\} / (2nr_1) + 0.356\rho / (mr_1^2)$	
z_3	$\rho m \{I_0(mr_2)K_1(mr_2) + K_0(mr_2)I_1(mr_2)\} / (2mr_2 D)$	$\{\rho m \coth(m\Delta)\} / (2mr_2) - \rho / \{2mr_2(r_2 + r_1)\}$	accurate for $(r_2 - r_1)/(r_2 + r_1) < 1/8$
z_4	$\rho / (2mr_2 r_2 D)$	$\{\rho \operatorname{cosech}(m\Delta)\} / \{\pi(r_2 + r_1)\}$	
z_5	$\rho m \{I_0(mr_3)K_1(mr_3) + K_0(mr_3)I_1(mr_3)\} / (2mr_3 D)$	$\{\rho \coth(m\Delta)\} / (2mr_3) + \rho / \{2mr_3(r_2 + r_1)\}$	accurate for $ mr_3 < 0.25$
z_7	see Section 2.5.2	$j\omega\mu\mu_0 \{-\ln(\gamma m r_4 / 2) + 1/2 - 4mh/3\} / (2\pi)$	

z_3, z_4 are given in eqn. 2.29
 ρ = resistivity of core or sheath as appropriate
 $m^2 = j\omega\mu\mu_0/\rho$
 $D = I_1(mr_2)K_1(mr_2) - I_1(mr_2)K_1(mr_2)$
 $\Delta = r_2 - r_1$
 h = depth of cable in earth
 γ = Euler's constant
 I_0, I_1, K_0, K_1 are the usual modified Bessel functions

it is apparent that all five impedances are strongly dependent on the frequency.

2.5.2 Cable systems

In cable systems consisting of a number of single-core cables it is assumed that these are disposed parallel to each other and the surface of the earth, and that the attenuation is negligible along a length of the system comparable with its lateral dimensions. With the usual spacing between cables the soil acts as an electrostatic shield so that there is no electrostatic coupling between them. The admittance matrix of the system is accordingly of diagonal form with the diagonal elements being the 2×2 admittance matrices of the individual cables discussed in the previous Section.

Similarly, the impedance matrix Z of the system can be partitioned in the form

$$Z = [Z_{ij}]$$

where the Z_{ij} are 2×2 submatrices. The diagonal submatrix Z_{ii} is then the 2×2 impedance matrix of the i th cable and is derivable from eqn. 2.32 of the previous section. However the soil does not act as an electromagnetic shield between cables i, j so that the off-diagonal terms are no longer zero. This coupling can be obtained by considering a current I at a point i a distance l_i below the surface of an earth of resistivity ρ . The electric field strength E_{ji} at the point j , separated horizontally from i by a distance x_{ji} and at a depth l_j , is expressed in the form

$$E_{ji} = z_{ji}I$$

For a cable at the point i , the current I is the sum of the core current i_1 and sheath current i_2 , and for a cable at the point j

e.m.f. induced in core j = e.m.f. induced in sheath j

$$\doteq E_{ji} = z_{ji}(i_1 + i_2)$$

Hence the submatrix Z_{ji} can be written

$$Z_{ji} = \begin{bmatrix} z_{ji} & z_{ji} \\ z_{ji} & z_{ji} \end{bmatrix}$$

and because of the reciprocity of mutual impedance it follows that

$$Z_{ji} = Z_{ij}$$

Both Pollaczek (1931) and Wedepohl and Wilcox (1973) derive equivalent expressions for z_{ji} as

$$z_{ji} = j\omega\mu_0(\mathcal{G}_1 + \mathcal{G}_2 - \mathcal{G}_3)/(2\pi) \quad (2.33)$$

where

$$\mathcal{G}_1 = \int_{-\infty}^{\infty} \frac{\exp\{j\alpha x_{ji} - (l_i + l_j)(\alpha^2 + m^2)^{1/2}\}}{|\alpha| + (\alpha^2 + m^2)^{1/2}} d\alpha$$

$$\mathcal{G}_2 = \int_{-\infty}^{\infty} \frac{\exp\{j\alpha x_{ji} - |l_i - l_j|(\alpha^2 + m^2)^{1/2}\}}{2(\alpha^2 + m^2)^{1/2}} d\alpha$$

$$\mathcal{G}_3 = \int_{-\infty}^{\infty} \frac{\exp\{j\alpha x_{ji} - (l_i + l_j)(\alpha^2 + m^2)^{1/2}\}}{2(\alpha^2 + m^2)^{1/2}} d\alpha$$

$$m^2 = j\omega\mu_0/\rho$$

If $s_{ji}^2 = x_{ji}^2 + (l_j - l_i)^2$ and $|ms_{ji}| < 0.25$ then eqn. 2.33 can be approximated by

$$z_{ji} = \frac{j\omega\mu_0}{2\pi} \left\{ -\ln \left(\frac{\gamma ms_{ji}}{2} \right) + \frac{1}{2} - \frac{2m}{3} (l_i + l_j) \right\} \quad (2.34)$$

where γ is Euler's constant, otherwise eqn. 2.33 is used.

By taking j to be a point on the outer surface of the i th cable so that $s_{ji} = r_a$ and $l_i + l_j = 2h$, say, the impedance of the earth surface surrounding the cable (i.e. z_7 of Section 2.5.1) is obtained.

Hence at any frequency ω , both the core and sheath voltages and currents are related by the transmission-line equations

$$\frac{dv}{dx} = -Zi; \quad \frac{di}{dx} = -Yv$$

and all the elements of Z, Y are now known. It should be noted that the column matrices v, i each contain $2N$ elements, where N is the number of cables.

Chapter 3

Transform methods of solution

In a general linear network with constant parameters the output $f(t)$ for an input $g(t)$ can be expressed in the form

$$F(D)f(t) = g(t), \quad D \equiv d/dt \quad (3.1)$$

However, in transmission line problems, as seen in Chapter 2, some of the parameters (i.e. the coefficients of eqn. 3.1) are frequency dependent, and in this case eqn. 3.1 should be modified to read

$$F(D, \omega)f(t) = g(t) \quad (3.2)$$

Hylten-Cavallius and Gjerlov (1959) proceeded by decomposing the input into its sinusoidal components, finding the corresponding components of the output, and reassembling these to give the solution. In mathematical terms this is equivalent to an application of the complex Fourier transform to eqn. 3.2, i.e. multiplying throughout by $\exp(-j\omega t)$ and integrating with respect to t over the range $(-\infty, \infty)$, thereby transforming the problem from the time to the frequency domain as

$$F(j\omega, \omega)\bar{f}(j\omega) = \bar{g}(j\omega) \quad (3.3)$$

where

$$\bar{f}(j\omega) = \int_{-\infty}^{\infty} f(t) \exp(-j\omega t) dt \quad (3.4)$$

and $\bar{g}(j\omega)$ is defined similarly. The reassembly to give the solution in the time domain is then achieved by taking the inverse complex Fourier transform,

$$f(t) = \frac{1}{2\pi} \int_{-\infty}^{\infty} \bar{f}(j\omega) \exp(j\omega t) d\omega \quad (3.5)$$

In practice it is seldom that the integral in eqn. 3.5 can be evaluated analytically and it is necessary to proceed numerically.

Suppose that

$$f(t) \equiv 0 \quad \text{for } t < 0,$$

that as $|\omega| \rightarrow \infty$, $\bar{f}(j\omega) \rightarrow 0$, and that the numerical integration is carried to a sufficiently large value of ω with a step length $\Delta\omega$. Then using the trapezoidal rule, an approximation $f^*(t)$ to $f(t)$ is obtained as

$$f^*(t) = \frac{\Delta\omega}{2\pi} \sum_{r=-\infty}^{\infty} \bar{f}(jr\Delta\omega) \exp(jr\Delta\omega t), \quad t > 0 \quad (3.6)$$

Define

$$T = 2\pi/(\Delta\omega) \quad \text{i.e. } \Delta\omega = 2\pi/T$$

and

$$C_r \equiv \frac{\Delta\omega}{2\pi} \bar{f}(jr\Delta\omega) = \frac{1}{T} \int_0^{\infty} f(\tau) \exp(-2\pi jr\tau/T) d\tau$$

so that eqn. 3.6 can be written

$$f^*(t) = \sum_{r=-\infty}^{\infty} C_r \exp(2\pi jr t/T) \quad (3.7)$$

i.e. $f^*(t)$ is a periodic function with period T .

Now C_r can be expressed in the form

$$C_r = \frac{1}{T} \sum_{k=0}^{\infty} \int_{kT}^{(k+1)T} f(\tau) \exp(-2\pi jr\tau/T) d\tau$$

and, interchanging the order of summation and integration,

$$C_r = \frac{1}{T} \int_0^T \left[\sum_{k=0}^{\infty} f(\tau + kT) \right] \exp(-2\pi jr\tau/T) d\tau \quad (3.8)$$

Eqns. 3.7, and 3.8 form a finite complex Fourier transform pair with

$$f^*(t) = \sum_{k=0}^{\infty} f(t + kT) \quad (3.9)$$

This phenomenon in eqn. 3.9 is known as aliasing (Blackman & Tukey, 1958), and for $f^*(t)$ to form a good approximation to $f(t)$ over the range $0 \leq t \leq T$ it is necessary that $f(t)$ should be negligibly small for $t > T$. This condition is fulfilled in the lightning surges dealt with by Hylten-Cavallius and Gjerlov (1959) but not in the case of such a phenomenon as line energisation. Here, where the output continues for long times, it is necessary to use some device to ensure that $f(t)$ tends to zero after a time T . This can be achieved mathematically by using the modified Fourier transform (Day *et al.*, 1966).

3.1 The modified Fourier transform

This transform can be constructed, for a function $\phi(t) \equiv 0$ for $t < 0$, (see eqn. 3.4) from the Fourier transform of $\{\phi(t) \exp(-at)\}$ with $a > 0$, i.e.

$$\int_0^{\infty} \phi(t) \exp\{-(a + j\omega)t\} dt = \bar{\phi}_+(a + j\omega) \quad (3.10)$$

whose inverse (see eqn. 3.5) is

$$\frac{1}{2\pi} \int_{-\infty}^{\infty} \bar{\phi}_+(a + j\omega) \exp(j\omega t) d\omega = \begin{cases} \phi(t) \exp(-at), & t > 0 \\ 0, & t < 0 \end{cases}$$

implying that

$$\left. \begin{array}{l} t > 0, \phi(t) \\ t < 0, 0 \end{array} \right\} = \frac{\exp(at)}{2\pi} \int_{-\infty}^{\infty} \bar{\phi}_+(a + j\omega) \exp(j\omega t) d\omega \quad (3.11)$$

Eqns. 3.10 and 3.11 form the one-sided modified Fourier transform pair and may be converted to the Laplace transform pair by the simple substitution $p = a + j\omega$ giving

$$\int_0^{\infty} \phi(t) \exp(-pt) dt = \bar{\phi}(p)$$

$$\frac{1}{2\pi j} \int_{a-j\infty}^{a+j\infty} \bar{\phi}(p) \exp(pt) dp = \begin{cases} \phi(t), & t > 0 \\ 0, & t < 0 \end{cases}$$

In the present context it is more convenient to use the modified Fourier transform since the transform parameter ω can be identified with the angular frequency.

If numerical integration is used to obtain an approximation $f^*(t)$ to the inverse modified Fourier transform

$$f(t) = \frac{\exp(at)}{2\pi} \int_{-\infty}^{\infty} \bar{f}_+(a + j\omega) \exp(j\omega t) d\omega$$

then it is readily shown, see Mullineux and Reed (1972), that for $0 \leq t \leq T$, eqn. 3.9 becomes

$$f^*(t) = f(t) + \sum_{k=1}^{\infty} f(t + kT) \exp(-akT) \quad (3.12)$$

and elsewhere by periodicity i.e.

$$f^*(t + nT) = f^*(t) \quad (3.13)$$

Clearly the effect of aliasing is reduced by the exponential terms, and by choosing aT sufficiently large in eqn. 3.12 $f^*(t)$ can be made to form a good approximation to $f(t)$ within the range $(0, T)$. The actual choice of a, T is discussed in Section 3.3.

One way of applying the modified Fourier transform to eqn. 3.2 would be to multiply the equation throughout by $\exp(-at)$

$$\exp(-at) F(D, \omega) f(t) = g(t) \exp(-at) \quad (3.14)$$

and use the rule of differential operators, viz.

$$\phi_1(D) \{\exp(\beta t) f(t)\} = \exp(\beta t) \phi_1(D + \beta) f(t)$$

or alternatively

$$\exp(\beta t) \phi_2(D) f(t) = \phi_2(D - \beta) \{\exp(\beta t) f(t)\}$$

to rewrite eqn. 3.14 in the form

$$F(D + a, \omega) \{f(t) \exp(-at)\} = g(t) \exp(-at) \quad (3.15)$$

The application of the complex Fourier transform has the effect of replacing the D -operator by $j\omega$ to yield

$$F(a + j\omega, \omega) \bar{f}_+(a + j\omega) = \bar{g}_+(a + j\omega) + f_0(a + j\omega, \omega) \quad (3.16)$$

where $f_0(a + j\omega, \omega)$ accounts for any initial conditions. It is seen that if the modified Fourier transform is applied in the usual manner, i.e. multiplying throughout by $\exp\{-(a + j\omega)t\}$ and integrating with respect to t over the range $(0, \infty)$, then apart from the term expressing the initial conditions, it is only necessary to replace the D -operator by $(a + j\omega)$. Furthermore, parameters which are known functions of ω are shown from eqn. 3.16 to remain the same functions of ω after the transform.

In Chapter 2 the dependence of the transmission line parameters on frequency is investigated on the implicit assumption that the frequency is positive. Now, however, the frequency covers the range $(-\infty, \infty)$ so that a meaning must be attached to $Z(-\omega)$. To this end consider

$$2W(\omega) \cos \omega t = W(\omega) \exp(j\omega t) + W(\omega) \exp(-j\omega t) \quad \omega > 0$$

where $W(\omega)$ can be put equal to $R(\omega), M(\omega)$ in turn. Then on treating each of the two terms on the right hand side of the equation separately it is necessary for consistency that

$$W(-\omega) = W(\omega)$$

i.e. W is even with respect to ω and can be treated as a function of the modulus of the frequency. Thus

$$Z_{rs}(\omega) = j\omega M'_{rs}(|\omega|) + R'_{rs}(|\omega|)$$

for all ω . On incorporating the internal self-impedance in Z_{rr} these form the elements of the complete impedance matrix Z at frequency ω . In eliminating the earth wire, and producing the Z -matrix of order equal to the number of phases, the matrix manipulation leaves the form of the elements unchanged as, say, the (r, s) th element of $Z = j\omega M'_{rs}(|\omega|) + R'_{rs}(|\omega|)$.

Denoting the elements of the corresponding admittance matrix Y at frequency ω by the (r, s) th element of $Y = j\omega C'_{rs} + G'_{rs}$ application of the modified Fourier transform to the line equations gives

$$\left. \begin{aligned} \frac{d\bar{v}}{dx} &= -\bar{Z}\bar{i}; & \frac{d\bar{i}}{dx} &= -\bar{Y}\bar{v} \\ \frac{d^2\bar{v}}{dx^2} &= \bar{P}\bar{v}; & \frac{d^2\bar{i}}{dx^2} &= \bar{P}\bar{i} \end{aligned} \right\} \quad (3.17)$$

with $\bar{P} = \bar{Z}\bar{Y}$ and \bar{Z}, \bar{Y} as square matrices of order equal to the number of phases with

$$(r, s)\text{th element of } \bar{Z} = (a + j\omega)M'_{rs}(|\omega|) + R'_{rs}(|\omega|)$$

$$(r, s)\text{th element of } \bar{Y} = (a + j\omega)C'_{rs} + G'_{rs}$$

where $M'_{rs}, R'_{rs}, C'_{rs}, G'_{rs}$ are real.

Thus the partial differential equations are now reduced to ordinary differential equations in the frequency domain, which when solved must be inverted to the time domain. Alternative methods of solution in the frequency domain are considered in the next Section and in Chapter 4.

3.2 Finite transforms for solution in the frequency domain

One method of solving ordinary differential equations is based upon a generalisation of the Fourier series in the form of finite integral transforms (e.g. Mullineux *et al.* 1970). The actual choice of transform is intimately dependent on the end-point conditions. The voltage equations of the line (eqn. 3.18) are conveniently solved in terms of the currents at the ends of the line. In general these currents are not known explicitly but the network elements connected to the ends provide further relations between these currents and the corresponding voltages. In this sense the approach is similar to the 2-port network representation discussed in Section 4.2. Since

$$\frac{d\bar{v}}{dx} = -\bar{Z}\bar{i}$$

and the \bar{i} at the ends are being regarded for the time being as known, the derivatives of the voltages are being considered as effectively given. Hence the finite cosine transform, viz.

$$\bar{f}(m) = \int_0^l f(x) \cos(m\pi x/l) dx$$

with inverse transform

$$f(x) = \frac{\bar{f}(0)}{l} + \frac{2}{l} \sum_{m=1}^{\infty} \bar{f}(m) \cos(m\pi x/l)$$

is indicated.

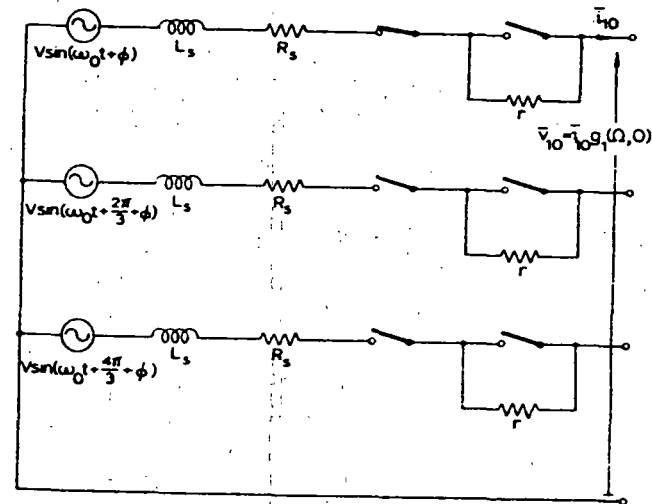


Fig. 3.1 Input circuit to a 3-phase line

The features of the method are best illustrated by means of the simple example illustrated in Fig. 3.1. Here the closure of the first pole of a switch from a source onto a charge-free, open-circuited 3-phase line of length l is considered. The closure of subsequent poles is discussed in Chapter 5. In the frequency domain, after bundling and elimination of the earth wire, the transmission line equations can be represented by

$$\frac{d^2 \bar{v}}{dx^2} = \bar{P} \bar{v} \quad (3.18)$$

where \bar{P} is a matrix of order 3×3 .

In the time domain the end-point conditions are, at $x=0$, $i_1 = i_{10}$, $i_2 = 0 = i_3$ for all time, and at $x=l$, $i_1 = 0 = i_2 = i_3$ for all time. Under the modified Fourier transform these conditions are expressed in terms of the transformed voltages as, at $x=0$,

$$\frac{d\bar{v}_1}{dx} = -\{(a+j\omega)M_{11} + R_1\}\bar{i}_{10}$$

$$\frac{d\bar{v}_2}{dx} = -(a+j\omega)M_{12}\bar{i}_{10}$$

$$\frac{d\bar{v}_3}{dx} = -(a+j\omega)M_{13}\bar{i}_{10}$$

at $x=l$

$$\frac{d\bar{v}_1}{dx} = \frac{d\bar{v}_2}{dx} = \frac{d\bar{v}_3}{dx} = 0$$

Since these end-point conditions are expressed in terms of first derivatives the finite cosine transform is appropriate. Accordingly, eqn. 3.18 is multiplied throughout by $\cos m\pi x/l$ (where m is an integer) and integrated over the range $(0, l)$, to give

$$[\bar{P} + (m\pi/l)^2 U] \bar{v} = \bar{i}_{10} \{(a+j\omega)M_{11} + R_1, (a+j\omega)M_{12}, (a+j\omega)M_{13}\} \quad (3.19)$$

where

$$\bar{v} = \int_0^l \bar{v} \cos(m\pi x/l) dx$$

and U is the unit 3×3 matrix.

With \bar{P} known, the solution to eqn. 3.19 can be written

$$\bar{v}_k = \bar{i}_{10} \bar{g}_k(m, a+j\omega), \quad k = 1, 2, 3 \quad (3.20)$$

where the \bar{g}_k are known functions. The inverse finite cosine transform with respect to m is

$$\bar{v}_k = \bar{i}_{10} g_k(x, a+j\omega) \quad (3.21)$$

where

$$g_k(x, a+j\omega) = \frac{2}{l} \left\{ \frac{\bar{g}_k(0, a+j\omega)}{2} + \sum_{m=1}^{\infty} \bar{g}_k(m, a+j\omega) \cos(m\pi x/l) \right\}$$

which can be computed sufficiently accurately by suitable truncation of the infinite sum, since there is no problem of convergence. The series is summed until the modulus of the last term is less than a prescribed percentage (related to the accuracy required) of the modulus of the partial sum.

It remains to find \bar{i}_{10} . For the system shown in Fig. 3.1, which includes resistor switching at $t = 0_+$, with v_1 at $x=0$ denoted by v_{10} , it follows that

$$V \sin(\omega_0 t + \phi) - v_{10} = (r + R_s) i_{10} + L_s \frac{di_{10}}{dt}$$

in the time domain and hence in the frequency domain

$$V \frac{(a+j\omega) \sin \phi + \omega_0 \cos \phi}{(a+j\omega)^2 + \omega_0^2} - \bar{v}_{10} = (r + R_s) \bar{i}_{10} + (a+j\omega) L_s \bar{i}_{10} \quad (3.22)$$

From eqn. 3.21 with $k=1$, $x=0$

$$\bar{v}_{10} = \bar{i}_{10} g_1(0, a+j\omega)$$

which when substituted in eqn. 3.22 gives

$$\bar{i}_{10} = \frac{V \{(a+j\omega) \sin \phi + \omega_0 \cos \phi\}}{\{(a+j\omega)^2 + \omega_0^2\} \{g_1(0, a+j\omega) + r + R_s + (a+j\omega) L_s\}} \quad (3.23)$$

Substitution in eqn. 3.21 then gives the solution in the frequency domain for all x .

3.3 Inversion to the time domain

In carrying out the inverse transform

$$f(t) = \frac{\exp(at)}{2\pi} \int_{-\infty}^{\infty} \bar{f}_+(a+j\omega) \exp(j\omega t) d\omega \quad (3.24)$$

numerically the integrand is sampled at discrete values of ω . This leads to aliasing as discussed in Section 3.1 and its effects are present no matter which integration technique is used. In fact de Balbine and Franklin (1966) have shown that the trapezoidal rule is at least as good as any other method. Thus with a step length $\Delta\omega$ over the whole range for which $\bar{f}_+(a+j\omega)$ is non-zero the aliasing effect shows itself in the form of eqns. 3.12 and 3.13. Suppose that the upper bound of $|f(t)|$ is M then eqn. 3.12 gives for $0 \leq t \leq T \equiv 2\pi/\Delta\omega$

$$|f^*(t) - f(t)| \leq \mathfrak{M} \sum_{k=1}^{\infty} \exp(-akT) = \frac{\mathfrak{M}}{\exp(aT) - 1} = \frac{\mathfrak{M}}{\exp(2\pi a/\Delta\omega) - 1} \quad (3.25)$$

Hence the aliasing can be reduced to arbitrarily small proportions by choosing (aT) sufficiently large. Other conditions on a and $\Delta\omega$ are generally more restrictive and ensure that aliasing errors are small. These conditions are now discussed.

Suppose that $a = 0$, so that the modified Fourier transform reduces to the complex Fourier transform and the integral to be evaluated numerically is that of eqn. 3.5. Physically it is known that unless all components of the solution are subject to considerable damping the integrand in eqn. 3.5 has poles (i.e. infinities) close to the line of integration. In the neighbourhood of these poles the integrand peaks sharply necessitating the use of a small step length for integration - a step length uneconomically small for the majority of the range.

It is also known that in a stable system none of the poles lie in the lower half of the $\zeta = \omega + j\eta$ plane, so that if the path of integration could be lowered, thus removing it further from the poles, the integrand would be smoothed. Further, since there is no pole in the lower half plane, the concepts of the calculus of residues show that the value of the integral remains unchanged by this shift.

The parameter $a > 0$ in the modified Fourier transform has precisely the desired effect of shifting the line of integration. This may be seen by making the substitution

$$a + j\omega = j\omega'$$

in the inverse modified Fourier transform of eqn. 3.11 which then becomes

$$\left. \begin{aligned} t > 0, \phi(t) \\ t < 0, 0 \end{aligned} \right\} = \frac{1}{2\pi} \int_{-ja}^{\infty - ja} \bar{\phi}_+(j\omega') \exp(j\omega' t) d\omega' \quad (3.26)$$

This is seen to be the inverse complex Fourier transform with the line of integration no longer the real axis in the ζ -plane but the parallel line $\text{Im } \zeta = -a$.

It might appear then that the larger the parameter a the better. However, in carrying out the numerical integration it is necessary to truncate the infinite range of the integral in eqn. 3.24 to some finite value, say $(-\Omega, \Omega)$. This introduces a truncation error which, being multiplied by $\exp(at)$, increases rapidly as (at) increases. This sets an upper bound to the choice of a and the best value to use is discussed later.

To examine the nature of the truncation error let $f_{\Omega}(t)$ be the value with the integration range truncated, i.e.

$$f_{\Omega}(t) = \frac{\exp(at)}{2\pi} \int_{-\Omega}^{\Omega} \bar{f}_+(a + j\omega) \exp(j\omega t) d\omega \quad (3.27)$$

or

$$\exp(-at) f_{\Omega}(t) = \frac{1}{2\pi} \int_{-\infty}^{\infty} \bar{\phi}(j\omega) \bar{f}_+(a + j\omega) \exp(j\omega t) d\omega \quad (3.28)$$

where

$$\bar{\phi}(j\omega) = \begin{cases} 1, & |\omega| < \Omega \\ 0, & |\omega| > \Omega \end{cases}$$

and is the complex Fourier transform of

$$\phi(t) = \frac{1}{2\pi} \int_{-\Omega}^{\Omega} \exp(j\omega t) d\omega = \frac{\sin(\Omega t)}{\pi t}$$

It will be recalled that $\bar{f}_+(a + j\omega)$ is the complex Fourier transform of $\exp(-at) f(t)$ so that the convolution theorem, viz.,

$$\frac{1}{2\pi} \int_{-\infty}^{\infty} \bar{\theta}(j\omega) \bar{\psi}(j\omega) \exp(j\omega t) d\omega = \int_{-\infty}^{\infty} \theta(\tau) \psi(t - \tau) d\tau$$

applied to eqn. 3.28 gives

$$\exp(-at) f_{\Omega}(t) = \int_0^{\infty} \{f(\tau) \exp(-a\tau)\} \frac{\sin \Omega(t - \tau)}{\pi(t - \tau)} d\tau \quad (3.29)$$

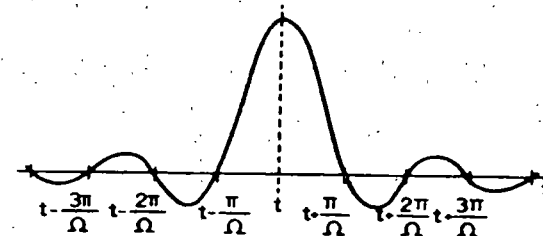


Fig. 3.2 The Dirichlet kernel $\sin[\Omega(t - \tau)]/[\Omega(t - \tau)]$

One interpretation of the right hand side of eqn. 3.29 is that the function $[\exp(-at) f(t)]$ is scanned (Guillemin, 1963) by the passage of the Dirichlet kernel $\sin(\Omega\tau)/(\pi\tau)$ over it. With Ω finite, the periodic nature of this kernel, which is shown in a normalised form in Fig. 3.2, gives rise to Gibbs' oscillations which mar the representation of the response. Only if $\Omega = \infty$ does the Dirichlet kernel reduce to a delta function which causes the oscillatory errors to disappear. Since the

period of the oscillations is $2\pi/\Omega$, a better representation of $f(t)$, say $f_o(t)$, is achieved by an averaging over this period in the following way:

$$\begin{aligned} \exp(-at)f_o(t) &= \frac{\Omega}{2\pi} \int_{t-\pi/\Omega}^{t+\pi/\Omega} \exp(-a\tau) f_\Omega(\tau) d\tau \\ &= \frac{\Omega}{(2\pi)^2} \int_{-\Omega}^{\Omega} \bar{f}_*(a+j\omega) d\omega \int_{t-\pi/\Omega}^{t+\pi/\Omega} \exp(j\omega\tau) d\tau \end{aligned}$$

Evaluation of the inner integral gives

$$f_o(t) = \frac{\exp(at)}{2\pi} \int_{-\Omega}^{\Omega} \bar{f}_*(a+j\omega) \sigma(\omega) \exp(j\omega t) d\omega \quad (3.30)$$

where

$$\sigma(\omega) = \frac{\sin(\pi\omega/\Omega)}{(\pi\omega/\Omega)} \quad (3.31)$$

is referred to as the sigma factor (Lanczos, 1957, Day *et al.*, 1965).

For numerical integration eqn. 3.30 can be further simplified. In Section 3.1 it is shown that the frequency dependence of the parameters can be incorporated in the usual modified Fourier transform through a dependence on $|\omega|$. Displaying this dependence, eqn. 3.10 becomes

$$\begin{aligned} \bar{f}_*(a+j\omega, |\omega|) &= \int_0^\infty f(t, |\omega|) \exp\{-(a+j\omega)t\} dt \\ &= \int_0^\infty f(t, |\omega|) \exp(-at) [\cos(\omega t) - j \sin(\omega t)] dt \end{aligned}$$

so that if the real and imaginary parts of $\bar{f}_*(a+j\omega, |\omega|)$ are $P(\omega, |\omega|)$, $Q(\omega, |\omega|)$ respectively, then

$$P(\omega, |\omega|) = \int_0^\infty f(t, |\omega|) \exp(-at) \cos \omega t dt$$

and is even with respect to ω and

$$Q(\omega, |\omega|) = \int_0^\infty f(t, |\omega|) \exp(-at) \sin \omega t dt$$

and this is odd with respect to ω .

For $t > 0$ eqn. 3.30 can be written

$$\exp(-at)f_o(t) = \frac{1}{2\pi} \int_{-\Omega}^{\Omega} \sigma(P+jQ)(\cos \omega t + j \sin \omega t) d\omega$$

and for $t < 0$

$$0 = \frac{1}{2\pi} \int_{-\Omega}^{\Omega} \sigma(P+jQ)(\cos \omega t + j \sin \omega t) d\omega$$

Replacing t by $-t$ in the second equation, and making use of the evenness of P and oddness of Q with respect to ω it follows on addition that

$$f_o(t) = \frac{2 \exp(at)}{\pi} \int_0^\Omega \sigma P \cos \omega t d\omega \quad (3.32)$$

Thus it is only necessary to compute P , the real part of $\bar{f}_*(a+j\omega)$, and to carry out the numerical integration over the half-range, $0 \leq \omega \leq \Omega$. Further, mechanisms have been built into the process for controlling the various sources of error. The best ways of using these mechanisms in practice is the subject of the next section.

It should be stated immediately that with

$$\omega = k \Delta\omega, \quad N = \Omega/\Delta\omega$$

eqn. 3.32 can be written, using the trapezoidal rule,

$$\exp(-at)f_o(t) = (2/\pi) \sum_{k=0}^{N-1} \sigma_k P_k \cos(rk\Omega/N)$$

where

$$\sigma_k P_k = \sigma(k\Delta\omega) P(k\Delta\omega, |k\Delta\omega|)$$

Hence, when $f_o(t)$ is required at a large number of points in the range $(0, T) = (0, 2\pi/\Delta\omega)$, the values $f_o(rT/N)$ can be obtained most efficiently using the fast Fourier transform developed by Cooley and Tukey (1965) and applied to this particular problem by Ametani (1972).

3.4 Choice of integration parameters, $a, \Delta\omega, \Omega$

In applying the trapezoidal rule for the numerical evaluation of eqn. 3.32 it is necessary to assign values to the smoothing parameter a , the step length $\Delta\omega$ and the range Ω . If the latter is too small it may limit the rate of rise. This is best seen by consideration of the Fourier integral for the step function $-\pi/2$ for $t < 0$, $\pi/2$ for $t > 0$, which may be represented by the integral

$$\int_0^\infty \frac{\sin(\omega t)}{\omega} d\omega$$

On truncating the range of integration the sine integral is obtained i.e.

$$\int_0^\Omega \frac{\sin(\omega t)}{\omega} d\omega = \text{Si}(\Omega t)$$

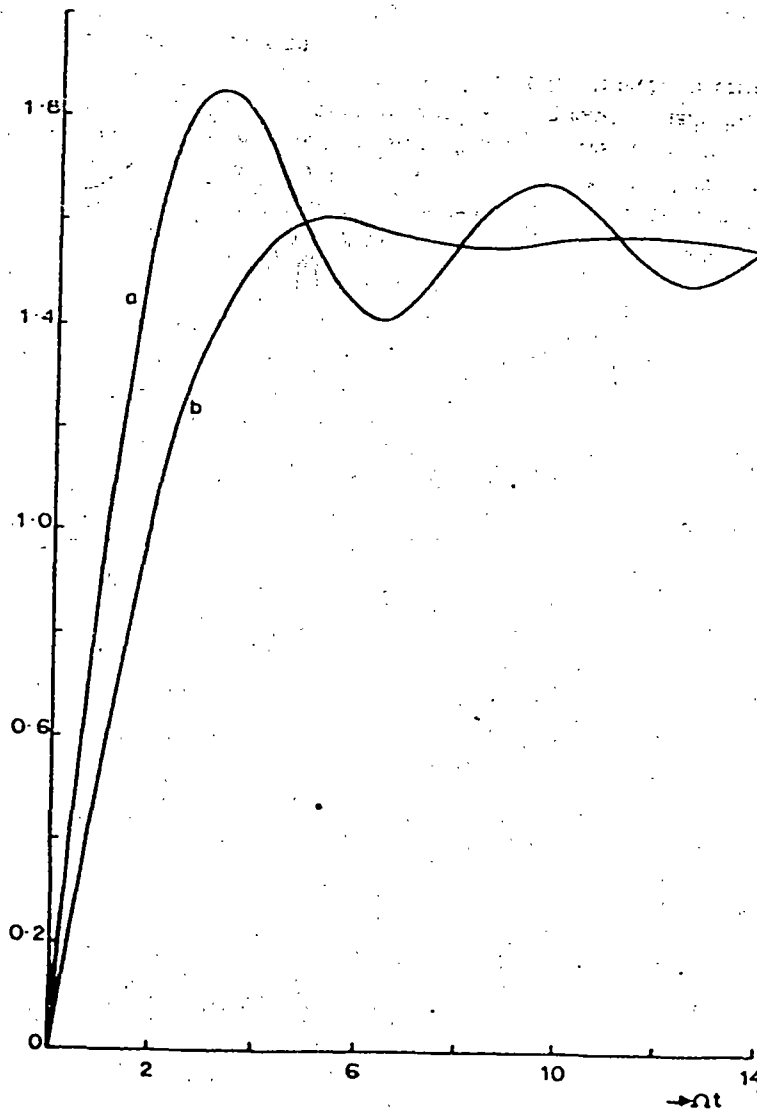


Fig. 3.3 Integral representation of step function of magnitude $\pi/2$
 a $\text{Si}(\Omega t)$
 b $\text{Si}(\Omega t)$ with sigma factor

and incorporating the σ -factor

$$\int_0^{\Omega} \frac{\sin(\omega t)}{\omega} \frac{\sin(\pi\omega/\Omega)}{(\pi\omega/\Omega)} d\omega = \text{Si}_{\sigma}(\Omega t), \text{ say}$$

These two functions are displayed in nondimensional form in Fig. 3.3 and it is apparent that the rise time t_r is given by

$$\Omega t_r = 4 \quad (3.33)$$

This represents the shortest rise time obtainable with a given Ω and is used as a guide in practical problems. For example, if with a given choice of Ω the rise time is found to be considerably greater than $t_r = 4/\Omega$, then it may be assumed that Ω has been chosen sufficiently high. On the other hand, if the rise time is of little importance and all that is required is a good overall representation, then an acceptable t_r may be chosen and used to estimate Ω , by choosing $\Omega > 4/t_r$.

The three parameters a , $\Delta\omega$, Ω are not only inter-related in a complex way but their choice depends on the time over which a solution is required. One way to obtain working rules is through mathematical experimentation and for this to be effective the subject of the experiment should be more testing than anything likely to be experienced in practice. For this reason a lightly damped, single-phase line is used with the parameters which are independent of frequency. Further, since aliasing errors cannot be fortuitously concealed for a function with a nonzero average, then the voltage at the open-circuited end of such a line energised by a unit step voltage is considered. Any rules adequate in this context can be applied with confidence in the practical situations in which they are used in Chapter 7.

It is readily shown (Day *et al.*, 1966) that for such a line $P(\omega, |\omega|)$ in eqn. 3.32 is

$$P = \text{Re}(a + j\omega)^{-1} \text{sech} \{ [R + (a + j\omega)M](a + j\omega)C \}^{1/2} \quad (3.34)$$

and for purposes of illustration the parameters are taken to be

$$l = 10 \text{ miles}; R = 2.74 \times 10^{-2} \text{ ohm/mile}; L = 1.386 \times 10^{-3} \text{ H/mile}; \\ C = 2.09 \times 10^{-8} \text{ F/mile.}$$

If the line were lossless then the voltage would take the castellated form shown in Fig. 3.4. This provides a check for the present calculation over the first few cycles and an upper bound for the voltage as $\mathcal{M} = 2$.

Since the travel time τ is $53.8 \mu\text{s}$, a reasonable overall representation can be achieved with a rise time $t_r = 5 \mu\text{s}$ say. Thus Ω is chosen such that

$$\Omega > 4/(5 \times 10^{-6}) = 0.8 \times 10^6$$

If $\Omega = 10^6$ and 500 integration steps are taken, so that $\Delta\omega = 2 \times 10^3$, then the greatest possible aliasing error is given in eqn. 3.25 as $\mathcal{M}/[\exp(aT) - 1]$, so that with $T = \pi \times 10^{-3} \text{ s}$ and its dependence on the choice of a can accordingly be tabulated.

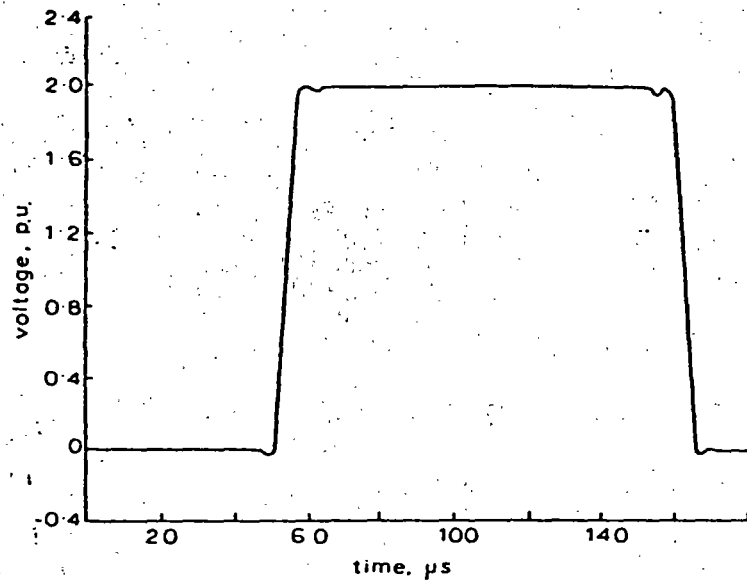


Fig. 3.4 Results with $\Omega = 10^4$, $\Delta\omega = 2 \times 10^3$, $a = 10^4$

Table 3.1

a	10^2	10^3	10^4	10^5
maximum possible aliasing error	5.4	0.09	4.6×10^{-12}	2.1×10^{-16}
error as percentage of $\mathcal{N} = 2$	270	4.5	2.3×10^{-10}	1.05×10^{-14}

The results of the numerical integration are shown in Figs. 3.4 and 3.5 for $10^2 \leq a \leq 10^5$. In view of the large aliasing factor for $a = 10^2$ (see Table 3.1) the poor representation is hardly surprising. For $a = 10^3$ the error is somewhat greater than Table 3.1 predicts since, in this case, the integrand is so peaky, as shown in Fig. 3.6, that the step length must be reduced to ensure an accurate solution. The choice $a = 10^4$ can be seen from Fig. 3.4 to give a very good representation, whereas with $a = 10^5$ a new oscillatory error, with period measurable from Fig. 3.4 as $c. 2\pi \times 10^{-6}$, has been introduced with an exponentially increasing amplitude. This error can be identified as the truncation error $\eta(t)$, since this is of the form

$$\eta(t) = \text{Re} \frac{2}{\pi} \exp(at) \int_{\Omega}^{\infty} P(\omega) \exp(j\omega t) d\omega$$

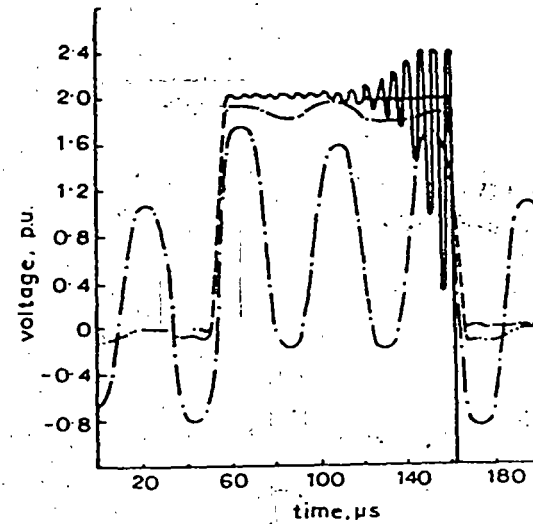


Fig. 3.5 Effect of smoothing parameter a
 $\Omega = 10^4$, $\Delta\omega = 2 \times 10^3$
 — $a = 10^2$
 - - $a = 10^3$
 - · - $a = 10^4$
 · · · $a = 10^5$

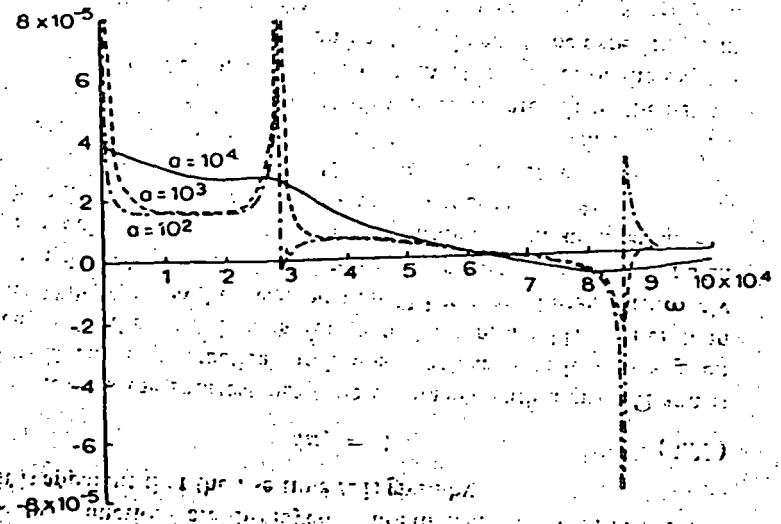


Fig. 3.6 Integrands for $a = 10^2, 10^3, 10^4$; $\tau = 100 \mu s$

$$\eta(t) = \operatorname{Re} \frac{2}{\pi} \exp(at) \exp(j\Omega t) \int_0^{\infty} P(\omega' - \Omega) \exp(j\omega' t) d\omega' \quad (3.35)$$

In eqn. 3.35 the integral is a relatively smooth function of t so that the truncation error has a basic period of $2\pi/\Omega$ [which is equal to $(2\pi \times 10^{-6})$ in this case] and the amplitude contains the factor $\exp(at)$.

Finally, the third parameter $\Delta\omega$ is considered in more detail. With $a = 10^4$ and $\Omega = 10^6$, which are values already found to give good results with $\Delta\omega = 2 \times 10^3$, $\Delta\omega$ is now varied. No distinguishable difference is found for $\Delta\omega \leq 2 \times 10^3$ over the first major period of 4τ .

Generalising, when an overall response is required over this first period of 4τ , a is chosen such that $a\tau$ is approximately equal to 1 in the middle of the time range (i.e. in this case $2a\tau \doteq 1$), $\Omega > 40/\tau$ (on the assumption that an acceptable rise time is $\tau/10$), and $\Delta\omega = \Omega/500$.

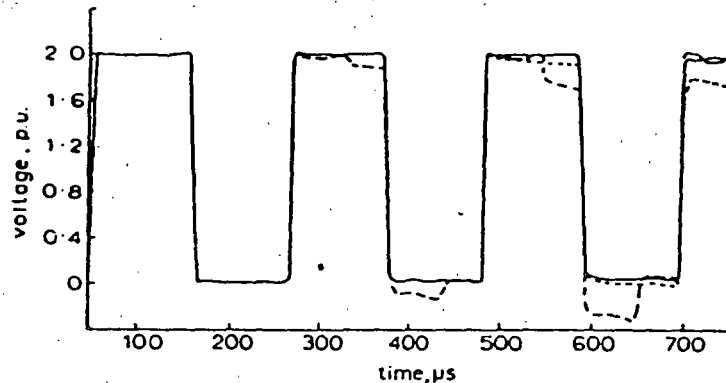


Fig. 3.7 Global response over several cycles

$$a = 10^4, \Omega = 10^6$$

$$a \text{ --- } \Delta\omega = 1000 \quad b \text{ --- } \Delta\omega = 2000$$

$$c \text{ - - - - } \text{Modified Simpson's rule with } \Delta\omega = 2000$$

While the parameter a smooths the term $P(\omega, |\omega|)$ in the integrand, the $\cos(\omega t)$ oscillates with a period in ω of $2\pi/t$. For a representation of this it is reasonable to expect that t should be restricted so that at least four points occur in each quarter cycle, i.e.

$$16 \Delta\omega < 2\pi/t$$

or

$$t < 0.4/\Delta\omega;$$

or with $\Delta\omega = \Omega/500$ and Ω chosen reasonably close to the lower bound of $\Omega > 40/\tau$, $t < 5\tau$.

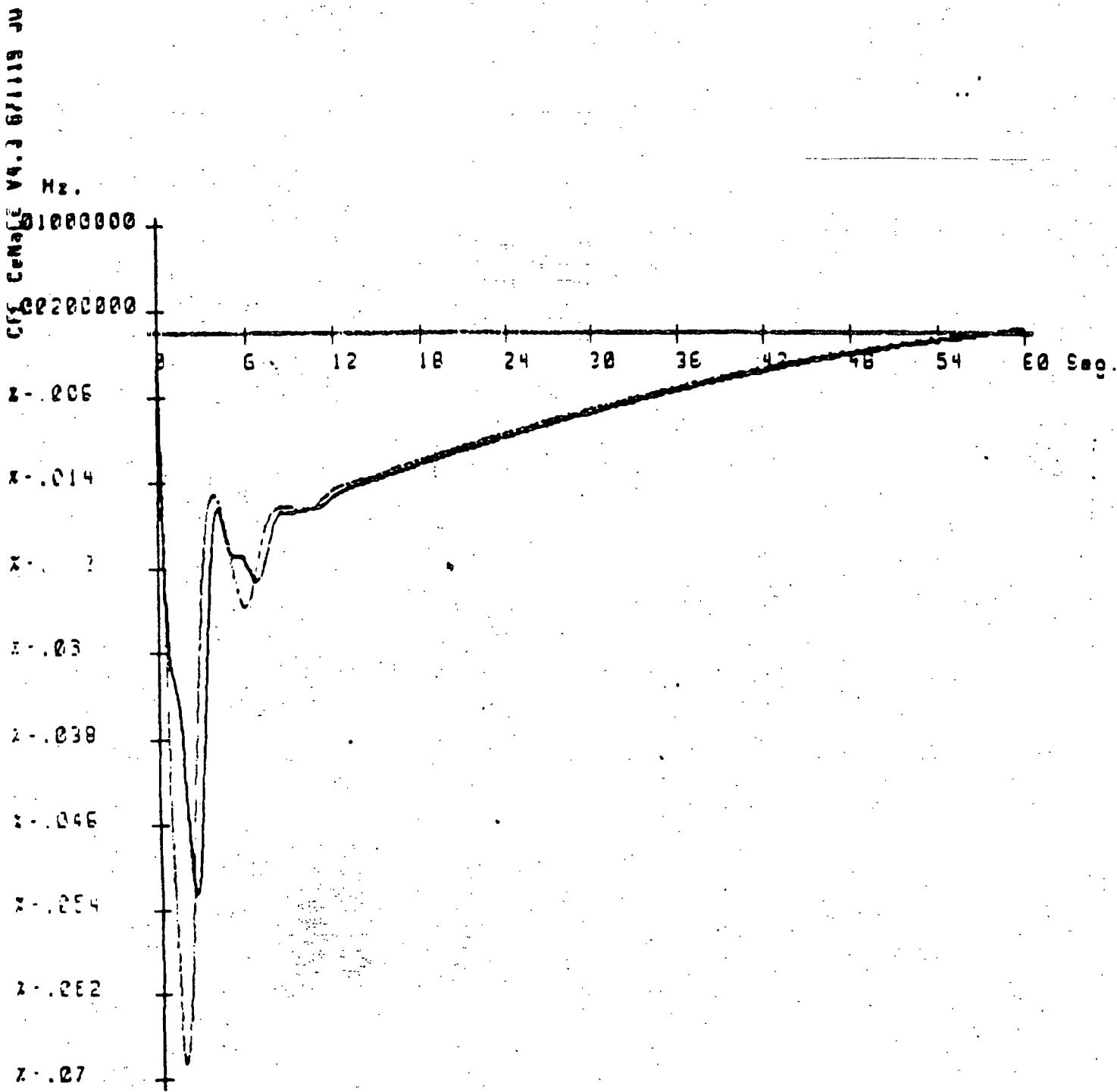
When the response is required over several periods it is necessary to reduce $\Delta\omega$. Fig. 3.7 shows that halving the step length with a and Ω unchanged gives a good representation over three complete periods i.e. 12τ . If the response is required over still longer times the range could be divided into two parts, the first covering the first few periods as described above. In the second part a new value of a is chosen such that $a\tau$ is approximately equal to 1 at the mid-point of the second range. By this means Battison *et al.* (1969) have given an example showing good representation over 12 complete periods i.e. 48τ . In this case the value of a will be comparatively low, but in order to comply with the inequality $t < 0.4/\Delta\omega$, $\Delta\omega$ must be correspondingly low. Hence according to eqn. 3.25 the aliasing errors are not increased.

Day *et al.* (1968) have shown that in systems composed of lines of different travel times the use of the above rules, based on that part of the system with the longest travel time, gives reasonable overall representation, provided that the ratio of the individual travel times does not exceed 10 to 1. Above this limit Ω must be increased further.

In all problems, having obtained an overall response using the working rules outlined, the fine detail in a subinterval which appears to be of special interest can, of course, be obtained using the same methods with new choices of the integration parameters, in particular a greater value of Ω .

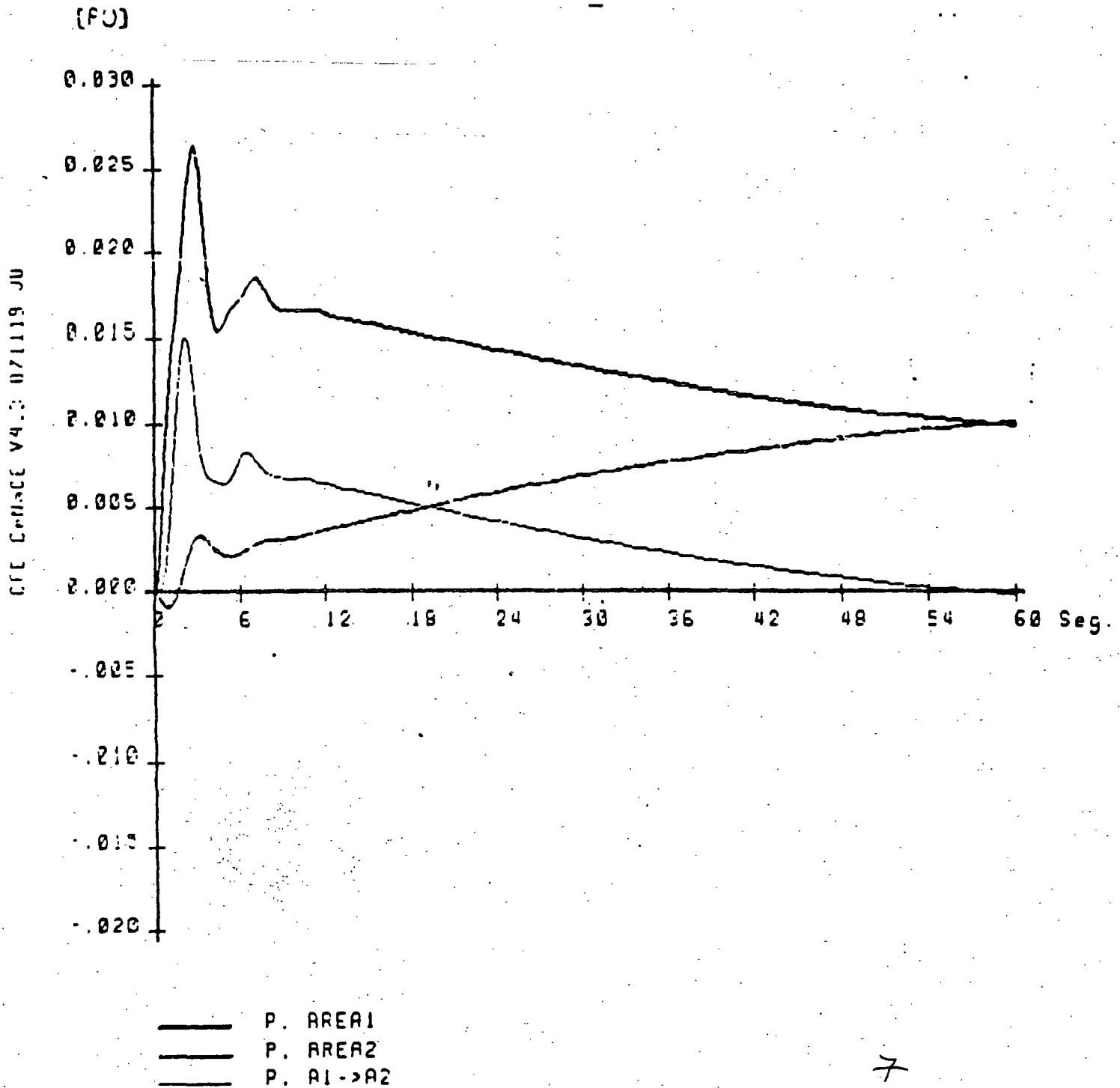
It may be useful to repeat that the rules given above are derived from a study of a particularly testing example. The fact that the example chosen is a single-phase line is irrelevant and the rules apply directly to multiphase problems. In fact, when realistic losses are included, some relaxation of the rules is generally possible. However, unless each case is to be treated on its merits, the safest way is to use the working rules described.

GRAFICAS DE VARIACION DE FRECUENCIA (caso 5A)



— OF AREA1
— OF AREA2

VARIACION DE POTENCIA MECANICA Y POTENCIA DE INTERCONEXION
(caso 5A)



CONCLUSIONES

Los estudios de estabilidad son un complemento a los estudios de flujos de potencia y de corto circuito en el objetivo de lograr un análisis más completo de un sistema eléctrico de potencia, permitiendo un conocimiento más amplio acerca de sus fortalezas y debilidades. Ellos se utilizan en las etapas de planeación y operación.

En la fase de planeación se aplican en algunas labores como:

- Diseño de la red.
- Selección de interruptores y esquemas de protección.
- Adición de elementos compensadores: CEV's, capacitores serie, etc.
- Determinación de los parámetros de los generadores síncronos: H, X', etc.
- Tipo y parámetros de los controles de velocidad y de voltaje: constantes de tiempo, ganancias, etc.

En la operación de los sistemas eléctricos, los estudios de estabilidad permiten establecer estrategias que proporcionen un mayor grado de seguridad, entre las que se pueden mencionar:

- Análisis de contingencias: generadores, líneas, carga, etc.
- Definición de límites de operación: líneas.
- Aplicación de controles discretos suplementarios: DAG, DAC, recierre monopolar, etc.

Aún cuando no se cuente con un simulador digital, para muchos fines existen técnicas sencillas que proporcionan en orden de magnitud el comportamiento del sistema.

El problema de inestabilidad puede ocurrir en un sistema en diversas magnitudes, desde la pérdida de sincronismo en una máquina, en un grupo de máquinas o un colapso generalizado.

Después de haber revisado los conceptos básicos sobre la Estabilidad de los Sistemas Eléctricos, fácilmente se puede dar respuesta a las preguntas que fueron planteadas al iniciar el tema:

¿Qué es la estabilidad de un sistema eléctrico?

¿En qué consisten los estudios de estabilidad?

¿Cuál es su utilidad?

¿Qué factores afectan la estabilidad de un sistema eléctrico?

- Fortaleza o robustez del sistema.
- Magnitud, duración y localización de la perturbación.
- Punto o condiciones de operación.

FINALMENTE, PUEDE DECIRSE QUE LOS ESTUDIOS DE ESTABILIDAD SON UNA ACTIVIDAD NECESARIA PARA LA ADECUADA PLANEACION Y OPERACION DE LOS SISTEMAS ELECTRICOS DE POTENCIA.

REFERENCIAS

- (1) F. Aboytes - G. Arroyo
TOPICOS DE ESTABILIDAD
CFE. Cenace, 1985.
- (2) F. Aboytes - F. Sánchez - M. Flores
SIMULADOR INTERACTIVO DE
SISTEMAS DE POTENCIA (SISP)
CFE-Cenace-Did, 1986.
- (3) Gerardo López S.
TOPICOS DE ESTABILIDAD EN SISTEMAS DE POTENCIA
Tesis Profesional, ESIME-IPN, 1987.
- (4) G. Villa
NOTAS SOBRE ESTABILIDAD
Curso Sistemas de Potencia II. Educ. Continua, 1987.
- (5) O. I. Elgerd
ELECTRIC ENERGY SYSTEMS. An introduction.
McGraw Hill, 1971.
- (6) E. W. Kimbark
POWER SYSTEM STABILITY
John Wiley & Sons, 1948.
- (7) Stagg - El Abiad
COMPUTER METHODS IN POWER SYSTEM ANALYSIS.
McGraw Hill, 1968.
- (8) Anderson and Fouad
POWER SYSTEM CONTROL AND STABILITY
Iowa State University Press, 1973.
- (9) Robin Padmore - Alain Germond
DEVELOP OF DINAMIC EQUIVALENTS FOR
TRANSIENT STABILITY STUDIES
Systems Control Inc., 1977.
- (10) Rubén Pérez R.
ANALISIS TRANSITORIO DE UN SEP
Proyecto Terminal, UAM, 1988.

Comportamiento del Voltaje en las Líneas de Transmisión Radiales

150.

Felipe Martínez Cruz

José Luis Martínez Menchaca

Compañía de Luz y Fuerza del Centro, S. A.
Operación Sistema

RESUMEN

Se presenta un método directo para determinar el comportamiento del voltaje de recepción en una línea de transmisión radial. El método resulta sencillo y práctico, y sustituye al procedimiento iterativo o de tanteos, que tradicionalmente se utilizaba cuando la carga es modelada como una potencia constante.

Se incluyen algunas aplicaciones del método, como son: La explicación del fenómeno de colapso de voltaje, la obtención del límite de estabilidad y la descripción de la relación entre la capacidad de transmisión y la longitud de la línea.

INTRODUCCION

En las líneas de transmisión radiales, como la mostrada en la figura 1, el voltaje en el punto de recepción (R), es la variable clave para analizar el comportamiento de la línea en estado estable equilibrado. El resto de las variables, como el voltaje en el extremo de envío (G), los parámetros de la línea y las características de la carga, son generalmente conocidos, y así se consideran en este trabajo.

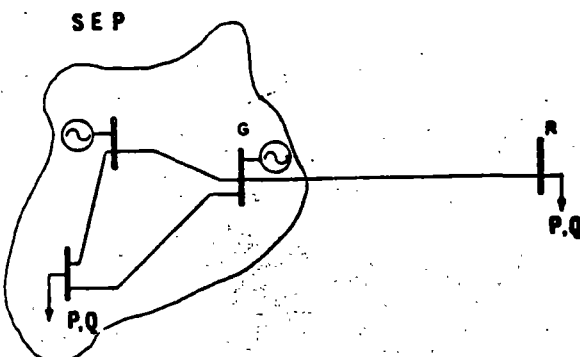


Figura 1.- Línea radial conectada a un bus robusto de un sistema eléctrico.

El voltaje de recepción, y la solución misma del problema, depende fundamentalmente del tipo de carga conectada y del modelo adoptado para representar la línea de

transmisión. Los párrafos siguientes se dedican a explicar el modelo de línea utilizado, los distintos modelos de cargas y su efecto en el comportamiento de la línea.

MODELADO DE LA LINEA

La línea de transmisión es modelada como una línea corta, esto es, despreciando el efecto capacitivo, como se muestra en la figura 2. Esta modelación simplifica notablemente el problema y aunque introduce un cierto error, éste influye hacia el lado conservador, es decir el comportamiento real de la línea, es ligeramente mejor que el obtenido a partir del método aquí expuesto.

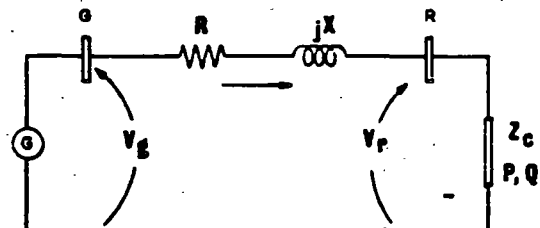


Figura 2.- Circuito equivalente de una línea radial.

MODELADO DE LA CARGA

Con el objeto de representar adecuadamente a las cargas en el análisis de un Sistema Eléctrico de Potencia (SEP), se han establecido tres modelos básicos, los cuales, combinados en diferentes proporciones, pueden representar con buena aproximación el comportamiento real de la carga [1]. Estos modelos quedan englobados en la ecuación:

$$S = V^k \quad (1)$$

donde

S = Potencia activa o reactiva demandada por la carga [p.u.]

V = Voltaje en el punto de carga [p.u.]

RECONOCIMIENTO

Los autores desean expresar su agradecimiento al Ing. Adolfo García García, Jefe de Operación Sistema de la CLFC, por el apoyo brindado en la realización de este trabajo.

- k = Exponente que determina el tipo de modelo
- 0 (modelo de potencia constante)
 - 1 (modelo de corriente constante)
 - 2 (modelo de impedancia constante)

El modelo de potencia constante se aproxima al comportamiento real de cargas rotativas, tales como motores de inducción y motores síncronos. Por otro lado, el modelo de impedancia constante se puede asociar a cargas estáticas, como por ejemplo: hornos, calefacción, alumbrado, etc. Las figuras 3 y 4 muestran de una manera más objetiva los modelos mencionados.

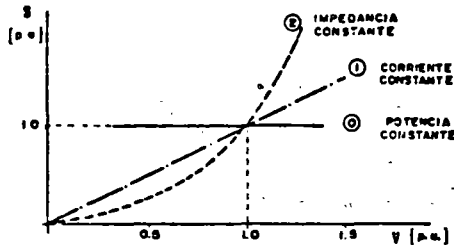


Figura 3.- Relación entre la carga y el voltaje para los modelos básicos.

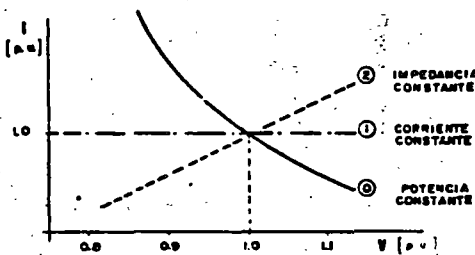


Figura 4.- Relación entre la corriente de la carga y el voltaje para los modelos básicos.

EFFECTO DEL TIPO DE CARGA EN LA SOLUCION

En una línea radial cuya carga puede suponerse una impedancia constante, el voltaje de recepción se obtiene con facilidad a partir de la ecuación:

$$\tilde{V}_r = \tilde{I} \tilde{Z}_c = \frac{\tilde{Z}_c}{\tilde{Z} + \tilde{Z}_c} \tilde{V}_g \text{ [volts]} \quad (2)$$

donde $\tilde{Z} = R + jX$ es la impedancia de la línea, \tilde{Z}_c la impedancia de la carga, y las demás variables, las asociadas al circuito de la figura 2.

Si la carga se considera modelada como una potencia constante, el problema ya no resulta tan sencillo, ya que la corriente demandada por la carga es función del voltaje de recepción, el cual a su vez depende de la caída de tensión en la línea, y ésta, de la corriente demandada. La determinación de las dos incógnitas (V_r e I) se realiza (ba) tradicionalmente utilizando el procedimiento iterativo mostrado en la figura 5. Los autores de este trabajo consideran que con el método aquí expuesto, el procedimiento iterativo no volverá a usarse (a menos que se quiera usar un modelo de la línea más completo).

MODELO DE CARGA ADOPTADO.

Una carga con impedancia constante contribuye a aliviar el problema de bajo voltaje demandando menor corriente, mientras que la carga con potencia constante es la más severa, ya que acentúa las caídas de tensión. Finalmente, un modelo de corriente constante tiene efectos intermedios, ya que es equivalente a 50% de carga con potencia constante y 50% de carga de impedancia constante.

Por tal motivo el problema del comportamiento del voltaje en líneas radiales se aborda utilizando el modelo más crítico, el de potencia constante.

INTENTOS DE RESOLVER EL PROBLEMA

Algunos autores han realizado esfuerzos para resolver el problema planteado, destacándose el método expuesto en las referencias [2] y [3], y que puede resumirse en la ecuación siguiente:

$$|V_r| = |V_g| - (R I \cos \theta + X I \sin \theta) \quad (3)$$

donde (θ) es el ángulo definido por el factor de potencia de la carga. En la ecuación (3) se considerará que la corriente es conocida e independiente del voltaje de recepción V_r . Esto es equivalente a suponer un modelo de carga de corriente constante.

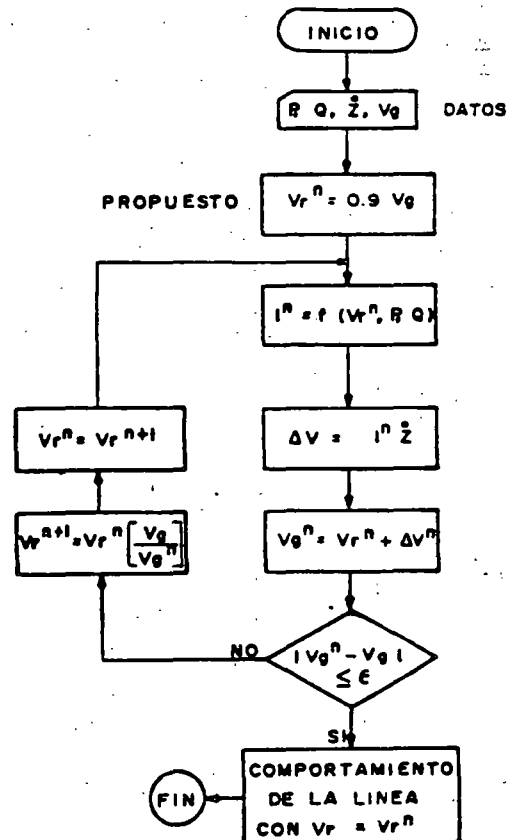


Figura 5.- Procedimiento iterativo para calcular el voltaje de recepción.

Es conveniente destacar que este método se basa también en el modelo de línea corta y supone que el ángulo (δ) entre los fasores V_r y V_g es pequeño, es decir $(XI \cos \theta - RI \sin \theta) \approx 0$.

METODO DIRECTO DE SOLUCION

Considérese la línea radial modelada de acuerdo con el circuito de la figura 2, donde:

- $\tilde{Z} = Z \angle \theta$ = Impedancia total de la línea.
- $\tilde{V}_g = V_g \angle \delta$ = Fesor asociado al voltaje de envío.
- $\tilde{V}_r = V_r \angle \alpha$ = Fesor asociado al voltaje de recepción.
- $\tilde{I} = I \angle \phi$ = Fesor asociado a la corriente demandada por la carga y que circula a través de la línea.
- $\hat{S} = P + jQ$ = Potencia compleja (por fase) de la carga conectada a la línea.

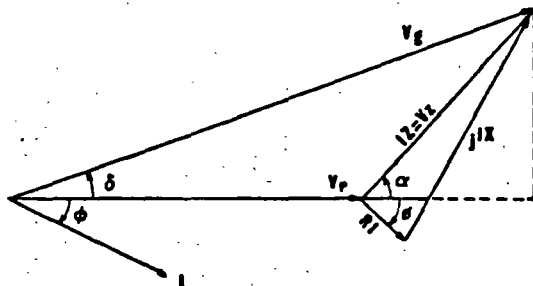


Figura 6.- Diagrama fasorial correspondiente al circuito monofásico de la línea de transmisión.

Del diagrama fasorial de la figura 6:

$$V_g^2 = (V_r + V_z \cos \alpha)^2 + (V_z \sin \alpha)^2 \quad (4)$$

Como:

$$\tilde{Z} = R + jX_L = Z \angle \theta \quad (5)$$

se tiene que:

$$\tilde{V}_z = (I \angle -\theta) (Z \angle \theta) = V_z \angle \theta - \theta \quad (6)$$

de modo que:

$$\alpha = \theta - \theta$$

Generalizando para cualquier factor de potencia:

$$\alpha = \theta + \theta \quad (7)$$

También,

$$I = \frac{P}{V_r \cos \theta} \quad (8)$$

De lo cual:

152.

$$V_z = IZ = \frac{PZ}{V_r \cos \theta} \quad (9)$$

Sustituyendo (9) en (4):

$$V_g^2 = \left(V_r + \frac{PZ}{V_r \cos \theta} \cos \alpha \right)^2 + \left(\frac{PZ}{V_r \cos \theta} \sin \alpha \right)^2 \quad (10)$$

Despejando V_r , se obtiene:

$$V_r = \sqrt{A + \sqrt{D}} \quad (11)$$

Donde:

$$A = \frac{V_g^2}{2} - B \cos \alpha \quad (12)$$

$$B = \frac{PZ}{\cos \theta} \quad (13)$$

$$D = A^2 - B^2 \quad (14)$$

La ecuación (11) es la que permite determinar de manera directa, el voltaje de recepción V_r .

Con el objeto de ilustrar el método, se presenta a continuación su aplicación a un caso real.

EJEMPLO 1.- La línea de 230 kV que une las Subestaciones de Puebla y Zapata, tiene los siguientes parámetros:

$$\tilde{Z} = 9.79 + j 63.32 = 64.07 \angle 81.2^\circ \text{ ohms}$$

$$l = 127.7 \text{ km}$$

Para el caso en que la Subestación Zapata quede radial de Puebla a través de la línea descrita, se desea saber el voltaje que se tendrá en el punto de recepción, si:

$$V_g = 241.5 \text{ kV}$$

$$P = 180 \text{ Mw (3\phi)}$$

$$\cos \theta = 0.90 \text{ (-)}$$

A partir de estos datos se tiene:

$$A = 2.1879 \times 10^{10}$$

$$B = 1.2814 \times 10^{10}$$

$$D = 3.1450 \times 10^{10}$$

$$V_r = 199 \text{ 031 volts.}$$

lo cual puede comprobarse, calculando secuencialmente \tilde{I} , \tilde{V}_z y \tilde{V}_g . Puede demostrarse también que la ecuación (11), funciona indistintamente con valores trifásicos, monofásicos o en por unidad, cuidando la homogeneidad de los valores.

APLICACIONES FUNDAMENTALES DEL METODO

El resto del trabajo se dedica a explicar el comportamiento del voltaje y sus repercusiones, tomando como base el método directo de solución explicado en la sección anterior.

COMPORTAMIENTO DEL VOLTAJE

Repetiremos la ecuación (11), con el objeto de analizarla con un poco más de profundidad.

$$V_r = \sqrt{A + \sqrt{D}}$$

Debido a que toda raíz cuadrada tiene dos soluciones, - el voltaje de recepción tiene también dos valores posibles.

$$V_{r_1} = +\sqrt{A + \sqrt{D}} \quad (15)$$

$$V_{r_2} = +\sqrt{A - \sqrt{D}} \quad (16)$$

donde las raíces negativas del radical externo no tienen sentido, ya que V_r es una magnitud.

Es interesante este resultado, ya que teóricamente es posible alimentar la carga con el valor bajo de voltaje (V_{r_2}), pero con una corriente demandada muy alta, de tal modo que su potencia se mantenga constante.

Para el caso de la línea del ejemplo 1, los valores posibles del voltaje de recepción son:

$$V_{r_1} = 199\ 031 \text{ volts} \quad \text{y} \quad V_{r_2} = 64\ 385 \text{ volts.}$$

Las ecuaciones (15) y (16) definen por lo tanto, el comportamiento del voltaje de recepción cuando se hace variar la carga conectada a la línea. La tabla 1 muestra dicho comportamiento para la línea del ejemplo 1, cuando la carga tiene un factor de potencia de 0.9 atrasado.

En la tabla 1, resultan de interés los casos siguientes

Caso (0) .- Si la línea está en vacío, el voltaje de recepción es igual al voltaje de envío.

Caso (9) .- Con 180 MVA de carga, se tiene el caso resuelto en el ejemplo 1.

Caso (14) .- Con 280 MW de carga, el problema ya no tiene solución.

LIMITE DE ESTABILIDAD EN ESTADO ESTABLE (LEEE)

Como pudo observarse del punto anterior, existe un cierto valor de carga con el cual el problema empieza a ser indeterminado. Desde el punto de vista matemático, éste se debe a que el discriminante (D), definido en la ecuación (14), se vuelve negativo y los valores V_{r_1} y V_{r_2} resultan números complejos. Desde el punto de vista eléctrico, ello se debe a que se ha rebasado el límite de estabilidad de la línea, es decir, la máxima potencia que puede enviarse a través de ella.

TABLA I
COMPORTAMIENTO DEL VOLTAJE DE RECEPCION
EN LA LINEA DE 230 kV PUE - ZAP
($\cos \phi = 0.90$)

CASO N°	P (Mw)	V_{R_1} (kV)	V_{R_2} (kV)
0	0	241.50	0.00
1	20	238.05	5.98
2	40	234.39	12.15
3	60	230.49	18.53
4	80	226.31	25.17
5	100	221.81	32.10
6	120	216.94	39.38
7	140	211.60	47.10
8	160	205.69	55.38
9	180	199.03	64.39
10	200	191.32	74.42
11	220	181.97	86.07
12	240	169.56	100.77
13	260	144.45	128.14
14	280	-	-

Si se grafican los resultados de la tabla 1, se obtiene la curva (A) de la figura 7. En ella se observan los dos valores posibles de V_r para cada valor de potencia. De los datos de la tabla, se desprende que el LEEE de la línea que ha servido como ejemplo, está entre 260 y 280 Mw, pero éste puede obtenerse directamente de la manera siguiente:

El LEEE se presenta en el vértice de la parábola, punto donde las soluciones V_{r_1} y V_{r_2} son iguales. Esto se presenta cuando el discriminante (D) es igual a cero. Por lo tanto si se iguala la ecuación (14) a cero y se despeja P, se tiene:

$$P_{\text{máx}} = \frac{Vg^2 \cos \phi}{2Z(\cos \alpha + 1)} = \text{LEEE} \quad (17)$$

o bien, en términos de potencia aparente:

$$S_{\text{máx}} = \frac{Vg^2}{2Z(\cos \alpha + 1)} \quad (18)$$

El límite, para la línea que se ha venido manejando como ejemplo es entonces de 261.20 Mw con un factor de potencia de 0.9 atrasado.

Una expresión muy conocida [4] para calcular el LEEE de una línea radial es:

$$P_{\text{máx}} = \frac{V^2}{2X} \quad (19)$$

donde se considera que la línea tiene resistencia cero y la carga, un factor de potencia unitario. Puede demostrarse que esta última ecuación es solo un caso particular de las ecuaciones (17) y (18), descritas anteriormente.

Es muy importante enfatizar que en el caso de líneas radiales, el LEEE no puede definirse únicamente en términos de potencia activa como normalmente ocurre, sino que se hace necesario asociar el factor de potencia correspondiente. Esto se debe a que en este tipo de líneas, la variable crítica es el voltaje de recepción, y éste se ve afectado no solo por el flujo de potencia

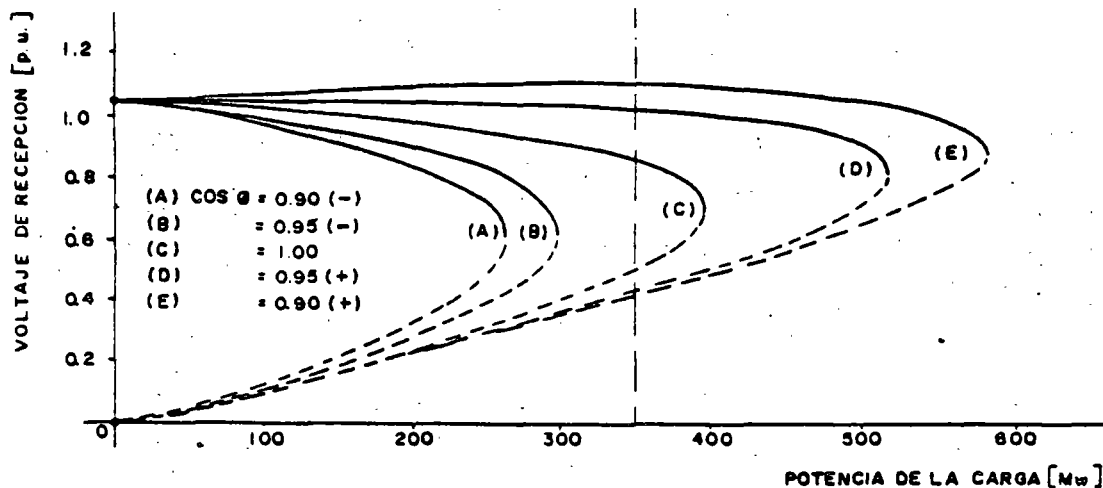


Figura 7.- Comportamiento (en estado estable) del voltaje en una línea radial (Caso típico: línea de 230 kV de 128 km).

activa, sino especialmente por el flujo de potencia reactiva, tal como se demuestra en la figura 8.

La tabla 2 muestra los límites de estabilidad para la línea Puebla - Zapata para diferentes factores de potencia de la carga, los cuales también pueden observarse en las curvas de la figura 7.

TABLA 2
LÍMITES DE ESTABILIDAD DE LA LÍNEA PUEBLA - ZAPATA PARA DIFERENTES FACTORES DE POTENCIA ($V_G = 241.5$ kV)

CASO	COS φ	LEEE (Mw)
A	0.90 (-)	261.2
B	0.95 (-)	297.4
C	1.00	394.8
D	0.95 (+)	516.7
E	0.90 (+)	579.5

Es oportuno en este momento justificar la instalación de capacitores en derivación, o cualquier otro equipo con el mismo efecto, con el objeto de mejorar el factor de potencia al que opera la línea. Los beneficios

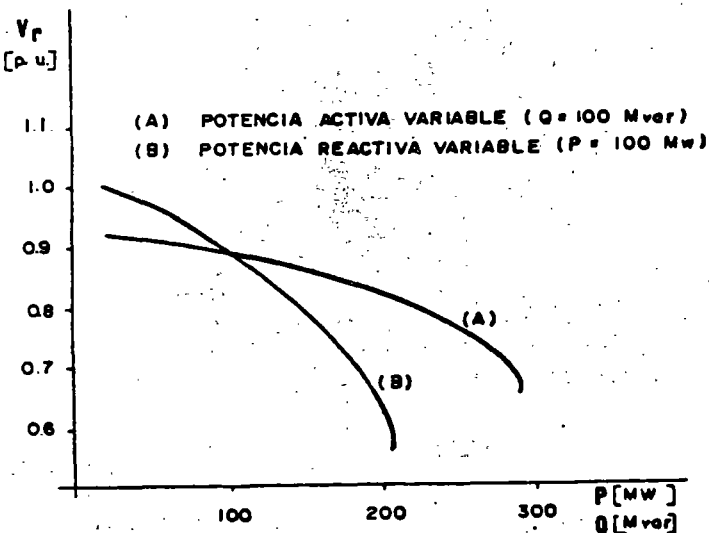


Figura 8.- Efecto de la transferencia de potencia reactiva a través de la línea.

asociados a la inyección local de potencia reactiva son importantes en la operación de un sistema eléctrico; entre ellos pueden mencionarse:

- Incremento del límite de estabilidad de la línea.
- Mejor regulación de voltaje.
- Reducción de las pérdidas de potencia activa y reactiva.

COLAPSO DE VOLTAJE

El colapso de voltaje es un fenómeno característico de las redes radiales y está íntimamente relacionado con la estabilidad de la carga. Puede ocurrir cuando el porcentaje de carga rotativa es alto.

Si se está operando la línea exactamente en su límite de estabilidad y llega a presentarse un aumento infinitesimal de carga, la estabilidad se pierde y el voltaje sufre el colapso, abatiéndose completamente como lo muestra la figura 9. Ello se debe a que el incremento de carga demanda mayor corriente, lo que a su vez produce una disminución en el voltaje, repitiéndose el ciclo hasta que el voltaje se hace cero en el punto de carga. Si se toma en cuenta que la carga rotativa se vuelve inestable (demandando mucho mayor potencia) cuando el voltaje se abate, entonces, podrá verse que el fenómeno se ve acentuado [5].

El colapso de voltaje no solo se presenta al conectar a la línea una carga rotativa superior a su límite de estabilidad, sino también debido a la disminución en el factor de potencia de la carga. Se recurrirá a la línea del ejemplo 1 para explicar esta posibilidad. Su póngase que se está operando a un factor de potencia unitario, con una carga de 280 Mw y con un voltaje de recepción de 0.93 pu. Si el banco de capacitores de la

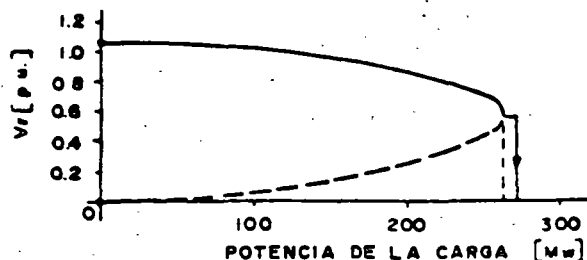


Figura 9.- Ocurrencia del colapso del voltaje por incremento de carga mas allá del límite de estabilidad.

Subestación receptora se desconectara y originara que el factor de potencia caiga a 0.90, ocurriría el colapso, ya que no habrá un punto de operación estable en la nueva curva de comportamiento.

PACIDAD DE TRANSMISION

En esta sección se enuncian las variables que determinan la capacidad de transmisión de potencia de una línea radial y se hace uso nuevamente del método directo de solución para describir cómo varía la capacidad de transmisión con la longitud de la línea de transmisión.

La capacidad de transmisión depende de tres límites, -- que son:

- Límite Térmico (Pt).
- Límite de Estabilidad (LEEE).
- Límite por Caída de Voltaje (Pv).

El límite térmico es función principalmente del calibre y material del conductor, de la temperatura de operación máxima y de las condiciones climatológicas (temperatura ambiente, velocidad del viento, etc.). Una vez definido el conductor de la línea y las demás condiciones de operación, el límite es constante e independiente de la longitud de la línea, tal como se muestra en la figura 10.

El límite de estabilidad, definido por la ecuación (17), puede escribirse como:

$$LEEE = \frac{V_g^2 \cos \theta}{2 Z l (1 + \cos \alpha)} \quad (20)$$

donde (Zl = Z) es la impedancia total de la línea, (z) impedancia por unidad de longitud y (l) la longitud de la línea. Una vez establecida la configuración de la línea, las características de la carga y el voltaje de envío, la única variable que resulta es la longitud (l) de la línea, de tal modo que la ecuación (20) puede expresarse de la siguiente manera:

$$LEEE = \frac{K_1}{l} \quad (21)$$

donde

$$K_1 = \frac{V_g^2 \cos \theta}{2 z (1 + \cos \alpha)} \quad (22)$$

La ecuación (21) corresponde a una hipérbola similar a la curva (B) de la figura 10. En dicha figura se muestra que existe una cierta longitud l_1 donde se presenta la frontera entre los dos límites descritos hasta el momento. Para una longitud menor a l_1 , la capacidad de transmisión está dada por el límite térmico, mientras que para una longitud mayor, la capacidad está determinada por el límite de estabilidad, el cual disminuye con la longitud. El valor de (l_1) puede obtenerse de la ecuación (21).

El límite por caída de voltaje puede también determinarse aplicando el método directo de solución descrito en este artículo. Despejando la potencia (P) de la ecuación (10) se tiene:

$$P = \frac{V_r \cos \theta}{Z} \left(\sqrt{V_g^2 - V_r^2 \sin^2 \alpha} - V_r \cos \alpha \right) \quad (23)$$

Si se expresa la impedancia total (Z) en términos de la impedancia por unidad de longitud y además se fija el valor mínimo permisible del voltaje de recepción V_r se-

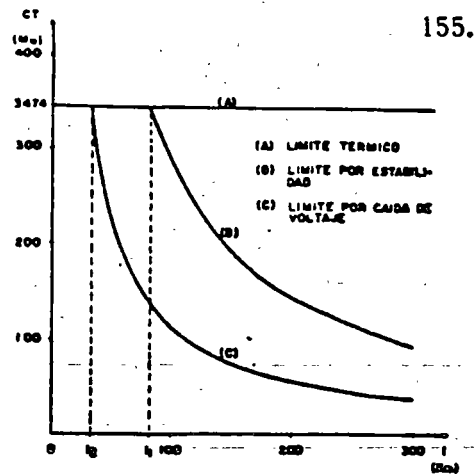


Figura 10. - Límites que determinan la capacidad de transmisión (CT) de una línea radial.

tiene que el flujo máximo de potencia activa es:

$$P_v = \frac{K_2}{l} \quad (24)$$

donde

$$K_2 = \frac{V_r \cos \theta}{z} \left(\sqrt{V_g^2 - V_r^2 \sin^2 \alpha} - V_r \cos \alpha \right) \quad (25)$$

De igual manera, la ecuación (24) describe una hipérbola como la curva (c) de la figura 10 con una longitud frontera (l_2), la cual puede obtenerse a partir de la ecuación (24). También, el flujo máximo de potencia activa disminuye con la longitud de la línea.

De manera que la capacidad de transmisión de una línea radial puede definirse como el valor mínimo de los tres límites descritos, es decir:

$$CT = \min [Pt, LEEE, P_v]$$

Normalmente se cumple que a partir de la longitud (l_2) el límite menor es el de caída de voltaje.

Como se mencionó en su oportunidad, el factor de potencia de la carga tiene gran influencia en el flujo máximo de potencia activa. La figura 11 muestra cómo se modifica la capacidad de transmisión con diferentes valores del factor de potencia. En esta figura ya no se incluye la curva correspondiente al LEEE por ser un límite intermedio.

EJEMPLO 2.- Una línea típica de 230 kV tiene los siguientes parámetros y valores de operación:

$$Z = 0.5283 / 68.54 \Omega/\text{km}$$

$$V_g = 1.05 V_n = 241.5 \text{ kV}$$

$$V_r = 0.95 V_n = 218.5 \text{ kV}$$

$$\cos \theta = 0.9 (-)$$

En estas condiciones se tiene:

$$\theta = 68.84^\circ$$

$$\beta = -25.842^\circ$$

$$\alpha = \theta + \beta = 42.998^\circ$$

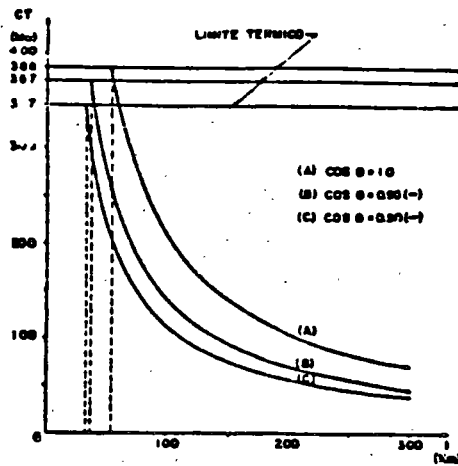


Figura 11.- Efecto del factor de potencia sobre la capacidad de transmisión (CT).

$$K_1 = 28\,692.910 \text{ Mw} \cdot \text{km}$$

$$K_2 = 11\,256.753 \text{ Mw} \cdot \text{km}$$

El límite térmico para las Líneas de 230 kV es

$$P_t = 386 \text{ Mva} \cdot (\cos \phi) = (386) (0.9) = 347.4 \text{ Mw}$$

Las longitudes frontera se calculan a partir de (21) y (24) considerando que:

$$P_t = LEEE = P_v$$

$$l_1 = \frac{K_1}{LEEE} = \frac{28\,692.910}{347.4} = 82.59 \text{ km}$$

$$l_2 = \frac{K_2}{P_v} = \frac{11\,256.753}{347.4} = 32.40 \text{ km}$$

Las ecuaciones que definen los tres límites de transferencia de potencia son entonces:

$$P_t = 347.4 \text{ Mw} = \text{cte.}$$

$$LEEE = \frac{K_1}{l} \text{ para } l \geq 82.59 \text{ km.}$$

$$P_v = \frac{K_2}{l} \text{ para } l \geq 32.40 \text{ km.}$$

y la capacidad de transmisión estará dada por el límite que se presente primero, tal como lo describe la ecuación (26).

Trabajo preparado para presentarse en la XI Conferencia Internacional de Investigación, Desarrollo y Aplicación de Ingeniería Eléctrica y Electrónica "MEXICON 83". No viembre de 1983.

Después del desarrollo del tema, es posible resumir su esencia con las siguientes conclusiones:

- 1.- Las condiciones de una transmisión radial de energía eléctrica puede presentarse con cierta frecuencia en un sistema eléctrico, no solo en condiciones normales de operación, sino también en el caso de falla de una de dos líneas que converjan en una subestación.
- 2.- El voltaje de recepción y su variación ante cambios de carga, determina prácticamente el comportamiento general de una línea radial.
- 3.- Dicho comportamiento se ve influenciado sobremanera por el tipo de carga conectada a la línea, siendo crítico el caso de carga rotativa o de potencia - constante.
- 4.- El método directo de solución aquí expuesto, para el caso de carga rotativa, resulta práctico y sencillo, sustituyéndose así el método iterativo anteriormente utilizado.
- 5.- El límite de estabilidad puede calcularse de una manera directa para cualquier factor de potencia de la carga. Este límite no es determinado por el ángulo entre los voltajes de envío y recepción, sino por la magnitud del voltaje (estabilidad de voltaje).
- 6.- El límite de estabilidad no puede definirse solamente en términos de potencia activa, sino que se debe incluir el factor de potencia, ya que el límite crece conforme dicho factor se mejora.
- 7.- El flujo de potencia reactiva por la línea abate notablemente el voltaje en el extremo de recepción, por lo que es recomendable la inyección local de potencia reactiva en el punto de carga.
- 8.- Si por algún motivo llega a rebasarse el límite de estabilidad de una línea radial, se presenta el fenómeno denominado "colapso" o inestabilidad de voltaje.

REFERENCIAS

- [1] Kent, Schmus, Mc Crackin and Wheeler. DYNAMIC MODELING OF LOADS IN STABILITY ESTUDIES. IEEE Transactions PAS, May 1969.
- [2] C. W. Brice. COMPARISON OF APPROXIMATE AND EXACT VOLTAGE DROP CALCULATIONS FOR DISTRIBUTION LINES. IEEE Transactions PAS, November 1982.
- [3] E. T. A. Rapson. ELECTRICAL TRANSMISSION AND DISTRIBUTION. Oxford University Press, London 1933.
- [4] O. I. Elgerd. ELECTRIC ENERGY SYSTEMS THEORY. AN INTRODUCTION. Mc. Graw Hill Book Company. 2nd Edition. 1981.
- [5] B. M. Weedy. ELECTRIC POWER SYSTEMS. John Wiley & Sons. 2nd. Edition. 1972

Desconexión de Carga por Baja Frecuencia en un Sistema Eléctrico de Potencia

Felipe Martínez Cruz

J. Leonel Hernández Grimaldo

Cfa. de Luz y Fuerza del Centro, S. A.
Universidad Autónoma Metropolitana

RESUMEN

En el trabajo se describe el comportamiento de un sistema eléctrico de potencia después de una pérdida de generación severa, incluyendo la desconexión de la carga por relevadores de frecuencia, la respuesta de los gobernadores, el amortiguamiento de la carga y la influencia de las constantes de tiempo de los componentes principales del sistema.

En la parte final del trabajo se muestra el programa digital desarrollado para simular el comportamiento mencionado, el cual ofrece la facilidad de modelar relevadores convencionales y/o relevadores de pendiente. El modelo del sistema utilizado es el de 1 Área - 1 Máquina.

INTRODUCCION

Todo sistema eléctrico de potencia (SEP) pasa durante su operación, por estados bien definidos [1, 2]:

- Normal (Durante más del 99% del tiempo).
- Alerta.
- Emergencia.
- Extremis (El más remoto).
- Restaurativo.

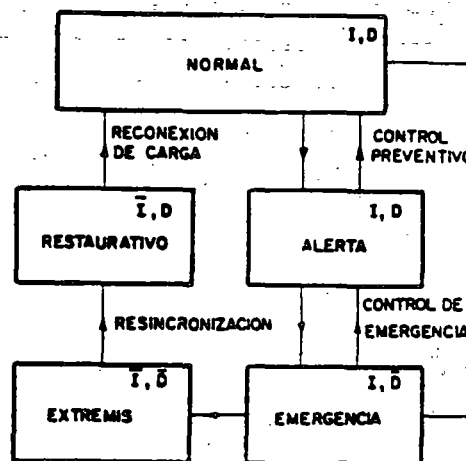
La figura 1 muestra la transición del sistema de un estado a otro. Si se desea, puede consultarse el anexo 1, donde los estados de operación se tratan con más de detalle.

La desconexión de carga por baja frecuencia es un evento que tiene lugar en el estado extremis y tiene por objeto llevar al sistema al estado restaurativo. Aunque la desconexión de carga es una medida que se aplica desde los años 30's, siempre resultará de interés abordar este tema, dada su importancia y efectividad.

RECONOCIMIENTO

Los autores desean expresar su agradecimiento al Ing. Adolfo García García, Jefe de Operación Sistema de la CLFC y al Ing. Agustín Flores Novelo, Jefe del Área Eléctrica de la UAM, por el apoyo brindado en la realización de este trabajo.

Trabajo preparado para presentarse en la Conferencia Internacional de Investigación, Desarrollo y Aplicación de Ingeniería Eléctrica y Electrónica "LATINCON" Julio de 1984.



I = RESTRICCIONES DE IGUALDAD.
D = RESTRICCIONES DE DESIGUALDAD.
- = NEGACION.

Figura 1.- Estados de operación de un SEP.

INTERACCION POTENCIA - FRECUENCIA

La desviación de la frecuencia en un SEP depende básicamente de las siguientes variables y parámetros:

- Magnitud del desbalance de potencia activa.
- Inercia del sistema.
- Coeficiente de amortiguamiento de la carga.
- Característica de regulación de los gobernadores.
- Reserva rodante en el momento del disturbio.

paulatinamente se irá explicando la influencia de cada una.

MODELO DEL SISTEMA.

Un SEP formado por los subsistemas de generación, transmisión y distribución, puede simplificarse para su estudio dinámico, de tal modo que solo se considere la generación y las cargas, éstas últimas conectadas en un solo nodo.

En la figura 2 se muestra este modelo, donde el generador y la turbina son un equivalente de todas las unidades generadoras del sistema, y la carga P_c es la suma de todas las cargas conectadas, más el total de pérdidas en la red. Considerando las pérdidas del generador equivalente incluidas también en la carga, la potencia mecánica P_m en la entrada de éste, será igual a la potencia eléctrica de generación P_g en la salida. Algunos autores le asignan a este modelo el nombre de "1 Area - 1 Máquina".

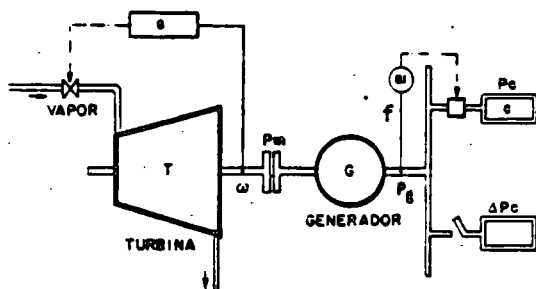


Figura 2.- Modelo del sistema.

CAUSAS Y EFECTOS DE UN DESBALANCE DE POTENCIA ACTIVA.

Las salidas forzadas de unidades generadoras, líneas de transmisión, etc. (denominados "disturbios"), pueden provocar que se produzca un fuerte desbalance entre la potencia de la carga P_c y la potencia eléctrica de generación P_g . Dos casos son los que ocurren:

- Deficiencia de generación.
- Exceso de generación.

Para explicar el caso de deficiencia, el cual es el que nos ocupa, supóngase que la carga excede a la generación debido a la conexión súbita de la carga ΔP_c . Después de la conexión, se presenta la siguiente secuencia de acontecimientos.

- La carga es alimentada instantáneamente.
- Debido a que los controles no han actuado, la potencia mecánica P_m y la de generación P_g no cambian.
- La nueva carga conectada, para satisfacerse, "toma prestada" una parte de la energía cinética que se encuentra almacenada en todas las masas rodantes del sistema.
- La velocidad angular de las masas rodantes (turbinas, generadores, excitatrices, etc.) decrece, es decir, se presenta una desaceleración.
- La frecuencia eléctrica del sistema, reflejo de la velocidad de rotación, decrece en igual proporción.

Bajo esta base, toda vez que se presente en el sistema baja frecuencia, es síntoma de que se tiene deficiencia de generación. En caso contrario, un valor alto de la frecuencia, es indicio de que sobra generación en el sistema.

En ambos casos el desbalance resulta ser:

$$P_a = P_m - P_c = P_g - P_c \quad (\text{Mw}) \quad (1)$$

Si el desbalance o potencia de aceleración P_a es positivo se produce una aceleración de las masas rodante y si es negativo el resultado es una desaceleración. - Recuérdese que para el modelo adoptado P_m y P_g son iguales.

SOBRECARGA DEL SISTEMA.

Cuando una pérdida de generación (desbalance negativo) ocurre, es común manejar el concepto de "sobrecarga" - en lugar de "desbalance de potencia" o "potencia de aceleración". La sobrecarga del sistema se define como:

$$SC = \frac{100|P_a|}{\text{Generación Final}} = \frac{|P_a|}{P_{go} - |P_a|} \times 100 \quad (2)$$

donde P_{go} es la potencia de generación antes del disturbio y $|P_a|$ el valor absoluto del desbalance.

EjemPlo 1.- Un sistema que tiene una generación inicial $P_{go} = 9000$ Mw y que sufre una pérdida de generación de 425 Mw (4.7%), estará soportando una sobrecarga de:

$$SC = \frac{425 \times 100}{9000 - 425} = \frac{425}{8575} \times 100 \approx 5\%$$

La expresión para calcular el desbalance en función de la sobrecarga puede deducirse a partir de la ecuación (2), obteniéndose:

$$|P_a| = \frac{SC}{100 + SC} P_{go} \quad (3)$$

Esta ecuación es válida solo para el caso en que la deficiencia haya sido producida por una pérdida de generación (lo más frecuente y real); no así para un aumento súbito de carga. En la tabla N° 1 se muestran algunos valores de desbalance con las sobrecargas correspondientes.

TABLA N° 1.
 DESBALANCES, SOBRECARGAS Y PENDIENTES

DESBALANCE DE POTENCIA (PERDIDA DE GENERACION)	SOBRECARGA	PENDIENTE
4.7%	5%	0.3 hz/s
9.1	10	0.6
16.7	20	1.2
23.1	30	1.8
33.3	50	3.0
50.0	100	6.0
66.7	200	12.0

CONSTANTE DE INERCIA

Al describir cualitativamente los efectos de un desbalance de potencia activa, se mencionó la energía cinética de las masas rodantes. La constante de inercia H de una unidad generadora es una medida de esa energía y se define como:

$$H \triangleq \frac{\text{Energía cinética de las masas [M Joules]}}{\text{Potencia de la Unidad [MVA]}} \quad (4)$$

Tal constante tiene la ventaja de tomar valores muy pa recidos, independientemente del tamaño de la unidad:

$$\begin{array}{ll} \text{Unidades Hidráulicas (400 rpm)} & H = 3.5s. \\ \text{Turbogeneradores (3600 rpm)} & H = 6 \text{ a } 8s. \end{array}$$

La constante de inercia de un conjunto de unidades - (sistema) puede obtenerse a partir de las constantes - individuales calculando un promedio ponderado de todas ellas, en función de la capacidad de las unidades.

$$H_s = H_1(S_1/S_B) + H_2(S_2/S_B) + \dots + H_n(S_n/S_B) \quad (5)$$

siendo $S_B = S_1 + S_2 + \dots + S_n$, la suma de las capacidades en MVA de todas las unidades.

Si todas las unidades del sistema fueran idénticas, H_s resultaría igual a la constante individual de las unidades. En la práctica H_s toma valores entre 4 y 6 segundos.

Cuando una pérdida de generación ocurre, la energía cinética en las masas rodantes del sistema se altera, por lo que se hace necesario corregir la constante de inercia del sistema.

$$H_s' = H_s \frac{P_{go} - |Pa|}{P_{go}} = H_s (1 - |\bar{Pa}|) \quad (6)$$

siendo $|\bar{Pa}|$ el desbalance de potencia, expresado en por unidad.

Se intuye que si un sistema tiene una alta inercia, o sea una gran energía cinética disponible, va a ser menos afectado por un desbalance de potencia activa. Esta propiedad es explotada en los sistemas interconectados, ya que un cierto desbalance impacta más a una área aislada, que a un sistema interconectado.

ECUACION DE OSCILACION.

La ecuación de oscilación es la expresión matemática que describe el comportamiento dinámico de una unidad generadora después de que se ha presentado un desbalance de potencia. Como el modelo adoptado consta de una unidad equivalente, será suficiente trabajar con una sola ecuación de oscilación.

En el anexo 2 se muestra cómo es posible transformar la expresión clásica de la ecuación de oscilación en una forma de mayor utilidad para nuestro problema, siendo ésta:

$$\dot{f} = \frac{df}{dt} = \frac{f_0}{2H_s'} \bar{Pa} \quad (7)$$

Con esta expresión es posible observar la variación de la frecuencia en el tiempo, a partir del valor de la constante de inercia modificada H_s' , de la frecuencia nominal del sistema f_0 y de la potencia de aceleración o desbalance Pa , expresada en por unidad.

1a. Solución. - La solución más simple al problema de encontrar la variación de la frecuencia al ocurrir un desbalance, se obtiene a partir de la ecuación (7) suponiendo que $Pa = P_g - P_c$ es constante. - Esto es cierto, si la carga P_c no cambia con la frecuencia y los gobernadores no actúan para variar la potencia de generación P_g . Dicha solución es:

$$f(t) = f_0 + (\dot{f}) t \quad (8)$$

la cual representa a una recta, siendo f_0 la ordenada al origen y (\dot{f}) , la pendiente.

En este caso particular de solución, la ecuación (7) puede transformarse a:

$$\dot{f} = \frac{df}{dt} = \frac{f_0}{2H_s'} (\bar{Pa}) \quad (9)$$

al sustituir en (7) el valor de la constante de inercia corregida H_s' , dado en (6). En este caso (9) indica la sobrecarga del sistema, expresada en por unidad.

La primera solución es la más pesimista, dadas las suposiciones que involucra. Aún con sus limitaciones, esta solución ofrece excelente información del fenómeno, tal como lo ilustra el siguiente ejemplo.

EJEMPLO 2. - Si en el sistema del ejemplo 1 se tiene una sobrecarga del 100% y se supone que la constante de inercia inicial es de 5 segundos, se tiene:

Desbalance:

$$|Pa| = \frac{sc}{100+sc} P_{go} = \frac{100}{200} 9000 = 4500 \text{ Mw}$$

Constante de Inercia Corregida:

$$H_s' = H_s (1 - |\bar{Pa}|) = 5 (1 - \frac{4500}{9000}) = 5(0.5) = 2.5s$$

Pendiente de Frecuencia.

$$\dot{f} = \frac{f_0}{2H_s'} \bar{Pa} = \frac{60}{(2)(2.5)} (-\frac{4500}{9000}) = -6 \text{ hz/s}$$

$$= \frac{f_0}{2H_s'} (\bar{Pa}) = \frac{60}{(2)(5)} (1.0) = 6 \text{ hz/s}$$

Ecuación de variación:

$$f(t) = 60 - 6.0t$$

Frecuencia 2 segundos después del disturbio.

$$f(2) = 60 - (6.0)(2) = 48 \text{ hz.}$$

La figura 3 y la tabla N° 1 incluyen el ejemplo anterior y proporcionan información objetiva del comportamiento de la frecuencia para otras sobrecargas.

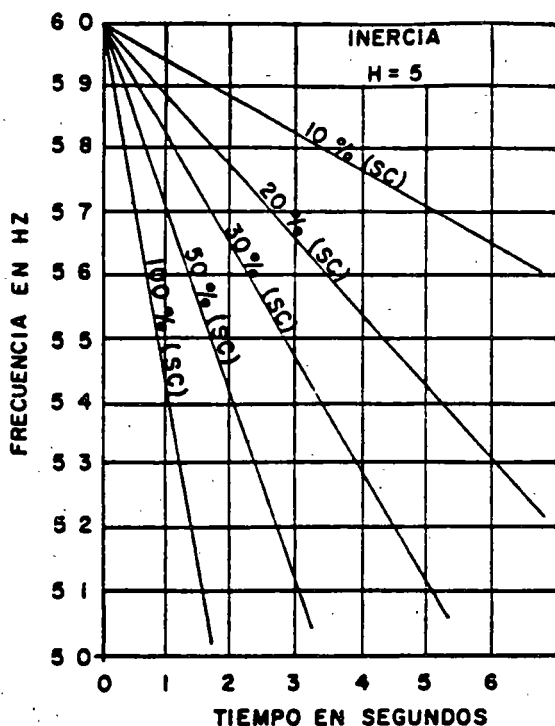


Figura 3.- Variación lineal de la frecuencia y efecto del grado de sobrecarga.

COEFICIENTE DE AMORTIGUAMIENTO DE LA CARGA.

En la primera solución se supuso constante la potencia de la carga P_c , sin embargo la carga real de un sistema (particularmente la rotatoria), varía con la frecuencia, tendiendo a disminuir conforme la frecuencia cae.

Esta característica se mide con el llamado "coeficiente de amortiguamiento", el cual se define como:

$$D = \frac{\Delta P_c}{\Delta f} \quad (10)$$

Existen varias versiones de este coeficiente, dependiendo de las unidades utilizadas, pero generalmente en todas ellas se supone que la variación de la carga es lineal:

$$D = \frac{\Delta P_c}{\Delta f} \quad \left[\frac{\text{Mw}}{\text{hz}} \right]$$

$$D = \frac{\Delta P_c}{10 \Delta f} \quad \left[\frac{\text{Mw}}{\text{dhz}} \right]$$

$$D = \frac{\Delta P_c / P_{g0}}{\Delta f} = \frac{\Delta P_c}{\Delta f} \quad \left[\frac{\text{pu Mw}}{\text{hz}} \right]$$

$$D = \frac{\Delta P_c / P_{g0}}{\Delta f / f_0} \quad [\%]$$

(11)

Esta última versión es la más popular y expresa el porcentaje que varía la carga para un 1% de variación en la frecuencia. Este coeficiente tiene un rango de 1 a 7, dependiendo de la mezcla de cargas, siendo el valor típico igual a 2% [4].

2a. Solución.- Esta solución considera que la carga es función del valor de la frecuencia, aunque supone todavía que no hay respuesta de los gobernadores, es decir, que la potencia de generación P_g no cambia. En estas condiciones se tiene:

$$\bar{P}_c = \bar{P}_{c0} + \Delta \bar{P}_c = \bar{P}_{c0} + \bar{D} \Delta f \quad (12)$$

La ecuación de oscilación dada en (7) es ahora:

$$\frac{df}{dt} = -\frac{f_0}{2H'_s} (\bar{P}_g - \bar{P}_c)$$

$$\frac{df}{dt} = -\frac{f_0}{2H'_s} [\bar{P}_{a0} - \bar{D}f + \bar{D}f_0] \quad (13)$$

donde

$\bar{P}_{a0} = \bar{P}_g - \bar{P}_{c0}$ es la potencia de aceleración en $t=0^+$.

La solución de la ecuación diferencial (13) es:

$$f(t) = f_0 + \frac{\bar{P}_{a0}}{\bar{D}} (1 - e^{-kt}) \quad (14)$$

con

$$k = \frac{f_0 \bar{D}}{2H'_s}$$

Esta solución es ya más realista; de ella puede observarse que la frecuencia no decae indefinidamente sino que tiende a estabilizarse en el valor:

$$f_{EE} = f(\infty) = f_0 + \frac{\bar{P}_{a0}}{\bar{D}}$$

EJEMPLO 3.- Si en el sistema de 9000 Mw que se ha venido manejando, se presenta una pérdida de generación de 420 Mw y la frecuencia se llega a estabilizar en 59.3 hz, se tiene:

$$D = \frac{420 \text{ Mw}}{0.7 \text{ hz}} = 600 \text{ Mw/hz} = 60 \text{ Mw/dhz} = 4\%$$

$$\bar{D} = \frac{420/9000}{0.7} = 0.0667 \text{ pu Mw/hz}$$

Si en este sistema se presentara una sobrecarga del 100% (comparar con el ejemplo 2), se tendría.

$$K = \frac{f_0 \bar{D}}{2H'_s} = \frac{60 \times 0.0667}{2 \times 2.5} = 0.8 \text{ s}^{-1}$$

$$f(t) = 60 - 7.5 (1 - e^{-0.8t})$$

La frecuencia, 2 segundos después del disturbio sería:

$$f(2) = 60 - 7.5 (1 - e^{-1.6}) = 60 - 6 = 54 \text{ hz.}$$

La frecuencia final, después del amortiguamiento de la carga:

$$f(\infty) = 60 - 7.5 = 52.5 \text{ hz.}$$

La pendiente de la frecuencia en $t=0^+$ coincidirá con la calculada en el ejemplo 2, ya que en ese momento el amortiguamiento de la carga es nulo; mientras que la pendiente final será cero, ya que la frecuencia se estabilizará en 52.5 hz.

RESERVA RODANTE Y RESPUESTA DE LOS GOBERNADORES (REGULACION PRIMARIA).

Tomar en cuenta las respuestas de los gobernadores introduce una gran complejidad en el problema, sin embargo con la ayuda de la computadora digital ya resulta alcanzable el objetivo de incluirla. Esta situación será tratada con detalle en la última parte del trabajo; por el momento, se describirá de manera breve el mecanismo de respuesta del control de velocidad o gobernador ante la baja frecuencia.

La figura 4 representa la curva de respuesta o característica de regulación (R) del gobernador de una unidad generadora. El punto O es el punto actual de operación, donde a 60 hz está entregando la unidad al sistema una potencia P_o y conservando una reserva rodante de $(P_n - P_o)$. Si la frecuencia se eleva por arriba de los 60 hz, la unidad disminuirá su generación (hasta cero, si la frecuencia llegara a un valor de f_1 , esto lógicamente ayuda a aliviar el problema, teniendo en cuenta que se tiene exceso de generación y que todas las unidades reaccionan en la misma forma. Por el contrario, si la frecuencia baja, es indicación de que falta generación y a medida que el decremento de frecuencia es mayor, la potencia generada aumenta hasta llegar a un valor de frecuencia f_2 , a partir del cual la unidad solo entrega su potencia nominal P_n , ya que su reserva se ha agotado.

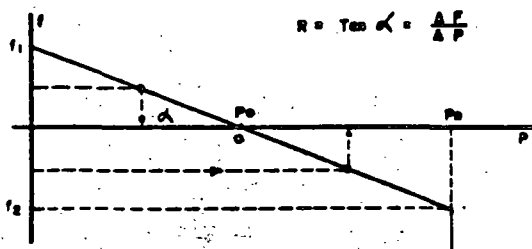


Figura 4.- Característica de regulación o estatismo del gobernador.

La característica de regulación (R) de un gobernador se define como el porcentaje que debe variar la frecuencia para que la potencia generada cambie de cero hasta la potencia nominal. Un valor típico resulta ser:

$$R = \frac{\Delta f}{\Delta P} = 4\%$$

o bien, en otras unidades:

$$R = 0.04 \times 60 = 2.4 \text{ hz/pu Mw}$$

PROTECCION DEL SISTEMA CONTRA BAJA FRECUENCIA

LIMITES DE FRECUENCIA.

En un SEP, el requisito ideal de mantener la frecuencia constante no se puede cumplir, dada la variabilidad incesante y aleatoria de la carga. No obstante, tal variable debe mantenerse dentro de márgenes muy estrechos, aunque en ocasiones por condiciones anormales, tales márgenes se vean excedidos.

Existen varias razones para justificar los límites estrictos en las fluctuaciones de la frecuencia del sistema:

- Efectos en la carga.
- Daño en las turbinas.
- Operación deficiente de auxiliares.
- Disparos en cascada.

Efectos en la carga.- Esta primera razón no pone fronteras estrictas en las desviaciones de frecuencia ya que la gran mayoría de las cargas manejadas por motores de corriente alterna no son sensibles a las fluctuaciones del orden de ± 2 hz [5].

Posibilidad de daño en las turbinas.- Cuando las turbinas de vapor o de gas operan con alta carga cerca de los 57.5 hz se presenta la resonancia mecánica en las dos últimas filas de álabes y éstos vibran severamente, produciéndose esfuerzos de fatiga en el material. Deben tomarse todas las precauciones para evitar a toda costa la operación abajo de los 57.5 y permitiendo solo desviaciones momentáneas abajo de los 59.4 hz. La frecuencia y tiempo límites para una turbina varían según el fabricante, pero resulta una buena guía los siguientes datos [6].

Frecuencia a Plena Carga	Tiempo máximo
59.4 hz	Operación continua
58.8	90 min.
58.2	10
57.6	1

estos tiempos son acumulativos durante la vida de la turbina.

Las turbinas hidráulicas prácticamente son inafectables a frecuencias hasta de 54 hz [7].

Operación Deficiente de Auxiliares.- Durante condiciones de baja frecuencia, los servicios auxiliares de una planta de vapor se ven afectados, provocando la reducción de la potencia de salida de la unidad. Por ejemplo: las bombas de agua de alimentación a la caldera, las bombas de agua de enfriamiento, el sistema de lubricación de chumaceras, etc. La operación es notoriamente deficiente a partir de los 56.5 hz.

Disparos en Cascada.- Si se alcanzan los límites de operación de una turbina, ésta será desconectada del sistema por la acción de su protección. Esto agrava el problema, ya que el desbalance de potencia crece, la frecuencia cae más rápidamente y el sistema se va desintegrando hasta llegar al colapso.

Aunque no existe ninguna reglamentación en cuanto a límites de frecuencia, por lo menos en nuestro país, es posible resumir lo expuesto, definiendo tres zonas características:

Zona Favorable:	60 ± 0.1 hz.
Zona Tolerable:	60 ± 0.6 hz.
Zona Extrema:	$57.5 < f < 61$ hz.

Los límites de la zona favorable son arbitrarios, aunque acordes con la práctica, como referencia se mencionará que en EUA tales límites son del orden de ± 0.05 hz [5]. La figura 5 resume lo expuesto en esta sección.

ESQUEMAS DE DESCONEXION AUTOMATICA DE CARGA (EDAC's).

Una vez que se ha presentado en el sistema una pérdida de generación importante y la frecuencia empieza a caer peligrosamente, la medida efectiva de salvar al sistema de males mayores, es desconectar la carga no prioritaria del sistema mediante relevadores de baja frecuencia (81's), con el fin de regresar al equilibrio entre generación y carga. Esta desconexión automática debe ser rápida y confiable.

El evento de desconexión de carga debe tener lugar en el intervalo de 0 a 2 segundos aproximadamente y sus efectos todavía se observan a los 5 ó 10 segundos después de ocurrida la pérdida de generación. En la figura 6 se muestra objetivamente este hecho y se compara el evento que nos ocupa con los problemas de estabilidad transitoria y estabilidad dinámica.

Un EDAC es un programa establecido de como ir desconectando la carga, de acuerdo con la severidad del desbalance de potencia que haya sufrido el sistema. Un EDAC debe cumplir los siguientes objetivos:

- Detectar a través del valor de baja frecuencia y/o su pendiente, que el sistema ha sufrido una pérdida de generación severa.
- Desconectar la carga necesaria (la mínima posible) para restablecer el balance entre generación y carga y asegurar que no se alcanzan valores críticos de baja frecuencia.
- Restablecer la frecuencia del sistema a su valor nominal, o por lo menos, a un valor dentro de la zona tolerable.
- Evitar un disturbio mayor o total del sistema (colapso), reduciendo la probabilidad de disparos en cascada de unidades generadoras.

Un esquema de desconexión de carga queda caracterizado, generalmente por:

- Máxima sobrecarga a proteger
- Frecuencia a la cual se inicia la desconexión
- Frecuencia mínima aceptable
- Número de pasos de desconexión y carga en cada uno.
- Ajuste de frecuencia y retardo, en cada paso.

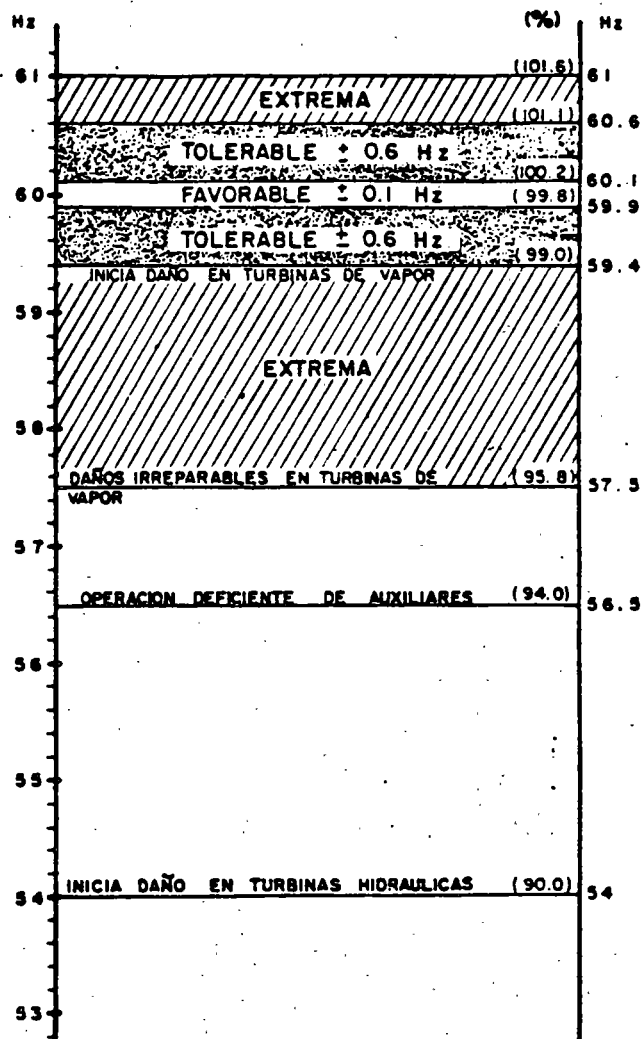


Figura 5.- Límites y zonas de frecuencia.

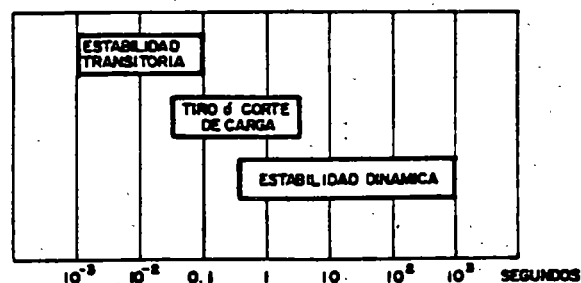


Figura 6.- Ubicación en el tiempo de la desconexión de carga.

SIMULACION DEL COMPORTAMIENTO DEL SISTEMA

REPRESENTACION DE SISTEMA

De acuerdo con el modelo adoptado (figura 2), el sistema está constituido por:

- . Grupo turbina - generador equivalente
- . Gobernador de velocidad (incluyendo sistema de válvulas).
- . Respuesta del sistema eléctrico de potencia.

Estos elementos ya interconectados forman el lazo de control potencia - frecuencia mostrado a continuación [5]:

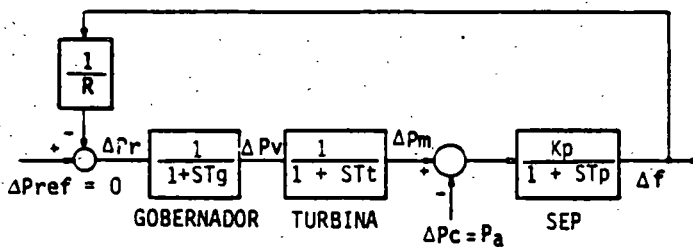


Figura 7.- Diagrama del lazo de control correspondiente a la regulación primaria.

Donde:

- Δf - variación de frecuencia
- ΔPr - variación de potencia en el gobernador
- $\Delta Pref$ - posición del cambiador de velocidad
- ΔPv - variación de potencia en las válvulas
- ΔPm - incremento de potencia mecánica
- ΔPc - incremento de potencia en la carga
- Tg - constante de tiempo del gobernador (≈ 0.1 s)
- Tt - constante de tiempo de la turbina (≈ 0.3 a 0.5 s)

$$Kp = \frac{1}{D}$$

$$Tp = \frac{2Hs}{f_0 D}$$

El diagrama del lazo de control o regulación primaria mostrado en la figura 7, se podría reducir a otro de menos bloques, pero para obtener su función de transferencia en el dominio del tiempo resultaría demasiado complicado. El método de solución adoptado es el de resolver las ecuaciones diferenciales - simultáneas mediante métodos numéricos.

Sistema de ecuaciones resultantes. Las ecuaciones - que representan matemáticamente al sistema en el dominio de Laplace son:

$$\Delta Pv(s) = -\frac{1}{R} \frac{1}{1+STg} \Delta f(s) \quad (15)$$

$$\Delta Pm(s) = \Delta Pv(s) \frac{1}{1+STt} \quad (16)$$

$$\Delta f(s) = [\Delta Pm(s) - \Delta Pc(s)] \frac{1}{1+STp} \quad (17)$$

con $\Delta Pref = 0$ dado que no se considera regulación secundaria.

Las ecuaciones (15), (16) y (17) están en el dominio de la variable(s); considerando las condiciones iniciales cero, es posible sustituir directamente S por $\frac{d}{dt}$ en las ecuaciones mencionadas, para así --

tenerlas en el dominio del tiempo como se muestra - a continuación:

$$\Delta Pv(t) + \Delta Pv(t) Tg = -\frac{1}{R} \Delta f(t) \quad (18)$$

$$\Delta Pm(t) + \Delta Pm(t) Tt = \Delta Pv(t) \quad (19)$$

$$\Delta f(t) + \Delta f(t) Tp = [\Delta Pm(t) - \Delta Pc(t)] Kp \quad (20)$$

Las expresiones anteriores constituyen un sistema de ecuaciones diferenciales de primer orden, que pueden resolverse por cualquier método aplicable a su solución (Euler, Trapezoidal, Runge-Kutta, etc.). En este caso se utilizó el método de Euler modificado de segundo orden y con un paso de integración de 0.01 s, tal como se recomienda en la referencia [5].

3a. Solución. Si se considera, por un lado que la -- carga tiene la característica de amortiguamiento, y por el otro, que los gobernadores responden instantáneamente (solución optimista), se tiene:

$$Tg = Tt = 0$$

En estas condiciones, es posible obtener la solución en el dominio del tiempo, a partir del diagrama de bloques del lazo de control primario; siendo esta:

$$f(t) = f_0 + \frac{RKp}{R+Kp} Pa (1 - e^{-\frac{R+Kp}{RTP} t}) \quad (21A)$$

$$\text{con } Kp = \frac{1}{D}$$

$$Tp = \frac{2Hs}{f_0 D}$$

Que sigue siendo una exponencial pura como la solución 2, solo que la frecuencia dada en (21A) se estabiliza en un valor superior, debido al incremento de generación originado por la respuesta de los gobernadores.

Ejemplo 4: Con esta nueva solución el ejemplo 3 -- resultaría:

$$R = 4\% = 2.4 \left[\frac{\text{Hz}}{\text{puMW}} \right] \text{ (valor típico)}$$

$$K_p = \frac{1}{D} = \frac{1}{0.0667} = 15 \frac{\text{Hz}}{\text{puMW}}$$

$$T_p = \frac{2Hs}{f_0 D} = \frac{2 \times 2.5}{60 \times 0.0667} = 1.25 \frac{\text{s}}{\text{puMW}}$$

$$f(t) = 60 - 1.0345 (1 - e^{-5.8t})$$

La frecuencia, 2 segundos después del disturbio, será:

$$f(2) = 60 - 1.0345(1 - e^{-11.6}) = 60 - 1.0345 = 58.96 \text{ Hz.}$$

La frecuencia final:

$$f(\infty) = 60 - 1.0345 = 58.96 \text{ Hz.}$$

Con esta solución, prácticamente la frecuencia alcanza su valor final antes de los 2 segundos. Este valor es mayor que el obtenido en los ejemplos anteriores, debido a la acción "instantánea" del gobernador.

IMPLEMENTACION DEL PROGRAMA

4a. Solución. La solución más completa al problema de determinar el comportamiento de la frecuencia después de una pérdida de generación (en base al modelo de 1 Area - 1 Máquina), es la obtenida al considerar todas las variables y parámetros que aparecen en el diagrama de control o regulación primaria (figura 7). Este objetivo se alcanza únicamente mediante métodos numéricos de solución de ecuaciones diferenciales y con la ayuda de una computadora digital.

Por tal motivo y para tal fin se desarrolló el programa de computadora que permite simular el comportamiento de la frecuencia del sistema después de una pérdida de generación. La figura 8 reúne las 4 soluciones tratadas en este trabajo, con el objeto de que el lector observe las diferencias entre ellas.

Una vez logrado esto, es fácil modelar la desconexión de carga, con solo variar el valor de ΔP_c o P_a cuando las condiciones de ajuste de los relevadores se han alcanzado.

El programa es interactivo y está estructurado en las siguientes partes:

- . Entrada de datos y parámetros
- . Solución del sistema de ecuaciones diferenciales.
- . Simulación de relevadores
- . Impresión de resultados

Entrada de datos y parámetros. Cuando se va a emplear el programa para una simulación, es necesario proporcionar:

- a) Número de pasos del esquema de desconexión de carga, el tipo de relevador (de magnitud o pendiente), su ajuste en Hz o Hz/s, el retardo y la potencia de la carga desconectable en cada paso.

b) La constante de inercia del sistema, el coeficiente de amortiguamiento de la carga, la característica de regulación del gobernador y las constantes de tiempo del gobernador la turbina.

c) La potencia de generación inicial o potencia base, la reserva rodante disponible, la pérdida de generación y el horario del evento.

d) Tiempo de estudio e intervalo de impresión.

Solución del sistema de ecuaciones resultantes. El programa cuenta con una rutina que resuelve ecuaciones diferenciales usando el método de Euler modificado de segundo orden, con un paso de integración de 0.01 segundos.

Simulación de relevadores. Dependiendo el tipo de relevador, se usan condicionales para discriminar entre los de magnitud y los de pendiente. Si algún contador de tiempo ya se inicializó, pero antes de que se cumpla su tiempo de operación la frecuencia o su derivada es mayor que su ajuste, dicho contador se restablece; es decir su conteo vuelve a ser cero segundos. Si uno ya alcanzó su tiempo de operación, se simula la pérdida de carga de ese paso modificando el desbalance.

Impresión de resultados. El programa imprime los valores de tiempo, frecuencia, derivada de la frecuencia, incremento de la potencia de generación, deficiencia de generación y valores de los contadores de tiempo de los relevadores.

CONSIDERACIONES PRACTICAS

En la simulación de corte de carga por baja frecuencia se toma en cuenta:

- . Pérdidas de generación en cascada
- . Horario del evento

Pérdidas de generación en cascada. Si por un desbalance inicial de potencia se alcanzan los valores críticos de frecuencia para las turbinas de vapor es posible que se produzcan salidas en cascada por acción de sus protecciones. El programa permite considerar tales eventos, tal como se muestran en la simulación de casos prácticos.

Horario del evento. La carga, como se sabe, tiene un comportamiento variable cíclico. Es por esto que determinada pérdida de generación no afecta de igual manera si esta se presenta en distinto horario. Por ejemplo en un sistema de 11000 MW, se pierden dos unidades de 300 MW en la hora pico produce una sobrecarga menor que en la hora de demanda mínima. Así mismo, la carga desconectable en cada paso del esquema también varía según el horario. Por esta razón, el programa corrige mediante un factor, dependiendo del horario del evento, la carga desconectable.

SIMULACION DE CASOS PRACTICOS.

Con el objeto de ilustrar la utilidad del programa digital, se incluyen algunas corridas de casos prácticos. La primera muestra se tiene en la figura 8 donde aunque no se presenta la desconexión de carga, se ilustran las cuatro variantes de la solución del modelo 1 Area - 1 Máquina.

El segundo caso es el mostrado en la figura 9, donde un sistema de 3800 Mw sufre una sobrecarga del 58%. Los datos para las corridas son:

. Esquema de Desconexión Automática de Carga.

Paso	Frec.	Retardo	Carga
1	59.2 hz	0.20 s	90 Mw
2	59.0	0.20	590
3	58.8	0.20	770
4	58.6	0.20	1170
5	58.4	0.20	1230
6	58.2	0.20	60

. Ajuste de las protecciones de Baja Frecuencia de las Unidades Generadoras.

No.	Frec.	Retardo	Generación
1	57.0 hz	2.0 s	590 Mw
2	57.0	3.0	510
3	57.0	4.0	700

. Parámetros Adicionales.

Hs = 5 s	Reserva = 0
D = 2%	Horario: Lunes (7AM)
R = 4%	Pa = -1400 Mw

La curva (1) corresponde a una operación correcta del esquema de desconexión, mientras que la curva (2) muestra el colapso del sistema por una operación deficiente del esquema de desconexión (solo se cortó el 20% de la carga desconectable).

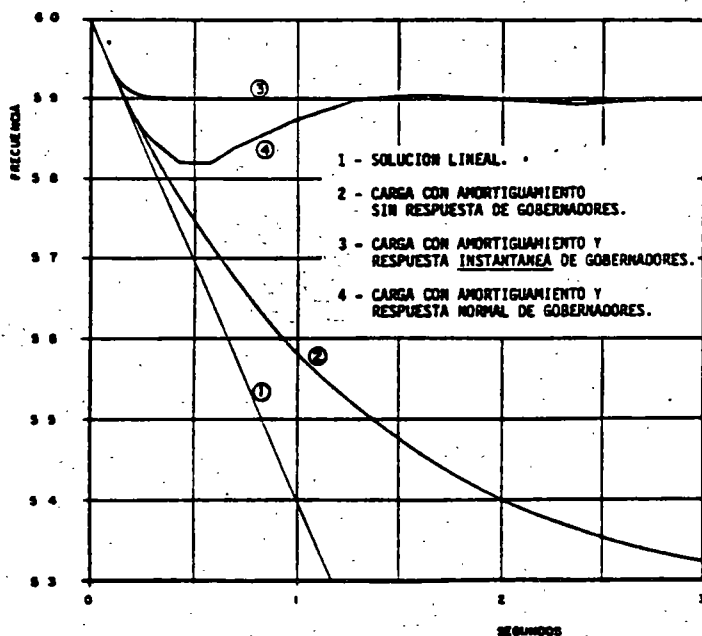


Figura 8.- Comparación del comportamiento de la frecuencia según la solución adoptada.

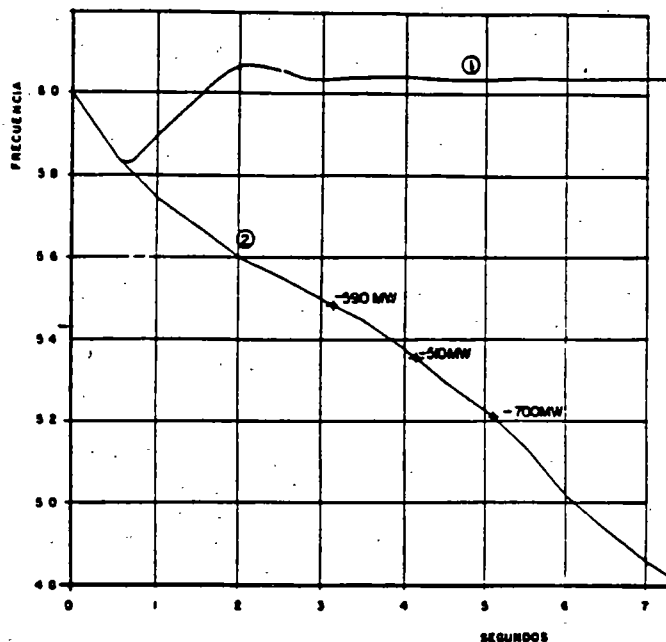


Figura 9.- Simulación de casos prácticos.

CONCLUSIONES

- 1.- La frecuencia del sistema no puede ser constante dada la incesante variabilidad de la carga, sin embargo, se debe procurar mantenerla dentro de límites muy estrechos, distinguiéndose tres zonas de desviación: la favorable, la tolerable y la extrema.
- 2.- La razón principal para limitar las desviaciones de frecuencia es evitar daños en las turbinas de vapor por resonancia mecánica y los disparos en cascada, una vez alcanzados los valores críticos para estas turbinas. Tales valores críticos se dan en la zona extrema.
- 3.- El comportamiento de la frecuencia, después de una pérdida de generación severa, depende fundamentalmente de la magnitud del desbalance de potencia activa, de la inercia del sistema, del amortiguamiento de la carga, de la respuesta de los gobernadores y de la magnitud de carga desconectada por los relevadores de frecuencia.
- 4.- El objetivo de la desconexión automática de carga por baja frecuencia es preservar la integridad del sistema, restableciendo el balance de potencia activa, antes de que la frecuencia alcance valores críticos y evitando así los disparos en cascada de las unidades generadoras.
- 5.- El grado de complejidad en la solución es susceptible de incrementarse tanto como se desee. En este caso, el modelo de 1 Area-1 Máquina ofrece una buena aproximación del comportamiento del sistema.
- 6.- Tener un medio de simulación siempre es ventajoso ya sea para analizar disturbios consumados, para revisar el esquema de desconexión o para capacitar al personal de operación en la comprensión del fenómeno y de las variables que intervienen.

ANEXO 1 ESTADOS DE OPERACION.

Como sugirió inicialmente Dy Liacco [1] y posteriormente ampliaron Fink y Carlsen [2], un SEP pasa durante su operación por varios estados (figura 1), los cuales se definen a continuación tomando como base la referencia [3].

ESTADO NORMAL. Este estado se caracteriza por: a) Conservarse un equilibrio entre la carga y la generación tanto en la parte activa, como en la reactiva (restricciones de igualdad), b) La corriente y voltaje en los elementos del sistema no excede los valores nominales de éstos (restricciones de desigualdad), y c) La reserva en generación rodante y en capacidad de transmisión son suficientes para proporcionar un nivel adecuado de seguridad.

ESTADO DE ALERTA. En este estado, las restricciones de igualdad y de desigualdad aún se satisfacen, pero la reserva es tal que el nivel de seguridad se ha reducido al grado de que algún disturbio pudiera provocar la violación de algunas restricciones de desigualdad.

ESTADO DE EMERGENCIA. Aquí las condiciones de desigualdad se han violado y el nivel de seguridad es cero. El sistema sin embargo todavía está intacto.

ESTADO EXTREMIS. En este estado, las restricciones de igualdad y las condiciones de desigualdad se han violado. El sistema no permanecerá intacto y se perderá un gran porcentaje de la carga del sistema.

ESTADO RESTAURATIVO. Este estado consistirá en reconectar el sistema y recuperar la carga.

ANEXO 2 TRANSFORMACION DE LA ECUACION DE OSCILACION.

La expresión clásica de la ecuación de oscilación es [11]:

$$\frac{d^2 \delta}{dt^2} = \frac{\omega_0}{2H} (\bar{P}_m - \bar{P}_c) = \frac{\omega_0}{2H} \bar{P}_a \quad (21)$$

donde: δ = Angulo del rotor con respecto a una referencia que gira a velocidad síncrona ω_0 , en radianes.

ω_0 = Velocidad angular síncrona, en rad/s.

\bar{P}_m = Potencia mecánica en la flecha de la turbina, en por unidad.

\bar{P}_c = Potencia eléctrica de la carga del sistema, en por unidad.

haciendo $\omega_0 = 2\pi f_0$ y sustituyendo en (21) se tiene:

$$\frac{d^2 \delta}{dt^2} = \frac{\pi f_0}{H} \bar{P}_a \quad (22)$$

La relación entre el ángulo y el ángulo real del rotor (θ), está dada por:

$$\theta = \omega_0 t + \delta$$

derivando sucesivamente:

$$\begin{aligned} \omega &= 2\pi f = \frac{d\theta}{dt} = \omega_0 + \frac{d\delta}{dt} \\ 2\pi \frac{df}{dt} &= \frac{d^2 \delta}{dt^2} \end{aligned} \quad (23)$$

igualando (22) y (23)

$$\frac{df}{dt} = \frac{f_0}{2H} \bar{P}_a$$

Esta última expresión es una versión de la ecuación de oscilación de mucha utilidad para cuando se desea observar el comportamiento de la frecuencia, en lugar del comportamiento del ángulo de los rotores.

REFERENCIAS

- [1] T.E. Dy Liacco
THE ADAPTIVE RELIABILITY CONTROL SYSTEM
IEEE Trans., PAS-86, May 1967.
- [2] L. Fink and K. Carlsen
OPERATING UNDER STRESS AND STRAIN
IEEE Spectrum, March 1978.
- [3] R. Guerrero, O. Hintze, G. Medina, F. Novas, L. Castanedo.
ESTRATEGIA DE DEFENSA DEL SIS. INTERCONECTADO MEXICANO.
- [4] H.E. Lokay, V. Burtnyk
APPLICATION OF UNDERFREQUENCY RELAYS FOR AUTOMATIC LOAD SHEDDING
IEEE Trans., March 1983.
- [5] O.I. Elgerd.
ELECTRIC ENERGY SYSTEMS THEORY. AN INTRODUCTION
Mc Graw Hill Book Company 1971.
- [6] J. Berdy
LOAD SHEDDING. AND APPLICATION GUIDE
General Electric Company
- [7] Warren C. New
LOAD CONSERVATION BY MEANS OF UNDERFREQUENCY RELAYS.
General Electric Co., 1966.
- [8] R.O. Bigelow, R.A. Thompson, P.L. Dandeno
AUTOMATIC LOAD RELIEF PRACTICES IN NORTHEASTERN UNITED STATES AND PROVINCE OF ONTARIO, CANADA.
- [9] Adolfo García G.
CONTROL DE FRECUENCIA Y GENERACION
Curso. Cia. de Luz y Fuerza del Centro, S.A. 1976.
- [10] Gonzalo Arroyo A.
EL CONTROL EN LOS SISTEMAS DE POTENCIA
Curso. Sección de Graduados ESIME - IPN, 1982.
- [11] Anderson and Fouad
POWER SYSTEM CONTROL AND STABILITY
Iowa State University Press.

DETERMINACION ANALITICA DE LA TRANSFERENCIA DE POTENCIA EN ESTADO ESTABLE

José Luis Martínez Menchaca.

Compañía de Luz y Fuerza del Centro, S. A.

RESUMEN

En este trabajo se presenta un método analítico para determinar la transferencia de potencia en estado estable en un sistema eléctrico de potencia.

El método contempla las dos formas de transferencia de potencia en estado estable:

- a) Con excitaciones constantes, y
- b) Con voltajes regulados.

Aun cuando con este método se puede calcular la potencia para un punto en particular, por ejemplo la $P_{\text{máx}}$ en estado estable con excitaciones constantes, la potencialidad del mismo radica en que al ser analítico se puede obtener toda la gama de valores de potencia, tanto de excitaciones constantes como de voltajes regulados, en el intervalo $0^\circ < \delta < 180^\circ$, y con ello obtener las gráficas de potencia-ángulo que son tan importantes para entender mejor la transferencia de potencia en estado estable. δ es el ángulo entre los voltajes internos E_G y E_M de las máquinas síncronas del modelo equivalente.

1.- INTRODUCCION

Determinar la transferencia óptima de potencia a través de las líneas de transmisión en un sistema eléctrico de potencia constituye uno de los aspectos más importantes para los ingenieros en redes eléctricas por las implicaciones económicas y de seguridad involucradas con el sistema.

Económicas, porque al transportar la mayor cantidad posible de energía eléctrica por las líneas de transmisión, se obtiene el beneficio óptimo por la inversión en el sistema generación-transmisión.

De seguridad, porque al tener un alto grado de certeza de estar operando las líneas de transmisión en los niveles de potencia adecuados, no se pone en riesgo la estabilidad del sistema, incluso para el caso de que ocurra alguna de las contingencias probables.

Uno de los elementos fundamentales para lograr la transferencia óptima de potencia por las líneas de transmisión, es el conocimiento de las curvas potencia-ángulo para el flujo de potencia en estado estable a través de las mismas, para las diferentes condiciones que presenta la red en el tiempo.

Para poder construir estas curvas es necesaria una ecuación, una ecuación de P en función de δ , donde P es la potencia real o activa y δ es el ángulo entre los voltajes internos E_G y E_M de las máquinas síncronas del modelo equivalente. Tal ecuación, y las ecuaciones necesarias para llegar a ella, constituyen la esencia de este trabajo, el cual tiene como objetivo principal darla a conocer y explicarla a partir de qué y cómo se obtuvo.

Para validarla se recurre a la comparación con el excelente método de Edith Clarke [1], en lo que a resultados se refiere.

Como aplicación se resuelven algunos casos de transferencia de potencia en estado estable, aprovechando la ocasión para ilustrar la forma en que se van aplicando las diferentes ecuaciones para llegar a los resultados finales.

2.- DESARROLLO DEL METODO

2.1. Modelo equivalente

Para analizar la transferencia de potencia eléctrica en estado estable entre dos nodos de una red nos valdremos del modelo de dos máquinas síncronas equivalentes, generador y motor, unidas o conectadas por la impedancia de una línea de transmisión. El efecto de las máquinas síncronas equivalentes se representa por sendas impedancias las cuales se obtienen en base a la robustez de los nodos, teniendo presente que para determinar dicha robustez de los nodos se deben considerar las reactancias síncronas en los generadores conectados al sistema.

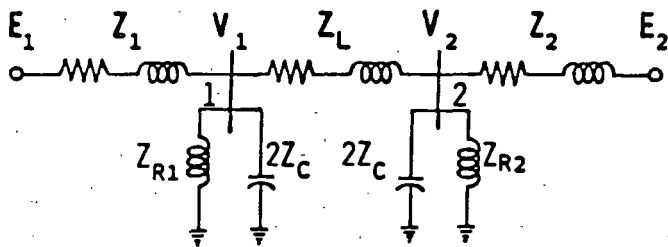


Fig. 1. Circuito equivalente original para analizar la transferencia de potencia.

En la Fig. 1:

- E_1 = Voltaje interno del generador síncrono.
- E_2 = Voltaje interno del motor síncrono.
- V_1 = Voltaje en los bornes del generador.
- V_2 = Voltaje en los bornes del motor.
- Z_1 = Impedancia del generador síncrono.
- Z_2 = Impedancia del motor síncrono.
- Z_L = Impedancia de la línea de transmisión.
- Z_C = Impedancia capacitiva de la línea de transmisión.
- Z_{R1} = Impedancia del reactor conectado al nodo 1 (en caso de que lo haya).
- Z_{R2} = Impedancia del reactor conectado al nodo 2 (en caso de que lo haya).

Haciendo uso del teorema de Thévenin, el circuito equivalente original de la Fig. 1 se

transforma en el circuito equivalente final de la Fig. 2.

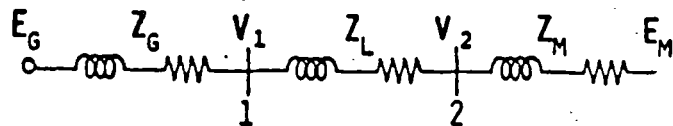


Fig. 2. Circuito equivalente final para el análisis de la transferencia de potencia.

Sean:

$$Z_{S1} = \frac{2Z_C Z_{R1}}{2Z_C + Z_{R1}} \quad (1)$$

y

$$Z_{S2} = \frac{2Z_C Z_{R2}}{2Z_C + Z_{R2}} \quad (2)$$

las impedancias en paralelo conectadas a los nodos 1 y 2 respectivamente.

Entonces:

La impedancia equivalente de Thévenin en el nodo 1 es:

$$Z_G = \frac{Z_1 Z_{S1}}{Z_1 + Z_{S1}} \quad (3)$$

La impedancia equivalente de Thévenin en el nodo 2 es:

$$Z_M = \frac{Z_2 Z_{S2}}{Z_2 + Z_{S2}} \quad (4)$$

La impedancia equivalente total del circuito es:

$$Z_T = Z_G + Z_L + Z_M \quad (5)$$

El voltaje interno en el generador está dado por:

$$E_G = \frac{Z_{S1}}{Z_1 + Z_{S1}} E_1 = \frac{Z_G}{Z_1} E_1 \quad (6)$$

De manera similar, el voltaje interno de Thévenin en el motor está dado por

$$E_M = \frac{Z_2}{Z_2 + Z_{S2}} E_2 = \frac{Z_M}{Z_2} E_2 \quad (7)$$

2.2. Expresión para la potencia Pvr en el nodo 2, considerando voltajes regulados.

En la Fig. 3 se representa el diagrama fasorial de Clarke del circuito equivalente de la Fig. 2. Se demuestra que el punto O se mueve sobre arcos de circunferencias que van de un extremo a otro de la de la caída de voltaje en la impedancia equivalente total. Los centros de estos arcos se localizan sobre la recta UV que es perpendicular a la caída en la impedancia equivalente total y pasa por su centro S. Para ángulos δ menores de 90° los centros se localizan a la izquierda de la caída total —como es el caso de la Fig. 3— y para ángulos δ mayores de 90° a la derecha. La caída en la impedancia total es una cuerda de dichos arcos, excepto para el caso particular de que δ sea igual a 90° , en cuyo caso es el diámetro de la semicircunferencia descrita por O.

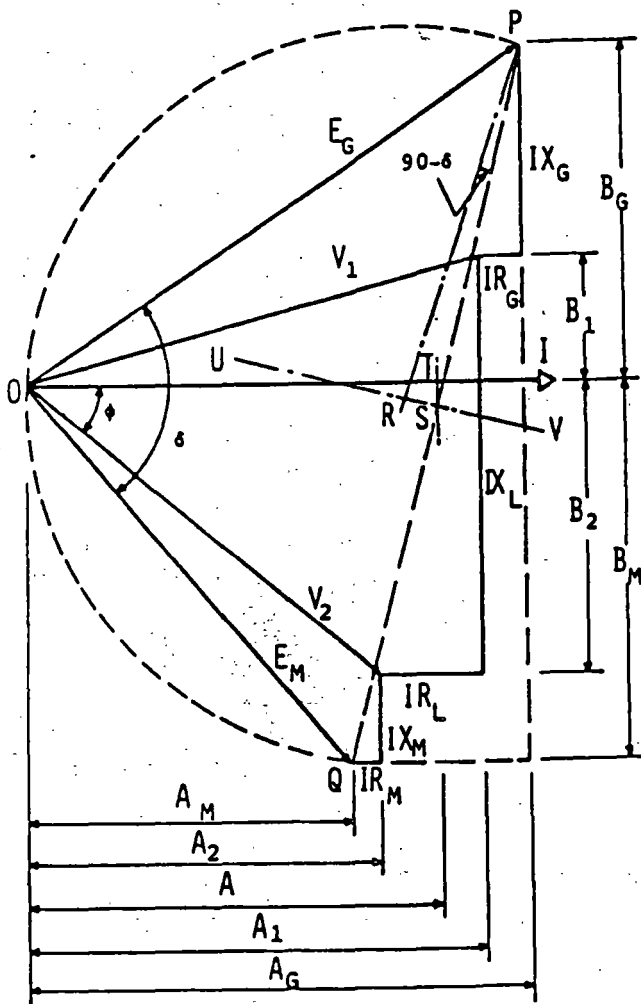


Fig. 3. Diagrama fasorial de Clarke del circuito equivalente de la Fig. 2.

Todos los elementos del diagrama fasorial de la Fig. 3 representan caídas de voltaje, excepto la corriente I , claro está, de tal suerte que si dividimos a todos y cada uno de dichos elementos entre la corriente I obtendremos un diagrama de impedancias a escala, con un valor para I igual a la unidad. Esto es precisamente lo que vamos a suponer para trabajar con elementos que representen resistencias y reactivancias y sólo cuando intervengan en el procedimiento caídas de voltaje haremos intervenir a la corriente I para hacer la conversión.

Así, refiriéndonos a la Fig. 3:

$$A = \overline{OT} \triangleq \frac{1}{2} Z_T \cot \left(\frac{\delta}{2} \right) \quad (8)$$

$$A_1 = A + \frac{1}{2} R_T - R_G \quad (9)$$

$$A_2 = A - \frac{1}{2} R_T + R_M \quad (10)$$

$$V_1^2 = (IA_1)^2 + (IB_1)^2 = I^2 (A_1^2 + B_1^2)$$

$$V_2^2 = (IA_2)^2 + (IB_2)^2 = I^2 (A_2^2 + B_2^2)$$

Dividiendo V_1^2 entre V_2^2 :

$$\frac{V_1^2}{V_2^2} = \frac{A_1^2 + B_1^2}{A_2^2 + B_2^2}$$

Sea

$$V = \frac{V_1^2}{V_2^2} \quad (11)$$

Entonces,

$$V = \frac{A_1^2 + B_1^2}{A_2^2 + B_2^2}$$

$$VA_2^2 + VB_2^2 = A_1^2 + B_1^2$$

$$VB_2^2 - B_1^2 = A_1^2 - VA_2^2$$

Pero

$$B_1 = X_L - B_2 \quad (12)$$

$$B_1^2 = X_L^2 - 2X_L B_2 + B_2^2$$

con lo que

$$VB_2^2 - X_L^2 + 2X_L B_2 - B_2^2 = A_1^2 - VA_2^2$$

$$(V-1)B_2^2 + 2X_L B_2 = X_L^2 + A_1^2 - VA_2^2$$

Ahora bien:

a) Si $V_1 = V_2$, entonces

$$B_2 = \frac{1}{2X_L} (X_L^2 + A_1^2 - A_2^2) \quad (13)$$

b) Si $V_1 \neq V_2$, entonces

$$B_2 = \frac{X_L}{V-1} \left[\sqrt{1 + \frac{V-1}{X_L^2} (X_L^2 + A_1^2 - VA_2^2)} - 1 \right] \quad (14)$$

Por otra parte,

$$V_2 \sin \phi = IB_2 \quad (15)$$

$$V_2 \cos \phi = IA_2 \quad (16)$$

Dividiendo (15) entre (16):

$$\tan \phi = \frac{B_2}{A_2} \quad (17)$$

de acuerdo con (17):

$$\cos \phi = \frac{A_2}{\sqrt{A_2^2 + B_2^2}} \quad (18)$$

De (16):

$$I = \frac{V_2}{A_2} \cos \phi = \frac{V_2}{\sqrt{A_2^2 + B_2^2}} \quad (19)$$

Finalmente, multiplicando (19) por V_2 y por $\cos \phi$ se obtiene la expresión buscada para la potencia P_{vr} en el nodo 2, considerando voltajes regulados; ésto es:

$$P_{vr} = V_2 I \cos \phi = V_2^2 \frac{A_2}{A_2^2 + B_2^2} \quad (20)$$

2.3. Expresión para la potencia P_{vn} en el nodo 2, considerando excitaciones constantes o voltajes no regulados.

Antes de comenzar el desarrollo de las ecuaciones necesarias para llegar a la expresión que determina la transferencia de potencia en estado estable con excitaciones constantes, haremos algunas consideraciones importantes.

Como ya lo demostró Edith Clarke [1], para un modelo de dos máquinas síncronas equivalentes y considerando constantes las corrientes de excitación, el ángulo de máxima transferencia de potencia α_c entre los voltajes internos E_G y E_M de las máquinas está dado por:

$$\alpha_c = \theta_T + 2(\theta_2 - \theta_M) \quad (21)$$

En donde:

θ_T = argumento de la impedancia total Z_T

$$= \text{áng. tan} \left(\frac{X_T}{R_T} \right)$$

θ_2 = argumento de la impedancia del motor original.

$$= \text{áng. tan} \left(\frac{X_2}{R_2} \right)$$

θ_M = argumento de la impedancia del motor final.

$$= \text{áng. tan} \left(\frac{X_M}{R_M} \right)$$

Dado que es recomendable considerar el efecto de la saturación en este análisis, es necesario que, para obtener las impedancias equivalentes Z_1 y Z_2 de las máquinas síncronas, se consideren las reactancias síncronas saturadas en los generadores conectados al sistema.

Refiriéndonos nuevamente al diagrama fasorial de la Fig. 3, tenemos:

$$A_G = A + \frac{1}{2} R_T \quad (22)$$

$$B_G = B_1 + X_G = X_L + X_G - B_2 \quad (23)$$

$$A_M = A - \frac{1}{2} R_T \quad (24)$$

$$B_M = B_2 + X_M \quad (25)$$

$$E_G^2 = (IA_G)^2 + (IB_G)^2 = I^2 (A_G^2 + B_G^2)$$

$$E_G = I \sqrt{A_G^2 + B_G^2}$$

Sustituyendo I dado por (19):

$$E_G = V_2 \frac{\sqrt{A_G^2 + B_G^2}}{\sqrt{A_2^2 + B_2^2}} \quad (26)$$

$$E_M^2 = (IA_M)^2 + (IB_M)^2 = I^2 (A_M^2 + B_M^2)$$

$$E_M = I \sqrt{A_M^2 + B_M^2}$$

Sustituyendo I dado por (19):

$$E_M = V_2 \frac{\sqrt{A_M^2 + B_M^2}}{\sqrt{A_2^2 + B_2^2}} \quad (27)$$

Por otra parte, tenemos que:

$$E_G = E_G \angle \delta$$

$$E_M = E_M \angle 0$$

$$I = \frac{E_G - E_M}{Z_T} = \frac{E_G}{Z_T} \angle \delta - \theta_T - \frac{E_M}{Z_T} \angle -\theta_T$$

$$V = E_M + Z_M I$$

$$= E_M \angle 0 + Z_M \angle \theta_M \left(\frac{E_G}{Z_T} \angle \delta - \theta_T - \frac{E_M}{Z_T} \angle -\theta_T \right)$$

$$= E_M \angle 0 + \frac{E_G Z_M}{Z_T} \angle \delta + \theta_M - \theta_T - \frac{E_M Z_M}{Z_T} \angle \theta_M - \theta_T$$

La potencia en el nodo 2 está dada por:

$$P = R (V \cdot I) = R (V I^*)$$

Desarrollando el segundo término se obtiene:

$$P = \frac{Z_M}{Z_T^2} (E_G^2 + E_M^2) \cos \theta_M - \frac{E_G^2}{Z_T} \cos \theta_T + \frac{E_G E_M}{Z_T} \cos (\delta - \theta_T) - \frac{2E_G E_M Z_M}{Z_T^2} \cos \theta_M \cos \delta$$

que es la expresión general para la potencia activa en el nodo 2.

Ahora bien, el hecho de considerar constantes las corrientes de excitación implica que también sean constantes los voltajes E_G y E_M de atrás de las reactancias síncronas de las máquinas equivalentes. De manera que, haciendo:

$$C = \frac{Z_M}{Z_T^2} (E_G^2 + E_M^2) \cos \theta_M - \frac{E_G^2}{Z_T} \cos \theta_T \quad (28)$$

$$D = \frac{E_G E_M}{Z_T} \quad (29)$$

y

$$E = \frac{2E_G E_M Z_M}{Z_T^2} \cos \theta_M = 2D \frac{Z_M}{Z_T} \cos \theta_M \quad (30)$$

se obtiene, finalmente, la expresión para la potencia P_{vn} en el nodo 2, considerando constantes las corrientes de excitación. Esto es:

$$P_{Vn} = C + D \cos(\delta - \theta_T) - E_r \cos \delta \quad (31)$$

3.- APLICACIONES DEL METODO.

Como aplicación, y sobre todo con el objeto de ilustrar el procedimiento del método, se resolverá, paso por paso, el mismo ejemplo de transferencia de potencia de dos maneras diferentes. La primera empleando las ecuaciones de la parte 2.2, y la segunda con las ecuaciones de la parte 2.3. A fin de comparar los resultados, este mismo ejemplo se resolverá con el método gráfico de Edith Clarke [1].

Para apreciar el método con mayor amplitud, a continuación, y siempre con el mismo caso, se obtendrán, mediante un programa de computadora, los valores para las dos funciones de potencia: con voltajes no regulados (P_{Vn}) y con voltajes regulados (P_{Vr}), para el intervalo $0 < \delta < 180$, así como sus respectivas curvas de potencia-ángulo.

Para finalizar esta tercera parte de aplicaciones del método, se obtendrán los resultados para el mismo ejercicio que nos ha venido sirviendo de ejemplo, pero despreciando las resistencias y considerando el caso de una máquina-bus infinito.

3.1. Determinar el límite de estabilidad en estado estable del sistema comprendido por dos máquinas síncronas equivalentes conectados por una línea de transmisión de 400 kV y 328 km de longitud.

Los datos del circuito equivalente original se muestran a continuación, aclarando que en la obtención de las impedancias Z_1 y Z_2 de las máquinas síncronas equivalentes se ha considerado el efecto de la saturación.

Los datos se encuentran en por unidad (pu) y en base de 100 MVA.

$$V_1 = 1.025$$

$$V_2 = 1.0$$

$$Z_1 = 0.0024833 + j0.0319089$$

$$Z_2 = 0.0013682 + j0.0175813$$

$$Z_L = 0.0066000 + j0.0848000$$

$$Z_C = 0 - j0.47270$$

$$Z_{R1} = 0 + j1.3333333$$

$$Z_{R2} = \text{ (no hay reactor en el nodo 2,)}$$

Cálculo del circuito equivalente final:

De la ecuación (1),

$$Z_{S1} = \frac{2Z_C \cdot Z_{R1}}{2Z_C + Z_{R1}} = 0 - j 3.2493583$$

De la ecuación (2):

$$Z_{S2} = 2Z_C = 0 - j0.94540$$

De la ecuación (3):

$$\begin{aligned} Z_G &= \frac{Z_1 Z_{S1}}{Z_1 + Z_{S1}} = 0.0025304 + j0.322235 \\ &= Z_G \angle \theta_G = 0.0323226 \angle 85.51 \end{aligned}$$

De la ecuación (4):

$$\begin{aligned} Z_M &= \frac{Z_2 Z_{S2}}{Z_2 + Z_{S2}} = 0.0014192 + j0.0179123 \\ &= Z_M \angle \theta_M = 0.0179684 \angle 85.47 \end{aligned}$$

De la ecuación (5):

$$\begin{aligned} Z_T &= Z_G + Z_L + Z_M \\ &= 0.0105496 + j0.1349358 \\ &= Z_T \angle \theta_T = 0.1353475 \angle 85.53 \end{aligned}$$

Ahora bien,

$$\theta_T = 85.53^\circ$$

$$\theta_2 = \text{áng tan} \left(\frac{X_2}{R_2} \right) = 85.55^\circ$$

$$\theta_M = 85.47^\circ$$

Entonces, el ángulo de máxima transferencia de potencia es, de acuerdo con (21):

$$\alpha_c = \theta_T + 2(\theta_2 - \theta_M) = 85.69^\circ$$

Hasta aquí son los datos que se requieren para resolver el problema ya sea por el método gráfico de Clarke o bien por el que se propone en este trabajo. Comencemos por el de nosotros.

Aplicando la ecuación (8) con $\delta = \alpha_c$, se tiene:

$$A = \frac{1}{2} Z_T \cot\left(\frac{\alpha_c}{2}\right) = 0.0729659$$

De la ecuación (9):

$$A_1 = A + \frac{1}{2} R_T - R_G = 0.0757103$$

De la ecuación (10):

$$A_2 = A - \frac{1}{2} R_T + R_M = 0.0691103$$

De la ecuación (11):

$$V = \frac{V_1^2}{V_2^2} = 1.050625$$

De la ecuación (14):

$$B_2 = \frac{X_L}{V-1} \left[\sqrt{1 + \frac{V-1}{X_L^2} (X_L^2 + A_1^2 - VA_2^2)} - 1 \right]$$

$$= 0.0459789$$

Finalmente, el límite de estabilidad en estado estable (P_{\max}) se obtiene aplicando la ecuación (20):

$$P_{\max} = V_2^2 \frac{A_2}{A_2^2 + B_2^2} = 10.03 \text{ pu}$$

$$= 1003 \text{ MW}$$

3.2. Calcular la P_{\max} del ejemplo anterior, pero aplicando las ecuaciones de la parte 2.3.

De la ecuación (22):

$$A_G = A + \frac{1}{2} R_T = 0.0782407$$

De la ecuación (23):

$$B_G = X_L + X_G - B_2 = 0.0710446$$

De la ecuación (24):

$$A_M = A - \frac{1}{2} R_T = 0.0676911$$

De la ecuación (25):

$$B_M = B_2 + X_M = 0.0638912$$

De la ecuación (26):

$$E_G = V_2 \frac{\sqrt{A_G^2 + B_G^2}}{\sqrt{A_2^2 + B_2^2}} = 1.2731723$$

De la ecuación (27):

$$E_M = V_2 \frac{\sqrt{A_M^2 + B_M^2}}{\sqrt{A_2^2 + B_2^2}} = 1.121359$$

De la ecuación (28):

$$C = \frac{Z_M}{Z_T^2} (E_G^2 + E_M^2) \cos\theta_M - \frac{E_M^2}{Z_T} \cos\theta_T$$

$$= -0.5010847$$

De la ecuación (29):

$$D = \frac{E_G E_M}{Z_T} = 10.548279$$

De la ecuación (30):

$$E = 2D \frac{Z_M}{Z_T} \cos\theta_M = 0.2212044$$

Finalmente, la P_{\max} se obtiene aplicando la ecuación (31):

$$P_{\max} = C + D \cos(\alpha_c - \theta_T) - E \cos\alpha_c$$

Resultado idéntico, como debe de ser para este único punto ($P_{\text{máx}}$), al encontrado con la ecuación (20),

$$IX_T = 1.6304348$$

De donde

$$I = \frac{1.6304348}{X_T} = 12.083041$$

3.3. Ahora se va a resolver el mismo ejemplo, pero aplicando el método gráfico de Edith - Clarke [1].

Finalmente:

Vamos a elegir una escala de 150 mm para la reactancia total X_T . Entonces, el factor de escala es:

$$P_{\text{máx}} = V_2 I \cos\phi = 10.03 \text{ pu}$$

$$= 1003 \text{ MW}$$

$$K = \frac{150}{X_T} = 1111.6398 \left(\frac{\text{mm}}{\text{pu}}\right)$$

Valor que concuerda con los resultados anteriores.

Con lo que:

$$KX_G = 35.82 \text{ mm}$$

$$KX_L = 94.27 \text{ "}$$

$$KX_M = 19.91 \text{ "}$$

$$KR_G = 2.81 \text{ "}$$

$$KR_L = 7.34 \text{ "}$$

$$KR_M = 1.58 \text{ "}$$

También,

$$\beta = 90 - \alpha_c = 4.31^\circ$$

y

$$\frac{V_1}{V_2} = 1.025$$

Con estos datos se traza el diagrama de Clarke (Fig. 4).

Del diagrama de Clarke (Fig. 4):

$$\cos\phi = \frac{OT}{V_2} = \frac{76.4}{92.0} = 0.8304347$$

$$\frac{V_2}{V_2} 150 = \frac{1.0}{92.0} 150 = 1.6304348$$

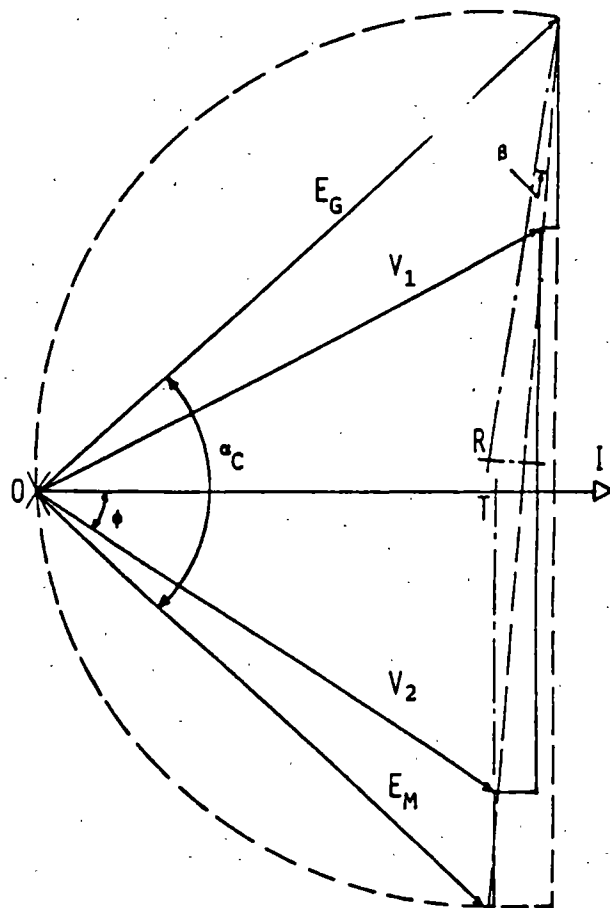
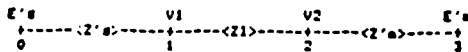


Fig. 4. Diagrama de Clarke para determinar la $P_{\text{máx}}$ del ejemplo 3.3. (dibujo fuera de escala).

3.4. Para apreciar la potencialidad del método, a continuación se presentan los resultados obtenidos a partir de los datos del ejemplo 3.1, para lo cual nos valemos de un programa de computadora.

Programa TDP para determinar y graficar la potencia activa en el nodo 2 de acuerdo con el siguiente circuito equivalente:



VERSION: 05. HECHA EL 26ABR88

NOMBRE DEL CASO

? Línea de 400 kV y 328 km de longitud.

ANOTE LOS DATOS SOLICITADOS EN P.U.!

CAPACIDAD DE C.C. EN EL NODO 1 ? 25.0713

VOLTAJE EN EL NODO 1 ? 1.025

CAPACIDAD DEL (LOS) REACTOR (ES) EN EL NODO 1 ? 0.75

IMPEDANCIA DE SEC. (+) DE LA LINEA (R,X) ? 0.0066,0.0848

SUCEPTANCIA DE SEC. (+) DE LA LINEA (B) ? 2.1155067

CAPACIDAD DE C.C. EN EL NODO 2 ? 45.5028

VOLTAJE EN EL NODO 2 ? 1.0

CAPACIDAD DEL (LOS) REACTOR (ES) EN EL NODO 2 ? 0

COLOQUE LA HOJA AL PRINCIPIO Y APLIQUE 'RETURN'

Tabla 1. Resultados del ejemplo 3.4.

RESULTADOS PARA: Línea de 400 kV y 328 km de longitud.

ANG	Pvn	Pvr	ANG	Pvn	Pvr	ANG	Pvn	Pvr	ANG	Pvn	Pvr
1	28	-1	46	748	346	91	1000	1005	136	637	997
2	47	-1	47	760	357	92	979	1013	137	623	785
3	65	-1	48	772	369	93	997	1020	138	609	971
4	83	-1	49	783	380	94	995	1027	139	594	957
5	101	45	50	794	392	95	992	1034	140	580	943
6	120	62	51	805	403	96	990	1041	141	565	926
7	138	77	52	816	414	97	986	1048	142	550	909
8	156	91	53	826	426	98	983	1054	143	535	892
9	174	104	54	836	437	99	979	1060	144	519	873
10	192	117	55	846	448	100	975	1066	145	504	854
11	210	129	56	855	459	101	971	1071	146	488	834
12	227	142	57	865	470	102	966	1076	147	472	814
13	245	154	58	874	482	103	961	1081	148	456	792
14	263	167	59	882	493	104	956	1086	149	440	770
15	280	179	60	891	504	105	950	1090	150	424	747
16	298	191	61	899	515	106	944	1094	151	407	723
17	315	203	62	907	526	107	938	1098	152	391	698
18	332	215	63	914	536	108	932	1101	153	374	673
19	349	228	64	921	547	109	925	1104	154	357	647
20	366	240	65	928	558	110	918	1107	155	340	620
21	383	252	66	935	569	111	910	1109	156	323	592
22	400	264	67	941	579	112	902	1111	157	305	563
23	416	276	68	947	589	113	894	1112	158	288	534
24	433	288	69	953	600	114	886	1113	159	271	504
25	449	299	70	959	611	115	878	1114	160	253	474
26	465	311	71	964	621	116	869	1114	161	235	443
27	481	323	72	969	631	117	860	1113	162	218	411
28	497	335	73	973	642	118	850	1113	163	200	379
29	512	347	74	977	652	119	841	1111	164	182	346
30	528	359	75	981	662	120	831	1109	165	164	312
31	543	371	76	985	672	121	820	1107	166	146	278
32	558	383	77	988	681	122	810	1104	167	128	244
33	573	394	78	991	691	123	799	1100	168	110	209
34	588	406	79	994	701	124	788	1096	169	92	174
35	602	418	80	996	710	125	777	1092	170	73	138
36	617	430	81	998	719	126	765	1086	171	55	103
37	631	441	82	1000	729	127	754	1080	172	37	66
38	645	453	83	1001	738	128	742	1074	173	18	30
39	658	465	84	1002	747	129	729	1067	174	0	-5
40	672	476	85	1003	756	130	717	1059	175	-17	-42
41	685	488	86	1003	764	131	704	1051	176	-34	-79
42	698	500	87	1003	773	132	691	1041	177	-54	-115
43	711	511	88	1003	781	133	678	1031	178	-72	-152
44	724	523	89	1002	789	134	665	1021	179	-91	-189
45	736	534	90	1002	797	135	651	1010	180	-109	-225

P_{vn} = Potencia considerando excitaciones constantes.

P_{vr} = Potencia considerando voltajes regulados.

GRAFICA POTENCIA-ANGULO PARA: Línea de 400 kV y 328 km de longitud.

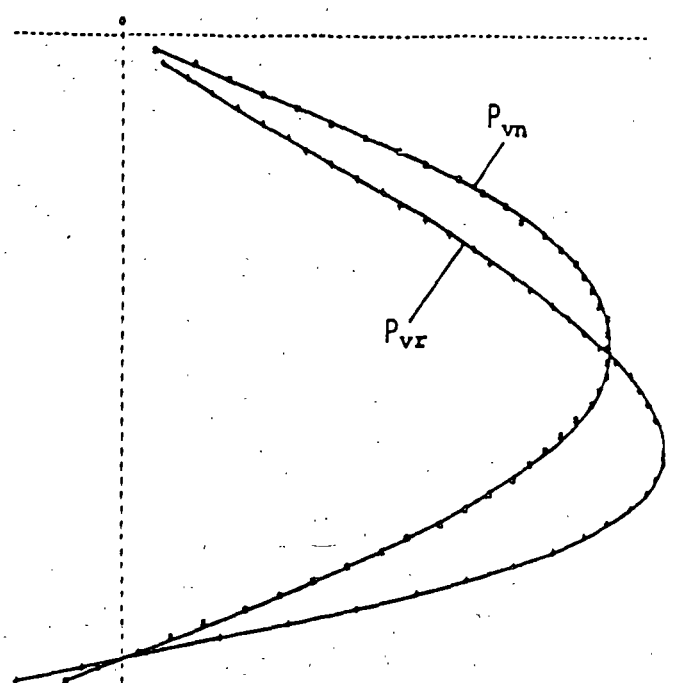
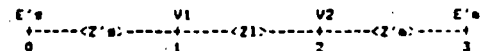


Fig. 5. Gráficas POTENCIA-ANGULO para el ejemplo 3.4.

3.5. Como ejemplo final de esta tercera parte se presentan los resultados del mismo ejemplo 3.1, pero despreciando las resistencias de los elementos y considerando el caso de máquina-bus infinito. Para ello se hace uso nuevamente del programa de computadora, y el objetivo es observar el comportamiento del método con respecto a los resultados teóricos esperados para este caso.

Programa TDP para determinar y graficar la potencia activa en el nodo 2 de acuerdo con el siguiente circuito equivalente:



VERSION: 05. HECHA EL 26ABR88

NOMBRE DEL CASO

? El ejemplo anterior pero sin resistencia.

ANOTE LOS DATOS SOLICITADOS EN P.U.!

CAPACIDAD DE C.C. EN EL NODO 1 ? 25.0713

VOLTAJE EN EL NODO 1 ? 1.025

CAPACIDAD DEL (LOS) REACTOR (ES) EN EL NODO 1 ? 0.75

IMPEDANCIA DE SEC. (+) DE LA LINEA (R,X) ? 0.0.0848

SUCEPTANCIA DE SEC. (+) DE LA LINEA (B) ? 2.1155067

CAPACIDAD DE C.C. EN EL NODO 2 ? 999999999999

VOLTAJE EN EL NODO 2 ? 1.0

CAPACIDAD DEL (LOS) REACTOR (ES) EN EL NODO 2 ? 0

COLOQUE LA HOJA AL PRINCIPIO Y APLIQUE 'RETURN'

Tabla 2. Resultados del ejemplo 3.5.

RESULTADOS PARA: El ejemplo anterior pero sin resistencia.

ANG	Pvr	Pvn	ANG	Pvr	Pvn	ANG	Pvr	Pvn	ANG	Pvr	Pvn
1	20	-1	46	827	641	91	1149	1119	136	799	1064
2	40	-1	47	841	654	92	1149	1126	137	784	1051
3	60	-1	48	854	667	93	1146	1143	138	769	1037
4	80	-1	49	868	680	94	1147	1149	139	754	1023
5	100	55	50	881	693	95	1145	1155	140	739	1008
6	120	74	51	893	706	96	1143	1161	141	723	993
7	140	90	52	906	719	97	1141	1167	142	708	977
8	160	104	53	918	732	98	1138	1172	143	692	960
9	180	121	54	930	745	99	1135	1177	144	676	943
10	200	136	55	942	757	100	1132	1181	145	659	925
11	219	151	56	953	770	101	1129	1186	146	643	907
12	239	166	57	964	782	102	1125	1190	147	626	888
13	259	181	58	975	795	103	1120	1193	148	609	868
14	278	195	59	985	807	104	1115	1196	149	592	848
15	298	210	60	996	819	105	1110	1199	150	575	827
16	317	224	61	1006	831	106	1105	1202	151	557	806
17	336	239	62	1015	843	107	1099	1204	152	540	784
18	355	253	63	1024	855	108	1093	1206	153	522	761
19	374	267	64	1033	867	109	1087	1207	154	504	738
20	393	282	65	1042	879	110	1080	1208	155	486	715
21	412	296	66	1050	890	111	1073	1209	156	468	691
22	431	310	67	1058	902	112	1066	1209	157	449	666
23	449	324	68	1066	913	113	1058	1208	158	431	641
24	468	339	69	1073	924	114	1050	1208	159	412	615
25	486	353	70	1080	936	115	1042	1206	160	393	589
26	504	367	71	1087	947	116	1033	1205	161	374	563
27	522	381	72	1093	957	117	1024	1203	162	355	536
28	540	395	73	1099	968	118	1015	1200	163	336	509
29	557	409	74	1105	979	119	1006	1197	164	317	481
30	575	423	75	1110	989	120	996	1194	165	298	453
31	592	437	76	1115	999	121	985	1189	166	278	424
32	609	451	77	1120	1009	122	975	1185	167	259	395
33	626	465	78	1125	1019	123	964	1180	168	239	366
34	643	478	79	1129	1029	124	953	1174	169	219	337
35	659	492	80	1132	1038	125	942	1168	170	200	307
36	676	506	81	1135	1048	126	930	1161	171	180	277
37	692	520	82	1138	1057	127	918	1154	172	160	247
38	708	533	83	1141	1066	128	906	1146	173	140	217
39	723	547	84	1143	1074	129	893	1138	174	120	186
40	739	561	85	1145	1082	130	881	1129	175	100	155
41	754	574	86	1147	1091	131	868	1120	176	80	124
42	769	588	87	1148	1099	132	854	1110	177	60	93
43	784	601	88	1149	1107	133	841	1099	178	40	62
44	799	614	89	1149	1115	134	827	1088	179	20	31
45	813	628	90	1150	1122	135	813	1076	180	0	0

P_{vn} = Potencia considerando excitaciones constantes.

P_{vr} = Potencia considerando voltajes regulados.

GRAFICA POTENCIA-ANGULO PARA: El ejemplo anterior pero sin resistencia.

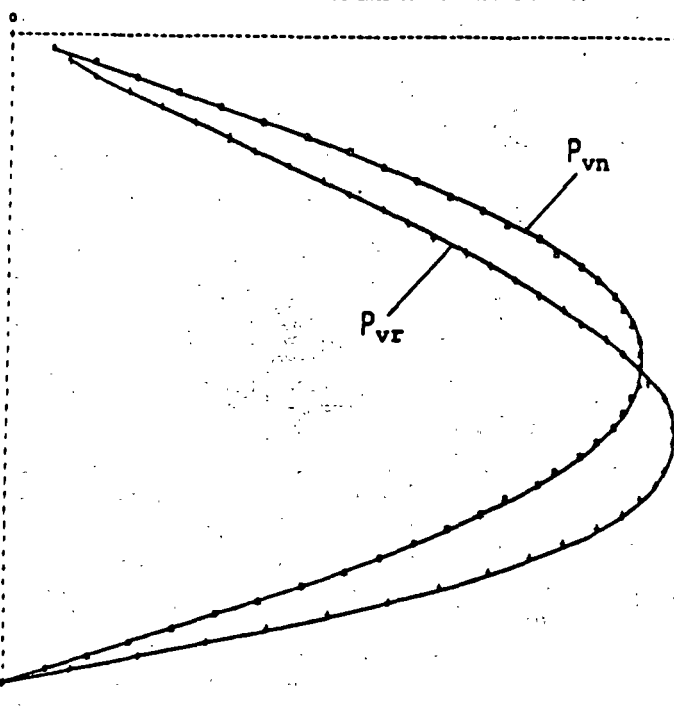


Fig. 6. Gráficas POTENCIA-ANGULO para el ejemplo 3.5.

4.- CONCLUSION.

Habremos observado que al resolver los ejemplos 3.1 y 3.2 llegamos a resultados iguales aunque en un caso utilizamos la ecuación (20) y en otro la (31).

Sabemos también que la ecuación (20) fue obtenida para encontrar la potencia con voltajes regulados y que la (31) lo fue para la potencia con excitaciones constantes; ambas funciones muy diferentes.

Sin embargo, la particularidad de estas dos funciones (P_{vr} y P_{vn}) es de que si se emplean los mismos valores de impedancias ambas tienen la misma solución en el punto máximo de la función P_{vn} , y esto sucede en el ángulo de máxima transferencia de potencia α_c ; de tal forma que si lo que deseamos obtener es el límite de estabilidad en estado estable considerando excitaciones constantes, la forma más práctica de lograrlo es empleando la ecuación (20).

Aun cuando el método ya resulta de gran utilidad al poderse determinar con él en forma analítica valores aislados de potencia (P_{vr} o P_{vn}) para determinados ángulos en particular, su potencialidad radica en poder calcular toda la gama de valores de potencia, tanto de P_{vr} como de P_{vn} , en función del ángulo δ , para el intervalo $0 < \delta < 180$, y de esta forma obtener las curvas de potencia-ángulo que finalmente son las que dan una mejor comprensión de la transferencia de potencia en estado estable.

AGRADECIMIENTOS

El autor expresa su agradecimiento al Ing. Adolfo García García, Subgerente del Area de Control Central, por el apoyo y por el impulso que siempre ha recibido por parte de él.

También se muestra agradecido con el Ing. Jorge León Aponte, Jefe de Operación Sistema, por las facilidades brindadas para la realización de este tipo de trabajos.

También agradece y felicita a la Sra. Arcelia Martínez Moreno, no tanto por su labor de corrección de los originales y mecanografía de

los mismos que ya es valiosa en sí, sino más bien por su alto espíritu de colaboración y su gran disposición al trabajo.

REFERENCIAS.

[1] EDITH CLARKE, "Steady-State Stability in Transmission Systems: Calculation by means of Equivalent Circuits or Circle Diagrams," - A. I. E. E. Trans., vol. 45, pp. 22-41, February, 1926, Disc., pp. 80-94.

[2] EDWARD WILSON KIMBARK, "Power System--Stability: Synchronous Machines," Dover Publications, Inc., 180 Varik Street, New York, - N. Y. 10014, Volume III, Chapter XV, "Stedy- - State Stability," pp. 247-314, 1968.

[3] JACINTO VIQUEIRA LANDA, "Redes Eléctricas Tercera Parte," Representaciones y Servicios de Ingeniería, S. A., AP 61-195, 06600 México, D. F., Volumen III, Capítulo V, "Estabilidad de los Sistemas de Energía Eléctrica en estado Permanente pp. 65-91, 1985.

APENDICE.

Convenciones.

● Las letras "negritas" representan los fasores asociados a las unidades eléctricas, por lo tanto son números complejos.

● Las letras "claras" o "normales" indican magnitudes escalares, por lo tanto son números reales.

Ejemplos:

$$1) \quad \underline{Z}_G = \underline{Z}_G \angle \theta_G = R_G + jX_G$$

con

$$Z_G = \sqrt{R_G^2 + X_G^2}$$

y

$$\theta_G = \text{áng} \tan \left(\frac{X_G}{R_G} \right)$$

$$2) \quad \underline{E}_M = \underline{E}_M \angle 0 = E_M$$

● En la ecuación (8), el símbolo $\underline{\quad}$ significa "igual por definición". Esto por no poder ofrecer una prueba rigurosa de esta ecuación, aun cuando el autor realizó pruebas exhaustivas en computadora para verificar su exactitud



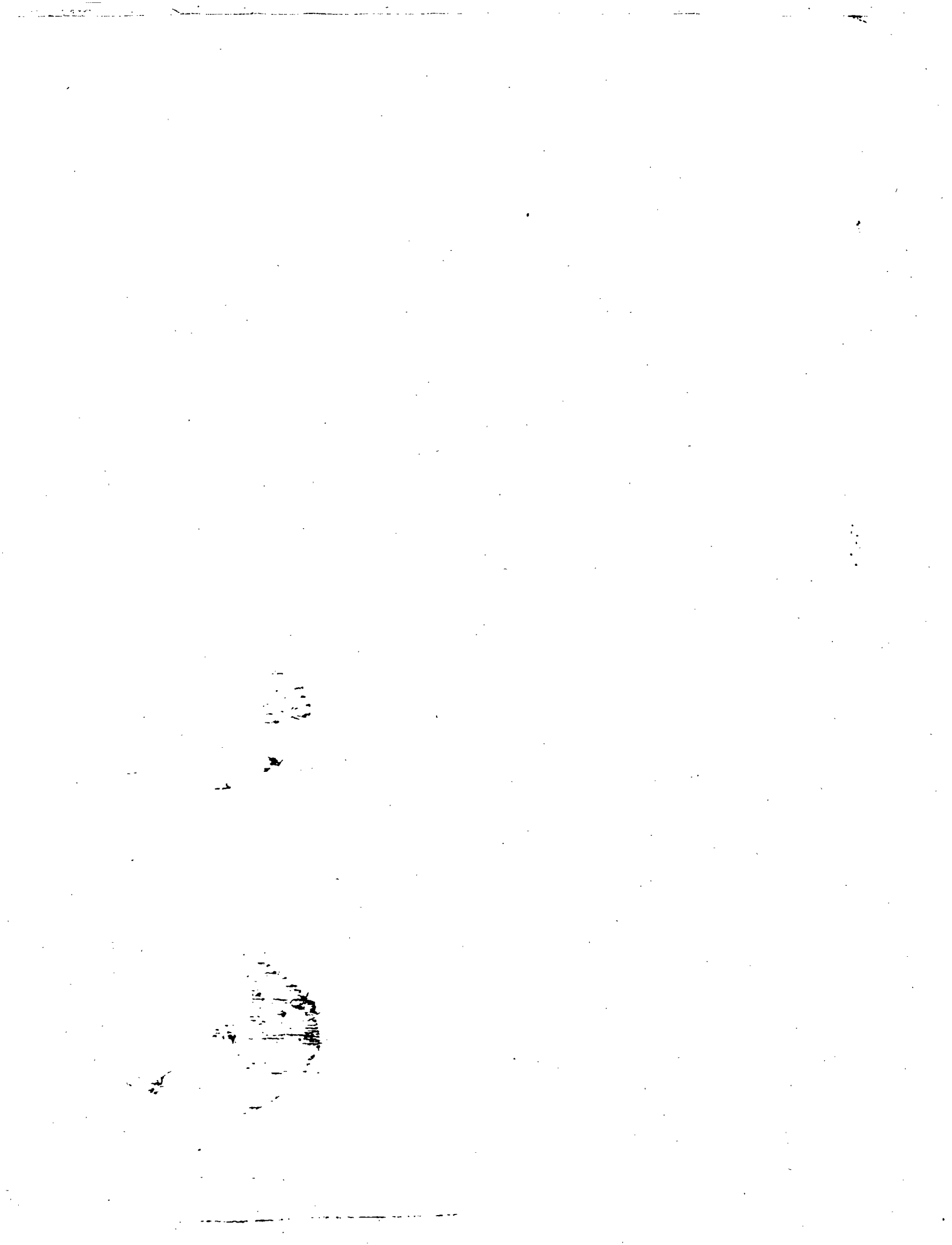
**FACULTAD DE INGENIERIA U.N.A.M.
DIVISION DE EDUCACION CONTINUA**

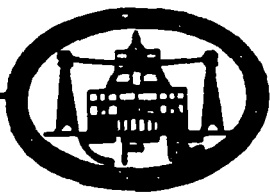
**V CURSO INTERNACIONAL DE SISTEMAS
ELECTRICOS DE POTENCIA**

MODULO II: SISTEMAS ELECTRICOS DE POTENCIA

**TEMA: DISTRIBUCION DE SALIDAS POR FALLA EN LINEAS DE
TRANSMISION**

EXPOSITOR: ING. ARTURO MORALES COLLANTES

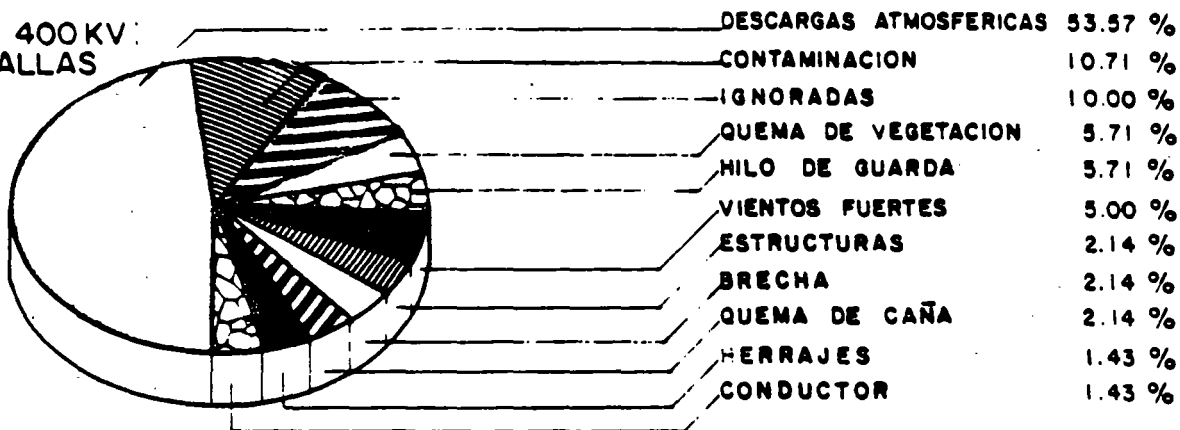




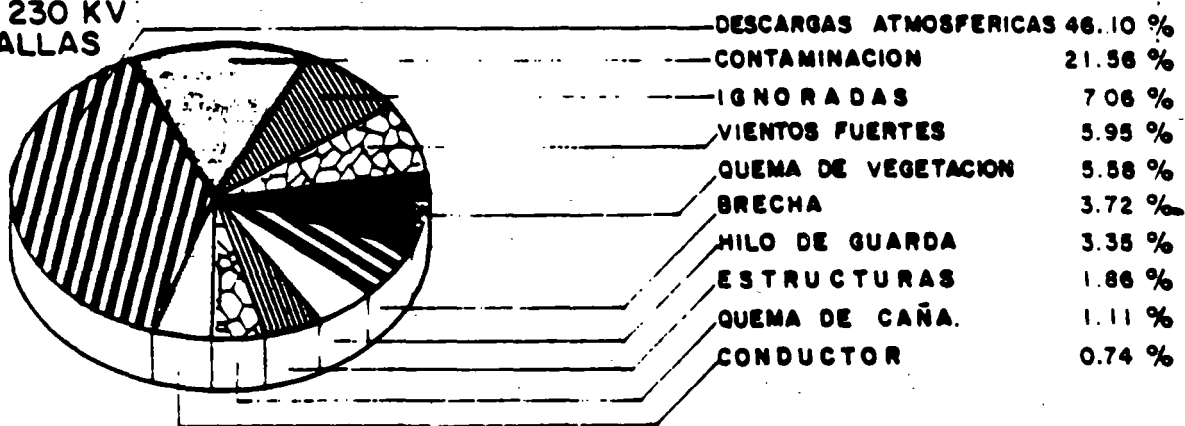
DISTRIBUCION DE SALIDAS POR FALLA EN LINEAS DE TRANSMISION PARA EL PERIODO 1990

FIG. No 20

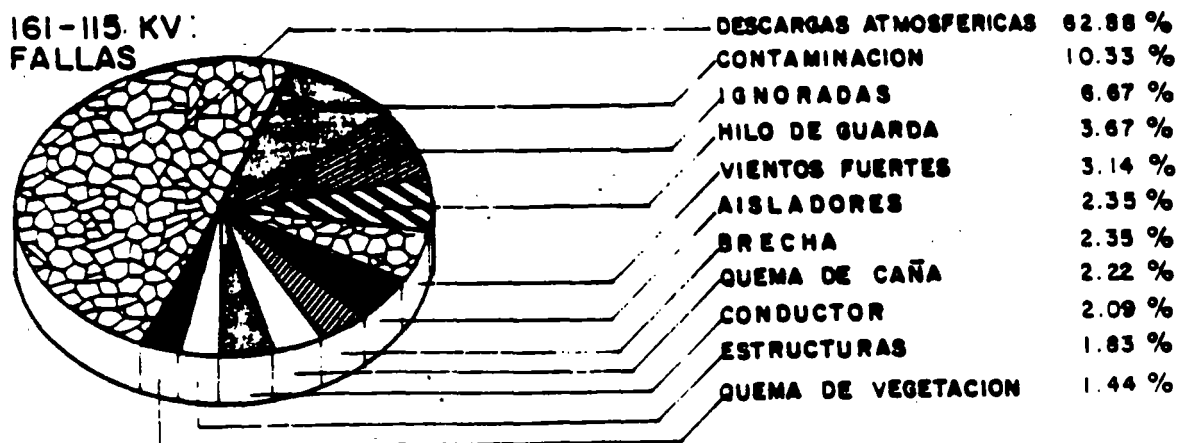
LT'S 400 KV:
140 FALLAS

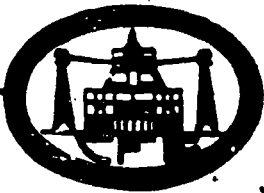


LT'S 230 KV:
269 FALLAS



LT'S 161-115 KV:
765 FALLAS

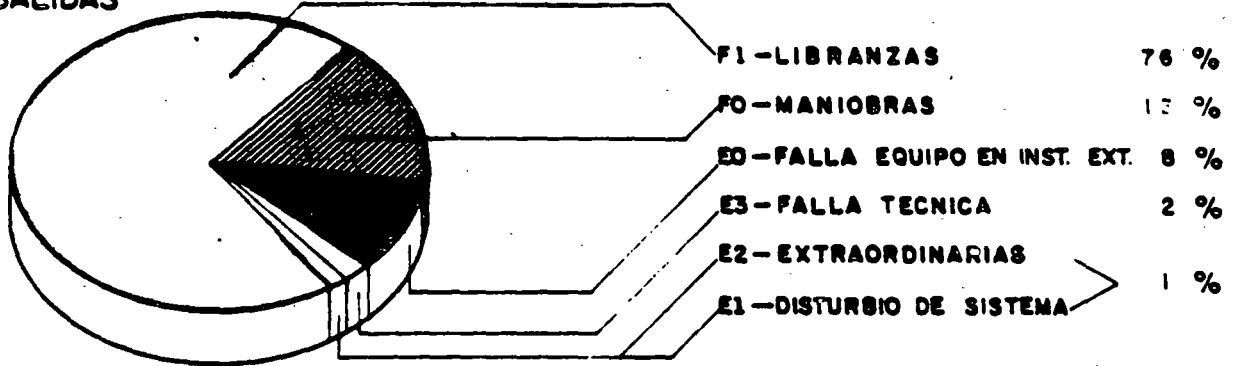




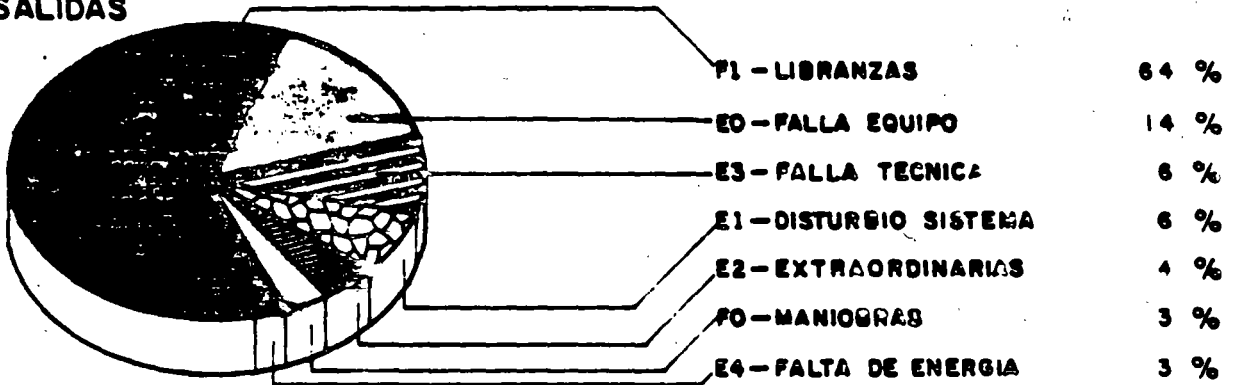
DISTRIBUCION DE SALIDAS POR CAUSAS AJENAS
Y MANIOBRAS EN LINEAS DE TRANSMISION
AÑO 1990

FIG. N.º 21

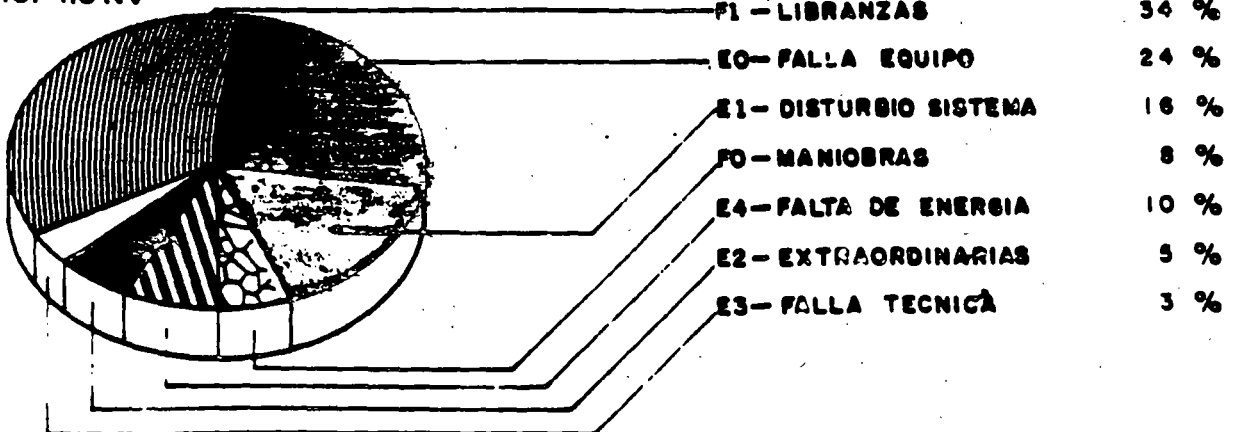
LT'S 400 KV
323 SALIDAS



LT'S 230 KV
522 SALIDAS



LT'S 161-115 KV



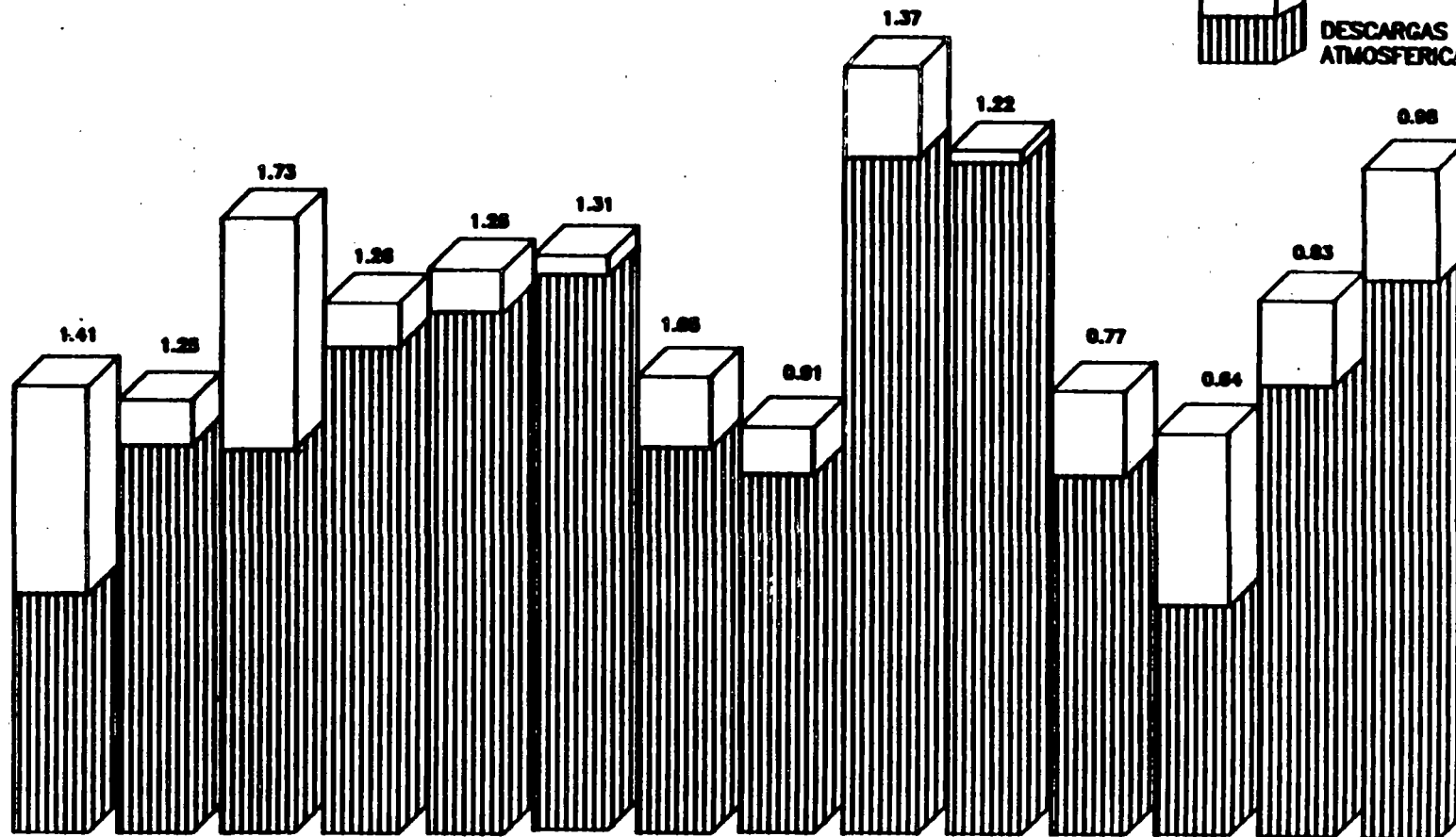


INDICE DE SALIDAS EN LINEAS DE TRANSMISION POR : DESCARGAS ATMOSFERICAS E IGNORADAS DE 400 kV

PERIODO 1977-1990

FIG. No. 10

IGNORADAS (Do)
DESCARGAS ATMOSFERICAS (Bo)



AÑO	1977	1978	1979	1980	1981	1982	1983	1984	1985	1986	1987	1988	1989	1990
No. SALIDAS (Bo)	32	53	51	65	70	75	53	49	92	91	49	31	61	75
No. SALIDAS (Do)	28	06	31	07	05	04	11	08	12	02	12	23	12	14
TOTAL	60	59	82	72	75	79	64	57	104	93	61	54	73	89
INDICE	1.41	1.25	1.73	1.26	1.25	1.31	1.05	0.91	1.37	1.22	0.77	0.64	0.83	0.98
KILOMETROS	4245	4737	4741	5695	5997	6035	6080	6287	7610	7855	7908	8378	8811.5	9099.1

Universidad Nacional Autónoma de México
División de Educación Continua

Curso: Sistemas de Potencia II

Tema: Sobretensiones y Coordinación de Aislamiento

Profesor: Víctor Federico Hermosillo Worley

M.S.E.E., Teck Lic. Elek

TEMARIO

1a Sesión:

1. Introducción

Fallas de L.T. en la Red Troncal del Sistema Mexicano
Clasificación de sobretensiones

2. Ondas viajeras en líneas de transmisión

Distorsión y atenuación de ondas viajeras

3. Modelos de líneas de transmisión

Componentes modales

4. Sobretensiones por descargas atmosféricas

Física y parámetros de descargas atmosféricas

Blindaje de líneas de transmisión

Modelo de una descarga directa

Descarga directa al hilo de guarda

Sobretensiones inducidas

2a Sesión:

5. Clasificación de sobretensiones por maniobra

Cierre y recierre de líneas de transmisión

Interrupción prematura de pequeñas corrientes inductivas

Interrupción de corrientes capacitivas

Sobretensiones temporales

Transitorios en subestaciones encapsuladas (SF6)

6. Coordinación de aislamiento

Nociones de probabilidad y estadística

Equipo de protección contra sobretensiones

Selección de apartarrayos

Nivel de aislamiento del equipo

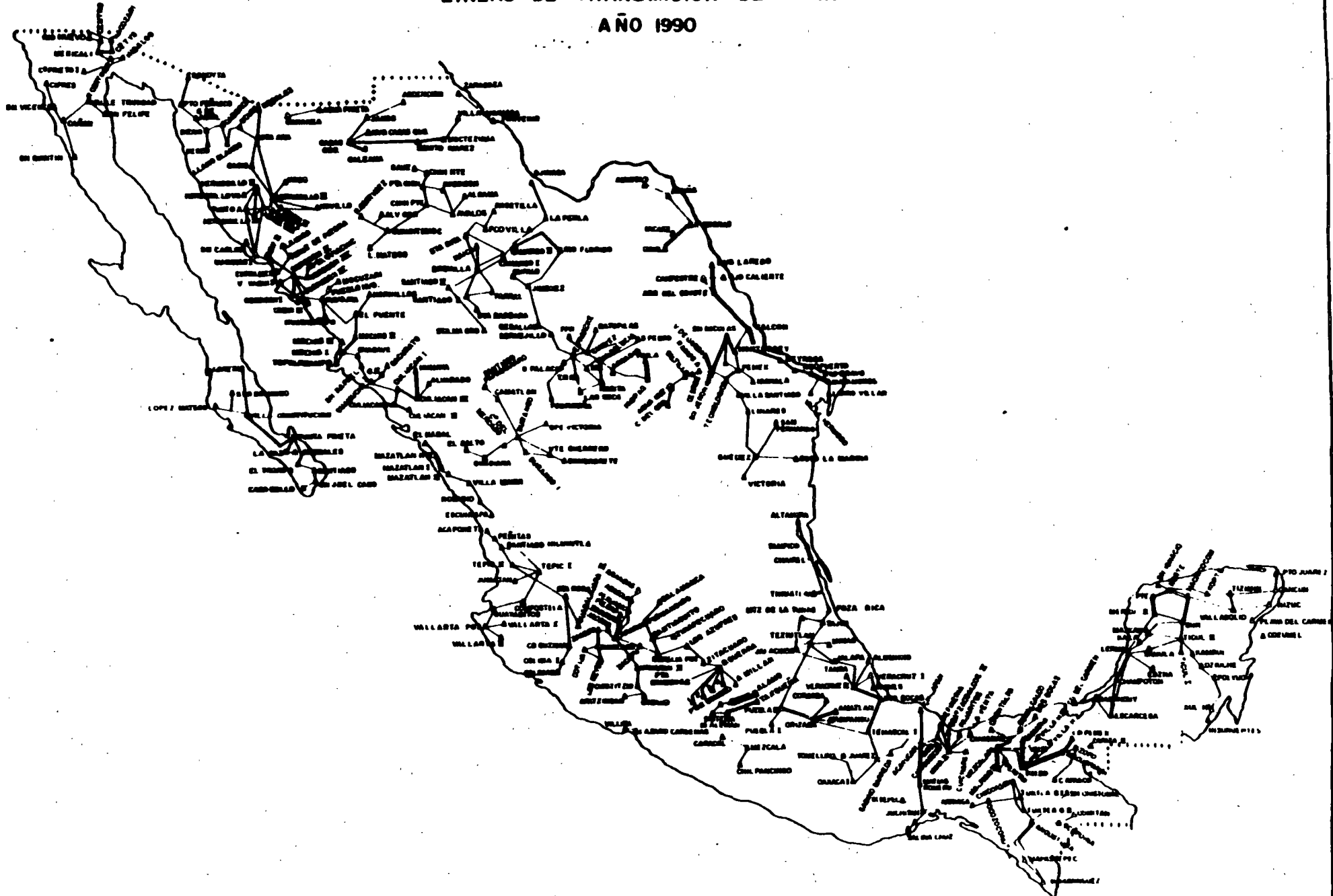
Estándares internacionales para coordinación de aislamiento

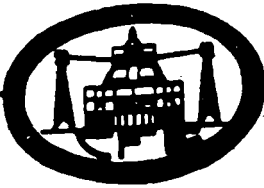


FIG. No. 3

LINEAS DE TRANSMISION DE 161-115 KV

AÑO 1990



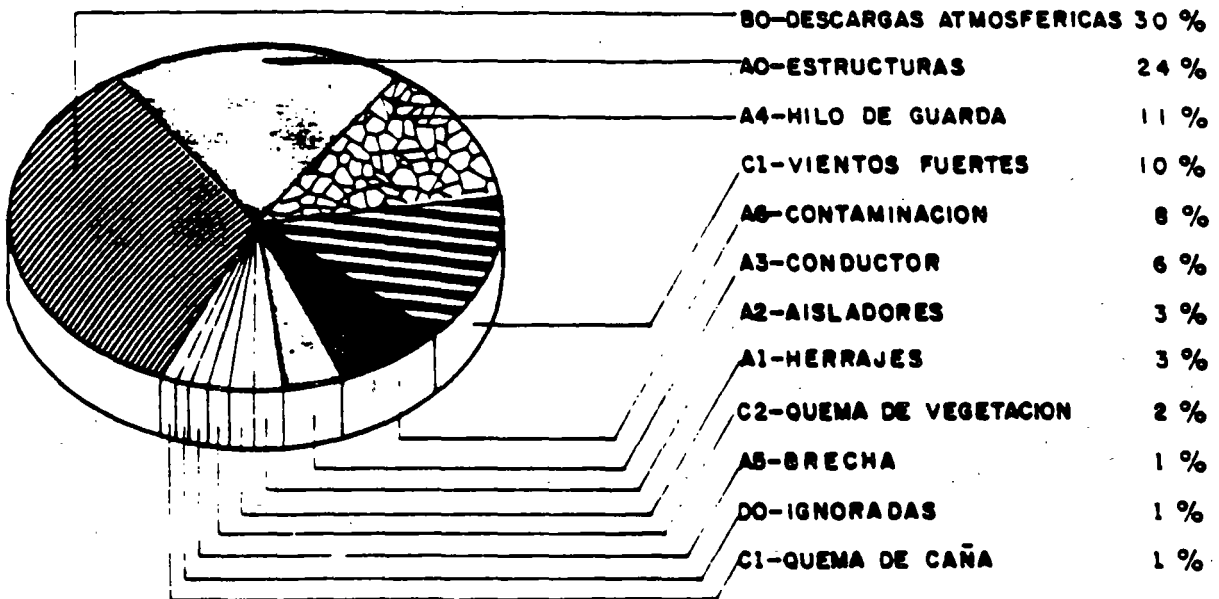


DISTRIBUCION EN PORCIENTO DEL TIEMPO QUE LAS LINEAS DE TRANSMISION, ESTUVIERON FUERA POR FALLA CAUSAS AJENAS, MANIOBRAS Y LIBRANZAS EN 1990

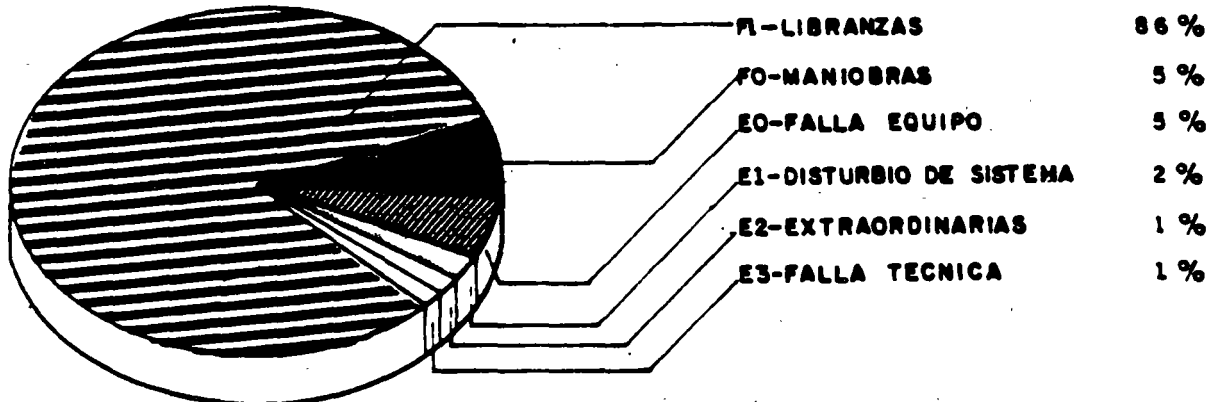
LT'S 400-115 KV

FIG. N° 22

TIEMPO FUERA POR FALLA: 2964:53 Hrs.: Min.



TIEMPO FUERA POR CAUSAS AJENAS, MANIOBRAS Y LIBRANZAS: 18953:12 Hr. Min.



1. WAVE PROPAGATION

1.1. INTRODUCTION

1.1.1. TYPES OF OVERVOLTAGES

- LIGHTNING STROKES
- SWITCHING SURGES
- ARCING GROUNDS
- RESONANCE VOLTAGES

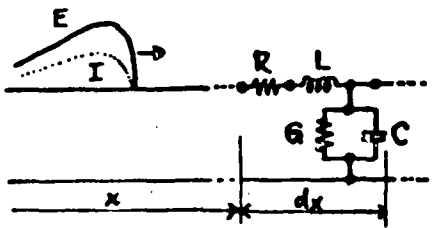
1.1.2. LIGHTNING STROKES

FREQUENCY OF OCCURRENCE
STATISTICAL DATA

MAGNITUDE
DURATION
RELEVANT PARAMETERS

1.1.3. MODELING LINES

DISTRIBUTED PARAMETERS
TRANSMISSION LINE DIFF. EQUATIONS



$$\frac{\partial^2 E}{\partial x^2} = \gamma^2 E$$

$$\frac{\partial^2 I}{\partial x^2} = \gamma^2 I$$

$$\gamma = \alpha + j\beta = \sqrt{(R+sL)(G+sC)}$$

1.2. IMPORTANT PARAMETERS

1.2.1. PROPAGATION CONSTANT

$$\gamma = \alpha + j\beta = \sqrt{Z_{LINE} Y_{LINE}}$$

α = ATTENUATION CONSTANT
 β = PHASE CONSTANT

1.2.2. CHARACTERISTIC (SURGE) IMPEDANCE

$$Z_0 = \sqrt{\frac{Z_{LINE}}{Y_{LINE}}} \quad e = Z_0 i \quad Y_0 = \frac{1}{Z_0}$$

1.2.3. LOSSLESS LINE: $R=0, G=0$

$$\gamma = s\sqrt{LC}$$

$$Z_0 = \sqrt{\frac{L}{C}}$$

1.2.4. DISTORTIONLESS LINE: $\frac{L}{R} = \frac{C}{G}$

1.3. LINE PARAMETERS, SIMPLE CASES

1.3.1. OVERHEAD CONDUCTOR

$$L = 2 \left(\frac{1}{4} + \ln \frac{2h}{r} \right) 10^{-4} \text{ H/km}$$

$$C = \frac{10^{-6}}{18 \ln \frac{2h}{r}} \text{ F/km}$$

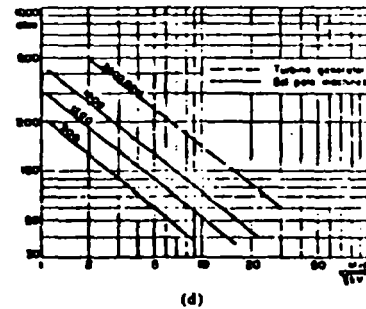
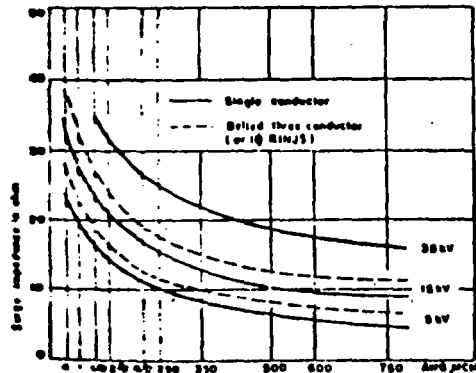
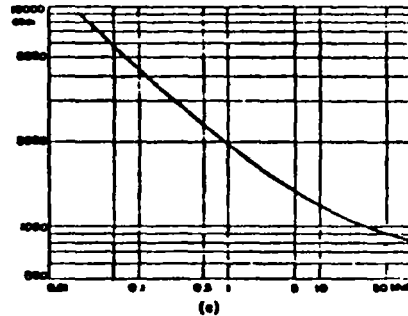
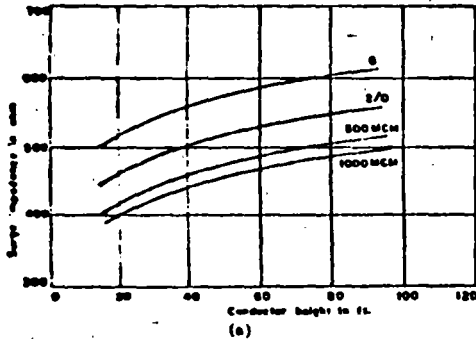
1.3.2. CABLE (ONE CONDUCTOR)

$$L \approx 2 \left(\frac{1}{4} + \ln \frac{R}{r} \right) 10^{-4} \text{ H/km}$$

$$C = k \frac{10^{-6}}{18 \ln \frac{R}{r}} \text{ F/km}$$

1.3.3. THREE PHASE SYSTEMS

1.4. SURGE IMPEDANCE CHARTS



POWER ENGINEER, TRANS. IGA, SEPT. 1965, 351
 (a) Surge impedance of overhead conductors (b) Surge impedance of paper insulated lead covered cables
 (c) Surge impedance per phase for transformers & high-voltage terms (d) Surge impedance per phase for synchronous machines

TYPICAL VALUES:

- OVERHEAD LINES: 400-600 OHMS
- CABLES: 10-40 OHMS, AROUND 25 OHMS
- TRANSFORMERS: THOUSANDS OF OHMS
- SYN. MACHINES: SEVERAL HUNDREDS OF OHMS

1.5. VELOCITY OF PROPAGATION

$$v \cong \frac{1}{\sqrt{LC}} = 300 \text{ m}/\mu\text{s}$$

$$v = \frac{V_{\text{LIGHT}}}{\sqrt{k \mu}}$$

1.6. MATHEMATICAL EXPRESSION OF E AND I

$$E = e^{\gamma x} f_1(t) + e^{-\gamma x} f_2(t)$$

$$I = -\frac{1}{Z_0} [e^{\gamma x} f_1(t) - e^{-\gamma x} f_2(t)]$$

$$E = f_1(t + \frac{x}{v}) + f_2(t - \frac{x}{v}) = E_{\text{BACKWARD}} + E_{\text{FORWARD}}$$

$$I = -\frac{1}{Z_0} [f_1(t + \frac{x}{v}) - f_2(t - \frac{x}{v})] = -I_{\text{BACKWARD}} + I_{\text{FORWARD}}$$

1.7. POLARITIES

FORWARD (INCIDENT) WAVES $E_f = Z_0 I_f$

BACKWARD (REFLECTED) WAVES $E_r = -Z_0 I_r$

1.8. SHAPE OF WAVES

1.81. SPECIFICATIONS

ANSI: 1.2 x 50

1.82. APPROXIMATIONS

1.9. ATTENUATION AND DISTORTION

- LOSSES
- CORONA
- GROUND
- SKIN EFFECT
- CHANGING L AND C

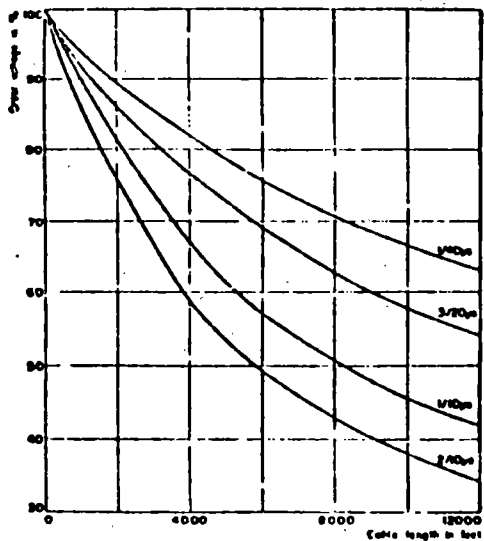
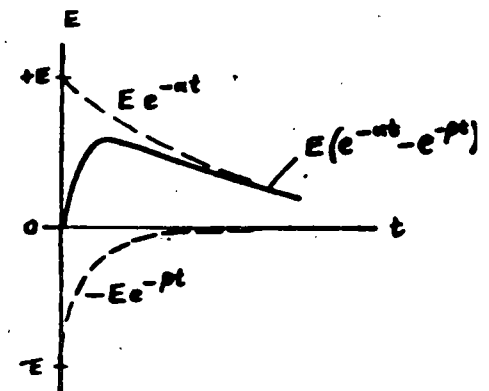
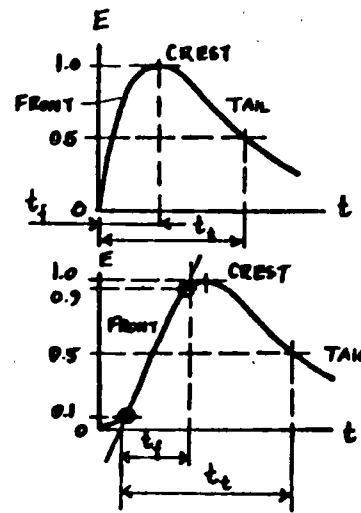


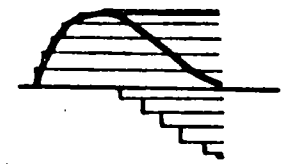
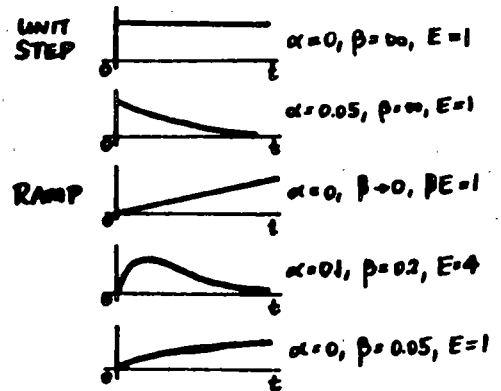
Fig. 4 Surge attenuation in cables as function of cable length. FOURTH EDITION, TROTTER, MGA, SEPT 1965, 35B

EFFECT OF DISTANCE



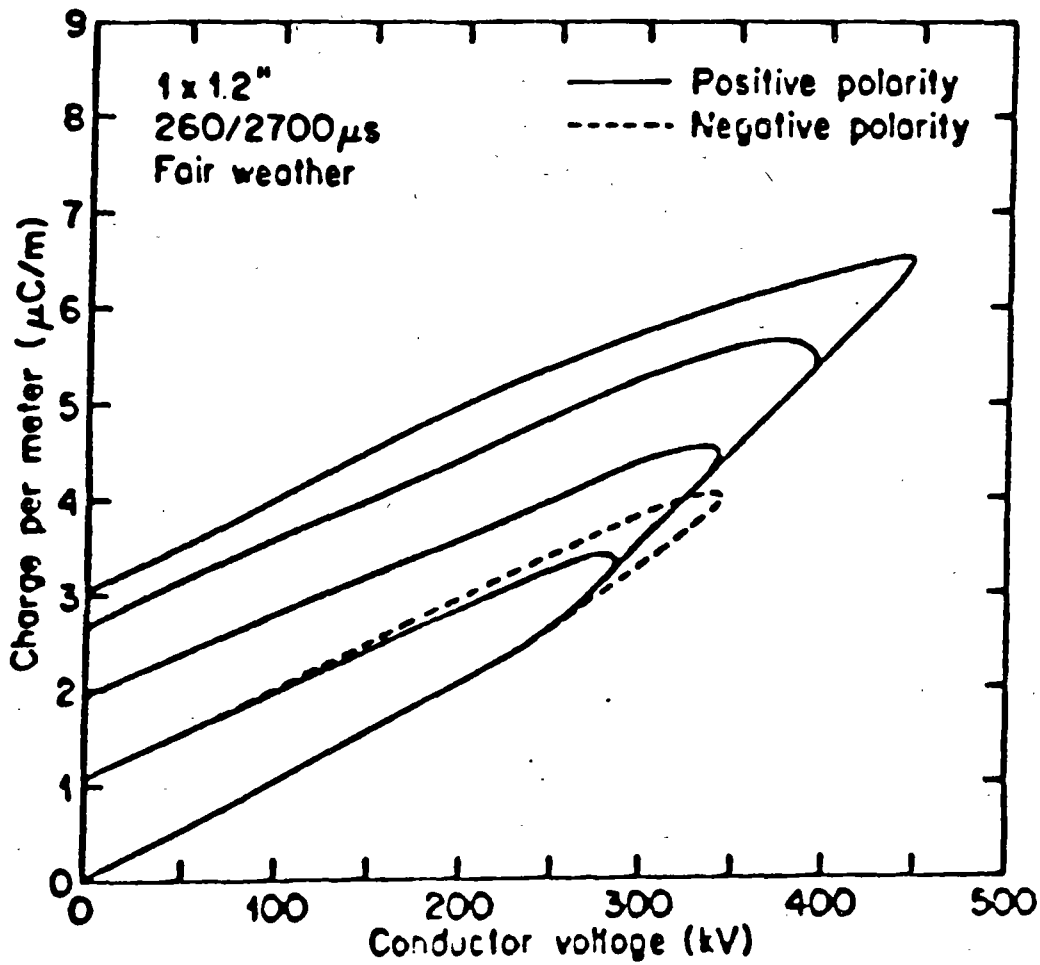
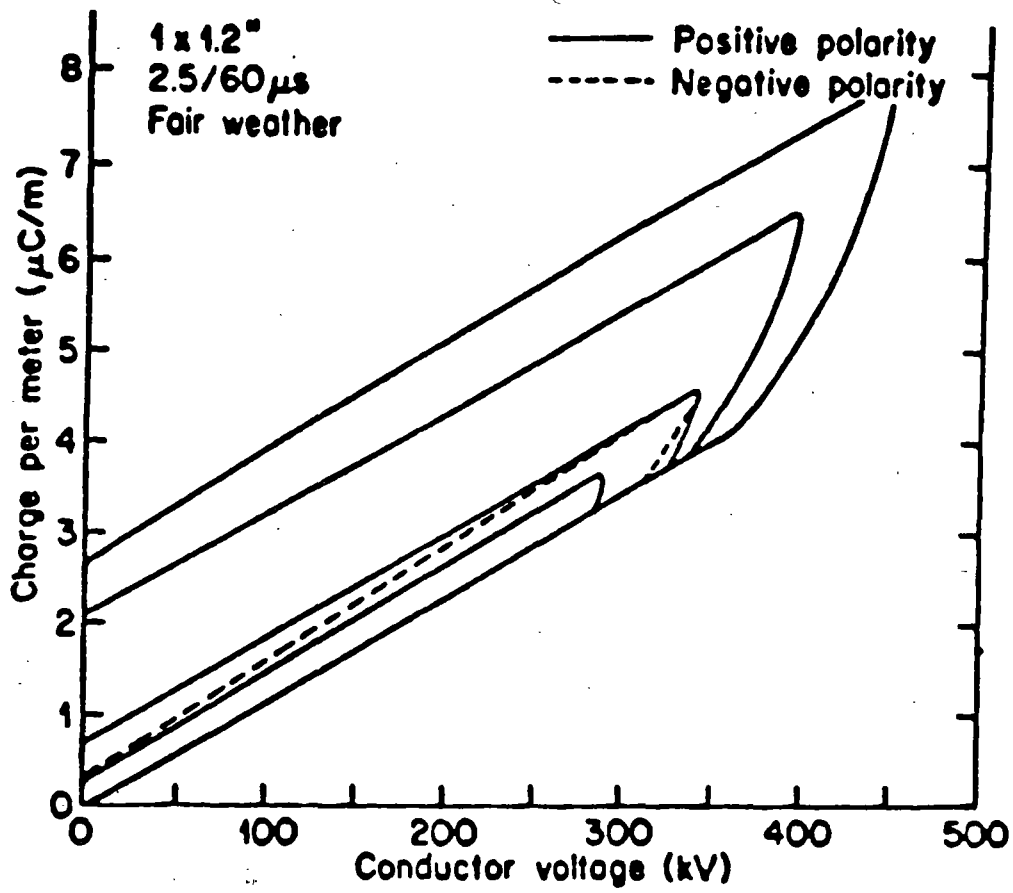
SPECIFICATION OF A TRAVELING WAVE:
 WAVE: $(t_f) \times (t_r)$ in microseconds:
 1.2 x 50; 5 x 10

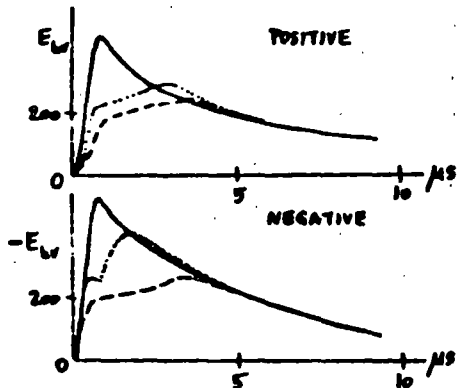
TRAVELING WAVE AS THE SUM OF TWO EXPONENTIAL FUNCTIONS



APPROXIMATION BY RECTANGULAR COMPONENTS

WAVESHAPES APPROXIMATED BY
 $e = E(e^{-at} - e^{-pt})$

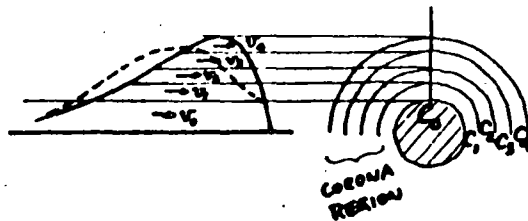




MODIFICATION OF CHARGES WITH DISTANCE TRAVELED:

- AT START (0 MI.)
- AT 1.5 MILES
- AT 5 MILES

EFFECT OF CORONA ON WAVE DISTORTION:



$$v_k = \frac{1}{\sqrt{LC_k}}$$

$$C_k: C_0 < C_1 < C_2 < C_3 < C_4 \dots$$

$$v_k: v_0 > v_1 > v_2 > v_3 > v_4 \dots$$

2. REFLECTION OF WAVES

2.1. GENERAL TRANSITION POINT

2.11. PRACTICAL CASES (NEXT PAGE)

TERMINAL CONDITIONS
 JUNCTIONS
 JUNCTIONS WITH SHUNT ELEMENT

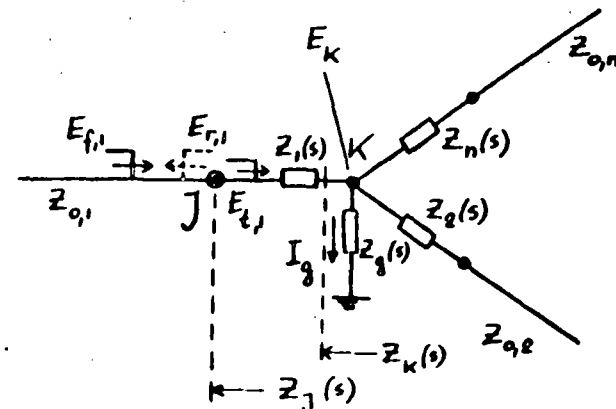
2.12. GENERAL TRANSITION POINT

$$\frac{E_{f,i}}{I_{f,i}} = Z_{0,i} \quad \frac{E_{r,i}}{I_{r,i}} = -Z_{0,i} \quad \frac{E_{t,i}}{I_{t,i}} = Z_0$$

$$E_{t,i} = E_{f,i} + E_{r,i}$$

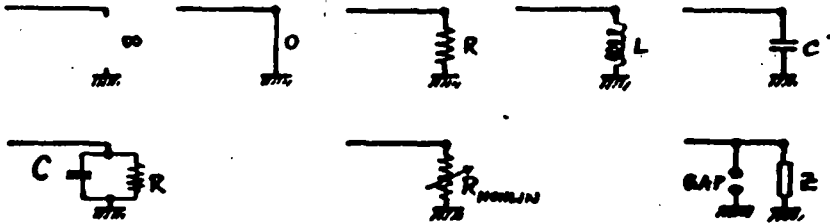
$$I_{t,i} = I_{f,i} + I_{r,i}$$

$$Z_j(s) = Z_1(s) + Z_k(s) = Z_1(s) + \frac{1}{\frac{1}{Z_0(s)} + \sum_{i=2}^n \frac{1}{Z_i(s)}}$$

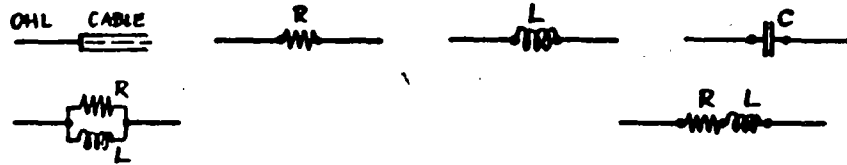


TYPICAL EXAMPLES:

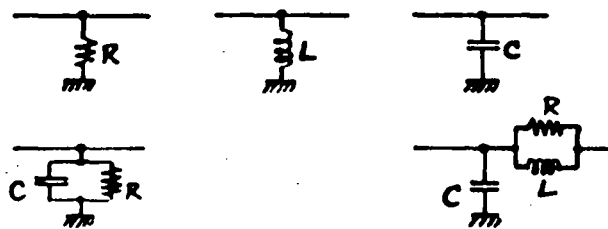
TERMINAL CONDITIONS:



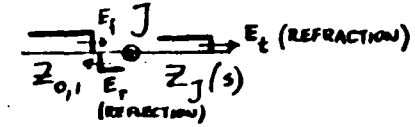
JUNCTIONS AND SERIES ELEMENTS:



JUNCTIONS AND SHUNT ELEMENTS:



2.13. REFLECTION COEFFICIENTS AT J



$$a_E = \frac{Z_j - Z_0}{Z_j + Z_0}$$

$$E_r = a_E E_f$$

$$a_I = -\frac{Z_j - Z_0}{Z_j + Z_0}$$

$$I_r = a_I I_f$$

2.14. REFRACTION COEFFICIENTS AT J

$$b_E = \frac{2Z_j}{Z_j + Z_0}$$

$$E_t = b_E E_f$$

$$b_I = \frac{2Z_0}{Z_j + Z_0}$$

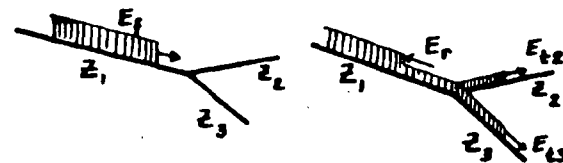
$$I_t = b_I I_f$$

2.15. a AND b RELATIONSHIPS

$$a_I = -a_E$$

$$b_I = 1 - a_E = 1 + a_I$$

$$b_E = 1 + a_E = 1 - a_I$$



2.2. LINE TERMINATED BY A RESISTANCE



R	∞ O.C.	Z_0	0 SH.C.
Z_j	∞	Z_0	0
a_E	1	0	-1
a_I	-1	0	1
b_E	2	1	0
b_I	0	1	2
E_r	E_f	0	$-E_f$
$E_f + E_r$	$2E_f$	E_f	0
I_r	$-I_f$	0	I_f
$I_f + I_r$	0	I_f	$2I_f$

DUALITY

CABLE - OVERHEAD LINE AND
OVERHEAD LINE - CABLE JUNCTIONS

2.3. INDUCTIVE AND CAPACITIVE ELEMENTS

2.31. ASSUMPTIONS

FRONT OF TRAVELING WAVE

$\omega \gg \omega_0$

$\omega L = \infty \quad \frac{1}{\omega C} = 0$

TAIL OF TRAVELING WAVE

$\omega \ll \omega_0$

$\omega L = 0 \quad \frac{1}{\omega C} = \infty$

2.32. TERMINATIONS

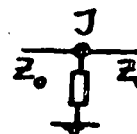
INDUCTIVE O.C. \rightarrow SH.C.

CAPACITIVE SH.C. \rightarrow O.C.

2.33. SHUNT ELEMENT AT JUNCTION

INDUCTIVE O.C. \rightarrow SH.C.

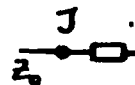
CAPACITIVE SH.C. \rightarrow O.C.



2.34. SERIES ELEMENT INSERTION

INDUCTIVE O.C. \rightarrow SH.C.

CAPACITIVE SH.C. \rightarrow O.C.



2.35. COMPUTATIONS, FLOWCHART

$Z_0 \quad Z_j(s)$

$a_E(s) \quad a_I(s) \quad b_E(s) \quad b_I(s)$

$\alpha [1/sec]$

$E_f(s) = \frac{E_f}{s}$

$E_r(s) = a_E(s) \cdot E_f(s) \longrightarrow e_r(t)$

$e_{total} = e_f(t) + e_r(t)$

$e_t(t)$

$e_{series}(t) = e_{total} - e_t(t)$

$i_r(t) = -\frac{e_r(t)}{Z_0}$

$i_{total} = i_f(t) + i_r(t)$

$i_t(t) = \frac{e_t(t)}{Z_0}$

$i_{shunt}(t) = i_{total} - i_t(t)$

CHARTS FOR

VOLTAGES AND CURRENTS VS. TIME

VOLTAGES AND CURRENTS ALONG LINE

2.4. SPECIAL CASES WITH AN INDUCTANCE OR A CAPACITANCE

2.41. INDUCTIVE TERMINATION

$Z_j(s) = sL$

$a = \frac{Z_j(s) - Z_0}{Z_j(s) + Z_0} = \frac{s - \alpha}{s + \alpha}$

$\alpha = \frac{Z_0}{L} \quad 1/sec$

$E_f(s) = \frac{E_f}{s}$

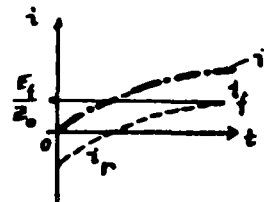
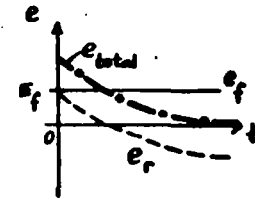
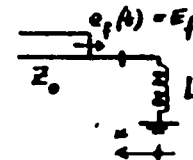
$E_r(s) = a E_f(s) = \frac{E_f}{s} \frac{s - \alpha}{s + \alpha}$

$e_r(t) = E_f (2e^{-\alpha t} - 1)$

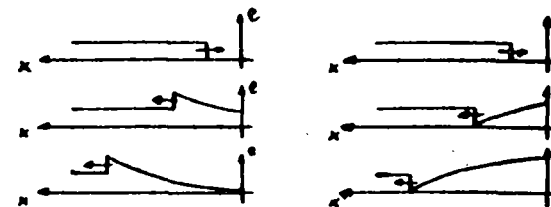
$e_{total} = e_f(t) + e_r(t) = 2E_f e^{-\alpha t}$

$i_r(t) = -\frac{e_r(t)}{Z_0} = \frac{E_f}{Z_0} (1 - 2e^{-\alpha t})$

$i_{total} = i_f(t) + i_r(t) = \frac{2E_f}{Z_0} (1 - e^{-\alpha t})$



VOLTAGES AND CURRENTS ALONG THE LINE



2.42. CAPACITIVE TERMINATION

$$Z_j(s) = \frac{1}{sC}$$

$$\alpha = \frac{\alpha - s}{\alpha + s}$$

$$\alpha = \frac{1}{Z_0 C} \quad 1/\text{sec}$$

$$E_f(s) = \frac{E_f}{s}$$

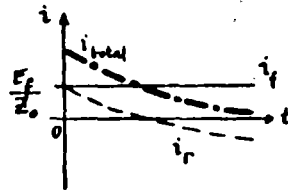
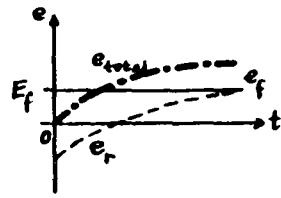
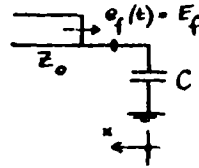
$$\rightarrow E_r(s) = \frac{E_f}{s} \frac{\alpha - s}{\alpha + s}$$

$$e_r(t) = E_f (1 - 2e^{-\alpha t})$$

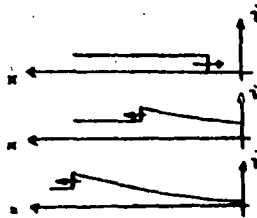
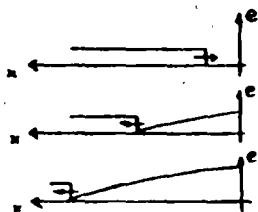
$$e_{\text{total}} = e_f(t) + e_r(t) = 2E_f (1 - e^{-\alpha t})$$

$$i_r(t) = \frac{E_f}{Z_0} (2e^{-\alpha t} - 1)$$

$$i_{\text{total}} = i_f(t) + i_r(t) = \frac{2E_f}{Z_0} e^{-\alpha t}$$



VOLTAGES AND CURRENTS ALONG THE LINE



2.43. SHUNT INDUCTANCE

$$Z_j(s) = \frac{sLZ_0}{sL + Z_0}$$

$$\alpha = -\frac{\alpha}{s + \alpha} \quad \alpha = \frac{Z_0}{2L}$$

$$E_f(s) = \frac{E_f}{s}$$

$$E_r(s) = -\frac{E_f}{s} \frac{\alpha}{s + \alpha}$$

$$e_r(t) = E_f (e^{-\alpha t} - 1)$$

$$e_{\text{total}} = e_f(t) + e_r(t) = E_f e^{-\alpha t}$$

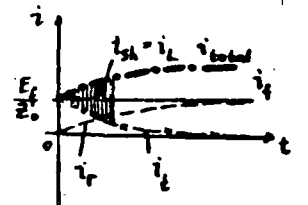
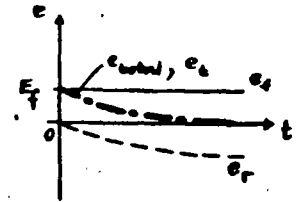
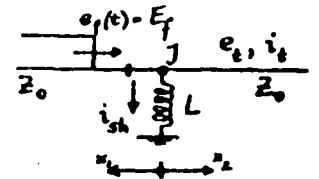
$$e_t(t) = e_{\text{total}}$$

$$i_r(t) = \frac{E_f}{Z_0} (1 - e^{-\alpha t})$$

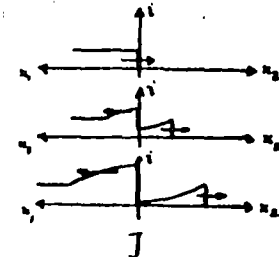
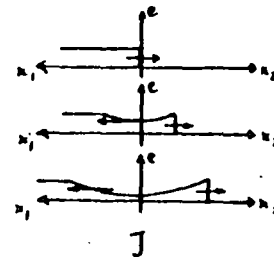
$$i_{\text{total}} = i_f(t) + i_r(t) = \frac{E_f}{Z_0} (2 - e^{-\alpha t})$$

$$i_t(t) = \frac{E_f}{Z_0} e^{-\alpha t}$$

$$i_{\text{sh}}(t) = i_{\text{total}} - i_t(t) = \frac{2E_f}{Z_0} (1 - e^{-\alpha t})$$



VOLTAGES AND CURRENTS ALONG THE LINE



2.44 SHUNT CAPACITANCE (MOTOR PROTECTION)

$$Z_j(s) = \frac{Z_0 / sC}{Z_0 + \frac{1}{sC}}$$

$$a = -\frac{s}{s+\alpha} \quad \alpha = \frac{2}{Z_0 C}$$

$$E_f(s) = \frac{E_f}{s}$$

$$E_r(s) = -E_f \frac{1}{s+\alpha}$$

$$e_r(t) = -E_f e^{-\alpha t}$$

$$e_{total} = e_f(t) + e_r(t) = E_f(1 - e^{-\alpha t})$$

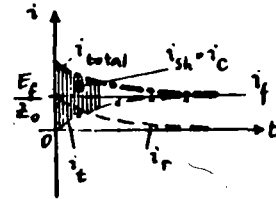
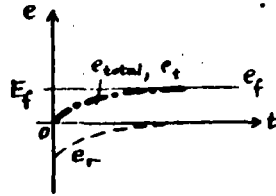
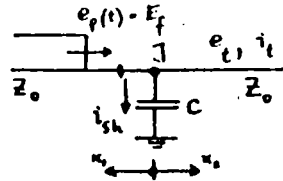
$$e_t(t) = e_{total}$$

$$i_r(t) = \frac{E_f}{Z_0} e^{-\alpha t}$$

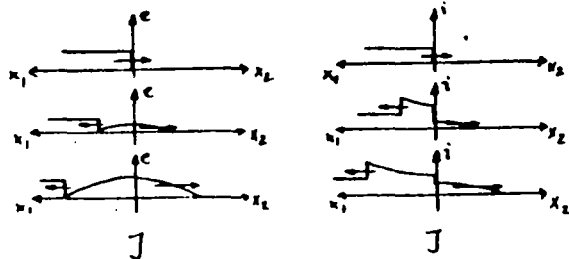
$$i_{total} = \frac{E_f}{Z_0} (1 + e^{-\alpha t})$$

$$i_t(t) = \frac{E_f}{Z_0} (1 - e^{-\alpha t})$$

$$i_{sh}(t) = \frac{2E_f}{Z_0} e^{-\alpha t}$$



VOLTAGES AND CURRENTS ALONG THE LINE



2.45. SERIES INDUCTANCE (MOTOR PROTECTION)

$$Z_j(s) = sL + Z_0$$

$$a = \frac{s}{s+\alpha} \quad \alpha = \frac{2Z_0}{L}$$

$$E_f(s) = \frac{E_f}{s}$$

$$E_r(s) = E_f \frac{1}{s+\alpha}$$

$$e_r(t) = E_f e^{-\alpha t}$$

$$e_{total} = e_f(t) + e_r(t) = E_f(1 + e^{-\alpha t})$$

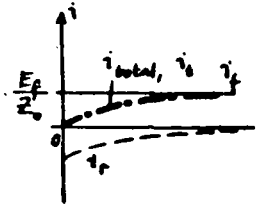
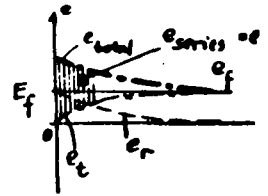
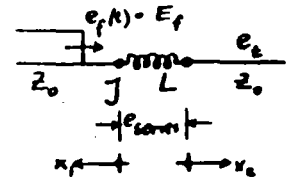
$$e_t(t) = E_f(1 - e^{-\alpha t})$$

$$e_{series} = e_{total} - e_t(t) = 2E_f e^{-\alpha t}$$

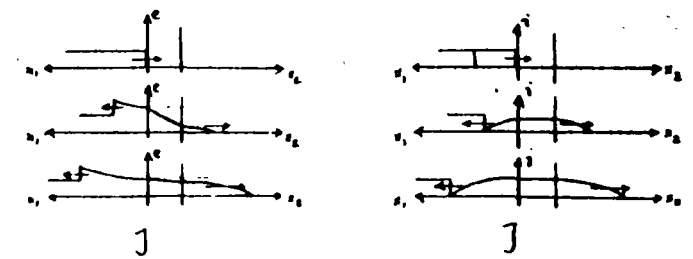
$$i_r(t) = -\frac{E_f}{Z_0} e^{-\alpha t}$$

$$i_{total} = i_f(t) + i_r(t) = \frac{E_f}{Z_0}(1 - e^{-\alpha t})$$

$$i_t(t) = \frac{E_f}{Z_0}(1 - e^{-\alpha t})$$



VOLTAGES AND CURRENTS ALONG THE LINE



2.46. SERIES CAPACITANCE

$$Z_j(s) = \frac{1}{sC} + Z_0$$

$$a = \frac{\alpha}{s+\alpha} \quad \alpha = \frac{1}{2Z_0 C}$$

$$E_f(s) = \frac{E_f}{s}$$

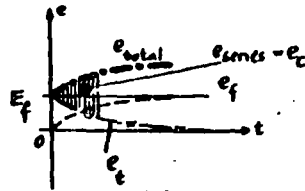
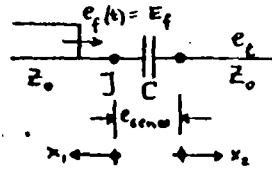
$$E_r(s) = \frac{E_f}{s} \frac{\alpha}{s+\alpha}$$

$$e_r(t) = E_f(1 - e^{-\alpha t})$$

$$e_{total} = e_f(t) + e_r(t) = E_f(2 - e^{-\alpha t})$$

$$e_t(t) = E_f e^{-\alpha t}$$

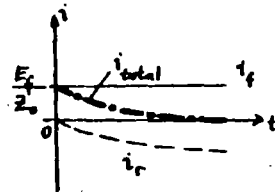
$$e_{series} = 2E_f(1 - e^{-\alpha t})$$



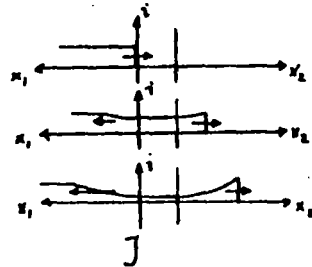
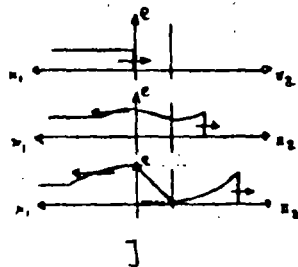
$$i_r(t) = \frac{E_f}{Z_0} (e^{-\alpha t} - 1)$$

$$i_{total} = i_f(t) + i_r(t) = \frac{E_f}{Z_0} e^{-\alpha t}$$

$$i_t(t) = \frac{E_f}{Z_0} e^{-\alpha t}$$



VOLTAGES AND CURRENTS ALONG THE LINE



2.5. SUCCESSIVE REFLECTIONS

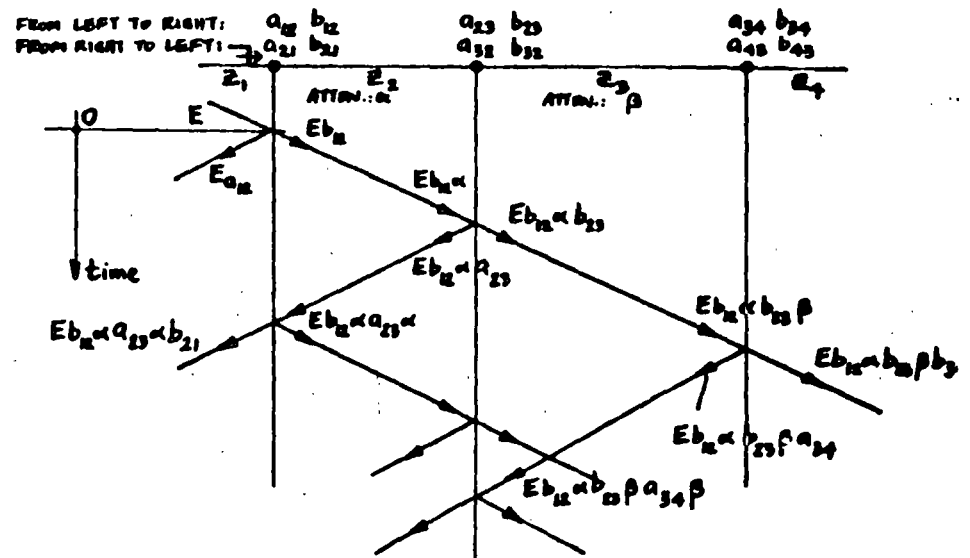
2.5.1. BEWLEY LATTICE

TIME-SPACE DIAGRAM
MULTIPLE REFLECTIONS

DISTANCE BETWEEN JUNCTIONS
IS PROPORTIONAL TO

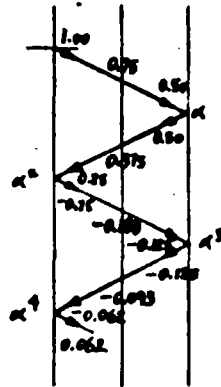
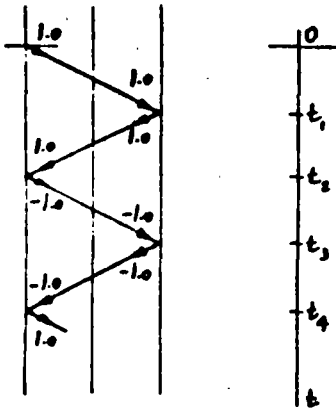
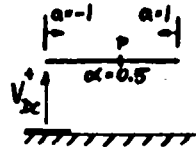
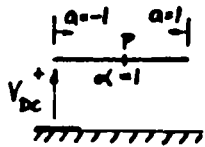
TIME OF WAVE PASSAGE
(DIAGONALS HAVE SAME SLOPE)

LENGTH BETWEEN JUNCTIONS
(SLOPES ARE DIFFERENT)

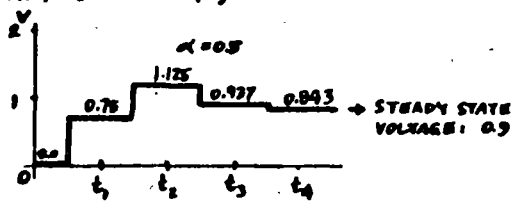
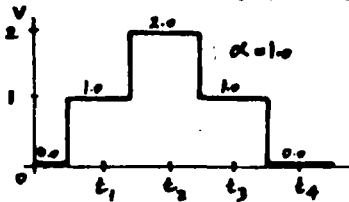


2.52. EXAMPLES

LINE CHARGING WITH DC



VOLTAGES AT MIDPOINT OF LINE (P):



VOLTAGE AT END WHEN $\alpha=0.5$:

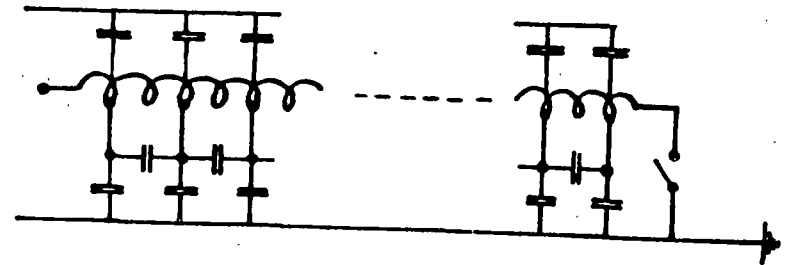
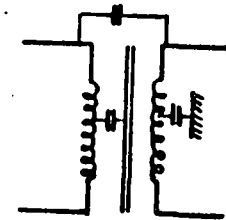
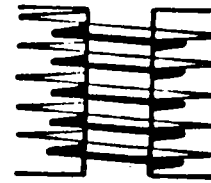
$$V = 2\alpha - 2\alpha^3 \pm \dots = 2\alpha (1 - \alpha^2 + \alpha^4 \mp \dots)$$

$$\text{STEADY STATE VOLTAGE: } \lim V = \frac{2\alpha}{1 + \alpha^2} = 0.8$$

3. TRANSFORMER WINDINGS UNDER TRANSIENT CONDITIONS

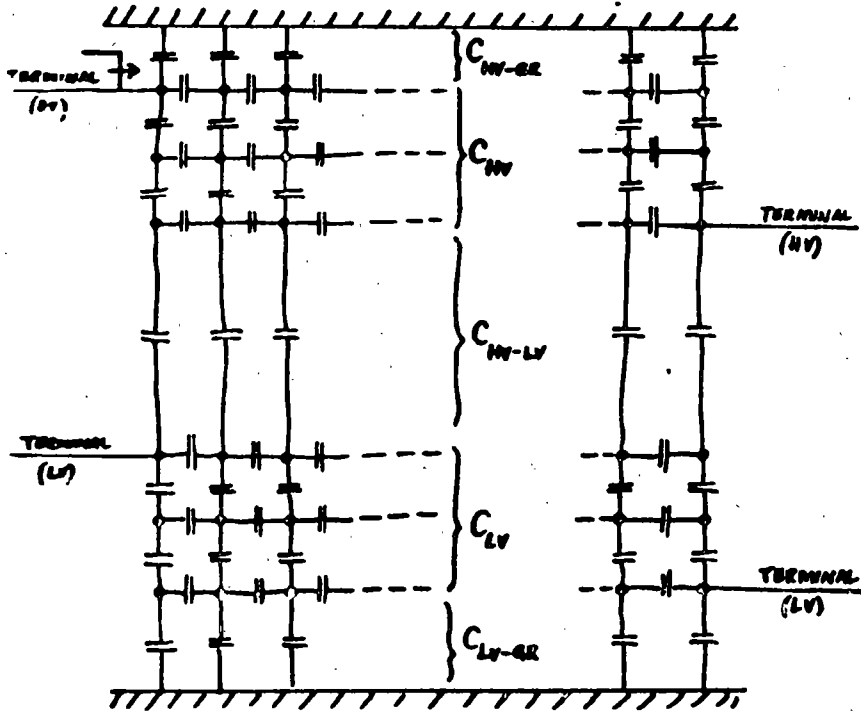
3.1. SCHEMATIC REPRESENTATION

- SELF INDUCTANCES
- MUTUAL INDUCTANCES
- CAPACITANCES: TO CORE
TO TANK
- CAPACITIVE COUPLING
- LOSSES (RESISTANCES)

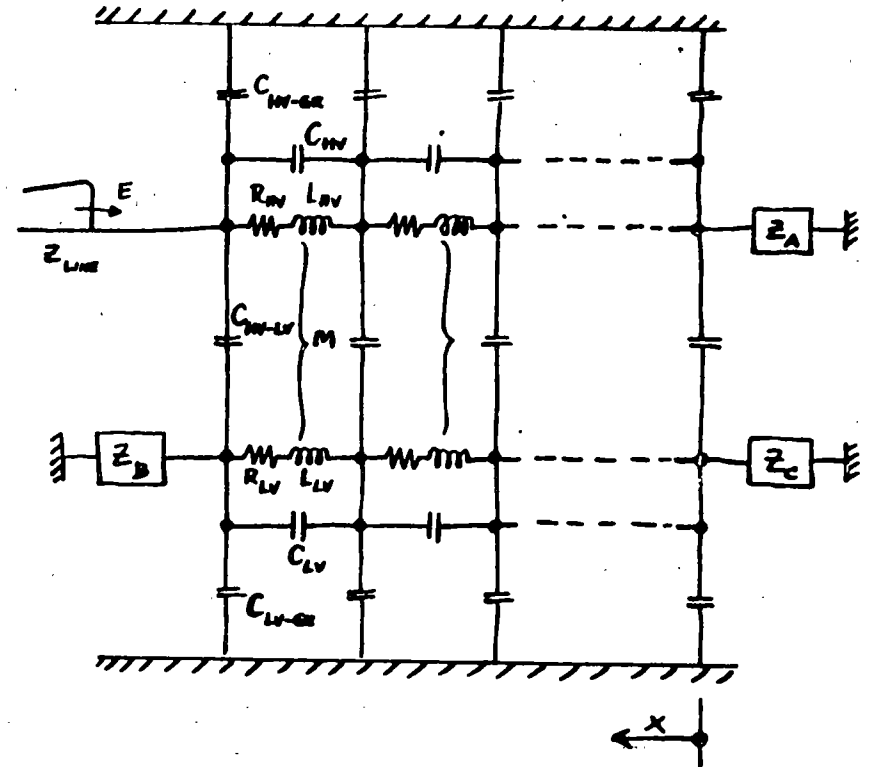


INITIAL VOLTAGE DISTRIBUTION IS DETERMINED BY THE CAPACITANCE NETWORK,

AT THE FRONT OF THE WAVE ($\omega \approx \infty$)
 $WL \approx \infty$, I.E., OPEN-CIRCUITED:



COMPLETE EQUIVALENT CIRCUIT FOR TRANSIENTS (ANALOG MODEL):



3.2. INITIAL VOLTAGE DISTRIBUTION

CAPACITANCE LADDER NETWORK

GROUND CAP. OF WINDING C_g

SERIES CAP. OF WINDING C_s

E = VOLTAGE TO GROUND AT ANY POINT

x = FROM NEUTRAL TO TERMINAL

l = LENGTH OF WINDING

$$\frac{\partial^2 E}{\partial x^2} - \frac{1}{l^2} \frac{C_g}{C_s} E = 0$$

$$E = Ae^{px} + Be^{-px}$$

$$p = \frac{1}{l} \left(\frac{C_g}{C_s} \right)^{\frac{1}{2}}$$

GROUNDING NEUTRAL

$$E = V \frac{\sinh(\alpha x/l)}{\sinh \alpha}$$

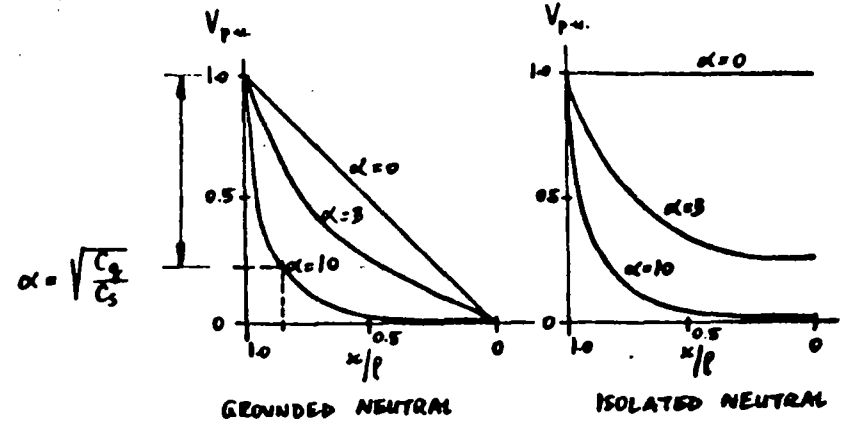
$$x=0: E=0 \quad x=l: E=V$$

$$\alpha = pl = \sqrt{\frac{C_g}{C_s}}$$

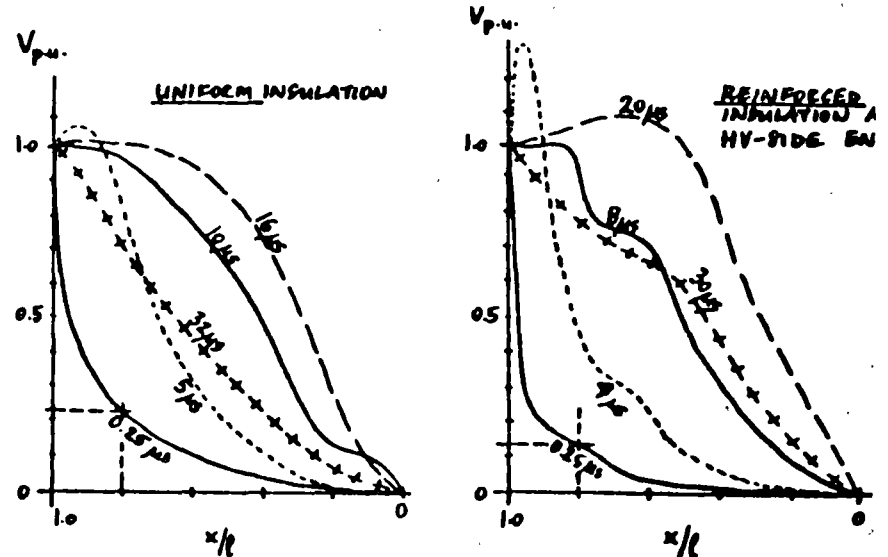
ISOLATED NEUTRAL

$$E = V \frac{\cosh(\alpha x/l)}{\cosh \alpha}$$

$$x=0: I=0 \quad x=l: E=V$$



INITIAL VOLTAGE DISTRIBUTION IN CASE OF STEP-FUNCTION FORWARD VOLTAGE



TRANSIENT VOLTAGE DISTRIBUTION IN CASE OF STEP-FUNCTION FORWARD VOLTAGE

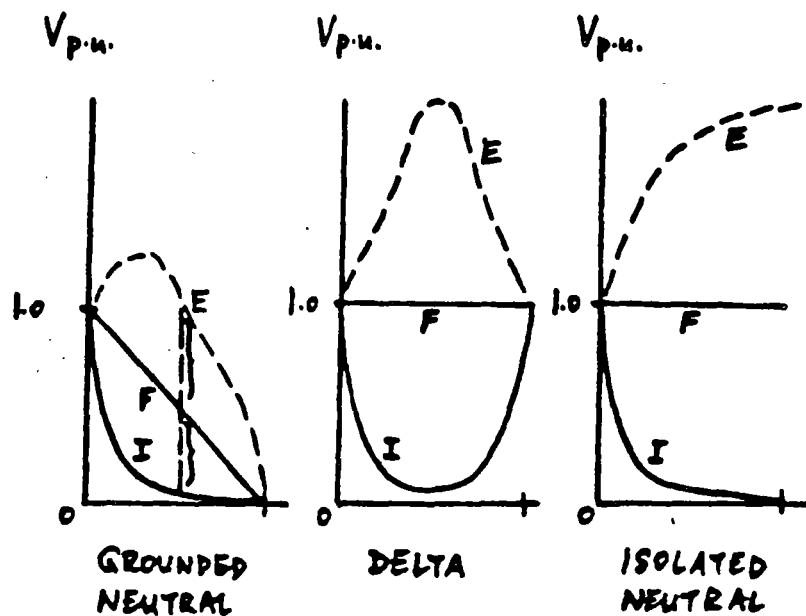
3.4. ENVELOPE CURVES

I - INITIAL DISTRIBUTION

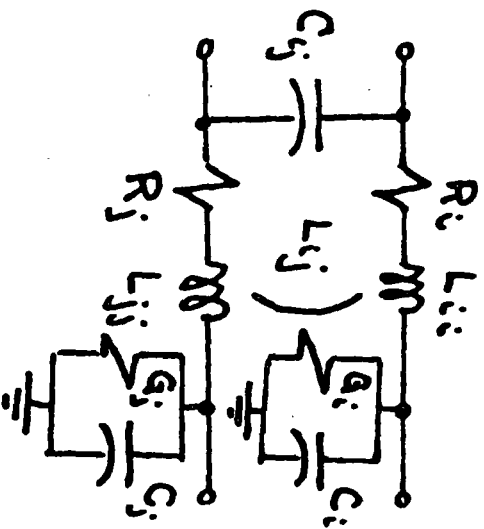
F - FINAL DISTRIBUTION

LC CIRCUITS \rightarrow OSCILLATIONS

E - ENVELOPES OF OSCILLATION



Líneas de Transmisión con Conductores Múltiples.



R_i, L_{ij}, G_i, C_i : resistencia, inductancia, conductancia a tierra y capacitancia a tierra, por unidad de longitud, para el conductor "i".

L_{ij}, C_{ij} : inductancia mutua y capacitancia, por unidad de longitud, entre los conductores "i" y "j".

$$\begin{cases} \frac{\partial v_i}{\partial x} = -\sum_{j=1}^n L_{ij} \frac{\partial i_j}{\partial t} - R_i i_i \\ \frac{\partial i_i}{\partial x} = -\sum_{j=1}^n C_{ij} \frac{\partial}{\partial t} (v_i - v_j) - C_i \frac{\partial v_i}{\partial t} - G_i v_i \end{cases}$$

$$\frac{\partial v_i}{\partial x} = -Z_{ij} i_j ; \quad \frac{\partial i_i}{\partial x} = -Y_{ij} v_j$$

⇓

$$\frac{\partial^2 v}{\partial x^2} = \vec{P} v ; \quad \frac{\partial^2 i}{\partial x^2} = \vec{P} i$$

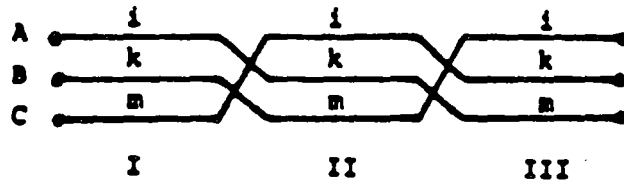
$$\vec{P} = Z Y, \quad \vec{P} = Y Z$$

Transposición de Lineas

$$d = 80 \rightarrow 160 \text{ km}$$

lineas con disposición triangular: 67 km

otras configuraciones: 33 km



- Transposition scheme for single three-phase circuit

$$\frac{1}{3} \begin{bmatrix} Z'_{ii} & Z'_{ik} & Z'_{im} \\ Z'_{ki} & Z'_{kk} & Z'_{km} \\ Z'_{mi} & Z'_{mk} & Z'_{mm} \end{bmatrix} + \begin{bmatrix} Z'_{kk} & Z'_{km} & Z'_{ki} \\ Z'_{mk} & Z'_{mm} & Z'_{mi} \\ Z'_{ik} & Z'_{im} & Z'_{ii} \end{bmatrix} + \begin{bmatrix} Z'_{mm} & Z'_{mi} & Z'_{mk} \\ Z'_{im} & Z'_{ii} & Z'_{ik} \\ Z'_{km} & Z'_{ki} & Z'_{kk} \end{bmatrix} = \begin{bmatrix} Z'_s & Z'_m & Z'_i \\ Z'_m & Z'_s & Z'_i \\ Z'_m & Z'_m & Z'_s \end{bmatrix}$$

with

$$Z'_s = \frac{1}{3} (Z'_{ii} + Z'_{kk} + Z'_{mm})$$

$$Z'_m = \frac{1}{3} (Z'_{ik} + Z'_{km} + Z'_{mi})$$

where Z, Y are square matrices of order n with

$$(r, s)\text{th element of } \bar{Z} = (a + j\omega)M'_{rs}(|\omega|) + R'_{rs}(|\omega|)$$

$$(r, s)\text{th element of } \bar{Y} = (a + j\omega)C'_{rs} + G'_{rs}$$

where $M'_{rs}, R'_{rs}, C'_{rs}, G'_{rs}$ are real.

If the parameter a is set to zero then the equations reduce to those of the steady-state problem at frequency ω . The theory to be developed therefore covers the steady state in which field modal analysis has found many uses e.g. Wedepohl (1965), Wedepohl and Wasley (1965, 1968), Hedman (1965). These authors give detailed treatments of modal analysis in the steady state. Here, however, attention is focused on those aspects necessary for transient analysis. As previously, eqn. 4.1 gives

$$\frac{d^2 \bar{v}}{dx^2} = \bar{P} \bar{v} \quad (4.2)$$

$$\frac{d^2 \bar{i}}{dx^2} = \bar{P} \bar{i} \quad (4.3)$$

where

$$\bar{P} = \bar{Z} \bar{Y}; \quad \bar{P} = \bar{Y} \bar{Z}$$

While \bar{Z}, \bar{Y} are symmetric matrices, \bar{P} is only symmetric in special cases such as the perfectly transposed line of Section 2.3. The general analysis must therefore be developed on the basis that \bar{P} is not symmetric i.e. $\bar{P} \neq \bar{P}$.

The following lemma is basic to the present approach.

Lemma 1. If $S^{-1} \bar{P} S$ is diagonal, then S can be formed from the eigenvectors of \bar{P} , and the elements of the diagonal matrix are the eigenvalues of \bar{P} .

Proof. Suppose that

$$S^{-1} \bar{P} S = \lambda = \text{diag}(\lambda_1, \dots, \lambda_n) \quad (4.4)$$

then

$$\bar{P} S = S \lambda \quad (4.5)$$

and writing S in the form of n columns vectors S_i

$$S = [S_1, S_2, \dots, S_n]$$

eqn. 4.5 gives

$$[\bar{P} S_1, \bar{P} S_2, \dots, \bar{P} S_n] = [\lambda_1 S_1, \lambda_2 S_2, \dots, \lambda_n S_n]$$

so that equating columns

Chapter 4

The theory of natural modes

In Section 2.3 it is shown that the transient behaviour of a perfectly transposed 3-phase line can be discussed in terms of three modes of propagation, each individually satisfying the equations of a single-phase line, whilst the combination satisfies the boundary (or input and output) conditions of the 3-phase line. Two of the modes are aerial in the sense that only in the third is the ground current nonzero.

This elementary example gives a physical interpretation to the common mathematical device of diagonalising a matrix by constructing a modal transformation matrix from its eigenvectors. In that particular situation the mathematical analysis is simplified by the symmetry of the \bar{P} matrix.

In this Chapter the analysis is first extended to deal with the general n -phase line in which \bar{P} is not symmetric but which is uniform in that the same equations apply throughout the length of the line. A computationally efficient 2-port network representation is developed. It is then shown how the basic concepts may be retained when different lines are interconnected to yield a non-uniform system and how these may be cascaded.

4.1 Modal analysis of a uniform n -phase line

In Section 3.1 the modified Fourier transform is used to reduce the partial differential equations of the transient problem to the ordinary differential equations of eqn. 3.17 in the frequency domain. For an n -phase line these may be restated as

$$\frac{d\bar{v}}{dx} = -\bar{Z}\bar{i}; \quad \frac{d\bar{i}}{dx} = -\bar{Y}\bar{v} \quad (4.1)$$

$$\bar{P}S_i = \lambda_i S_i, \quad 1 \leq i \leq n \quad (4.6)$$

Eqn. 4.6 defines the scalars λ_i as the unique eigenvalues of \bar{P} and the column matrices S_i as the corresponding eigenvectors, unique to within a multiplicative constant. The matrix S so constructed is the modal transformation matrix of \bar{P} .

Under the transformation
$$v = S\bar{v}_m \quad (4.7)$$

with S nonsingular, eqn. 4.2 becomes

$$\frac{d^2 \bar{v}_m}{dx^2} = S^{-1} \bar{P} S \bar{v}_m$$

so that if S is now chosen to be the modal transformation matrix of \bar{P}

$$\frac{d^2 \bar{v}_m}{dx^2} = \lambda \bar{v}_m \quad (4.8)$$

i.e. the matrix eqn. 4.2 is reduced to n independent scalar differential equations.

Transposition of eqn. 4.4 yields

$$\tilde{S} \tilde{P} \tilde{S}^{-1} = \tilde{\lambda} = \lambda$$

so that on introducing

$$Q = \tilde{S}^{-1} \quad (4.9)$$

$$Q^{-1} \bar{P} Q = \lambda$$

i.e. Q is seen as the modal transformation matrix of \bar{P} (lemma 1). Hence on setting

$$\bar{i} = Q \bar{i}_m \quad (4.10)$$

eqn. 4.3 reduces to
$$\frac{d^2 \bar{i}_m}{dx^2} = Q^{-1} \bar{P} Q \bar{i}_m = \lambda \bar{i}_m \quad (4.11)$$

again representing n independent scalar differential equations.

As in the case of the perfectly transposed line of Section 2.3 the elements of \bar{v}_m, \bar{i}_m are the components of the modes of propagation. To show that these modes act independently it is necessary to show that the two equations of eqn. 4.1 each transform into n scalar differential equations in the same variables. Under the transformations of eqns. 4.7 and 4.10, eqn. 4.1 becomes

$$\frac{d\bar{v}_m}{dx} = -(S^{-1} \bar{Z} Q) \bar{i}_m = -\bar{Z}_m \bar{i}_m, \text{ say} \quad (4.12)$$

$$\frac{d\bar{i}_m}{dx} = -(Q^{-1} \bar{Y} S) \bar{v}_m = -\bar{Y}_m \bar{v}_m, \text{ say} \quad (4.13)$$

so that it is necessary to show that \bar{Z}_m, \bar{Y}_m are both diagonal matrices.

To this end it is noted that from eqn. 4.4

$$\lambda = S^{-1} \bar{P} S = S^{-1} \bar{Z} \bar{Y} S = (S^{-1} \bar{Z} Q)(Q^{-1} \bar{Y} S) = \bar{Z}_m \bar{Y}_m$$

and from eqn. 4.9

$$\lambda = Q^{-1} \bar{P} Q = Q^{-1} \bar{Y} \bar{Z} Q = (Q^{-1} \bar{Y} S)(S^{-1} \bar{Z} Q) = \bar{Y}_m \bar{Z}_m$$

i.e.

$$\bar{Z}_m \bar{Y}_m = \bar{Y}_m \bar{Z}_m = \lambda \quad (4.14)$$

The conditions under which eqn. 4.14 implies that \bar{Z}_m, \bar{Y}_m are themselves diagonal are given in the following lemma:-

Lemma 2. If

$$AB = BA = \lambda = \text{diag}(\lambda_1, \lambda_2, \dots, \lambda_n) \quad (4.15)$$

where $\lambda_i \neq \lambda_j$ for $i \neq j$ and B is nonsingular, then A, B are diagonal.

Proof. Let $B^{-1} = C$ so that eqn. 4.15 becomes

$$A = \lambda C = C \lambda; \quad (4.16)$$

on writing C in the form of row and column vectors as

$$C = \begin{bmatrix} C_1 \\ C_2 \\ \vdots \\ C_n \end{bmatrix} = [C'_1, C'_2, \dots, C'_n]$$

substitution for λ in eqn. 4.16 yields

$$\lambda C = \begin{bmatrix} \lambda_1 C_1 \\ \lambda_2 C_2 \\ \vdots \\ \lambda_n C_n \end{bmatrix} = [\lambda_1 C'_1, \lambda_2 C'_2, \dots, \lambda_n C'_n] = C \lambda$$

Equating the (i, j) th element in the square matrix gives

$$\lambda_i C_{ij} = \lambda_j C_{ij}$$

so that if $\lambda_i \neq \lambda_j$ for $i \neq j$ it follows that $C_{ij} = 0$ and C is diagonal. Hence B, A are diagonal.

In eqn. 4.14 the diagonal elements of λ are the eigenvalues of \bar{P} . These are distinct in all except those special cases, such as the perfectly transposed line, where other properties yield the same result.

Thus it is apparent that, as in the case of the perfectly transposed line, the behaviour of any uniform line can be discussed in terms of independent modes of propagation. Again from eqns. 4.7 and 4.10 the distribution between the phases of voltage and current within each mode is the same throughout the line but now, since in general $Q \neq S$, the distribution of voltage in a given mode is not the same as that of the current in the same mode.

If the i th elements of $\bar{v}_m, \bar{i}_m, \bar{Z}_m, \bar{Y}_m, \lambda$ are denoted by $\bar{v}_{mi}, \bar{i}_{mi}, \bar{z}_{mi}, \bar{y}_{mi}, \lambda_i$ the behaviour of the magnitude of the i th mode is given by the scalar equations

$$\frac{d\bar{v}_{mi}}{dx} = -\bar{z}_{mi}\bar{i}_{mi}; \quad \frac{d\bar{i}_{mi}}{dx} = -\bar{y}_{mi}\bar{v}_{mi}$$

$$\frac{d^2\bar{v}_{mi}}{dx^2} = \lambda_i\bar{v}_{mi}; \quad \frac{d^2\bar{i}_{mi}}{dx^2} = \lambda_i\bar{i}_{mi}$$

with

$$\lambda_i = \bar{z}_{mi}\bar{y}_{mi}$$

and so may be interpreted as the steady-state behaviour in a notional single-phase line with series impedance \bar{z}_{mi} and shunt admittance \bar{y}_{mi} .

If

$$\lambda_i = \gamma_i^2$$

and

$$\gamma_i = \alpha_i + j\beta_i$$

with α_i, β_i real and $\alpha_i > 0$, it follows that both $\bar{v}_{mi}, \bar{i}_{mi}$ are of the form

$$A \exp(-\alpha_i x) \exp(-j\beta_i x) + B \exp(\alpha_i x) \exp(j\beta_i x) \quad (4.17)$$

Let $A^*(x) = A \exp(-\alpha_i x) \exp(-j\beta_i x)$ then $A^*(x)$ gives the magnitude and phase of a sinusoidal wave at the point x . At the point $x + x_0$

$$A^*(x + x_0) = A^*(x) \exp(-\alpha_i x_0) \exp(-j\beta_i x_0)$$

so that the wave has undergone an attenuation $\alpha_i x_0$ and experienced a further phase shift of $\beta_i x_0$. This means that its peak is delayed by a time $\beta_i x_0 / \omega$, and in this sense the wave has travelled forward with a propagation velocity $u = \omega / \beta_i$. Similarly, the remaining term in eqn. 4.17 can be interpreted as a backward travelling wave with the same attenuation and propagation velocity. It is convenient to refer to β_i as the velocity factor and the combination $\alpha_i + j\beta_i = \gamma_i$ as the propagation constant for the mode. It will be recognised as the steady-state equivalent of the parameter k used in Section 2.2 for a single-phase line.

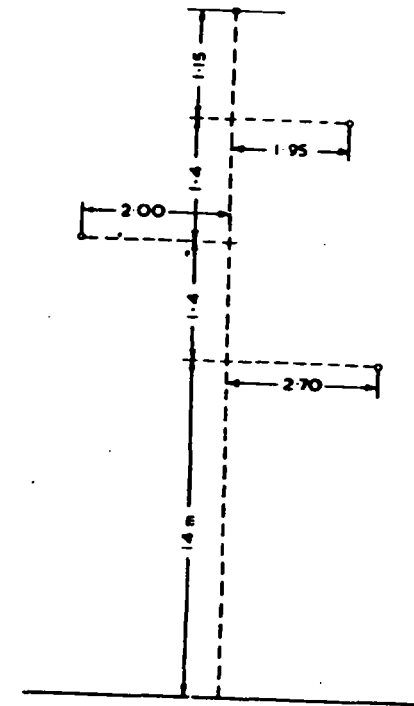


Fig. 4.1 Configuration of Bodio-Cunardo line
Conductor 7/5.2 mm Al
Earth wire 7/2.67 mm steel
Mean sag, 6 m

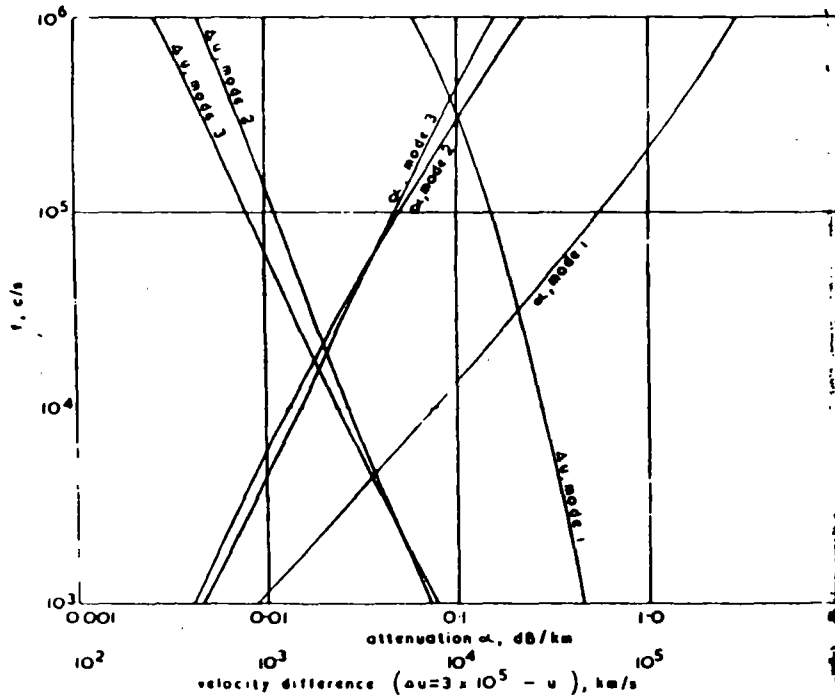
It should perhaps be noted that, since the parameters of the original line are frequency dependent, and additionally the use of the modified Fourier transform introduces the parameter a , the A, B, α_i, β_i in eqn. 4.17 are complicated functions of $a, \omega, |\omega|$. If however a is set to zero all the equations in transform space are identical with the steady-state equations at the fixed frequency ω . Then the α_i, β_i do in fact represent the attenuation and velocity factor for the i th mode of a sinusoidal voltage of frequency ω in the original line. For the line having the configuration shown in Fig. 4.1 with the following constants

Conductor resistivity	$3.21 \times 10^{-8} \Omega m$
Earth wire resistivity	$20 \times 10^{-8} \Omega m$
Earth resistivity	$100 \Omega m$
Relative permeability of earth wire	10^3

Galloway *et al.* (1964) give the modal distribution and propagation constants at 100 kHz shown in Table 4.1.

Table 4.1 Calculated mode-distribution vectors and propagation constants

Mode number	Mode-distribution vectors		Attenuation dB/km	Velocity km/s
	Voltage	Current		
1	0.291 - j0.002	1.489 + j0.044	0.559	284 550
	0.257 - j0.005	1.306 + j0.014		
	0.231 - j0.005	1.000 + j0.000		
2	0.092 - j0.127	3.581 - j0.495	0.0498	298 850
	-0.127 - j0.015	-4.956 + j0.515		
	0.028 + j0.006	1.000 + j0.000		
3	-0.383 - j0.006	-0.605 - j0.010	0.0480	299 180
	-0.130 + j0.021	-0.213 + j0.024		
	0.741 + j0.000	1.000 + j0.000		



Mode parameters for Bodio-Cunardo line

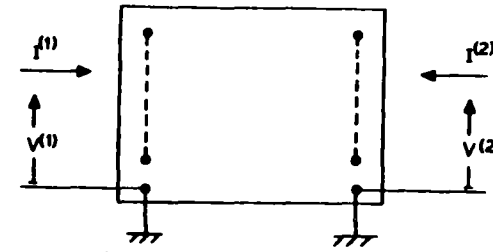


Fig. 4.3 2-port network representation of multiphase line

Since the velocity approaches that of light $c_0 (= 3 \times 10^5 \text{ km/s})$ it is convenient to display the variation in modal velocity u in terms of the velocity difference $\Delta u = c_0 - u$. The variation in this and the attenuation with frequency are displayed for the three modes in Fig. 4.2. The similarity of the three modes to the ground and aerial modes discussed in Section 2.3 should be noted. The same authors showed the close agreement between measured and calculated values of attenuation.

4.2 The uniform line as a 2-port network

The modal equations in transform space, viz. eqns. 4.8, 4.11, 4.12 and 4.13 are conveniently solved by viewing the line as a 2-port network with modal input current and voltages $I_m^{(1)}, \bar{V}_m^{(1)}$ at $x = 0$ and $I_m^{(2)}, \bar{V}_m^{(2)}$ at the other end, say $x = l$ as illustrated in Fig. 4.3.

From eqn. 4.11, with $\lambda = \gamma^2$, it follows that

$$\bar{i}_m = [\text{sh} \gamma x] K_1 + [\text{ch} \gamma x] K_2$$

where K_1, K_2 are column matrices arising from the constants of integration, and eqn. 4.13 then yields, on using eqn. 4.14

$$v_m = \bar{Z}_m \gamma^{-1} \{ [\text{ch} \gamma x] K_1 + [\text{sh} \gamma x] K_2 \}$$

The input conditions at $x = 0$ then give

$$I_m^{(1)} = K_2$$

$$\bar{V}_m^{(1)} = -\bar{Z}_m \gamma^{-1} K_1$$

and at $x = l$

$$-I_m^{(2)} = [\text{sh} \gamma l] K_1 + [\text{ch} \gamma l] K_2$$

$$\bar{V}_m^{(2)} = -\bar{Z}_m \gamma^{-1} \{ [\text{ch} \gamma l] K_1 + [\text{sh} \gamma l] K_2 \}$$

On noting that \bar{Z}_m, γ and the matrices arising from the sh or ch terms are diagonal, and eliminating the unknown matrices K_1, K_2

result can be expressed as

$$\begin{bmatrix} I_m^{(1)} \\ I_m^{(2)} \end{bmatrix} = \begin{bmatrix} A_m & -B_m \\ -B_m & A_m \end{bmatrix} \begin{bmatrix} \bar{V}_m^{(1)} \\ \bar{V}_m^{(2)} \end{bmatrix} \quad (4.18)$$

where

$$A_m = \bar{Z}_m^{-1} \gamma [\coth \gamma l]$$

$$B_m = \bar{Z}_m^{-1} \gamma [\operatorname{cosech} \gamma l]$$

with A_m, B_m diagonal matrices.

On transforming to phase quantities with $\bar{I} = Q I_m$, $\bar{V} = S \bar{V}_m$ eqn. 4.18 becomes

$$\begin{bmatrix} I^{(1)} \\ I^{(2)} \end{bmatrix} = \begin{bmatrix} A & -B \\ -B & A \end{bmatrix} \begin{bmatrix} \bar{V}^{(1)} \\ \bar{V}^{(2)} \end{bmatrix} \quad (4.19)$$

with, after some manipulation and introducing

$$\Psi = S \gamma S^{-1}$$

$$\bar{Y}_0 = \bar{Z}^{-1} S \gamma S^{-1},$$

$$Q A_m S^{-1} = A = \bar{Y}_0 [\coth \Psi l] \quad (4.20)$$

$$Q B_m S^{-1} = B = \bar{Y}_0 [\operatorname{cosech} \Psi l] \quad (4.21)$$

the square matrix in eqn. 4.19 is known as the nodal admittance matrix. It should be noted that since A_m, B_m are diagonal and $Q = \bar{S}^{-1}$

$$\tilde{A} = \tilde{S}^{-1} A_m \tilde{Q} = Q A_m S^{-1} = A$$

i.e. A, B are symmetric matrices of order n .

4.3 Example

As a very simple example, first pole closure of a source on to an open circuit 3-phase line is considered, as illustrated in Fig. 4.4. When the sub-conductors are bundled and the earth wire is eliminated, the series impedance and shunt admittance are known functions of $|\omega|$. Hence by choosing the parameter a in the modified Fourier transform as suggested in Section 3.4

$$\bar{P} = \bar{Z} \bar{Y}$$

is computed at any chosen ω . The eigenvalues and eigenvectors are then found. Of the several standard methods available that suggested by Galloway *et al.* (1964) has proved reliable. It is based on a root-squaring technique which has been improved to separate nearly equal eigenvalues

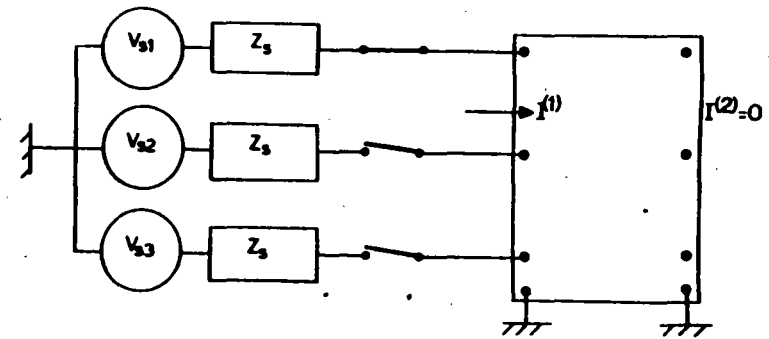


Fig. 4.4 First pole closure on 3-phase line

as outlined in Section 4.4.

The sub-matrices A, B in eqn. 4.19, viz.

$$\begin{bmatrix} I^{(1)} \\ I^{(2)} \end{bmatrix} = \begin{bmatrix} A & -B \\ -B & A \end{bmatrix} \begin{bmatrix} \bar{V}^{(1)} \\ \bar{V}^{(2)} \end{bmatrix} \quad (4.19)$$

are computed using eqns. 4.20, 4.21.

The end-point conditions of the problem may be expressed as

$$I^{(2)} = 0 \quad (4.22)$$

$$I^{(1)} = \begin{bmatrix} \bar{V}_{s1} \bar{Z}_s^{-1} \\ 0 \\ 0 \end{bmatrix} - F \bar{V}^{(1)} \quad (4.23)$$

where

$$F = \begin{bmatrix} \bar{Z}_s^{-1} & 0 & 0 \\ 0 & 0 & 0 \\ 0 & 0 & 0 \end{bmatrix}$$

Elimination of $I^{(1)}, I^{(2)}, \bar{V}^{(1)}$ from eqns. 4.19, 4.22 and 4.23 yields

$$[(F + A)B^{-1}A - B] \bar{V}^{(2)} = \begin{bmatrix} \bar{V}_{s1} \bar{Z}_s^{-1} \\ 0 \\ 0 \end{bmatrix}$$

from which $\bar{V}^{(2)}$ at the chosen frequency follows.

This process is repeated at a sufficient number of frequencies to permit inversion to the time domain as described in Section 3.4. In

carrying out the computation, the hyperbolic terms appearing in the nodal admittance matrix should be formulated in terms of exponentials with negative exponents, in order to avoid overflow in the computer.

The understanding of the results is sometimes aided by consideration of the contributions of the individual modes of propagation. In this event it is necessary to find the contributions first in transform space and invert each separately.

4.4 Eigenvalues, -vectors of the matrix \bar{P} .

Standard methods for finding the eigenvalues, and eigenvectors of a matrix require the eigenvalues to be well separated. In the \bar{P} matrix such separation arises solely from the finite conductivity of the ground and Galloway *et al.* (1964) showed that for computational purposes the separation may be increased by expressing the matrix $Z(\omega)$ in the form

$$Z(\omega) = R_c(|\omega|) + R_g(|\omega|) + j\omega\{L_c(|\omega|) + L_g(|\omega|) + L_0\} \quad (4.24)$$

where subscript c denotes the conductor internal impedances, subscript g those arising from the lossy ground (i.e. from the integral in eqns. 2.24 and 2.25) and subscript zero the external inductance with a loss-free ground.

Then it is well known that

$$L_0 C = \mu_0 \epsilon_0 U$$

so that

$$\bar{Z}_0 \bar{Y} = (a + j\omega)^2 \mu_0 \epsilon_0 U \quad (4.25)$$

where U is the unit diagonal matrix, and writing

$$\bar{Z} = \bar{Z}_c + \bar{Z}_g + \bar{Z}_0$$

the matrix \bar{P} becomes

$$\bar{P} = \bar{Z} \bar{Y} = (\bar{Z}_c + \bar{Z}_g) \bar{Y} + (a + j\omega)^2 \mu_0 \epsilon_0 U \quad (4.26)$$

It is apparent that the eigenvectors of \bar{P} are the eigenvectors of $(\bar{Z}_c + \bar{Z}_g) \bar{Y}$, whilst the eigenvalues differ by $(a + j\omega)^2 \mu_0 \epsilon_0$. Hence if the eigenvalues of $(\bar{Z}_c + \bar{Z}_g) \bar{Y}$ are Λ_i then

$$\lambda_i = \Lambda_i + (a + j\omega)^2 \mu_0 \epsilon_0 \quad (4.27)$$

and the Λ_i/Λ_j are better separated than the λ_i/λ_j and are more readily computed.

The matrix product $(\bar{Z}_c + \bar{Z}_g) \bar{Y}$ is dependent on frequency so that it is necessary to find the eigenvalues, and eigenvectors at each

frequency. However, Paul (1975) has pointed out that, for a horizontal line configuration, all the elements of $R_g(|\omega|)$ and of $L_g(|\omega|)$ are approximately equal. Making the assumption of equality the matrix \bar{Z}_g may be written

$$\bar{Z}_g = z_g(a + j\omega, |\omega|) N \quad (4.28)$$

where N is a square matrix in which every element is unity and $z_g(a + j\omega, |\omega|)$ is a scalar. Then on setting \bar{Z}_c to zero, eqn. 4.26 gives

$$\begin{aligned} \lambda &= z_g S^{-1} N \bar{Y} S + (a + j\omega)^2 \mu_0 \epsilon_0 U \\ &= z_g \Lambda + (a + j\omega)^2 \mu_0 \epsilon_0 U \end{aligned} \quad (4.29)$$

where now $(N \bar{Y})$ is independent of frequency so that its eigenvalues and eigenvectors need be calculated once only.

To a poorer degree of approximation, but one which still retains the main features of the frequency dependent parameters, the same idea could be applied to other line configurations. Of course, in such cases the elements of the matrix N in eqn. 4.28 would no longer be unity.

4.5 Interconnection of 2-port networks

In Section 4.2 the nodal admittance matrix of a uniform n -phase line is derived as

$$\begin{bmatrix} A & -B \\ -B & A \end{bmatrix}$$

with A, B symmetric matrices of order n . When a number of different lines are connected in series, and the nonuniform combination is regarded as a 2-port network, then the nodal admittance matrix takes the more complicated form common to all linear passive networks,

$$\begin{bmatrix} A & -B \\ -\tilde{B} & C \end{bmatrix} \quad (4.30)$$

However A, C are still symmetric matrices, thus retaining the symmetry of the whole matrix.

In cascading a number of such nonuniform combinations it is usual to express the 2-port equations in the form

$$\begin{bmatrix} V^{(1)} \\ I^{(1)} \end{bmatrix} = T \begin{bmatrix} V^{(2)} \\ -I^{(2)} \end{bmatrix} \quad (4.31)$$

where the transfer or chain matrix T is readily shown to be

$$T = \begin{bmatrix} \tilde{B}^{-1}C & \tilde{B}^{-1} \\ A\tilde{B}^{-1}C-B & A\tilde{B}^{-1} \end{bmatrix} \quad (4.32)$$

The output from each 2-port network is the input to the succeeding one so that the overall transfer matrix is the product of the transfer matrices of the separate 2-port networks taken in the order in which they are cascaded.

In crossbonded cable systems each major section, comprising a complete sequence of transpositions, is nonuniform, and accordingly has a nodal admittance matrix of the form given in eqn. 4.30, and systems generally contain a very large number of such major sections. Wedepohl and Indulkar (1974) found that computation based on classical methods of analysis is prohibitively long. For the same reason the lattice approach for solving the problem directly in the time domain is impracticable. However it should be noted that the transfer matrix T of eqn. 4.32 has the property that the inverse of its transpose contains the same submatrices as T , i.e.

$$\tilde{T}^{-1} = \begin{bmatrix} A\tilde{B}^{-1} & B-A\tilde{B}^{-1}C \\ -\tilde{B}^{-1} & \tilde{B}^{-1}C \end{bmatrix} \quad (4.33)$$

Hence \tilde{T}^{-1} can be obtained from T by an elementary transformation represented in this case by a matrix K defined by

$$K = \begin{bmatrix} O & U \\ -U & O \end{bmatrix}; \quad K^{-1} = \tilde{K} \quad (4.34)$$

in which all the submatrices are of order $n \times n$ and U is the unit diagonal matrix and O the zero matrix. It is readily shown that

$$\begin{aligned} \tilde{T}^{-1}K &= KT \\ \text{or} \quad K^{-1}\tilde{T}^{-1}K &= T \end{aligned} \quad (4.35)$$

If Q is the modal transformation matrix of T and if the resulting $2n \times 2n$ diagonal matrix of eigenvalues is expressed in terms of two $n \times n$ diagonal submatrices, then T may be written as

$$T = Q \begin{bmatrix} \lambda_1 & O \\ O & \lambda_2 \end{bmatrix} Q^{-1}$$

with λ_1 containing the n eigenvalues with the largest moduli. It follows that

$$\tilde{T}^{-1} = \tilde{Q}^{-1} \begin{bmatrix} \lambda_1^{-1} & O \\ O & \lambda_2^{-1} \end{bmatrix} \tilde{Q}$$

and, on noting that

$$K^{-1} \begin{bmatrix} \lambda_1^{-1} & O \\ O & \lambda_2^{-1} \end{bmatrix} K = \begin{bmatrix} \lambda_2^{-1} & O \\ O & \lambda_1^{-1} \end{bmatrix}$$

eqn. 4.35 gives

$$\begin{aligned} T &= K^{-1}\tilde{T}^{-1}K = K^{-1}\tilde{Q}^{-1}KK^{-1} \begin{bmatrix} \lambda_1^{-1} & O \\ O & \lambda_2^{-1} \end{bmatrix} KK^{-1}\tilde{Q}K \\ &= (K^{-1}\tilde{Q}^{-1}K) \begin{bmatrix} \lambda_2^{-1} & O \\ O & \lambda_1^{-1} \end{bmatrix} (K^{-1}\tilde{Q}^{-1}K)^{-1} \end{aligned} \quad (4.36)$$

which is a second diagonalisation of T . Accordingly, on using lemma 1, the diagonal matrix $\text{diag}(\lambda_2^{-1}, \lambda_1^{-1})$ contains all the eigenvalues of T i.e. all the elements of $\text{diag}(\lambda_1, \lambda_2)$. Hence the eigenvalues occur in reciprocal pairs and since λ_1 contains the n eigenvalues with the largest moduli, λ_2 contains their reciprocals. If the eigenvalues are ordered in both λ_1, λ_2 according to the magnitude of their moduli then it follows that

$$\lambda_2 = \lambda_1^{-1} \quad (4.37)$$

By construction, λ_1 contains the n eigenvalues with the largest moduli, so that the first n columns of Q are the corresponding eigenvectors. If the remaining n columns of Q could be computed in terms of the eigenvalues in λ_1 , then a highly efficient computational process would result. To this end it is noted that the modal transformation matrix used so far is composed of column eigenvectors satisfying

$$Tx_1 = \lambda_1 x_1$$

and leading to

$$Q^{-1}TQ = \lambda$$

However the row eigenvectors satisfying

$$y_1 T = \lambda_1 y_1$$

lead to a transformation matrix S whose rows are the y_1 and for which

$$STS^{-1} = \lambda$$

Since the y_1 are indeterminate to within a multiplicative constant it is possible to choose S as Q^{-1} . Using lemma 1 on eqn. 4.36, $(K^{-1}\tilde{Q}^{-1}K)$

is seen as a modal transformation matrix of T and since Q is defined as such a matrix the columns of $(K^{-1}\tilde{Q}^{-1}K)$ and Q must be equal to within a multiplicative constant, i.e.

$$K^{-1}\tilde{Q}^{-1}K = QD$$

where D is some diagonal matrix. Then, writing

$$Q = \begin{bmatrix} Q_{11} & Q_{12} \\ Q_{21} & Q_{22} \end{bmatrix}; \quad S = \begin{bmatrix} S_{11} & S_{12} \\ S_{21} & S_{22} \end{bmatrix}; \quad D = \begin{bmatrix} D_1 & 0 \\ 0 & D_2 \end{bmatrix}$$

where $\{Q_{11}, Q_{21}\}$ and $\{S_{11}, S_{12}\}$ are the n column and row eigenvectors associated with the eigenvalues in λ_1 , it is readily shown that

$$\tilde{Q}^{-1} = \begin{bmatrix} Q_{22}D_2 & -Q_{21}D_1 \\ -Q_{12}D_2 & Q_{11}D_1 \end{bmatrix} \quad (4.38)$$

Hence, on using

$$S = Q^{-1} \quad (4.39)$$

and identifying corresponding submatrices, there results

$$\begin{bmatrix} Q_{12} \\ Q_{22} \end{bmatrix} = \begin{bmatrix} -\tilde{S}_{12} \\ \tilde{S}_{11} \end{bmatrix} D_2^{-1}$$

Since the eigenvectors are indeterminate to within a multiplicative constant, the modal transformation matrix may be written as

$$Q = \begin{bmatrix} Q_{11} & -\tilde{S}_{12} \\ Q_{21} & \tilde{S}_{11} \end{bmatrix} \quad (4.40)$$

i.e. entirely in terms of the column and row eigenvectors associated with the eigenvalues in λ_1 . As pointed out by Wedepohl and Indulkar (1974), this is not only computationally efficient but has the following advantage.

The eigenvalues are ordered

$$|\lambda_1| > |\lambda_2| > \dots > |\lambda_n| > 1 > |\lambda_n^{-1}| > \dots > |\lambda_1^{-1}|$$

so that the range is $|\lambda_1|^2$. In crossbonded cable systems this range is so large that numerical instabilities occur. In the above method the range is reduced to $|\lambda_1/\lambda_n| (< |\lambda_1|)$ and thus these instabilities are avoided. For an illuminating discussion on the significance of the ratio of the highest to the lowest moduli of the eigenvalues (the condition number) Lanzcos (1961).

her, from eqns. 4.38 and 4.39 it follows that

$$S_{21} = -D_1\tilde{Q}_{21}; \quad S_{22} = D_1\tilde{Q}_{11}$$

so that S may be written

$$S = \begin{bmatrix} S_{11} & S_{12} \\ -D_1\tilde{Q}_{21} & D_1\tilde{Q}_{11} \end{bmatrix}$$

and

$$SQ = \begin{bmatrix} S_{11}Q_{11} + S_{12}Q_{21} & -S_{11}\tilde{S}_{12} + S_{12}\tilde{S}_{11} \\ D(\tilde{Q}_{11}Q_{21} - \tilde{Q}_{21}Q_{11}) & D(\tilde{Q}_{11}\tilde{S}_{11} + \tilde{Q}_{21}\tilde{S}_{12}) \end{bmatrix}$$

$$= U, \text{ from eqn. 4.39.}$$

By construction

$$\begin{bmatrix} S_{11} & S_{12} \end{bmatrix} \begin{bmatrix} Q_{11} \\ Q_{21} \end{bmatrix} = S_{11}Q_{11} + S_{12}Q_{21} = U$$

so that for $D(\tilde{Q}_{11}\tilde{S}_{11} + \tilde{Q}_{21}\tilde{S}_{12})$ to be equal to U it is necessary that $D = U$ and hence S' reduces to

$$S = \begin{bmatrix} S_{11} & S_{12} \\ -\tilde{Q}_{21} & \tilde{Q}_{11} \end{bmatrix} \quad (4.41)$$

and $S(=Q^{-1})$ is obtained without additional computation.

When n identical 2-port networks are cascaded the overall transfer matrix may be expressed as

$$T^n = (Q\lambda Q^{-1})^n = Q\lambda^n S = \begin{bmatrix} T_{11} & T_{12} \\ T_{21} & T_{22} \end{bmatrix} \quad (4.42)$$

where

$$\left. \begin{aligned} T_{11} &= Q_{11}\lambda_1^n S_{11} + \tilde{S}_{12}\lambda_1^{-n}\tilde{Q}_{21} \\ T_{12} &= Q_{11}\lambda_1^n S_{12} - \tilde{S}_{12}\lambda_1^{-n}\tilde{Q}_{11} \\ T_{21} &= Q_{21}\lambda_1^n S_{11} - \tilde{S}_{11}\lambda_1^{-n}Q_{21} \\ T_{22} &= Q_{21}\lambda_1^n S_{12} + \tilde{S}_{11}\lambda_1^{-n}\tilde{Q}_{11} \end{aligned} \right\} \quad (4.43)$$

on using eqns. 4.37, 4.40 and 4.41.

However in crossbonded cable systems it is impracticable to achieve realistic results because the dominant eigenvalue in λ_1^n swamps all others although this mode has the greatest attenuation and contributes least to the transfer of energy. Accordingly, Wedepohl and Indulkar (1974) form the nodal admittance matrix of the n -fold cascade from the transfer matrix of eqn. 4.42. Since the cascade is a passive network, the nodal admittance matrix involves only three matrices A_n, B_n, C_n say, and elementary analysis gives the matrix as

The theory of natural modes

$$\begin{bmatrix} A_n & -B_n \\ -\tilde{B}_n & C_n \end{bmatrix} = \begin{bmatrix} T_{22}T_{12}^{-1} & -(T_{22}T_{12}^{-1}T_{11} - T_{21}) \\ -T_{12}^{-1} & T_{12}^{-1}T_{11} \end{bmatrix} \quad (4.44)$$

Use of eqn. 4.43 together with some manipulation yields

$$\begin{aligned} A_n &= [Q_{21}Q_{11}^{-1} + \tilde{S}_{11}\lambda_1^{-n}\tilde{Q}_{11}S_{12}^{-1}\lambda_1^{-n}Q_{11}^{-1}] \times [U - \tilde{S}_{12}\lambda_1^{-n}\tilde{Q}_{11}S_{12}^{-1}\lambda_1^{-n}Q_{11}^{-1}]^{-1} \\ \tilde{B}_n &= S_{12}^{-1}\lambda_1^{-n}Q_{11}^{-1} [U - \tilde{S}_{12}\lambda_1^{-n}\tilde{Q}_{11}S_{12}^{-1}\lambda_1^{-n}Q_{11}^{-1}]^{-1} \quad (4.45) \\ C_n &= [S_{11}^{-1}S_{12} - S_{11}^{-1}\lambda_1^{-n}Q_{11}^{-1}\tilde{S}_{12}\lambda_1^{-n}\tilde{Q}_{11}]^{-1} \\ &\quad \times [U + S_{11}^{-1}\lambda_1^{-n}Q_{11}^{-1}\tilde{S}_{12}\lambda_1^{-n}\tilde{Q}_{11}] \end{aligned}$$

Since these equations involve only λ_1^{-n} the low loss modes receive greatest prominence and the numerical difficulties disappear.

$$-\left[\frac{dV_{\text{phase}}}{dx}\right] = \begin{bmatrix} Z'_s & Z'_m & Z'_m \\ Z'_m & Z'_s & Z'_m \\ Z'_m & Z'_m & Z'_s \end{bmatrix} [I_{\text{phase}}]$$

↓ $\alpha, \beta, 0$

$$-\begin{bmatrix} dV_0/dx \\ dV_\alpha/dx \\ dV_\beta/dx \end{bmatrix} = \begin{bmatrix} Z'_s + 2Z'_m & 0 & 0 \\ 0 & Z'_s - Z'_m & 0 \\ 0 & 0 & Z'_s - Z'_m \end{bmatrix} \begin{bmatrix} I_0 \\ I_\alpha \\ I_\beta \end{bmatrix}$$

$$Z'_{\text{zero}} = Z'_s + 2Z'_m$$

$$Z'_{\text{pos}} = Z'_s - Z'_m$$

↓

$$-dV_{\text{zero}}/dx = Z'_{\text{zero}} I_{\text{zero}}$$

$$-dV_\alpha/dx = Z'_{\text{pos}} I_\alpha$$

$$-dV_\beta/dx = Z'_{\text{pos}} I_\beta$$

$$[v_{\text{OAB}}] = [T]^{-1} [v_{\text{phase}}]$$

$$[i_{\text{OAB}}] = [T]^{-1} [i_{\text{phase}}]$$

$$[T] = \frac{1}{\sqrt{3}} \begin{bmatrix} 1 & \sqrt{2} & 0 \\ 1 & -\frac{1}{\sqrt{2}} & \frac{\sqrt{3}}{\sqrt{2}} \\ 1 & -\frac{1}{\sqrt{2}} & -\frac{\sqrt{3}}{\sqrt{2}} \end{bmatrix} \quad \text{and} \quad [T]^{-1} = \frac{1}{\sqrt{3}} \begin{bmatrix} 1 & 1 & 1 \\ \sqrt{2} & -\frac{1}{\sqrt{2}} & -\frac{1}{\sqrt{2}} \\ 0 & \frac{\sqrt{3}}{\sqrt{2}} & -\frac{\sqrt{3}}{\sqrt{2}} \end{bmatrix}$$

$$\begin{bmatrix} z_{1, \text{pos}} \\ \vdots \\ z_{2, \text{pos}} \\ \vdots \\ z_{n, \text{pos}} \\ \vdots \\ z_{1, \text{zero}} \\ \vdots \\ z_{m, \text{zero}} \end{bmatrix}$$



$$\begin{bmatrix} 1 & 1 & 1 & 1 & 1 & 1 & 1 & 1 \\ -1 & -1 & -1 & -1 & -1 & -1 & -1 & -1 \\ 0 & 0 & 0 & 0 & 0 & 0 & 0 & 0 \\ 0 & \sqrt{3} & \sqrt{3} & \sqrt{3} & \sqrt{3} & \sqrt{3} & \sqrt{3} & \sqrt{3} \\ 0 & 0 & 0 & 0 & 0 & 0 & 0 & 0 \\ 0 & 0 & -2 & 0 & 0 & 0 & 0 & 0 \\ 0 & 0 & 0 & 1 & -\sqrt{3} & 1 & -\sqrt{3} & 1 \\ 0 & 0 & 0 & 0 & 0 & 1 & 0 & 0 \\ 0 & 0 & 0 & 0 & 0 & 0 & 1 & 0 \end{bmatrix}$$

$$[Z]^{-1} = \frac{1}{\sqrt{6}} [Z]$$

$$z_{1, \text{pos}} - z_{1, \text{zero}} = z_{1, \text{pos}}$$

$$z_{2, \text{zero}} + (M-1)z_{2, \text{pos}} = z_{2, \text{zero}}$$

$$[Z]^{-1} = [Z]$$

where again

$$\begin{bmatrix} \frac{1}{\sqrt{M}} & 0 & 0 & \dots & 0 & 0 & \dots & \frac{1}{\sqrt{M}} \\ \vdots & \vdots & \vdots & \vdots & \vdots & \vdots & \vdots & \vdots \\ 0 & \frac{(1-j)(1-j)}{(1-j)} & \dots & \dots & \dots & \dots & \dots & 0 \\ \vdots & \vdots & \vdots & \vdots & \vdots & \vdots & \vdots & \vdots \\ \frac{1}{\sqrt{M}} & \frac{1}{\sqrt{2}} & \frac{1}{\sqrt{2}} & \dots & \frac{1}{\sqrt{2}} & \frac{1}{\sqrt{2}} & \dots & \frac{1}{\sqrt{M}} \\ \vdots & \vdots & \vdots & \vdots & \vdots & \vdots & \vdots & \vdots \\ \frac{1}{\sqrt{M}} & \frac{1}{\sqrt{2}} & \frac{1}{\sqrt{2}} & \dots & \frac{1}{\sqrt{2}} & \frac{1}{\sqrt{2}} & \dots & \frac{1}{\sqrt{M}} \end{bmatrix} = [Z]$$

J-th col.

J-th row

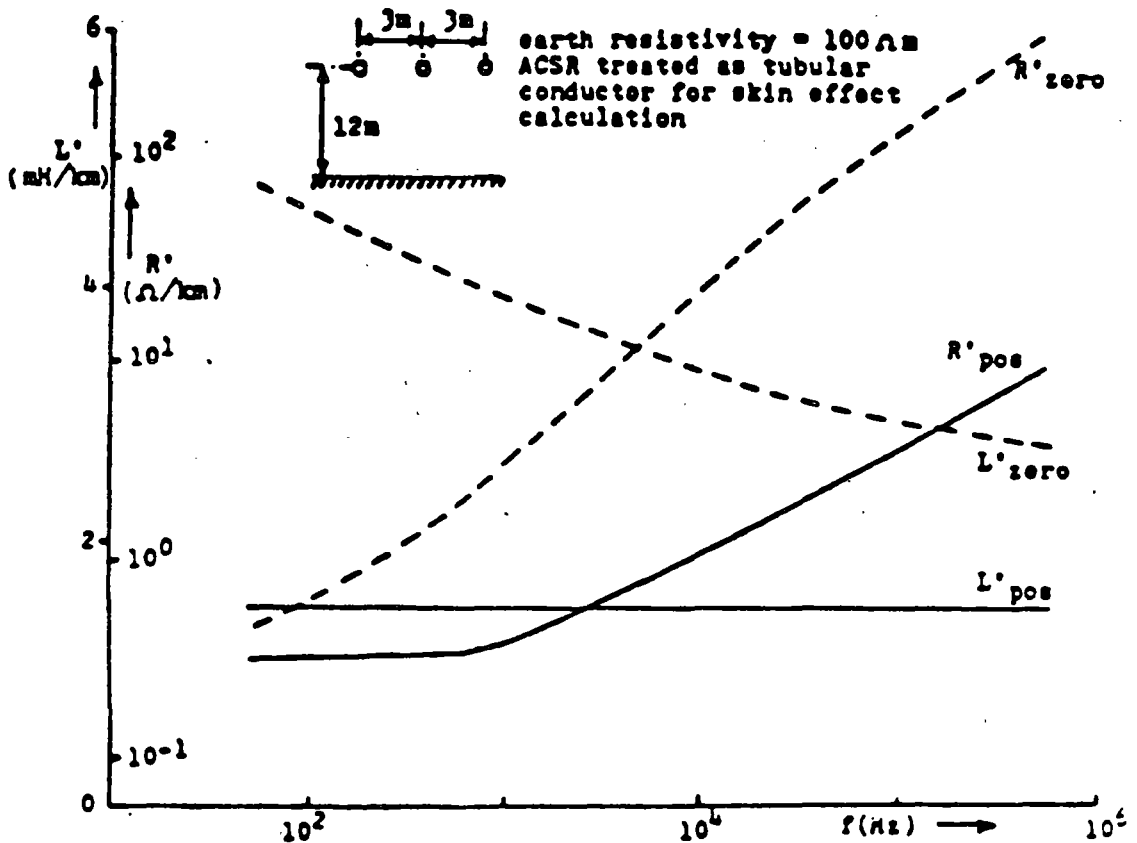
transformator ...

$$Z_{pos} = R_{pos}(\omega) + j\omega L_{pos}(\omega)$$

$$= Z_s - Z_m$$

$$Z_{zero} = R_{zero}(\omega) + j\omega L_{zero}(\omega)$$

$$= Z_s + 2Z_m$$



Positive and zero sequence resistance and inductance of a three-phase line

Conductividad Finita del terreno

Teoría de Imágenes Complejas

Fórmula de Carson

$$\bar{d} = \frac{2}{\sqrt{j\omega\mu_0\sigma_e}}$$

$$Z_{ii} = R_{int} + j\omega(L' + L_{int})$$

$$Z_{int} = \frac{\sqrt{j\omega\mu_0 R_e}}{2\pi r_e}$$

$$L' = \frac{\mu_0}{2\pi} \log \frac{2h'}{r_e}$$

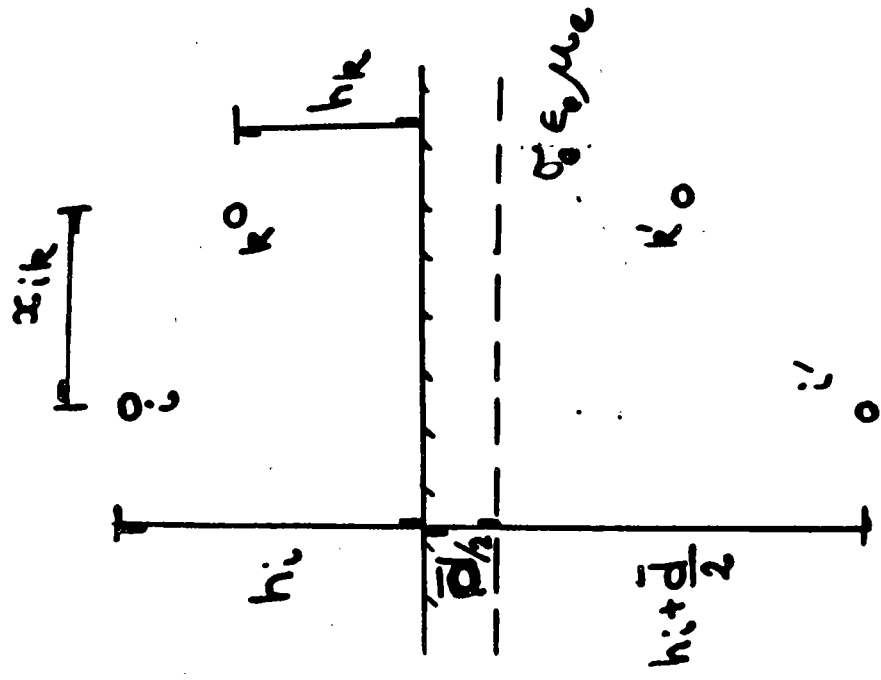
$$h' = h_i + \frac{1}{\sqrt{j\omega\mu_0\sigma_e}}$$

$$Z_{ik} = j\omega \frac{\mu_0}{2\pi} \log \frac{\sqrt{(h_i + h_k + \bar{d})^2 + x_{ik}^2}}{d_{ik}}$$

$$d_{ik} = \sqrt{(h_i - h_k)^2 + x_{ik}^2}$$

máx dif 9%

• para varios estratos $\sigma_e(\omega)$



Fórmula de Carson

$$\bar{Z}_{ii} = (R_{int} + \Delta R_i) + j\omega (L_i + L_{int} + \Delta L_i)$$

$$\bar{Z}_{int} = R_{int} + j\omega L_{int}$$

$$L_i = \frac{\mu_0}{2\pi} \log \frac{2h_i}{r}$$

$$\bar{Z}_{ik} = \Delta R_{ik} + j\omega (L_m + \Delta L_m)$$

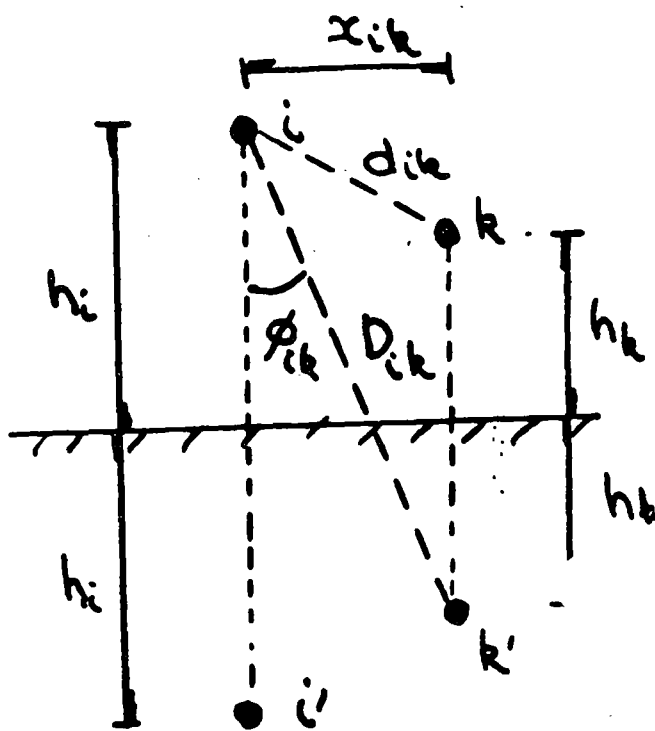
$$L_m = \frac{\mu_0}{2\pi} \log \frac{D_{ik}}{d_{ik}}$$

$$a = 4\pi \sqrt{5} \times 10^4 D \sqrt{\frac{f}{\rho_e}}$$

$$D = \begin{cases} 2h_i \\ D_{ik} \end{cases}$$

$$\Delta R = \left[\frac{\cos \phi}{a} - \frac{\sqrt{2} \cos 2\phi}{a^2} + \frac{\cos 3\phi}{a^3} + \frac{3 \cos 5\phi}{a^5} - \frac{45 \cos 7\phi}{a^7} \right] \frac{4\omega \times 10^4}{\sqrt{2}}$$

$$\Delta L = \left[\frac{\cos \phi}{a} - \frac{\cos 3\phi}{a^3} + \frac{3 \cos 5\phi}{a^5} + \frac{45 \cos 7\phi}{a^7} \right] \frac{4\omega \times 10^4}{\sqrt{2}}$$



SOBRETENSIONES Y ESFUERZOS ELECTRICOS EN SISTEMAS DE POTENCIA

**Víctor F. Hermosillo
Comisión Federal de Electricidad
DEPFI - UNAM**

1. INTRODUCCION

El diseño apropiado del nivel de aislamiento eléctrico de un sistema de potencia debe llegar a un balance entre el aguante, el costo y la fiabilidad de los elementos del sistema ante un esfuerzo eléctrico determinado. El aguante ante un cierto esfuerzo eléctrico puede requerir de aislamiento adicional, que incrementa la fiabilidad pero implica mayores costos. Comúnmente, el costo representa un factor limitante mayor que la factibilidad técnica.

La ruptura o deterioro del aislamiento eléctrico depende de la magnitud, forma y duración del esfuerzo eléctrico a que éste se sujeta. Los fenómenos físicos involucrados en la ruptura de un aislamiento son diferentes para distintos tipos de esfuerzo. Debido a lo anterior, las normas internacionales han propuesto clasificar los esfuerzos típicos encontrados en sistemas de potencia, definiendo características de aguante del aislamiento en base a cada tipo de esfuerzo.

La clasificación de esfuerzos eléctricos y sobretensiones de acuerdo a la norma IEC-71 se muestra en la Figura 1. Cada clase incluye la definición de una forma del esfuerzo respecto al tiempo, un rango de valores para las frecuencias y períodos de tiempo involucrados, así como una forma y prueba estandarizada.

2. VOLTAJES CONTINUOS EN EL SISTEMA

El voltaje nominal se define como el voltaje efectivo (rms), entre fases, a la frecuencia de operación de un sistema de potencia, bajo condiciones normales. A diferencia de voltajes transitorios y temporales, que ocurren bajo condiciones anormales de operación, el voltaje nominal del sistema representa un esfuerzo eléctrico continuo aplicado al aislamiento. Es importante considerarlo en procesos de envejecimiento del aislamiento y en problemas de contaminación.

En ocasiones un sistema eléctrico opera al voltaje máximo del sistema (v.g. 5 a 10% mayor al nominal). Las normas internacionales incluyen valores recomendados para el voltaje máximo de operación para efectos de estandarización del equipo y sistemas, por ejemplo, la norma IEC-71 contiene tablas en dos rangos: 1 kV a 245 kV y mayores de 245 kV.

3. SOBRETENSIONES

Una sobretensión es cualquier voltaje entre fases o entre fase y tierra, cuyo valor de cresta sea mayor que el valor de cresta del voltaje máximo del sistema, es decir, $V_m \sqrt{2} / \sqrt{3}$ entre fase y tierra o $V_m \sqrt{2}$ entre fases.

Las sobretensiones se expresan en valores por unidad (Vpu), utilizando el voltaje máximo del sistema (V_m) como base. Por ejemplo, una sobretensión entre fase y tierra con valor máximo V_{f-t}

$$V_{pu} = \frac{V_{f-t} \sqrt{3}}{V_m \sqrt{2}} \quad \dots(1)$$

4. SOBRETENSIONES TEMPORALES

Es un voltaje oscilatorio, con una duración relativamente larga, no amortiguado o ligeramente amortiguado. La magnitud y duración de este tipo de sobretensiones somete a los apartarrayos a requerimientos severos en su capacidad de descarga y su estabilidad térmica. Una estimación correcta de su probabilidad de ocurrencia es esencial para determinar las características necesarias en los apartarrayos.

Las sobretensiones temporales son de carácter probabilístico debido a los factores aleatorios involucrados en los fenómenos que las producen. Estos factores están asociados con la forma en que se opera el sistema y la configuración del mismo (maniobras de interrupción, variaciones de voltaje, la aleatoriedad de los puntos sobre la línea donde ocurre una falla, etc.). En la práctica, estas sobretensiones ocurren como consecuencia de maniobras o debido a fallas y acciones correctivas, por lo tanto, hay una alta probabilidad de coincidencia de sobretensiones temporales y por maniobra.

Las sobretensiones temporales se pueden clasificar en tres diferentes grupos, de acuerdo a los componentes de frecuencia de la sobretensión:

Grupo 1. Sobretensiones temporales con una frecuencia de oscilación muy cercana a la frecuencia de operación del sistema. Producidas por fenómenos tan variados como: pérdida repentina de carga, corto circuitos asimétricos, efecto capacitivo en líneas largas con el extremo de entrega abierto (efecto Ferranti), resonancia en circuitos lineales producida por fases abiertas o por operación no sincronizada de interruptores, resonancia inducida entre circuitos acoplados y oscilaciones armónicas en circuitos no lineales.

En la Figura 2 se muestran distribuciones de frecuencia acumuladas para magnitudes de sobretensiones temporales debidas a maniobras en líneas sin carga, maniobras en el secundario y maniobras en líneas terminadas en transformadores.

Si se conocen las magnitudes máxima y mínima de sobretensiones temporales que pueden ocurrir en un sistema (ver Figura 2), es posible calcular la distribución de sus valores utilizando la siguiente fórmula:

$$P(V_e \geq V) = k \left((1/AV - E)^{m+1} - (1 - 1/AV_{\min})^{m+1} \right) \dots (2)$$

$$k = \frac{1}{(1 - 1/AV_{\max})^{m+1} - (1 - 1/AV_{\min})^{m+1}}$$

$$E = 1/AV_{\min} + 1/AV_{\min} - 1$$

Esta fórmula empírica es producto de ochenta mil mediciones realizadas en los sistemas de la URSS. $P(V_e \geq V)$ es la probabilidad de que la sobretensión V_e en el extremo abierto de la línea sea mayor que un valor V . El factor A es la razón entre el voltaje en el nodo de envío y el voltaje en el extremo abierto de la línea ($A \leq 1$), podemos suponer $A=1$. El exponente m depende de la forma de conexión de los reactores en paralelo, una línea de transmisión con estos elementos conectados permanentemente, con reactores que se desconectan por medio de un controlador durante cada recierre automático o para líneas sin reactores en paralelo, consideramos $m = 2$. Si los reactores en paralelo se conectan y desconectan de acuerdo a la potencia transmitida, $m = 0$.

La duración de las sobretensiones transitorias para el caso de maniobras producto de fallas (corto circuito, recierre automático, etc.) con operación simultánea de ambos lados de la línea con señales en micro-ondas o carrier, tiene valores típicos entre 0.02 y 0.15 s. Si actúa una protección de distancia o de respaldo, esta duración es entre 0.3 y 0.5 s.

Grupo 2. Sobretensiones temporales con frecuencia de oscilación mayor a la frecuencia de operación del sistema. Este tipo de sobretensiones se deben a oscilaciones forzadas con armónicas superiores pares o impares. Existen dos casos de importancia práctica:

a) **Resonancia de estado estable:** un circuito típico en el que puede ocurrir este fenómeno se muestra en la Figura 3. La corriente de magnetización que fluye por la inductancia no lineal L_m , contiene componentes a la frecuencia fundamental y componentes con armónicas superiores impares. Su probabilidad de ocurrencia es muy baja.

b) Resonancia transitoria: se presentan durante maniobras en líneas terminadas en un transformador sin carga, maniobras en el secundario de un transformador en el extremo de entrega de una línea (Figura 4), produciendo armónicas pares e impares.

Grupo 3. Sobretensiones temporales subarmónicas. Son características en líneas aéreas con compensación en serie. En algunas ocasiones su probabilidad de ocurrencia llega a 10%; aunque para un sistema bien diseñado, esta probabilidad es cercana a cero.

De acuerdo a la experiencia en campo obtenida de distintos países, la magnitud de sobretensiones transitorias en sistemas de potencia reales no llega a valores mayores de 2.0 pu.

4.1 FALLAS A TIERRA

Una falla a tierra produce una sobretensión temporal no amortiguada que persiste hasta que el el esquema de protección produce una maniobra que suprime la falla.

El tipo más común de falla se produce entre una fase y tierra, causando una sobretensión en las fases sanas, que se sostiene hasta que se corrige la situación. La magnitud de la sobretensión en las fases sanas depende de la relación entre la impedancia de secuencia cero y de secuencia positiva del sistema, vistas desde el punto donde ocurre la falla. Por lo tanto, su magnitud esta relacionada con el aterrizamiento del sistema. Esta sobretensión será menor de 1.4 pu para sistemas aterrizados efectivamente y puede llegar a 1.73 pu o más en sistemas no aterrizados.

Un sistema aterrizado efectivamente se define como aquél en el que el máximo voltaje efectivo entre fase y tierra en una de las fases sanas durante una falla es 80% o menor que el voltaje nominal entre fases en el sistema donde se localiza la falla.

La norma IEC-71 incluye gráficas para obtener el factor de aterrizamiento k, en base a las relaciones entre la resistencia de secuencia positiva, la resistencia y la reactancia de secuencia cero, con la reactancia de secuencia positiva, $R1/X1$, $Ro/X1$ y $Xo/X1$, desde el punto donde ocurre la falla (Figura 5). El factor de aterrizamiento es la razón entre el voltaje efectivo máximo de fase a tierra en una fase sana durante una falla y el voltaje efectivo de operación del sistema entre fase y tierra. Para un sistema aterrizado efectivamente $k = \sqrt{3} (0.8) = 1.4$.

4.2 CAMBIOS REPENTINOS EN LA CARGA

El peor caso de este tipo de sobretensiones ocurre cuando se produce un rechazo o pérdida de carga, al abrirse el interruptor remoto de una línea por la que se transmite una parte substancial de la potencia de una central generadora (Figura 6). El voltaje tiende a subir al disminuir la caída de potencial en la impedancia equivalente en serie del sistema y al producirse una aceleración del generador.

La sobretensión en el generador está determinada por el nivel de corto circuito del sistema, la velocidad del generador (respuesta del gobernador de velocidad, sistema de excitación), las características de la carga antes y después del evento, las longitudes de las líneas conectadas y la cantidad de reactivos generados por la línea (incluyendo compensación en serie o paralelo). Se puede lograr un cálculo preciso de las sobretensiones por rechazo de carga utilizando una simulación digital que incluya las características dinámicas de las máquinas, sus sistemas de control, así como el modelado de las líneas y cargas.

En pruebas de rechazo de carga en sistemas de potencia reales se han obtenido sobretensiones con magnitudes máximas de 1.45 pu.

4.3 EFECTO FERRANTI

Este efecto ocurre debido a la corriente capacitiva, producida por la carga de una línea de transmisión, fluye por la impedancia en serie cuando se abre el extremo lejano de una línea larga no compensada (Figura 7). En estas condiciones el voltaje en el extremo abierto (V_2) es siempre mayor que el voltaje en el nodo de envío (V_1). El voltaje senoidal en el extremo abierto está dado por

$$V_2 = \frac{V_1}{\cos(\beta l)} \quad \dots(3)$$

($\beta = 7.2^\circ$ cada 100 km a 60 Hz, l : longitud de la línea, km)

El efecto Ferranti se puede disminuir mediante compensación inductiva en paralelo o compensación capacitiva en serie.

4.4 RESONANCIA

Algunas de las más severas sobretensiones temporales ocurren debido a condiciones de resonancia. En su forma más simple, el circuito equivalente de un sistema resonante consiste de una fuente, un interruptor y un circuito resonante RCL. La sobretensión se produce al cerrar el interruptor, limitada por pérdidas y efectos de saturación de algunos componentes.

Ignorando las pérdidas, la sobretensión se puede aproximar con la siguiente ecuación

$$V_2 = \frac{V_1 X_c}{X_L + X_c} \quad \dots(4)$$

donde V_1 es el voltaje en el nodo de envío y V_2 es el voltaje en el nodo de recepción.

En la práctica se pueden producir condiciones cercanas a la resonancia. Un ejemplo es el caso de la apertura de una fuente de alta tensión que alimenta a un circuito de baja tensión por medio de un cable y un transformador, si la reactancia inductiva del transformador es cercana a la reactancia capacitiva del cable. Otro caso de resonancia es cuando las armónicas asociadas a la saturación de un transformador tienen frecuencias cercanas a la frecuencia natural de resonancia del sistema. Las sobretensiones debidas a resonancia pueden evitarse cambiando las impedancias de elementos del sistema. Esta consideración debe formar parte de los criterios de diseño del mismo.

4.5 FERRORESONANCIA

Este tipo de sobretensiones ocurre cuando un elemento magnético saturable del sistema es excitado por una capacitancia. La capacitancia puede representar, por ejemplo, al capacitor de graduación entre los contactos abiertos de un interruptor o la capacitancia a tierra de un cable (Figura 8).

Este fenómeno puede producirse también cuando solamente una o dos fases de un sistema se encuentran energizadas debido a la operación de fusibles o interruptores (Figura 9). El elemento saturable puede representar transformadores de potencial (con reactancias altas) conectados al bus abierto, o bien, un transformador con terciario conectado en delta que a su vez alimenta transformadores auxiliares.

La sobretensión en las terminales depende de la magnitud y forma de la corriente que fluye por el elemento magnético, a su vez, esta corriente depende del estado magnético del elemento. Al entrar y salir éste de la región de saturación (Figura 10), su inductancia efectiva cambia, resultando en voltajes con multitud de armónicas. Estos voltajes pueden presentar componentes con frecuencias mayores o menores de la frecuencia de operación del sistema (Figura 11). Diversos estudios efectuados con TNA muestran que existe mayor posibilidad de que se presente ferresonancia en sistemas en los que la reactancia capacitiva equivalente sea menor a veinte veces la reactancia inductiva, $X_c < 20X_L$.

Las sobretensiones por ferresonancia se pueden controlar operando los transformadores a una densidad de flujo reducida, también se pueden implementar procedimientos de maniobra que eviten energizar un transformador sin carga a través de elementos capacitivos.

4.6 ENERGIZACION DE UNA LINEA TERMINADA EN UN TRANSFORMADOR

Este tipo de maniobras producen sobretensiones temporales ligeramente amortiguadas. Se originan durante la energización o recierre de una línea terminada en un transformador. Después del transitorio inicial (que se clasifica como sobretensión por maniobra), la corriente de excitación del transformador produce un sobrevoltaje sostenido durante varios segundos (Figura 12). Su magnitud depende del instante en que se cierre el interruptor, la impedancia equivalente de la fuente, los parámetros de la línea y el transformador y del flujo residual de éste último.

5. SOBRETENSIONES POR MANIOBRA

Son voltajes transitorios, amortiguados y de relativamente corta duración, producidos por acciones de conexión o desconexión por medio de elementos de interrupción del sistema. La magnitud de una sobretensión por maniobra depende del voltaje de operación del sistema. Actualmente se clasifican como sobretensiones transitorias de frente lento.

5.1 CIERRE Y RECIERRE DE LINEAS DE TRANSMISION

La energización de una línea en vacío, no terminada en un transformador, produce sobretensiones debido a las ondas viajeras en los conductores, estas ondas son producidas por el cierre del interruptor o pueden ser causadas por acoplamiento entre fases. Los tiempos relativos de cierre entre los polos del interruptor son importantes para determinar este tipo de sobretensiones, otros factores involucrados son la longitud de la línea, el grado de compensación en paralelo, las características de la fuente equivalente en el nodo de envío, la utilización de resistencias de preinserción y el tipo de terminación en el extremo de la línea. En general las sobretensiones son mayores en el extremo de entrega de la línea.

La apertura de una línea puede dejar un voltaje remanente en la línea desenergizada. A menos que la carga atrapada sea drenada a tierra por medio de un transformador o reactor, puede permanecer en la línea durante varios segundos. La cantidad de carga dependerá de la capacitancia equivalente de la línea y del valor de la resistencia de preinserción (Figura 13), su decremento en el tiempo varía según las condiciones atmosféricas (Figura 14).

Si ocurre un recierre de una línea con carga atrapada y, en el instante en que el interruptor cierra, el voltaje de la fuente tiene polaridad opuesta al voltaje en la línea abierta, se pueden producir sobretensiones muy altas.

Como resultado de un estudio realizado en conjunto por los comités 13 y 33 de CIGRE, se elaboró un diagrama que condensa información sobre factores de sobretensión producidos por el cierre y recierre de líneas (Figura 15). Este diagrama incluye resultados de simulaciones digitales, TNA y mediciones en campo. Se muestran valores mínimos, medios y máximos para una combinación de condiciones del sistema, en forma de un árbol de decisiones. Las opciones son: cierre o recierre trifásico, con o sin resistencia de preinserción, con una fuente inductiva o compleja (sistemas con cables, en los que debe añadirse una capacitancia en paralelo en el equivalente de Thévenin), compensación en paralelo mayor o menor al 50%.

5.2 MANIOBRAS EN CIRCUITOS INDUCTIVOS

Este tipo de sobretensiones puede analizarse con un circuito sencillo, presentado en la Figura 16. Si la reactancia del elemento inductivo de la carga L_c es menor que la reactancia de la capacitancia en paralelo C_c , la mayor parte de la corriente que circula por el circuito fluye por la inductancia L_c y se encuentra atrasada 90° respecto al voltaje de la fuente; además, se supone que la reactancia de la fuente es pequeña comparada con la correspondiente a la carga, $L_s \ll L_c$.

Al iniciarse la apertura de los contactos del interruptor, el arco entre éstos conduce la corriente de la carga. El arco tenderá a extinguirse cuando la corriente alterna llegue a un valor de cero. Debido a que el circuito es puramente inductivo, en el momento de interrupción el voltaje en la fuente y el voltaje en la carga tendrán valores cercanos al máximo.

La interrupción del arco separa al circuito en dos secciones. El voltaje en el contacto del lado del generador tiene dos componentes: una de 60 Hz y una oscilación amortiguada superpuesta cuya frecuencia tiene valores entre 0.5 y 100 kHz, dependiendo de los valores de los parámetros L_s y C_s . El voltaje en el contacto del lado de la carga es oscilatorio amortiguado con una frecuencia dependiendo de C_c y L_c . El voltaje de recuperación transitoria se puede calcular obtenido la diferencia entre los voltajes que aparecen entre los contactos del interruptor, se inicia una carrera entre las propiedades dieléctricas del medio entre los contactos y este voltaje.

5.2.1 REIGNICION DEL ARCO

Existe la posibilidad de una reignición del arco que produce el flujo de corriente con frecuencia mayor a la de operación del sistema y causa una escalación en el voltaje en la carga. Si la corriente se interrumpe de nuevo al llegar al valor de cero, pueden aparecer varios ciclos de reignición e interrupción, con escalaciones de voltaje cada vez mayores (Figura 17).

5.2.2 CORTE DE PEQUEÑAS CORRIENTES INDUCTIVAS

El arco que se forma entre los contactos de un interruptor durante una apertura en un sistema con carga inductiva, se encuentra sujeto a inestabilidades conforme la corriente que fluye por él tiende a cero. Estas se presentan en forma de oscilaciones en la corriente y el voltaje entre los contactos. Si la inestabilidad es seguida de una repentina caída de la corriente a cero, se produce un fenómeno que se conoce como corte prematuro de una pequeña corriente inductiva (Figura 18).

En el modelo más simplificado del arco, suponemos que la transición entre un estado y otro se realiza de modo exponencial con una cierta constante de tiempo. Se desprecian las inductancias del lado de la carga y del lado de la fuente L_s y L_c , obteniéndose un circuito equivalente formado por dos ramas: una contiene una inductancia L_a en serie con una resistencia R_i , la segunda incluye una capacitancia C en paralelo con una resistencia R_a . C es la capacitancia equivalente de C_s y C_c en serie. En la Figura 19 se muestra la simplificación del circuito y la solución de la ecuación diferencial, de la cual obtenemos una expresión para la corriente en el arco. La condición para inestabilidad se da cuando el factor exponencial es creciente. Lo anterior resulta en una relación entre la corriente de corte (i_{ch}) y la raíz cuadrada de la capacitancia equivalente (C), en la que está involucrado un factor que depende del tipo de interruptor. Para una capacitancia típica de $C = 10 \text{ nF}$ los valores de esta corriente son:

tipo de interruptor	i_{ch}
pequeño volumen de aceite	7 a 10 A
hexafluoruro de azufre SF ₆	4 a 17 A
aire comprimido	15 a 20 A

La sobretensión generada del lado de la carga una vez ocurrido el corte prematuro de la corriente, depende de los valores de i_{ch} , L_c y C_c . La energía almacenada en estos elementos antes del corte, se convierte en energía electrostática. Haciendo un balance de energía, se puede

obtener la siguiente fórmula para el factor de la sobretensión

$$k_s = \sqrt{1 + \left(\frac{I_{ch}}{U_0}\right)^2 \frac{L_s}{C_s} \eta_m} \quad \dots(5)$$

donde U_0 es el voltaje pico de operación del sistema y η_m es la eficiencia magnética en el sistema, y toma valores entre 0.3 y 0.5.

5.2.3 CORTE VIRTUAL DE UNA CORRIENTE INDUCTIVA

En circuitos trifásicos, la reignición del arco en un polo del interruptor puede producir un corte virtual de corriente que causa mayores sobretensiones que el corte prematuro de corriente, descrito anteriormente. Como se ilustra en la Figura 20, el primer polo en abrir corresponde a la fase A, la corriente i_a llega a cero y, si la carga no está aterrizada, las corrientes en las otras fases son iguales y tienden normalmente a cero $i_b = i_c$. Si ocurre una reignición del arco en la fase A, se producirán corrientes oscilatorias de frecuencia mayor a la nominal del sistema en las tres fases, que pudieran ser interrumpidas al pasar por cero. Esta interrupción es semejante a un corte prematuro de una corriente inductiva.

5.3 MANIOBRAS EN CIRCUITOS CAPACITIVOS

Consideremos un circuito sencillo formado por una carga capacitiva suministrada por una fuente inductiva. La corriente en la carga adelanta al voltaje en 90° . Cuando se interrumpe la corriente, al llegar a cero, el voltaje del sistema se encuentra en un valor cercano al máximo (marcado con un 1 en la Figura 21). El voltaje de recuperación transitoria en el interruptor es muy pequeño, por lo que no ocurre reignición del arco, y la carga capacitiva queda cargada al voltaje pico de operación del sistema. Al pasar medio ciclo, el voltaje de recuperación llegará al doble del voltaje pico del sistema, 2 pu. Si en ese momento ocurre una reignición del arco en el interruptor (marcado con un 2 en la Figura 21). Entonces, despreciando las pérdidas, el voltaje en el capacitor podría subir hasta 3 pu. Al interrumpirse de nuevo el circuito, el capacitor queda cargado a 3 pu, repitiéndose el ciclo indefinidamente.

En un sistema trifásico este fenómeno es más complejo, particularmente si alguno de los interruptores opera antes que los otros dos. Las mayores sobretensiones ocurren cuando solo una de las fases abre y su valor depende de la relación entre la capacitancia de secuencia positiva y la capacitancia de secuencia cero del sistema, ver Figura 22.

6. SOBRETENSIONES POR DESCARGAS ATMOSFERICAS

Dentro de la clasificación actual, éstas se consideran como sobretensiones de frente rápido. Producidas como consecuencia de descargas entre la nube y tierra, se pueden dividir en sobretensiones producidas por descargas directas y sobretensiones inducidas.

La descarga atmosférica consta de varias fases, iniciando con una guía descendente que viaja desde la nube hacia tierra, dando saltos de 50 m, a velocidad promedio de 150km/s, cubre una distancia promedio de 3 km en 20 ms. La guía descendente puede ser encontrada por una guía ascendente originada en una estructura alta. La guía descendente se encuentra al potencial de la nube, al llegar a tierra, se drenan las cargas en el canal y los paquetes de cargas en la nube hacia tierra, durante lo se denomina el rayo de retorno (Figura 23). Mediciones de las corrientes del rayo de retorno han resultado en su caracterización con una forma de doble exponencial con un frente rápido, adquiriendo su valor máximo en 1 a 30 μ s, seguido de un decremento al 50% de su valor pico, que toma de 10 a 250 μ s. Para descargas negativas, que representan el 90% de las descargas a tierra, el valor medio de la amplitud de la corriente durante el rayo de retorno es de 30 kA, con valores máximos de 100 kA. Existen publicaciones con distribuciones acumuladas de distintos parámetros relacionados con descargas a tierra, ver Figura 24.

En una línea de transmisión sin hilos de guarda o, si ocurre una falla en el blindaje, la corriente producida por el rayo de retorno es inyectada directamente a una de las fases. Esta corriente $i(t)$ se va a dividir en dos ondas viajeras que se propagan hacia extremos opuestos de la línea, cuya impedancia característica es Z_0 . La sobretensión producida $v(t)$ esta dada por la siguiente ecuación:

$$v(t) = Z_0/2 i(t) \quad \dots(6)$$

Por ejemplo, una corriente inyectada en una fase, con magnitud de 10 kA, produciría un voltaje con magnitud de 2MV en una línea con impedancia característica de 400 Ω .

Si la descarga incide en el hilo de guarda, se puede producir un flameo inverso, al subir el potencial de la torre. La Figura 25 muestra los porcentajes de la corriente total que fluyen por las torres de una línea de transmisión, por descargas directas a la mitad de la distancia interpostal y directas a una de las torres, siendo éste último el peor caso.

Cuando la descarga atmosférica cae en el punto en que se une el hilo de guarda y la torre, la corriente se divide en tres componentes, dos que viajan en sentidos opuestos sobre el hilo de guarda, la tercera que se propaga por la torre hacia la base, donde se produce una reflexión. La Figura 26 muestra las formas típicas de las sobretensiones producidas en la torre, las cuales producen un esfuerzo en las cadenas de aisladores.

7. SOBRETENSIONES EN SUBESTACIONES ENCAPSULADAS EN SF6

Este tipo de sobretensiones se conocen también como sobretensiones transitorias muy rápidas. Ocurren como consecuencia de maniobras con cuchillas e interruptores en subestaciones encapsuladas en hexafluoruro de azufre y son importantes en sistemas con voltajes nominales mayores a 300kV. Se caracterizan por tiempos de frente en el rango de decenas y cientos de nanosegundos.

La componente de mayor frecuencia de estas sobretensiones esta determinada por el tiempo en el que se produce el colapso en el voltaje entre los electrodos, que a su vez depende de la presión de trabajo del gas SF6. Se ha propuesto la siguiente fórmula para estimar el tiempo mínimo en el frente de la sobretensión

$$t_f = 1 \text{ a } 1.5 \frac{1}{p} \quad (\text{ns}) \quad \dots(7)$$

esta expresión puede obtenerse a partir de la ecuación de Toepler para un arco eléctrico. El tiempo de frente de la sobretensión se reduce bajo la presencia de protuberancias o asperezas en la superficie de los electrodos y por partículas en el gas.

Al analizar estas sobretensiones es necesario utilizar la teoría de ondas viajeras, considerando cierta velocidad de propagación en un medio con una impedancia característica. La forma y valor máximo de la sobretensión en algún punto de interés dependen de la configuración misma de la subestación, como resultado de una serie de reflexiones y refracciones de la onda viajera en transiciones y ramificaciones.

Otros factores que determinan la forma y magnitud de estas sobretensiones es el diseño de los contactos del interruptor o cuchilla desconectadora (la asimetría trae consigo una dependencia de la descarga en la polaridad del voltaje) y su velocidad de operación (la carga atrapada en el extremo desconectado depende de esta velocidad).

Otro fenómeno que ocurre en subestaciones en SF6 son las tensiones transitorias en la carcaza, que producen arqueo entre las partes aterrizadas de la subestación. Este es un fenómeno de baja energía, no hay evidencia de peligro para el personal, puede causar daño a equipo de control y protección. Las sobretensiones en la carcaza pueden controlarse mediante el diseño apropiado de las conexiones a tierra.

Este tipo de transitorios produce radiación a frecuencias de 10 a 20 MHz, con magnitudes de campo eléctrico de 10 kV/m.

La distribución no lineal de voltaje que producen en transformadores sujeta a esfuerzos adicionales las primeras vueltas del devanado, las conexiones y taps. En algunos casos es necesario proteger los cambiadores de taps con varistores. Se considera que la prueba de impulso cortado sujeta a este equipo a esfuerzos semejantes.

En cuanto a cuchillas e interruptores, existen pruebas de impulso en posiciones abierta y cerrada, es necesario considerar posiciones intermedias.

En la Figura 27 se muestran algunas sobretensiones por maniobra medidas en subestaciones encapsuladas en SF6.

REFERENCIAS

[1] International Electrotechnical Commission, Publication IEC 71-2, Insulation Coordination Part II: Applications Guide, Geneve, Switzerland.

[2] Gert, T., Glavitsch, H., Tikhodeyev, N., Shur, S. & Thoren, B., CIGRE, International Conference on Large High Tension Electric Systems, Temporary Overvoltages, their classification, magnitude, duration, shape and frequency of occurrence, Report of Study Committee No.33, 33-12, 1972 Session, August 28-September 6, p. 1-14.

[3] EPRI, Electric Power Research Institute, Transmission Line Reference Book, 345 kV and above, 2nd. edition, Publication No. EL-2500, Palo Alto, CA 94303, 1982, p. 421-445, 545-597.

[4] Catenacci, G. & Palva, V., Switching Overvoltages in EHV and UHV Systems with special reference to closing and reclosing transmission lines, ELECTRA, No. 30, p. 70-121.

[5] Slamecka, E., Interruption of Small Inductive Currents, Chapters 1 and 2, CIGRE Working group 13.02, ELECTRA, No.72, 1974, p. 73-103.

[6] Berger, K., Anderson, R. & Kroninger, H., Parameters of Lightning Flashes, CIGRE Working group No. 33, ELECTRA, No.41, p. 23-69.

[7] CIGRE Working group 33/13-09, Very Fast Transient Phenomena Associated with Gas Insulated Substations, International Conference on Large High Voltage Electric Systems, 1988 Session, August 28-September 3, p. 1-20.

CLASS	LOW FREQUENCY		TRANSIENT		
	CONTINUOUS	TEMPORARY	SLOW-FRONT	FAST-FRONT	VERY-FAST-FRONT
voltage shape					
range of voltage shapes	$f = 50 \text{ or } 60 \text{ Hz}$ $T_d \geq 1 \text{ hr}$	$50 < f < 500 \text{ Hz}$ $0.03 < T_d < 3600 \text{ s}$	$30 < T_f < 3000 \mu\text{s}$ $0.3 < T_d < 30 \text{ ms}$	$0.3 < T_f < 30 \mu\text{s}$ $3 < T_d < 300 \mu\text{s}$	$3 < T_f < 300 \text{ ns}$ $0.3 < f_1 < 100 \text{ kHz}$ $30 < f_2 < 300 \text{ kHz}$ $0.03 < T_d < 3 \text{ ns}$
standard voltage shape	$f = 50 \text{ or } 60 \text{ Hz}$ $T_d = (\text{°})$	$48 \leq f \leq 62 \text{ Hz}$ $T_d = 1 \text{ min}$	$T_f = 250 \mu\text{s}$ $T_d = 2500 \mu\text{s}$	$T_f = 1.2 \mu\text{s}$ $T_d = 50 \mu\text{s}$	under consideration
standard withstand test	long-duration power-frequency test	short-duration power-frequency test	switching impulse test	lightning impulse test	(chopped impulse) under consideration

Figura 1. Clasificación de esfuerzos eléctricos y sobretensiones de acuerdo a la norma IEC-71.

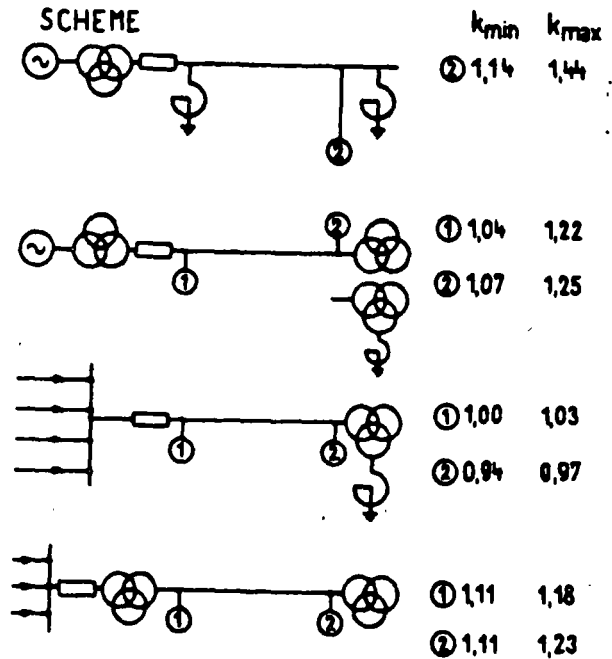
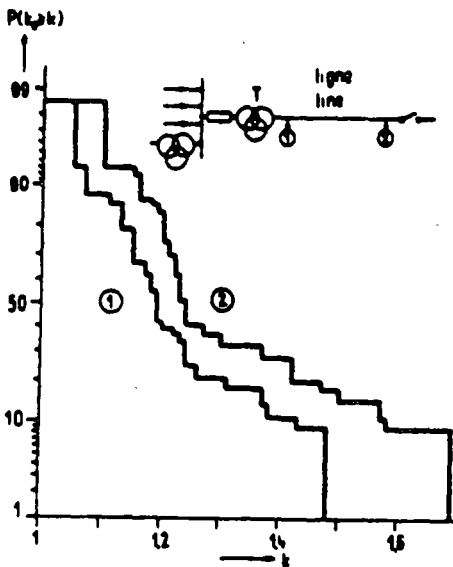
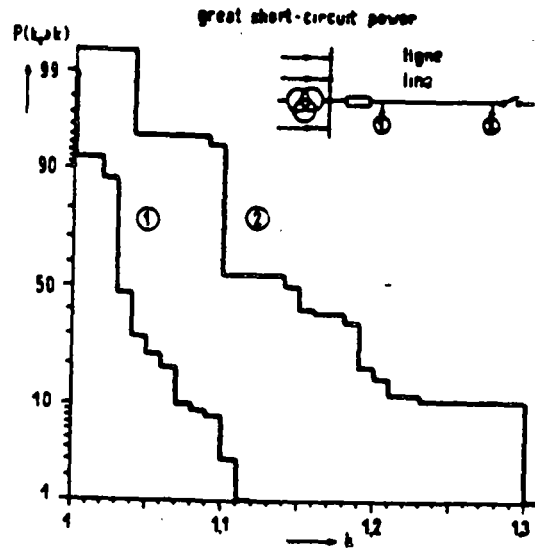
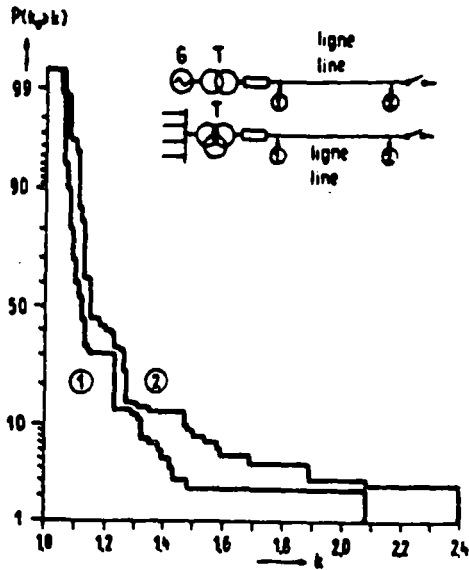
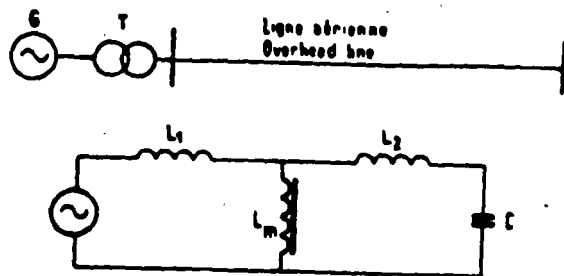


Figura 2. Curvas de distribución de frecuencia acumulada para magnitudes de sobretensiones temporales en el extremo de envío (1) y en el extremo de recepción (2): a) fuente con bajo nivel de corto circuito (230 mediciones/curva), b) fuente con alto nivel de corto circuito (100 mediciones/curva), maniobras en el secundario (70 mediciones/curva), c) rango de magnitudes medidas para diferentes circuitos.



L_1, L_2 - short-circuit and magnetizing inductance of the transformer
 L_2, C - inductance and capacitance of the overhead line.

Figura 3. Circuito en el que ocurre resonancia en estado estable con componentes fundamental y armónicas superiores.

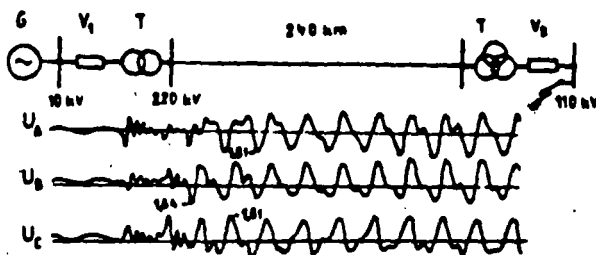


Figura 4. Circuito en el que ocurre resonancia transitoria al eliminar una falla trifásica en el secundario de un transformador. El interruptor en V2 esta abriendo.

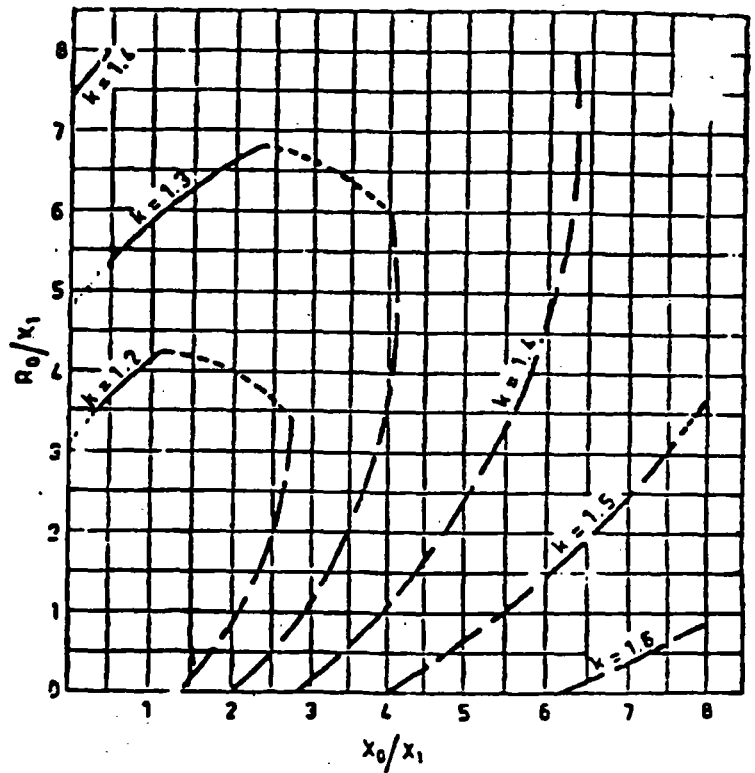
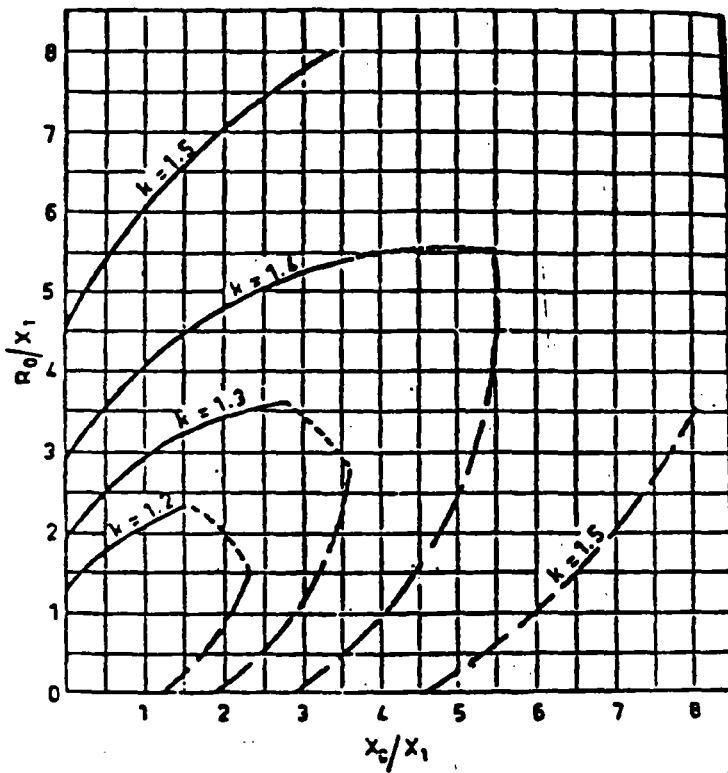
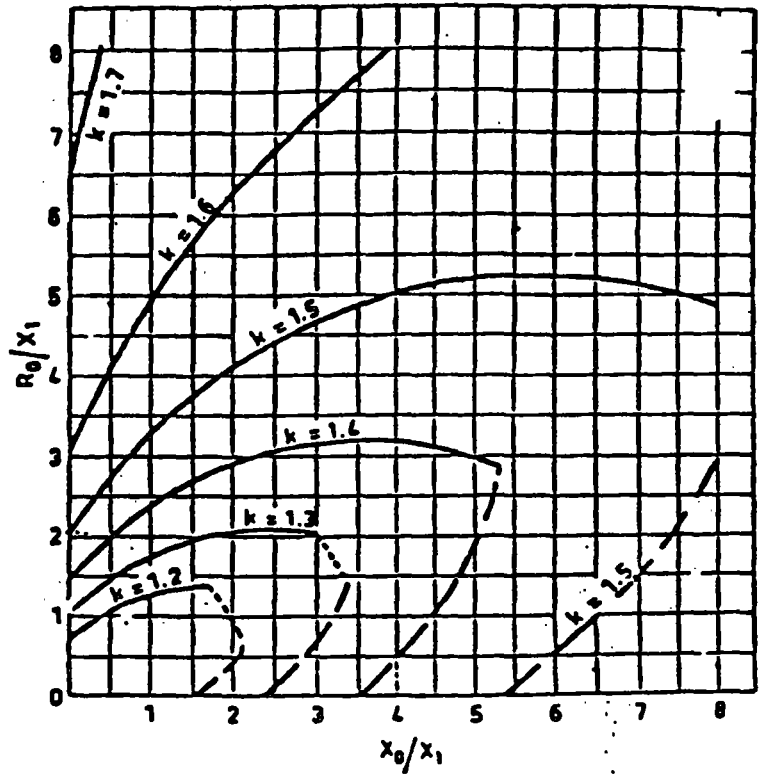
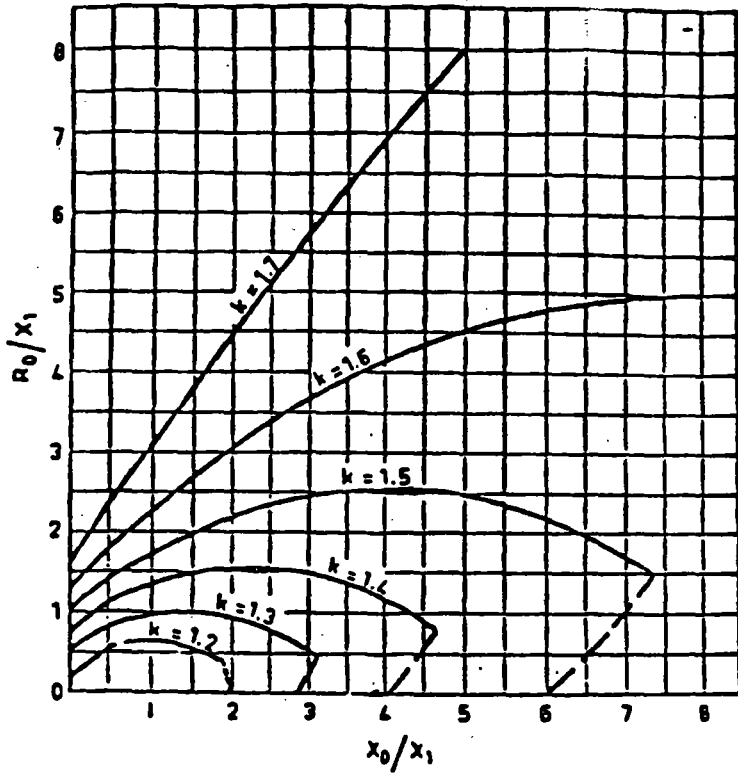


Figura 5. Factores de aterrizamiento para: a) $R_1 = 2X_1$, b) $R_1 = X_1$, c) $R_1 = 0.5X_1$ y d) $R_1 = 0$.

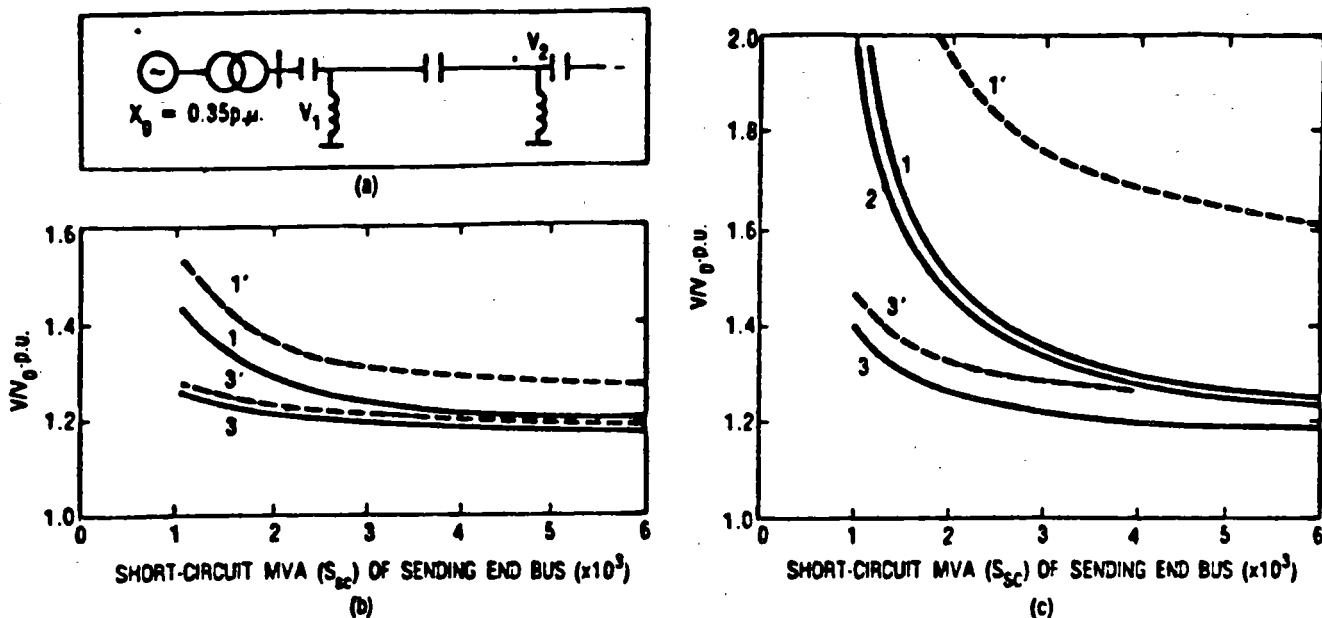


Figura 6. Sobretensiones a frecuencia nominal causados por rechazo de carga: a) diagrama, b) línea de 300 km de longitud, c) línea de 600 km de longitud. 1 y 1' sin compensación, 2 con compensación capacitiva en serie de 50%, 3 y 3' con 50% de compensación en serie y 70% de compensación en paralelo. 1, 2 y 3 son voltajes en el nodo de envío, 1' y 3' son voltajes en el nodo de recepción. Voltaje nominal 400 kV, carga inicial 33% del nivel de corto circuito del nodo de envío. Se supone un incremento en la velocidad del generador de 10% y se desprecian pérdidas.

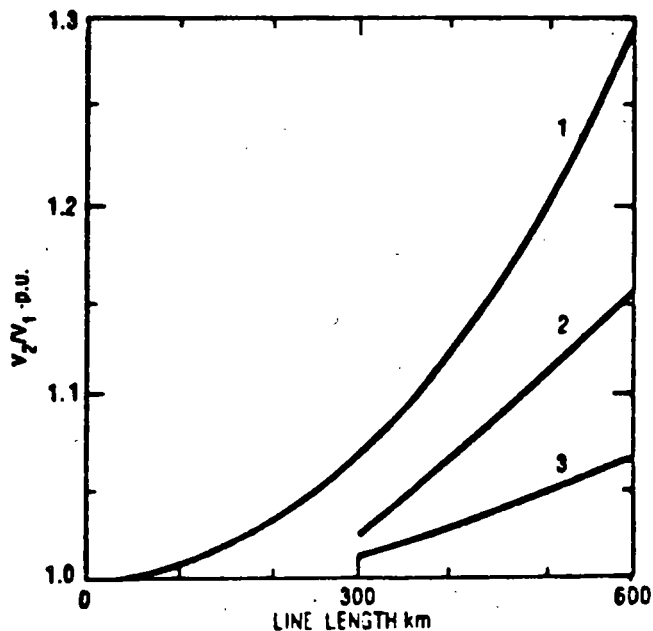


Figura 7. Magnitud de sobretensiones debidas al Efecto Ferranti: (1) sin compensación, (2) compensación en serie de 50% y (3) 50% de compensación en serie, 70% de compensación en paralelo.

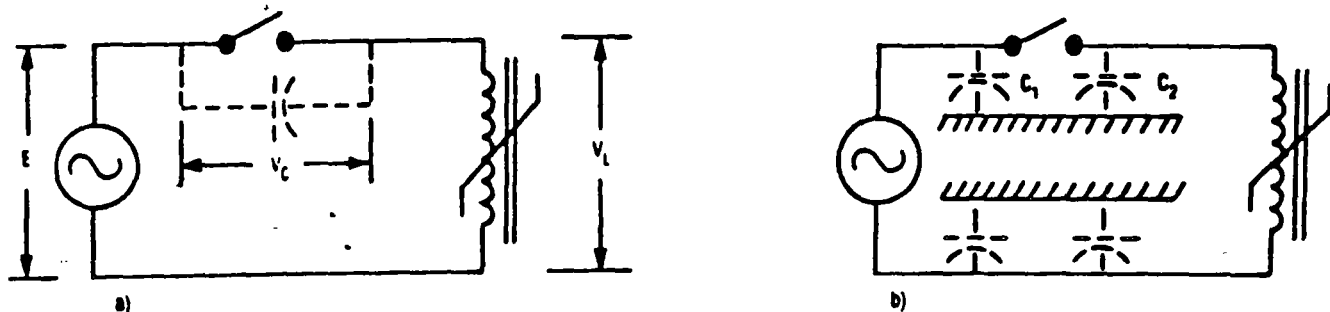


Figura 8. Circuitos sujetos a ferrorsonancia: a) excitación por medio de la capacitancia entre los contactos de un interruptor abierto, b) excitación por medio de una capacitancia a tierra.

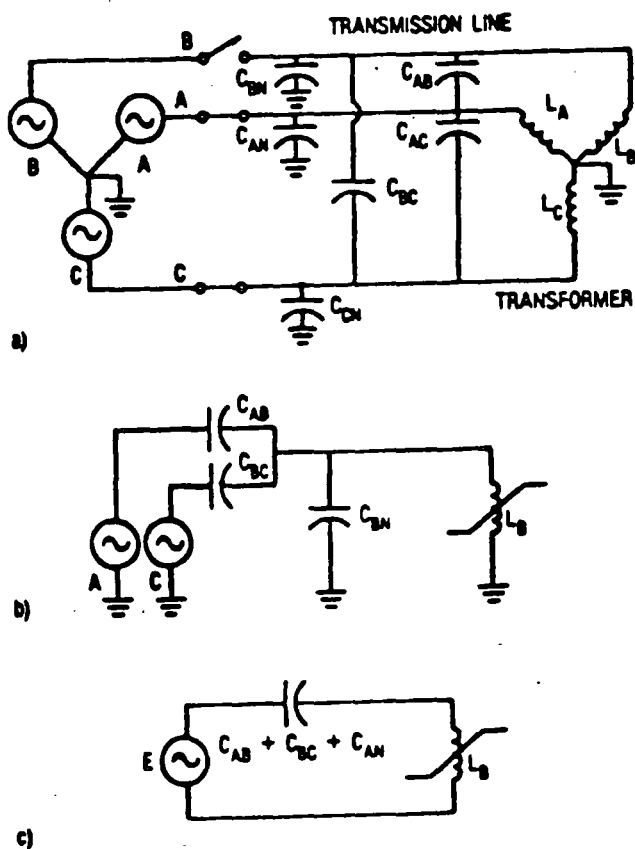


Figura 9. Circuito trifásico con fase B abierta, sujeto a ferrorsonancia: a) representación trifásica, b) y c) circuitos equivalentes simplificados.

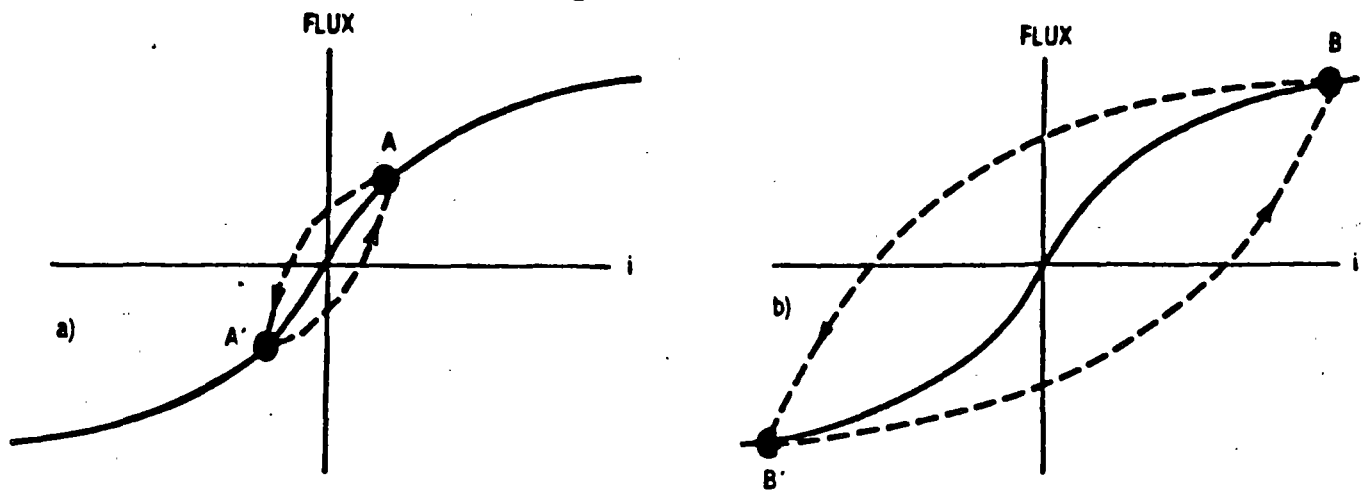


Figura 10. Operación de un elemento ferromagnético: a) en la región lineal y b) en la región saturada.

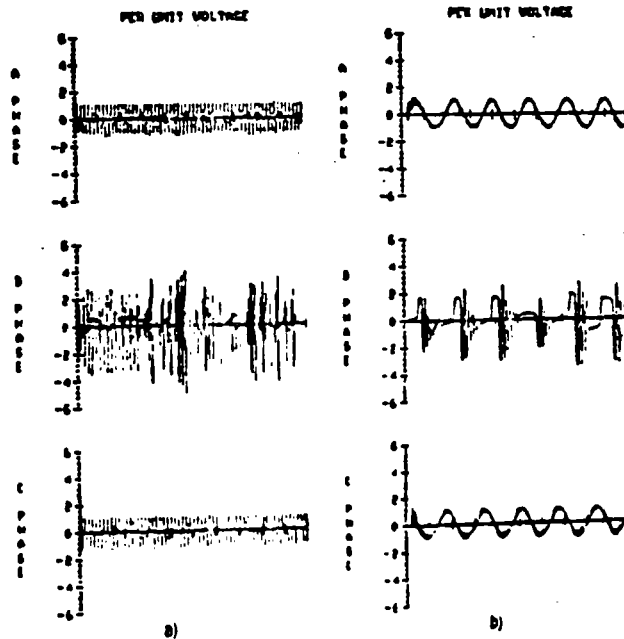


Figura 11. Voltajes ferroresonantes producidos por la apertura de la fase B (ver Figura 9): a) escala 100 ms/div b) escala 10 ms/div.

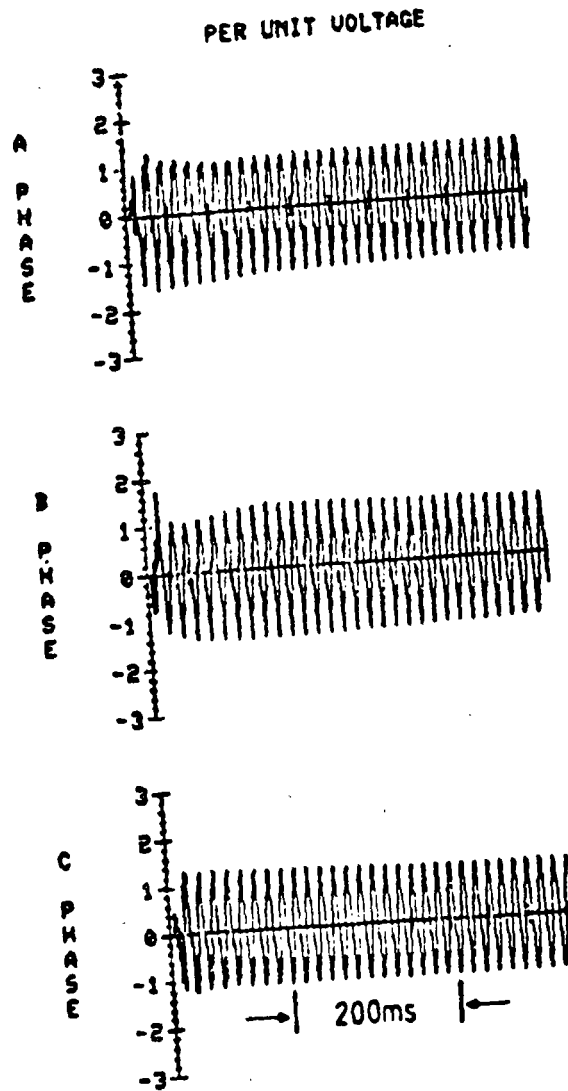


Figura 12. Sobretensión temporal producida al energizar una línea terminada en un transformador.

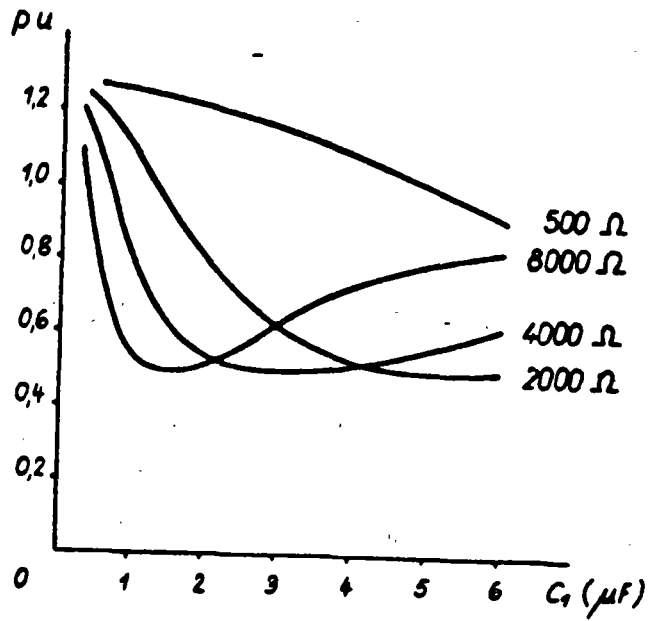


Figura 13. Variación del valor en por unidad de la carga atrapada, en función de la capacitancia total de la línea y el valor de la resistencia de preinserción.

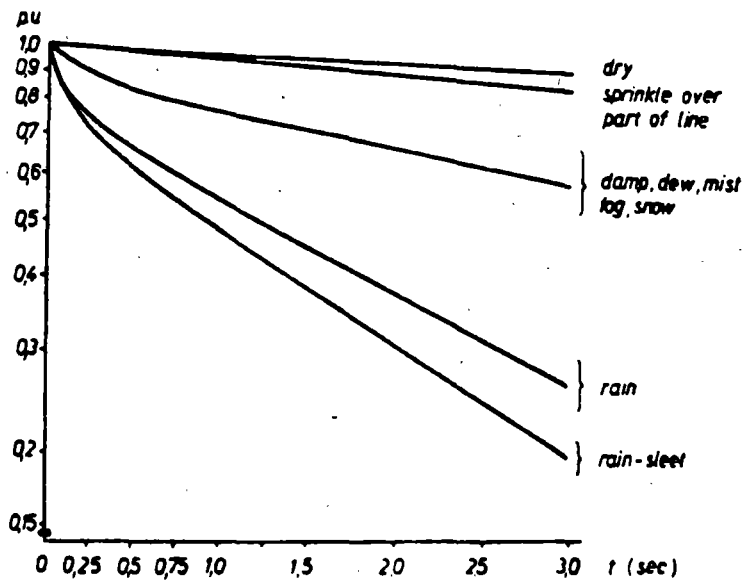


Figura 14. Variación del valor por unidad de la carga atrapada en una línea en función del tiempo y las condiciones atmosféricas.

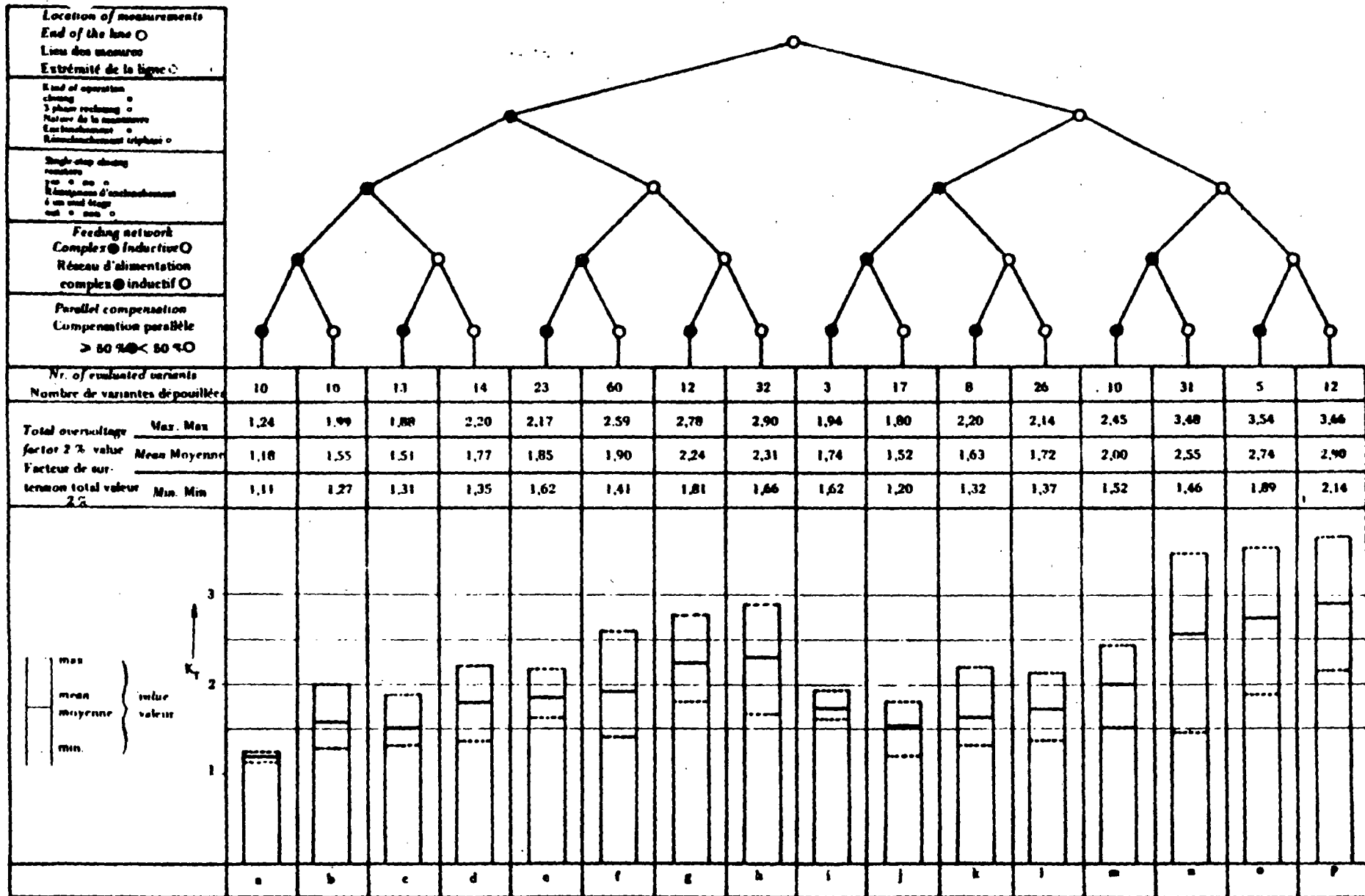


Figura 15. Factores de sobretensión debidos a cierre y recierre de líneas de transmisión.

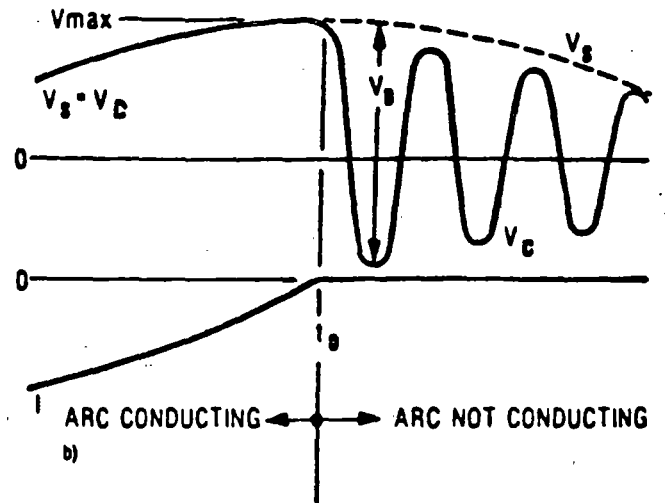
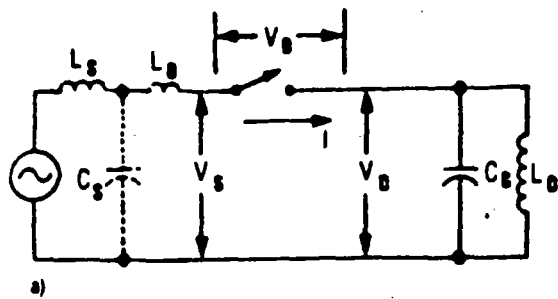


Figura 16. Circuito elemental para analizar las sobretensiones por maniobras en sistemas con cargas inductivas: a) circuito, b) voltajes y corrientes.

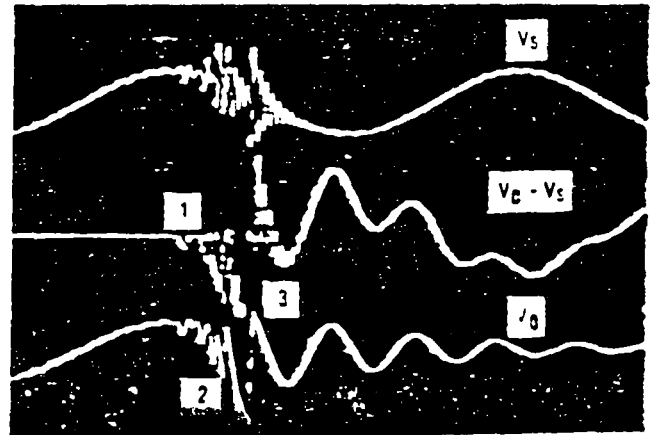
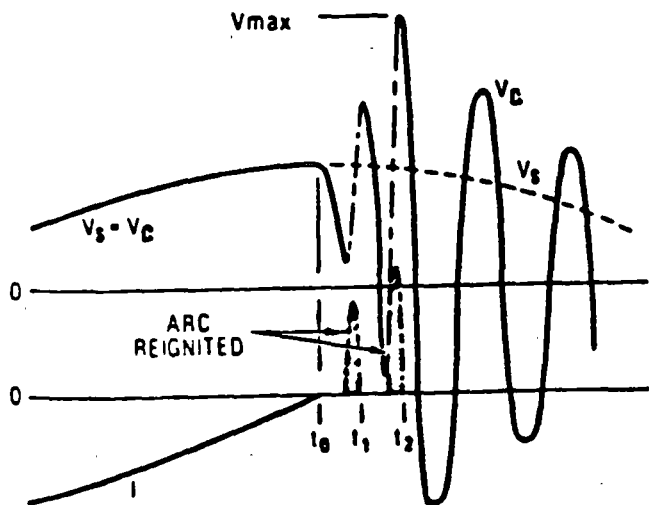


Figura 17. Reignición del arco en el interruptor y escalación en el voltaje.

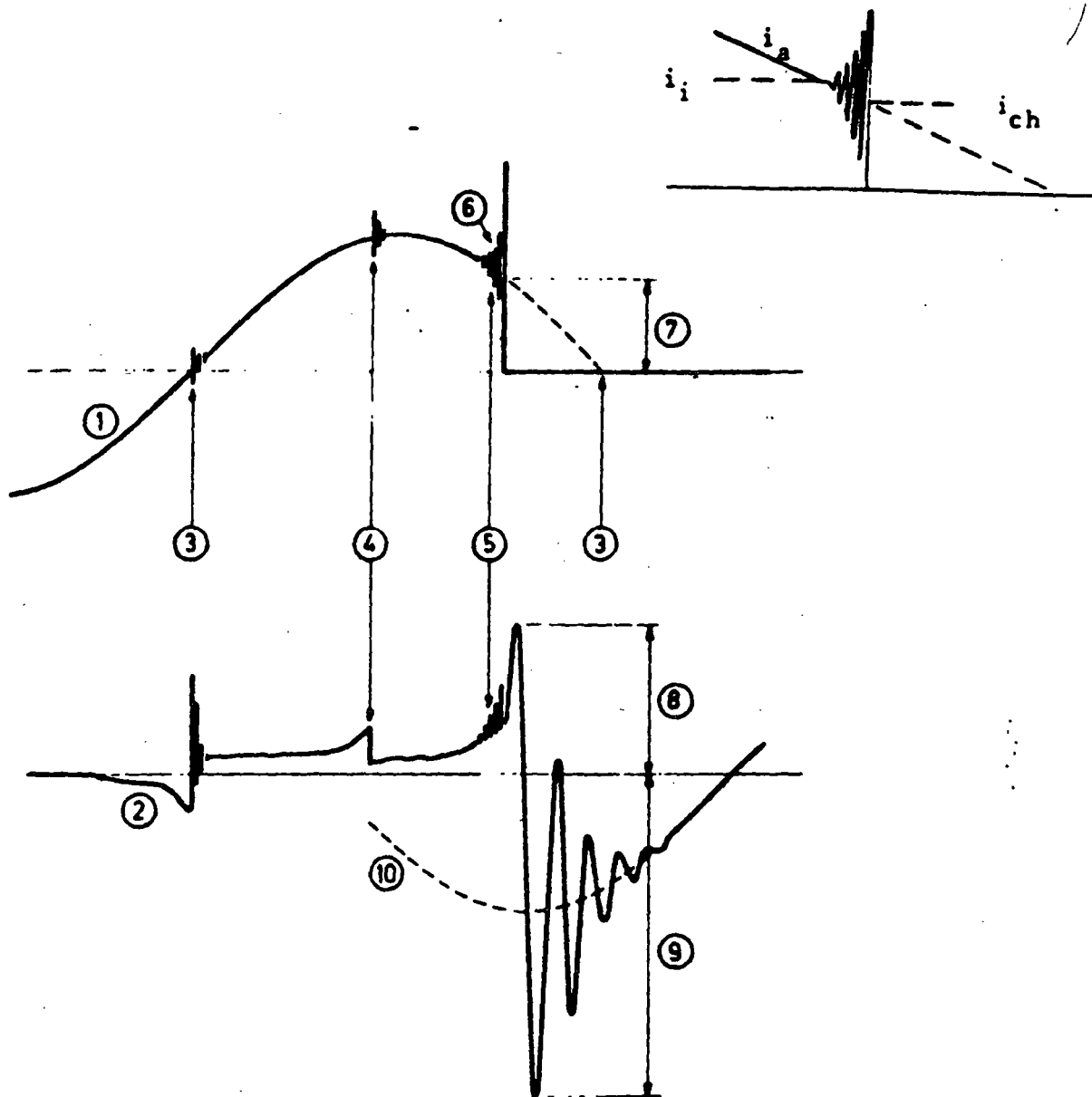
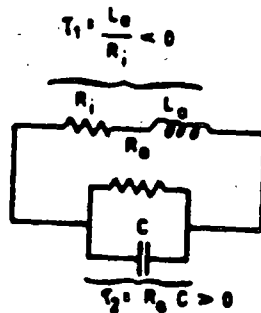
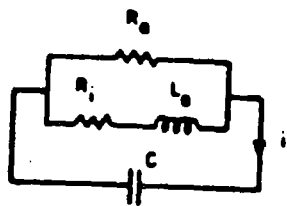
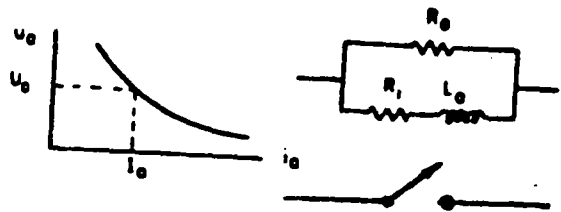
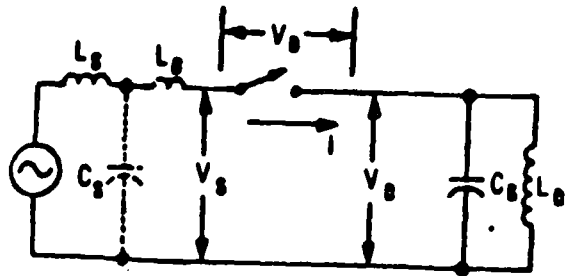


Figura 18. Corriente y voltaje en el arco entre los contactos de un interruptor, para el caso de una interrupción prematura de la corriente

Definiciones:

- (1) Corriente circulando por el interruptor ($i_a(t)$)
- (2) Voltaje entre los contactos del interruptor
- (3) Disminución normal de la corriente a cero
- (4) Inestabilidad en el arco que no causa corte prematuro
- (5) Inestabilidad en el arco con corte prematuro
- (6) Oscilación inestable
- (7) Magnitud de la corriente al momento de corte (i_{ch})
- (8) Voltaje de supresión
- (9) Voltaje máximo de recuperación
- (10) Voltaje de alimentación



$$R_0 = \frac{U_0}{i_0}$$

$$R_1 = \frac{-\alpha R_0}{1 + \alpha}$$

$$L_0 = \frac{\Theta R_0}{1 + \alpha}$$

$$\frac{d^2 i}{dt^2} + \left(\frac{1}{\tau} + \frac{1}{\tau_2} \right) \frac{di}{dt} + \omega_0^2 i = 0$$

$$\tau_1 = L_0/R_1; \tau_2 = R_0 C; \omega_0^2 = \frac{R_0 + R_1}{R_0} \cdot \frac{1}{L_0 C}$$

$$i(t) = I e^{-t/\tau} \cos(\omega_i t + \phi)$$

$$1/\tau = \frac{1}{2} (1/\tau_1 + 1/\tau_2); \omega_i = \sqrt{(\omega_0^2 - 1/\tau^2)}$$

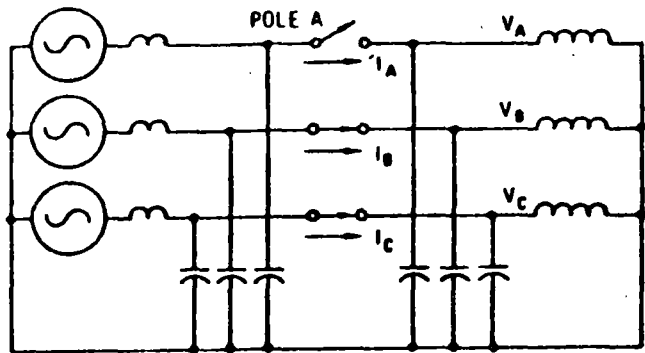
$$R_0 = \eta I_0^{-(\alpha+1)}$$

$$i_{ch}^{\alpha+1} = \frac{\alpha \eta C}{\theta}$$

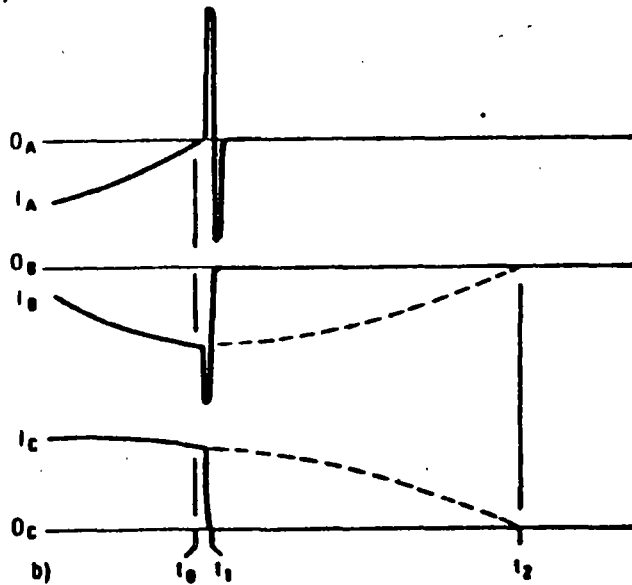
$$i_{ch} = \sqrt{\frac{\eta C}{\theta}}$$

$$\sqrt{\frac{\eta C}{\theta}} = \begin{cases} \text{oil-minimum} & (7 \dots 10) \times 10^4 \\ \text{SF}_6 & (4 \dots 17) \times 10^4 \\ \text{air-blast} & (15 \dots 20) \times 10^4 \end{cases}$$

Figura 19. Circuito equivalente y análisis del modelo estático del arco en un interruptor sujeto a corte prematuro de una pequeña corriente inductiva.



a)



b)

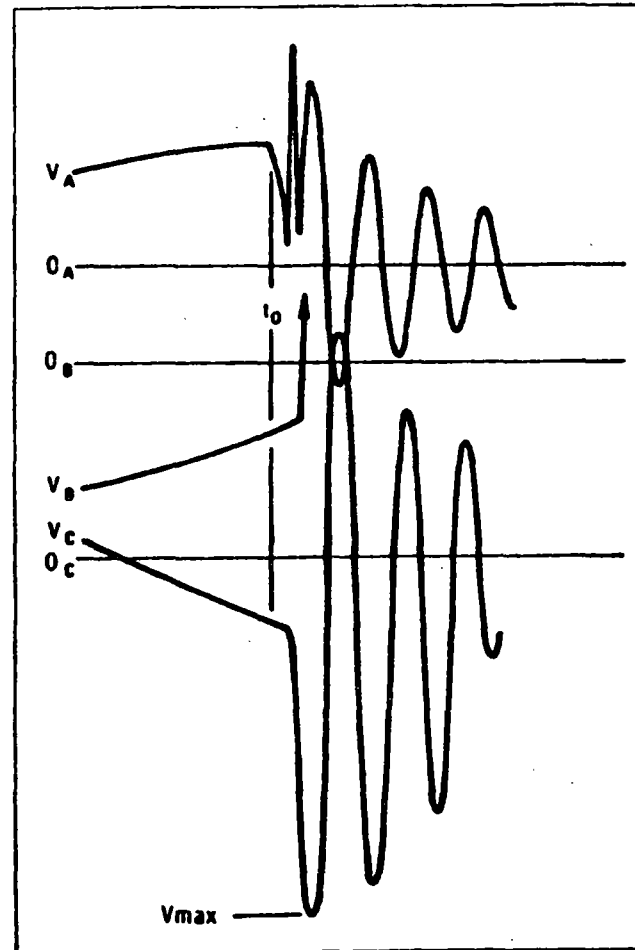


Figura 20. Corte virtual de corriente en un circuito trifásico con carga inductiva: a) circuito, b) corrientes, c) voltajes.

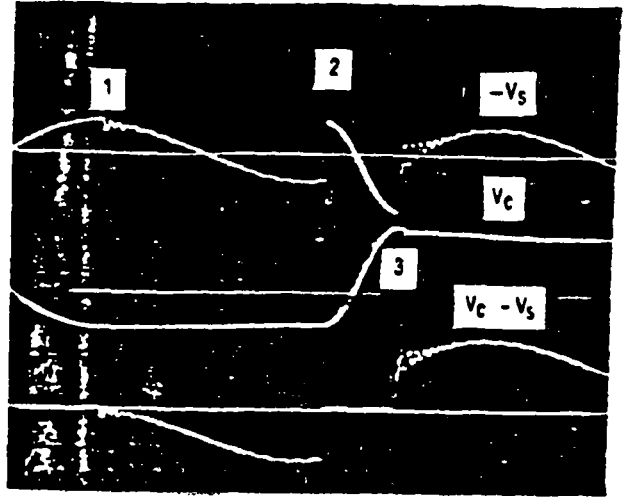
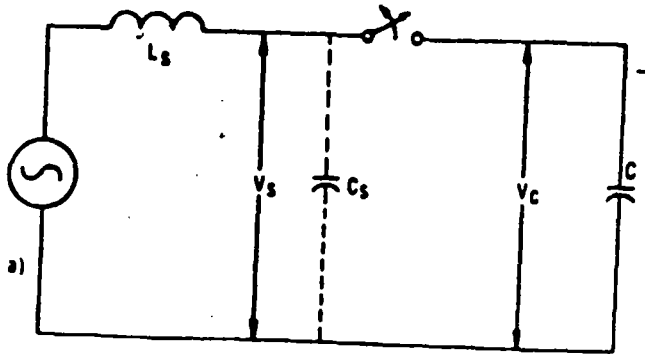


Figura 21. Maniobra en un circuito capacitivo a) circuito, b) voltajes en la fuente V_s , la carga V_c y voltaje de recuperación transitoria en el interruptor $V_c - V_s$.

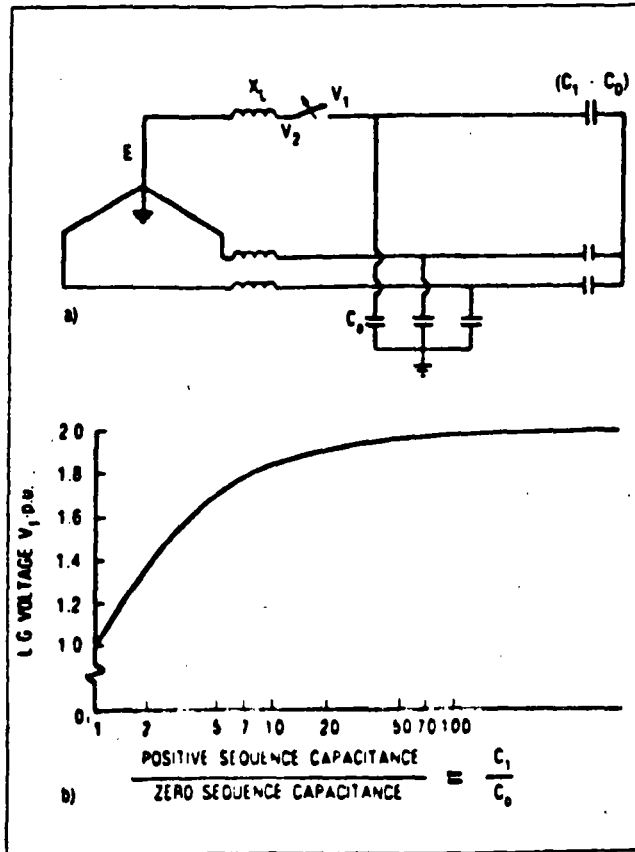


Figura 22. Factor de sobretensión producido al abrir una de las fases de un sistema trifásico con carga capacitiva, suponiendo que no hay reignición del arco: a) circuito, b) relación entre la sobretensión y las capacitancias de secuencias positiva y cero.

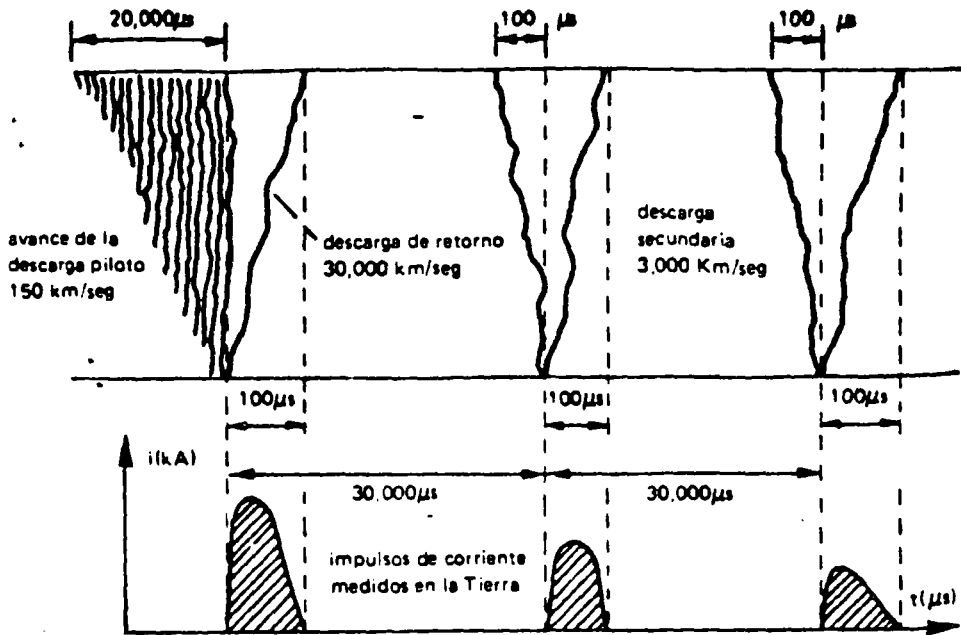


Figura 23. Representación gráfica de una descarga atmosférica formada por una guía descendente, primer rayo de retorno, guía flecha y rayos de retorno subsiguientes.

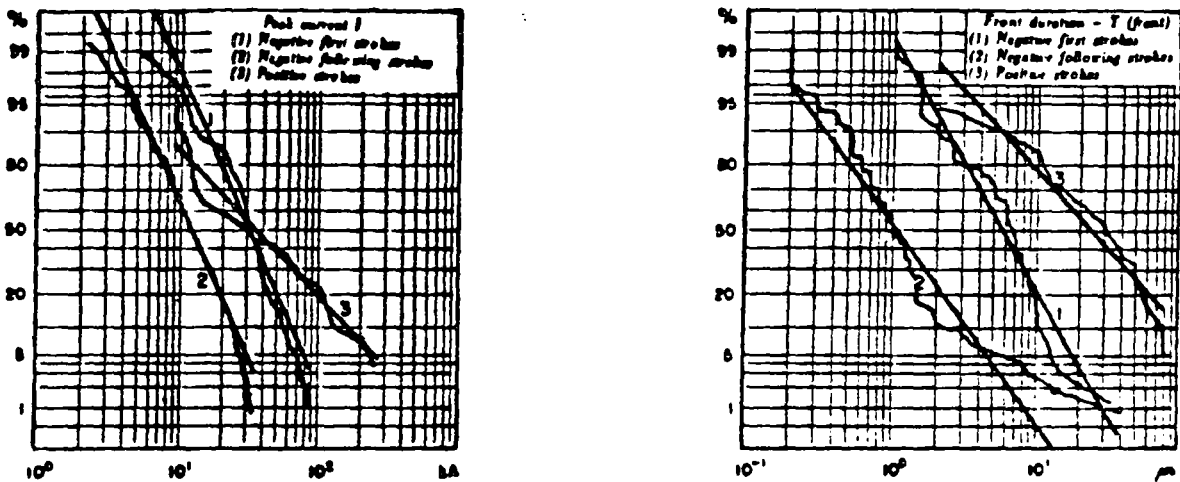


Figura 24. Distribuciones acumuladas de frecuencias para las magnitudes y tiempos en el frente de corrientes de rayos de retorno (obtenidas por Berger).

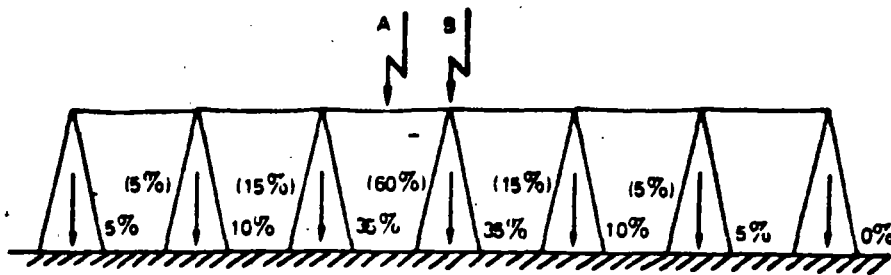


Figura 25. Distribución de la corriente inyectada a una línea de transmisión por una descarga atmosférica directa a la mitad de la distancia entre torres y directa a una de las torres.

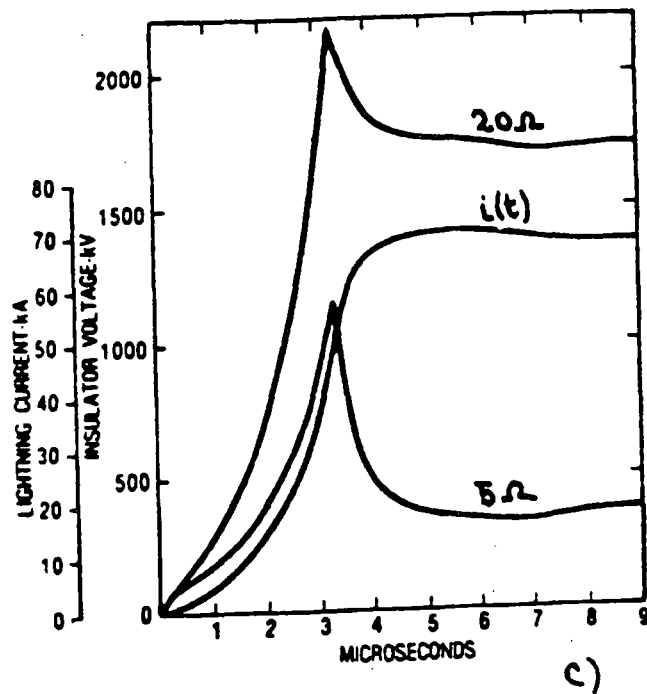
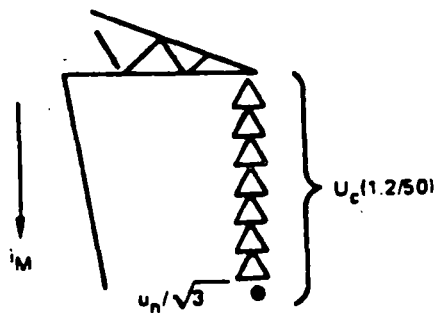
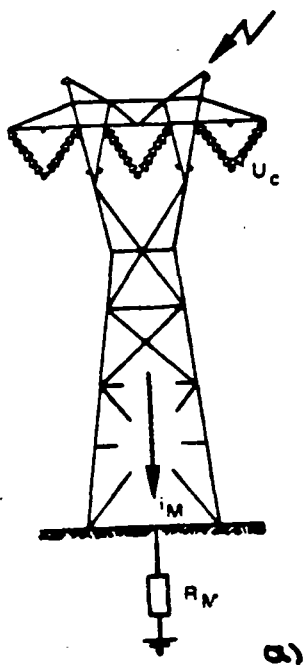


Figura 26. Descarga directa al hilo de guarda y la torre de transmisión: a) esquema, b) circuito equivalente, c) forma típica de la sobretensión producida en la torre para resistencias a tierra de 5 y 20 Ω y forma de onda de la corriente.

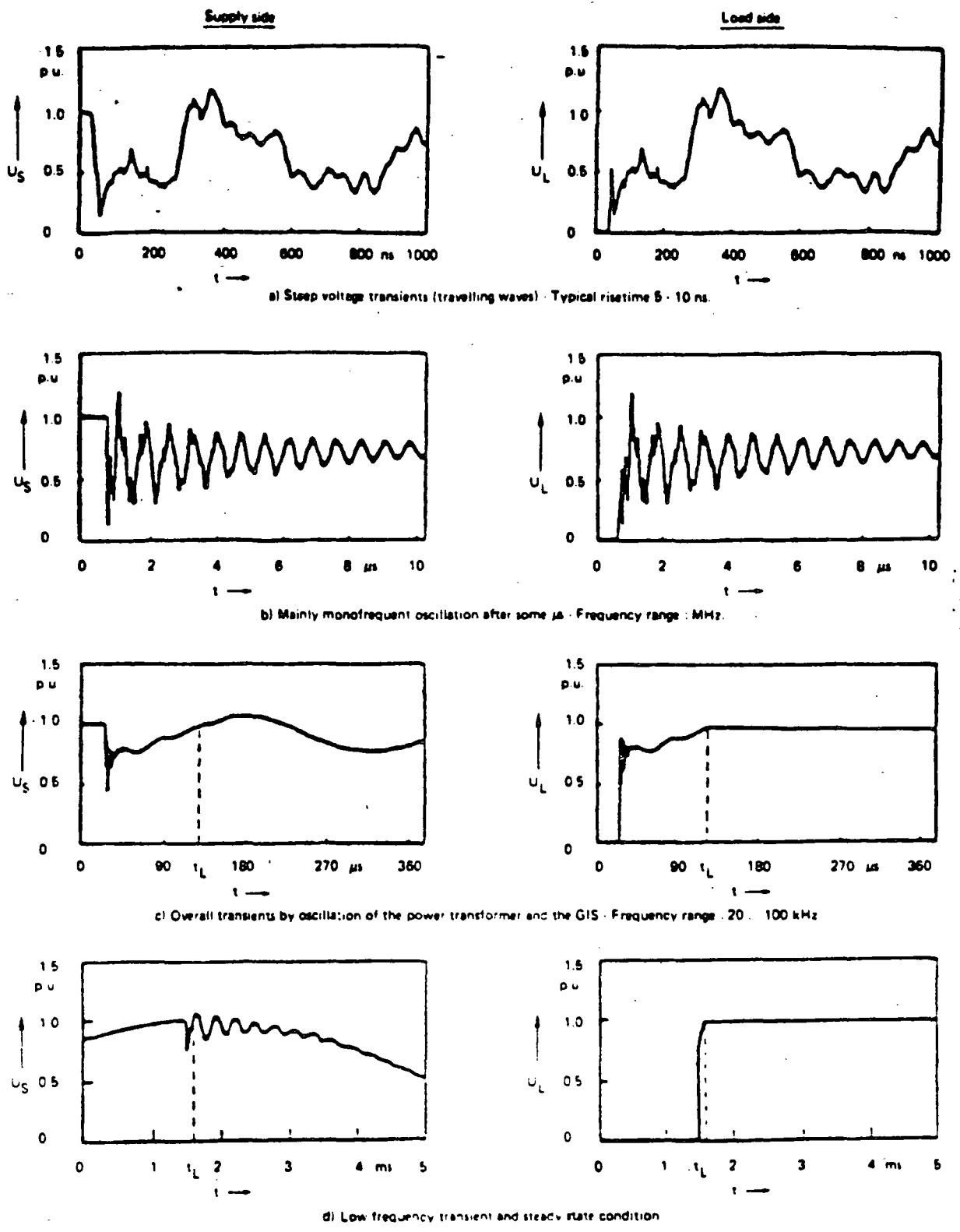


Figura 27. Algunas sobretensiones por maniobra, medidas en subestaciones aisladas con SF6.

LIGHTNING PERFORMANCE OF TRANSMISSION LINES

by J. G. Anderson

12.1 INTRODUCTION

The initiation of an insulator flashover by a lightning stroke is a very complex electromagnetic event. It involves poorly defined gas discharge physics, rapidly changing electromagnetic fields in which retardation plays a major role, nonlinear effects due to corona development on the conductors and on the tower itself, and frequency- and current-dependent impedances of the earth. To evaluate the problem, it must be simplified and linearized somehow. The degree of simplification depends on the availability of computational power and on the skills of the user in understanding what is really being done with the computational power available. A realistic simplification of the problem is also affected by the limited precision of the information about the problem excitation function, i.e., the lightning stroke itself. There is little point in computing the lightning response of a transmission tower with great accuracy if one knows only in a vague way what the lightning stroke is. Since the first edition of this book, substantial progress has been made by Uman *et al.* (1), Anderson (2) in South Africa, and others (3-6) in resolving the physical characteristics of the lightning flash and refining the statistics of its current waveshapes and magnitudes. Lightning statistics are notoriously non-Gaussian and imperfect, and much scientific intuition resides in the curves presently used by the industry. The complexity and multitudinous nature of these statistics spurred the successful development of computer Monte Carlo techniques to predict transmission-line lightning flashover probabilities (7). However, the techniques require the utilization of digital computers with substantial number-crunching capabilities and high speeds.

In this edition, the author has endeavored to supply the user with a step-by-step, linearized numerical solution that can be realized with nothing more powerful than a hand calculator. However, the repetitious nature of these calculations, which require that voltage be examined phase by phase and waveshape by waveshape, makes it almost mandatory that a programmable hand calculator be utilized to avoid setting up each equation over and over. The foundations of each step in the method are reviewed, with the more complicated mathematics relegated to appendices, and a step-by-step numerical example for a double-circuit tower is provided to guide the user. The procedure is fairly long, but not overly complicated, and utilizes all the rigor that appears feasible for a hand calculator.

12.2 PROBLEMS OF ACCURACY

There are few absolutes in the computation of lightning flashovers of transmission lines. For the most part the engineer is dealing in statistics. A line with a computed average flashover rate of 1.0 per 100 miles per year may easily exhibit 2.0 per 100 miles for the first year, none for the second year, and 3.0 for the third year, and still have a long term average of 2.0. In terms of protective relaying and reliability planning, it is important to know the probability of the actual flashover rate exceeding some specified value in any given year. To determine these probabilities, one must turn to binomial statistics.

When a lightning flash makes contact with a line, there are only two possible outcomes: success (no flashover) or failure (flashover). A basic theorem of binomial statistics states that if the probability of success (no flashover) for a single flash is p , then for n flashes to the line, the probability that there will be exactly k successes and $n - k$ failures is given by

$$P_k = \frac{n!}{k!(n-k)!} p^k q^{n-k} \quad (12.2.1)$$

where p is the probability of a success and q equals $1 - p$, which is the probability of a flashover.

Equation 12.2.1 provides the key to evaluating the theoretical flashover probabilities for any given year. Under service conditions, one can determine an actual flashover rate only by keeping outage records from year to year and gradually gaining an impression of the effectiveness of the design. However, until one accumulates enough data, these impressions may be misleading, sometimes resulting in initiation of corrective actions to a line that was actually of good design but was subject to unfortunate circumstances after it was first energized. As a practical case, assume that a new line with a length of 100 miles is built, that the line is designed to have a flashover rate of 1.0 per 100 miles per year, and that the line is located in an area with a keramic level such that 100 flashes contact the line in an average year. Then, the probability, q , of a flash causing flashover is $1/100 = 0.01$.

For the total sample size, n , of 100 flashes, Eq. 12.2.1 yields the following probabilities:

Flashover Rate ($n-k$) Per 100 Miles Per Year	Probability (P_k) That This Rate Will Be Observed
0	0.366
1	0.369
2	0.185
3	0.061
4	0.015

Thus, the probability of observing a flashover rate of zero is about the same as of observing the true flashover rate of 1.0 per 100 miles per year. If one sums the probabilities, then about 27% of the time there would be a flashover rate of at least double the true rate. This, of course, is for a constant sample size of 100 flashes to the line each year. But ground-flash density varies from year to year over a range of 2.0 to 1.0 or even more, thus further expanding the observed flashover rates. Curve A of Figure 12.2.1 shows the lightning flash incidence to a 110-kV line observed by Popolansky (8) over a period of 10 years. The average incidence was 46.8 flashes per 100 kilometers per year, varying between a minimum of 20 and a maximum of 92. If the line had been designed to have a true flashover probability of $P = 0.01$ per flash, then the most probable flashover rate over the 10-year period would have been 0.468 per 100 kilometers per year. However, whenever the lightning flash incidence to the line dips below 50 in a given year, the probability of even one lightning flashover occurring in that year drops below 0.5. Consequently, the observer may record none at all. At most, one could expect only about one flashover a year in those years of higher lightning incidence. If the assumption is made that one flashover occurs in each year designated as a higher-lightning-incidence year, there would be four flashovers in the 10 years, resulting in a flashover rate of 0.4 per year, which is not far from the most probable or ideal rate of 0.468. However, if one kept a running tally of the observed flashover rate, it would appear as curve B of Figure 12.2.1. The observed flashover rate begins to converge on its true value in about 10 years. It should be noted that for the first 2 years the line had no flashovers at all.

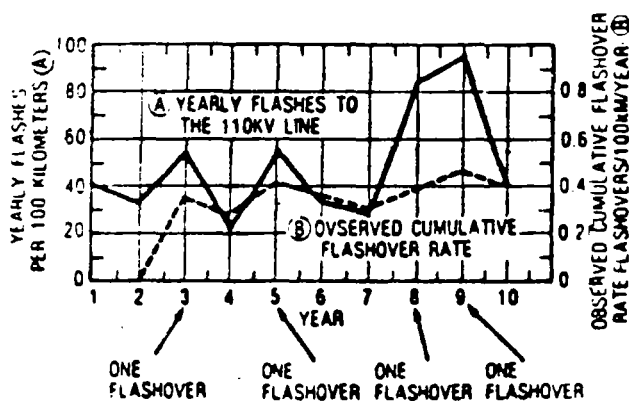


Figure 12.2.1. Observations of lightning performance of a 110-kV line by Popolansky (8).

From the application viewpoint, the conclusion is that good accuracy at low flashover rates is not possible, either from digital models (statistically) or from observation in the field. Precision in statistics requires a large data base, but for lightning flashover calculations this large data base is simply not available. Despite this, observable or computable trends may still serve to guide the user in choosing among the alternatives to achieve the lowest possible outage rate consistent with economic reality. There are trade-offs in cost (as well as in flashover rates) between adding insulation and reducing footing resistance that may be considered so as to gain the greatest improvement for the least money. Flashover calculations may also guide other choices, such as choice of tower height, of additional ground wires, and of tower construction.

12.3 TERMINOLOGY

Over the last century, a plethora of terms has evolved to describe the physics of lightning and lightning effects. The same words have been defined differently, and different words have been applied to the same referents. Especially in the United States, the engineering terminology has been neither specific nor concise. In this chapter, European usage is followed whenever feasible, and, in particular, one should note the following terms:

- Flash—a term encompassing the entire electrical discharge from cloud to stricken object.
- Flashover—an electrical discharge completed from an energized conductor to a grounded support. It may clear itself and not trip a circuit breaker.
- Stroke—the high-current components in a flash. A single flash may contain several strokes.
- Tripout—a flashover of a line that does not clear itself. It must be cleared by operation of a circuit breaker.

12.4 LIGHTNING FLASH PARAMETERS

The basic concepts that appear in any computation of lightning flashovers of transmission lines divide broadly into the concepts of incidence (the appearance of lightning on the line) and the concepts of response (the voltages created on the line by the flash when it occurs). Knowledge of the latter concepts is more complete because they are more easily studied in the laboratory, whereas knowledge of the former relies primarily on incidental observations and inferences both from records and from field measurements.

KERAUNIC LEVELS AND ISOKERAUNIC MAPS

Any locality through which transmission lines must pass may be said to have a certain keraunic level, or isokeraunic level, as it is usually called. The level represents the average number of thunder days per year at that locality, i.e., the average number of days per year on which thunder will be heard during a 24-hour period. The keraunic level may be determined by referring to the isokeraunic maps prepared by the U.S. Weather Bureau (Figure 12.4.1) in which lines of constant keraunic level are plotted in a manner similar to the altitude contour lines on a topographic map. These lines of constant keraunic level are known as isoke-

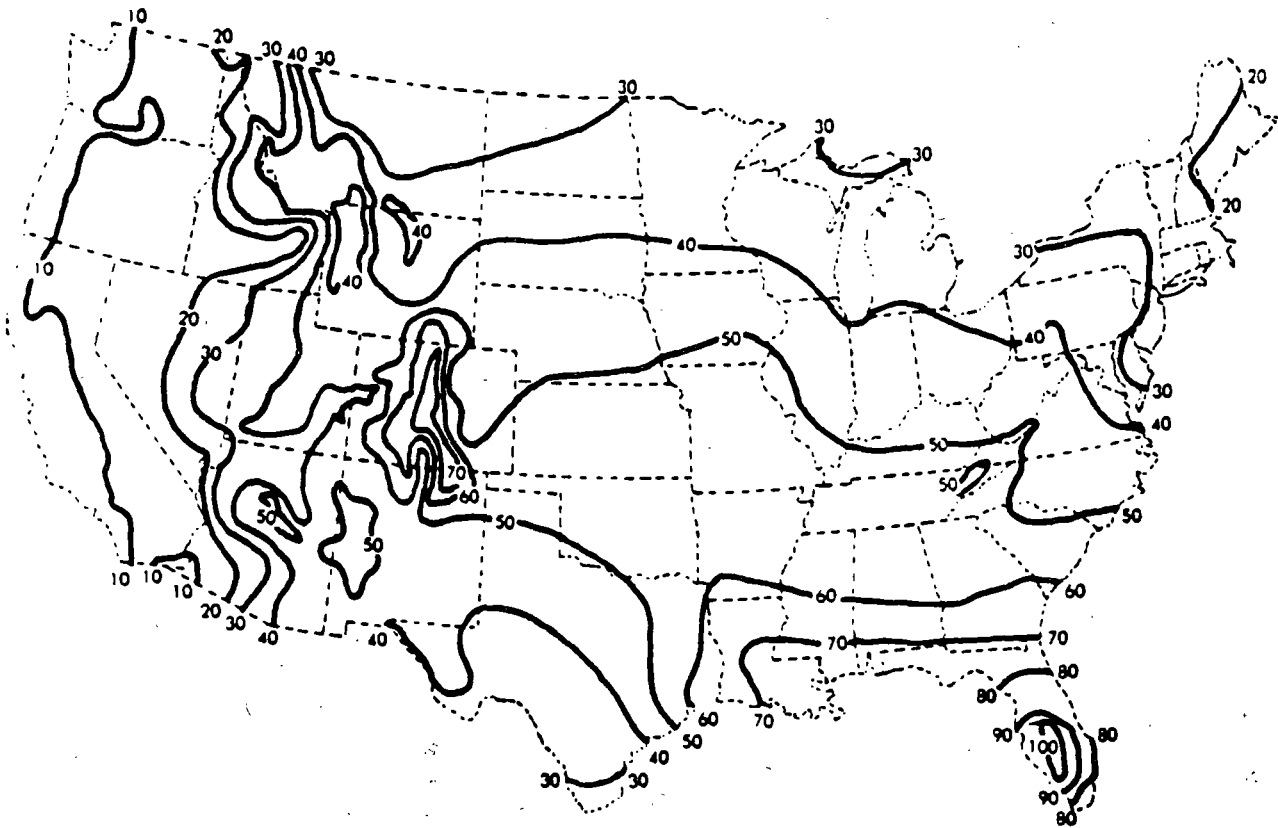


Figure 12.4.1. Isokeraunic map showing mean annual days of thunderstorm activity within the continental United States.

raunic lines, and the keraunic level in any region may be approximated by interpolating between the isokeraunic lines on these maps.

The keraunic level is a statistic that obviously depends on the hearing ability of the weather observers, on ambient noise backgrounds and local geography, and on a conscientious completion of weather records. If two thunderstorms occur in any day, the day is still classified as one thunder-day, and the deviation of the number of thunder-days about the mean and their duration—statistics important in establishing confidence limits for a design—are not usually reported.

The U.S. Weather Bureau now keeps hourly weather records at all first-order weather stations, and these records are available on magnetic tapes or punched cards. Such observations permit the construction of isokeraunic maps based on thunder-hours rather than days and, when such maps are ultimately developed, the finer resolution should sharpen the lightning computation processes. The finest resolution will occur when research is completed on counting the actual number of cloud-to-ground strokes in thunderstorms.

The keraunic level is the basic statistic that must be known for a given geographical region before the lightning incidence to earth and to any transmission line in that region can be computed. To a first approximation, the error in determining this important parameter will make a proportionate error in calculation of lightning performance.

NUMBER OF FLASHES TO EARTH

For simplicity, it has usually been assumed that the number of flashes to earth or to a transmission line in a specified locality

is roughly proportional to the keraunic level (annual thunder-days) in that locality. Prentice (9) has presented a comprehensive summation of the research on relationships between flash counts to earth and the keraunic level. Table 12.4.1, taken from Prentice, shows that most researchers have arrived at a proportional relationship ranging from 0.17 to 0.19T ground flashes per square kilometer per year where T is the keraunic level in annual thunder-days. The average ground-flash density in Table 12.4.1 is 0.14T for those observations with no exponent for T. The first edition of this book used a value of 0.17, which made an allowance for reduced numbers of flashes to lines due to shielding by trees and undulating terrain (10). In open country, the 0.14T relationship would hold. As a compromise, it is suggested that

$$N = 0.12T \tag{12.4.1}$$

where N is the number of flashes to earth per square kilometer per year and T is the keraunic level in thunder-days per year in the area or,

$$N_m = 0.31T \tag{12.4.2}$$

where N_m is the number of flashes to earth per square mile per year. For all lightning calculations in this chapter (and in most published methods), the number of lightning flashes to earth or to a transmission line will be proportional to the keraunic level.

INTERCEPTION OF FLASHES BY THE LINE

A transmission line passing above the earth may be said to throw an electrical shadow on the land beneath. Lightning

Table 12.4.1
EMPIRICAL RELATIONSHIPS BETWEEN LIGHTNING GROUND-FLASH DENSITY AND ANNUAL THUNDER-DAYS (*T*)

Location	Ground-Flash Density (km ² yr ⁻¹)	Reference
India	0.17	Aiya (1968)
Rhodesia	0.147	Anderson and Jenner (1954)
South Africa	0.0237 ^{1.03}	Anderson/Eriksson (1981)
Sweden	0.0047 ^{1.0} (approx.)	Müller-Hillebrand (1964)
U.K.	a ^{0.9}	Stringfellow (1974) [a = 2.6 ± 0.2 × 10 ⁻² ; b = 1.9 ± 0.1]
U.S.A. (North)	0.117	Horn and Ramsey (1951)
U.S.A. (South)	0.177	Horn and Ramsey (1951)
U.S.A.	0.17	Anderson and others (1968)
U.S.A.	0.157	Brown and Whitehead (1963)
U.S.S.R.	0.0367 ^{1.03}	Kolokolov and Pavlov (1972)
World (temperate climate)	0.197	Brooks (1950)
World (temperate climate)	0.157	Goide (1966)
World (tropical climate)	0.137	Brooks (1950)

flashes that would generally terminate on the land inside the shadow will strike the line instead, whereas flashes outside this shadow will miss the line entirely. Figure 12.4.2 shows a simple approximation for the width, *W*, of this shadow for a line with two shield wires. For a line with only one shield wire, *b* becomes zero. The height, *h*, in Figure 12.4.2 is the mean shield wire height of the line, not the towers, and is given by

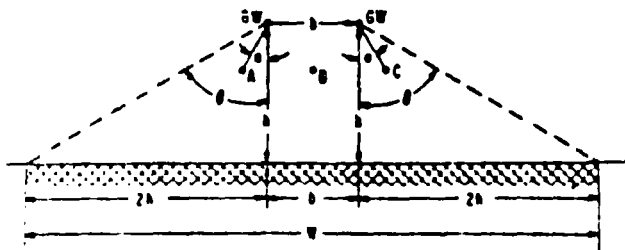
$$h = h_g - 2/3 (h_g - h_{pm}) \quad (12.4.3)$$

where *h_g* is the height of shield wires at the tower and *h_{pm}* is the shield wire midspan clearance to ground. After *h* has been determined, then the shadow width is given by

$$W = b + 4h \quad (12.4.4)$$

The preceding is a simplistic representation of the shadow width justified only by the meager, available knowledge of the true mechanism involved. Whitehead (11) has reviewed other more complicated approximations for this shadow width and has suggested a modification of Eq. 12.4.4 that yields a better correlation with magnetic link data. This revised relation is

$$W = b + 4h^{1.09} \text{ m} \quad (12.4.5)$$



- θ - shadow angle (assumed 63°; degrees)
- γ - shield angle between shield wire and phase conductor
- W - shadow width on earth's surface
- GW - shield wire location
- A, B, C - phase wires

Figure 12.4.2 Width of right-of-way, shielded from lightning strokes (horizontal single-circuit line with two shield wires).

Equation 12.4.5 is used for subsequent calculations, and combining it with Eq. 12.4.1, the relationship for the number of flashes to the line becomes

$$N_L = 0.0127 (b + 4h^{1.09}) \quad (12.4.6)$$

where *N_L* is the number of flashes to the line per 100 kilometers per year and *T* is the keraunic level in thunder-days per year.

LIGHTNING FLASHES TO SHIELD WIRES AND TOWERS

All the equations in this chapter and in most of the chapter appendices are based on the assumption that the lightning flash contacts the tower top. In fact, the equations for flash frequency to the line, e.g., Eq. 12.4.6, are derived on the basis of equal probabilities of flashes appearing anywhere along the line, including midspan. However, the towers tend to attract a somewhat greater proportion of strokes because they are higher, and the midspan area attracts less because it is closer to the earth. The towers are also more massive, tending to increase their proportionate share. The farther the flash terminates away from the tower (on the shield wire), the less is the stroke current eventually entering the tower top, and, in midspan, the current splits and only half of it arrives at the towers at the ends of the stricken span. At first glance, it appears that a stroke to a shield wire at midspan would very likely create a midspan flashover to the nearest phase conductor. However, Wagner and Hileman (12,13) examined this process in 1964 and found that the very heavy predischARGE currents that develop must inhibit midspan flashover long enough for current reflections to arrive from the adjacent towers, thus reducing the midspan voltage below the flashover level. This process has since been confirmed for larger conductor-to-conductor gaps (14), and it is fairly certain that midspan lightning flashovers are quite uncommon.

For lack of a better procedure, the author has adopted guidelines assuming that 60% of the flashes contacting a line are near enough to a tower to be considered a tower flash and that the remaining 40% are far enough out on the span to cause no damage. The actual flash frequency to towers is then

$$N_T = 0.6 (N_L - N_S) \quad (12.4.6A)$$

where N_L is the total number of flashes to the line per 100 kilometers per year and N_S is the total number of flashes causing shielding failure per 100 kilometers per year. For wood pole lines, the 60% tower flashes must be reduced because of the lessened attractive effects of the wood structures. A value of 40% is suggested.

FLASHES TO TALL STRUCTURES

Relationships such as that expressed by Eq. 12.4.5 are substantially lower for very tall objects. For example, New York City has a keraunic level of about 27, and, in 1947, the Empire State Building was about 396m high to the top of its mast. Using the same concepts presented in Figure 12.4.2, the number of flashes to the building per year would be 1.35. However, the author has observed as many as 12 flashes to the building in a single storm, and the yearly average is almost an order of magnitude higher than 1.35. The discrepancy is partially due to the changing of the flash mechanism for very high objects: above 60m flashes can trigger from the stricken object itself instead of from the cloud overhead. Consequently, flash frequency increases sharply. However, Eq. 12.4.6 should be adequate for all except the tallest transmission towers, such as those at river crossings.

PROBABILITY DISTRIBUTION OF STROKE AMPLITUDES

The stroke-current amplitudes within a lightning flash are described in terms of probabilities. These probabilities become more sharply resolved each year as the increasing volume of data on stroke-current amplitudes from various research projects enter the main stream of evaluation work. Particular attention should be called to the work of Berger and others in Switzerland (3), Anderson and his associates in South Africa (5), Uman and his associates (1), Cianos and Pierce (4), Popolansky (8), and Szpor and his associates (15).

The following material is based largely on a summation of the present knowledge of stroke-current amplitudes and waveshapes prepared by Anderson and Eriksson (5) in 1979 for presentation to CIGRE Study Committee 33 on overvoltages and insulation coordination.

- Multiple Stroke Flashes: About 55% of flashes have more than one stroke, and about 90% of the flashes will not exceed eight strokes. The mean number of strokes per flash may be assumed to be three.
- Flash Peak Current Amplitudes: In 1972, Popolansky (16) published a cumulative probability curve of 624 peak current measurements of lightning flashes from investigations in Europe, Australia, and the United States. A log normal approximation of this curve is shown in Figure 12.4.3, in which the approximate median current, \bar{I} , is 25 kA and $\sigma_{\log I}$ is 0.39. This evaluation was used in the first edition of this book for shielding failure strike distance determinations. However, over 50% of these measurements were on chimneys of unspecified height and also included positive peak currents from Mount San Salvatore, which were not really downward flashes of the type expected to transmission lines in open country. Therefore, Anderson and Eriksson (5) recently developed a modified curve containing only downward flashes to structures less than 60 m in height, for which 338 records were available. The resulting curve is also shown in Figure 12.4.3. This log normal approximation has a median current, \bar{I} , of 31 kA and a $\sigma_{\log I}$ of 0.30.

mal approximation has a median current, \bar{I} , of 31 kA and a $\sigma_{\log I}$ of 0.30.

For lightning flashover computations using a small calculator, the statistical log normal curve is much too complex, but these log normal curves may be approximated with quite reasonable accuracy between 5 kA and 200 kA with two simple equations. For the Popolansky curve,

$$P_f = \frac{1}{1 + \left(\frac{I}{25}\right)^2} \tag{12.4.7}$$

and for the Anderson-Eriksson curve,

$$P_f = \frac{1}{1 + \left(\frac{I}{31}\right)^{2.6}} \tag{12.4.8}$$

where P_f is the probability that the peak current in any flash will exceed I in kiloamperes. Equation 12.4.8 is used as the basis for all stroke-current magnitude calculations in this chapter, for both back-flashover and shielding failure. Positive flashes are comparatively rare and are not included in the analysis.

STROKE WAVESHAPES PARAMETERS INFLUENCING FLASHOVER

The waveshapes of the stroke currents within lightning flashes to power lines play an important role in the development of voltages across the line insulators, particularly for taller structures, for which the surge impedance has a magnifying effect.

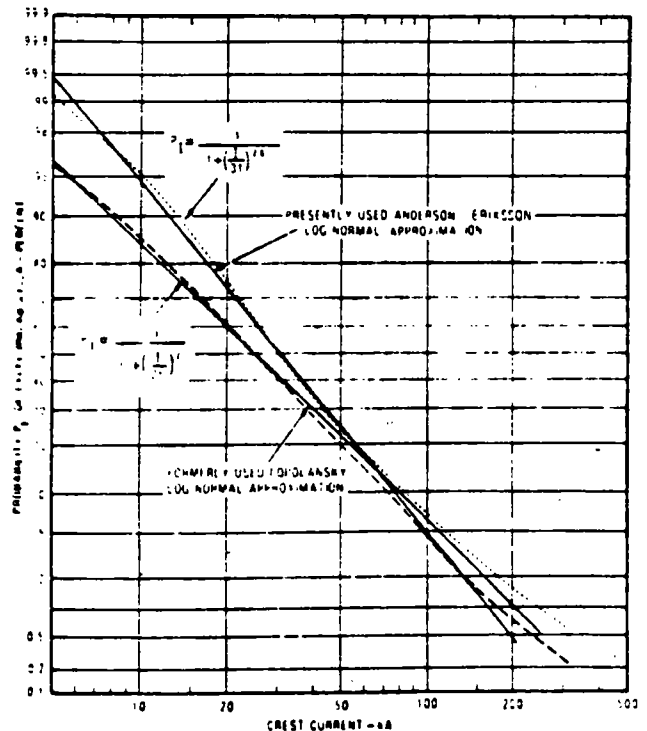


Figure 12.4.3. Cumulative frequency distribution of peak current amplitudes in downward negative flashes.

The most comprehensive waveshape data for these high current peaks have come from the work of Berger and associates (3) at San Salvatore. These data have been augmented by records from many other localities (2). The following material is primarily derived from Berger's negative-flash-to-earth data because negative flashes are the principal troublemakers for transmission lines.

COMPOSITE WAVESHAPES

The first stroke-current waveshape in a flash tends to rise more gradually to crest than the waveshapes in subsequent strokes. Figure 12.4.4 shows composite waveshapes of the first and subsequent strokes developed by Anderson and Eriksson from a computer blending of many Mount San Salvatore strokes and other records. Clearly, the subsequent stroke wavefront has the capability to create higher voltage on a transmission tower during its rise to crest than the first stroke, provided it has sufficient amplitude. However, it also has a tail that tends to fall off rapidly, helping to relieve any voltage that is developed. Weck and Hileman (17) have shown that the amplitudes of the first and subsequent strokes were statistically independent in 29 records examined. The amplitudes of subsequent strokes are much lower, having a median value of approximately 12 kA.

In the general case, there may be times when the first stroke dominates the flashover phenomenon, as well as times when the subsequent stroke is dominant, usually for tall towers. The inclusion of both in an algorithm for flashover computations is quite practical, but only if one has, in advance, some estimate of the likelihood that a subsequent stroke will occur at all. The re-

ported incidence of single-stroke flashes varies from 76% in Switzerland (3) to about 25% in South Africa (5), and an average, weighted single-stroke incidence of 45% is suggested (5). Consequently, a subsequent stroke would appear 55% of the time. However, it certainly will not be dominant every time it appears. The author has concluded by numerical experimentation that, for typical transmission lines, the subsequent stroke is not likely to be dominant more than 20% of the time primarily because its overvoltage-generating effects are of fractional microsecond duration at a time when the volt-time strength of an insulator string is extremely high.

Figure 12.4.5 shows one example of numerical experimentation for voltages across an insulator string on a transmission tower when strokes with various front times, but equal crest amplitudes, contact the tower. A standard volt-time curve is adjusted so that it just touches curve C, cresting in 1.8 μs (18, 19). The voltage waves for the shorter stroke front times, then, do not reach the volt-time curve at which flashover could occur. In addition, volt-time curves are usually obtained with a constant 1.2 × 50-μs waveshape. The author's experience suggests that, if the volt-time curve had been obtained by changing the applied waveshape according to waves A, B and C, then the volt-time curve at A would have been even higher. Hence, for all practical calculations, this chapter ignores the contribution of second strokes to transmission-line lightning performance. However, the computational routine has been made sufficiently general so that effects of second strokes may be included whenever desired, particularly for river crossings.

If a computer is to resolve the voltage effects of the current waveshapes of Figure 12.4.4, there is great merit in representing the waveshapes by expressions that are as simple as possible, yet consistent with reality. This is particularly true for a hand calculator. For the practical case, the meanderings of the currents down near the beginning of the stroke-current waveshape have little effect on the flashover of the line insulators; it is the crest current and the rapidly rising frontal currents near crest that play the key role. Hence, a realistic, but very simple, approximation to the composite current waveshape is possible by using the ramp current wave shown in Figure 12.4.6. The ramp should be selected so that its slope is approximately equal to the maximum, or near maximum, observed di/dt on the front of the actual wave. The front time, t_f , is then fixed.

However, the probabilities for the maximum di/dt of the stroke front are reasonably well defined (see Figure 12.4.7). Again, a relatively simple equation provides a reasonable approximation:

$$P_{di} = \frac{1}{1 + \left(\frac{di/dt}{24}\right)^4} \quad (12.4.9)$$

where P_{di} is the probability that a specified value of di/dt will be exceeded and di/dt is the specified maximum rise time in kiloamperes per microsecond.

In lightning voltage analysis of transmission lines, a front time, t_f , must be selected in advance. Voltages will then be directly proportional to stroke-current amplitude. However, if t_f is fixed and a ramp-function, idealized stroke current is used, then selecting a stroke-current amplitude in accordance with the probability relationship of Figure 12.4.3 also fixes the frontal di/dt , but this must then meet the probability relationship in Figure 12.4.7. Hence, to meet both probability relationships,

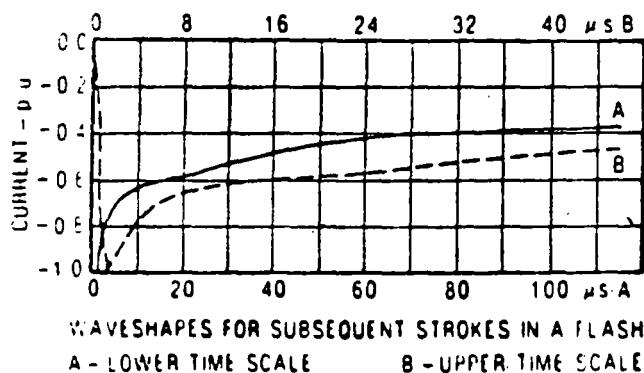
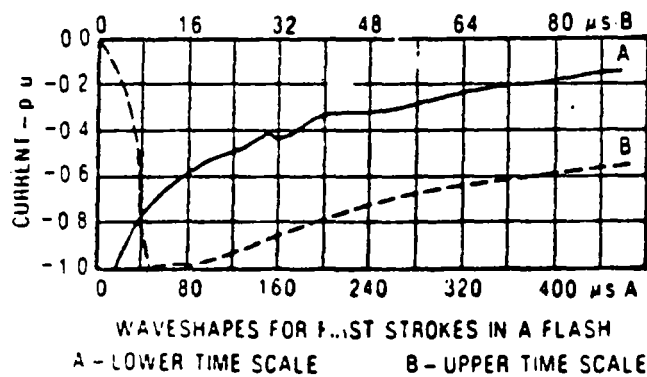


Figure 12.4.4 Mean current waveshapes from lightning to Mount San Salvatore, Switzerland.

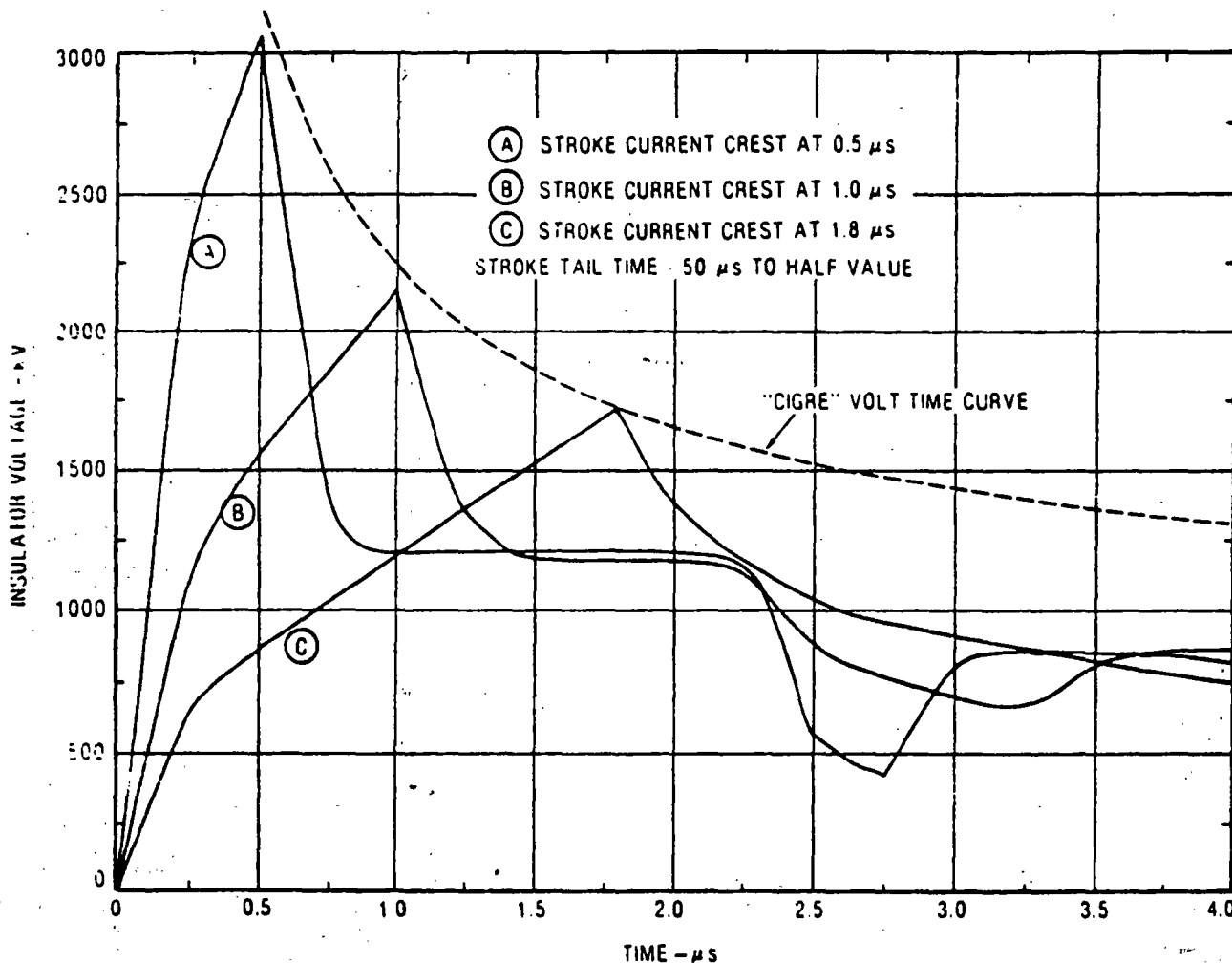


Figure 12.4.5. Effect on insulator voltages of stroke currents with various front times but equal amplitudes.

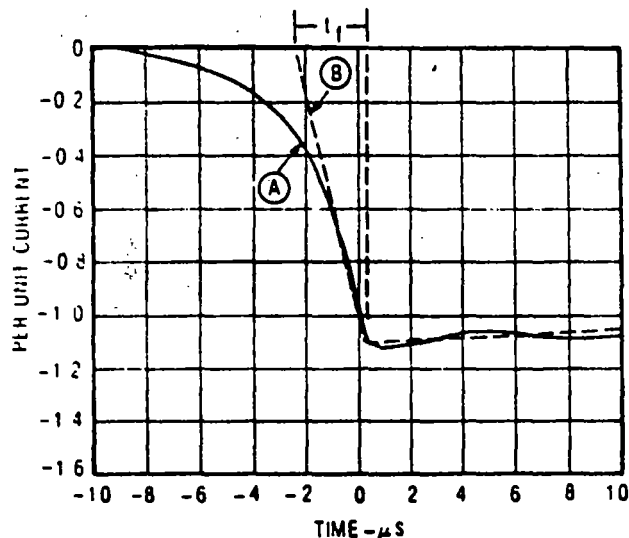


Figure 12.4.6. Anderson-Eriksson computer synthesis of a median current wavefront for negative first strokes. A, and a ramp current approximation to it, B.

t_f may have certain unique values only. Figure 12.4.8 shows the relationship that must exist. For example, assume that a ramp-function wave with a front time of 1.5 μs to crest is selected, that stroke-crest amplitudes are then varied according to the probability curve of Figure 12.4.3, and that one observes the resulting probabilities of occurrence of the front di/dt . Then, only at a stroke current of 47.5 kA will the rate of rise probability required by Figure 12.4.7 be met, and this rate of rise will be about 32 kA/ μs . Fortunately, for analysis with a hand calculator, the currents causing flashover of a transmission tower usually range from about 50 kA to 200 kA (beyond 200 kA no adequate data exist). Figure 12.4.8 shows that these currents require a front time somewhere between 1.5 and 2.5 μs for the calculations. Flashover effects do not exhibit great front-time sensitivity within this range.

FRONT AND TAIL CONSTANTS

Regardless of the choice of front time, the stroke-current waveshape, when reflection from the adjacent towers are not present, may be expressed for mathematical convenience as the sum of two simple ramp functions having slopes A_1 and A_2 (see

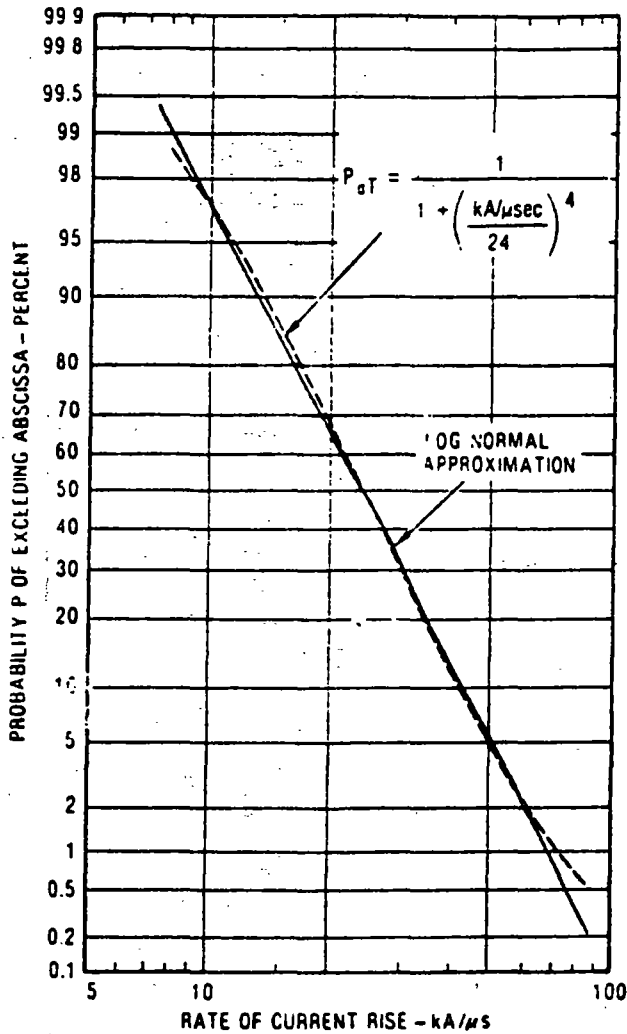


Figure 12.4.7. Log normal approximation from data (75 observations) on maximum rate of rise of negative first strokes (Anderson-Eriksson) and a simple approximation of it.

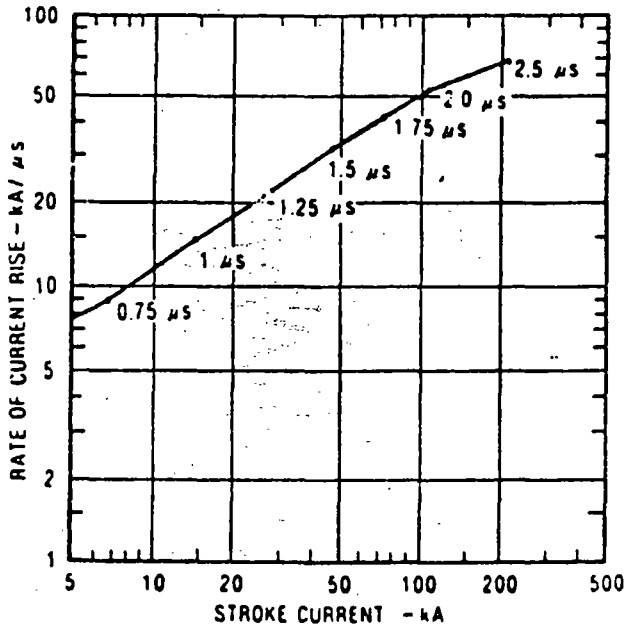


Figure 12.4.8 Required relationships between crest current, frontal rate-of-rise and time-to-crest of a ramp-function, stroke-current wave to meet probability requirements. Curve computed from the approximation equations of Figures 12.4.3 and 12.4.7.

Figure 12.4.9) where A_1 is the slope, or rate of rise, of the front and A_1 plus A_2 is the slope of the tail. Table 12.4.2 shows values of A_1 and A_2 for a per unit current wave having a crest of 1 kA and various front times, t_f . The time-to-half value of the tail, t_x , is assumed to be 50 μ s.

For an infinite tail A_2 equals $-A_1$. For any combination of A_1 , front time, t_f , and time-to-half value, t_x

$$A_2 = \frac{0.5 - A_1 t_f}{t_x - t_f} \quad (12.4.10)$$

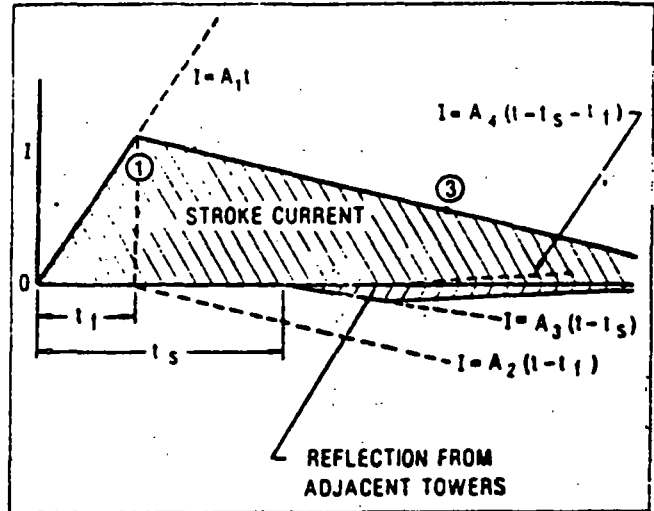


Figure 12.4.9. The total stroke current can be reduced to the sum of four ramp functions: t_f = time-to-crest; t_s = round-trip travel time (at the velocity of light) between the stricken tower and an adjacent tower.

Table 12.4.2
CHOICE OF WAVES OF A_1 AND A_2

Front Time, t_f (μ s)	A_1 (kA/ μ s)	A_2 (kA/ μ s)
0.75	1.33	-1.34
1.0	1.00	-1.01
1.25	0.80	-0.81
1.50	0.67	-0.68
1.75	0.57	-0.58
2.00	0.50	-0.51
3.00	0.33	-0.34

12.5 CIRCUIT ELEMENTS INVOLVED IN COMPUTATION OF FLASHOVER PERFORMANCE

After the stroke probabilities and waveshape requirements have been established, the circuit components that affect the lightning response can be quantified. Figure 12.5.1 shows the basic elements involved in establishing the voltages across the insulator strings. Some of these elements are influential in establishing the back-flashover rate (due to a stroke to the tower or shield wires), and others influence the shielding failure performance (when a stroke misses the shield wires and strikes a phase conductor instead). The step-by-step procedure presented next is

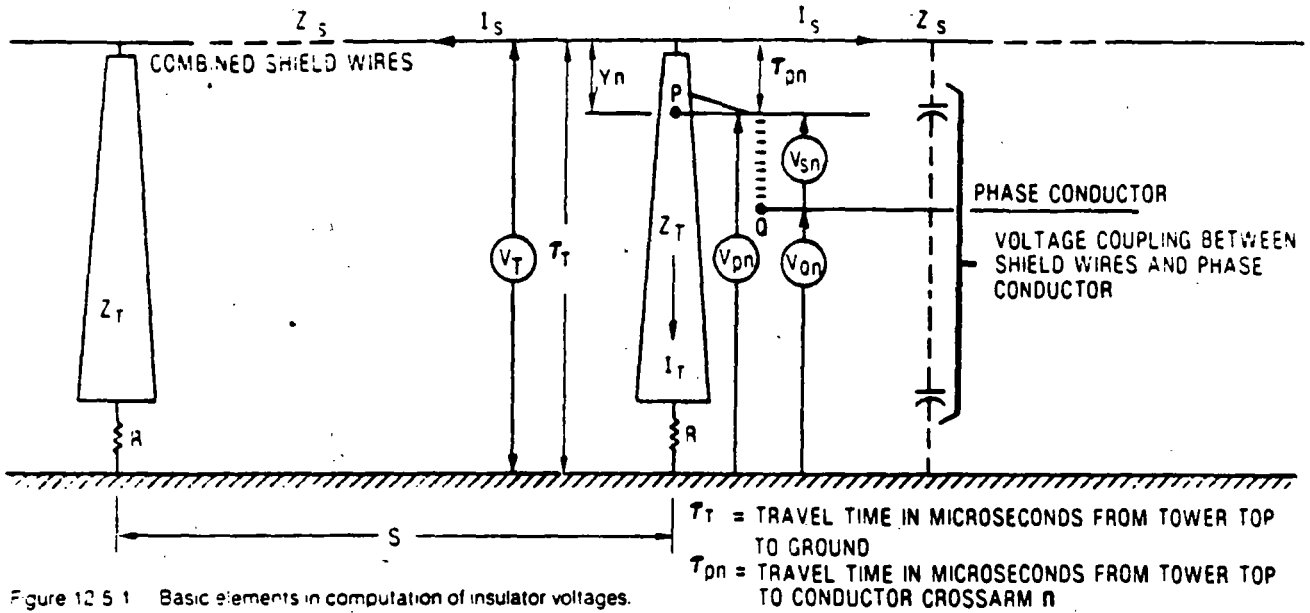


Figure 12.5.1 Basic elements in computation of insulator voltages.

more or less in the order one would follow to solve for the flashover rate.

REDUCING BUNDLE CONDUCTORS TO EQUIVALENT SINGLE CONDUCTORS

To make the problem more tractable, it is suggested that each bundle conductor be reduced to an equivalent single conductor.

This is done by assuming that the single conductor will carry the same charge and voltage to ground as the bundle and will be located where the center of the bundle was located. The derivation is found in Appendix 12.1. Figure 12.5.2 provides a conversion curve for two-, three-, or four-conductor bundles having conventional 18-in. subconductor spacing. The more general formula derived in Appendix 12.1 for symmetrical bundles is

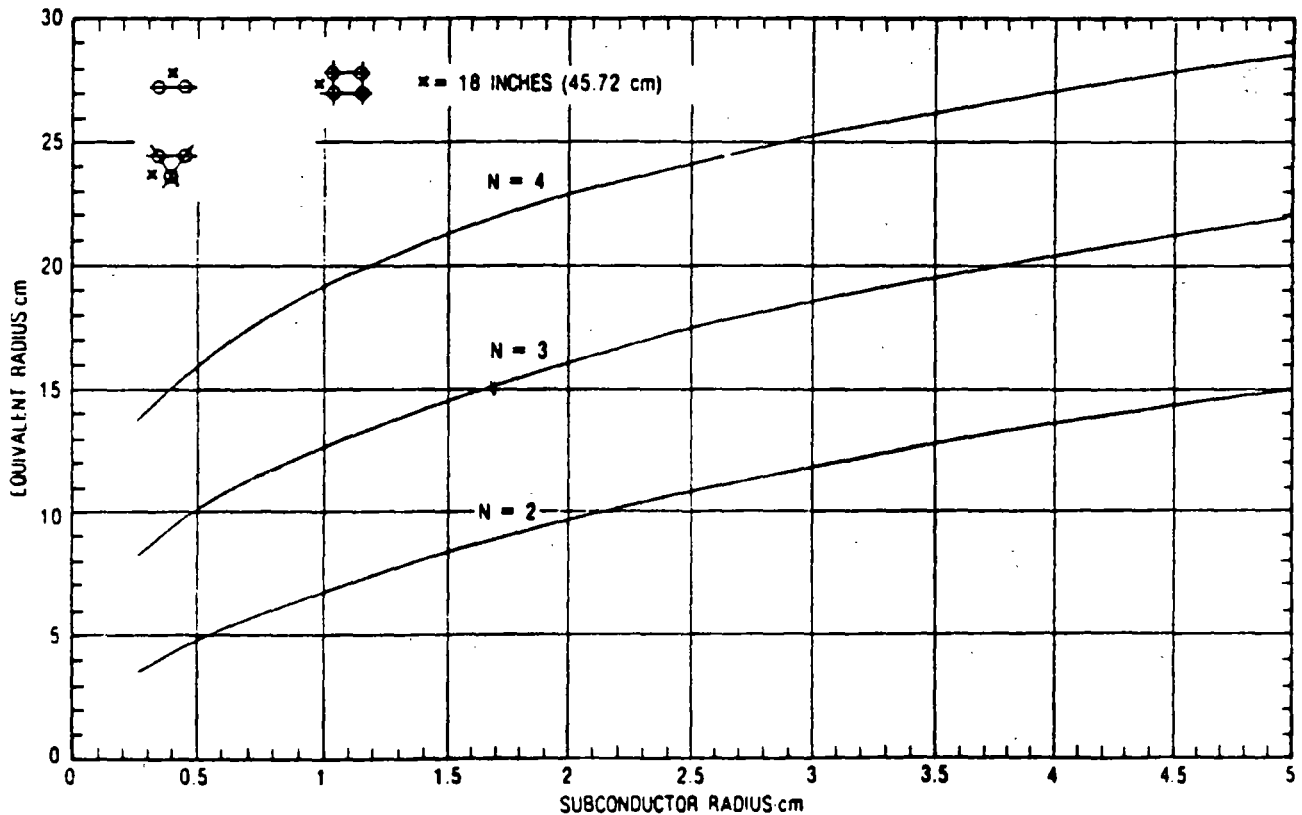


Figure 12.5.2. Conversion of bundle conductors to equivalent single conductors.

$$R_{eq} = \sqrt[3]{r_{11}r_{12}r_{13} \dots r_{1n}} \quad (12.5.1)$$

where R_{eq} is the radius of the equivalent single conductor, r_{11} is the radius of subconductor 1, r_{1n} is the distance from conductor 1 to conductor n , and N is the number of subconductors.

FINDING EFFECTIVE RADII OF SHIELD WIRES AND PHASE CONDUCTORS WITH CORONA PRESENT

After each bundle conductor is reduced to an equivalent single conductor, a further adjustment should be made to account for the effects of the corona envelope that forms when high voltage appears. In the case of the shield wires, the corona envelope may be over a meter in diameter, and its effect on the voltages induced on the phase conductors may be very significant. Similarly, for a phase conductor, the corona envelope that forms when a flash contacts the phase conductor directly may be sufficiently large to help limit the overvoltage and improve the shielding failure performance. The electrical coupling effects of conductors with corona envelopes vary more or less as the logarithm of the radius, so even a rough approximation will usually be adequate. Appendix 12.2 provides a simplistic derivation of the single conductor radius of this envelope from Gauss's law. The resulting equation is

$$R \ln \frac{2h}{R} = \frac{V}{E_0} \quad (12.5.2)$$

where R is the radius of the corona envelope (m), h is the height of the conductor above ground (m), V is the voltage applied to the conductor (kV), and E_0 is the limiting corona gradient below which the envelope can no longer grow (kV/m). A plot of corona sheath diameters as a function of V/E_0 and h is shown in Figure 12.5.3.

The envelope radius, R , is strongly influenced by the value of E_0 that is selected. Brown (20) recently analyzed test data of

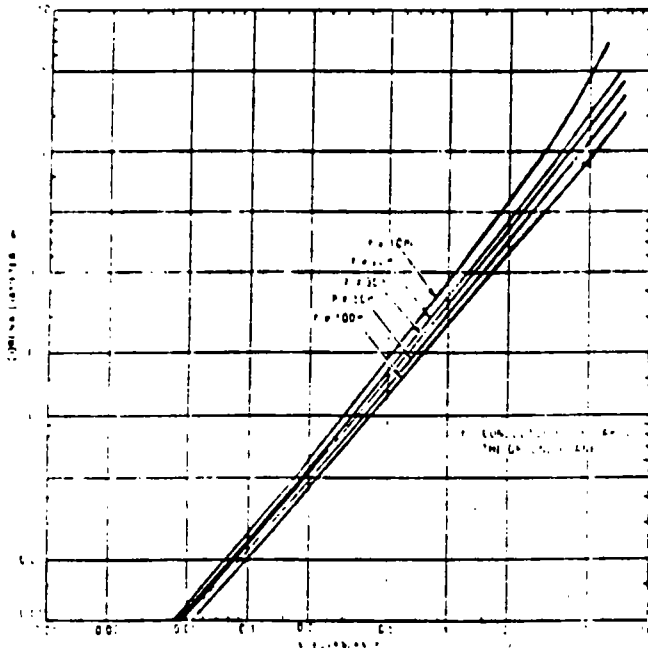


Figure 12.5.3 Approximate diameter of the corona sheath around a conductor at high voltage

McCann (22) and has suggested a value of 1500 kV/m (15 kV/cm). The author concluded that the critical gradient for the shield wires should be about 20 kV/cm because of the shielding effects of the tower and 12 kV/cm for the phase conductors because of the attractive effects of the tower. However, 15 kV/cm is a reasonable average value, and it is utilized in all subsequent calculations.

The corona envelope modifies only the capacitance of the conductor. It has little effect on the inductance. As pointed out in Appendix 12.2, the effective radius of a single conductor should be taken as the geometric mean of its effects with and without the corona envelope. Therefore, the self-surge impedance of a single conductor in heavy corona is given by

$$Z_{sn} = 60 \sqrt{\ln \frac{2h}{r} \cdot \ln \frac{2h}{R}} \quad (12.5.3)$$

where Z_{sn} is the self-surge impedance of conductor n (Ω), h is the height of conductor above ground (m), r is the radius of the metallic conductor (m), and R is the radius of the corona sheath around the conductor (m). (See Figure 12.5.3.)

For a bundle conductor, the presence of multiple subconductors causes major reductions in the effective corona diameter of each subconductor (23). However, as a rough rule of thumb, the equivalent single conductor radius of the bundle may be determined without corona from Figure 12.5.2 or from Eq. 12.5.1. The effective corona radius for each subconductor is determined from Figure 12.5.3, and the two radii are then summed to establish a working value of corona radius for the bundle. Equation 12.5.3 then yields the bundle surge impedance. From Eq. 12.5.3 the effective diameter, D_E , (including corona effects) is

$$\ln D_E = \ln 4h - \sqrt{\ln \frac{4h}{d} \cdot \ln \frac{4h}{D_c}} \quad (12.5.4)$$

For the case of the shield wire corona, the voltage to be used in Eq. 12.5.2 must be the tower top voltage. This voltage will be greater than the critical flashover voltage of the insulators because the latter are reduced by the coefficient of coupling (the voltage coupled electromagnetically onto the phase conductors). Conversely, for a direct stroke to a phase conductor, no coefficient of coupling is considered. This leads to the following rough guide: To solve for the self-surge impedance of a shield wire with corona effects included, use a voltage equal to approximately 1.8 times the flashover voltage of the tower insulator at about 2 μ s. For a direct stroke to a phase conductor (a shielding failure), use the flashover voltage of the insulator at about 6 μ s. For the limiting corona gradient, E_0 , use 1500 kV/m.

REDUCTION OF SHIELD WIRE SURGE IMPEDANCES TO EQUIVALENT SINGLE-WIRE SURGE IMPEDANCES

It is obvious from Figure 12.5.4 that when a stroke, I , contacts a tower, part of the current is diverted from the tower and passes out the shield wires. The amount of this diverted current is controlled by the shield wire and tower surge impedances. The self-surge impedance of a single conductor is the ratio of the voltage to the current in the conductor as a wave travels along it. The standard formula for this surge impedance for a conductor, n , parallel to the earth is

$$Z_{sn} = 60 \ln \left(\frac{4h_n}{D_n} \right) \quad (12.5.5)$$

where D is the effective conductor diameter. The mutual impedance between the two shield wires, Z_{mn} , is

$$Z_{mn} = 60 \ln \left(\frac{a_{mn}}{b_{mn}} \right) \quad (12.5.5A)$$

where a_{mn} is the distance from conductor m to the image of n in the earth and b_{mn} is the direct distance between conductor m and n (See Appendix 12.3.)

Equations 12.5.5 and 12.5.5A were derived from the condition of a transverse electromagnetic mode of wave propagation along the line. The effects of electric- and magnetic-field travel times between the conductor and the earth beneath it are assumed to be negligible. However, practically all workers computing line lightning performance concur that the travel times of waves traveling down the tower are not negligible, and yet these travel times are nearly the same as from the shield wires to ground out on the span. This inconsistency is firmly ingrained in the many analytical approaches to the problem. In actual fact, the electric fields that are involved in the evaluation of surge impedance (or tower voltage) are propagating and are not conservative. The voltage one observes depends greatly on the path selected to measure it, and consequently the surge impedance is a variable, not a constant.

In reality, the shield wire acts as a linear radiator carrying a progressive wave, and it exhibits radiation resistance, particularly during the rapidly changing front (24). It also develops a charge into the corona sheath around it. Equation 12.5.5 only relates to the principal mode of propagation.

One of the driving forces in the development of nano- and geometrical models was to avoid making such simplistic assumptions and to measure effects as they really were, not as idealized (25). Fortunately, in 1960 Wagner and Hileman (26) published a fundamental paper showing that classical values of conductor surge impedances were an acceptable approximation, provided a particular value of tower surge impedance was also selected. They derived this tower surge impedance for a right cylinder. Therefore, in this chapter the conventional concept of

surge impedances is adopted, as is generally done by the industry. Appendix 12.3 then shows that the equivalent surge impedance of two shield wires (connected to the same level on the tower) is

$$Z_S = \frac{Z_{11} + Z_{12}}{2} \quad (12.5.6)$$

where Z_{11} is the self-surge impedance of one of the shield wires and Z_{12} is the mutual surge impedance between conductor 1 and conductor 2 (see Appendix 12.3). For one shield wire, Eq. 12.5.5 is used.

COMPUTATION OF TOWER SURGE IMPEDANCES

The tower surge impedance is not so much a surge impedance as it is a transfer function. It is essentially the voltage developed across an insulator string at the tower top (in the absence of shield wires) per unit of lightning current entering the tower. This insulator voltage is created by the changing electromagnetic fields around the tower, and studies of this electromagnetic induction have been conducted by many engineers over the past 20 years (27). If the problem is to be reduced to manageable size, the equivalent tower surge impedance, which represents this electromagnetic induction, must be utilized because a solution using Maxwell's field equations is formidable indeed. The tower then becomes a simple, short transmission line with a constant surge impedance, grounded through its footing resistance at the base. The travel time, τ_T , of a wave down the tower is then the tower height divided by the velocity of light (300 m/ μ s). In 1960, Wagner and Hileman (26) published their fundamental paper deriving a theoretical value of tower surge impedance and found typical values ranging from 200 to 280 Ω for right cylinders.

In 1963, Kawai (28) made full-scale measurements of the surge response of transmission towers varying in height from 26 to 214 m. A fast current surge was inserted between the tower top and either a vertical wire suspended from a balloon or a horizontal shield wire disconnected from the tower. The surge impedance was observed to be a variable with a final value of approximately 100 Ω , somewhat lower than anticipated. However, the measured velocity of propagation of the surge was about 0.7 to 0.9 of the velocity of light (also lower), and it is the combination of these two variables that creates the insulator stresses.

In 1968, Sargent and Darveniza (29) published an important paper in which they computed equivalent tower surge impedances for a variety of shapes and compared them with actual measurements on nanosecond geometrical models. Key results that are relevant to this analysis are shown in Figure 12.5.5. The value $2r$ in the Class 2 profile is the diameter of the down lead for the case of a wood pole or the diameter of the metal pole if it is a metal structure. The surge impedance for the Class 3 profile is an approximation from the surge impedance of a right cylinder. Surge impedances of other classes of structures may be determined either by estimates from Classes 1, 2, or 3, or by measurements on geometrical models. Values will usually range from 100 to 300 Ω .

Some engineers have preferred to use tower inductance rather than surge impedance because it greatly simplifies the calculations. There is a direct relationship between surge impedance and tower inductance. This relationship is examined in Section 12.9 and in Appendix 12.7, and if it is used, the results will be as accurate as for surge impedances in most practical cases.

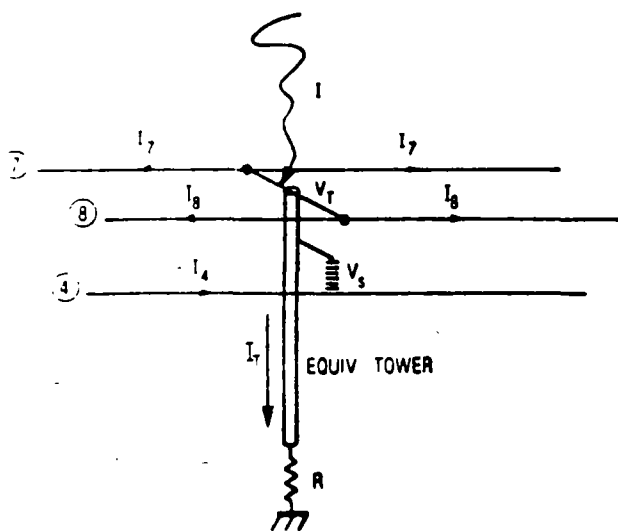
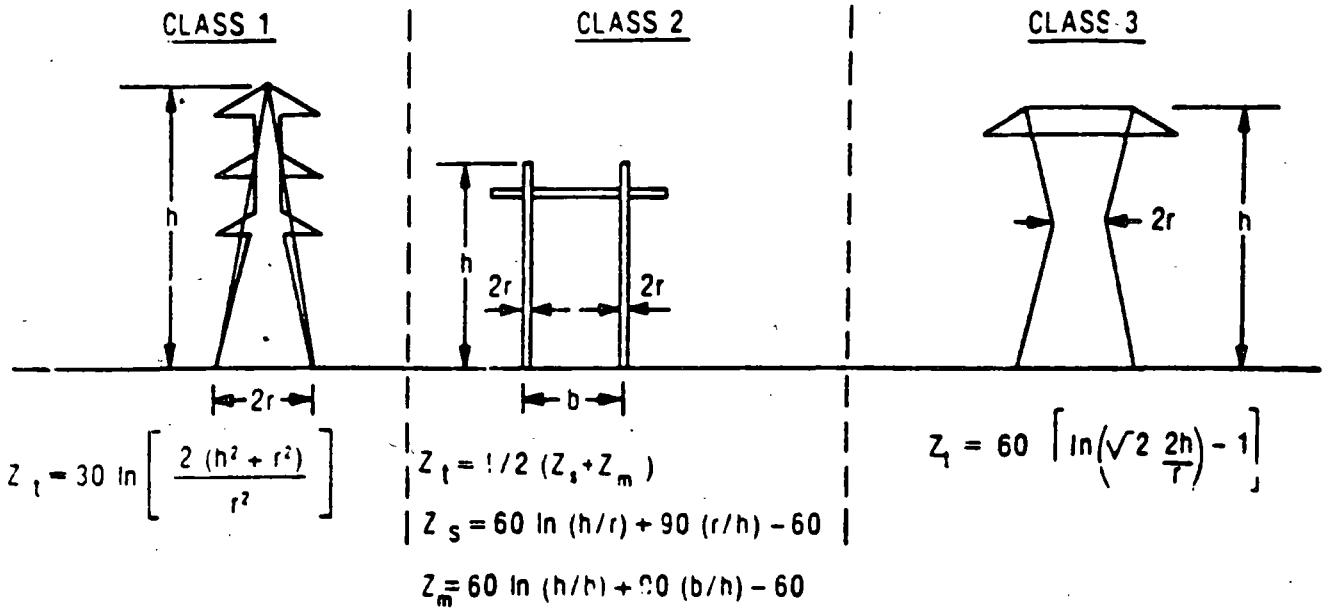


Figure 12.5.4 Stroke current at a tower splits between shield wires and ground



FOR EACH CASE, THE TRAVEL TIME T FROM TOWER TOP TO GROUND IS: $T = h/300 \mu s$

Figure 12.5.5. Approximations for tower surge impedance.

DETERMINATION OF COUPLING FACTORS FOR PHASE CONDUCTORS

That portion of the stroke current flowing outward over the shield wires induces a voltage called the coupled voltage in each phase conductor, and the ratio of the total induced voltage on phase conductor n to the tower top voltage is known as the coefficient of coupling, K_n . It is derived from the classical conductor equations in Appendix 12.3 and is expressed for the case of two shield wires at equal height above ground as

$$K_n = \frac{Z_{n1} + Z_{n2}}{Z_{11} + Z_{12}} \tag{12.5.7}$$

where Z_{nm} is the mutual impedance between conductor m and conductor n and Z_{11} is equal to Z_{22} which equals Z_{nn} , the self-surge impedance of each shield wire (1 and 2 are the shield wires, and n is the phase conductor). If only a single shield wire exists, then

$$K_n = \frac{Z_{1n}}{Z_{11}} \tag{12.5.7A}$$

If propagation effects are to be assumed up and down the tower, then consistency requires that propagation effects also be assumed to occur for the coupling effects. This ensures that one is not using one time scale for one effect and a different time scale for the other. A simple approximation is to use as the shield wire voltage, not the tower top voltage, V_T , at a time, t , but the voltage $V_T(t - T_{pn})$ that existed at a previous time, $t - T_{pn}$, where T_{pn} is the propagation time down the tower from the tower top to the insulator crossarm, n . This same travel time, T_{pn} , is also used to derive the cross-arm potentials, which may differ significantly from the tower top potentials for tall towers or fast stroke currents.

SELECTION OF FOOTING RESISTANCE

The tower footing resistance is an extremely important parameter in the determination of lightning flashover rates. Unfortunately, it is a fluctuating statistical variable the magnitude of which is governed not only by geography but also by nonlinear conduction physics in the earth. It may swing over a two to one range or more owing to changes in stroke current, and even with constant current it will change with time. An advantage of the Monte Carlo method of analysis (7) is that these widely fluctuating values may easily be accounted for, but in the analytical approach necessary for a hand calculator, an equivalent fixed value of footing resistance must be selected. Prior to making this selection, some of the fundamentals are reviewed. The following is a condensation of material in the first edition of this book—material organized primarily by F. A. Fisher (10).

The simplest electrode configuration to analyze is a spherical electrode that either is buried completely in the ground or has only the lower hemisphere buried (30). In the latter case, assuming uniform soil resistivity, a current, I , flowing from the hemisphere into the ground produces a current density in the surrounding soil of

$$i = \frac{I}{2\pi\lambda^2} \tag{12.5.8}$$

where i is the current density, I is the total current, and λ is the distance from the center line of the electrode. According to Ohm's law, such a current produces in the soil an electric field strength of

$$E = \rho i = \frac{\rho I}{2\pi\lambda^2} \tag{12.5.9}$$

where ρ is the soil resistivity. The voltage, as the line integral of the field strength from the surface of the conducting sphere to any distance, X , is

$$V = \int_a^X E dX = \frac{\rho I}{2\pi} \int_a^X \frac{dX}{X^2} = \frac{\rho I}{2\pi} \left(\frac{1}{a} - \frac{1}{X} \right) \quad (12.5.10)$$

where a is the radius of the hemisphere. The total voltage between the hemisphere and a far distant point with $X \approx \infty$ is then

$$V = \frac{\rho I}{2\pi a} \quad (12.5.11)$$

The total resistance experienced by the flux lines diverging from the hemisphere becomes

$$R = \frac{V}{I} = \frac{\rho}{2\pi a} \quad (12.5.12)$$

As an example, a hemisphere of radius $a = 1$ m embedded in soil of resistivity $\rho = 100 \Omega \cdot \text{m}$ will have a ground resistance of

$$R = \frac{100 \Omega \cdot \text{m}}{2\pi \cdot 1 \text{ m}} = 16 \Omega$$

This is the resistance experienced by current flowing through the entire surrounding space. Most of this resistance is encountered in the region immediately around the electrode. From Eq. 12.5.8, 50% of the total resistance is contained in the first meter beyond the electrode ($X = 2a$) and 90% is contained in the first nine meters beyond the electrode ($X = 10a$).

Figure 12.5.6 from Rudenberg (30) shows the resistance of several simple electrodes that are buried at an extreme depth in the earth. If these electrodes are buried with only half their vertical dimension in the earth, the resistance will be twice that given in Figure 12.5.6. The resistance will be only somewhat less than twice that given in Figure 12.5.6 if the electrodes are buried at a depth that is shallow compared to their length. Tabulations of ground resistance of other electrodes as a function of burial depth are given by Dwight (31), Fink and Beaty (32), and Sunde (33).

The most useful form of ground electrode is the driven ground rod. Ground rods are usually supplied in 8- to 12-ft lengths, and they may be joined by couplings for longer depths. Rod diameters are generally less than 3 cm. Sunde has derived the resistance of a driven ground rod as

$$R = \frac{\rho}{2\pi l} \left[\ln \left(\frac{4l}{a} \right) - 1 \right] \text{ when } l \gg a \quad (12.5.13)$$

where R is the resistance (Ω), ρ is the ground resistivity ($\Omega \cdot \text{m}$), l is the length of rod (m), and a is the rod radius.

The diameter of the rod is of some significance because it affects the logarithmic term $4l/a$, but the length is more important. However, the resistance does not decrease directly with length, and a condition may arise in which a further increase in length is accompanied by only a minor reduction in footing resistance.

A careful examination of both Eq. 12.5.13 from Sunde and the equation for the resistance of a deeply buried rod from

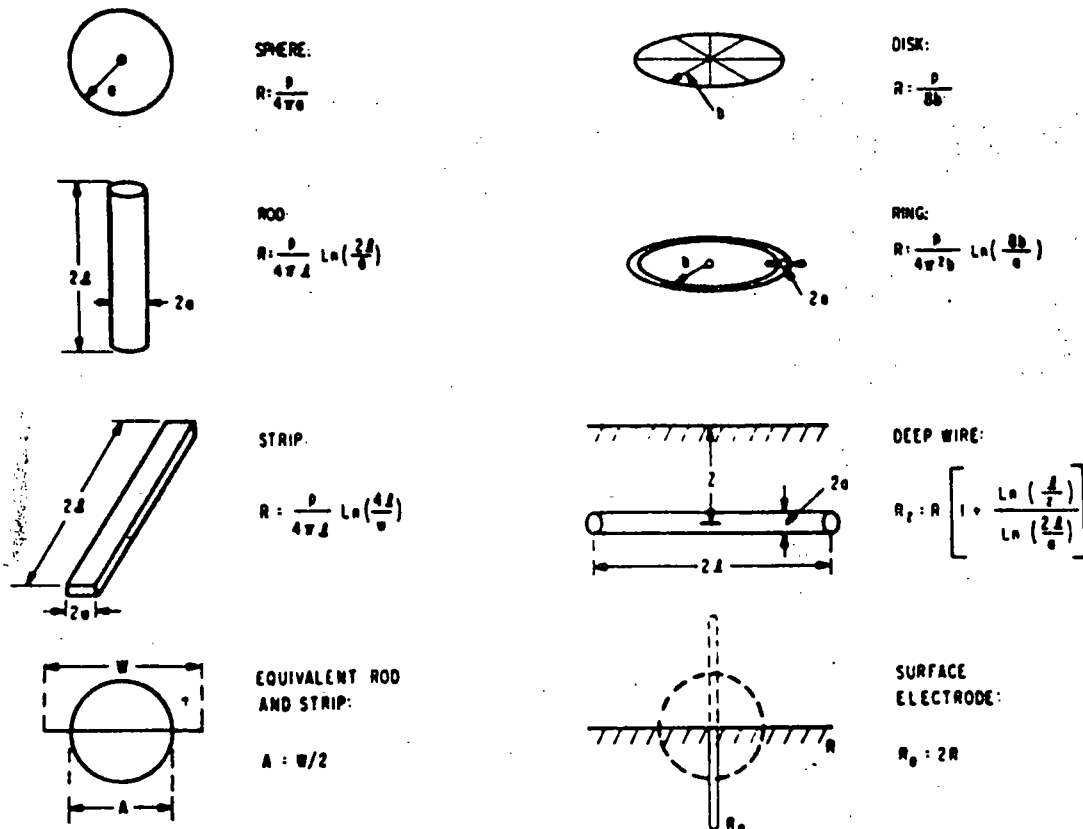


Figure 12.5.6. Ground resistance of elementary electrodes.

Rudenberg in Figure 12.5.6 reveals a moderate discrepancy. For a driven ground rod, the theoretical expression by Rudenberg in Figure 12.5.6 would have to be doubled because half the resistive material would not exist. Making this correction and allowing l to now equal the length of rod driven into the ground, Rudenberg's expression becomes

$$R = \frac{\rho}{2\pi l} \ln \left(\frac{2l}{a} \right) \quad (12.5.13A)$$

Part of the discrepancy between Eq. 12.5.13 and Eq. 12.5.13A is due to the different approaches to the approximations. Generally, Eq. 12.5.13 is used, and it is the same as that given by Dwight (31) when Dwight's equation is modified so that l represents the length of the rod driven into the ground. There is also some difference in the derivations of the resistance of a buried strip. Rudenberg and Sundt agree fairly well, though not exactly, and both differ from Dwight. Figure 12.5.7 shows the variation of resistance with rod length for various diameters. The curves are drawn for a ground resistivity of 100 $\Omega \cdot m$.

Ground resistance may also be lowered by connecting driven ground rods in parallel. If the spacing between rods is great compared with the length of the individual rods, the resistance will be reduced in proportion to the number of rods. If the rods are close together, each rod will be in the intense electrical field of its neighbor. If the rods are very close together, then the overall resistance becomes

$$R = \frac{\rho}{2\pi l} \ln \left(\frac{2l}{a} \right) \quad (12.5.14)$$

where a represents the radius of an equivalent rod.

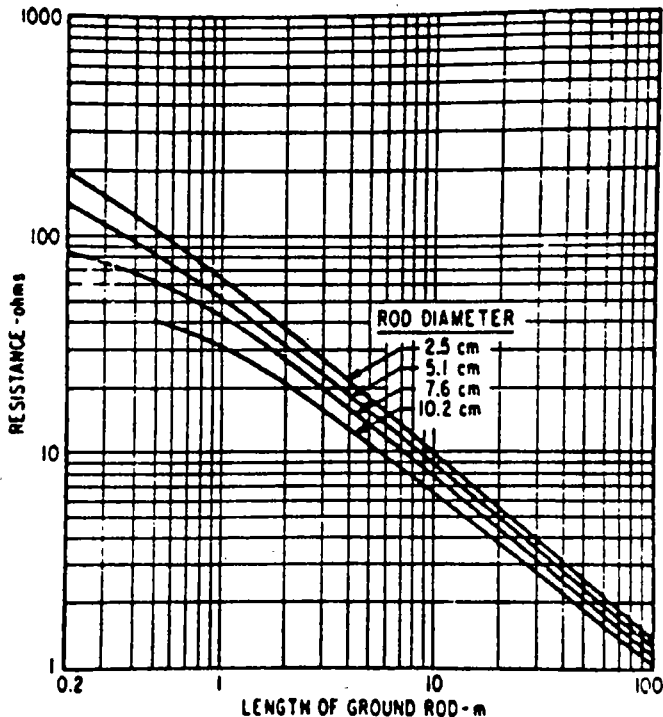


Figure 12.5.7 Resistance of vertical ground rods as a function of length and diameter. Soil resistivity = 100 $\Omega \cdot m$.

Figure 12.5.8 shows how the equivalent radius depends on rod geometry. If the rods are moderately close to each other, the overall resistance will be more than if the same number of rods were spaced far apart. The increase in resistance depends on the number of rods involved. Two rods, with 1.9-cm diameter and 3-m length, in parallel and spaced 3 m apart will have a resistance 1.14 times greater than they would if they were an infinite distance apart. Four rods in a square would have to be 9.15 m apart to have the same resistance ratio. Lewis (34) gives additional information on ground rods in parallel as a function of spacing.

Table 12.5.1 shows an example of the ground resistance that could be obtained on an area of 20,000 ft (100 ft \times 200 ft).

The resistance of a single buried horizontal wire is, from Sundt,

$$R = \frac{\rho}{\pi l} \left(\ln \frac{2l}{\sqrt{4ad}} - 1 \right) \text{ when } d \ll l \quad (12.5.15)$$

where l is the length of wire (m), a is the wire radius (m), and d is the burial depth (m). Figure 12.5.9 shows how this resistance varies with the length and diameter of the buried wire.

Equation 12.5.15 assumes that the potential is uniform over the entire length of the wire, which could be true only if the wire had perfect conductivity. If the wire is very long, it will not be at the same potential all along its length, and Eq. 12.5.15 will be in error. If allowance is made for wire resistance, the overall ground resistance becomes

$$R_o = \sqrt{rR} \text{Coth } l \sqrt{\frac{r}{R}} \quad (12.5.16)$$

Table 12.5.1
GROUND RESISTANCE OF RODS IN PARALLEL

Number of Rods 1.9 cm Diam \times 3.05 m Long	Relative Ground Resistance
1	1.000
5	0.200
10	0.110
20	0.070
50	0.042

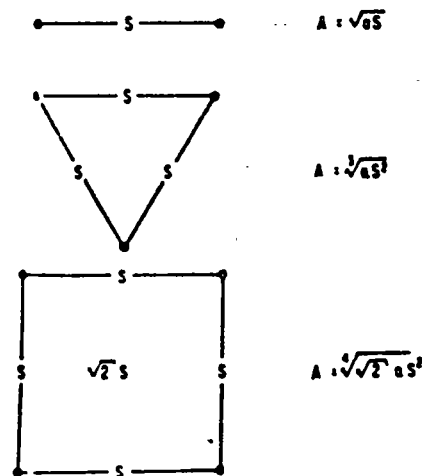


Figure 12.5.8. Equivalent radius, A , of groups of ground rods of radius a .

and if $\sqrt{\frac{l}{R}}$ is large, then

$$R_0 = \sqrt{lR} \quad (12.5.17)$$

where l is the resistance of wire ($\Omega \cdot m$), R is the ground resistivity ($\Omega \cdot m$), and l is the length (m). As a practical matter, a ground wire long enough for the wire resistance to cause serious error in Eq. 12.5.15 would be so long that its transient response would have little to do with the computed resistance.

If a lightning current surge is applied to a counterpoise, or buried wire, the effective resistance is initially quite high, on the order of 150 Ω . This value is the surge impedance of the wire. As the surge propagates along the wire, the resistance decreases as the current spans more and more of the wire, thus making more effective contact with the ground. The surge propagates in the ground at roughly one-third the speed of light. Hence, current does not span a 300-m wire for approximately 3 μs . For a given length of buried wire, the transient resistance will reduce to the steady-state resistance faster if the wire is arranged as several, shorter, radial wires than if it is laid as one long wire. Bewley (35) has shown how the transient response of buried wires varies for several configurations of counterpoise. In the case of driven ground rods, the final resistance would be attained quite quickly because the rods would be fairly short. Widely spaced ground rods would not attain their final resistance until a surge current reached the most distant rod. As a practical matter for the grounding of lightning currents, the first 250 ft of buried conductor is the most effective.

Ground resistance decreases with increasing current, at least until the current dries out the soil. The proportional reduction is less for grounds of low resistance than it is for grounds of high resistance. Figure 12.5.10, from Bellaschi *et al.* (36), shows typical measured values of ground resistance as a function of impulse current. In 1974, Liew and Darveniza (37) developed a new dynamic resistance model based on surge-current measurements in a variety of earth conditions. They found that the reduction of crest voltage across the earth resistor due to stroke current was larger than previously assumed. Figure 12.5.11 is reproduced

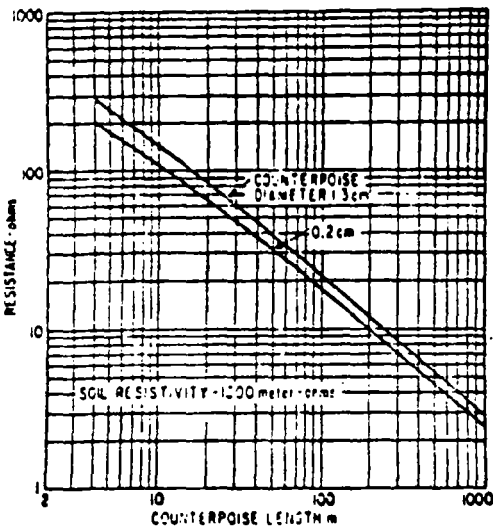


Figure 12.5.9 Resistance of counterpoise as a function of length

from their paper. In 1978, Darveniza and others (38) published a correction curve that the author has since adopted as the best compromise for performance calculations. Figure 12.5.12 displays this curve. Whitehead (39) also developed a dynamic model that has good representation of the tests made by Darveniza.

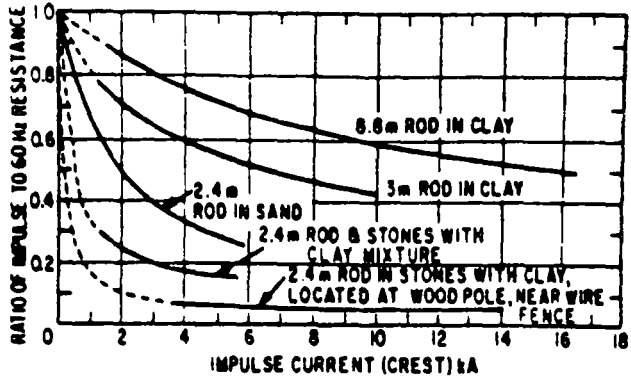


Figure 12.5.10. Impulse current resistance of various ground rods.

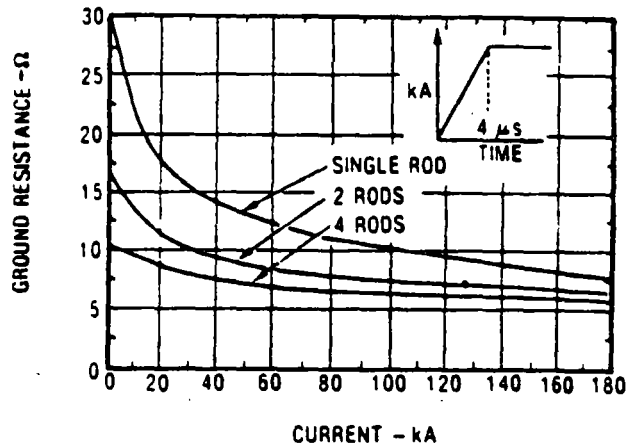


Figure 12.5.11. Ground resistance reductions found by Liew and Darveniza. (Depth of rods = 3.3m; $\rho = 1000 \Omega \cdot m$; separation of rods = 3.3 m.)

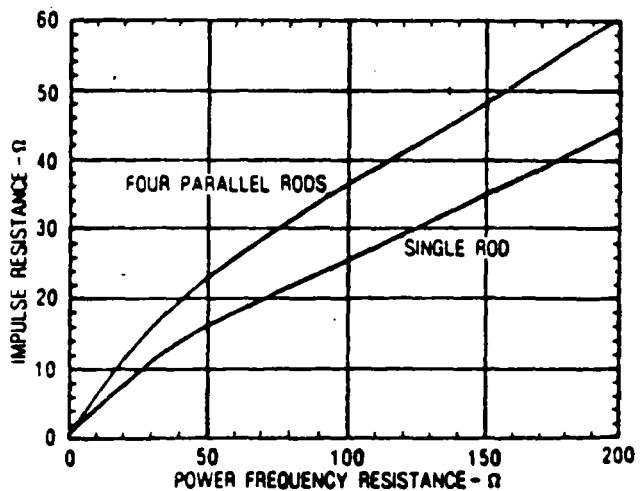


Figure 12.5.12 Suggested reduction of impulse resistance to use for lightning calculations from Darveniza and others (38)

The fundamental method of measuring ground resistance is shown in Figure 12.5.13. Current is circulated between the ground under test and an auxiliary ground. Preferably, the auxiliary ground should be located at a distance that is great compared with the dimensions of the ground under test because it is not desirable to have interaction of the ground current distributions at the two electrodes. A voltage is then measured between the ground under test and a reference ground located between the two current-carrying electrodes. The reference ground should also be located so that it is not in the electric field of either of the current-carrying electrodes. Assuming that the current density is negligible at the reference electrode, the resistance of the ground under test is

$$R = \frac{V}{I} \quad (12.5.18)$$

The measurement may be made using a voltmeter and ammeter with the current supplied by a transformer energized from the power lines. Alternatively, a bridge may be used for the measurement. Most often, however, ground resistance is measured with self-contained instruments such as a ground megger.

The resistivity of earth may vary over extremely wide limits, depending on the composition of the soil and its moisture content. Representative values are shown in Table 12.5.2.

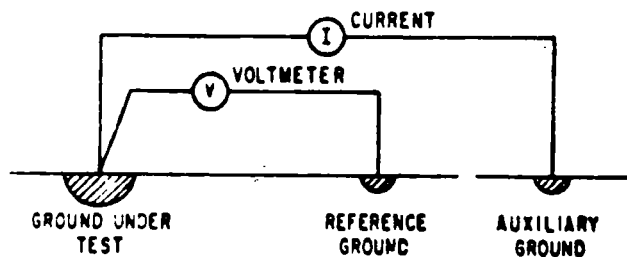


Figure 12.5.13 Fundamental method of ground-resistance measurement.

Table 12.5.2
EARTH RESISTIVITY

Material	$\Omega\text{-m}$
General average	100
Sea water	0.01-1.0
Swampy ground	10-100
Dry earth	1000
Pure slate	10^7
Sandstone	10^8

EFFECTS OF A STATISTICAL DISTRIBUTION OF FOOTING RESISTANCE VALUES

In practice, a transmission line does not have a constant value of footing resistance but has, instead, a range of values, depending on tower location. Usually, towers in swampland or on moisture-bearing soil have low footing resistances, whereas towers on rocky soil have high resistances. Most design procedures, including those in this book, compute tripout rates for a constant value of footing resistance, and it is of some importance to examine the

best procedure for using the results calculated with this simplified assumption. In practice, the disparity is easily overcome by using the following rules:

- If the expected variation of footing resistance about a mean value is not extreme (i.e., if the coefficient of variation, σ , for the distribution is less than half the average value), then use the average value of footing resistance for a computation that will be usually of acceptable error (less than 20%). A. R. Hileman has suggested that the average, plus one or two σ , be used, thereby yielding a somewhat more conservative value.
- If the footing resistances fall into two or more widely different classes, each one a significant part of the total, then split the computation into sections of high and low resistance, and, for the length of line in each section, compute the outage rate using the average resistance for the section. Then sum to find the total by the relation

$$T = \frac{T_1L_1 + T_2L_2 + \dots + T_NL_N}{L} \quad (12.5.19)$$

where T is the total line tripout per 100 miles per year; T_N is the tripout rate per 100 miles per year of section N with a length, L_N , and with a tripout rate determined from the curves by using the average footing resistance for the section; and L is the length, in miles, of the entire line.

12.6 RESPONSE OF A TRANSMISSION TOWER TO A LIGHTNING FLASH

Referring to Figure 12.5.1 and Figure A12.4.1 in Appendix 12.4 will show that the insulator voltage for any phase is the difference between the crossarm voltage, V_{ph} , and the voltage induced on the phase conductor, V_{Qn} . In addition, the tower top voltage, V_T , must be computed for the most severe stroke in a flash so that V_{Qn} may be determined by using the appropriate coefficient of coupling. There are also current waves that reflect off the adjacent towers on each side of the stricken tower, and these waves eventually arrive to reduce the stricken tower insulator voltages. All these components may be determined by classical traveling wave theory, provided the proper value of tower surge impedance is chosen (26). After each insulator surge voltage is computed, the additional contribution of 60-Hz voltages on the insulators must be included. The stress so produced is then compared with the insulator volt-time curves to find the stroke amplitudes required for flashover. Without the aid of a minicomputer, the computation is tedious, but straightforward.

COMPUTATION OF TOWER TOP VOLTAGE

The author's arrangement of the traveling wave solution for tower top voltage, V_T , is derived in Appendix 12.4 as follows:

$$V_T(t) = Z_T I(t) - Z_0 \sum_{n=1}^N [I(t - 2nT_T) \psi^{n-1}] \quad (12.6.1)$$

where

$V_T(t)$ = tower top voltage in kilovolts at any selected time, t , in microseconds;

- $I(t)$ = stroke current into the equivalent circuit in kiloamperes at the same time, t , in microseconds;
 Z_i = the intrinsic circuit impedance in ohms encountered by the stroke current at the instant it enters the equivalent circuit (see Figure 12.5.1):

$$Z_i = \frac{Z_s Z_T}{Z_s + 2Z_T} \quad (12.6.1A)$$

- Z_s = a constant wave impedance on which all traveling wave current components operate to provide components of tower top voltage:

$$Z_s = \left[\frac{2Z_s^2 Z_T}{(Z_s + 2Z_T)^2} \right] \left[\frac{Z_i - R}{Z_i + R} \right] \quad (12.6.1B)$$

- T_T = travel time in microseconds from tower top to base: the height of the tower in meters divided by 300

- $I(t - 2nT_T)$ = the stroke current that entered the equivalent circuit at a previous time, $t - 2nT_T$, where n is a whole number, called the wave number, that defines the component.

- ψ = a damping constant that successively reduces the contribution of reflections:

$$\psi = \left(\frac{2Z_T - Z_s}{2Z_T + Z_s} \right) \left(\frac{Z_T - R}{Z_T + R} \right) \quad (12.6.1C)$$

- N = the largest value that the wave number, n , can reach: the largest whole number $\leq t/2T_T$

To use Eq. 12.6.1, one first selects a time at which the tower top voltage is to be computed and then computes each current component inside the summation sign until n reaches its largest permitted value, N . Except for educational purposes, it is not necessary to compute the entire voltage waveshape because most of it contributes little to the insulator flashover process. Tower top voltages should always be computed in the vicinity of the stroke current crest because that is where tower voltage can have the highest magnitude. In addition, when high values of footing resistance are involved, voltages out at 3 to 6 μ s are usually of interest because the volt-time strength of the insulator will be weaker in that region. Figure 12.6.1 includes a tower top waveshape computed with Eq. 12.6.1 for a representative set of circuit impedances and a ramp-function, stroke-current waveshape having a time-to-crest of 1.8 μ s, a tail time-to-half value of 50 μ s, and a unit crest amplitude. (See Figure 12.4.9.)

If the stroke-current waveshape is of the ramp-function form $I = At$, then Appendix 12.4 shows that the tower top voltage on the front or at the crest of the wave, $V_T(t)$, takes the form

$$V_T(t) = At \left[Z_i - Z_s \left(\frac{1 - \psi^N}{1 - \psi} \right) \right] + 2AT_T Z_s \left[\frac{1 - \psi^N}{(1 - \psi)^2} - \frac{N\psi^N}{1 - \psi} \right] \quad (12.6.2)$$

When the stroke-current wave is assumed to be composed of a sum of several ramp functions, as shown in Figure 12.4.8, one simply uses Eq. 12.6.2 for each ramp function with the proper value of A inserted. Then, the tower top voltage, $V_T(t)$, will be the sum of the voltages obtained. Brown (21) provides a somewhat different version of the tower top voltage equation, which could be used.

COMPUTATION OF CROSSARM VOLTAGES

When insulator voltages must be determined, it will usually be necessary to compute all the crossarm voltages. Hence, a numerical routine requiring the least computation is highly desirable. Because the tower top voltage, $V_T(t)$, must be computed to find the coupled voltages on the phase conductors, the simplest crossarm voltage procedure is to compute the voltage at the base of the tower (across the footing resistance) and then to interpolate between these two end voltages for each crossarm, assuming the voltage changes linearly along the tower from top to bottom. (A linear interpolation is not strictly rigorous, but it gives acceptable accuracy after about the first 0.3 μ s for a typical tower.) Appendix 12.5 shows that the voltage at the tower base is

$$V_R(t + T_T) = \bar{\alpha}_R Z_i \sum_{n=0}^N I(t - 2nT_T) \psi^n \quad (12.6.3)$$

where $V_R(t + T_T)$ is the voltage across footing resistance, R , at a time $(t + T_T)$, and

$$\bar{\alpha}_R = \frac{2R}{Z_T + R} \quad (12.6.4)$$

The footing resistance voltage to be used is the voltage created at a time, $(t + T_T)$, where t is the time at which the voltage is computed at the tower top. As explained in Appendix 12.5, the tower base voltage is computed at a later time than the tower top voltage to allow for the fact that the tower base voltage lags the tower top voltage by one tower travel time, T_T . (It also simplifies the equations.) Once again, if the incoming stroke-current wave is a ramp function, $I(t) = At$, Eq. 12.6.3 may be expanded in the same manner as Eq. 12.6.1, the tower top voltage equation. Appendix 12.5 shows that the tower base voltage on the front or at the crest of the stroke-current wave is

$$V_R(t + T_T) = \bar{\alpha}_R Z_i A \left[\left(\frac{1 - \psi^{N+1}}{1 - \psi} \right) t - 2\psi \left(\frac{1 - \psi^N}{(1 - \psi)^2} - \frac{N\psi^N}{1 - \psi} \right) T_T \right] \quad (12.6.5)$$

After the base voltage is determined, the interpolated voltage for any crossarm, n , is

$$V_{pn}(t + T_{pn}) = V_R(t + T_T) + \frac{h - y_n}{h} [V_T(t) - V_R(t + T_T)] \quad (12.6.6)$$

where h is the tower height (m) and y_n is the distance from the tower top down to the crossarm (m). Figure 12.6.1 includes an example of computed crossarm voltages for the 345-kV, vertical double-circuit tower in Section 12.10.

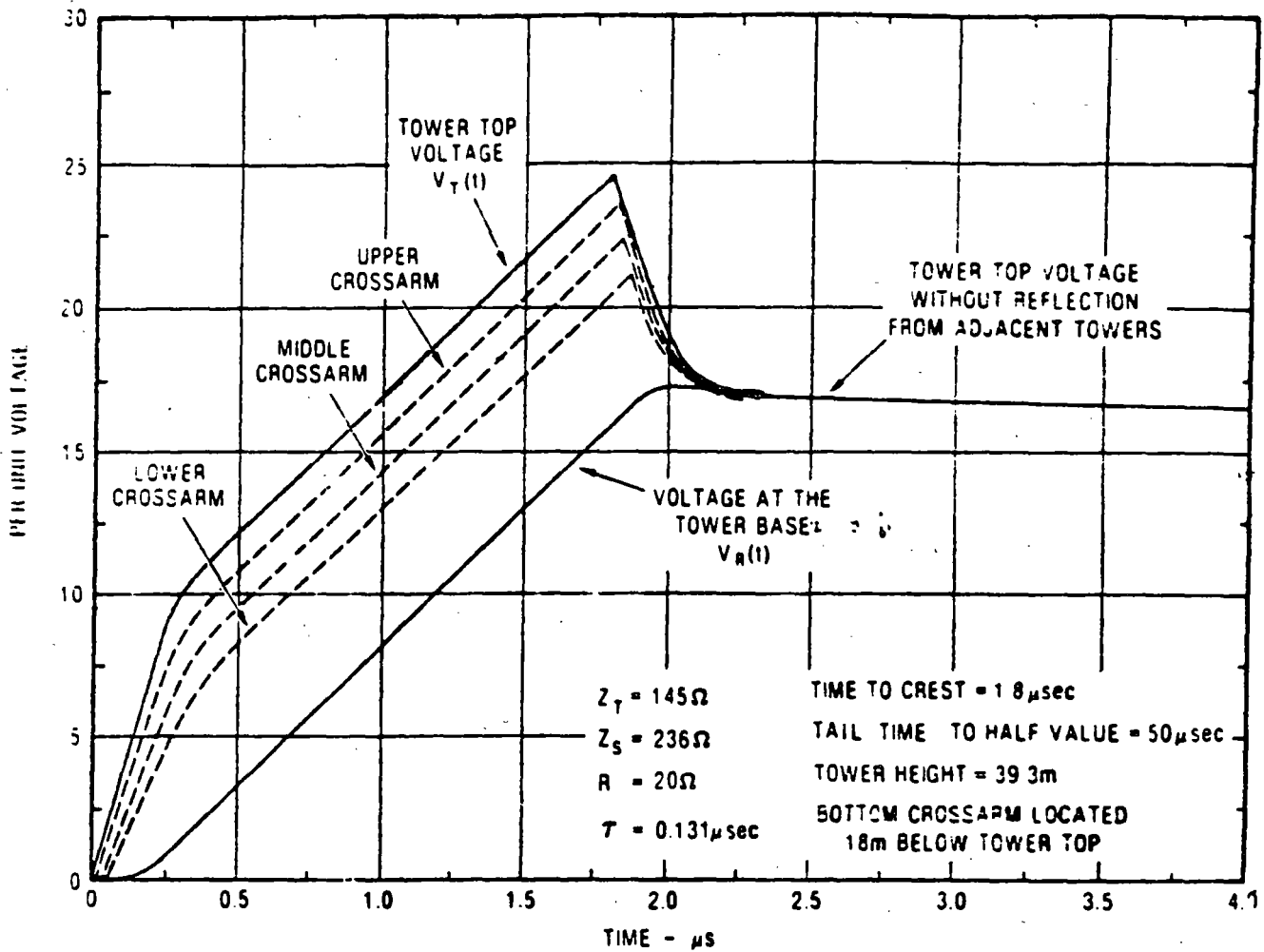


Figure 12.6.1. Per unit voltage (kV) per unit crest stroke current (kA) for tower top and crossarms of a tower similar to that on work sheet 1-A, Section 12.10. R is the linearized surge resistance.

COMPUTATION OF INSULATOR SURGE VOLTAGES

As mentioned previously, if the stroke current entering the tower top changes its magnitude at some time, t , the finite velocity of light creates a condition (Figure 12.6.1) in which the crossarm voltage cannot be affected by this change until a time T_{pa} later, and the footing resistance voltage drop will not be affected until a time T_T later. This finite velocity of light makes these nonsimultaneous voltages work together, the tower top voltage at a time t , the crossarm voltage at a time $(t + T_{pa})$, and the footing resistance, or tower base voltage, at a time $(t + T_T)$. Keeping this in mind, one will note from Figure 12.6.1 that, if propagation at the velocity of light across the insulator string itself is ignored, the insulator string surge voltage is the difference between the crossarm voltage, V_{pa} , and the voltage coupled to the phase conductor from the tower top.

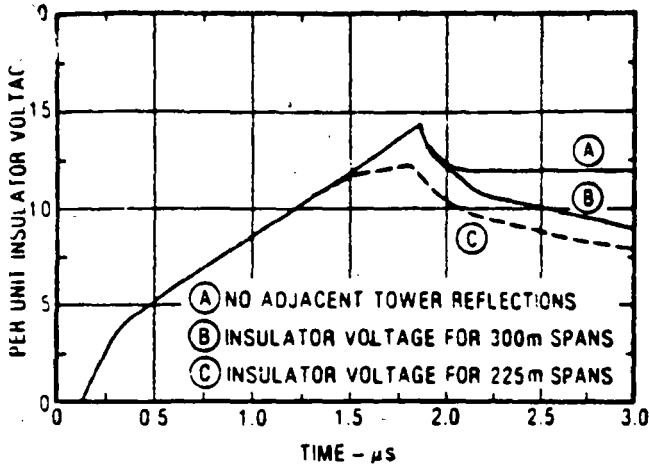
$$V_{in}(t + T_{pa}) = V_{pa}(t + T_{pa}) - K_n V_T(t + T_{pa}) \quad (12.6.7)$$

where K_n is the coupling factor and T_{pa} is the time from tower top to crossarm. Combining the equations yields

$$V_{in}(t + T_{pa}) = V_R(t + T_T) + \frac{T_T - T_{pa}}{T_T} [V_T(t) - V_R(t + T_T)] - K_n V_T(t) \quad (12.6.8)$$

Equation 12.6.8 will be utilized in solutions for the magnitudes of insulator voltages. One may make this interpolation with good accuracy once a few tower reflections have occurred. It clearly cannot apply during the first travel time. An equation accurate for all times is derived in Appendix 12.5.

Figure 12.6.2 presents one set of insulator voltages for the vertical circuit tower shown in Section 12.10. The figure shows that the bottom phase insulators have greater voltage across them than the top phase insulators because the coefficient of coupling is less for the bottom insulators. It is quite common for the lower phases on vertical circuit towers to have higher lightning flashover rates than the upper phases, and differences in coupling are invariably responsible. For tall structures with only one shield wire and low footing resistances, the upper phases may sometimes experience the greatest stress and the largest tripout rate.



12.6.6. Reflections from adjacent towers reduce the crest insulator voltage.

length, these reflections may arrive before or after the crest voltage that would otherwise occur at the stricken tower. The magnitude of the reflections is not easily determined by simple analytical means because the reflected waves are badly distorted by corona and resistance losses, which are functions of voltage, rise time, and distance. Many multiple reflections and refractions may be involved. However, consideration of these reflections is required because they can reduce the tripout rate if they arrive soon enough.

An approximation strategy used by the author with some success in earlier work replaces each adjacent tower surge impedance and its footing resistance with an equivalent impedance that is a function of the stroke waveshape. If the tower top voltage, $V_T(t_0)$, is computed without reflections from adjacent towers at a time, t_0 (the time-to-crest of the stroke-current wave), then the ratio of $V(t_0)/I(t_0)$ is, at that moment in time, the total impedance, $Z(t_0)$, encountered by the stroke current. This impedance, $Z(t_0)$, is the parallel combination of $Z_s/2$ and a varying tower impedance, $Z'_T(t)$, where

$$Z'_T(t) = \frac{Z_s Z(t_0)}{Z_s - 2Z(t_0)} \quad (12.6.9)$$

An assumption is then made that the tower surge impedance and footing resistance on each side of the stricken tower may also be replaced with this same equivalent tower impedance, $Z'_T(t_0)$, except, of course, delayed in time. With this assumption, which is not strictly true but is a fair approximation, an application of the classical traveling wave equations will show that the sum of the reflecting voltage components arriving at the stricken tower from both sides is

$$V''_T(t) = \beta_s V_T(t - 2T_s) \quad (12.6.10)$$

where

- $V''_T(t)$ = voltage from adjacent towers appearing across the stricken tower at time, t ;
- $V_T(t - 2T_s)$ = tower top voltage that existed at the stricken tower at a time, $(t - 2T_s)$

- β_s = span voltage reflection factor:
 - $$\beta_s = \frac{-4Z(t_0)[Z_s - 2Z(t_0)]K_s}{Z_s^2}$$
 - Z_s = shield wire surge impedance (Ω)
 - $Z(t_0)$ = $V_T(t_0)/I(t_0)$
 - $V_T(t_0)$ = tower top voltage at current crest time, t_0 ;
 - $I(t_0)$ = stroke current at crest time, t_0 (usually 1.0 p.u.);
 - K_s = an attenuation factor (assume 0.85 unless better information is available)
- (12.6.11)

But on a per unit basis $I(t_0) = 1.0$ and $Z(t_0)$ will have the same numeric value as $V_T(t_0)$. Therefore, the reflected voltage arriving at the tower top at crest time, t_0 is approximately equal in magnitude (but not dimensionally) to

$$V'_T(t_0) = \frac{-4K_s[V_T(t_0)]^2}{Z_s} \left[1 - \frac{2V_T(t_0)}{Z_s} \right] \left[\frac{t_0 - 2T_s}{t_0} \right] \quad (12.6.12)$$

where

- $V'_T(t_0)$ = sum of the reflected voltage waves from adjacent towers appearing at the tower top at crest time, t_0 ;
- $V_T(t_0)$ = crest tower top voltage at time, t_0 without reflections from adjacent towers;
- $2T_s$ = travel time for a wave to travel to the adjacent tower and return (μs);
- = (twice the span distance in meters)/(300 × 0.9);
- Z_s = shield wire surge impedance, (Ω);

if

$$t_0 < 2T_s, V'_T(t_0) = 0$$

Equation 12.6.11 is constructed on the premise that corona distortion reduces the reflected voltage wave to something approaching a ramp function. The attenuation constant, K_s , may be assumed to be about 0.85 if no specific data are available. The total tower top voltage at stroke crest time, t_0 , is then

$$V_T(t_0) = V_T(t_0) - V'_T(t_0) \quad (12.6.13)$$

Because the insulator voltages have a similar shape to the tower top voltage, Eq. 12.6.11 may also be used for them with $V_T(t_0)$ replacing $V'_T(t_0)$ wherever it occurs.

After crest time, t_0 , when the stroke current has flattened out and the towers have rung down, the effect of voltage reflections from the two adjacent towers may be treated as in Eq. 12.6.12, except that the computed tower top voltage at $6 \mu s$ is used instead of $V_T(t_0)$, and the ratio $(t_0 - 2T_s)/t_0$ is set equal to 2.0. For that case, K_s is approximately 1.0. Just as the voltages reflected from adjacent towers reduce the tower top voltage at the stricken tower, so do they also reduce the voltage across the stricken tower footing resistance, and by nearly the same ratio.

EFFECTS OF POWER-FREQUENCY VOLTAGE

The previous analysis arrived at a critical value of stroke current, I_{cn} , for each phase, n , that must be exceeded if a flashover is to occur on that phase. However, this analysis did not account for any power-frequency voltage. The power-frequency voltage across each insulator continuously adds to or subtracts from the stresses created across the insulator by the lightning stroke, thus continuously changing the amplitude of the stroke current required to cause flashover. This power-frequency voltage may make a significant change in the lightning tripout rate, and it is a major reason why observed tripouts are not all on the phase having the lowest critical current, I_{cn} . In the old AIEE method, the effect of power-frequency voltage was ignored, possibly because it greatly increased the complexity of the graphical method and was different for different tower geometries. In the Monte Carlo method, the inclusion of phase voltage effects is automatic. However, in analytical methods it is a fairly complicated problem, different for each tower configuration and for each phasing arrangement.

As the power-frequency voltage on phase n varies with the instantaneous voltage angle θ_n , it adds to or subtracts from the

flashover voltage, V_{cn} , for that insulator string. At any instant, the critical stroke current, I_{cn} , required to create a flashover on phase n with power-frequency voltage superimposed is

$$I_{cn} = \left[\frac{V_{cn} - V_{on} \sin(\theta_n - \alpha_n)}{V_{cn}} \right] I_{cn} \quad (12.6.14)$$

where V_{on} is the crest phase-to-ground voltage for phase n , θ_n is the instantaneous voltage angle for phase A (the reference phase), α_n is the phase angle of phase n (either 0° , -120° , or $+120^\circ$), I_{cn} is the critical stroke current without power-frequency voltage, and V_{cn} is the insulator flashover voltage at the time of I_{cn} from Figure 12.6.3.

In Eq. 12.6.14, I_{cn} is no longer a constant because power-frequency voltage is present. Instead, I_{cn} is sinusoidal. The numerical example in Figure 12.6.7 is for a three-phase case that might be representative of a 345-kV, vertical single circuit in a region of high footing resistance. Phase C is closest to the shield wire, and consequently, it has the greatest coupling factor. The surge voltage across it is the lowest for a given stroke, thus requiring the highest critical stroke current, I_{cc} (69 kA), if no power-frequency voltage is present. The phase having the lowest

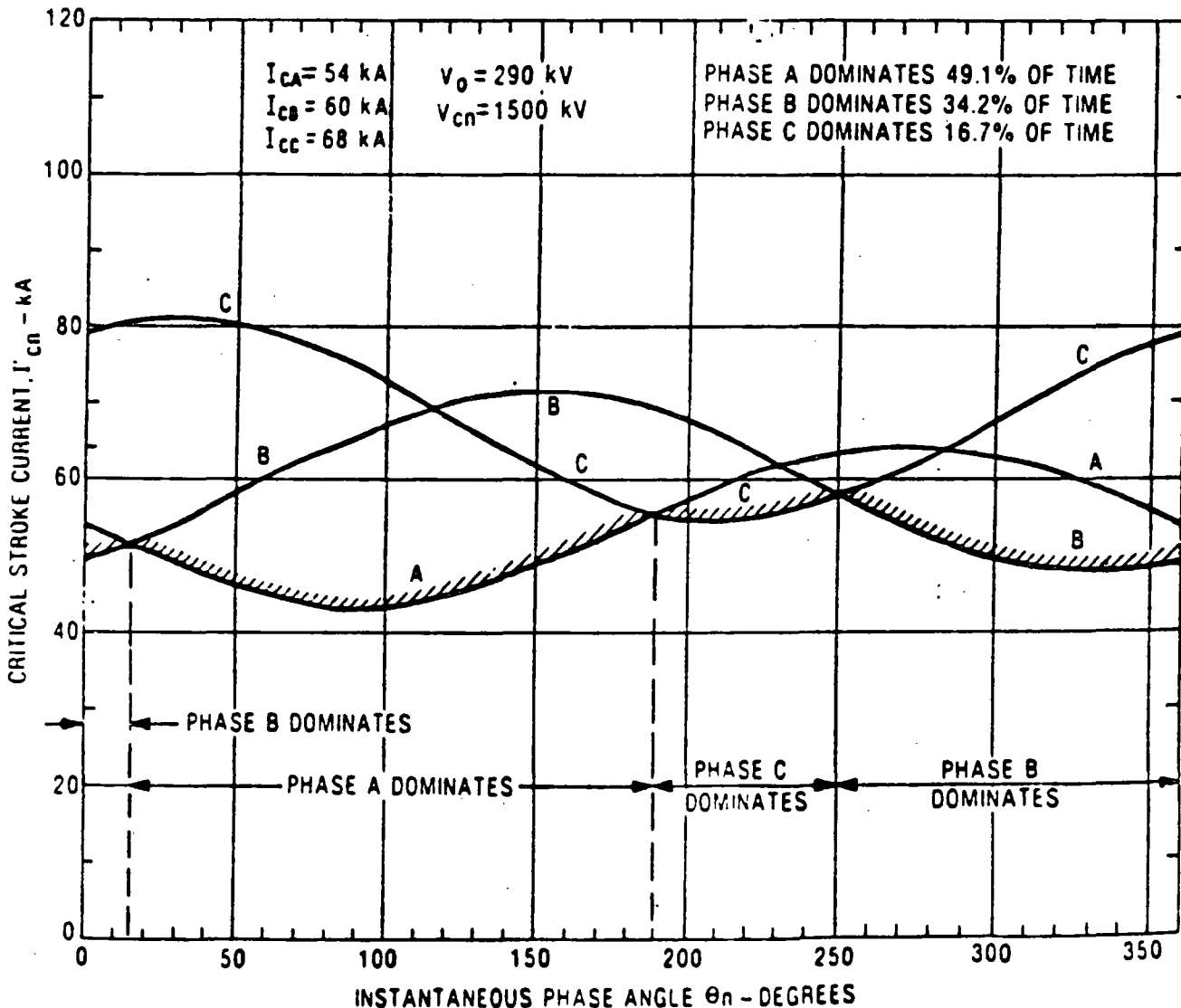


Figure 12.6.7 Fluctuation of the critical stroke current, I'_{cn} required to cause flashover of phase n .

I_{cn} is the most likely to flash over first. It may be called the dominant phase. When it flashes, it suddenly is connected to the tower, becoming the equivalent of another shield wire. This inhibits (but not entirely prevents) flashovers on the other phases. The percentage of time that each phase is dominant (most likely to flash over first) is determined in Figure 12.6.7 by simply measuring the proportion of 360° for which each of the crosshatched phases is dominant.

One must know not only the percentage of time that each phase, n , is dominant, but also the average I_{cn} for that phase during that time because this is used to compute the ultimate tripout rate. If wave n dominates between instantaneous phase angle θ_2 and θ_1 , where θ_2 is the greater, then the average value of I_{cn} for phase n during the dominant interval is symbolized by \bar{I}_{cn} and may be computed from

$$\bar{I}_{cn} = I_{cn} \left\{ 1 + \frac{V_{cn}}{V_{cn}} \left[\frac{\cos(\theta_2 - \alpha_n) - \cos(\theta_1 - \alpha_n)}{\theta_2 - \theta_1} \right] \right\} \quad (12.6.15)$$

where $(\theta_2 - \theta_1)$ must be in radians. As an example for phase C, $\alpha = 190^\circ$, $\theta_2 = 250^\circ$, $\theta_1 = 120^\circ$

$$\bar{I}_{cn} = 68 \left\{ 1 + \frac{290}{1500} \left[\frac{\cos(250^\circ - 120^\circ) - \cos(190^\circ - 120^\circ)}{1.047} \right] \right\} = 55.7 \text{ kA}$$

Once the average critical currents and the percentage have been established for the time each phase dominates, the next step is to construct a back-flash table.

Table 12.6.1 displays a simplified example of a back-flash table. This table provides the back-flash rate of each phase of a transmission line. Table 12.6.1 is an example for three phases (often six may be involved). Even though phase A requires the lowest critical stroke current, I_{cA} , to cause flashover, the power-frequency voltages distribute the flashovers within all three phases, as shown in item 7 of the table. Detailed procedures are presented in the complete numerical example in Section 12.10.

12.7 SHIELDING FAILURES OF TRANSMISSION LINES

Previous sections of this chapter have dealt primarily with flashover of insulators when lightning contacts the tower top or the shield wires close to the tower. Shielding failures are another flashover mechanism that must be considered. These failures occur when a flash misses the shield wires or tower and terminates directly on the phase conductor. Extremely high voltages will quickly develop at the contact point, and they will travel in both directions along the phase conductor, eventually reaching one or more insulators and causing a flashover. The probabilities of occurrence of shielding failures must be computed for each design because such failures represent a significant proportion of the total tripout rate of some lines, particularly lines with only one shield wire.

THE ELECTROGEOMETRIC THEORY

To analyze the frequency of shielding failures on lines, various electrogeometric theories are often used by the industry. In 1963, Young, Clayton, and Hileman (42) authored a basic paper (somewhat difficult to obtain because it was published as an IEEE supplement) that laid the foundation for much of what is now the electrogeometric theory. Whitehead and his colleagues (43,44) have made significant recent contributions to this approach, both in fieldwork and in analytical evaluations.

Table 12.6.1
EXAMPLE OF BACK-FLASH TABLE

Item	Value	⊙A	⊙B	⊙C
1 Total strokes to line per 100 km/year (shielding failure strokes not included)	95	—	—	—
2 Strokes to tower (item 1 times 0.60)	57	—	—	—
3 Percentage of dominance for each phase	—	49.1	34.2	16.7
4 Strokes to tower per year (item 3 times item 2 divided by 100) while each phase is dominant	—	25.0	21.3	8.5
5 I_{cn} required to cause flashover (Eq. 12.6.15)	—	47.4	51.0	55.7
6 Probability that I_{cn} will be exceeded (from Figure 12.4.3)	—	0.26	0.24	0.20
7 Number of strokes per year exceeding flashover level (item 6 times item 4) equals flashover rate per phase	—	6.5	5.1	1.7
8 Total back-flashover rate per 100 km per year (sum of columns in item 7)	13.3	—	—	—

12

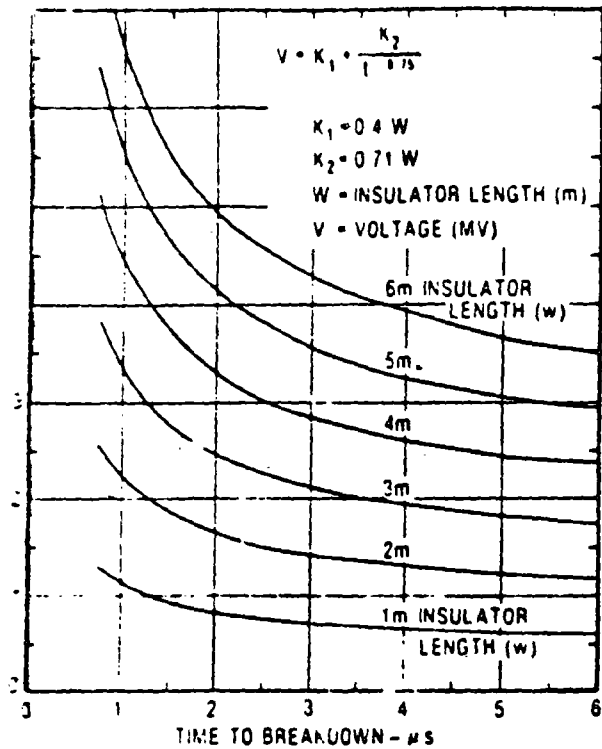


Figure 12.6.3 CIGRE volt-time curve for flashover of line insulators from Carvenza, Popolansky, and Whithead.

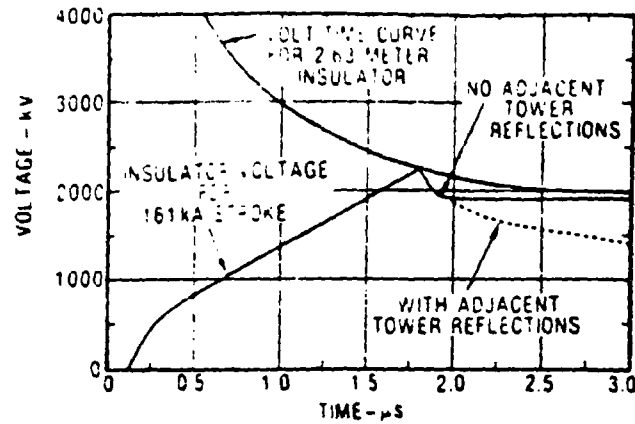


Figure 12.6.5. Increasing stroke current to 161 kA increases insulator voltage until it reaches the flashover volt-time curve.

the stroke crest time and at about 6 μs. It then to work with the lowest of the two critical stroke currents thus obtained.

Caldwell and Darveniza (40) and others have pointed out that it is inaccurate to assume that flashover will occur when a voltage wave just touches the volt-time curve. However, when using only a hand calculator, the additional complexity in computing severity factors is generally not worth the effort if some corrective multiplier can be found instead. There are several influences that argue for a penetration above the volt-time curve. These include the following:

- In reality, the maximum stroke current, di/dt , does not exist at the crest of the current wave but shortly before it. This reduces the insulator voltage and requires more stroke current
- The tower goes into heavy corona during part of the breakdown process. This reduces its surge impedance and the insulator voltage, again requiring more stroke current
- Some flashes terminate on the shield wires, a short or moderate distance away from the tower top. This reduces the current entering the tower top and requires more stroke current to create flashover.

There is one influence that pushes in the opposite direction: the additional voltage on each phase conductor due to the release of bound charge as the lightning flash return stroke occurs. This additional voltage has been ignored thus far in the analysis. The author adopts the compromise of allowing the two curves to just touch. However, the stroke current so derived may, if preferred by other investigators, be multiplied by whatever penetration factor one prefers.

The stroke current required for the insulator voltage in any phase, n , to reach the insulator volt-time curve is defined as the critical stroke current, I_{cn} , for that phase. In this chapter it is computed at the crest time of the stroke current and at 6 μs. The lowest of the two critical currents is used to compute the tripout rate for that phase.

REFLECTIONS FROM ADJACENT TOWERS

Reflections from adjacent towers can drive down the insulator voltages at the stricken tower by reflected current waves, as shown in Figures 12.4.9 and 12.6.6. Depending on the span

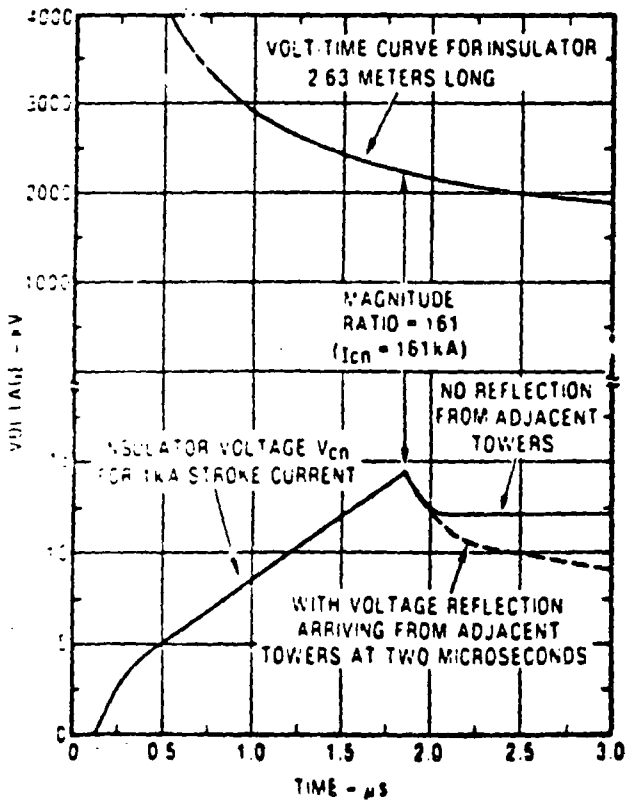


Figure 12.6.4. Per unit insulator voltage under the volt-time curve.

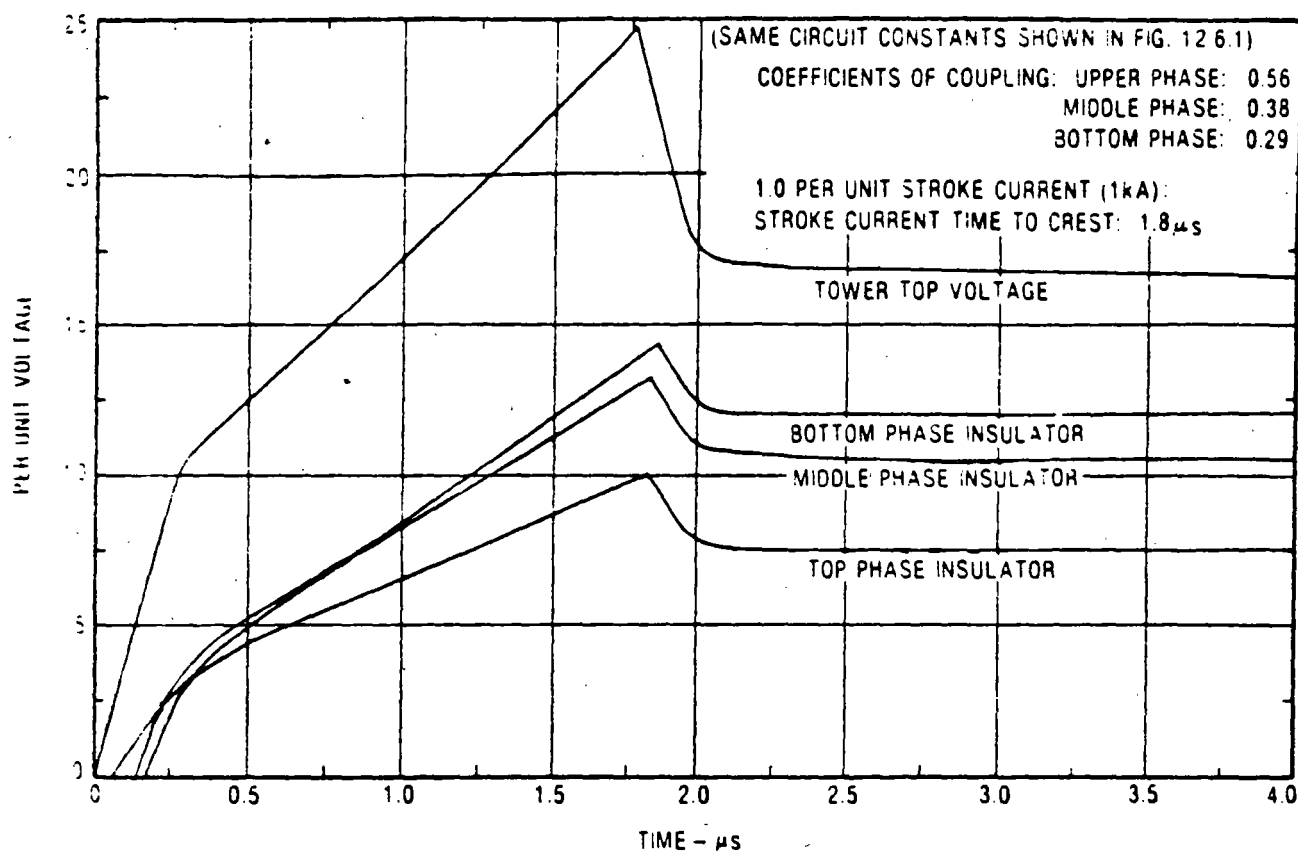


Figure 12.6.2. Examples of insulation voltages in per-unit of crest-stroke current for a flash to the double-circuit tower. (See work sheet 1-A, page 12.10.)

PENETRATION OF INSULATOR VOLTAGE INTO THE VOLT-TIME CURVE

To this point, all lightning voltage calculations have been per unit (e.g., kV of voltage per 1 kA crest stroke current entering the tower). The insulator voltages presented have all been derived for the ramp function of stroke current (Section 12.4). To fit probability requirements it has been shown that this ramp function should crest somewhere between about $1.25 \mu\text{s}$ and $2.5 \mu\text{s}$ (Figure 12.4.8). Next, the stroke current required to cause flashover must be determined from the per unit voltages and from the insulator volt-time curves or the air-gap, volt-time curve if the air gap is weaker than the insulator.

The surge voltage level at which an insulator or air gap will flash over is not a constant; it is a function of time. The shorter the time at which failure occurs, the greater this voltage must be. Figure 12.6.3 presents a mathematically convenient set of insulator volt-time curves published by Darveniza and others (19). The upper left portion, for long insulator strings and short times, is primarily an extrapolation because very few data are available. As a first approximation, use the air-gap length if the air gap is less than the length of the insulator.

As previously stated, the voltage waves shown in Figure 12.6.2 are per unit, as are all calculations thus far. If the stroke has a crest current of 1 kA at $1.8 \mu\text{s}$, then the bottom insulator develops a crest voltage of 14 kV at $1.8 \mu\text{s}$. However, an 18-unit insulator for 345 kV is about 2.63 m long, and Figure 12.6.3 re-

quires that the voltage for flashover at $1.8 \mu\text{s}$ be 2250 kV. Therefore, for a flashover to develop, the stroke current, I_{cr} , must be increased by $2250/14$ (161 times) or 161 kA. This current, I_{cr} , the critical current to cause the phase n insulator to flash over, may have a different value for each phase. Consequently, all phases should be computed. This translation to a stroke current necessary for flashover is diagrammed in Figure 12.6.4 for the bottom phase insulator waveshape of Figure 12.6.2. As shown in Figure 12.6.5, the two curves just touch at $1.8 \mu\text{s}$, but the insulator voltage curve cuts through the volt-time curve beyond $2.7 \mu\text{s}$, at which point one would infer that flashover is more likely to occur.

However, the insulator voltages in Figure 12.6.2 were computed for the case of no reflections arriving from adjacent towers. Adjacent towers will usually be about 300 m or less from the stricken tower, and current reflections will arrive from these towers on both sides of the stricken tower in about $2 \mu\text{s}$ or less (the velocity of light is $300 \text{ m}/\mu\text{s}$) after the stroke makes contact. These reflections are in the direction to drive down the voltages at the stricken tower, as shown by the dotted lines in Figures 12.6.4 and 12.6.5 (discussed subsequently).

In general, the location of the juncture of the insulator voltage curve with the insulator volt-time curve will be at the same time as the crest time of the stroke current if footing resistances are moderate or low. However, if footing resistances are high or the towers are short, the juncture may occur beyond the crest time. Therefore, it is advisable to compute the juncture both at

Figure 12.7.1 shows a simplified model of the postulated shielding failure mechanism for one shield wire and one phase conductor above a horizontal earth. In Figure 12.7.1A, three flashes of equal current magnitude are shown nearing the line. As a flash approaches within a certain distance, s , of the earth and the line, it is influenced by what is below it and jumps the distance, s , to make contact. This distance, s , is called the strike distance, and it is a key concept in the electrogeometric theory. The strike distance is a function of the charge (and consequently the current) in the channel of the approaching flash. Use of the equation developed by Love (45) to find this distance is recommended:

$$S = 10 I^{0.65} \quad (12.7.1)$$

$$I = 0.029 S^{1.54} \quad (12.7.1A)$$

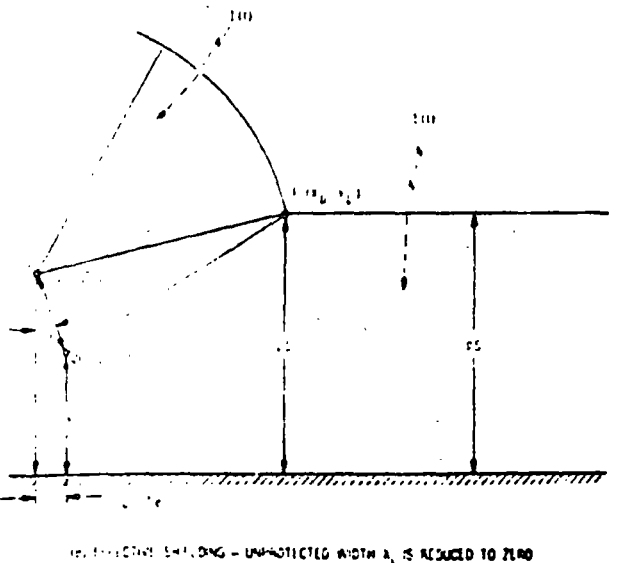
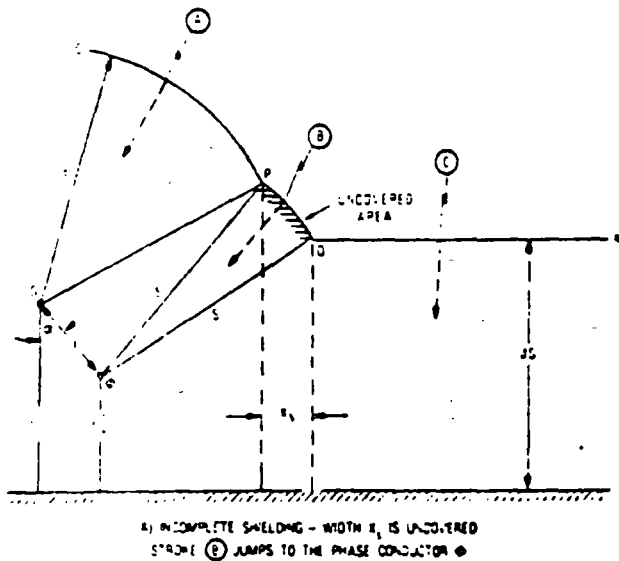


Figure 12.7.1 An electrogeometric model for shielding failures.

where S is the strike distance (m), and where I is the stroke current (kA).

In Figure 12.7.1A, flash A may make its final jump only to the shield wire because anywhere on the arc OP the distance to the phase conductor, ϕ , exceeds s . Flash C may jump only the distance, βs , to the earth because anywhere on line QR the distance to the phase conductor is too great. The coefficient β allows for the strong likelihood that the final strike distance to the horizontal ground plane, with its widespread attractive effects, will be significantly different from the strike distance to a wire suspended above the plane. The value of β used by the author is 0.8 for EHV lines and 0.67 for UHV lines. Note that flash B, as soon as it reaches the arc PQ , may jump only to the phase conductor, ϕ , because distances to the shield wire and earth will exceed the strike distance. For vertical flashes, the width X_1 then establishes the uncovered area of the earth in which flashes that generally would reach the earth contact the phase conductor instead. Whitehead and Brown (44) expanded the electrogeometric analysis to include the effects of flashes coming in from other than a vertical direction and showed that, depending on the flash angular distribution probabilities one assumes, the width X_1 will change. This width should also be adjusted for undulating terrain, nearby trees, and locations along the span (because of sag). In view of these uncertainties, the author will utilize the simplistic assumption of only vertical flashes until the industry arrives at a consensus for the corrections. In all shielding failure calculations, use average conductor heights, i.e., height at the tower minus two-thirds of the sag. If the shield wire is moved more nearly over the phase conductor (Figure 12.7.1B), a condition will be reached in which the uncovered arc PQ disappears and any incoming stroke cannot reach the phase conductor. This results in an effective shielding angle, α_0 . If S is known, and if $\beta S > Y_0$, a trigonometric solution for the uncovered width X_1 is

$$X_1 = S[\cos \theta + \sin(\alpha_0 - \omega)] \quad (12.7.2)$$

where

$$\theta = \arcsin \frac{\beta S - Y_0}{S}$$

$$\omega = \arccos \frac{F}{2S}$$

$$\alpha_0 = \arctan \left(\frac{X_0 - X_G}{-Y_G - Y_0} \right)$$

If $\beta S < Y_0$, $\cos \theta$ is set equal to unity and,

$$X_1 = S[1 + \sin(\alpha_0 - \omega)] \quad (12.7.3)$$

ATTAINMENT OF EFFECTIVE SHIELDING

To attain an effective shielding condition (Figure 12.7.1B), the designer would usually hold the phase conductor fixed and move the shield wire horizontally until the unprotected width, X_1 , is reduced to zero. For good shielding, if the X coordinate of the phase conductor is taken as zero, the X_G coordinate of the shield wire, X_0 , with respect to it, is then

$$X_0 = \sqrt{S^2 - (\beta S - Y_0)^2} - \sqrt{S^2 - (\beta S - Y_G)^2} \quad (12.7.4)$$

In this case the effective shield angle, α_g , becomes

$$\alpha_g = \arctan \left(\frac{Y_G}{Y_S - Y_G} \right) \quad (12.7.5)$$

Note that for positive shield angles, Y_G will be negative because the shield wire will be to the left of the phase conductor in Figure 12.7.1.

SHIELDING FAILURE RATE COMPUTATION

If the line is not effectively shielded, shielding failures will occur, and Eq. 12.7.2 or Eq. 12.7.3 applies. To solve for the shielding failure rate, first compute the magnitude of stroke current, I_{min} , to phase β (the most exposed phase) just sufficient to flash over its insulator:

$$I_{min} = \frac{2V}{Z_s} \quad (12.7.6)$$

where I_{min} is the minimum shielding failure stroke current (kA), V is the insulator critical flashover voltage (kV) (see Figure 12.6.3), and Z_s is the surge impedance of the phase conductor, including corona effects (see Appendixes 12.2 and 12.3). Next, insert I_{min} into Eq. 12.7.1 and solve for the minimum strike distance, S_{min} , to that phase. With S_{min} determined, compute the unshielded width, X_S , from Eq. 12.7.2 or Eq. 12.7.3.

Although not apparent at first, as the distance S in Figure 12.7.1A is increased, the arc PQ decreases. If S is sufficiently large, arc PQ becomes zero, and it becomes equivalent to Figure 12.7.1B. This distance, designated S_{max} , is the strike distance corresponding to the maximum value of stroke current, I_{max} , that can cause a shielding failure. Only flashes having stroke currents between I_{min} and I_{max} can cause a shielding failure according to the electrogeometric theory, and these currents must terminate within the unprotected area. The solution for S_{max} is equivalent to solving Eq. 12.7.4 for S .

However, in Figure 12.7.2, the length of line OP approaches S_{max} for most practical cases, $\beta/10$. If it is assumed that line OP is approximately the same as S_{max} (an assumption at least as valid as most of the other assumptions on which the electrogeometric theory is based), then the quadratic solution for S_{max} is much simplified, and it is easy to show that

$$S_{max} = Y_G \left(\frac{-B_1 - \sqrt{B_1^2 + A_1 C_1}}{A_1} \right) = Y_G S \quad (12.7.7)$$

where

$$Y_G = \frac{Y_0 Y_S}{2}$$

$$A_1 = m^2 - m\beta + \beta^2$$

$$B_1 = \beta(m^2 + 1)$$

$$C_1 = (m + 1)$$

m = slope of line OP in Figure 12.7.2:

$$m = \frac{X_G - X_G}{Y_G - Y_0}$$

Figure 12.7.2 provides the value S by which Y_G must be multiplied to obtain the approximate value of S_{max} . It is a function only of m and the coefficient β . For EHV lines, the author uses $\beta = 0.8$ and for UHV lines 0.67. However, these values are by no means firmly established by the industry.

At this point, the minimum and maximum stroke currents that can cause a shielding failure flashover have been determined, as has the unshielded width, X_S , associated with the minimum current. For the maximum current, I_{max} , X_S shrinks to zero. The average unshielded width is $X_S/2$, and this width X_S is used for the shielding failure computation. The number of flashes causing shielding failure is then determined by computing the most probable number of flashes per 100 per year falling within X_S (by Eq. 12.4.1) and multiplying this number by the difference of the probabilities of the I_{min} and the I_{max} flashes occurring, or

$$N_{SF} = 0.012 T \frac{X_S}{2} (P_{min} - P_{max}) \quad (12.7.8)$$

where N_{SF} is the number of shielding failures per 100 km per year, T is the keraunic level (thunder-days), X_S is the unprotected width (m), P_{min} is the probability that a stroke will exceed I_{min} , and P_{max} is the probability that a stroke will exceed I_{max} .

Note that Eq. 12.7.8 is for one shield wire and one phase conductor. There may be other phase conductors that are also exposed, or there may be one phase conductor that is exposed on

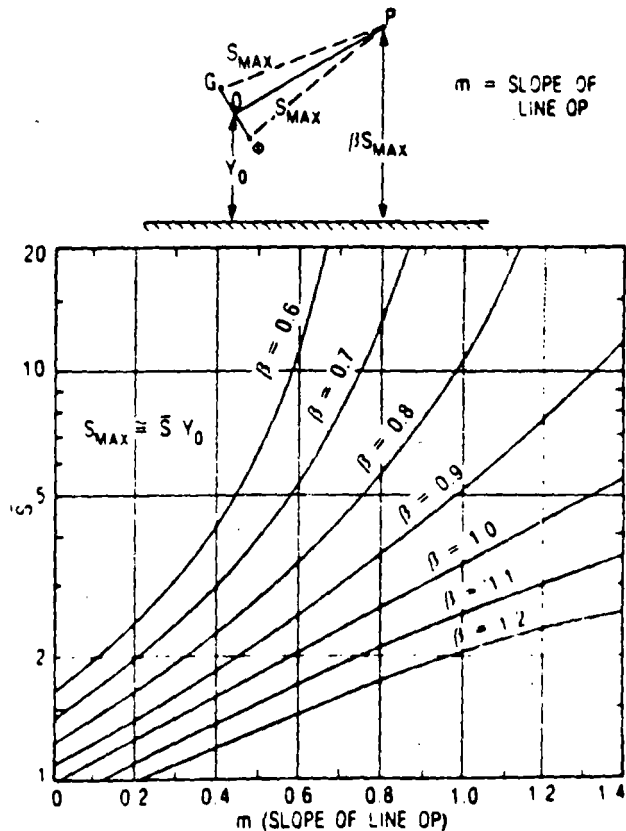


Figure 12.7.2 The value of S by which Y_G must be multiplied to find S_{max} , the maximum possible striking distance

where $(V_T)_2$ is the magnitude of tower top voltage at 2 μ s for a one-per-unit stroke current cresting at 2 μ s. Z_L , Z_s , T_T , and ψ are defined in Equation 12.6.1. (The damping constant ψ usually will not exceed about 0.2 and N in Eq. 12.6.2 will usually be about 4 or 5. Consequently, ψ^N and $N\psi^N$ are very small.) The magnitude of the footing resistance voltage, $V_R/(1 + T_T)$, is closely approximated from Eq. 12.6.5:

$$(V_R)_2 = \left[\frac{\bar{\alpha}_R Z_L}{1 - \psi} \left(1 - \frac{\psi T_T}{1 - \psi} \right) \right] I \quad (12.10.2)$$

where $(V_R)_2$ is the magnitude of voltage across the footing resistance at $(2 + T_T)$ μ s for a one-per-unit stroke current cresting at 2 μ s. From Eq. 12.6.12, the voltage reflection from adjacent towers, which appears across the stricken tower at 2 μ s (provided $2T_T < 2$), is

$$(V_T)_2 = \frac{-4K_S (V_T)_2^2}{Z_S} \left[\frac{1 - 2(V_T)_2}{Z_S} \right] (1 - T_S) \quad (12.10.3)$$

where K_S is the span attenuation factor (defined under Eq. 12.6.11). If $T_T > 1.0$ μ s, there is no voltage reflection at 2 μ s. The total tower top voltage magnitude is

$$(V_T)_2 = (V_T)_2 + (V_T)_2 \quad (12.10.4)$$

The voltage, $(V_{pn})_2$ at crossarm n at 2 μ s is still determined by interpolation, as in Eq. 12.6.8:

$$(V_{pn})_2 = (V_R)_2 + \frac{T_T - T_{pn}}{T_T} \quad (12.10.5)$$

$$\left[(V_T)_2 - (V_R)_2 \right]$$

The insulator surge voltage for phase n at 2 μ s is the difference between the crossarm surge voltage and the phase conductor surge voltage:

$$(V_{in})_2 = (V_{pn})_2 - K_n (V_T)_2 \quad (12.10.6)$$

After the current wave has crested and the towers have rung down and after the effect of tower surge impedance disappears, the equations of Section 12.6 yield the following for the voltages developed at 6 μ s:

$$(V_T)_6 = (V_R)_6 = (V_{pn})_6 = \left[\frac{Z_L R}{Z_L + 2R} \right] I \quad (12.10.7)$$

The reflections from the adjacent towers have not rung down completely. For simplification, only the first set of reflections is used. Then Eq. 12.6.11 applies and becomes

$$(V_T)_6 = -4K_S Z_L \left(\frac{R}{Z_L + 2R} \right)^2 \left[1 - \frac{2R}{Z_L + 2R} \right] I \quad (12.10.8)$$

The total per unit insulator voltage at 6 μ s is

$$(V_{in})_6 = [(V_T)_6 + (V_T)_6] (1 - K_n) \quad (12.10.9)$$

From Figure 12.6.3 the dielectric strengths of an insulator string at 2 and 6 μ s are

$$(V_I)_2 = 820W \quad (12.10.10)$$

and

$$(V_I)_6 = 585W \quad (12.10.11)$$

where $(V_I)_2$ is the insulator flashover strength at 2 μ s (kV), $(V_I)_6$ is the insulator flashover strength at 6 μ s (kV), and W is the insulator length (m). The critical stroke currents required to flash over insulator n at 2 and 6 μ s respectively (in the absence of power-frequency voltage) are

$$(I_{cn})_2 = \frac{820W}{(V_{in})_2} = \frac{(V_I)_2}{(V_{in})_2} \quad (12.10.12)$$

and

$$(I_{cn})_6 = \frac{585W}{(V_{in})_6} = \frac{(V_I)_6}{(V_{in})_6} \quad (12.10.13)$$

6. A general analysis of power-frequency effects is included to obtain a good simulation of the way power-frequency voltages influence the sharing among the various phases of the tripouts that occur and because the presence of power-frequency voltages can make a noticeable increase in total tripouts observed. The approach is that presented in Section 12.6 (Eq. 12.6.11). Combining Eq. 12.6.14 with Eq. 12.10.2 and Eq. 12.6.12 yields

$$(I'_{cn})_2 = \left[\frac{820W - V_{on} \sin(\theta_n - \alpha_n)}{(V_{in})_2} \right] (I_{cn})_2 \quad (12.10.14)$$

and

$$(I'_{cn})_6 = \left[\frac{585W - V_{on} \sin(\theta_n - \alpha_n)}{(V_{in})_6} \right] (I_{cn})_6 \quad (12.10.15)$$

where $(I'_{cn})_m$ is the critical stroke current required to cause flashover of insulator n at m μ s with power-frequency voltage present, V_{on} is the crest phase-to-ground voltage for phase n , θ_n is the instantaneous voltage angle, α_n is the phase angle of phase n (either 0° , -120° , or $+120^\circ$), and W is the length of the insulator string (m) [820 W is $(V_T)_2$, flashover strength of the insulator string at 2 μ s (kV) and 585 W is $(V_T)_6$, the flashover strength of the insulator string at 6 μ s (kV)].

7. Probabilities of flashover are determined directly from the stroke probability curves. After the critical stroke currents (with power-frequency effects included) are determined, the probability of a stroke equaling or exceeding this value is found directly from the stroke probability distribution curve of Figure 12.4.3. The Anderson-Eriksson curve is used. Knowing this prob-

$$V_L(t) = \left(\frac{2R' + Z_i'}{Z_i'} \right) V_T(t) - R'I(t) \quad (12.9.5)$$

where $V_L(t)$ is the voltage at any time, t , across L and $V_T(t)$ is the tower top voltage at time t . Also,

$$V_R(t) = V_T(t) - V_L(t) \quad (12.9.6)$$

where $V_R(t)$ is the voltage at time t across the equivalent footing resistance R' . Then,

$$V_{pn}(t) = \left[1 - \frac{Y_n}{h} \left(\frac{2R' + Z_i'}{Z_i'} \right) \right] V_T(t) + \frac{Y_n}{h} R'I(t) \quad (12.9.7)$$

where $V_{pn}(t)$ is the voltage at crossarm n at time t . Y_n is the distance from the tower top down to the crossarm n in meters, and h is the tower height in meters. R' and Z_i' are given by Eqs. 12.9.1 and 12.9.2. L is given by Eq. 12.9.3. The term within brackets is fixed and is computed once. The insulator voltage, $V_{in}(t)$, for insulator n is

$$V_{in}(t) = V_{pn}(t) - K_n V_T(t) \quad (12.9.8)$$

where K_n is the coefficient of coupling from tower top to phase n . If Eqs. 12.9.7 and 12.9.8 are combined, then

$$V_{in}(t) = \left[1 - K_n - \frac{Y_n}{h} \left(\frac{2R' + Z_i'}{Z_i'} \right) \right] V_T(t) + \frac{Y_n}{h} R'I(t) \quad (12.9.9)$$

Eq. 12.9.9 is the basic equation for insulator voltage using the R-L equivalent circuit. To utilize it, the tower top voltage, $V_T(t)$, must be determined first. If the differential equation of Figure 12.9.4 is solved for $V_T(t)$ when $I(t) = At$ (a ramp function), then

$$V_T(t) = \frac{AL(Z_i')^2}{(2R' + Z_i')^2} (1 - e^{-at}) + \frac{Z_i' R' At}{(2R' + Z_i')} \quad (12.9.10)$$

where

$$a = \frac{2R' + Z_i'}{2L}$$

Both Eqs. 12.9.9 and 12.9.10 may be set up on a programmable hand calculator. Eq. 12.9.9 cannot exactly duplicate the computed response with a traveling wave solution because it assumes instantaneous communication between both ends of the tower

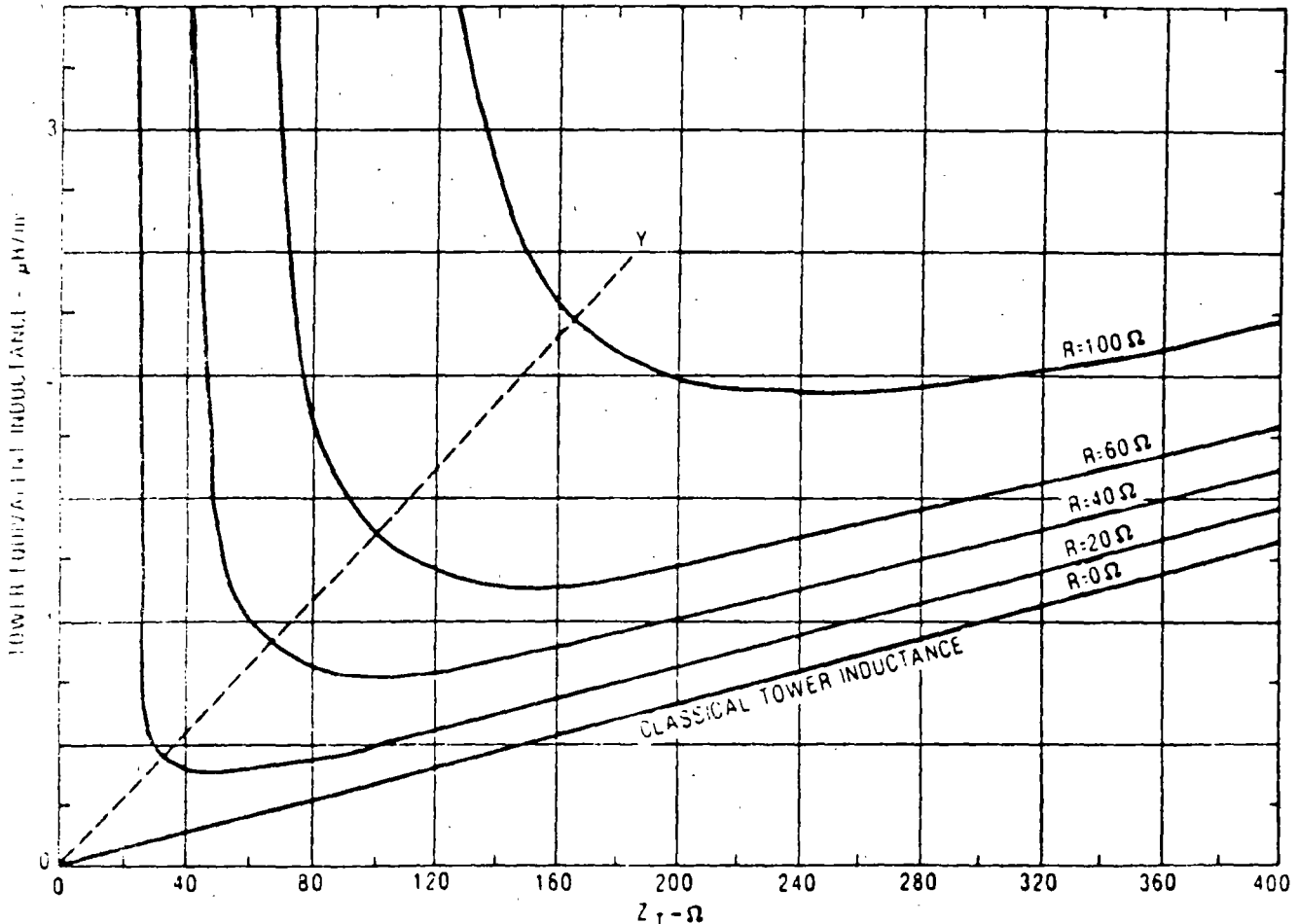


Figure 12.9.2. Effective tower inductance per meter of length as a function of tower surge impedance and tower footing resistance ($Z_s = 400 \Omega$).

both sides. In these cases, each shielding failure rate is added separately to find the total shielding failure rate. After the shielding failure rate is computed, this rate is subtracted from the total number of strokes, N_s , to the line (Eq. 12.4.6) to determine the total number of strokes available to be used in back-flashover calculations.

12.8 LIGHTNING PERFORMANCE OF UHV LINES

The lightning performance of UHV lines has been estimated by Anderson (10) and by Darveniza and others (19). In summary, because of the large air gaps and insulator lengths, lines above 800 kV should be practically lightning proof, provided that attention is paid to proper shield angles and that the footing resistances are maintained below 50 Ω. There are substantial uncertainties regarding the value of β to use for adequate shield angles, and consequently the author has used $\beta = 0.64$ to be conservative. Also, the volt-time flashover for these large gaps is ill defined, and no field experience is available. However, proper design should provide extremely good lightning performance. The preceding references provide more details.

12.9 EQUIVALENT R-L CIRCUITS OF TRANSMISSION TOWERS

Representation of the lightning response of transmission towers by lumped resistance-inductance circuits has distinct advantages in that the traveling wave equations are eliminated and voltage solutions may be determined by conventional circuit analysis. Such representations are particularly appropriate when the greater precision of the traveling wave solution is not justified because of meager or ill-defined problem parameters, as is usually the case. The key problem that arises is the choice of proper values of tower inductance and footing resistance for best accuracy.

Figure 12.9.1 presents the conventional equivalent circuit using a tower surge impedance representation on the left and an R-L representation on the right. Appendix 12.7 shows that, if both circuits are to have the same initial and final voltage responses, Z'_s and R' must be selected so that

$$Z'_s = \frac{2Z_s Z_T}{Z_s + 2Z_T} \quad (12.9.1)$$

and

$$R' = \frac{RZ_T}{Z_T - R} \quad (12.9.2)$$

A unique value of L must also be chosen. The author uses a value such that the area under the R-L volt-time response curve to a step function of stroke current is equal to the area under the tower volt-time response of the conventional traveling wave circuit. Appendix 12.7 provides a derivation for this equivalent inductance

$$L = \left(\frac{Z'_s + 2R'}{Z'_s} \right)^2 \frac{2Z_s \tau_T}{(1 - \psi)^2} \quad (12.9.3)$$

where L is the total tower inductance (μH), τ_T is the tower travel time (μs), Z_s is the tower wave impedance (not the tower surge

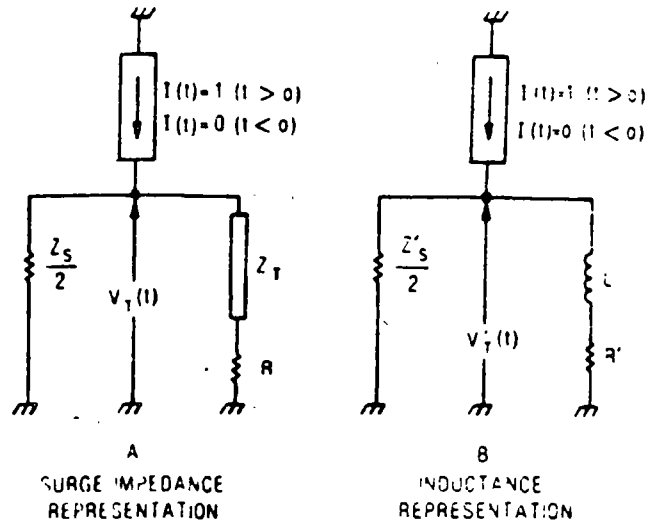


Figure 12.9.1. Two equivalent circuits of a transmission tower, and shield wire subjected to a step-function lightning stroke.

impedance), and ψ is the damping factor (see Eq. 12.6.1C). Only when the footing resistance is zero ($R = R' = 0$), does Eq. 12.9.3 reduce to

$$L = Z_T \tau_T \quad (12.9.4)$$

which is the classical formula for tower inductance. The travel time, τ_T , establishes the height of the tower, and the total inductance is directly proportional to the height. Figure 12.9.2 presents an example of how the tower equivalent inductance is related to the tower surge impedance for nonzero values of footing resistance. To the left of line OY , the inductance values turn toward infinity and become infinite when the footing resistance is equal to the tower surge impedance. To the right of line OY , the values tend to vary linearly, but are always above the classical value for $R > 0$. The classical value of tower inductance, which is independent of the terminations, is the best equivalent value only when the footing resistance is zero.

Figure A12.7.2 of Appendix 12.7 shows the response of equivalent R-L circuits as well as traveling wave (tower surge impedance) circuits when a step-function stroke current is applied. The ringing of the latter is not duplicated by the R-L circuit. However, the settling time is roughly simulated and is only a few tower round-trip travel times—for conventional towers, a few tenths of a microsecond. It is therefore of interest to see how well an R-L circuit using this value of inductance duplicates the response of a tower to a ramp-function stroke current. An example is shown in Figure 12.9.3 for a standard stroke-current ramp function. The agreement is extremely good in all regions of significance.

It can be shown by numerical experiment that the value of L given by Eq. 12.9.3 is the only value that permits the inductive solution to be asymptotic to the traveling wave solution before and at the crest of the wave.

The R-L equivalent circuit has another advantage in that a good approximation for any crossarm voltage is easily obtained. First, the assumption is made that the tower inductance per unit length does not change with tower height. The crossarm may be considered to be connected partway down on the tower inductance, as shown in Figure 12.9.4. Then, the differential equation of Figure 12.9.4 reveals that

12.10 A SIMPLIFIED TWO-POINT METHOD FOR COMPUTING LIGHTNING PERFORMANCE OF TRANSMISSION LINES

The previous sections provided the foundations for computing lightning trippouts with about all the rigor that is justified considering the sparsity of data and the uncertainties of the statistics of lightning, climate, and geology. The preceding is clearly too complex for convenient solution with a hand calculator, and simplifications are required. In this section, a step-by-step hand calculation method is developed, and a numerical example for a double-circuit tower is presented. Step-by-step schedules are provided to help the user keep track of computations and to store intermediate values that will be used later.

BASIS OF THE METHOD

The method is based on the following concepts:

1. Only one waveshape is utilized. Section 12.4 showed that, although stroke-crest currents and rise times have different probability distributions, they are not independent once one selects the time-to-crest of a ramp function used to simulate the stroke waveshape. Figure 12.4.8 shows the relationship that must then exist to meet probability requirements. Most lightning trippouts from back-flashovers are caused by strokes with magnitudes of 80 kA or higher (frequently much higher), and Figure 12.4.8 indicates that a stroke waveshape time-to-crest in the 1.8- to 2.0- μ s range or more would simulate field observations reasonably well. However, Figure 12.4.5 demonstrates that, even if one errs by selecting a somewhat faster rise time than observed in field measurements, the effect of the error is minimized because of the increase in dielectric strength of the insulator volt-time curve. Therefore, for this simplified method, the standard wave will be a ramp function cresting at 2 μ s, with a flat top.
2. Reflections from adjacent towers are included. Reflections from adjacent towers can reduce tower top potentials and significantly reduce the line flashover rate. As reviewed in Section 12.6, these reflections are distorted by corona currents, and their velocity of propagation is slowed appreciably by resistance and corona effects. (The author has often used a velocity of 0.9C for waves from adjacent towers, where C is 300 m/ μ s, the velocity of light, although in reality different parts of these reflected waves travel with different velocities.) Thus if an adjacent tower is 300 m (984 ft) away, these slowed reflections would start arriving at the stricken tower at about 2.2 μ s. Even for a 200-m (656-ft) span, about 1.5 μ s will elapse before refractions start reducing the voltages at the stricken tower. Because most EHV transmission spans average 200 m or more in length, one may simply select a stroke front time of 2 μ s as a standard waveshape from Figure 12.4.8 and then correct for reflections from the nearest towers according to Eq. 12.6.11 and Eq. 12.6.12 in Section 12.6.
3. Penetrations into the volt-time curve are computed at only two points. Figure 12.10.1 shows the per unit

stroke-current wave adopted as the standard and the two points, A and B, at which the critical stroke current required to make the insulator voltage penetrate into the volt-time curve is computed. The lower of the two stroke currents is then used as the true critical stroke current for flashover calculations. No penetration factor (see Section 12.6) is used. Flashovers beyond 6 μ s are assumed to be infrequent because of the flattening of the volt-time curve. The two voltages, A and B, are computed for each insulator on the tower unless it is determined by inspection that the insulators have identical stresses.

4. Subsequent strokes are ignored. The analysis suggests that as far as the severity of voltage across the insulators is concerned, subsequent strokes in the same flash are no worse than the first stroke. Subsequent strokes create more insulator voltage but at shorter times where the insulator strength is higher.
5. By selecting the two penetration points at times of 2 and 6 μ s, all the voltage equations are greatly simplified. With t_0 equal to 2 μ s (A in Figure 12.10.1) and no reflections from adjacent towers, Eq. 12.6.2 reduces to the following good approximation:

$$(V_T)2 = \left[Z_I - \frac{Z_v}{1-\psi} \left(1 - \frac{\tau_T}{1-\psi} \right) \right] I \tag{12.10.1}$$

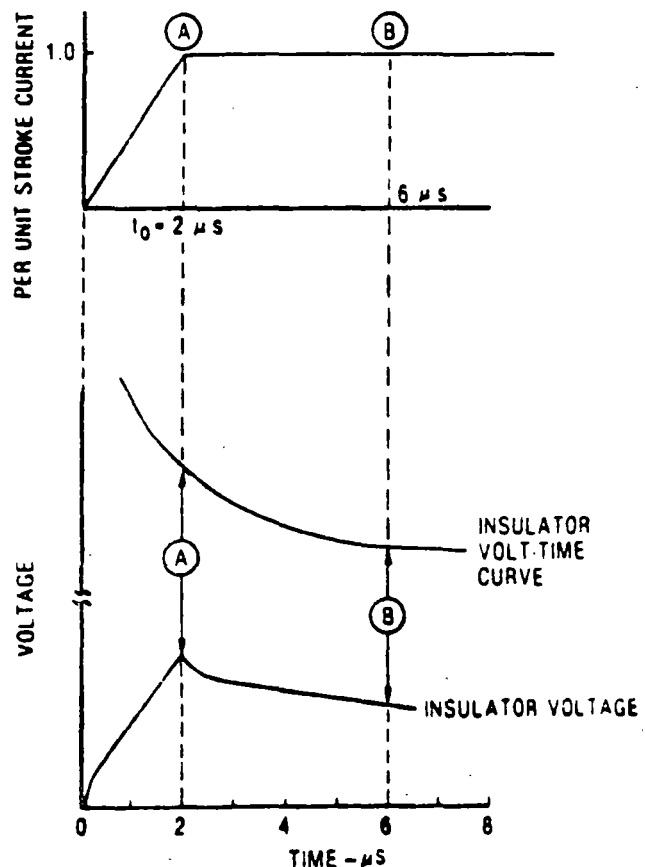


Figure 12.10.1. A simple ramp-function stroke current is used, and insulator voltages computed at only two points in time.

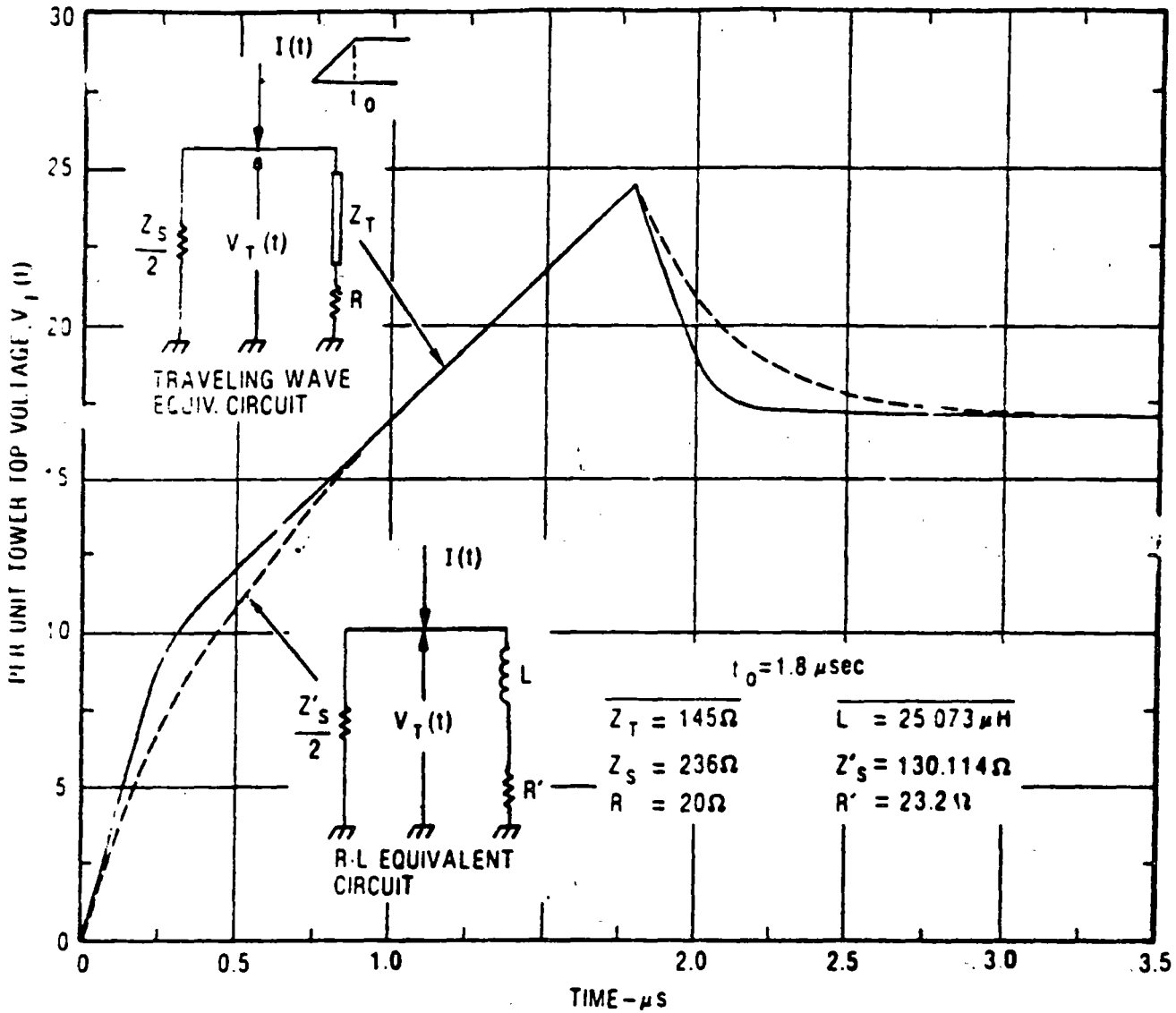


Figure 12.9.3. Computed tower top voltages for two different equivalent circuits.

and the crossarm. However, it is close enough for practical purposes if fast second strokes are not being applied. It should be clear from Figure 12.9.3 that unless footing resistance is very high, the voltages need to be computed only at or near the crest time of the applied current wave. For this case, $e^{-t/\tau}$ is usually so small that the equation for tower top voltage becomes

$$V_T(t) = \frac{IZ'_S}{2R' + Z'_S} \left(\frac{LZ'_S}{2R' + Z'_S} - R't \right) \quad (12.9.11)$$

For all practical purposes, an R-L equivalent circuit may be used to represent the lightning response of a tower provided the values of R' , Z'_S , and L are chosen according to Eqs. 12.9.1 through 12.9.3.

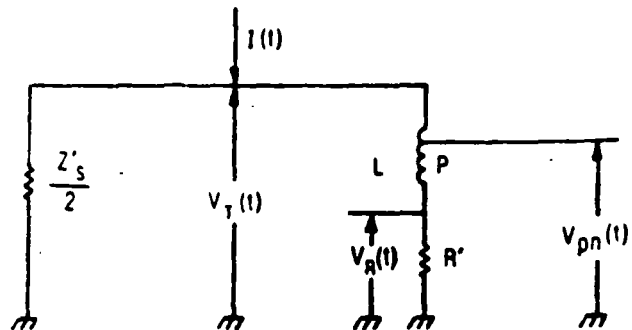


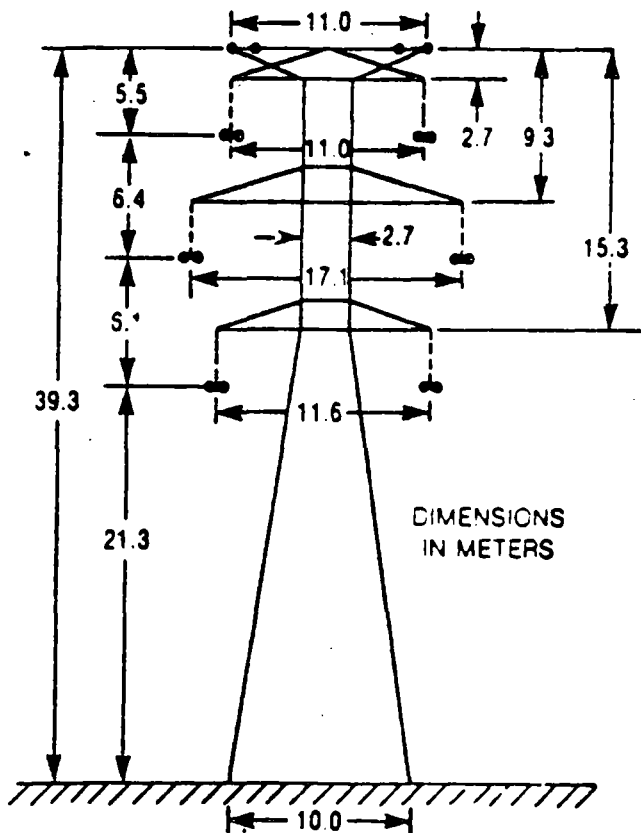
Figure 12.9.4. Crossarm connects partway down the tower inductance.

ability and the number of strokes to the line (with shielding failure strokes deleted), the expected number of flashovers per 100 miles per year immediately follows.

3. Shielding failures are included. The equations of Section 12.7 are applied to establish the shielding failure rate for the phase conductors on each side of the center line. The shielding failure rates are then summed to find the total shielding failure rate.
4. Schedules are provided to facilitate a step-by-step solution for the lightning performance of practically any transmission line. Schedules 1 and 2 provide a step-by-step guide for using the concepts and equations in this chapter to find the lightning outage rate of a transmis-

sion line. One begins by drawing the supporting towers to scale, defining all the dimensions, and computing lightning incidence and concludes with the expected lightning flashover rate for each phase and for the entire line. The schedules shown are filled in with a specific example of a double-circuit, 345-kV tower in a region with a keraunic level of 30. To use these schedules for any other case, reproduce them with a copier and mask out the handwritten entries with typist's white correction fluid. Then copy them once again. From the length of the schedules, it would appear that the solution is the result of a long and laborious process. However, once all the input is available (as it must be for any method), the solution will emerge reasonably well. Worksheets begin on the following page.

WORK SHEET 1-A. 345 kV, VERTICAL DOUBLE-CIRCUIT, TWO GROUND WIRES



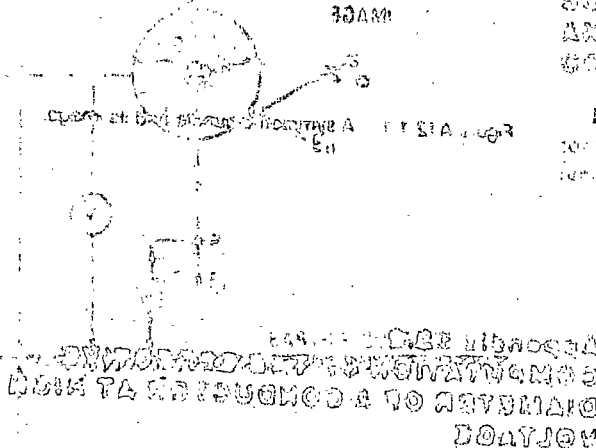
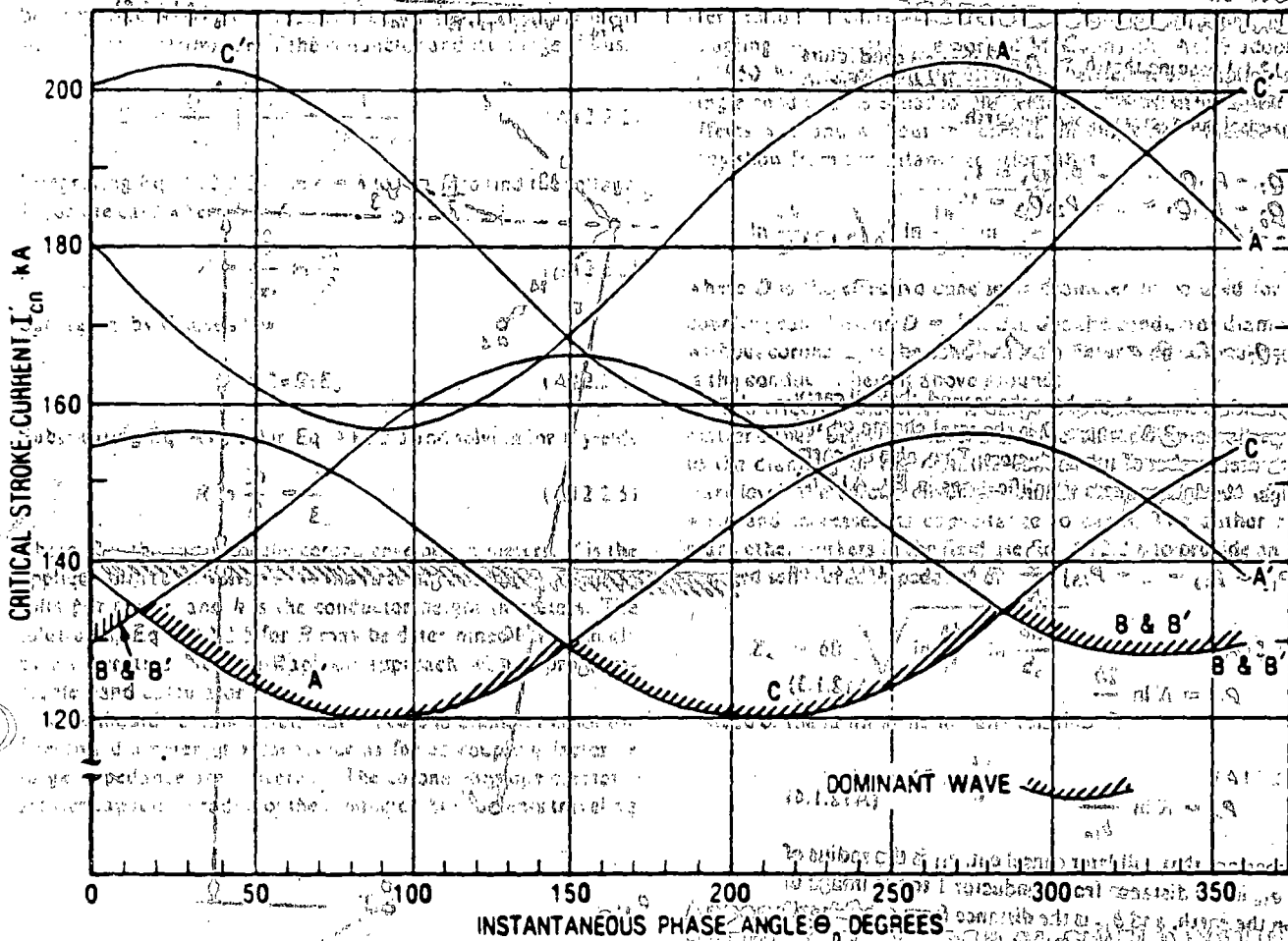
Tower Sketch

Conductor No.	Function	Phase Coordinates		Conductor Radius (cm)	Bundle Spacing (cm)	Operating Phase-Phase (kV)	α Phase Angle (degrees)
		X (m)	Y (m)				
1	Shield	-5.5	39.3	0.45	—	0	—
2	Shield	5.5	39.3	0.45	—	0	—
3	A	-5.5	33.8	1.48	45.7	345	0
4	B	-8.6	27.4	1.48	45.7	345	-120
5	C	-5.8	21.3	1.48	45.7	345	120
6	C'	5.5	33.8	1.48	45.7	345	120
7	B'	8.6	27.4	1.48	45.7	345	-120
8	A'	5.8	21.3	1.48	45.7	345	0

W = Insulator length (m) 2.63
 h = Tower height (m) 39.3
 b = Spacing between shield wires (m) 11
 S = span distance (m) 335

Shield height at midspan (m)
 Conductor sag (m) 7.0
 Tower width at base (m)
 Distance from tower top to phase conductor (m)—
 Upper: 5.5; Middle: 11.9; Lower: 18.0.

WORK SHEET 2-A. PLOTTING I_{cn} IN STEP 31 FOR EXAMPLE CASE



AND VOLTAGES APPLIED TO THE PHASE CONDUCTORS (P. 151A)

For any ray of horizontal incidence (same angle theta) the critical stroke current I_{cn} is a function of the phase angle theta and is related to the critical stroke current I_{cn0} by the following equation:

$$I_{cn} = I_{cn0} \left(\frac{1 + \cos \theta}{2} \right)^{0.5}$$

$$I_{cn} = I_{cn0} \left(\frac{1 + \cos \theta}{2} \right)^{0.5}$$

$$I_{cn} = I_{cn0} \left(\frac{1 + \cos \theta}{2} \right)^{0.5}$$

$$I_{cn} = I_{cn0} \left(\frac{1 + \cos \theta}{2} \right)^{0.5}$$

The complete analytical model consists of this geometry together with an associated set of basic assumptions and mathematical relations. The basic assumptions are listed below.

(a) The mean conductor height \bar{Y} can be computed from profile drawings or, alternatively, estimated for preliminary purposes from the following broad relations:

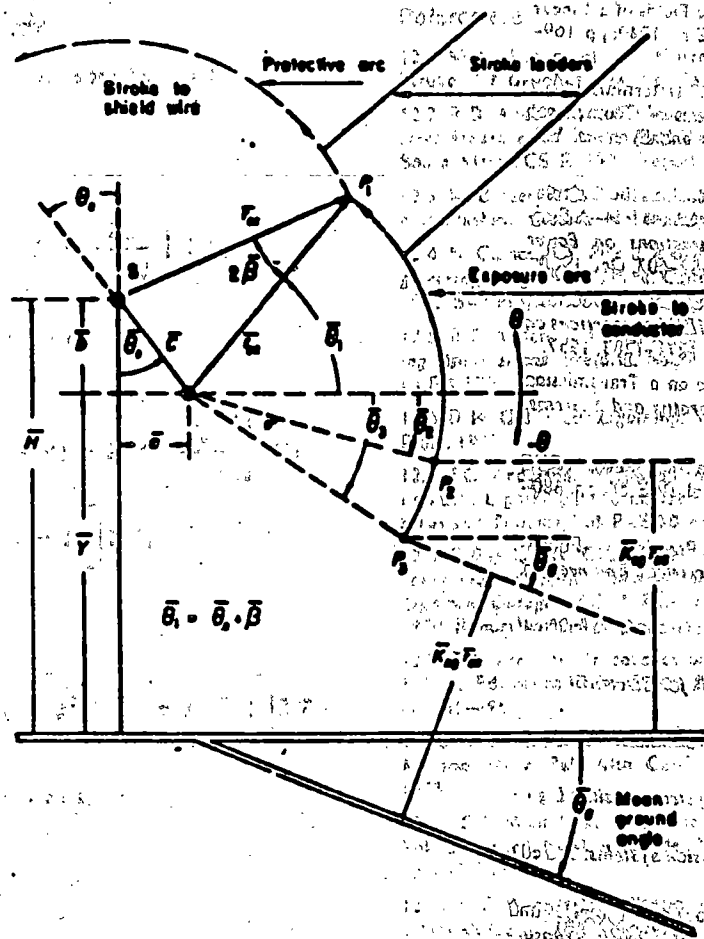
flat profile

$$\bar{Y}_f = Y_i - (2/3)(S_c)$$

(1)

Y_i = height of conductor at the tower;

S_c = sag of the conductor;



Geometry of the reference model for shielding failure.

rolling profile

$$\bar{Y}_r = Y_i$$

(2)

mountainous profile

$$\bar{Y}_m = 2Y_i$$

(3)

for all cases

$$R = \bar{Y} + b$$

(4)

$$b = b_1 + (2/3)(S_s - S_c)$$

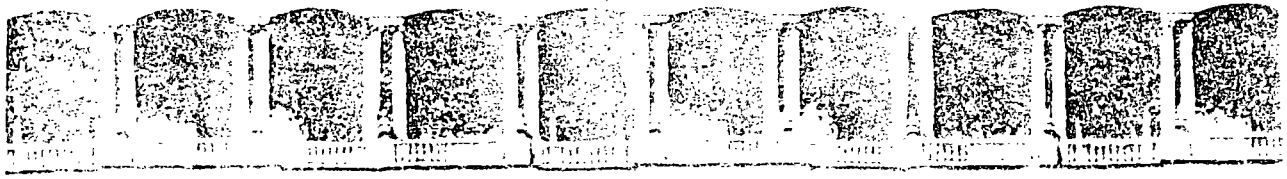
(5)

$$b_1 = H_i - Y_i$$

(6)

H_i = height of the shield wire at the tower;

S_s = sag of the shield wire.



FACULTAD DE INGENIERIA U.N.A.M.
DIVISION DE EDUCACION CONTINUA

V CURSO INTERNACIONAL DE SISTEMAS ELECTRICOS DE POTENCIA

MODULO II: SISTEMAS ELECTRICOS DE POTENCIA

TEMA: WAVE PROPAGATION

EXPOSITOR: ING. ARTURO MORALES COLLANTES

I. WAVE PROPAGATION

I.1. INTRODUCTION

I.1.1. TYPES OF OVERVOLTAGES

LIGHTNING STROKES
SWITCHING SURGES
ARCING GROUNDS
RESONANCE VOLTAGES

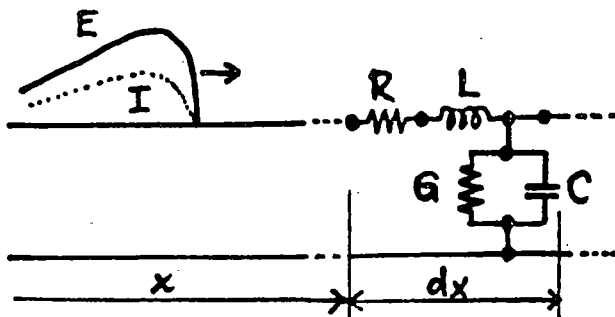
I.1.2. LIGHTNING STROKES

FREQUENCY OF OCCURRENCE
STATISTICAL DATA

MAGNITUDE
DURATION
RELEVANT PARAMETERS

I.1.3. MODELING LINES

DISTRIBUTED PARAMETERS
TRANSMISSION LINE DIFF. EQUATIONS



$$\frac{\partial^2 E}{\partial x^2} = \gamma^2 E$$
$$\frac{\partial^2 I}{\partial x^2} = \gamma^2 I$$

$$\gamma = \alpha + j\beta = \sqrt{(R+sL)(G+sC)}$$

1.2. IMPORTANT PARAMETERS

1.21. PROPAGATION CONSTANT

$$\gamma = \alpha + j\beta = \sqrt{Z_{\text{LINE}} Y_{\text{LINE}}}$$

α = ATTENUATION CONSTANT

β = PHASE CONSTANT

1.22. CHARACTERISTIC (SURGE) IMPEDANCE

$$Z_0 = \sqrt{\frac{Z_{\text{LINE}}}{Y_{\text{LINE}}}} \quad e = Z_0 i \quad Y_0 = \frac{1}{Z_0}$$

1.23. LOSSLESS LINE: $R = 0, G = 0$

$$\gamma = s\sqrt{LC}$$

$$Z_0 = \sqrt{\frac{L}{C}}$$

1.24. DISTORTIONLESS LINE: $\frac{L}{R} = \frac{C}{G}$

1.3. LINE PARAMETERS, SIMPLE CASES

1.31. OVERHEAD CONDUCTOR

$$L = 2 \left(\frac{1}{4} + \ln \frac{2h}{r} \right) 10^{-4} \text{ H/km}$$

$$C = \frac{10^{-6}}{18 \ln \frac{2h}{r}} \text{ F/km}$$

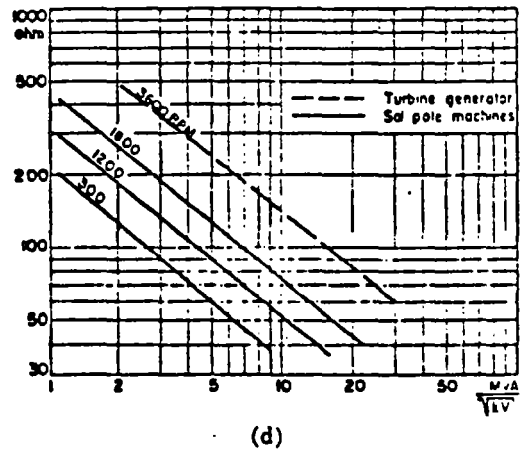
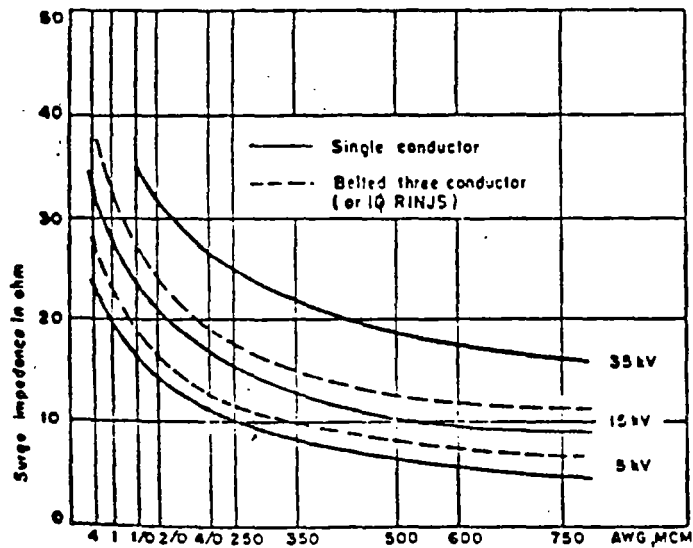
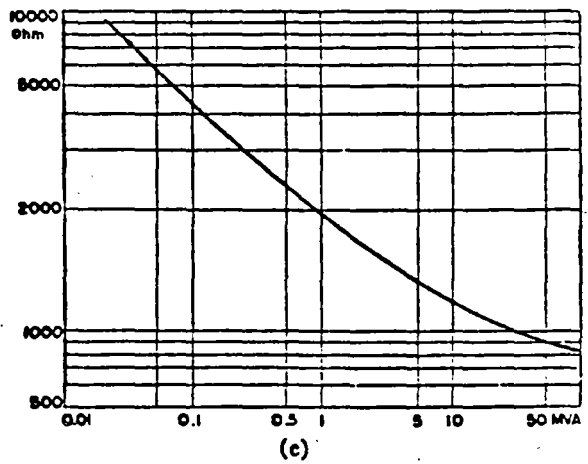
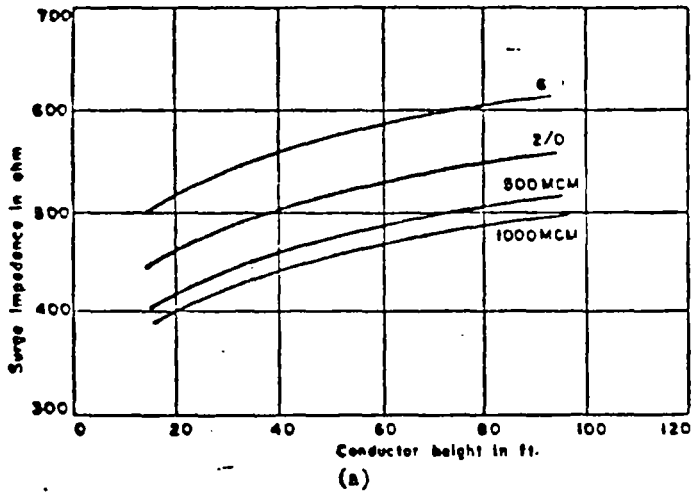
1.32. CABLE (ONE CONDUCTOR)

$$L \cong 2 \left(\frac{1}{4} + \ln \frac{R}{r} \right) 10^{-4} \text{ H/km}$$

$$C = k \frac{10^{-6}}{18 \ln \frac{R}{r}} \text{ F/km}$$

1.33. THREE PHASE SYSTEMS

1.4. SURGE IMPEDANCE CHARTS



(b) FORSTMAIER, TRANS. IGA, SEPT. 1965, 351
 (a) Surge impedance of overhead conductors. (b) Surge impedance of paper insulated lead covered cables. (c) Surge impedance per phase for transformers α (high-voltage term). (d) Surge impedance per phase for synchronous machines

TYPICAL VALUES:

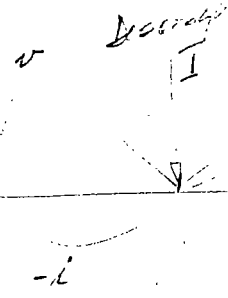
OVERHEAD LINES: 400-600 OHMS
 CABLES: 10-40 OHMS, AROUND 25 OHMS
 TRANSFORMERS: THOUSANDS OF OHMS
 SYN. MACHINES: SEVERAL HUNDREDS OF OHMS

1.5. VELOCITY OF PROPAGATION

$$v \cong \frac{1}{\sqrt{LC}} = 300 \text{ m}/\mu\text{s}$$

$$v = \frac{v_{\text{LIGHT}}}{\sqrt{k\mu}}$$

1.6. MATHEMATICAL EXPRESSION OF E AND I



$$E = e^{\gamma x} f_1(t) + e^{-\gamma x} f_2(t)$$

$$I = -\frac{1}{Z_0} [e^{\gamma x} f_1(t) - e^{-\gamma x} f_2(t)]$$

$$E = f_1\left(t + \frac{x}{v}\right) + f_2\left(t - \frac{x}{v}\right) = E_{\text{BACKWARD}} + E_{\text{FORWARD}}$$

$$I = -\frac{1}{Z_0} \left[f_1\left(t + \frac{x}{v}\right) - f_2\left(t - \frac{x}{v}\right) \right] = -I_{\text{BACKWARD}} + I_{\text{FORWARD}}$$

1.7. POLARITIES

FORWARD (INCIDENT) WAVES

$$E_f = Z_0 I_f$$

BACKWARD (REFLECTED) WAVES

$$E_r = -Z_0 I_r$$

1.8. SHAPE OF WAVES

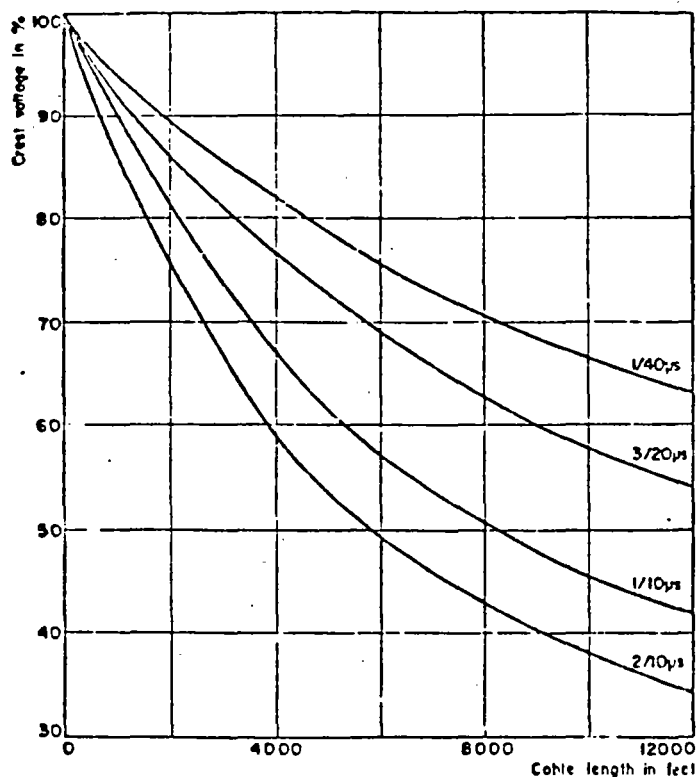
1.81. SPECIFICATIONS

ANSI: 1.2×50

1.82. APPROXIMATIONS

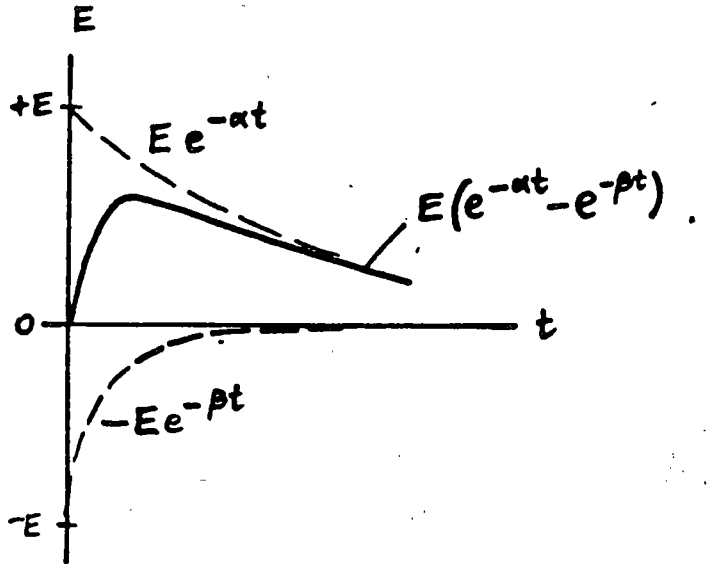
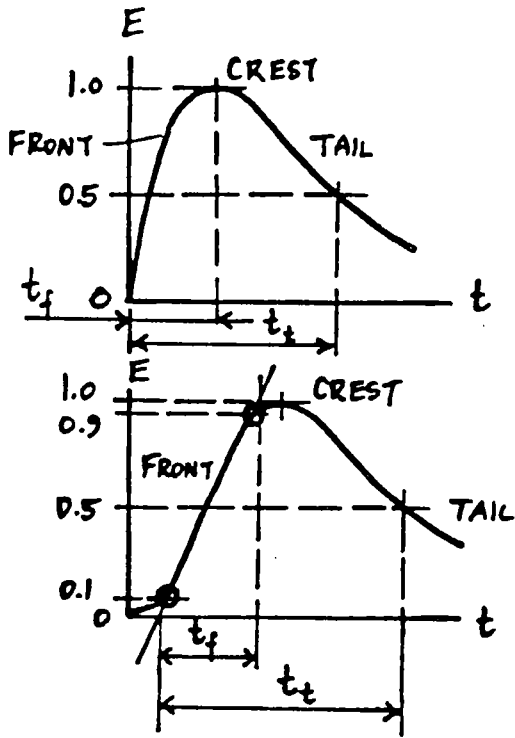
1.9. ATTENUATION AND DISTORTION

LOSSES
 CORONA
 GROUND
 SKIN EFFECT
 CHANGING L AND C



EFFECT OF
 DISTANCE

Fig. 4. Surge attenuation in cables as function of cable length.
 FORTMAYER, TRANS. ICA, SEPT. 1965, 352

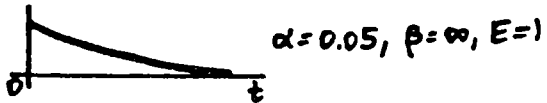
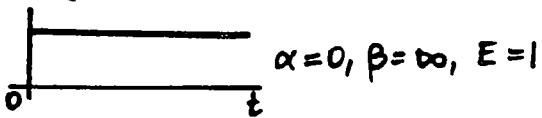


SPECIFICATION OF A TRAVELING WAVE:
 WAVE: $(t_f) \times (t_t)$ in μ seconds:

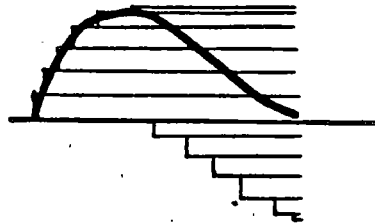
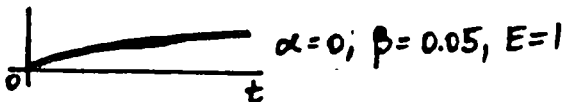
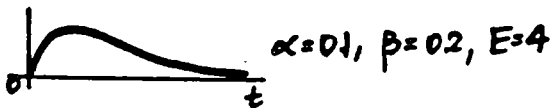
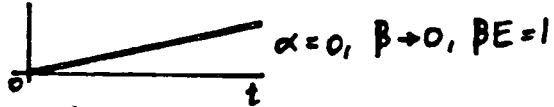
$1.2 \times 50, \quad 5 \times 10$

TRAVELING WAVE AS THE SUM OF TWO EXPONENTIAL FUNCTIONS

UNIT STEP



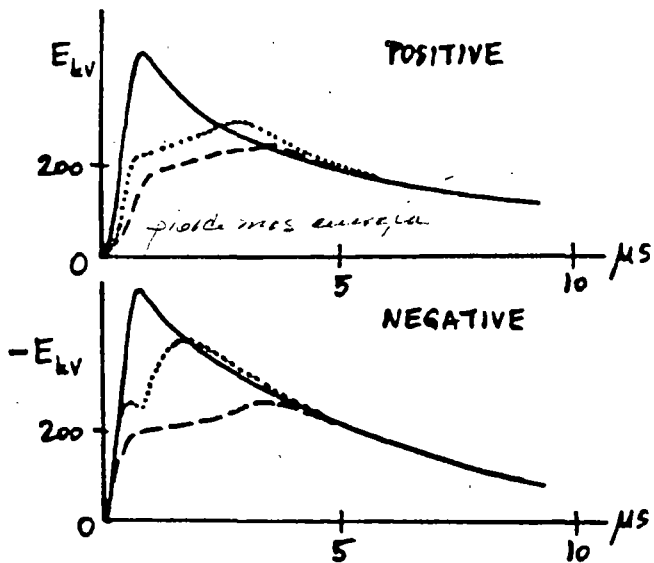
RAMP



APPROXIMATION BY RECTANGULAR COMPONENTS

WAVESHAPES APPROXIMATED BY
 $e = E(e^{-\alpha t} - e^{-\beta t})$

FORNIA IEC 71

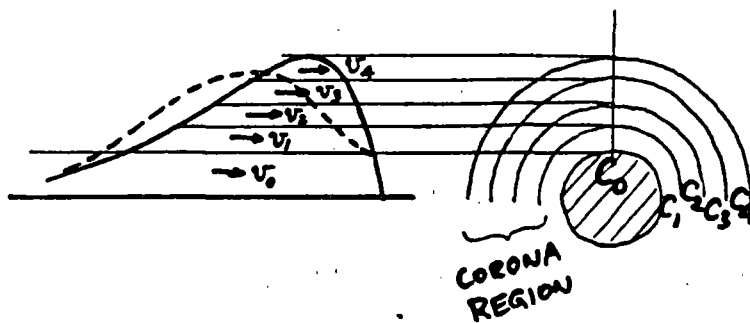


MODIFICATION OF PULSES WITH DISTANCE TRAVELED:

- AT START (0 MI.)
- AT 1.5 MILES
- AT 5 MILES

La diferencia producida entre ambos se justifica por presencia del efecto corona (gran grado de fenomenos de ionizacion) y de carga en gases
Pulsos Trichel

EFFECT OF CORONA ON WAVE DISTORTION:



como:

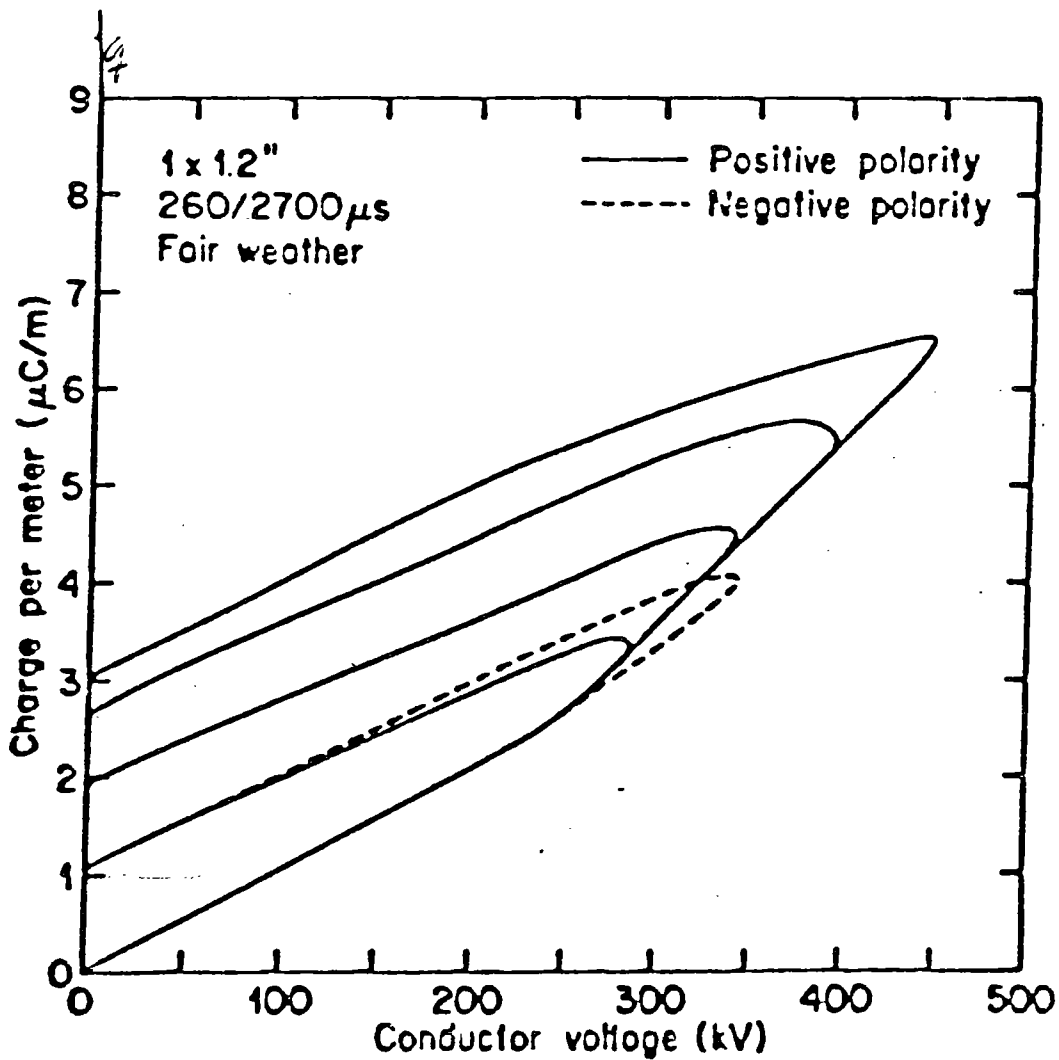
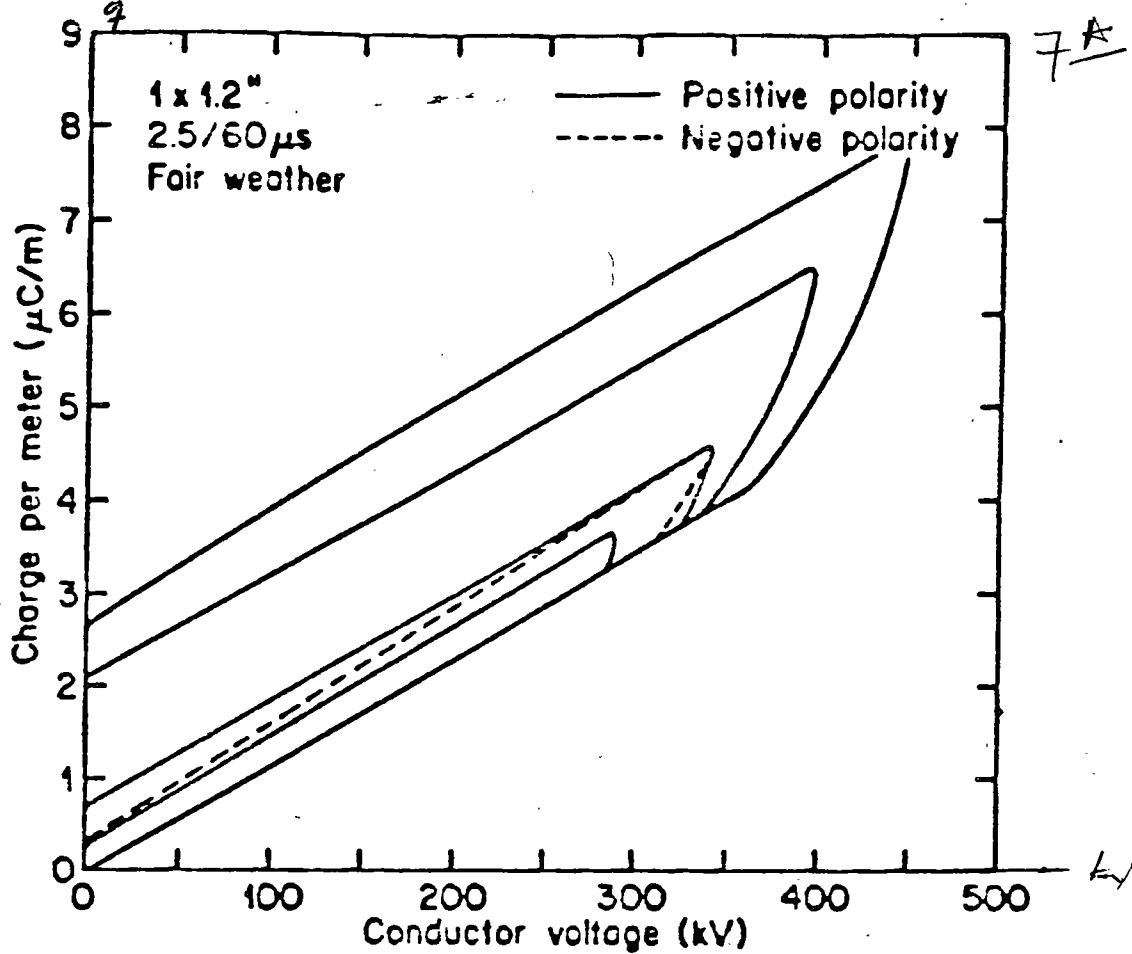
$$v_k = \frac{1}{\sqrt{LC_k}}$$

si

$$C_k: C_0 < C_1 < C_2 < C_3 < C_4 \dots$$

$$v_k: v_0 > v_1 > v_2 > v_3 > v_4 \dots$$

1988 Electricite France realizo estudio de efecto corona



2. REFLECTION OF WAVES

2.1. GENERAL TRANSITION POINT

2.11. PRACTICAL CASES (NEXT PAGE)

TERMINAL CONDITIONS

JUNCTIONS

JUNCTIONS WITH SHUNT ELEMENTS

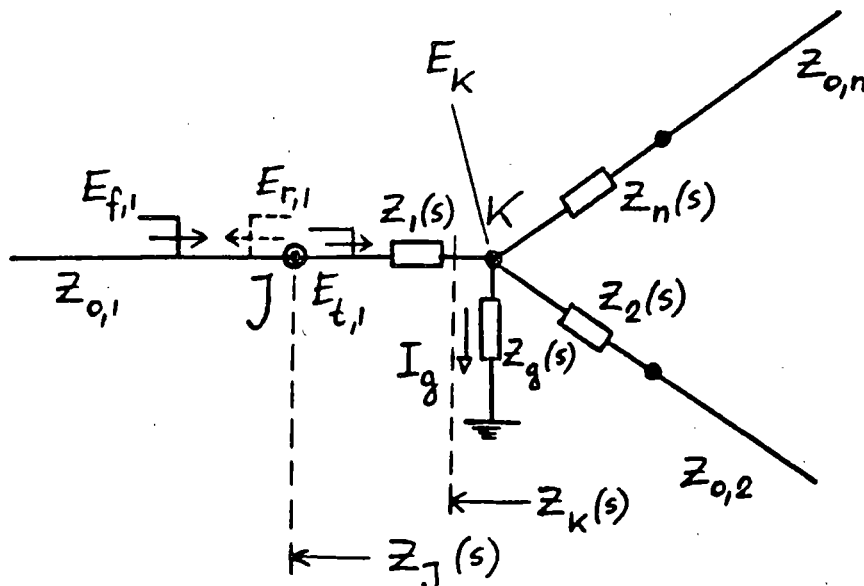
2.12. GENERAL TRANSITION POINT

$$\frac{E_{f,i}}{I_{f,i}} = Z_{0,i} \quad \frac{E_{r,i}}{I_{r,i}} = -Z_{0,i} \quad \frac{E_{t,i}}{I_{t,i}} = Z_{0,i}$$

$$E_{t,1} = E_{f,1} + E_{r,1}$$

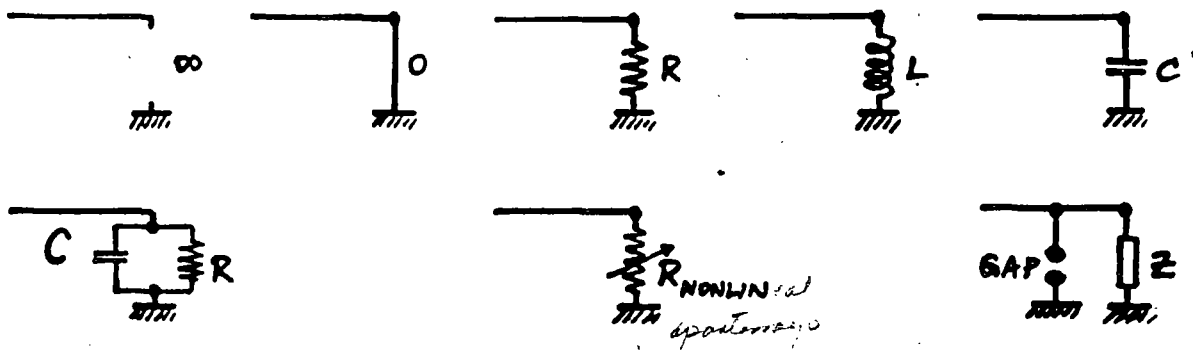
$$I_{t,1} = I_{f,1} + I_{r,1}$$

$$Z_j(s) = Z_1(s) + Z_k(s) = Z_1(s) + \frac{1}{\frac{1}{Z_g(s)} + \sum_{i=2}^n \frac{1}{Z_i(s) + Z_{0,i}}}$$

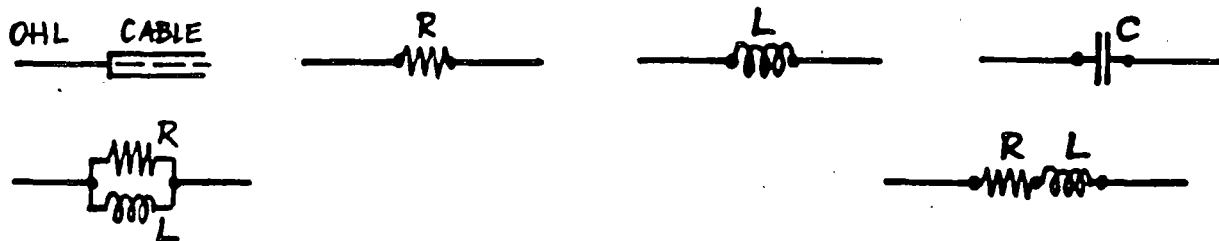


TYPICAL EXAMPLES:

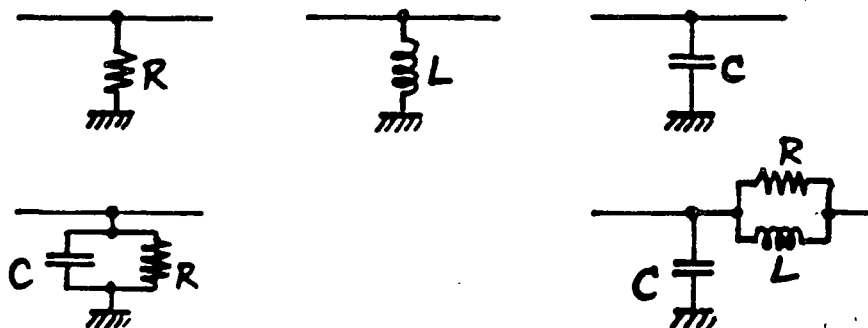
TERMINAL CONDITIONS:



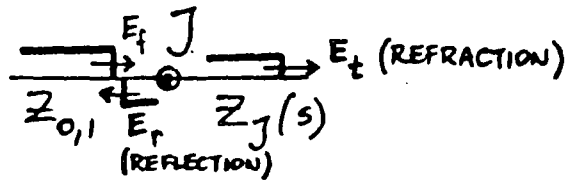
JUNCTIONS AND SERIES ELEMENTS:



JUNCTIONS AND SHUNT ELEMENTS:



2.13. REFLECTION COEFFICIENTS AT J



$$a_E = \frac{z_J - z_0}{z_J + z_0}$$

$$E_r = a_E E_f$$

$$a_I = -\frac{z_J - z_0}{z_J + z_0}$$

$$I_r = a_I I_f$$

2.14. REFRACTION COEFFICIENTS AT J

$$b_E = \frac{2z_J}{z_J + z_0}$$

$$E_t = b_E E_f$$

$$b_I = \frac{2z_0}{z_J + z_0}$$

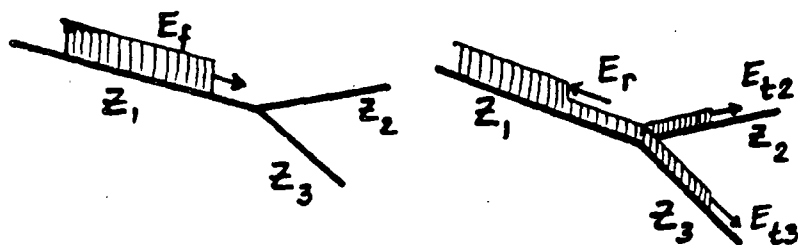
$$I_t = b_I I_f$$

2.15. a AND b RELATIONSHIPS

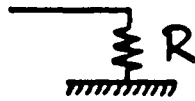
$$a_I = -a_E$$

$$b_I = 1 - a_E = 1 + a_I$$

$$b_E = 1 + a_E = 1 - a_I$$



2.2. LINE TERMINATED BY A RESISTANCE



R	∞ O.C.	Z_0	0 S.H.C.
Z_J	∞	Z_0	0
a_E	1	0	-1
a_I	-1	0	1
b_E	2	1	0
b_I	0	1	2
E_r	E_f	0	$-E_f$
$E_f + E_r$	$2E_f$	E_f	0
I_r	$-I_f$	0	I_f
$I_f + I_r$	0	I_f	$2I_f$

DUALITY

CABLE - OVERHEAD LINE AND
OVERHEAD LINE - CABLE JUNCTIONS

2.3. INDUCTIVE AND CAPACITIVE ELEMENTS

de l'aspect de la ligne

2.31. ASSUMPTIONS

FRONT OF TRAVELING WAVE

$$\omega \approx \infty$$

$$\omega L = \infty \quad \frac{1}{\omega C} = 0$$

TAIL OF TRAVELING WAVE

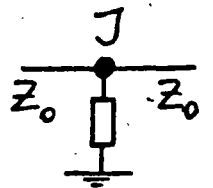
$$\omega \approx 0$$

$$\omega L = 0 \quad \frac{1}{\omega C} = \infty$$

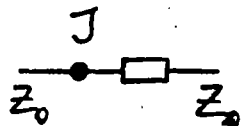
2.32. TERMINATIONS

INDUCTIVE O.C. \rightarrow SH.C.CAPACITIVE SH.C. \rightarrow O.C.

2.33. SHUNT ELEMENT AT JUNCTION

INDUCTIVE O.C. \rightarrow SH.C.CAPACITIVE SH.C. \rightarrow O.C.

2.34. SERIES ELEMENT INSERTION

INDUCTIVE O.C. \rightarrow SH.C.CAPACITIVE SH.C. \rightarrow O.C.

2.35. COMPUTATIONS, FLOWCHART

$$Z_0 \quad Z_j(s)$$

$$a_E(s) \quad a_I(s) \quad b_E(s) \quad b_I(s)$$

$$\alpha \text{ [1/sec]}$$

$$E_f(s) = \frac{E_f}{s}$$

$$E_r(s) = a_E(s) \cdot E_f(s) \quad \longrightarrow \quad e_r(t)$$

$$e_{\text{total}} = e_f(t) + e_r(t)$$

$$e_t(t)$$

$$e_{\text{series}}(t) = e_{\text{total}} - e_t(t)$$

$$i_r(t) = - \frac{e_r(t)}{Z_0}$$

$$i_{\text{total}} = i_f(t) + i_r(t)$$

$$i_t(t) = \frac{e_t(t)}{Z_0}$$

$$i_{\text{shunt}}(t) = i_{\text{total}} - i_t(t)$$

CHARTS FOR

VOLTAGES AND CURRENTS VS. TIME

VOLTAGES AND CURRENTS ALONG LINE

2.4. SPECIAL CASES WITH AN INDUCTANCE OR A CAPACITANCE

2.4.1. INDUCTIVE TERMINATION

$$Z_j(s) = sL$$

$$a = \frac{Z_j(s) - Z_0}{Z_j(s) + Z_0} = \frac{s - \alpha}{s + \alpha}$$

$$\alpha = \frac{Z_0}{L} \quad 1/\text{sec}$$

$$E_f(s) = \frac{E_f}{s}$$

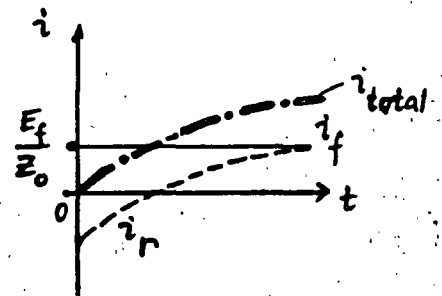
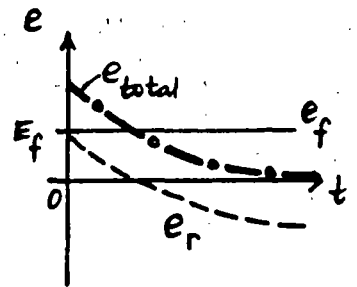
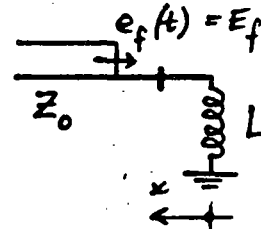
$$E_r(s) = a E_f(s) = \frac{E_f}{s} \frac{s - \alpha}{s + \alpha}$$

$$e_r(t) = E_f (2e^{-\alpha t} - 1)$$

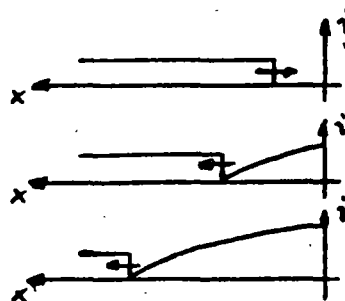
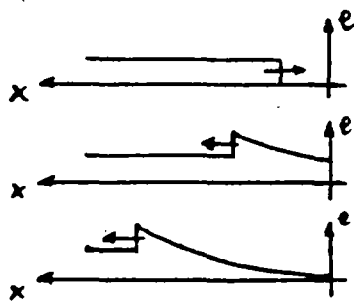
$$e_{\text{total}} = e_f(t) + e_r(t) = 2E_f e^{-\alpha t}$$

$$i_r(t) = -\frac{e_r(t)}{Z_0} = \frac{E_f}{Z_0} (1 - 2e^{-\alpha t})$$

$$i_{\text{total}} = i_f(t) + i_r(t) = \frac{2E_f}{Z_0} (1 - e^{-\alpha t})$$



VOLTAGES AND CURRENTS ALONG THE LINE



2.42. CAPACITIVE TERMINATION

$$Z_j(s) = \frac{1}{sC}$$

$$a = \frac{\alpha - s}{\alpha + s}$$

$$\alpha = \frac{1}{Z_0 C} \quad 1/\text{sec}$$

$$E_f(s) = \frac{E_f}{s}$$

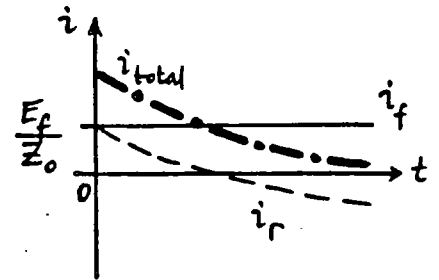
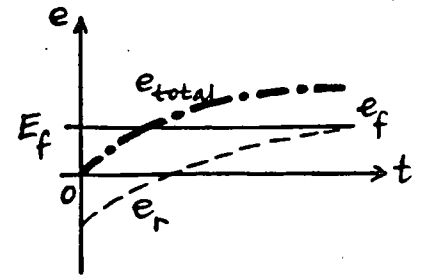
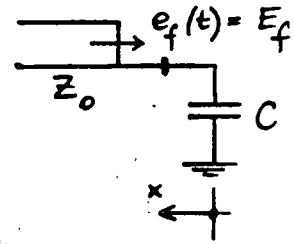
$$\rightarrow E_r(s) = \frac{E_f}{s} \frac{\alpha - s}{\alpha + s}$$

$$e_r(t) = E_f (1 - 2e^{-\alpha t})$$

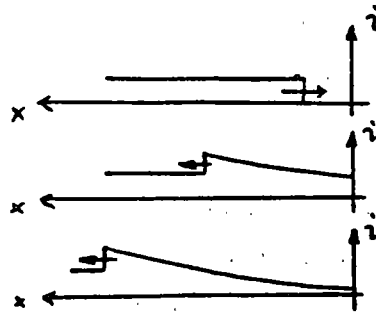
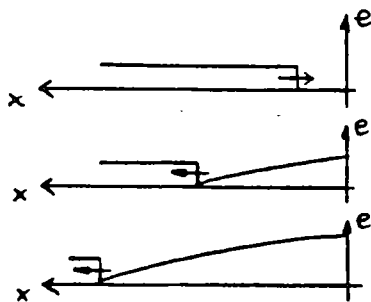
$$e_{\text{total}} = e_f(t) + e_r(t) = 2E_f(1 - e^{-\alpha t})$$

$$i_r(t) = \frac{E_f}{Z_0} (2e^{-\alpha t} - 1)$$

$$i_{\text{total}} = i_f(t) + i_r(t) = \frac{2E_f}{Z_0} e^{-\alpha t}$$



VOLTAGES AND CURRENTS ALONG THE LINE



2.43. SHUNT INDUCTANCE

$$Z_J(s) = \frac{SLZ_0}{SL + Z_0}$$

$$a = -\frac{\alpha}{s + \alpha} \quad \alpha = \frac{Z_0}{2L}$$

$$E_f(s) = \frac{E_f}{s}$$

$$E_r(s) = -\frac{E_f}{s} \frac{\alpha}{s + \alpha}$$

$$e_r(t) = E_f (e^{-\alpha t} - 1)$$

$$e_{total} = e_f(t) + e_r(t) = E_f e^{-\alpha t}$$

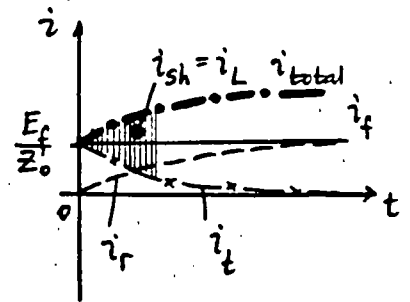
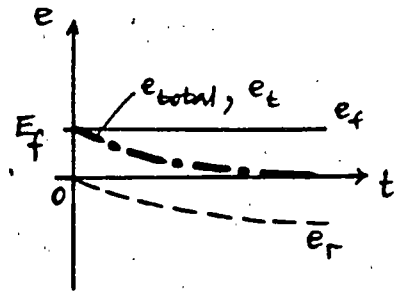
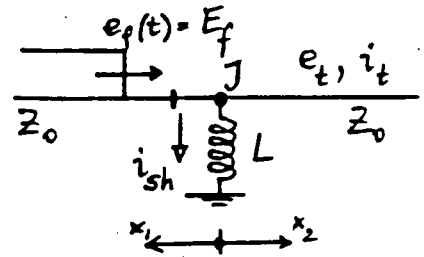
$$e_t(t) = e_{total}$$

$$i_r(t) = \frac{E_f}{Z_0} (1 - e^{-\alpha t})$$

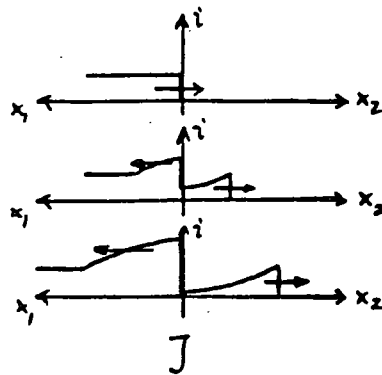
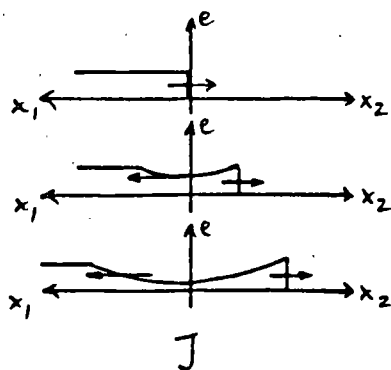
$$i_{total} = i_f(t) + i_r(t) = \frac{E_f}{Z_0} (2 - e^{-\alpha t})$$

$$i_t(t) = \frac{E_f}{Z_0} e^{-\alpha t}$$

$$i_{sh}(t) = i_{total} - i_t(t) = \frac{2E_f}{Z_0} (1 - e^{-\alpha t})$$



VOLTAGES AND CURRENTS ALONG THE LINE



2.44. SHUNT CAPACITANCE (MOTOR PROTECTION)

$$Z_J(s) = \frac{Z_0 / sC}{Z_0 + \frac{1}{sC}}$$

$$a = -\frac{s}{s+\alpha} \quad \alpha = \frac{2}{Z_0 C}$$

$$E_f(s) = \frac{E_f}{s}$$

$$E_r(s) = -E_f \frac{1}{s+\alpha}$$

$$e_r(t) = -E_f e^{-\alpha t}$$

$$e_{total} = e_f(t) + e_r(t) = E_f (1 - e^{-\alpha t})$$

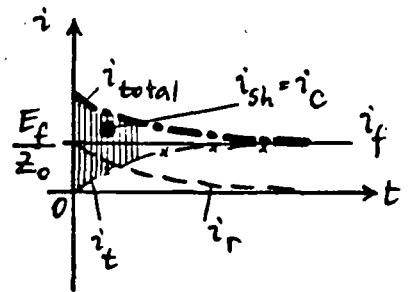
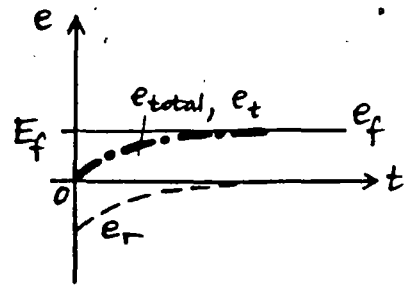
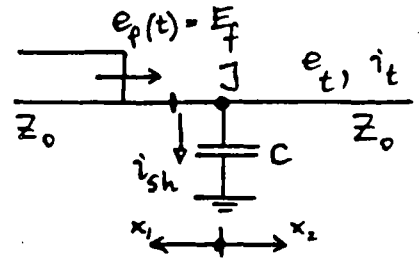
$$e_t(t) = e_{total}$$

$$i_r(t) = \frac{E_f}{Z_0} e^{-\alpha t}$$

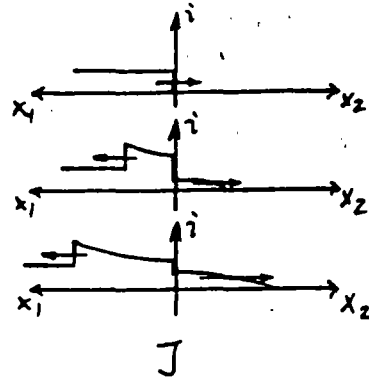
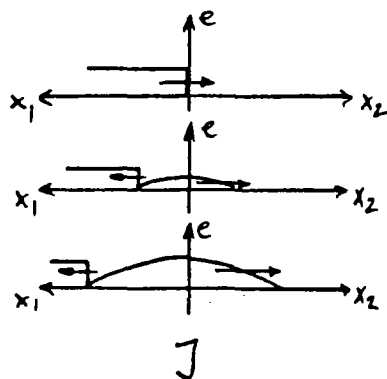
$$i_{total} = \frac{E_f}{Z_0} (1 + e^{-\alpha t})$$

$$i_t(t) = \frac{E_f}{Z_0} (1 - e^{-\alpha t})$$

$$i_{sh}(t) = \frac{2E_f}{Z_0} e^{-\alpha t}$$



VOLTAGES AND CURRENTS ALONG THE LINE



2.45. SERIES INDUCTANCE (MOTOR PROTECTION)

$$Z_j(s) = sL + Z_0$$

$$a = \frac{s}{s+\alpha} \quad \alpha = \frac{2Z_0}{L}$$

$$E_f(s) = \frac{E_f}{s}$$

$$E_r(s) = E_f \frac{1}{s+\alpha}$$

$$e_r(t) = E_f e^{-\alpha t}$$

$$e_{total} = e_f(t) + e_r(t) = E_f (1 + e^{-\alpha t})$$

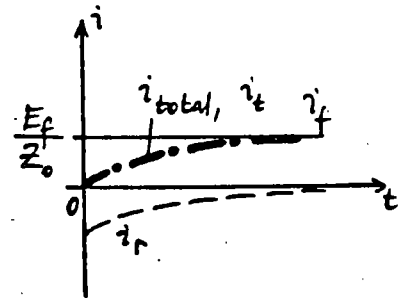
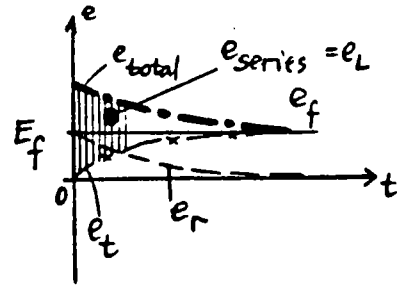
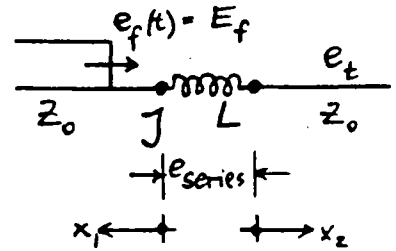
$$e_t(t) = E_f (1 - e^{-\alpha t})$$

$$e_{series} = e_{total} - e_t(t) = 2E_f e^{-\alpha t}$$

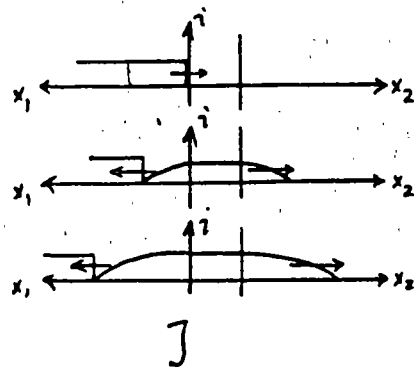
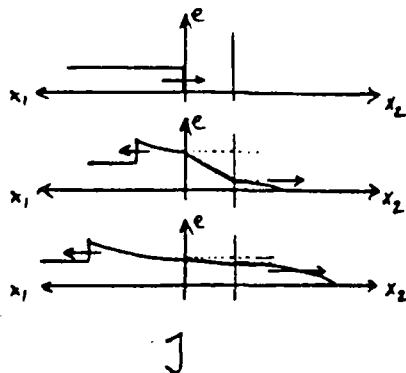
$$i_r(t) = -\frac{E_f}{Z_0} e^{-\alpha t}$$

$$i_{total} = i_f(t) + i_r(t) = \frac{E_f}{Z_0} (1 - e^{-\alpha t})$$

$$i_t(t) = \frac{E_f}{Z_0} (1 - e^{-\alpha t})$$



VOLTAGES AND CURRENTS ALONG THE LINE



2. 46. SERIES CAPACITANCE

$$Z_J(s) = \frac{1}{sC} + Z_0$$

$$a = \frac{\alpha}{s + \alpha} \quad \alpha = \frac{1}{2Z_0 C}$$

$$E_f(s) = \frac{E_f}{s}$$

$$E_r(s) = \frac{E_f}{s} \frac{\alpha}{s + \alpha}$$

$$e_r(t) = E_f(1 - e^{-\alpha t})$$

$$e_{total} = e_f(t) + e_r(t) = E_f(2 - e^{-\alpha t})$$

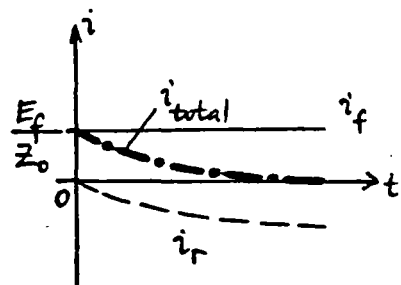
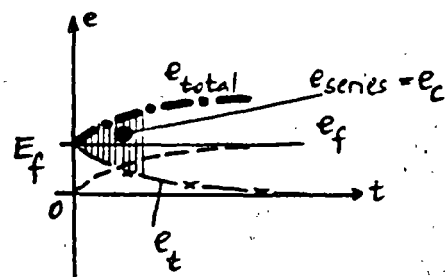
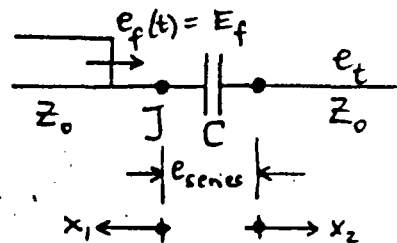
$$e_t(t) = E_f e^{-\alpha t}$$

$$e_{series} = 2E_f(1 - e^{-\alpha t})$$

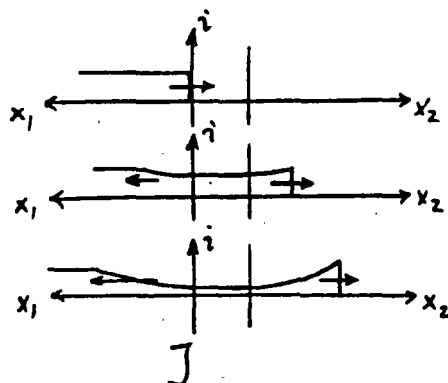
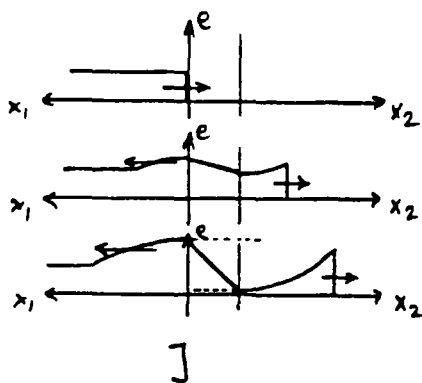
$$i_r(t) = \frac{E_f}{Z_0} (e^{-\alpha t} - 1)$$

$$i_{total} = i_f(t) + i_r(t) = \frac{E_f}{Z_0} e^{-\alpha t}$$

$$i_t(t) = \frac{E_f}{Z_0} e^{-\alpha t}$$



VOLTAGES AND CURRENTS ALONG THE LINE



2.5. SUCCESSIVE REFLECTIONS

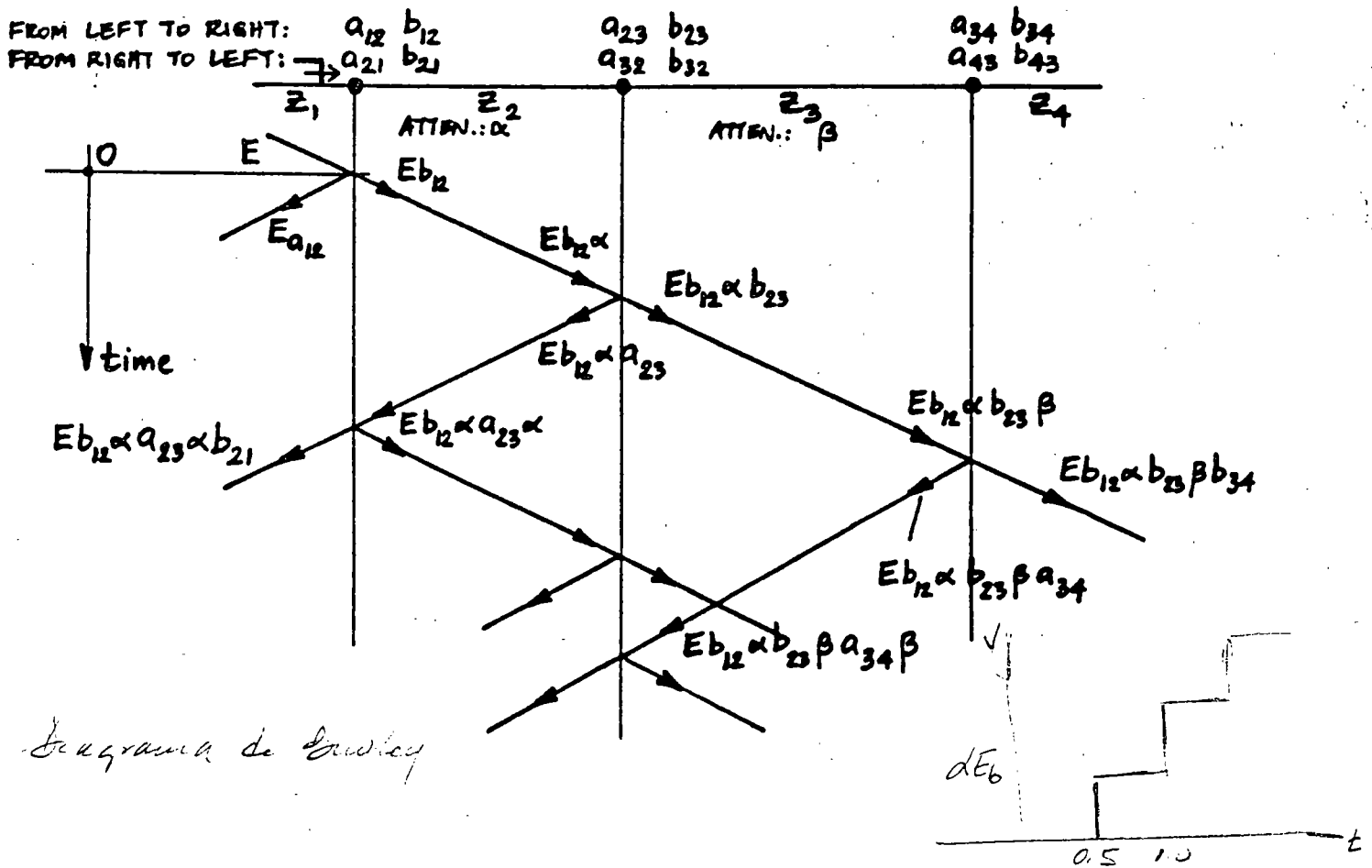
2.5.1. BEWLEY LATTICE

TIME - SPACE DIAGRAM
MULTIPLE REFLECTIONS

DISTANCE BETWEEN JUNCTIONS
IS PROPORTIONAL TO

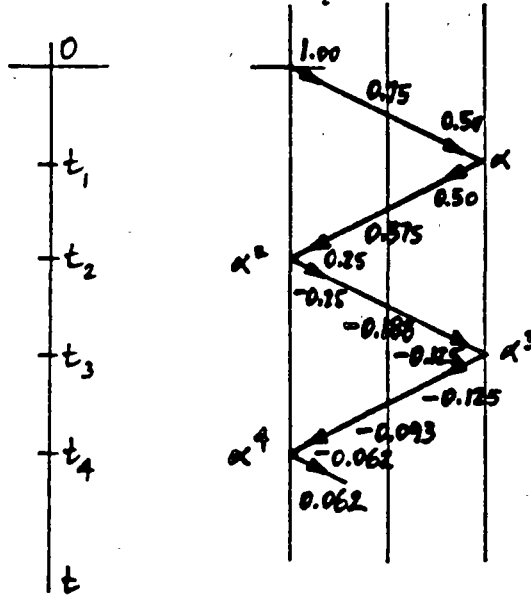
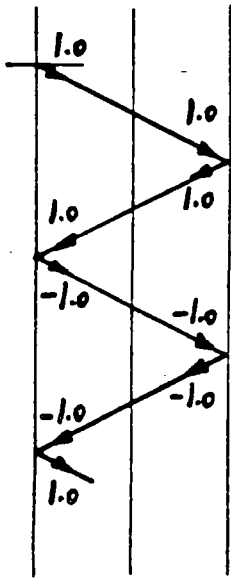
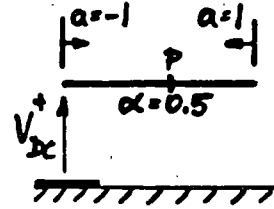
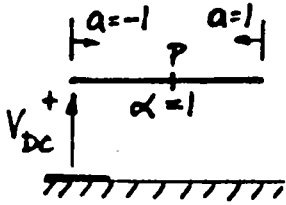
TIME OF WAVE PASSAGE
(DIAGONALS HAVE SAME SLOPE)

LENGTH BETWEEN JUNCTIONS
(SLOPES ARE DIFFERENT)

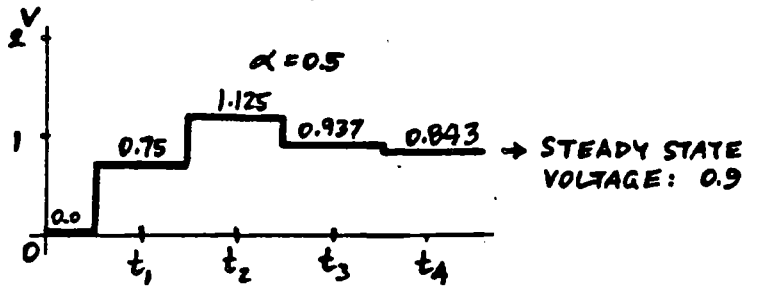
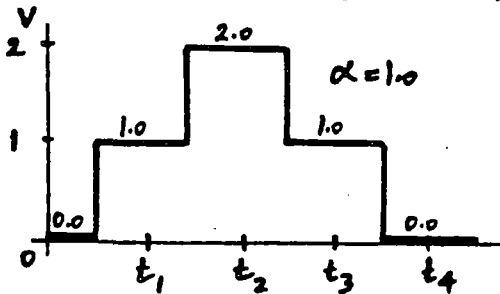


2.52. EXAMPLES

LINE CHARGING WITH DC



VOLTAGES AT MIDPOINT OF LINE (P):



VOLTAGE AT END WHEN $\alpha=0.5$:

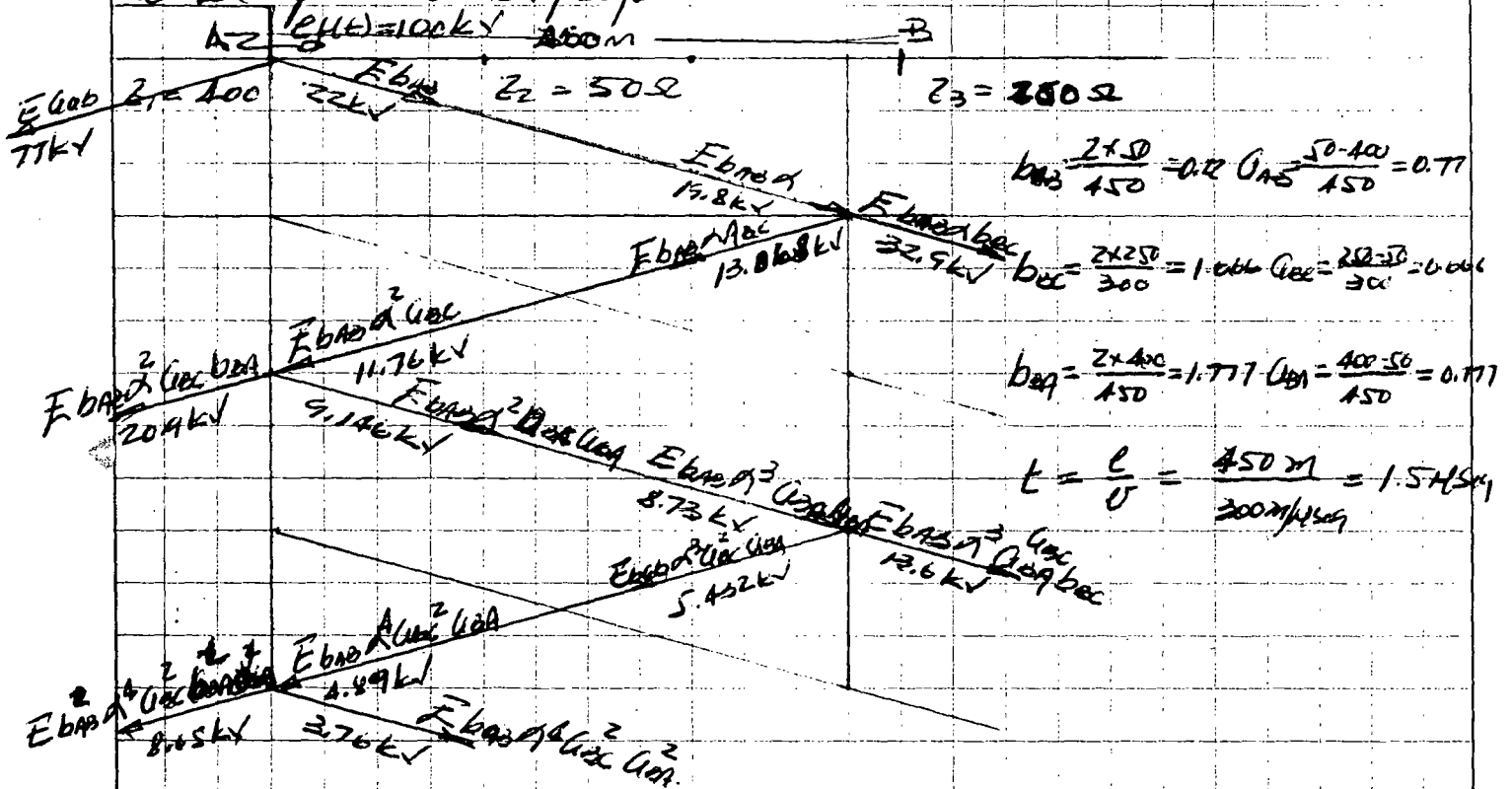
$$V = 2\alpha - 2\alpha^3 \pm \dots = 2\alpha (1 - \alpha^2 + \alpha^4 \mp \dots)$$

$$\text{STEADY STATE VOLTAGE: } \lim V = \frac{2\alpha}{1 + \alpha^2} = 0.8$$

Tarea 1 Sobretensiones y Coordinación de Caisamiento

Antonio Morales Callentes Profesor Ing Victor F Bermosillo Worley.

Se utiliza el diagrama de Bewley para encontrar los valores de voltaje producidos por un escalon con amplitud 100kV en la dos transiciones (A, B) de la línea de transmisión mostrada en la fig. Considere $\alpha = 0.9$ y $v = 300 \text{ m/}\mu\text{s}$ en el transitorio, calcule voltajes incidentes, transmitidos y reflejados, dibuje el voltaje en cada transición durante los primeros 6 μs segs.



$E_{BA} = 100 \times 0.22 = 22 \text{ kV}$ $E_{AB} = 100 \times 0.77 = 77 \text{ kV}$

$E_{BA}^2 = 22 \times 0.9 = 19.8 \text{ kV}$, $E_{AB}^2 = 19.8 \times 1.066 = 32.9 \text{ kV}$, $E_{BA}^3 = 19.8 \times 0.77 = 15.246 \text{ kV}$

$E_{BA}^3 = 13.068 \times 0.9 = 11.76 \text{ kV}$, $E_{AB}^3 = 11.76 \times 0.77 = 20.9 \text{ kV}$, $E_{BA}^4 = 11.76 \times 0.77 = 9.146 \text{ kV}$

$E_{BA}^4 = 9.146 \times 0.9 = 8.23 \text{ kV}$, $E_{AB}^4 = 8.23 \times 1.066 = 13.6 \text{ kV}$, $E_{BA}^5 = 8.23 \times 0.77 = 5.49 \text{ kV}$

$E_{BA}^5 = 5.49 \times 0.9 = 4.94 \text{ kV}$, $E_{AB}^5 = 4.94 \times 0.77 = 3.76 \text{ kV}$, $E_{BA}^6 = 4.94 \times 0.77 = 3.76 \text{ kV}$

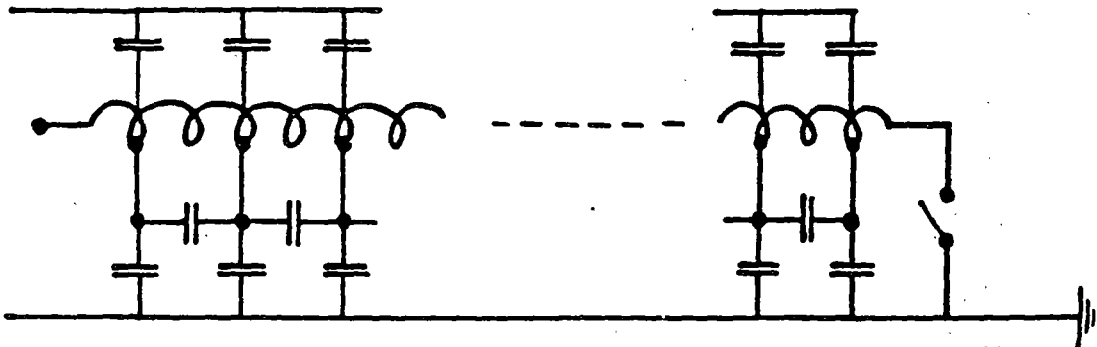
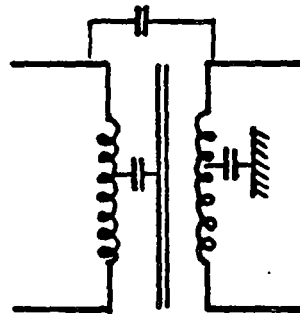
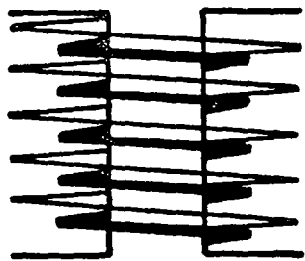
3. TRANSFORMER WINDINGS UNDER TRANSIENT CONDITIONS

3.1. SCHEMATIC REPRESENTATION

SELF INDUCTANCES
 MUTUAL INDUCTANCES
 CAPACITANCES: TO CORE
 TO TANK
 CAPACITIVE COUPLING
 LOSSES (RESISTANCES)

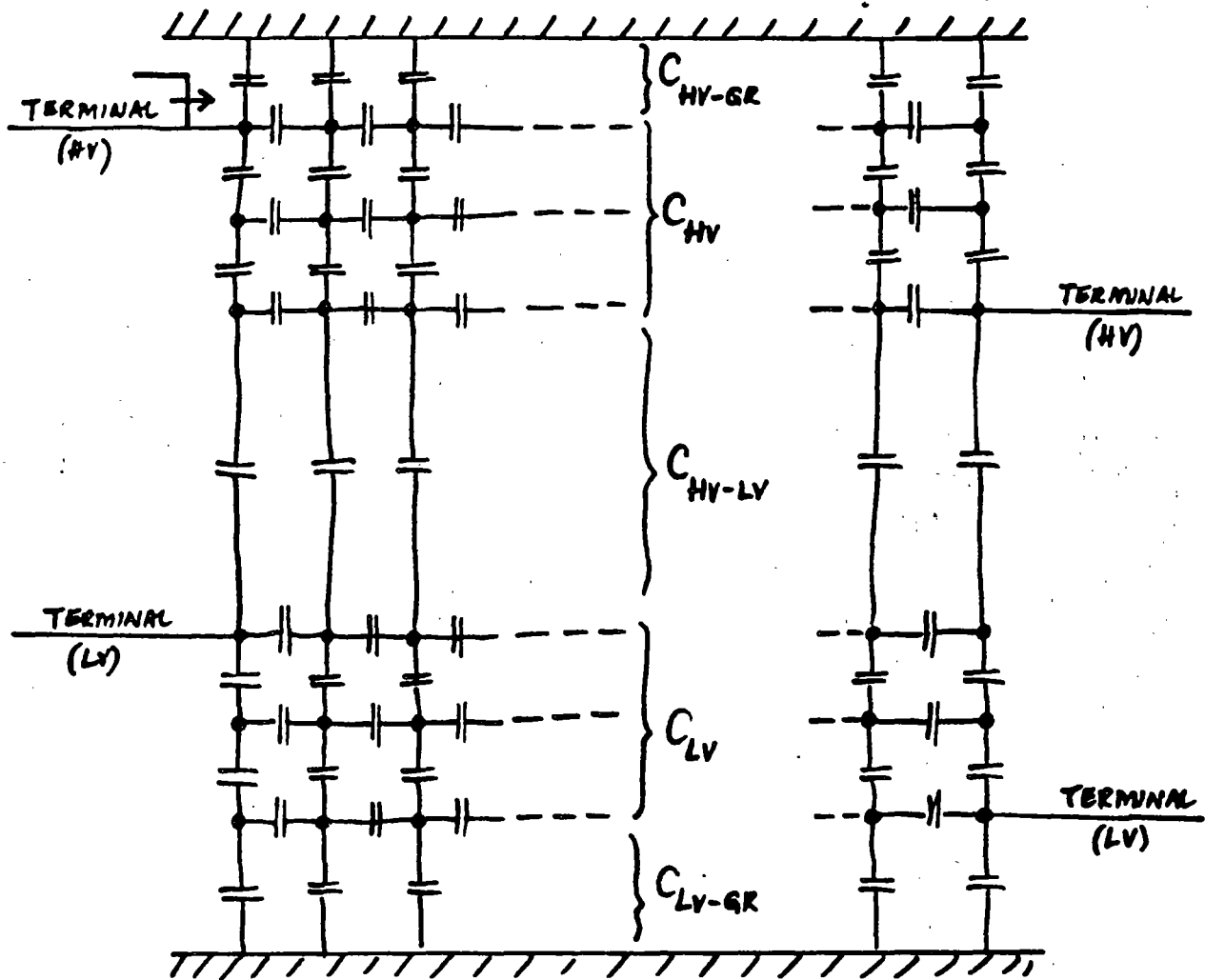


CONSIDERATIONS

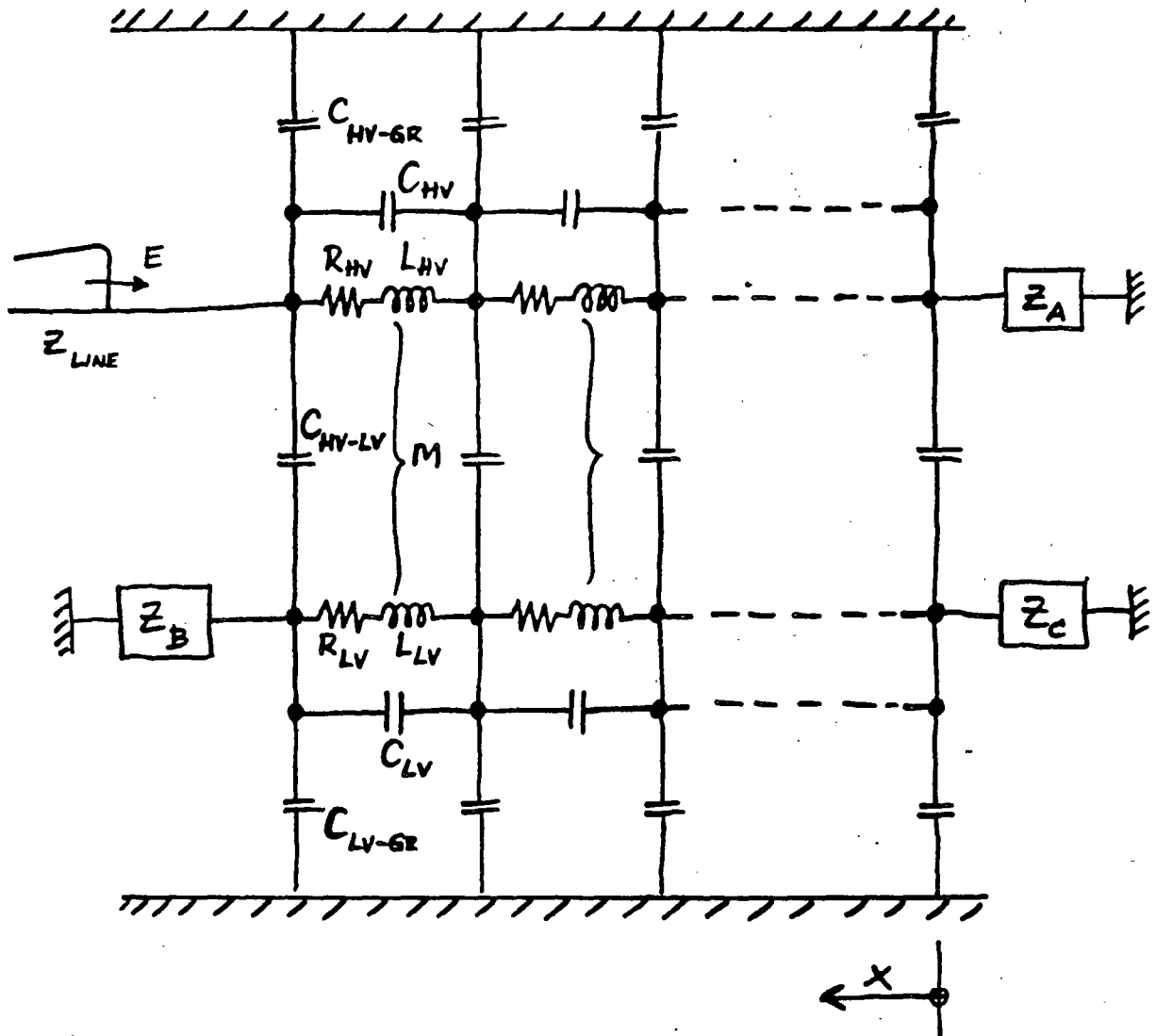


INITIAL VOLTAGE DISTRIBUTION IS DETERMINED BY THE CAPACITANCE NETWORK,

AT THE FRONT OF THE WAVE ($\omega \approx \infty$)
 $WL \approx \infty$, I.E., OPEN-CIRCUITED:



COMPLETE EQUIVALENT CIRCUIT FOR TRANSIENTS
(ANALOG MODEL):



3.2. INITIAL VOLTAGE DISTRIBUTION

CAPACITANCE LADDER NETWORK

GROUND CAP. OF WINDING C_g SERIES CAP. OF WINDING C_s E = VOLTAGE TO GROUND AT ANY POINT x = FROM NEUTRAL TO TERMINAL l = LENGTH OF WINDING

$$\frac{\partial^2 E}{\partial x^2} - \frac{1}{l^2} \frac{C_g}{C_s} E = 0$$

$$E = A e^{px} + B e^{-px}$$

$$p = \frac{1}{l} \left(\frac{C_g}{C_s} \right)^{\frac{1}{2}}$$

GROUNDED NEUTRAL

$$E = V \frac{\sinh(\alpha x/l)}{\sinh \alpha}$$

$$\alpha = pl = \sqrt{\frac{C_g}{C_s}}$$

$$x=0: E=0$$

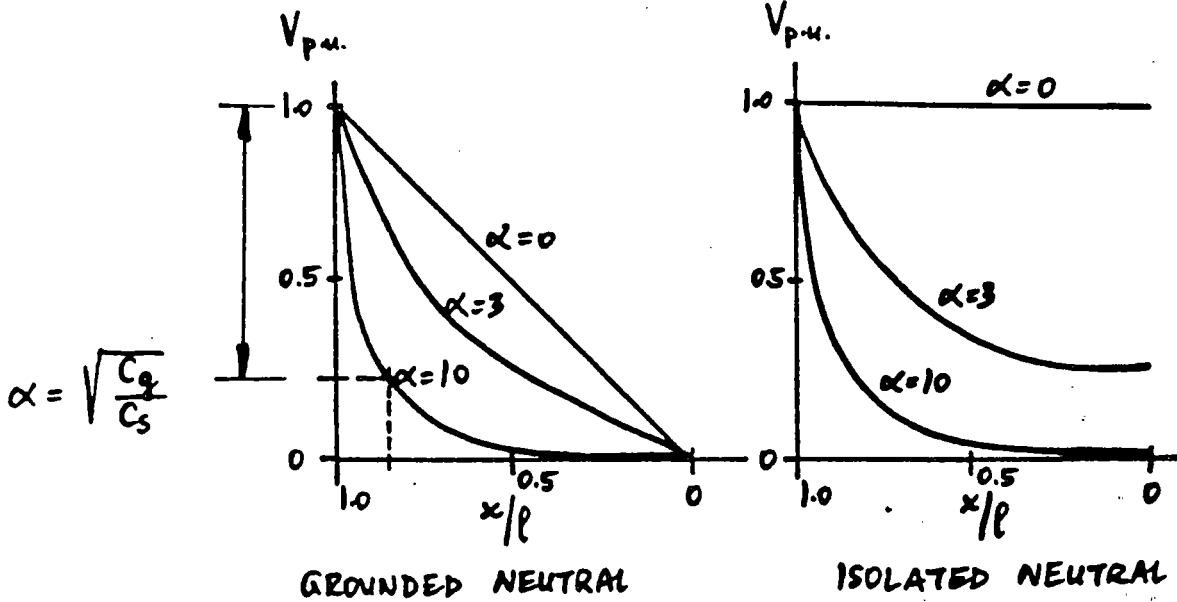
$$x=l: E=V$$

ISOLATED NEUTRAL

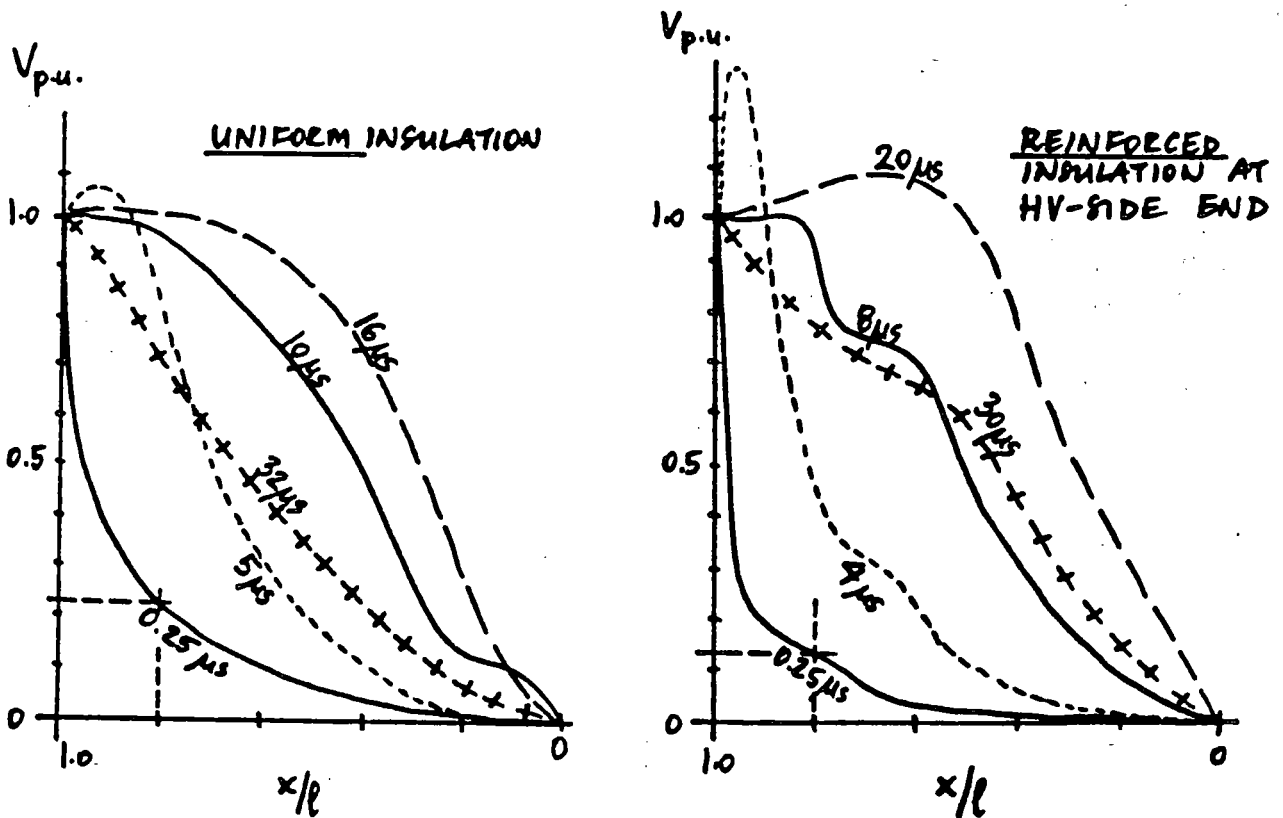
$$E = V \frac{\cosh(\alpha x/l)}{\cosh \alpha}$$

$$x=0: I=0$$

$$x=l: E=V$$



INITIAL VOLTAGE DISTRIBUTION IN CASE OF STEP-FUNCTION FORWARD VOLTAGE



TRANSIENT VOLTAGE DISTRIBUTION IN CASE OF STEP-FUNCTION FORWARD VOLTAGE

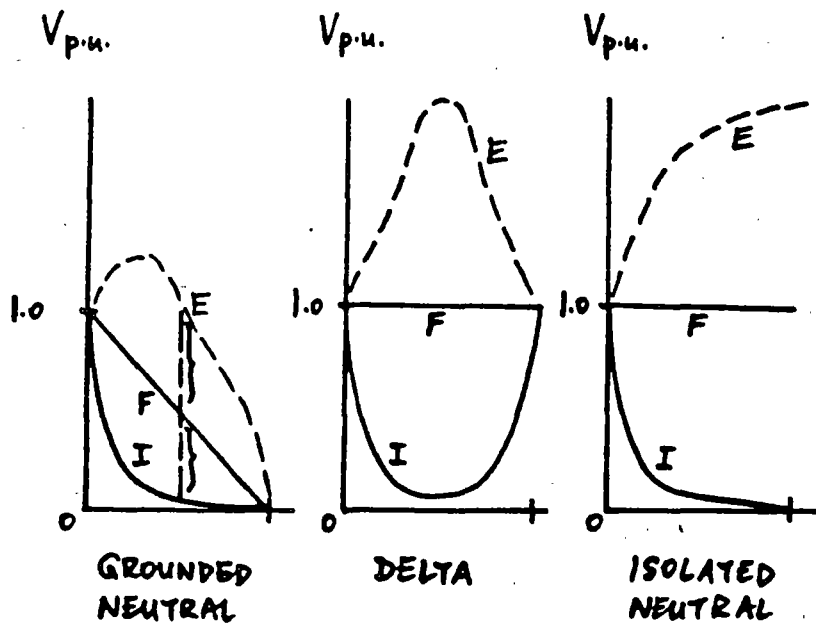
3.4. ENVELOPE CURVES

I - INITIAL DISTRIBUTION

F - FINAL DISTRIBUTION

LC CIRCUITS \rightarrow OSCILLATIONS

E - ENVELOPES OF OSCILLATION



4. PROTECTION OF OVERHEAD LINES AGAINST OVERVOLTAGES

4.1. LIGHTNING STROKES

INITIAL DISCHARGE, FROM 10kV/cm
STEPPED LEADER TOWARDS EARTH
RETURN STREAMER FROM EARTH

CURRENTS ARE UP TO 200KA OR MORE
VOLTAGES

WAVESHAPE, STANDARD WAVESHAPE
POLARITY OF 90% OF STROKES IS NEGATIVE
CHARGE 2-200 COULOMB

FREQUENCY

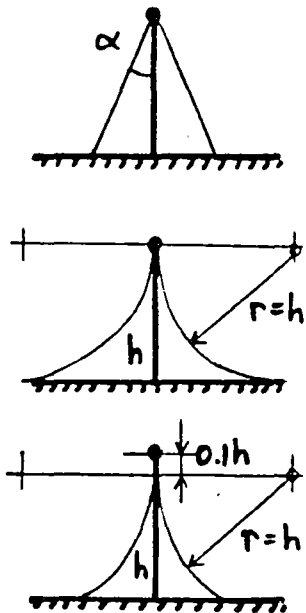
ISOKERAUNIC MAP - NEXT PAGE
(ANNUAL NUMBER OF DAYS WITH
THUNDERSTORMS)

ISOKERAUNIC LEVEL, MEAN IKL = 30,
IKL = 30 CORRESPONDS TO ABOUT
13-14 STROKES / SQ. MILE / YEAR,
OR 1 STROKE / 100 TR. LINE MILES / YEAR

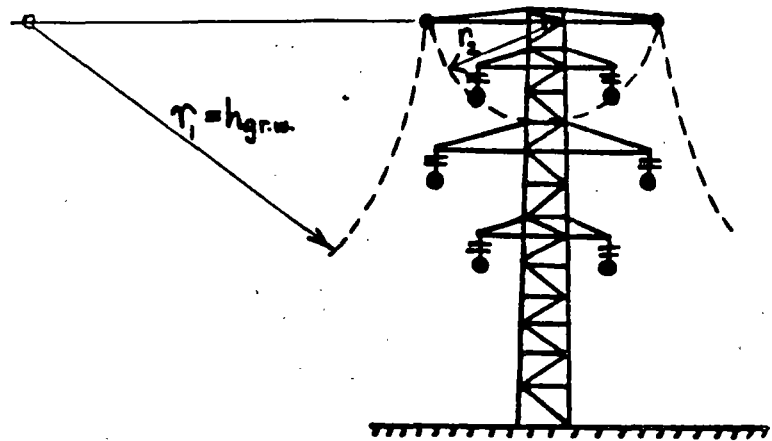
DIRECT STROKES

INDUCED STROKES

4.2. GROUND WIRES.



PROTECTIVE ZONE OF A GROUND WIRE



PROTECTIVE ZONE OF TWO GROUND WIRES

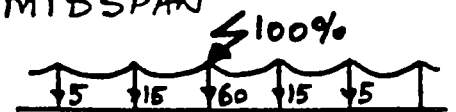
INTERCEPTION OF STROKES

STROKES TO TOWER OR AT MIDSPAN

SHIELDING

TOWER GROUNDING

END EFFECTS



OTHER FEATURES:

GROUND WIRE LOSSES

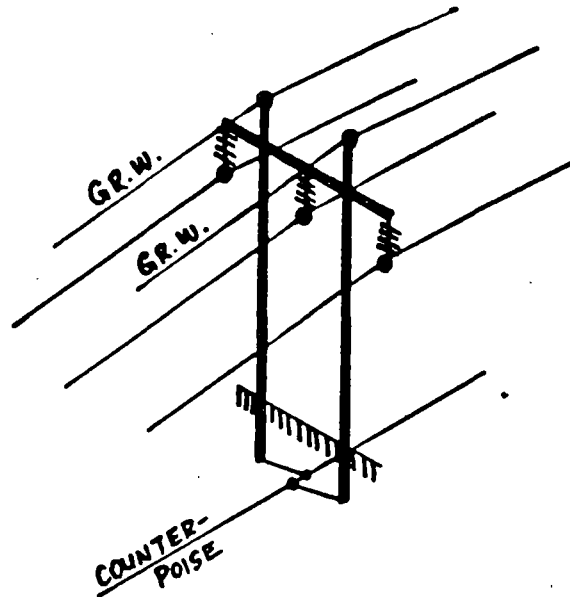
INFLUENCE ON FAULT CURRENTS, RELAYING

ISOLATED GROUND WIRES

CAPACITIVE COUPLING → INDUCED VOLTAGES

INTERFERENCE

4.3. COUNTERPOISE



USED IN CASE OF HIGH SOIL RESISTIVITY AND
TOWER GROUNDING RESISTANCES (20-500 Ω)

LEAKAGE RESISTANCE VALUES

LADDER NETWORK

TYPICAL WIRE: $\frac{1}{4}$ -IN DIAMETER, 2-FT DEPTH



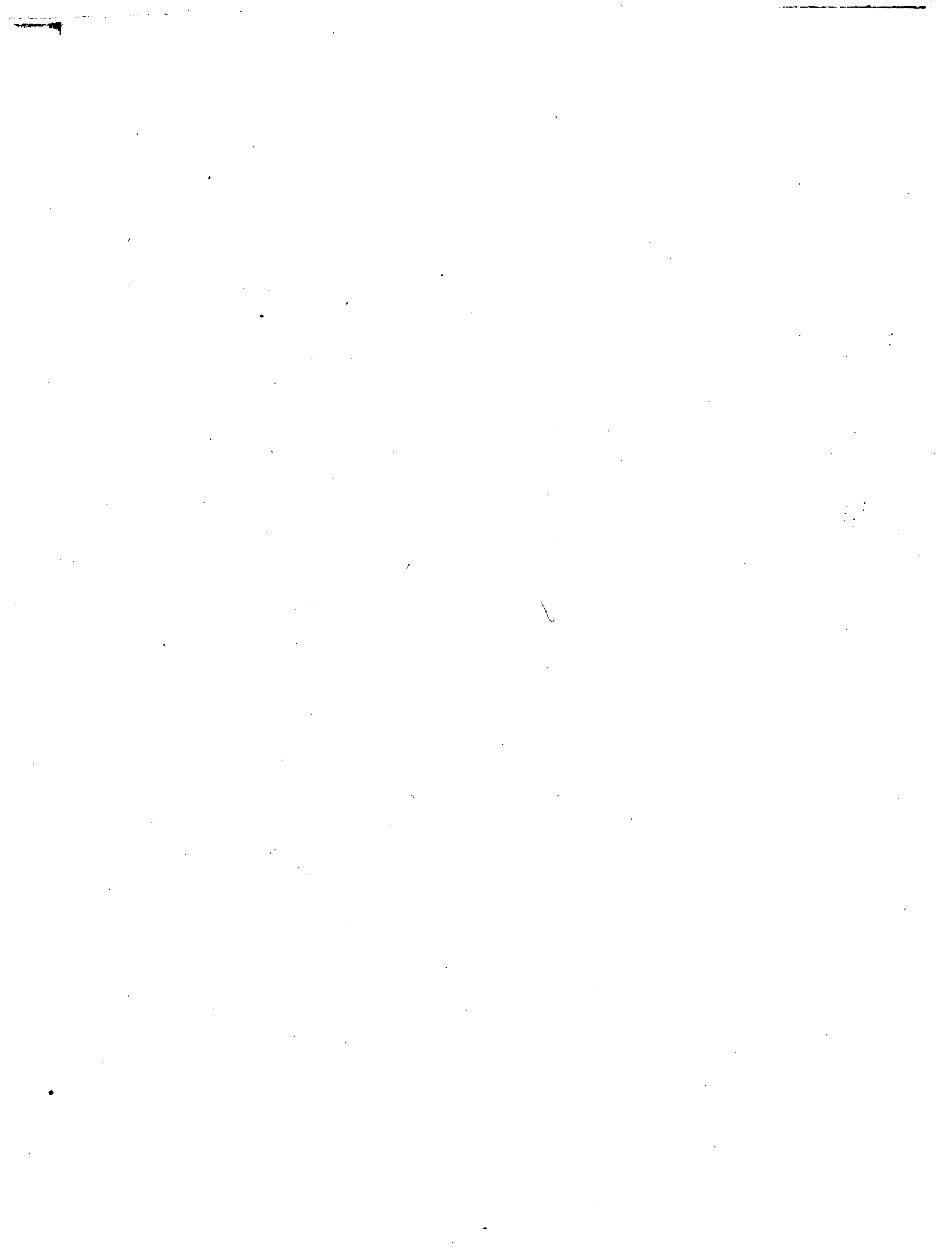
**FACULTAD DE INGENIERIA U.N.A.M.
DIVISION DE EDUCACION CONTINUA**

**V CURSO INTERNACIONAL DE SISTEMAS
ELECTRICOS DE POTENCIA**

MODULO II: SISTEMAS ELECTRICOS DE POTENCIA

TEMA: INTRODUCCION

EXPOSITOR: ING. ARTURO MORALES COLLANTES



Introduction

1.1 PURPOSE OF COURSE

The objectives of a first-year, one-semester graduate course in electric power generation, operation, and control include the desire to

1. Acquaint electric power engineering students with power generation systems, their operation in an economic mode, and their control.
2. Introduce students to the important "terminal" characteristics for thermal and hydroelectric power generation systems.
3. Introduce mathematical optimization methods and apply them to practical operating problems.
4. Introduce methods for solving complicated problems involving both economic analysis and network analysis and illustrate these techniques with relatively simple problems.
5. Introduce methods that are used in modern control systems for power generation systems.

1.2 COURSE SCOPE

Topics to be addressed include

1. Power generation characteristics.
 2. Economic dispatch and the general economic dispatch problem.
 3. The economic dispatch problem for thermal units.
-

4. Methods of solution of the thermal dispatch problem.
5. Transmission losses.
6. Introduction to network transformation methods.
7. Loss formula in the economic dispatch, coordination equations.
8. Methods for solution of the coordination equations.
9. Unit commitment problem and an introduction to dynamic programming.
10. Economic dispatching in systems with limited energy availability.
11. The hydrothermal coordination problem.
12. Examples of solution methods for hydrothermal systems.
13. Probabilistic production cost calculations.
14. Power system control.
15. Capacity and energy interchange pricing analysis.
16. Techniques of analyzing power system security.
17. An introduction to least-squares techniques for power system state estimation.

In many cases this will be only an introduction to the topic area. Many additional problems and topics that represent important, practical problems would require more time and space than is available. Still other problems, such as those involving light-water nuclear reactors, would require several chapters to lay a firm foundation. These topics can only be the subject of a brief overview.

1.3 ECONOMIC IMPORTANCE

The efficient and optimum economic operation and planning of electric power generation systems have always occupied an important position in the electric power industry. Prior to 1973 and the oil embargo that signaled the rapid escalation in fuel prices, electric utilities in the United States spent about 20% of their total revenues on fuel for the production of electrical energy. By 1980, that figure had risen to more than 40% of total revenues. In the 5 years after 1973, U.S. electric utility fuel costs escalated at a rate that averaged 25% compounded on an annual basis. The efficient use of the available fuel is growing in importance both monetarily and because most of the fuel used represents irreplaceable natural resources.

An idea of the magnitude of the amounts of money under consideration can be obtained by considering the annual operating expenses of a large utility for purchasing fuel. Assume the following parameters for a moderately large system.

Annual peak load: 10,000 MW

Annual load factor: 60%

Average annual heat rate for converting fuel to electric energy: 10,500 Btu/kWh

Average fuel cost: \$2.00 per million Btu (MBtu)

With these assumptions the total annual fuel cost for this system is as follows.

Annual energy produced: $10^7 \text{ kW} \times 8760 \text{ h/yr} \times 0.60 = 5.256 \times 10^{10} \text{ kWh}$

Annual fuel consumption: $10,500 \text{ Btu/kWh} \times 5.256 \times 10^{10} \text{ kWh}$
 $= 55.188 \times 10^{13} \text{ Btu}$

Annual fuel cost: $55.188 \times 10^{13} \text{ Btu} \times 2 \times 10^{-6} \text{ \$/Btu} = \$1.104 \text{ billion}$

To put this cost in perspective, it represents a direct requirement for revenues from the average customer of this system of 2.1 cents per kWh just to recover the expense for fuel.

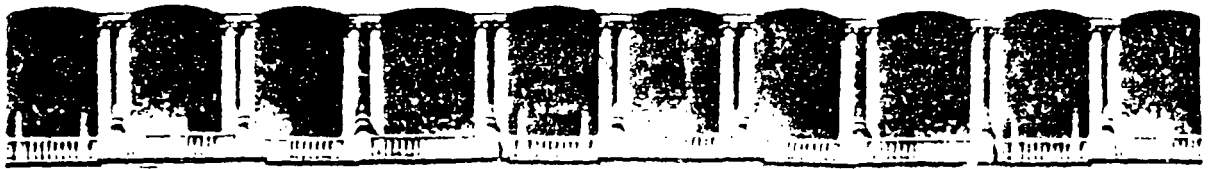
A savings in the operation of this system of a small percent represents a significant reduction in operating cost as well as in the quantities of fuel consumed. It is no wonder that this area has warranted a great deal of attention from engineers through the years.

Periodic increases in basic fuel price levels serve to accentuate the problem and increase its economic significance. Inflation also causes problems in developing and presenting methods, techniques, and examples of the economic operation of electric power generating systems. Actually, recent fuel costs always seem to be ancient history and entirely inappropriate to current conditions. To avoid leaving false impressions about the actual value of the methods to be discussed, all the examples and problems that are in the text are expressed in a nameless, fictional monetary unit to be designated as an "R".

1.4 PROBLEMS SOLVED AND UNSOLVED

This text represents a progress report in an engineering area that has been and is still undergoing rapid change. It concerns established engineering problem areas (i.e., economic dispatch and control of interconnected systems) that have taken on new importance in recent years. The original problem of economic dispatch for thermal systems was solved by numerous methods years ago. Recently there has been a rapid growth in applied mathematical methods and the availability of computational capability for solving problems of this nature so that more involved problems have been successfully solved.

The classic problem is the economic dispatch of fossil-fired generation systems to achieve minimum operating cost. This problem area has taken on a subtle twist as the public has become increasingly concerned with environmental matters, so that "economic dispatch" now includes the dispatch of systems to minimize pollutants and conserve various forms of fuel as well as to achieve minimum costs. In addition, there is a need to expand the limited economic optimization problem to incorporate constraints on system operation to ensure the "security" of the system, thereby preventing the collapse of the system due to unforeseen conditions. The hydrothermal coordination problem is another optimum operating problem area that has received a great deal of attention. Even so, there are difficult problems involving hydrothermal coordination that cannot be solved in a theoretically satisfying fashion in a rapid and efficient computational manner.



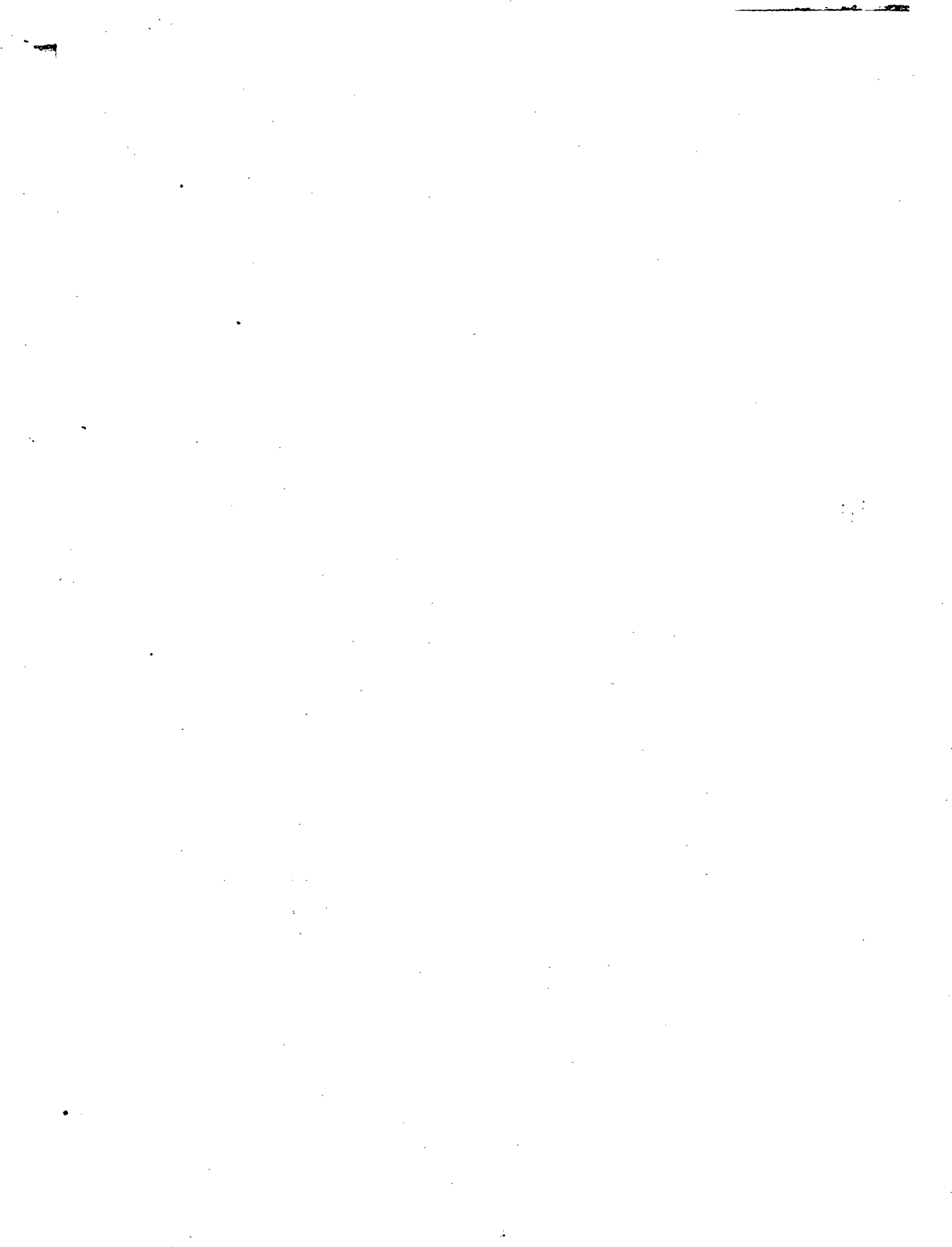
**FACULTAD DE INGENIERIA U.N.A.M.
DIVISION DE EDUCACION CONTINUA**

**V CURSO INTERNACIONAL DE SISTEMAS
ELECTRICOS DE POTENCIA**

MODULO II: SISTEMAS ELECTRICOS DE POTENCIA

**TEMA: CARACTERISTICAS DE LAS UNIDADES DE GENERACION
DE PODER**

EXPOSITOR: ING. ARTURO MORALES COLLANTES



The post World War II period saw the increasing installation of pumped-storage hydroelectric plants in the U.S. and a great deal of interest in energy storage systems. These storage systems involve another difficult aspect of the optimum economic operating problem. Methods are available for solving coordination of hydroelectric, thermal, and pumped-storage electric systems. However, closely associated with this economic dispatch problem is the problem of the proper commitment of an array of units out of a total array of units to serve the expected load demands in an "optimal" manner. This unit commitment problem can only be solved approximately for practical-sized systems at the present time.

There are other unsolved problems in the area of power generation, operation, and control. For example, we would like to be able to schedule maintenance outages of units on an "optimum" basis. However, at this time, we are not even sure what we mean by the term "optimum." In interconnected system operations there are control, economic dispatch, and accounting problems that need further work and resolution. Many researchers are still working on solutions to the "optimal load flow" problem that promise to extend economic dispatch to include the optimal setting of generator voltages, transformer taps, and reactive power sources. The list is long and undoubtedly will expand as new problems arise and will contract as new methodologies are developed, tested, and utilized on a routine basis.

FURTHER READING

The following books are suggested as sources of information for this general area. The first four are the "classics"; the remainder are either specialized to a limited number of topics or else represent collections of articles or chapters on varied topics related to this broad subject.

1. Steinberg, M. J., Smith, T. H., *Economy Loading of Power Plants and Electric Systems*, Wiley, New York, 1943.
2. Kirchmayer, L. K., *Economic Operation of Power Systems*, Wiley, New York, 1958.
3. Kirchmayer, L. K., *Economic Control of Interconnected Systems*, Wiley, New York, 1959.
4. Cohn, N., *Control of Generation and Power Flow On Interconnected Systems*, Wiley, New York, 1961.
5. Hano, I., *Operating Characteristics of Electric Power Systems*, Denki Shoin, Tokyo, 1967.
6. Handschin, E. (ed.), *Real-Time Control of Electric Power Systems*, Elsevier, Amsterdam, 1972.
7. Savulescu, S. C. (ed.), *Computerized Operation of Power Systems*, Elsevier, Amsterdam, 1976.
8. Sterling, M. J. H., *Power System Control*, Peregrinus, London, 1978.
9. El-Hawary, M. E., Christensen, G. S., *Optimal Economic Operation of Electric Power Systems*, Academic, New York, 1979.

Characteristics of Power Generation Units

2.1 CHARACTERISTICS OF STEAM UNITS

In analyzing the problems associated with the controlled operation of power systems, there are many possible parameters of interest. Fundamental to the economic operating problem is the set of input-output characteristics of a thermal power generation unit. A typical boiler-turbine-generator unit is sketched in Figure 2.1. This unit consists of a single boiler that generates steam to drive a single turbine generator set. The electrical output of this set is connected not only to the electric power system but also to the auxiliary power system in the power plant. A typical steam turbine unit may require 2 to 6% of the gross output of the unit for the auxiliary power requirements necessary to drive boiler feed pumps, fans, condenser circulating water pumps, and so on. In defining the unit characteristics, we will talk about *gross* input versus *net* output. That is, gross input to the plant represents the total input whether measured in terms of dollars per hour or tons of coal per hour or millions of cubic feet of gas per hour, or any other units. The net output of the plant is the electrical power output available to the electric utility system. Occasionally engineers

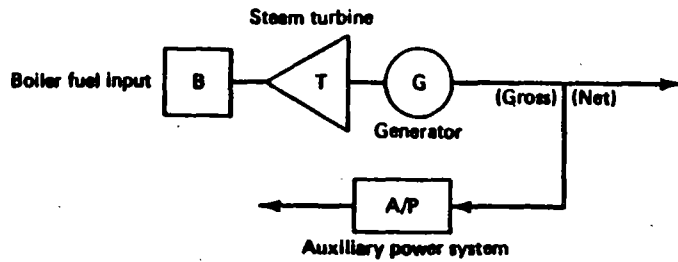


FIG. 2.1 Boiler-turbine-generator unit.

will develop gross input-gross output characteristics. In such situations, the data should be converted to net output to be more useful in scheduling the generation.

In defining the characteristics of steam turbine units, the following terms will be used.

H: Btu per hour heat input to the unit (or MBtu/h)

F: Fuel cost times **H** is the \$ per hour (\$/h) input to the unit for fuel.

Occasionally the dollar per hour operating cost of a unit will include prorated operation and maintenance costs. That is, the labor cost for the operating crew will be included as part of the operating cost if this cost can be expressed directly as a function of the power output of the unit. The output of the generation unit will be designated by **P**, the megawatt net output of the unit.

Figure 2.2 shows the input-output characteristic of a steam unit in idealized form. The input to the unit shown on the ordinate may be either in terms of heat energy requirements [millions of Btu per hour (MBtu/h)] or in terms of total

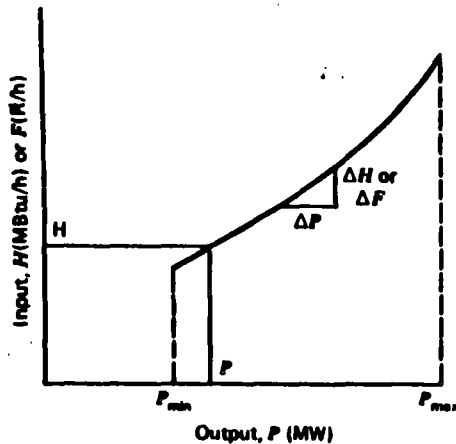


FIG. 2.2 Input-output curve of a steam turbine generator.

cost per hour (dollars per hour). The output is normally the net electrical output of the unit. The characteristic shown is idealized in that it is presented as a smooth, convex curve.

These data may be obtained from design calculations or from heat rate tests. When heat rate test data are used, it will usually be found that the data points do not fall on a smooth curve. Steam turbine generating units have several critical operating constraints. Generally, the minimum load at which a unit can operate is influenced more by the steam generator and the regenerative cycle than by the turbine. The only critical parameters for the turbine are shell and rotor metal differential temperatures, exhaust hood temperature, and rotor and shell expansion. Minimum load limitations are generally caused by fuel combustion stability and inherent steam generator design constraints. For example, most supercritical units cannot operate below 30% of design capability. A minimum flow of 30% is required to cool the tubes in the furnace of the steam generator adequately. Turbines do not have any inherent overload capability, so that the data shown on these curves normally do not extend much beyond 5% of the manufacturer's stated valve-wide-open capability.

The incremental heat rate characteristic for a unit of this type is shown in Figure 2.3. This incremental heat rate characteristic is the slope (the derivative) of the input-output characteristic, ($\Delta H/\Delta P$ or $\Delta F/\Delta P$). The data shown on this curve are in terms of Btu per kilowatt hour (or dollars per kilowatt hour) versus the net power output of the unit in megawatts. This characteristic is widely used in economic dispatching of the unit. It is converted to an incremental fuel cost characteristic by multiplying the incremental heat rate in Btu per kilowatt hour by the equivalent fuel cost in terms of dollars per Btu. Frequently this characteristic is approximated by a sequence of straight-line segments.

The last important characteristic of a steam unit is the unit (net) heat rate characteristic shown in Figure 2.4. This characteristic is H/P versus **P**. It is the reciprocal of the usual efficiency characteristic developed for machinery. The unit

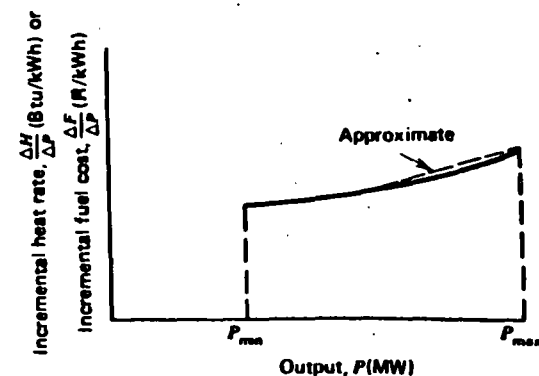


FIG. 2.3 Incremental heat (cost) rate characteristic.

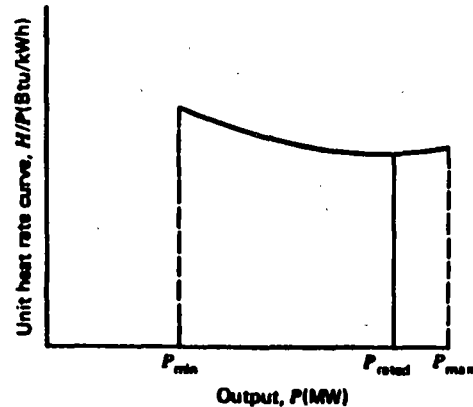


FIG. 24 Net heat rate characteristic of a steam turbine generator unit.

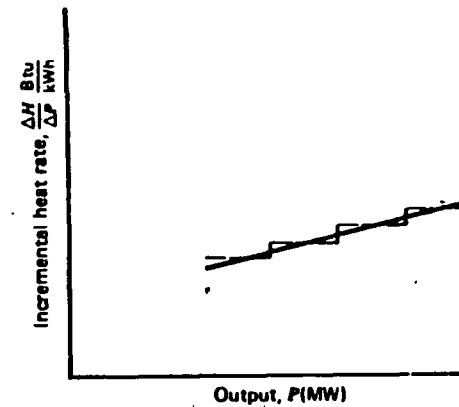


FIG. 25 Approximate representations of the incremental heat rate curve.

heat rate characteristic shows the heat input per kilowatt hour of output versus the megawatt output of the unit. Conventional steam turbine units are between 30 and 35% efficient, so that their unit heat rates range between approximately 11,400 Btu/kWh and 9800 Btu/kWh. (A kilowatt hour has a thermal equivalent of approximately 3412 Btu.) Unit heat rate characteristics are a function of unit design parameters such as initial steam conditions, stages of reheat and the reheat temperatures, condenser pressure, and the complexity of the regenerative feed-water cycle. These are important considerations in the establishment of the unit's efficiency. For purposes of estimation, a typical heat rate of 10,500 Btu/kWh may be used occasionally to approximate actual unit heat rate characteristics.

Many different formats are used to represent the input-output characteristic shown in Figure 2.2. The data obtained from heat rate tests or from the plant design engineers may be fitted by a polynomial curve. In many cases quadratic characteristics have been fit to these data. A series of straight-line segments may also be used to represent the input-output characteristics. The different representations will, of course, result in different incremental heat rate characteristics. Figure 2.5 shows two such variations. The solid line shows the incremental heat rate characteristic that results when the input versus output characteristic is a quadratic curve or some other continuous, smooth, convex function. This incremental heat rate characteristic is monotonically increasing as a function of the power output of the unit. The dashed lines in Figure 2.5 show a stepped incremental characteristic that results when a series of straight-line segments are used to represent the input-output characteristics of the unit. The use of these different representations may require that different scheduling methods be used for establishing the optimum economic operation of a power system. Both formats are useful, and both may be represented by tables of data. Only the first, the solid line, may be represented by a continuous analytic function, and only the first

has a derivative that is nonzero. (That is, d^2F/dP^2 equals zero if dF/dP is constant.)

2.2 VARIATIONS IN STEAM UNIT CHARACTERISTICS

A number of different steam unit characteristics exist. For large steam turbine generators the input-output characteristics shown on Figure 2.2 are not always as smooth as indicated there. Large steam turbine generators will have a number of steam admission valves that are opened in sequence to obtain ever-increasing output of the unit. Figure 2.6 shows both an input-output and an incremental heat rate characteristic for a unit with four valves. As the unit loading increases, the input to the unit increases and the incremental heat rate decreases between opening points for any two valves. However, when a valve is first opened, the throttling losses increase rapidly and the incremental heat rate rises suddenly. This gives rise to the discontinuous type of incremental heat rate characteristic shown in Figure 2.6. It is possible to use this type of characteristic in order to schedule steam units, although it is usually not done. This type of input-output characteristic is nonconvex; hence optimization techniques that require convex characteristics may not be used with impunity.

Another type of steam unit that may be encountered is the *common-header plant*, which contains a number of different boilers connected to a common steam line (called a common header). Figure 2.7 is a sketch of a rather complex common-header plant. In this plant there are not only a number of boilers and turbines each connected to the common header but also a "topping turbine" connected to the common header. A *topping turbine* is one in which steam is exhausted from the turbine and fed not to a condenser but to the common steam header.

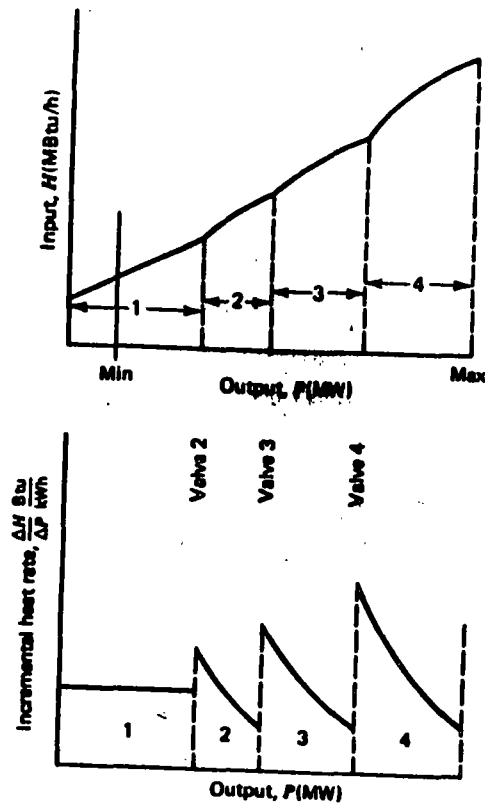


FIG. 26 Characteristics of a steam turbine generator with four steam admission valves.

A common-header plant will have a number of different input-output characteristics that result from different combinations of boilers and turbines connected to the header. Steinberg and Smith (*Economy Loading of Power Plants and Electric Systems*, Wiley, 1943) treats this type of plant quite extensively. Common-header plants were constructed originally not only to provide a large electrical output from a single plant but also to provide steam sendout for the heating and cooling of buildings in dense urban areas. After World War II, a number of these plants were modernized by the installation of the type of topping turbine shown in Figure 2.7. For a period of time during the 1960s, these common-header plants were being dismantled and replaced by modern, efficient plants. However, as urban areas began to reconstruct, a number of metropolitan utilities found that their steam loads were growing and that the common-header plants could not be dismantled but had to be expanded to provide steam supplies to new buildings.

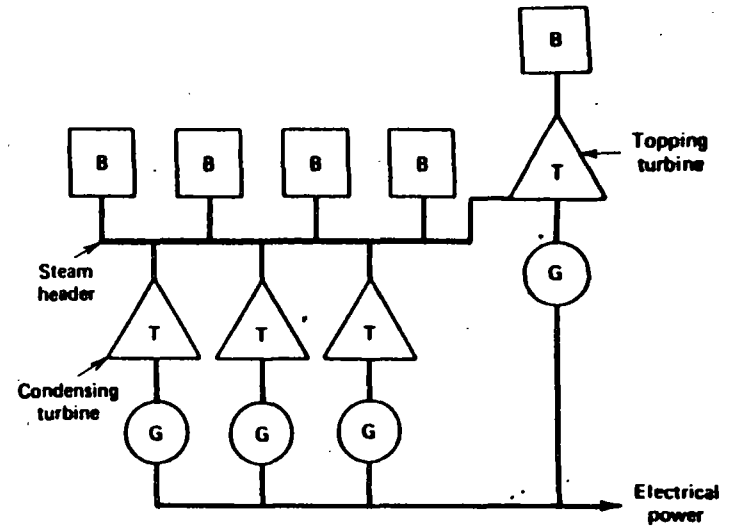


FIG. 27 A common-header steam plant.

In the late 1960s, a new type of steam plant configuration began to find favor, the *combined cycle plant*. A simple cycle gas turbine unit consists of a gas turbine and compressor connected on a single shaft to a generating unit. Simple cycle gas turbines have efficiencies in the range of 25 to 30% (i.e., unit heat rate of 13,600 to 11,400 MBtu/kWh based on the higher heating value of the fuel), require oil or gas for fuel, and are used primarily for peaking duty in electric power systems. The high temperature exhaust from a simple cycle unit is discharged to the atmosphere. The combined cycle plant utilizes the high temperature exhaust of gas turbines in heat recovery steam generators (HRSG) to generate steam to drive a separate steam turbine generating unit. The advantage of this type of plant is that it has a high thermal cycle efficiency. Figure 2.8 is a schematic diagram of this type of plant with four gas turbines and a single steam turbine. Figure 2.9 shows the resulting unit heat rate characteristic for the combined cycle plant.

It appears from data available from various manufacturers of combined cycle units that unit heat rates of 8500 Btu/kWh may be achievable with this type of plant. The incremental heat rate characteristics are very difficult to ascertain from the available data. It appears that the incremental heat rate characteristics are monotonically decreasing (or at least nonincreasing) as a function of the power output of the plant. The existence of this type of discontinuous characteristic as well as the negative-sloping incremental characteristic make the optimum economic scheduling of this type of unit somewhat difficult. When conventional economic dispatching methods are utilized to schedule this type of plant, it may be found that these plants are operating at full load all the time that they are available. It is an open question as to whether or not this type of plant is

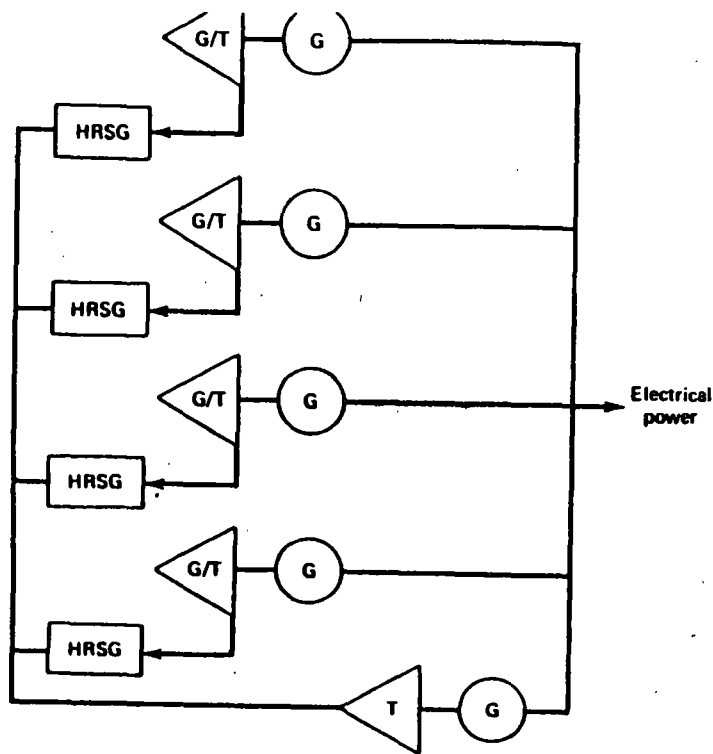


FIG. 28 A combined cycle plant with four gas turbines and a steam turbine generator.

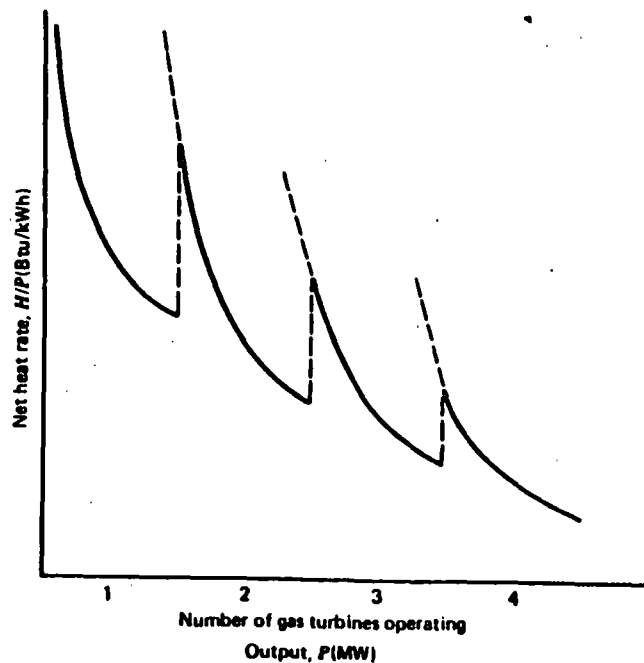


FIG. Combined cycle plant heat rate characteristic

designed to operate at full load for 6000 to 7000 h/yr. Of course, the actual operation of this type of plant will depend on relative fuel costs as well as on the unit generating mix available in the system.

Variations in the design of combined cycle plants have been utilized in recent years. There is, for example, a design configuration using a single shaft that contains two gas turbines driving a single electric generator. The exhaust gases from these two jet engines are then utilized in a heat recovery steam generator. Designs of heat recovery steam generators have been proposed that make use of additional fuel supplies to augment the steam-generating capability of the HRSG. Most combined cycle plants can utilize the gas turbines as simple cycle units when the HRSG and/or steam turbine generating units are out of service. These plants require a bypass around the HRSGs for the exhaust gases.

2.3 LIGHT-WATER MODERATED NUCLEAR REACTOR UNITS

U.S. utilities have adopted the light-water moderated reactor as the "standard" type of nuclear steam supply system. These reactors are either pressurized water reactors (PWRs) or boiling water reactors (BWRs) and use slightly enriched uranium as the basic energy supply source. The uranium that occurs in nature contains approximately seven-tenths of 1% by weight of U_{235} . This natural uranium must be enriched so that the content of U_{235} is in the range of 2 to 4% for use in either a PWR or a BWR.

The enriched uranium must be fabricated into fuel assemblies by various manufacturing processes. At the time the fuel assemblies are loaded into the nuclear reactor core there has been a considerable investment made in this fuel. During the period of time in which fuel is in the reactor and is generating heat and steam, and electrical power is being obtained from the generator, the amount of usable fissionable material in the core is decreasing. At some point the reactor core is no longer able to maintain a critical state at a proper power level, so the core must be removed and new fuel reloaded into the reactor. Commercial power reactors are normally designed to replace one third to one fifth of the fuel in the core during reloading.

At this point the nuclear fuel assemblies that have been removed are highly radioactive and must be treated in some fashion. Originally it was intended that these assemblies would be reprocessed in commercial plants and that valuable materials would be obtained from the reprocessed core assemblies. At this time (1983) it is questionable if the U.S. reactor industry will develop an economically viable reprocessing system that is acceptable to the public in general. If this is not done, either these radioactive cores will need to be stored for some indeterminate period of time or the U.S. government will have to take over these fuel assemblies for storage and eventual reprocessing. In any case, an additional amount of money will need to be invested either in reprocessing the fuel or in storing it for some period of time.

The calculation of "fuel cost" in a situation such as this involves economic and accounting considerations and is really an investment analysis. Simply speaking, there will be a total dollar investment in a given core assembly. This dollar investment includes the cost of mining the uranium, milling the uranium core, converting it into a gaseous product that may be enriched, fabricating fuel assemblies, and delivering them to the reactor plus the cost of removing the fuel assemblies after they have been irradiated and either reprocessing them or storing them. Each of these fuel assemblies will have generated a given amount of electrical energy. A pseudo fuel cost may be obtained by dividing the total investment in dollars by the total amount of electrical energy generated by the assembly. Of course there are refinements that may be made in this simple computation. For example, it is possible using nuclear physics calculations to compute more precisely the amount of energy generated by a specific fuel assembly in the core in a given stage of operation of a reactor.

In the remainder of this text nuclear units will be treated as if they are ordinary thermal-generating units fueled by a fossil fuel. The considerations and computations of exact fuel reloading schedules and enrichment levels in the various fuel assemblies are beyond the scope of a one-semester graduate course because they require a background in nuclear engineering as well as detailed understanding of the fuel cycle and its economic aspects.

2.4 HYDROELECTRIC UNITS

Hydroelectric units have input-output characteristics similar to steam turbine units. The input is in terms of volume of water per unit time; the output is in terms of electrical power. Figure 2.10 shows a typical input-output curve for a hydroelectric plant where the net hydraulic head is constant. This characteristics

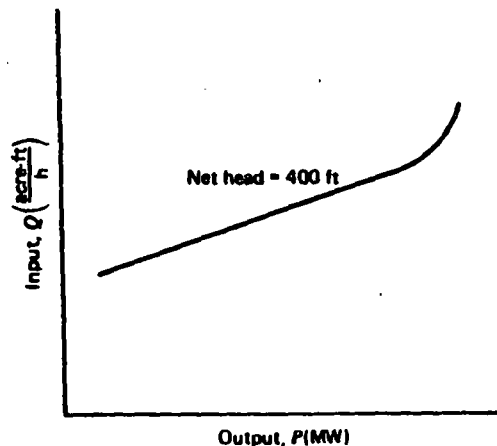


FIG. 2.10 Hydroelectric unit input-output curve.

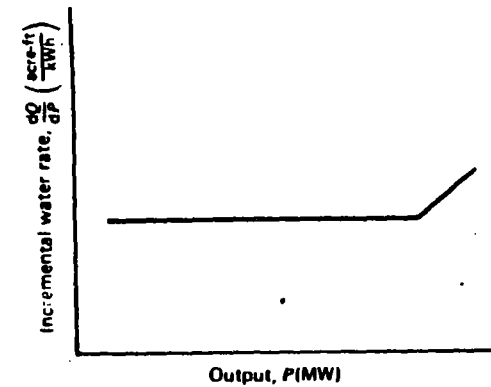


FIG. 2.11 Incremental water rate curve for hydroelectric plant.

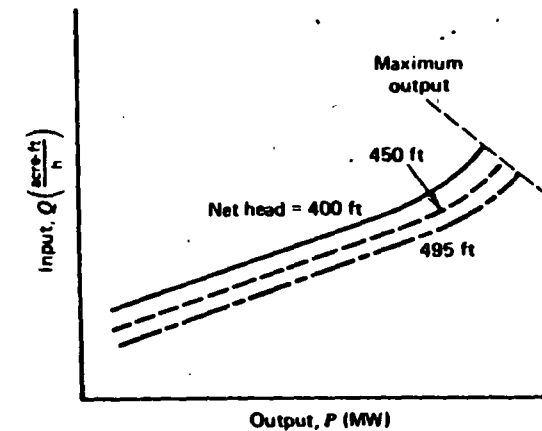


FIG. 2.12 Input-output curves for hydroelectric plant with a variable head.

shows an almost linear curve of input water volume requirements per unit time as a function of power output as the power output increases from minimum to rated load. Above this point the volume requirements increase as the efficiency of the unit falls. The incremental water rate characteristics are shown in Figure 2.11. The units shown on both these curves are English units. That is, volume is shown as acre-feet (an acre of water a foot deep). If necessary, net hydraulic heads are shown in feet. Metric units are also used as are thousands of cubic feet per second (kft^3/sec) for the water rate.

Figure 2.12 shows the input-output characteristics of a hydroelectric plant with variable head. This type of characteristic occurs whenever the variation in the storage pond (i.e., forebay) and/or afterbay elevations is a fairly large percentage of the net hydraulic head. Scheduling hydroelectric plants with

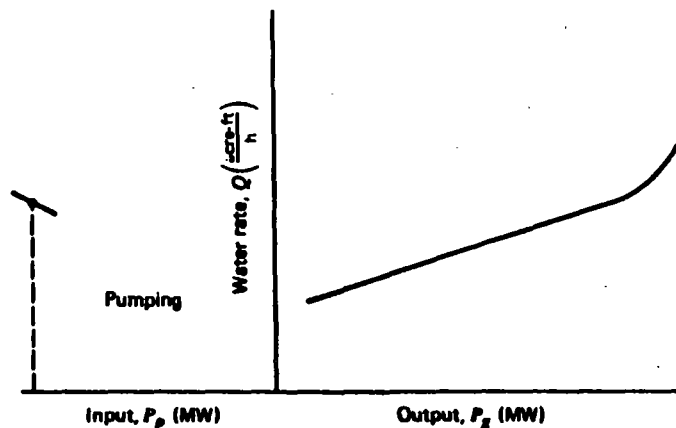


FIG. 2.13 Input-output characteristics for a pumped storage hydro plant with a fixed, net hydraulic head.

variable head characteristics is more difficult than scheduling hydroelectric plants with fixed heads. This is true not only because of the multiplicity of input-output curves that must be considered, but also because the maximum capability of the plant will also tend to vary with the hydraulic head. In Figure 2.12 the volume of water required for a given power output decreases as the head increases. (That is, $\partial Q/\partial \text{head}$ or $\partial Q/\partial \text{volume}$ are negative for a fixed power.) In a later section methods are discussed that have been proposed for the optimum scheduling of hydrothermal power systems where the hydroelectric systems exhibit variable head characteristics.

Figure 2.13 shows the type of characteristics exhibited by pumped-storage hydroelectric plants. These plants are designed so that water may be stored by pumping it against a net hydraulic head for discharge at a more propitious time. This type of plant was originally installed with separate hydraulic turbines and electric motor driven pumps. In recent years reversible, hydraulic pump turbines have been utilized. These reversible pump turbines exhibit normal input-output characteristics when utilized as turbines. In the pumping mode, however, the efficiency of operation tends to fall off when the pump is operated away from the rating of the unit. For this reason most plant operators will only operate these units in the pumping mode at a fixed pumping load. The incremental water characteristics when operating as a turbine are, of course, similar to the conventional units illustrated previously.

The scheduling of pumped-storage hydroelectric plants may also be complicated by the necessity of recognizing the variable-head effects. These effects may be most pronounced in the variation of the maximum capability of the plant rather than in the presence of multiple input-output curves. This variable maximum capability may have a significant effect on the requirements for selecting capacity to run on the system, since these pumped-storage hydro plants may usually be considered as spinning-reserve capability. That is, they will be used

only during periods of highest cost generation on the thermal units; at other times they may be considered as readily available ("spinning reserve"). That is, during periods when they would normally be pumping, they may be shut off to reduce the demand. When idle, they may be started rapidly. In this case the maximum capacity available will have a significant impact on the requirements for having other units available to meet the systems total spinning-reserve requirements.

These hydroelectric plants and their characteristics (both the characteristics for the pumped-storage and the conventional storage hydroelectric plants) are affected greatly by the hydraulic configuration that exists where the plant is installed and by the requirements for water flows that may have nothing to do with power production. The characteristics just illustrated are for single, isolated plants. In many river systems plants are connected in both series and in parallel (hydraulically speaking). In this case the release of an upstream plant contributes to the inflow of downstream plants. There may be tributaries between plants that contribute to the water stored behind a downstream dam. The situation becomes even more complex when pumped-storage plants are constructed in conjunction with conventional hydroelectric plants. The problem of the optimum utilization of these resources involves the complicated problems associated with the scheduling of water as well as the optimum operation of the electric power system to minimize production cost. We can only touch on these matters in this text and introduce the subject. Because of the importance of the hydraulic coupling between plants, it is safe to assert that no two hydroelectric systems are exactly the same.

APPENDIX Typical Generation Data

Up until the early 1950s, most U.S. utilities installed units of less than 100 MW. These units were relatively inefficient (about 950 psi steam and no reheat cycles). During the early 1950s, the economics of reheat cycles and advances in materials technology encouraged the installation of reheat units having steam temperatures of 1000°F and pressures in the range of 1450 to 2150 psi. Unit sizes for the new design reheat units ranged to 225 MW. In the late 1950s and early 1960s, U.S. utilities began installing larger units ranging up to 300 MW in size. In the late 1950s, U.S. utilities began installing larger, more efficient units (about 2400 psi with single reheat) ranging in size to 700 MW. In addition, in the late 1960s, some U.S. utilities began installing more efficient supercritical units (about 3500 psi, some with double reheat) ranging in size to 1300 MW. The bulk of these supercritical units range in size from 500 to 900 MW. However, many of the newest supercritical units range in size from 1150 to 1300 MW.

Typical heat rate data for these classes of fossil generation are shown in Table 2.1. These data are based on Federal Power Commission reports and other design data for U.S. utilities (see *Heat Rates for General Electric Steam*

TABLE 2.1 Typical Fossil Generation Unit Heat Rates

Fossil unit-description	Unit rating (MW)	100% output (Btu/kWh)	80% output (Btu/kWh)	60% output (Btu/kWh)	40% output (Btu/kWh)	25% output (Btu/kWh)
Steam-coal	50	11000	11088	11429	12166	13409*
Steam-oil	50	11500	11592	11949	12719	14019*
Steam-gas	50	11700	11794	12156	12940	14262*
Steam-coal	200	9500	9576	9871	10507	11581*
Steam-oil	200	9900	9979	10286	10949	12068*
Steam-gas	200	10050	10130	10442	11115	12251*
Steam-coal	400	9000	9045	9252	9783	10674*
Steam-oil	400	9400	9447	9663	10218	11148*
Steam-gas	400	9500	9548	9766	10327	11267*
Steam-coal	600	8900	8989	9265	9843	10814*
Steam-oil	600	9300	9393	9681	10286	11300*
Steam-gas	600	9400	9494	9785	10396	11421*
Steam-coal	800-1200	8750	8803	9048	9625*	
Steam-oil	800-1200	9100	9155	9409	10010*	
Steam-gas	800-1200	9200	9255	9513	10120*	

* For study purposes, units should not be loaded below the points shown.

TABLE 2.2 Approximate Unit Heat Rate Increase Over Valve-Best-Point Turbine Heat Rate in %

Unit size (MW)	Coal	Oil	Gas
50	22	28	30
200	20	25	27
400	16	21	22
600	16	21	22
800-1200	16	21	22

Turbine-Generators 100,000 kW and Larger, Large Steam Turbine Generator Department, G.E.

The shape of the heat rate curves is based on the locus of design, "valve-best-points" for the various sizes of turbines. The magnitude of the turbine heat rate curve has been increased to obtain the unit heat rate, adjusting for the mean of the valve loops, boiler efficiency, and auxiliary power requirements. The resulting approximate increase from design turbine heat rate to obtain the generation unit heat rate in Table 2.1 is summarized in Table 2.2 for the various types and sizes of fossil units. Typical fossil unit maintenance requirements and forced outage rate (F.O.R.) data are shown in Table 2.3.

The annual maintenance requirements, based on a fairly recent report (1975) of the Edison Electric Institute on equipment availability, includes both scheduled and unscheduled maintenance (or maintenance outages). A maintenance outage occurs when a unit is taken out of service to repair a problem. Supercritical units have more complicated equipment than subcritical units; therefore

TABLE 2.3 Typical Fossil Unit Maintenance Requirements and Forced Outage Rates

Unit size (MW)	Maintenance requirements (Day/Yr)			Full outage			Partial outage data			Effective outage		
	Scheduled	Unscheduled	Total	F.O.R. (%)	Avg. repair time (Day)	Avg. derating (% Unit)	Avg. partial F.O.R. (%)	Avg. repair time (Day)	Effective F.O.R. (%)	Avg. repair time (Day)	Effective F.O.R. (%)	Avg. repair time (Day)
50	17	7	24	2.3	2.2	15	2.4	0.9	2.7	2.4	2.7	2.4
200	24	12	36	5.3	2.2	24	8.9	3.2	7.4	3.0	7.4	3.0
400	31	14	45	9.5	2.5	22	14.0	4.9	13.0	3.6	13.0	3.6
600	31	14	45	16.0	2.7	21	25.0	8.8	21.0	4.5	21.0	4.5
800-1200	34	15	49	18.0	3.0	21	29.0	9.5	24.0	5.0	24.0	5.0

TABLE 2.4 Typical Nuclear Generation Unit Heat Rates

	100% Output (Btu/kWh)	75% Output (Btu/kWh)	50% Output (Btu/kWh)
Light-water reactor	10400	10442*	10951*

* Nuclear units are usually dispatched at fixed output.

the maintenance requirements have been increased 19% over the EEI data for units larger than 600 MW, which is based mainly on subcritical unit maintenance requirements.

The forced outage rate and outage duration data for the fossil units are also based on the cited EEI report. Full and partial outage data are presented as well as the resulting effective outage rate data. The forced outage rates increase significantly as the unit size and initial steam conditions increase. The EEI report does not separate the forced outage rates of supercritical units from the subcritical units greater than 600 MW. Since the steam pressure is much higher and the unit size will be larger for supercritical units, it is assumed that the forced outage data would be 10% higher than the 600 MW subcritical unit data, which represent larger subcritical unit forced outage rates.

Typical nuclear generation heat rate data are shown in Table 2.4. One set of typical characteristics can represent both types of light-water reactors for generation studies. The typical shape of the heat rate curve for light-water reactors is based on the locus of design valve-best-points, adjusted upward 8% to obtain the unit net heat rates. The additional 8% accounts for auxiliary power requirements and heat losses in the reactor auxiliary equipment. Maintenance and forced outage rate data shown in Table 2.5 are based on EEI data for the existing nuclear units.

Gas turbines range in size from a few megawatts to 100 MW for some of the newer units. Gas turbines are designed to burn liquid or gaseous fuels, mostly light distillate oil or natural gas. Typical gas turbine heat rates are shown in Table 2.6. Heat rate data based on the same sources as the fossil and nuclear units are presented only for full-load operation because these units are not normally operated at partial loads.

Typical gas turbine maintenance and forced outage data are presented in Table 2.7. The maintenance requirements are approximately the same for both industrial and jet engine plants, based on the EEI report. The effective forced outage rates shown in Table 2.7 are also about the same for both types of gas turbines if the EEI definition of forced outage rate is modified as follows.

$$\text{EEI F.O.R.} = \frac{\text{Time on forced outage}}{\text{Time in service} + \text{Time on forced outage}}$$

$$\text{Modified F.O.R.} = \frac{\text{Time on forced outage}}{\text{Time available for service} + \text{Time on forced outage}}$$

TABLE 2.5 Typical Nuclear Unit Maintenance Requirements and Forced Outage Rates

Nuclear unit size	Maintenance requirements (Day/Yr)		Full outage		Partial outage data			Effective outage	
	Scheduled	Unscheduled Total	F.O.R. (%)	Avg. repair time (Day)	Avg. derating (% Unit)	Avg. partial F.O.R. (%)	Avg. repair time (Day)	Effective F.O.R. (%)	Avg. repair time (Day)
All	35	49	11	3.7	23	16	5	15	5

TABLE 2.6 Typical Gas Turbine Generation Unit Heat Rates

Unit type	Heat rate (Btu/kWh)
Industrial	13,600
Jet	16,000

TABLE 2.7 Typical Gas Turbine Maintenance Requirements and Forced Outage Rates

Unit type	Maintenance requirements (Day/Yr)		Full outage		Partial outage data			Effective outage	
	Scheduled	Unscheduled Total	F.O.R. (%)	Avg. repair time (Day)	Avg. derating (% Unit)	Avg. partial F.O.R. (%)	Avg. repair time (Day)	Effective F.O.R. (%)	Avg. repair time (Day)
All	8	10	—	—	—	—	—	24	2



**FACULTAD DE INGENIERIA U.N.A.M.
DIVISION DE EDUCACION CONTINUA**

**V CURSO INTERNACIONAL DE SISTEMAS
ELECTRICOS DE POTENCIA**

MODULO II: SISTEMAS ELECTRICOS DE POTENCIA

**TEMA: ECONOMIC DISPATCH OF THERMAL UNITES AND
METHODS OF SOLUTION**

EXPOSITOR: ING. ARTURO MORALES COLLANTES

Since turbines are generally operated as peaking units due to high fuel cost and high unit heat rates, their actual running time is very small. The conventionally calculated forced outage rates for gas turbines are approximately 33% for industrial units and 48% for jet engines. However, if the service time is replaced by the time the peaking units are available, the forced outage rates reduce to about 24% for both types of gas turbines. It is recommended that the modified forced outage rate data be used for these peaking units. It is almost impossible to specify "typical" data for a hydroelectric plant since the essential characteristics depend on the hydraulic parameters associated with each plant site.

Economic Dispatch of Thermal Units and Methods of Solution

This chapter introduces techniques of power system optimization. For a complete understanding of how optimization problems are carried out, first read the appendix to this chapter where the concepts of the LaGrange multiplier and the Kuhn-Tucker conditions are introduced.

3.1 THE ECONOMIC DISPATCH PROBLEM

Figure 3.1 shows the configuration that will be studied in this section. This system consists of N thermal-generating units connected to a single busbar serving a received electrical load P_R . The input to each unit, shown as F_i , represents the cost rate* of the unit. The output of each unit, P_i , is the electrical power generated by that particular unit. The total cost rate of this system is, of course, the sum of the costs of each of the individual units. The

* Generating units consume fuel at a specific rate (e.g., MBtu/h), which as noted in Chapter 2 can be converted to R/h , which represents a cost rate. Starting in this chapter and throughout the remainder of the text, we will simply use the term generating unit "cost" to refer to R/h .

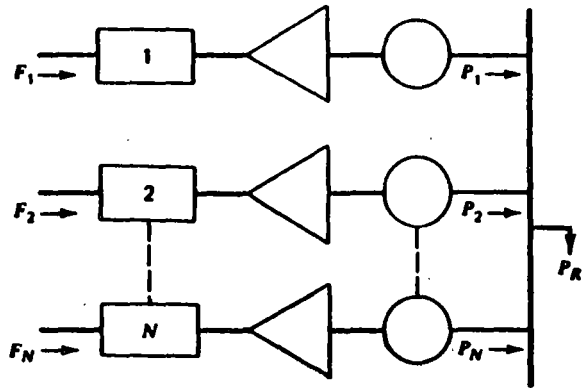


FIG. 3.1 N thermal units committed to serve a load of P_R .

essential constraint on the operation of this system is that the sum of the output powers must equal the load demand.

Mathematically speaking, the problem may be stated very concisely. That is, an objective function, F_T , is equal to the total cost for supplying the indicated load. The problem is to minimize F_T subject to the constraint that the sum of the powers generated must equal the received load. Note that any transmission losses are neglected and any operating limits are not explicitly stated when formulating this problem. That is,

$$F_T = F_1 + F_2 + F_3 + \dots + F_N$$

$$= \sum_{i=1}^N F_i(P_i) \quad (3.1)$$

$$\phi = 0 = P_R - \sum_{i=1}^N P_i \quad (3.2)$$

This is a constrained optimization problem that may be attacked formally using advanced calculus methods that involve the LaGrange function.

In order to establish the necessary conditions for an extreme value of the objective function, add the constraint function to the objective function after the constraint function has been multiplied by an undetermined multiplier. This is known as the LaGrange function and is shown in Eq. 3.3.

$$\mathcal{L} = F_T + \lambda \phi \quad (3.3)$$

The necessary conditions for an extreme value of the objective function result when we take the first derivative of the LaGrange function with respect to each of the independent variables and set the derivatives equal to zero. In this case there are $N + 1$ variables, the N values of power output, P_i , plus the undetermined LaGrange multiplier, λ . The derivative of the LaGrange function with respect to the undetermined multiplier merely gives back the constraint equation. On the other hand, the N equations that result when we take the partial

derivative of the LaGrange function with respect to the power output values one at a time give the set of equations shown as Eq. 3.4.

$$\frac{\partial \mathcal{L}}{\partial P_i} = \frac{dF_i(P_i)}{dP_i} - \lambda = 0 \quad (3.4)$$

or

$$0 = \frac{dF_i}{dP_i} - \lambda$$

That is, the necessary condition for the existence of a minimum cost-operating condition for the thermal power system is that the incremental cost rates of all the units be equal to some undetermined value, λ . Of course, to this necessary condition we must add the constraint equation that the sum of the power outputs must be equal to the power demanded by the load. In addition, there are two inequalities that must be satisfied for each of the units. That is, the power output of each unit must be greater than or equal to the minimum power permitted and must also be less than or equal to the maximum power permitted on that particular unit.

These conditions and inequalities may be summarized as shown in the set of equations making up Eq. 3.5.

$$\frac{dF_i}{dP_i} = \lambda \quad N \text{ equations}$$

$$P_{i,\min} \leq P_i \leq P_{i,\max} \quad 2N \text{ inequalities} \quad (3.5)$$

$$\sum_{i=1}^N P_i = P_R \quad 1 \text{ constraint}$$

When we recognize the inequality constraints, then the necessary conditions may be expanded slightly as shown in the set of equations making up Eq. 3.6.

$$\frac{dF_i}{dP_i} = \lambda \quad \text{for } P_{i,\min} < P_i < P_{i,\max}$$

$$\frac{dF_i}{dP_i} \leq \lambda \quad \text{for } P_i = P_{i,\max} \quad (3.6)$$

$$\frac{dF_i}{dP_i} \geq \lambda \quad \text{for } P_i = P_{i,\min}$$

Several of the examples in this chapter use the following three generator units.

Unit 1: Coal-fired Steam Unit:

Max output = 600 MW

Min output = 150 MW

Input-output curve:

$$H_1 \left(\frac{\text{MBtu}}{\text{h}} \right) = 510.0 + 7.2 P_1 + 0.00142 P_1^2$$

Unit 2: Oil-fired Steam Unit:

Max output = 400 MW

Min output = 100 MW

Input-output curve:

$$H_2 \left(\frac{\text{MBtu}}{\text{h}} \right) = 310.0 + 7.85 P_2 + 0.00194 P_2^2$$

Unit 3: Oil-fired Steam Unit:

Max output = 200 MW

Min output = 50 MW

Input-output curve:

$$H_3 \left(\frac{\text{MBtu}}{\text{h}} \right) = 78.0 + 7.97 P_3 + 0.00482 P_3^2$$

EXAMPLE 3A

Suppose that we wish to determine the economic operating point for these three units when delivering a total of 850 MW. Before this problem can be solved, the fuel cost of each unit must be specified. Let the following fuel costs be in effect.

Unit 1: Fuel cost = 1.1 R/MBtu

Unit 2: Fuel cost = 1.0 R/MBtu

Unit 3: Fuel cost = 1.0 R/MBtu

Then

$$F_1(P_1) = H_1(P_1) \times 1.1 = 561 + 7.92 P_1 + 0.001562 P_1^2 \text{ R/h}$$

$$F_2(P_2) = H_2(P_2) \times 1.0 = 310 + 7.85 P_2 + 0.00194 P_2^2 \text{ R/h}$$

$$F_3(P_3) = H_3(P_3) \times 1.0 = 78 + 7.97 P_3 + 0.00482 P_3^2 \text{ R/h}$$

Using Eq. 3.5, the conditions for an optimum dispatch are

$$\frac{dF_1}{dP_1} = 7.92 + 0.003124 P_1 = \lambda$$

$$\frac{dF_2}{dP_2} = 7.85 + 0.00388 P_2 = \lambda$$

$$\frac{dF_3}{dP_3} = 7.97 + 0.00964 P_3 = \lambda$$

and

$$P_1 + P_2 + P_3 = 850 \text{ MW}$$

Solving for λ , one obtains

$$\lambda = 9.148 \text{ R/MWh}$$

and then solving for P_1 , P_2 , and P_3 ,

$$P_1 = 393.2 \text{ MW}$$

$$P_2 = 334.6 \text{ MW}$$

$$P_3 = 122.2 \text{ MW}$$

Note that all constraints are met, that is, each unit is within its high and low limit and the total output when summed over all three units meets the desired 850 MW total.

EXAMPLE 3B

Suppose the price of coal decreased to 0.9 R/MBtu. The fuel cost function for unit 1 becomes

$$F_1(P_1) = 459 + 6.48 P_1 + 0.00128 P_1^2$$

If one goes about the solution exactly as done here, the results are

$$\lambda = 8.284 \text{ R/MWh}$$

and

$$P_1 = 704.6 \text{ MW}$$

$$P_2 = 111.8 \text{ MW}$$

$$P_3 = 32.6 \text{ MW}$$

This solution meets the constraint requiring total generation to equal 850 MW, but units 1 and 3 are not within limit. To solve for the most economic dispatch while meeting unit limits, use Eq. 3.6.

Suppose unit 1 is set to its maximum output and unit 3 to its minimum output. The dispatch becomes

$$P_1 = 600 \text{ MW}$$

$$P_2 = 200 \text{ MW}$$

$$P_3 = 50 \text{ MW}$$

From Eq. 3.6, we see that λ must equal the incremental cost of unit 2 since it is not at either limit. Then

$$\lambda = \left. \frac{dF_2}{dP_2} \right|_{P_2=200} = 8.626 \text{ R/MWh}$$

Next, calculate the incremental cost for units 1 and 3 to see if they meet the conditions of Eq. 3.6.

$$\left. \frac{dF_1}{dP_1} \right|_{P_1=600} = 8.016 \text{ R/MWh}$$

$$\left. \frac{dF_3}{dP_3} \right|_{P_3=50} = 8.452 \text{ R/MWh}$$

Note that the incremental cost for unit 1 is less than λ , so unit 1 should be at its maximum. However, the incremental cost for unit 3 is not greater than λ , so unit 3 should not be forced to its minimum. Thus, to find the optimal dispatch, allow the incremental cost at units 2 and 3 to equal λ as follows.

$$P_1 = 600 \text{ MW}$$

$$\frac{dF_2}{dP_2} = 7.85 + 0.00388 P_2 = \lambda$$

$$\frac{dF_3}{dP_3} = 7.97 + 0.00964 P_3 = \lambda$$

$$P_2 + P_3 = 850 - P_1 = 250 \text{ MW}$$

which results in

$$\lambda = 8.576 \text{ R/MWh}$$

and

$$P_2 = 187.1 \text{ MW}$$

$$P_3 = 62.9 \text{ MW}$$

Note that this dispatch meets the conditions of Eq. 3.6 since

$$\left. \frac{dF_1}{dP_1} \right|_{P_1=600 \text{ MW}} = 8.016 \text{ R/MWh}$$

which is less than λ , while

$$\frac{dF_2}{dP_2} \text{ and } \frac{dF_3}{dP_3}$$

both equal λ .

3.2 THERMAL SYSTEM DISPATCHING WITH NETWORK LOSSES CONSIDERED

Figure 3.2 shows symbolically an all thermal power generation system connected to an equivalent load bus through a transmission network. The economic-dispatching problem associated with this particular configuration is slightly more complicated to set up than the previous case. This is because the constraint

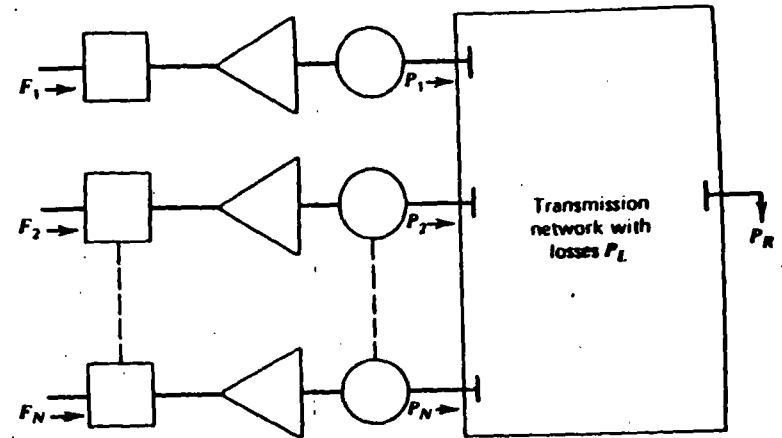


FIG. 3.2 N thermal units serving load through transmission network.

equation is now one that must include the network losses. The objective function, F_T , is the same as that defined for Eq. 3.1. However, the constraint equation previously shown in Eq. 3.2 must now be expanded to the one shown in Eq. 3.7.

$$P_R + P_L - \sum_{i=1}^N P_i = \phi = 0 \quad (3.7)$$

The same procedure is followed in the formal sense to establish the necessary conditions for a minimum cost operating solution. The LaGrange function is shown in Eq. 3.8. In taking the derivative of the LaGrange function with respect to each of the individual power outputs, P_i , it must be recognized that the loss in the transmission network, P_L , is a function of the network impedances and the currents flowing in the network. For our purposes, the currents will be considered only as a function of the independent variables P_i and the load P_R . Taking the derivative of the LaGrange function with respect to any one of the N values of P_i results in Eq. 3.9. There are N equations of this type to be satisfied along with the constraint equation shown in Eq. 3.7. This collection, Eq. 3.9 plus Eq. 3.7, is known collectively as the *coordination equations*.

$$\mathcal{L} = F_T + \lambda \phi \quad (3.8)$$

$$\frac{\partial \mathcal{L}}{\partial P_i} = \frac{dF_i}{dP_i} - \lambda \left(1 - \frac{\partial P_L}{\partial P_i} \right) = 0 \quad (3.9)$$

or

$$\frac{dF_i}{dP_i} + \lambda \frac{\partial P_L}{\partial P_i} = \lambda$$

$$P_R + P_L - \sum_{i=1}^N P_i = 0$$

It is much more difficult to solve this set of equations than the previous set with no losses since this second set involves the computation of the network loss in order to establish the validity of the solution in satisfying the constraint equation. There have been two general approaches to the solution of this problem. The first is the development of a mathematical expression for the losses in the network solely as a function of the power output of each of the units. This is the loss-formula method discussed at some length in Kirchmayer (*Economic Operation of Power Systems*, Wiley, 1958). The other basic approach to the solution of this problem is to incorporate the load-flow equations as essential constraints in the formal establishment of the optimization problem. This general approach is known as the *optimal load flow*.

EXAMPLE 3C

Starting with the same units and fuel costs as in Example 3A, we will include a simplified loss expression.

$$P_L = 0.00003 P_1^2 + 0.00009 P_2^2 + 0.00012 P_3^2$$

This simplified loss formula will suffice to show the difficulties in calculating a dispatch for which losses are accounted. Note that real-world loss formulas are more complicated than the one used in this example (See Chapter 4).

Applying Eqs. 3.8 and 3.9,

$$\frac{dF_1}{dP_1} = \lambda \left(1 - \frac{\partial P_L}{\partial P_1} \right)$$

becomes

$$7.92 + 0.003124 P_1 = \lambda [1 - 2(0.00003)P_1]$$

Similarly for P_2 and P_3 ,

$$7.85 + 0.00388 P_2 = \lambda [1 - 2(0.00009)P_2]$$

$$7.97 + 0.00964 P_3 = \lambda [1 - 2(0.00012)P_3]$$

and

$$P_1 + P_2 + P_3 - 850 - P_L = 0$$

We no longer have a set of linear equations as in Example 3A. This necessitates a more complex solution procedure as follows.

Step 1 Pick a set of starting values for P_1 , P_2 , and P_3 that sum to the load.

Step 2 Calculate the incremental losses $\partial P_L / \partial P_i$ as well as the total losses P_L . The incremental losses and total losses will be considered constant until we return to step 2.

Step 3 Calculate the value of λ that causes P_1 , P_2 , and P_3 to sum to the total load plus losses. This is now as simple as the calculations in Example 3A since the equations are again linear.

Step 4 Compare the P_1 , P_2 , and P_3 from step 3 to the values used at the start of step 2. If there is no significant change in any one of the values, go to step 5, otherwise go back to step 2.

Step 5 Done.

Using this procedure, we obtain

Step 1 Pick the P_1 , P_2 , and P_3 starting values as

$$P_1 = 400.0 \text{ MW}$$

$$P_2 = 300.0 \text{ MW}$$

$$P_3 = 150.0 \text{ MW}$$

Step 2 Incremental losses are

$$\frac{\partial P_L}{\partial P_1} = 2(0.00003)400 = 0.0240$$

$$\frac{\partial P_L}{\partial P_2} = 2(0.00009)300 = 0.0540$$

$$\frac{\partial P_L}{\partial P_3} = 2(0.00012)150 = 0.0360$$

Total losses are 15.6 MW

Step 3 We can now solve for λ using the following.

$$7.92 + 0.003124 P_1 = \lambda [1 - 0.0240] = \lambda(0.9760)$$

$$7.85 + 0.00388 P_2 = \lambda [1 - 0.0540] = \lambda(0.9460)$$

$$7.97 + 0.00964 P_3 = \lambda [1 - 0.0360] = \lambda(0.9640)$$

and

$$P_1 + P_2 + P_3 - 850 - 15.6 = P_1 + P_2 + P_3 - 865.6 = 0$$

These equations are now linear, so we can solve for λ directly. The results are

$$\lambda = 9.5252 \text{ R/MWh}$$

and the resulting generator outputs are

$$P_1 = 440.68$$

$$P_2 = 299.12$$

$$P_3 = 125.77$$

Step 4 Since these values for P_1 , P_2 , and P_3 are quite different from the starting values, we will return to step 2.

Step 2 The incremental losses are recalculated with the new generation values.

$$\frac{\partial P_L}{\partial P_1} = 2(0.00003)440.68 = 0.0264$$

$$\frac{\partial P_L}{\partial P_2} = 2(0.00009)299.12 = 0.0538$$

$$\frac{\partial P_L}{\partial P_3} = 2(0.00012)125.77 = 0.0301$$

Total losses are 15.78 MW.

Step 3 The new incremental losses and total losses are incorporated into the equations, and a new value of λ and P_1 , P_2 , and P_3 are solved for

$$7.92 + 0.003124 P_1 = \lambda(1 - 0.0264) = \lambda(0.9736)$$

$$7.85 + 0.00388 P_2 = \lambda(1 - 0.0538) = \lambda(0.9462)$$

$$7.97 + 0.00964 P_3 = \lambda(1 - 0.0301) = \lambda(0.9699)$$

$$P_1 + P_2 + P_3 - 850 - 15.78 = P_1 + P_2 + P_3 - 865.78 = 0$$

resulting in $\lambda = 9.5275$ R/MWh and

$$P_1 = 433.94 \text{ MW}$$

$$P_2 = 300.11 \text{ MW}$$

$$P_3 = 131.74 \text{ MW}$$

⋮

Table 3.1 summarizes the iterative process used to solve this problem.

TABLE 3.1 Iterative Process Used to Solve Example 3.

Iteration	P_1 (MW)	P_2 (MW)	P_3 (MW)	Losses (MW)	Lambda (R/MWh)
Start	400.00	300.00	150.00	15.60	9.5252
1	440.68	299.12	125.77	15.78	9.5275
2	433.94	300.11	131.74	15.84	9.5285
3	435.87	299.94	130.42	15.83	9.5283
4	435.13	299.99	130.71	15.83	9.5284

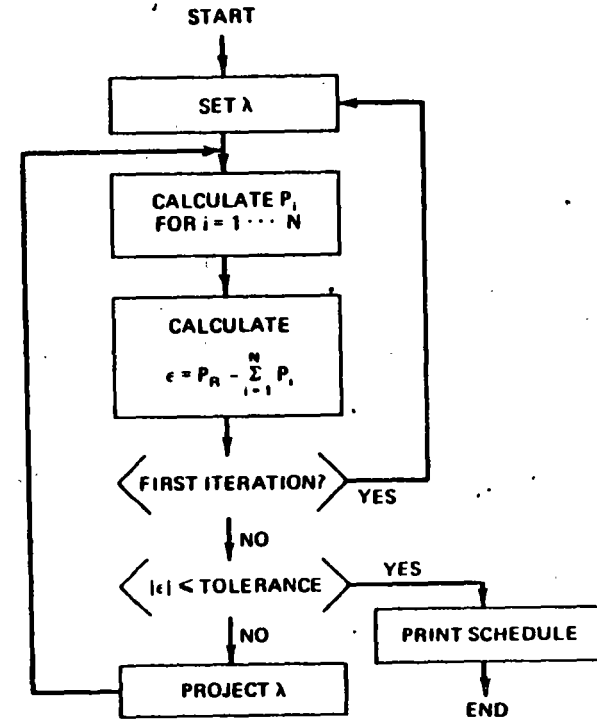


FIG. 3.3 Economic dispatch by the Lambda-iteration method.

3.3 THE LAMBDA-ITERATION METHOD

Figure 3.3 is a block diagram of the lambda-iteration method of solution for the all thermal, dispatching problem-neglecting losses. We can approach the solution to this problem by considering a graphical technique for solving the problem and then extending this into the area of computer algorithms.

Suppose we had a three-machine system and wish to find the optimum economic operating point. One approach would be to plot the incremental cost characteristics for each of these three units on the same graph, such as sketched in Figure 3.4. In order to establish the operating points of each of these three units such that we have minimum cost and at the same time satisfy the specified demand, we could use this sketch and a ruler to find the solution. That is, we could assume an incremental cost rate (λ) and find the power outputs of each of the three units for this value of incremental cost.

Of course, our first estimate will be incorrect. If we have assumed the value of incremental cost such that the total power output is too low, we must increase the λ value and try another solution. With two solutions, we can extrapolate (or

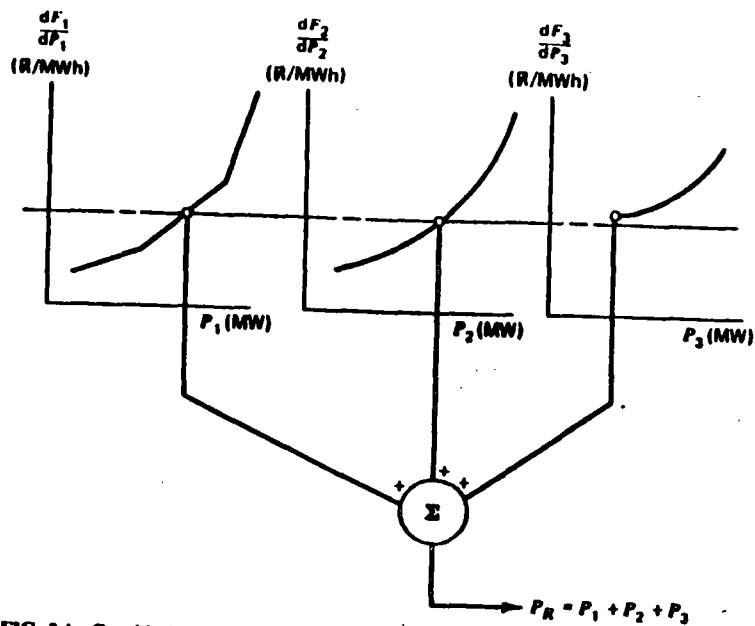


FIG. 3.4 Graphical solution to economic dispatch.

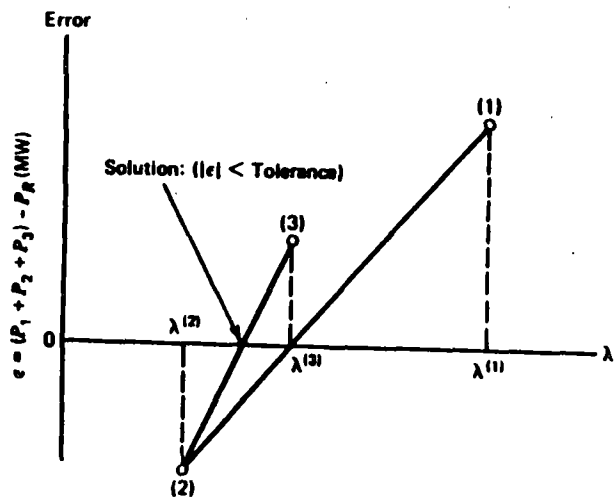


FIG. 3.5 Lambda projections.

interpolate) the two solutions to get closer to the desired value of total received power (see Figure 3.5).

By keeping track of the total demand versus the incremental cost, we can rapidly find the desired operating point. If we wished, we could manufacture a whole series of tables that would show the total power supplied for different incremental cost levels and combinations of units.

This same procedure can be adopted for a computer implementation as shown in Figure 3.3. That is, we will now establish a set of logical rules that would enable us to accomplish the same objective as we have just done with ruler and graph paper. The actual details of how the power output is established as a function of the incremental cost rate are of very little importance. We could, for example, store tables of data within the computer and interpolate between the stored power points to find exact power output for a specified value of incremental cost rate. Another approach would be to develop an analytical function for the power output as a function of the incremental cost rate, store this function (or its coefficients) in the computer, and use this to establish the output of each of the individual units.

This procedure is an iterative type of computation, and we must establish stopping rules. Two general forms of stopping rules seem appropriate for this application. The first is shown in Figure 3.3 and is essentially a rule based on finding the proper operating point within a specified tolerance. The other, not shown in Figure 3.3, involves counting the number of times through the iterative loop and stopping when a maximum number is exceeded.

The lambda-iteration procedure converges very rapidly for this particular type of optimization problem. The actual computational procedure is slightly more complex than that indicated in Figure 3.3 since it is necessary to observe the operating limits on each of the units during the course of the computation. The well-known Newton-Raphson method may be used to project the incremental cost value to drive the error between the computed and desired generation to zero.

EXAMPLE 3D

Assume that one wishes to use cubic functions to represent the input/output characteristics of generating plants as follows.

$$H \text{ (MBtu/h)} = A + BP + CP^2 + DP^3 \quad (P \text{ in MW})$$

For the three units, find the optimum schedule using the lambda-iteration method.

	A	B	C	D
Unit 1	749.55	695	9.68×10^{-6}	1.27×10^{-7}
Unit 2	1285.0	7051	7.375×10^{-6}	6.453×10^{-8}
Unit 3	1531.0	6531	1.04×10^{-5}	9.98×10^{-8}

Assume the fuel cost to be 1.0 R/MBtu for each unit and unit limits as follows.

$$320 \text{ MW} \leq P_1 \leq 800 \text{ MW}$$

$$300 \text{ MW} \leq P_2 \leq 1200 \text{ MW}$$

$$275 \text{ MW} \leq P_3 \leq 1100 \text{ MW}$$

Two sample calculations are shown, both using the flowchart in Figure 3.3. In this calculation, the value for λ on the second iteration is always set at 10% above or below the starting value depending on the sign of the error; for the remaining iterations, lambda is projected as in Figure 3.5.

The first example shows the advantage of starting λ near the optimum value.

$$P_R = 2500 \text{ MW}$$

$$\lambda_{\text{start}} = 8.0 \text{ R/MWh}$$

The second example shows the oscillatory problems that can be encountered with a lambda-iteration approach.

$$P_R = 2500 \text{ MW}$$

$$\lambda_{\text{start}} = 10.0 \text{ R/MWh}$$

Iteration	Lambda	Total generation (MW)	P_1	P_2	P_3
1	8.0000	1731.5	494.3	596.7	640.6
2	8.8000	2795.0	800.0	1043.0	952.0
3	8.5781	2526.0	734.7	923.4	867.9
4	8.5566	2497.5	726.1	911.7	859.7
5	8.5586	2500.0	726.9	912.7	860.4

Iteration	Lambda	Total generation (MW)	P_1	P_2	P_3
1	10.0000	3100.0	800.0	1200.0	1100.0
2	9.0000	2974.8	800.0	1148.3	1026.5
3	5.2068	895.0	320.0	300.0	275.0
4	8.1340	1920.6	551.7	674.5	694.4
5	9.7878	3100.0	800.0	1200.0	1100.0
6	8.9465	2927.0	800.0	1120.3	1006.7
7	6.8692	895.0	320.0	300.0	275.0
8	8.5099	2435.0	707.3	886.1	841.7
9	8.5791	2527.4	735.1	924.0	868.3
10	8.5586	2500.1	726.9	912.8	860.4

3.4 FIRST-ORDER GRADIENT METHOD

Many optimization procedures are nothing more than directed enumeration, or search, procedures. Such is the case with the methods that are known as *gradient*

methods. These methods are well suited for the type of problem where there is a great deal of physical understanding of the nature of the problem and the behavior of the objective function as the independent variables are adjusted. Gradient methods have one very strong desirable characteristic. That is, gradient search techniques always start off with a feasible solution and search for the optimum solution along a trajectory that maintains a feasible solution at all times. By "feasible solution" is meant a solution in which all the constraint conditions are met.

There may be other methods of gradient search that start from nonfeasible solutions and search for solutions that are both optimal and feasible. However, the most commonly used gradient search techniques always provide feasible answers. This is a very desirable characteristic since the computational procedure may be interrupted at any time and the most recent solution point will still be a reasonable operating point of which to make use. If the method is such that the objective function is monotonically changing as each new operating point is established, then the most recent solution is the best one found to that particular stage of the computation. The disadvantage of this type of optimization procedure is that there is no clear "stopping rule." That is, the establishment of "the" optimum point is difficult. Usually, the gradient search method is allowed to continue until the search procedure can find no additional "significant" gain in the objective function or until the number of iterations has exceeded some reasonably high value.

To start the gradient technique, begin with the objective function of Eq. 3.1 and/or the constraint equation (Eq. 3.2). Next, assume that the power system is operating at a feasible operating point. That is, the sum of the power outputs of the units is equal to the load demand. Next, assume that the power outputs of each of these units is changed by some small amount and that a new feasible operating point is found.

Equation 3.10 is the Taylor-series expansion of the objective function of Eq. 3.1, expanded about the initial feasible operating point. Terms are shown in this Taylor-series expansion up to and including the second order. To a first order the change in the objective function is shown in Eq. 3.11. We have obtained this relationship by assuming that all second-order and higher terms may be neglected relative to the first-order terms and by subtracting the initial operating cost from the perturbed equation.

$$F_T + \Delta F_T = F_1(P_1) + F_2(P_2) + \dots + F_N(P_N)$$

$$+ \frac{dF_1}{dP_1} \Delta P_1 + \frac{dF_2}{dP_2} \Delta P_2 + \dots + \frac{dF_N}{dP_N} \Delta P_N + \frac{1}{2} \left(\frac{d^2 F_1}{dP_1^2} [\Delta P_1]^2 + \frac{d^2 F_2}{dP_2^2} [\Delta P_2]^2 + \dots \right) + \dots \quad (3.10)$$

$$\Delta F_T = \frac{dF_1}{dP_1} \Delta P_1 + \frac{dF_2}{dP_2} \Delta P_2 + \dots + \frac{dF_N}{dP_N} \Delta P_N \quad (3.11)$$

Next, consider the constraint equation (Eq. 3.2) and allow each of the powers to be perturbed some small amount. The constraint equation is as follows.

$$\sum_{i=1}^N \Delta P_i = 0 \quad (3.12)$$

In this relationship again the initial values have been subtracted so that the constraint equation now merely states that the sum of the changes in all the power outputs must be zero. This constraint relationship removes one degree of freedom from the problem so that at least one unit must be selected as a dependent variable. Let us call this dependent unit the x^{th} unit. In that case, the change in power output for this dependent unit is a negative sum of the change in power outputs of the remaining $N - 1$ units as shown in Eq. 3.13.

$$\Delta P_x = - \sum_{i \neq x} \Delta P_i \quad (3.13)$$

These two equations may be combined to establish an equation that gives the change in the objective function, F_T , as a function of the change in the power output of each of the $N - 1$ independent machines. This is shown in Eq. 3.14. The procedure for using this equation is indicated in Figure 3.6, which is a functional block diagram of a first-order gradient search method.

$$\Delta F_T = \sum_{i \neq x} \left[\frac{dF_i}{dP_i} - \frac{dF_x}{dP_x} \right] \Delta P_i = \sum_{i \neq x} \frac{\partial F_T}{\partial P_i} \Delta P_i \quad (3.14)$$

The technique starts with any feasible solution, that is, a solution that satisfies the constraint equation (Eq. 3.2). Next, the coefficients in Eq. 3.14 are evaluated for this operating point after the dependent machine, x , has been selected. The results in the numerical expression of Eq. 3.14, and the coefficients of each of the $N - 1$ power variables indicate the gain in objective function that may be achieved for a unit move in the power of that particular machine. Obviously, the machine that gains the most reduction in the operating cost function is the one to move first. This unit can be obtained by finding the maximum of the absolute values of the various coefficients of the changes in the power output.

When a move is selected, the amount to move the power must be checked carefully so that neither the independent unit (the i^{th} unit) nor the dependent unit (the x^{th} unit) is moved beyond its operating constraints. Both units must be moved in an equal and opposite manner so that the new operating point is still feasible.

As Figure 3.6 shows, the operating points should be checked after each step, or preferably before each step is made permanently. If the dependent unit comes up against an operating limit or an operating limit for the dependent unit is violated, then it is time to return to that stage of the computation where the dependent unit is selected. This procedure is quite simple and straightforward. It does require, however, a large number of iterations to come to a satisfactory convergence.

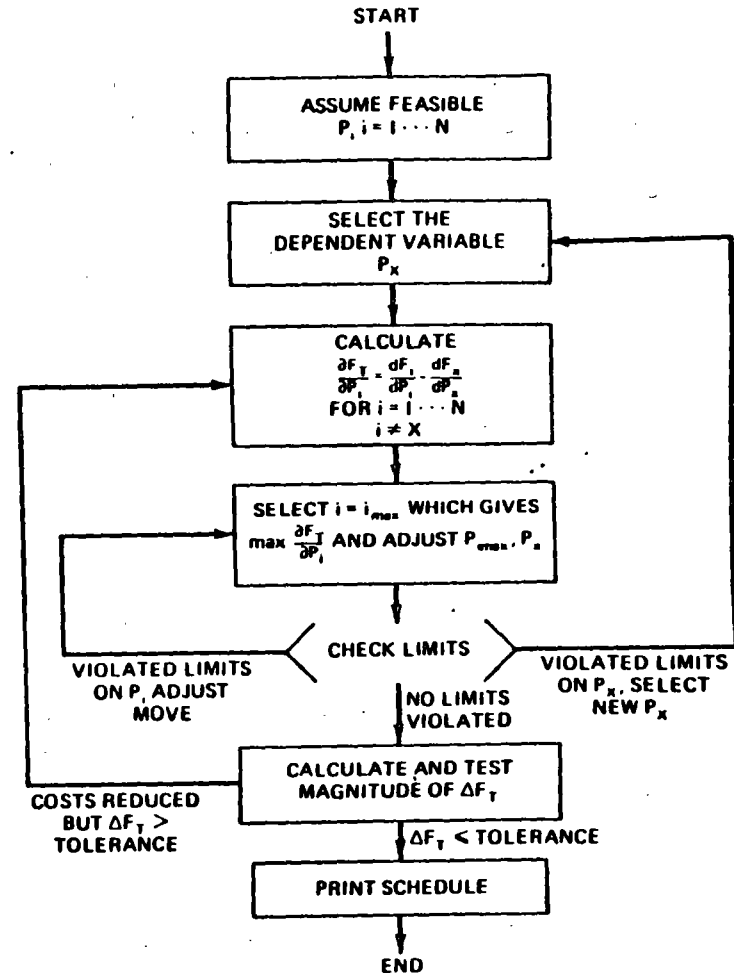


FIG. 3.6 Economic dispatch by first-order gradient search.

Other procedures may be used to augment this first-order gradient search method. For example, in the coefficients shown in Eq. 3.14 the difference in incremental costs is a function of the operating point of the units taken two at a time. That is, given an initial set of operating points, these coefficients may be established. They will change, however, as the operating points of the unit are varied so that they are in fact functions of the changes in the operating power output, the ΔP_i values. Regarded in this way, you may look at the changes in the operating power point of each of the units.

If we now select a particular pair of units to move (that is, both i and x), then we can drive the coefficient as close to zero as is possible. Neglecting any operating limits of the units, it would be possible to move the power of the i^{th} unit and x^{th} unit such that the two incremental costs will be equal and that the coefficient of the change in the output would vanish. This may easily be done for practical scheduling algorithms, particularly if the incremental cost characteristics are simple analytic functions or simple tabulated values. In that case, we can easily determine the "optimum step size" to take in each step of the gradient method. We would, however, restrict our movements so that we only moved in one direction at a time.

EXAMPLE 3E

Again, taking the data of Example 3A, solve for an economic dispatch of generation by the first-order gradient technique shown in Figure 3.6. The search will be started as follows.

$$\left. \begin{array}{l} P_1 = 400 \text{ MW} \\ P_2 = 300 \text{ MW} \\ P_3 = 150 \text{ MW} \end{array} \right\} \text{Iteration 1}$$

We can use this starting point since it meets the condition that $P_1 + P_2 + P_3 = 850 \text{ MW}$. The dependent variable, x , will be unit 3 output P_3 . Then

$$\begin{aligned} \Delta F &= \left(\frac{dF_1}{dP_1} - \frac{dF_3}{dP_3} \right) \Delta P_1 + \left(\frac{dF_2}{dP_2} - \frac{dF_3}{dP_3} \right) \Delta P_2 \\ &= (-0.2464) \Delta P_1 + (-0.4020) \Delta P_2 \end{aligned}$$

and

$$F_T = 8200.47 \text{ R/h.}$$

Since the larger coefficient appears with ΔP_2 , we will move P_2 up. That is, we wish to decrease F (ΔF negative), so increasing P_2 (ΔP_2 positive) will achieve this since its coefficient is negative. The next iteration's conditions are (after increasing P_2 by 50 MW and decreasing P_3 by 50 MW)

$$\left. \begin{array}{l} P_1 = 400 \text{ MW} \\ P_2 = 350 \text{ MW} \\ P_3 = 100 \text{ MW} \end{array} \right\} \text{Iteration 2}$$

which results in

$$\Delta F = (0.2356) \Delta P_1 + (0.2740) \Delta P_2$$

$$F_T = 8197.27 \text{ R/h}$$

Succeeding iterations are shown in the following table.

Iteration	P_1 (MW)	P_2 (MW)	P_3 (MW)	F (R/h)	ΔF	ΔP_1 (MW)	ΔP_2 (MW)	ΔP_3 (MW)
1	400	300	150	8200.47	$(-0.2464)\Delta P_1 + (-0.4020)\Delta P_2$	0	+50	-50
2	400	350	100	8197.27	$(0.2356)\Delta P_1 + (0.2740)\Delta P_2$	0	-25	+25
3	400	325	125	8194.65	$(-0.0054)\Delta P_1 + (-0.064)\Delta P_2$	0	+12.5	-12.5
4	400	337.5	112.5	8194.90	$(0.1151)\Delta P_1 + (0.105)\Delta P_2$	-10	0	+10
5	390	337.5	122.5	8194.38	$(-0.01254)\Delta P_1 + (-0.00861)\Delta P_2$	+5	0	-5
6	395	337.5	117.5	8194.48	$(0.05128)\Delta P_1 + (0.0568)\Delta P_2$	0	-2.5	+2.5
7	395	335	120	8194.38	$(0.0272)\Delta P_1 + (0.023)\Delta P_2$			

3.5 SECOND-ORDER GRADIENT METHOD

Let us return to the problem of finding the economic schedule for a given single level of demand. The gradient method shown in Section 3.4 may be refined and made more efficient by using the second-order terms of the Taylor series expansion of the total generation cost given in Eq. 3.10.

$$\begin{aligned}
 F_T + \Delta F_T &= F_1(P_1) + F_2(P_2) + \cdots + F_N(P_N) \\
 &+ \frac{dF_1}{dP_1} \Delta P_1 + \frac{dF_2}{dP_2} \Delta P_2 + \cdots + \frac{dF_N}{dP_N} \Delta P_N \\
 &+ \frac{1}{2} \left(\frac{d^2 F_1}{dP_1^2} (\Delta P_1)^2 + \frac{d^2 F_2}{dP_2^2} (\Delta P_2)^2 + \cdots + \frac{d^2 F_N}{dP_N^2} (\Delta P_N)^2 \right) \\
 &+ \cdots
 \end{aligned} \tag{3.15}$$

Recall again that there are no mixed, second partial derivatives in the usual case. That is, the second derivative of the fuel cost rate of a given unit is normally only explicitly dependent on the power output of that unit, itself. That is,

$$\frac{\partial^2 F_i}{\partial P_i \partial P_j} = 0$$

for $i \neq j$. Also, the constraint requiring the sum of the power outputs of the individual units to equal the total demand must be treated as in Eqs. 3.12 and 3.13 in order that the schedule developed will not alter the frequency of the system. These are

$$\sum_{i=1}^N \Delta P_i = 0 \tag{3.16}$$

$$\Delta P_x = - \sum_{i \neq x} \Delta P_i \tag{3.17}$$

If we substitute the relationship of Eq. 3.17 into Eq. 3.15 keeping both the first- and second-order terms involving the perturbed powers, then we obtain

$$\begin{aligned}
 \Delta F_T &= \sum_{i \neq x} \left(\frac{dF_i}{dP_i} - \frac{dF_x}{dP_x} \right) \Delta P_i \\
 &+ \frac{1}{2} \left\{ \sum_{i \neq x} \left[\frac{d^2 F_i}{dP_i^2} (\Delta P_i)^2 + \frac{d^2 F_2}{dP_2^2} (\Delta P_2)^2 + \cdots \right] \right. \\
 &\left. + \frac{d^2 F_x}{dP_x^2} (\Delta P_x^2 + \Delta P_2^2 + \cdots + 2\Delta P_1 \Delta P_2 + 2\Delta P_1 \Delta P_3 + \cdots) \right\} \tag{3.18}
 \end{aligned}$$

The change in the total operating cost, ΔF_T , can be treated using ordinary calculus methods since it is a function of the $N - 1$ independent changes in the power output levels, ΔP_i . There are no constraint conditions other than the limits on the plant outputs, which we will ignore at present. The best operating point

will be achieved when the partial derivative of ΔF_T with respect to each independent variable, ΔP_i , is zero. That is, the partial derivatives $\partial \Delta F_T / \partial \Delta P_i$ must be zero for all i , $i \neq x$. These derivatives result in a set of simultaneous equations.

$$\begin{aligned}
 \frac{\partial \Delta F_T}{\partial \Delta P_1} = 0 &= \left(\frac{dF_1}{dP_1} - \frac{dF_x}{dP_x} \right) + \frac{d^2 F_1}{dP_1^2} \Delta P_1 + \frac{d^2 F_x}{dP_x^2} \sum_{i \neq x} \Delta P_i \\
 \frac{\partial \Delta F_T}{\partial \Delta P_2} = 0 &= \left(\frac{dF_2}{dP_2} - \frac{dF_x}{dP_x} \right) + \frac{d^2 F_2}{dP_2^2} \Delta P_2 + \frac{d^2 F_x}{dP_x^2} \sum_{i \neq x} \Delta P_i
 \end{aligned} \tag{3.19}$$

The presentation may be made somewhat clearer by letting

$$F_i = \frac{dF_i}{dP_i} \tag{3.20}$$

and

$$F_i' = \frac{d^2 F_i}{dP_i^2}$$

both be evaluated for the initial operating point. Then the $N - 1$ simultaneous equations may be written in matrix form as

$$\begin{bmatrix} F_1' + F_x' & & & F_x' & \cdots \\ F_x' & F_2' + F_x' & & F_x' & \cdots \\ F_x' & & F_3' + F_x' & & \cdots \\ \vdots & \vdots & \vdots & \vdots & \ddots \end{bmatrix} \begin{bmatrix} \Delta P_1 \\ \Delta P_2 \\ \Delta P_3 \\ \vdots \end{bmatrix} = - \begin{bmatrix} F_1 - F_x \\ F_2 - F_x \\ F_3 - F_x \\ \vdots \end{bmatrix} \tag{3.21}$$

The second-order gradient search method yields the multidimensional components of the gradient of the cost function by the following steps.

1. Start with a feasible solution and compute the elements of the matrix equation.
2. Invert the matrix to solve for the amounts to shift each generator.
3. Verify that the solution does not violate any constraint.
4. Check the value of the vector $(F_i - F_x)$ at the new operating point to see that all the incremental costs are equal given the operating limitations of each unit.

If the incremental costs are not equal, the procedure is repeated.

With a quadratic objective function, the second-order method will converge in one step assuming an unconstrained situation. The examples used in this text may lead you to the impression that the second-order method is one that always converges in a single step and does not seem to have any of the computational problems associated with the first-order methods. Don't you believe it! These methods all have their difficulties. Generally, in using gradient techniques it is the constraints that give rise to computational problems. (In some other optimization techniques these very same constraints are a blessing and serve to reduce the dimensionality of the problem.)

EXAMPLE 3F

We will solve the same dispatch problem (Example 3A) from the same starting conditions as in Example 3E using the second-order gradient method. The starting conditions are

$$P_1 = 400 \text{ MW}$$

$$P_2 = 300 \text{ MW}$$

$$P_3 = 150 \text{ MW}$$

$$F'_1 = 9.1696 \text{ R/MWh} \quad F''_1 = 0.003124 \text{ (R/MWh)/MW}$$

$$F'_2 = 9.0140 \text{ R/MWh} \quad F''_2 = 0.00388 \text{ (R/MWh)/MW}$$

$$F'_3 = 9.4160 \text{ R/MWh} \quad F''_3 = 0.00964 \text{ (R/MWh)/MW}$$

Then using Eq. 3.21,

$$\begin{bmatrix} F'_1 + F'_3 & F'_3 \\ F'_3 & F'_2 + F'_3 \end{bmatrix} \begin{bmatrix} \Delta P_1 \\ \Delta P_2 \end{bmatrix} = - \begin{bmatrix} F_1 - F_3 \\ F_2 - F_3 \end{bmatrix}$$

or

$$\begin{bmatrix} 0.012764 & 0.00964 \\ 0.00964 & 0.01352 \end{bmatrix} \begin{bmatrix} \Delta P_1 \\ \Delta P_2 \end{bmatrix} = - \begin{bmatrix} -0.2464 \\ -0.4020 \end{bmatrix}$$

The solution of which is

$$\begin{bmatrix} \Delta P_1 \\ \Delta P_2 \end{bmatrix} = \begin{bmatrix} -6.8301 \\ 34.603 \end{bmatrix}$$

Then

$$P_1 = 400 - 6.83 = 393.17 \text{ MW}$$

$$P_2 = 300 + 34.6 = 334.6 \text{ MW}$$

and by definition $P_3 = 850 - P_1 - P_2 = 122.23 \text{ MW}$.

3.6 BASE POINT AND PARTICIPATION FACTORS

This method assumes that the economic dispatch problem has to be solved repeatedly by moving the generators from one economically optimum schedule to another as the load changes by a reasonably small amount. We start from a given schedule—the *base point*. Next, the scheduler assumes a load change and investigates how much each generating unit needs to be moved (i.e., “participate” in the load change) in order that the new load be served at the most economic operating point.

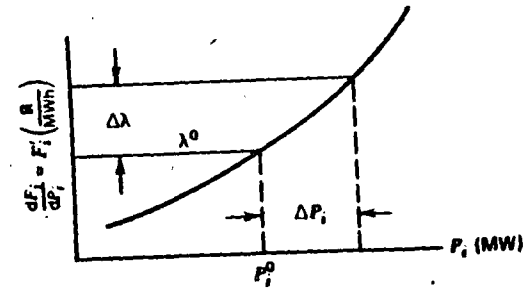


FIG. 3.7 Relationship of $\Delta\lambda$ and ΔP_i .

Assume that both the first and second derivatives in the cost versus power output function are available (i.e., both F'_i and F''_i exist). The incremental cost curve of the i^{th} unit is given in Figure 3.7. As the unit load is changed by an amount ΔP_i , the system incremental cost moves from λ^0 to $\lambda^0 + \Delta\lambda$. For a small change in power output on this single unit,

$$\Delta\lambda_i = \Delta\lambda \approx F''_i(P_i^0) \Delta P_i \quad (3.22)$$

This is true for each of the N units on the system so that,

$$\Delta P_1 = \frac{\Delta\lambda}{F''_1}$$

$$\Delta P_2 = \frac{\Delta\lambda}{F''_2}$$

⋮

$$\Delta P_N = \frac{\Delta\lambda}{F''_N}$$

The total change in generation (= change in total system demand) is, of course, the sum of the individual unit changes. Let P_D be the total demand on the generators (where $P_D = P_R + \text{losses}$), then

$$\begin{aligned} \Delta P_D &= \Delta P_1 + \Delta P_2 + \dots + \Delta P_N \\ &= \Delta\lambda \sum_i \left(\frac{1}{F''_i} \right) \end{aligned} \quad (3.23)$$

The earlier equation, 3.22, can be used to find the *participation factor* for each unit as follows.

$$\left(\frac{\Delta P_i}{\Delta P_D} \right) = \frac{(1/F''_i)}{\sum_i (1/F''_i)} \quad (3.24)$$

The computer implementation of such a scheme of economic dispatch is straightforward. It might be done by provision of tables of the values of F''_i as a

function of the load levels and devising a simple scheme to take the existing load plus the projected increase to look up these data and compute the factors.

A somewhat less elegant scheme to provide participation factors would involve a repeat economic dispatch calculation at $P_D^0 + \Delta P_D$. The base-point economic generation values are then subtracted from the new economic generation values and the difference divided by ΔP_D to provide the participation factors. This scheme works well in computer implementations where the execution time for the economic dispatch is short and will always give consistent answers when units reach limits or pass through break points on piecewise linear incremental cost functions.

EXAMPLE 3G

Starting from the optimal economic solution found in Example 3A, use the participation factor method to calculate the dispatch for a total load of 900 MW. Using Eq. 3.24,

$$\frac{\Delta P_1}{\Delta P_D} = \frac{(0.003124)^{-1}}{(0.003124)^{-1} + (0.00388)^{-1} + (0.00964)^{-1}} = \frac{320.10}{681.57} = 0.47$$

Similarly,

$$\frac{\Delta P_2}{\Delta P_D} = \frac{(0.00388)^{-1}}{681.57} = 0.38$$

$$\frac{\Delta P_3}{\Delta P_D} = \frac{103.73}{681.57} = 0.15$$

$$\Delta P_D = 900 - 850 = 50$$

The new value of generation is calculated using

$$P_{new,i} = P_{base,i} + \left(\frac{\Delta P_i}{\Delta P_D} \right) \Delta P_D \quad \text{for } i = 1, 2, 3$$

Then for each unit

$$P_{new,1} = 393.2 + (0.47)(50) = 416.7$$

$$P_{new,2} = 334.6 + (0.38)(50) = 353.6$$

$$P_{new,3} = 122.2 + (0.15)(50) = 129.7$$

3.7 ECONOMIC DISPATCH VERSUS UNIT COMMITMENT

At this point it may be well to emphasize the essential difference between the unit commitment and economic dispatch problem. The economic dispatch problem assumes that there are N units already connected to the system. The purpose of the

economic dispatch problem is to find the optimum operating policy for these N units. This is the problem that we have been investigating so far in this text.

On the other hand, the unit commitment problem is more complex. We may assume that we have N units available to us and that we have a forecast of the demand to be served. The question that is asked in the unit commitment problem area is approximately as follows.

Given that there are a number of subsets of the complete set of N generating units that would satisfy the expected demand, which of these subsets should be used in order to provide the minimum operating cost?

This unit commitment problem may be extended over some period of time, such as the 24 h of a day or the 168 h of a week. The unit commitment problem is a much more difficult problem to solve. The solution procedures involve the economic dispatch problem as a subproblem. That is, for each of the subsets of the total number of units that are to be tested, for any given set of them connected to the load the particular subset should be operated in optimum economic fashion. This will permit finding the minimum operating cost for that subset, but it does not establish which of the subsets is in fact the one that will give minimum cost over a period of time.

A later chapter will consider the unit commitment problem in some detail. The problem is more difficult to solve mathematically since it involves integer variables. That is, generating units must be either all on or all off. (How can you turn a switch half on?) Methods of solving optimization problems with integer variables have developed in recent years. The two most widely used techniques are *integer programming* and *dynamic programming*. A later section will explore the use of dynamic programming for the solution of a restricted range of unit commitment problems.

At this point (1983), there is no satisfactory, theoretically correct solution procedure for solving the unit commitment problem for a large system.

APPENDIX

Optimization Within Constraints

Suppose you are trying to maximize or minimize a function of several variables. It is relatively straightforward to find the maximum or minimum using rules of calculus. First, of course, you must find a set of values for the variables where the first derivative of the function with respect to each variable is zero. In addition, the second derivatives should be used to determine whether the solution found is a maximum, minimum, or a saddle point.

In optimizing a real-life problem one is usually confronted with a function to be maximized or minimized as well as numerous constraints that must be met. The

constraints, sometimes called *side conditions*, can be other functions with conditions that must be met or they can be simple conditions such as limits on the variables themselves.

Before we begin this discussion on constrained optimization, we will put down some definitions. Since the objective is to maximize or minimize a mathematical function, we will call this function the *objective function*. The constraint functions and simple variable limits will be lumped under the term *constraints*. The region defined by the constraints is said to be the *feasible region* for the independent variables. If the constraints are such that no such region exists, that is, there are no values for the independent variables that satisfy all the constraints, then the problem is said to have an *infeasible solution*. When an optimum solution to a constrained optimization problem occurs at the boundary of the feasible region defined by a constraint, we say the constraint is *binding*. If the optimum solution lies away from the boundary, the constraint is *nonbinding*.

To begin, let us look at a simple elliptical objective function.

$$f(x_1, x_2) = 0.25x_1^2 + x_2^2 \quad (3A.1)$$

This is shown in Figure 3.8 for various values of f .

Note that the minimum value f can attain is zero, but that it has no finite maximum value. The following is an example of a constrained optimization problem.

$$\begin{aligned} \text{Minimize:} & \quad f(x_1, x_2) = 0.25x_1^2 + x_2^2 \\ \text{Subject to the Constraint:} & \quad \omega(x_1, x_2) = 0 \\ \text{Where:} & \quad \omega(x_1, x_2) = 5 - x_1 - x_2. \end{aligned} \quad (3A.2)$$

This optimization problem can be pictured as in Figure 3.9.

We need to observe that the optimum pictured gives the minimum value for our objective function, f , while also meeting the constraint function, ω . This optimum

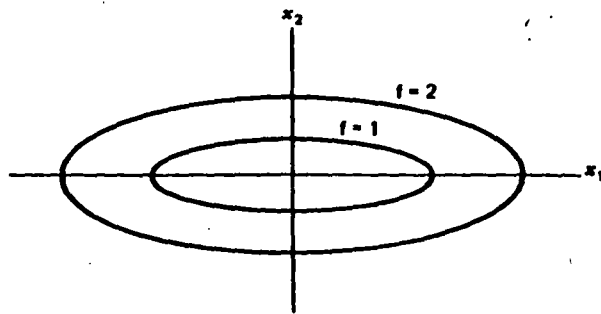


FIG. 3.8 Elliptical objective function.

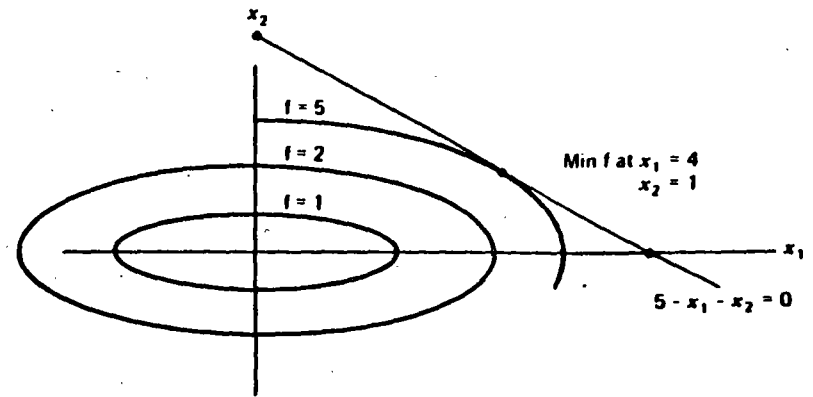


FIG. 3.9 Elliptical objective function with equality constraint.

point occurs where the function f is exactly tangent to the function ω . Indeed, this observation can be made more rigorous and will form the basis for our development of LaGrange multipliers.

First, redraw the function f for several values of f around the optimum point. At the point (x_1^*, x_2^*) calculate the gradient vector of f . This is pictured in Figure 3.10 as $\nabla f(x_1^*, x_2^*)$. Note that the gradient at (x_1^*, x_2^*) is perpendicular to f but not to ω and therefore has a nonzero component along ω . Similarly, at the point (x_1^*, x_2^*) the gradient of f has a nonzero component along ω . The nonzero component of the

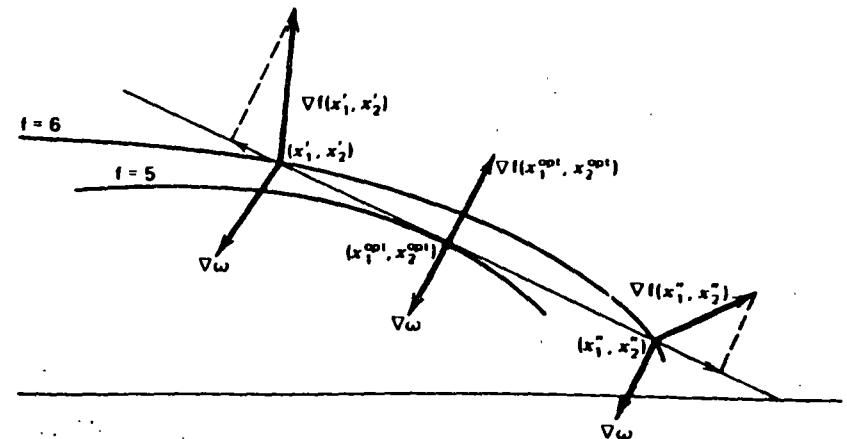


FIG. 3.10 Gradients near a constrained optimum.

gradient along ω tells us that a small move along ω in the direction of this component will increase the objective function. Therefore, to minimize f we should go along ω in the opposite direction to the component of the gradient projected onto ω . At the optimum point, the gradient of f is perpendicular (mathematicians say "normal") to ω and therefore there can be no improvement in f by moving off this point. We can solve for this optimum point mathematically by using this "normal" property at the optimum. To guarantee that the gradient of f , (i.e. ∇f), is normal to ω we simply require that ∇f and the gradient of ω , $\nabla \omega$, be linearly dependent vectors. Vectors that are linearly dependent must "line up" with each other (i.e., they point in exactly the same or exactly the opposite direction) although they may be different in magnitude. Mathematically, we can then set up the following equation.

$$\nabla f + \lambda \nabla \omega = 0 \quad (3A.3)$$

That is, the two gradients can be added together in such a way that they cancel each other as long as one of them is scaled. The scaling variable, λ , is called a *LaGrange multiplier*, and instead of using the gradients as shown in Eq. 3A.3, we will restate them as

$$\mathcal{L}(x_1, x_2, \lambda) = f(x_1, x_2) + \lambda \omega(x_1, x_2) \quad (3A.4)$$

This equation is called the *LaGrange equation* and consists of three variables, x_1 , x_2 , and λ . When we solve for the optimum values for x_1 and x_2 , we will automatically calculate the correct value for λ . To meet the conditions set down in Eq. 3A.3, we simply require that the partial derivative of \mathcal{L} with respect to each of the unknown variables, x_1 , x_2 , and λ , be equal to zero. That is,

At the Optimum

$$\begin{aligned} \frac{\partial \mathcal{L}}{\partial x_1} &= 0 \\ \frac{\partial \mathcal{L}}{\partial x_2} &= 0 \\ \frac{\partial \mathcal{L}}{\partial \lambda} &= 0 \end{aligned} \quad (3A.5)$$

To show how this works, solve for the optimum point for the sample problem using LaGrange's method.

$$\begin{aligned} \mathcal{L}(x_1, x_2, \lambda) &= 0.25 x_1^2 + x_2^2 + \lambda(5 - x_1 - x_2) \\ \frac{\partial \mathcal{L}}{\partial x_1} &= 0.5 x_1 - \lambda = 0 \\ \frac{\partial \mathcal{L}}{\partial x_2} &= 2 x_2 - \lambda = 0 \\ \frac{\partial \mathcal{L}}{\partial \lambda} &= 5 - x_1 - x_2 = 0 \end{aligned} \quad (3A.6)$$

Note that the last equation in (3A.6) is simply the original constraint equation. The solution to Eq. 3A.6 is

$$\begin{aligned} x_1 &= 4 \\ x_2 &= 1 \\ \lambda &= 2 \end{aligned} \quad (3A.7)$$

When there is more than one constraints present in the problem, the optimum point can be found in a similar manner to that just used. Suppose there were three constraints to be met, then our problem would be as follows,

$$\begin{aligned} \text{Minimize:} & \quad f(x_1, x_2) \\ \text{Subject to:} & \quad \omega_1(x_1, x_2) = 0 \\ & \quad \omega_2(x_1, x_2) = 0 \\ & \quad \omega_3(x_1, x_2) = 0 \end{aligned} \quad (3A.8)$$

The optimum point would possess the property that the gradient of f and the gradients of ω_1 , ω_2 , and ω_3 are linearly dependent. That is,

$$\nabla f + \lambda_1 \nabla \omega_1 + \lambda_2 \nabla \omega_2 + \lambda_3 \nabla \omega_3 = 0 \quad (3A.9)$$

Again, we can set up a LaGrangian equation as before.

$$\mathcal{L} = f(x_1, x_2) + \lambda_1 \omega_1(x_1, x_2) + \lambda_2 \omega_2(x_1, x_2) + \lambda_3 \omega_3(x_1, x_2) \quad (3A.10)$$

whose optimum occurs at

$$\begin{aligned} \frac{\partial \mathcal{L}}{\partial x_1} &= 0 & \frac{\partial \mathcal{L}}{\partial x_2} &= 0 \\ \frac{\partial \mathcal{L}}{\partial \lambda_1} &= 0 & \frac{\partial \mathcal{L}}{\partial \lambda_2} &= 0 & \frac{\partial \mathcal{L}}{\partial \lambda_3} &= 0 \end{aligned} \quad (3A.11)$$

Up until now we have assumed that all the constraints in the problem were equality constraints, that is, $\omega(x_1, x_2, \dots) = 0$. In general, however, optimization problems involve inequality constraints, that is, $g(x_1, x_2, \dots) \leq 0$ as well as equality constraints. The optimal solution to such problems will not necessarily require all the inequality constraints to be binding. Those that are binding will result in $g(x_1, x_2, \dots) = 0$ at the optimum.

The fundamental rule that tells when the optimum has been reached is presented in a famous paper by Kuhn and Tucker (3). *The Kuhn-Tucker conditions*, as they are called, are presented here.

$$\begin{aligned} \text{Minimize:} & \quad f(x) \\ \text{Subject to:} & \quad \omega_i(x) = 0 \quad i = 1, 2, \dots, N\omega \\ & \quad g_i(x) \leq 0 \quad i = 1, 2, \dots, Ng \\ & \quad x = \text{vector of real numbers, dimension} = N \end{aligned}$$

Then forming the LaGrange function,

$$\mathcal{L}(x, \lambda, \mu) = f(x) + \sum_{i=1}^{N\omega} \lambda_i \omega_i(x) + \sum_{i=1}^{N\mu} \mu_i g_i(x)$$

The conditions for an optimum for the point x^0, λ^0, μ^0 are

1. $\frac{\partial \mathcal{L}}{\partial x_i}(x^0, \lambda^0, \mu^0) = 0$ for $i = 1 \cdots N$
2. $\omega_i(x^0) = 0$ for $i = 1 \cdots N\omega$
3. $g_i(x^0) \leq 0$ for $i = 1 \cdots N\mu$
4. $\left. \begin{array}{l} \mu_i^0 g_i(x^0) = 0 \\ \mu_i^0 \geq 0 \end{array} \right\}$ for $i = 1 \cdots N\mu$

The first condition is simply the familiar set of partial derivatives of the LaGrange function that must equal zero at the optimum. The second and third conditions are simply a restatement of the constraint conditions on the problem. The fourth condition, often referred to as *the complimentary slackness condition*, provides a concise mathematical way to handle the problem of binding and nonbinding constraints. Since the product $\mu_i^0 g_i(x^0)$ equals zero, either μ_i^0 is equal to zero or $g_i(x^0)$ is equal to zero, or both are equal to zero. If μ_i^0 is equal to zero, $g_i(x^0)$ is free to be nonbinding; if μ_i^0 is positive, then $g_i(x^0)$ must be zero. Thus we have a clear indication of whether the constraint is binding or not by looking at μ_i^0 .

To illustrate how the Kuhn-Tucker equations are used, we will add an inequality constraint to the sample problem used earlier in this appendix. The problem we will solve is as follows.

Minimize: $f(x_1, x_2) = 0.25x_1^2 + x_2^2$
 Subject to: $\omega(x_1, x_2) = 5 - x_1 - x_2 = 0$
 $g(x_1, x_2) = x_1 + 0.2x_2 - 3 \leq 0$

which can be illustrated as in Figure 3.11.

First, set up the LaGrange equation for the problem.

$$\begin{aligned} \mathcal{L} &= f(x_1, x_2) + \lambda[\omega(x_1, x_2)] + \mu[g(x_1, x_2)] \\ &= 0.25x_1^2 + x_2^2 + \lambda(5 - x_1 - x_2) + \mu(x_1 + 0.2x_2 - 3) \end{aligned}$$

The first condition gives

$$\frac{\partial \mathcal{L}}{\partial x_1} = 0.5x_1 - \lambda + \mu = 0$$

$$\frac{\partial \mathcal{L}}{\partial x_2} = 2x_2 - \lambda + 0.2\mu = 0$$

The second condition gives

$$5 - x_1 - x_2 = 0$$

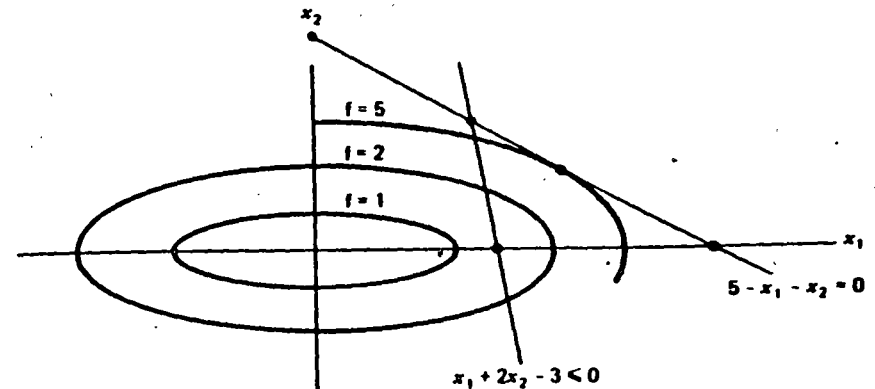


FIG. 3.11 Elliptical objective function with equality and inequality constraints.

The third condition gives

$$x_1 + 0.2x_2 - 3 \leq 0$$

The fourth condition gives

$$\begin{aligned} \mu(x_1 + 0.2x_2 - 3) &= 0 \\ \mu &\geq 0 \end{aligned}$$

At this point we are confronted with the fact that the Kuhn-Tucker conditions only give necessary conditions for a minimum, not a precise procedure as to how that minimum is to be found. To solve the problem just presented we must literally experiment with various solutions until we can verify that one of the solutions meets all four conditions. First, let $\mu = 0$, which implies that $g(x_1, x_2)$ can be less than or equal to zero. However, if $\mu = 0$, we can see that the first and second conditions give the same solution as we had previously without the inequality constraint. But the previous solution violates our inequality constraint; and therefore the four Kuhn-Tucker conditions do not hold with $\mu = 0$. In summary

If $\mu = 0$, then by conditions 1 and 2

$$x_1 = 4$$

$$x_2 = 1$$

$$\lambda = 2$$

but

$$g(x_1, x_2) \Big|_{\substack{x_1=4 \\ x_2=1}} = 4 + 0.2(1) - 3 = 1.2 \not\leq 0$$

Now we will try a solution in which $\mu > 0$. In this case $g(x_1, x_2)$ must be exactly zero and our solution can be found by solving for the intersection of $g(x_1, x_2)$ and

$\omega(x_1, x_2)$, which occurs at $x_1 = 2.5, x_2 = 2.5$. Further, condition 1 gives $\lambda = 5.9375$ and $\mu = 4.6875$ and all four of the Kuhn-Tucker conditions are met. In summary

If $\mu > 0$, then by conditions 2 and 3

$$x_1 = 2.5$$

$$x_2 = 2.5$$

by condition 1

$$\lambda = 5.9375$$

$$\mu = 4.6875$$

and

$$\theta(x_1, x_2)|_{x_1=x_2=2.5} = 2.5 + 0.2(2.5) - 3 = 0$$

All conditions are met.

Considerable insight can be gained into the characteristics of optimal solutions through use of the Kuhn-Tucker conditions. One important insight comes from formulating the optimization problem so that it reflects our standard power system economic dispatch problems. Specifically, we will assume that the objective function consists of a sum of individual cost functions each of which is a function of only one variable. For example,

$$f(x_1, x_2) = C_1(x_1) + C_2(x_2)$$

Further, we will restrict this problem to have one equality constraint of the form

$$\omega(x_1, x_2) = L - x_1 - x_2 = 0$$

and a set of inequality constraints that act to restrict the problem variables within an upper and lower limit. That is,

$$x_1 \leq x_1 \leq x_1^+ \rightarrow \begin{cases} \theta_1(x_1) = x_1 - x_1^+ \leq 0 \\ \theta_2(x_1) = x_1^- - x_1 \leq 0 \end{cases}$$

$$x_2^- \leq x_2 \leq x_2^+ \rightarrow \begin{cases} \theta_3(x_2) = x_2 - x_2^+ \leq 0 \\ \theta_4(x_2) = x_2^- - x_2 \leq 0 \end{cases}$$

Then the LaGrange function becomes

$$\begin{aligned} &= f(x_1, x_2) + \lambda\omega(x_1, x_2) + \mu_1\theta_1(x_1) + \mu_2\theta_2(x_1) + \mu_3\theta_3(x_2) + \mu_4\theta_4(x_2) \\ &= C_1(x_1) + C_2(x_2) + \lambda(L - x_1 - x_2) + \mu_1(x_1 - x_1^+) + \mu_2(x_1^- - x_1) \\ &\quad + \mu_3(x_2 - x_2^+) + \mu_4(x_2^- - x_2) \end{aligned}$$

Condition 1 gives

$$C_1'(x_1) - \lambda + \mu_1 - \mu_2 = 0$$

$$C_2'(x_2) - \lambda + \mu_3 - \mu_4 = 0$$

Condition 2 gives

$$L - x_1 - x_2 = 0$$

Condition 3 gives

$$x_1 - x_1^+ \leq 0$$

$$x_1^- - x_1 \leq 0$$

$$x_2 - x_2^+ \leq 0$$

$$x_2^- - x_2 \leq 0$$

Condition 4 gives

$$\mu_1(x_1 - x_1^+) = 0 \quad \mu_1 \geq 0$$

$$\mu_2(x_1^- - x_1) = 0 \quad \mu_2 \geq 0$$

$$\mu_3(x_2 - x_2^+) = 0 \quad \mu_3 \geq 0$$

$$\mu_4(x_2^- - x_2) = 0 \quad \mu_4 \geq 0$$

Case 1

If the optimum solution occurs at values for x_1 and x_2 that are not at either an upper or a lower limit, then all μ 's are equal to zero and

$$C_1'(x_1) = C_2'(x_2) = \lambda$$

That is, the incremental costs associated with each variable are equal and this value is exactly the λ we are interested in.

Case 2

Now suppose that the optimum solution requires that x_1 be at its upper limit (i.e., $x_1 - x_1^+ = 0$) and that x_2 is not at its upper or lower limit. Then

$$\mu_1 \geq 0$$

and $\mu_2, \mu_3,$ and μ_4 will each equal zero. Then, from condition 1,

$$C_1'(x_1) = \lambda - \mu_1 \rightarrow C_1'(x_1) \leq \lambda$$

$$C_2'(x_2) = \lambda$$

Therefore, the incremental cost associated with the variable that is at its upper limit will always be less than or equal to λ , whereas the incremental cost associated with the variable that is not at limit will exactly equal λ .

Case 3

Now suppose the optimum solution of Case 2 obtains, that is, let the optimum solution require x_1 to be at its lower limit (i.e., $x_1^- - x_1 = 0$) and again assume that x_2 is

not at its upper or lower limit. Then

$$\mu_2 \geq 0$$

and $\mu_1, \mu_3,$ and μ_4 will each equal zero. Then from condition 1

$$C_1(x_1) = \lambda + \mu_2 \Rightarrow C_1(x_1) \geq \lambda$$

$$C_2(x_2) = \lambda$$

Therefore, the incremental cost associated with a variable at its lower limit will be greater than or equal to λ whereas, again, the incremental cost associated with the variable that is not at limit will equal λ .

Case 4

If the optimum solution requires that both x_1, x_2 are at limit and the equality constraint can be met, then λ and the nonzero μ 's are indeterminate. For example, suppose the optimum required that

$$x_1 - x_1^+ = 0$$

and

$$x_2 - x_2^+ = 0$$

Then

$$\mu_1 \geq 0 \quad \mu_3 \geq 0 \quad \mu_2 = \mu_4 = 0$$

Condition 1 would give

$$C_1(x_1) = \lambda - \mu_1$$

$$C_2(x_2) = \lambda - \mu_3$$

and the specific values for $\lambda, \mu_1,$ and μ_3 would be undetermined. In summary, for the general problem of N variables

Minimize: $C_1(x_1) + C_2(x_2) + \dots + C_N(x_N)$

Subject to: $L - x_1 - x_2 - \dots - x_N = 0$

And: $\left. \begin{array}{l} x_i - x_i^+ \leq 0 \\ x_i^- - x_i \leq 0 \end{array} \right\} \text{ for } i = 1 \dots N$

Let the optimum lie at $x_i = x_i^{\text{opt}} \quad i = 1 \dots N$ and assume that at least one x_i is not at limit. Then

If $x_i^{\text{opt}} < x_i^+$ and $x_i^{\text{opt}} > x_i^-$, then $C_i(x_i^{\text{opt}}) = \lambda$

If $x_i^{\text{opt}} = x_i^+$ $C_i(x_i^{\text{opt}}) \leq \lambda$

If $x_i^{\text{opt}} = x_i^-$ $C_i(x_i^{\text{opt}}) \geq \lambda$

Slack Variable Formulation

An alternate approach to the optimization problem with inequality constraints requires that all inequality constraints be made into equality constraints. This is done by adding slack variables in the following way.

If: $g(x_1) = x_1 - x_1^+ \leq 0$

Then: $g(x_1, S_1) = x_1 - x_1^+ + S_1^2 = 0$

We add S_1^2 rather than S_1 so that S_1 need not be limited in sign.

Making all inequality constraints into equality constraints eliminates the need for conditions 3 and 4 of the Kuhn-Tucker conditions. However, as we will see shortly, the result is essentially the same. Let us use our two variable problem again.

Minimize: $f(x_1, x_2) = C_1(x_1) + C_2(x_2)$

Subject to: $\omega(x_1, x_2) = L - x_1 - x_2 = 0$

And: $g_1(x_1) = x_1 - x_1^+ \leq 0$ or $g_1(x_1, S_1) = x_1 - x_1^+ + S_1^2 = 0$

$g_2(x_1) = x_1^- - x_1 \leq 0$ $g_2(x_1, S_2) = x_1^- - x_1 + S_2^2 = 0$

$g_3(x_2) = x_2 - x_2^+ \leq 0$ $g_3(x_2, S_3) = x_2 - x_2^+ + S_3^2 = 0$

$g_4(x_2) = x_2^- - x_2 \leq 0$ $g_4(x_2, S_4) = x_2^- - x_2 + S_4^2 = 0$

The resulting LaGrange function is

$$\mathcal{L} = f(x_1, x_2) + \lambda_0 \omega(x_1, x_2) + \lambda_1 g_1(x_1, S_1) + \lambda_2 g_2(x_1, S_2) + \lambda_3 g_3(x_2, S_3) + \lambda_4 g_4(x_2, S_4)$$

Note that all constraints are now equality constraints, so we have used only λ 's as LaGrange multipliers.

Condition 1 Gives: $\frac{\partial \mathcal{L}}{\partial x_1} = C_1(x_1) - \lambda_0 + \lambda_1 - \lambda_2 = 0$

$$\frac{\partial \mathcal{L}}{\partial x_2} = C_2(x_2) - \lambda_0 + \lambda_3 - \lambda_4 = 0$$

$$\frac{\partial \mathcal{L}}{\partial S_1} = 2 \lambda_1 S_1 = 0$$

$$\frac{\partial \mathcal{L}}{\partial S_2} = 2 \lambda_2 S_2 = 0$$

$$\frac{\partial \mathcal{L}}{\partial S_3} = 2 \lambda_3 S_3 = 0$$

$$\frac{\partial \mathcal{L}}{\partial S_4} = 2 \lambda_4 S_4 = 0$$

Condition 2 Gives:

$$\begin{aligned} L - x_1 - x_2 &= 0 \\ (x_1 - x_1^* + S_1^2) &= 0 \\ (x_1 - x_1^* + S_1^2) &= 0 \\ (x_2 - x_2^* + S_2^2) &= 0 \\ (x_2 - x_2^* + S_2^2) &= 0 \end{aligned}$$

We can see that the derivatives of the LaGrange function with respect to the slack variables provide us once again with a complimentary slackness rule. For example, if $2\lambda_1 S_1 = 0$, then either $\lambda_1 = 0$ and S_1 is free to be any value or $S_1 = 0$ and λ_1 is free (or λ_1 and S_1 can both be zero). Since there are as many problem variables whether one uses the slack variable form or the inequality constraint form, there is little advantage to either other than perhaps a conceptual advantage to the student.

PROBLEMS

3.1 Assume that the fuel inputs in Btu per hour for units 1 and 2, which are both on-line, are given by

$$\begin{aligned} H_1 &= 8 P_1 + 0.024 P_1^2 + 80 \\ H_2 &= 6 P_2 + 0.04 P_2^2 + 120 \end{aligned}$$

where

H_n = fuel input to unit n in MBtu per hour (millions of Btu per hour)

P_n = unit output in megawatts

- Plot the input-output characteristics for each unit expressing input in MBtu per hour and output in megawatts. Assume that the minimum loading of each unit is 20 MW and that the maximum loading is 100 MW.
- Calculate the net heat rate in Btu/kWh, and plot against output in megawatts.
- Assume that the cost of fuel is 1.5 R/MBtu. Calculate the incremental production cost in R/MWh of each unit, and plot against output in megawatts.

3.2 Dispatch with Three Segment Piecewise Linear Incremental Heat Rate Function

Given: Two generating units with incremental heat rate curves (IHR) specified as three connected line segments (four points as shown in Figure 3.12).

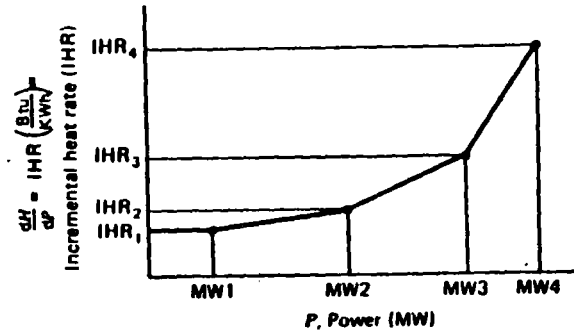


FIG. 3.12 Piecewise linear incremental heat rate curve for Problem 3.2.

Unit 1

Point	MW	IHR (Btu/kWh)
1	100	7000
2	200	8200
3	300	8900
4	400	11000

Fuel cost for unit 1 = 1.60 R/MBtu.

Unit 2

Point	MW	IHR (Btu/kWh)
1	150	7500
2	275	7700
3	390	8100
4	450	8500

Fuel cost for unit 2 = 2.10 R/MBtu.

Both units are running. Calculate the optimum schedule (i.e., the unit megawatt output for each unit) for various total megawatt values to be supplied by the units. Find the schedule for these total megawatt values.

300 MW
500 MW
700 MW
840 MW

Notes: Piecewise linear increment cost curves are quite common in digital computer executions of economic dispatch. The problem is best solved by using a "search" technique. In such a technique, the incremental cost is given a value

and the units are scheduled to meet this incremental cost. The megawatt outputs for the units are added together and compared to the desired total. Depending on the difference, and whether the resulting total is above or below the desired total, a new value of incremental cost is "tried." This is repeated until the incremental cost is found that gives the correct desired value. The trick is to search in an efficient manner so that the number of iterations is minimized.

3.3 Assume the system load served by the two units of Problem 3.1 varies from 50 to 200 MW. For the data of Problem 3.1 plot the outputs of units 1 and 2 as a function of total system load when scheduling generation by equal incremental production costs. Assume that both units are operating.

3.4 As an exercise, obtain the optimum loading of the two generating units in Problem 3.1 using the following technique. The two units are to deliver 100 MW. Assume both units are on-line and delivering power. Plot the total fuel cost for 100 MW of delivered power as generation is shifted from one unit to the other. Find the minimum cost. The optimum schedule should check with the schedule obtained by equal incremental production costs.

3.5 This problem demonstrates the complexity involved when we must commit (turn on) generating units as well as dispatch them economically. This problem is known as the *unit commitment problem* and is the subject of Chapter 5.

Given the two generating units in Problem 3.1, assume that they are both off-line at the start. Also assume that load starts at 50 MW and increases to 200 MW. The most economic schedule to supply this varying load will require committing one unit first, followed by commitment of the second unit when the load reaches a higher level.

Determine which unit to commit first and at what load the remaining unit should be committed. Assume no "start-up" costs for either unit.

3.6 The system to be studied consists of two units described in Problem 3.1. Assume a daily load cycle as follows.

Time Band	Load (MW)
0000-0600	50
0600-1800	150
1800-0000	50

Also, assume that a cost of 180 R is incurred in taking either unit off line and returning it to service after 12 h. Consider the 24-h period from 0600 one morning to 0600 the next morning.

a. Would it be more economical to keep both units in service for this 24-h period or to remove one of the units from service for the 12-h period from 1800 one evening to 0600 the next morning?

- b. What is the economic schedule for the period of time from 0600 to 1800 (load = 150 MW)?
- c. What is the economic schedule for the period of time from 1800 to 0600 (load = 50 MW)?

3.7 Assume that all three of the thermal units described in the following table are running. Find the economic dispatch schedules as requested in each part. Use the method and starting conditions given

Unit Data	Minimum (MW)	Maximum (MW)	Fuel Cost (R/MBtu)
$H_1 = 225 + 8.4 P_1 + 0.0025 P_1^2$	45	350	0.80
$H_2 = 729 + 6.3 P_2 + 0.0081 P_2^2$	45	350	1.02
$H_3 = 400 + 7.5 P_3 + 0.0025 P_3^2$	47.5	450	0.90

- a. Use the lambda-iteration method to find the economic dispatch for a total demand of 450 MW.
- b. Use the base-point and participation factor method to find the economic schedule for a demand of 495 MW. Start from the solution to part a.
- c. Use a gradient method to find the economic schedule for a total demand of 500 MW assuming the initial conditions (i.e., loadings) on the three units are

$$P_1 = P_3 = 100 \text{ MW} \quad \text{and} \quad P_2 = 300 \text{ MW}$$

Give the individual unit loadings and cost per hour as well as the total cost per hour to supply each load level. (MBtu = millions of BTU; H_i = heat input in MBtu/h; P_i = electric power output in MW; $i = 1, 2, 3$.)

3.8 Thermal Scheduling with Straight-Line Segments for Input-Output Curves

The following data apply to three thermal units. Compute and sketch the input-output characteristics and the incremental heat rate characteristics. Assume the unit input-output curves consist of straight-line segments between the given power points.

Unit No.	Power Output (MW)	Net Heat Rate (Btu/kWh)
1	45	13,512.5
	300	9,900.0
	350	9,918.0
2	45	22,764.5
	200	11,465.0
	300	11,060.0
3	350	11,117.9
	47.5	16,039.8
	200	10,000.0
	300	9,583.3
	450	9,513.9

Fuel costs are

Unit No.	Fuel Cost (₹/MBtu)
1	0.61
2	0.75
3	0.75

Compute the economic schedule for system demands of 300, 460, 500, and 650 MW, assuming all three units are on-line. Give unit loadings and costs per hour as well as total costs in ₹ per hour.

3.9 Environmental Dispatch

Recently there has been concern that optimum economic dispatch was not the best environmentally. The principles of economic dispatch can fairly easily be extended to handle this problem. Following is a problem based on a real situation that occurred in the midwestern United States in 1973. Other cases have arisen with "NOX" emission in Los Angeles.

Two steam units have input-output curves as follows.

$$H_1 = 400 + 5P_1 + 0.01P_1^2, \text{ MBtu/h}, 20 \leq P_1 \leq 200 \text{ MW}$$

$$H_2 = 600 + 4P_2 + 0.015P_2^2, \text{ MBtu/h}, 20 \leq P_2 \leq 200 \text{ MW}$$

The units each burn coal with a heat content of 11,500 Btu/lb that costs 13.50 ₹ per ton (2000 lb). The combustion process in each unit results in 11.75% of the coal by weight going up the stack as fly ash.

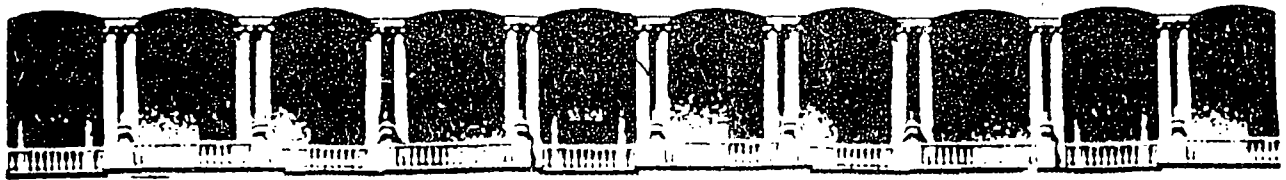
- Calculate the net heat rates of both units at 200 MW.
- Calculate the incremental heat rates; schedule each unit for optimum economy to serve a total load of 250 MW with both on-line.
- Calculate the cost of supplying that load.
- Calculate the rate of emission of fly ash for that case in lb/h, assuming no fly ash removal devices are in service.
- Unit 1 has a precipitator installed that removes 85% of the fly ash; unit 2's precipitator is 89.0% efficient. Reschedule the two units for the minimum total fly ash emission rate with both on-line to serve a 250 MW load.
- Calculate the rate of emission of ash and the cost for this schedule to serve the 250 MW load. What is the cost penalty?
- Where does all that fly ash go?

FURTHER READING

Since this chapter introduces several optimization concepts it would be useful to refer to some of the general works on optimization such as references 1 and 2. The importance of the Kuhn-Tucker theorem is given in their paper (3). A very thorough discussion of the Kuhn-Tucker theorem is found in Chapter 1 of reference 4.

For an overview of recent power system optimization practices see references 5 and 6. Several other applications of optimization have been presented. Reference 7 discusses the allocation of regulating margin while dispatching generator units. References 8-10 discuss how to formulate the dispatch problem as one that minimizes air pollution from power plants.

- Application of Optimization Methods in Power System Engineering*, IEEE Tutorial Course Text 76CH1107-2-PWR, IEEE, New York, 1976.
- Wilde, P. J., Beightler, C. S., *Foundations of Optimization*, Prentice-Hall, Englewood Cliffs, N.J., 1967.
- Kuhn, H. W., Tucker, A. W., "Nonlinear Programming", in *Second Berkeley Symposium on Mathematical Programming Statistics and Probability*, 1950, University of California Press, Berkeley, 1951.
- Wismer, D. A., *Optimization Methods for Large-Scale Systems With Applications*, McGraw-Hill, New York, 1971.
- IEEE Committee Report, "Present Practices in the Economic Operation of Power Systems," *IEEE Transactions on Power Apparatus and Systems*, Vol. PAS-90, July/August 1971, pp. 1768-1775.
- Najaf-Zadeh, K., Nikolas, J. T., Anderson, S. W., "Optimal Power System Operation Analysis Techniques," *Proceedings American Power Conference*, 1977.
- Stadlin, W. O., "Economic Allocation of Regulating Margin," *IEEE Transactions on Power Apparatus and Systems*, Vol. PAS-90, July/August 1971, pp. 1777-1781.
- Gent, M. R., Lamont, J. W., "Minimum Emission Dispatch," *IEEE Transactions on Power Apparatus and Systems*, Vol. PAS-90, November/December 1971, pp. 2650-2260.
- Sullivan, R. L., "Minimum Pollution Dispatching," IEEE Summer Power Meeting, Paper C-72-468, 1972.
- Friedman, P. G., "Power Dispatch Strategies for Emission and Environmental Control," *Proceedings of the Instrument Society of America*, Vol. 16, 1973.



**FACULTAD DE INGENIERIA U.N.A.M.
DIVISION DE EDUCACION CONTINUA**

**V CURSO INTERNACIONAL DE SISTEMAS
ELECTRICOS DE POTENCIA**

MODULO II: SISTEMAS ELECTRICOS DE POTENCIA

TEMA: TRANSMISSION LOSSES

EXPOSITOR: ING. ARTURO MORALES COLLANTES

Transmission Losses

This chapter introduces the concept of the steady-state transmission network solution or load flow and the relationship of losses in the transmission network to economic dispatch. *Load flow* is the name given to a network solution that shows currents, voltages, and power flows at every bus in the system. It is normally assumed that the system is balanced and the common use of the term load flow implies a positive sequence solution only. Full three-phase load-flow solution techniques are available for special purpose calculations. As used here, we are only interested in balanced solutions. Load flow is not a single calculation such as $E = IR$ or $E = [Z]I$ involving linear circuit analysis. Such circuit analysis problems start with a given set of currents or voltages, and one must solve for the linearly dependent unknowns. In the load-flow problem we are given a nonlinear relationship between voltage and current at each bus and we must solve for all voltages and currents such that these nonlinear relationships are met. The nonlinear relationships involve, for example, the real and reactive power consumption at a bus, or the generated real power and scheduled voltage magnitude at a generator bus. As such, the load flow gives us the electrical response of the transmission system to a particular set of loads and generator unit outputs. Load flows are an important part of power system design procedures (system planning). Modern digital computer load-flow programs are routinely run for systems up to 5000 or more buses

and also are used widely in power system control centers to study unique operating problems and provide accurate calculations of bus penalty factors.

One of the quantities available from a load-flow solution is the electrical losses of the network. The electrical losses are important in economically dispatching generation. However, it is not simply the value of the losses but the derivatives of losses with respect to generator outputs that are important. Before the advent of large, fast digital computers, the losses were treated by various approximate methods. Present state-of-the-art system-control centers build the economic dispatch problem around the load flow itself.

4.1 THE LOAD-FLOW PROBLEM AND ITS SOLUTION

The load-flow problem consists of a given transmission network where all lines are represented by a Pi-equivalent circuit and transformers by an ideal voltage transformer in series with an impedance. Generators and loads represent the boundary conditions of the solution. Generator or load real and reactive power involves products of voltage and current. Mathematically, the load flow requires a solution of a system of simultaneous nonlinear equations.

4.1.1 The Load-Flow Problem on a Direct Current Network

The problems involved in solving a load flow can be illustrated by the use of direct current circuit examples. The circuit shown in Figure 4.1 has a resistance of 0.25Ω tied to a constant voltage of 1.0 V (called the *reference voltage*). We wish to find the voltage at bus 2 that results in a net inflow of 1.2 W . Buses are electrical nodes. Power is said to be "injected" into a network; therefore, loads are simply negative injections.

The current from bus 2 to bus 1 is

$$I_{21} = (E_2 - 1.0) \times 4 \quad (4.1)$$

Power P_2 is

$$P_2 = 1.2 = E_2 I_{21} = E_2 (E_2 - 1) \times 4 \quad (4.2)$$

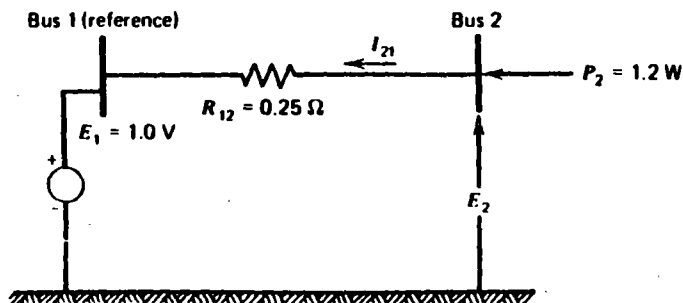


FIG. 4.1 Two-bus dc network.

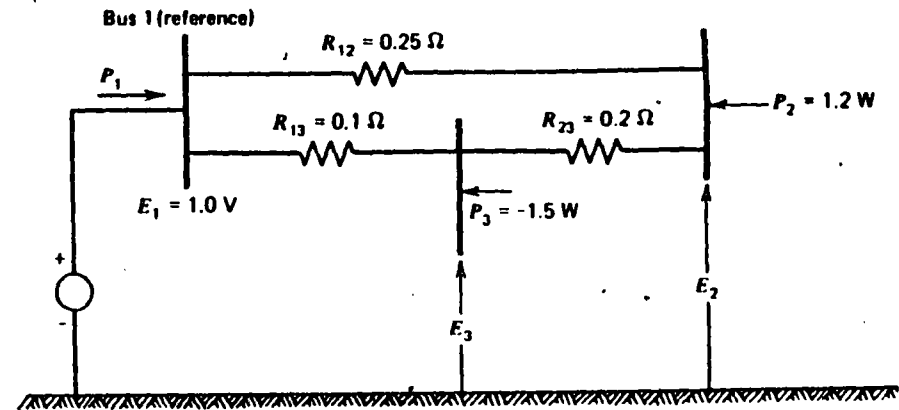


FIG. 4.2 Three-bus dc network.

or

$$4E_2^2 - 4E_2 - 1.2 = 0 \quad (4.3)$$

The solutions to this quadratic equation are $E_2 = 1.24162 \text{ V}$ and $E_2 = -0.24162 \text{ V}$. Note that 1.2 W enter bus 2, producing a current of 0.96648 A ($E_2 = 1.24162$), which means that 0.96648 W enter reference bus and 0.23352 W are consumed in the 0.25Ω resistor.

Let us complicate the problem by adding a third bus and two more lines (see Figure 4.2). The problem is more complicated because we cannot simply write out the solutions using a quadratic formula. The admittance equations are

$$\begin{bmatrix} I_1 \\ I_2 \\ I_3 \end{bmatrix} = \begin{bmatrix} 14 & -4 & -10 \\ -4 & 9 & -5 \\ -10 & -5 & 15 \end{bmatrix} \begin{bmatrix} E_1 \\ E_2 \\ E_3 \end{bmatrix} \quad (4.4)$$

In this case we know the power injected at buses 2 and 3 and we know the voltage at bus 1. To solve for the unknowns (E_2 , E_3 , and P_1), we write Eqs. 4.5, 4.6, and 4.7. The solution procedure is known as the *Gauss-Seidel procedure*, wherein a calculation for a new voltage at each bus is made based on the most recently calculated voltages at all neighboring buses.

Bus 2:

$$I_2 = \frac{P_2}{E_2} = -4(1.0) + 9E_2 - 5E_3$$

$$E_2^{\text{new}} = \frac{1}{9} \left(\frac{1.2}{E_2^{\text{old}}} + 4 + 5E_3^{\text{old}} \right) \quad (4.5)$$

where E_2^{old} and E_3^{old} are the initial values for E_2 and E_3 , respectively.

Bus 3:

$$I_3 = \frac{P_3}{E_3} = -10(1.0) - E_2^{\text{new}} + 15E_3$$

$$E_3^{\text{new}} = \frac{1}{15} \left[\frac{-1.5}{E_3^{\text{old}}} + 10 + 5E_2^{\text{new}} \right] \quad (4.6)$$

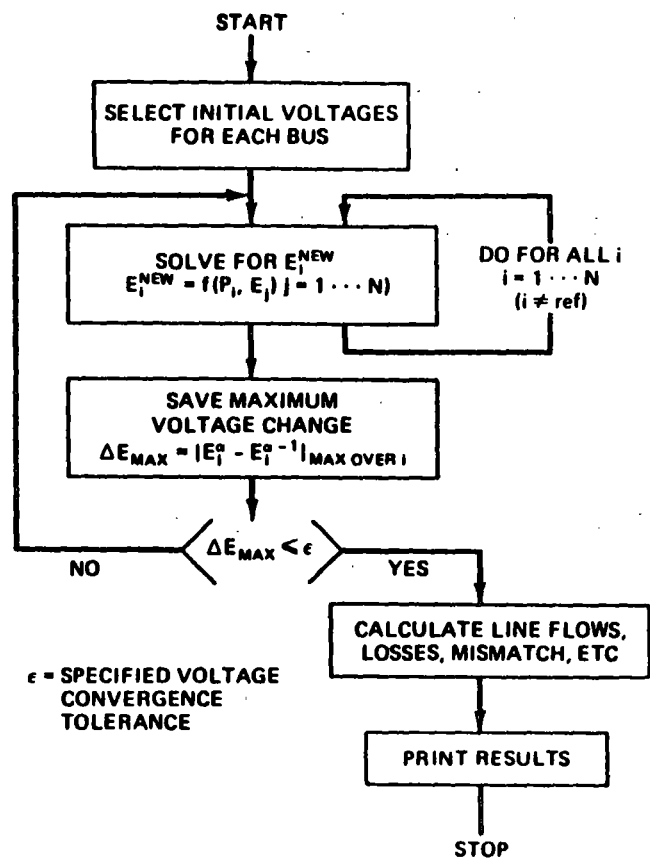


FIG. 4.3 Gauss-Seidel load-flow solution.

where E_2^{new} is the voltage found in solving Eq. 4.5 and E_3^{old} is the initial value of E_3 .

Bus 1: $P_1 = E_1 I_1^{new} = 1.0 I_1^{new} = 14 - 4 E_2^{new} - 10 E_3^{new}$ (4.7)

The Gauss-Seidel method first assumes a set of voltages at buses 2 and 3 and then uses Eqs. 4.5 and 4.6 to solve for new voltages. The new voltages are compared to the old's most recent values, and the process continues until the change in voltage is very small. This is illustrated in the flowchart in Figure 4.3 and Eqs. 4.8 and 4.9.

First Iteration: $E_2^{(0)} = E_3^{(0)} = 1.0$
 $E_2^{(1)} = \frac{1}{9} \left(\frac{1.2}{1.0} + 4 + 5 \right) = 1.133$ (4.8)

$E_3^{(1)} = \frac{1}{15} \left[\frac{-1.5}{1.0} + 10 + 5(1.133) \right] = 0.944$

$\Delta E_{max} = 0.133$ too large

NOTE: In calculating $E_3^{(1)}$ we used the new value of E_2 found in the first correction.

Second Iteration: $E_2^{(2)} = \frac{1}{9} \left[\frac{1.2}{1.133} + 4 + 5(0.944) \right] = 1.087$

$E_3^{(2)} = \frac{1}{15} \left[\frac{-1.5}{0.944} + 10 + 5(1.087) \right] = 0.923$ (4.9)

$\Delta E_{max} = 0.046$

And so forth until $\Delta E_{max} < \epsilon$.

4.1.2 The Formulation of the AC Load Flow

AC load flows involve several types of bus specifications, as shown in Figure 4.4. Note that $[P, \theta]$, $[Q, |E|]$, and $[Q, \theta]$ combinations are generally not used.

The transmission network consists of complex impedances between buses and from the buses to ground. An example is given in Figure 4.5. The equations are written in matrix form as

$$\begin{bmatrix} I_1 \\ I_2 \\ I_3 \\ I_4 \end{bmatrix} = \begin{bmatrix} y_{12} & -y_{12} & 0 & 0 \\ -y_{12} & (y_{12} + y_{2g} + y_{23}) & -y_{23} & 0 \\ 0 & -y_{23} & (y_{23} + y_{3g} + y_{34}) & -y_{34} \\ 0 & 0 & -y_{34} & (y_{34} + y_{4g}) \end{bmatrix} \begin{bmatrix} E_1 \\ E_2 \\ E_3 \\ E_4 \end{bmatrix} \quad (4.10)$$

(All I 's, E 's, y 's complex)

This matrix is called the *network Y matrix*, which is written as

$$\begin{bmatrix} I_1 \\ I_2 \\ I_3 \\ I_4 \end{bmatrix} = \begin{bmatrix} Y_{11} & Y_{12} & Y_{13} & Y_{14} \\ Y_{21} & Y_{22} & Y_{23} & Y_{24} \\ Y_{31} & Y_{32} & Y_{33} & Y_{34} \\ Y_{41} & Y_{42} & Y_{43} & Y_{44} \end{bmatrix} \begin{bmatrix} E_1 \\ E_2 \\ E_3 \\ E_4 \end{bmatrix} \quad (4.11)$$

The rules for forming a Y matrix are

If a line exists from i to j
 $Y_{ij} = -y_{ij}$
 and
 $Y_{ii} = \sum_j y_{ij} + y_{ig}$
 j over all lines connected to i .

Bus Type	✓	Q	E	θ	Comments
Load	✓	✓			Usual load representation
Voltage Controlled	✓		✓		Assume E is held constant no matter what Q is
Generator or Synchronous Condenser	✓		✓		Generator or synchronous condenser (P = 0) has VAR limits
	✓	✓			Q ⁻ minimum VAR limit Q ⁺ maximum VAR limit E is held as long as Q _s is within limit
Fixed Z to Ground					Only Z is given
Reference			✓	✓	"Swing bus" must adjust net power to hold voltage constant (essential for solution)

FIG. 4.4 Load-flow bus specifications (quantities checked are the bus boundary conditions).

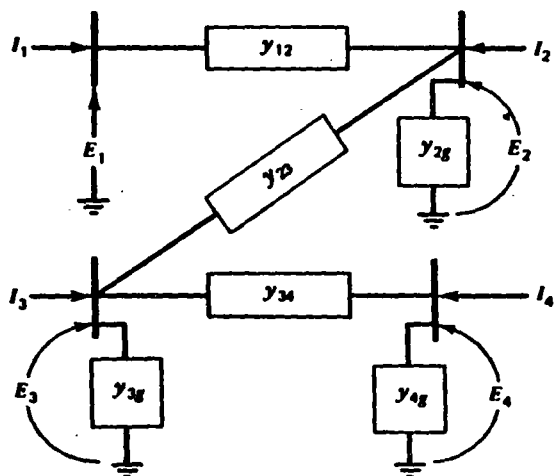


FIG. 4.5 Four-bus ac network.

The equation of net power injection at a bus is usually written as

$$\frac{P_k - jQ_k}{E_k^*} = \sum_{j=1}^n Y_{jk} E_j + Y_{kk} E_k \quad (4.12)$$

4.1.2.1 The Gauss-Seidel Method

The voltages at each bus can be solved for by using the Gauss-Seidel method. The equation in this case is

$$E_k^{(\alpha)} = \frac{1}{Y_{kk}} \frac{(P_k - jQ_k)}{E_k^{(\alpha-1)*}} - \frac{1}{Y_{kk}} \left[\sum_{j < k} Y_{jk} E_j^{(\alpha-1)} + \sum_{j > k} Y_{jk} E_j^{(\alpha-1)} \right] \quad (4.13)$$

Voltage at iteration α

The Gauss-Seidel method was the first ac load-flow method to be developed for solution on digital computers. This method is characteristically long in solving due to its slow convergence and often difficulty is experienced with unusual network conditions such as negative reactance branches. The solution procedure is the same as shown in Figure 4.3.

4.1.2.2 The Newton-Raphson Method

One of the disadvantages of the Gauss-Seidel method lies in the fact that each bus is treated independently. Each correction to one bus requires subsequent correction to all the buses to which it is connected. The Newton-Raphson method is based on the idea of calculating the corrections while taking account of all the interactions.

Newton's method involves the idea of an error in a function $f(x)$ being driven to zero by making adjustments Δx to the independent variable associated with the function. Suppose we wish to solve

$$f(x) = K \quad (4.14)$$

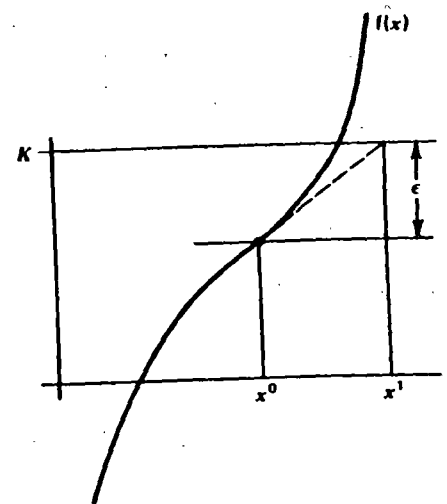


FIG. 4.6 Newton's method.

In Newton's method we pick a starting value of x and call it x^0 . The error is the difference between K and $f(x^0)$. Call the error ϵ . This is shown in Figure 4.6 and given in Eq. 4.15.

$$f(x^0) + \epsilon = K \quad (4.15)$$

To drive the error to zero, we use a Taylor expansion of the function about x^0 .

$$f(x^0) + \frac{df(x^0)}{dx} \Delta x + \epsilon = K \quad (4.16)$$

Setting the error to zero we calculate

$$\Delta x = \left(\frac{df(x^0)}{dx} \right)^{-1} [K - f(x^0)] \quad (4.17)$$

When we wish to solve a load flow we extend Newton's method to the multivariable case (the multivariable case is called the *Newton-Raphson method*). An equation is written for each bus "i."

$$P_i + jQ_i = E_i I_i^* \quad (4.18)$$

where

$$I_i = \sum_{k=1}^N Y_{ik} E_k$$

then

$$P_i + jQ_i = E_i \left[\sum_{k=1}^N Y_{ik} E_k \right]^* \\ = |E_i|^2 Y_{ii}^* + \sum_{k=1, k \neq i}^N Y_{ik}^* E_i E_k^*$$

As in the Gauss-Seidel method, a set of starting voltages is used to get things going. The $P + jQ$ calculated is subtracted from the scheduled $P + jQ$ at the bus and the resulting errors stored in a vector. As shown following, we will assume that the voltages are in polar coordinates and that we are going to adjust each voltage's magnitude and phase angle as separate independent variables. Each bus injection equation is differentiated with respect to all independent variables. Note that at this point two equations are written for each bus: one for real power and one for reactive power. For each bus

$$\Delta P_i = \sum_{k=1}^N \frac{\partial P_i}{\partial \theta_k} \Delta \theta_k + \sum_{k=1}^N \frac{\partial P_i}{\partial |E_k|} \Delta |E_k| \\ \Delta Q_i = \sum_{k=1}^N \frac{\partial Q_i}{\partial \theta_k} \Delta \theta_k + \sum_{k=1}^N \frac{\partial Q_i}{\partial |E_k|} \Delta |E_k| \quad (4.19)$$

All the terms are arranged in a matrix (the Jacobian matrix) as follows.

$$\begin{bmatrix} \Delta P_1 \\ \Delta Q_1 \\ \Delta P_2 \\ \Delta Q_2 \\ \vdots \end{bmatrix} = \underbrace{\begin{bmatrix} \frac{\partial P_1}{\partial \theta_1} & \frac{\partial P_1}{\partial |E_1|} & \dots \\ \frac{\partial Q_1}{\partial \theta_1} & \frac{\partial Q_1}{\partial |E_1|} & \dots \\ \vdots & \vdots & \ddots \end{bmatrix}}_{\text{Jacobian matrix}} \begin{bmatrix} \Delta \theta_1 \\ \Delta |E_1| \\ \vdots \end{bmatrix} \quad (4.20)$$

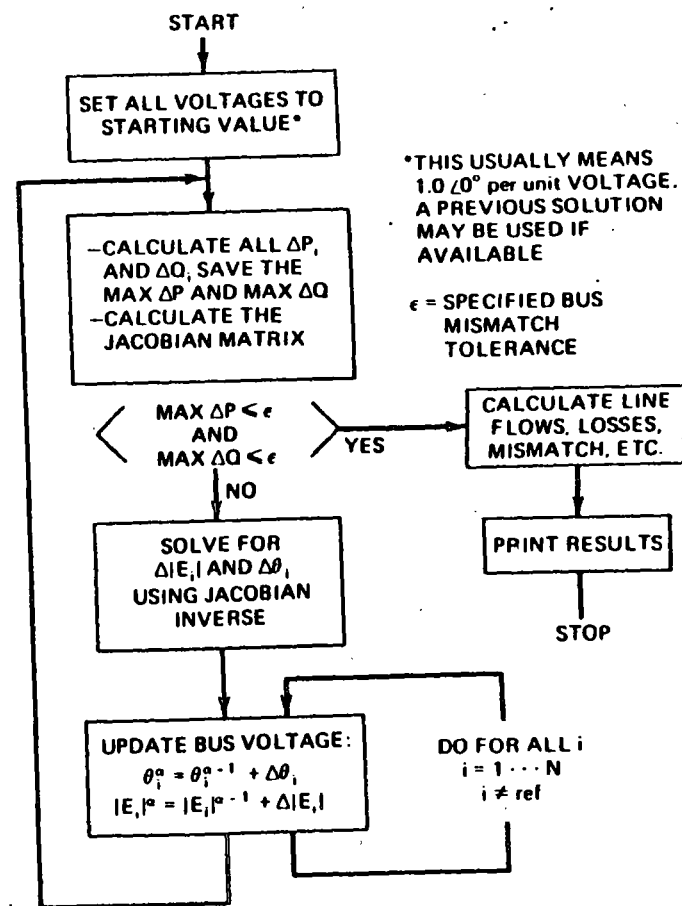


FIG. 4.7 Newton-Raphson load-flow solution.

The solution to the Newton-Raphson load flow runs according to the flowchart in Figure 4.7. Solving for $\Delta\theta$ and $\Delta|E|$ requires the solution of a set of linear equations whose coefficients make up the Jacobian matrix. (See Appendix C for details of the Jacobian matrix.) The Jacobian matrix generally has only a

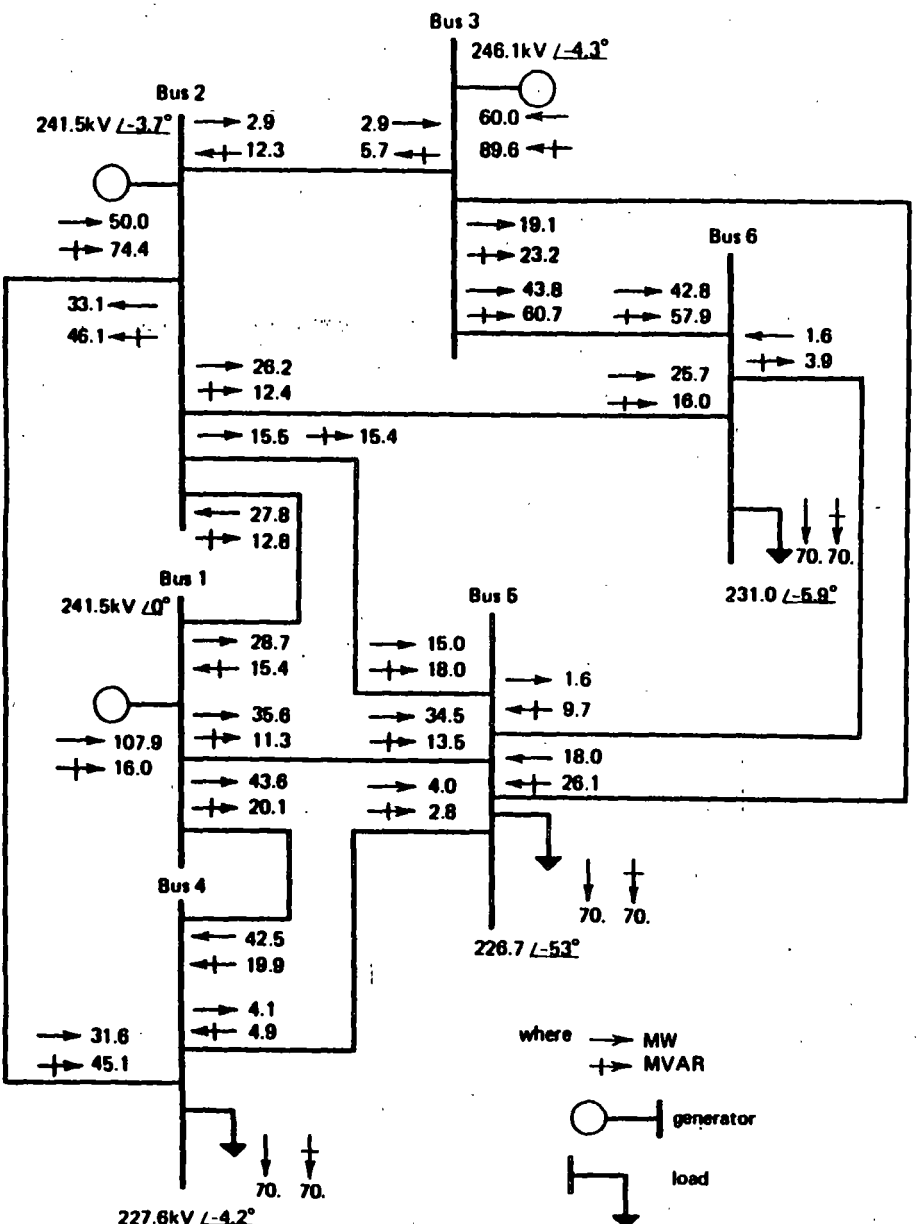


FIG. 4.8 Six-bus network base case ac load flow.

few percent of its entries that are nonzero. Programs that solve ac load flow using the Newton-Raphson method are successful because they take advantage of the Jacobian's "sparsity." The solution procedure uses Gaussian elimination on the Jacobian matrix and does not calculate J^{-1} explicitly. (See reference 3 for introduction to "sparsity" techniques.)

EXAMPLE 4A

The six-bus network shown in Figure 4.8 will be used to demonstrate several aspects of load flows and transmission loss factors. The voltages and flows shown are for the "base case" of 210 MW total load. The impedance values and other data for this system may be found in Appendix A.

4.1.3 The "DC" Load Flow

A very widely used approximation of the AC load flow is the "linearized" or "DC" load flow, which converts the AC solution into a simple linear circuit analysis problem. Assume we are given a transmission line Pi-equivalent circuit as shown in Figure 4.9. The equation for power flowing through the line calculated at bus i can be written as

$$\begin{aligned}
 P_{ij} + jQ_{ij} &= E_i[(E_i - E_j)y_{ij}]^* + E_i[E_i y_{cap,ij}]^* \\
 &= |E_i|e^{j\theta_i}[(|E_i|e^{j\theta_i} - |E_j|e^{j\theta_j})(G_{ij} + jB_{ij})]^* - j|E_i|^2 B_{cap,ij} \\
 &= (|E_i|^2 - |E_i||E_j| \cos(\theta_i - \theta_j) - |E_i||E_j|j \sin(\theta_i - \theta_j)) \\
 &\quad \times (G_{ij} + jB_{ij})^* - j|E_i|^2 B_{cap,ij}
 \end{aligned}
 \tag{4.21}$$

Then

$$P_{ij} = G_{ij}|E_i|^2 - G_{ij}|E_i||E_j| \cos(\theta_i - \theta_j) - B_{ij}|E_i||E_j| \sin(\theta_i - \theta_j)
 \tag{4.22}$$

Assuming

1. $|E_i| = |E_j| = 1$
 2. $x_{ij} \gg r_{ij} \rightarrow G_{ij} = \frac{r_{ij}}{r_{ij}^2 + x_{ij}^2} \approx 0$
- $$B_{ij} = \frac{-x_{ij}}{r_{ij}^2 + x_{ij}^2} = \frac{-1}{x_{ij}}$$

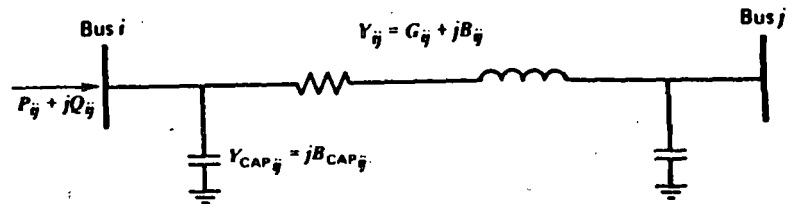


FIG. 4.9 Transmission line Pi-equivalent circuit.

$\lambda (\theta_i - \theta_j)$ is quite small.

$$\cos(\theta_i - \theta_j) \cong 1$$

$$\sin(\theta_i - \theta_j) \cong (\theta_i - \theta_j)$$

Then

$$P_{ij} = \frac{1}{x_{ij}} (\theta_i - \theta_j) \quad (4.23)$$

This linearized form may be used to calculate all bus phase angles in a network.

$$P_i = \sum_j P_{ij} = \sum_j \frac{1}{x_{ij}} (\theta_i - \theta_j) \quad (4.24)$$

j over all nodes connected directly to *i*

Then in matrix form,

$$\begin{bmatrix} P_1 \\ P_2 \\ \vdots \end{bmatrix} = [B_x] \begin{bmatrix} \theta_1 \\ \theta_2 \\ \vdots \end{bmatrix} \quad (4.25a)$$

or

$$\begin{bmatrix} \theta_1 \\ \theta_2 \\ \vdots \end{bmatrix} = [X] \begin{bmatrix} P_1 \\ P_2 \\ \vdots \end{bmatrix} \quad (4.25b)$$

where $B_{x_{ii}} = \sum_j \frac{1}{x_{ij}}$ for $i \neq \text{ref}$
j over all lines connected to *i*

$$B_{x_{ii}} = 0.0 \quad \text{for } i = \text{ref}$$

$$B_{x_{ij}} = \frac{-1}{x_{ij}} \quad \text{for } i \neq \text{ref and } j \neq \text{ref}$$

$$B_{x_{ij}} = 0.0 \quad \text{for } i = \text{ref or } j = \text{ref}$$

Strictly speaking, $[B_x]$ has no inverse since the row and column corresponding to the reference bus contain all zeros. If there are N buses, we only have $N - 1$ linearly independent equations. Thus, we have an $(N - 1) \times (N - 1)$ submatrix of $[B_x]$, which can be inverted. Therefore, when we refer to the matrix $[X]$, we will mean that matrix with the inverse of the submatrix of $[B_x]$ plus a zero row and column corresponding to the reference bus. See Example 4B. We have written $[B_x]$ and $[X]$ in this way so that the vectors θ and P can contain all buses. Note that we must

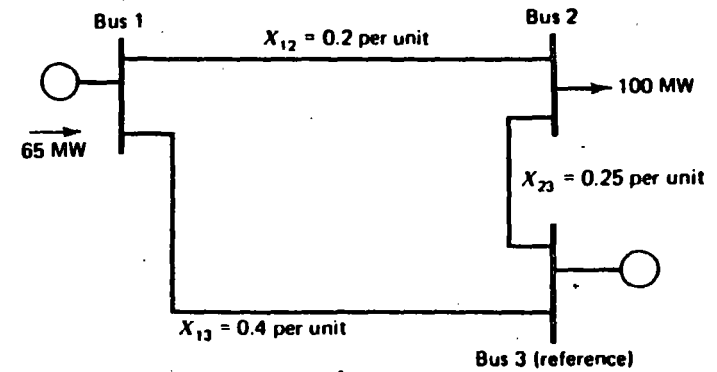


FIG. 4.10 Three-bus network.

always assume a value for the phase angle at the reference bus. Usually we assign this value to be zero radians.

EXAMPLE 4B

The megawatt flows on the network in Figure 4.10 will be solved using the DC load flow. The B_x matrix equation is

$$\begin{bmatrix} 7.5 & -5.0 & 0 \\ -5.0 & 9.0 & 0 \\ 0 & 0 & 0 \end{bmatrix} \begin{bmatrix} \theta_1 \\ \theta_2 \\ 0 \end{bmatrix} = \begin{bmatrix} P_1 \\ P_2 \\ P_3 \end{bmatrix}$$

$\theta_3 = 0$

Note that all megawatt quantities and network quantities are expressed in pu (per unit, 100 MVA base). All phase angles will then be in radians.

The solution to the preceding matrix equation is

$$\begin{bmatrix} \theta_1 \\ \theta_2 \\ 0 \end{bmatrix} = \begin{bmatrix} 0.2118 & 0.1177 & 0 \\ 0.1177 & 0.1765 & 0 \\ 0 & 0 & 0 \end{bmatrix} \begin{bmatrix} 0.65 \\ -1.00 \\ 0.35 \end{bmatrix} = \begin{bmatrix} 0.02 \\ -0.1 \\ 0 \end{bmatrix}$$

The resulting flows are shown in Figure 4.11 and calculated using Eq. 4.24. Note that all flows in Figure 4.11 were converted to actual megawatt values.

EXAMPLE 4C

The network of Example 4A was solved using the dc load flow with resulting power flows as shown in Figure 4.12. The dc load flow is useful for rapid calculations of real power flows, and, as will be shown later, it can be used to calculate incremental losses.

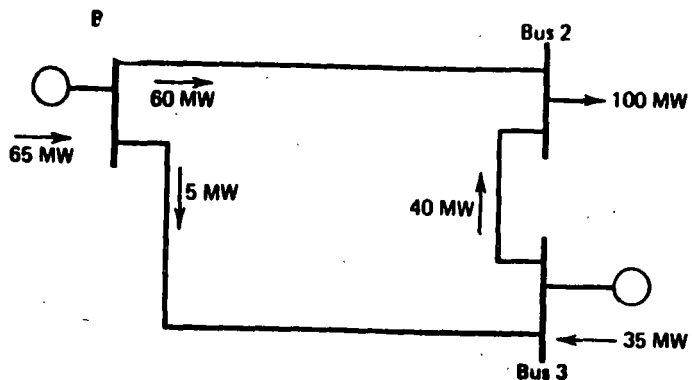
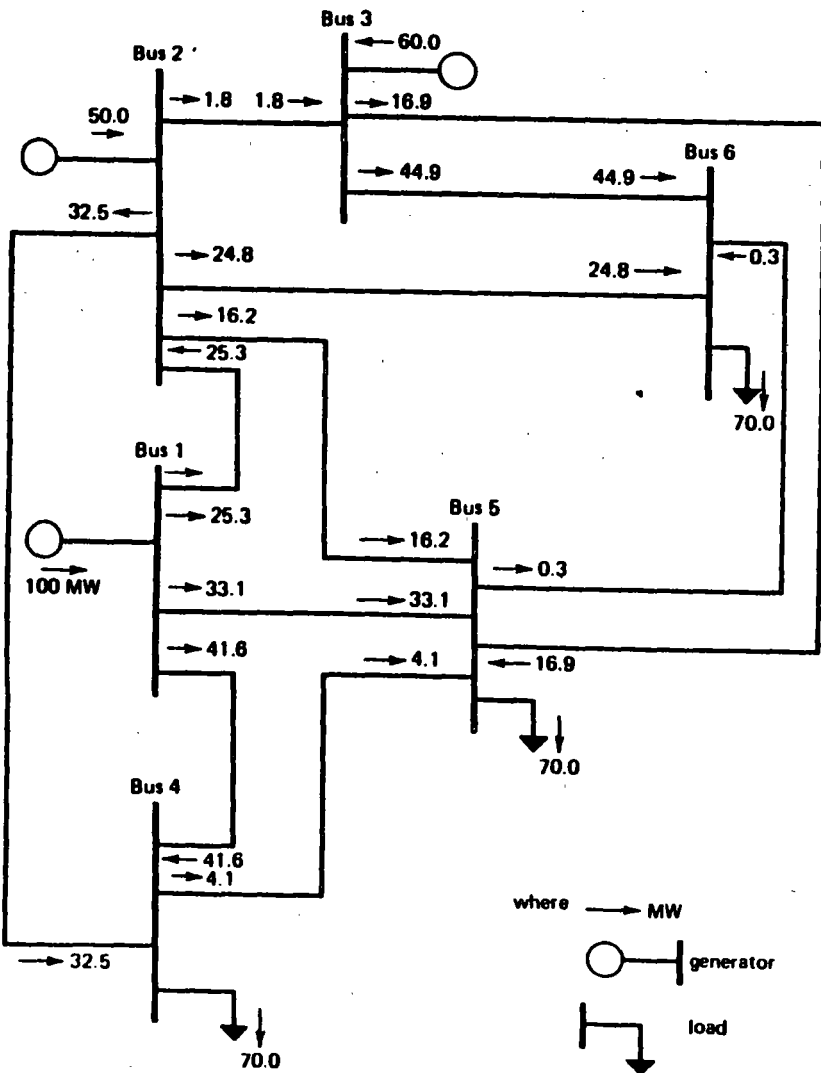


FIG. 4.11 Three-bus network showing flows calculated by dc load flow.



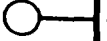

where → MW
 generator
 load

FIG. 4.12 Six-bus network base case dc load flow for Example 4C.

4.2 TRANSMISSION LOSSES

4.2.1 A Two-Generator System

We are given the power system in Figure 4.13. The losses on the transmission line are proportional to the square of the power flow. The generating units are identical, and the production cost modeled using the quadratic curve shown. If both units were loaded to 250 MW, we would fall short of the 500 MW load value by 12.5 MW lost on the transmission line, as shown in Figure 4.14.

Where should the extra 12.5 MW be generated? Solve the LaGrange equation that was given in Chapter 3, Eqs. 3.7, 3.8, and 3.9.

$$\mathcal{L} = F_1(P_1) + F_2(P_2) + \lambda(500 + P_{\text{loss}} - P_1 - P_2) \quad (4.26)$$

where

$$P_{\text{loss}} = 0.0002 P_1^2$$

Then

$$\begin{aligned} \frac{\partial \mathcal{L}}{\partial P_1} &= \frac{dF_1(P_1)}{dP_1} - \lambda \left(1 - \frac{\partial P_{\text{loss}}}{\partial P_1} \right) = 0 \\ \frac{\partial \mathcal{L}}{\partial P_2} &= \frac{dF_2(P_2)}{dP_2} - \lambda \left(1 - \frac{\partial P_{\text{loss}}}{\partial P_2} \right) = 0 \\ P_1 + P_2 - 500 - P_{\text{loss}} &= 0 \end{aligned} \quad (4.27)$$

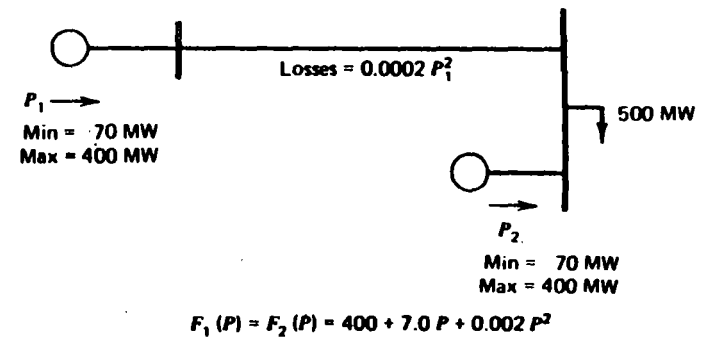


FIG. 4.13 Two-generator system.

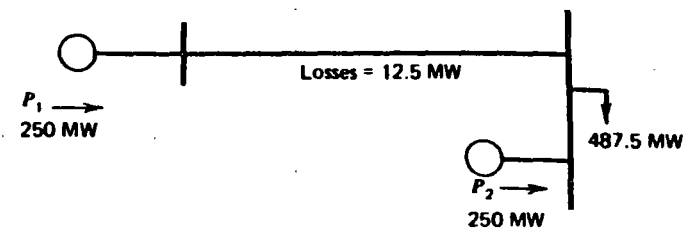


FIG. 4.14 Two-generator system with both generators at 250 MW output.

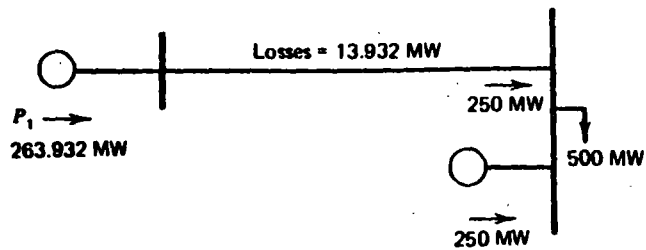


FIG. 4.15 Two-generator system with generator 1 supplying all losses.

Substituting into Eq. 4.27,

$$7.0 + 0.004 P_1 - \lambda(1 - 0.0004 P_1) = 0$$

$$7.0 + 0.004 P_2 - \lambda = 0$$

$$P_1 + P_2 - 500 - 0.0002 P_1^2 = 0$$

Solution: $P_1 = 178.882$

$$P_2 = 327.496$$

Production cost: $F_1(P_1) + F_2(P_2) = 4623.15 \text{ ₹/h}$

Losses: 6.378 MW

Suppose we had decided simply to ignore the economic influence of losses and ran unit 1 up until it supplied all the losses. It would need to be run at 263.932 MW as shown in Figure 4.15. In this case, the total production cost would be

$$F_1(263.932) + F_2(250) = 4661.84 \text{ ₹/h}$$

Note that the optimum dispatch tends toward supplying the losses from the unit close to the load, and it also resulted in a lower value of losses. Also note that best economics are not necessarily attained at minimum losses. The minimum loss solution for this case would simply run unit 1 down and unit 2 up as far as possible. The result is unit 2 on high limit.

$$P_1 = 102.084 \text{ MW}$$

$$P_2 = 400.00 \text{ MW (high limit)}$$

The minimum loss production cost would be

$$F_1(102.084) + F_2(400) = 4655.43 \text{ ₹/h}$$

$$\text{Min losses} = 2.084 \text{ MW}$$

4.2.2 Coordination Equations, Incremental Losses, and Penalty Factors

The classic LaGrange multiplier solution to the economic dispatch problem was given in Chapter 3, Eqs. 3.7, 3.8, and 3.9. These are repeated here and expanded.

Minimize: $\mathcal{L} = F_T + \lambda \phi$

Where: $F_T = \sum_{i=1}^N F_i(P_i)$

$$\phi = P_R + P_L(P_1, P_2, \dots, P_N) - \sum_{i=1}^N P_i$$

Load Losses Generation

Solution: $\frac{\partial \mathcal{L}}{\partial P_i} = 0$ for all $P_{i\min} \leq P_i \leq P_{i\max}$

Then

$$\frac{\partial \mathcal{L}}{\partial P_i} = \frac{dF_i}{dP_i} - \lambda \left(1 - \frac{\partial P_L}{\partial P_i} \right) = 0$$

The equations are rearranged

$$\left(\frac{1}{1 - \frac{\partial P_L}{\partial P_i}} \right) \frac{dF_i(P_i)}{dP_i} = \lambda \tag{4.28}$$

where

$$\frac{\partial P_L}{\partial P_i}$$

is called the *incremental loss* for bus i , and

$$Pf_i = \left(\frac{1}{1 - \frac{\partial P_L}{\partial P_i}} \right)$$

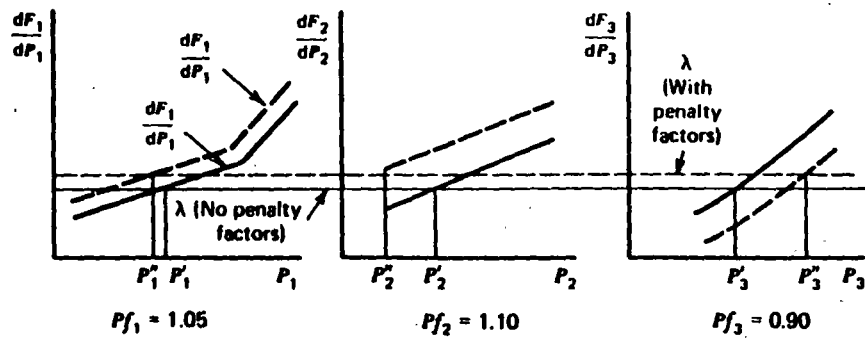
is called the *penalty factor* for bus i . Note that if the losses increase for an increase in power from bus i , the incremental loss is positive and the penalty factor is greater than unity.

When we did not take account of transmission losses, the economic dispatch problem was solved by making the incremental cost at each unit the same. We can still use this concept by observing that the penalty factor, Pf_i , will have the following effect. For

$$Pf_i > 1$$

(Positive increase in P_i results in increase in losses.)

$$Pf_i \frac{dF_i(P_i)}{dP_i}$$



P'_i = Dispatch ignoring losses
 P_i = Dispatch with penalty factors

FIG. 4.16 Economic dispatch with and without penalty factors.

acts as if

$$\frac{dF_i(P_i)}{dP_i}$$

had been slightly increased (moved up). For $Pf_i < 1$ (positive increase in P_i results in decrease in losses).

$$Pf_i \frac{dF_i(P_i)}{dP_i}$$

acts as if

$$\frac{dF_i(P_i)}{dP_i}$$

had been slightly decreased (moved down). The resulting set of equations look like

$$Pf_i \frac{dF_i(P_i)}{dP_i} = \lambda \quad \text{for all } P_{i\min} \leq P_i \leq P_{i\max} \quad (4.29)$$

and are called *coordination equations*. The P_i values that result when penalty factors are used will be somewhat different from the dispatch, which ignores the losses (depending on the Pf_i and $dF_i(P_i)/dP_i$ values). This is illustrated in Figure 4.16.

4.2.3 The B Matrix Loss Formula

The B matrix loss formula was originally introduced in the early 1950s as a practical method for loss and incremental loss calculations. At the time, automatic

dispatching was performed by analog computers and the loss formula was "stored" in the analog computers by setting precision potentiometers. The equation for the B matrix loss formula is as follows.

where \mathbf{P} = vector of all generator bus net MW
 $[\mathbf{B}]$ = square matrix of the same dimension as \mathbf{P}
 \mathbf{B}_0 = vector of the same length as \mathbf{P}
 B_{00} = constant

$$P_L = \mathbf{P}^T [\mathbf{B}] \mathbf{P} + \mathbf{P}^T \mathbf{B}_0 + B_{00} \quad (4.30)$$

This can be written:

$$P_L = \sum_i \sum_j P_i B_{ij} P_j + \sum_i B_{i0} P_i + B_{00} \quad (4.31)$$

Before we discuss the calculation of the B coefficients, we will discuss how the coefficients are used in an economic dispatch calculation. Substitute Eq. 4.31 into Eqs. 3.7, 3.8, and 3.9.

$$\phi = \sum_{i=1}^N P_i - P_R - \left(\sum_i \sum_j P_i B_{ij} P_j + \sum_i B_{i0} P_i + B_{00} \right) \quad (4.32)$$

Then

$$\frac{\partial \phi}{\partial P_i} = \frac{dF_i P_i}{dP_i} - \lambda \left(1 - 2 \sum_j B_{ij} P_j - B_{i0} \right) \quad (4.33)$$

Note that the presence of the incremental losses has coupled the coordination equations; this makes solution somewhat more difficult. A method of solution that is often used is shown in Figure 4.17.

EXAMPLE 4D

The B matrix loss formula for the network in Example 4A is given here. (Note that all P_i 's must be per unit on 100 MVA base, which results in P_{loss} in per unit on 100 MVA base.)

$$P_{\text{loss}} = [P_1 \quad P_2 \quad P_3] \begin{bmatrix} 0.0676 & 0.00953 & -0.00507 \\ 0.00953 & 0.0521 & 0.00901 \\ -0.00507 & 0.00901 & 0.0294 \end{bmatrix} \begin{bmatrix} P_1 \\ P_2 \\ P_3 \end{bmatrix} + [-0.0766 \quad -0.00342 \quad 0.0189] \begin{bmatrix} P_1 \\ P_2 \\ P_3 \end{bmatrix} + 0.040357$$

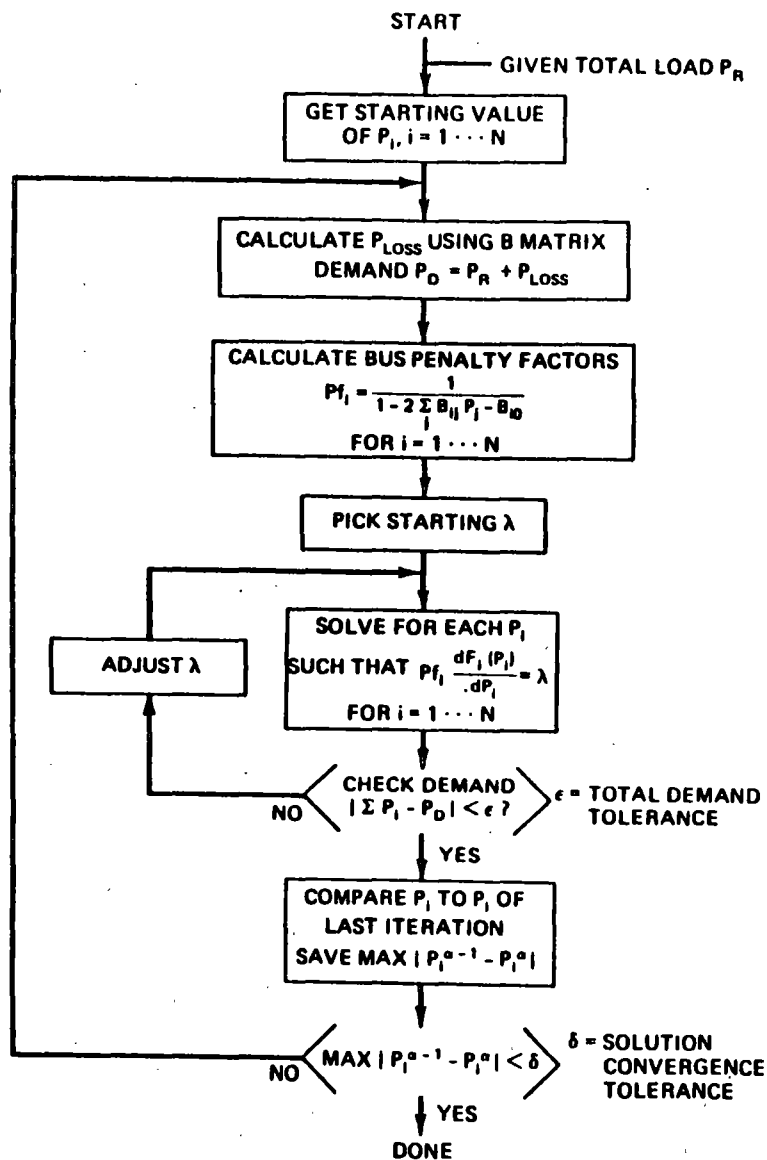


FIG. 4.17 Economic dispatch with updated penalty factors.

From the base case load flow we have

$$P_1 = 107.9 \text{ MW}$$

$$P_2 = 50.0 \text{ MW}$$

$$P_3 = 60.0 \text{ MW}$$

$$P_{\text{loss}} = 7.9 \text{ MW (as calculated by the load flow)}$$

With these generation values placed in the B matrix, we see a very close agreement with the load flow calculation.

$$P_{\text{loss}} = [1.079 \quad 0.50 \quad 0.60] \begin{bmatrix} 0.0676 & 0.00953 & -0.00507 \\ 0.00953 & 0.0521 & 0.00901 \\ -0.00507 & 0.00901 & 0.0294 \end{bmatrix} \begin{bmatrix} 1.079 \\ 0.50 \\ 0.60 \end{bmatrix} \\ + [-0.0766 \quad -0.00342 \quad 0.0189] \begin{bmatrix} 1.079 \\ 0.50 \\ 0.60 \end{bmatrix} + 0.040357 \\ = 0.07877 \text{ pu (or 7.877 MW) loss}$$

EXAMPLE 4E

Let the fuel cost curves for the three units in the six-bus network of Example 4A be given as

$$F_1(P_1) = 213.1 + 11.669 P_1 + 0.00533 P_1^2 \text{ R/h}$$

$$F_2(P_2) = 200.0 + 10.333 P_2 + 0.00889 P_2^2 \text{ R/h}$$

$$F_3(P_3) = 240.0 + 10.833 P_3 + 0.00741 P_3^2 \text{ R/h}$$

With unit dispatch limits

$$50.0 \text{ MW} \leq P_1 \leq 200 \text{ MW}$$

$$37.5 \text{ MW} \leq P_2 \leq 150 \text{ MW}$$

$$45.0 \text{ MW} \leq P_3 \leq 180 \text{ MW}$$

A computer program using the method of Figure 4.17 was run using the following starting conditions from the load-flow solution.

$$P_1 = 107.9 \text{ MW}$$

$$P_2 = 50.0 \text{ MW}$$

$$P_3 = 60.0 \text{ MW}$$

and

$$P_R \text{ (total load to be supplied)} = 210 \text{ MW}$$

The resulting iterations (Table 4.1) show how the program must redispatch again and again to account for the changes in losses and penalty factors.

Note that the flowchart of Figure 4.17 shows a "two-loop" procedure. The "inner" loop adjusts λ until total demand is met; then the outer loop recalculates the penalty factors. (Under some circumstances the penalty factors are quite sensitive to changes in dispatch. If the incremental costs are relatively "flat," this procedure may be unstable and special precautions may need to be employed to ensure convergence.)

TABLE 4.1 Iterations for Example 4E

Iteration	P_{loss}	P_D	P_1	P_2	P_3
1	11.9626	7.8771	217.8771	50.0000	91.6545
2	12.6500	10.8536	220.8535	50.0000	48.2477
3	13.2807	10.5843	220.5843	60.5845	79.6274
4	13.2772	9.9045	219.9044	60.2852	79.4562
5	13.2771	9.8672	219.8672	60.2686	79.4467
6	13.2770	9.8651	219.8651	60.2677	79.4462
7	13.2770	9.8650	219.8650	60.2677	79.4462
8	13.2770	9.8650	219.8650	60.2677	79.4462

4.2.3.1 Derivation of the B Matrix Loss Formula

The derivation of the B matrix loss formula involves the concept of network reference-frame transformations. A *reference frame* is nothing more than a set of voltages and currents that completely describe the electrical network. At any bus i in an electric power network, power "injected" into the network is defined as

$$P_i + jQ_i = E_i I_i^* \quad (4.34)$$

Injected
power

Let the charging capacitance and all other impedances to ground be removed. Then whatever power goes into the network equals the power taken out of the network plus the losses in the network. If we count power put into the network as a positive injection and power taken from the network as a negative injection, we can express losses as

$$P + jQ = \sum_{\text{All network buses}} P_i + jQ_i \quad (4.35)$$

Losses

If we express the injected power as a function of the voltage and injected current at each bus we have

$$P + jQ = \sum_{\text{All network buses}} E_i I_i^* \quad (4.36)$$

Losses

Equation 4.36 can be written in terms of the voltage vector and current vector as follows.

$$E = \begin{bmatrix} E_1 \\ \vdots \\ E_N \end{bmatrix} \quad I = \begin{bmatrix} I_1 \\ \vdots \\ I_N \end{bmatrix}$$

Then

$$P + jQ = E^T I^*$$

Losses

where

E^T is the transpose of E
 I^* is the conjugate of I

so

$$E^T = [E_1 \cdots E_N]$$

$$I^* = \begin{bmatrix} I_1^* \\ \vdots \\ I_N^* \end{bmatrix} \quad (4.37)$$

We are going to transform the voltages and currents so that the network losses remain constant. First we define a matrix $[C]$ that contains both real and complex numbers. We transform using the following matrix multiplications.

$$E_{\text{new}} = [C]^T E_{\text{old}} \quad (4.38)$$

$$I_{\text{old}} = [C] I_{\text{new}}$$

where $[C]^T$ is the transpose conjugate of $[C]$. Let E_{old} and I_{old} be the original voltage and current vectors. From Eq. 4.37

$$P + jQ = E^T I^* = E_{\text{old}}^T I_{\text{old}}^* \quad (4.39)$$

Losses

what we want is

$$P + jQ = E_{\text{new}}^T I_{\text{new}}^* \quad (4.40)$$

Losses

substituting into Eq. 4.40,

$$P + jQ = ([C]^T E_{\text{old}})^T I_{\text{new}}^* \quad (4.41)$$

Losses

$$= E_{\text{old}}^T [C]^* I_{\text{new}}^*$$

$$= E_{\text{old}}^T ([C] I_{\text{new}})^*$$

$$= E_{\text{old}}^T I_{\text{old}}^*$$

REMEMBER: (1) The transpose of a product of matrices is the product of the transpose of each written in reverse order. (2) The conjugate of the product of matrices is the product of their conjugates in the same order.

Furthermore, we can express the impedance matrix as a new matrix referenced to the new voltage and currents. First,

$$\mathbf{E}_{\text{old}} = [\mathbf{Z}_{\text{old}}]\mathbf{I}_{\text{old}} \quad (4.42)$$

Then

$$\begin{aligned} \mathbf{E}_{\text{new}} &= [\mathbf{C}]^T \mathbf{E}_{\text{old}} = [\mathbf{C}]^T [\mathbf{Z}_{\text{old}}] \mathbf{I}_{\text{old}} \\ &= \underbrace{[\mathbf{C}]^T [\mathbf{Z}_{\text{old}}] [\mathbf{C}]}_{[\mathbf{Z}_{\text{new}}]} \mathbf{I}_{\text{new}} \end{aligned}$$

or

$$[\mathbf{Z}_{\text{new}}] = [\mathbf{C}]^T [\mathbf{Z}_{\text{old}}] [\mathbf{C}]$$

and

$$\mathbf{E}_{\text{new}} = [\mathbf{Z}_{\text{new}}]\mathbf{I}_{\text{new}} \quad (4.43)$$

EXAMPLE 4F

A simple DC circuit example will be used to show how the transforms are used. The circuit is given in Figure 4.18. Note that one bus is the reference and is grounded. Then the Y and Z matrix equations are:

$$\mathbf{I} = [\mathbf{Y}]\mathbf{E}$$

$$\begin{bmatrix} I_1 \\ I_2 \\ I_3 \end{bmatrix} = \begin{bmatrix} 5 & -5 & 0 \\ -5 & 7 & -2 \\ 0 & -2 & 3 \end{bmatrix} \begin{bmatrix} E_1 \\ E_2 \\ E_3 \end{bmatrix} \quad (4.44)$$

$$\mathbf{E} = [\mathbf{Z}]\mathbf{I}$$

$$\begin{bmatrix} E_1 \\ E_2 \\ E_3 \end{bmatrix} = \begin{bmatrix} 1.7 & 1.5 & 1 \\ 1.5 & 1.5 & 1 \\ 1 & 1 & 1 \end{bmatrix} \begin{bmatrix} I_1 \\ I_2 \\ I_3 \end{bmatrix} \quad (4.45)$$

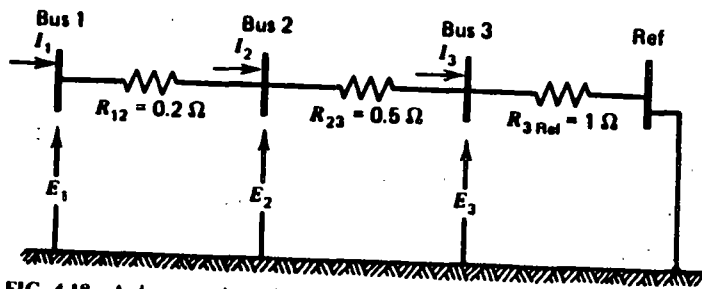


FIG. 4.18 A dc network used to illustrate reference transformations.

Let the currents be given as

$$\begin{bmatrix} I_1 \\ I_2 \\ I_3 \end{bmatrix} = \begin{bmatrix} +10 \\ -4 \\ -6 \end{bmatrix}$$

The voltages are (using Eq. 4.45)

$$\begin{bmatrix} E_1 \\ E_2 \\ E_3 \end{bmatrix} = \begin{bmatrix} 5 \\ 3 \\ 0 \end{bmatrix}$$

The net losses are (we will write the conjugate but ignore it since all quantities here are real numbers):

$$P_{\text{loss}} = \mathbf{E}^T \mathbf{I}^* = [5 \ 3 \ 0] \begin{bmatrix} 10 \\ -4 \\ -6 \end{bmatrix} = 38 \text{ W} \quad (4.46)$$

Think of I_2 and I_3 as load currents that are always in the same proportion of an equivalent total load current $I_{L_{\text{eq}}}$. (Such loads in a power system are said to be "conforming.") Similarly, let I_1 be thought of as a generator current. Then for our example here let

$$I_2 = 0.4 I_{L_{\text{eq}}} \quad (4.47)$$

$$I_3 = 0.6 I_{L_{\text{eq}}}$$

The vector relationship between \mathbf{I}_{old} and \mathbf{I}_{new} becomes

$$\begin{aligned} \mathbf{I}_{\text{old}} &= [\mathbf{C}]\mathbf{I}_{\text{new}} \\ \begin{bmatrix} I_1 \\ I_2 \\ I_3 \end{bmatrix} &= \begin{bmatrix} 1 & 0 \\ 0 & 0.4 \\ 0 & 0.6 \end{bmatrix} \begin{bmatrix} I_1 \\ I_{L_{\text{eq}}} \end{bmatrix} \end{aligned} \quad (4.48)$$

Then by definition

$$\begin{aligned} \mathbf{E}_{\text{new}} &= [\mathbf{C}]^T \mathbf{E}_{\text{old}} \\ \begin{bmatrix} E_1 \\ E_{L_{\text{eq}}} \end{bmatrix} &= \begin{bmatrix} 1 & 0 & 0 \\ 0 & 0.4 & 0.6 \end{bmatrix} \begin{bmatrix} E_1 \\ E_2 \\ E_3 \end{bmatrix} \end{aligned} \quad (4.49)$$

and $[\mathbf{Z}_{\text{new}}]$ is

$$\begin{aligned} [\mathbf{Z}_{\text{new}}] &= \begin{bmatrix} 1 & 0 & 0 \\ 0 & 0.4 & 0.6 \end{bmatrix} \begin{bmatrix} 1.7 & 1.5 & 1 \\ 1.5 & 1.5 & 1 \\ 1 & 1 & 1 \end{bmatrix} \begin{bmatrix} 1 & 0 \\ 0 & 0.4 \\ 0 & 0.6 \end{bmatrix} \\ &= \begin{bmatrix} 1.7 & 1.2 \\ 1.2 & 1.08 \end{bmatrix} \end{aligned} \quad (4.50)$$

Let us calculate the losses for a total equivalent load current of -10 A. (Note that $I_{L_{eq}} = -10$ results in $I_2 = -4$, $I_3 = -6$, as before.) Then

$$\begin{bmatrix} E_1 \\ E_{L_{eq}} \end{bmatrix} = \begin{bmatrix} 1.7 & 1.2 \\ 1.2 & 1.08 \end{bmatrix} \begin{bmatrix} I_1 \\ I_{L_{eq}} \end{bmatrix} = \begin{bmatrix} 1.7 & 1.2 \\ 1.2 & 1.08 \end{bmatrix} \begin{bmatrix} 10 \\ -10 \end{bmatrix} = \begin{bmatrix} 5 \\ 1.2 \end{bmatrix} \quad (4.51)$$

and the losses are

$$E_{new}^T I_{new}^* = [5 \quad 1.2] \begin{bmatrix} 10 \\ -10 \end{bmatrix} = 38 \text{ W} \quad (4.52)$$

If we further make the assumption that $I_L = -I_1$, that is, the equivalent load current will always be the negative of the generator current. [Note: The next new reference frame is designed with a prime (I' , E' , etc.)] Then

$$I_{new} = [C] I_{new}' \quad (4.53)$$

$$\begin{bmatrix} I_1 \\ I_{L_{eq}} \end{bmatrix} = \begin{bmatrix} 1 \\ -1 \end{bmatrix} I_1'$$

$$E_{new} = [1 \quad -1] \begin{bmatrix} E_1 \\ E_{L_{eq}} \end{bmatrix}$$

$$[Z'_{new}] = [1 \quad -1] \begin{bmatrix} 1.7 & 1.2 \\ 1.2 & 1.08 \end{bmatrix} \begin{bmatrix} 1 \\ -1 \end{bmatrix} = 0.38$$

if as before $I_1 = 10$ A. Then

$$E_{new} = 3.8 \text{ V}$$

and

$$E_{new}^T I_{new}' = (3.8)(10) = 38 \text{ W} \quad (4.54)$$

By following this procedure we have reduced the effort to compute losses. As long as the load currents "conform" as in the derivation, the losses can be calculated using only the generator input current itself. This concept is extended to an electric power system to allow losses to be calculated using only the megawatt input for each of the system's generators.

4.2.3.2 Loss-Matrix Calculation

There are different methods for calculating a loss matrix. One of these methods is shown in detail in Appendix B to this chapter. This discussion will simply highlight some of the types of transformations and calculations used in loss-matrix algorithms. The first assumption usually made is that the load at each bus

conforms to the total load. That is,

$$P_{load_i} = \ell_i P_{total\ load} + P_{load_i}^0 \quad (4.55)$$

Since the load on the network buses is represented by complex load currents, we can more properly write

$$I_i^L = \ell_i I_L + I_i^0 \quad (4.56)$$

where I_i^L = load current at bus i

ℓ_i = complex load distribution factor for bus i

I_L = total system load current

I_i^0 = base or constant load current at bus i

Similarly, the generator real and reactive powers are assumed to be related to each other by a constant, S_i .

$$Q_i^G = Q_i^{G0} + S_i P_i^G \quad (4.57)$$

The S_i , Q_i^{G0} , ℓ_i , and I_i^0 quantities are derived from two load-flow calculations, one called the "base" the other called the "off-base." These load-flow calculations are run at loading conditions typically found on the network. The base-load flow may, for example, correspond to the system's peak load conditions and the off-base to its low load conditions.

The ℓ_i factors are used in a series of transformations on the network impedance matrix to eliminate the individual load currents (see Example 4F). The S_i factors together with the voltage magnitudes and phase angles at the generator buses are used to convert generator bus currents to generator bus real powers. Thus, the basic system voltage-current relationship

$$V = [Z]I \quad (4.58)$$

is used to set up an equation for losses.

$$\begin{aligned} P_{loss} &= R_e \{ P_{loss} - jQ_{loss} \} \\ &= R_e \{ I^* [Z] I \} \end{aligned} \quad (4.59)$$

and the transformations just described give a final expression:

$$P_{loss} = P^G [B] P^G + B_0 P^G + B_{00} \quad (4.60)$$

where P^G is a vector of generator real powers and B , B_0 , B_{00} are the loss-matrix terms that are a function of the $[Z]$ matrix elements, the base-case load flow, voltages and phase angles, as well as the ℓ_i 's, and S_i 's.

The calculations are not simple, as even a casual reading of Appendix B will show. Further, it must be remembered that the assumptions of conforming load and conforming generator reactive power are never seen exactly on a real system; therefore, the loss matrix will always remain an approximation. Nonetheless, loss

matrices are widely used because of their convenience and the speed with which losses and incremental losses can be calculated.

4.2.4 Other Methods of Calculating Penalty Factors

4.2.4.1 A Discussion of Reference Bus versus Load Center Penalty Factors

The B matrix assumes that all load currents conform to an equivalent total load current and that the equivalent load current is the negative of the sum of all generator currents. When incremental losses are calculated, something is implied.

$$\text{Total loss} = \mathbf{P}^T[\mathbf{B}]\mathbf{P} + \mathbf{B}_0\mathbf{P} + B_{00}$$

$$\text{Incremental loss at generator bus } i = \frac{\partial P_{\text{loss}}}{\partial P_i}$$

The incremental loss is the change in losses when an increment is made in generation output. As just derived, the incremental loss for bus i assumed that all the other generators remained fixed. By the original assumption, however, the load currents all conform to each other and always balance with the generation, then the implication in using a B matrix is that an incremental increase in generator output is matched by an equivalent increment in load.

An alternative approach to economic dispatch is to use a reference bus that always moves when an increment in generation is made. Figure 4.19 shows a power system with several generator buses and a reference-generator bus. Suppose we change the generation on bus i by ΔP_i ,

$$P_i^{\text{new}} = P_i^{\text{old}} + \Delta P_i \quad (4.61)$$

Furthermore, we will assume that load stays constant and that to compensate for the increase in ΔP_i the reference bus just drops off by ΔP_{ref} .

$$P_{\text{ref}}^{\text{new}} = P_{\text{ref}}^{\text{old}} + \Delta P_{\text{ref}} \quad (4.62)$$

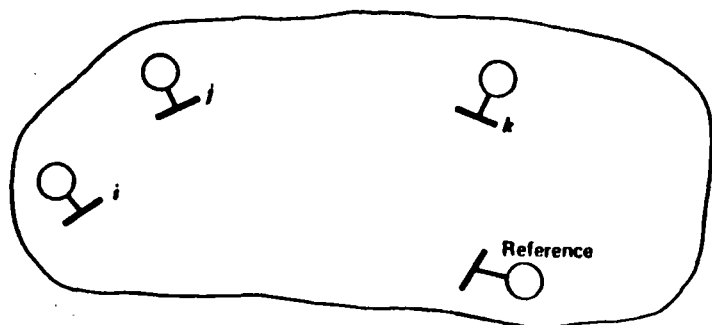


FIG. 4.19 Power system with reference generator.

If nothing else changed, ΔP_{ref} would be the negative of ΔP_i ; however, the flows on the system can change as a result of the two generation adjustments. The change in flow is apt to cause a change in losses so that ΔP_{ref} is not necessarily equal to ΔP_i . That is,

$$\Delta P_{\text{ref}} = -\Delta P_i + \Delta P_{\text{loss}} \quad (4.63)$$

Next, we can define β_i as the ratio of the negative change in the reference-bus power to the change ΔP_i .

$$\beta_i = \frac{-\Delta P_{\text{ref}}}{\Delta P_i} = \frac{(\Delta P_i - \Delta P_{\text{loss}})}{\Delta P_i} \quad (4.64)$$

or

$$\beta_i = 1 - \frac{\partial P_{\text{loss}}}{\partial P_i} \quad (4.65)$$

We can define economic dispatch as follows.

All generators are in economic dispatch when a shift of ΔP MW from any generator to the reference bus results in no change in net production cost. Where ΔP is arbitrarily small.

That is,

$$\text{if total production cost} = \sum F_i(P_i)$$

then the change in production cost with a shift ΔP_i from plant i is

$$\Delta \text{Production cost} = \frac{dF_i(P_i)}{dP_i} \Delta P_i + \frac{dF_{\text{ref}}(P_{\text{ref}})}{dP_{\text{ref}}} \Delta P_{\text{ref}} \quad (4.66)$$

But

$$\Delta P_{\text{ref}} = -\beta_i \Delta P_i$$

Then

$$\Delta \text{Production cost} = \frac{dF_i(P_i)}{dP_i} \Delta P_i - \beta_i \frac{dF_{\text{ref}}(P_{\text{ref}})}{dP_{\text{ref}}} \Delta P_i \quad (4.67)$$

To satisfy the economic conditions,

$$\Delta \text{Production cost} = 0$$

or

$$\frac{dF_i(P_i)}{dP_i} = \beta_i \frac{dF_{\text{ref}}(P_{\text{ref}})}{dP_{\text{ref}}} \quad (4.68)$$

which could be written

$$\frac{1}{\beta_i} \frac{dF_i(P_i)}{dP_i} = \frac{dF_{ref}(P_{ref})}{dP_{ref}} \quad (4.69)$$

This is very similar to Eq. 4.28. To obtain an economic dispatch solution, pick a value of generation on the reference bus and then set all other generators according to Eq. 4.69 and check for total demand and readjust reference generation as needed until a solution is reached.

Note further that this method is exactly the first-order gradient method (Section 4) with losses. Where (see Eq. 3.14 and substitute *ref* for *x*)

$$\Delta F_T = \sum_{i=ref} \left[\frac{dF_i}{dP_i} - \beta_i \frac{dF_{ref}}{dP_{ref}} \right] \Delta P_i \quad (4.70)$$

4.2.4 Reference-Bus Penalty Factors Direct from the AC Load Flow

The reference-bus penalty factors may be derived using the Newton-Raphson load flow. What we wish to know is the ratio of change in power on the reference bus when a change ΔP_i is made.

where P_{ref} is a function of the voltage magnitude and phase angle on the network. When a change in ΔP_i is made, all phase angles and voltages in the network will change

then

$$\begin{aligned} \Delta P_{ref} &= \sum_T \frac{\partial P_{ref}}{\partial \theta_i} \Delta \theta_i + \sum_T \frac{\partial P_{ref}}{\partial |E_i|} \Delta |E_i| \\ &= \sum_T \frac{\partial P_{ref}}{\partial \theta_i} \frac{\partial \theta_i}{\partial P_i} \Delta P_i + \sum_T \frac{\partial P_{ref}}{\partial |E_i|} \frac{\partial |E_i|}{\partial P_i} \Delta P_i \end{aligned} \quad (4.71)$$

To carry out the matrix manipulations, we will also need the following.

$$\begin{aligned} \Delta P_{ref} &= \sum_T \frac{\partial P_{ref}}{\partial \theta_i} \Delta \theta_i + \sum_T \frac{\partial P_{ref}}{\partial |E_i|} \Delta |E_i| \\ &= \sum_T \frac{\partial P_{ref}}{\partial \theta_i} \frac{\partial \theta_i}{\partial Q_i} \Delta Q_i + \sum_T \frac{\partial P_{ref}}{\partial |E_i|} \frac{\partial |E_i|}{\partial Q_i} \Delta Q_i \end{aligned} \quad (4.72)$$

The terms $\partial P_{ref}/\partial \theta_i$ are derived by differentiating Eq. 4.18 for the reference bus. The terms $\partial \theta_i/\partial P_i$ and $\partial |E_i|/\partial P_i$ are from the inverse Jacobian matrix (see Eq. 4.20). We can write Eqs. 4.71 and 4.72 for every bus *i* in the network. The resulting equation is

$$\begin{aligned} &\begin{bmatrix} \frac{\partial P_{ref}}{\partial P_1} & \frac{\partial P_{ref}}{\partial Q_1} & \frac{\partial P_{ref}}{\partial P_2} & \frac{\partial P_{ref}}{\partial Q_2} & \dots & \frac{\partial P_{ref}}{\partial P_N} & \frac{\partial P_{ref}}{\partial Q_N} \end{bmatrix} \\ &= \begin{bmatrix} \frac{\partial P_{ref}}{\partial \theta_1} & \frac{\partial P_{ref}}{\partial |E_1|} & \frac{\partial P_{ref}}{\partial \theta_2} & \frac{\partial P_{ref}}{\partial |E_2|} & \dots & \frac{\partial P_{ref}}{\partial \theta_N} & \frac{\partial P_{ref}}{\partial |E_N|} \end{bmatrix} [J^{-1}] \end{aligned} \quad (4.73)$$

By transposing we get

$$\begin{bmatrix} \frac{\partial P_{ref}}{\partial P_1} \\ \frac{\partial P_{ref}}{\partial Q_1} \\ \frac{\partial P_{ref}}{\partial P_2} \\ \frac{\partial P_{ref}}{\partial Q_2} \\ \vdots \\ \frac{\partial P_{ref}}{\partial P_N} \\ \frac{\partial P_{ref}}{\partial Q_N} \end{bmatrix} = [J^T]^{-1} \begin{bmatrix} \frac{\partial P_{ref}}{\partial \theta_1} \\ \frac{\partial P_{ref}}{\partial |E_1|} \\ \frac{\partial P_{ref}}{\partial \theta_2} \\ \frac{\partial P_{ref}}{\partial |E_2|} \\ \vdots \\ \frac{\partial P_{ref}}{\partial \theta_N} \\ \frac{\partial P_{ref}}{\partial |E_N|} \end{bmatrix}$$

In practice, instead of calculating J^T explicitly, we use Gaussian elimination on J^T in the same way we operate on J in the Newton load-flow solution.

4.2.4.3 Reference-Bus Penalty Factors Using the DC Load Flow

The real (MW) losses on a transmission line (where $R_r(\)$ = real part of) are

$$R_r(\text{loss}_{ij}) = [|E_i|^2 + |E_j|^2 - 2|E_i||E_j| \cos(\theta_i - \theta_j)] R_r(Y_{ij}) \quad (4.74)$$

Taking the derivatives with respect to θ_i and θ_j ,

$$\begin{aligned} \frac{\partial P_{\text{loss}_{ij}}}{\partial \theta_i} &= 2|E_i||E_j| \sin(\theta_i - \theta_j) R_r(Y_{ij}) \\ \frac{\partial P_{\text{loss}_{ij}}}{\partial \theta_j} &= -2|E_i||E_j| \sin(\theta_i - \theta_j) R_r(Y_{ij}) \end{aligned} \quad (4.75)$$

We can calculate incremental losses for the entire system by first obtaining the change in phase angle at every bus with a change in bus power injection and then multiplying these derivatives times the derivative in Eq. 4.75 and adding the contribution for all lines. That is,

$$\Delta P_{\text{loss}} = \sum_{\text{All lines } l} \frac{\partial P_{\text{loss on line } l}}{\partial \theta_j} \frac{\partial \theta_j}{\partial P_i} \Delta P_i \quad (4.76)$$

To facilitate matrix operations, we will sum over all buses and then over all lines attached to each bus.

$$\frac{\Delta P_{\text{loss}}}{\Delta P_i} = \sum_j \left[\sum_{\substack{\text{All lines } \ell \\ \text{attached to} \\ \text{bus } j}} \frac{\partial P_{\text{loss line } \ell}}{\partial \theta_j} \right] \frac{\partial \theta_j}{\partial P_i} \quad (4.77)$$

The terms $\partial \theta_j / \partial P_i$ are in the columns of the X matrix given in Eq. 4.25b. That is,

$$\begin{bmatrix} \Delta \theta_1 \\ \Delta \theta_2 \\ \vdots \end{bmatrix} = \begin{bmatrix} \partial \theta_1 / \partial P_1 & \partial \theta_1 / \partial P_2 & \cdots \\ \vdots & \vdots & \vdots \end{bmatrix} \begin{bmatrix} \Delta P_1 \\ \Delta P_2 \\ \vdots \end{bmatrix} \quad (4.78)$$

Then Eq. 4.77 can be written

$$\begin{bmatrix} \frac{\partial P_{\text{loss}}}{\partial P_1} \\ \frac{\partial P_{\text{loss}}}{\partial P_2} \\ \vdots \end{bmatrix} = \begin{bmatrix} \partial \theta_1 & \partial \theta_2 & \cdots \\ \vdots & \vdots & \vdots \end{bmatrix}^T \begin{bmatrix} \frac{\partial P_{\text{loss}}}{\partial \theta_1} \\ \frac{\partial P_{\text{loss}}}{\partial \theta_2} \\ \vdots \end{bmatrix} \quad (4.79)$$

where the right-hand side vector terms come from the bracketed terms in Eq. 4.77. Where

$$\frac{\partial P_{\text{loss}}}{\partial \theta_j} = \sum_{\substack{\text{All lines } \ell \\ \text{attached to} \\ \text{bus } j}} \frac{\partial P_{\text{loss line } \ell}}{\partial \theta_j} \quad (4.80)$$

Also note that the matrix in Eq. 4.79 is the transpose of the $[X]$ matrix. Incremental losses derived by Eq. 4.79 are very nearly the same as those derived by Eq. 4.73, but the solution of Eq. 4.79 is much faster.

4.2.4.4 Mathematical Relationship of Loss-Matrix Penalty Factors and Reference-Bus Penalty Factors

Suppose we are given a loss matrix from which we can calculate incremental losses $\partial P_{\text{loss}} / \partial P_i$ for each generator bus in a network. Assume that for a change ΔP_i in generation at bus i a compensating change in load, $\Delta P_{\text{load},i}$, will take place at an "equivalent load center" bus. We are going to look at such a shift for two separate generator buses with each shift taken independently. We will call the first generator bus, bus i , and the second, bus r . For the first shift, from bus i , see Figure 4.20, where

$$\Delta P_i = \Delta P_{\text{loss},i} + \Delta P_{\text{load},i} \quad (4.81)$$

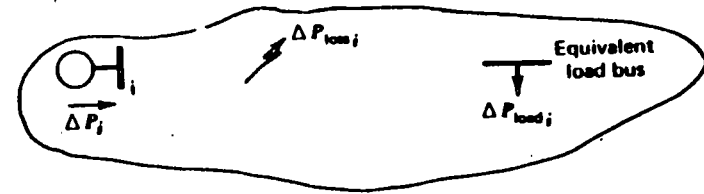


FIG. 4.20 Change at equivalent load bus and bus i .

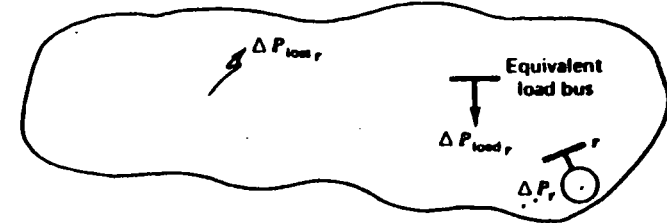


FIG. 4.21 Change at equivalent load bus and reference bus.

If we approximate $\Delta P_{\text{loss},i} / \Delta P_i$ using $\partial P_{\text{loss}} / \partial P_i$ from the loss matrix, we can write Eq. 4.81 as

$$\Delta P_{\text{load},i} = \left(1 - \frac{\partial P_{\text{loss}}^*}{\partial P_i} \right) \Delta P_i \quad (4.82)$$

where the asterisk (*) indicates an incremental loss calculated from a loss matrix. Similarly, we can do the same thing, independently, for bus r (see Figure 4.21), where

$$\Delta P_r = \Delta P_{\text{loss},r} + \Delta P_{\text{load},r} \quad (4.83)$$

and again we approximate $\Delta P_{\text{loss},r} / \Delta P_r$ as $\partial P_{\text{loss}} / \partial P_r$ from the loss matrix. Then,

$$\Delta P_{\text{load},r} = \left(1 - \frac{\partial P_{\text{loss}}^*}{\partial P_r} \right) \Delta P_r \quad (4.84)$$

Now suppose we carry out these two steps in sequence as follows. First, we carry out the step shown in Eq. 4.82 so that $\Delta P_{\text{load},i}$ exactly compensates for the change ΔP_i and the change in losses. Then we adjust ΔP_r so that $\Delta P_{\text{load},r}$ is precisely the negative of $\Delta P_{\text{load},i}$. That is,

$$\Delta P_{\text{load},r} = -\Delta P_{\text{load},i} \quad (4.85)$$

Then,

$$\left(1 - \frac{\partial P_{\text{loss}}^*}{\partial P_r} \right) \Delta P_r = -\left(1 - \frac{\partial P_{\text{loss}}^*}{\partial P_i} \right) \Delta P_i \quad (4.86)$$

By performing this sequence, we have artificially created the actions that constitute the basis for reference-bus penalty factors. That is, we have increased generation at bus i by ΔP_i and compensated with a change ΔP_r at a reference bus while holding load constant. By definition (see Eq. 4.64),

$$\beta_i = \frac{-\Delta P_r}{\Delta P_i} \quad (4.87)$$

but by manipulating Eq. 4.86,

$$\beta_i = \frac{-\Delta P_r}{\Delta P_i} = \frac{(1 - \partial P_{\text{loss}}^* / \partial P_i)}{(1 - \partial P_{\text{loss}}^* / \partial P_r)} \quad (4.88)$$

If we define penalty factors as

$$Pf_i^{\text{loss matrix}} = \frac{1}{1 - \frac{\partial P_{\text{loss}}^*}{\partial P_i}} \quad (4.89)$$

and

$$Pf_i^{\text{ref bus}} = \frac{1}{\beta_i} \quad (4.90)$$

Then,

$$\begin{aligned} Pf_i^{\text{ref bus}} &= \left(1 - \frac{\partial P_{\text{loss}}^*}{\partial P_r}\right) \left(\frac{1}{1 - \frac{\partial P_{\text{loss}}^*}{\partial P_i}}\right) \\ &= \left(1 - \frac{\partial P_{\text{loss}}^*}{\partial P_r}\right) Pf_i^* \end{aligned} \quad (4.91)$$

Thus we can see that the reference-bus penalty factors are simply a constant times the loss-matrix penalty factors. Furthermore, it should be realized that this means that an economic dispatch calculation performed with either reference-bus penalty factors or loss-matrix penalty factors will produce the same generation dispatch and only differ in the value of λ .

APPENDIX A Load Flow Input Data

Figure 4.22 lists the input data to the six-bus sample power system used in the examples in Chapter 4.

LINE DATA

FROM	TO	R	X	BCAP*
1	2	0.1000	0.2000	0.0200
1	4	0.0500	0.2000	0.0200
1	5	0.0800	0.3000	0.0300
2	3	0.0500	0.2500	0.0300
2	4	0.0500	0.1000	0.0100
2	5	0.1000	0.3000	0.0200
2	6	0.0700	0.2000	0.0250
3	5	0.1200	0.2600	0.0250
3	6	0.0200	0.1000	0.0100
4	5	0.2000	0.4000	0.0400
5	6	0.1000	0.3000	0.0300

BUS DATA

BUS NO.	GEN (PU MW)	VOLTAGE (PU KV)	P LOAD (PU MW)	Q LOAD (PU MVAR)
SWING 1	0.00	1.050	0.00	0.00
2	0.50	1.050	0.00	0.00
3	0.60	1.070	0.00	0.00
4	0.00	1.000	0.70	0.70
5	0.00	1.000	0.70	0.70
6	0.00	1.000	0.70	0.70

* BCAP = 1/2 Total line charging

FIG. 4.22 Input data to a six-bus sample power system.

APPENDIX B Derivation of the B Matrix Loss Formula

The B matrix loss formula is developed using a series of transformations on the full-impedance matrix of the transmission system network. The derivation that follows is taken from the paper by Meyer (7). A computer program based on this technique was used to derive the loss formula shown in Example 4D. The derivation in Meyer's paper is related to much earlier pioneering work by Kron (4) and Early and Watson (6), which should be consulted to appreciate Meyer's method fully.

To start, assume that the N transmission system buses are divided up into M generator buses and $N - M$ load buses. The generator buses are ordered $1 \cdots M$, and the load buses $M + 1 \cdots N$. The network is shown in Figure 4.23. The basic relationships between the voltages and currents will be stated throughout the derivation using the impedance (Z) matrix. Meyer's paper should be consulted for specific computational details involving the Z matrix terms.

Our first relationship is then

$$V = [Z]I \quad (4B.1)$$

where V and I are $N \times 1$ vectors and $[Z]$ is an $N \times N$ matrix. The total real and reactive losses in the network may be expressed as

$$P_{\text{loss}} + jQ_{\text{loss}} = I^*TV = I^*[Z]I \quad (4B.2)$$

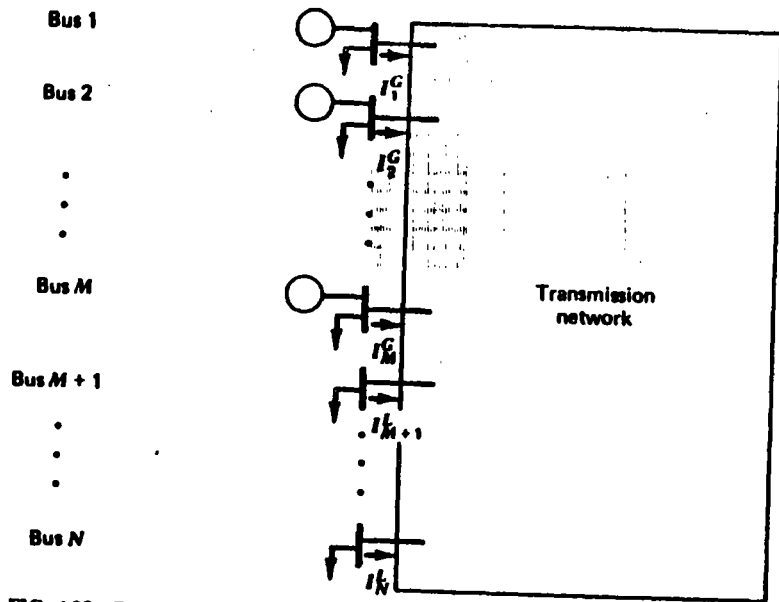


FIG. 4.23 Representation of loads and generators attached to a transmission network.

Since we are only interested in the real power losses, we will use

$$P_{\text{loss}} = R_s \{ \mathbf{I}^{*T} [\mathbf{Z}] \mathbf{I} \} \quad (4B.3)$$

Each bus-current injection consists of two components, the generation component and the load component designated I_i^G and I_i^L , respectively. Then

$$I_i = I_i^G + I_i^L \quad \text{for } i = 1 \cdots N \quad (4B.4)$$

where by our ordering of buses $I_i^G = 0$ for $i = M + 1 \cdots N$.

Further, the load currents will be modeled as a linear function of the total load current I_L . This is similar to the "conforming load" assumption used in Example 4F. Then

$$I_i^L = \ell_i I_L + I_i^0 \quad (4B.5)$$

where I_i^L = load current at bus i

ℓ_i = load distribution factor for bus i (ℓ_i is complex)

I_L = total system load current

I_i^0 = constant or base-load current at bus i

Now we can begin to use transformations as follow.

$$\mathbf{I} = [\mathbf{C}_1] \mathbf{I}_2 + \mathbf{I}^0 \quad (4B.6)$$

or

$$\begin{bmatrix} I_1 \\ \vdots \\ I_M \\ I_{M+1} \\ \vdots \\ I_N \end{bmatrix} = \begin{bmatrix} \diagdown & & & & \\ & \diagdown & & & \\ & & \diagdown & & \\ & & & \diagdown & \\ & & & & 0 \end{bmatrix} \begin{bmatrix} I_1 \\ \vdots \\ I_M \\ I_{M+1} \\ \vdots \\ I_N \end{bmatrix} + \begin{bmatrix} I_1^G \\ \vdots \\ I_M^G \\ I_L \\ \vdots \\ I_N^G \end{bmatrix} + \begin{bmatrix} I_1^0 \\ \vdots \\ I_M^0 \\ I_{M+1}^0 \\ \vdots \\ I_N^0 \end{bmatrix}$$

where \mathbf{I}_2 is a vector as shown with the first N elements equal to the N generator currents and the $N + 1$ element equal to the total load current I_L . Substituting (4B.6) into (4B.3), gives

$$P_{\text{loss}} = R_s \{ (\mathbf{I}_2^{*T} [\mathbf{C}_1]^{*T} + \mathbf{I}^{0*T}) [\mathbf{Z}] ([\mathbf{C}_1] \mathbf{I}_2 + \mathbf{I}^0) \} \quad (4B.7)$$

which on being expanded has four terms.

$$P_{\text{loss}} = R_s \{ H_1 + H_2 + H_3 + H_4 \} \quad (4B.8)$$

where $H_1 = \mathbf{I}_2^{*T} [\mathbf{C}_1]^{*T} [\mathbf{Z}] [\mathbf{C}_1] \mathbf{I}_2$

$$H_2 = \mathbf{I}^{0*T} [\mathbf{Z}] \mathbf{I}^0$$

$$H_3 = \mathbf{I}^{0*T} [\mathbf{Z}] [\mathbf{C}] \mathbf{I}_2$$

$$H_4 = \mathbf{I}_2^{*T} [\mathbf{C}]^{*T} [\mathbf{Z}] \mathbf{I}^0$$

It should be observed here that the H_1 term contributes only to the quadratic part (B_{ij}) of the loss formula, H_2 contributes to the constant part (B_{00}), and H_3 and H_4 contribute to the linear part (B_{i0}).

Before proceeding, we will observe two assumptions that are built into this loss-formula derivation. The first assumes that each generator's reactive power is a linear function of its real power output. That is,

$$Q_i^G = Q_i^{G0} + S_i P_i^G \quad (4B.9)$$

The value of S_i is quite important and must be obtained carefully. The usual procedure is to run base and off-base load-flow calculations that differ by the amount of load on the network. Each generator's S_i value and each load's ℓ_i and I_i^0 values are derived from the two load flows.

We use the S_i factors together with the bus voltage magnitudes and phase angles from the base-load flow as follows:

$$I_i^G = \left(\frac{d_1}{|V_i|} + j \frac{d_2}{|V_i|} \right) P_i^G \quad (4B.10)$$

Note that we have ignored the Q_i^{G0} by simply lumping it into the load bus reactive power. The d_1 and d_2 terms are

$$d_1 = \cos \theta_i + S_i \sin \theta_i \quad (4B.11)$$

$$d_2 = \sin \theta_i + S_i \cos \theta_i$$

The second assumption built into the calculation concerns the reference-bus voltage. This voltage is assumed known and constant as loading varies on the system. Let $i = r$ be the reference bus for the network. It is normal practice to have r be one of the generator buses. Then

$$V_r = \sum_{i=1}^M z_{ri} I_i^G + I_L \sum_{i=1}^N z_{ri} + \sum_{i=1}^N z_{ri} I_i^D \quad (4B.12)$$

We can use 4B.12 to eliminate I_L from our equations.

$$I_L = - \sum_{i=1}^M T_i I_i^G + T^* \bar{V}_r \quad (4B.13)$$

where $T_i = \frac{z_{ri}}{\sum_{j=1}^N z_{rj}}$

$$T^* = \frac{1}{\sum_{j=1}^N z_{rj}}$$

$$\bar{V}_r = V_r - \sum_{i=1}^M z_{ri} I_i^G$$

Using 4B.13, we can build another transformation on I_2 .

$$I_2 = [C_2] I_2' \quad (4B.14)$$

or

$$\begin{bmatrix} I_1^G \\ \vdots \\ I_M^G \\ I_L \end{bmatrix} = \begin{bmatrix} 1 & & 0 \\ & \ddots & \\ & & 1 & 0 \\ -T_1 & \cdots & -T_M & T^* \end{bmatrix} \begin{bmatrix} I_1^G \\ \vdots \\ I_M^G \\ V_r \end{bmatrix}$$

Now we can start to reduce H_1 through H_4 . First, H_1 ; using 4B.14, H_1 becomes

$$\begin{aligned} H_1 &= I_2^{*T} [C_2]^{*T} [C_1]^{*T} [Z] [C_1] [C_2] I_2' \\ &= I_2^{*T} [Z^3] I_2' \end{aligned} \quad (4B.15)$$

where

$$[Z^3] = [C_2]^{*T} [C_1]^{*T} [Z] [C_1] [C_2]$$

We can reduce H_2 to

$$H_2 = I^{0*T} V^A \quad (4B.16)$$

where

$$V^A = [Z] I^0$$

Then

$$R_e \{H_2\} = \sum_{i=1}^M R_e \{I_i^{0*} V_i^A\} \quad (4B.17)$$

H_3 and H_4 will be treated together. First, since H_3 and H_4 are scalars,

$$\begin{aligned} R_e \{H_3 + H_4\} &= R_e \{H_3^T + H_4^T\} \\ &= R_e \{I_2^{*T} [C_1]^{*T} [Z] I^{0*} + I_2^{*T} [C_1]^{*T} [Z]^{*} I^{0*}\} \\ &= R_e \{I_2^{*T} \underbrace{([C_1]^{*T} [Z] I^{0*} + [C_1]^{*T} [Z]^{*} I^{0*})}_{V^D}\} \end{aligned} \quad (4B.18)$$

where

$$V^D = [C_1]^{*T} \underbrace{[Z] I^{0*}}_{V^D} + \underbrace{[Z]^{*} I^{0*}}_{V^A} \quad (4B.19)$$

Then

$$\begin{aligned} R_e \{H_3 + H_4\} &= R_e \{I_2^{*T} V^D\} \\ &= R_e \left\{ \sum_{i=1}^M I_i^G V_i^D + V_{M+1}^D I_2 \right\} \end{aligned} \quad (4B.20)$$

and using 4B.13,

$$R_e \{H_3 + H_4\} = R_e \left\{ \sum_{i=1}^M (V_i^D - V_{M+1}^D T_i) I_i^G + V_{M+1}^D T^* \bar{V}_r \right\} \quad (4B.21)$$

We can now write out the terms in the loss matrix.

$$\begin{aligned} B_{ij} &= \frac{(R_{ij}^3 + R_{ji}^3)}{2} \left[\frac{(1 + S_i S_j) \cos(\theta_i - \theta_j) + (S_i - S_j) \sin(\theta_i - \theta_j)}{|V_i| |V_j|} \right] \\ &\quad + \frac{(X_{ij}^3 - X_{ji}^3)}{2} \left[\frac{(1 + S_i S_j) \sin(\theta_i - \theta_j) + (S_i - S_j) \cos(\theta_i - \theta_j)}{|V_i| |V_j|} \right] \end{aligned} \quad (4B.22)$$

$$\begin{aligned} B_{i0} &= \frac{1}{|V_i|} [(R_e \{\bar{V}_r\} d_{i0} - I_m \{\bar{V}_r\} d_{i0} + R_e \{\zeta\} d_i \\ &\quad + R_e \{\bar{V}_r\} d_{i0} + I_m \{\bar{V}_r\} d_{i0} - I_m \{\zeta\} d_i] \\ B_{00} &= |\bar{V}_r|^2 R_e \{\Psi\} + \sum_{i=1}^M R_e \{I_i^{0*} V_i^A\} + R_e \{V_{M+1}^D T^* \bar{V}_r\} \end{aligned}$$

where R^3, X^3 are elements from $[Z^3]$ [see Eq. 4B.15].

S_i, S_j are as defined in Eq. 4B.9.

\bar{V}_r is defined in Eq. 4B.13.

$|V_i|, |V_j|, \theta_i, \theta_j$ are from the base-load flow.

$$d_{i0} = R_e \{T^*(a_i - T_i^* \omega) + T^{**}(b_j - T_j^* \omega)\}$$

$$d_{00} = I_m \{T^*(a_i - T_i^* \omega) + T^{**}(b_j - T_j^* \omega)\}$$

$$\text{where } a_i = \sum_{j=1}^N z_{ij} f_j$$

$$b_j = \sum_{i=1}^N z_{ij} f_i^2$$

$$\omega = \sum_{i=1}^N l_i^2 a_i$$

$$\zeta = V_i^D - T_i V_{M+1}^D \quad \text{where } V^D \text{ is defined in Eq. 4B.19}$$

$$\Psi = T^* T^* \omega$$

and V^A is defined in Eq. 4B.16

APPENDIX C

Jacobian Matrix in the Newton Power Flow

The Jacobian matrix in Eq. 4.20 and the transpose Jacobian shown in Eq. 4.73 both start with the equation for the real and reactive power at each bus. This equation, shown in the text as Eq. 4.18, is repeated here.

$$P_i + jQ_i = E_i \sum_{k=1}^N Y_{ik}^* E_k^* \quad (4C.1)$$

This can be expanded as

$$P_i + jQ_i = \sum_{k=1}^N |Y_{ik}| |E_i| |E_k| e^{j(\theta_i - \theta_k - \theta_{ik})} \quad (4C.2)$$

where θ_i, θ_k = phase angle at buses i and k , respectively

$$\theta_{ik} = \arctan \frac{B_{ik}}{G_{ik}}$$

$|E_i|, |E_k|$ = magnitude of E_i and E_k , respectively

$$|Y_{ik}| = \sqrt{G_{ik}^2 + B_{ik}^2}$$

General practice in solving load flows by the Newton method has been to use $\Delta|E_i|/|E_i|$ instead of simply $\Delta|E_i|$. This simplifies writing the equations. The derivatives are

For $i \neq k$:

$$\begin{aligned} \frac{\partial P_i}{\partial \theta_k} &= |Y_{ik}| |E_i| |E_k| \sin(\theta_i - \theta_k - \theta_{ik}) \\ &= (a_k f_i - b_k e_i) \\ \frac{\partial P_i}{\partial |E_k|} &= |Y_{ik}| |E_i| |E_k| \cos(\theta_i - \theta_k - \theta_{ik}) \\ &= (a_k e_i + b_k f_i) \end{aligned} \quad (4C.3)$$

$$\text{where } a_k + jb_k = (e_k + jf_k)(G_{ik} + jB_{ik})$$

$$e_k = R_{ik}(E_k)$$

$$f_k = I_{ik}(E_k)$$

and

$$\frac{\partial Q_i}{\partial \theta_k} = -\frac{\partial P_i}{\partial |E_k|} \frac{|E_k|}{|E_i|}$$

$$\frac{\partial Q_i}{\partial |E_k|} = \frac{\partial P_i}{\partial \theta_k}$$

For $i = k$:

$$\frac{\partial P_i}{\partial \theta_i} = -Q_i - B_{ii} E_i^2$$

$$\frac{\partial P_i}{\partial |E_i|} = P_i + G_{ii} E_i^2$$

$$\frac{\partial Q_i}{\partial \theta_i} = P_i - G_{ii} E_i^2$$

$$\frac{\partial Q_i}{\partial |E_i|} = Q_i - B_{ii} E_i^2$$

Equation 4.20 now becomes

$$\begin{bmatrix} \Delta P_1 \\ \Delta Q_1 \\ \Delta P_2 \\ \Delta Q_2 \\ \vdots \end{bmatrix} = [J] \begin{bmatrix} \Delta \theta_1 \\ \frac{\Delta |E_1|}{|E_1|} \\ \Delta \theta_2 \\ \frac{\Delta |E_2|}{|E_2|} \\ \vdots \end{bmatrix}$$

Similarly for Eq. 4.73.

PROBLEMS

4.1 The circuit elements in the 138 kV circuit in Figure 4.24 are in per unit on a 100 MVA base with the nominal 138 kV voltage as base. The $P + jQ$ load is scheduled to be 170 MW and 50 MVAR.

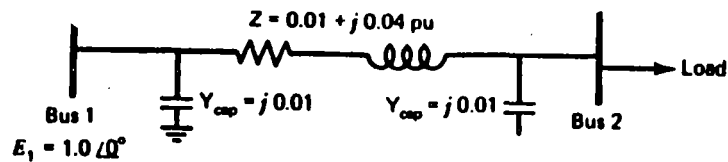


FIG. 4.24 Two-bus ac system for Problem 4.1.

- Write the Y matrix for this two-bus system.
- Assume bus 1 as the reference bus and set up the Gauss-Seidel correction equation for bus 2. (Use $1.0 \angle 0^\circ$ as the initial voltage on bus 2.) Carry out two or three iterations and show that you are converging.
- Apply the "DC" load flow conventions to this circuit and solve for the phase angle at bus 2 for the same load real power of 1.7 per unit.

4.2 Given the network in Figure 4.25 (base = 100 MVA):

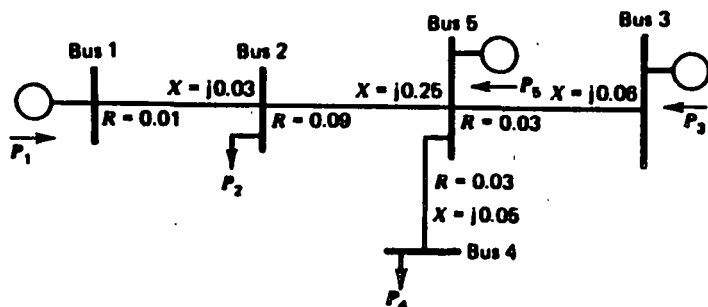


FIG. 4.25 Four-bus network for Problem 4.2.

- Develop the $[B_x]$ matrix for this system.

$$\begin{bmatrix} P_1 \\ P_2 \\ P_3 \\ P_4 \\ P_5 \end{bmatrix} = [B_x] \begin{bmatrix} \theta_1 \\ \theta_2 \\ \theta_3 \\ \theta_4 \\ \theta_5 \end{bmatrix}$$

P in per unit MW
 θ in radians

- Assume bus 5 as the reference bus. To carry out a "DC" load flow, we will set $\theta_5 = 0$ rad. Row 5 and column 5 will be zeroed.

$$\begin{bmatrix} P_1 \\ P_2 \\ P_3 \\ P_4 \\ P_5 \end{bmatrix} = \begin{bmatrix} & & & & 0 \\ & \text{Remainder} & & & 0 \\ & \text{of } B_x & & & 0 \\ & & & & 0 \\ 0 & 0 & 0 & 0 & 0 \end{bmatrix} \begin{bmatrix} \theta_1 \\ \theta_2 \\ \theta_3 \\ \theta_4 \\ \theta_5 \end{bmatrix}$$

Solve for the X matrix.

$$\begin{bmatrix} \theta_1 \\ \theta_2 \\ \theta_3 \\ \theta_4 \\ \theta_5 \end{bmatrix} = [X] \begin{bmatrix} P_1 \\ P_2 \\ P_3 \\ P_4 \\ P_5 \end{bmatrix}$$

- Calculate the phase angles for the set of power injections.

$$P_1 = 100 \text{ MW generation}$$

$$P_2 = 120 \text{ MW load}$$

$$P_3 = 150 \text{ MW generation}$$

$$P_4 = 200 \text{ MW load}$$

- Calculate P_5 according to the "DC" load flow.
- Calculate all power flows on the system using the phase angles found in part c.
- (Optional) Calculate the reference-bus penalty factors for buses 1, 2, 3, and 4. Assume all bus voltage magnitudes are 1.0 per unit.

4.3 Given the following loss formula (use P 's in MW):

$$B_{ij} = \begin{matrix} & \begin{matrix} 1 & 2 & 3 \end{matrix} \\ \begin{matrix} 1 \\ 2 \\ 3 \end{matrix} & \begin{bmatrix} 1.36255 \cdot 10^{-4} & 1.753 \cdot 10^{-5} & 1.8394 \cdot 10^{-4} \\ 1.753 \cdot 10^{-5} & 1.5448 \cdot 10^{-4} & 2.82765 \cdot 10^{-4} \\ 1.8394 \cdot 10^{-4} & 2.82765 \cdot 10^{-4} & 1.6147 \cdot 10^{-3} \end{bmatrix} \end{matrix}$$

B_{10} and B_{00} are neglected.

Assume three units are on line and have the following characteristics:

Unit 1: $H_1 = 312.5 + 8.25 P_1 + 0.005 P_1^2$, MBtu/h

$$50 \leq P_1 \leq 250 \text{ MW}$$

Fuel cost = 1.05 $\text{\$/MBtu}$

Unit 2: $H_2 = 112.5 + 8.25 P_2 + 0.005 P_2^2$, MBtu/h

$$5 \leq P_2 \leq 150 \text{ MW}$$

Fuel cost = 1.217 $\text{\$/MBtu}$

Unit 3: $H_3 = 50 + 8.25 P_3 + 0.005 P_3^2$, MBtu/h

$$15 \leq P_3 \leq 100 \text{ MW}$$

Fuel cost = 1.1831 $\text{\$/MBtu}$

- a. No Losses Used in Scheduling
 - i. Calculate the optimum dispatch and total cost neglecting losses for $P_D = 190 \text{ MW}$.*
 - ii. Using this dispatch and the loss formula, calculate the system losses.
- b. Losses Included in Scheduling
 - i. Find the optimum dispatch for a total generation of $P_D = 109 \text{ MW}$ * using the coordination equations and the loss formula.
 - ii. Calculate the cost rate.
 - iii. Calculate the total losses using the loss formula.
 - iv. Calculate the resulting load supplied.

4.4 Given the network in Figure 4.26:

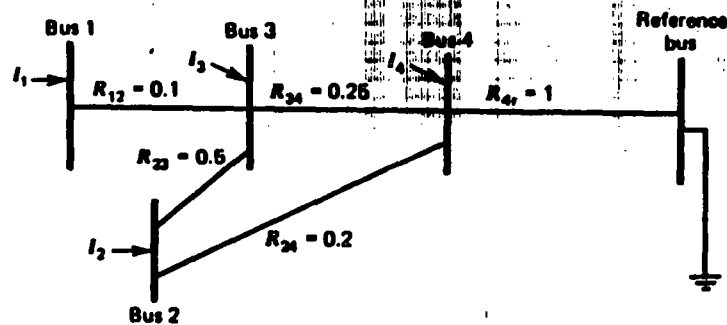


FIG. 4.26 Network for Problem 4.4.

- a. Develop the Y matrix and Z matrix equations for this network.
- b. Assume I_3 and I_4 are load-bus currents. Transform E 's and I 's and $[Z]$ to reflect a conforming load assumption.

$$I_3 = 0.35I_{L_{\text{eq}}}$$

$$I_4 = 0.65I_{L_{\text{eq}}}$$

- c. Transform to eliminate $I_{L_{\text{eq}}}$. That is, $I_{L_{\text{eq}}} = -(I_3 + I_4)$
- d. Calculate network losses for each "frame," assuming the following initial currents.

$$I_1 = 10$$

$$I_2 = 15$$

$$I_3 = -8.75$$

$$I_4 = -16.25$$

* $P_{\text{demand}} = P_1 + P_2 + P_3 = P_D$.

P_L = power loss.

$P_N = P_D - P_L$ = net load.

- e. Calculate the incremental losses for a change in current ΔI_1 at bus 1 with $I_2 = 15 \text{ A}$.

Compare the incremental loss just calculated with an approximation obtained by setting $I_1 = 11 \text{ A}$ (leave $I_2 = 15 \text{ A}$ and assuming the load currents compensate this 1-A adjustment as described in the text).

4.5 This problem requires the use of a load-flow program. Set up and solve the load-flow base case shown in Appendix A and Example 4A. You should be able to match the solution shown in Figure 4.8.

- a. Resolve the load flow with each load set to 71 MW, 71 MVAR. Require that bus 1 be the swing bus so that any change in generation will appear on bus 1 (i.e., keep generator 2 at 50 MW and generator 3 at 60 MW).
- b. Resolve the load flow with loads set as in (a). Require that bus 2 be the swing bus so that all generation change appears on bus 2 (i.e., keep generator 1 at 107.9 MW and generator 3 at 60 MW).
- c. Set all loads back to their base-case conditions of 70 MW, 70 MVAR. Increase the generation on bus 2 to 55 MW. Require bus 1 to be the swing bus and resolve the load flow (bus 3 remains at 60 MW).

In each of these three load-flow runs, you perturbed the network in some way. For each solution, you should notice a difference in the network losses as compared to the base case.

From the data of part (a) calculate

$$\frac{\Delta P_{\text{losses}}}{\Delta P_1}$$

From the data of part (b) calculate

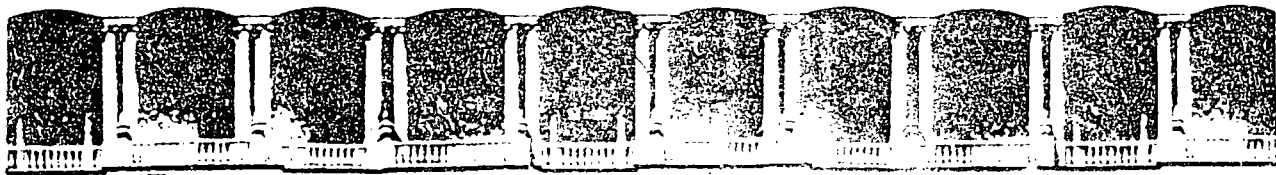
$$\frac{\Delta P_{\text{losses}}}{\Delta P_2}$$

All loads were perturbed equally in parts (a) and (b) to simulate a slight increase in total load. Compare the incremental losses as calculated from the load flow to the incremental losses calculated from the B matrix shown in Example 4D.

The perturbation in part (c) is to demonstrate the change in losses on the network for a shift of generation such as proposed in Section 4.2.4.4. Calculate B_i and P_f for bus 2 from the data of part (c).

FURTHER READING

The basic papers on solution of the load flow can be found in references 1-3. The development of the loss-matrix equations is based on the work of Kron (4), who developed the reference-frame transformation theory. Other developments of the transmission-loss



**FACULTAD DE INGENIERIA U.N.A.M.
DIVISION DE EDUCACION CONTINUA**

**V CURSO INTERNACIONAL DE SISTEMAS
ELECTRICOS DE POTENCIA**

MODULO II: SISTEMAS ELECTRICOS DE POTENCIA

TEMA: UNIT COMMITMENT

EXPOSITOR: ING. ARTURO MORALES COLLANTES

formula are seen in references 5 and 6. Meyer's paper (7) is representative of recent adaptation of sparsity programming methods to calculation of the loss matrix.

The development of the reference-bus penalty factor method can be seen in references 8 and 9. Reference 10 gives an excellent derivation of the reference-bus penalty factors derived from the Newton load-flow equations. Reference 10 provides an excellent summary of recent developments in power system dispatch.

1. Ward, J. B., Hale, H. W., "Digital Computer Solution of Power-Flow Problems," *AIEE Transactions, Part III Power Apparatus and Systems*, Vol. 75, June 1956, pp. 398-404.
2. VanNess, J. E., "Iteration Methods for Digital Load Flow Studies," *AIEE Transactions on Power Apparatus and Systems*, Vol. 78A, August 1959, pp. 583-588.
3. Tinney, W. F., Hart, C. E., "Power Flow Solution by Newton's Method," *IEEE Transactions on Power Apparatus and Systems*, Vol. PAS-86, November 1967, pp. 1449-1460.
4. Kron, G., "Tensorial Analysis of Integrated Transmission Systems—Part I: The Six Basic Reference Frames," *AIEE Transactions*, Vol. 70, Part I, 1951, pp. 1239-1248.
5. Kirchmayer, L. K., Stagg, G. W., "Analysis of Total and Incremental Losses in Transmission Systems," *AIEE Transactions*, Vol. 70, Part I, 1951, pp. 1197-1205.
6. Early, E. D., Watson, R. E., "A New Method of Determining Constants for the General Transmission Loss Equation," *AIEE Transactions on Power Apparatus and Systems*, Vol. PAS-74, February 1956, pp. 1417-1423.
7. Meyer, W. S., "Efficient Computer Solution for Kron and Kron-Early Loss Formulas," *Proc 1973 PICA Conference*, IEEE 73 CHO 740-1, PWR, pp. 428-432.
8. Shipley, R. B., Hochdorf, M., "Exact Economic Dispatch—Digital Computer Solution," *AIEE Transactions on Power Apparatus and Systems*, Vol. PAS-75, November 1956, pp. 1147-1152.
9. Dommel, H. W., Tinney, W. F., "Optimal Power Flow Solutions," *IEEE Transactions on Power Apparatus and Systems*, Vol. PAS 87, October 1968, pp. 1866-1876.
10. Happ, H. H., "Optimal Power Dispatch," *IEEE Transactions on Power Apparatus and Systems*, Vol. PAS-93, May/June 1974, pp. 820-830.

Unit Commitment

5.1 INTRODUCTION

Because human activity follows cycles, most systems supplying services to a large population will experience cycles. This includes transportation systems, communication systems, as well as electric power systems. In the case of an electric power system, the total load on the system will generally be higher during the daytime and early evening when industrial loads are high, lights are on, and so forth and lower during the late evening and early morning when most of the population is asleep. In addition, the use of electric power has weekly cycles, the load being lower over weekend days than weekdays. But why is this a problem in the operation of an electric power system? Why not just simply commit enough units to cover the maximum system load and leave them running? Note that to "commit" a generating unit is to "turn it on," that is, to bring the unit up to speed, synchronize it to the system, and connect it so it can deliver power to the network. The problem with "commit enough units and leave them on line" is one of economics. As will be shown in Example 5A, it is quite expensive to run too many generating units. A great deal of money can be saved by turning units off (decommitting them) when they are not needed.

EXAMPLE 5A

Suppose one had the three units given here.

Unit 1: Min = 150 MW

Max = 600 MW

$$H_1 = 510.0 + 7.2 P_1 + 0.00142 P_1^2 \text{ MBtu/h}$$

Unit 2: Min = 100 MW

Max = 400 MW

$$H_2 = 310.0 + 7.85 P_2 + 0.00194 P_2^2 \text{ MBtu/h}$$

Unit 3: Min = 50 MW

Max = 200 MW

$$H_3 = 78.0 + 7.97 P_3 + 0.00482 P_3^2 \text{ MBtu/h}$$

with fuel costs:

$$F_1 = 1.1 \text{ R/MBtu}$$

$$F_2 = 1.0 \text{ R/MBtu}$$

$$F_3 = 1.2 \text{ R/MBtu}$$

If we are to supply a load of 550 MW, what unit or combination of units should be used to supply this load most economically? To solve this problem, simply try all combinations of the three units. Some combinations will be infeasible if the sum of all maximum MW for the units committed is less than the load or if the sum of all minimum MW for the units committed is greater than the load. For each feasible combination, the units will be dispatched using the techniques of Chapter 3. The results are presented in Table 5.1.

TABLE 5.1 Unit Combinations and Dispatch for 550 MW Load Example 5A

Unit 1	Unit 2	Unit 3	Max Generation	Min Generation	P_1	P_2	P_3	F_1	F_2	F_3	Total Generation Cost	$F_1 + F_2 + F_3$
OFF	OFF	OFF	0	0							Infeasible	
OFF	OFF	ON	200	50							Infeasible	
OFF	ON	OFF	400	100							Infeasible	
OFF	ON	ON	600	150	0	400	150	0	3760	1658	5418	
ON	OFF	OFF	600	150	550	0	0	5389	0	0	5389	
ON	OFF	ON	800	200	500	0	50	4911	0	586	5497	
ON	ON	OFF	1000	250	295	255	0	3030	2440	0	5471	
ON	ON	ON	1200	300	267	233	50	2787	2244	586	5617	

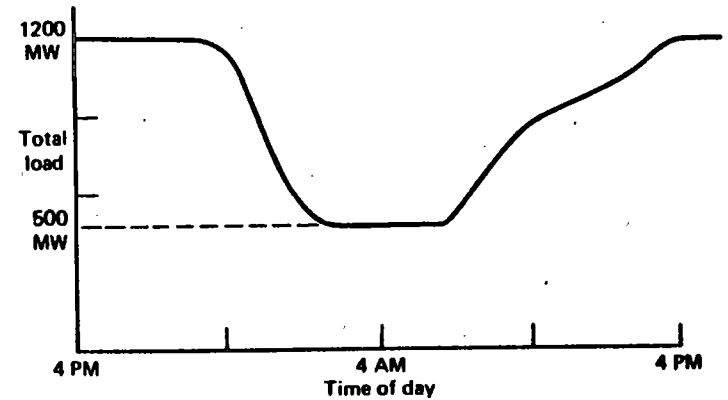


FIG. 5.1a Simple "peak-valley" load pattern.

Note that the least expensive way to supply the generation is not with all three units running, or even any combination involving two units. Rather, the optimum commitment is to only run unit 1, the most economic unit. By only running the most economic unit, the load can be supplied by that unit operating closer to its best efficiency. If another unit is committed, both unit 1 and the other unit will be loaded further from the best efficiency point such that the net cost is greater than unit 1 alone.

Suppose the load follows a simple "peak-valley" pattern as shown in Figure 5.1a. If the operation of the system is to be optimized, units must be shut down as the load goes down and then recommitted as it goes back up. We would like to know which units to drop and when. As we will show later, this problem is far from trivial when real generating units are considered. One approach to this solution is demonstrated in Example 5B, where a simple priority list scheme is developed.

EXAMPLE 5B

Suppose we wish to know which units to drop as a function of system load. Let the units and fuel costs be the same as in Example 5A with the load varying from a peak of 1200 MW to a valley of 500 MW. To obtain a "shut-down rule," simply use a brute-force technique wherein all combinations of units will be tried (as in Example 5A) for each load value taken in steps of 50 MW from 1200 to 500. The results of applying this brute-force technique are given in Table 5.2. Our shut-down rule is quite simple.

When load is above 1000 MW, run all three units; between 1000 MW and 600 MW, run units 1 and 2; below 600 MW, run only unit 1.

TABLE 5.2 "Shut-down Rule" Derivation for Example 5B

Load	Optimum combination		
	Unit 1	Unit 2	Unit 3
1200	ON	ON	ON
1150	ON	ON	ON
1100	ON	ON	ON
1050	ON	ON	ON
1000	ON	ON	OFF
950	ON	ON	OFF
900	ON	ON	OFF
850	ON	ON	OFF
800	ON	ON	OFF
750	ON	ON	OFF
700	ON	ON	OFF
650	ON	ON	OFF
600	ON	OFF	OFF
550	ON	OFF	OFF
500	ON	OFF	OFF

Figure 5.1b shows the unit commitment schedule derived from this shut-down rule as applied to the load curve of Figure 5.1a.

So far, we have only obeyed one simple constraint: *Enough units will be committed to supply the load.* If this were all that was involved in the unit commitment problem, that is, just meeting the load, we could stop here and state that the problem was "solved." Unfortunately, other constraints and other phenomena must be taken into account in order to claim an optimum solution. These constraints will be discussed in the next section followed by a description of some of the presently used methods of solution.

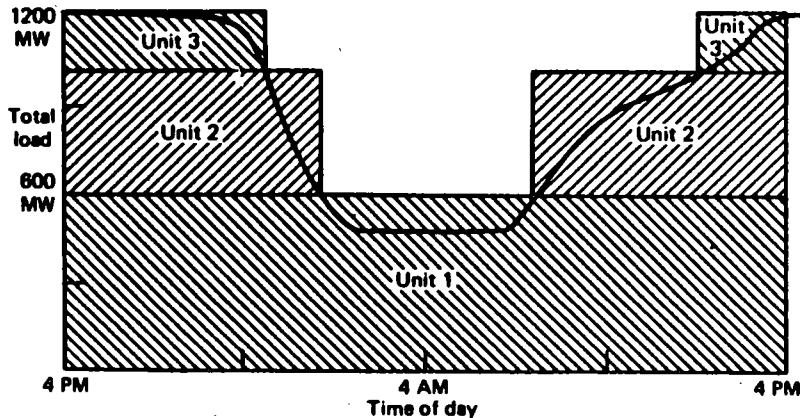


FIG. 5.1b Unit commitment schedule using shut-down rule.

5.1.1 Constraints in Unit Commitment: Introduction

Many constraints can be placed on the unit commitment problem. The list presented here is by no means exhaustive. Each individual power system, power pool, reliability council, and so forth may impose different rules on the scheduling of units, depending on the generation makeup, load-curve characteristics, and such.

5.1.2 Spinning Reserve

Spinning reserve is the term used to describe the total amount of generation available from all units synchronized (i.e., spinning) on the system minus the present load plus losses being supplied. Spinning reserve must be carried so that the loss of one or more units does not cause too far a drop in system frequency (see Chapter 9). Quite simply, if one unit is lost, there must be ample reserve on the other units to make up for the loss in a specified time period.

Spinning reserve must be allocated to obey certain rules, usually set by regional reliability councils (in the United States) that specify how the reserve is to be allocated to various units. Typical rules specify that reserve must be a given percentage of forecasted peak demand, or that reserve must be capable of making up the loss of the most heavily loaded unit in a given period of time, or such. Others calculate reserve requirements as a function of the probability of not having sufficient generation to meet the load.

Not only must the reserve be sufficient to make up for a generation unit failure, but the reserves must be allocated among fast-responding units and slow-responding units. This allows the automatic generation control system (see Chapter 9) to restore frequency and interchange quickly in the event of a generating-unit outage.

Beyond spinning reserve, the unit commitment problem may involve various classes of "scheduled reserves" or "off-line" reserves. These include quick-start diesel or gas-turbine units as well as most hydro and pumped-storage hydro units that can be brought on line, synchronized, and brought up to full capacity quickly. As such, these units can be "counted" in the overall reserve assessment as long as their time to come up to full capacity is taken into account.

Reserves, finally, must be spread around the power system to avoid transmission system limitations (often called "bottling" of reserves) and to allow various parts of the system to run as "islands," should they become electrically disconnected.

EXAMPLE 5C

Suppose a power system consisted of two isolated regions: a western region and an eastern region. Five units have been committed to supply 3090 MW as shown in Figure 5.2. The two regions are separated by transmission tie lines that can together transfer a maximum of 550 MW in either direction. This is shown in Figure 5.2. What can we say about the allocation of spinning reserve in this system?

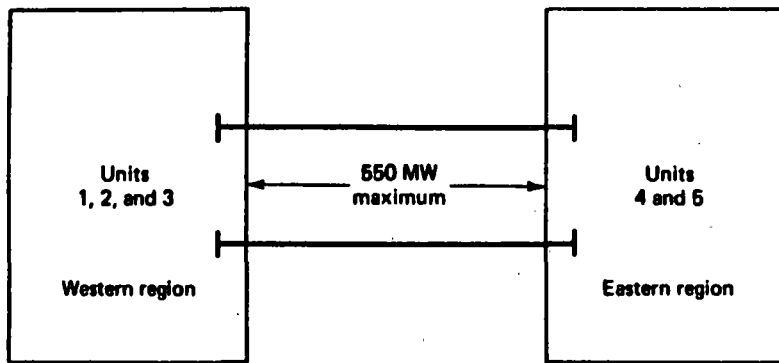


FIG. 5.2 Two-region system.

The data for the system in Figure 5.2 are given in Table 5.3. With the exception of unit 4, the loss of any unit on this system can be covered by the spinning reserve on the remaining units. Unit 4 presents a problem, however. If unit 4 were to be lost and unit 5 were to be run to its maximum of 600 MW, the eastern region would still need 590 MW to cover the load in the eastern region. The 590 MW would have to be transmitted over the tie lines from the western region, which can easily supply 590 MW from its reserves. However, the tie capacity of only 550 MW limits the transfer. Therefore, the loss of unit 4 cannot be covered even though the entire system has ample reserves. The only solution to this problem is to commit more units to operate in the eastern region.

5.1.3 Thermal Unit Constraints

Thermal units require a crew to operate them, especially when turned on and turned off. A thermal unit can undergo only gradual temperature changes, and this translates into a time period of some hours required to bring the unit on line. As a result of such restrictions in the operation of a thermal plant, various constraints

TABLE 5.3 Data for the System in Figure 5.2

Region	Unit	Unit capacity (MW)	Unit output (MW)	Regional generation (MW)	Spinning reserve	Regional load (MW)	Interchange (MW)
Western	1	1000	900	1740	100	1900	160 ^{out}
	2	800	420		380		
	3	800	420		380		
Eastern	4	1200	1040	1350	160	1190	160 ^{out}
	5	600	310		290		
Total		4400	3090	3090	1310	3090	

arise such as

- **Minimum Up Time:** Once the unit is running, it should not be turned off immediately.
- **Minimum Down Time:** Once the unit is decommitted, there is a minimum time before it can be recommitted.
- **Crew Constraints:** If a plant consists of two or more units, they cannot both be turned on at the same time.

In addition, because the temperature and pressure of the thermal unit must be moved slowly, a certain amount of energy must be expended to bring the unit on line. This energy does not result in any MW generation from the unit and is brought into the unit commitment problem as a *start-up cost*.

The start-up cost can vary from a maximum "cold-start" value to a much smaller value if the unit was only turned off recently and is still relatively close to normal temperature. There are two approaches to treating a thermal unit during its down period. The first allows the unit's boiler to cool down and then heat back up to operating temperature in time for a scheduled turn on. The second (called *banking*) requires that sufficient energy be input to the boiler to just maintain operating temperature. The costs for the two can be compared so that, if possible, the best approach (cooling or banking) can be chosen.

$$\text{Start-up cost when cooling} = C_c(1 - e^{-t/\alpha}) \cdot F + C_f$$

where C_c = cold-start cost (MBtu)

F = fuel cost

C_f = fixed cost (includes crew expense, maintenance expenses) (in R)

α = thermal time constant for the unit

t = time in hours the unit was cooled

$$\text{Start-up cost when banking} = C_i \cdot t \cdot F + C_f$$

where C_i = cost (MBtu/h) of maintaining unit at operating temperature

Up to a certain number of hours the cost of banking will be less than the cost of cooling, as is illustrated in Figure 5.3.

Finally, the capacity limits of thermal units may change frequently due to maintenance or unscheduled outages of various equipment in the plant; this must also be taken into account in unit commitment.

5.1.4 Other Constraints

5.1.4.1 Hydro Constraints

Unit commitment cannot be completely separated from the scheduling of hydro units. In this text we will assume that the hydrothermal scheduling (or "coordination") problem can be separated from the unit commitment problem. We,

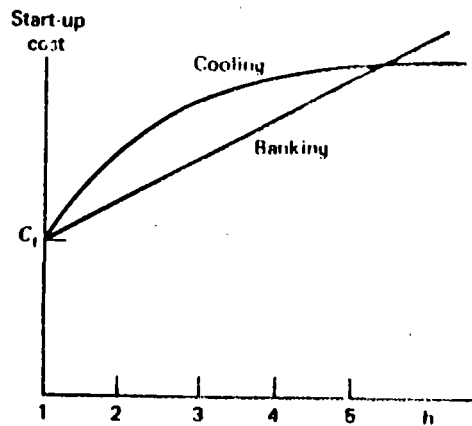


FIG. 5.3 Time-dependent Start-up costs.

of course, cannot assert flatly that our treatment in this fashion will always result in an optimal solution.

5.1.4.2 Must Run

Some units are given a must-run status during certain times of the year for reason of voltage support on the transmission network or for such purposes as supply of steam for uses outside the steam plant itself.

5.1.4.3 Fuel Constraints

We will treat the "fuel scheduling" problem briefly in Chapter 6. A system in which some units have limited fuel, or else have constraints that require them to burn a specified amount of fuel in a given time, presents a most challenging unit commitment problem for which no completely general solution (that works on a practical utility system) exists.

5.2 UNIT COMMITMENT SOLUTION METHODS

The commitment problem can be very difficult. As a theoretical exercise, let us postulate the following situation.

- We must establish a loading pattern for M periods.
- We have N units to commit and dispatch.
- The M load levels and operating limits on the N units are such that any one unit can supply the individual loads and that any combination of units can also supply the loads.

Next, assume we are going to establish the commitment by enumeration (brute force). The total number of combinations we need to try each hour is

$$C(N, 1) + C(N, 2) + \dots + C(N, N-1) + C(N, N) = 2^N - 1$$

where $C(N, j)$ is the combination of N items taken j at a time. That is,

$$C(N, j) = \frac{N!}{(N-j)! j!}$$

$$j! = 1 \times 2 \times 3 \times \dots \times j$$

For the total period of M intervals, the maximum number of possible combinations is $(2^N - 1)^M$, which can become a horrid number to think about.

For example, take a 24-h period (e.g., 24 one-hour intervals) and consider systems with 5, 10, 20, and 40 units. The value of $(2^N - 1)^{24}$ becomes the following.

N	$(2^N - 1)^{24}$
5	6.2×10^{15}
10	1.73×10^{22}
20	3.12×10^{44}
40	(Too big)

These very large numbers are the upper bounds for the number of enumerations required. Fortunately, the constraints on the units and the load-capacity relationships of typical utility systems are such that we do not approach these large numbers. Nevertheless, the real practical barrier in the optimized unit commitment problem is the high dimensionality of the possible solution space.

The most talked about techniques for the solution of the unit commitment problem are

- Priority-list schemes.
- Dynamic programming (DP).
- Mixed integer-linear programming (MILP).

Of these, priority-list schemes are the most popular. DP algorithms are the only ones that approach an optimum solution for large systems. MILP algorithms are just beginning to be researched and are not widely used on large-system problems.

5.2.1 Priority-List Methods

The simplest unit commitment solution method consists of creating a priority list of units. As we saw in Example 5B, a simple shut-down rule or priority-list scheme could be obtained after an exhaustive enumeration of all unit combinations at each load level. The priority list of Example 5B could be obtained in a much simpler manner by noting the full-load average production cost of each unit, where the full-load average production cost is simply the net heat rate at full load times the fuel cost.

EXAMPLE 5D

Construct a priority list for the units of Example 5A. (Use the same fuel costs as in Example 5A.) First, the full load average production cost will be calculated

Unit	Full load average production cost (¢/MWh)
1	9.79
2	9.40
3	11.188

A strict priority order for these units based on the average production cost would order them as follows.

Unit	¢/MWh	Min MW	Max MW
2	9.40	100	400
1	9.79	150	600
3	11.40	50	200

and the commitment scheme would (ignoring min up/down time, start-up costs, etc.) simply use only the following combinations.

Combination	Min MW from combination	Max MW from combination
2 + 1 + 3	300	1200
2 + 1	250	1000
2	150	400

Note that such a scheme would not completely parallel the shut-down sequence described in Example 5B where unit 2 was shut down at 600 MW leaving unit 1. With the priority-list scheme, both units would be held on until load reached 400 MW, then unit 1 would be dropped.

Most priority-list schemes are built around a simple shut-down algorithm that might operate as follows.

- At each hour when load is dropping, determine whether dropping the next unit on the priority list will leave sufficient generation to supply the load plus spinning-reserve requirements. If not, continue operating as is, if yes, go on to the next step.
- Determine the number of hours, H , before the unit will be needed again. That is, assuming that the load is dropping and will then go back up some hours later.
- If H is less than the minimum shut-down time for the unit, keep commitment as is. If not, go to next step.
- Calculate two costs. The first is the sum of the hourly production costs from the next H hours with the unit up. Then recalculate the same sum for the unit down and add in the start-up cost for either cooling the unit or banking it, whichever is

less expensive. If there is sufficient savings from shutting down the unit, it should be shut down, otherwise keep it on.

- Repeat this entire procedure for the next unit on the priority list. If it is also dropped, go to the next and so forth.

Various enhancements to the priority-list scheme can be made by grouping of units to ensure that various constraints are met. We will note later that dynamic-programming methods usually create the same type of priority list for use in the DP search.

5.2.2 Dynamic-Programming Solution

5.2.2.1 Introduction

Dynamic programming has many advantages over the enumeration scheme, the chief advantage being a reduction in the dimensionality of the problem. Suppose we have four units on a system and any combination of them could serve the (single) load. There would be a maximum of $2^4 - 1 = 15$ combinations to test. However, if a strict priority order is imposed, there are only four combinations to try:

Priority 1 Unit

Priority 1 Unit + Priority 2 Unit

Priority 1 Unit + Priority 2 Unit + Priority 3 Unit

Priority 1 Unit + Priority 2 Unit + Priority 3 Unit + Priority 4 Unit

The imposition of a priority list arranged in order of the full-load average-cost rate would result in a theoretically correct dispatch and commitment only if

1. No load costs are zero.
2. Unit input-output characteristics are linear between zero output and full load.
3. There are no other restrictions.
4. Start-up costs are a fixed amount.

In the dynamic programming approach that follows, we assume that

1. A *state* consists of an array of units with specified units operating and the rest off-line.
2. The start-up cost of a unit is independent of the time it has been off-line (i.e., it is a fixed amount).
3. There are no costs for shutting down a unit.
4. There is a strict priority order, and in each interval a specified minimum amount of capacity must be operating.

A feasible state is one in which the committed units can supply the required load and that meets the minimum amount of capacity each period.

5.2.2.2 Backward DP Approach

The first dynamic-programming approach uses a backward (in time) approach in which the solution starts at the last interval and proceeds back to the initial point. There are M intervals in the period to be considered. The dynamic-programming equations for the computation of the minimum total fuel cost during a time period, K , are given here.

$$F_{\text{cost}}(K, I) = \min_{\{J\}} [P_{\text{cost}}(K, I) + S_{\text{cost}}(I, K; J, K+1) + F_{\text{cost}}(K+1, J)] \quad (5.1)$$

$$F_{\text{cost}}(M, I) = P_{\text{cost}}(M, I)$$

where

$F_{\text{cost}}(K, I)$ = minimum total fuel cost from state I in interval K to the last interval M

and

$P_{\text{cost}}(K, I)$ = minimum generation cost in supplying the load during interval K given state I

$S_{\text{cost}}(I, K; J, K+1)$ = incremental start-up cost going from state I in the K^{th} interval to state J in the $(K+1)^{\text{th}}$ interval

$\{J\}$ = set of feasible states in interval $K+1$

The production cost $P_{\text{cost}}(K, I)$ is obtained by economically dispatching the units on-line in state I .

A path is a schedule starting from a state in an interval K to the final interval M . An optimal path is one for which the total fuel cost is minimum. Equation 5.1 asserts that, given the optimal paths starting from all the individual states in the $(K+1)^{\text{th}}$ interval, the optimal path originating from any state in the K^{th} interval can be found. This is the main advantage of the dynamic-programming method. The procedure for determining the optimal schedule and the minimum total fuel cost is shown by the flowchart in Figure 5.4.

5.2.2.3 Forward DP Approach

The backward dynamic-programming approach does not cover many practical situations. For example, if the start-up cost of a unit is a function of the time it has been off-line (i.e., its temperature), then a forward dynamic program approach is more suitable since the previous history of the unit can be computed at each stage. There are other practical reasons for going forward. The initial conditions are easily specified and the computations can go forward in time as long as required and as long as computer storage is available. A forward dynamic-programming algorithm similar to the previously given backward approach is shown by the flowchart in Figure 5.5.

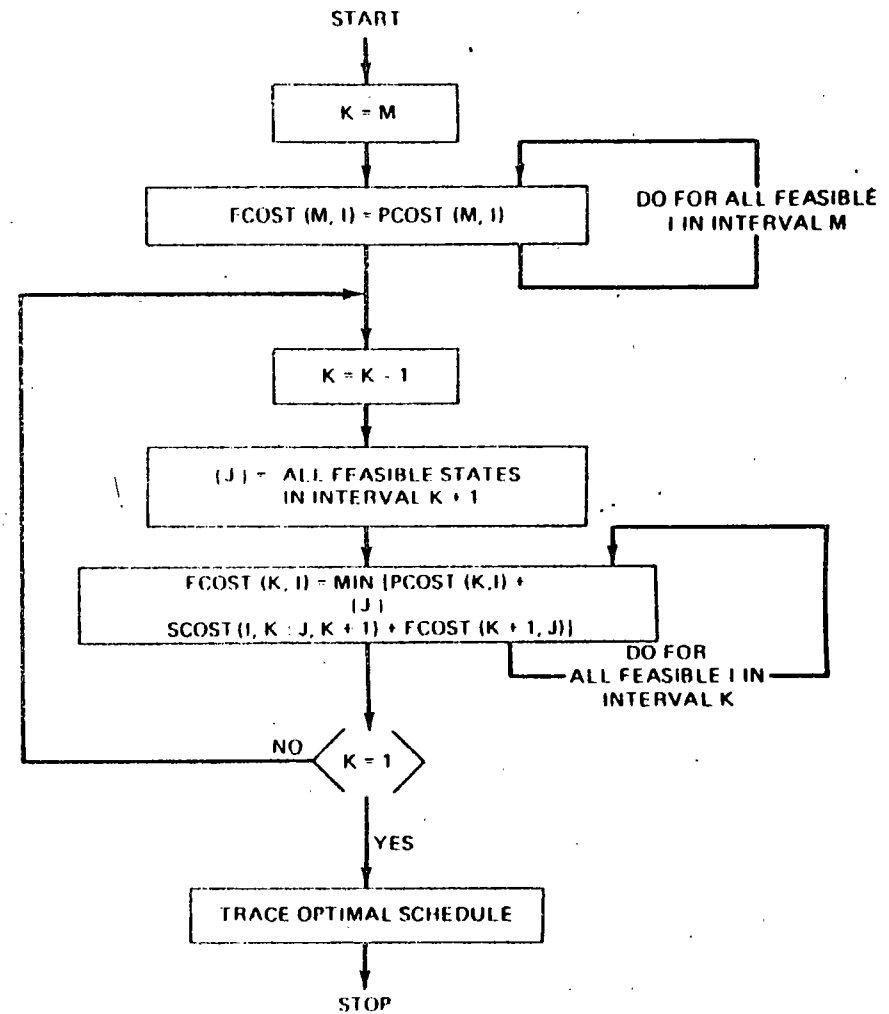


FIG. 5.4 Unit commitment via backward dynamic programming.

The recursive algorithm to compute the minimum cost in hour K with combination I is

$$F_{\text{cost}}(K, I) = \min_{\{L\}} [P_{\text{cost}}(K, I) + S_{\text{cost}}(K-1, L; K, I) + F_{\text{cost}}(K-1, L)]$$

where $F_{\text{cost}}(K, I)$ = least total cost to arrive at state (K, I)

$P_{\text{cost}}(K, I)$ = production cost for state (K, I)

$S_{\text{cost}}(K-1, L; K, I)$ = transition cost from state $(K-1, L)$ to state (K, I)

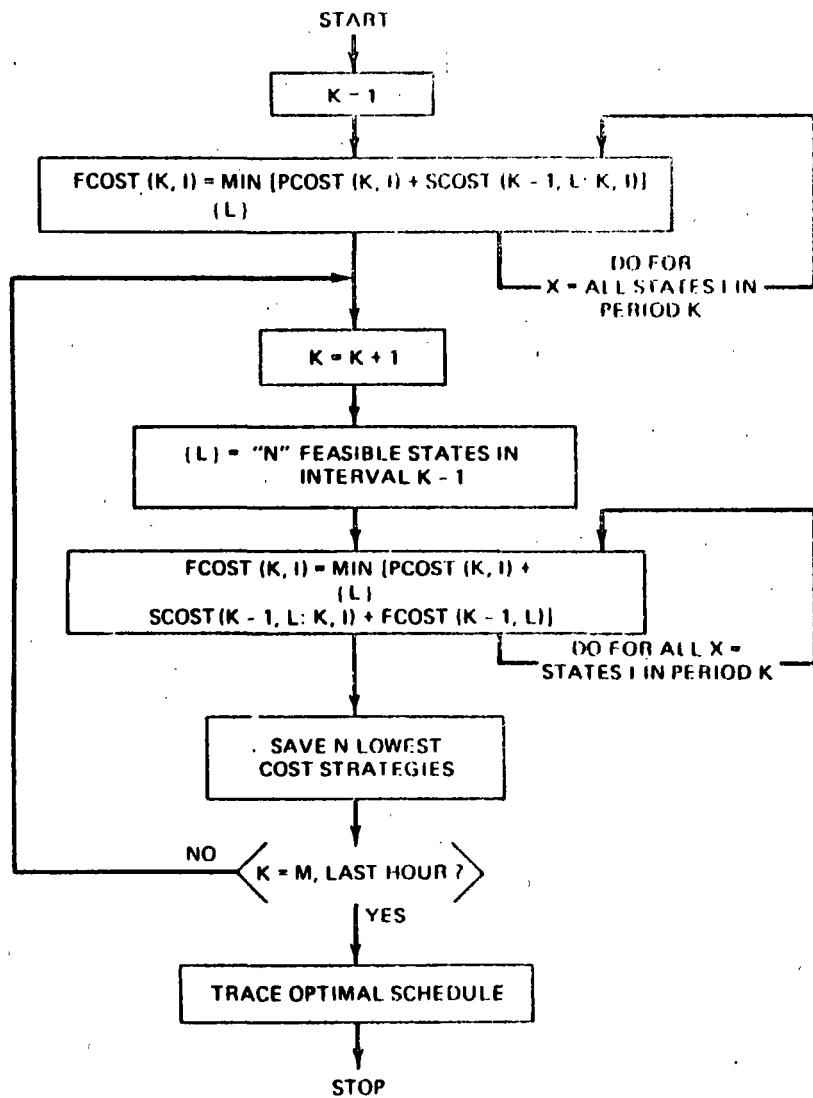


FIG. 5.5 Unit commitment via forward dynamic programming.

where state (K, I) is the I^{th} combination in hour K . For the forward dynamic-programming approach, we define a *strategy* as the transition, or path, from one state at a given hour to a state at the next hour.

Note that two new variables, X and N , have been introduced in Figure 5.5.

X = Number of states to search each period

N = Number of strategies, or paths, to save at each step

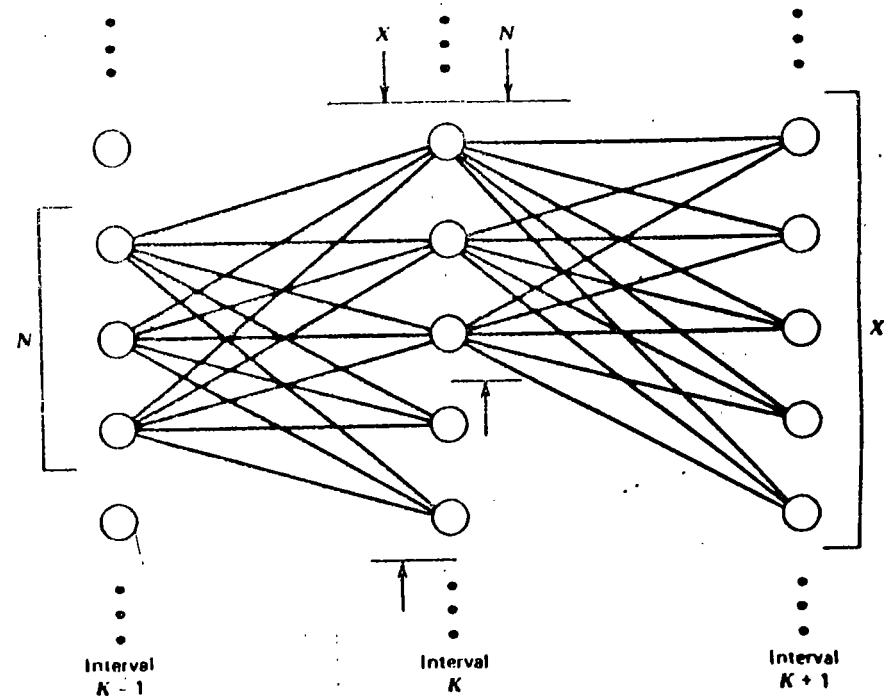


FIG. 5.6 Restricted search paths in DP algorithm with $N = 3$ and $X = 5$.

These variables allow control of the computational effort (see Figure 5.6). For complete enumeration, the maximum number of the value of X or N is $2^n - 1$.

For example, with a strict priority-list ordering, the upper bound on X is n , the number of units. Reducing the number N means that we are discarding the highest cost schedules at each time interval and saving only the lowest N paths or strategies. There is no assurance that the theoretical optimal schedule will be found using a reduced number of strategies and search range (the X value); only experimentation with a particular program will indicate the potential error associated with limiting the values of X and N below their upper bounds.

EXAMPLE 5E

For this example, the complete search range will be used and three cases will be studied. The first is a priority-list schedule, the second is the same example with complete enumeration. Both of the first two cases ignore hot-start costs and minimum up and down times. The third case includes the hot-start costs as well as the minimum up and down times. Four units are to be committed to serve an 8-h load pattern. Data on the units and the load pattern are contained in Table 5.4.

In-order to make the required computations more efficiently, a simplified model of the unit characteristics is used. In practical applications, two or three section

TABLE 5.4 Characteristics, Load Pattern, and Initial Status for the Cases in Example SE

Unit	Max (MW)	Min (MW)	Incremental heat rate (Btu/kWh)	No-load* cost (₹/h)	Full-load ave cost (₹/MWh)	Minimum Times (h)	
						Up	Down
1	80	25	10,440	213.00	23.54	4	2
2	250	60	9,000	585.62	20.34	5	3
3	300	75	8,730	684.74	19.74	5	4
4	60	20	11,900	252.00	28.00	1	1

Unit	Initial conditions		Startup costs		
	Hours off-line (-) or on-line (+)	Hot (₹)	Cold (₹)	Cold start (h)	
1	-5	150	350	4	
2	8	170	400	5	
3	8	500	1,100	5	
4	-6	0	0.02	0	

Load pattern	
Hour	Load (MW)
1	450
2	530
3	600
4	540
5	400
6	280
7	290
8	500

* This is the cost when the (P) function (in this case a straight line) is extended to $P = 0$ MW. Note that we do not allow the unit to operate at zero output. That is, if the unit is on-line, it must be loaded between its min and max. If it is off-line, it must have zero output and its operating cost will be zero ₹/h. Fuel costs are 2.00 ₹/MBtu.

stepped incremental curves might be used, as shown in Figure 5.7. For our example, only a single step between minimum and the maximum power points is used. Start-up costs for the first two cases are taken as the cold-start costs. The priority order for the four units in the example is: Unit 3, Unit 2, Unit 1, Unit 4. For the first two cases the minimum up and down times are taken as 1 h for all units.

In all three cases we will refer to the capacity ordering of the units. This is shown in Table 5.5 where the unit combinations or states are ordered by maximum net capacity for each combination.

Case 1

In Case 1 the units are scheduled according to a strict priority order. That is, units are committed in order until the load is satisfied. The total cost for the interval is the sum of the eight dispatch costs plus the transitional costs for starting any units. In this first case, a maximum of 24 dispatches must be considered.

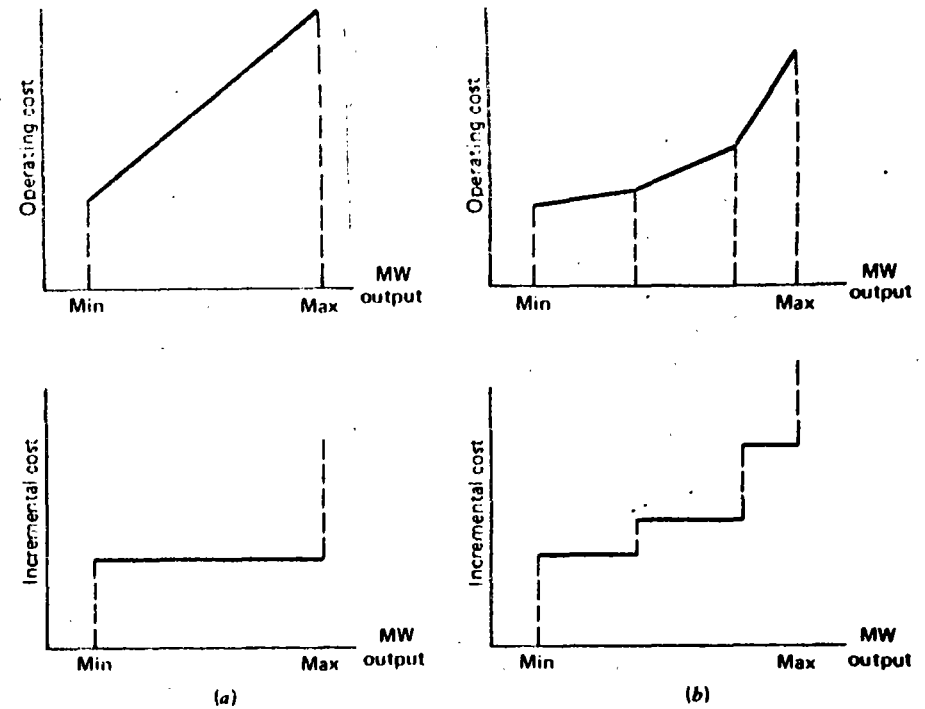


FIG. 5.7 (a) Single-step incremental cost curve and (b) multiple-step incremental cost curve.

TABLE 5.5 Capacity Ordering of the Units

State	Unit combination*	Maximum net capacity for combination
15	1111	690
14	1110	630
13	0111	610
12	0110	550
11	1011	440
10	1101	390
9	1010	380
8	0011	360
7	1100	330
6	0101	310
5	0010	300
4	0100	250
3	1001	140
2	1000	80
1	0001	60
0	0000	0
	Unit 1 2 3 4	

* 1 = Committed (unit operating)
0 = Uncommitted (unit shut down)

For case 1 the only states examined each hour consist of

State no.	Unit status	Capacity (MW)
5	0010	400
12	0110	550
14	1110	630
15	1111	690

Note that this is the priority order, that is, state 5 = unit 3, state 12 = units 3 + 2, state 14 = unit 3 + 2 + 1, and state 15 = units 3 + 2 + 1 + 4. For the first 4 h only the last three states are of interest. The sample calculations illustrate the technique. All possible commitments start from state 12 since this was given as the initial condition. For hour 1 the minimum cost is state 12 and so on. The results for the priority-ordered case are as follows.

Hour	State with min total cost	Pointer for previous hour
1	12 (9208)	12
2	12 (19857)	12
3	14 (32472)	12
4	12 (43300)	14
⋮	⋮	⋮

Note that State 13 is not reachable in this strict priority ordering.

Sample Calculations for Case 1

$$F_{\text{cost}}(J, K) = \min_{(L)} [P_{\text{cost}}(J, K) + S_{\text{cost}}(J-1, L, J, K) + F_{\text{cost}}(J-1, L)]$$

Allowable states are

$$\{ \} = \{0010, 0110, 1110, 1111\} = \{5, 12, 14, 15\}$$

In hour 0 $\{L\} = \{12\}$, initial condition

$J = 1$: 1st hour

$$\begin{aligned} \frac{K}{15} \quad F_{\text{cost}}(1, 15) &= P_{\text{cost}}(1, 15) + S_{\text{cost}}(0, 12; 1, 15) \\ &= 9861 + 350 = 10211 \end{aligned}$$

$$14 \quad F_{\text{cost}}(1, 14) = 9493 + 350 = 9843$$

$$12 \quad F_{\text{cost}}(1, 12) = 9208 + 0 = 9208$$

$J = 2$: 2nd hour

Feasible states are $\{12, 14, 15\} = \{K\}$

So $X = 3$

Suppose two strategies are saved at each stage,

So $N = 2$ and

$$\{L\} = \{12, 14\}$$

$$\begin{aligned} \frac{K}{15} \quad F_{\text{cost}}(2, 15) &= \min_{(12, 14)} [P_{\text{cost}}(2, 15) + S_{\text{cost}}(1, L; 2, 15) + F_{\text{cost}}(1, L)] \\ &= 11301 + \min \left[\begin{array}{l} (350 + 9208) \\ (0 + 9843) \end{array} \right] = 20860 \end{aligned}$$

and so on.

Case 2

In case 2 complete enumeration is tried with a limit of $(2^4 - 1) = 15$ dispatches each of the 8 hours, so that there is a theoretical maximum of $15^8 = 2.56 \times 10^9$ possibilities. Fortunately, most of these are not feasible because they do not supply sufficient capacity and can be discarded with little analysis required.

Figure 5.8 illustrates the computational process for the first 4 h for case 2. On the figure itself the circles denote states each hour. The numbers within the circles are the "pointers." That is, they denote the state number in the previous hour that provides the path to that particular state in the current hour. For example, in hour 2, the minimum costs for states 12, 13, 14, and 15 all result from transitions from state 12 in hour 1. Costs shown on the connections are the start-up costs. At each state the figures shown are the hourly cost/total cost.

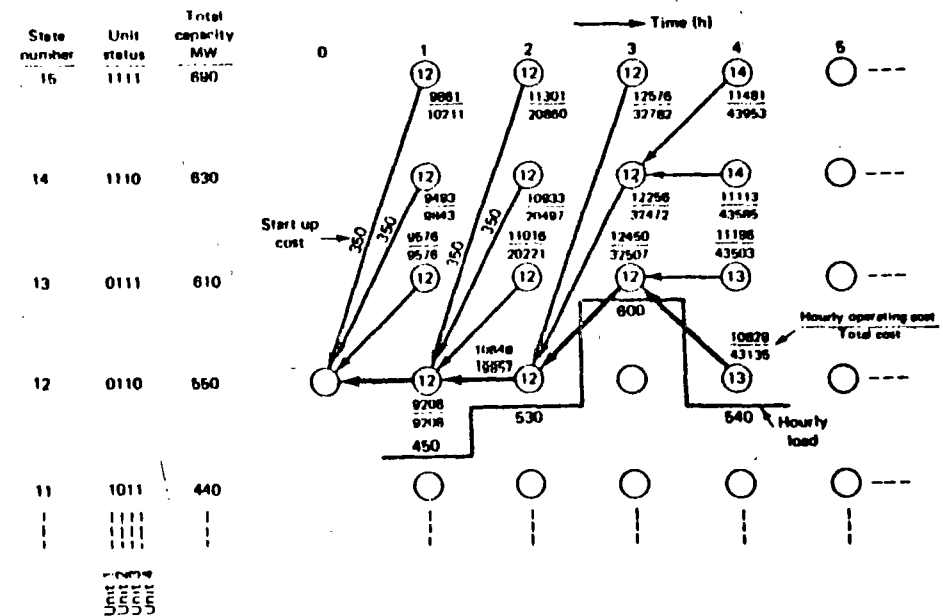


FIG. 5.8 Example 5D cases 1 and 2 (first 4 h).

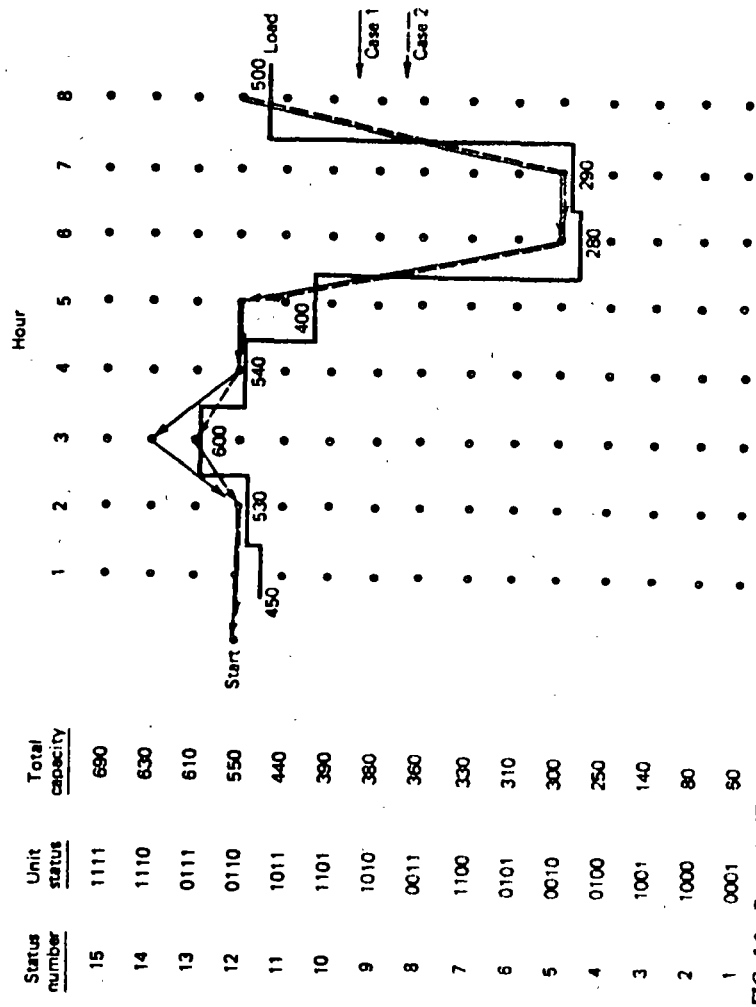


FIG. 5.9 Example 5D cases 1 and 2 (complete solutions).

In case 2 the true optimal commitment is found. That is, it is less expensive to turn on the less efficient peaking unit, number 4, for hour 3 than to start up the more efficient unit 1 for that period. By hour 3 the difference in total cost is R165, or R0.104/MWh. This is not an insignificant amount when compared with the fuel cost per MWh for an average thermal unit with a net heat rate of 10,000 Btu/kWh and a fuel cost of R2.00 MBtu. A savings of R165 every 3 h is equivalent to R481,800/yr.

The total 8-h trajectories for cases 1 and 2 are shown in Figure 5.9. The neglecting of start-up and shutdown restrictions in these two cases permits the shutting down of all but unit 3 in hours 6 and 7. The only difference in the two trajectories occurs in hour 3 as discussed in the previous paragraph.

Case 3

In case 3 the original unit data are used so that the minimum shutdown and operating times are observed. The forward dynamic-programming algorithm was repeated for the same 8-h period. Complete enumeration was used. That is, the upper bound on X shown in the flowchart was 15. Three different values for N , the number of strategies saved at each stage, were taken as 4, 8, and 10. The same trajectory was found for values of 8 and 10. This trajectory is shown in Figure 5.10. However, when only four strategies were saved, the procedure flounders (i.e., fails to find a feasible path) in hour 8 because the lowest cost strategies in hour 7 have shutdown units that cannot be restarted in hour 8 because of minimum unit downtime rules.

The practical remedy for this deficiency in the method shown in Figure 5.5 is to return to a period prior to the low-load hours and temporarily keep more (i.e., higher cost) strategies. This will permit keeping a nominal number of strategies at each stage. The other alternative is, of course, the method used here, run the entire period with more strategies saved.

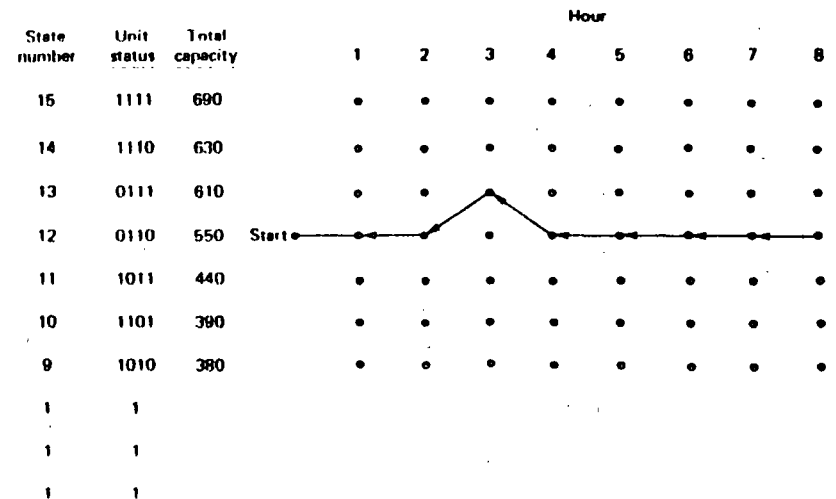


FIG. 5.10 Example 5D case 3.

TABLE 5.6 Summary of Cases 1-3

Case	Conditions	Total cost (R)
1	Priority order. Up and down times neglected	73,439
2	Enumeration ($X \leq 15$) with 4 strategies (N) saved. Up and down times neglected	73,274
3	$X \leq 15$. Up and down times observed	No solution
	$N = 4$ strategies	74,110
	$N = 8$ strategies	74,110
	$N = 10$ strategies	74,110

These cases can be summarized in terms of the total costs found for the 8-h period, as shown in Table 5.6. These cases illustrate the forward dynamic-programming method and also point out the problems involved in the practical application of the method.

5.2.3.4 Restricted Search Ranges, Strategies, and Time-Dependent Problems

We can make use of the simple four-unit 8-h problem in Example 5E to illustrate the use of the heuristic methods to reduce the number of computations. We saw from the first two cases that the strict priority-list computation is apt to miss the optimal commitment. This is even more true when time-dependent effects are included. The most frequent of these are the inclusion of start-up costs, which are a function of the time a unit has been down, the inclusion of minimum downtimes, and the restriction on the maximum number of unit starts through the imposition of maximum start-ups per interval per plant and/or the imposition of minimum running-time requirements.

The heuristic approach, which restricts the number of strategies saved and the number of feasible states at each stage, is intermediate between the strict-priority ordering and a complete enumeration. The two facets of this approach are restrictions on the search range, X , and the number of strategies, N , preserved at each step. Let us consider the effect of restricting the number of strategies by considering one of the examples used in the appendix to this chapter.

Suppose on the first example in the appendix, the transportation problem, we had kept only a limited number of strategies at each stage. Now suppose we had attempted to solve this dynamic-programming problem in a backward fashion starting at the terminal node N and saving only the least costly path at each stage as the search proceeded toward the starting node A . Figure 5.11 illustrates the path we would have found. With this limited dynamic-programming approach, the minimum cost path found would have been ADGKMN, with a path cost of 21 units.

Next consider that two strategies are saved at each stage. Figure 5.12 shows the two paths. The minimum cost path found is the true optimal path, ACEILN, with a cost of 19.

The reduction in computational effort for this problem is, of course, trivial. (Would it be if there were 40 nodes at each stage?) However, we managed to find the

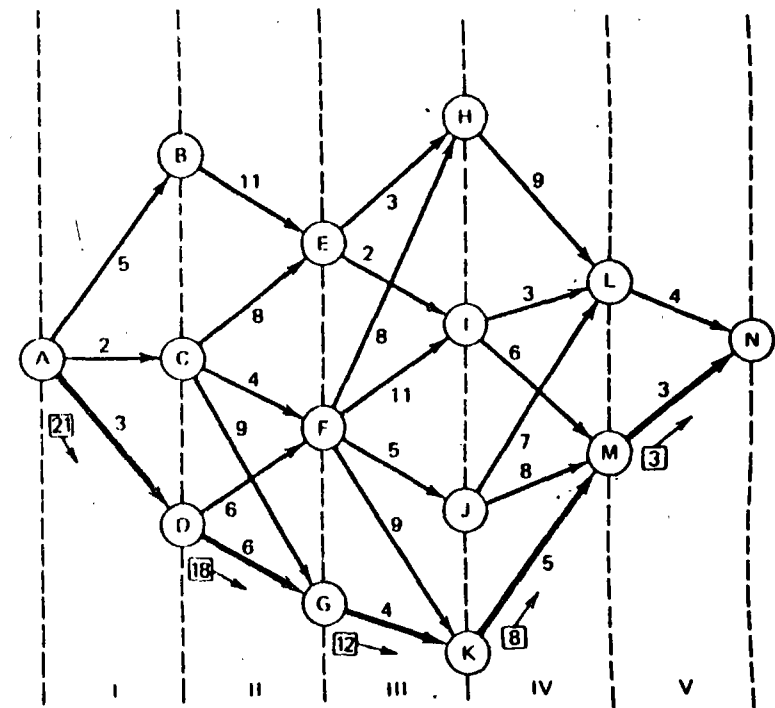


FIG. 5.11 Saving least-cost path each interval (backward from N).

optimal path with only two strategies at each stage. If this problem were being programmed on a computer, in order to ensure finding the optimal path, the maximum number of paths saved would have to be equal to the maximum number of nodes in any stage. For this problem, that would be four paths. (As an exercise, try this particular problem in a forward direction to establish the number of strategies needed in order to find the optimal path.)

As an observation it might be pointed out that the cost savings for finding the true optimal path is 10% of the total. This is usually not true for most scheduling problems. Unfortunately, the difference (savings in costs, in profit, and so forth) between the true optimum and a satisfactory near-optimal schedule is more apt to be less than 0.5 to 0.1% of the total. Since this is a heuristic method (i.e., one we have every reason to believe will work), it is necessary to try it out numerically in order to evaluate the benefit in added computational effort for saving more strategies.

The other heuristic technique that has been tried successfully in the unit commitment problem is that of using a limited "search range" in place of a strict priority order or complete enumeration. This is accomplished by making a unit selection list based on the priority-list concept modified by engineering judgment. There are always some units that are must-run, base-load units. Either these are so much more economical than the others that they always run or else they are constrained from shutting down. Some other units may be of the other extreme

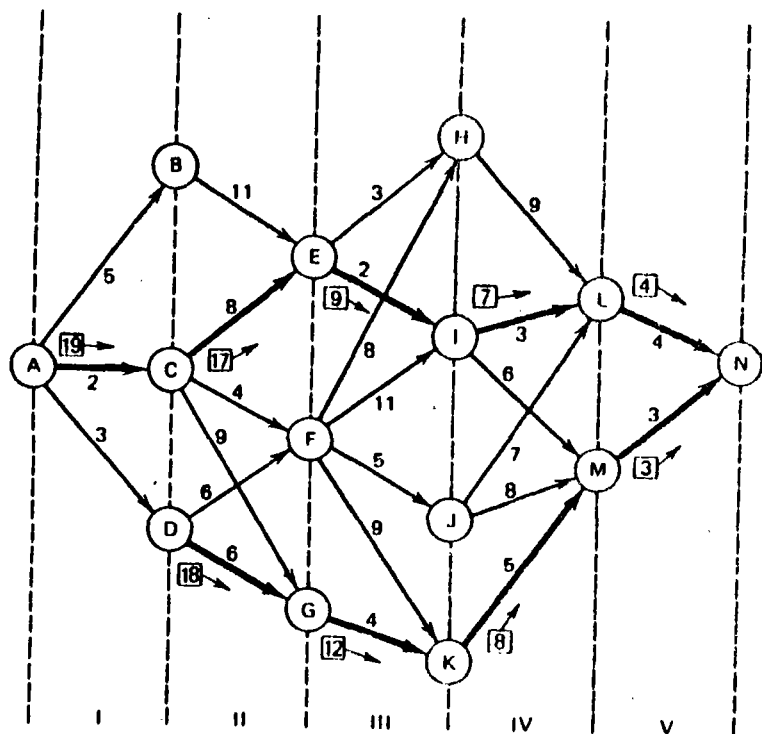


FIG. 5.12 Saving two strategies.

nature and are "must-not-run" units. Perhaps they are on maintenance or are so uneconomic that they are run only during emergencies. When these restrictions are considered along with the priority-list concept and the requirement that schedules must be feasible (i.e., they must meet the load plus spinning reserve and not violate any other constraint), the possible number of states is quite reduced.

The idea of a search range is illustrated in Figure 5.13. If complete enumeration was used, you would have to search over nine states at each interval. Suppose, however, that the load plus spinning-reserve requirement in a given interval could be met by committing the first eight units in priority order. We could then consider searching over states involving units 7 through 10 for our optimal commitment procedure. This will greatly reduce the computational effort.

Take as another example the four-unit, 8-h case of Example 5E. Priority-list ordering gave us 24 dispatches, whereas the complete enumeration gave us 2.56×10^9 . Suppose we were to cut the search range down from four to two each hour. The upper bound to the number of dispatches would now become $(2^2 - 1)^8 = 6561$, which is six orders of magnitude less than $(2^4 - 1)^8$.

This method of unit commitment works well with small and moderate sized systems. For large systems, further heuristic techniques must be applied to reduce the computational effort.

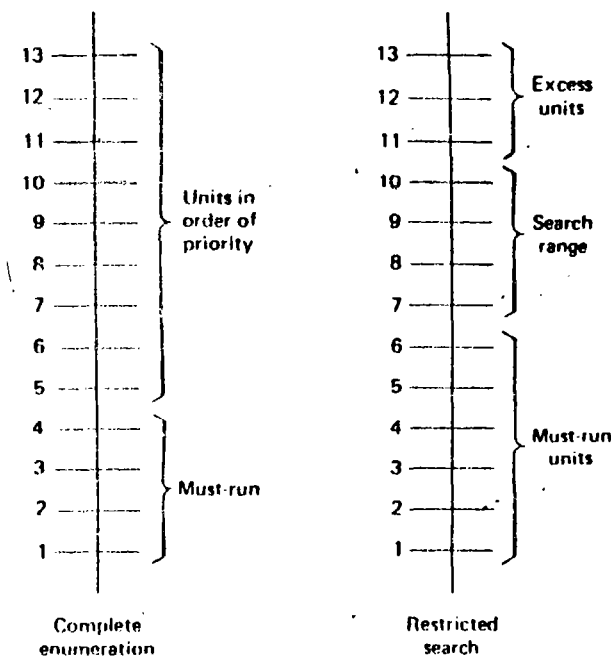


FIG. 5.13 Example of a unit selection list.

EXAMPLE 5E

Figures 5.14 and 5.15 show computer output from a typical unit commitment program. This program has the ability to include maintenance costs as a separate cost from generating cost and start-up costs. The unit statuses shown at the bottom of Figure 5.14 are

- 1 = OFF-FOUT: Unit is off-line due to a forced outage
- 2 = OFF-MAIN: Unit is off-line for maintenance work
- 3 = OFF-TIME:
- 4 = OFF-AVAL: Unit is off-line but available for start-up
- 5 = ON-MUST: Unit is on-line and must be running
- 6 = ON-TIME:
- 7 = ON-CBSD: Unit is on-line and can be shut down

Unit commitment programs, such as shown in Figures 5.14 and 5.15, are used for many different kinds of economic studies such as

1. **Costing a generator unit outage strategy.** In this type of study the user wishes to know if there is a significant difference in total generating cost between taking one unit off-line for maintenance versus another unit. A similar, but different, study would answer the question "Is it cheaper to take a given unit off for maintenance today or tomorrow?"

UNIT COMMITMENT OUTPUT

UNIT STARTUP AND SHUTDOWN SCHEDULE

		SAT 08-DEC-79		SUN 09-DEC-79		MON 10-DEC-79		TUE 11-DEC-79	
TOTAL COST \$ =		397152.		339440.		387107.		387122.	
FUEL COST \$ =		379243.		326991.		370328.		370245.	
MAINT COST \$ =		16799.		12669.		15869.		15747.	
START COST \$ =		1110.		0.		1110.		1110.	

UNIT ID	STATUS	111	111111122222	111	111111122222	111	111111122222	111	111111122222
NO.	NAME	IN	FM	123456789012	345678901234	123456789012	345678901234	123456789012	345678901234
1	LAKE 01	5	5	XXXXXXXXXX	XXXXXXXXXX	XXXXXXXXXX	XXXXXXXXXX	XXXXXXXXXX	XXXXXXXXXX
2	LAKE 02	5	5	XXXXXXXXXX	XXXXXXXXXX	XXXXXXXXXX	XXXXXXXXXX	XXXXXXXXXX	XXXXXXXXXX
3	LAKE 03	5	5	XXXXXXXXXX	XXXXXXXXXX	XXXXXXXXXX	XXXXXXXXXX	XXXXXXXXXX	XXXXXXXXXX
4	LAKE 04	5	5	XXXXXXXXXX	XXXXXXXXXX	XXXXXXXXXX	XXXXXXXXXX	XXXXXXXXXX	XXXXXXXXXX
5	LAKE PKR	4	4	XXXXXXXXXX	XXXXXXXXXX	XXXXXXXXXX	XXXXXXXXXX	XXXXXXXXXX	XXXXXXXXXX
6	ZENITH 1	4	4	XXXXXXXXXX	XXXXXXXXXX	XXXXXXXXXX	XXXXXXXXXX	XXXXXXXXXX	XXXXXXXXXX
7	ZENITH 2	7	3	XXXXXXXXXX	XXXXXXXXXX	XXXXXXXXXX	XXXXXXXXXX	XXXXXXXXXX	XXXXXXXXXX
8	ZENITH 3	4	3	XXXXXXXXXX	XXXXXXXXXX	XXXXXXXXXX	XXXXXXXXXX	XXXXXXXXXX	XXXXXXXXXX
9	ZENITH 4	4	3	XXXXXXXXXX	XXXXXXXXXX	XXXXXXXXXX	XXXXXXXXXX	XXXXXXXXXX	XXXXXXXXXX
10	ZENITH T	4	4	XXXXXXXXXX	XXXXXXXXXX	XXXXXXXXXX	XXXXXXXXXX	XXXXXXXXXX	XXXXXXXXXX
11	RI PKR 1	4	4	XXXXXXXXXX	XXXXXXXXXX	XXXXXXXXXX	XXXXXXXXXX	XXXXXXXXXX	XXXXXXXXXX
12	RI PKR 2	4	4	XXXXXXXXXX	XXXXXXXXXX	XXXXXXXXXX	XXXXXXXXXX	XXXXXXXXXX	XXXXXXXXXX
13	RI PKR 3	4	4	XXXXXXXXXX	XXXXXXXXXX	XXXXXXXXXX	XXXXXXXXXX	XXXXXXXXXX	XXXXXXXXXX
14	BR PKR 1	4	4	XXXXXXXXXX	XXXXXXXXXX	XXXXXXXXXX	XXXXXXXXXX	XXXXXXXXXX	XXXXXXXXXX
15	BR PKR 6	4	4	XXXXXXXXXX	XXXXXXXXXX	XXXXXXXXXX	XXXXXXXXXX	XXXXXXXXXX	XXXXXXXXXX
16	STRK PKR	4	4	XXXXXXXXXX	XXXXXXXXXX	XXXXXXXXXX	XXXXXXXXXX	XXXXXXXXXX	XXXXXXXXXX
17	JOINT M2	5	5	XXXXXXXXXX	XXXXXXXXXX	XXXXXXXXXX	XXXXXXXXXX	XXXXXXXXXX	XXXXXXXXXX
305	DIS TRAN	1	5	XXXXXXXXXX	XXXXXXXXXX	XXXXXXXXXX	XXXXXXXXXX	XXXXXXXXXX	XXXXXXXXXX
308	DIS TRAN	5	5	XXXXXXXXXX	XXXXXXXXXX	XXXXXXXXXX	XXXXXXXXXX	XXXXXXXXXX	XXXXXXXXXX
FIX	NET PUR	1	5	XXXXXXXXXX	XXXXXXXXXX	XXXXXXXXXX	XXXXXXXXXX	XXXXXXXXXX	XXXXXXXXXX
FIX	NET SALE	0	0	XXXXXXXXXX	XXXXXXXXXX	XXXXXXXXXX	XXXXXXXXXX	XXXXXXXXXX	XXXXXXXXXX

STUDY PERIOD TOTALS:		UNIT STATUS:		LEGEND:	
TOTAL COST \$ =	1511240.	(INIT/FINAL)	1 = OFF-FOUR	5 = DN-MUST	F = FIXED MW
FUEL COST \$ =	1444824.		2 = OFF-MAIN	6 = DN-TIME	S = DISPATCHED
MAINT COST \$ =	61084.		3 = OFF-TIME	7 = DN-CBSD	L = DN @ LOW
START COST \$ =	3330.		4 = OFF-AVAL		U = DN @ HIGH
					BLANK = OFF

FIG. 5.14 Sample output from a unit commitment program. (Courtesy of Power Technologies, Inc.)

UNIT COMMITMENT OUTPUT

HOURLY MW SCHEDULES FOR SAT 08-DEC-79

NAME	01	02	03	04	05	06	07	08	09	10	11	12	13	14	15	16	17	18	19	20	21	22	23	24
LAKE 01	129	129	129	129	129	129	129	131	129	129	129	129	129	130	131	131	131	134	132	133	134	134	135	136
LAKE 02	130	131	131	132	132	132	131	135	135	135	135	135	135	135	135	135	135	135	135	135	135	135	135	135
LAKE 03	138	138	138	138	138	138	138	138	138	138	138	138	138	138	138	138	138	138	138	138	138	138	138	139
LAKE 04	209	209	209	209	209	209	209	209	209	209	209	209	209	209	209	209	209	209	209	209	209	209	209	209
LAKE PKR	0	0	0	0	0	0	0	0	0	0	0	0	0	0	0	0	0	0	0	0	0	0	0	0
ZENITH 1	0	0	0	0	0	0	0	0	0	0	0	0	0	0	0	0	0	0	0	0	0	0	0	0
ZENITH 2	60	41	25	25	25	25	28	42	60	60	60	60	60	60	36	30	40	60	60	60	60	60	37	60
ZENITH 3	0	0	0	0	0	0	0	0	0	0	0	0	0	0	0	0	0	0	0	0	0	0	0	0
ZENITH 4	0	0	0	0	0	0	0	22	51	77	77	77	47	28	22	22	22	72	77	77	62	40	22	77
ZENITH T	0	0	0	0	0	0	0	0	0	0	0	0	0	0	0	0	0	0	0	0	0	0	0	0
RI PKR 1	0	0	0	0	0	0	0	0	0	0	0	0	0	0	0	0	0	0	0	0	0	0	0	0
RI PKR 2	0	0	0	0	0	0	0	0	0	0	0	0	0	0	0	0	0	0	0	0	0	0	0	0
RI PKR 3	0	0	0	0	0	0	0	0	0	0	0	0	0	0	0	0	0	0	0	0	0	0	0	0
BR PKR 1	0	0	0	0	0	0	0	0	0	0	0	0	0	0	0	0	0	0	0	0	0	0	0	0
BR PKR 6	0	0	0	0	0	0	0	0	0	0	0	0	0	0	0	0	0	0	0	0	0	0	0	0
STRK PKR	0	0	0	0	0	0	0	0	0	0	0	0	0	0	0	0	0	0	0	0	0	0	0	0
JOINT M2	132	132	124	109	107	117	132	132	132	132	132	132	132	132	132	132	132	132	132	132	132	132	132	132
305 TRAN	0	0	0	0	0	0	0	0	0	0	0	0	0	0	0	0	0	0	0	0	0	0	0	0
308 TRAN	12	0	0	0	0	0	0	0	0	0	3	1	0	0	0	0	0	0	0	0	0	0	0	0
FIX PUR	0	0	0	0	0	0	0	0	0	0	0	0	0	0	0	0	0	0	0	0	0	0	0	0
FIX SALE	0	0	0	0	0	0	0	0	0	0	0	0	0	0	0	0	0	0	0	0	0	0	0	-166
TOT GEN	798	780	756	742	740	750	767	809	854	880	880	880	852	832	803	797	807	843	925	903	884	862	822	942
NET INT	12	0	0	0	0	0	0	0	0	0	3	1	0	0	0	0	0	0	0	0	0	0	0	-166
TOT LOAD	808	778	754	740	738	748	745	807	852	878	881	879	850	830	801	795	803	891	923	901	882	860	820	774
OPER RES	105	104	104	103	103	103	104	105	107	107	107	107	107	106	105	105	105	108	109	108	107	107	106	104
SPIN RES	28	27	27	26	26	26	27	28	30	30	30	30	30	29	28	28	28	31	32	31	30	30	29	27

FIG. 5.15 Sample output from a unit commitment program. (Courtesy of Power Technologies, Inc.)

2. Evaluating change power (see Chapter 10). Here the user of the unit commitment program wishes to study the change in operating cost incurred if a block of power were sold or purchased over tie lines to a neighboring system. Often, these sales or purchases require a different unit commitment to give optimum economic operation.

Of course, both types of studies are in addition to using such a unit commitment simply to work out the commit/decommit schedules for the system operators to use in the daily operation of the power system.

APPENDIX Dynamic Programming Applications

The application of digital methods to solve a wide variety of control and dynamic optimization problems in the late 1950s led Dr. Richard Bellman and his associates to the development of dynamic programming. These techniques are useful in solving a variety of problems and can greatly reduce the computational effort in finding optimal trajectories or control policies.

The theoretical mathematical background, based on the calculus of variations, is somewhat difficult. The applications are not, however, since they depend on a willingness to express the particular optimization problem in terms appropriate for a dynamic programming (DP) formulation.

In the scheduling of power generation systems, DP techniques have been developed for

- The economic dispatch of thermal systems.
- The solution of hydrothermal economic-scheduling problems.
- The practical solution of the unit commitment problem.

This text will touch on all three areas.

First, however, it will be well to introduce some of the notions of DP by means of some one-dimensional examples. Figure 5.16 represents the cost of transporting a unit shipment from Node A to Node N. The values on the arcs are the costs, or values, of shipping the unit from the originating to the terminating node of the arc. The problem is to find the minimum cost route from A to N. The method to be illustrated is that of dynamic programming. The first two examples are from reference 12 and are used by permission.

Starting at A, the minimum cost path to N is ACEILN.

Starting at C, the least cost path to N is CEILN.

Starting at E, the least cost path to N is EILN.

Starting at I, the least cost path to N is IILN.

Starting at L, the least cost path to N is LN.

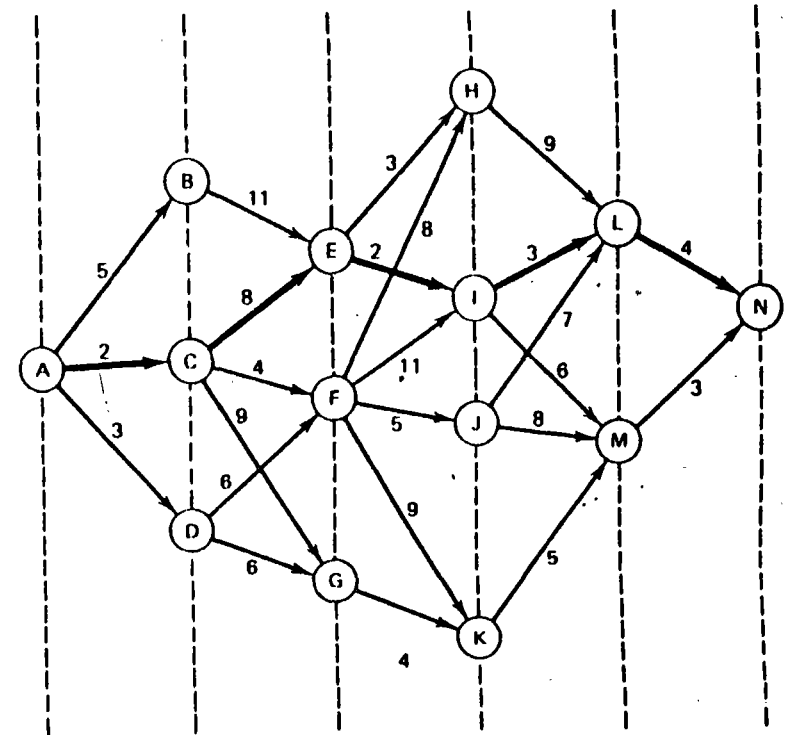


FIG. 5.16 Dynamic-programming example.

The same type of statements could be made about the maximum cost path from A to N (ABEHLN). That is, the maximum cost to N, starting from any node on the original maximal path, is contained in that original path.

The choice of route is made in sequence. There are various stages traversed. The optimum sequence is called the *optimal policy*. Any subsequence is a *subpolicy*. From this it may be seen that the optimal policy (i.e., the minimum cost route) contains only optimal subpolicies. This is the *Theorem of Optimality*.

An optimal policy must contain only optimal subpolicies.

In Reference 15, Bellman and Dreyfus call it the "Principle of Optimality" and state it as

A policy is optimal if, at a stated stage, whatever the preceding decisions may have been, the decisions still to be taken constitute an optimal policy when the result of the previous decisions is included.

We continue with the same example, only now let us find the minimum cost path. Figure 5.17 identifies the stages (I, II, III, IV, V). At the terminus of each stage there is a set of choices of nodes $\{X_i\}$ to be chosen [$\{X_3\} = \{H, I, J, K\}$]. The symbol $V_a(X_i, X_i + 1)$ represents the "cost" of traversing stage a ($= 1, \dots, V$) and depends on the variables selected from the sets $\{X_i\}$ and $\{X_i + 1\}$. That is, the cost, V_a , depends on the starting and terminating nodes. Finally, $f_a(X_i)$ is the minimum cost for stages I through a to arrive at some particular node X_i at the end of that stage, starting from A. The numbers in the node circles in Figure 5.17 represent this minimum cost.

$\{X_0\}$: A $\{X_2\}$: E, F, G $\{X_4\}$: L, M
 $\{X_1\}$: B, C, D $\{X_3\}$: H, I, J, K $\{X_5\}$: N

$f_1(X_1)$: Minimum cost for the first stage is obvious:

$$\begin{aligned} f_1(B) &= V_1(A, B) = 5 \\ f_1(C) &= V_1(A, C) = 2 \\ f_1(D) &= V_1(A, D) = 3 \end{aligned}$$

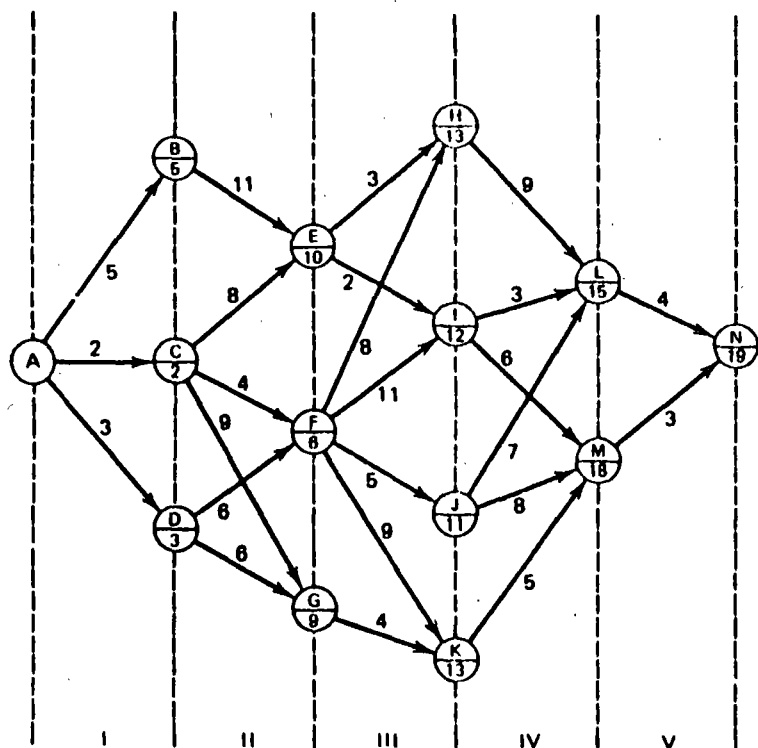


FIG. 5.17 Dynamic-programming example showing minimum cost at each node.

$f_{II}(X_2)$: Minimum cost for stages I and II as a function of X_2 :

$$\begin{aligned} f_{II}(E) &= \min_{(X_1)} [f_1(X_1) + V_{II}(X_1, E)] \\ &= \min [5 + 11, 2 + 8, 3 + \infty] = 10 \\ X_1 &= B = C = D \quad X_1 = C \end{aligned}$$

The cost is infinite for node D since there is no path from D to E:

$$f_{II}(F) = \min_{(X_1)} [f_1(X_1) + V_{II}(X_1, F)] = \min[\infty, 6, 9] = 6, X_1 = C$$

$$f_{II}(G) = \min_{(X_1)} [f_1(X_1) + V_{II}(X_1, G)] = \min[\infty, 11, 9] = 9, X_1 = D$$

Thus, at each stage we should record the minimum cost and the termination starting the stage to achieve the minimum cost path for each of the nodes terminating the current stage.

(X_2)	E	F	G
$f_{II}(X_2)$	10	6	9
Path X_0X_1	AC	AC	AD

$f_{III}(X_3)$: Minimum cost of stages I, II, and III as a function of X_3 :

$$f_{III}(H) = \min_{(X_2)} (f_{II}(X_2) + V_{III}(X_2, H)) = \min(13, 14, \infty) = 13 \quad \text{with } X_2 = E$$

In general,

$$f_{III}(X_3) = \min_{(X_2)} [f_{II}(X_2) + V_{III}(X_2, X_3)]$$

Giving,

X_3	H	I	J	K
$f_{III}(X_3)$	13	12	11	13
Path $X_0X_1X_2$	ACE	ACE	ACF	ADG

$f_{IV}(X_4)$: Minimum cost of stages I through IV as a function of X_4 :

$$f_{IV}(X_4) = \min_{X_3} (f_{III}(X_3) + V_{IV}(X_3, X_4))$$

$$f_{IV}(L) = \min(13 + 9, 12 + 3, 11 + 7, 13 + \infty) = 15 \quad X_3 = I$$

$$X_3 = H \quad I \quad J \quad K$$

$$f_{IV}(M) = \min(13 + \infty, 12 + 6, 11 + 8, 13 + 5) = 18 \quad X_3 = I \text{ or } K$$

$$H \quad I \quad J \quad K$$

f_V : Minimum cost of I \rightarrow V as a function of X_5 :

$$f_V(N) = \min_{(X_4)} (f_{IV}(X_4) + V_V(X_4, X_5))$$

$$\begin{aligned} &= \min(15 + 4, 18 + 3) = 19 \quad X_4 = L \\ X_4 &= L = M \end{aligned}$$

Tracing back path of minimum cost is found as follows:

Stage I	$\{X_i\}$	f_i
1	B, C, D	5, 2, 3
2	E, F, G	10, 6, 9
3	H, I, J, K	13, 12, 11, 13
4	L, M	15, 18
5	N	19

It would be possible to carry out this procedure in the opposite direction just as easily.

An Allocation Problem

Table 5.7 lists the profits to be made in each of four ventures as a function of the investment in the particular venture. Given a limited amount of money to allocate, the problem is to find the optimal investment allocation. The only restriction is that investments must be made in integer amounts. For instance, if one had 10 units to invest and the policy were to put

- 3 in I
- 1 in II
- 5 in III
- 1 in IV

$$\text{Profit} = 0.65 + 0.25 + 0.65 + 0.20 = 1.75.$$

The problem is to find an allocation policy that yields the maximum profit. Let

X_1, X_2, X_3, X_4 be investments in I through IV

$V(X_1), V(X_2), V(X_3), V(X_4)$ be profits

$X_1 + X_2 + X_3 + X_4 = 10$ is the constraint. That is, 10 units must be invested.

TABLE 5.7 Profit Versus Investment

Investment amount	Profit from venture			
	I	II	III	IV
0	0	0	0	0
1	0.28	0.25	0.15	0.20
2	0.45	0.41	0.25	0.33
3	0.65	0.55	0.40	0.42
4	0.78	0.65	0.50	0.48
5	0.90	0.75	0.65	0.53
6	1.02	0.80	0.73	0.56
7	1.13	0.85	0.82	0.58
8	1.23	0.88	0.90	0.60
9	1.32	0.90	0.96	0.60
10	1.38	0.90	1.00	0.60

To transform this into a multistage problem, let the stages be

$$X_1, U_1, U_2, A$$

$$\begin{aligned} \text{where } U_1 &= X_1 + X_2 & U_1 &\leq A & U_2 &\leq A \\ U_2 &= U_1 + X_3 & \{A\} &= 0, 1, 2, 3, \dots, 10 \\ A &= U_2 + X_4 \end{aligned}$$

The total profit is

$$f(X_1, X_2, X_3, X_4) = V_1(X_1) + V_2(X_2) + V_3(X_3) + V_4(X_4)$$

which can be written

$$f(X_1, U_1, U_2, A) = V_1(X_1) + V_2(U_1 - X_1) + V_3(U_2 - U_1) + V_4(A - U_2)$$

At the second stage, we can compute

$$f_2(U_1) = \max_{X_1=0, 1, \dots, U_1} [V_1(X_1) + V_2(U_1 - X_1)]$$

$X_1, X_2, \text{ or } U_1$	$V_1(X_1)$	$V_2(X_2)$	$f_2(U_1)$	Optimal subpolicies I & II
0	1	0	0	(0, 0)
1	0.28	0.25	0.28	(1, 0)
2	0.45	0.41	0.53	(1, 1)
3	0.65	0.55	0.70	(2, 1)
4	0.78	0.65	0.90	(3, 1)
5	0.90	0.75	1.06	(3, 2)
6	1.02	0.80	1.20	(3, 3)
7	1.13	0.85	1.33	(4, 3)
8	1.23	0.88	1.45	(5, 3)
9	1.32	0.90	1.57	(6, 3)
10	1.38	0.90	1.68	(7, 3)

Next, at the third stage,

$$f_3(U_2) = \max_{U_1=0, 1, 2, \dots, U_2} [f_2(U_1) + V_3(U_2 - U_1)]$$

$U_1, U_2, \text{ or } X_3$	$f_2(U_1)$	$V_3(X_3)$	$f_3(U_2)$	Optimal subpolicies	
				For I & II	For I, II & III
0	0	0	0	0, 0	0, 0, 0
1	0.28	0.15	0.28	1, 0	1, 0, 0
2	0.53	0.25	0.53	1, 1	1, 1, 0
3	0.70	0.40	0.70	2, 1	2, 1, 0
4	0.90	0.50	0.90	3, 1	3, 1, 0
5	1.06	0.62	1.06	3, 2	3, 2, 0
6	1.20	0.73	1.21	3, 3	3, 2, 1
7	1.33	0.82	1.35	4, 3	3, 3, 1
8	1.45	0.90	1.48	5, 3	4, 3, 1
9	1.57	0.96	1.60	6, 3	5, 3, 1 or 3, 3, 3
10	1.68	1.00	1.73	7, 3	4, 3, 3

Finally, the last stage is

$$f_4(A) = \max_{(U_2)} [f_3(U_2) + V_4(A - U_2)]$$

U_2, A or X_4	$f_3(U_2)$	$V_4(X_4)$	$f_4(A)$	Optimal subpolicy for I, II, III	Optimal policy
0	0	0	0	0, 0, 0	0, 0, 0, 0
1	0.28	0.20	0.28	1, 0, 0	1, 0, 0, 0
2	0.53	0.33	0.53	1, 1, 0	1, 1, 0, 0
3	0.70	0.42	0.73	2, 1, 0	1, 1, 0, 1
4	0.90	0.48	0.90	3, 1, 0	3, 1, 0, 0 or 2, 1, 0, 1
5	1.06	0.53	1.10	3, 2, 0	3, 1, 0, 1
6	1.21	0.56	1.26	3, 2, 1	3, 2, 0, 1
7	1.35	0.58	1.41	3, 3, 1	3, 2, 1, 1
8	1.48	0.60	1.55	4, 3, 1	3, 3, 1, 1
9	1.60	0.60	1.68	5, 3, 1 or 3, 3, 3	4, 3, 1, 1 or 3, 3, 1, 2
10	1.73	0.60	1.81	4, 3, 3	4, 3, 1, 2

Consider the procedure and solution:

1. It was not necessary to enumerate all possible solutions. Instead we used an orderly, stagewise search, the form of which was the same at each stage.
2. The solution was obtained not only for $A = 10$, but for the complete set of A 's $\{A\} = 0, 1, 2, \dots, 10$
3. The optimal policy contains only optimal subpolicies. For instance, $A = 10$, (4, 3, 1, 2) is the optimal policy. For stages I, II, III and $U_2 = 8$, (4, 3, 1) is the optimal subpolicy. For stages I and II and $U_1 = 7$, (4, 3) is the optimal subpolicy. For stage I only, $X_1 = 4$ fixes the policy.
4. Notice also, that by storing the intermediate results, we could work a number of different variations of the same problem with the data already computed.

Economic Dispatch of Thermal Systems Using Dynamic Programming

The problem of finding the economic dispatch of a system of thermal units can be expressed in such a fashion that it is amenable to solution using dynamic-programming methods. Assume:

1. All the units to be considered are to be on-line (i.e., the unit commitment problem is solved, or ignored.)
2. Losses are neglected.
3. It will be satisfactory to find the economic dispatch at discrete load steps rather than for continuous load levels.

In order to use the DP formulation, the units to be dispatched must be ordered. For this particular problem the loading order is arbitrary. Let i represent the order number of a unit and then define

$$P_i = \text{loading (MW) on unit } i$$

$$F_i(P_i) = \text{cost (₹/h) for generating } P_i \text{ MW on unit } i$$

$$f_i(D) = \text{stage cost of supplying a demand of } D \text{ MW with } i \text{ units}$$

At each stage the recursive relationship that may be used to find the optimal economic operating schedule (i.e., operating policy) is

$$f_i(D) = \min_{(P_i)} [f_{i-1}(D - P_i) + F_i(P_i)]$$

It is easier to see by example. We will use a three-unit example with the following data.

Unit no.	Min MW	Max MW
1	100	500
2	100	500
3	200	1000

Unit costs in ₹ per hour are given in Table 5.8. Infinite costs are assigned for outputs below the minimum and above the maximum ratings.

The method is quite appropriate to the computation of a whole range of schedules. Let us illustrate the process by finding the optimum schedule for a total demand, D , of 800 MW. The first stage with only one machine is obviously nothing more than a reproduction of the first column from Table 5.8. Therefore, let us proceed directly to stage 2.

$$f_2(D) = \min_{(P_2)} [f_1(D - P_2) + F_2(P_2)]$$

$$= \min_{(P_2)} [F_1(D - P_2) + F_2(P_2)]$$

TABLE 5.8 Unit Costs in ₹ per hour

P_i (MW)	$F_i(P_i)$: Costs in ₹/h		
	F_1	F_2	F_3
0	∞	∞	∞
100	500	400	∞
200	950	1000	1020
300	1400	1440	1450
400	1840	1800	1900
500	2320	2400	2350
600	∞	∞	2800
700			3240
800			3680
900			4130
1000			4570

TABLE 5.9 ge 2 (Two Machines) Generation Dispatch

D	F ₁ (D)	F ₁ (D - P ₂) + F ₂ (P ₂)					Optimum Schedules		
		P ₂ = 0 F ₂ (P ₂) = ∞	100	200	300	400	500	f ₂	P ₂ *
0	∞	∞							
100	500		∞						
200	950		900	∞			900	100	
300	1400		1350	1500	∞		1350	100	
400	1840		1800	1950	1940	∞	1800	100	
500	2320		2240	2400	2390	2300	∞	2240	100
600	∞		2720	2840	2840	2750	2900	2720	100
700			∞	3320	3280	3200	3350	3200	400
800			∞	∞	3760	3640	3800	3640	400
900					∞	4120	4240	4120	400
1000						∞	4720	4720	500

P₂* = value of P₂ that results in the minimum. The minimum costs and loading on unit 2 for serving the various load levels {D} are contained in the two right-hand columns of Table 5.9. If we need a finer tuning of the schedule, we might be able to expand these tables in smaller steps in the range of the coarse optimum. This will work if the functions are smooth and convex in the neighborhood of the coarse optimum. If not, we need to cover the entire range with the finer grid.

For three machines the minimum cost is found from

$$f_3(D) = \min_{(P_3)} [F_3(P_3) + f_2(D - P_3)]$$

The table for three machines could easily be set up for a number of different demand levels. Instead, it is set up in Table 5.10 only for D = 800 MW. The data for 600 < P₃ < 200 MW are omitted for obvious reasons. Therefore, f₃(800) = 3690 and P₃* = 300 MW. The resulting demand on units 1 and 2 is 500 MW, and from Table 5.9, P₂* = 100 MW so that P₁* = 400 MW. Note that the schedules were finally found by looking up data in the three tables for the f_i(D) in sequence. Therefore, in setting up a computerized routine only a moderate amount of data need be saved.

TABLE 5.10 Stage 3 (Three Machines) Generation Dispatch

D = 800 MW				
P ₃ (MW)	F ₃ (R/h)	800 - P ₃ (MW)	f ₂ (800 - P ₃) (R/h)	F ₃ (P ₃) + f ₂ (800 - P ₃) (R/h)
200	1020	600	2720	3740
300	1450	500	2240	3690
400	1900	400	1800	3700
500	2350	300	1350	3700
600	2800	200	900	3700
700	∞	∞	∞	∞
800	∞	∞	∞	∞

The two significant items to note about this economic dispatch method are

1. Nothing is demanded of the individual unit cost characteristics. They do not have to be convex, smooth, or even possess derivatives.
2. The order in which the units are considered is not important as long as all three units are assumed to be committed. (Note that unit 3 alone could serve the 800 MW demand at less cost.)

The first point permits this method to be used for economic dispatching problems in which unit characteristics may be represented in detail to simulate increased friction losses when turbine valves are first opened. The second point is worth making since it separates the economic dispatching problem from the unit commitment problem.

PROBLEMS

5.1 You have been assigned the job of building an oil pipeline from the West Coast of the United States to the East Coast. You are told that any one of the three West Coast sites is satisfactory and any of the East Coast sites is satisfactory. The numbers in Figure 5.18 represent relative cost in hundreds of millions (R · 10⁶). Find the cheapest West Coast to East Coast pipeline.

5.2 The Stagecoach Problem

A mythical salesman who had to travel west by stagecoach through unfriendly country wished to take the safest route. His starting point and destination were

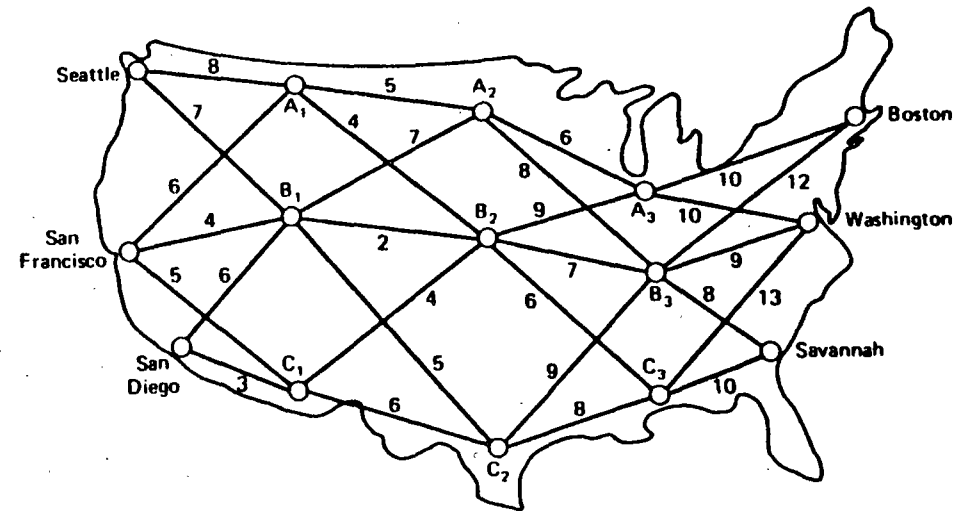


FIG. 5.18 Possible oil pipeline routes for Problem 5.1.

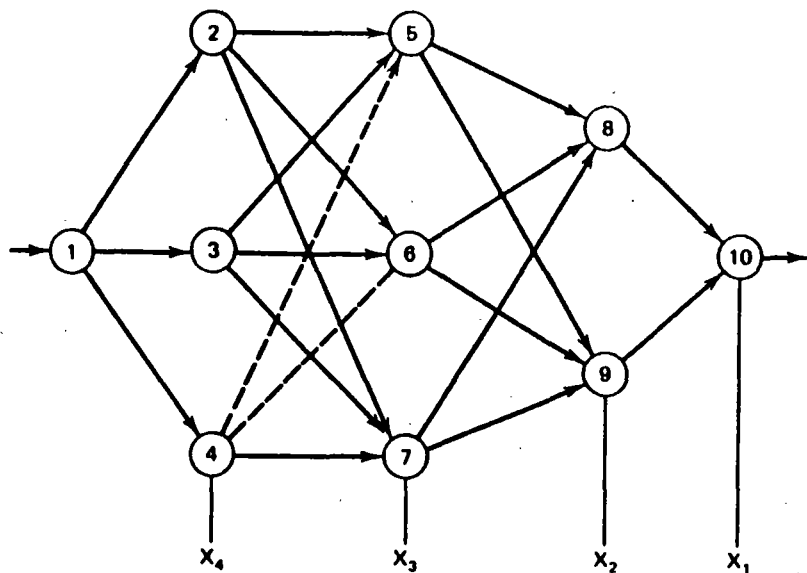


FIG. 5.19 Possible stagecoach routes for Problem 5.2.

fixed, but he had considerable choice as to which states he would travel through enroute. The possible stagecoach routes are shown in Figure 5.19. After some thought the salesman deduced a clever way of determining his safest route. Life insurance policies were offered to passengers, and since the cost of each policy was based on a careful evaluation of the safety of that run, the safest route should be the one with the cheapest policy. The cost of the standard policy on the stagecoach run from state i to state j , denoted as C_{ij} , is given in Figure 5.20. Find the safest path(s) for the salesman to take.

$i \backslash j$	1	2	3	4	5	6	7	8	9	10
1		2	4	3						
2					7	4	6			
3				3	2	4				
4				4	1	5				
5							1	4		
6							6	3		
7							3	2		
8									3	
9									4	
10										

FIG. 5.20 Cost to go from state i to state j in Problem 5.2. Costs not shown are infinite.

5.3 Economic Dispatch Problem

Consider three generating units that do not have convex input-output functions. (This is the type of problem one encounters when considering valve points in the dispatch problem.)

Unit 1:

$$H_1(P_1) = \begin{cases} 80 + 8P_1 + 0.024P_1^2 & 20 \text{ MW} \leq P_1 \leq 60 \text{ MW} \\ 196.4 + 3P_1 + 0.075P_1^2 & 60 \text{ MW} \leq P_1 \leq 100 \text{ MW} \end{cases}$$

Generation limits are $20 \text{ MW} \leq P_1 \leq 100 \text{ MW}$.

Unit 2:

$$H_2(P_2) = \begin{cases} 120 + 6P_2 + 0.04P_2^2 & 20 \text{ MW} \leq P_2 \leq 40 \text{ MW} \\ 157.335 + 3.3333P_2 + 0.08333P_2^2 & 40 \text{ MW} \leq P_2 \leq 100 \text{ MW} \end{cases}$$

Generation limits are $20 \text{ MW} \leq P_2 \leq 100 \text{ MW}$.

Unit 3:

$$H_3(P_3) = \begin{cases} 100 + 4.6666P_3 + 0.13333P_3^2 & 20 \text{ MW} \leq P_3 \leq 50 \text{ MW} \\ 316.66 + 2P_3 + 0.1P_3^2 & 50 \text{ MW} \leq P_3 \leq 100 \text{ MW} \end{cases}$$

Generation limits are $20 \text{ MW} \leq P_3 \leq 100 \text{ MW}$. Fuel costs = 1.5 $\text{\$/MBtu}$ for all units.

- Plot the cost function for each unit (see Problem 3.1).
- Plot the incremental cost function for each unit.
- Find the most economical dispatch for the following total demands assuming all units are on line:

$$P_D = 100 \text{ MW}$$

$$P_D = 140 \text{ MW}$$

$$P_D = 180 \text{ MW}$$

$$P_D = 220 \text{ MW}$$

$$P_D = 260 \text{ MW}$$

$$\text{Where } P_D = P_1 + P_2 + P_3.$$

Solve using dynamic programming using discrete load steps of 20 MW starting at 20 MW through 100 MW for each unit.

- Can you solve these dispatch problems without dynamic programming? If think you know how, try solving for $P_D = 100 \text{ MW}$.

5.4 Unit Commitment

Given the unit data in Tables 5.11 and 5.12 use forward dynamic-programming to find the optimum unit commitment schedules covering the 8-h period.

E.5.11 Unit Commitment Data for Problem 5.4

Unit	Max MW	Min MW	Incremental heat rate (Btu/kWh)	No-load energy input (MBtu/h)	Start-up energy (MBtu)
1	500	70	9,950	300	800
2	250	40	10,200	210	380
3	150	30	11,000	120	110
4	150	30	11,000	120	110

Load data (all time periods = 2 h):

Time period	Load (MW)
1	600
2	800
3	700
4	950

Start-up and shut-down rules

Unit	Minimum uptime (h)	Minimum downtime (h)
1	2	2
2	2	2
3	2	4
4	2	4

Fuel cost = 1.00 R/MBtu.

TABLE 5.12 Unit Combinations and Operating Cost for Problem 5.5

Combination	Unit				Operating cost (R/h)			
	1	2	3	4	Load 600 MW	Load 700 MW	Load 800 MW	Load 950 MW
A	1	1	0	0	6505	7525	x	x
B	1	1	1	0	6649	7669	8705	x
C	1	1	1	1	6793	7813	8833	10475

1 = up; 0 = down

Table 5.12 gives all the combinations you need as well as the operating cost for each at the loads in the load data. An "X" indicates that a combination cannot supply the load. The starting conditions are: At the beginning of the first period units 1 and 2 are up, units 3 and 4 are down and have been down for 8 h.

5.5 Unit Commitment

Table 5.13 presents the unit characteristics and load pattern for a five-unit—four time period problem. Each time period is 2 h long. The input-output characteristics are approximated by a straight line from min to max generation so that the incremental heat rate is constant. Unit no-load and start-up costs are given in terms of heat energy requirements.

TABLE 5.13 The Unit Characteristic and Load Pattern for Problem 5.5

Unit	Max (MW)	Net full-load heat rate (Btu/kWh)	Incremental heat rate (Btu/kWh)	Min (MW)	No-load cost* (MBtu/h)	Start-up cost (MBtu)	Min up/down time (h)
1	200	11,000	9,900	50	220	400	8
2	60	11,433	10,100	15	80	150	8
3	50	12,000	10,800	15	60	105	4
4	40	12,900	11,900	5	40	0	4
5	25	13,500	12,140	5	34	0	4

Load pattern

Hours	MW load	Conditions
1-2	250	1. Initially (prior to hour 1) only unit 1 is on and has been on for 4 hr.
3-4	320	2. Ignore losses, spinning reserve, etc. The only requirement is that the generation be able to supply the load.
5-6	110	
7-8	75	3. Fuel costs for all units may be taken as 1.40 R/MBtu

* See footnote on Table 5.4

- Develop the priority list for these units and solve for the optimum unit commitment. Use a strict priority list with a search range of three ($X = 3$) and save no more than three strategies ($N = 3$). Ignore min up/min down times for units.
- Solve the same commitment problem using the strict priority list with $X = 3$ and $N = 3$ as in (a), but obey the min up/min down time rules.
- (Optional) Find the optimum unit commitment without use of a strict priority list (i.e., all 32 unit on/off combinations are valid). Restrict the search range to decrease your effort. Obey the min up/min down time rules.

When using a dynamic-programming method to solve a unit commitment problem with minimum up- and downtime rules, one must save an additional piece of information at each state each hour. This information simply tells whether any units are ineligible to be shut down or started up at that state. If such units exist at a particular state, the transition cost, S_{cost} , to a state that violates the start-up/shut-down rules should be given a value of infinity.

FURTHER READING

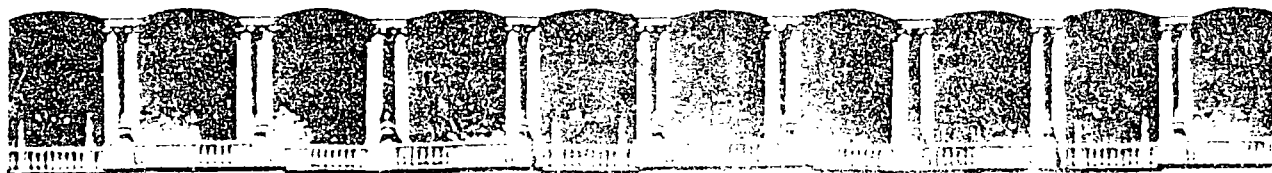
Some good introductory references to the unit commitment problem are found in references 1-3. A survey of the state-of-the-art (as of 1975) of unit commitment solutions is found in reference 4. References 5 and 6 provide a good look at two commercial unit commitment programs in present use.

References 7-11 deal with unit commitment as an integer-programming problem. Much of the pioneering work in this area was done by Garver (7), who also sounded a note of pessimism in a discussion of reference 8 written together with Happ in 1968. Further research 9-11 has refined the unit commitment solution by integer programming but has never really

overcome the Garver-Happ limitations presented in the 1968 discussion, thus leaving dynamic programming as the only viable solution technique to large-scale unit commitment problems.

References 12-16 should be consulted for a deeper study of the mathematical programming technique known as dynamic programming, which was introduced in the Appendix of this chapter. The reader should see references 17 and 18 for a discussion of valve-point loading and for a thorough development of economic dispatch via dynamic programming.

1. Baldwin, C. J., Dale, K. M., Dittrich, R. F., "A Study of Economic Shutdown of Generating Units in Daily Dispatch," *AIEE Transactions on Power Apparatus and Systems* Vol. PAS-78, December 1959, pp. 1272-1284.
2. Burns, R. M., Gibson, C. A., "Optimization of Priority Lists for a Unit Commitment Program," IEEE Power Engineering Society Summer Meeting, Paper A75 453-1, 1975.
3. Davidson, P. M., Kohrman, F. J., Master, G. L., Schafer, G. R., Evans, J. R., Lovewell, K. M., Payne, T. B., "Unit Commitment Start-Stop Scheduling in the Pennsylvania-New Jersey-Maryland Interconnection," 1967 PICA Conference Proceedings, 1967, pp. 127-132.
4. Gruhl, J., Schweppe, F., Ruane, M., "Unit Commitment Scheduling of Electric Power Systems," *Systems Engineering for Power: Status and Prospects*, Henniker, N. H., August 1975. U.S. Government Printing Office Washington D.C.
5. Pang, C. K., Chen, H. C., "Optimal Short-Term Thermal Unit Commitment," *IEEE Transactions on Power Apparatus and Systems*, Vol. PAS-95, July/August 1976, pp. 1336-1346.
6. Happ, H. H., Johnson, P. C., Wright, W. J., "Large Scale Hydro-Thermal Unit Commitment—Method and Results," *IEEE Transactions on Power Apparatus and Systems*, Vol. PAS-90, May/June 1971, pp. 1373-1384.
7. Garver, L. L., "Power Generation Scheduling by Integer Programming—Development of Theory," *AIEE Transactions on Power Apparatus and Systems*, February 1963, pp. 730-735.
8. Muckstadt, J. A., Wilson, R. C., "An Application of Mixed-Integer Programming Duality to Scheduling Thermal Generating Systems," *IEEE Transactions on Power Apparatus and Systems*. December 1968, pp. 1968-1978.
9. Ohuchi, A., Kaji, I., "A Branch-and-Bound Algorithm for Start-up and Shut-down Problems of Thermal Generating Units," *Electrical Engineering in Japan*, Vol. 95, No. 5, 1975, pp. 54-61.
10. Dillon, T. S., Egan, G. T., "Application of Combinational Methods to the Problems of Maintenance Scheduling and Unit Commitment in Large Power Systems," Proceedings of IFAC Symposium on Large Scale Systems Theory and Applications, Udine, Italy, 1976.
11. Dillon, T. S., Edwin, K. W., Kochs, H. D., Taud, R. J., "Integer Programming Approach to the Problem of Optimal Unit Commitment with Probabilistic Reserve Determination," *IEEE Transactions on Power Apparatus and Systems*, Vol. 97, November/December 1978, pp. 2154-2166.
12. Kaufmann, A., *Graphs, Dynamic Programming and Finite Games*, Academic Press, New York, 1967.
13. Kaufmann, A., Cruon, R., *Dynamic Programming: Sequential Scientific Management*, Academic Press, New York, 1967.
14. Howard, R. A., *Dynamic Programming and Markov Processes*, Wiley and Technology Press, New York, 1960.
15. Bellman, R. E., Dreyfus, S. E., *Applied Dynamics Programming*, Princeton University Press, Princeton, N.J., 1962.
16. Neuhauser, G. L., *Introduction to Dynamic Programming*, Wiley, New York, 1966.
17. Happ, H. H., Ille, W. B., Reisinger, R. M., "Economic System Operation Considering Valve Throttling Losses, I.—Method of Computing Valve-Loop Heat Rates on Multivalve Turbines," *IEEE Transactions on Power Apparatus and Systems*, Vol. PAS-82, February 1963, pp. 609-615.
18. Ringlee, R. J., Williams, D. D., "Economic Dispatch Operation Considering Valve Throttling Losses, II—Distribution of System Loads by the Method of Dynamic Programming," *IEEE Transactions on Power Apparatus and Systems*, Vol. PAS-82, February 1963, pp. 615-622.



**FACULTAD DE INGENIERIA U.N.A.M.
DIVISION DE EDUCACION CONTINUA**

**V CURSO INTERNACIONAL DE SISTEMAS
ELECTRICOS DE POTENCIA**

MODULO II: SISTEMAS ELECTRICOS DE POTENCIA

TEMA: GENERATION WITH LIMITED ENERGY SUPPLY

EXPOSITOR: ING. ARTURO MORALES COLLANTES

Generation with Limited Energy Supply

6.1 INTRODUCTION

The economic operation of a power system requires that expenditures for fuel be minimized over a period of time. When there is no limitation on the fuel supply to any of the plants in the system, the economic dispatch can be carried out with only the present conditions as data in the economic dispatch algorithm. In such a case the fuel costs are simply the incoming price of fuel with, perhaps, adjustments for fuel handling and maintenance of the plant.

When the energy resource available to a particular plant (be it coal, oil, gas, water, or nuclear fuel) is a limiting factor in the operation of the plant, the entire economic dispatch calculation must be done differently. Each economic dispatch calculation must account for what happened before and what will happen in the future.

This chapter begins the development of solutions to the dispatching problem "over time." The techniques used are an extension of the familiar LaGrange formulation. Concepts involving slack variables and penalty functions are introduced to allow solution under certain conditions.

The example chosen to start is a fixed fuel supply that must be paid for whether or not it is consumed.

We might have started with a limited fuel supply of natural gas that must be used as boiler fuel because it has been declared as "surplus." The take-or-pay fuel supply contract is probably the simplest of these possibilities.

Alternatively, we might have started directly with the problem of economic scheduling of hydroelectric plants with their stored supply of water or with light-water-moderated nuclear reactors supplying steam to drive turbine generators. Hydroelectric plant scheduling involves the scheduling of water flows, impoundments (storage), and releases into what usually prove to be a rather complicated hydraulic network (namely, the water shed). The treatment of nuclear unit scheduling requires some understanding of the physics involved in the reactor core and is really beyond the scope of this current text (the methods useful for optimizing the unit outputs are, however, quite similar to those used in scheduling other limited energy systems).

6.2 TAKE-OR-PAY FUEL SUPPLY CONTRACT

Assume there are N normally fueled thermal plants plus one turbine generator fueled under a "take-or-pay" agreement. We will interpret this type of agreement as being one in which the utility agrees to use a minimum amount of fuel during a period (the "take") or, failing to use this amount, it agrees to pay the minimum charge. This last clause is the "pay" part of the "take-or-pay" contract.

While this unit's cumulative fuel consumption is below the minimum, the system excluding this unit should be scheduled to minimize the total fuel cost subject to the constraint that the total fuel consumption for the period for this particular unit is equal to the specified amount. Once the specified amount of fuel has been used, the unit should be scheduled normally. Let us consider a special case where the minimum amount of fuel consumption is also the maximum. The system is shown in Figure 6.1. We will consider the operation of the system over

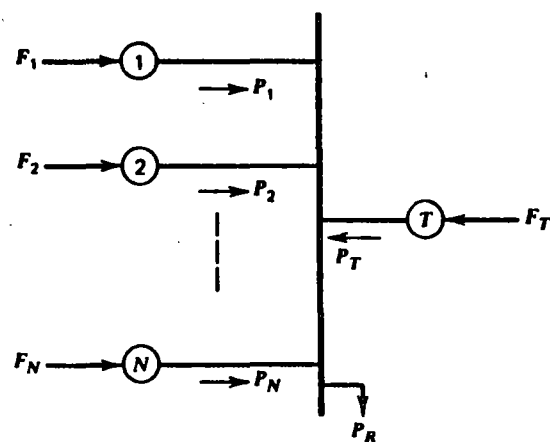


FIG. 6.1 $N + 1$ unit system with take-or-pay fuel supply at unit T .

j_{\max} time intervals j where $j = 1, \dots, j_{\max}$, so that

$$P_{1j}, P_{2j}, \dots, P_{Tj} \quad (\text{Power outputs})$$

$$F_{1j}, F_{2j}, \dots, F_{Nj} \quad (\text{Fuel cost rate})$$

and

$$q_{T1}, q_{T2}, \dots, q_{Tj} \quad (\text{Take-or-pay fuel input})$$

are the power outputs, fuel costs, and take-or-pay fuel inputs.

where $P_{ij} \triangleq$ power from i^{th} unit in the j^{th} time interval

$F_{ij} \triangleq$ $\$/\text{h}$ cost for i^{th} unit during the j^{th} time interval

$q_{Tj} \triangleq$ fuel input for unit T in j^{th} time interval

$F_{Tj} \triangleq$ $\$/\text{h}$ cost for unit T in j^{th} time interval

$P_{Rj} \triangleq$ total load in the j^{th} time interval

$n_j \triangleq$ Number of hours in the j^{th} time interval

Mathematically, the problem is as follow.

$$\min \sum_{j=1}^{j_{\max}} n_j \sum_{i=1}^N F_{ij} + \sum_{j=1}^{j_{\max}} n_j F_{Tj} \quad (6.1)$$

subject to

$$\phi = \sum_{j=1}^{j_{\max}} n_j q_{Tj} - q_{TOT} = 0 \quad (6.2)$$

and

$$\psi_j = P_{Rj} - \sum_{i=1}^N P_{ij} - P_{Tj} = 0 \quad \text{for } j = 1 \dots j_{\max} \quad (6.3)$$

or in words

We wish to determine the minimum production cost for units 1 to N subject to constraints that ensure that fuel consumption is correct and also subject to the set of constraints to ensure that power supplied is correct each interval.

Note that (for the present) we are ignoring high and low limits on the units themselves. It should also be noted that the term

$$\sum_{j=1}^{j_{\max}} n_j F_{Tj}$$

is constant because the total fuel to be used in the "T" plant is fixed. Therefore the total cost of that fuel will be constant and we can drop this term from the objective function.

The Lagrange function is

$$\mathcal{L} = \sum_{j=1}^{j_{\max}} n_j \sum_{i=1}^N F_{ij} + \sum_{j=1}^{j_{\max}} \lambda_j \left(P_{Rj} - \sum_{i=1}^N P_{ij} - P_{Tj} \right) + \gamma \left(\sum_{j=1}^{j_{\max}} n_j q_{Tj} - q_{TOT} \right) \quad (6.4)$$

The independent variables are the powers P_{ij} and P_{Tj} , since $F_{ij} = F_i(P_{ij})$ and $q_{Tj} = q_T(P_{Tj})$.

For any given time period, $j = k$,

$$\frac{\partial \mathcal{L}}{\partial P_{ik}} = 0 = n_k \frac{dF_{ik}}{dP_{ik}} - \lambda_k \quad \text{for } i = 1, \dots, N \quad (6.5)$$

and

$$\frac{\partial \mathcal{L}}{\partial P_{Tk}} = -\lambda_k + \gamma n_k \frac{dq_{Tk}}{dP_{Tk}} = 0 \quad (6.6)$$

Note that if one analyzes the dimensions of γ , it would be $\text{\$/unit of } q$ (e.g., $\text{\$/ft}^3$, $\text{\$/bbl}$, $\text{\$/ton}$). As such, γ has the units of a "fuel price" expressed in volume units rather than MBtu as we have used up to now. Because of this, γ is often referred to as a "pseudoprice" or "shadow price." In fact, once it is realized what is happening in this analysis it becomes obvious that we could solve fuel-limited dispatch problems by simply adjusting the price of the limited fuel(s), thus, the terms "pseudoprice" and "shadow price" are quite meaningful.

Since γ appears unsubscripted in Eq. 6.6, γ would be expected to be a constant value over all the time periods. This is true unless the fuel-limited machine is constrained by fuel-storage limitations. We will encounter such limitations in hydro-plant scheduling in Chapter 7. The appendix to Chapter 7 shows when to expect a constant γ and when to expect a discontinuity in γ .

Figure 6.2a shows how the load pattern may look. The solution to a fuel-limited dispatching problem will require dividing the load pattern into time intervals as in

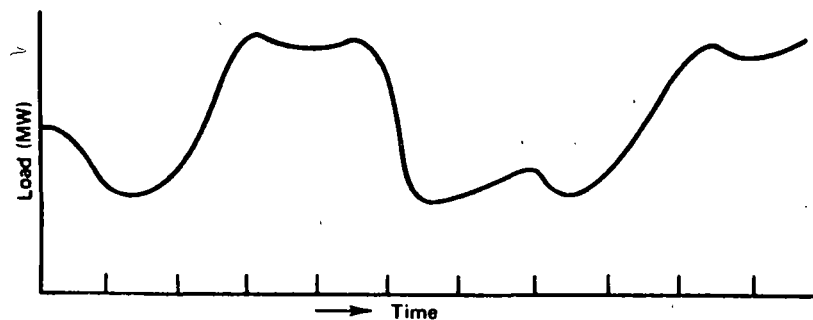


FIG. 6.2a Load pattern.

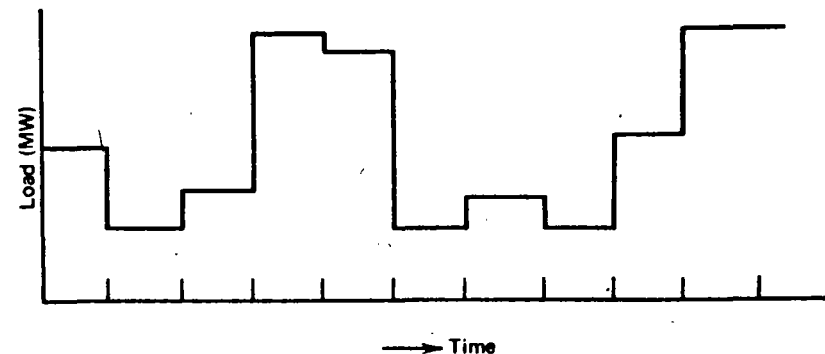


FIG. 6.2b Discrete load pattern.

Figure 6.2b and assuming load to be constant during each interval. Assuming all units are on-line for the period, the optimum dispatch could be done using a simple search procedure for γ as is shown in Figure 6.3. Note that the procedure shown in Figure 6.3 will only work if the fuel-limited unit does not hit either its high or its low limit in any time interval.

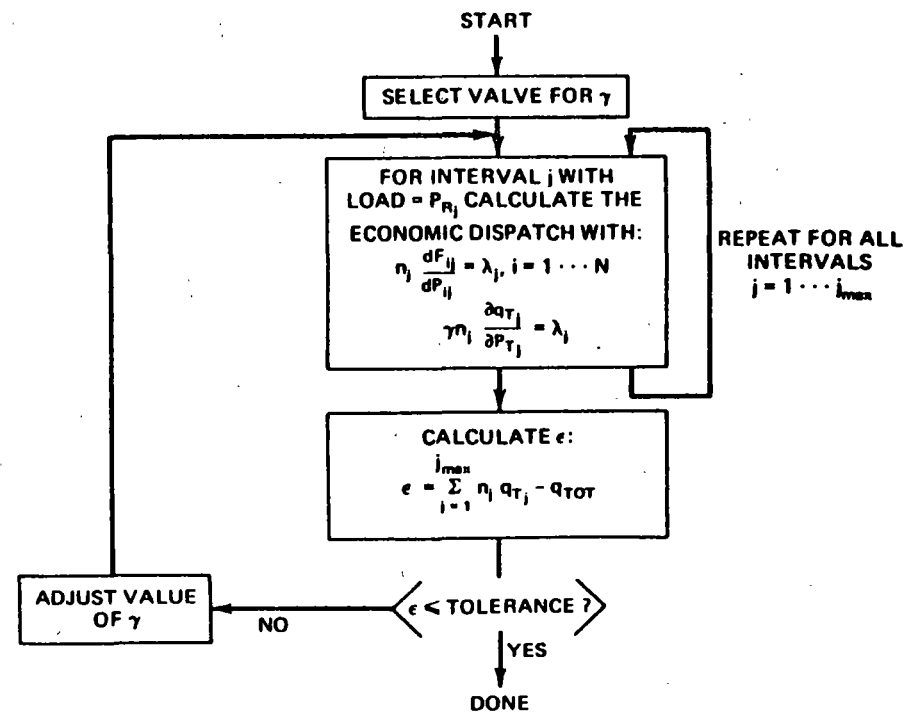


FIG. 6.3 γ search method.

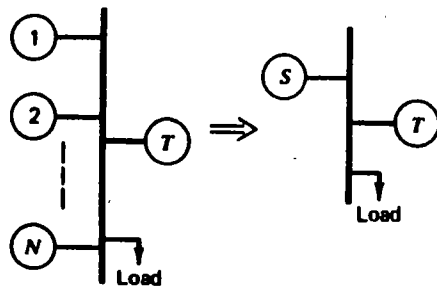


FIG. 6.4 Composite generator unit.

6.3 COMPOSITE GENERATION PRODUCTION COST FUNCTION

A useful technique to facilitate the take-or-pay fuel supply contract procedure is to develop a composite generation production cost curve for all the non-fuel-constrained units. For example, suppose there were N non-fuel-constrained units to be scheduled with the fuel-constrained unit as shown in Figure 6.4. Then a composite cost curve for units 1, 2, ..., N can be developed.

$$F_A(P_s) = F_1(P_1) + \dots + F_N(P_N) \quad (6.7)$$

where

$$P_s = P_1 + \dots + P_N$$

and

$$\frac{dF_1}{dP_1} = \frac{dF_2}{dP_2} = \dots = \frac{dF_N}{dP_N} = \lambda$$

If one of the units hits a limit, its output is held constant, as in Chapter 3, Eq. 3.6.

A simple procedure to allow one to generate $F_A(P_s)$ consists of adjusting λ from λ^{\min} to λ^{\max} in specified increments, where

$$\lambda^{\min} = \min \left[\frac{dF_i}{dP_i}, i = 1 \dots N \right]$$

$$\lambda^{\max} = \max \left[\frac{dF_i}{dP_i}, i = 1 \dots N \right]$$

At each increment, calculate the total fuel consumption and the total power output for all the units. These points represent points on the $F_A(P_s)$ curve. The points may be used directly by assuming $F_A(P_s)$ consists of straight-line segments between the points or a smooth curve may be fit to the points using a least-squares fitting program. Be aware, however, that such smooth curves may have undesirable properties such as nonconvexity (e.g., the first derivative is not monotonically increasing). The procedure to generate the points on $F_A(P_s)$ is shown in Figure 6.5.

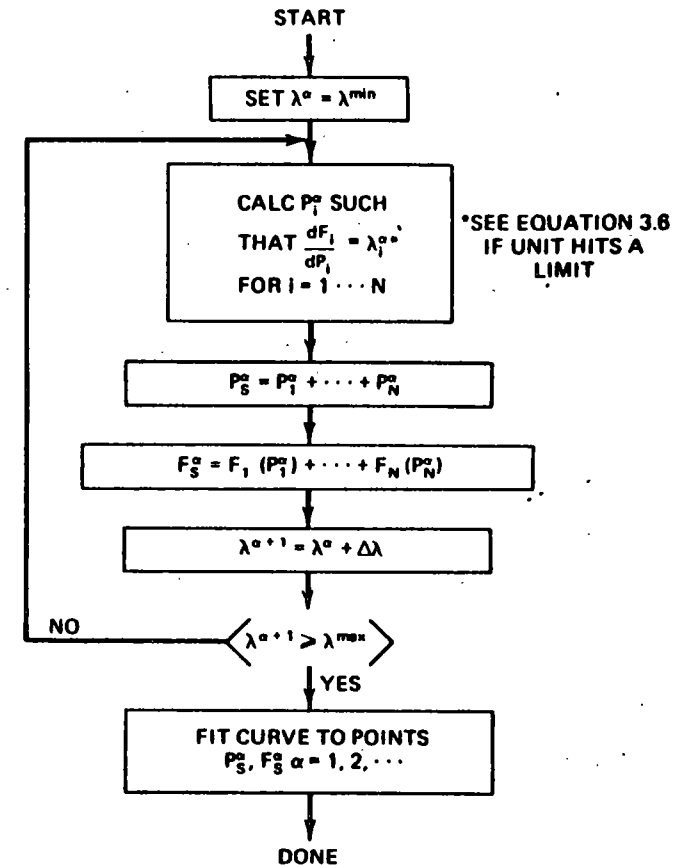


FIG. 6.5 Procedure for obtaining composite cost curve.

EXAMPLE 6A

The three generating units from Example 3A are to be combined into a composite generating unit. The fuel costs assigned to these units will be

Fuel cost for unit 1 = 1.1 ¢/MBtu

Fuel cost for unit 2 = 1.4 ¢/MBtu

Fuel cost for unit 3 = 1.5 ¢/MBtu

Figure 6.6a shows the individual unit incremental costs, which range from 8.3886 to 14.847 ¢/MWh. A program was written based on Figure 6.5, and lambda was stepped from 8.3886 to 14.847.

At each increment the three units are dispatched to the same lambda and then outputs and generating costs are added as shown in Figure 6.5. The results are given

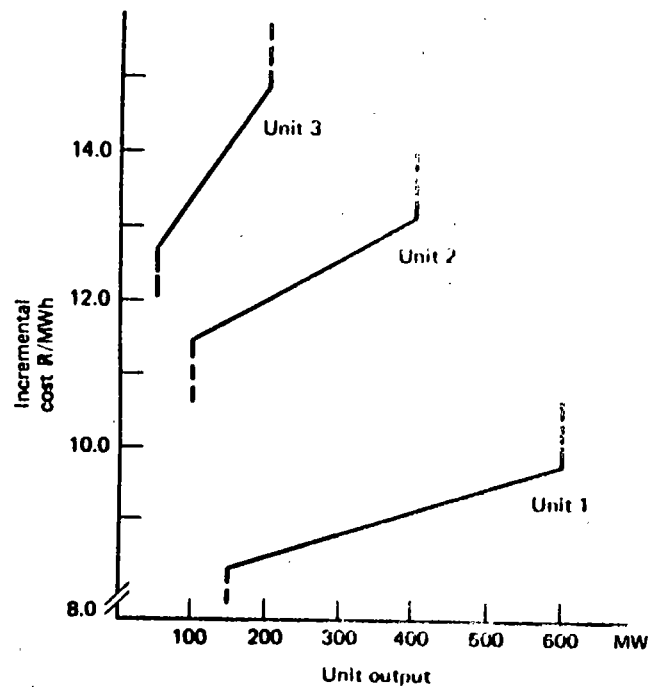


FIG. 6.6a Unit incremental costs.

TABLE 6.1 Lambda Steps Used in Constructing Composite Cost Curve for Example 6A

Step	lambda	P_i	F_i	F_i approx
1	8.3886	300.0	4077.12	4137.69
2	8.7115	403.4	4743.92	4924.39
3	9.0344	506.7	5878.10	5799.07
4	9.3574	610.1	6828.66	6761.72
5	9.6803	713.5	7812.59	7812.35
6	10.0032	750.0	8168.30	8204.68
7	11.6178	765.6	8346.58	8375.29
8	11.9407	825.0	9048.81	9044.86
9	12.2636	884.5	9768.28	9743.54
10	12.5866	943.9	10506.92	10471.31
12	12.9095	1019.4	11469.56	11436.96
13	13.2324	1088.4	12369.40	12360.58
14	13.5553	1110.67	12668.51	12668.05
15	13.8782	1133.00	12974.84	12979.63
16	14.2012	1155.34	13288.37	13295.30
17	14.5241	1177.67	13609.12	13615.09
18	14.8470	1200.00	13937.07	13938.98

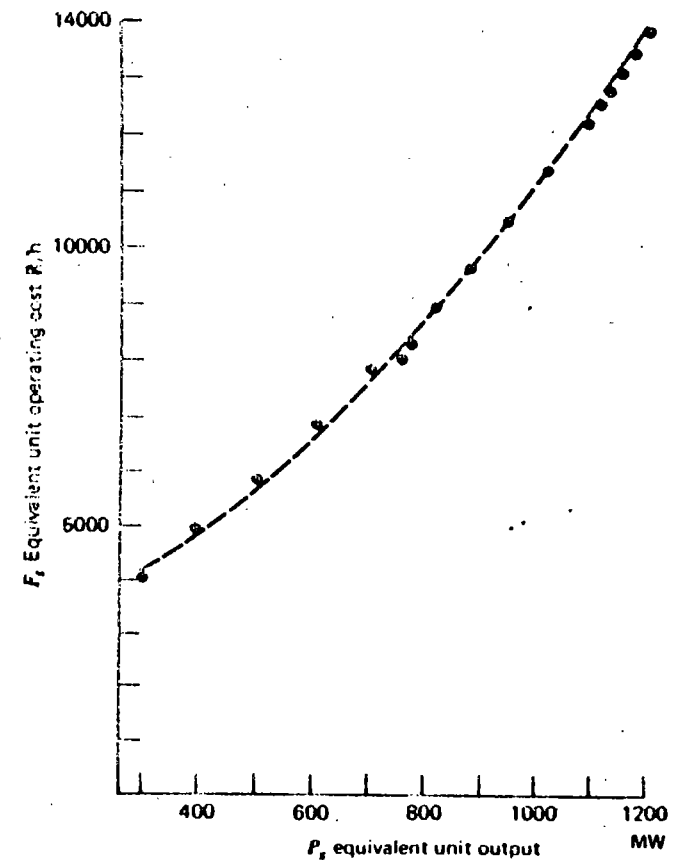


FIG. 6.6b Equivalent unit input/output curve.

in Table 6.1. The result, called F_i approx in Table 6.1 and shown in Figure 6.6b, was calculated by fitting a second-order polynomial to the P_i and F_i points using a least-squares fitting program. The equivalent unit function is

$$F_i \text{ approx}(P_i) = 2352.65 + 4.7151 P_i + 0.0041168 P_i^2$$

(k/h) 300 MW $\leq P_i \leq$ 1200 MW

The reader should be aware that when fitting a polynomial to a set of points many choices can be made. The preceding function is a good fit to the total operating cost of the three units, but it is not that good at approximating the incremental cost. More advanced fitting methods should be used if one desires to match total operating cost as well as incremental cost. See Problem 6.2 for an alternative procedure.

EXAMPLE 6B

Find the optimal dispatch for a gas-fired steam plant given the following.

Gas-fired Plant:

$$H_T(P_T) = 300 + 6.0 P_T + 0.0025 P_T^2 \text{ MBtu/h}$$

Fuel cost for gas = 2.0 R/ccf (where 1 ccf = 10^3 ft^3)

The gas is rated at 1100 Btu/ft³

$$50 \leq P_T \leq 400$$

Composite of Remaining Units:

$$H_s(P_s) = 200 + 8.5 P_s + 0.002 P_s^2 \text{ MBtu/h}$$

Equivalent fuel cost = 0.6 R/MBtu

$$50 \leq P_s \leq 500$$

The gas-fired plant must burn $40 \cdot 10^6 \text{ ft}^3$ of gas. The load pattern is shown in Table 6.2. If the gas constraints are ignored, the optimum economic schedule for these two plants appears as is shown in Table 6.3. Operating cost of the composite unit over the entire 24-h period is 52,128.03 R. The total gas consumption is $21.8 \cdot 10^6 \text{ ft}^3$. Since the gas-fired plant must burn $40 \cdot 10^6 \text{ ft}^3$ of gas, the cost will be $2.0 \text{ R}/1000 \text{ ft}^3 \times 40 \cdot 10^6 \text{ ft}^3$, which is 80,000 R for the gas. Therefore, the total cost will be 132,128.03 R. The solution method shown in Figure 6.3 was used with γ values ranging from 0.500 to 0.875. The final value for γ is 0.8742 R/ccf with an optimal schedule as shown in Table 6.4. This schedule has a fuel cost for the composite unit of 34,937.47 R. Note that the gas unit is run much harder and that it

TABLE 6.2 Load Pattern

Time period	Load
1. 12 PM - 4 AM	400 MW
2. 4 AM - 8 AM	650 MW
3. 8 AM - 12 AM	800 MW
4. 12 AM - 4 PM	500 MW
5. 4 PM - 8 PM	200 MW
6. 8 PM - 12 PM	300 MW

Where: $n_j = 4, j = 1 \dots 6$.

TABLE 6.3 Optimum Economic Schedule (Gas Constraints Ignored)

Time period	P_s	P_T
1	350	50
2	500	150
3	500	300
4	450	50
5	150	50
6	250	50

TABLE 6.4 Optimal Schedule (Gas Constraints Met)

Time period	P_s	P_T
1	197.3	202.6
2	353.2	296.8
3	446.7	353.3
4	259.7	240.3
5	72.6	127.4
6	135.0	165.0

does not hit either limit in the optimal schedule. Further note that the total cost is now

$$34,937.47 \text{ R} + 80,000 \text{ R} = 114,937.47 \text{ R}$$

so we have lowered the total fuel expense by properly scheduling the gas plant.

6.4 SOLUTION BY GRADIENT SEARCH TECHNIQUES

An alternative solution procedure to the one shown in Figure 6.3 makes use of Eqs. 6.5 and 6.6.

$$n_k \frac{dF_{ik}}{dP_{ik}} = \lambda_k$$

and

$$\lambda_k = \gamma n_k \frac{dq_{Tk}}{dP_{Tk}}$$

then

$$\gamma = \left(\frac{\frac{dF_{ik}}{dP_{ik}}}{\frac{dq_{Tk}}{dP_{Tk}}} \right) \tag{6.8}$$

For an optimum dispatch, γ will be constant for all hours $j, j = 1, \dots, j_{max}$.

We can make use of this fact to obtain an optimal schedule using the procedures shown in Figure 6.7a or Figure 6.7b. Both these procedures attempt to adjust fuel-limited generation so that γ will be constant over time. The algorithm shown in Figure 6.7a differs from the algorithm shown in Figure 6.7b in the way the problem is started and in the way various time intervals are selected for adjustment. The algorithm in Figure 6.7a requires an initial feasible but not optimal schedule and then finds an optimal schedule by "pairwise" trade-offs of fuel consumption while maintaining problem feasibility. The algorithm in Figure 6.7b does not require an

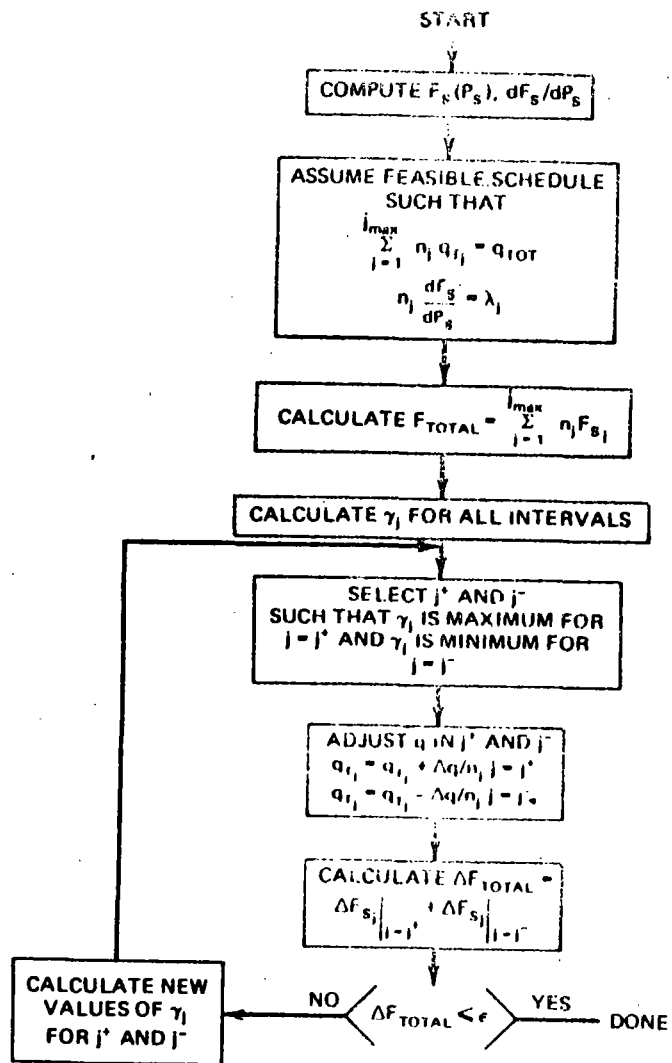


FIG. 6.7a Gradient method based on relaxation technique.

initial feasible fuel usage schedule but achieves this while optimizing. These two methods may be called gradient methods because q_{Tj} is treated as a vector and the γ_j 's indicate the gradient of the objective function with respect to q_{Tj} .

EXAMPLE 6C

Use the method of Figure 6.7b to obtain an optimal schedule for the problem given in Example 6B. Assume that the starting schedule is the economic dispatch schedule shown in Example 6A.

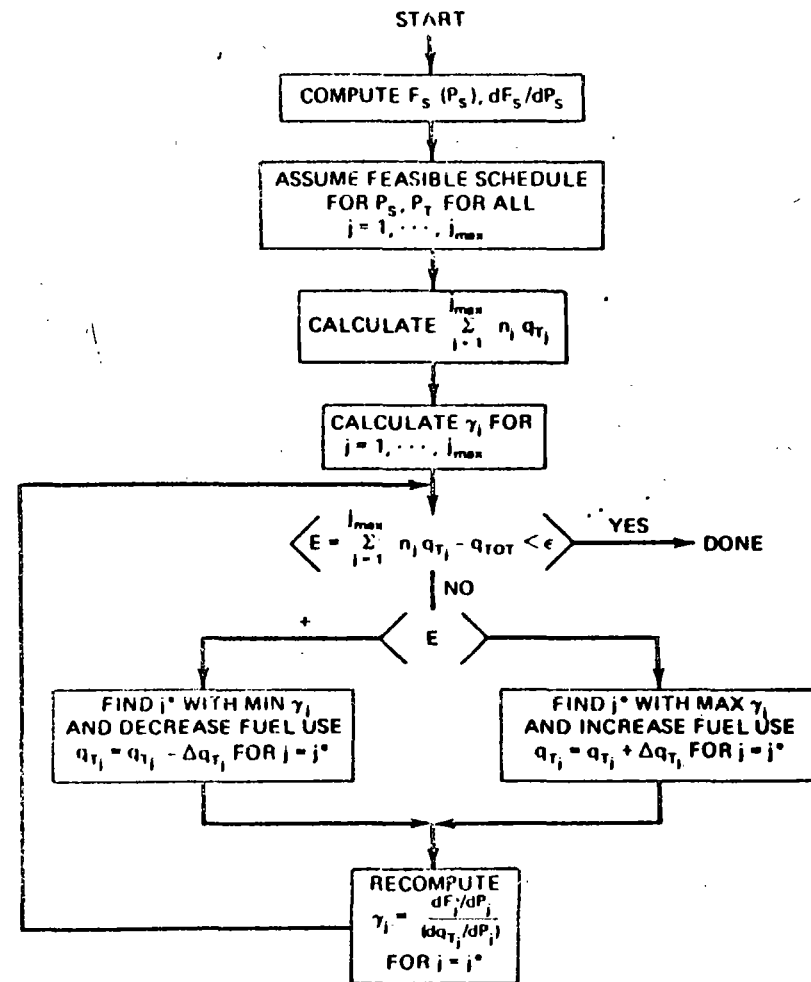


FIG. 6.7b Gradient method based on a simple search.

Initial Dispatch

Time period	1	2	3	4	5	6
P_s	350	500	500	450	150	250
P_T	50	150	300	50	50	50
γ	1.0454	1.0266	0.9240	1.0876	0.9610	1.0032

$$\sum q_T = 21.84 \cdot 10^6 \text{ ft}^3$$

Since we wish to burn $40.0 \cdot 10^6 \text{ ft}^3$ of gas, the error is negative, therefore we must increase fuel usage in the time period having maximum γ , that is, period 4. As a star increase P_T to 150 MW and drop P_s to 350 MW in period 4.

Result of Step 1

Time period	1	2	3	4	5	6
P_s	350	500	500	350	150	250
P_T	50	150	300	150	50	50
γ	1.0454	1.0266	0.9240	0.9680	0.9610	1.0032

$$\sum q_T = 24.2 \cdot 10^6 \text{ h}^2.$$

The error is still negative, so we must increase fuel usage in the period with maximum γ , which is now period 1. Increase P_T to 200 MW and drop P_s to 200 MW in period 1.

Result of Step 2

Time period	1	2	3	4	5	6
P_s	200	500	500	350	150	250
P_T	200	150	300	150	50	50
γ	0.8769	1.0266	0.9240	0.9680	0.9610	1.0032

$$\sum q_T = 27.8 \cdot 10^6 \text{ h}^2.$$

and so on. After 11 steps, the schedule looks like:

Time period	1	2	3	4	5	6
P_s	200	350	450	250	75	140
P_T	200	300	350	250	125	160
γ	0.8769	0.8712	0.8772	0.8648	0.8767	0.8794

$$\sum q_T = 40.002 \cdot 10^6 \text{ h}^2.$$

which is beginning to look similar to the optimal schedule generated in Example 6A.

6.5 HARD LIMITS AND SLACK VARIABLES

This section takes account of hard limits on the take-or-pay generating unit. The limits are

$$P_T \geq P_{T\min} \quad (6.9)$$

and

$$P_T \leq P_{T\max} \quad (6.10)$$

These may be added to the LaGrangian by the use of two constraint functions and two new variables called *slack variables* (see Appendix, Chapter 3). The constraint functions are

$$\psi_{1j} = P_{Tj} - P_{T\max} + S_{1j}^2 \quad (6.11)$$

and

$$\psi_{2j} = P_{T\min} - P_{Tj} + S_{2j}^2 \quad (6.12)$$

where S_{1j} and S_{2j} are slack variables that may take on any real value including zero.

The new LaGrangian then becomes

$$\begin{aligned} \mathcal{L} = & \sum_{j=1}^{J_{\max}} n_j \sum_{i=1}^N F_{ij} + \sum_{j=1}^{J_{\max}} \lambda_j \left(P_{Rj} - \sum_{i=1}^N P_{ij} - P_{Tj} \right) \\ & + \gamma \left(\sum_{j=1}^{J_{\max}} n_j q_{Tj} - Q_{TOT} \right) \\ & + \sum_{j=1}^{J_{\max}} \alpha_{1j} (P_{Tj} - P_{T\max} + S_{1j}^2) + \sum_{j=1}^{J_{\max}} \alpha_{2j} (P_{T\min} - P_{Tj} + S_{2j}^2) \end{aligned} \quad (6.13)$$

where α_{1j}, α_{2j} are LaGrange multipliers. Now, the first partial derivatives for the k^{th} period are

$$\begin{aligned} \frac{\partial \mathcal{L}}{\partial P_{1k}} = 0 &= n_j \frac{dF_{1j}}{dP_{1k}} - \lambda_k \\ \frac{\partial \mathcal{L}}{\partial P_{Tk}} = 0 &= -\lambda_k + \alpha_{1k} - \alpha_{2k} + \gamma n_j \frac{dq_{Tk}}{dP_{Tk}} \\ \frac{\partial \mathcal{L}}{\partial S_{1k}} = 0 &= 2\alpha_{1k} S_{1k} \\ \frac{\partial \mathcal{L}}{\partial S_{2k}} = 0 &= 2\alpha_{2k} S_{2k} \end{aligned} \quad (6.14)$$

As was noted in the Appendix to Chapter 3, when the constrained variable (P_{Tk} in this case) is within bounds, the new LaGrange multipliers $\alpha_{1k} = \alpha_{2k} = 0$ and S_{1k} and S_{2k} are nonzero. When the variable is limited, one of the slack variables, S_{1k} or S_{2k} , becomes zero and the associated LaGrange multiplier will take on a non-zero value.

Suppose in some interval k , $P_{Tk} = P_{\max}$, then $S_{1k} = 0$ and $\alpha_{1k} \neq 0$. Thus

$$-\lambda_k + \alpha_{1k} + \gamma n_j \frac{dq_{Tk}}{dP_{Tk}} = 0 \quad (6.15)$$

and if

$$\lambda_k > \gamma n_j \frac{dq_{Tk}}{dP_{Tk}}$$

the value of α_{2k} will take on the value just sufficient to make the equality true.

EXAMPLE 6D

Repeat Example 6B with the maximum generation on P_T reduced to 300 MW. Note that the optimum schedule in Example 6A gave a $P_T = 353.3$ MW in the third time

TABLE Resulting Optimal Schedule with $P_{i,max} = 300$ MW

Time period j	P_{ij}	P_{Tj}	λ_j	$\gamma_j \frac{\partial q_j}{\partial P_{ij}}$	α_{2j}
1	183.4	216.6	5.54	5.54	0
2	350.0	300.0	5.94	5.86	0.08
3	300.0	300.0	24.80 6.03	5.86	19.14 0.17
4	345.4	254.6	5.69	5.69	0
5	59.5	140.5	5.24	5.24	0
6	121.4	178.6	5.39	5.39	0

period. When the limit is reduced to 300 MW, the gas-fired unit will have to burn more fuel in other time periods to meet the $40 \cdot 10^3$ ft³ gas consumption constraint.

Table 6.5 shows the resulting optimal schedule where $\gamma = 0.2151$ and total cost = 122,984.83 R.

6.6 FUEL SCHEDULING BY LINEAR PROGRAMMING

Figure 6.8 shows the major elements in the chain making up the delivery system that starts with raw fuel suppliers and ends up in delivery of electric power to individual customers. The basic elements of the chain are

The Suppliers: Coal, oil, and gas companies with which the utility must negotiate contracts to acquire fuel. The contracts are usually written for a long term (10 to 20 yr) and may have stipulations such as the minimum and maximum limits on the quantity of fuel delivered over a specified time period. The time period may be as long as a year, a month, a week, a day, or even for a period of only a few minutes. Prices may change as subject to the renegotiation provisions of the contracts.

Transportation: Railroads, unit trains, river barges, gas pipeline companies, and such all present problems in scheduling of deliveries of fuel.

Inventory: Coal piles, oil storage tanks, underground gas storage facilities. Inventories must be kept at proper levels to forestall fuel shortages when load levels exceed forecast or suppliers or shippers are unable to deliver. Price fluctuations also complicate the decisions on when and how much to add or subtract from inventories.

The remainder of the system—generators, transmission, and loads—are covered in other chapters.

One of the most useful tools for solving large fuel-scheduling problems is linear programming (LP). If the reader is not familiar with LP, an easily understood algorithm is provided in the Appendix of this chapter.

Linear programming is an optimization procedure that minimizes a linear objective function with variables that are also subject to linear constraints. Because

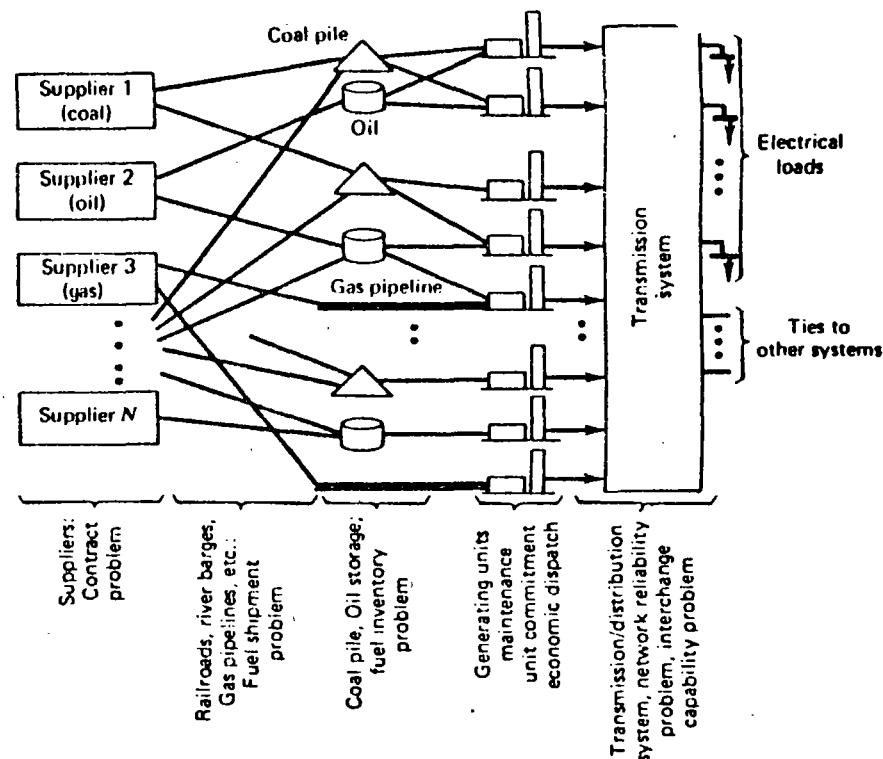


FIG. 6.8 Energy delivery system.

of this limitation, any nonlinear functions either in the objective or in the constraint equations will have to be approximated by linear or piecewise linear functions.

To solve a fuel-scheduling problem with linear programming, we must break the total time period involved into discrete time increments as was done in Example 6B. The LP solution will then consist of an objective function that is made up of a sum of linear or piecewise linear functions each of which is a function of one or more variables from only one time step. The constraints will be linear functions of variables from each time step. Some constraints will be made up of variables drawn from one time step whereas others will span two or more time steps. The best way to illustrate how to set up an LP to solve a fuel-scheduling problem will be to use an example.

EXAMPLE 6E

We are given two coal-burning generating units that must both remain on-line for a 3-wk period. The combined output from the two units is to supply the following loads (loads are assumed constant for 1 wk).

Week	Load (MW)
1	1200
2	1500
3	800

The two units are to be supplied by one coal supplier who is under contract to supply 40,000 tons of coal per week to the two plants. The plants have existing coal inventories at the start of the 3-wk period. We must solve for the following.

1. How should each plant be operated each week?
2. How should the coal deliveries be made up each week?

The data for the problem are as follows.

Coal: Heat value = 11,500 Btu/lb = 23 MBtu/ton
(1 ton = 2000 lb)

Coal can be delivered to one plant or the other or it can be split, some going to one plant, some to the other, as long as the total delivery in each week is equal to 40,000 tons. The coal costs 30 R/ton or 1.3 R/MBtu

Inventories: Plant 1: has an initial inventory of 70,000 tons, its final inventory is not restricted
Plant 2: has an initial inventory of 70,000 tons, its final inventory is not restricted

Both plants have a maximum coal storage capacity of 200,000 tons of coal.

Generating Units:

Unit	Min (MW)	Max (MW)	Heat input at min (MBtu/h)	Heat input at max (MBtu/h)
1	150	600	1620	5340
2	400	1000	3850	8750

The input versus output function will be approximated by a linear function for each unit.

$$H_1(P_1) = 380.0 + 8.267 P_1$$

$$H_2(P_2) = 583.3 + 8.167 P_2$$

The unit cost curves are

$$F_1(P_1) = 1.3 \text{ R/MBtu} \times H_1(P_1) = 495.65 + 10.78 P_1 \text{ (R/h)}$$

$$F_2(P_2) = 1.3 \text{ R/MBtu} \times H_2(P_2) = 760.8 + 10.65 P_2 \text{ (R/h)}$$

The coal consumption q (tons/h) for each unit is

$$q_1(P_1) = \frac{1}{23} \left(\frac{\text{Tons}}{\text{MBtu}} \right) \times H_1(P_1) = 16.52 + 0.3594 P_1 \text{ tons/h}$$

$$q_2(P_2) = \frac{1}{23} \left(\frac{\text{Tons}}{\text{MBtu}} \right) \times H_2(P_2) = 25.36 + 0.3551 P_2 \text{ tons/h}$$

To solve this problem with linear programming, assume that the units are to be operated at a constant rate during each week and that the coal deliveries will each take place at the beginning of each week. Therefore, we will set up the problem with 1-wk time periods and the generating unit cost functions and coal consumption functions will be multiplied by 168 h to put them on a "per week" basis, then

$$F_1(P_1) = 83,269.2 + 1811 P_1 \text{ R/wk}$$

$$F_2(P_2) = 127,814.4 + 1789 P_2 \text{ R/wk}$$

$$q_1(P_1) = 2775.4 + 60.4 P_1 \text{ tons/wk}$$

$$q_2(P_2) = 4260.5 + 59.7 P_2 \text{ tons/wk}$$

(6.16)

We are now ready to set up the objective function and the constraints for our linear programming solution.

Objective Function: To minimize the operating cost over the 3-wk period. The objective function is

$$\begin{aligned} \text{Minimize } Z = & F_1[P_1(1)] + F_2[P_2(1)] + F_1[P_1(2)] + F_2[P_2(2)] \\ & + F_1[P_1(3)] + F_2[P_2(3)] \end{aligned} \quad (6.17)$$

where $P_i(j)$ is the power output of the i^{th} unit during the j^{th} week, $j = 1 \dots 3$.

Constraints: During each time period, the total power delivered from the units must equal the scheduled load to be supplied, then

$$P_1(1) + P_2(1) = 1200$$

$$P_1(2) + P_2(2) = 1500 \quad (6.18)$$

$$P_1(3) + P_2(3) = 800$$

Similarly, the coal deliveries, D_1 and D_2 , made to plant 1 and plant 2, respectively, during each week must sum to 40,000 tons. Then

$$D_1(1) + D_2(1) = 40,000$$

$$D_1(2) + D_2(2) = 40,000 \quad (6.19)$$

$$D_1(3) + D_2(3) = 40,000$$

The volume of coal at each plant at the beginning of each week plus the delivery of coal to that plant minus the coal burned at the plant will give the coal remaining at

week of

$$V_1(1) = 70,000 \text{ tons}$$

$$V_2(1) = 70,000 \text{ tons}$$

The solution is

<i>t</i>	P_1	P_2	D_1	D_2	V_1	V_2
1	200	1000	0	40000	70000	70000
2	500	1000	0	40000	55144.6	46039.5
3	150	650	0	40000	22169.2	22079.0
4					10333.8	19013.5

Total operating cost = 6,913,449.00 ₪

In this case, there are no constraints on the coal deliveries to either plant and the system can run in the most economic manner. Since unit 2 has a lower incremental cost, it is run at its maximum when possible. Furthermore, since no restrictions were placed on the coal pile levels at the end of the third week, the coal deliveries could have been shifted a little from unit 2 to unit 1 with no effect on the generation dispatch.

The next case solved was purposely structured to create a fuel shortage at unit 2. The beginning inventory at plant 2 was set to 50,000 tons, and a requirement was imposed that at the end of the third week the coal pile at unit 2 be no less than 8000 tons. The solution was made by changing the right-hand side of the fourth constraint from -65739.5 (i.e., $4260.5 - 70,000$) to -45739.5 (i.e., $4260.5 - 50,000$) and placing a lower bound on $V_2(4)$ (i.e., variable X_{18}) of 8000. The solution is

<i>t</i>	P_1	P_2	D_1	D_2	V_1	V_2
1	200	1000	0	40000	70000	50000
2	600	900	0	40000	55144.6	26039.5
3	200.5	599.5	0	40000	16129.2	8049.0
4					1241.93	8000.0

Total operating cost = 6,916,760.00 ₪

Note that this solution requires unit 2 to drop off its generation in order to meet the end-point constraint on its coal pile. In this case, all the coal must be delivered to plant 2 to minimize the overall cost.

The final case was constructed to show the interaction of the fuel deliveries and the economic dispatch of the generating units. In this case, the initial coal piles were set to 10,000 tons and 150,000 tons, respectively. Furthermore, a restriction of 30,000 tons minimum in the coal pile at unit 1 at the end of the third week was imposed.

To obtain the most economic operation of the two units over the 3-wk period, the coal deliveries will have to be adjusted to ensure both plants have sufficient coal. The

solution was obtained by setting the right-hand side of the third and fourth constraint equations to -7224.6 and -145739.5 , respectively, as well as imposing a lower bound of 30,000 on $V_1(4)$ (i.e., variable X_{17}).

The solution is

<i>t</i>	P_1	P_2	D_1	D_2	V_1	V_2
1	200	1000	4855.4	35144.6	10000	150000
2	500	1000	34810.8	5189.2	0	121184.1
3	150	650	40000	0	1835.4	62412.8
4					30000	19347.3

Total operating cost = 6,913,449.00 ₪

The LP was able to find a solution that allowed the most economic operation of the units while still directing enough coal to unit 1 to allow it to meet its end-point coal pile constraint. Note that in practice we would probably not wish to let the coal pile at unit 1 go to zero. This could be prevented by placing an appropriate lower bound on all the volume variables (i.e., X_5 , X_8 , X_{11} , X_{14} , X_{17} , and X_{18}).

This example has shown how a fuel-management problem can be solved with linear programming. The important factor in being able to solve very large fuel-scheduling problems is to have a linear-programming code capable of solving large problems having perhaps tens of thousands of constraints and as many or more problem variables. Using such codes, elaborate fuel-scheduling problems can be optimized out over several years and play a critical role in utility fuel-management decisions.

APPENDIX

Linear Programming

Linear programming is perhaps the most widely applied mathematical programming technique. Simply stated, linear programming seeks to find the optimum value of a linear objective function while meeting a set of linear constraints. That is, we wish to find the optimum set of x 's that minimize the following objective function.

$$Z = c_1x_1 + c_2x_2 + \dots + c_Nx_N$$

Subject to a set of linear constraints:

$$a_{11}x_1 + a_{12}x_2 + \dots + a_{1N}x_N \leq b_1$$

$$a_{21}x_1 + a_{22}x_2 + \dots + a_{2N}x_N \leq b_2$$

⋮

In addition variables themselves may have specified upper and lower limits.

$$x_i^{\min} \leq x_i \leq x_i^{\max} \quad i = 1 \cdots N$$

There are a variety of solutions to the LP problem. Many of these solutions are tailored to a particular type of problem. This appendix will not try to develop the theory of alternate LP solution methods. Rather, it will present a simple LP algorithm that can be used (or programmed on a computer) to solve the applicable power-system sample problems given in this text.

The algorithm is presented in its simplest form. There are alternative formulations, and these will be indicated when appropriate. If the student has access to a standard LP program, such a standard program may be used to solve any of the problems in this book.

The LP technique presented here is properly called an *upper-bounding dual linear programming algorithm*. The "upper-bounding" part of its name refers to the fact that variable limits are handled implicitly in the algorithm. Dual refers to the theory behind the way in which the algorithm operates. For a complete explanation of the primal and dual algorithms, refer to the references cited at the end of this chapter.

In order to proceed in an orderly fashion to solve a dual upper-bound linear programming problem, we must first add what is called a *slack variable* to each constraint. The slack variable is so named because it equals the difference or slack between a constraint and its limit. By placing a slack variable into an inequality constraint, we can transform it into an equality constraint. For example, suppose we are given the following constraint.

$$2x_1 + 3x_2 \leq 15 \quad (6A.1)$$

We can transform this constraint to an equality constraint by adding a slack variable, x_3 .

$$2x_1 + 3x_2 + x_3 = 15 \quad (6A.2)$$

If x_1 and x_2 were to be given values such that the sum of the first two terms in Eq. 6A.2 added to less than 15, we could still satisfy Eq. 6A.2 by setting x_3 to the difference. For example, if $x_1 = 1$, $x_2 = 3$, then $x_3 = 4$ would satisfy Eq. 6A.2. We can go even further, however, and restrict the values of x_3 so that Eq. 6A.2 still acts as an inequality constraint such as Eq. 6A.1. Note that when the first two terms of Eq. 6A.2 add to exactly 15, x_3 must be set to zero. By restricting x_3 to always be a positive number, we can force Eq. 6A.2 to yield the same effect as Eq. 6A.1. Thus:

$$\left. \begin{array}{l} 2x_1 + 3x_2 + x_3 = 15 \\ 0 \leq x_3 \leq \infty \end{array} \right\} \text{is equivalent to: } 2x_1 + 3x_2 \leq 15$$

Note that we could change a "less than or equal to" constraint to a "greater than or equal to" constraint by changing the sign on the slack variable. Then

$$\left. \begin{array}{l} 2x_1 + 3x_2 - x_3 = 15 \\ 0 \leq x_3 \leq \infty \end{array} \right\} \text{is equivalent to: } 2x_1 + 3x_2 \geq 15$$

Because of the way the dual upper-bounding algorithm is initiated, we will always require slack variables in every constraint. In the case of an equality constraint, we will add a slack variable and then require its upper and lower bounds to both equal zero.

To solve our linear programming algorithm, we must arrange the objective function and constraints in a tabular form as follows.

$$\begin{array}{rcl} a_{11}x_1 + a_{12}x_2 + \cdots + x_{\text{slack}_1} & = & b_1 \\ a_{21}x_1 + a_{22}x_2 + \cdots + x_{\text{slack}_2} & = & b_2 \\ c_1x_1 + c_2x_2 + \underbrace{\hspace{10em}}_{\text{Basis variables}} - Z & = & 0 \end{array} \quad (6A-3)$$

Because we have added slack variables to each constraint, we automatically have arranged the set of equations into what is called *canonical form*. In canonical form, there is at least one variable in each constraint whose coefficient is zero in all the other constraints. These variables are called the *basis variables*. The entire solution procedure for the linear programming algorithm centers on performing "pivot" operations that can exchange a nonbasis variable for a basis variable. A pivot operation may be shown by using our tableau in Eq. 6A.3. Suppose we wished to exchange variable x_1 , a nonbasis variable for x_{slack_2} , a slack variable. This could be accomplished by "pivoting" on column 1 row 2. To carry out the pivoting operation we execute the following steps.

Pivoting on Column 1 Row 2

Step 1 Multiply row 2 by $1/a_{21}$

That is, each a_{2j} , $j = 1 \cdots N$ in row 2 becomes

$$a'_{2j} = \frac{a_{2j}}{a_{21}} \quad j = 1 \cdots N$$

and

$$b_2 \text{ becomes } b'_2 = \frac{b_2}{a_{21}}$$

Step 2 For each row i ($i \neq 2$), multiply row 2 by a_{i1} and subtract from row i . That is, each coefficient a_{ij} in row i ($i \neq 2$) becomes

$$a'_{ij} = a_{ij} - a_{i1}a'_{2j} \quad j = 1 \cdots N$$

and

$$b_i \text{ becomes } b'_i = b_i - a_{i1}b'_2$$

Step 3 Last of all, we also perform the same operations in step 2 on the cost row. That is, each coefficient c_j becomes

$$c'_j = c_j - c_1a'_{2j} \quad j = 1 \cdots N$$

The result of carrying out the pivot operation will look like

$$\begin{aligned} a'_{12}x_2 + \cdots x_{\text{slack}_1} + a'_{1s_2}x_{\text{slack}_2} &= b'_1 \\ x_1 + a'_{22}x_2 + \cdots + a'_{2s_2}x_{\text{slack}_2} &= b'_2 \\ c'_2x_2 + \cdots + c'_{s_2}x_{\text{slack}_2} - Z &= Z' \end{aligned}$$

Notice that the new basis for our tableau is formed by variable x_1 and x_{slack_1} . x_{slack_2} no longer has nonzero coefficients in row 1 or the cost row.

The dual upper-bounding algorithm proceeds in simple steps wherein variables that are in the basis are exchanged for variables out of the basis. When an exchange is made, a pivot operation is carried out at the appropriate row and column. The nonbasis variables are held equal to either their upper or their lower value while the basis variables are allowed to take any value without respect to their upper or lower bounds. The solution terminates when all the basis variables are within their respective limits.

In order to use the dual upper-bound LP algorithm, follow these rules.

Start:

1. Each variable that has a nonzero coefficient in the cost row (i.e., the objective function) must be set according to the following rule.

$$\text{If } C_j > 0, \quad \text{set } x_j = x_j^{\min}$$

$$\text{If } C_j < 0, \quad \text{set } x_j = x_j^{\max}$$

2. If $C_j = 0$, x_j may be set to any value, but for convenience set it to its minimum also.
3. Add a slack variable to each constraint. Using the x_j values from steps 1 and 2, set the slack variables to make each constraint equal to its limit.

Variable exchange:

1. Find the basis variable with the greatest violation, this determines the row to be pivot on. Call this row R . If there are no limit violations among the basis variables, we are done. The most violated variable leaves the basis and is set equal to the limit that was violated.
2. Select the variable to enter the basis using one of the following column selection procedures.

Column Selection Procedure P1 (Most violated variable below its minimum)

Given constraint row R , whose basis variable is below its minimum and is the worst violation. Pick column S , so that, $c_S/(-a_{R,S})$ is minimum for all S that meet the following rules.

- a. S is not in the current basis.
- b. $a_{R,S}$ is not equal to zero.
- c. If x_S is at its minimum, then $a_{R,S}$ must be negative and c_S must be positive or zero.
- d. If x_S is at its maximum, then $a_{R,S}$ must be positive and c_S must be negative or zero.

Column Selection Procedure P2 (Most violated variable above its maximum)

Given constraint row R , whose basis variable is above its maximum and is the worst violation. Pick column S , so that, $c_S/a_{R,S}$ is the minimum for all S that meet the following rules:

- a. S is not in the current basis.
 - b. $a_{R,S}$ is not already zero.
 - c. If x_S is at its minimum, then $a_{R,S}$ must be positive and c_S must be positive or zero.
 - d. If x_S is at its maximum, then $a_{R,S}$ must be negative and c_S must be negative or zero.
3. When a column has been selected, pivot at the selected row R (from step 1) and column S (from step 2). The pivot column's variable, S goes into the basis.

If no column fits the column selection criteria, we have an infeasible solution. That is, there are no values for $x_1 \cdots x_N$ that will satisfy all constraints simultaneously. In some problems, the cost coefficient c_S associated with column S will be zero for several different values of S . In such a case, $c_S/a_{R,S}$ will be zero for each such S and none of them will be the minimum. The fact that c_S is zero means that there will be no increase in cost if any of the S 's are pivoted into the basis; therefore the algorithm is indifferent to which one is chosen.

Setting the Variables After Pivoting

1. All nonbasis variables, except x_S remain as they were before pivoting.
2. The most violated variable is set to the limit that was violated.
3. Since all nonbasis variables are determined, we can proceed to set each basis variable to whatever value is required to make the constraints balance. Note that this last step may move all the basis variables to new values, and some may now end up violating their respective limits (including the x_S variable).

Go back to step 1 of the variable exchange procedure.

These steps are shown in flowchart form in Figure 6.10. To help you understand the procedures involved, a sample problem is solved using the dual upper-bounding algorithm. The sample problem, shown in Figure

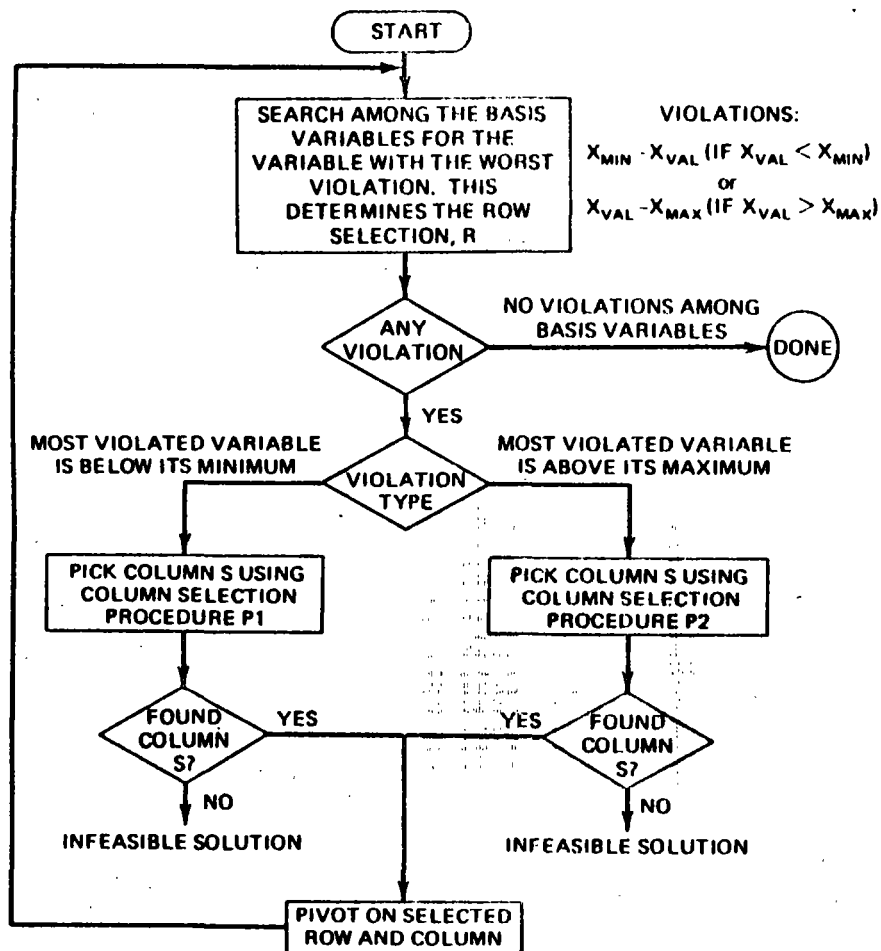
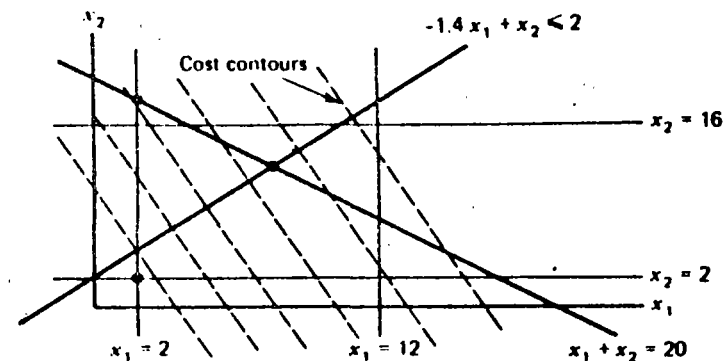


FIG. 6.10 Dual upper-bound linear programming algorithm.

consists of a two-variable objective with one equality constraint and one inequality constraint.

First, we must put the equations into canonical form by adding slack variables x_3 and x_4 . These variables are given limits corresponding to the type of constraint into which they are placed. x_3 is the slack variable in the equality constraint, so its limits are both zero; x_4 is in an inequality constraint so it is restricted to be a positive number. To start the problem, the objective function must be set to the minimum value it can attain, and the algorithm will then seek the minimum constrained solution by increasing the objective just enough to reach the constrained solution. Thus we set x_1 and x_2 both at their minimum values since the cost coefficients are



Minimize: $Z = 2x_1 + x_2$
 Subject to: $x_1 + x_2 = 20$ constraint 1
 $-1.4x_1 + x_2 \leq 2$ constraint 2
 $2 \leq x_1 \leq 12$
 $2 \leq x_2 \leq 16$

FIG. 6.11 Sample LP problem.

both positive. These conditions are shown here

Constraint 1:	$x_1 + x_2$	$+ x_3$		$= 20 - R$
Constraint 2:	$-1.4x_1 + x_2$		$+ x_4$	$= 2$
Cost:	$2x_1 + x_2$			$- Z = 0$
				$0 \leq x_3 \leq 0$
				$0 \leq x_4 \leq \infty$
Minimum:	2	2	0	0
Present value:	2	2	16	2.8 6
Maximum:	12	16	0	∞

Basis variable 1
 Basis variable 2
 ↑
 Most-violated variable

We can see from these conditions that variable x_3 is the worst-violated variable and that it presently exceeds its maximum limit of zero. Thus we must use column procedure P2 on constraint number 1. This is summarized as follows.

Using selection procedure P2 on constraint 1:

$$i = 1 \quad a_1 > 0 \quad x_1 = x_1^{\min} \quad c_1 > 0 \quad \text{then } \frac{c_1}{a_1} = \frac{2}{1} = 2$$

$$i = 2 \quad a_2 > 0 \quad x_2 = x_2^{\min} \quad c_1 > 0 \quad \text{then } \frac{c_1}{a_2} = \frac{1}{1} = 1$$

$\min c_i/a_i$ is 1 at $i = 2$

Pivot at column 2 row 1

To carry out the required pivot operations on column 2 row 1, we need merely subtract the first constraint from the second constraint and from the objective function. This results in:

Constraint 1:	x_1	$+ x_2 + x_3$		$= 20$
Constraint 2:	$-2.4 x_1$	$- x_3$	$+ x_4$	$= -18 \leftarrow R$
Cost:	x_1	$- x_3$		$- Z = -20$
Minimum:	2	2	0	0
Present value:	2	18	0	-13.2 22
Maximum:	12	16	0	∞
		Basis variable	Basis variable	
		1	2	
			Most-violated variable	

We can see now that the variable with the worst violation is x_4 and that x_4 is below its minimum. Thus we must use selection procedure P1 as follows.

Using selection procedure P1 on constraint 2

$$i = 1 \quad a_1 < 0 \quad x_1 = x_1^{\min} \quad c_1 > 0 \quad \text{then } \frac{c_1}{-a_1} = \frac{1}{-(-2.4)} = 0.4166$$

$$i = 3 \quad a_3 < 0 \quad x_3 = x_3^{\min} = x_3^{\max} \quad c_3 < 0 \quad \text{then } x_3 \text{ is not eligible}$$

Pivot at column 1 row 2

Which after pivoting results in

Constraint 1:		$x_2 + 0.5833 x_3 + 0.4166 x_4$	$= 12.5$
Constraint 2:	x_1	$+ 0.4166 x_3 - 0.4166 x_4$	$= 7.5$
Cost:		$- 1.4166 x_3 + 0.4166 x_4$	$- Z = -27.5$
Minimum:	2	2	0
Present value:	7.5	12.5	0
Maximum:	12	16	0
	Basis variable	Basis variable	
	1	2	

At this point we have no violations among the basis variables, so the algorithm can stop at the optimum.

$$\left. \begin{array}{l} x_1 = 7.5 \\ x_2 = 12.5 \end{array} \right\} \text{cost} = 27.5$$

See Figure 6.11 to verify that this is the optimum. The dots in Figure 6.11 show the solution points beginning at the starting point $x_1 = 2, x_2 = 2, \text{cost} = 6.0$ then going to $x_1 = 2, x_2 = 18, \text{cost} = 22.0$ and finally to the optimum $x_1 = 7.5, x_2 = 12.5, \text{cost} = 27.5$

How does this algorithm work? At each step two decisions are made.

1. Select the most-violated variable.
2. Select a variable to enter the basis.

The first decision will allow the procedure to eliminate, one after the other, those constraint violations that exist at the start as well as those that happen during the variable-exchange steps. The second decision (using the column selection procedures) guarantees that the rate of increase in cost to move the violated variable to its limit is minimized. Thus the algorithm starts from a minimum cost, infeasible solution (constraints violated), toward a minimum cost, feasible solution, by minimizing the rate of cost increase at each step.

PROBLEMS

6.1 Three units are on-line all 720 h of a 30-day month. Their characteristics are as follows.

$$H_1 = 225 + 8.47 P_1 + 0.0025 P_1^2, 50 \leq P_1 \leq 350$$

$$H_2 = 729 + 6.20 P_2 + 0.0081 P_2^2, 50 \leq P_2 \leq 350$$

$$H_3 = 400 + 7.50 P_3 + 0.0025 P_3^2, 50 \leq P_3 \leq 450$$

In these equations the H_i are in MBtu/h and the P_i are in MW.

Fuel costs for units 2 and 3 are 0.60R/MBtu. Unit 1, however, is operated under a take-or-pay fuel contract where 60,000 tons of coal are to be burned and/or paid for each 30-day period. This coal costs 12R/ton delivered and has an average heat content of 12,500 Btu/lb (1 ton = 2000 lb).

The system monthly load-duration curve may be approximated by three steps as follows.

Load (MW)	Hours duration	Energy (MWh)
800	50	40,000
500	550	275,000
300	120	36,000
Total	720 h	351,000 Mwh

- Compute the economic schedule for the month assuming all three units are on-line all the time and that the coal must be consumed. Show the MW loading for each load period, the MWh of each unit, and the value of gamma (the pseudo-fuel cost).
- What would be the schedule if unit 1 was burning the coal at 12 R/ton with no constraint to use 60,000 tons? Assume the coal may be purchased on the spot market for that price and compute all the data asked for in (a). In addition, calculate the amount of coal required for the unit.

6.2 Refer to Example 6A, where three generating units are combined into a single composite generating unit. Repeat the example, except develop an equivalent incremental cost characteristic using only the incremental characteristics of the three units. Using this composite incremental characteristic plus the zero-load intercept costs of the three units, develop the total cost characteristic of the composite. (Suggestion: Fit the composite incremental cost data points using a linear approximation and a least-squares fitting algorithm.)

6.3 Refer to Problem 3.8, where three generator units have input/output curves specified as a series of straight-line segments. Can you develop a composite input/output curve for the three units? Assume all three units are on-line and that the composite input/output curve has as many linear segments as needed.

6.4 Refer to Example 6E. The first problem solved in Example 6E left the end-point restrictions at zero to 200,000 tons for both coal piles at the end of the 3-wk period. Resolve the first problem ($V_1(1) = 70,000$ and $V_2(1) = 70,000$) with the

added restriction that the final volume of coal at plant 2 a end of the third week be at least 20,000 tons.

6.5 Refer to Example 6E. In the second case solved with the LP algorithm (starting volumes equal to 70,000 and 50,000 for plant 1 and plant 2, respectively), we restricted the final volume of the coal pile at plant 2 to be 8000 tons. What is the optimum schedule if this final volume restriction is relaxed (i.e., the final coal pile at plant 2 could go to zero)?

6.6 An oil-fired power plant (Figure 6.12) has the following fuel consumption curve.

$$q(\text{bbl/h}) = \begin{cases} 50 + P + 0.005 P^2 & \text{for } 100 \leq P \leq 500 \text{ MW} \\ 0 & \text{for } P = 0 \end{cases}$$

The plant is connected to an oil storage tank with a maximum capacity of 4000 bbl. The tank has an initial volume of oil of 3000 bbl. In addition, there is a pipeline supplying oil to the plant. The pipeline terminates in the same storage tank and must be operated by contract at 500 bbl/h. The oil-fired power plant supplies energy into a system along with other units. The other units have an equivalent cost curve of

$$F_{eq} = 300 + 6 P_{eq} + 0.0025 P_{eq}^2 \\ 50 \leq P_{eq} \leq 700 \text{ MW}$$

The load to be supplied is given as follows.

Period	Load (MW)
1	400
2	900
3	700

Each time period is 2 h in length. Find the oil-fired plant's schedule using dynamic programming such that the operating cost on the equivalent plant is minimized and the final volume in the storage tank is 2000 bbl at the end of the third period. When solving, you may use 2000, 3000, and 4000 bbl as the storage volume states for the tank. The q versus P function values you will need are included in the following table.

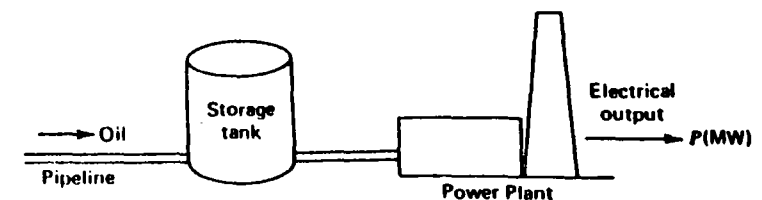


FIG. 6.12 Oil-fired power plant with storage tank for Problem 6.6.



**FACULTAD DE INGENIERIA U.N.A.M.
DIVISION DE EDUCACION CONTINUA**

**V CURSO INTERNACIONAL DE SISTEMAS
ELECTRICOS DE POTENCIA**

MODULO II: SISTEMAS ELECTRICOS DE POTENCIA II

TEMA : OPERACION DE SISTEMAS DE POTENCIA. ANEXO

EXPOSITOR: M EN I. RAMON VILA VIVALDO

ESTADOS DE OPERACION

A las condiciones de un sistema de potencia las describen 5 estados de operación, tal y como se muestra en la fig. 1. Tres juegos de ecuaciones genéricas uno diferencial y dos algebraicos gobiernan la operación del sistema de potencia. El juego diferencial describe el comportamiento dinámico de los componentes del sistema. Los juegos algebraicos comprenden: "restricciones de igualdad" que se refieren a la carga total y a la generación total y "restricciones de desigualdad" que establecen que ciertas variables, como son corrientes, voltajes y frecuencia, no deben exceder ciertos valores representativos de las limitaciones físicas del equipo.

EN ESTADO NORMAL DE OPERACION.

Todas las restricciones se satisfacen indicando: que la generación es la adecuada para alimentar la demanda total existente y que ningún elemento del sistema está sobrecargado. En este estado los márgenes tanto de generación como de transmisión son suficientes y proveen de un nivel adecuado de seguridad con respecto al esfuerzo al cual el sistema puede ser sometido.

Si el nivel de seguridad cae por debajo de cierto valor de una escala, indicando que dejó de ser adecuado, o si la probabilidad de que ocurra algún disturbio aumenta, entonces el sistema ha entrado en un:

ESTADO DE ALERTA

En este estado todas las restricciones aún se satisfacen, pero los márgenes o la reserva existente es tal, que algún disturbio bien pudiera resultar en violación de algunas "restricciones de desigualdad", o sea que algún elemento del sistema se verá sobrecargado en forma más o menos severa. En este estado de alerta (inseguro) se deberá tomar alguna acción preventiva para restablecer al sistema al estado normal.

Si antes de concluir con la acción correctiva, ocurre un disturbio suficientemente severo, el sistema entra en un:

ESTADO DE EMERGENCIA

Aquí las "condiciones de desigualdad" se han violado y la seguridad del sistema se ha fracturado, el nivel de seguridad es cero o es prácticamente inexistente. El sistema, sin embargo, todavía está intacto por lo que deberán ser tomadas medidas de emergencia (medidas heróicas) cuya finalidad será recuperar, cuando menos, el estado de alerta.

Si estas medidas no se toman a tiempo o son inefectivas y si el disturbio inicial o uno subsecuente son de gran severidad, entonces el sistema empieza a desintegrarse y entra en un estado llamado:

IN EXTREMIS

En este estado las "condiciones de igualdad" y las "condiciones de desigualdad" han sido violadas; el sistema no permanecerá intacto y se perderá un gran porcentaje de la carga total del sistema. La estrategia o las acciones de control de emergencia deben tener como finalidad salvar tantas partes del sistema como sea posible, de un colapso total. Una vez que el colapso se ha detenido se puede emprender un:

ESTADO DE RECUPERACION

Este estado consistirá en reconectar el sistema y recuperar la carga. Es obvio que a partir de este estado el sistema puede pasar al de alerta o al normal, dependiendo de las circunstancias.

Resumiendo:

I. TRANSICIONES SIN CONTROL

NORMAL ---> ALERTA

- Naturaleza de la transición:

Se refleja en una reducción en el nivel de seguridad; mlo anterior puede explicarse de otro modo: a partir del estado de alerta puede pasarse al estado normal, pero mientras eso está ocurriendo, el sistema es mucho más vulnerable a las consecuencias de un disturbio subsecuente.

- Causas posibles:

- 1.- Reducción en la capacidad de generación debida a: indisponibilidad de combustible, pérdida de alguna unidad generadora, falla de auxiliares, reprogramación del mantenimiento.

2.- Reducción en la capacidad de transmisión debida a: pérdida de una línea por contaminación o falla permanente; falla de un banco, limitaciones por condiciones ambientales, etc.

3.- Aumento de la probabilidad de ocurrencia de algún disturbio debido a cercanía de tormentas u otros accidentes.

ALERTA ----> EMERGENCIA

- Naturaleza de la transición:
violación de las "restricciones de desigualdad"
- Restricciones importantes:
Flujos de potencia, niveles de voltaje, frecuencia, ángulos de máquina y buses.
- Causas posibles:
mal funcionamiento o pérdida temporal o permanente de un elemento primordial de la red principal.

- Causa potencial que desencadenaría el problema:

Fallas internas mecánicas o eléctricas, funcionamiento equivocado de dispositivos de protección o control, eventos externos tales como descargas atmosféricas, etc.

EMERGENCIA ----> IN EXTREMIS

- Naturaleza de la transición:

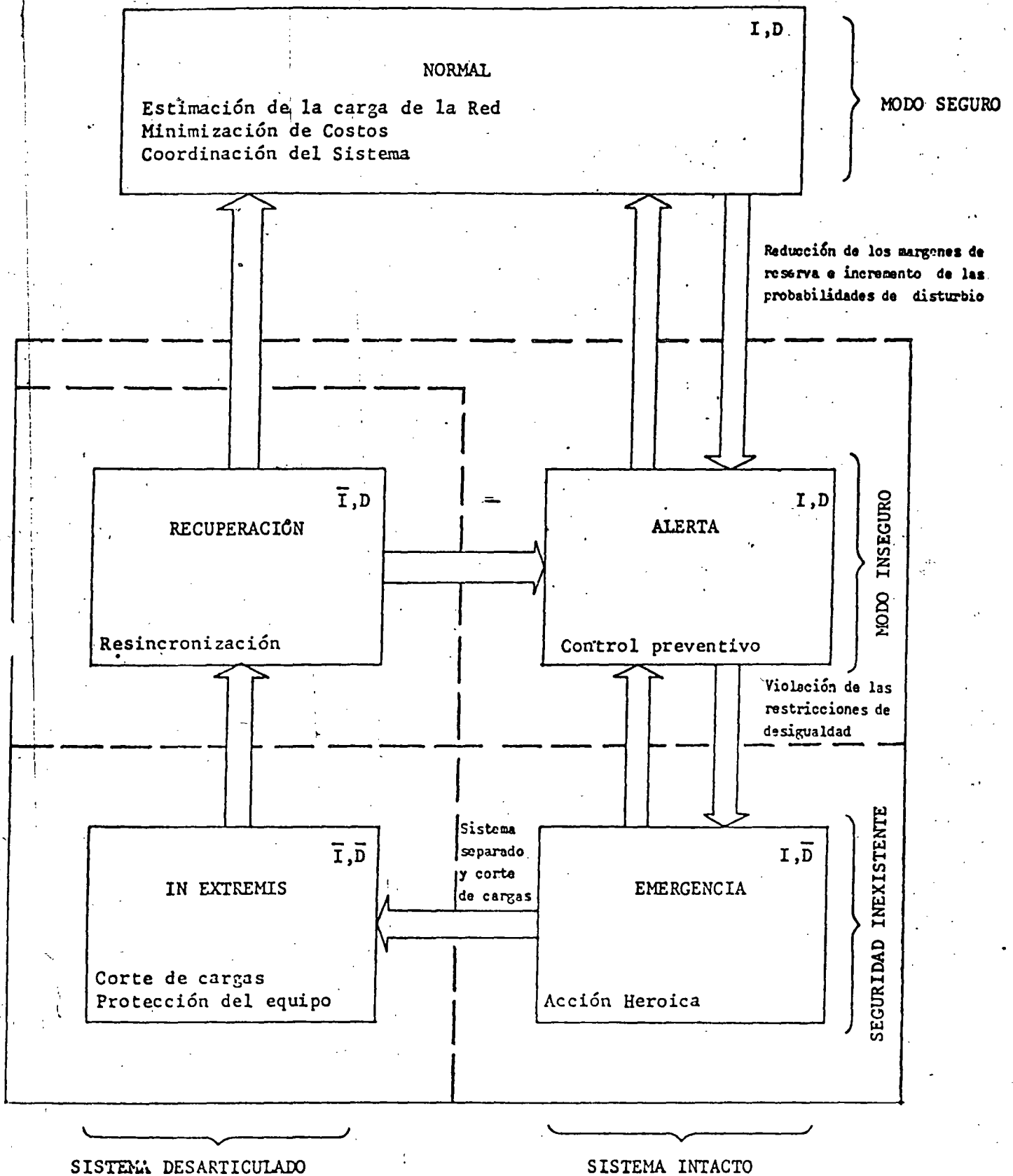
Pérdida de integridad del sistema y violación de las restricciones de igualdad" (carga total \neq generación total).

- Causas posibles:

Pérdida de enlaces, formación -sin control- de sistemas aislados no suficientes (carga \neq generación).

- Causas potenciales que desencadenarían el problema:

Sobrecargas prolongadas en enlaces importantes, operación equivocada de protecciones, disturbios sucesivos durante la emergencia.



I: Restricciones de igualdad
 D: Restricciones de desigualdad

FIG. 1

I.I. MODOS DE CONTROL

A).- ESTADO DE ALERTA:

Se aplicaría un método deliberado o preventivo para recuperar los márgenes de seguridad; las medidas serían: relocalización de generación y de subestaciones, reducción de voltaje y/o frecuencia (no siempre tan efectivo como se desearía).

B).- ESTADO DE EMERGENCIA:

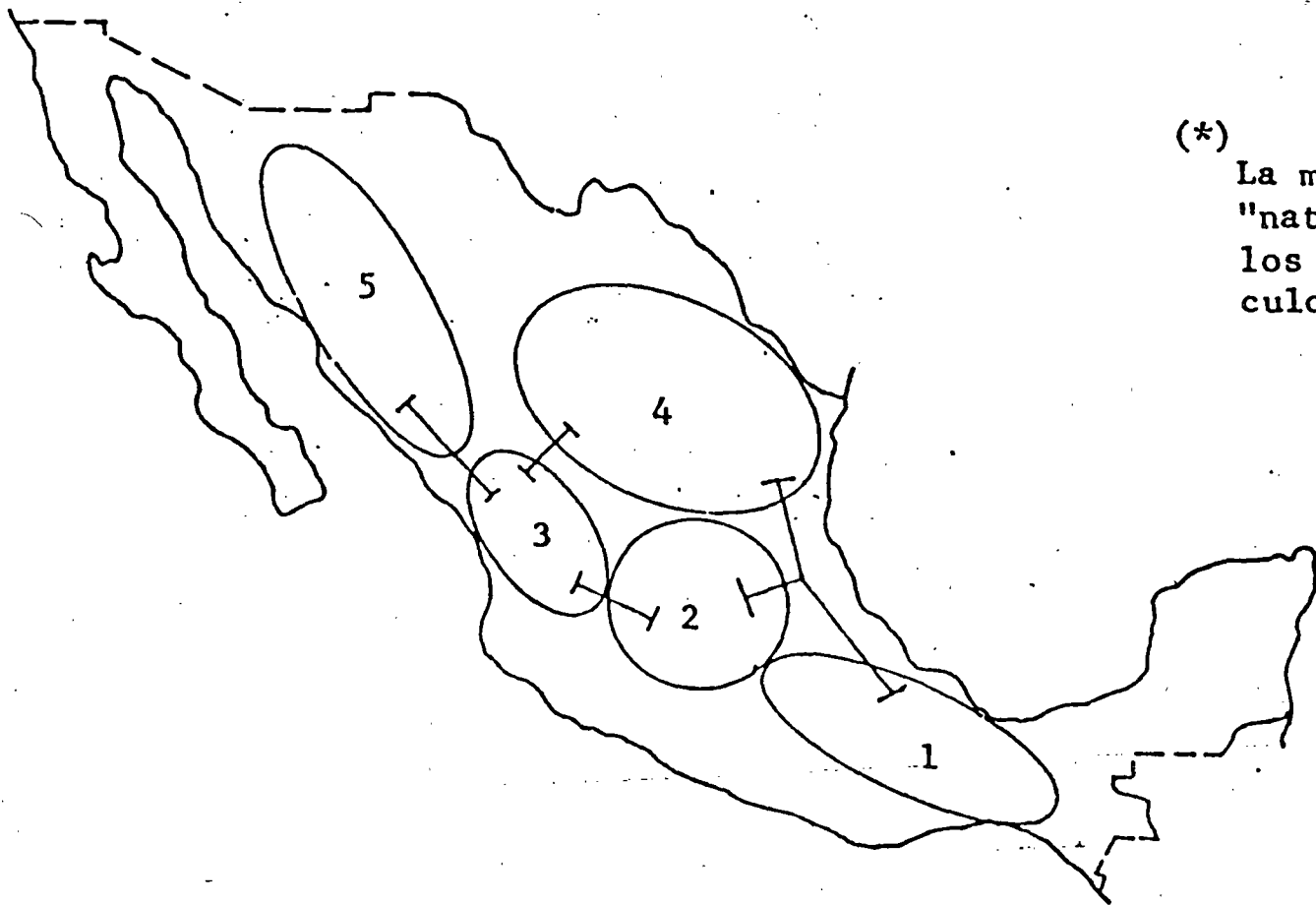
Se aplicaría un método que permitiera de manera inmediata librar de sobrecargas a el o a los elementos principales de la red; las medidas serían: libramiento rápido de elementos fallados, "fast valving", resistencias de freno, control de excitación, modulación mediante control de convertidores de CD, control de la carga, switcheo de capacitores, más todo lo indicado en el estado de alerta.

C) .- IN EXTREMIS:

El método usaría medidas heroicas para contener la total degradación del sistema. Contemplaría todas las medidas de los estados A) y B), más un programa de disparo de carga por relés de baja frecuencia y segregación controlada del sistema.

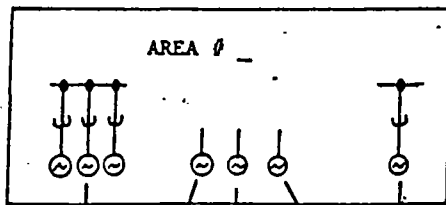
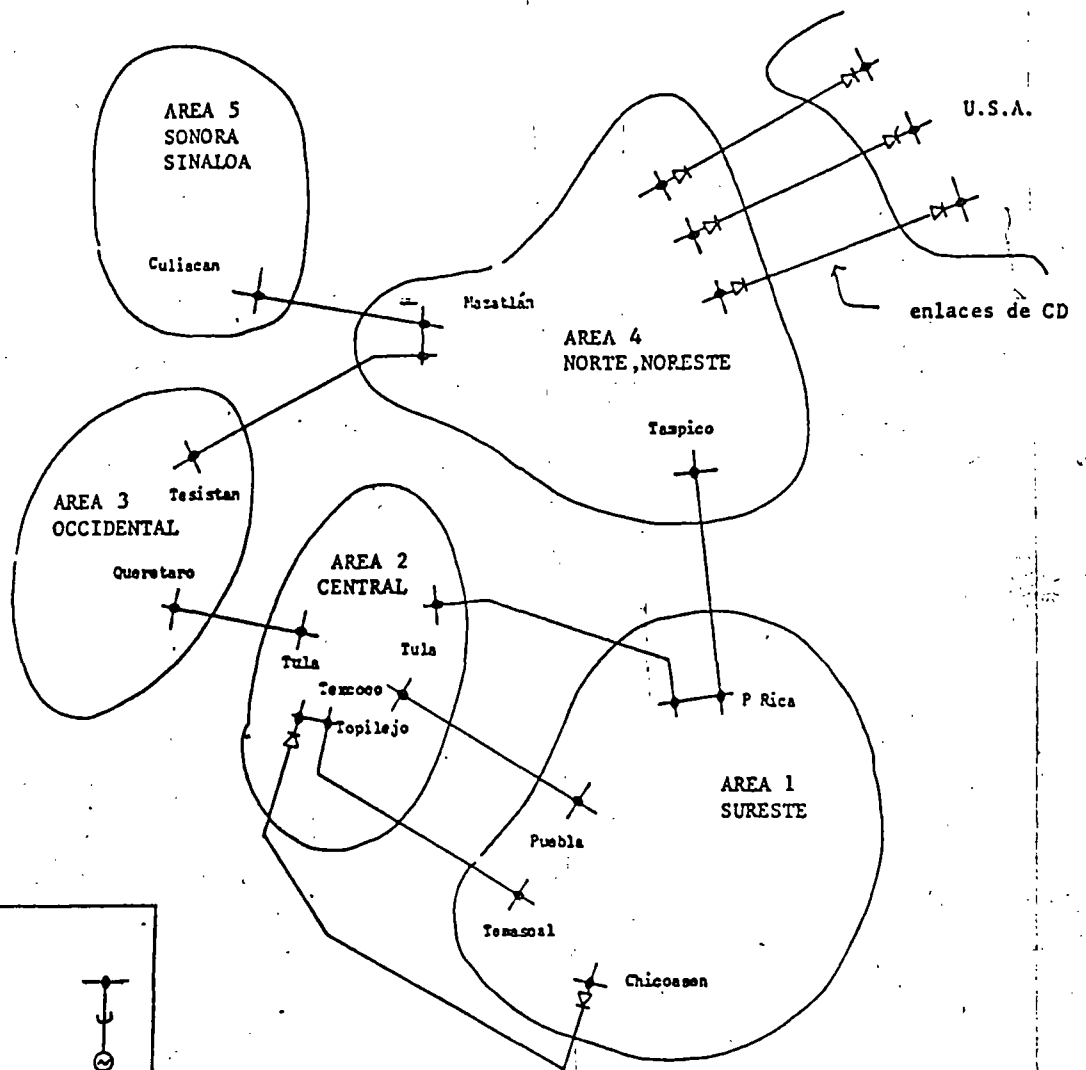
D) .- ESTADO DE RESTAURACION:

El método de control sería deliberado (correctivo) para restaurar el sistema y llegar a un modo viable de funcionamiento. Contemplaría: rodar de nueva cuenta las unidades y sincronizarlas, reconectar cargas y la re-sincronización de las diferentes islas o áreas.

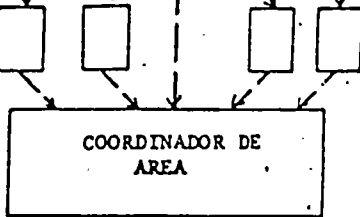


(*)

La manera o modo de selección es "natural" ; Tal y como lo definen los equivalentes durante el cálculo de cortos-circuitos

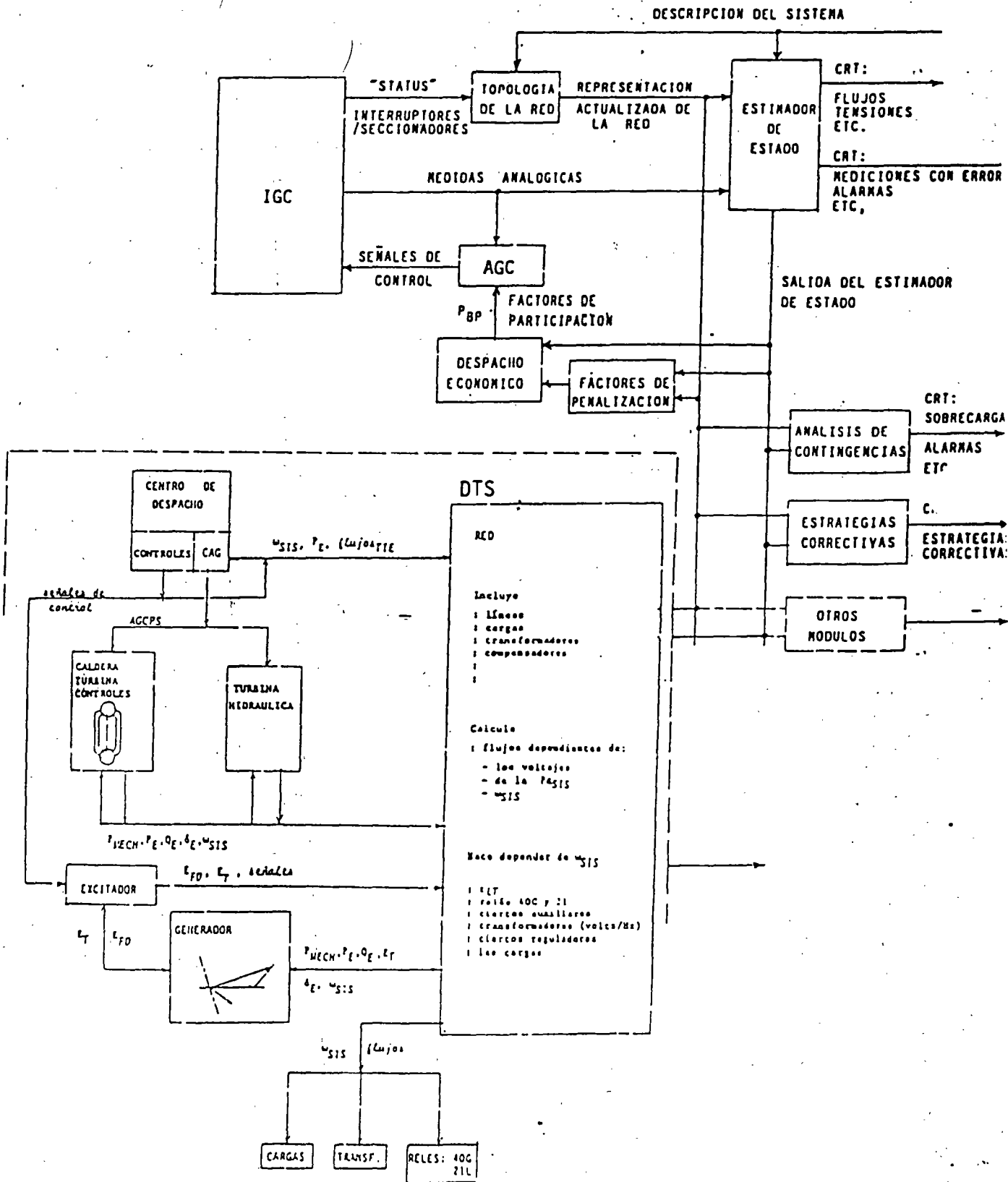


Controladores Locales



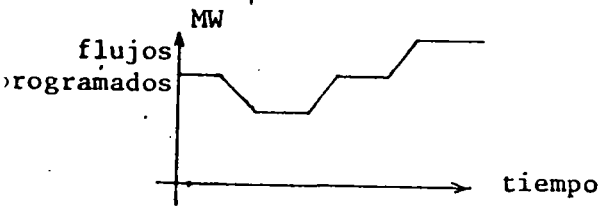
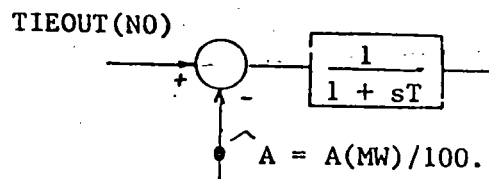
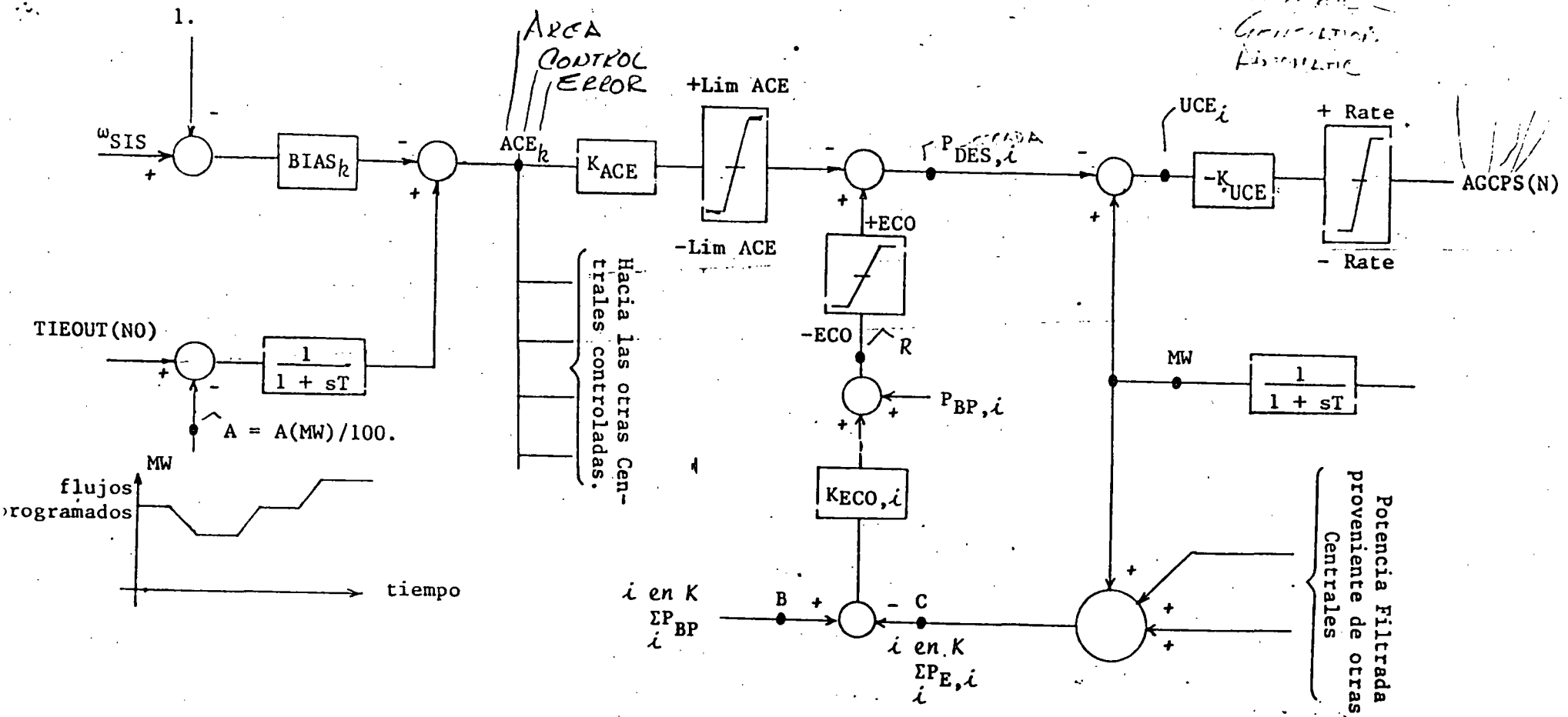
CONTROL EN ESTADO DE EMERGENCIA
- DOS NIVELES JERARQUICOS

DIAGRAMA FUNCIONAL
(UNA CONFIGURACION):



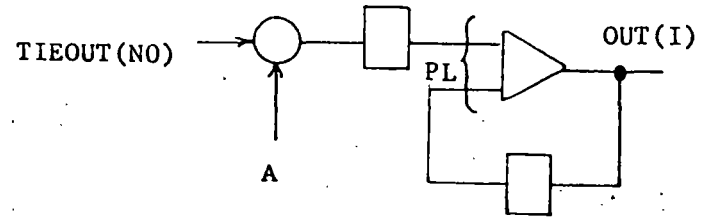
OPTIMAL POWER FLOW

Control Generation Automatic

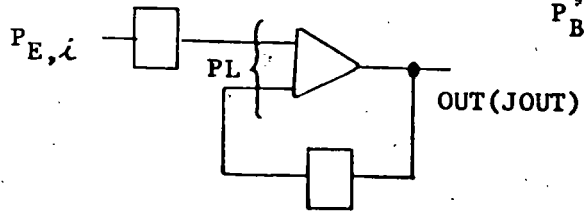


Hacia las otras Centrales controladas.

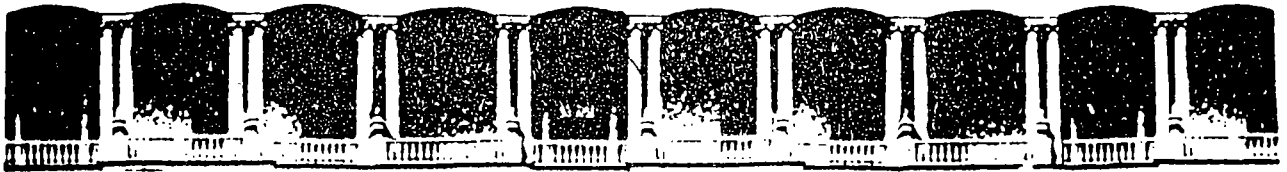
Potencia Filtrada proveniente de otras Centrales



SAVE = STOR
OUT_o = STORO



$k = Area$
 $i = Unidad$
 $P_{BP,i} = 0$ indica que la unidad esta fuera del AGC.



**FACULTAD DE INGENIERIA U.N.A.M.
DIVISION DE EDUCACION CONTINUA**

**V CURSO INTERNACIONAL DE SISTEMAS
ELECTRICOS DE POTENCIA**

MODULO II: SISTEMAS ELECTRICOS DE POTENCIA II

TEMA : PROTECCION DE SISTEMAS ELECTRICOS DE POTENCIA

**EXPOSITOR: ING. AUGUSTO O. HINTZE V.
1996**

RELEVADORES DE PROTECCION Y
SISTEMAS DE PROTECCION POR RELEVADORES.

Son circuitos analógicos compactos, conectados a varias partes del -- Sistema de Potencia, para detectar condiciones de operación no deseadas ó intolerables dentro de su área asignada.

Su función principal es iniciar la desconexión del área en problema, - esta desconexión se lleva a cabo mediante los interruptores.

Por lo tanto: Los relevadores y los interruptores forman un equipo, - ambos deben ser planeados juntos.

CINCO PRINCIPIOS BASICOS PARA
LA APLICACION DE RELEVADORES.

- 1.- CONFIABILIDAD Mide el grado en el que el relevador o el sistema de protección se comporta correctamente:
 - a). Confianza (Dependability).
 - b). Seguridad

- 2.- SELECTIVIDAD Máxima continuidad del servicio con desconexión mínima del sistema.

- 3.- RAPIDEZ Mínimo tiempo de falla y de daño al equipo.

- 4.- SIMPLICIDAD Mínimo equipo y alambrado (Circuitry).

- 5.- ECONOMIA Máxima protección a mínimo costo.

FACTORES IMPORTANTES EN LA APLICACION

1.- ECONOMIA.-

Inicial, de operación, mantenimiento.

2.- PRACTICAS DE OPERACION.-

De acuerdo a los estándares y prácticas.
Permiten una operación eficiente del sistema.
Flexibilidad para el futuro.

3.- EXPERIENCIAS PREVIAS.-

La protección se enfoca hacia problemas previos ó anticipando otros.

4.- MEDICIONES DISPONIBLES DE FALLAS A PROBLEMAS.-

Magnitudes de falla, localizaciones de TC'S
ó de TP'S.

CLASES DE RELEVADORES POR ANSI

I.- POR FUNCION

- | | |
|----------------|------------------|
| 1). Protección | 4). Programación |
| 2). Regulación | 5). Auxiliar |
| 3). Monitoreo | |

II.- POR SEÑAL DE ENTRADA

- | | | |
|---------------|-----------------|-----------|
| 1). Corriente | 4). Presión | 7). |
| 2). Voltaje | 5). Frecuencia | 8). Flujo |
| 3). Potencia | 6). Temperatura | |

III.- SEGUN PRINCIPIO DE OPERACION O ESTRUCTURA

- | | |
|------------------------------|---------------------|
| 1). Por ciento | 4). Estado sólido |
| 2). Restricción
Múltiple. | 5). Electromecánico |
| 3). Producto | 6). Térmico |

IV.- POR CARACTERISTICA DE COMPORTAMIENTO

- | | |
|---------------------------------|---------------------------|
| 1).- Distancia | 5). Bajo Voltaje |
| 2).- Sobrecorriente Direccional | 6). Tierra, Fase |
| 3). Tiempo Inverso | 7). Alta ó Baja Velocidad |
| 4). Tiempo Definido | 8). Comparación de Fase |

CLASIFICACION DEL COMPORTAMIENTO DEL RELEVADOR

- 1.- Correcta.
- 2.- Sin conclusión.
- 3.- Incorrecta
 - a). No disparó
 - b). Disparó en falso.

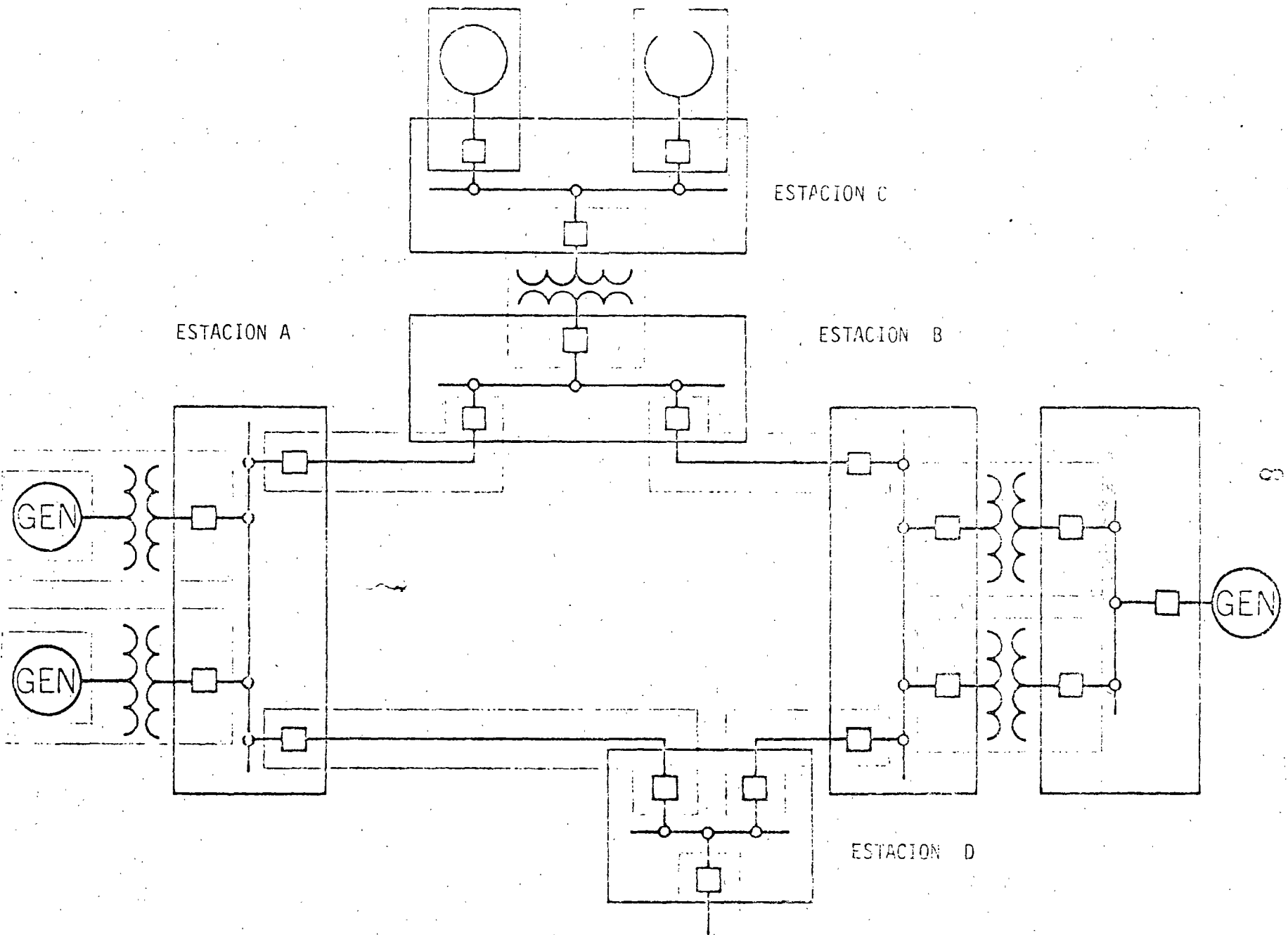
RAZONES DE OPERACION INCORRECTA

- 1.- Aplicación
- 2.- Ajuste.
- 3.- Personal.
- 4.- Equipo (TC'S, TP'S, Interruptor, Cable y Alambrado, Relevador, Canal, Bateria, Otros).

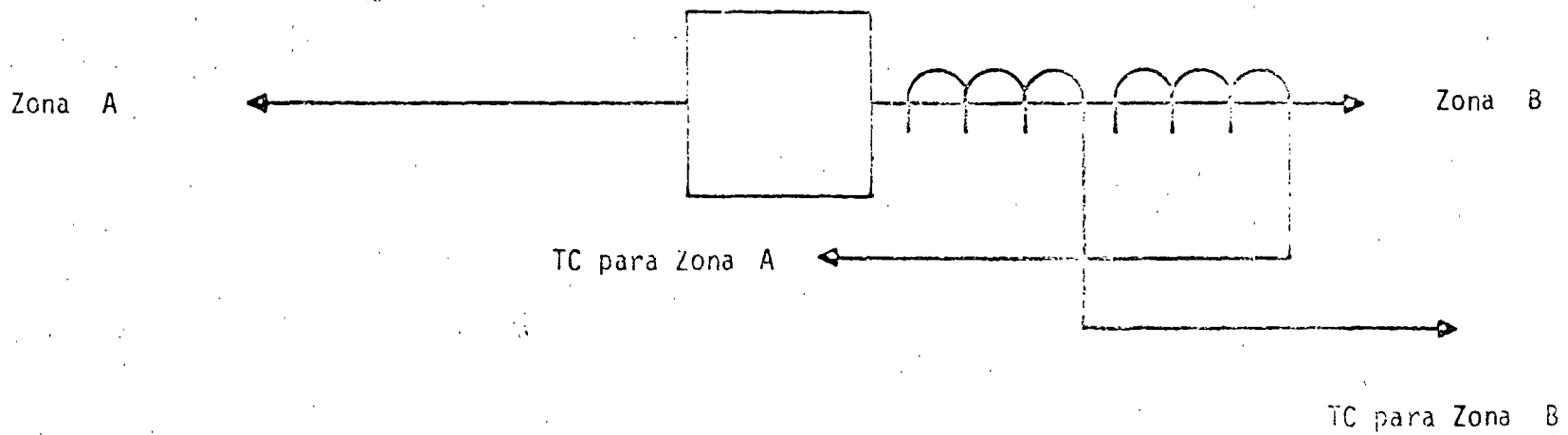
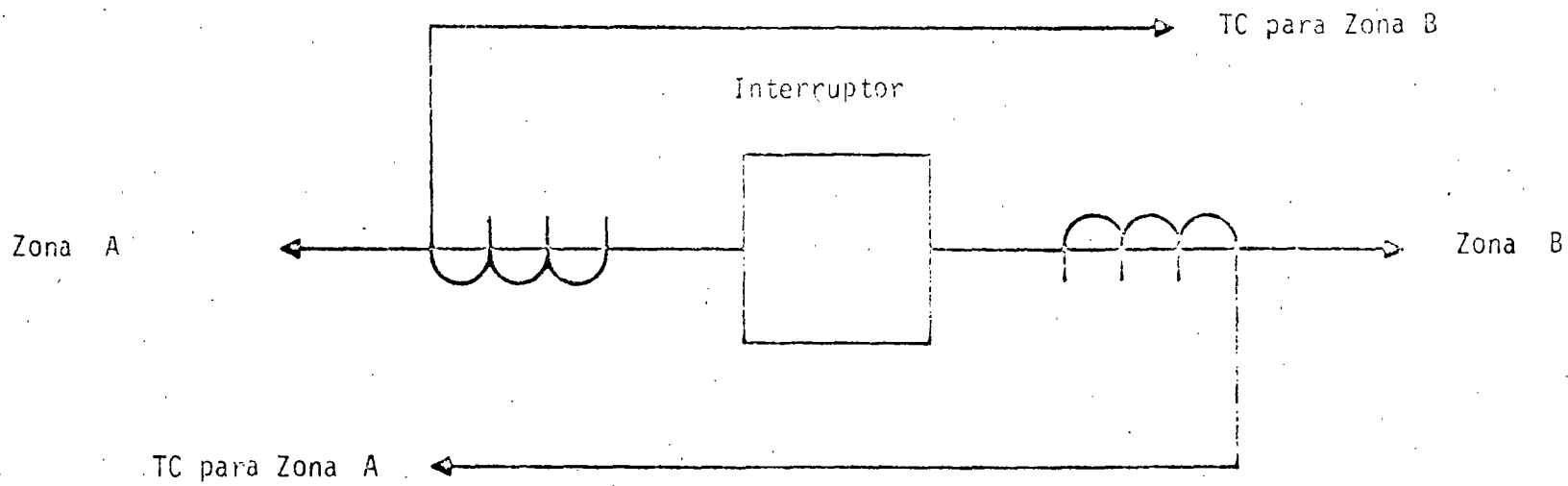
FILOSOFIA GENERAL
DE LA APLICACION DE RELEVADORES

Dividir el sistema de potencia en zonas que pueden ser protegidas adecuadamente con un mínimo de interrupción para el sistema.

- 1.- Generador y Unidad Generador-Transformador.
- 2.- Transformadores.
- 3.- Buses.
- 4.- Circuitos de Transmisión y de Distribución.
- 5.- Motores.



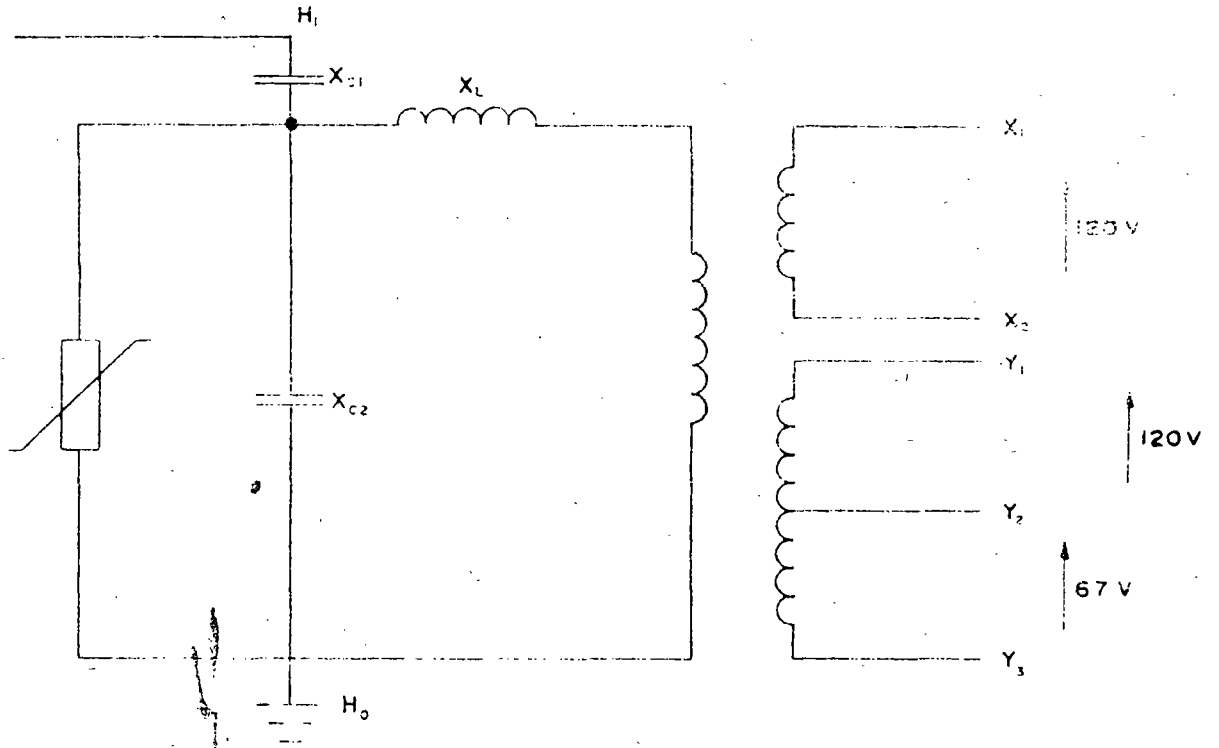
8



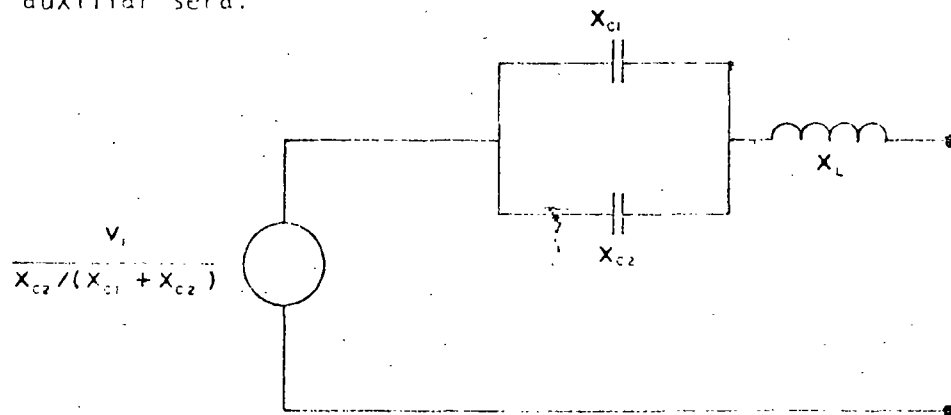
INFORMACION REQUERIDA
PARA LA APLICACION DE RELEVADORES

- 1.- Configuración del Sistema.
- 2.- Protección actual del sistema y sus dificultades.
- 3.- Grado de Protección requerida.
- 4.- Preferencias Existentes, operación, procedimientos, prácticas.
- 5.- Expansiones Futuras.
- 6.- Estudios de corto circuito y Cargas Máximas compatibles.
- 7.- Localización de TC'S, TP'S, conexión y relación de transformación.
- 8.- Impedancias de líneas y transformadores.

Lo cual resultaría en una regulación muy alta. Para poder evitar este problema, se utiliza un circuito resonante al que además para tener aislamiento eléctrico, se le añade un transformador auxiliar, tal como se muestra en seguida:



De tal manera, el equivalente visto desde las terminales del transformador auxiliar será:

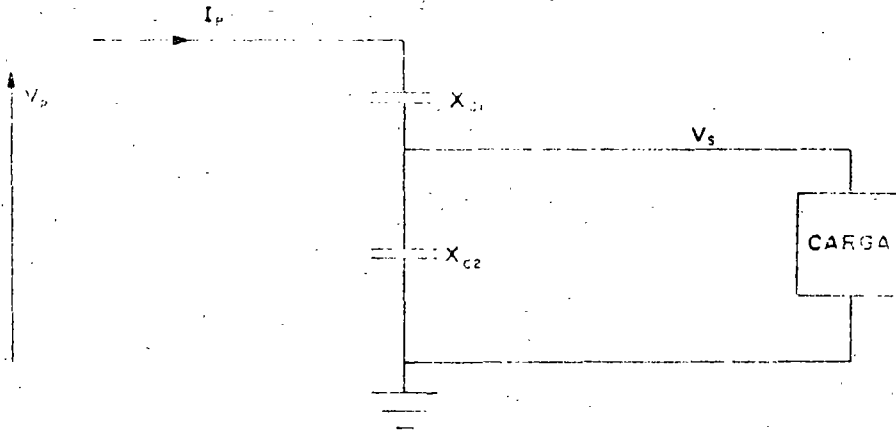


FUENTES DE POTENCIAL

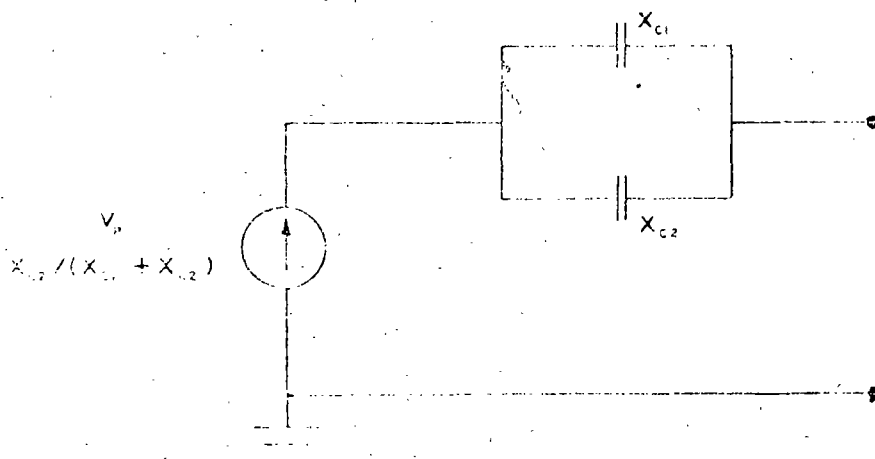
Dispositivos capacitivos de potencial

Transformadores de potencial

Un dispositivo de potencial podría ser simplemente



Pero esto limitaría muy seriamente la capacidad que se pudiera alimentar; ya que el equivalente de Thevenin sería:



2.- TRANSFORMADORES DE INSTRUMENTO

Seleccionando $X_L = \frac{X_{C1} \cdot X_{C2}}{X_{C1} + X_{C2}}$ se logra una regulación prácticamente cero;

sin embargo, esto no es sin costo. En este caso, el costo es el hecho de que, si se llegara a provocar un corto circuito en las terminales secundarias del DP, el voltaje a través del reactor y a través de los capacitores crecerá enormemente, y, con excepción de X_{C1} , el nivel de aislamiento no será suficiente. Es por ésto que es necesario proveerlo de un apartartrayos que sea capaz de proteger el aislamiento pero que no opere durante medio ciclo en caso de descargas atmosféricas.

Los transformadores de potencial efectúan la reducción de la señal en forma muy similar a la de los transformadores de distribución con la diferencia principal de que el hierro del núcleo es suficiente para soportar mayores voltajes sin que su saturación sea apreciable.

Como son elementos que trabajan a flujo reducido todo el tiempo, generalmente los efectos no lineales de la saturación se puede despreciar.

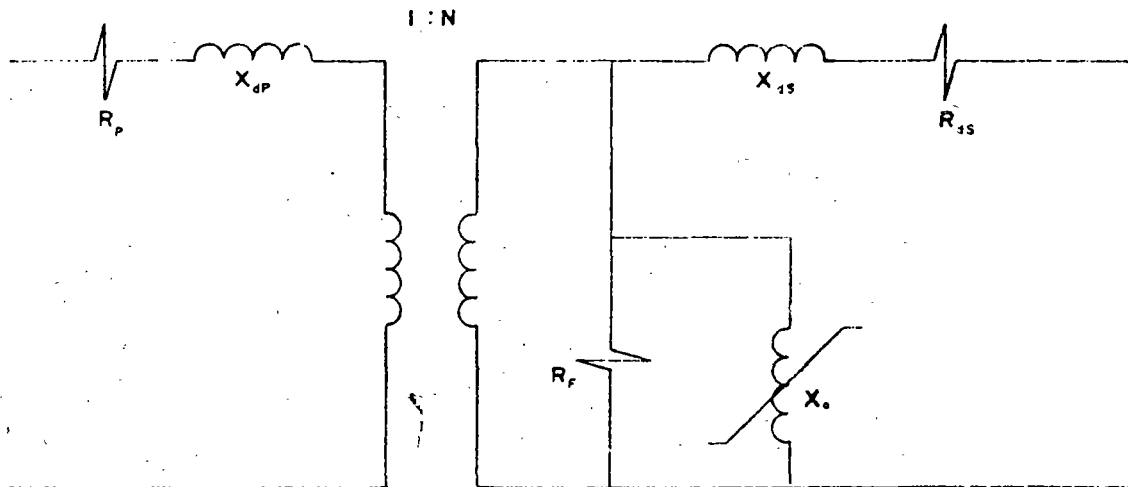
Igualmente los errores de relación de transformación (en magnitud y ángulo) son despreciables para los fines de protección; no siendo este el caso con los equipos de medición a menos que se tenga cuidado con la carga secundaria del TP ó DP.

FUENTES DE CORRIENTE

La obtención de una señal representativa de la corriente primaria se --- lleva a cabo por medio de transformadores de corriente. Es en estos aparatos en donde el rango dinámico de las señales por manejar es más grande, y, por tanto, es en ellos donde se tienen los mayores problemas de manejo de señal. Generalmente los problemas los causa la saturación del núcleo y es por eso que el mayor esfuerzo se dedica a conocer y tratar este fenómeno.

Debido a que el manejo de fenómenos no lineales no es fácil, generalmente se procura simplificar el fenómeno antes de representarlo.

Partiendo del diagrama equivalente del transformador



Tanto R_p como X_{dp} o sea la resistencia del primario como la reactancia de dispersión del primario no tienen ningún efecto sobre la precisión de la relación de transformación.

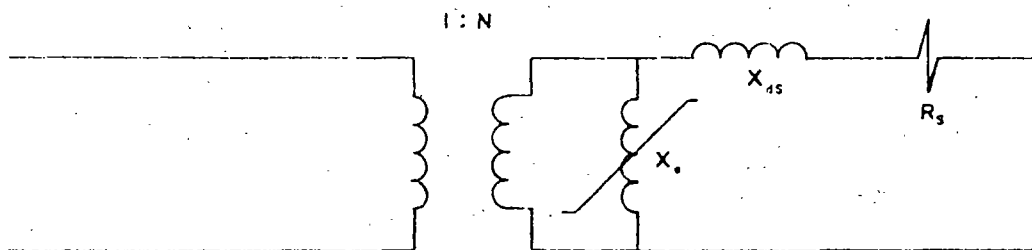
Su efecto se deja sentir únicamente en la necesidad del voltaje primario para sostener una corriente de falla y esto solo afectaría a sistemas de voltajes muy reducidos.

Es por lo anterior que estos dos elementos no se incluyen en los cálculos de relación de transformación.

Para la precisión requerida para la protección, la resistencia paralelo con la que se representan las pérdidas en el hierro, se puede despreciar.

Lo que es muy importante representar es la inductancia de excitación, ya que su efecto puede ser decisivo, sobre todo para corrientes elevadas.

Tras las simplificaciones mencionadas, el modelo del transformador de corriente será:



Dependiendo de la construcción del transformador de corriente, puede ---
lograrse tener una baja impedancia de dispersión secundaria o no. Si --
ésto se logra, el comportamiento del TC es calculable; en caso contrario,
este comportamiento se deberá encontrar por medio de pruebas en las que -
simulen (o dupliquen) las condiciones que se espera encontrar.

Lo anterior da lugar a la clasificación de TC's en función de la impedancia
de dispersión y del voltaje de saturación de la impedancia de excita-
ción. Esta clasificación es de la forma:

	<u>C 400</u>	
C	calculable	voltaje de
T	se debe probar	saturación

La literal solo puede ser C ó T; si es C esto implica que la reactancia
de dispersión es despreciable y que por tanto el comportamiento es ---
calculable. Si es T, la reactancia de dispersión es apreciable y solo -
por medio de pruebas se podrá determinar el comportamiento. La T pro-
viene de la palabra "Tested"

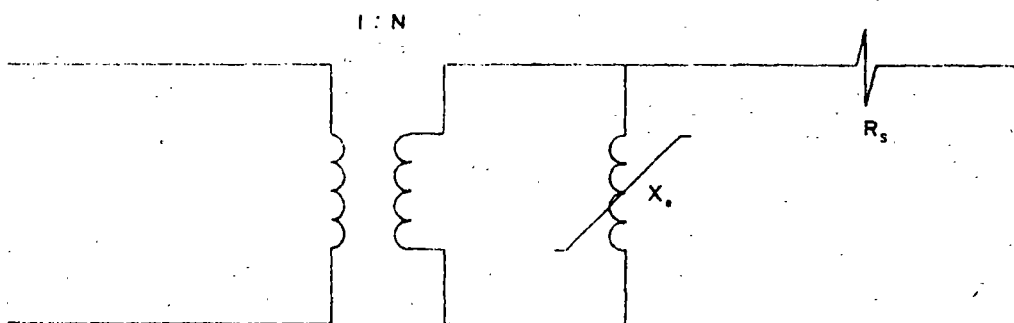
El voltaje de saturación se define como "El voltaje máximo RMS en las --
terminales secundarias para el que el TC, con una corriente primaria de
20 veces el valor nominal, entrega una corriente secundaria con un error
no mayor del 10%".

Los valores de voltaje de saturación se encuentran normalizados a las --
siguientes clases:

- 50 V
- 100 V
- 200 V
- 400 V
- 800 V

de tal suerte, si un determinado TC es capaz de sostener el error dentro de 10% para 500 V; deberá ser clasificado como clase 400.

Debido a que solo se pueden calcular los TC's con impedancia de dispersión despreciable, el modelo que se usará para ellos será el siguiente:



y, en este modelo, la X_e se da por medio de la curva $V - I$, ya que no es una constante.

Existen tres métodos generalmente empleados para calcular el comportamiento de los TC's.

- 1.- Se calcula la densidad de flujo en el núcleo y se compara con la densidad que se puede tener en el acero del núcleo.

Para élllo, suponiendo que lá relación de transformación es perfecta, se calcula la corriente secundaria y, con ella y las impedancias de las cargas, se calcula el voltaje en el secundario del TC. Con este voltaje, y sabiendo que

$$V = 4.44 f N \phi \times 10^{-8}$$

se puede calcular ϕ y con él y el área de sección transversal del TC se puede calcular β pues

$$\beta = \frac{\phi}{A}$$

Una vez calculada la β , se compara con la densidad permisible para la clase de acero de que esté hecho el núcleo, la cual es generalmente del orden de 11 000 a 19 000 líneas/cm². (75 000 a 125 000 líneas/pulg²).

Esta prueba solo es cualitativa en realidad, pues solo indica si habría o no saturación pero no indica la imprecisión que esto causaría. Además no siempre se tiene disponible la información del tipo de acero del núcleo ni del área de sección transversal. Esto orilla al ingeniero de protecciones a usar alguno de los dos métodos siguientes.

- 2.- Una vez calculado el voltaje secundario del TC tal como se describió en el método 1, se procede simplemente a compararlo con el voltaje de clasificación del TC y, si lo excede, la aplicación implicará

saturación (aunque no necesariamente pues como se mencionó antes, un TC con voltaje de saturación V_{gr} 700 volts se clasificaría como -- clase 400).

Este método es también cualitativo únicamente ya que es solo una -- comprobación permisiva; además, no es muy precisa para corrientes diferentes de 20 veces la corriente nominal (tanto mayores como menores).

Cuando se desea mayor detalle o precisión se debe entrar al método -- que aquí se da como número 3.

- 3.- Utilizar el modelo eléctrico del (o los) TC teniendo la curva de -- excitación para tomar en cuenta correctamente el elemento no lineal. Este método solo se puede utilizar para TC's con impedancia baja de dispersión secundaria. Cabe hacer notar además, que, debido a la -- presencia de fenómenos no lineales, no se pueden obtener soluciones generales sino solamente soluciones particulares, lo cual implica -- que cada caso se deberá analizar individualmente y con los métodos -- numéricos adecuados.

Debido a que un TC no se debe aplicar si esto está al borde de no -- resultar satisfactorio, en la aplicación de este método se toma un punto de vista pesimista y se asume que todos los componentes son resistivos puros con lo que las corrientes y las caídas de tensión se pueden manejar aritméticamente en lugar de fasorialmente.

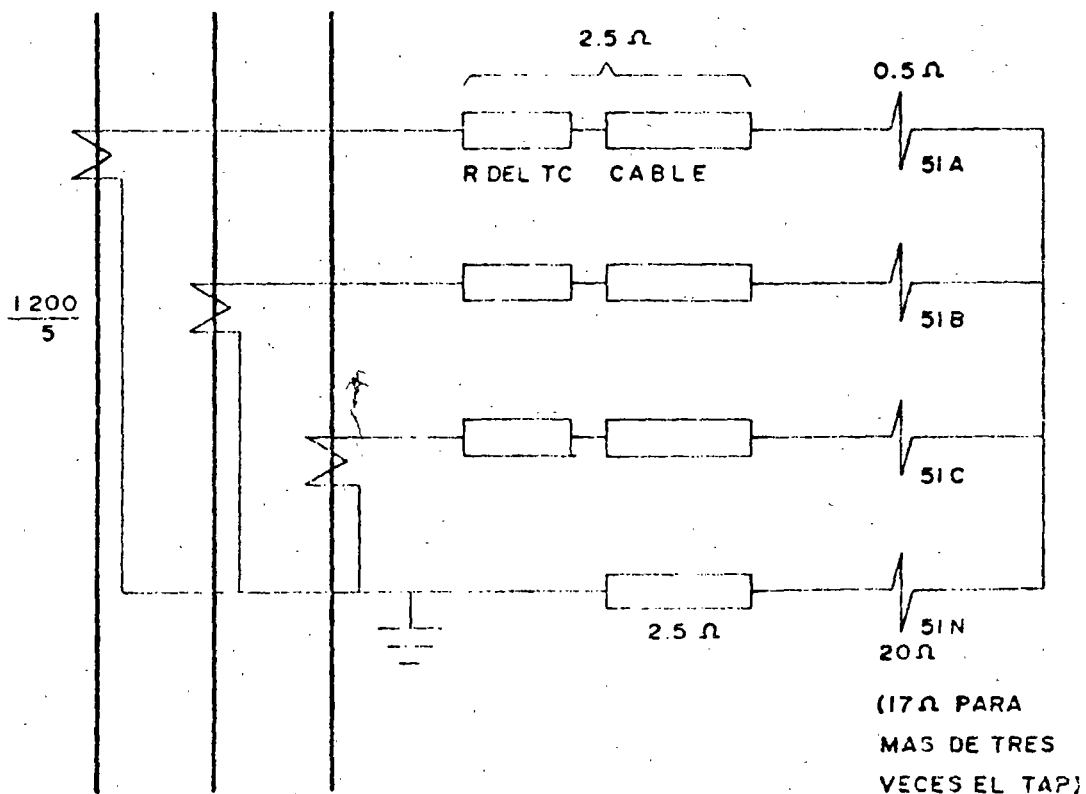
Esto simplifica la labor de por sí pesada de manejar por prueba y -- error los elementos no lineales, además de que el concepto de reactancia se diluye un poco por el hecho de que se tiene un contenido de armónicas generalmente alto.

A continuación se resuelve un problema que ejemplifica los dos tipos de problema que generalmente se encuentran y que son:

- Conocida una corriente secundaria deseada, cual deberá ser la corriente primaria que la produzca.
- Conocida una corriente primaria, que corriente secundaria circulará.

En el ejemplo se han exagerado las resistencias del cableado. Además se ha representado un TC de muy baja calidad (tiene una corriente de excitación alta y se satura pronto) para ilustrar más claramente el efecto de la corriente de excitación.

Primera mente se plantea el problema más fácil de resolver y que es: conocida la corriente secundaria, encontrar la corriente primaria.



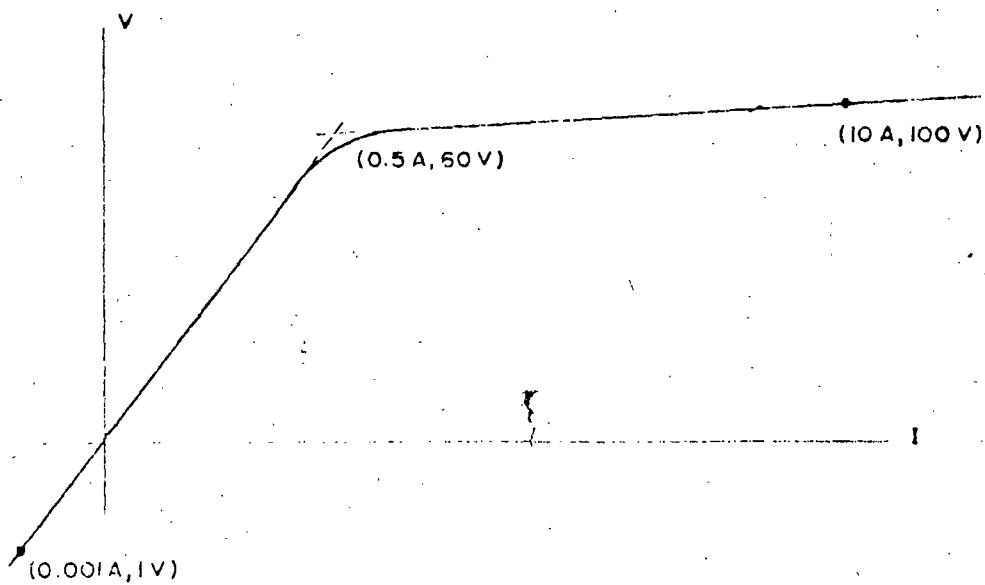
Sabiendo que los ajustes son:

51's de fase — TAP = 5 amp.

51 N — TAP = 0.5 amp.

Se desea saber cual es la corriente trifásica primaria con la que operan los 51's de fase y cual es la corriente primaria monofásica con la que operará el 51N. Para ello se cuenta, además del conocimiento de la RIG, con el conocimiento de la curva de saturación de los TC's.

La curva de excitación es:



y, aproximándola con dos líneas rectas, las ecuaciones que la definen son:

$$\begin{aligned} \text{a) Para } & 0.001 \leq I_e \leq 0.5 \\ & \delta \quad \quad \quad 1 \leq V \leq 60 \end{aligned}$$

$$V = 94.7278 I_e^{65883}$$

$$\delta \quad I_e = 0.001 V^{1.5179}$$

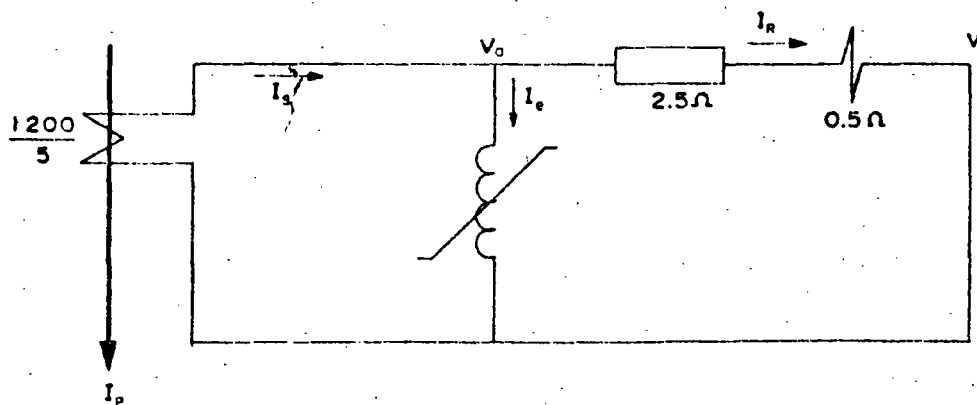
$$\text{b) Para } \quad 0.5 \leq I_e \quad \delta \quad 60 \leq V$$

$$V = 67.528 I_e^{0.17052}$$

$$\delta \quad I_e = 1.8665 \times 10^{-11} V^{5.8645}$$

SOLUCION

Para corriente trifásica no circulará corriente por el 5Ω y así no habrá caída de tensión ni en él ni en el cableado de neutro. Entonces, como $T = 5$ amps., $I_R = 5$ para que opere. Así:



Si $I_R = 5$, como $V_1 = 0$

$$V_a = 5 \times (2.5 + 0.5) = 15 \text{ V}$$

De la curva, para $V = 15$, $I_e = 0.061$ amps.

entonces

$$I_s = I_e + I_R = 5 + 0.061 = 5.061$$

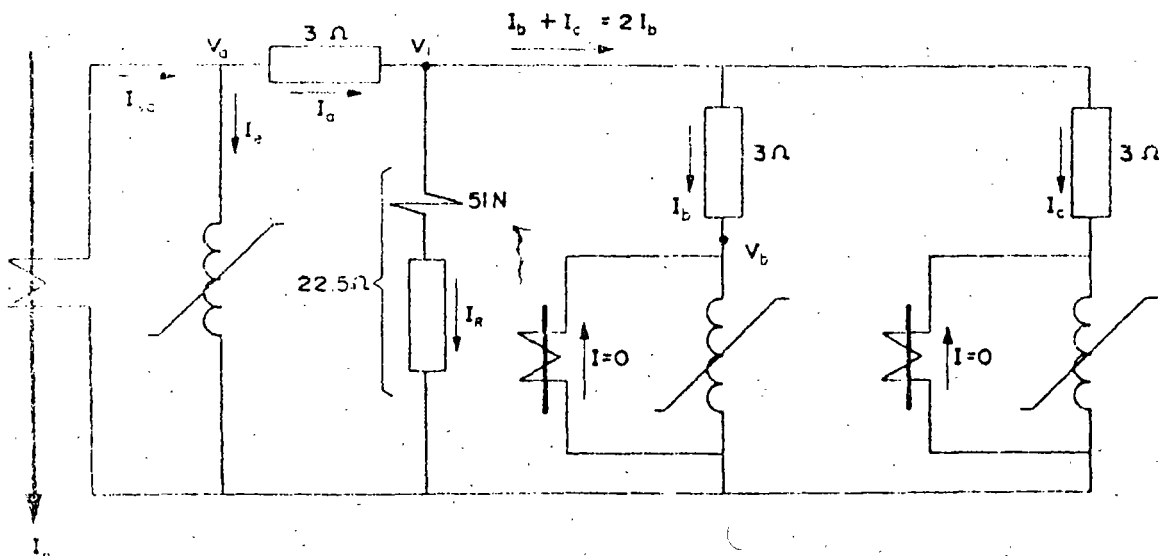
y así

$$I_p = \frac{1200}{5} \times 5.061 = 1214.6 \text{ amps.}$$

O sea

$$I_p = 1215 \text{ Amps.}$$

Para el caso de corriente monofásica, habrá necesidad de representar el - circuito completo pues el voltaje del neutro de los relés será diferente de cero. El diagrama equivalente será:



Como $T = 0.5$ y $K = 8$, $I_R = 0.5 \times 8 = 4.0$ amps.

$$V_1 = 4.0 \times (17 + 2.5) = 78 \text{ V}$$

efectuando nuevamente el proceso iterativo para encontrar I_b , iniciando con $V_b = V_1$

V_b	I_b	
78.00	2.329	
71.01	1.343	
73.97	1.706	
72.88	1.5642	
73.31	1.6187	
73.144	1.5976	
73.21	1.606	-- valor suficientemente aproximado

Conocida $I_b = I_e = 1.606$

$$I_a = I_R + I_b + I_c = 4.0 + 1.606 + 1.606 = 7.2052$$

con lo que

$$V_a = V_1 + 3 * I_a$$

$$= 78 + 3 \times 7.20522$$

$V_a = 99.616$ y, entrando a la curva con este voltaje

$$I_e = 9.777$$

86

y, entrando a la curva,

para $V = 12.983$, $I_e = 0.04897$

y así,

$$I_s = I_a + I_e = 0.578 + 0.04897$$

$$I_s = 0.6265$$

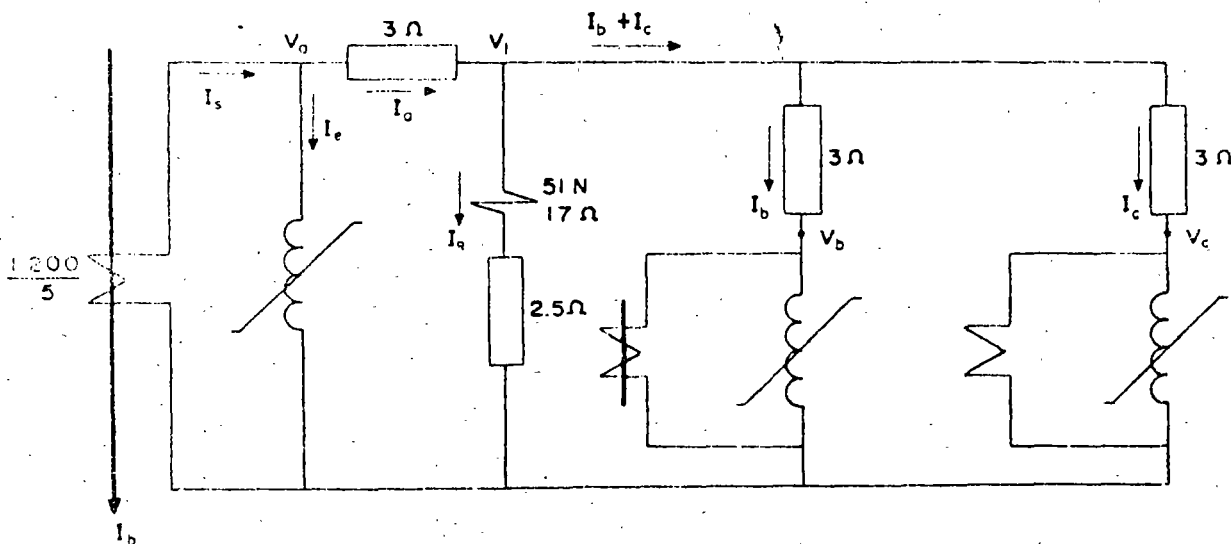
y entonces

$$I_p = \frac{1200}{5} \times 0.6265$$

$$I_p = 150.37 \text{ amps.}$$

(teóricamente $I_p = 120 \text{ amps}$)

Para corriente de falla monofásica, se desea conocer el valor de la corriente primaria que haga circular por el 51N, una corriente ocho veces superior a la del tap. (con lo cual la resistencia del 51N baja a 17Ω)



Como $T = 0.5$; $I_R = 0.5$ entonces

$$V_1 = 22.5 \times 0.5 = 11.25 \text{ V}$$

Con este valor de voltaje, se encontrará I_b por aproximaciones sucesivas así; suponiendo $V_b = V_1$

— para $V_b = 11.25$; $I_e = 0.03940$

Con I_e conocida, se calcula $V_b = V_1 - I_e \times 3$

$$V_b = 11.25 - 3 \times 0.03940 = 11.132 \text{ y nuevamente se entra a la curva}$$

— para $V_b = 11.132$, $I_e = 0.03877$ y, con esta nueva I_e , se recalcula V_b y se vuelve a la curva.

— para $V_b = 11.134$, $I_e = 0.03878$

Como ya el valor en dos aproximaciones sucesivas es prácticamente igual, se considera correcto, con lo cual y sabiendo que $I_b = I_c$

$$I_a = I_R + I_b + I_c = 0.5 - 0.039 + 0.039$$

$$I_a = 0.578$$

con lo que ahora se puede calcular V_a pues

$$V_a = V_1 + I_a \times 3$$

$$= 11.25 + 3 \times 0.578$$

$$V_a = 12.983$$

88

así,

$$I_s = I_a + I_e = 7.2052 + 9.777 = 169819$$

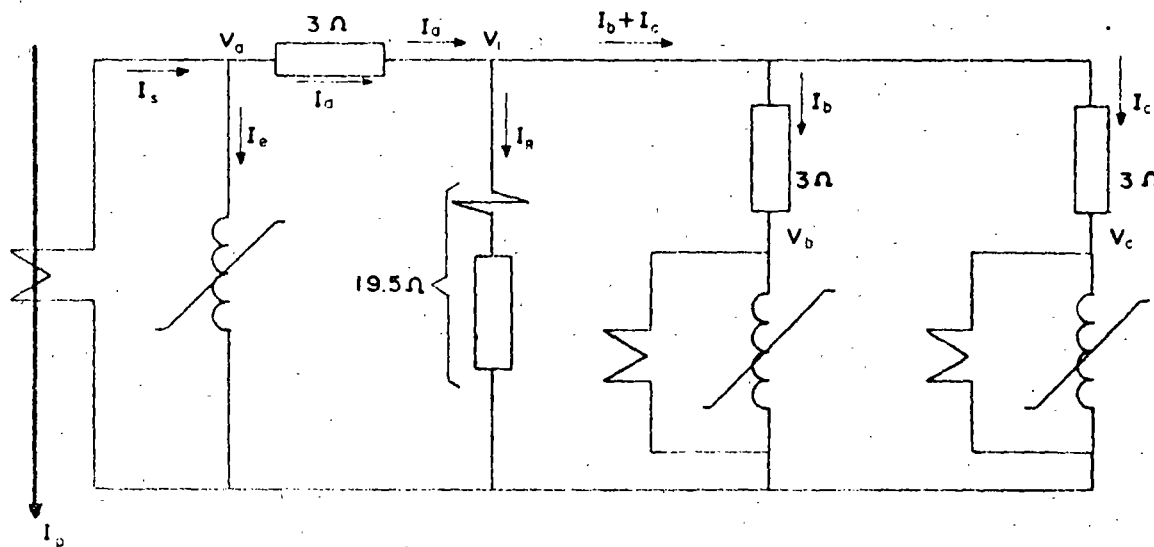
con lo que

$$I_p = \frac{1200}{5} \times 16.9819$$

$$I_p = 4075.7 \text{ Amps.}$$

teóricamente $I_p = 960 \text{ Amps.}$

Ahora, para una corriente primaria de 20 veces la corriente nominal, se desea conocer la corriente en el 51N.



$$I_p = 20 \times 1200 = 24\ 000 \text{ Amps.}$$

$$I_s = 24\ 000 / \left(\frac{1200}{5}\right) = 100 \text{ Amps.}$$

89

Asumiendo el límite del error

$$I_e = 10 \text{ y } V_a = 100 \text{ y así } I_a = 90$$

con lo que

$$V_1 = 100 - 90 \times 3 = 100 - 270 = 170 \text{ lo que no puede}$$

ser.

Suponiendo entonces una corriente mucho más alta de excitación

$$I_e = 70, \quad V_a = 139.35 \text{ (de la curva); } I_a = 30$$

$$\text{y así } V_1 = 139.35 - 30 \times 3 = 49.349$$

Con V_1 conocido, se puede calcular I_R

$$I_R = V_1/19.5 = 49.349/19.5 = 2.531$$

y con I_R se puede calcular I_b pues

$$I_b = \frac{I_a - I_R}{2} = \frac{30 - 2.531}{2} = \frac{12.469}{2} = I_b$$

y entonces $V_b = V_1 - 3 \times I_b$

$$V_b = 49.349 - 3 \times 12.469 = 11.942$$

y para este voltaje, según la curva

$I_b = 0.043$ que es inferior a la calculada arriba

Probando con una saturación más alta

$$I_e = 80, \quad V_a = 142.56 \text{ (de la curva) y así } I_a = 20A$$

entonces, con I_a conocido

$$V_1 = V_a - 3 \times I_a = 142.56 - 3 \times 20 = 82.558$$

con lo que

$$I_R = V_1/19.5 = \frac{82.558}{19.5} = 4.234$$

$$\text{para obtener } I_b = \frac{I_a - I_R}{2} = \frac{20 - 4.234}{2} = \frac{7.883}{2} = I_b$$

$$V_b = V_1 - I_b \times 3 = 82.558 - 3 \times 7.883 = 58.909$$

y, con este voltaje, la curva arroja $I_b = 0.486$ que es aún inferior a la calculada anteriormente.

--- Probando con saturación aún mayor

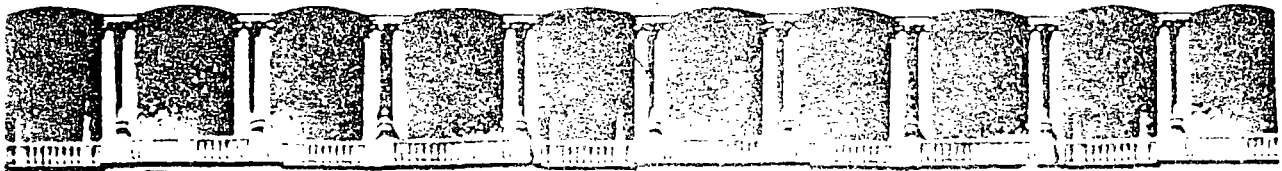
$$I_e = 90, \quad V_a = 145.451 \text{ (de la curva), así } I_a = 10A$$

Con esto,

$$V_1 = V_a - 3 I_a = 145.451 - 3 \times 10 = 115.451$$

$$\text{con lo que } I_R = \frac{115.451}{19.5} = 5.921$$

$$\text{entonces } I_b = \frac{10 - 5.921}{2} = \frac{2.040}{2}$$



**FACULTAD DE INGENIERIA U.N.A.M.
DIVISION DE EDUCACION CONTINUA**

**V CURSO INTERNACIONAL DE SISTEMAS
ELECTRICOS DE POTENCIA**

MODULO II: SISTEMAS ELECTRICOS DE POTENCIA II

TEMA : PROTECCION DE MOTORES

**EXPOSITOR: ING. AUGUSTO O. HINTZE V.
1996**

PROTECCION DE MOTORES

El arte de la protección de motores está bien alejado de estar tan estandarizado como el de los generadores, aunque el National Electric Code y los Estandares de la NEMA tienen requerimientos específicos básicos de protección.

Estos no pueden proporcionar protección adecuada en todas las aplicaciones, así que hay muchos esquemas y grados de protección variables en servicio exitoso. La principal razón de esto es los numerosos y diferentes tipos y tamaños de motores, su aplicación tan variada a través de los vastos campos que utilizan la energía eléctrica. También aquí, el costo y el grado de protección debe ser sopesado contra el riesgo de eventualidades, de tal forma que el tamaño y el tipo de servicio tendrán una gran influencia en la protección.

Las eventualidades por las que se aplican protecciones a los motores son:

- 1.- Fallas en las bobinas ó circuitos asociados.
- 2.- Sobrecargas excesivas.
- 3.- Reducción y pérdida del voltaje de alimentación.
- 4.- Inversión de fase
- 5.- Desbalance de fases.
- 6.- Pérdida de excitación o sincronismo en motores

Hay algo de traslape, particularmente en las dos primeras, ya que un corto circuito es una sobrecarga muy severa. Así una protección apli

cada para una eventualidad puede operar con otras.

La protección puede proporcionarse por dispositivos de protección en los controles y directamente en los motores. Excepto en los motores pequeños que tienen varios tipos de protección térmica en su interior, la protección usualmente se incluye como parte de los controles. Los motores de hasta 600 V usualmente se protegen con fusibles. Arriba de 600 V y hasta alrededor de 2200 V, se usan dispositivos de sobrecorriente de acción directa, asociados con interruptores. En voltajes más altos se aplican relevadores de sobrecorriente por separado.

Se recomienda protección diferencial en motores grandes de 1500 HP ó más, ó en motores de 5 KV ó más. Donde no se usa protección diferencial, la protección para las dos primeras eventualidades consiste en relevadores de sobrecorriente de tiempo e instantáneos con relevadores térmicos para una protección de sobrecarga más sensible.

PROTECCION POR SOBRECARGA Y CONTRA CORTO CIRCUITO

Es difícil obtener las curvas de calentamiento del motor y varían -- considerablemente con los tamaños y diseños. Además, son un promedio aproximado de una zona térmica difícil de definir donde pueden -- ocurrir diversos grados de daño o envejecimiento prematuro del aislamiento. Así se vuelve difícil para un esquema de protección acercarse adecuadamente a estas curvas que varían sobre el rango completo desde sobrecargas pequeñas sostenidas hasta severas sobrecargas -- con motor bloqueado.

Los relevadores térmicos de sobrecarga ofrecen buena protección en -- los casos de sobrecargas cortas y medianas (en largo tiempo) pero --

frecuentemente no pueden proporcionar adecuada protección en sobrecargas fuertes, como se vé en la figura 5-1. El relevador de inducción de sobrecorriente de tiempo, proporciona protección en estos casos, -- pero sobreproteje en sobrecargas pequeñas y medianas. Por lo que se requiere un compromiso. Algunas de las aplicaciones más comunes se dan en la tabla IV.

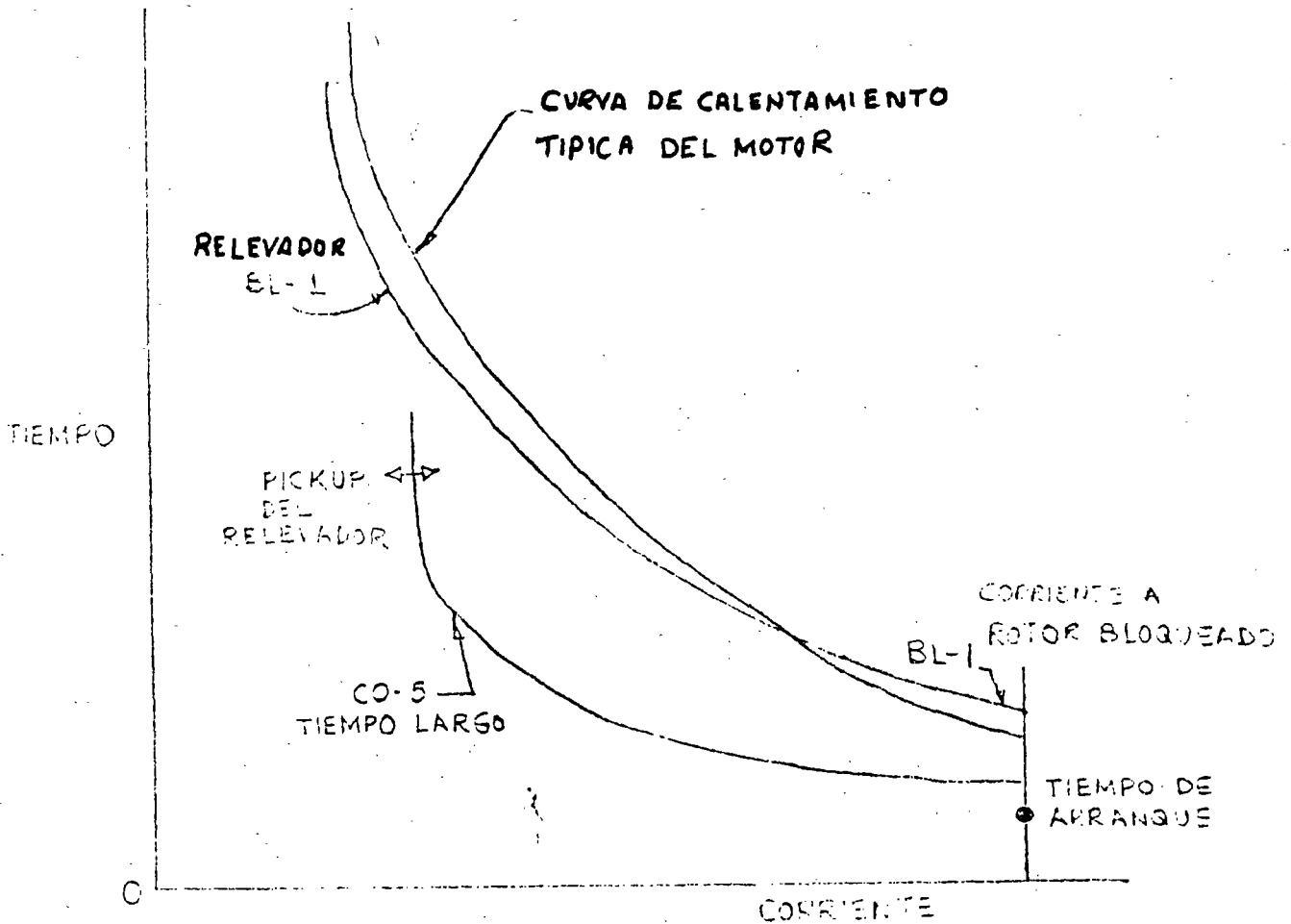


FIG. 5-1 CARACTERÍSTICAS TÍPICAS DE CORRIENTES DEL ARROLLO Y DEL MOTOR.

La aplicación de ambos tipos de relevadores (esquema 1) es recomendada, ya que ofrece la mejor protección. Cuando se usa la protección de sobrecarga térmica, el relevador de tiempo puede ser ajustado alto para reducir la sobreprotección inherente a cargas pequeñas con esta característica.

En motores grandes (200 - 300 HP) existe una tendencia para que el tiempo de arranque sea mayor que el tiempo del rotor bloqueado. Esto hace que los relevadores de sobrecorriente queden imposibilitados para distinguir ó proporcionar protección adecuada con estas altas corrientes.

TABLA IV
PROTECCION DE MOTORES POR SOBRECORRIENTE
(LOS RELEVADORES DE TIERRA SE CONSIDERAN POR SEPARADO)

ESQUEMA	RELEVADORES APLICADOS	ACCION (NOTA 4)	AJUSTES TIPICOS
1	2 RELEVADORES TERMICOS	DISPARO O ALARMA	100% Ir (Nota 1)
	1 SOBRECORRIENTE DE INDUCCION - TIEMPO LARGO	DISPARO O ALARMA	300-350% Ir (Nota 2)
	3 SOBRECORRIENTE INSTANTANEOS	DISPARO	ARRIBA DE LA MAXIMA I DE ARRANQUE (Nota 3)
2	2 SOBRECORRIENTE DE INDUCCION - TIEMPO LARGO	DISPARO	300-350% Ir (Nota 2)
	1 SOBRECORRIENTE DE INDUCCION - TIEMPO LARGO	ALARMA	115-125% Ir

39.

2 SOBRECORRIENTE INSTANTANEO	DISPARO	ARRIBA DE LA MAXIMA I DE ARRANQUE (Nota 3)
------------------------------	---------	--

3 2 SOBRECORRIENTE DE INDUCCION - TIEMPO LARGO	DISPARO O ALARMA	125-150% Ir (Nota 2)
--	------------------	----------------------

2 SOBRECORRIENTE INSTANTANEOS	DISPARO	ARRIBA DE LA MAXIMA I DE ARRANQUE (Nota 3)
-------------------------------	---------	--

4 2 RELEVADORES TERMICOS	DISPARO O ALARMA	100% Ir (Nota 1)
--------------------------	------------------	------------------

2 SOBRECORRIENTE INSTANTANEOS	DISPARO	ARRIBA DE LA MAXIMA I DE ARRANQUE (Nota 3)
-------------------------------	---------	--

Ir es la corriente nominal (carga plena) del motor

NOTA 1: Relevador tipo réplica como el BL-1. El ajuste se cambia en el ajuste del contacto. Un ajuste normal proporciona operación en 60 minutos a 125% Ir. Puede ser ajustado para que opere en 15 minutos con 125% de Ir.

NOTA 2: El tiempo seleccionado es tal que la operación ocurre con corriente de rotor bloqueado, pero no cuando el motor arranca cuando el tiempo de arranque es menor que el tiempo de rotor bloqueado. Cuando no se tenga este dato, este ajuste se obtiene arrancando el motor varias veces y aumentando el ajuste del tiempo hasta que la operación del relé no suceda, luego agregue entre 1 y 5 segundos al tiempo de operación del relevador. Un ajuste típico puede ser de 10 seg.

para la magnitud de corriente con rotor bloqueado. Si los relevadores son para alarma, los ajustes se reducen a 115%, excepto donde se tienen valores cortos en los factores de servicio ó en las capacidades nominales para sobrecarga.

NOTA 3: Como es difícil determinar como ocurren offset de las corrientes de directa particularmente al arrancar grandes motores, el ajuste se obtiene mejor con arranques sucesivos para determinar el ajuste de no operación y entonces incrementar el pick-up en 10% aproximadamente. Ajustes típicos pueden ser de 160 a 170% de la corriente de rotor bloqueado, aunque pueden requerirse valores tan altos como 250%. Esto puede ser de 12 a 15 veces la corriente nominal del motor.

NOTA 4: La decisión para disparo a alarma depende del énfasis dado a la continuidad del servicio y a protección de motores. En motores esenciales como auxiliares de planta de fuerza (donde una falla podría causar la salida del generador) se usan alarmas frecuentemente, para que el operador pueda tomar medidas correctivas y evitar la salida ó transferir la generación antes de un disparo.

DESCRIPCION DE RELEVADORES TERMICOS

Los relevadores térmicos son de dos tipos: uno opera con bobinas exploradoras embebidas en los devanados de la máquina, como los tipos CT y DT-3, y el otro directamente de la corriente que pasa por la máquina como el tipo BL-1.

Los primeros se aplican sólo en motores grandes, usualmente entre 1000, 1500 HP y más donde las bobinas exploradoras están disponibles. El -

segundo tipo es el relevador réplica de sobrecorriente térmica, aplicado como se indica en la Tabla IV.

Las bobinas exploradoras forman parte de un puente de Wheatstone que se balancea a una temperatura particular. Al variar la temperatura del motor, el puente se desbalancea y opera el relevador. El tipo CT ó DT-3 son los aplicados; con el CT se usan dos bobinas exploradoras como vemos en la figura 5-2.

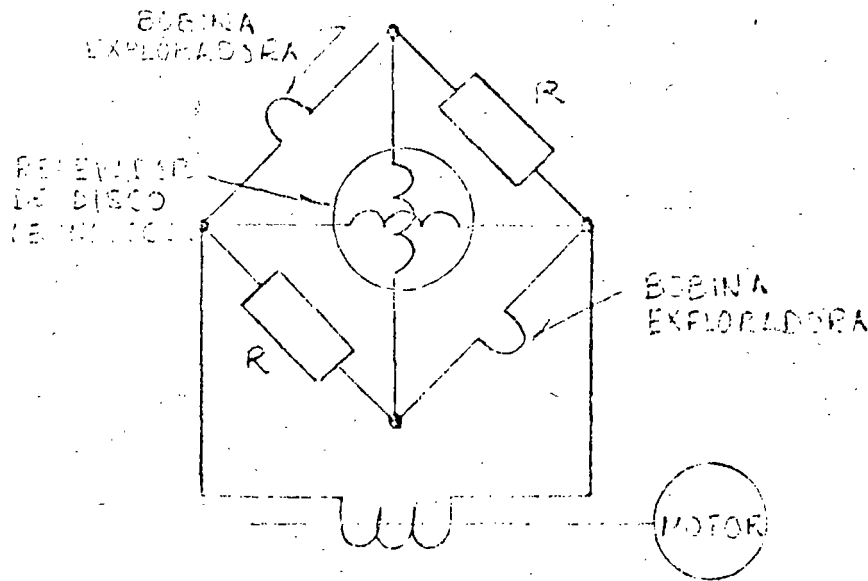


FIG. 5-2 CONEXIÓN DEL RELEVADOR CON BOBINAS EXPLORADORAS

La unidad de operación es un disco de inducción con dos bobinas productoras de Par conectadas a través del puente. Se usa la corriente de una de las fases de la máquina a través de un TC para suministrar ener-

gía al puente. El relevador cierra sus contactos cuando la temperatura de las bobinas del estator y la corriente calculando en una línea, -- alcanzan un valor predeterminado. Durante el arranque el disparo se previene si el ciclo de arranque queda dentro de la capacidad de la máquina porque tanto la alta temperatura como una sobrecorriente deben estar presentes para que el relevador opere. Además, se previene el disparo con sobrecarga térmica donde la sobrecarga sea de corta duración.

El relevador DT-3 es un miliampermetro tipo d'Arsonval, de CD que cierra sus contactos al operar y que puede ser conectado a través del puente donde una bobina exploradora forma parte del puente. En esta aplicación el puente es energizado con CD, 125 ó 250 VCD. La escala del relé se calibra de 60° a 120°C. con el puente balanceado (sin corriente por el relevador) normalmente a 90°C. Los contactos izquierdo y derecho cierran cuando la temperatura baja ó sube del valor 90° a los valores ajustados entre 60 y 120°C.

Los relevadores tipo réplica intentan duplicar en una pequeña escala -- dentro del relevador las características de calentamiento de la máquina. Entonces, cuando la corriente del secundarios del TC pasa por el relevador, su característica tiempo-corriente sigue aproximadamente la de la máquina como se ilustra en la figura 5-1. El relevador BL-1 tiene dos resortes bimetálicos enrollados en espiral. Uno es actuado por el calor producido por la corriente aplicada mientras que el otro por la temperatura ambiente del relevador. Esto proporciona una compensación por temperatura ambiente, así que el relevador opera aproximadamente en la misma curva corriente-tiempo, independientemente de la temperatura del aire alrededor del relevador.

El relevador BC-1 esta disponible en una o dos unidades de sobrecarga --

térmica con accesorios de disparo instantáneo para cuando se aplica - como se dice en la tabla IV.

PROTECCION DE FALLA A TIERRA

Cuando la fuente de alimentación está a tierra, se conecta en el TC - del neutro un relevador de inducción de tiempo inverso, muy inverso, - ó de corto tiempo. Estas fuentes tienen normalmente impedancias de neutro para limitar la corriente de tierra así que se requieren ajustes muy sensibles de los relevadores de tierras. Ajustes típicos -- son 1/5 de la corriente de falla mínima para una falla sólida en las terminales de la máquina. Se usan ajustes del tiempo en el dial de alrededor de 1 y se tienen operaciones de 4 a 5 ciclos para 500% de pick-up, cuando se usa el relevador CO-2 (COH).

Ocasionalmente una corriente alta de arranque en motores grandes que se arrancan directamente a la línea, causarán la operación del relevador de tierra. Esto sucede cuando hay saturación desigual en los -- TC'S que origina una corriente residual falsa en los circuitos secundarios o del relevador. El usar dos y no tres relevadores de fase ó ajustes diferentes entre los tres relevadores de fases tenderá a -- aumentar el efecto.

Como una regla de dedo, no habrá problemas si los burdens de fase están limitados de tal manera que el voltaje desenrollado por el TC durante el arranque es menor que el 75% de la precisión nominal 10H del TC. Una solución práctica para prevenir la operación del relevador, debido a un problema de estos, es aumentar el burden en el relevador de tierra, usando un tap menor. Esto hace que los tres TC'S se sa-

lunen más uniformemente juntos y reducen efectivamente la corriente residual falsa. Una solución alternativa es conectar una resistencia a reactor en serie con el relevador de tierra.

La tendencia en estaciones de servicio y sistemas de potencia industriales entre 2300 y 14400 Volts es aumentar la impedancia de neutro y obtener apreciablemente menores corrientes de falla a tierra. Esto aumenta el problema de obtener un ajuste muy sensible en los relevadores, que no opere con las falsas corrientes residuales durante el arranque. Esto se resuelve mejor usando un TC tipo ventana que tiene un sólo secundario rodeando los tres conductores. Esto elimina la corriente residual falsa, y permite aplicar un relevador de tierra instantáneo muy sensible. Una alternativa es usar relevadores direccionales de sobrecorriente con la bobina de polarización por corriente o voltaje conectada en el neutro de la fuente ó entre las terminales de la resistencia de neutro.

PROTECCION POR BAJO VOLTAJE

El bajo voltaje no permite que los motores alcancen su velocidad nominal en el arranque ó es la causa de que pierdan velocidad y de que tomen pesadas sobrecargas. Mientras que los relevadores de sobrecarga eventualmente detectan esta condición, el motor debe ser desconectado rápidamente cuando se tiene una sévera condición de bajo voltaje. La protección contra bajo voltaje en la línea es una característica estándar de los controles de motores que operan con C.A. Usualmente se aplican relevadores de bajo voltaje, con retraso de tiempo, tal como el tipo CV. Donde es esencial una operación continua, como en los auxiliares de estación a procesos de manufactura continuos, estos relevadores ó son omitidos ó se usan solamente como alarma.

PROTECCION DE ROTACION DE FASE (SECUENCIA)

En donde un arranque en reversa puede provocar un daño serio, un relevador en fase inversa como el CP debe aplicarse. Este es un relevador de inducción operado como un voltmetro polifásico con contactos para bajo voltaje y para alto voltaje. Los contactos de bajo voltaje son los de disparo y se mantienen cerrados por un resorte. Si la rotación de fases es correcta y están presentes los tres voltajes este contacto abre y se mantiene abierto. Si los voltajes aplicados están suficientemente desbalanceados el relevador operará, aunque el relevador no proporciona protección por desbalance de fase con una fase abierta, si la rotación del motor y la carga son tales que el voltaje se mantiene en la fase abierta.

PROTECCION CONTRA OPERACION DESBALANCEADA DE CORRIENTE O CON UNA SOLA FASE.

Este tipo de protección se aplica en motores grandes donde la operación en una fase es un riesgo peligroso. El caso típico es el suministro a través de fusibles y uno de éstos está abierto. En estas aplicaciones, el relevador tipo CM es el recomendado. Contiene dos unidades de disco de inducción. Una balancea I_a contra I_b y la otra I_b contra I_c . Cuando las corrientes se desbalancean suficientemente, se produce un par en una de las dos unidades, tendiendo a cerrar sus contactos que están en paralelo en el circuito de disparo. Un relevador protegerá una ó dos máquinas en paralelo. Su rango entre sensibilidad máxima a mínima de 3 a 1 no puede permitir proteger un número grande de motores polifásicos. Por ejemplo, si la corriente de plena carga de una máquina es de 2 amperes, y la corriente de otras es de 4 amperes, el relevador CM puede ser ajustado en el tap de 2 amperes donde la corriente térmica continua nominal es 6 amperes. Esto propor-

conará protección para la máquina más pequeña cuando opere sola, en tanto tiene 2 amperes en una o dos fases y cero en la tercer fase.

Protección contra operación monofásica con cargas pequeñas es difícil de lograr, ya que las magnitudes de la corriente para una condición de fase abierta son pequeñas.

Donde se requiere más sensibilidad, el relevador POQ de secuencia negativa es el indicado. Opera con 0.5 amperes de secuencia negativa (I_2) y soporta 5 amperes de corriente de carga continua. Con una fase --- abierta las otras dos corrientes quedan a 180° y la corriente de fase es $\sqrt{3} I_2$, así la comparación es 0.866 amperes para el POQ contra los 2 amperes del CM. El POQ opera en uno ó dos ciclos, así un relé de tiempo debe ser usado para prevenir su operación a menos que persista esa condición.

En motores de 1000 HP ó más, el COQ se aplica. Donde fueron establecidos los estándares para generadores sincrónicos no se obtuvo ningún acuerdo en las constantes aplicadas a los motores sincrónicos ó motores de inducción. Se diseñan motores para soportar una cantidad más grande de corriente inducida en el propio rotor, así como en el devanado amortiguador durante el período de arranque. Por consiguiente, parece razonable usar un valor de I^2t igualmente alto que en generadores convencionales y cuando menos de 40.

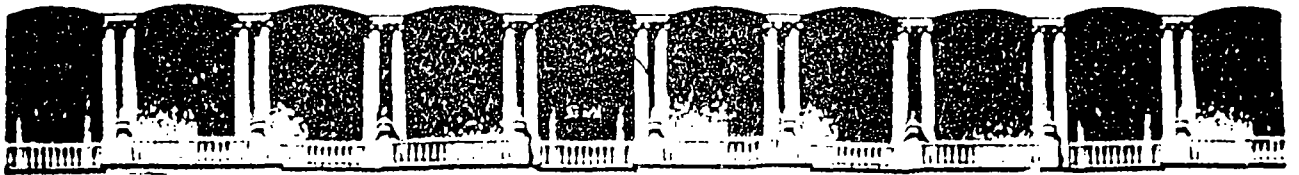
PROTECCION CONTRA OSCILACIONES O PERDIDAS DE SINCRONISMO

Este tipo de protección generalmente no es aplicado a equipo rotativo, excepto en cambiadores sincrónicos de frecuencia que interconectan dos sistemas, y en motores sincrónicos ó grupos motor generador donde caídas de voltaje severas pueden provocar que la máquina pierda sincronismo. Donde se requiere esta protección se usa el relevador tipo notching

CRH, el cual cuenta una sucesión de variaciones de potencia inversa y si un determinado número de ellas ocurre dentro de un intervalo especificado de tiempo, el relevador envía una alarma ó un disparo para parar la máquina. El relevador CRH es un relevador de sobrecorriente bidireccional que opera con cada impulsor de oscilación. Estos impulsos operan una cadena de relevadores auxiliares que los cuentan y el último opera después de 3 1/2 ciclos de deslizamiento. El Timer puede ser ajustado entre 0 y 10 segundos y a menos que los 3 1/2 ciclos de deslizamiento ocurren dentro de este tiempo, todas las unidades de notching son restablecidas.

PERDIDA DE EXCITACION

La protección contra pérdida de excitación puede obtenerse en motores síncronos, con un relevador de baja corriente conectado en el campo. Debe tener retraso de tiempo para el disparo ó alarmar al operador si los reguladores automáticos de voltaje no son usados. El relevador ILLF también se aplica con grandes motores. La habilidad del circuito de suministro para proporcionar potencia inductiva al motor cuando pierda su campo es un factor importante en esta protección. Si el voltaje cae con el incremento de potencia reactiva, el par puede reducirse causando que el motor pierda sincronismo, y cualquier relevador, el de pérdida de campo ó el de pérdida de sincronismo proporcionarán una protección.



**FACULTAD DE INGENIERIA U.N.A.M.
DIVISION DE EDUCACION CONTINUA**

**V CURSO INTERNACIONAL DE SISTEMAS
ELECTRICOS DE POTENCIA**

MODULO II: SISTEMAS ELECTRICOS DE POTENCIA II

TEMA : PROTECCION DE LINEAS

**EXPOSITOR: ING. AUGUSTO O. HINTZE V.
1996**

PROTECCION DE LINEAS

Las líneas se pueden proteger contra fallas por medio de relevadores de sobrecorriente; sin embargo, esto solo se puede lograr si la corriente de carga es inferior a la mínima corriente de falla. Tiene este método a su favor el poder proporcionar respaldo remoto sin instalaciones adicionales.

Debido a que no es una protección selectiva en cuanto a detección, la selectividad se debe lograr en base a coordinación de tiempos. Esto hace que los tiempos de libramiento de fallas cercanas a la fuente sean, en general, altos.

Cuando hay pluralidad de fuentes de suministro en la red, se hace necesario dotar de direccionalidad a la protección de sobrecorriente para poder lograr la coordinación. A pesar de ello, en algunos casos, principalmente en los que se forman anillos se dificulta mucho el lograr la coordinación o, inclusive, puede resultar imposible. Esto obligará a operar el anillo abierto o a utilizar una protección más selectiva.

La protección de distancia es una protección más selectiva y por lo mismo puede ser más rápida.

Según la longitud de la línea, la resistencia de arco esperable y la carga que se espera transportar por la línea se deberá seleccionar la protección adecuada, ya sea de admitancia, de reactancia, de paralelogramo, etc.

Debido a que la protección de distancia no puede ser tan precisa que ---
discierna entre fallas a un lado y otro del interruptor remoto, la protec-
ción de la línea se lleva a cabo por medio de dos zonas:

La primera zona se utiliza para detectar fallas en el primer 80% a 85% de
la línea protegida utilizándose la detección para provocar disparo instan-
táneo.

La segunda zona se utiliza para detectar fallas en la porción restante de
línea. Para asegurarse de éllo, se le da un ajuste de alcance tal que --
sea cuando menos el 115% de la línea protegida, aunque la costumbre es --
dar el ajuste de alcance tal que cubra la totalidad de la línea protegida
más la mitad de la línea siguiente.

Cuando se desea dar respaldo remoto de distancia, se emplea una tercera -
zona, cuyo ajuste de alcance deberá ser tal que cubra no solo la línea --
protegida sino además, la línea mas larga que salga de la estación remota
y ésto con un margen de seguridad de 10 a 15%; o sea que

$$\text{Zona 3} \geq 1.15 (L1 + L2 \text{ más larga})$$

En ocasiones este alcance tan largo puede provocar problemas, ya que ---
también se debe evitar que la Zona 3 alcance porciones protegidas por la
estación remota en Zona 3; o sea que

$$\text{Zona 3} < L1 + L2 \begin{matrix} \text{más} \\ \text{corta} \end{matrix} + L3 \begin{matrix} \text{más} \\ \text{corta} \end{matrix}$$

Estos dos criterios limitantes del ajuste de alcance de la Zona 3 puede reducir demasiado el margen de ajuste o inclusive cancelarlo, lo que imposibilitaría el uso de la Zona 3 para dar respaldo remoto.

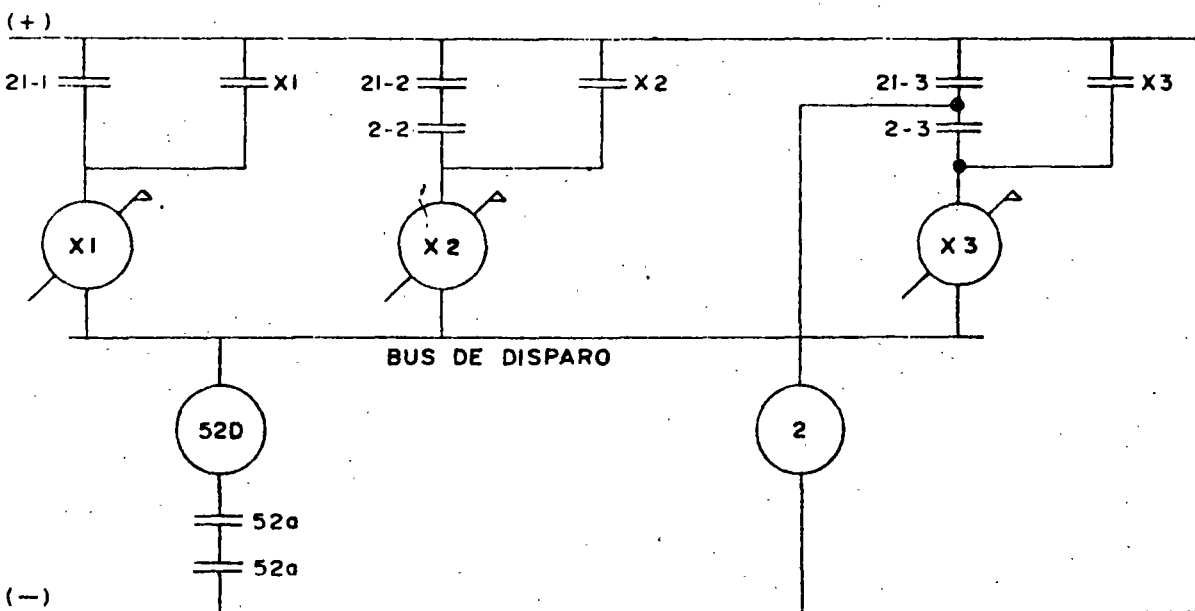
Debido a los sobrealcances introducidos intencionalmente en las Zonas 2 y 3, la selectividad se debe lograr nuevamente en base de tiempo.

El tiempo de la Zona 1 será cero para el retraso intencional puesto que esta Zona sí es selectiva.

El tiempo de la Zona 2 deberá ser tal que, para la porción sobrealcanzada, no opere antes que la protección propia de ella. Dependiendo de la protección propia de la porción sobrealcanzada, el tiempo se ajustará usualmente entre 0.2 y 0.5 segundos.

El tiempo de la Zona 3 también deberá permitir que primeramente dispare la protección primaria. Como la protección primaria pudiera ser lenta, generalmente el ajuste de tiempo de la Zona 3 es muy alto; usualmente entre 0.8 y 2 segundos.

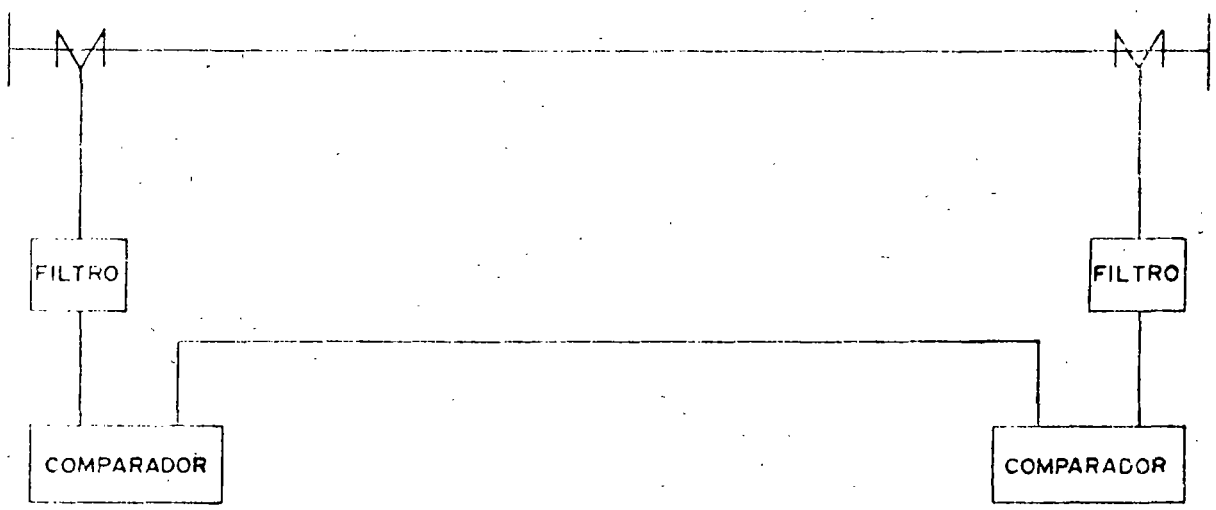
El diagrama simplificado de control de la protección de distancia de tres zonas se muestra a continuación.



F. S.

Existe para la protección de líneas un dispositivo eminentemente selectivo y que por lo tanto puede tener disparo instantáneo. Esta protección es el "hilo piloto".

PROTECCION POR HILO PILOTO

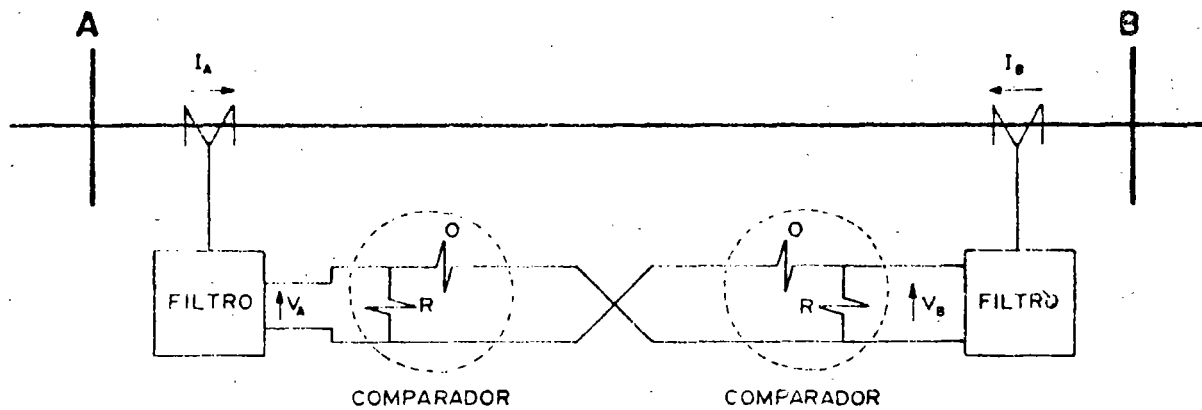


Para ahorro de canal de comunicaciones, por él se envía una señal que es una mezcla (en proporciones ajustables) de las tres componentes de la corriente primaria.

Para líneas muy cortas, en que el canal puede ser una pareja física de conductores, la señal empleada es analógica y puede ser de voltaje o de corriente. A continuación se muestran estos dos tipos de comparación.

F.3

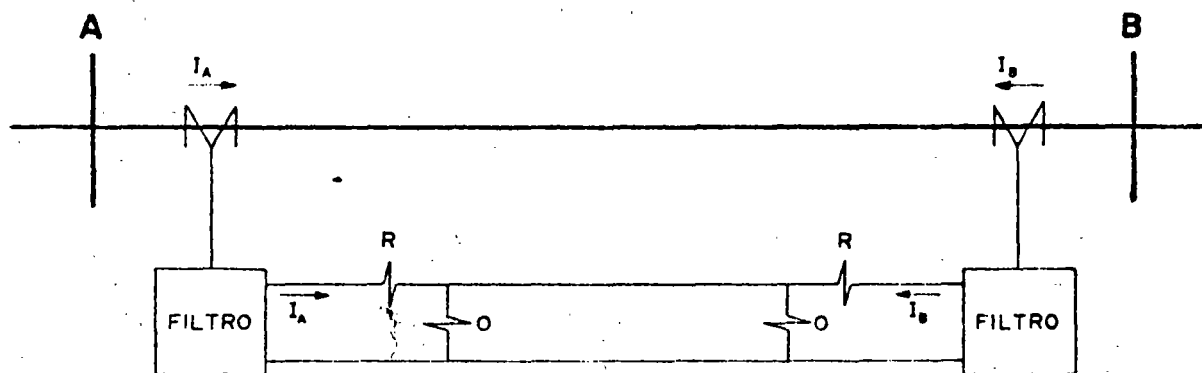
a) COMPARACION DE VOLTAJES



$$V_A = K_1 I_{A1} + K_2 I_{A2} + K_0 I_{A0}$$

$$V_B = K_1 I_{B1} + K_2 I_{B2} + K_0 I_{B0}$$

b) COMPARACION DE CORRIENTES

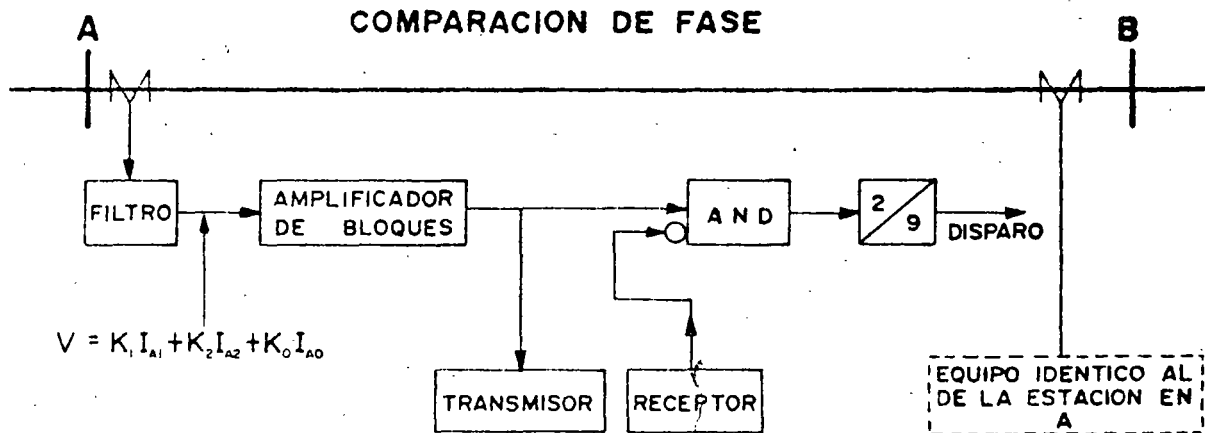


$$I_A = K_1 I_{A1} + K_2 I_{A2} + K_0 I_{A0}$$

$$I_B = K_1 I_{B1} + K_2 I_{B2} + K_0 I_{B0}$$

En caso de que el hilo piloto se abra, el de comparación de voltajes no disparará para fallas internas mientras que el de comparación de corrientes disparará en falso para fallas externas. Por el contrario, en caso de que el hilo piloto se cortocircuite, el esquema de comparación de voltajes disparará en falso para fallas externas, mientras que el de comparación de corriente, si el corto circuito es muy severo, podrá ser que no dispare para fallas internas.

Cuando se desea protección eminentemente selectiva en líneas en que por su longitud o por otras causas no se pueda emplear pareja física de conductores, entonces se emplea comparación de fase entre las señales y esta comparación se hace entre bloques representativos de la salida del filtro, tal como se muestra (grandemente simplificado) a continuación.



El canal de comunicación entre A y B puede ser por onda portadora, por micro-ondas o por UHF, su único requisito es que sea lo suficientemente rápido para poder reproducir en la estación remota los pulsos o bloques generados localmente.

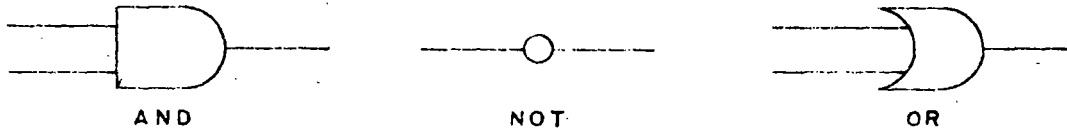
PROTECCIONES ESTATICAS

En las protecciones estáticas se trabajan las señales, en forma interna, a través de circuitos lógicos. Esto va en contraste con el proceso analógico que de la señal se hace en los relevadores electromagnéticos.

Las señales analógicas obtenidas del sistema primario a través de TC's y/o TP's se hacen pasar por dispositivos a través de los cuales se disminuye el nivel de señal, se aísla del exterior y, en caso necesario, se convierten a señales de voltaje.

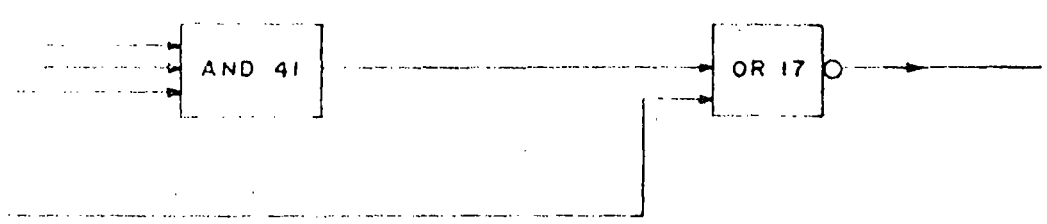
Estas señales de voltaje se harán pasar por dispositivos que las convertirán en pulsos o en bloques o señal permanente para después utilizar esto en la lógica del esquema.

Los símbolos de los operadores lógicos son:

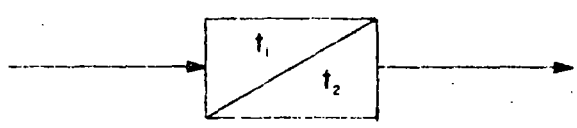


pero generalmente se acostumbra representar solamente con un paralelogramo en el que se escribe el identificador del operador y generalmente un número que lo distingue de otros operadores lógicos iguales.

Ejemplo:

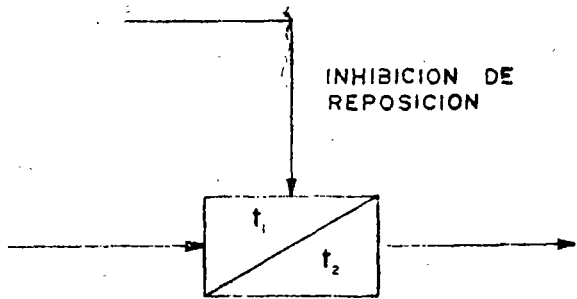


Otro dispositivo muy empleado lo constituye la unidad temporizadora, la cual se representa generalmente como sigue:



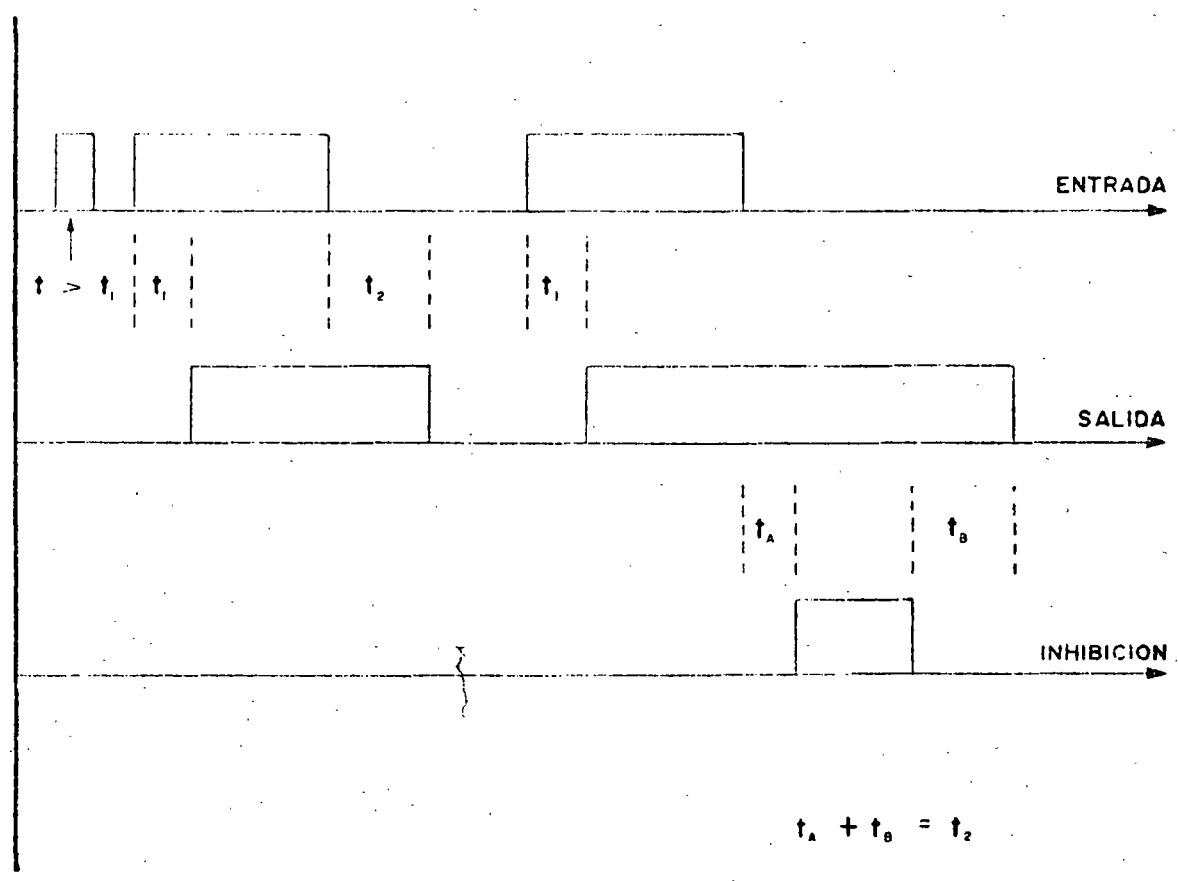
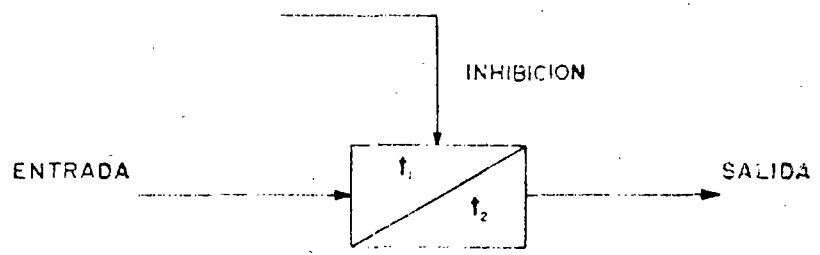
En el diagrama, t_1 representa el tiempo mínimo (en mseg) que debe tener valor "verdadero" la señal de entrada para que se produzca señal de salida mientras que t_2 representa el tiempo que permanecerá la señal de salida después que haya desaparecido la de entrada. También t_2 se da generalmente en mseg.

Una variante interesante de las unidades temporizadas se logra añadiéndoles una señal inhibidora de la reposición.



5"

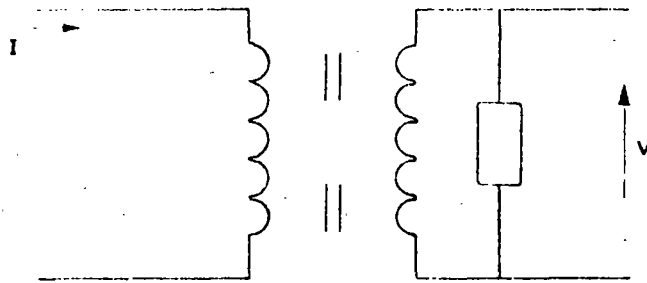
El efecto que esto tiene es el suspender el proceso de reposición durante todo el tiempo que permanezca la señal de inhibición de tal suerte que el tiempo de reposición será la suma del tiempo que transcurra entre la desaparición de la señal de entrada y la aparición de la de inhibición sumado al tiempo que permanezca la de inhibición más el que transcurra tras su desaparición. Esto se ilustra más claramente enseguida.



53

Como se mencionó antes, las señales analógicas que se utilizarán para -- obtener señales lógicas son siempre de voltaje. En el caso de señales de voltaje originalmente, solo se les reducirá el nivel por medio de trans-- formadores de aislamiento, los cuales generalmente también servirán para ajustes por medio de derivaciones.

El manejo de señales de corriente se hace a través de transactores, que - en realidad son transformadores con entrehierro en el núcleo y una carga en el secundario, de tal manera que muestran un voltaje secundario propor-- cional a la corriente primaria, siendo compleja la constante de proporció-- nalidad. Su representación habitual es:

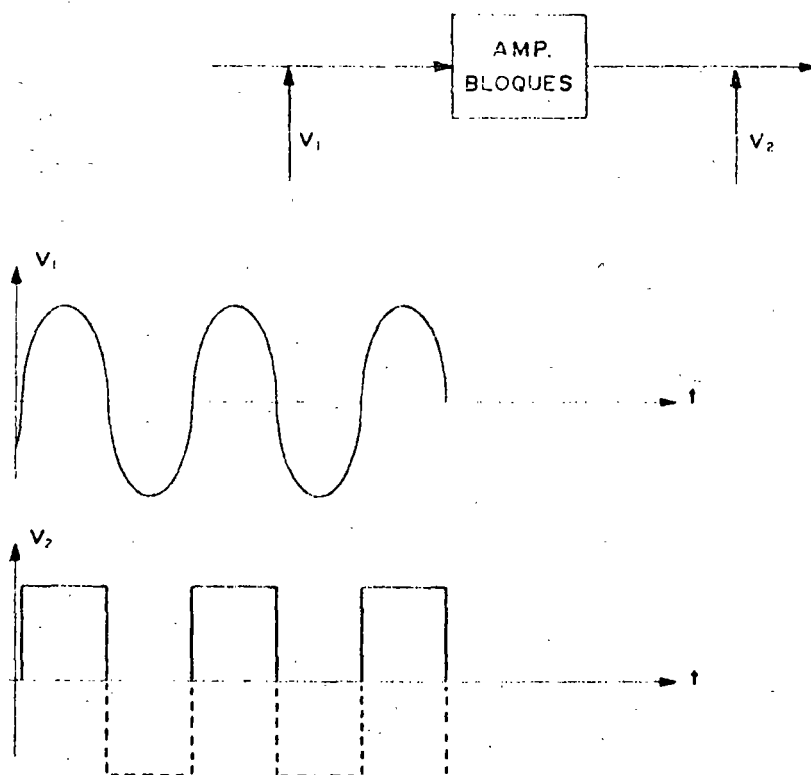


$$\frac{V}{I} = Z_T$$

La "impedancia" del transactor, Z_T , es función de la construcción del --- mismo y de la carga que se le aplique.

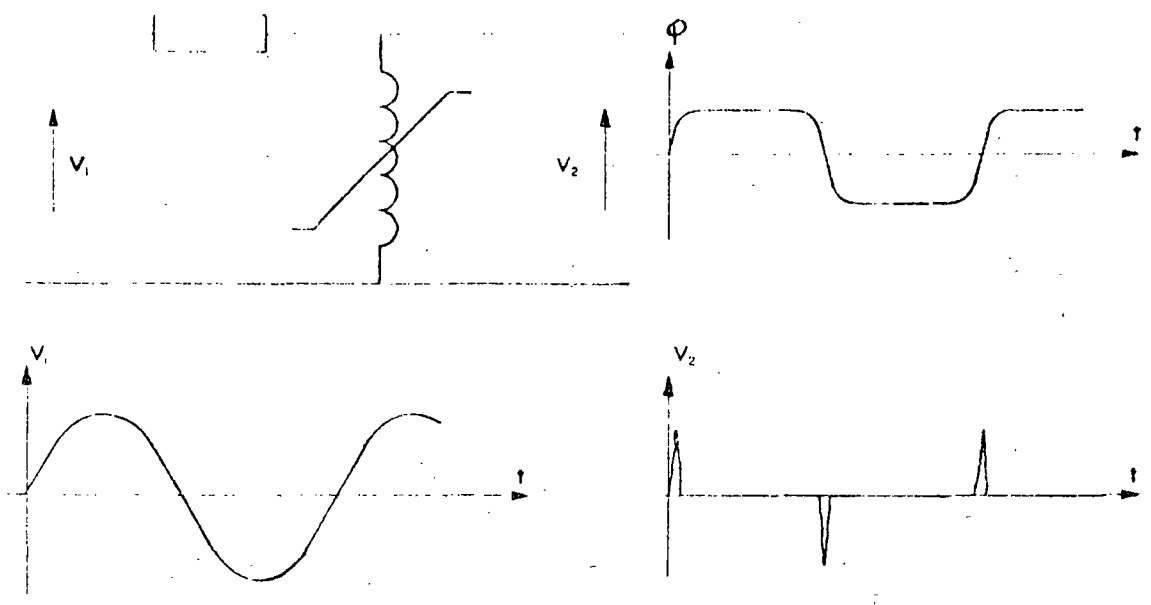
53

Las señales analógicas de voltaje se hacen pasar posteriormente por amplificadores de pulsos o de bloques que, en el caso de estos últimos se trata de un amplificador llevado intencionalmente a saturación por medio de la señal de entrada y una amplificación muy alta. Su operación se ilustra enseguida.

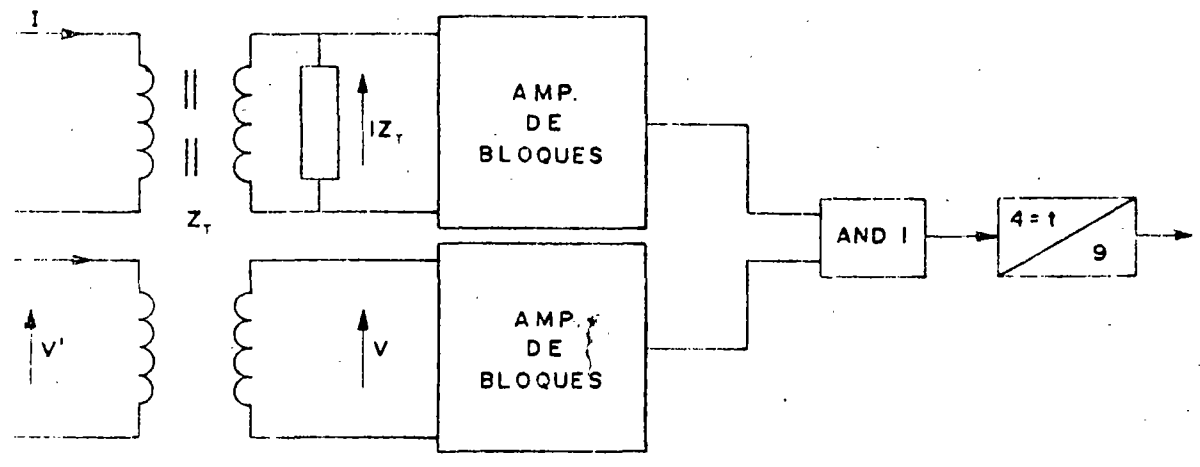


Los amplificadores de pulsos se basan: o en un núcleo sumamente saturado, o en un derivador a la salida de un amplificador de bloques.

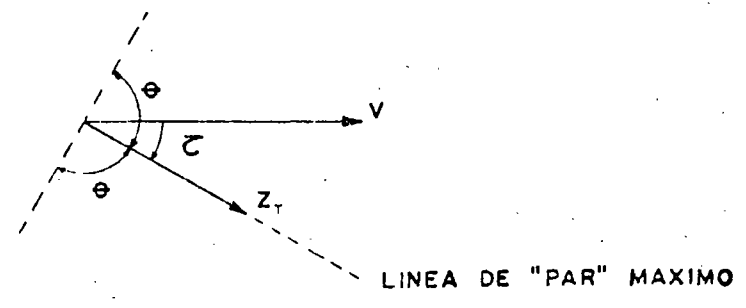
El primer método se ilustra enseguida por ser el más empleado.



A continuación se ilustra con una aplicación de los elementos vistos un "elemento" direccional.



$$\theta = \frac{360^\circ}{T} \cdot t_1$$

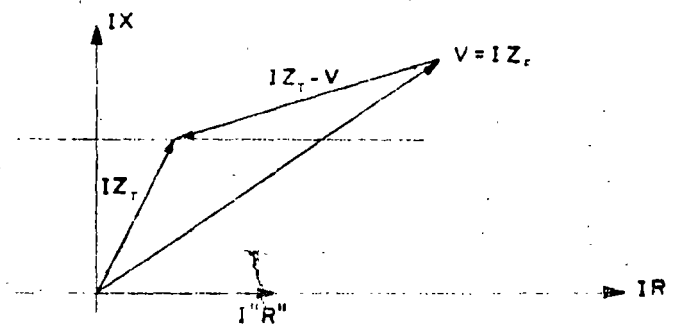
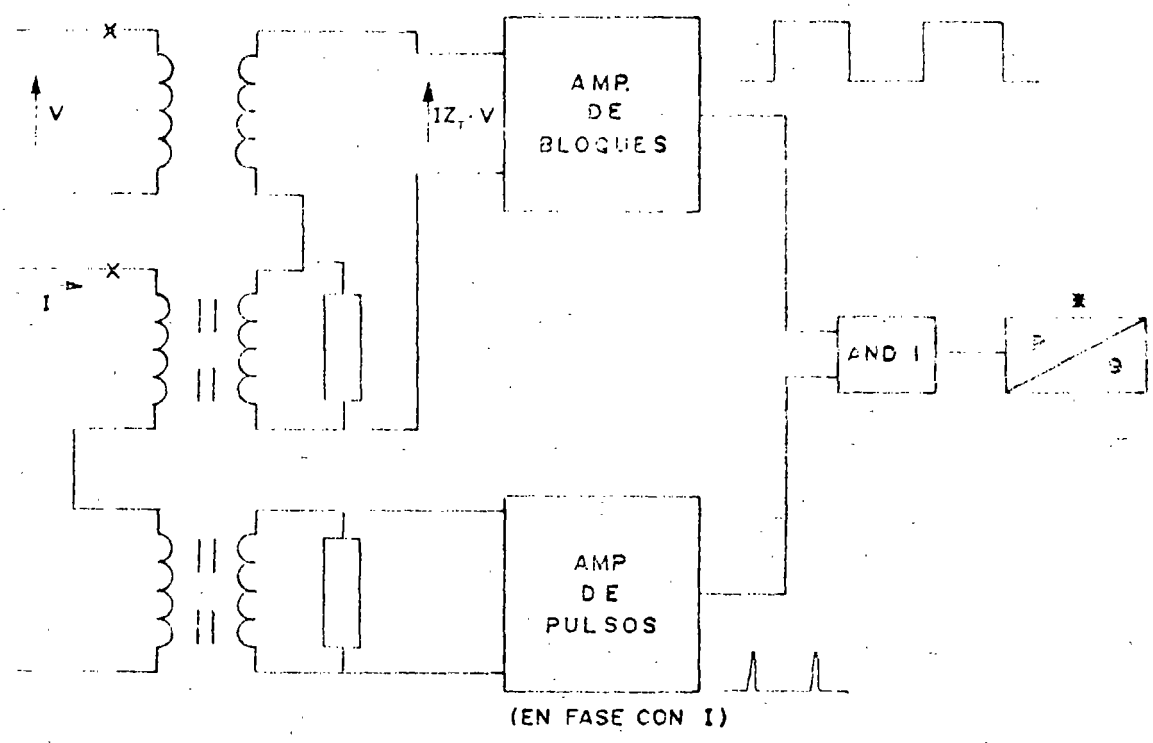


LINEA DE "PAR" MAXIMO

61

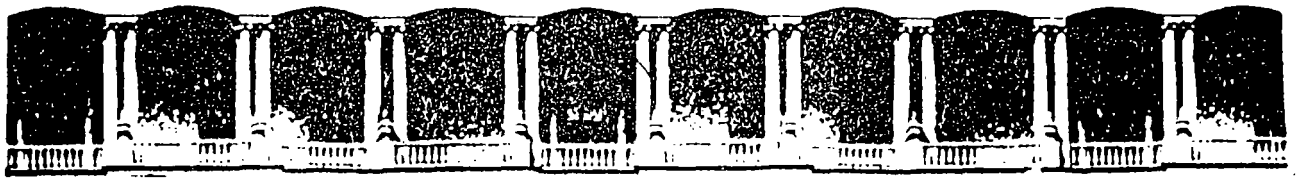
Generalmente $t_1 = 4.16$, así $\phi = 90^\circ$ con lo que la línea divisoria -- entre operación y no operación es una recta.

Otra operación es la constituida por el relevador de reactancia.



Los pulsos coincidirán con la existencia de bloques siempre y cuando el defasamiento entre $IZ_T - V$ e $I'R''$ este comprendido entre 0° y 180° y esto define la recta de reactancia constante mostrada.

* LA P en el temporizador implica $t_1 \rightarrow 0$



**FACULTAD DE INGENIERIA U.N.A.M.
DIVISION DE EDUCACION CONTINUA**

**V CURSO INTERNACIONAL DE SISTEMAS
ELECTRICOS DE POTENCIA**

MODULO II: SISTEMAS ELECTRICOS DE POTENCIA II

TEMA : PROTECCION DE GENERADORES

**EXPOSITOR: ING. AUGUSTO O. HINTZE V.
1996**

PROTECCION DE GENERADORES

La frecuencia de falla en máquinas es pequeña, éste es el resultado de los diseños modernos y de los materiales cada vez mejores. Aún así - las fallas ocurren con las consecuencias serias y los daños severos -- que dejan a las unidades fuera de servicio por tiempos largos. Así - que es muy importante que se detecten rápidamente las condiciones anor- males y que las áreas afectadas sean prontamente aisladas.

El equipo rotatorio esta sujeto a varias condiciones anormales, algu- nas de las cuales son:

- a). Fallas en los devanados
- b). Sobrecargas
- c). Sobrecalentamientos (devanados o chumaceras).
- d). Sobrevelócidad
- e). Falla ó pérdida de campo
- f). Motorización del Generador.
- g). Operación en una fase ó desbalanceado.
- h). Pérdida de sincronismo.

Algunas de estas condiciones pueden no requerir disparo automático de la máquina, ya que pueden ser corregidas en una estación apropiadamen- te atendida, mientras que la máquina permanece en operación. Aquí, - los dispositivos de protección actuan sobre alarmas. Otras condicio- nes, como las fallas, requieren que la máquina sea rápidamente desco- nectada.

64

En cualquier caso es importante evaluar el costo (inicial, de operación y de mantenimiento) y grado de protección proporcionada contra el riesgo encontrado si no se aplica alguna protección para ese caso particular. El juicio ingenieril determinará que tanta protección aplicar, y si esta cantidad variará con el tamaño e importancia de la máquina.

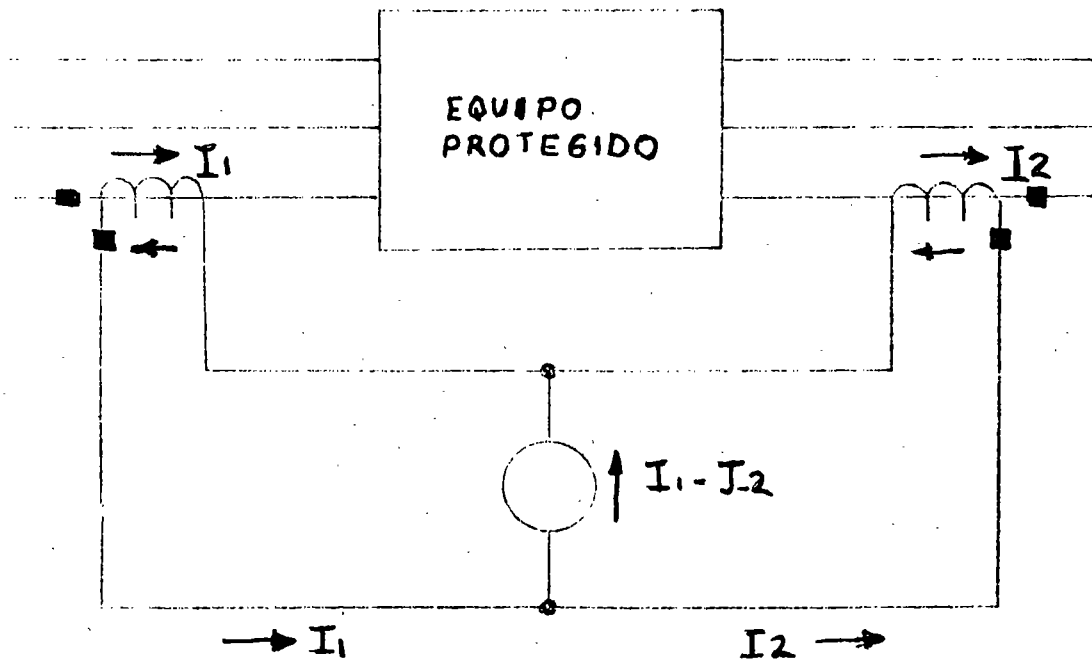


FIGURA 4-1
PROTECCION DIFERENCIAL BASICA

Las fallas dentro de la máquina generalmente tienden a poner a tierra -- uno de los bobinados de fase y con frecuencia tienden a involucrar a -- las otras fases. La protección más efectiva para tales casos es la --

60

protección diferencial. En este esquema, las corrientes en cada fase ó en cualquier lado de la máquina son comparadas en un circuito diferencial y cualquier desbalance ó corriente diferencial se usa para operar el relevador. En operación normal ó en una falla externa a los dos juegos de TC'S, I_1 entrando a la máquina es igual a I_2 que sale de la máquina en cualquier fase (despreciando las pequeñas pérdidas internas) y suponiendo que los TC'S son perfectos.

La corriente en el relevador $I_1 - I_2$, es pequeña, y el relevador puede ser ajustado arriba de su valor máximo durante la operación normal de la unidad y prevenir una operación del relevador. Cuando ocurre una falla dentro de los grupos de TC'S, una ó más de las corrientes I_1 aumenta repentinamente, mientras que la corriente I_2 puede disminuir ó aumentar rápidamente y circular en la dirección contraria. En cualquier caso, la corriente de falla fluye ahora a través del relevador haciéndolo operar.

Este arreglo podría ser ideal y el relevador de sobrecorriente en el circuito diferencial sería ajustado muy sensibilmente y muy rápido, si los TC'S fueran perfectos. Sin embargo en la realidad, los TC'S no siempre dan exactamente la misma corriente secundaria para la misma corriente primaria, aún cuando sean comercialmente idénticos.

Esta diferencia es a causa de variaciones en el proceso de manufactura y a diferencia del burden, es decir, desigual longitud de cables al relevador y cargas desiguales de medidores e instrumentos que pueden ser conectados en uno ó ambos secundarios. La corriente diferencial producida fluye a través del relevador. Mientras que ellas son normalmente pequeñas, pueden llegar a ser apreciables cuando corrientes de corto circuito sean transmitidas a una falla externa. Entonces el relevador de sobrecorriente debe ser ajustado arriba del valor de la corriente de error máxima, que puede circular por él durante una falla externa.

66

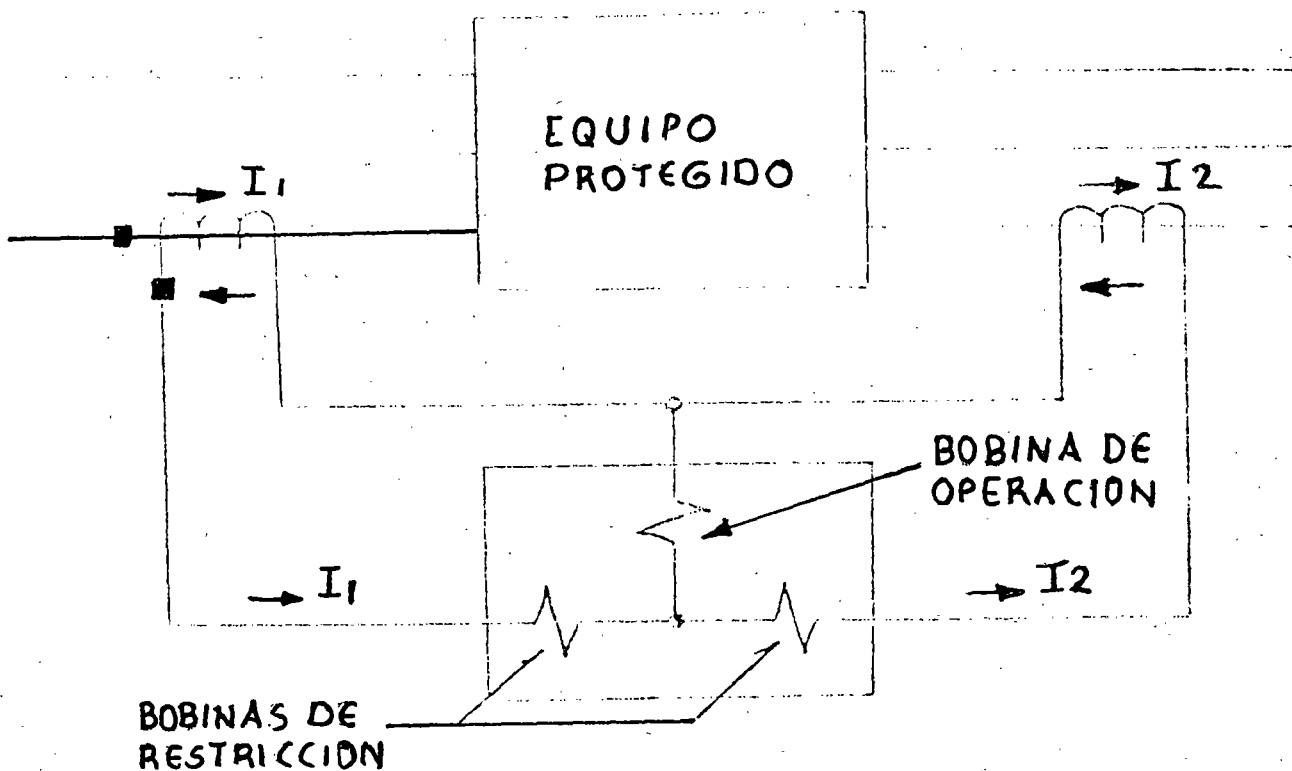


FIGURA 4-2

DIAGRAMA ESQUEMATICO DE UN RELEVADOR DIFERENCIAL DE PORCENTAJE. SE MUESTRAN SOLO LAS CONEXIONES DE UNA FASE.

El relevador diferencial con porcentaje, Fig. 4.2, resuelve este problema sin sacrificar sensibilidad. Los devanados reciben la corriente secundaria de los TC y funcionan para desensibilizar la bobina de operación, particularmente con altas corrientes. Esto se hace comúnmente con bobinas en el mismo electromágneto ó en un elemento separado bobinado en forma -- tal que produce un par que abre el contacto oponiéndose al par de cierre de la bobina de operación. En otras palabras, la corriente requerida pa

67

na operar aumenta si la corriente de falla externa aumenta. Este incremento puede ser un incremento porcentual constante, como en el caso del relevador diferencial con porcentaje tipo CA para protección de generadores, ó con un incremento porcentual variable (más grande con corrientes más altas) como se usa en el relevador tipo HA, de alta velocidad (1 ciclo). El efecto de las bobinas de restricción es despreciable en fallas internas, ya que la bobina de operación tiene más amper-vueltas netas y recibe la corriente secundaria total.

El relevador CA esta disponible en dos tipos: de 10% y de 25%. Este valor representa el porciento de corriente desbalanceada necesario para operar el relevador expresado en términos de la corriente más pequeña que hace operar el relevador. El relevador de 10% tiene un pick-up mínimo de 0.18 ampers y el de 25%, 0.45 ampers. Esta es la corriente que debe circular por una bobina de restricción y por la de operación para hacer operar el relevador. Con 3 ampers ó más en el relevador de 10% ó 7 ampers ó más en el de 25%, el tiempo de operación es de 10 ciclos ó menos, con un tiempo mínimo de 5-6 ciclos. Hablando en general, este relevador puede dejar pasar los transitorios de C.D. No se ha experimentado ninguna dificultad en este aspecto excepto en casos muy extremos.

El tipo HA ha sido diseñado de tal manera que no es afectado por los transitorios de CD asociados con corrientes asimétricas de falla externa, y puede ser aplicado con una considerable diferencia de comportamiento de los TC'S en ambos lados de la máquina. El porcentaje de desbalance varía entre 5% a 5 ampers y 20 % a 60 ampers. Como se indicó antes el HA opera en 1 ciclo y cuesta aproximadamente 20% más que el CA, comparando 3 CA'S monofásicos contra un HA trifásico.

En todos los esquemas diferenciales es buena práctica usar TC'S de las

68

mismas características, siempre que sea posible y evitar la conexión de otros equipos en estos circuitos.

La mayoría de los generadores tienen sus devanados conectados en estrella. Así los tres relevadores conectados a los TC'S también conectados en estrella proporcionan protección contra fallas entre fases y de fase a tierra (Fig. 4-2). Una protección similar se obtiene para generadores en delta con el esquema de la Fig. 4-3.

Esto requiere que los devanados sean traídos al exterior para que sean instalados los TC'S dentro de la delta. Los generadores que tienen bobinas divididas (split-phase) se protegen con dos juegos de relevadores diferenciales, uno conectado entre dos bobinas paralelas y el otro completo como en la Fig. 4-2. Este arreglo hace posible proteger contra todo tipo de fallas internas, incluyendo cortos entre espiras una bobina abierta. Un esquema alternativo es el de la Fig. 4-4. Las relaciones de los TC'S deben ser de dos a uno, ó conectar un juego de transformadores auxiliares para proporcionar un balanceo durante la operación normal.

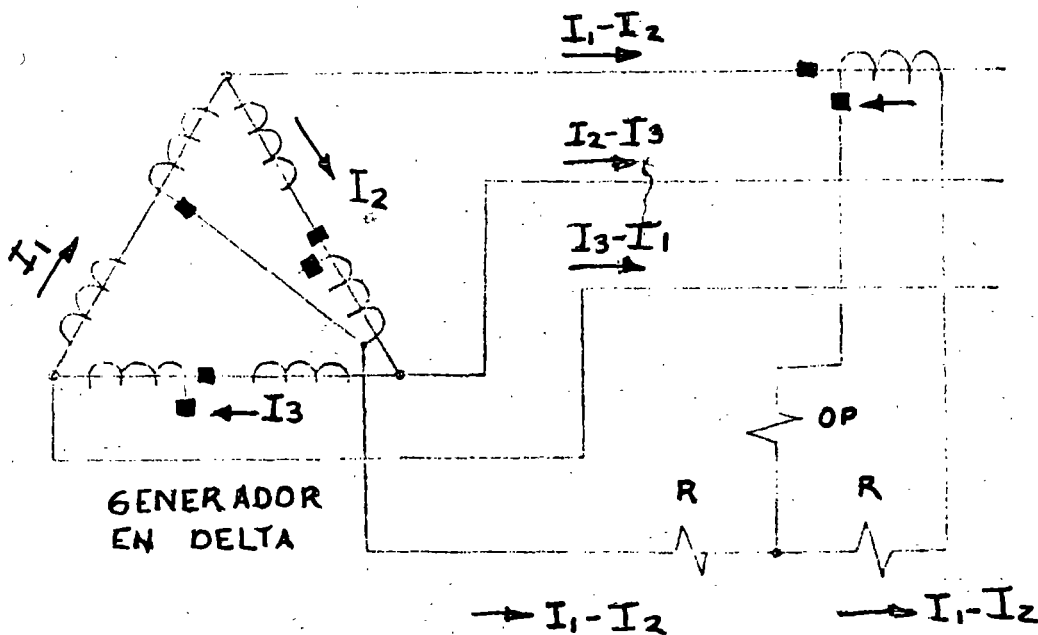


FIGURA 4-3

DIAGRAMA ESQUEMATICO DE UN RELEVADOR DIFERENCIAL PARA UNA UNIDAD CONECTADA EN DELTA

R.C.

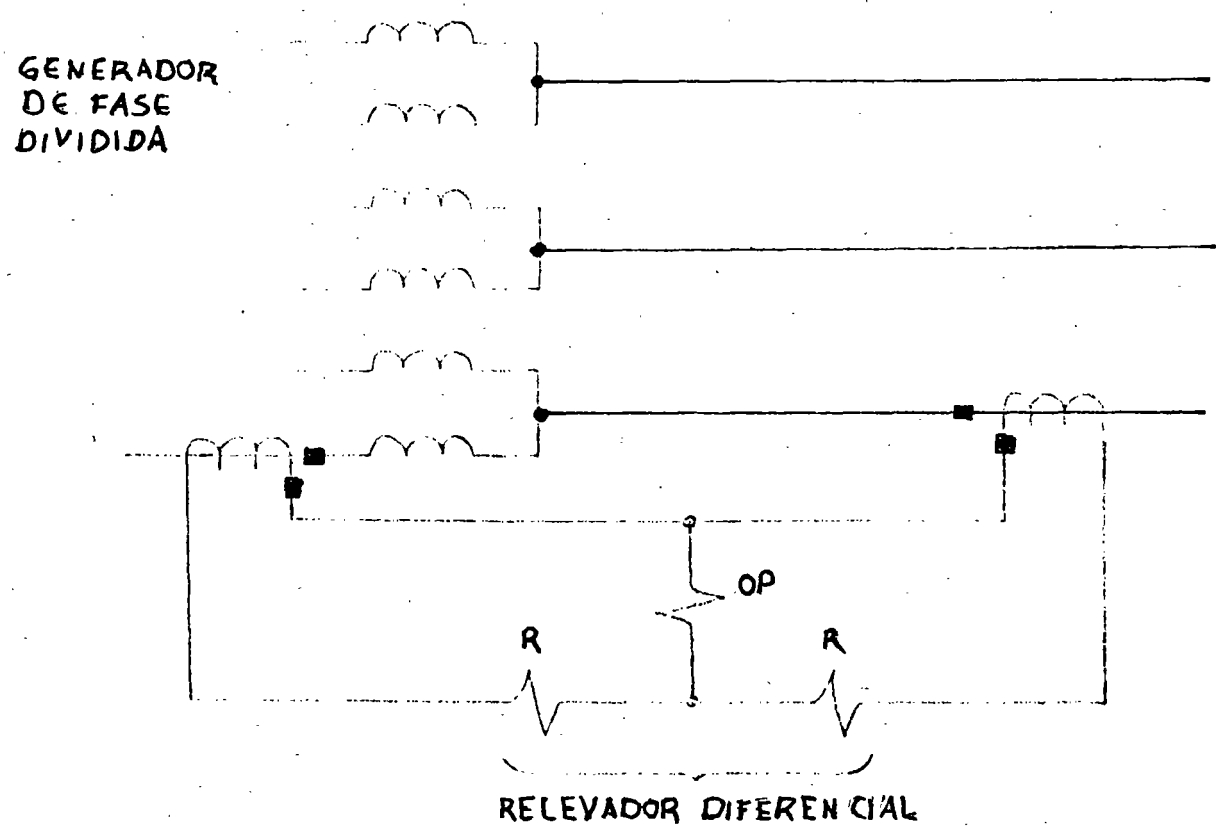


FIGURA 4-9'

DIAGRAMA ESQUEMATICO, MONTADO EN UNA SOLA FASE PARA LA PROTECCION DE UNA UNIDAD CON BOBINAS DE FASE DIVIDIDAS

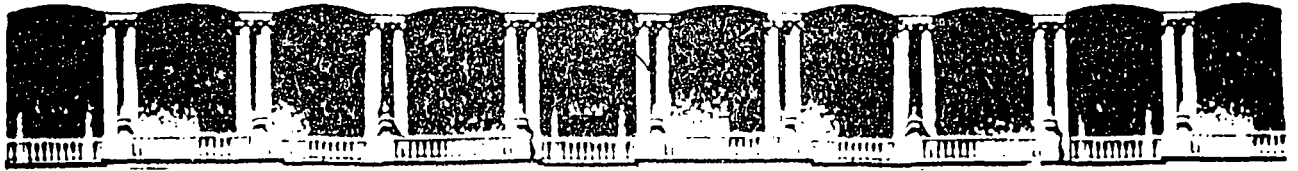
PROTECCION CONTRA FALLAS A TIERRA

El método de conexión a tierra afecta la protección proporcionada por los relevadores diferenciales. Entre más grande es la impedancia de conexión, más pequeña es la magnitud de la corriente de falla y más difícil es para el relevador diferencial detectar las fallas pequeñas. Un relevador conectado en la trayectoria del neutro a tierra proporcionará protección más sensitiva, ya que puede ser ajustado en forma correspondiente de la corriente de carga. Al aumentar la impedancia de conexión a tierra, se hace más difícil aplicar un relevador de corrien-

76

te. Entre más bajo sea el pick-up, más grande es el burden en el TC y más difícil es distinguir entre fallas a tierra y desbalanceo de tercera armónica que también circula por el neutro. Esta tercera armónica puede llegar a ser del orden del 10 al 15% de la capacidad máxima del generador.

El relevador de tierra puede operar para fallas a tierra más allá del generador, y por lo tanto, debe incluir un retraso de tiempo para que coincida con otros relevadores. Un caso típico es el generador conectado directamente al bus con otros circuitos. Una falla en cualquiera de los circuitos no debe disparar la máquina, sino que éste debe ser liberado por la protección correspondiente en el circuito fallado. Un transformador conectado en estrella delta bloquea la circulación de corriente de tierra y así las fallas en el lado opuesto a estos bancos no operará relevadores de tierra. El generador tipo unitario es un ejemplo típico donde el transformador limita la operación del relevador de tierra al generador y cables terminales hasta el banco.



**FACULTAD DE INGENIERIA U.N.A.M.
DIVISION DE EDUCACION CONTINUA**

**V CURSO INTERNACIONAL DE SISTEMAS
ELECTRICOS DE POTENCIA**

MODULO II: SISTEMAS ELECTRICOS DE POTENCIA II

TEMA : PROTECCION DE TRANSFORMADORES

**EXPOSITOR: ING. AUGUSTO O. HINTZE V.
1996**

PROTECCION DE TRANSFORMADORES

Problemas a considerar:

- 1.- Diferencias en corrientes de plena carga.
- 2.- Relaciones de Transformación discretas en los TC'S.
- 3.- Corriente de Magnetización al energizar (Inrush).
- 4.- Variaciones de Taps.
- 5.- Defasamiento Vectorial.
- 6.- Varios Devanados.
- 7.- Corriente de Excitación.
- 8.- Diferencia en relaciones de corriente para diferentes tipos de fallas.

La protección de transformadores de 1 MVA ó más, se obtiene principalmente con relevadores del tipo diferencial. La protección diferencial no puede ser tan sensible como en los generadores, porque se tienen:

- 1.- Diferentes voltajes, incluyendo taps, y por lo tanto: corrientes primarias diferentes en los circuitos de conexión.
- 2.- Diferentes tipos de TC'S, relaciones de transformación, y características con posible desacople en las relaciones de los TC'S, en algunos casos y en algunos taps. Diferente comportamiento de -- los TC'S, particularmente en altas corrientes.
- 3.- La corriente de magnetización al energizar que aparece como falla interna al relé diferencial.

Las conexiones Delta-estrella introducen defasamientos que se deben considerar al aplicar los relevadores diferenciales en los bancos de transformación. Los transformadores defasadores y reguladores introducen problemas adicionales que requieren atención cuidadosa.

CORRIENTE DE MAGNETIZACIÓN

Cuando se energiza un transformador, una corriente transitoria de magnetización o de excitación circula de tal forma, que aparece como falla interna para los relevadores conectados diferencialmente. Corrientes pico de magnetización llegan a ser del orden de 8 a 10 veces del valor de la I nominal.

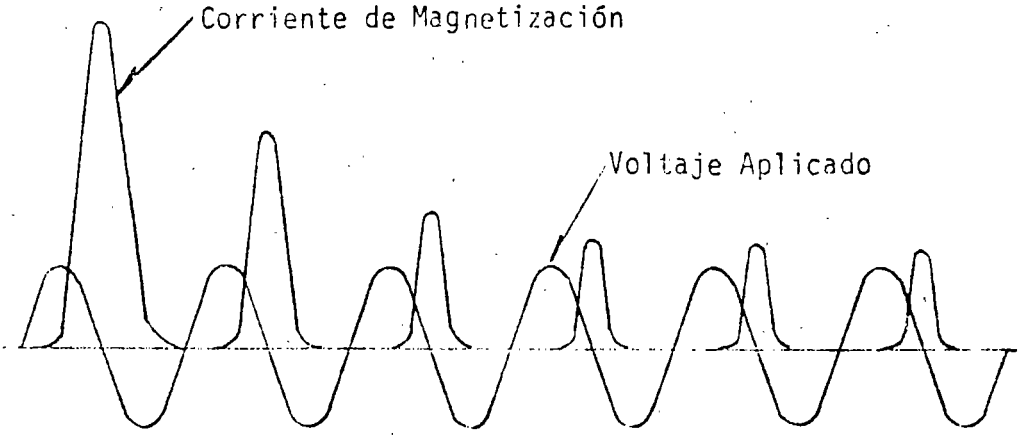
190

Los factores que controlan la magnitud y duración de la corriente de magnetización, son:

- 1.- Tamaño del banco de transformación.
- 2.- Tamaño del sistema de potencia.
- 3.- Resistencia en el sistema desde la fuente hasta el banco.
- 4.- Tipo de fierro usado en el transformador.
- 5.- Historia anterior del banco (flujo residual).
- 6.- Como se energiza el banco (por primera vez, restablecimiento --- o benevolamente).

La corriente de inrush máxima ocurre si el transformador se energiza cuando la onda de voltaje esta cerca del valor cero. En este momento, la corriente y el flujo deben tener un valor máximo en el altamente inductivo circuito, y una media onda de voltaje requiere un cambio de flujo del doble del máximo flujo. Si existe flujo residual en el banco, dejado por una energización anterior, puede ser que se sume o se reste del flujo total, aumentando ó disminuyendo la corriente de magnetización. Los transformadores se operan normalmente cerca de la rodilla de la curva de saturación, así que el flujo adicional, requerido por una energización cuando cuando el voltaje es cero, más el flujo residual saturarán definitivamente el núcleo e incrementarán los componentes de la corriente de magnetización.

Una curva típica de corriente de magnetización es:

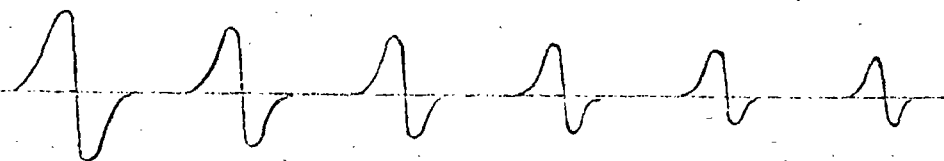


La corriente de magnetización decae rápidamente en los primeros ciclos, y luego lentamente, tardando hasta 4 ó 5 segundos para tomar un valor final, cuando la resistencia es baja. La constante de tiempo del circuito (L/R) no es constante porque L varía debido a la saturación del transformador. Durante los primeros ciclos, la saturación es alta, por lo tanto L es baja. Como las pérdidas amortiguan el circuito, la saturación disminuye y L aumenta. De acuerdo al reporte de 1949 del AIEE, las constantes de tiempo para las corrientes de inrush varían de 10 ciclos en unidades pequeñas a 1 minuto en unidades grandes.

La resistencia desde la fuente hasta el banco determina el amortiguamiento de la onda de corriente. Por lo que los bancos cercanos a los generadores tendrán una corriente de inrush más grande. En subestaciones alejadas de los generadores, el inrush no es tan severo, ya que la resistencia de la línea de interconexión amortigua rápidamente la corriente.

1.24

La forma de onda de la corriente de inrush que va hacia un bobinado conectado en delta es influenciada por dos condiciones adicionales a las que se tienen en el caso de los bobinados monofásicos. La primera es que más de un núcleo puede experimentar un inrush. Como los picos de la corriente de inrush en cada núcleo que experimenta un inrush estarán defasados por 60° ó por un múltiplo, la forma de onda senoidal de un inrush monofásico se distorsionará, ó la forma de onda será oscilatoria:



El segundo factor que afecta la forma de la onda cuando se trata de un bobinado delta, es que la corriente de línea es el resultado de sumar vectoralmente las dos corrientes del devanado del banco. Dependiendo de la naturaleza del inrush, suponiendo que sólo uno de los núcleos se ha saturado, se pueden experimentar las ondas oscilatorias o la distorsión de la forma monofásica. Si por suerte hay un tercer bobinado delta en este banco, el inrush puede ser influenciado por el acoplamiento entre los diferentes embobinados. Si el banco es trifásico, dependiendo de la construcción del núcleo, el acoplamiento entre fases está presente y puede afectar el inrush.

125

Formas de onda similares también se encuentran al energizar el bobinado estrella de un banco estrella-delta ó cuando se energiza un auto-transformador. En este caso la forma de onda monofásica se distorsiona debido al acoplamiento entre fases proporcionado por el embobinado delta (o terciario).

Una corriente máxima de inrush no ocurrirá cada vez que se energiza el banco ya que es poca la probabilidad de que se tenga voltaje cero. Si se energiza con voltaje máximo, no se producirá un inrush sin residual. En un banco trifásico, el inrush variará apreciablemente en las 3 fases.

El inrush más grande ocurre cuando un banco no energizado es conectado al sistema. Sin embargo, puede ocurrir un inrush, después de que una falla externa al banco es librada y el voltaje recobra el valor normal. En este caso, el transformador esta parcialmente energizado, así que el inrush al recobrase el voltaje es menor que el inrush cuando se energiza en forma completa.

Cuando un banco es conectado en paralelo con otro ya energizado, este último puede experimentar un inrush benévolo. La corriente de inrush en el banco que se conecta a la línea encontrará una trayectoria en paralelo por el transformador energizado y la componente de C.D. puede saturar su fierro, causando un inrush aparente. Nuevamente este inrush es menor que el inrush cuando se energiza en forma completa y su magnitud depende del valor relativo de la impedancia del transformador a la impedancia del resto del sistema que forma un circuito paralelo adicional.

En conexión serie generador-transformador, no hay problema por inrush inicial, ya que la unidad es energizada gradualmente hasta llegar al voltaje nominal. Aquí los inrush debidos a voltajes recobrados ó a energizaciones benévolas pueden ser problema, pero son menos severos que el inicial.

Como la corriente de inrush aparece como falla interna a los relevadores diferenciales, es necesario emplear algunos medios para desensibilizarlos durante el inrush. Entre ellos tenemos:

- 1.- Un relevador diferencial con reducida sensibilidad a la onda del inrush (Un ajuste más alto para la onda offset, más un retraso de tiempo para dejar pasar los altos picos iniciales).
- 2.- Una unidad operada con voltaje que suprime automáticamente el disparo junto con el relevador diferencial.
- 3.- Una unidad desensibilizante de armónicas junto con el relevador diferencial.
- 4.- Desensibilizando el relevador diferencial durante la energización del banco.

El relevador diferencial de transformador tipo CA es un buen ejemplo del método 1. Esta aplicación es la menos compleja, más económica, y hay cientos en servicio exitoso.

Este relevador para bancos de dos devanados es similar al relevador tipo CA para generador, excepto que tiene una característica de desbalance con 50% del porcentaje, una corriente de disparo mínima de 2.8 amperes, y los taps para una diferencia de 2/1 en las relaciones de los TC'S principales. Los taps son 5-5, 5-5.5, 5-6, 5-6.6, 5-7.3, 5-8, 5-9 y 5-10. Cuando las relaciones son tales que el relevador debería balancear en una falla externa con 5 y 10 amperes, el tap 5-10 se usa en la distribución de corrientes como se muestra en la figura No. 1. Para el caso de tap 7.3-5 la distribución se muestra en la figura No. 2. En todos los casos los amper-vueltas netos se

197

cancelan en la bobina de operación, por lo que no se produce par de --
operación.

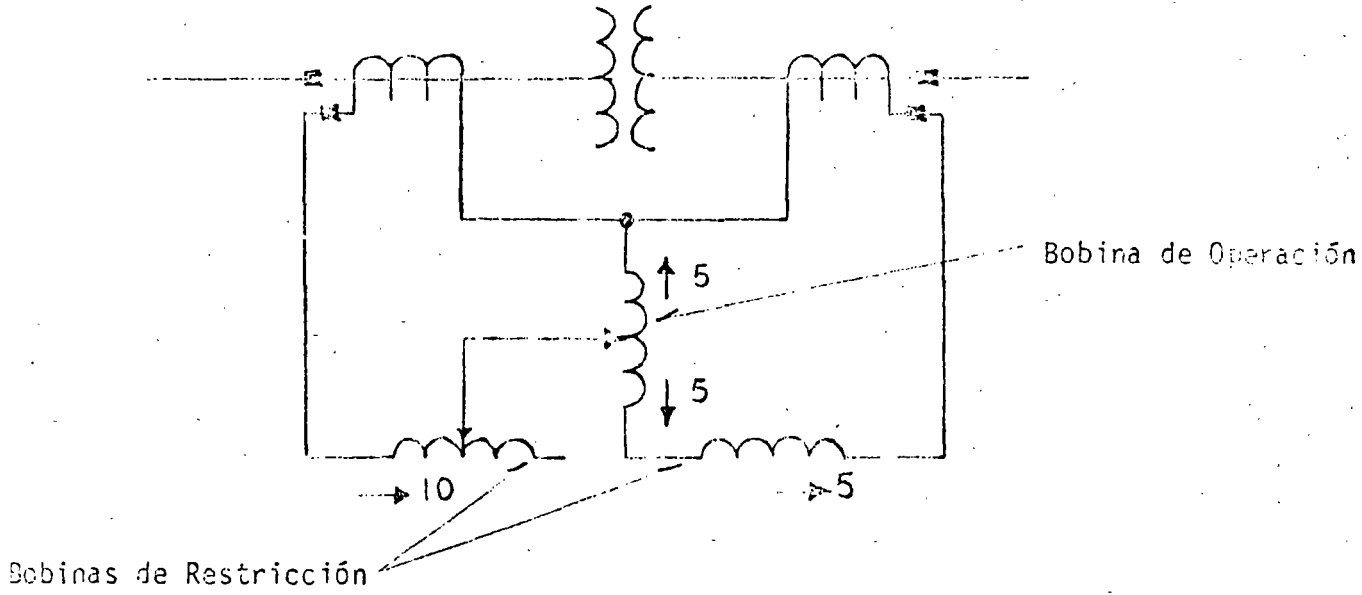


FIGURA No. 1.- Distribución de corrientes en el relevador tipo CA conectado en el tap 5-10.

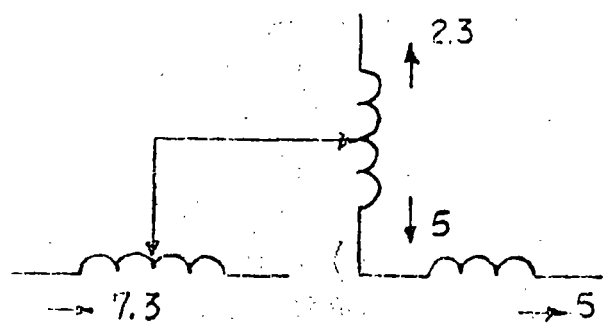


FIGURA No. 2.- Distribución de corrientes en el relevador tipo CA conectado en el tap 5.7.3.

1.5.1

Para los bancos de transformación de tres devanados, se aplica el relevador CA-4. Este relevador tiene 4 unidades de inducción operando en 2 discos. Tres de las unidades se usan para restricción en cada una de las tres bobinas del banco, y una se usa para la unidad de operación conectada en el circuito diferencial.

Se dispone de taps para las características de 15-25-40% con un ajuste de corriente mínima de 4.0, 2.5 ó 1.3 amperes, 60 ciclos, respectivamente dependiendo del tap de porcentaje. El tiempo de operación es de 2 a 6 ciclos.

El tipo CA-6 ha sido usado para proteger transformadores aunque fué diseñado para proteger buses. Reconociendo esto se diseñó el relevador CA-5 el cual tiene una restricción y el elemento de operación del CA-6. Estos relevadores tienen una característica de porcentaje variable, poco porcentaje para fallas pequeñas, donde el comportamiento de los TC'S es bueno y un porcentaje alto en fallas severas, donde la saturación de los TC'S puede ser un problema. Las bobinas de restricción están en el mismo elemento, así que ellos se suman para incrementar la restricción en todas las fallas externas y se restan cancelando la restricción en todas las fallas internas. Por lo tanto, el efecto de la carga en el pick-up es minimizado, y es posible obtener tiempos de operación más rápidos con valores mínimos de pick-up. El pick-up mínimo es ajustable entre 0.75 y 2 amperes, con un tiempo de operación de 2 a 6 ciclos.

Las características variables se obtienen mediante un transformador saturable en el circuito de operación que también tiende a desviar la componente de C.D. de la bobina de operación.

La corriente de magnetización de inrush esta formada por armónicas pares, particularmente la 2a. El relevador del tipo de inducción, tal

100

como el CA, es menos sensitivo a este tipo de onda. Esta característica junto con un tiempo de operación entre 5 y 6 ciclos, significa que el relevador tipo CA no operará con las corrientes de inrush, excepto en los casos extremos de grandes transformadores adyacentes a grandes fuentes generadoras. Este relevador tiene más del doble de insensibilidad si se conecta de tal manera que reciba la corriente de inrush en la bobina con taps.

La unidad operada con voltaje, método 2, se conoce como tipo TSI (Supresor de Disparo por Corriente de Magnetización de Inrush). Se aplica más frecuentemente con el relevador tipo CA-4 para bancos con tres devanados, pero puede ser usado con el CA. El voltaje trifásico se usa como el criterio para distinguir entre una falla o un inrush. Una falla se distingue por una reducción de voltaje en una ó más de las fases, mientras que el inrush ocurre a voltaje pleno. Este método no desensibiliza directamente el propio relevador y cualquier falla interna que reduce uno ó más de los voltajes hacer operar la unidad de voltaje que permite un disparo inmediato si los contactos del relevador diferencial están cerrados.

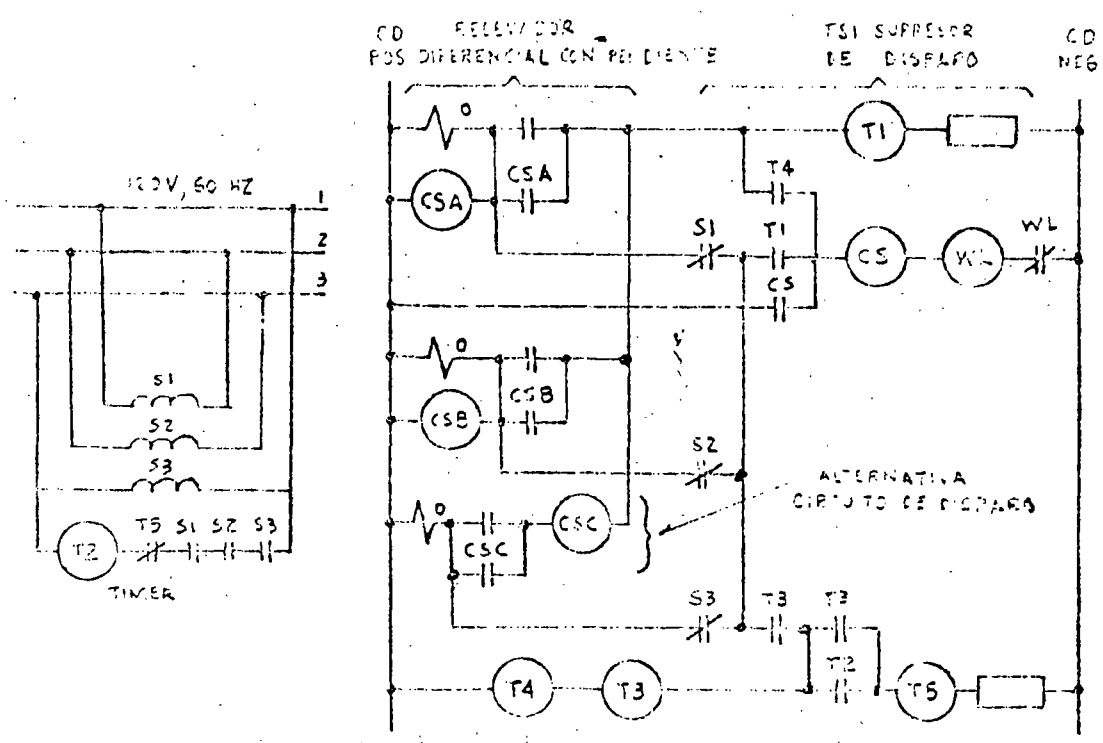
En un inrush todas las unidades de voltaje abren antes que las unidades diferenciales puedan operar y energizar T-1; si cualquiera de las unidades de voltaje (S-1, S-2, ó S-3) no abre indicando una falla, el disparo es inmediato a través de los contactos S-1, S-2 ó S-3 y T-1.

Un timer, T-2, ajustable hasta 5 segundos, restablece la trayectoria de disparo normal a través de los contactos del relevador diferencial, cerrando el contacto T-4. T-3 y T-5 son unidades auxiliares para sellar la unidad T-4 y desenergizar el timer respectivamente.

Las unidades de voltaje deben ser energizadas con, ó al mismo tiempo -- que, el banco. Esto requiere una fuente de potencial trifásico dentro

de la zona diferencial] ó el uso de contactos "a" en el interruptor que esta entre el transformador y los transformadores de potencial. Cuando se conecta el supresor en el lado delta del banco, se usan los voltajes entre líneas. Cuando se conectan en el lado de la estrella se prefiere tomar los 120 volts de línea a neutro, aunque los voltajes en tre fases se usan comunmente.

Los elementos de voltaje operan con un pick-up de 100 volts y sueltan entre 90 y 95 volts. Por lo tanto, el relevador de diferencial es de sensibilizado indirectamente sólo hasta el punto en que la falla interna haga caer el voltaje desde 120 ó 115 volts hasta 90 ó 95 volts.



13

El tercer método es aprovechar las armónicas que forman parte de la corriente para retención, desensibilizando así al relevador. Este método tiene su mérito pero no carece de problemas. Es necesario proporcionar suficiente restricción durante los inrushes y dar cierto grado de sensibilidad para fallas internas que también pueden contener una gran cantidad de armónicas debido a la naturaleza de la falla ó debido a la combinación de una falla ligera con un inrush.

Los relevadores diferenciales con porcentaje variable y con supervisión para restricción con segunda armónica, tipos HU y HU-1, para dos y tres devanados respectivamente, resuelven en forma adecuada los problemas mencionados. Las conexiones se muestran en la figura No. 3. La unidad diferencial consiste de Air-gap transformadores, que alimentan los circuitos de restricción y de un Non-air-gap transformador para energizar el circuito de la bobina de operación. Las señales de restricción son rectificadas y conectadas en paralelo, de tal forma, que la restricción es proporcionada por la corriente de restricción más grande de las que circulan por los circuitos de restricción.

La característica de porcentaje variable proporciona un valor bajo (del orden de 15%) en fallas ligeras donde el comportamiento de los TC'S es bueno y un porcentaje alto (del orden de 50-60%) en fallas severas donde la saturación de los TC'S puede ser un problema. Esto se obtiene en el transformador saturable en el circuito de la bobina de operación. Se tienen taps para balancear las diferencias en relación de transformación. Estos son 2.9, 3.2, 3.5, 3.8, 4.2, 4.6, 5.0, 8.7 con una corriente mínima de pick-up de 30% del valor del tap. Esta es justamente la corriente necesaria para cerrar los contactos de la unidad diferencial (DU) con la bobina de operación y una de las de restricción energizadas. Las bobinas de restricción pueden soportar continuamente 10 amperes en cualquier tap.

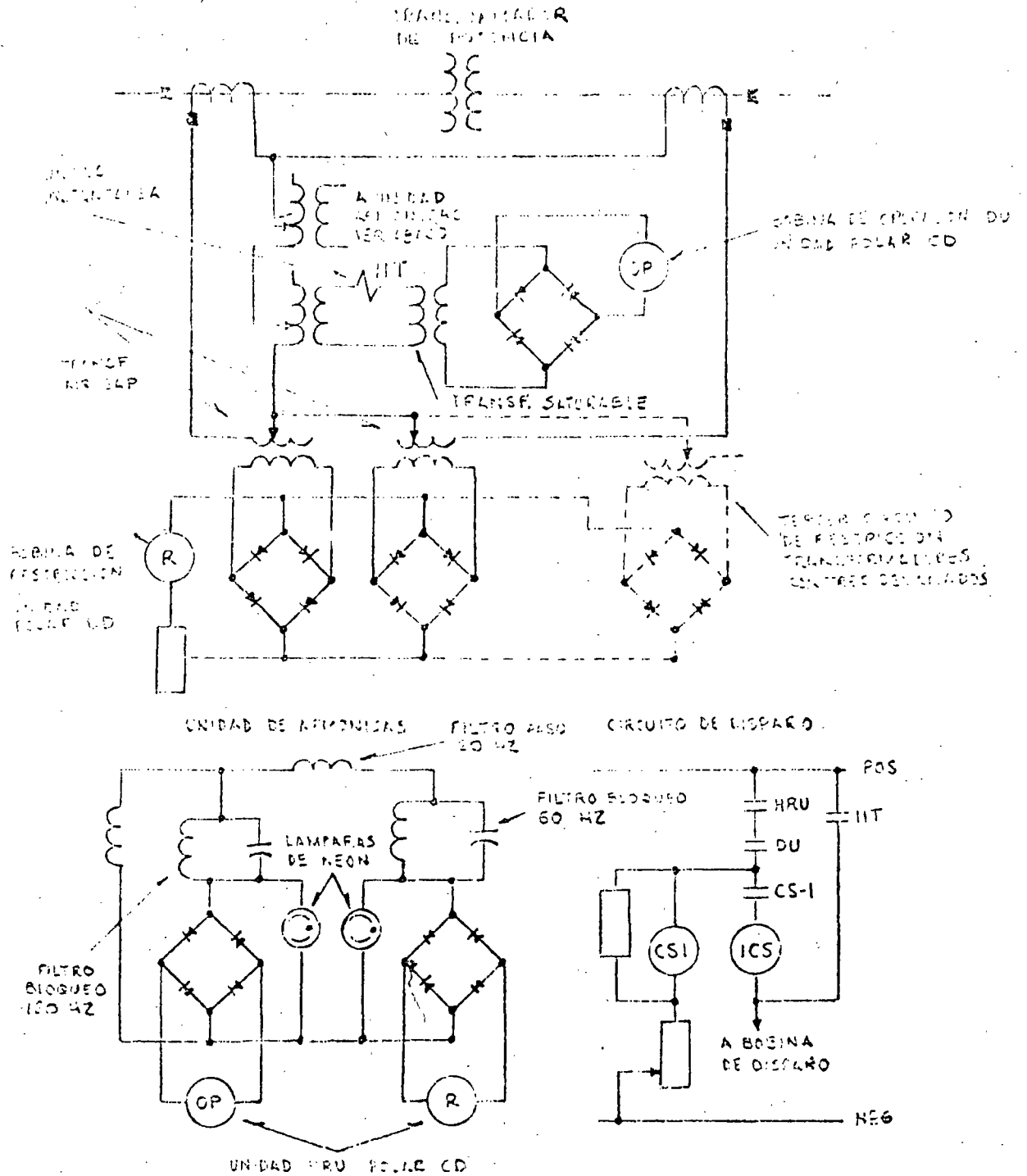
138

La unidad de armónica contiene un filtro de bloqueo de 120 ciclos (2a. armónica) en el circuito de la bobina de operación y un filtro de paso de 120 ciclos y bloqueo de 60 ciclos en el circuito de la bobina de restricción. Cuando ocurre un inrush con su segunda armónica como predominante característica, amplia restricción con energía de operación mínima, existe en la unidad. Se diseña el circuito para mantener abiertos sus contactos cuando la magnitud de la componente de segunda armónica es aproximadamente 15% de la fundamental. Los estudios indican que esta restricción es adecuada para manejar los inrushes que pueden encontrarse en la práctica. El contenido mínimo de la segunda armónica encontrado en el análisis de un gran número de corrientes reales de inrush fué del 23% de la fundamental.

Para fallas internas existe bastante energía de operación a partir de la onda fundamental de 60 ciclos y de todas las armónicas, excepto la segunda, la cual tiene poco predominio durante una falla. Además, la fundamental produce energía de restricción en mínima cantidad. Por lo tanto, en ausencia de segunda armónica, esta unidad (HRU) operará el mismo pick-up que la unidad diferencial, permitiendo que ésta (DU) opere sensiblemente en fallas internas como se muestra en la circuito de disparo de la figura No. 3. En fallas externas la unidad diferencial (DU) tendrá restricción. En condiciones de inrush, la unidad armónica (HRU) tendrá retención y la unidad diferencial (DU) puede ó no operar, dependiendo de la severidad de la falla. El tiempo de operación del relevador es de 1.5 a 2.5 ciclos.

En el circuito de operación se tiene una unidad instantánea (IIT) para proporcionar una operación de un ciclo para fallas internas realmente severas. Su pick-up es de 10 veces el valor del tap. Esto proporciona un ajuste adecuado para dejar pasar los picos del inrush y las máximas corrientes diferenciales falsas en fallas externas.

133



151

El método 4 es, desensibilizar el relevador diferencial (como los tipos CA, CA-4, CA-5) durante el tiempo que el transformador es energizado. - Esto se hace conmutando una resistencia en paralelo con la bobina de operación, para elevar temporalmente el pick-up del relevador a un valor del doble ó del triple. Las resistencias pueden ser conectadas manualmente cuando se cierra el interruptor del banco, ó automáticamente mediante relevadores de sobrevoltaje, que sueltan con retraso de tiempo. - Este último método soluciona los inrushes de recuperación en los pocos casos en que estos sean un problema.

RECOMENDACIONES GENERALES

Qué relevador o qué método aplicar es siempre una buena pregunta, y como previamente anotamos, en el campo de la protección no hay respuestas categóricas. Todos los métodos anteriores se están usando en forma exitosa. Sin embargo como una regla general los relevadores diferenciales con disco de inducción (CA, CA-5, CA-6) deben aplicarse en subestaciones alejadas de fuentes de generación grandes, donde el inrush sea despreciable. Los relevadores de armónicas (HU, HU-1) que son más complejos y más caros deben usarse en plantas generadoras y en grandes transformadores instalados cerca de fuentes generadoras. En estos casos existe una gran probabilidad de tener un inrush severo.

Hay un mérito considerable en la aplicación de un simple relevador diferencial ajustado para ser insensible al inrush, con el advenimiento de un relevador confiable que detecta presión de gases. Este es el SPR, relevador de presión súbita que opera en una relación de incremento de gas en el transformador. Puede aplicarse en todos los transformadores que tengan una cámara de aire sellada arriba del nivel de aceite. El dispositivo es unido al tanque ó a la cubierta del Hoyo-Hombre, arriba del nivel de aceite. Opera con el incremento en la relación de presión y no es afectado por la presión estática ó por los cambios de presión que resultan de una operación normal del transformador.

El relevador SPR se recomienda para todas las unidades de 5 MVA ó mayores y ha sido ampliamente probado contra ondas de falla externa e impactos externos. Es muy sensible a fallas pequeñas ya que él opera con un incremento tan bajo como 0.33 Lb/Pulg^2 de aumento en la pre

130

sión de gas. En un caso esto representa una falla de 50 amperes. De este modo es más sensible a una falla pequeña ligera similar a una falla entre espiras que el mismo relevador diferencial. Sin embargo el relevador diferencial es aún requerido para fallas en los bushings y en otras áreas fuera del tanque. El tiempo de operación varió de 1/2 ciclo a 37 ciclos en una instalación de prueba dependiendo de la magnitud de la falla. La unidad puede ser probada removiendo un pequeño plug mientras que el espacio de gas del transformador esta a una presión de 1/2 Lb/Pulg² ó mayor.

CONECTANDO RELEVADORES DIFERENCIALES

En bancos estrella-delta, los TC'S en el lado de la estrella se conectan en delta y los TC'S en el lado de la delta se conectan en estrella. Esto se hace para corregir el ángulo de fase y para eliminar la secuencia cero del circuito del relevador diferencial cuando la estrella está puesta a tierra. Si la estrella no esta puesta a tierra, entonces se pueden usar conexiones opuestas, pero no son --convencionales.

A.- BANCOS CON DOS DEVANADOS

Las conexiones en los relevadores diferenciales son muy impor--tantes. Deben ser hechas correctamente. Se pueden hacer y revisar en dos pasos: 1) Faseando, y 2) Revisando la relación. En seguida tenemos una hoja de trabajo para conectar un releva--dor diferencial en un banco de dos devanados:

1.- Revisando el Faseo: Empezando en el lado de la estrella del transformador de potencia, supongase que Ia, Ib e Ic estan circulando a través del banco hacia una carga ó hacia una fa--lla externa. Dibuje las corrientes en las bobinas del lado --del transformador conectado en delta, y luego dibuje las co---rrientes a través de los TC'S conectados en estrella y determi--ne las corrientes que circulan hacia el relevador. Esto nos dice que corrientes deben circular en las bobinas de restric--ción del lado conectado en estrella y nos permite conectar en la delta apropiada los TC'S del lado estrella del transformador asegurando así el correcto faseo para todas las condicio--nes.

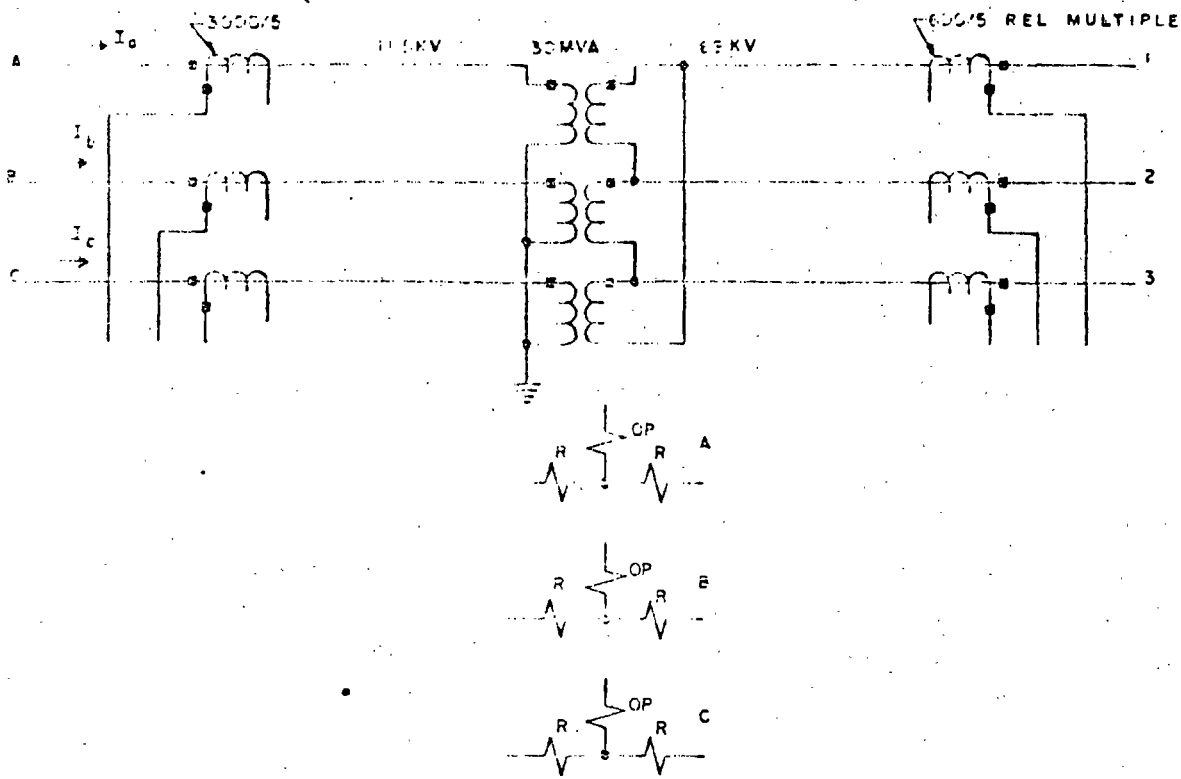


Fig. 6-7 Hoja de trabajo para conectar relevadores diferenciales en un banco de dos devanados.

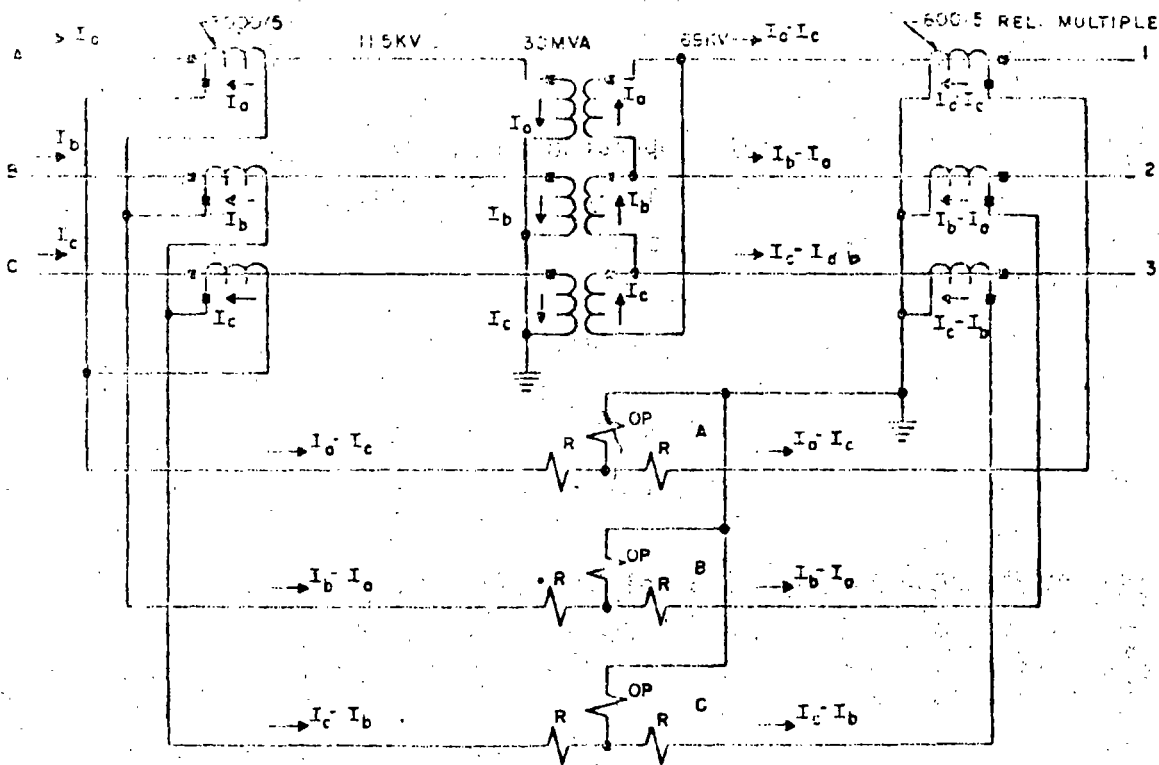


Fig. 6-8 Revisión completa de fases para el Ejemplo de la Fig. 6-7.

2.- Revisando la Relación de Transformación: Suponga una corriente trifásica del orden de la corriente de carga máxima. Esto supone haber elegido las relaciones de los TC'S de tal manera que la capacidad de las bobinas de restricción para llevar una corriente en forma continua no será excedida. La relación total mínima del primario al secundario del TC, proporcionará la máxima sensibilidad. Por conveniencia esta corriente puede ser la misma que la corriente primaria de un grupo de TC'S. Revise las relaciones a través del banco y de los TC'S, seleccionando el TC o Taps adecuados para un balance. Se prefiere que las corrientes se balancen en cada lado, pero frecuentemente existirá una pequeña diferencia. Esto es satisfactorio, ya que el CA -- puede tolerar hasta el 50%, CA-4 hasta 15, 25 ó 40%, etc. Esto es reservado para diferencias en el comportamiento del TC. Donde el transformador tiene cambiador de taps bajo carga las diferenciales se ajustan en la mitad del rango, y se recomienda usar el tap de 40% en este caso. Con taps de más ó menos 10%, el margen de 40% se reduce alrededor del 30% para los taps extremos.

REVISION PARA EL EJEMPLO DE LA FIGURA 6-7

Suponga que la corriente de carga máxima es para 30 MVA, la capacidad del banco:

En el lado de 11.5 KV:

$$I \text{ pri.} = \frac{30,000}{\sqrt{3} \times 11.5} = 1,505 \text{ Amperes}$$

$$I \text{ sec.} = \frac{1505}{600} = 2.51 \text{ Amperes}$$

$$I \text{ fuera de la delta} = 2.51 \cdot \sqrt{3} = 4.35 \text{ Amperes}$$

140

En el lado de 69 KV

$$I_{pri.} = \frac{30,000}{\sqrt{3} \times 69} = 251 \text{ Amperes}$$

La relación apropiada para el transformador de corriente de relación múltiple (600/5 máximo) sería:

$$251/4.35 = 57.7 \quad \text{Así use el tap: } 300/5 = 60$$

Usando este tap, la corriente de restricción del lado de 11.5 KV es de 4.35 y del lado de 69 KV es de $251/60 = 4.19$ amperes. Así la corriente diferencial de 0.16 circula por la bobina de operación. El desbalance es de $0.16/4.19 = 3.82\%$ que es bastante satisfactorio para un relevador con 50% de pendiente, dejando inclusive un margen de casi 46% para considerar un comportamiento desigual de los TC'S, etc.

141

B.- BANCOS DE TRES DEVANADOS

El mismo procedimiento de revisión del faseo y relación de transformación se usan transformadores de tres devanados. Para la revisión de faseo, suponga que uno de los lados del transformador es el primario y que los otros dos devanados son secundarios y determine la dirección y fase correctas de las corrientes de restricción. Para revisar la relación es importante ir revisando de 2 en 2 devanados (como si el banco fuera una unidad de dos devanados) considerando corriente cero en el terciario. Así todas las relaciones estarán correctas para cualquier distribución de corriente, ya sea de carga ó de falla.

En la figura 6-9 se tiene una hoja de trabajo para conectar un relevador diferencial a un transformador típico de tres devanados.

En la figura 6-10 se muestra la solución del problema de la figura 6-9.

REVISION DE LAS RELACIONES DE TRANSFERENCIA DEL BANCO DE TRES DEVANADOS DE LA FIGURA 6-9.

Donde las relaciones no son correctas para el relevador CA-4 se requieren autotransformadores de balanceo auxiliares ó bien TC'S auxiliares. En el caso general se requieren dos juegos para un banco de tres devanados. De nuevo la mínima relación total de la corriente primaria a la corriente del relé nos proporciona la máxima sensibilidad para fallas.

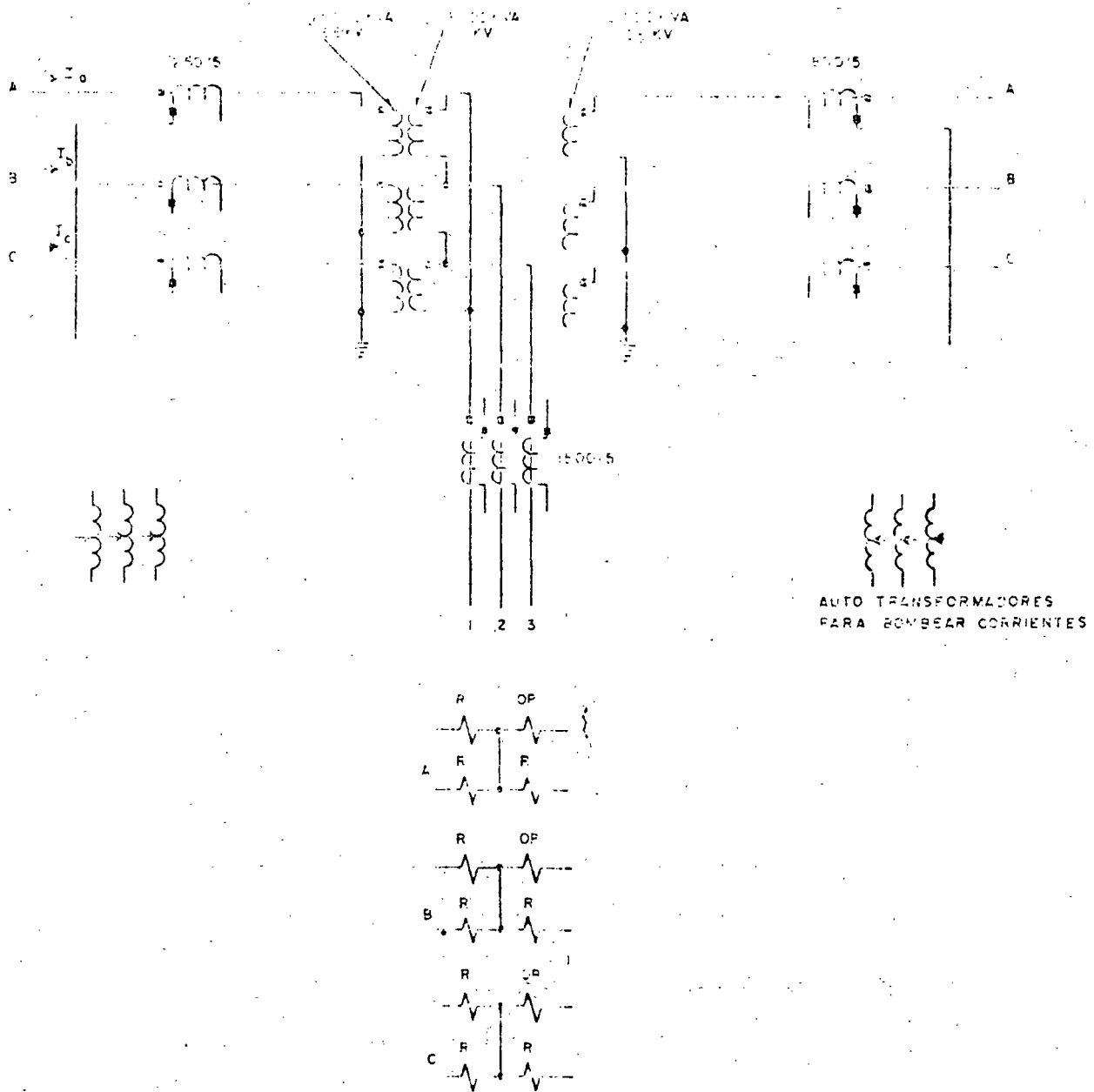


Fig. 6-9 Hoja de Trabajo para Conectar Relevadores Diferenciales en bancos de tres devanados.

140

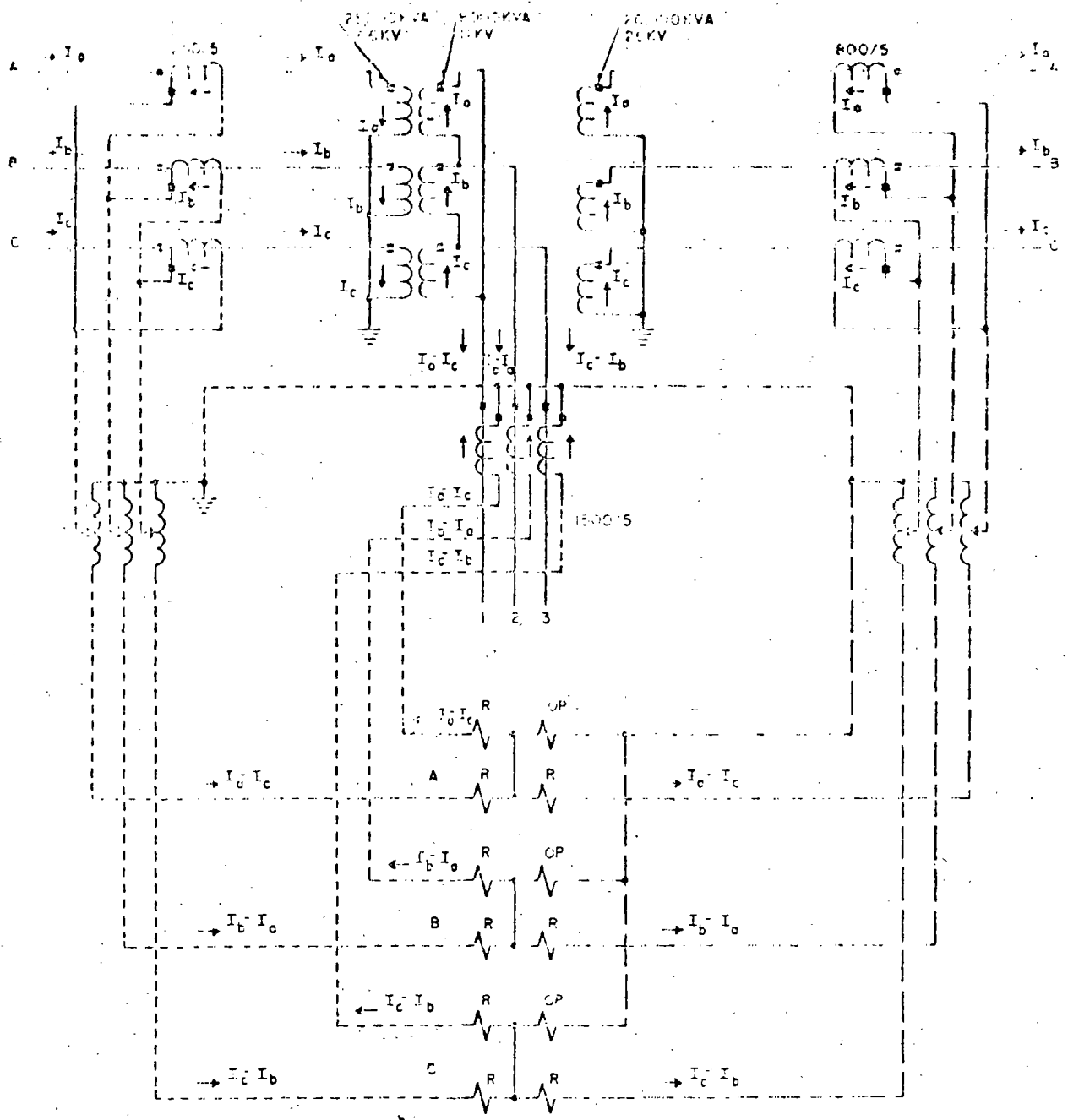


Fig. 6-10 Revisión completa para el faseo del ejemplo de la Fig. 6-9. Las líneas punteadas cortas muestran el faseo entre los devanados de 66 y 11 KV. Las líneas punteadas largas muestran el faseo entre los devanados de 66 y 26 KV suponiendo que el circuito de 11 KV no existe. Con este método el faseo es correcto para cualquier distribución de corriente entre los 3 devanados.

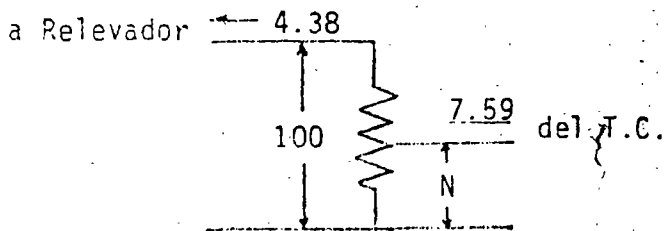
144

Suponga que 25 MVA circulan a través del banco: las corrientes para esta carga en cada devanado serán:

<u>KV</u>	<u>RTC</u>	<u>AMPERES PRIMARIOS</u>	<u>AMPERES SECUNDARIOS</u>	<u>AMPERES RELEVADOR</u>
66 KV	250/5	$\frac{25,000}{\sqrt{3} \times 66} = 219$	$\frac{219}{50} = 4.38$	$4.38 \times \sqrt{3} = 7.59$
11 KV	1500/5	$\frac{25,000}{\sqrt{3} \times 11} = 1310$	$\frac{1310}{300} = 4.38$	4.38
26 KV	800/5	$\frac{25,000}{\sqrt{3} \times 26} = 555$	$\frac{555}{160} = 3.47$	$3.47 \times \sqrt{3} = 6.01$

A. Si se usan autotransformadores para balancear la corriente, deben conectarse para disminuir la corriente hacia el relevador. Supongamos que los autotransformadores tienen 100 vueltas. Otra vez los ajustes deben ser hechos en la base de corrientes iguales a través de los dos devanados en estudio, con corrientes cero en el tercero.

GRUPO 66 KV

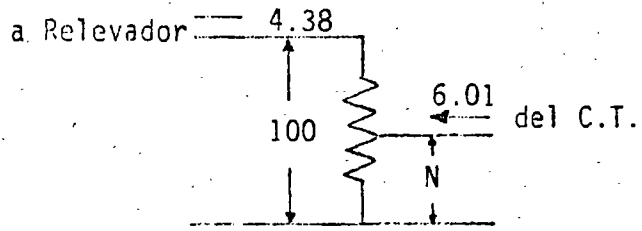


$$4.38 \times 100 = 7.59 N$$

$$N = \frac{4.38}{7.59} = 57.8 \text{ Vueltas}$$

Use N = 58 Vueltas

GRUPO 26 KV



$$4.38 \times 100 = 6.01 N$$

$$N = \frac{4.38}{6.01} = 72.9 \text{ Vueltas}$$

Use N = 73 Vueltas

Con los autotransformadores de balanceo ajustados como se muestra, de mostramos que el balance es correcto para cualquier distribución de corriente, supongamos que del devanado de 26 KV salen 20 MVA y que del enbobinado de 11 KV salen 5 MVA. En estas condiciones:

Lado 66 KV 25 MVA Entrada

$$\begin{aligned}
 I \text{ pri.} &= 219 \text{ Amperes} \\
 I \text{ sec.} &= 4.38 \text{ Amperes} \\
 I \text{ Fuera de la delta} &= 7.59 \text{ Amperes} \\
 I \text{ Relevador} &= \frac{7.59 \times 58}{100} = 4.4 \text{ Amperes}
 \end{aligned}$$

Lado 26 KV 20 MVA Fuera

$$\begin{aligned}
 I \text{ pri.} &= \frac{20,000}{\sqrt{3} \times 26} = 445 \text{ Amperes} \\
 I \text{ sec.} &= \frac{445}{160} = 2.78 \text{ Amperes} \\
 I \text{ Fuera de la delta} &= 2.78 \sqrt{3} = 4.82 \text{ Amperes} \\
 I \text{ Relevador} &= \frac{4.82 \times 73}{100} = 3.51 \text{ Amperes}
 \end{aligned}$$

Lado 11 KV 5 MVA Fuera

$$\begin{aligned}
 I \text{ pri.} &= \frac{5,000}{\sqrt{3} \times 11} = .262 \text{ Amperes} \\
 I \text{ sec.} &= \frac{262}{300} = .875 \text{ Amperes} \\
 I \text{ Relevador} &= .875 \text{ Amperes}
 \end{aligned}$$

140

Entonces el balance es correcto, ya que 4.4 amperes es un valor muy cercano a la suma de 3.51 + 0.875 = 4.385.

B. Si se usa el relevador HU-1 elija el tap de balanceo más cercano a la corriente más alta del relevador y obtenga las relaciones siguientes:

KV	<u>CORRIENTE DISPONIBLE</u>	<u>TAP ELEGIDO EN EL RELE</u>	<u>RELACION DE LA CORRIENTE AL TAP</u>
	<u>EN EL RELEVADOR</u>	<u>HU-1</u>	
66	7.59	5	$\frac{7.59}{5} = 1.52$
26	6.01	3.8	$\frac{6.01}{3.8} = 1.58$
11	4.38	2.9	$\frac{4.38}{2.9} = 1.51$

Las relaciones indican que los taps seleccionados quedan dentro del 5% del ideal, lo que es bastante satisfactorio. Para obtener la sensibilidad máxima, el valor más pequeño posible del tap debe ser usado.

No se requieren otros ajustes en el relevador HU-1.

PROTECCION DIFERENCIAL CON RELEVADORES DE SOBRECORRIENTE

Como previamente dijimos no se recomienda una proteccion diferencial sin algun tipo de restriccion. Sin embargo se usan relevadores de sobrecorriente conectados diferencialmente y su aplicacion involucra compromisos. Un gran sistema del Oeste aplica relevadores de sobrecorrientes muy inversos, tipo CO-9, con rangos de 2-6 amperes, y de 10 a 40 instantaneos, para proteger transformadores universalmente sin restricciones. La unidad CO se ajusta usualmente en 40% de la corriente nominal y un dial de 0.5. La unidad instantanea se ajusta entre 200 y 300% de la corriente nominal. Al instalarse se hacen pruebas de inrush para asegurar la no operacion de ambas unidades, energizando el banco entre 8 y 10 veces. La experiencia en este sistema particular ha indicado que la unidad CO raramente requiere mas del 40% de ajuste, aunque el dial algunas veces anda en un valor cercano al 1. El ajuste de la unidad instantanea es mas critico con un ajuste promedio de 250% de la corriente nominal. La experiencia ha indicado tambien que si el relevador no opera con el inrush tampoco operara con fallas externas.

Los compromisos con esta proteccion son: Mas pruebas de campo para determinar los ajustes y tiempo de disparo algo mas largo. Mientras que el costo del relevador de sobrecorriente puede ser del 50% o menos que el del diferencial con frecuencia se requeriran transformadores de balanceo auxiliares. El costo de esto aumentado al costo de la instalacion probable eliminara cualquier ventaja en costos.

148

PROTECCION DE TRANSFORMADORES REGULADORES

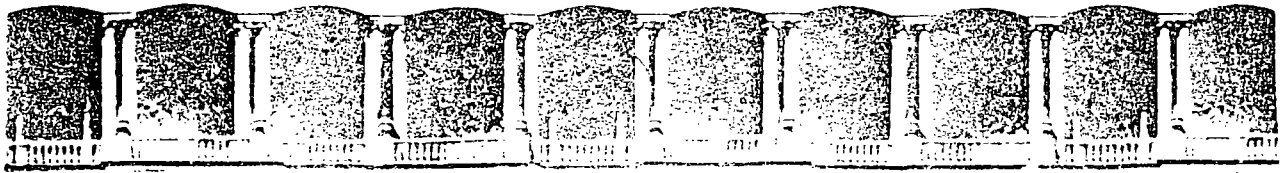
El transformador regulador con un devanado para excitación en paralelo para controlar voltaje y/o ángulo de fase, presenta un problema especial en la protección del devanado paralelo. Sus KVA nominales son sólo el 10% de los del devanado serie; por lo tanto su impedancia es alta. La alta capacidad del devanado serie dicta una RTC alta para los relevadores diferenciales, por lo que la sensibilidad del relevador para fallos en el devanado serie, es muy limitado. En otras palabras el relevador CA de la figura 6.11 no puede detectar fallas medianas o pequeñas en el devanado serie ó en el equipo del cambiador de taps, donde es más usual que las fallas comiencen. Debido a esto se desarrolló el relevador diferencial con característica de porcentaje tipo CAM para suplementar los relés diferenciales convencionales. El relevador tiene una bobina de operación y una de restricción, y una característica de 15%. El pick-up mínimo es de 1.0 amperes cuando no hay restricción. Cuando la corriente en la bobina de operación excede a la corriente por cerca de 15% y los contactos cierran. Al aplicar el relevador los RTC'S se eligen de tal manera que ambas bobinas reciben la misma corriente secundaria con carga balanceada y alrededor de 5 amperes para una corriente máxima a través del transformador.

Cuando el devanado paralelo se conecta en estrella y se conecta a tierra los TC'S del relevador CA debén de conectarse en delta para evitar la operación con fallas a tierra externas. Un relevador de sobrecorriente debe ser aplicado en este devanado de excitación aterrizado y ajustado selectivamente para que no opera con fallas externas, antes que los relevadores de tierra apropiados hayan tenido la oportunidad de librar la falla externa. Si el secundario del devanado de

149

excitación se conecta en estrella a tierra, debe aplicarse un relevador de sobrecorriente en este neutro. Y si este devanado se conecta en delta una pierna de la delta puede ser puesta a tierra y un relevador de sobrecorriente se conecta en este circuito, como se ilustra en la siguiente figura.

El relevador de presión súbita es particularmente recomendable para estas unidades, ya que la probabilidad de una falla con arco en el equipo del cambiador de taps es alta.



**FACULTAD DE INGENIERIA U.N.A.M.
DIVISION DE EDUCACION CONTINUA**

**V CURSO INTERNACIONAL DE SISTEMAS
ELECTRICOS DE POTENCIA**

MODULO II: SISTEMAS ELECTRICOS DE POTENCIA II

TEMA : PROTECCION DE BUSES

**EXPOSITOR: ING. AUGUSTO O. HINTZE V.
1996**

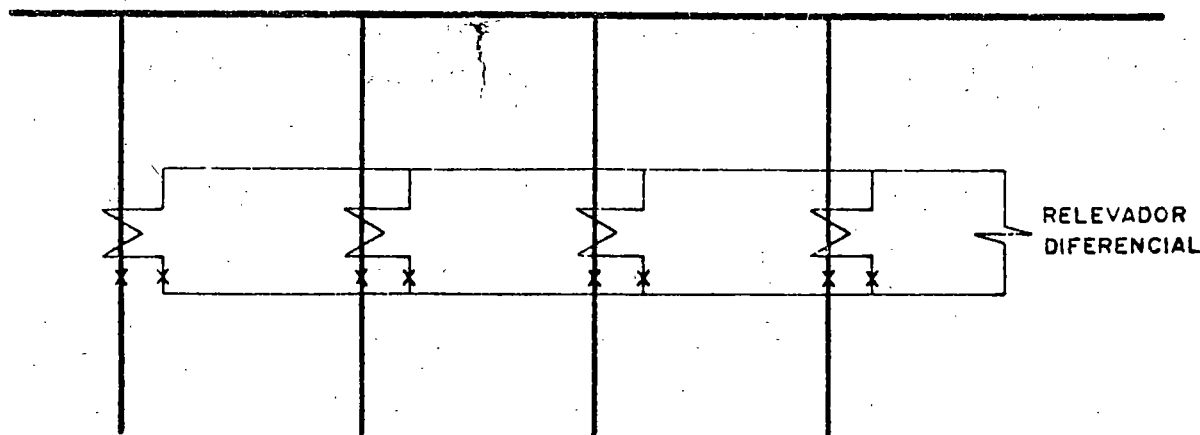
181

PROTECCION DE BARRAS

La forma más antigua de protección a las barras la constituye el sobrealcance de las protecciones de los elementos que confluyen a una misma barra. Esto por supuesto es protección remota y como tal, requerirá de tiempo para suplir la falta de información respecto a la localización de la falla. Este factor, tiempo, aunado al hecho de que se hace necesario desconectar una cantidad muy grande de equipo para lograr aislar la falla, puede convertir en inaplicable este método para la protección de barras.

Cuando este es el caso, será necesario utilizar protección y detección local. El principal problema para llevar a cabo la detección local con seguridad y confiabilidad lo constituyen los transformadores de corriente, ya que la barra en si no presenta características peculiares como es el caso en los transformadores de potencia.

Cuando las corrientes de falla interna y externa no crean problemas graves de imprecisión por saturación en los transformadores de corriente, la protección se puede lograr por medio de detección de corriente diferencial tal como se muestra a continuación.



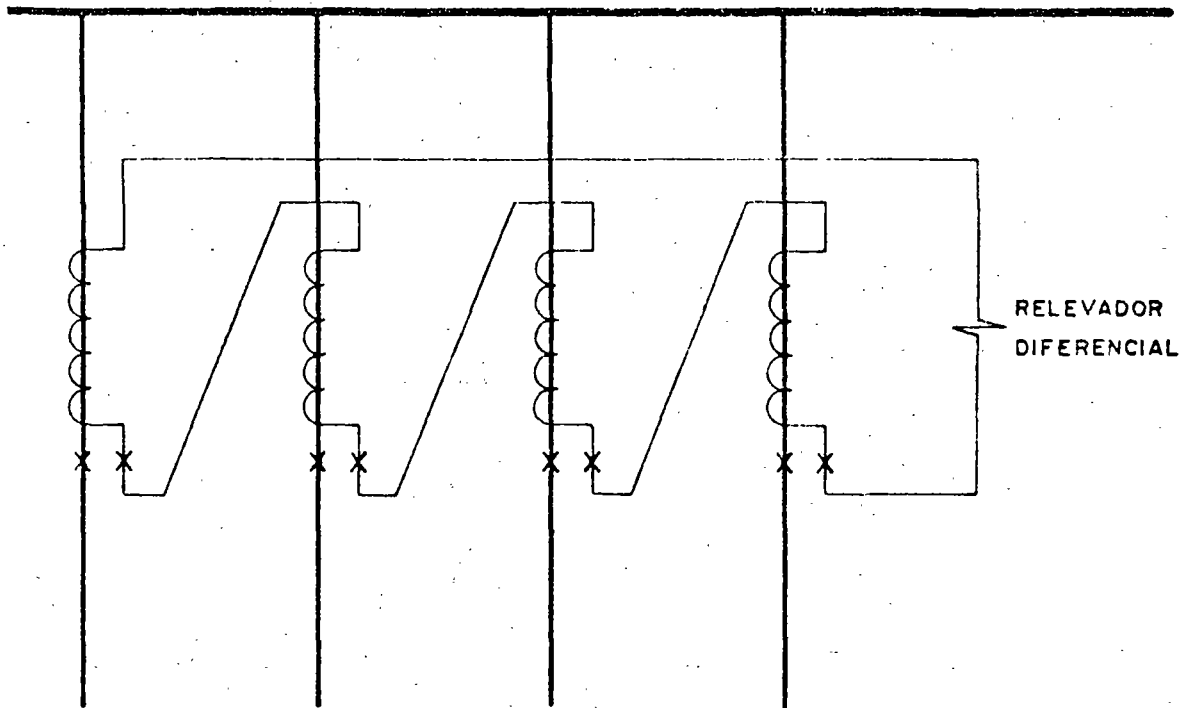
De acuerdo con la ley de kirchoff de corrientes, si el bus está sano, la suma de corrientes que llegan a él deberá ser cero. Si las imágenes secundarias de las corrientes no difieren mucho de sus valores ideales, la suma de ellas será muy cercana a cero con lo que el relevador diferencial no operará.

Si las corrientes de falla son tan altas que provoquen saturación desigualmente entre los TC's, este método no será aplicable pues la suma de corrientes secundarias no será cero para fallas externas, lo que provocaría la operación en falso del relevador diferencial. La solución que se viene a la mente es el mejorar los TC's para evitar este problema; sin embargo cuando las corrientes de falla son verdaderamente altas y/o tienen una componente de corriente directa que dure demasiado, esta solución resulta prohibitivamente costosa.

una solución similar a la de mejorar los TC's la constituye su sustitución por "acopladores lineales" que son dispositivos similares pero sin núcleo de hierro y con un número muy grande de vueltas en el secundario, de tal manera que para todo fin práctico, en el secundario se obtiene un voltaje proporcional a la corriente primaria; usualmente esta proposición es de 5 volts secundarios para cada 1000 amperes primarios y se mantiene aún para corrientes muy elevadas, ya que no hay hierro que se sature.

Debido a que la señal secundaria es ahora un voltaje, la suma de ellos se efectuará conectando en serie todos los secundarios de los acopladores lineales tal como se muestra.

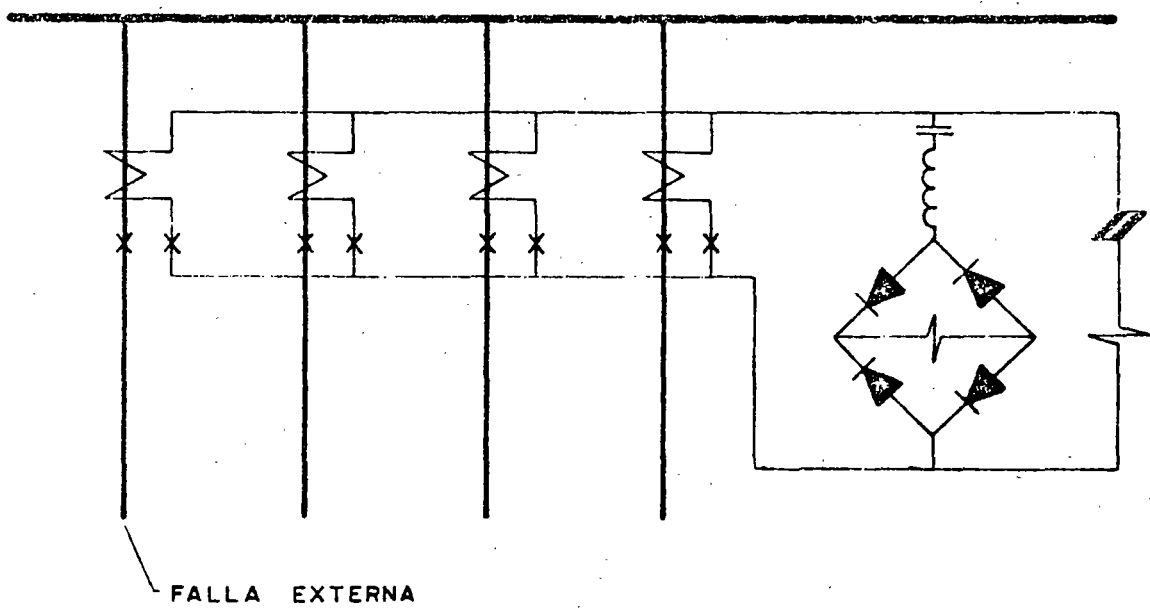
158



La aplicación de este método es muy simple y solo requiere que el relevador diferencial se ajuste por arriba del error más grande que se presentará debido a las tolerancias de fabricación de los AL's durante la falla externa más severa. El inconveniente más grave lo presenta el punto de vista práctico de que es necesario contar con acopladores lineales en todos los elementos conectados a la barra protegida y esto no siempre es posible de lograr, especialmente cuando una estación sufre ampliaciones o adiciones o cambios en el tipo de interruptores en algunos de los elementos conectados a la barra.

150

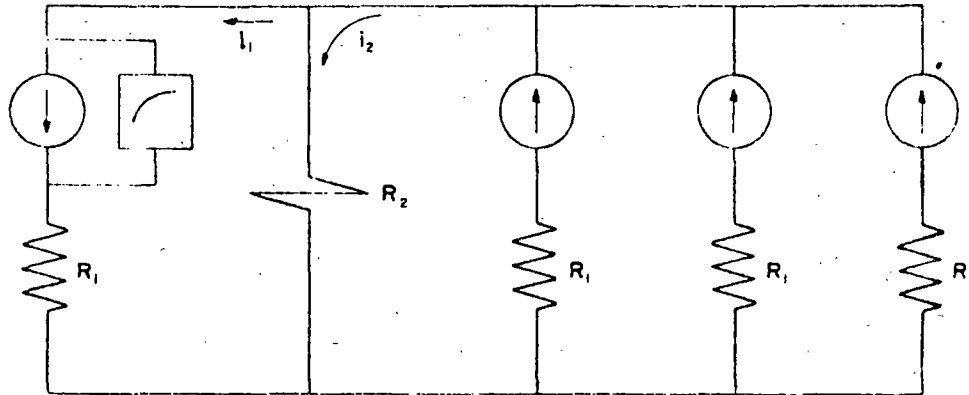
Una solución más realista al problema de la saturación de los TC's consiste en basar en ella el funcionamiento de la protección diferencial. Para ello, el relevador diferencial es de alta impedancia y responde a voltaje. Para lograr que la impedancia aparezca como resistencia, en ocasiones la bobina se alimenta por medio de un puente de onda completa. Sus conexiones se muestran enseguida.



Debido a la saturación del TC del elemento fallado, este solo producirá su voltaje de saturación pero presentará una impedancia muy baja, prácticamente solo la resistencia de su secundario y la del cableado. Además presentará voltaje en oposición al de los demás TC's por lo que la mayor parte de la corriente producida por ellos circulará por el TC saturado y no por la bobina del relevador, ya que esta tiene una resistencia muy alta (del orden de 3000Ω) comparada con la saturación del TC. Esto se aprecia más claramente en el diagrama del circuito equivalente que se

157

muestra:



Como $R_2 > R_1$ entonces $i_1 > i_2$ y, para lograr evitar la operación en falso bastará con ajustar el relevador por arriba del voltaje producido por i_1 en la resistencia R_1 , ya que ésto, en el caso más pesimista supone un TC tan saturado que solo presenta la resistencia de devanado y de cableado.

Existen varios otros métodos, pero de ellos el que amerita mención es el que logra la operación correcta basándose en velocidad, lo cual a su vez se apoya en el hecho de que la saturación no ocurre instantáneamente sino que es un proceso que toma varios milisegundos en alcanzar niveles problemáticos. El relevador diferencial a que se alude también es de alta impedancia, sin embargo su operación en caso de ser necesaria ocurre durante los primeros 2 a 3 milisegundos después de iniciada la corriente de falla, ya que es durante este tiempo cuando aún la corriente secundaria es un reflejo fiel de la primaria, aún cuando posteriormente el TC se vaya a saturar.

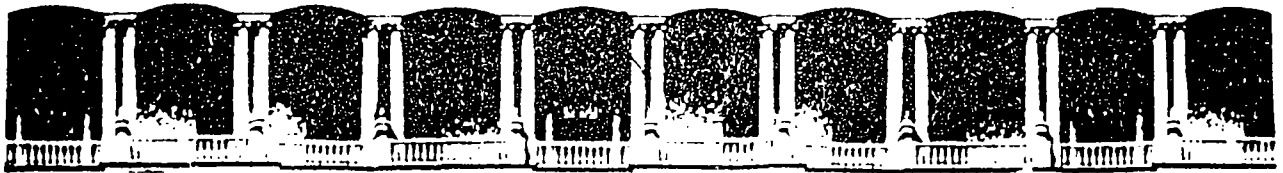
9.- PROTECCION DE BUSES

8.- PROTECCION DE TRANSFORMADORES

6.- PROTECCION DE GENERADORES

5.- PROTECCION DE LINEAS

4.- PROTECCION DE MOTORES



**FACULTAD DE INGENIERIA U.N.A.M.
DIVISION DE EDUCACION CONTINUA**

SISTEMAS ELECTRICOS DE POTENCIA

MODULO II

SISTEMA ELECTRICOS DE POTENCIA II

TEMA: SOBRETENSIONES Y COORDINACION DE ASISLAMIENOS

1996

Universidad Nacional Autónoma de México
División de Educación Continua

Curso: Sistemas de Potencia II
Tema: Sobretensiones y Coordinación de Aislamiento
Profesor: Víctor Federico Hermosillo Worley
M.S.E., Teck Lic. Elek

TEMARIO

1a Sesión:

1. Introducción
Fallas de L.T. en la Red Troncal del Sistema Mexicano
Clasificación de sobretensiones
2. Ondas viajeras en líneas de transmisión
Distorsión y atenuación de ondas viajeras
3. Modelos de líneas de transmisión
Componentes modales
4. Sobretensiones por descargas atmosféricas
Física y parámetros de descargas atmosféricas
Blindaje de líneas de transmisión
Modelo de una descarga directa
Descarga directa al hilo de guarda
Sobretensiones inducidas

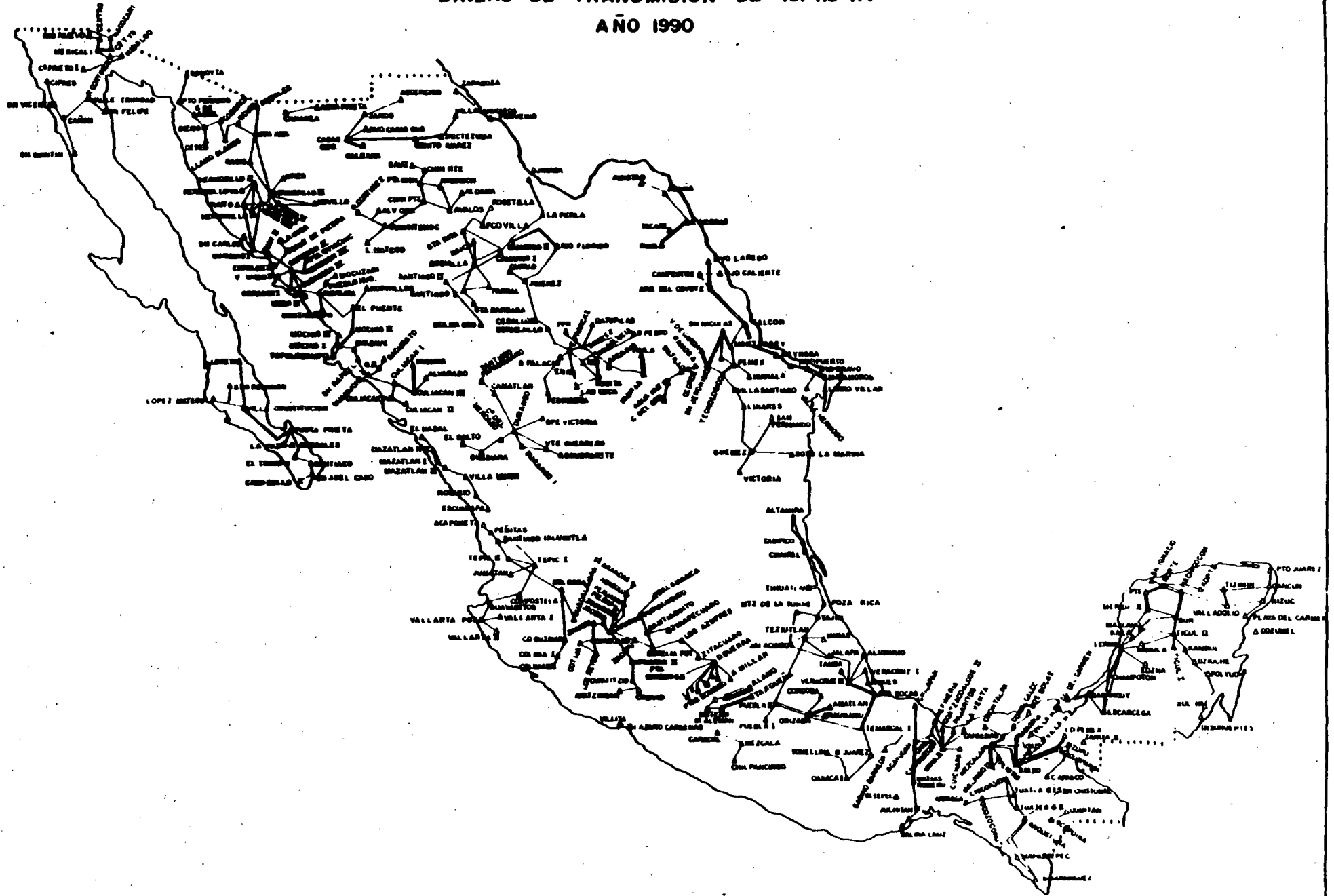
2a Sesión:

5. Clasificación de sobretensiones por maniobra
Cierre y recierre de líneas de transmisión
Interrupción prematura de pequeñas corrientes inductivas
Interrupción de corrientes capacitivas
Sobretensiones temporales
Transitorios en subestaciones encapsuladas (SF6)
6. Coordinación de aislamiento
Nociones de probabilidad y estadística
Equipo de protección contra sobretensiones
Selección de apartarrayos
Nivel de aislamiento del equipo
Estándares internacionales para coordinación de aislamiento



FIG. No. 3

LINEAS DE TRANSMISION DE 161-115 KV
AÑO 1990

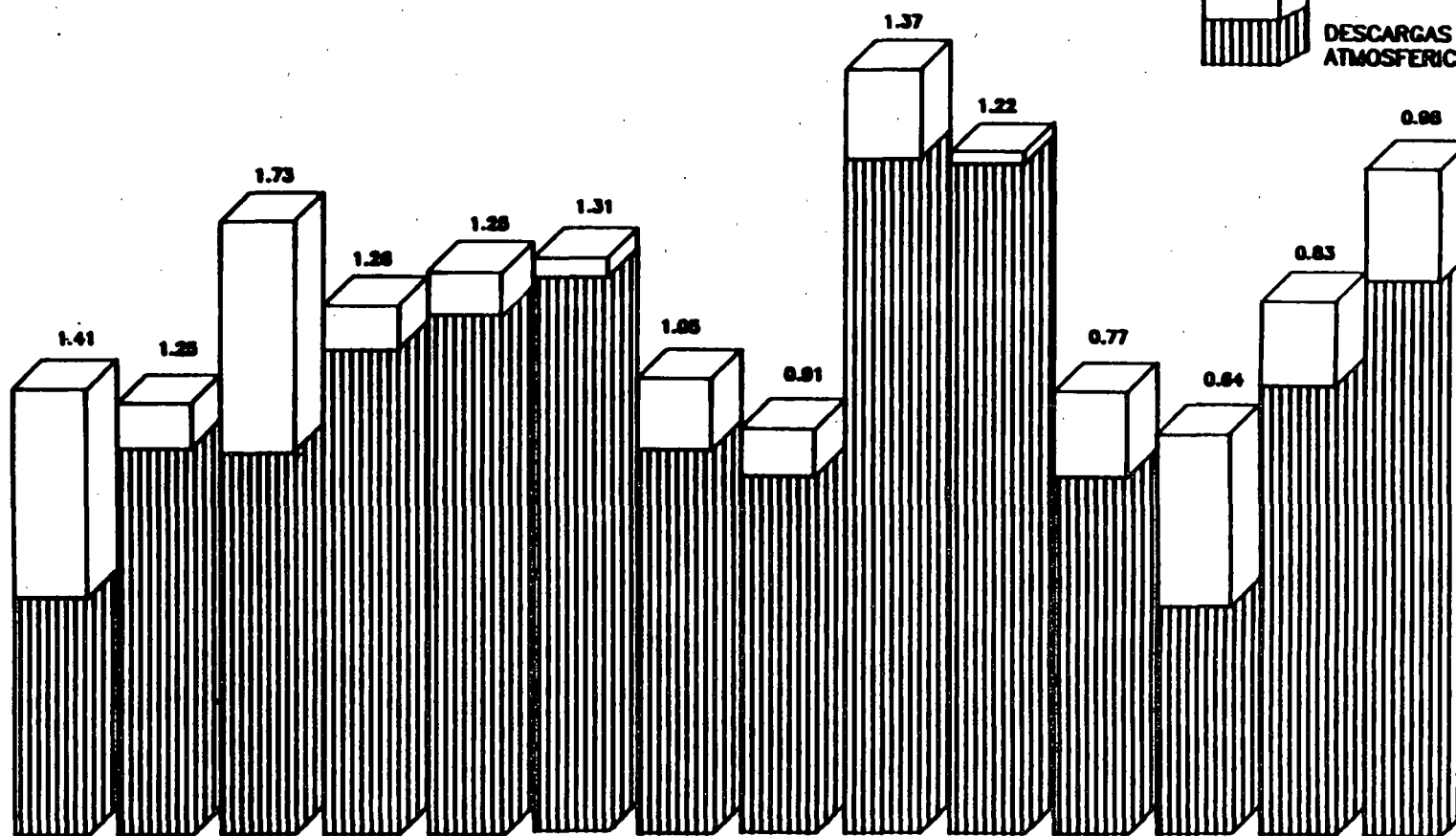




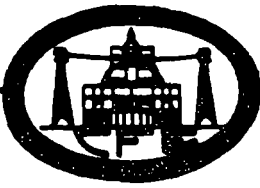
INDICE DE SALIDAS EN LINEAS DE TRANSMISION POR : DESCARGAS ATMOSFERICAS E IGNORADAS DE 400 kV

PERIODO 1977-1990

FIG. No. 10



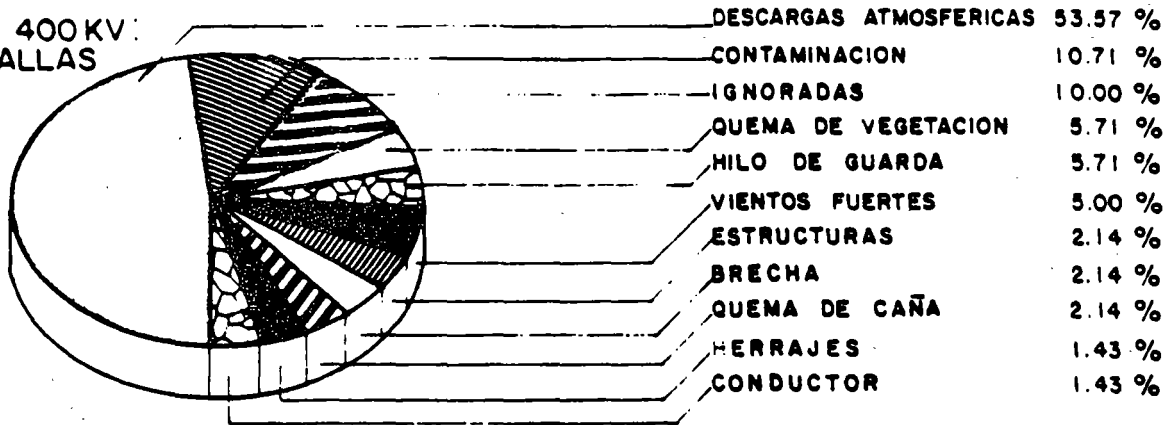
AÑO	1977	1978	1979	1980	1981	1982	1983	1984	1985	1986	1987	1988	1989	1990
No. SALIDAS (Bo)	32	53	51	65	70	75	53	49	92	91	49	31	61	75
No. SALIDAS (Do)	28	08	31	07	05	04	11	08	12	02	12	23	12	14
TOTAL	60	59	82	72	75	79	64	57	104	93	61	54	73	89
INDICE	1.41	1.25	1.73	1.28	1.25	1.31	1.05	0.91	1.37	1.22	0.77	0.64	0.83	0.98
KILOMETROS	4245	4737	4741	5895	5997	6035	6080	6287	7610	7855	7908	8378	8811.5	9099.1



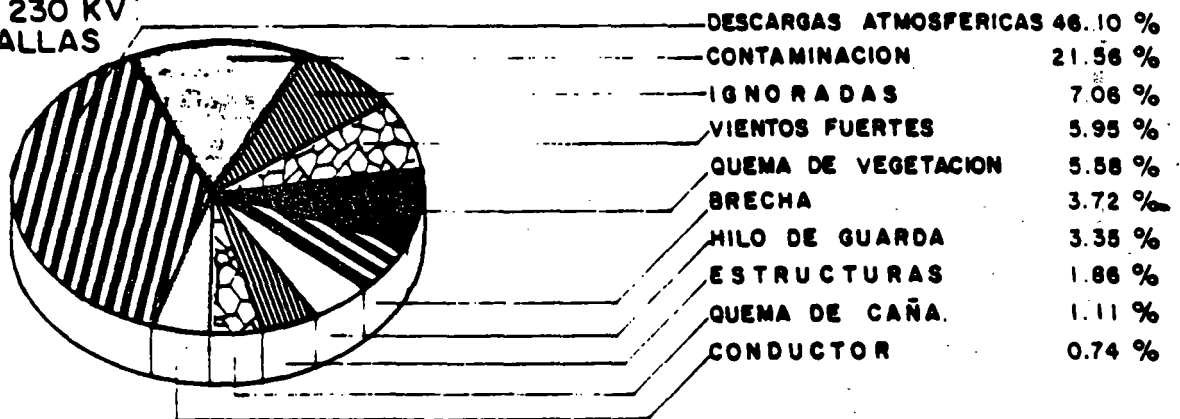
DISTRIBUCION DE SALIDAS POR FALLA EN
LINEAS DE TRANSMISION PARA EL PERIODO 1990

FIG. N° 20

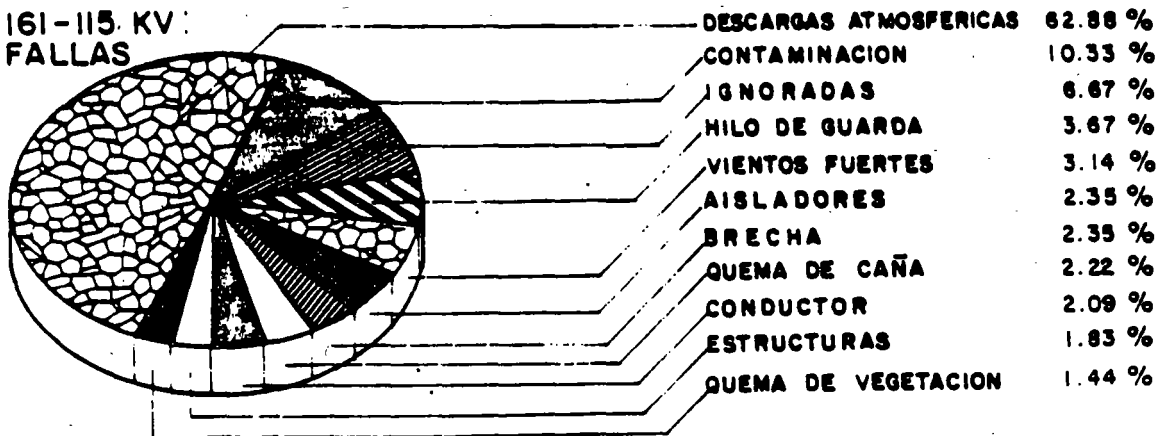
LT'S 400 KV:
140 FALLAS

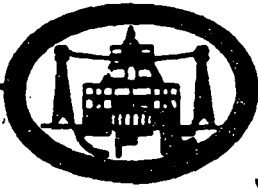


LT'S 230 KV:
269 FALLAS



LT'S 161-115 KV:
765 FALLAS

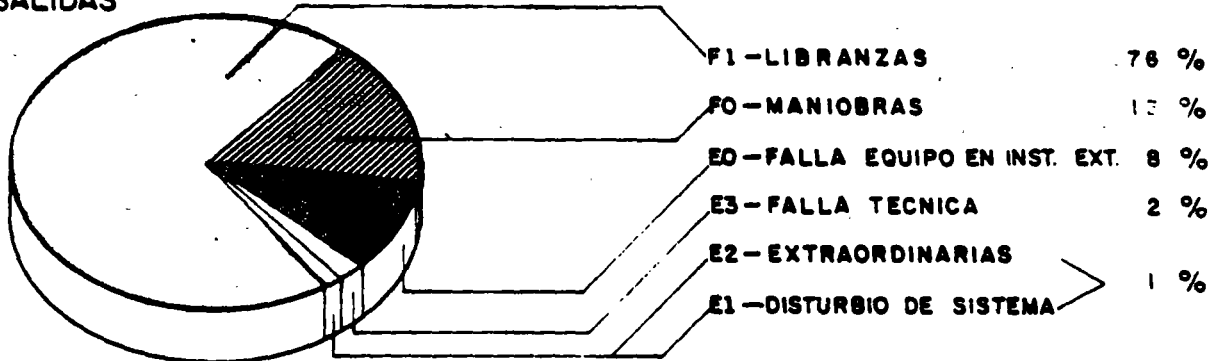




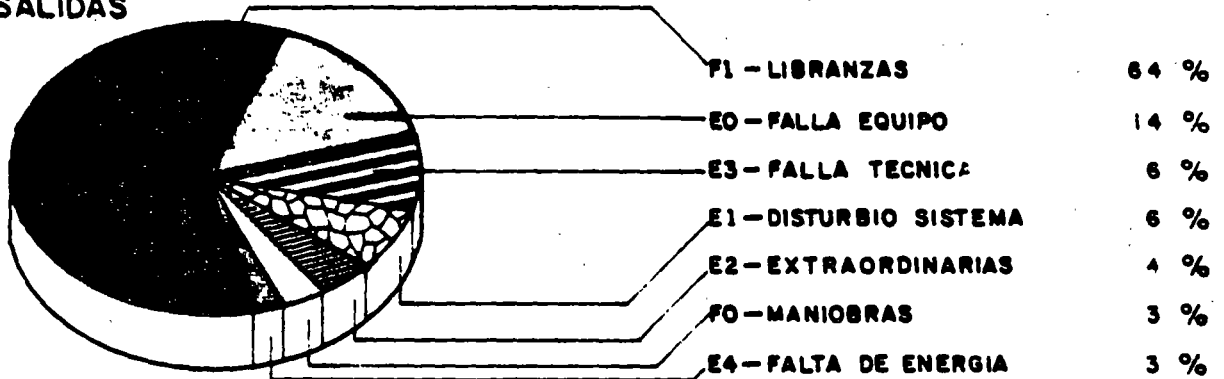
DISTRIBUCION DE SALIDAS POR CAUSAS AJENAS Y MANIOBRAS EN LINEAS DE TRANSMISION AÑO 1990

FIG. N.º 21

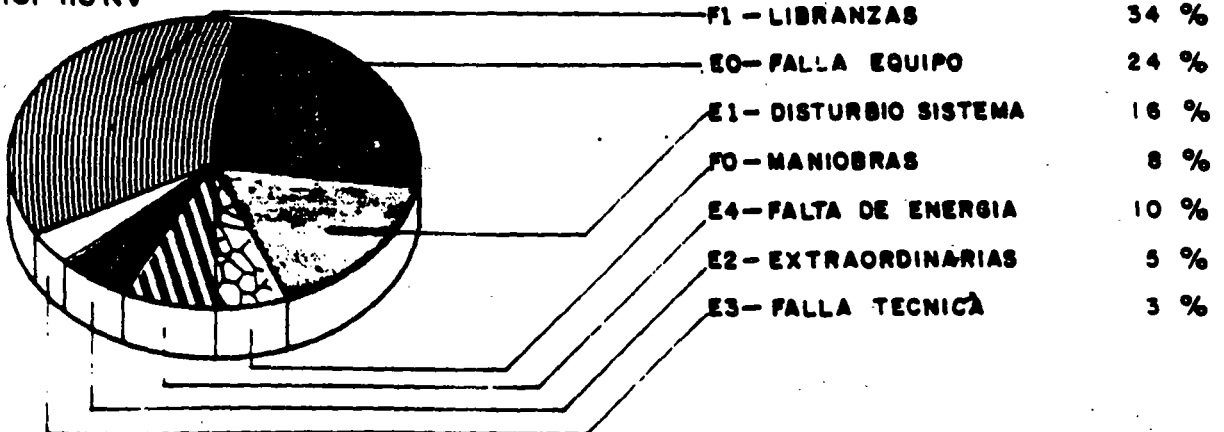
LT'S 400 KV
323 SALIDAS

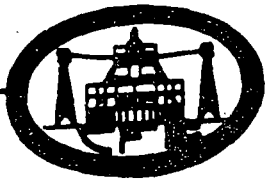


LT'S 230 KV
522 SALIDAS



LT'S 161-115 KV



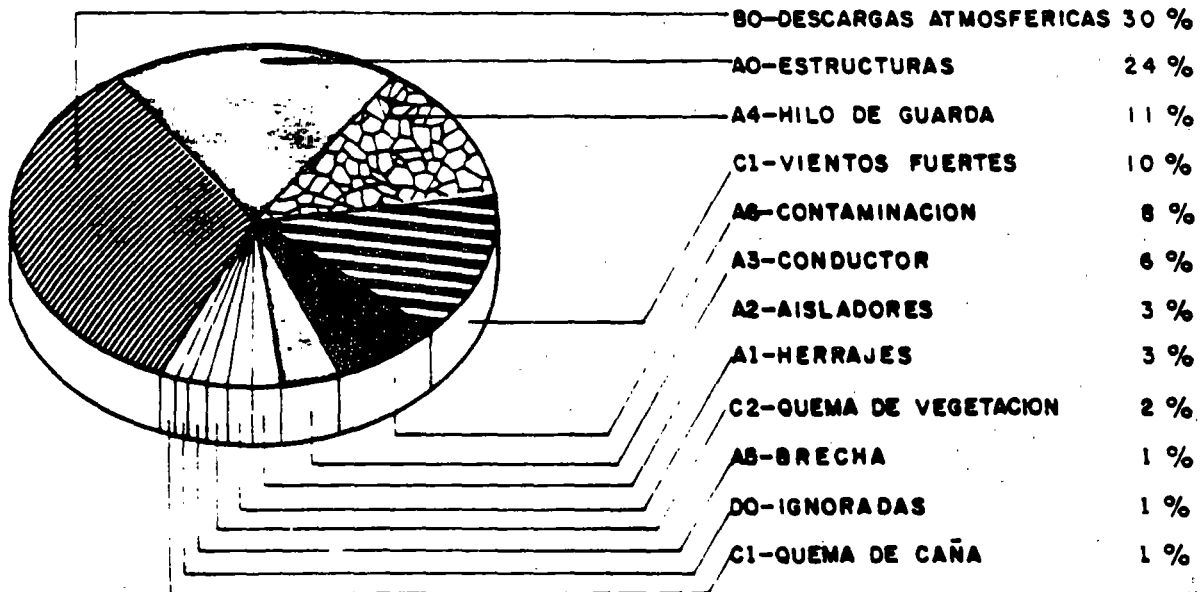


DISTRIBUCION EN PORCIENTO DEL TIEMPO QUE LAS LINEAS DE TRANSMISION, ESTUVIERON FUERA POR FALLA CAUSAS AJENAS, MANIOBRAS Y LIBRANZAS EN 1990

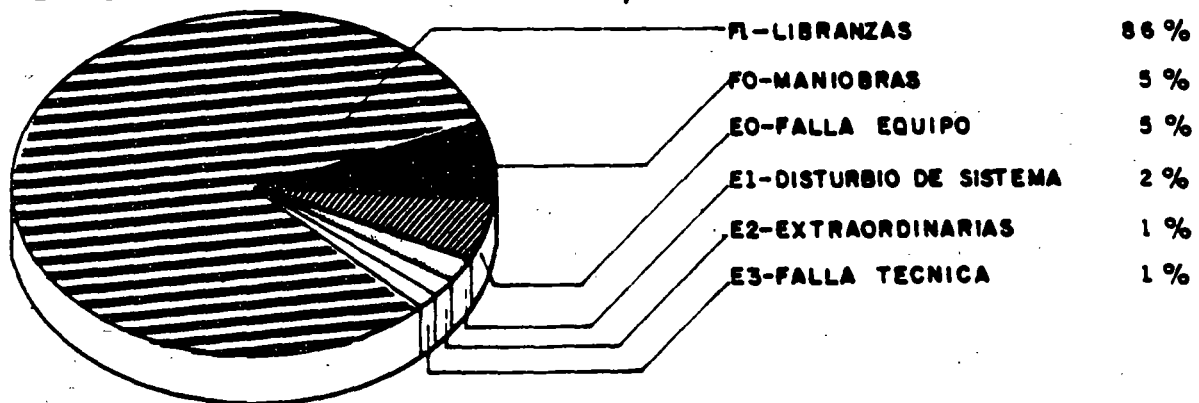
LT'S 400-115 KV

FIG. N° 22

TIEMPO FUERA POR FALLA: 2964:53 Hrs.: Min.



TIEMPO FUERA POR CAUSAS AJENAS, MANIOBRAS Y LIBRANZAS: 18953:12 Hr. Min.



I. WAVE PROPAGATION

I.1. INTRODUCTION

I.1.1. TYPES OF OVERVOLTAGES

- LIGHTNING STROKES
- SWITCHING SURGES
- ARCING GROUNDS
- RESONANCE VOLTAGES

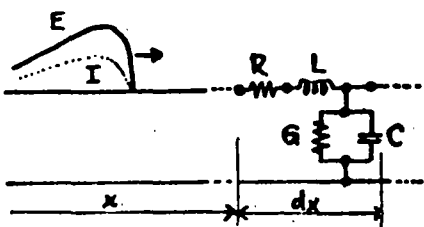
I.1.2. LIGHTNING STROKES

FREQUENCY OF OCCURRENCE
STATISTICAL DATA

MAGNITUDE
DURATION
RELEVANT PARAMETERS

I.1.3. MODELING LINES

DISTRIBUTED PARAMETERS
TRANSMISSION LINE DIFF. EQUATIONS



$$\frac{\partial^2 E}{\partial x^2} = \gamma^2 E$$

$$\frac{\partial^2 I}{\partial x^2} = \gamma^2 I$$

$$\gamma = \alpha + j\beta = \sqrt{(R+sL)(G+sC)}$$

I.2. IMPORTANT PARAMETERS

I.2.1. PROPAGATION CONSTANT

$$\gamma = \alpha + j\beta = \sqrt{Z_{LINE} Y_{LINE}}$$

α = ATTENUATION CONSTANT
 β = PHASE CONSTANT

I.2.2. CHARACTERISTIC (SURGE) IMPEDANCE

$$Z_0 = \sqrt{\frac{Z_{LINE}}{Y_{LINE}}} \quad e = Z_0 i \quad Y_0 = \frac{1}{Z_0}$$

I.2.3. LOSSLESS LINE: $R = 0, G = 0$

$$\gamma = s\sqrt{LC}$$

$$Z_0 = \sqrt{\frac{L}{C}}$$

I.2.4. DISTORTIONLESS LINE: $\frac{L}{R} = \frac{C}{G}$

I.3. LINE PARAMETERS, SIMPLE CASES

I.3.1. OVERHEAD CONDUCTOR

$$L = 2 \left(\frac{1}{4} + \ln \frac{2h}{r} \right) 10^{-4} \text{ H/km}$$

$$C = \frac{10^{-6}}{18 \ln \frac{2h}{r}} \text{ F/km}$$

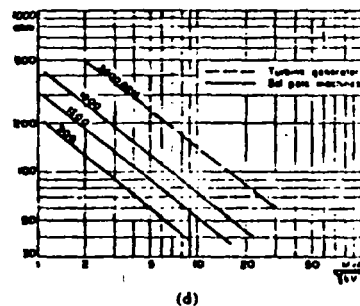
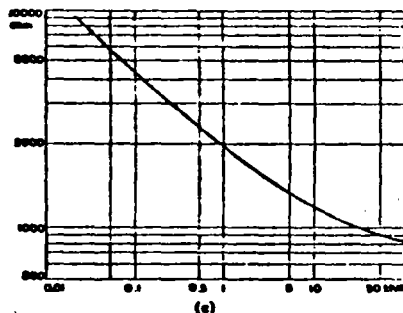
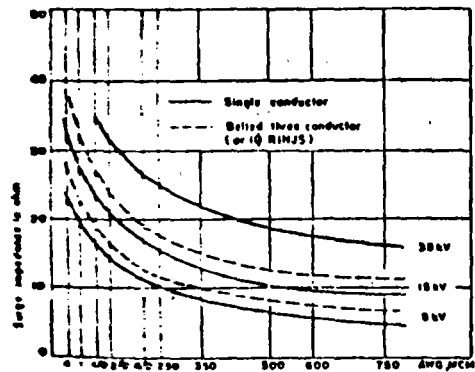
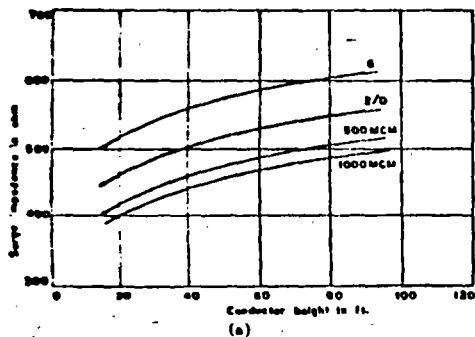
I.3.2. CABLE (ONE CONDUCTOR)

$$L \approx 2 \left(\frac{1}{4} + \ln \frac{R}{r} \right) 10^{-4} \text{ H/km}$$

$$C = k \frac{10^{-6}}{18 \ln \frac{R}{r}} \text{ F/km}$$

I.3.3. THREE PHASE SYSTEMS

1.4. SURGE IMPEDANCE CHARTS



PROCEEDINGS, TRANS. ICA, SEPT. 1965, 35
 Surge impedances: (a) Surge impedance of overhead conductors (b) Surge impedance of paper insulated lead covered cables
 (c) Surge impedance per phase for transformers in high-voltage terms (d) Surge impedance per phase for synchronous machines

TYPICAL VALUES:

- OVERHEAD LINES: 400-600 OHMS
- CABLES: 10-40 OHMS, AROUND 25 OHMS
- TRANSFORMERS: THOUSANDS OF OHMS
- SYN. MACHINES: SEVERAL HUNDREDS OF OHMS

1.5. VELOCITY OF PROPAGATION

$$v \approx \frac{1}{\sqrt{LC}} = 300 \text{ m}/\mu\text{s}$$

$$v = \frac{V_{\text{LIGHT}}}{\sqrt{k \mu}}$$

1.6. MATHEMATICAL EXPRESSION OF E AND I

$$E = e^{\gamma x} f_1(t) + e^{-\gamma x} f_2(t)$$

$$I = -\frac{1}{Z_0} [e^{\gamma x} f_1(t) - e^{-\gamma x} f_2(t)]$$

$$E = f_1(t + \frac{x}{v}) + f_2(t - \frac{x}{v}) = E_{\text{BACKWARD}} + E_{\text{FORWARD}}$$

$$I = -\frac{1}{Z_0} [f_1(t + \frac{x}{v}) - f_2(t - \frac{x}{v})] = -I_{\text{BACKWARD}} + I_{\text{FORWARD}}$$

1.7. POLARITIES

FORWARD (INCIDENT) WAVES $E_f = Z_0 I_f$

BACKWARD (REFLECTED) WAVES $E_r = -Z_0 I_r$

1.8. SHAPE OF WAVES

1.81. SPECIFICATIONS

ANSI: 1.2 x 50

1.82. APPROXIMATIONS

1.9. ATTENUATION AND DISTORTION

LOSSES
CORONA
GROUND
SKIN EFFECT
CHANGING L AND C

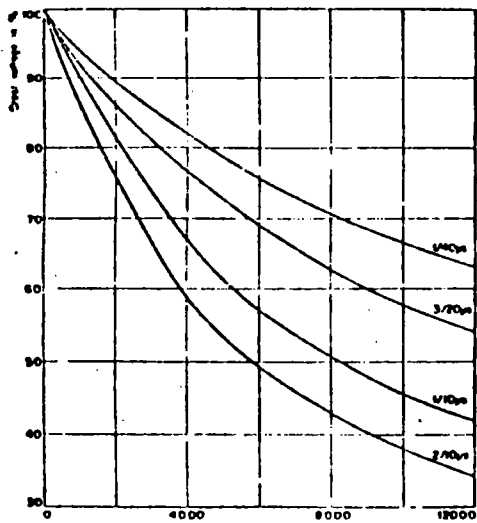
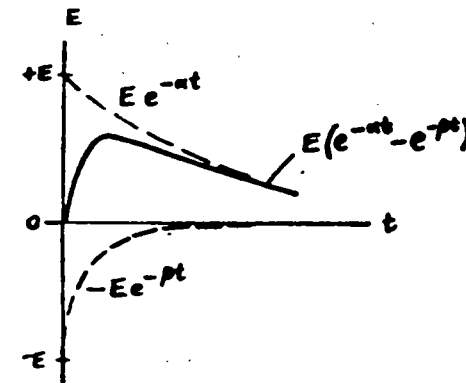
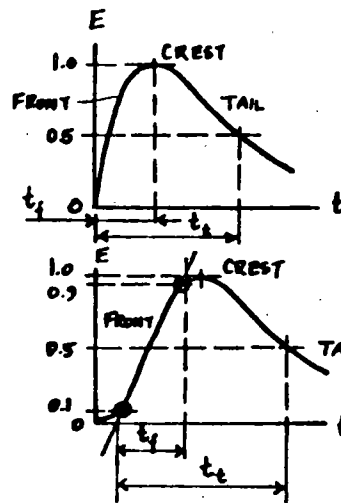
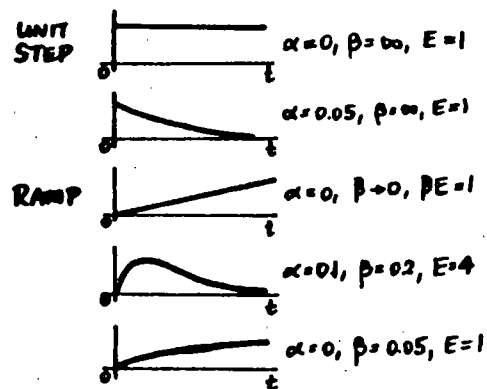


Fig. 4. Surge attenuation in cables as function of cable length. POWERLINE, TRANS. MAG., SEPT 1965, 352

EFFECT OF DISTANCE

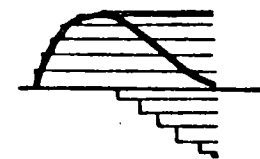


SPECIFICATION OF A TRAVELING WAVE:
 $(t_f) \times (t_r)$ in μ seconds:
1.2 x 50, 5 x 10

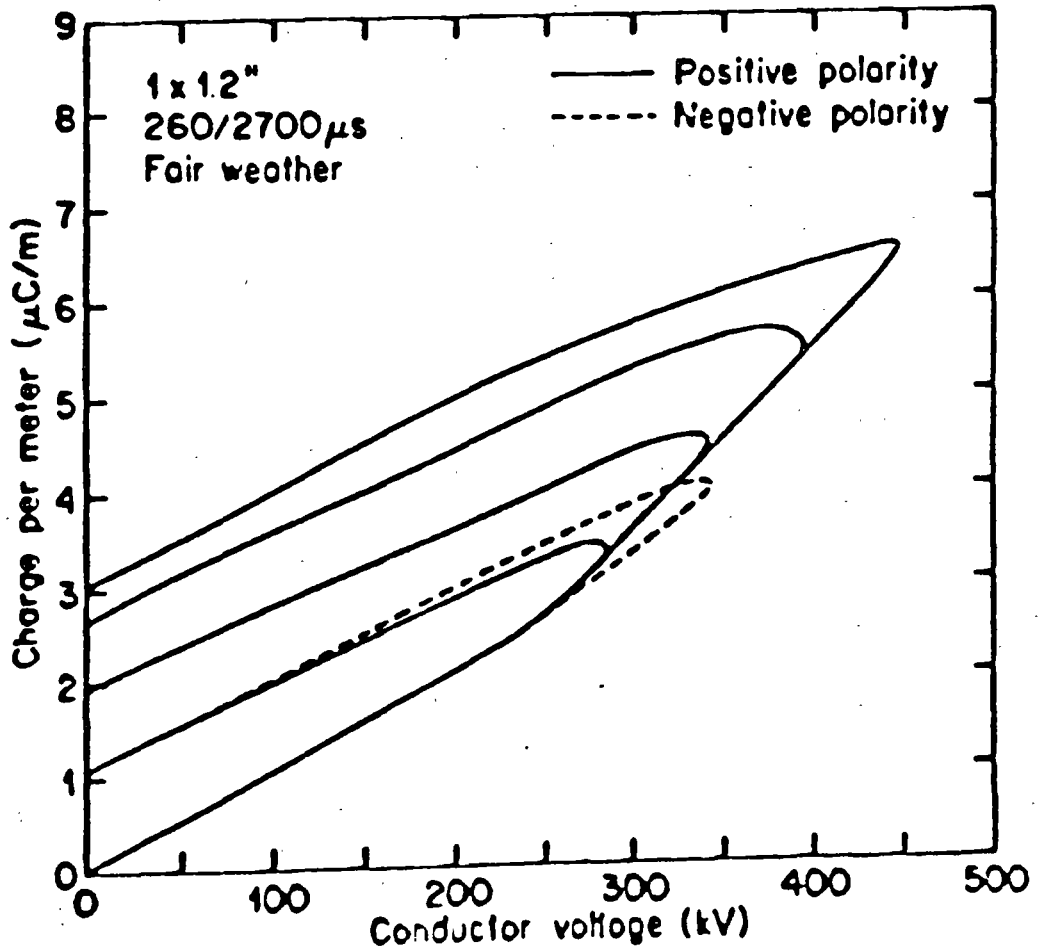
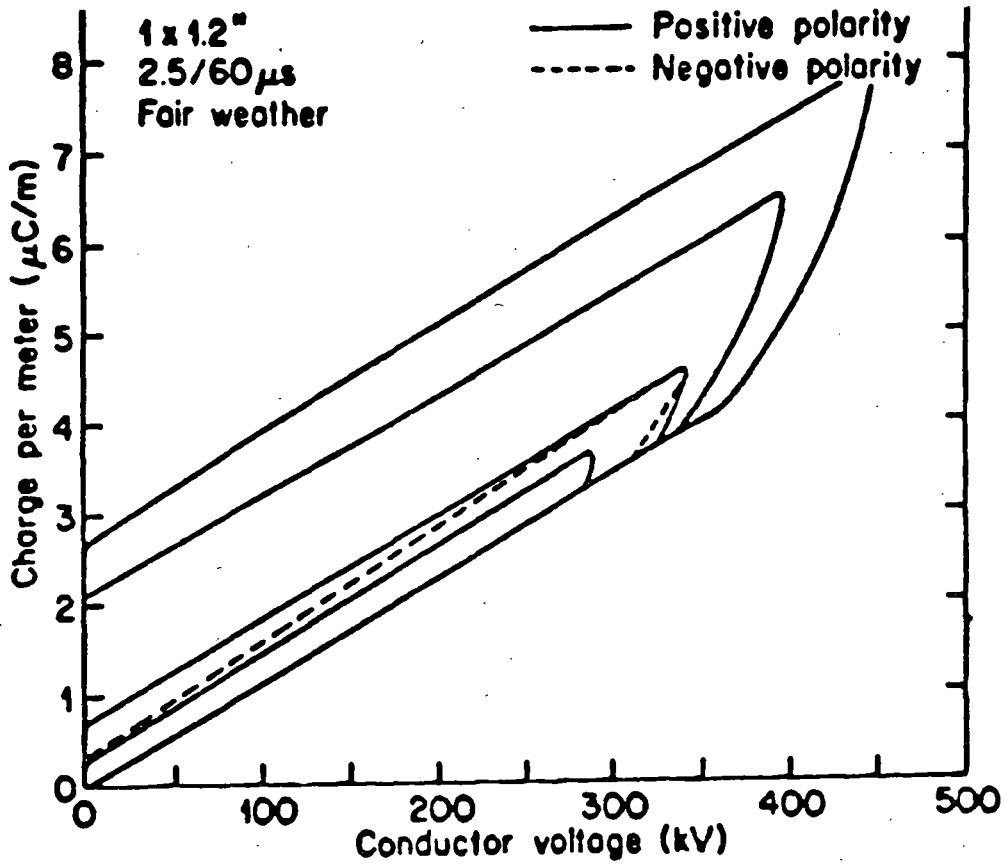


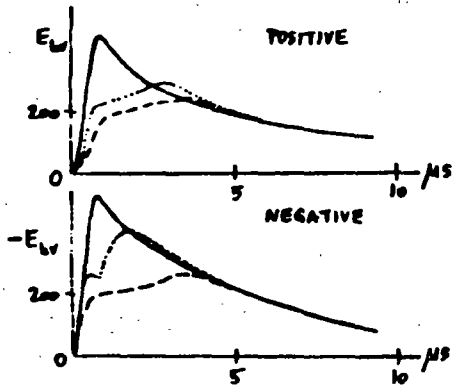
WAVESHAPES APPROXIMATED BY
 $e = E(e^{-at} - e^{-bt})$

TRAVELING WAVE AS THE SUM OF TWO EXPONENTIAL FUNCTIONS



APPROXIMATION BY RECTANGULAR COMPONENTS

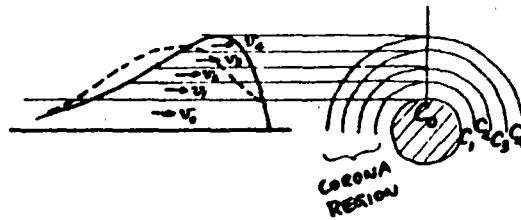




MODIFICATION OF PULSES WITH DISTANCE TRAVELED:

- AT START (0 MI.)
- AT 1.5 MILES
- - - AT 5 MILES

EFFECT OF CORONA ON WAVE DISTORTION:



$$v_k = \frac{1}{\sqrt{LC_k}}$$

$$C_k: C_0 < C_1 < C_2 < C_3 < C_4 \dots$$

$$v_k: v_0 > v_1 > v_2 > v_3 > v_4 \dots$$

2. REFLECTION OF WAVES

2.1. GENERAL TRANSITION POINT

2.11. PRACTICAL CASES (NEXT PAGE)

TERMINAL CONDITIONS
 JUNCTIONS
 JUNCTIONS WITH SHUNT ELEMENT

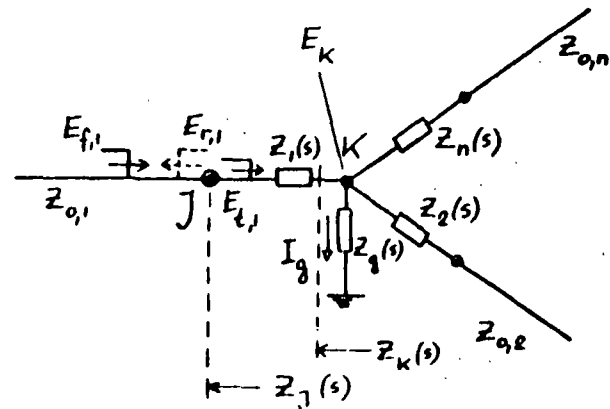
2.12. GENERAL TRANSITION POINT

$$\frac{E_{f,i}}{I_{f,i}} = Z_{0,i} \quad \frac{E_{r,i}}{I_{r,i}} = -Z_{0,i} \quad \frac{E_{t,i}}{I_{t,i}} = Z_0$$

$$E_{t,i} = E_{f,i} + E_{r,i}$$

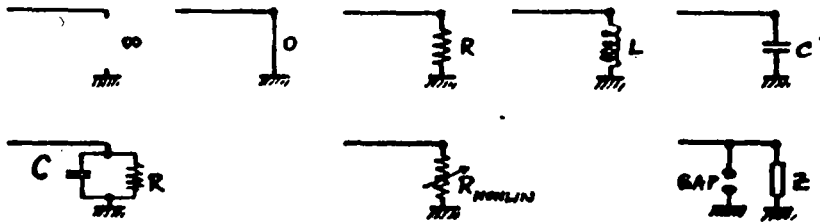
$$I_{t,i} = I_{f,i} + I_{r,i}$$

$$Z_j(s) = Z_1(s) + Z_k(s) = Z_1(s) + \frac{1}{\frac{1}{Z_0(s)} + \sum_{i=2}^n \frac{1}{Z_i(s)}}$$

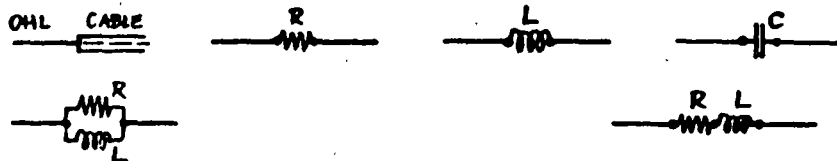


TYPICAL EXAMPLES:

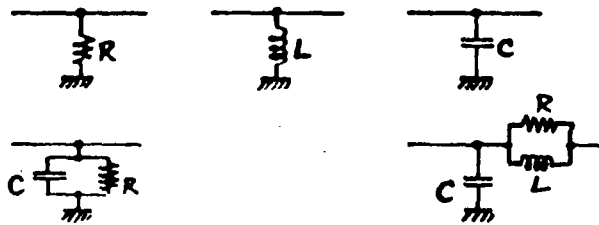
TERMINAL CONDITIONS:



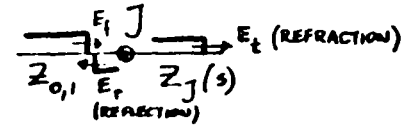
JUNCTIONS AND SERIES ELEMENTS:



JUNCTIONS AND SHUNT ELEMENTS:



2.13. REFLECTION COEFFICIENTS AT J



$$a_E = \frac{Z_J - Z_0}{Z_J + Z_0}$$

$$E_r = a_E E_f$$

$$a_I = -\frac{Z_J - Z_0}{Z_J + Z_0}$$

$$I_r = a_I I_f$$

2.14. REFRACTION COEFFICIENTS AT J

$$b_E = \frac{2Z_J}{Z_J + Z_0}$$

$$E_t = b_E E_f$$

$$b_I = \frac{2Z_0}{Z_J + Z_0}$$

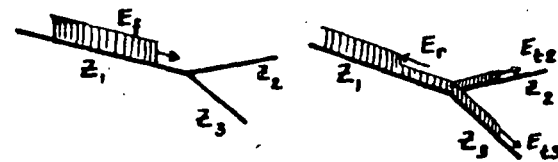
$$I_t = b_I I_f$$

2.15. a AND b RELATIONSHIPS

$$a_I = -a_E$$

$$b_I = 1 - a_E = 1 + a_I$$

$$b_E = 1 + a_E = 1 - a_I$$



2.2. LINE TERMINATED BY A RESISTANCE



R	∞ O.C.	Z_0	0 SH.C.
Z_j	∞	Z_0	0
a_E	1	0	-1
a_I	-1	0	1
b_E	2	1	0
b_I	0	1	2
E_r	E_f	0	$-E_f$
$E_f + E_r$	$2E_f$	E_f	0
I_r	$-I_f$	0	I_f
$I_f + I_r$	0	I_f	$2I_f$

DUALITY

CABLE - OVERHEAD LINE AND
OVERHEAD LINE - CABLE JUNCTIONS

2.3. INDUCTIVE AND CAPACITIVE ELEMENTS

2.31. ASSUMPTIONS

FRONT OF TRAVELING WAVE

$\omega \approx \infty$

$\omega L = \infty \quad \frac{1}{\omega C} = 0$

TAIL OF TRAVELING WAVE

$\omega \approx 0$

$\omega L = 0 \quad \frac{1}{\omega C} = \infty$

2.32. TERMINATIONS

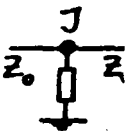
INDUCTIVE O.C. \rightarrow SH.C.

CAPACITIVE SH.C. \rightarrow O.C.

2.33. SHUNT ELEMENT AT JUNCTION

INDUCTIVE O.C. \rightarrow SH.C.

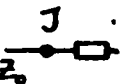
CAPACITIVE SH.C. \rightarrow O.C.



2.34. SERIES ELEMENT INSERTION

INDUCTIVE O.C. \rightarrow SH.C.

CAPACITIVE SH.C. \rightarrow O.C.



2.35. COMPUTATIONS, FLOWCHART

Z_0 $Z_j(s)$

$a_E(s)$ $a_I(s)$ $b_E(s)$ $b_I(s)$

α [1/sec]

$E_f(s) = \frac{E_f}{s}$

$E_r(s) = a_E(s) \cdot E_f(s) \rightarrow e_r(t)$

$e_{total} = e_f(t) + e_r(t)$

$e_t(t)$

$e_{series}(t) = e_{total} - e_t(t)$

$i_r(t) = -\frac{e_r(t)}{Z_0}$

$i_{total} = i_f(t) + i_r(t)$

$i_t(t) = \frac{e_t(t)}{Z_0}$

$i_{shunt}(t) = i_{total} - i_t(t)$

CHARTS FOR

VOLTAGES AND CURRENTS VS. TIME

VOLTAGES AND CURRENTS ALONG LINE

2.4. SPECIAL CASES WITH AN INDUCTANCE OR A CAPACITANCE

2.41. INDUCTIVE TERMINATION

$Z_j(s) = sL$

$a = \frac{Z_j(s) - Z_0}{Z_j(s) + Z_0} = \frac{s - \alpha}{s + \alpha}$

$\alpha = \frac{Z_0}{L}$ 1/sec

$E_f(s) = \frac{E_f}{s}$

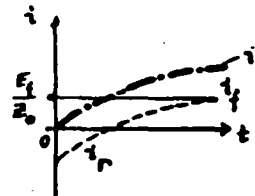
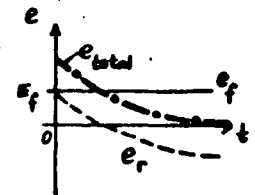
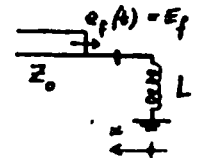
$E_r(s) = a E_f(s) = \frac{E_f}{s} \frac{s - \alpha}{s + \alpha}$

$e_r(t) = E_f (2e^{-\alpha t} - 1)$

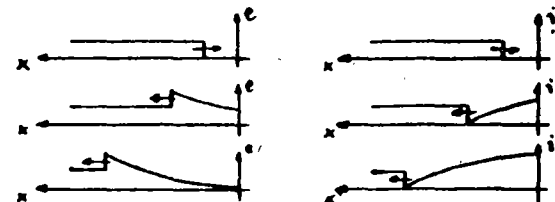
$e_{total} = e_f(t) + e_r(t) = 2E_f e^{-\alpha t}$

$i_r(t) = -\frac{e_r(t)}{Z_0} = \frac{E_f}{Z_0} (1 - 2e^{-\alpha t})$

$i_{total} = i_f(t) + i_r(t) = \frac{2E_f}{Z_0} (1 - e^{-\alpha t})$



VOLTAGES AND CURRENTS ALONG THE LINE



2.42. CAPACITIVE TERMINATION

$$Z_j(s) = \frac{1}{sC}$$

$$\alpha = \frac{\alpha - s}{\alpha + s}$$

$$\alpha = \frac{1}{Z_0 C} \quad 1/\text{sec}$$

$$E_f(s) = \frac{E_f}{s}$$

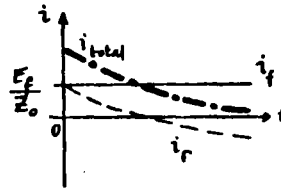
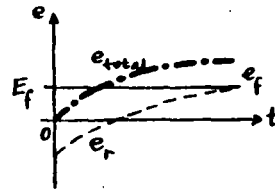
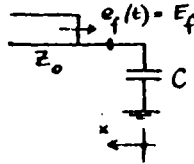
$$\rightarrow E_r(s) = \frac{E_f}{s} \frac{\alpha - s}{\alpha + s}$$

$$e_r(t) = E_f (1 - 2e^{-\alpha t})$$

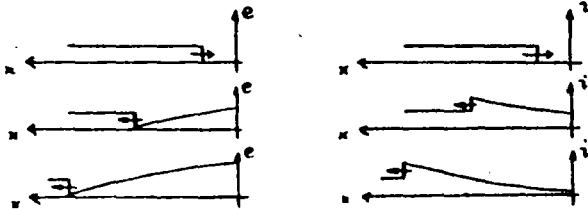
$$e_{\text{total}} = e_f(t) + e_r(t) = 2E_f (1 - e^{-\alpha t})$$

$$i_r(t) = \frac{E_f}{Z_0} (2e^{-\alpha t} - 1)$$

$$i_{\text{total}} = i_f(t) + i_r(t) = \frac{2E_f}{Z_0} e^{-\alpha t}$$



VOLTAGES AND CURRENTS ALONG THE LINE



2.43. SHUNT INDUCTANCE

$$Z_j(s) = \frac{sLZ_0}{sL + Z_0}$$

$$\alpha = -\frac{\alpha}{s + \alpha} \quad \alpha = \frac{Z_0}{2L}$$

$$E_f(s) = \frac{E_f}{s}$$

$$E_r(s) = -\frac{E_f}{s} \frac{\alpha}{s + \alpha}$$

$$e_r(t) = E_f (e^{-\alpha t} - 1)$$

$$e_{\text{total}} = e_f(t) + e_r(t) = E_f e^{-\alpha t}$$

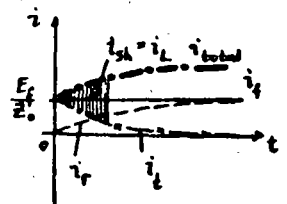
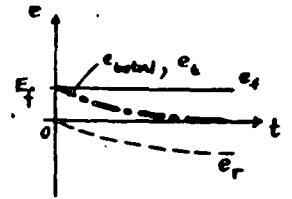
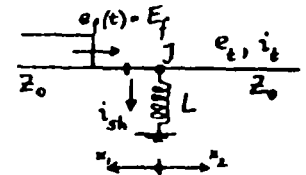
$$e_t(t) = e_{\text{total}}$$

$$i_r(t) = \frac{E_f}{Z_0} (1 - e^{-\alpha t})$$

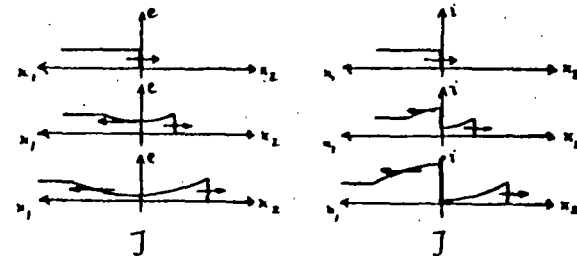
$$i_{\text{total}} = i_f(t) + i_r(t) = \frac{E_f}{Z_0} (2 - e^{-\alpha t})$$

$$i_t(t) = \frac{E_f}{Z_0} e^{-\alpha t}$$

$$i_{\text{sh}}(t) = i_{\text{total}} - i_t(t) = \frac{2E_f}{Z_0} (1 - e^{-\alpha t})$$



VOLTAGES AND CURRENTS ALONG THE LINE



2.44 SHUNT CAPACITANCE (MOTOR PROTECTION)

$$Z_j(s) = \frac{Z_0 / sC}{Z_0 + sC}$$

$$a = -\frac{s}{s+\alpha} \quad \alpha = \frac{2}{Z_0 C}$$

$$E_f(s) = \frac{E_f}{s}$$

$$E_r(s) = -E_f \frac{1}{s+\alpha}$$

$$e_r(t) = -E_f e^{-\alpha t}$$

$$e_{total} = e_f(t) + e_r(t) = E_f(1 - e^{-\alpha t})$$

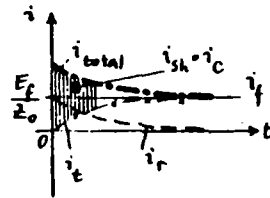
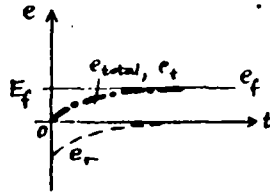
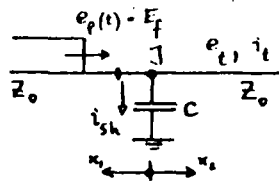
$$e_t(t) = e_{total}$$

$$i_r(t) = \frac{E_f}{Z_0} e^{-\alpha t}$$

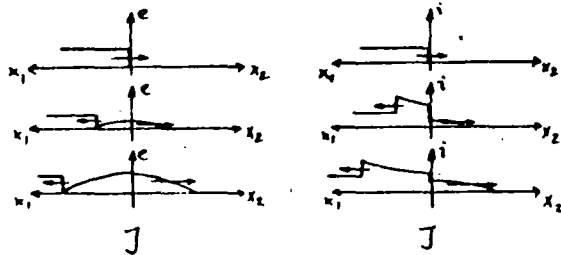
$$i_{total} = \frac{E_f}{Z_0} (1 + e^{-\alpha t})$$

$$i_t(t) = \frac{E_f}{Z_0} (1 - e^{-\alpha t})$$

$$i_{sh}(t) = \frac{2E_f}{Z_0} e^{-\alpha t}$$



VOLTAGES AND CURRENTS ALONG THE LINE



2.45. SERIES INDUCTANCE (MOTOR PROTECTION)

$$Z_j(s) = sL + Z_0$$

$$a = \frac{s}{s+\alpha} \quad \alpha = \frac{2Z_0}{L}$$

$$E_f(s) = \frac{E_f}{s}$$

$$E_r(s) = E_f \frac{1}{s+\alpha}$$

$$e_r(t) = E_f e^{-\alpha t}$$

$$e_{total} = e_f(t) + e_r(t) = E_f(1 + e^{-\alpha t})$$

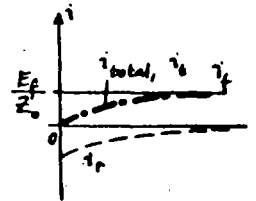
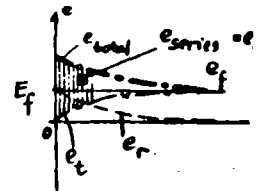
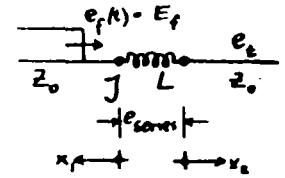
$$e_t(t) = E_f(1 - e^{-\alpha t})$$

$$e_{series} = e_{total} - e_t(t) = 2E_f e^{-\alpha t}$$

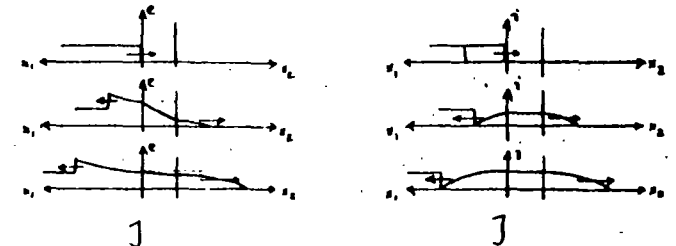
$$i_r(t) = -\frac{E_f}{Z_0} e^{-\alpha t}$$

$$i_{total} = i_f(t) + i_r(t) = \frac{E_f}{Z_0} (1 - e^{-\alpha t})$$

$$i_t(t) = \frac{E_f}{Z_0} (1 - e^{-\alpha t})$$



VOLTAGES AND CURRENTS ALONG THE LINE



2.46. SERIES CAPACITANCE

$$Z_j(s) = \frac{1}{sC} + Z_0$$

$$a = \frac{\alpha}{s+\alpha} \quad \alpha = \frac{1}{2Z_0C}$$

$$E_f(s) = \frac{E_f}{s}$$

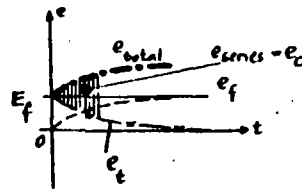
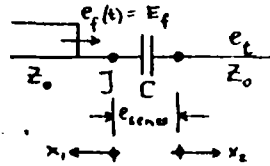
$$E_r(s) = \frac{E_f}{s} \frac{\alpha}{s+\alpha}$$

$$e_r(t) = E_f(1 - e^{-\alpha t})$$

$$e_{total} = e_f(t) + e_r(t) = E_f(2 - e^{-\alpha t})$$

$$e_t(t) = E_f e^{-\alpha t}$$

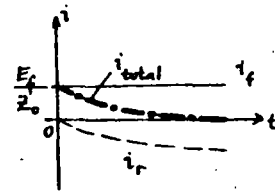
$$e_{series} = 2E_f(1 - e^{-\alpha t})$$



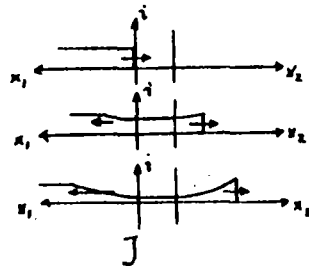
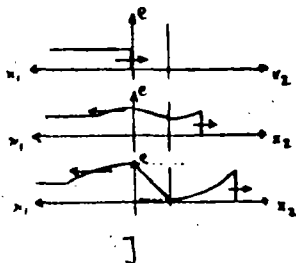
$$i_r(t) = \frac{E_f}{Z_0} (e^{-\alpha t} - 1)$$

$$i_{total} = i_f(t) + i_r(t) = \frac{E_f}{Z_0} e^{-\alpha t}$$

$$i_t(t) = \frac{E_f}{Z_0} e^{-\alpha t}$$



VOLTAGES AND CURRENTS ALONG THE LINE



2.5. SUCCESSIVE REFLECTIONS

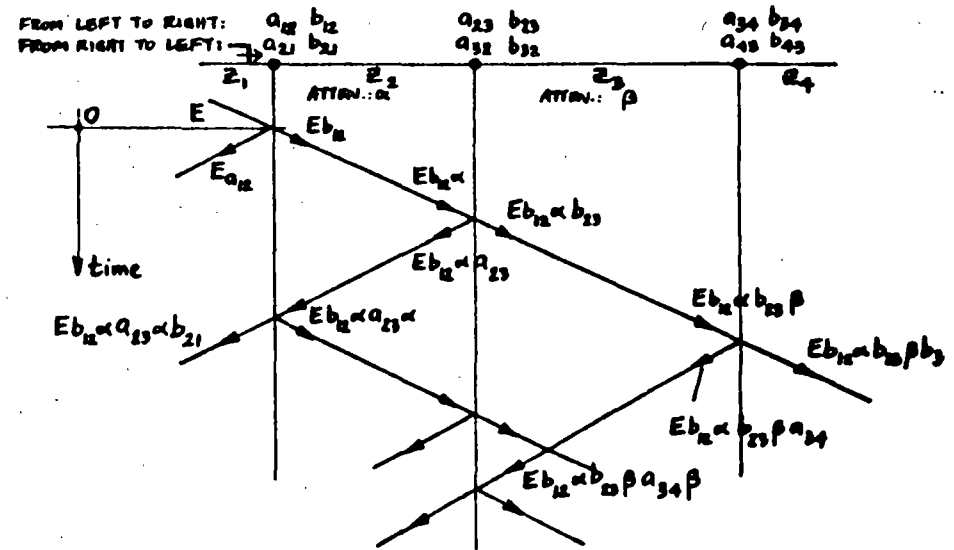
2.51. BEWLEY LATTICE

TIME - SPACE DIAGRAM
MULTIPLE REFLECTIONS

DISTANCE BETWEEN JUNCTIONS
IS PROPORTIONAL TO

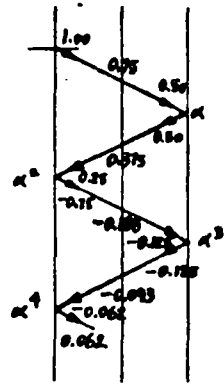
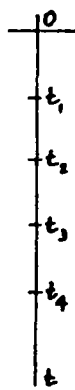
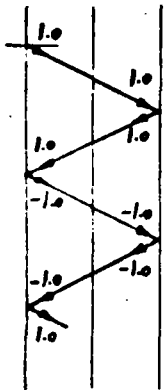
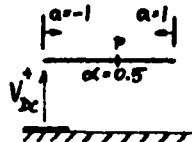
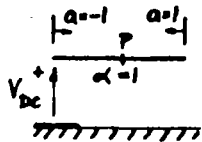
TIME OF WAVE PASSAGE
(DIAGONALS HAVE SAME SLOPE)

LENGTH BETWEEN JUNCTIONS
(SLOPES ARE DIFFERENT)

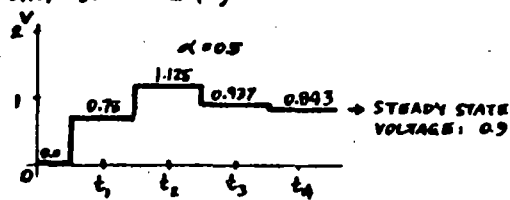
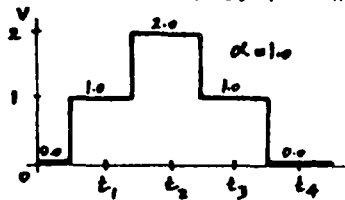


2.52. EXAMPLES

LINE CHARGING WITH DC



VOLTAGES AT MIDPOINT OF LINE (P):



VOLTAGE AT END WHEN $\alpha = 0.5$:

$$V = 2\alpha - 2\alpha^3 \pm \dots = 2\alpha (1 - \alpha^2 + \alpha^4 \mp \dots)$$

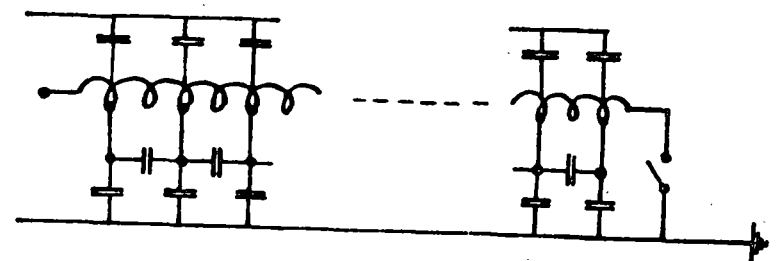
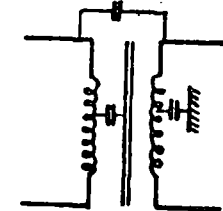
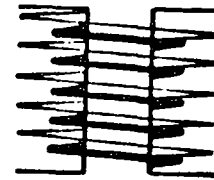
STEADY STATE VOLTAGE: $\lim V = \frac{2\alpha}{1 + \alpha} = 0.8$

21

3. TRANSFORMER WINDINGS UNDER TRANSIENT CONDITIONS

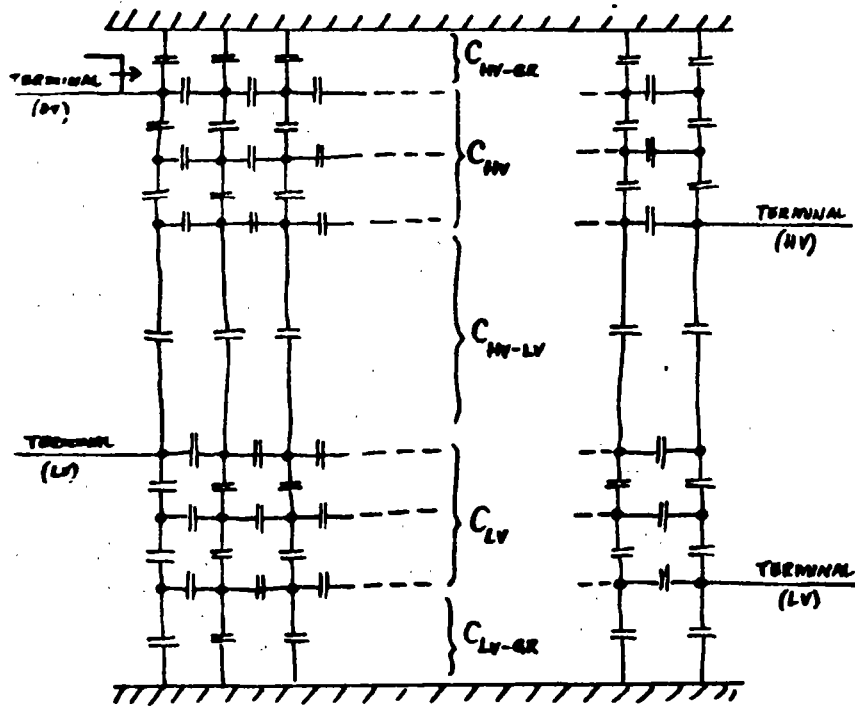
3.1. SCHEMATIC REPRESENTATION

- SELF INDUCTANCES
- MUTUAL INDUCTANCES
- CAPACITANCES: TO CORE
TO TANK
- CAPACITIVE COUPLING
- LOSSES (RESISTANCES)

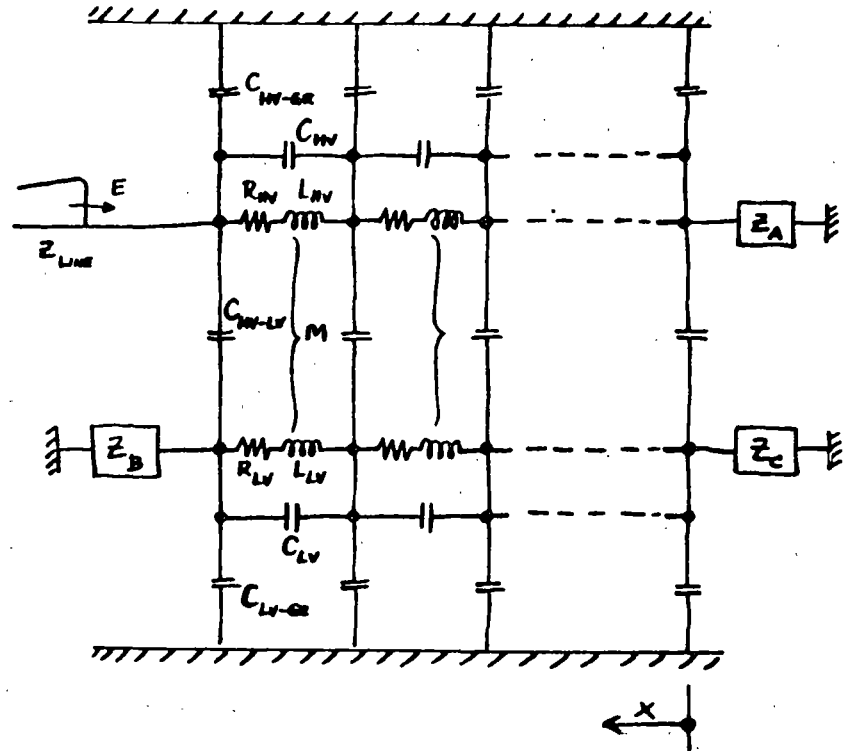


INITIAL VOLTAGE DISTRIBUTION IS DETERMINED BY THE CAPACITANCE NETWORK,

AT THE FRONT OF THE WAVE ($\omega \approx \infty$)
 $\omega L \approx \infty$, I.E., OPEN-CIRCUITED:



COMPLETE EQUIVALENT CIRCUIT FOR TRANSIENTS (ANALOG MODEL):



3.2. INITIAL VOLTAGE DISTRIBUTION

CAPACITANCE LADDER NETWORK

GROUND CAP. OF WINDING C_g

SERIES CAP. OF WINDING C_s

E = VOLTAGE TO GROUND AT ANY POINT

x = FROM NEUTRAL TO TERMINAL

l = LENGTH OF WINDING

$$\frac{\partial^2 E}{\partial x^2} - \frac{1}{l^2} \frac{C_g}{C_s} E = 0$$

$$E = Ae^{px} + Be^{-px}$$

$$p = \frac{1}{l} \left(\frac{C_g}{C_s} \right)^{\frac{1}{2}}$$

GROUNDING NEUTRAL

$$E = V \frac{\sinh(\alpha x/l)}{\sinh \alpha}$$

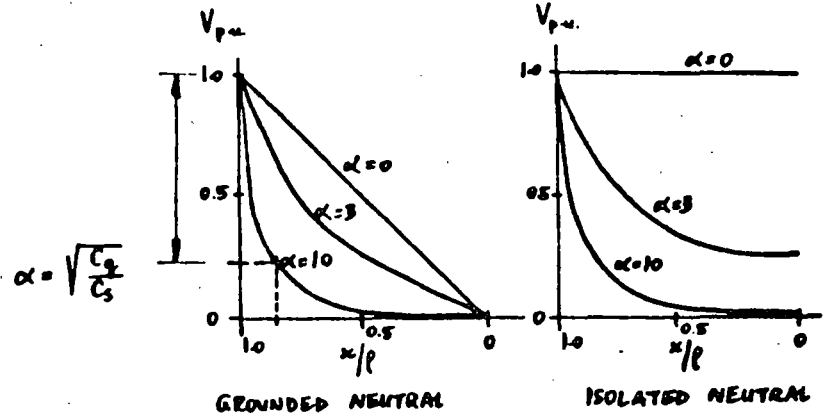
$$\alpha = pl = \sqrt{\frac{C_g}{C_s}}$$

$$x=0: E=0 \quad x=l: E=V$$

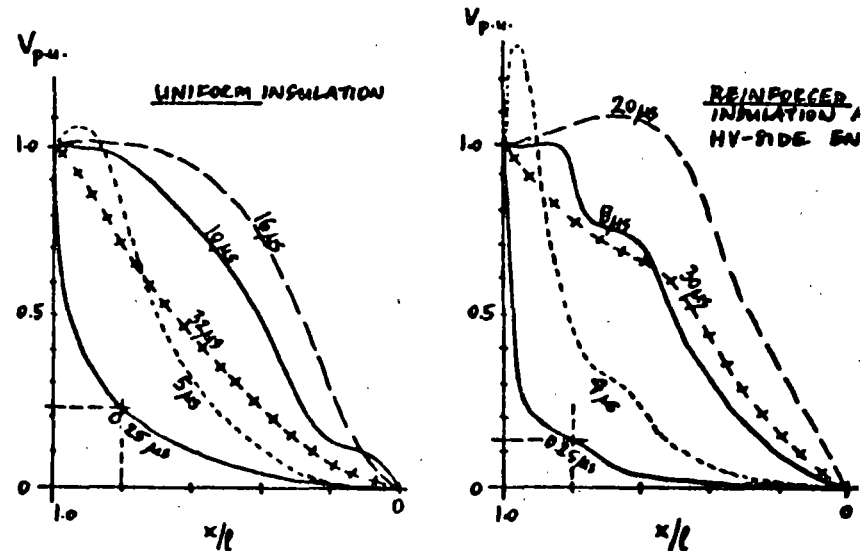
ISOLATED NEUTRAL

$$E = V \frac{\cosh(\alpha x/l)}{\cosh \alpha}$$

$$x=0: E=V \quad x=l: E=0$$



INITIAL VOLTAGE DISTRIBUTION IN CASE OF STEP-FUNCTION FORWARD VOLTAGE



TRANSIENT VOLTAGE DISTRIBUTION IN CASE OF STEP-FUNCTION FORWARD VOLTAGE

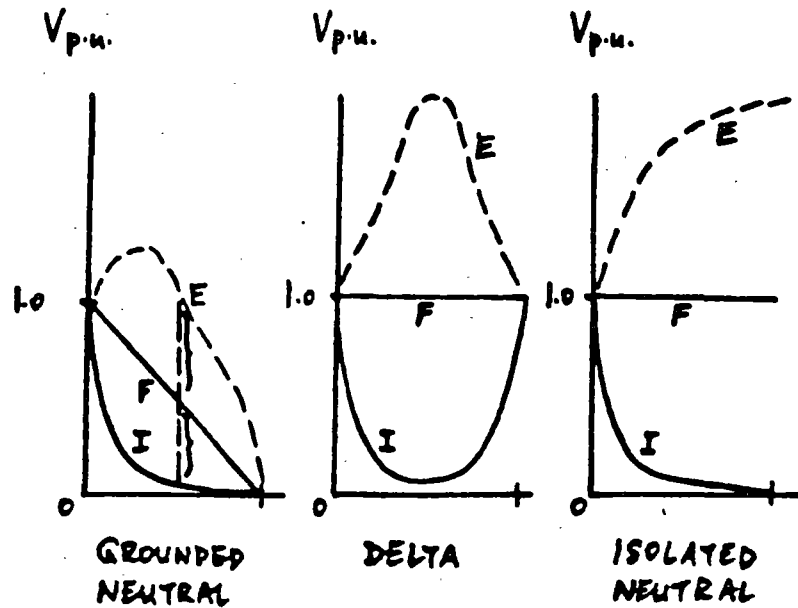
3.4. ENVELOPE CURVES

I - INITIAL DISTRIBUTION

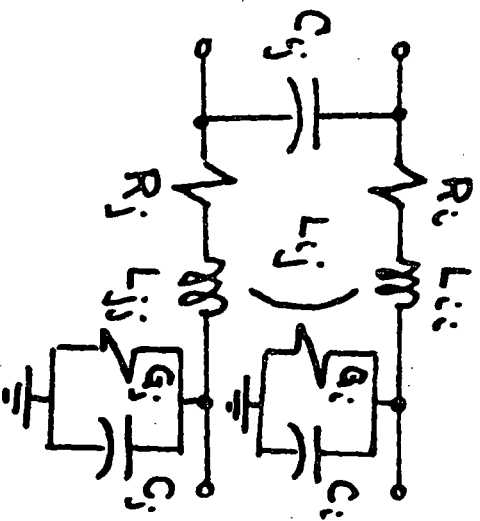
F - FINAL DISTRIBUTION

LC CIRCUITS → OSCILLATIONS

E - ENVELOPES OF OSCILLATION



Líneas de Transmisión con Conductores Múltiples.



R_i, L_{ij}, G_i, C_i : resistencia, inductancia, conductancia a tierra y capacitancia a tierra, por unidad de longitud, para el conductor "i".

L_{ij}, C_{ij} : inductancia mutua y capacitancia, por unidad de longitud, entre los conductores "i" y "j".

$$\begin{cases} \frac{\partial v_i}{\partial x} = -\sum_{j=1}^n L_{ij} \frac{\partial i_j}{\partial t} - R_i i_i \\ \frac{\partial i_i}{\partial x} = -\sum_{j=1}^n C_{ij} \frac{\partial}{\partial t} (v_i - v_j) - C_i \frac{\partial v_i}{\partial t} - G_i v_i \end{cases}$$

$$\frac{\partial v''}{\partial x} = -Z' i' ; \quad \frac{\partial i'_i}{\partial x} = -Y' v''$$

⇓

$$\frac{\partial^2 v''}{\partial x^2} = P' v'' ; \quad \frac{\partial^2 i'_i}{\partial x^2} = P' i'_i$$

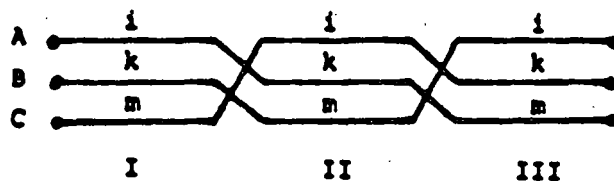
$$P' = Z' Y', \quad P' = Y' Z'$$

Transposición de Líneas

$$d = 80 \rightarrow 160 \text{ km}$$

líneas con disposición triangular: 67 km

otras configuraciones: 33 km



- Transposition scheme for single three-phase circuit

$$\frac{1}{3} \begin{bmatrix} Z'_{11} & Z'_{1k} & Z'_{1m} \\ Z'_{k1} & Z'_{kk} & Z'_{km} \\ Z'_{m1} & Z'_{mk} & Z'_{mm} \end{bmatrix} + \begin{bmatrix} Z'_{kk} & Z'_{km} & Z'_{k1} \\ Z'_{mk} & Z'_{mm} & Z'_{m1} \\ Z'_{1k} & Z'_{1m} & Z'_{11} \end{bmatrix} + \begin{bmatrix} Z'_{mm} & Z'_{m1} & Z'_{mk} \\ Z'_{1m} & Z'_{11} & Z'_{1k} \\ Z'_{km} & Z'_{k1} & Z'_{kk} \end{bmatrix} = \begin{bmatrix} Z'_s & Z'_m & Z'_m \\ Z'_m & Z'_s & Z'_m \\ Z'_m & Z'_m & Z'_s \end{bmatrix}$$

with

$$Z'_s = \frac{1}{3} (Z'_{11} + Z'_{kk} + Z'_{mm})$$

$$Z'_m = \frac{1}{3} (Z'_{1k} + Z'_{km} + Z'_{m1})$$

SOBRETENSIONES Y ESFUERZOS ELECTRICOS EN SISTEMAS DE POTENCIA

Victor F. Hermosillo
Comisión Federal de Electricidad
DEPFI - UNAM

1. INTRODUCCION

El diseño apropiado del nivel de aislamiento eléctrico de un sistema de potencia debe llegar a un balance entre el aguante, el costo y la fiabilidad de los elementos del sistema ante un esfuerzo eléctrico determinado. El aguante ante un cierto esfuerzo eléctrico puede requerir de aislamiento adicional, que incrementa la fiabilidad pero implica mayores costos. Comúnmente, el costo representa un factor limitante mayor que la factibilidad técnica.

La ruptura o deterioro del aislamiento eléctrico depende de la magnitud, forma y duración del esfuerzo eléctrico a que éste se sujeta. Los fenómenos físicos involucrados en la ruptura de un aislamiento son diferentes para distintos tipos de esfuerzo. Debido a lo anterior, las normas internacionales han propuesto clasificar los esfuerzos típicos encontrados en sistemas de potencia, definiendo características de aguante del aislamiento en base a cada tipo de esfuerzo.

La clasificación de esfuerzos eléctricos y sobretensiones de acuerdo a la norma IEC-71 se muestra en la Figura 1. Cada clase incluye la definición de una forma del esfuerzo respecto al tiempo, un rango de valores para las frecuencias y períodos de tiempo involucrados, así como una forma y prueba estandarizada.

2. VOLTAJES CONTINUOS EN EL SISTEMA

El voltaje nominal se define como el voltaje efectivo (rms), entre fases, a la frecuencia de operación de un sistema de potencia, bajo condiciones normales. A diferencia de voltajes transitorios y temporales, que ocurren bajo condiciones anormales de operación, el voltaje nominal del sistema representa un esfuerzo eléctrico continuo aplicado al aislamiento. Es importante considerarlo en procesos de envejecimiento del aislamiento y en problemas de contaminación.

En ocasiones un sistema eléctrico opera al voltaje máximo del sistema (v.g. 5 a 10% mayor al nominal). Las normas internacionales incluyen valores recomendados para el voltaje máximo de operación para efectos de estandarización del equipo y sistemas, por ejemplo, la norma IEC-71 contiene tablas en dos rangos: 1 kV a 245 kV y mayores de 245 kV.

3. SOBRETENSIONES

Una sobretensión es cualquier voltaje entre fases o entre fase y tierra, cuyo valor de cresta sea mayor que el valor de cresta del voltaje máximo del sistema, es decir, $V_m \sqrt{2} / \sqrt{3}$ entre fase y tierra o $V_m \sqrt{2}$ entre fases.

Las sobretensiones se expresan en valores por unidad (Vpu), utilizando el voltaje máximo del sistema (V_m) como base. Por ejemplo, una sobretensión entre fase y tierra con valor máximo V_{f-t}

$$V_{pu} = \frac{V_{f-t} \sqrt{3}}{V_m \sqrt{2}} \quad \dots(1)$$

4. SOBRETENSIONES TEMPORALES

Es un voltaje oscilatorio, con una duración relativamente larga, no amortiguado o ligeramente amortiguado. La magnitud y duración de este tipo de sobretensiones somete a los apartarrayos a requerimientos severos en su capacidad de descarga y su estabilidad térmica. Una estimación correcta de su probabilidad de ocurrencia es esencial para determinar las características necesarias en los apartarrayos.

Las sobretensiones temporales son de carácter probabilístico debido a los factores aleatorios involucrados en los fenómenos que las producen. Estos factores están asociados con la forma en que se opera el sistema y la configuración del mismo (maniobras de interrupción, variaciones de voltaje, la aleatoriedad de los puntos sobre la línea donde ocurre una falla, etc.). En la práctica, estas sobretensiones ocurren como consecuencia de maniobras o debido a fallas y acciones correctivas, por lo tanto, hay una alta probabilidad de coincidencia de sobretensiones temporales y por maniobra.

Las sobretensiones temporales se pueden clasificar en tres diferentes grupos, de acuerdo a los componentes de frecuencia de la sobretensión:

Grupo 1. Sobretensiones temporales con una frecuencia de oscilación muy cercana a la frecuencia de operación del sistema. Producidas por fenómenos tan variados como: pérdida repentina de carga, corto circuitos asimétricos, efecto capacitivo en líneas largas con el extremo de entrega abierto (efecto Ferranti), resonancia en circuitos lineales producida por fases abiertas o por operación no sincronizada de interruptores, resonancia inducida entre circuitos acoplados y oscilaciones armónicas en circuitos no lineales.

En la Figura 2 se muestran distribuciones de frecuencia acumuladas para magnitudes de sobretensiones temporales debidas a maniobras en líneas sin carga, maniobras en el secundario y maniobras en líneas terminadas en transformadores.

Si se conocen las magnitudes máxima y mínima de sobretensiones temporales que pueden ocurrir en un sistema (ver Figura 2), es posible calcular la distribución de sus valores utilizando la siguiente fórmula:

$$P(V_e \geq V) = k \left((1/AV - E)^{m+1} - (1 - 1/AV_{\min})^{m+1} \right) \dots (2)$$

$$k = \frac{1}{(1 - 1/AV_{\max})^{m+1} - (1 - 1/AV_{\min})^{m+1}}$$

$$E = 1/AV_{\min} + 1/AV_{\min} - 1$$

Esta fórmula empírica es producto de ochenta mil mediciones realizadas en los sistemas de la URSS. $P(V_e \geq V)$ es la probabilidad de que la sobretensión V_e en el extremo abierto de la línea sea mayor que un valor V . El factor A es la razón entre el voltaje en el nodo de envío y el voltaje en el extremo abierto de la línea ($A \leq 1$), podemos suponer $A=1$. El exponente m depende de la forma de conexión de los reactores en paralelo, una línea de transmisión con estos elementos conectados permanentemente, con reactores que se desconectan por medio de un controlador durante cada recierre automático o para líneas sin reactores en paralelo, consideramos $m = 2$. Si los reactores en paralelo se conectan y desconectan de acuerdo a la potencia transmitida, $m = 0$.

La duración de las sobretensiones transitorias para el caso de maniobras producto de fallas (corto circuito, recierre automático, etc.) con operación simultánea de ambos lados de la línea con señales en micro-ondas o carrier, tiene valores típicos entre 0.02 y 0.15 s. Si actúa una protección de distancia o de respaldo, esta duración es entre 0.3 y 0.5 s.

Grupo 2. Sobretensiones temporales con frecuencia de oscilación mayor a la frecuencia de operación del sistema. Este tipo de sobretensiones se deben a oscilaciones forzadas con armónicas superiores pares o impares. Existen dos casos de importancia práctica:

a) **Resonancia de estado estable:** un circuito típico en el que puede ocurrir este fenómeno se muestra en la Figura 3. La corriente de magnetización que fluye por la inductancia no lineal L_m , contiene componentes a la frecuencia fundamental y componentes con armónicas superiores impares. Su probabilidad de ocurrencia es muy baja.

b) Resonancia transitoria: se presentan durante maniobras en líneas terminadas en un transformador sin carga, maniobras en el secundario de un transformador en el extremo de entrega de una línea (Figura 4), produciendo armónicas pares e impares.

Grupo 3. Sobretensiones temporales subarmónicas. Son características en líneas aéreas con compensación en serie. En algunas ocasiones su probabilidad de ocurrencia llega a 10%; aunque para un sistema bien diseñado, esta probabilidad es cercana a cero.

De acuerdo a la experiencia en campo obtenida de distintos países, la magnitud de sobretensiones transitorias en sistemas de potencia reales no llega a valores mayores de 2.0 pu.

4.1 FALLAS A TIERRA

Una falla a tierra produce una sobretensión temporal no amortiguada que persiste hasta que el el esquema de protección produce una maniobra que suprime la falla.

El tipo más común de falla se produce entre una fase y tierra, causando una sobretensión en las fases sanas, que se sostiene hasta que se corrige la situación. La magnitud de la sobretensión en las fases sanas depende de la relación entre la impedancia de secuencia cero y de secuencia positiva del sistema, vistas desde el punto donde ocurre la falla. Por lo tanto, su magnitud esta relacionada con el aterrizamiento del sistema. Esta sobretensión será menor de 1.4 pu para sistemas aterrizados efectivamente y puede llegar a 1.73 pu o más en sistemas no aterrizados.

Un sistema aterrizado efectivamente se define como aquél en el que el máximo voltaje efectivo entre fase y tierra en una de las fases sanas durante una falla es 80% o menor que el voltaje nominal entre fases en el sistema donde se localiza la falla.

La norma IEC-71 incluye gráficas para obtener el factor de aterrizamiento k , en base a las relaciones entre la resistencia de secuencia positiva, la resistencia y la reactancia de secuencia cero, con la reactancia de secuencia positiva, $R1/X1$, $R0/X1$ y $X0/X1$, desde el punto donde ocurre la falla (Figura 5). El factor de aterrizamiento es la razón entre el voltaje efectivo máximo de fase a tierra en una fase sana durante una falla y el voltaje efectivo de operación del sistema entre fase y tierra. Para un sistema aterrizado efectivamente $k = \sqrt{3}(0.8) = 1.4$.

4.2 CAMBIOS REPENTINOS EN LA CARGA

El peor caso de este tipo de sobretensiones ocurre cuando se produce un rechazo o pérdida de carga, al abrirse el interruptor remoto de una línea por la que se transmite una parte substancial de la potencia de una central generadora (Figura 6). El voltaje tiende a subir al disminuir la caída de potencial en la impedancia equivalente en serie del sistema y al producirse una aceleración del generador.

La sobretensión en el generador está determinada por el nivel de corto circuito del sistema, la velocidad del generador (respuesta del gobernador de velocidad, sistema de excitación), las características de la carga antes y después del evento, las longitudes de las líneas conectadas y la cantidad de reactivos generados por la línea (incluyendo compensación en serie o paralelo). Se puede lograr un cálculo preciso de las sobretensiones por rechazo de carga utilizando una simulación digital que incluya las características dinámicas de las máquinas, sus sistemas de control, así como el modelado de las líneas y cargas.

En pruebas de rechazo de carga en sistemas de potencia reales se han obtenido sobretensiones con magnitudes máximas de 1.45 pu.

4.3 EFECTO FERRANTI

Este efecto ocurre debido a la corriente capacitiva, producida por la carga de una línea de transmisión, fluye por la impedancia en serie cuando se abre el extremo lejano de una línea larga no compensada (Figura 7). En estas condiciones el voltaje en el extremo abierto (V_2) es siempre mayor que el voltaje en el nodo de envío (V_1). El voltaje senoidal en el extremo abierto está dado por

$$V_2 = \frac{V_1}{\cos(\beta l)} \quad \dots(3)$$

($\beta = 7.2^\circ$ cada 100 km a 60 Hz, l : longitud de la línea, km)

El efecto Ferranti se puede disminuir mediante compensación inductiva en paralelo o compensación capacitiva en serie.

4.4 RESONANCIA

Algunas de las más severas sobretensiones temporales ocurren debido a condiciones de resonancia. En su forma más simple, el circuito equivalente de un sistema resonante consiste de una fuente, un interruptor y un circuito resonante RCL. La sobretensión se produce al cerrar el interruptor, limitada por pérdidas y efectos de saturación de algunos componentes.

Ignorando las pérdidas, la sobretensión se puede aproximar con la siguiente ecuación

$$V_2 = \frac{V_1 X_c}{X_L + X_c} \quad \dots(4)$$

donde V_1 es el voltaje en el nodo de envío y V_2 es el voltaje en el nodo de recepción.

En la práctica se pueden producir condiciones cercanas a la resonancia. Un ejemplo es el caso de la apertura de una fuente de alta tensión que alimenta a un circuito de baja tensión por medio de un cable y un transformador, si la reactancia inductiva del transformador es cercana a la reactancia capacitiva del cable. Otro caso de resonancia es cuando las armónicas asociadas a la saturación de un transformador tienen frecuencias cercanas a la frecuencia natural de resonancia del sistema. Las sobretensiones debidas a resonancia pueden evitarse cambiando las impedancias de elementos del sistema. Esta consideración debe formar parte de los criterios de diseño del mismo.

4.5 FERRORESONANCIA

Este tipo de sobretensiones ocurre cuando un elemento magnético saturable del sistema es excitado por una capacitancia. La capacitancia puede representar, por ejemplo, al capacitor de graduación entre los contactos abiertos de un interruptor o la capacitancia a tierra de un cable (Figura 8).

Este fenómeno puede producirse también cuando solamente una o dos fases de un sistema se encuentran energizadas debido a la operación de fusibles o interruptores (Figura 9). El elemento saturable puede representar transformadores de potencial (con reactancias altas) conectados al bus abierto, o bien, un transformador con terciario conectado en delta que a su vez alimenta transformadores auxiliares.

La sobretensión en las terminales depende de la magnitud y forma de la corriente que fluye por el elemento magnético, a su vez, esta corriente depende del estado magnético del elemento. Al entrar y salir éste de la región de saturación (Figura 10), su inductancia efectiva cambia, resultando en voltajes con multitud de armónicas. Estos voltajes pueden presentar componentes con frecuencias mayores o menores de la frecuencia de operación del sistema (Figura 11). Diversos estudios efectuados con TNA muestran que existe mayor posibilidad de que se presente ferresonancia en sistemas en los que la reactancia capacitiva equivalente sea menor a veinte veces la reactancia inductiva, $X_c < 20X_L$.

Las sobretensiones por ferresonancia se pueden controlar operando los transformadores a una densidad de flujo reducida, también se pueden implementar procedimientos de maniobra que eviten energizar un transformador sin carga através de elementos capacitivos.

4.6 ENERGIZACION DE UNA LINEA TERMINADA EN UN TRANSFORMADOR

Este tipo de maniobras producen sobretensiones temporales ligeramente amortiguadas. Se originan durante la energización o recierre de una línea terminada en un transformador. Después del transitorio inicial (que se clasifica como sobretensión por maniobra), la corriente de excitación del transformador produce un sobrevoltaje sostenido durante varios segundos (Figura 12). Su magnitud depende del instante en que se cierre el interruptor, la impedancia equivalente de la fuente, los parámetros de la línea y el transformador y del flujo residual de éste último.

5. SOBRETENSIONES POR MANIOBRA

Son voltajes transitorios, amortiguados y de relativamente corta duración, producidos por acciones de conexión o desconexión por medio de elementos de interrupción del sistema. La magnitud de una sobretensión por maniobra depende del voltaje de operación del sistema. Actualmente se clasifican como sobretensiones transitorias de frente lento.

5.1 CIERRE Y RECIERRE DE LINEAS DE TRANSMISION

La energización de una línea en vacío, no terminada en un transformador, produce sobretensiones debido a las ondas viajeras en los conductores, estas ondas son producidas por el cierre del interruptor o pueden ser causadas por acoplamiento entre fases. Los tiempos relativos de cierre entre los polos del interruptor son importantes para determinar este tipo de sobretensiones, otros factores involucrados son la longitud de la línea, el grado de compensación en paralelo, las características de la fuente equivalente en el nodo de envío, la utilización de resistencias de preinserción y el tipo de terminación en el extremo de la línea. En general las sobretensiones son mayores en el extremo de entrega de la línea.

La apertura de una línea puede dejar un voltaje remanente en la línea desenergizada. A menos que la carga atrapada sea drenada a tierra por medio de un transformador o reactor, puede permanecer en la línea durante varios segundos. La cantidad de carga dependerá de la capacitancia equivalente de la línea y del valor de la resistencia de preinserción (Figura 13), su decremento en el tiempo varía según las condiciones atmosféricas (Figura 14).

Si ocurre un recierre de una línea con carga atrapada y, en el instante en que el interruptor cierra, el voltaje de la fuente tiene polaridad opuesta al voltaje en la línea abierta, se pueden producir sobretensiones muy altas.

Como resultado de un estudio realizado en conjunto por los comités 13 y 33 de CIGRE, se elaboró un diagrama que condensa información sobre factores de sobretensión producidos por el cierre y recierre de líneas (Figura 15). Este diagrama incluye resultados de simulaciones digitales, TNA y mediciones en campo. Se muestran valores mínimos, medios y máximos para una combinación de condiciones del sistema, en forma de un árbol de decisiones. Las opciones son: cierre o recierre trifásico, con o sin resistencia de preinserción, con una fuente inductiva o compleja (sistemas con cables, en los que debe añadirse una capacitancia en paralelo en el equivalente de Thévenin), compensación en paralelo mayor o menor al 50%.

5.2 MANIOBRAS EN CIRCUITOS INDUCTIVOS

Este tipo de sobretensiones puede analizarse con un circuito sencillo, presentado en la Figura 16. Si la reactancia del elemento inductivo de la carga L_c es menor que la reactancia de la capacitancia en paralelo C_c , la mayor parte de la corriente que circula por el circuito fluye por la inductancia L_c y se encuentra atrasada 90° respecto al voltaje de la fuente; además, se supone que la reactancia de la fuente es pequeña comparada con la correspondiente a la carga, $L_s \ll L_c$.

Al iniciarse la apertura de los contactos del interruptor, el arco entre éstos conduce la corriente de la carga. El arco tenderá a extinguirse cuando la corriente alterna llegue a un valor de cero. Debido a que el circuito es puramente inductivo, en el momento de interrupción el voltaje en la fuente y el voltaje en la carga tendrán valores cercanos al máximo.

La interrupción del arco separa al circuito en dos secciones. El voltaje en el contacto del lado del generador tiene dos componentes: una de 60 Hz y una oscilación amortiguada superpuesta cuya frecuencia tiene valores entre 0.5 y 100 kHz, dependiendo de los valores de los parámetros L_s y C_s . El voltaje en el contacto del lado de la carga es oscilatorio amortiguado con una frecuencia dependiendo de C_c y L_c . El voltaje de recuperación transitoria se puede calcular obtenido la diferencia entre los voltajes que aparecen entre los contactos del interruptor, se inicia una carrera entre las propiedades dieléctricas del medio entre los contactos y este voltaje.

5.2.1 REIGNICION DEL ARCO

Existe la posibilidad de una reignición del arco que produce el flujo de corriente con frecuencia mayor a la de operación del sistema y causa una escalación en el voltaje en la carga. Si la corriente se interrumpe de nuevo al llegar al valor de cero, pueden aparecer varios ciclos de reignición e interrupción, con escalaciones de voltaje cada vez mayores (Figura 17).

5.2.2 CORTE DE PEQUEÑAS CORRIENTES INDUCTIVAS

El arco que se forma entre los contactos de un interruptor durante una apertura en un sistema con carga inductiva, se encuentra sujeto a inestabilidades conforme la corriente que fluye por él tiende a cero. Estas se presentan en forma de oscilaciones en la corriente y el voltaje entre los contactos. Si la inestabilidad es seguida de una repentina caída de la corriente a cero, se produce un fenómeno que se conoce como corte prematuro de una pequeña corriente inductiva (Figura 18).

En el modelo más simplificado del arco, suponemos que la transición entre un estado y otro se realiza de modo exponencial con una cierta constante de tiempo. Se desprecian las inductancias del lado de la carga y del lado de la fuente L_s y L_c , obteniéndose un circuito equivalente formado por dos ramas: una contiene una inductancia L_a en serie con una resistencia R_i , la segunda incluye una capacitancia C en paralelo con una resistencia R_a . C es la capacitancia equivalente de C_s y C_c en serie. En la Figura 19 se muestra la simplificación del circuito y la solución de la ecuación diferencial, de la cual obtenemos una expresión para la corriente en el arco. La condición para inestabilidad se da cuando el factor exponencial es creciente. Lo anterior resulta en una relación entre la corriente de corte (i_{ch}) y la raíz cuadrada de la capacitancia equivalente (C), en la que está involucrado un factor que depende del tipo de interruptor. Para una capacitancia típica de $C = 10 \text{ nF}$ los valores de esta corriente son:

tipo de interruptor	i_{ch}
pequeño volumen de aceite	7 a 10 A
hexafluoruro de azufre SF ₆	4 a 17 A
aire comprimido	15 a 20 A

La sobretensión generada del lado de la carga una vez ocurrido el corte prematuro de la corriente, depende de los valores de i_{ch} , L_c y C_c . La energía almacenada en estos elementos antes del corte, se convierte en energía electrostática. Haciendo un balance de energía, se puede

obtener la siguiente fórmula para el factor de la sobretensión

$$k_s = \sqrt{1 + \left(\frac{I_{ch}}{U_o}\right)^2 \frac{L_e}{C_e} \eta_m} \quad \dots (5)$$

donde U_o es el voltaje pico de operación del sistema y η_m es la eficiencia magnética en el sistema, y toma valores entre 0.3 y 0.5.

5.2.3 CORTE VIRTUAL DE UNA CORRIENTE INDUCTIVA

En circuitos trifásicos, la reignición del arco en un polo del interruptor puede producir un corte virtual de corriente que causa mayores sobretensiones que el corte prematuro de corriente, descrito anteriormente. Como se ilustra en la Figura 20, el primer polo en abrir corresponde a la fase A, la corriente i_a llega a cero y, si la carga no está aterrizada, las corrientes en las otras fases son iguales y tienden normalmente a cero $i_b = i_c$. Si ocurre una reignición del arco en la fase A, se producirán corrientes oscilatorias de frecuencia mayor a la nominal del sistema en las tres fases, que pudieran ser interrumpidas al pasar por cero. Esta interrupción es semejante a un corte prematuro de una corriente inductiva.

5.3 MANIOBRAS EN CIRCUITOS CAPACITIVOS

Consideremos un circuito sencillo formado por una carga capacitiva suministrada por una fuente inductiva. La corriente en la carga adelanta al voltaje en 90° . Cuando se interrumpe la corriente, al llegar a cero, el voltaje del sistema se encuentra en un valor cercano al máximo (marcado con un 1 en la Figura 21). El voltaje de recuperación transitoria en el interruptor es muy pequeño, por lo que no ocurre reignición del arco, y la carga capacitiva queda cargada al voltaje pico de operación del sistema. Al pasar medio ciclo, el voltaje de recuperación llegará al doble del voltaje pico del sistema, 2 pu. Si en ese momento ocurre una reignición del arco en el interruptor (marcado con un 2 en la Figura 21). Entonces, despreciando las pérdidas, el voltaje en el capacitor podría subir hasta 3 pu. Al interrumpirse de nuevo el circuito, el capacitor queda cargado a 3 pu, repitiéndose el ciclo indefinidamente.

En un sistema trifásico este fenómeno es más complejo, particularmente si alguno de los interruptores opera antes que los otros dos. Las mayores sobretensiones ocurren cuando solo una de las fases abre y su valor depende de la relación entre la capacitancia de secuencia positiva y la capacitancia de secuencia cero del sistema, ver Figura 22.

6. SOBRETENSIONES POR DESCARGAS ATMOSFERICAS

Dentro de la clasificación actual, éstas se consideran como sobretensiones de frente rápido. Producidas como consecuencia de descargas entre la nube y tierra, se pueden dividir en sobretensiones producidas por descargas directas y sobretensiones inducidas.

La descarga atmosférica consta de varias fases, iniciando con una guía descendente que viaja desde la nube hacia tierra, dando saltos de 50 m, a velocidad promedio de 150km/s, cubre una distancia promedio de 3 km en 20 ms. La guía descendente puede ser encontrada por una guía ascendente originada en una estructura alta. La guía descendente se encuentra al potencial de la nube, al llegar a tierra, se drenan las cargas en el canal y los paquetes de cargas en la nube hacia tierra, durante lo se denomina el rayo de retorno (Figura 23). Mediciones de las corrientes del rayo de retorno han resultado en su caracterización con una forma de doble exponencial con un frente rápido, adquiriendo su valor máximo en 1 a 30 μ s, seguido de un decremento al 50% de su valor pico, que toma de 10 a 250 μ s. Para descargas negativas, que representan el 90% de las descargas a tierra, el valor medio de la amplitud de la corriente durante el rayo de retorno es de 30 kA, con valores máximos de 100 kA. Existen publicaciones con distribuciones acumuladas de distintos parámetros relacionados con descargas a tierra, ver Figura 24.

En una línea de transmisión sin hilos de guarda o, si ocurre una falla en el blindaje, la corriente producida por el rayo de retorno es inyectada directamente a una de las fases. Esta corriente $i(t)$ se va a dividir en dos ondas viajeras que se propagan hacia extremos opuestos de la línea, cuya impedancia característica es Z_0 . La sobretensión producida $v(t)$ esta dada por la siguiente ecuación

$$v(t) = Z_0/2 i(t) \quad \dots(6)$$

Por ejemplo, una corriente inyectada en una fase, con magnitud de 10 kA, produciría un voltaje con magnitud de 2MV en una línea con impedancia característica de 400 Ω .

Si la descarga incide en el hilo de guarda, se puede producir un flameo inverso, al subir el potencial de la torre. La Figura 25 muestra los porcentajes de la corriente total que fluyen por las torres de una línea de transmisión, por descargas directas a la mitad de la distancia interpostal y directas a una de las torres, siendo éste último el peor caso.

Cuando la descarga atmosférica cae en el punto en que se une el hilo de guarda y la torre, la corriente se divide en tres componentes, dos que viajan en sentidos opuestos sobre el hilo de guarda, la tercera que se propaga por la torre hacia la base, donde se produce una reflexión. La Figura 26 muestra las formas típicas de las sobretensiones producidas en la torre, las cuales producen un esfuerzo en las cadenas de aisladores.

7. SOBRETENSIONES EN SUBESTACIONES ENCAPSULADAS EN SF6

Este tipo de sobretensiones se conocen también como sobretensiones transitorias muy rápidas. Ocurren como consecuencia de maniobras con cuchillas e interruptores en subestaciones encapsuladas en hexafluoruro de azufre y son importantes en sistemas con voltajes nominales mayores a 300kV. Se caracterizan por tiempos de frente en el rango de decenas y cientos de nanosegundos.

La componente de mayor frecuencia de estas sobretensiones esta determinada por el tiempo en el que se produce el colapso en el voltaje entre los electrodos, que a su vez depende de la presión de trabajo del gas SF6. Se ha propuesto la siguiente fórmula para estimar el tiempo mínimo en el frente de la sobretensión

$$t_f = 1 \text{ a } 1.5 \frac{1}{p} \quad (\text{ns}) \quad \dots(7)$$

esta expresión puede obtenerse a partir de la ecuación de Toepler para un arco eléctrico. El tiempo de frente de la sobretensión se reduce bajo la presencia de protuberancias o asperezas en la superficie de los electrodos y por partículas en el gas.

Al analizar estas sobretensiones es necesario utilizar la teoría de ondas viajeras, considerando cierta velocidad de propagación en un medio con una impedancia característica. La forma y valor máximo de la sobretensión en algún punto de interés dependen de la configuración misma de la subestación, como resultado de una serie de reflexiones y refracciones de la onda viajera en transiciones y ramificaciones.

Otros factores que determinan la forma y magnitud de estas sobretensiones es el diseño de los contactos del interruptor o cuchilla desconectadora (la asimetría trae consigo una dependencia de la descarga en la polaridad del voltaje) y su velocidad de operación (la carga atrapada en el extremo desconectado depende de esta velocidad).

Otro fenómeno que ocurre en subestaciones en SF6 son las tensiones transitorias en la carcaza, que producen arqueo entre las partes aterrizadas de la subestación. Este es un fenómeno de baja energía, no hay evidencia de peligro para el personal, puede causar daño a equipo de control y protección. Las sobretensiones en la carcaza pueden controlarse mediante el diseño apropiado de las conexiones a tierra.

Este tipo de transitorios produce radiación a frecuencias de 10 a 20 MHz, con magnitudes de campo eléctrico de 10 kV/m.

La distribución no lineal de voltaje que producen en transformadores sujeta a esfuerzos adicionales las primeras vueltas del devanado, las conexiones y taps. En algunos casos es necesario proteger los cambiadores de taps con varistores. Se considera que la prueba de impulso cortado sujeta a este equipo a esfuerzos semejantes.

En cuanto a cuchillas e interruptores, existen pruebas de impulso en posiciones abierta y cerrada, es necesario considerar posiciones intermedias.

En la Figura 27 se muestran algunas sobretensiones por maniobra medidas en subestaciones encapsuladas en SF6.

REFERENCIAS

- [1] International Electrotechnical Commission, Publication IEC 71-2, Insulation Coordination Part II: Applications Guide, Geneve, Switzerland.
- [2] Gert, T., Glavitsch, H., Tikhodeyev, N., Shur, S. & Thoren, B, CIGRE, International Conference on Large High Tension Electric Systems, Temporary Overvoltages, their classification, magnitude, duration, shape and frequency of occurrence, Report of Study Committee No.33, 33-12, 1972 Session, August 28-September 6, p. 1-14.
- [3] EPRI, Electric Power Research Institute, Transmission Line Reference Book, 345 kV and above, 2nd. edition, Publication No. EL-2500, Palo Alto, CA 94303, 1982, p. 421-445, 545-597.
- [4] Catenacci, G. & Palva, V., Switching Overvoltages in EHV and UHV Systems with special reference to closing and reclosing transmission lines, ELECTRA, No. 30, p. 70-121.
- [5] Slamecka, E., Interruption of Small Inductive Currents, Chapters 1 and 2, CIGRE Working group 13.02, ELECTRA, No.72, 1974, p. 73-103.
- [6] Berger, K., Anderson, R. & Kroninger, H., Parameters of Lightning Flashes, CIGRE Working group No. 33, ELECTRA, No.41, p. 23-69.
- [7] CIGRE Working group 33/13-09, Very Fast Transient Phenomena Associated with Gas Insulated Substations, International Conference on Large High Voltage Electric Systems, 1988 Session, August 28-September 3, p. 1-20.

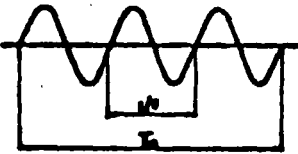
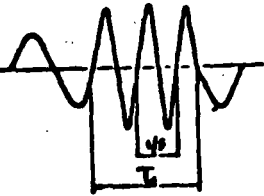
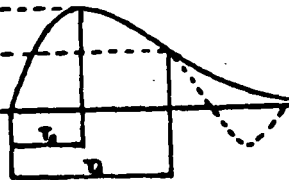
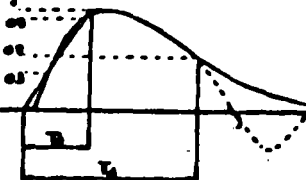
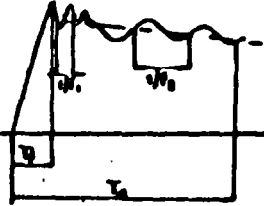
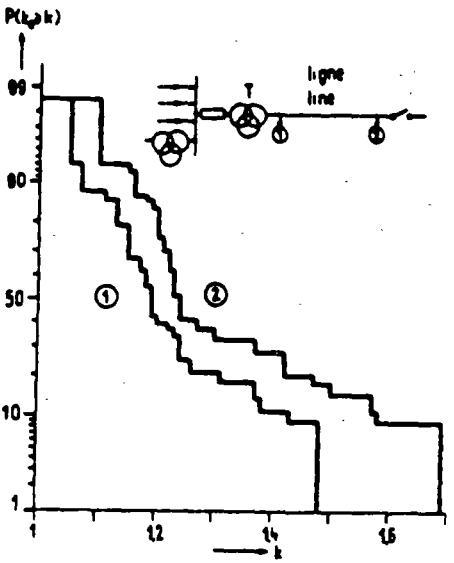
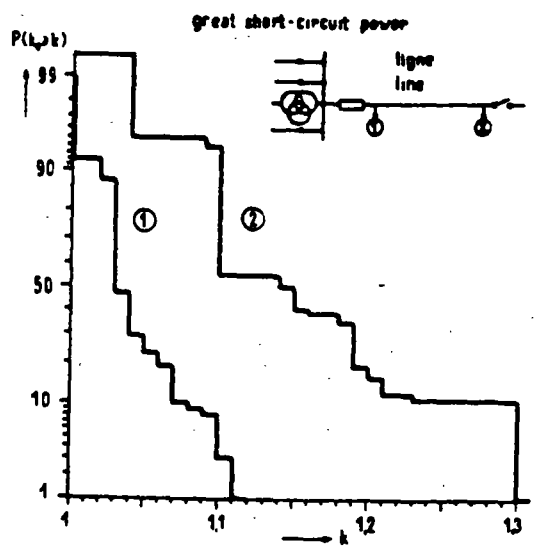
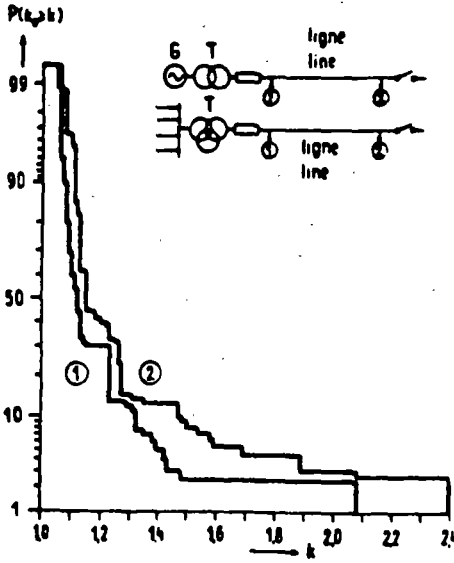
CLASS	LOW FREQUENCY		TRANSIENT		
	CONTINUOUS	TEMPORARY	SLOW-FRONT	FAST-FRONT	VERY-FAST-FRONT
voltage shape					
range of voltage shape	$f = 50 \text{ or } 60 \text{ Hz}$ $T_d \geq 1 \text{ hr}$	$50 < f < 500 \text{ Hz}$ $0.03 < T_d < 3600 \text{ s}$	$30 < T_f < 3000 \mu\text{s}$ $0.3 < T_d < 30 \text{ ms}$	$0.3 < T_f < 30 \mu\text{s}$ $3 < T_d < 300 \mu\text{s}$	$3 < T_f < 300 \text{ ns}$ $0.3 < f_1 < 100 \text{ kHz}$ $30 < f_2 < 300 \text{ kHz}$ $0.03 < T_d < 3 \text{ ns}$
standard voltage shape	$f = 50 \text{ or } 60 \text{ Hz}$ $T_d = (*)$	$48 \leq f \leq 62 \text{ Hz}$ $T_d = 1 \text{ min}$	$T_f = 250 \mu\text{s}$ $T_d = 2500 \mu\text{s}$	$T_f = 1.2 \mu\text{s}$ $T_d = 50 \mu\text{s}$	under consideration
standard withstand test	long-duration power-frequency test	short-duration power-frequency test	switching impulse test	lightning impulse test	(chopped impulse) under consideration

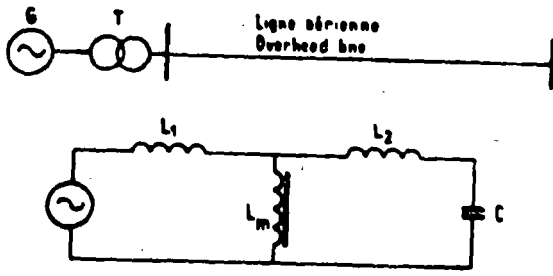
Figura 1. Clasificación de esfuerzos eléctricos y sobretensiones de acuerdo a la norma IEC-71.



SCHEME

	k_{min}	k_{max}
	② 1,14	1,44
	① 1,04	1,22
	② 1,07	1,25
	① 1,00	1,03
	② 0,94	0,97
	① 1,11	1,18
	② 1,11	1,23

Figura 2. Curvas de distribución de frecuencia acumulada para magnitudes de sobretensiones temporales en el extremo de envío (1) y en el extremo de recepción (2): a) fuente con bajo nivel de corto circuito (230 mediciones/curva), b) fuente con alto nivel de corto circuito (100 mediciones/curva), maniobras en el secundario (70 mediciones/curva), c) rango de magnitudes medidas para diferentes circuitos.



L_1, L_m - short-circuit and magnetizing inductance of the transformer
 L_2, C - inductance and capacitance of the overhead line.

Figura 3. Circuito en el que ocurre resonancia en estado estable con componentes fundamental y armónicas superiores.

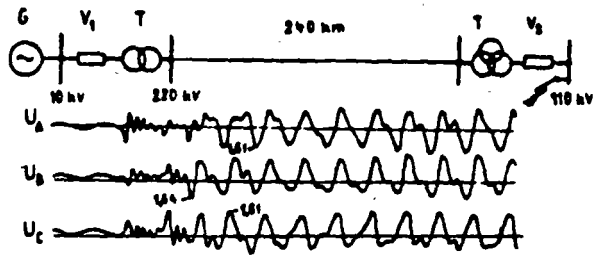


Figura 4. Circuito en el que ocurre resonancia transitoria al eliminar una falla trifásica en el secundario de un transformador. El interruptor en V2 esta abriendo.

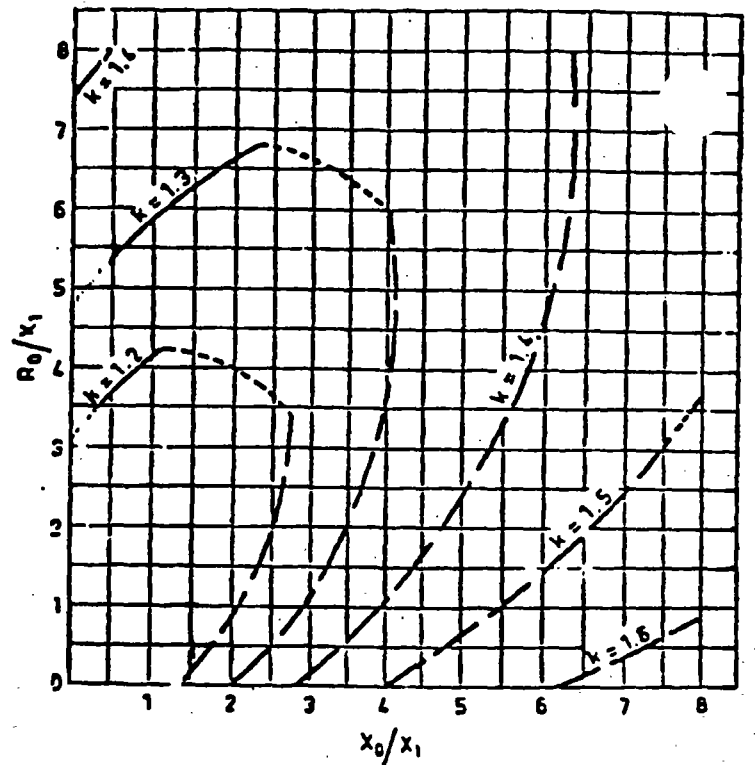
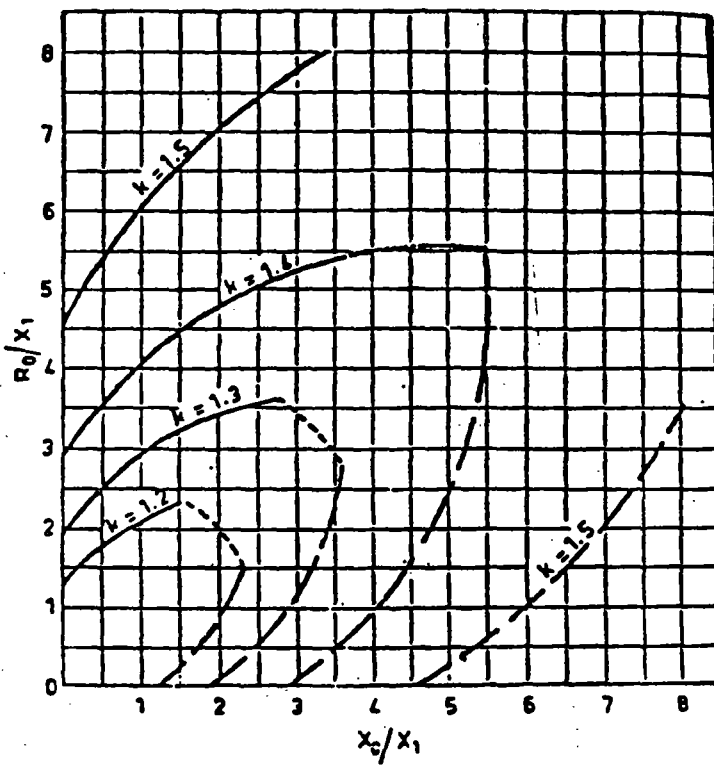
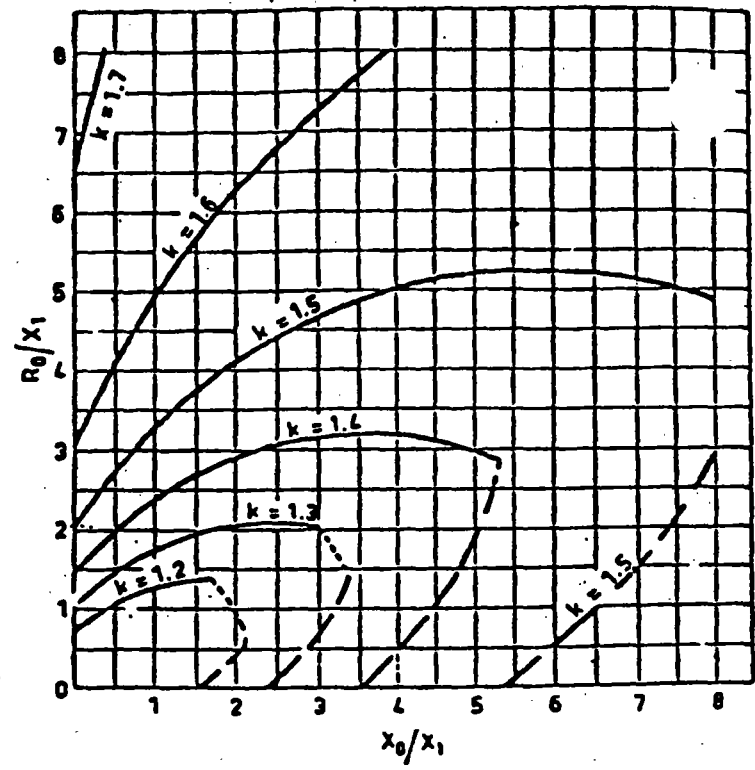
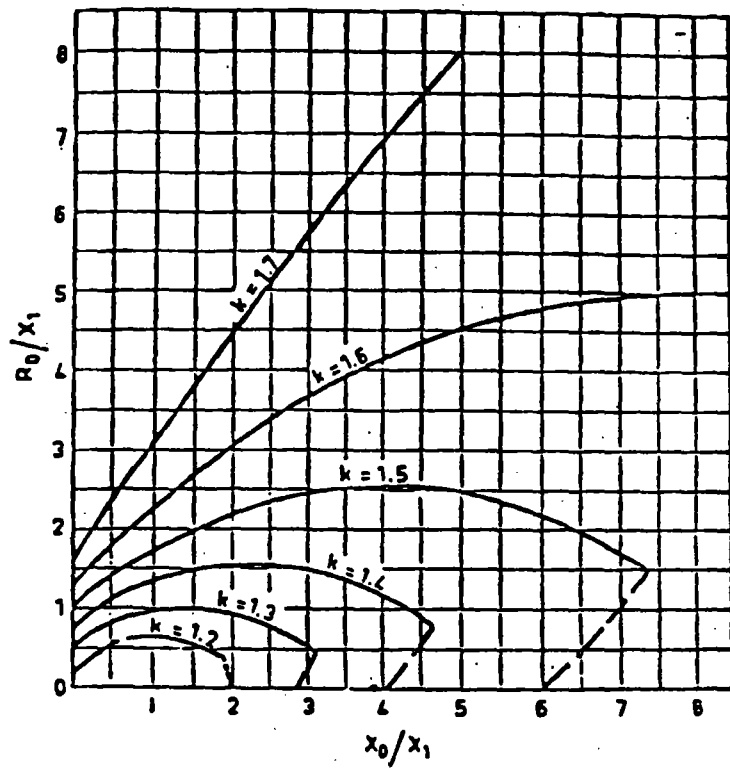


Figura 5. Factores de aterrizamiento para: a) $R_1 = 2X_1$, b) $R_1 = X_1$, c) $R_1 = 0.5X_1$ y d) $R_1 = 0$.

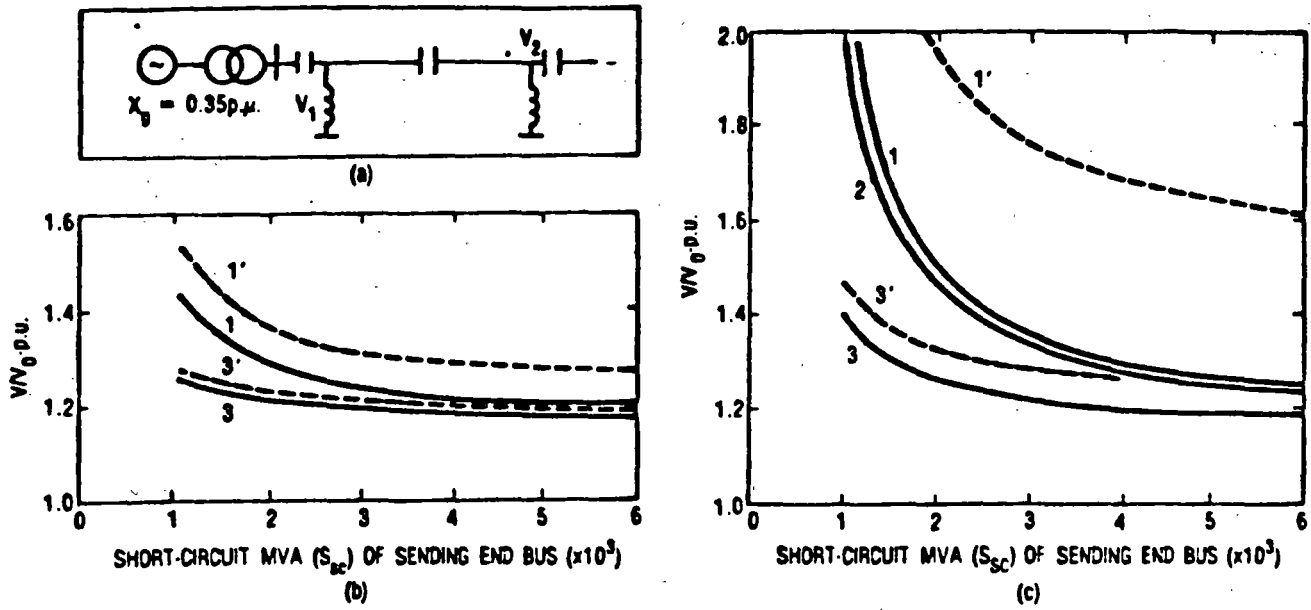


Figura 6. Sobretensiones a frecuencia nominal causados por rechazo de carga: a) diagrama, b) línea de 300 km de longitud, c) línea de 600 km de longitud. 1 y 1' sin compensación, 2 con compensación capacitiva en serie de 50%, 3 y 3' con 50% de compensación en serie y 70% de compensación en paralelo. 1, 2 y 3 son voltajes en el nodo de envío, 1' y 3' son voltajes en el nodo de recepción. Voltaje nominal 400 kV, carga inicial 33% del nivel de corto circuito del nodo de envío. Se supone un incremento en la velocidad del generador de 10% y se desprecian pérdidas.

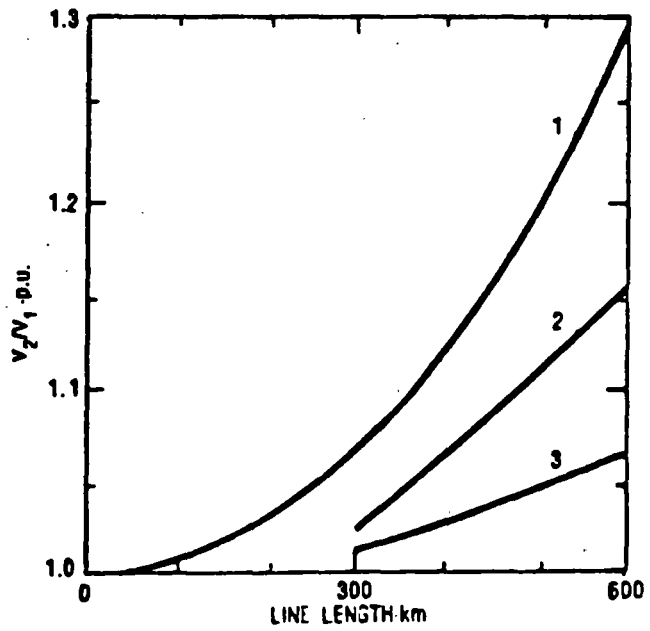


Figura 7. Magnitud de sobretensiones debidas al Efecto Ferranti: (1) sin compensación, (2) compensación en serie de 50% y (3) 50% de compensación en serie, 70% de compensación en paralelo.

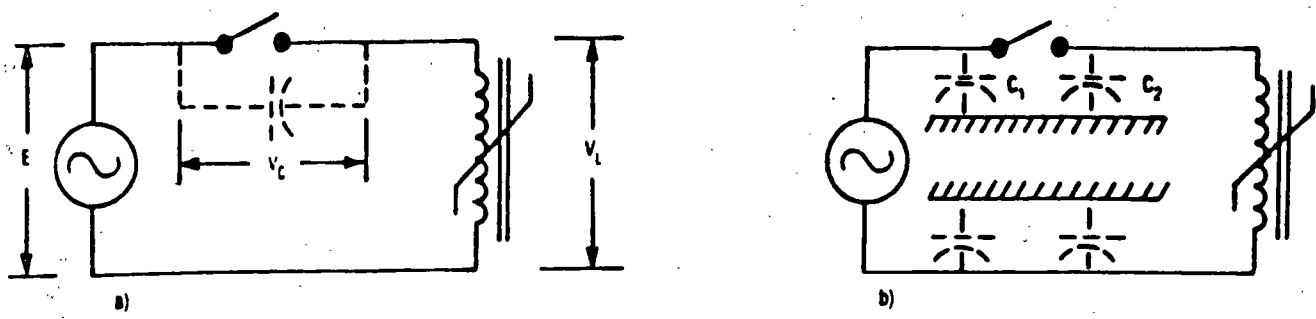


Figura 8. Circuitos sujetos a ferros resonancia: a) excitación por medio de la capacitancia entre los contactos de un interruptor abierto, b) excitación por medio de una capacitancia a tierra.

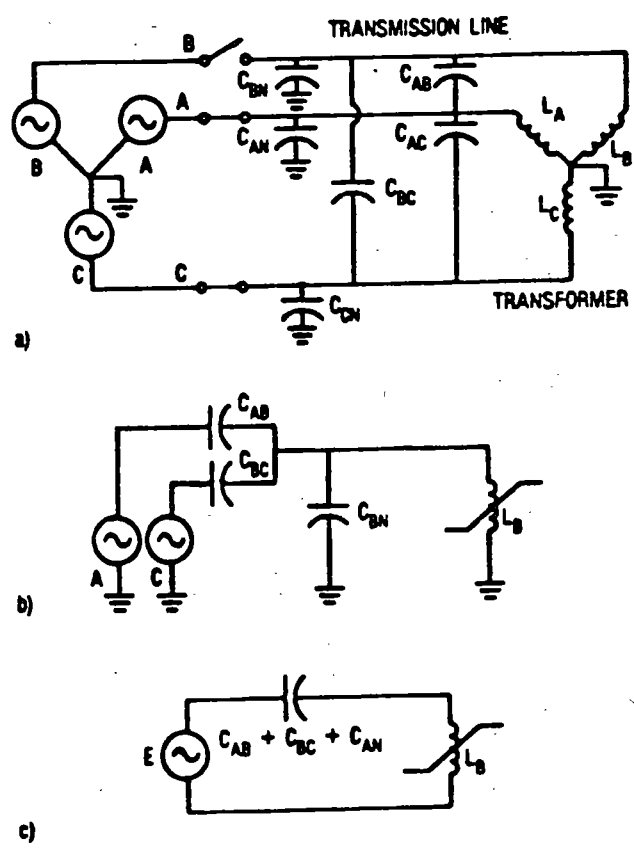


Figura 9. Circuito trifásico con fase B abierta, sujeto a ferros resonancia: a) representación trifásica, b) y c) circuitos equivalentes simplificados.

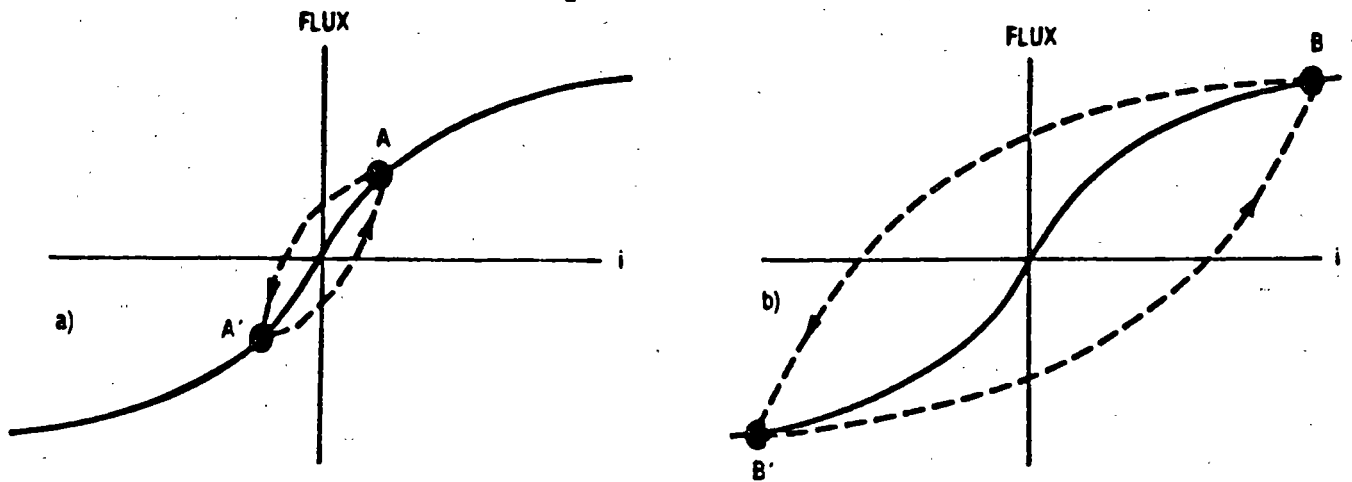


Figura 10. Operación de un elemento ferromagnético: a) en la región lineal y b) en la región saturada.

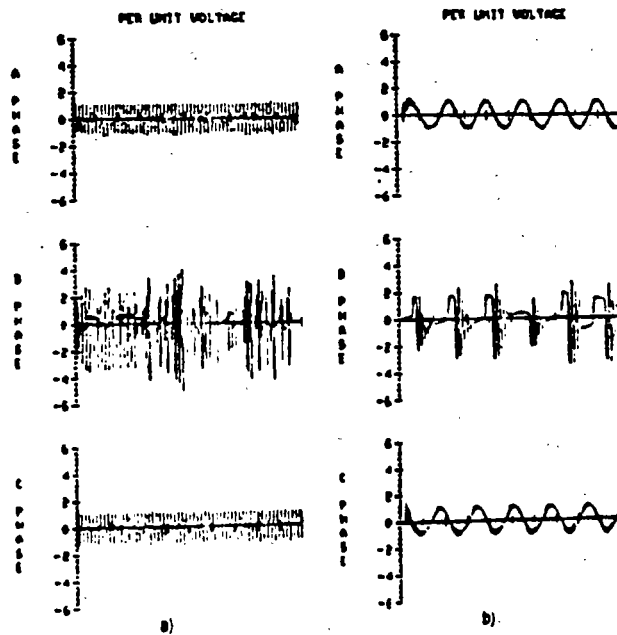


Figura 11. Voltajes ferroresonantes producidos por la apertura de la fase B (ver Figura 9): a) escala 100 ms/div b) escala 10 ms/div.

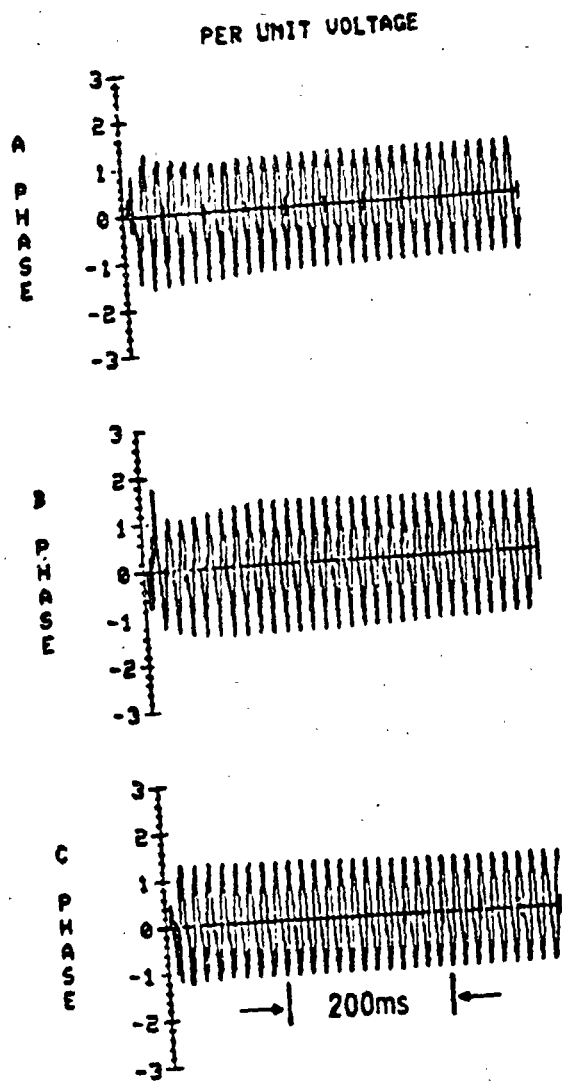


Figura 12. Sobretensión temporal producida al energizar una línea terminada en un transformador.

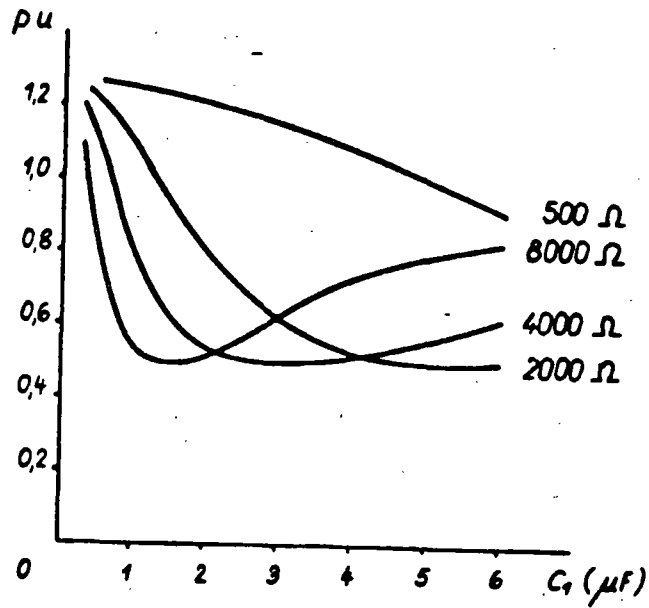


Figura 13. Variación del valor en por unidad de la carga atrapada, en función de la capacitancia total de la línea y el valor de la resistencia de preinserción.

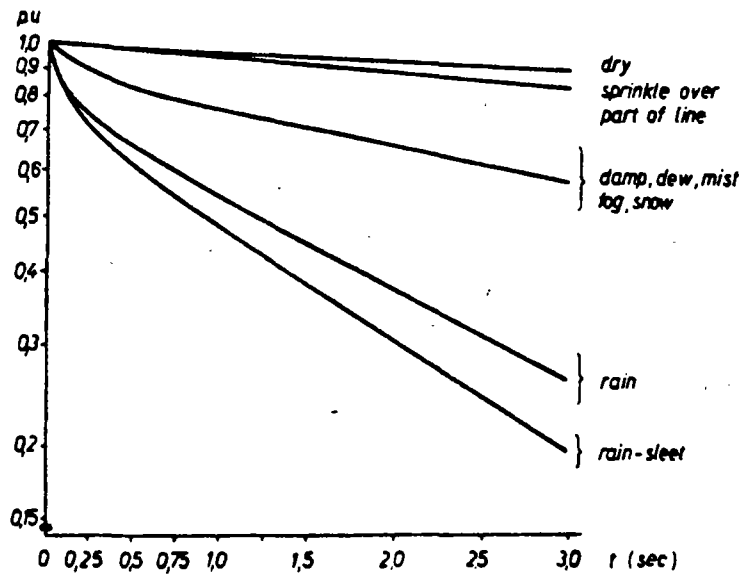


Figura 14. Variación del valor por unidad de la carga atrapada en una línea en función del tiempo y las condiciones atmosféricas.

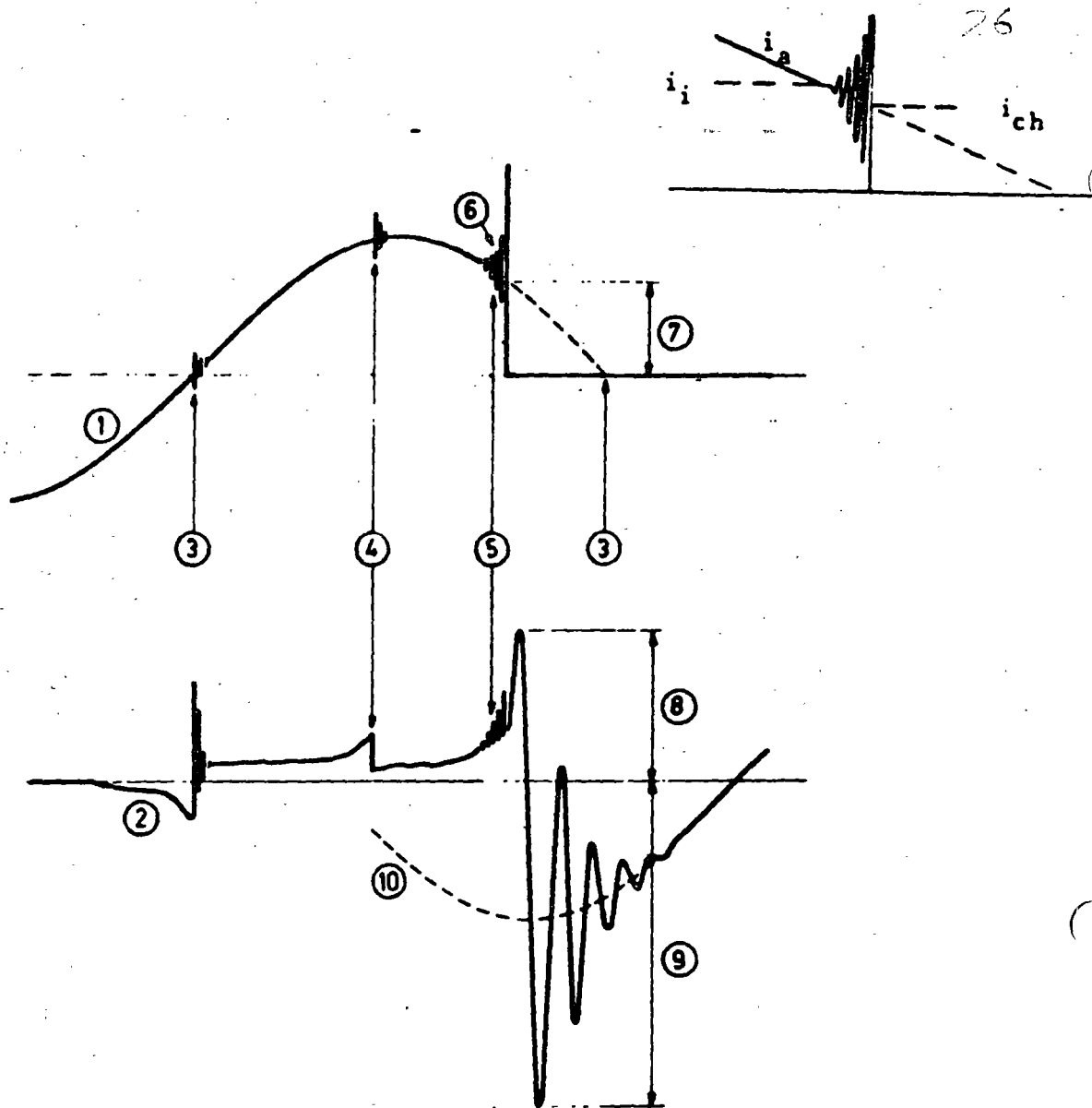
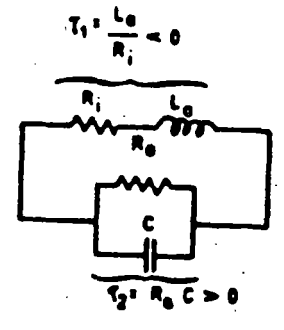
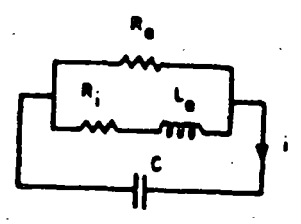
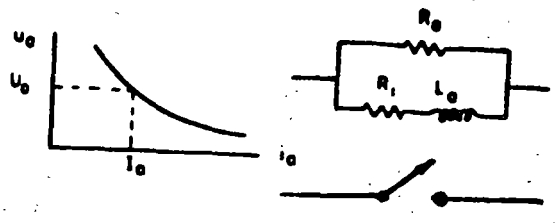
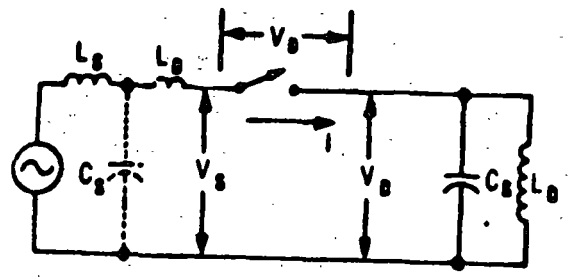


Figura 18. Corriente y voltaje en el arco entre los contactos de un interruptor, para el caso de una interrupción prematura de la corriente

Definiciones:

- (1) Corriente circulando por el interruptor ($i_a(t)$)
- (2) Voltaje entre los contactos del interruptor
- (3) Disminución normal de la corriente a cero
- (4) Inestabilidad en el arco que no causa corte prematuro
- (5) Inestabilidad en el arco con corte prematuro
- (6) Oscilación inestable
- (7) Magnitud de la corriente al momento de corte (i_{ch})
- (8) Voltaje de supresión
- (9) Voltaje máximo de recuperación
- (10) Voltaje de alimentación



$$R_a = \frac{U_a}{I_a}$$

$$R_i = \frac{-\alpha R_a}{1 + \alpha}$$

$$L_a = \frac{\Theta R_a}{1 + \alpha}$$

$$\frac{d^2 i}{dt^2} + \left(\frac{1}{\tau} + \frac{1}{\tau_2}\right) \frac{di}{dt} + \omega_0^2 i = 0$$

$$\tau_1 = L_a/R_i; \tau_2 = R_a C; \omega_0^2 = \frac{R_a + R_i}{R_a} \cdot \frac{1}{L_a C}$$

$$i(t) = I e^{-t/\tau} \cos(\omega_i t + \phi)$$

$$1/\tau = \frac{1}{2} (1/\tau_1 + 1/\tau_2); \omega_i = \sqrt{(\omega_0^2 - 1/\tau^2)}$$

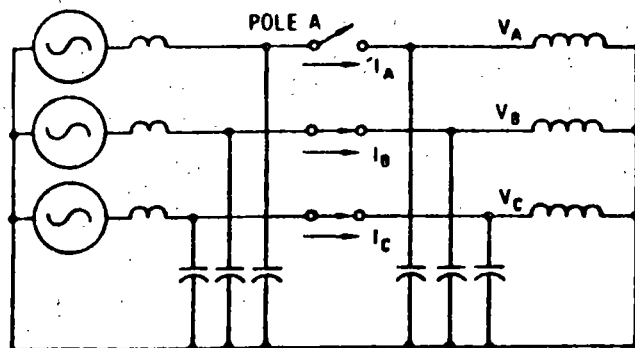
$$R_a = \eta I_a^{-(\alpha+1)}$$

$$I_{ch}^{\alpha+1} = \frac{\alpha \eta C}{\theta}$$

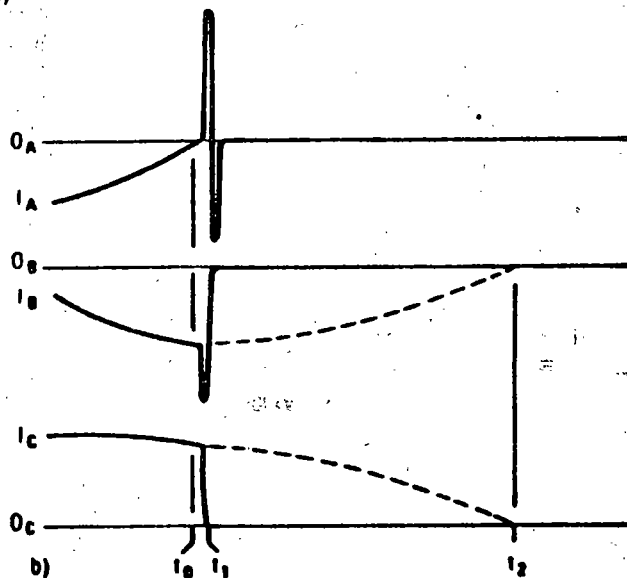
$$I_{ch} = \sqrt{\frac{\eta C}{\theta}}$$

$$\sqrt{\frac{\eta}{\theta}} = \begin{cases} \text{oil-minimum} & (7 \dots 10) \times 10^4 \\ SF_6 & (4 \dots 17) \times 10^4 \\ \text{air-blast} & (15 \dots 20) \times 10^4 \end{cases}$$

Figura 19. Circuito equivalente y análisis del modelo estático del arco en un interruptor sujeto a corte prematuro de una pequeña corriente inductiva.



a)



b)

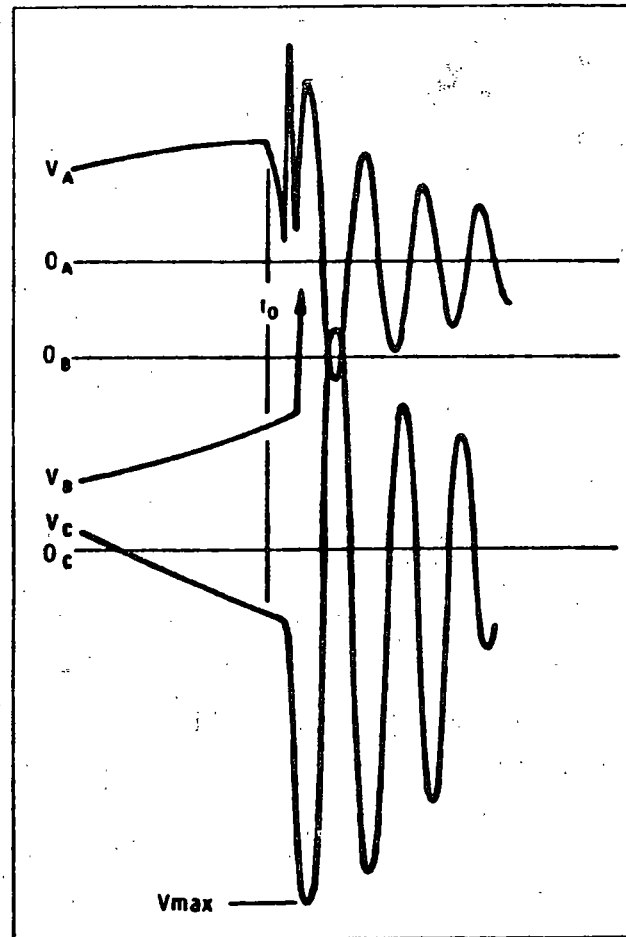


Figura 20. Corte virtual de corriente en un circuito trifásico con carga inductiva: a) circuito, b) corrientes, c) voltajes.

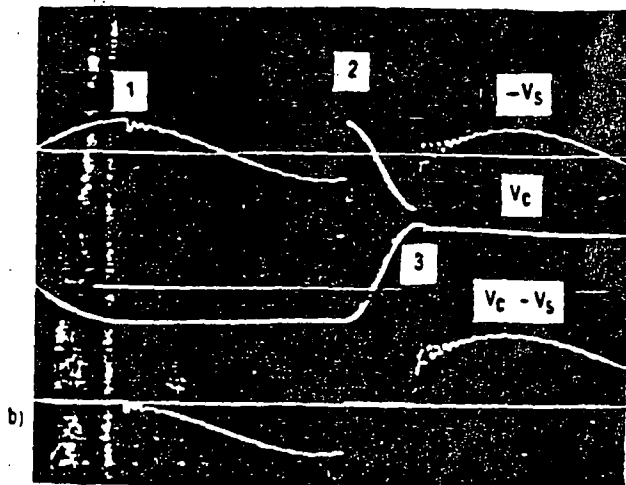
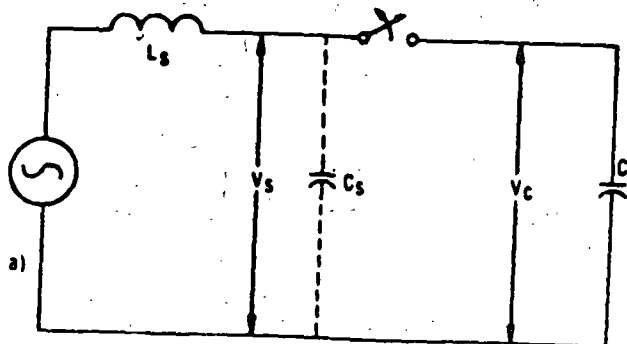


Figura 21. Maniobra en un circuito capacitivo a) circuito, b) voltajes en la fuente V_s , la carga V_c y voltaje de recuperación transitoria en el interruptor $V_c - V_s$.

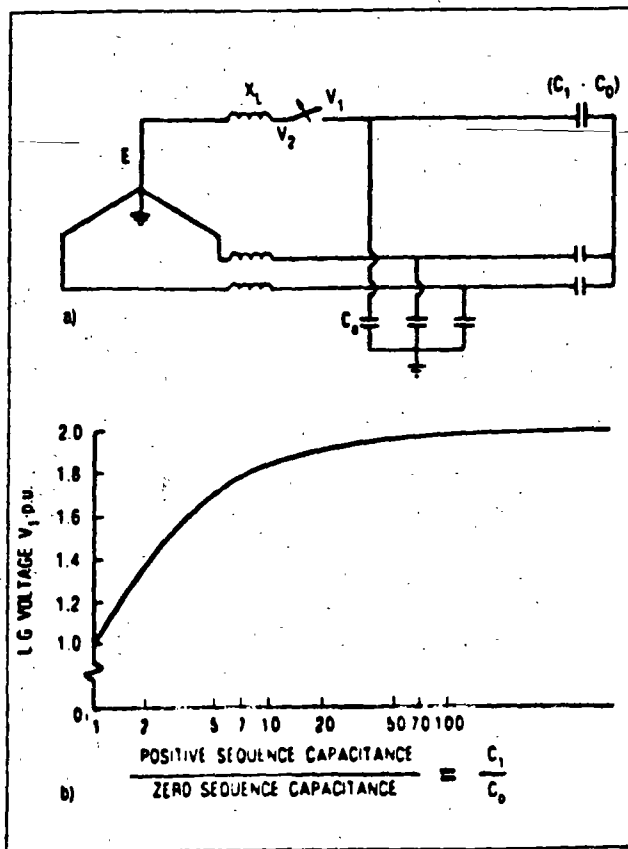


Figura 22. Factor de sobretensión producido al abrir una de las fases de un sistema trifásico con carga capacitiva, suponiendo que no hay reignición del arco: a) circuito, b) relación entre la sobretensión y las capacitancias de secuencias positiva y cero.

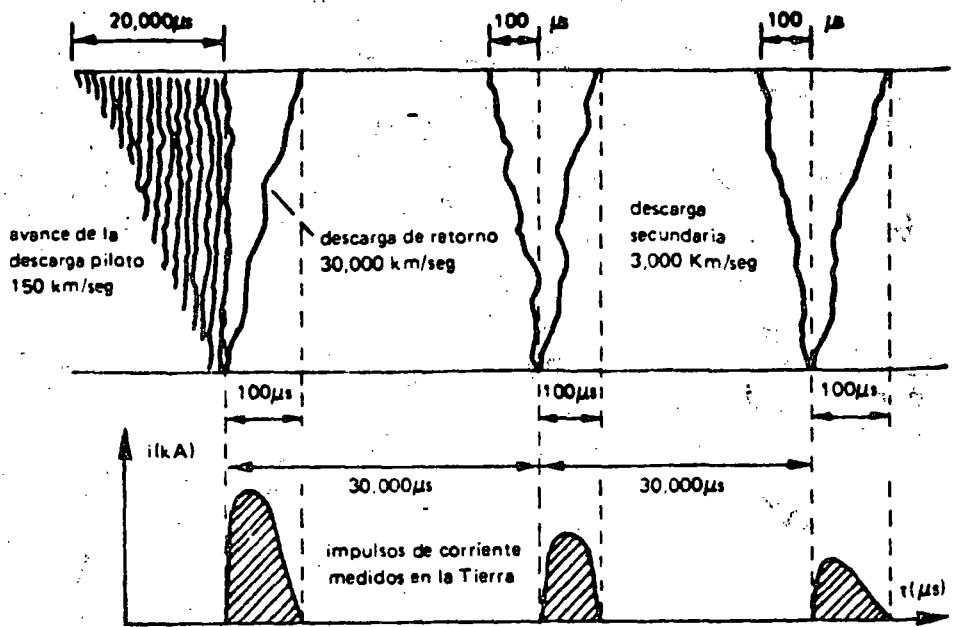


Figura 23. Representación gráfica de una descarga atmosférica formada por una guía descendente, primer rayo de retorno, guía flecha y rayos de retorno subsecuentes.

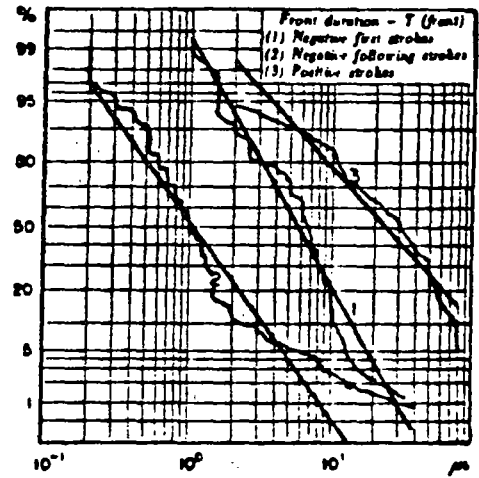
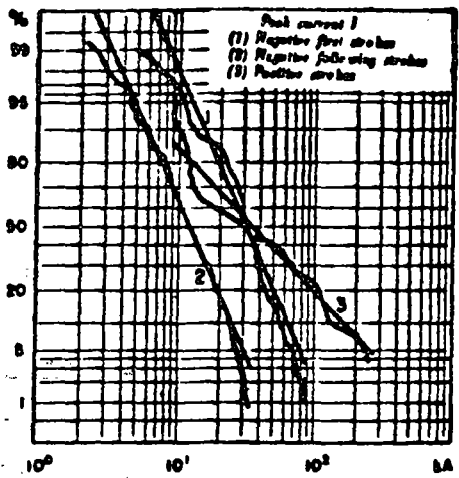


Figura 24. Distribuciones acumuladas de frecuencias para las magnitudes y tiempos en el frente de corrientes de rayos de retorno (obtenidas por Berger).

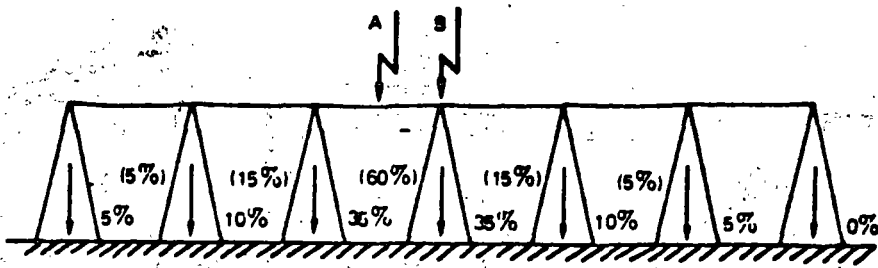
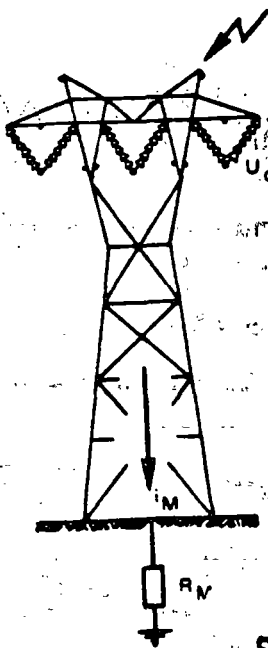
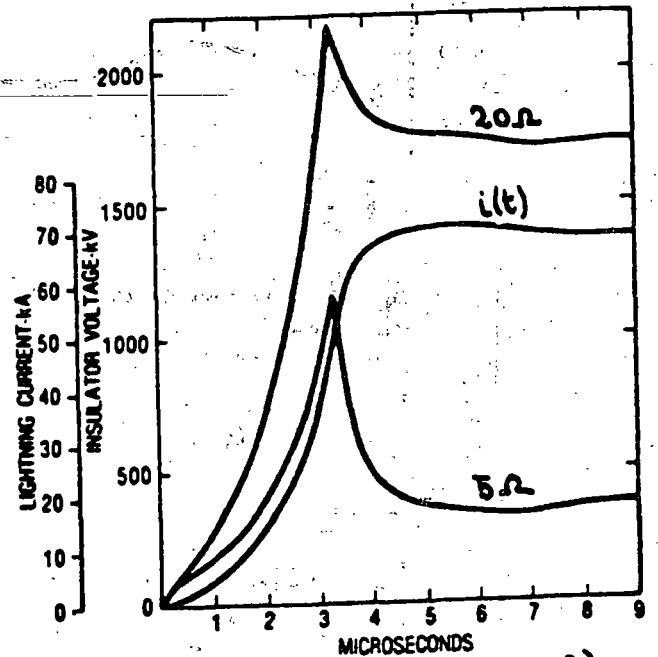
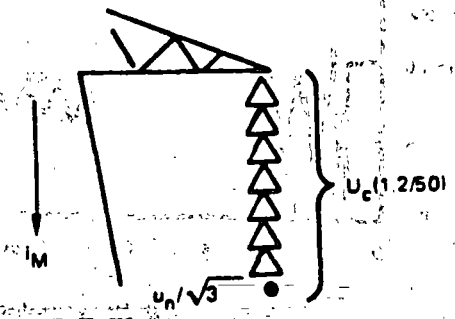


Figura 25. Distribucion de la corriente inyectada a una línea de transmisión por una descarga atmosférica directa a la mitad de la distancia entre torres y directa a una de las torres.

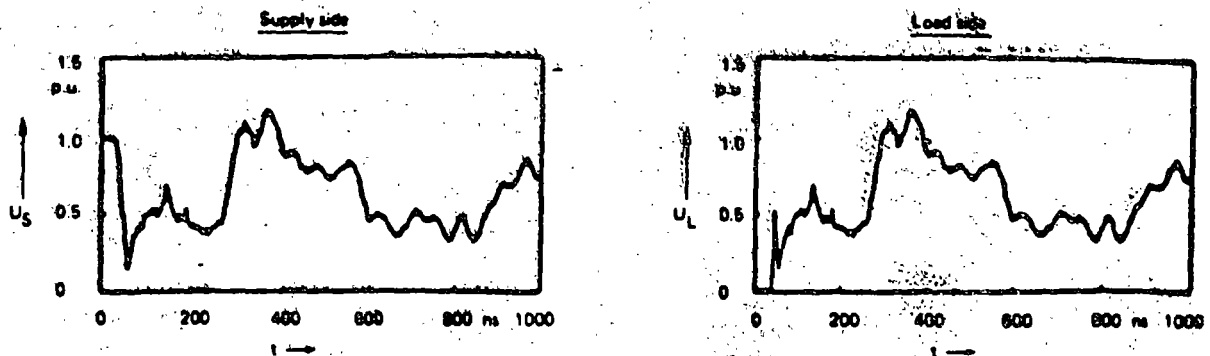


a)

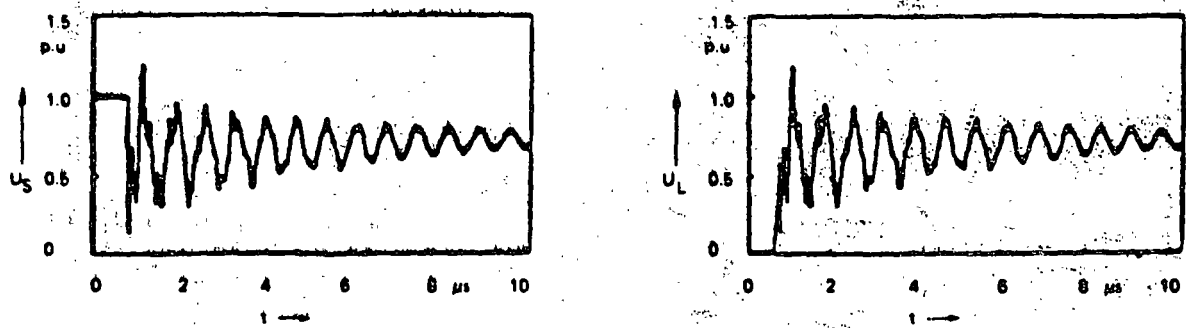


c)

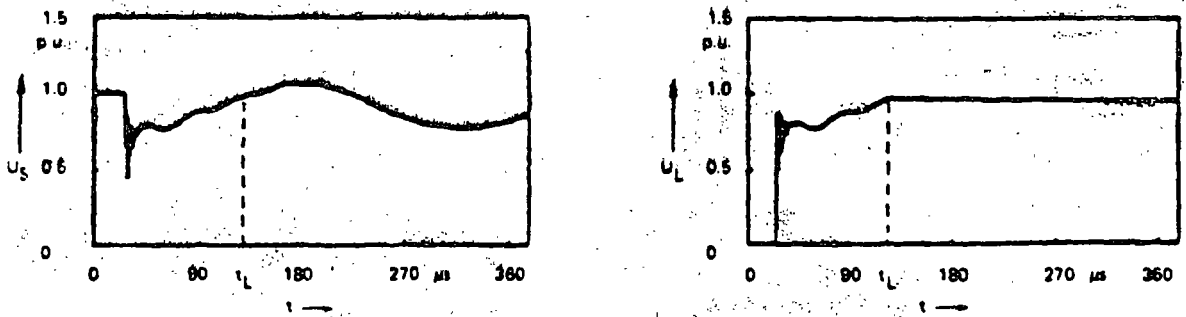
Figura 26. Descarga directa al hilo de guarda y la torre de transmisión: a) esquema, b) circuito equivalente, c) forma típica de la sobretensión producida en la torre para resistencias a tierra de 5 y 20 Ω y forma de onda de la corriente.



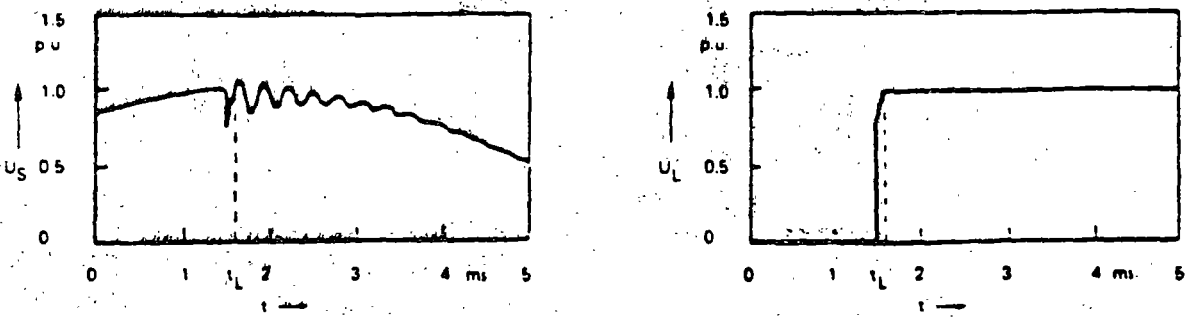
a) Steep voltage transients (traveling waves). Typical risetime 5 - 10 ns.



b) Mainly monofrequent oscillation after about 100 ns. Frequency range: MHz.



c) Overall transient by oscillation of the power transformer and the GIS. Frequency range: 20 - 100 kHz.



d) Low frequency transient and steady state condition.

Figura 27. Algunas sobretensiones por maniobra, medidas en subestaciones aisladas con SF6.